Enzyme Engineering

XIII

Editors

Jonathan S. Dordick

Alan J. Russell

Annals of the
New York
Academy of
Sciences

ANNALS OF
THE NEW YORK ACADEMY
OF SCIENCES

Volume 799

REPORT DOCUMENTATION PAGE

Form Approved
OMB NO. 0704-0188

1. AGENCY USE ONLY *(Leave blank)*	2. REPORT DATE July 1997	3. REPORT TYPE AND DATES COVERED Final 1 Sep 95 - 31 Aug 96

4. TITLE AND SUBTITLE

Engineering Foundation Conference on Enzyme Engineering XII

5. FUNDING NUMBERS

DAAH04-95-1-0507

6. AUTHOR(S)

Alan J. Russell, principal investigator

7. PERFORMING ORGANIZATION NAMES(S) AND ADDRESS(ES)

United Engineering Trustees, Inc.
New York, NY 10017

8. PERFORMING ORGANIZATION REPORT NUMBER

9. SPONSORING / MONITORING AGENCY NAME(S) AND ADDRESS(ES)

U.S. Army Research Office
P.O. Box 12211
Research Triangle Park,, NC 27709-2211

10. SPONSORING / MONITORING AGENCY REPORT NUMBER

ARO 34550.1-LS-CF

11. SUPPLEMENTARY NOTES

The views, opinions and/or findings contained in this report are those of the author(s) and should not be construed as an official Department of the Army position, policy or decision, unless so designated by other documentation.

12a. DISTRIBUTION / AVAILABILITY STATEMENT

Approved for public release; distribution unlimited.

12 b. DISTRIBUTION CODE

13. ABSTRACT *(Maximum 200 words)*

14. SUBJECT TERMS

15. NUMBER IF PAGES

16. PRICE CODE

17. SECURITY CLASSIFICATION OR REPORT UNCLASSIFIED	18. SECURITY CLASSIFICATION OF THIS PAGE UNCLASSIFIED	19. SECURITY CLASSIFICATION OF ABSTRACT UNCLASSIFIED	20. LIMITATION OF ABSTRACT UL

ENZYME ENGINEERING XIII

19970912 064

Cover: The illustration on the softcover edition of this volume depicts the lipase from Rhizomucor miehei complexed with substrate after minimization. (Courtesy of Susan Linko and coworkers.)

ENZYME ENGINEERING XIII[a]

Editors and Conference Organizers
JONATHAN S. DORDICK and ALAN J. RUSSELL

CONTENTS

Part II. Biopolymer Structure and Function

Introduction

JONATHAN S. DORDICK[a] AND ALAN J. RUSSELL[b]

[a]Department of Chemical and Biochemical Engineering
University of Iowa
Iowa City, Iowa 52242

[b]Department of Chemical and Petroleum Engineering
University of Pittsburgh
Pittsburgh, Pennsylvania 15261

Enzyme technology is an interdisciplinary field that has had a broad impact in biotechnology, synthetic chemistry, pharmaceutical discovery and development, and agriculture. In addition to fundamental enzymology, enzymes are used routinely in the development of new biologically active compounds and their intermediates, in the preparation of materials with unique functional properties, and in the evolution of novel processes for synthesizing and purifying enzyme-derived products. The repertoire of biocatalysts has expanded beyond conventional natural enzymes and now encompasses the generation of new biocatalysts with highly selective properties that function under rigorous environments previously accessible only to hardy chemical catalysts.

This volume contains the proceedings of the Thirteenth International Enzyme Engineering Conference, which was held in San Diego, California, on October 15–20, 1995. The conference was sponsored by the Engineering Foundation, New York, and supported by 4 government agencies and 17 companies, without whose support the conference would not have been possible. Enzyme Engineering XIII focused on both fundamental and applied aspects of enzyme technology, including the preparation of novel enzyme systems isolated from nature or engineered by investigators, and the uses of enzymes in a wide variety of industrial processes. The main themes of the papers presented at the meeting were as follows:

- preparation and properties of designed biocatalysts
- biopolymer structure and function
- biocatalysts under extreme environments
- application of protein expression in biocatalysis
- biochemical engineering of enzyme systems
- biomaterials synthesis and design
- enzymes in organic synthesis.

Papers presented herein are compiled from both oral and poster presentations, the latter from topics included in the aforementioned list.

The executive committee in charge of organizing the conference was composed as follows:

- Chairpersons—Jonathan S. Dordick and Alan J. Russell
- Members—Douglas S. Clark, Thomas Graycar, Isao Karube, Allen Laskin (ex officio), Marie-Dominique Legoy, Onno Missett, Frieder Scheller, Itaru Urabe, and Li Gao Xiang.

The Enzyme Engineering Award

The Enzyme Engineering Award was established in 1982 to recognize exceptional achievements in enzyme engineering research and applications. It recognizes new discoveries, research, process or device developments in enzyme engineering, and outstanding contributions of a scientific or engineering nature in the design, operation, and management of facilities, processes, or devices based primarily on enzyme engineering.

The first award in 1983 was to Ichiro Chibata, Japan. Subsequent recipients were as follows—1985: Klaus Mosbach, Sweden; 1987: Ephraim Katchalski-Katzir, Israel; 1989: Saburo Fukui, Japan; 1991: Alexander M. Klibanov, United States; 1993: Malcolm D. Lilly, England; 1995: Maria-Regina Kula jointly with Christian Wandrey, Germany.

The award committee for the 1995 award consisted of Klaus Mosbach (chair), Frances H. Arnold, Ephraim Katchalski-Katzir, Alexander M. Klibanov, Malcolm D. Lilly, and Tetsuya Tosa.

Strategy for the Directed Evolution of a Peptide Ligase

HUIMIN ZHAO, YOU LI, AND FRANCES H. ARNOLD

Division of Chemistry and Chemical Engineering
California Institute of Technology
Pasadena, California 91125

INTRODUCTION

Available natural resources are being tailored to fulfill increasing demands for new biocatalysts. A practical strategy for altering enzyme properties is to introduce random base substitutions into the gene sequence and then select or screen for variants that express the desired phenotype(s). Features that have been enhanced by random mutagenesis include catalytic activity,[1] activity in organic solvents,[2,3] thermostability[4] and alkaline stability,[5] and substrate specificity.[1,6] Once the genes are sequenced, effective mutations can be accumulated by site-directed mutagenesis.[4,7] An attractive alternative to sequencing and site-directed mutagenesis is to accumulate beneficial mutations in sequential rounds of random mutagenesis,[2,3] following a "directed evolution" strategy.[8] Directed evolution is likely to prove useful for enhancing enzyme performance in "nonnatural" environments[2,3] as well as for obtaining new features never required by nature, provided an efficient selection or screening method can be found to channel the enzyme's evolution towards the desired properties. A significant advantage of this approach over "rational" design methods is that neither structural information nor a mechanistic road map is required to guide the desired evolution experiment.

Subtilisin is a useful catalyst for organic synthesis, particularly in the presence of organic solvents. Subtilisin can catalyze regioselective[9] and stereoselective[10] acylations in organic media. The enzyme also catalyzes peptide synthesis, either by direct reversal of the hydrolytic process or by aminolysis of N-protected amino-acid or peptide esters.[11] The addition of water-miscible organic solvents shifts the reaction direction to favor aminolysis and also increases the solubility of the substrate and products. Compared to chemical peptide synthesis, enzymatic peptide synthesis offers several advantages, including high efficiency, mild reaction conditions that can minimize problems of undesired side reactions, minimal use of noxious chemicals, and simple scale-up after optimization of the process. Most importantly, enzymes have high selectivity, including enantioselectivity, chemoselectivity, and regioselectivity, which can be invaluable for fine chemical, pharmaceutical, and agricultural applications. To make full use of these advantages, a broadly applicable peptide ligase functioning in organic solvents is needed.

Here, we report the successful application of the directed evolution approach to

1

improve the activity of subtilisin in the presence of a polar organic solvent, dimethyl-
formamide (DMF). A *B. subtilis–E. coli* shuttle vector has been developed to
facilitate establishment of the mutant library in *B. subtilis*. The resulting evolved 13M
subtilisin is 471 times more active than wild-type subtilisin E in 60% DMF. A new,
direct method for rapid screening of peptide ligase activity in a random mutant
library is also described.

RESULTS

B. subtilis–E. coli *Shuttle Expression Vector pBE2*

Successful application of directed enzyme evolution requires the screening of
large numbers of variants for the desired feature(s). The size of the mutant library
that can be established in *E. coli* is not generally a limiting factor for screening.
However, the direct cloning of mutant subtilisin E genes into *B. subtilis*–competent
cells occurs with low efficiency relative to *E. coli*. The *B. subtilis–E. coli* shuttle vector
pBE2 was designed to increase the size of the mutant library that could be
established in *B. subtilis*. As shown in FIGURE 1, the shuttle vector was constructed by
ligating three DNA fragments from plasmids pUB110 and pUC19 containing the
replication origin region and the kanamycin resistance gene of pUB110, the portion
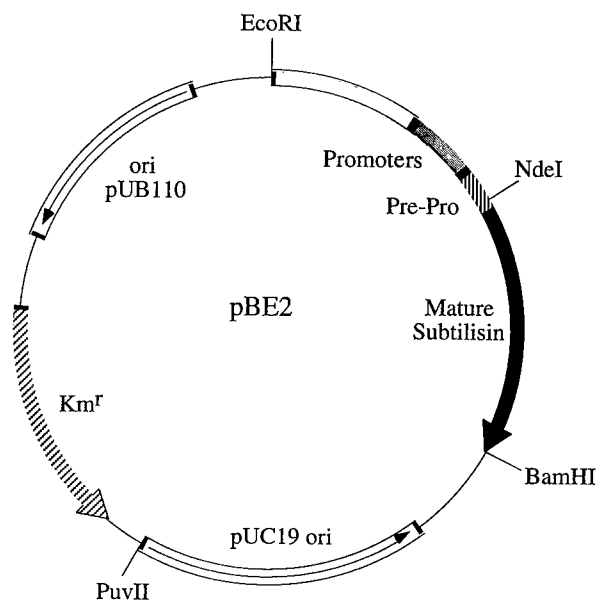
FIGURE 1. The *B. subtilis–E. coli* shuttle vector pBE2 was constructed by ligating three DNA
fragments from plasmids pUB110 and pUC19 containing the replication origin and the
kanamycin resistance gene of pUB110.[3]

TABLE 1. Kinetic Parameters k_{cat}, K_M, and k_{cat}/K_M for Hydrolysis of suc-Ala-Ala-Pro-Phe-*p*-Nitroanilide by Subtilisin E Variants in 0.1 M Tris-HCl/10 mM CaCl$_2$ (pH 8.0) Containing 0%, 20%, and 60% (v/v) DMF (37 °C)

	0% DMF			20% DMF			60% DMF	
Variant	K_M (mM)	k_{cat} (s^{-1})	k_{cat}/K_M (M^{-1}-s^{-1} × 10^{-3})	K_M (mM)	k_{cat} (s^{-1})	k_{cat}/K_M (M^{-1}-s^{-1} × 10^{-3})	k_{cat}/K_M (M^{-1}-s^{-1} × 10^{-3})	
WT	0.56	21	38	12	17	1.4	0.014	1[a]
10M	0.1	27	270	0.7	73	104	2.2	157[a]
13M	0.067	39	582	0.4	98	245	6.6	471[a]

[a]Catalytic efficiency relative to wild-type (WT) subtilisin E.

of pUB110 covering the minus-strand replication origin, and the replication origin region of pUC19. The subtilisin E gene was subcloned from pKWZ.

Catalytic Activities of the "Evolved" Enzyme

Starting with the gene for 10M subtilisin E,[2] two additional generations of PCR-based random mutagenesis and screening were conducted. As shown in TABLE 1, the specific catalytic efficiency k_{cat}/K_M of the resulting evolved 13M subtilisin E is greater than that of its parent 10M and much greater than that of the wild-type enzyme in the presence of DMF cosolvent. For instance, in 60% DMF, k_{cat}/K_M for 13M subtilisin E is 3-fold higher than 10M and 471-fold higher than the wild-type subtilisin E. The increase in catalytic efficiency reflects an increase in k_{cat} as well as a decrease in K_M. The crystallographic model of 13M subtilisin E is shown in FIGURE 2. The ten amino-acid substitutions in the parent 10M enzyme (shown in white) are on the surface and are clustered on the enzyme face that harbors the active site and substrate binding pocket. The two new amino-acid substitutions found in 13M subtilisin E (shown in black) also appear more or less on the same face. Interestingly, most of the twelve amino-acid substitutions already exist in subtilisins from different species.[2,3]

In Situ *Screening Method for Peptide Ligase Activity*

In this method, one amino-acid ester is tethered to a cellulose filter paper, while a fluorescent dye is attached to the second amino acid. Protease-catalyzed coupling of these two amino acids results in the attachment of dye to the paper. The location and intensity of the fluorescence can be used to identify protease variants with improved activity. In this case, L-methionine methyl ester was tethered to the paper through linker-1, while L-methionine was attached to fluorescein isothiocyanate (FITC) through linker-2. Tetraethylene glycol derivative linkers serve as spacer arms to make the amino acids accessible to the enzyme. The assay scheme is outlined in FIGURE 3. Preliminary results indicate that a fluorescent spot above background corresponding to the position of active enzyme occurred on the derivatized filter paper. Further quantification and optimization are under way.

FIGURE 2. Model of subtilisin E showing the ten amino-acid mutations in 10M (white) and the two additional mutations identified in the 13M variant (black) evolved for increased activity in aqueous DMF. Peptide substrate s-AAPF-pNA is shown in the CPK model.
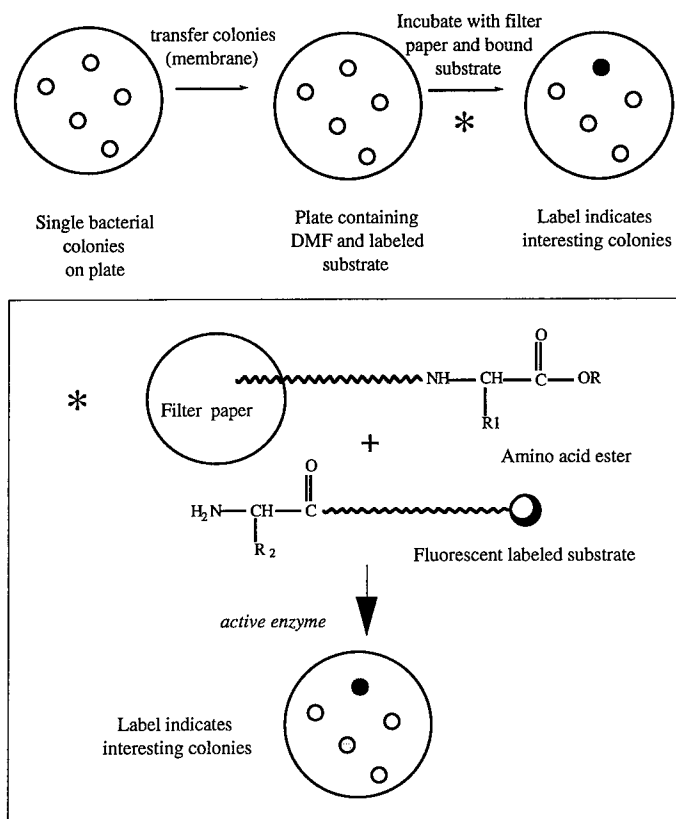
FIGURE 3. Scheme of the *in situ* screening method for peptide ligase activity.

REFERENCES

1. GRAHAM, L. D., K. D. HAGGETT, P. A. JENNINGS, D. S. LE BROCQUE & R. G. WHITTAKER. 1993. Biochemistry **32:** 6250–6258.
2. CHEN, K. Q. & F. H. ARNOLD. 1993. Proc. Natl. Acad. Sci. U.S.A. **90:** 5618–5622.
3. LI, Y. & F. H. ARNOLD. 1996. Protein Eng. **9:** 77–83.
4. JOYET, P., N. DECLERCK & C. GAILARDIN. 1992. Bio/Technology **10:** 1579–1583.
5. CUNNINGHAM, B. C. & J. A. WELLS. 1987. Protein Eng. **1:** 319–325.
6. OLIPHANT, A. R. & K. STRUHL. 1989. Proc. Natl. Acad. Sci. U.S.A. **86:** 9094–9098.
7. STRAUSBERG, S. L., P. A. ALEXANDER, D. T. GALLAGHER, G. L. GILLILAND, B. L. BARNETT & P. N. BRYAN. 1995. Bio/Technology **13:** 669–673.
8. ARNOLD, F. H. 1996. Chem. Eng. Sci. In press.
9. RIVA, S. & A. M. KLIBANOV. 1988. J. Am. Chem. Soc. **110:** 3291–3295.
10. MARGOLIN, A. L., P. A. FITZPATRICK, P. L. DUBIN & A. M. KLIBANOV. 1991. J. Am. Chem. Soc. **113:** 4693–4694.
11. WONG, C-H. & K-T. WANG. 1991. Experientia **47:** 1123–1129.

Towards Engineering an Improved Morphine Dehydrogenase

EDWARD H. WALKER AND NEIL C. BRUCE[a]

Institute of Biotechnology
University of Cambridge
Cambridge CB2 1QT, United Kingdom

INTRODUCTION

Bacterial morphine dehydrogenase (MDH), discovered in *Pseudomonas putida* M10,[1] catalyzes the NADP$^+$-dependent oxidation of the 6-hydroxyl group of morphine and certain close analogues.[2] It is a monomeric protein with a molecular weight of 31.99 kDa, encoded on a large plasmid (165 kb).[3] The gene has been cloned[3] and the comparison of the predicted primary sequence with those in the Swissprot database indicates that it is a member of the aldo-keto reductase family that includes aldose reductase and rat liver 3α-hydroxysteroid dehydrogenase.[4]

MDH is a key component of two systems: first, in combination with a novel heroin esterase, it is used as part of a biosensor for the detection of illicit heroin;[5] second, in combination with morphinone reductase (MR), it is used for the production of the powerful analgesic hydromorphone and the antitussive hydrocodone.[6,7] Both of these applications could benefit if the properties of MDH were modified.

FAMILY RELATIONSHIPS

MDH has 40% identity with aldose reductase and 31% identity with rat 3α-hydroxysteroid dehydrogenase.[4] The tertiary structure of both of these enzymes has been reported,[8,9] together with evidence of the residues involved in the catalytic mechanism.[10] Close examination of the aligned primary structures of the superfamily led to the conclusion that the nicotinamide coenzyme binding and substrate reduction/oxidation occur in all the known enzymes of the superfamily by broadly analogous mechanisms, among which some probable differences were identified.[4] From this, MDH was deduced to be a β/α-barrel protein, in which active site residues could be expected to be located in the loops that connect a β-strand to the following α-helix, and the active site to be formed in the C-terminal half of the barrel.[4] The tertiary structure of aldose reductase with bound cofactor reveals that it binds NADPH in a unique, extended conformation.[8] Both aldose reductase and rat 3α-hydroxysteroid dehydrogenase have activity with NAD$^+$.

SITE-DIRECTED MUTAGENESIS OF MDH

To confirm that MDH is truly related to these enzymes, site-directed mutagenesis has been used to alter the residues in the active site. Work by Bohren *et al.*[10] on

---

[a] To whom all correspondence should be addressed.

the catalytic mechanism of aldose reductase has shown that three residues in the active site are involved in catalysis. These are tyrosine 48, lysine 77, and aspartic acid 43, where tyrosine acts as the proton donor.

Site-directed mutagenesis was performed according to the method of Deng and Nickoloff[11] using the primers shown in FIGURE 1 and the plasmid containing the gene for MDH, pMDH1.7.[3] The selectable primer was designed to remove the *Sca* I site from the β-lactamase gene and the mutagenic primer was designed to change tyrosine 52 into phenylalanine (mutant Y52F) or serine. Phenylalanine would conserve the spatial fit and hydrophobic properties of tyrosine, but is incapable of acting as the proton donor as it lacks the hydroxyl group of the tyrosine. Serine contains a hydroxyl group that could possibly act as the proton donor in the reaction.

Selectable mutation primer

5′   GG TGA GTA T̲TC AAC CAA GTC ATT C   3′

Wild type sequence
                Sca I

5′C TGG TGA GTA C̲TC AAC CAA GTC ATT CA   3′

Mutagenic primer

5′   CC GCC AGG TCG TT̲/C̲T AAC AAT GAG GC   3′
        T   A   R   S   S/F   N   N   E   A

Wild type sequence
5′ C ACC GCC AGG TCG TA̲T AAC AAT GAG GCT A 3′
     T   A   R   S   Y   N   N   E   A

FIGURE 1. The primers used for the site-directed mutagenesis of MDH.

This mutant has not yet been identified. Sequencing was performed using an Applied Biosystems Model 373A automated sequencer.

The mutant Y52F was purified to homogeneity using two affinity chromatography steps, based on the method of Bruce *et al.,*[2] using a 0.0–2.0 M KCl gradient to elute the protein. In both cases, the mutant protein eluted at a higher salt concentration than did the wild type. Fractions containing the mutant enzyme were identified using dot blots with antibodies raised against wild-type MDH.[3] No activity was detectable with this mutation, as seen with aldose reductase and 3α-hydroxysteroid dehydrogenase,[10,12] indicating that these enzymes are related.

BIOTRANSFORMATION OF MORPHINE

The biotransformation of morphine into hydromorphone via morphinone re-
quires MDH and MR (FIGURE 2). MDH exclusively uses $NADP^+$ as its cofactor,
whereas MR uses NADH. This has two consequences for the reaction: first, in a
whole cell system, depletion of the endogenous cofactors limits the amount of

Morphine, R_1=OH

Codeine, R_1=CH$_3$O

Dihydromorphine, R_1=OH

Dihydrocodeine, R_1=CH$_3$O

NADP$^+$

MDH   MDH

NADPH

Morphinone, R_1=OH

Codeinone, R_1=CH$_3$O

NADH

MR

NAD$^+$

Hydromorphone, R_1=OH

Hydrocodone, R_1=CH$_3$O
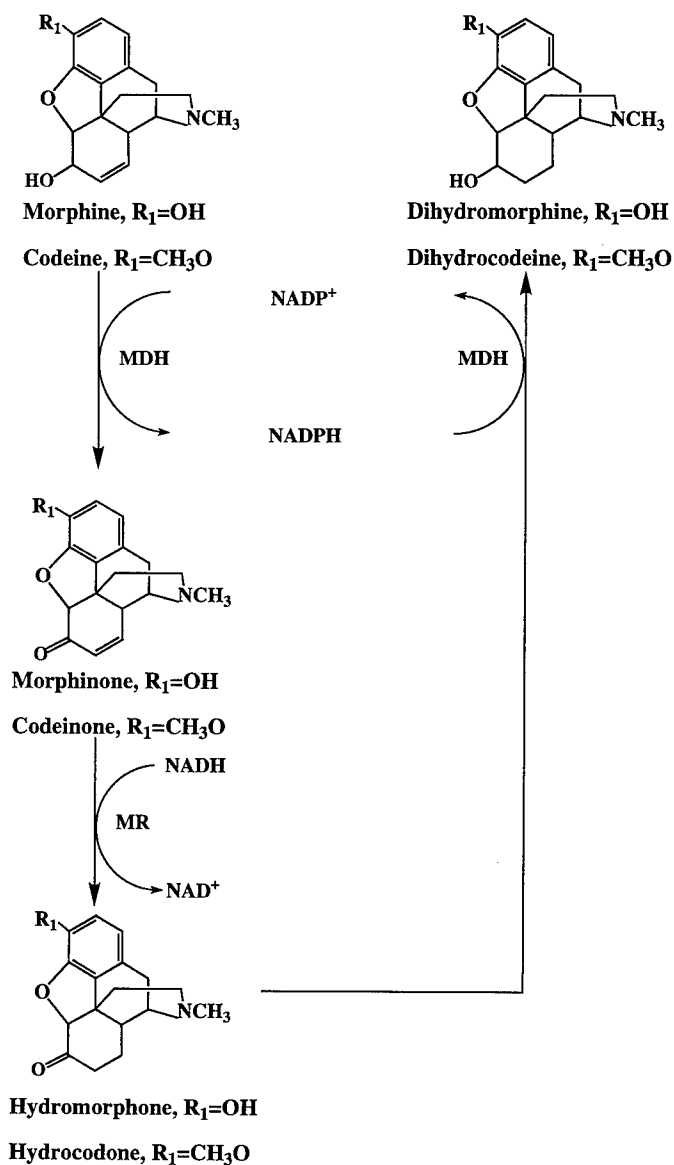
FIGURE 2. Biotransformation route for the production of hydromorphone.

Morphine, R_1=OH

Codeine, R_1=CH$_3$O

Hydromorphone, R_1=OH

Hydrocodone, R_1=CH$_3$O

Morphinone, R_1=OH

Codeinone, R_1=CH$_3$O
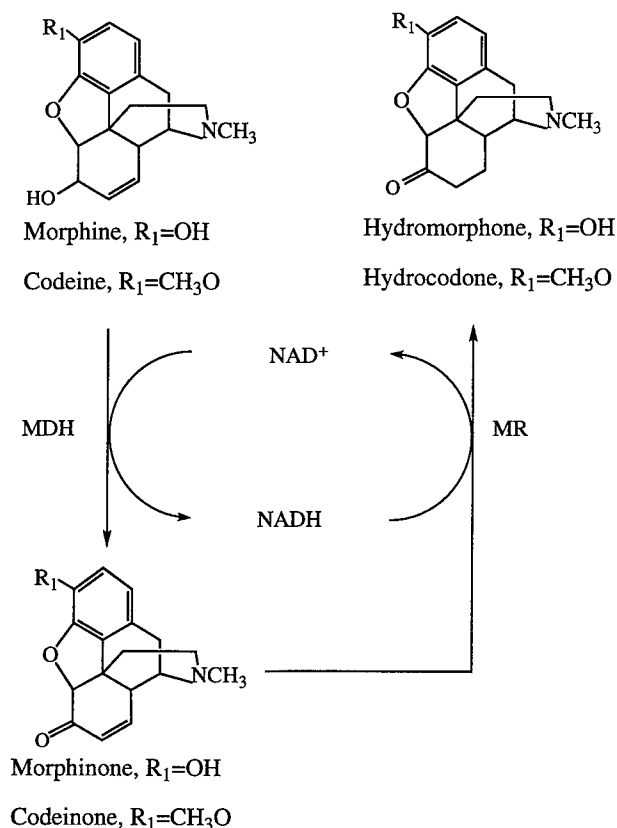
FIGURE 3. A proposed engineered route for the production of hydromorphone.

morphine that can be converted; second, the buildup of NADPH as the reaction proceeds leads to a side reaction where hydromorphone is reduced to dihydromorphine by MDH (FIGURE 2). This is an undesirable reaction as dihydromorphine is easily produced chemically. The use of an NAD$^+$-dependent morphine dehydrogenase would be of benefit to this system, allowing for catalytic use of the cells due to cofactor recycling, resulting in higher yields of hydromorphone (FIGURE 3).

MDH has no activity with NAD$^+$, whereas aldose reductase has $<5\%$ of the activity with NAD$^+$ compared to the activity with the same concentration of NADP$^+$;[13] rat 3α-hydroxysteroid dehydrogenase has similar affinity for NAD$^+$ and NADP$^+$.[10] Homology modeling, site-directed mutagenesis, and the production of chimeric enzymes are currently being used to investigate the differences in cofactor and substrate specificities in these enzymes with the aim of producing an NAD$^+$-dependent MDH.

REFERENCES

1. BRUCE, N. C., C. J. WILMOT, K. N. JORDAN, A. E. TREBILCOCK, L. D. GRAY STEPHENS & C. R. LOWE. 1990. Arch. Microbiol. **154:** 465–470.

2. BRUCE, N. C., C. J. WILMOT, K. N. JORDAN, L. D. GRAY STEPHENS & C. R. LOWE. 1991. Biochem. J. **274:** 875–880.
3. WILLEY, D. L., D. A. CASWELL, C. R. LOWE & N. C. BRUCE. 1993. Biochem. J. **290:** 539–544.
4. BRUCE, N. C., D. L. WILLEY, A. F. W. COULSON & J. JEFFERY. 1994. Biochem. J. **299:** 805–811.
5. HOLT, P-J., L. D. GRAY STEPHENS, N. C. BRUCE & C. R. LOWE. 1995. Biosens. Bioelectronics **10:** 517–526.
6. BRUCE, N. C., C. E. FRENCH, A. M. HAILES, M. T. LONG & D. A. RATHBONE. 1995. TIBTECH **13:** 200–205.
7. FRENCH, C. E., A. M. HAILES, D. A. RATHBONE, M. T. LONG, D. L. WILLEY & N. C. BRUCE. 1995. Bio/Technology **13:** 674–676.
8. HOGG, S. S., J. E. PAWLOWSKI, P. M. ALZARI, T. M. PENNING & M. LEWIS. 1994. Proc. Natl. Acad. Sci. U.S.A. **91:** 2517–2521.
9. WILSON, D. K., K. M. BOHREN, K. H. GABBAY & F. A. QUIOCHO. 1992. Science **257:** 81–84.
10. BOHREN, K. M., C. E. GRIMSHAW, C-J. LAI, D. H. HARRISON, D. RINGE, G. A. PETSKO & K. H. GABBAY. 1994. Biochemistry **33:** 2021–2032.
11. DENG, W. P. & J. A. NICKOLOFF. 1992. Anal. Biochem. **200:** 81–88.
12. PAWLOWSKI, J. E. & T. M. PENNING. 1994. J. Biol. Chem. **269:** 13502–13510.
13. WERMUTH, B., H. BÜRGISSER, K. BOHREN & J-P. VON WARTBURG. 1982. J. Biochem. **127:** 279–284.

Production and Modification of *E. coli* Transketolase for Large-Scale Biocatalysis[a]

CAROL FRENCH AND JOHN M. WARD

Department of Biochemistry and Molecular Biology
University College London
London WC1E 6BT, United Kingdom

INTRODUCTION

Asymmetric carbon-carbon bond formation is at the heart of modern organic synthesis. Because of their inherent production of chiral centers, recent attention has focused on enzyme-catalyzed C-C bond reactions. Fructose-1,6-diphosphate aldolase from rabbit muscle has been shown to possess a wide substrate specificity[1] and has been used as a catalyst in the stereospecific synthesis of deoxynojirimycin, an antiviral glycosidase inhibitor.[2] However, the use of aldolase as a biocatalyst suffers from the disadvantage that there is an absolute requirement for one of the reactants, usually dihydroxyacetone, to be phosphorylated.

Other carbon-carbon bond forming reactions involving transketolase enzymes from yeast,[3,4] spinach,[5,6] and *E. coli*[7-9] have recently been investigated. The substrate specificity of these enzymes has been shown to be broad enough for them to be considered as useful biocatalysts. The yeast enzyme has been used in a synthetic pathway to form (+)-*exo*-brevicom, a naturally occurring beetle pheromone.[10]

In vivo, *E. coli* transketolase catalyzes a stereospecific carbon-carbon bond formation reaction at two points in the pentose phosphate pathway.[11] It transfers a two-carbon ketol group from D-xylulose-5-phosphate to D-ribose-5-phosphate to generate D-sedoheptulose-7-phosphate and from D-xylulose-5-phosphate to erythrose-4-phosphate to form fructose-6-phosphate. The reaction *in vivo* is freely reversible; however, by using hydroxypyruvate as a synthetic ketol donor *in vitro*, carbon dioxide is produced and the reaction becomes irreversible, leading to compounds containing a new carbon-carbon bond and a chiral hydroxy group.[7] Moreover, transketolase works efficiently when neither substrate is phosphorylated. This makes transketolase a valuable tool in biocatalysis as the reaction can go to 100% completion, without the additional problems of separating a mixture of products.

This report describes the strategies used to increase the production of *E. coli* transketolase to a level suitable for biotransformations, as well as the modification of the enzyme to alter its biocatalytic properties.

ENZYME PRODUCTION

Transketolase can be obtained commercially from two sources, *Saccharomyces cerevisiae* and spinach. However, these yields are not sufficient for a large-scale biotransformation. Draths and Frost[12] originally cloned the *E. coli tkt* gene (1991 bp) on a 5-kb fragment in a low copy number vector pBR325. Sprenger has recently sequenced the *tkt* gene and the flanking regions on the 5-kb fragment. These regions have been shown to encode three other genes: *speB* and ORF1, which are involved in putrescine synthesis, and *cmt*B.[13–15]

HIGH COPY NUMBER VECTORS

We excised the BamHI 5-kb fragment and subcloned it into the high copy number vectors pUC18[16] and pBGS19.[17] The resultant constructs, pQR182 (pUC18) and pQR700 (pBGS19), were transformed into the *E. coli* K12 strain JM107 (FIGURE 1). These strains expressed very high levels of transketolase up to 82 mg/mL of culture, after overnight growth in complex medium (TABLE 1; FIGURE 2).[18] These constructs were then used for large-scale fermentation studies. However, the pUC-based construct, pQR182, produced very low levels of transketolase as it was segregationally unstable in the fermentor and could not be maintained under selective pressure. The plasmid instability was thought to be due to the mechanism of antibiotic resistance. The high copy number of pUC leads to a large amount of periplasmic β-lactamase leaking to the medium, where it will inactivate the ampicillin antibiotic. The pBGS-based constructs, although similar in copy number to the pUC vectors, were far more stable during growth. These constructs are selectively maintained by kanamycin, which is inactivated within the host cell by phosphorylation. JM107 pQR700 has been used to produce 4 g/L of soluble intracellular transketolase equivalent to 43% of the total cell protein in a fed-batch, 1000-L fermentation.[19]

PCR AMPLIFICATION

Higher levels of transketolase have been produced by constructs that contain the *tkt* gene only. The *tkt* gene was amplified by PCR to remove the extraneous fragments of DNA on the 5-kb fragment encoding the *speB*, ORF1, and *cmt*B genes.[14,15] Two N-terminal primers were designed, one to incorporate the whole *tkt* promoter region and the other to fuse the *tkt* gene and its RBS in frame to the *lac*Z promoter. The amplification products of 2.2 kb were cloned into pCR script SK(+), forming the constructs pQR706 and pQR728 (FIGURE 1). After overnight growth in complex medium, JM107 pQR706, under the control of the *tkt* gene promoter, produced higher levels of transketolase than the original 5-kb fragment constructs, pQR182 and pQR700 (TABLE 1). However, JM107 pQR728 produced very low levels of transketolase from the *lac*Z promoter as shown on the SDS-PAGE gel. Although the *lac*Z promoter was not induced by lactose or IPTG, we did expect a higher level of expression due to the high copy number of the plasmid titrating out the *lac*I[q] repressor.[20] The pQR728 construct was sequenced and the *tkt* gene was shown to be in frame with the *lac*Z promoter.
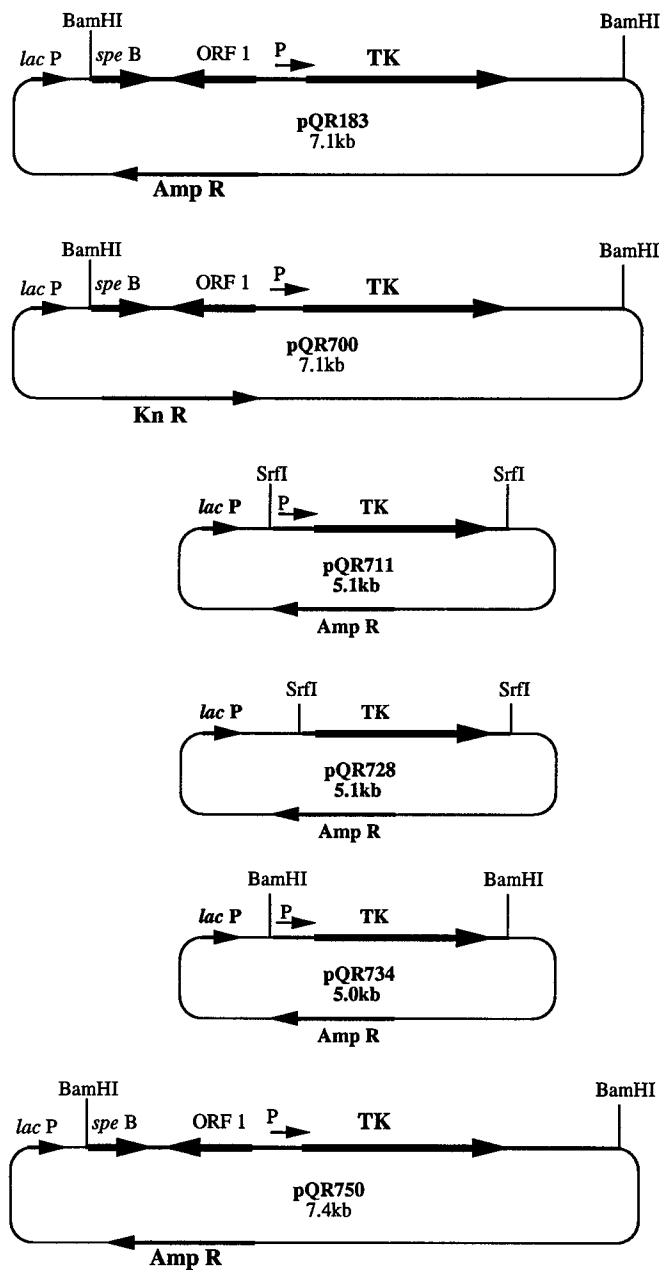
FIGURE 1. Restriction enzyme map of transketolase-expressing plasmids obtained from subcloning and PCR experiments. The arrows represent the orientation of the genes and **P** represents the *tkt* promoter.

TABLE 1. Transketolase Production in Shake-Flask Culture[a]

Construct	Transketolase (U/mL)	Specific Activity (U/mg)	Yield (mg/mL)
JM107	0.12	0.31	3.8 (1%)[b]
pQR182	1.38	3.91	53 (15%)
pQR700	1.51	3.87	55 (14%)
pQR706	4.50	6.43	156 (24%)
pQR728	0.40	1.05	14.8 (4%)
pQR734	2.40	4.12	58 (15%)
pQR750	3.84	5.34	137 (19%)

[a]Transketolase activity was monitored using a linked enzyme assay.[27]
[b]Figures in parentheses represent the % of total cell protein.

PLASMID STABILITY

The *tkt* gene has also been subcloned into a pUC-based vector, pKS450, that encodes the *cer* region from *Col*E1.[21] It has been shown that the segregational instability of vectors, such as pUC, resulted from a reduction in the number of independently segregating units.[22] The recombination site *cer* reduces plasmid multimers to monomers, thereby increasing the number of independent segregating units and enabling the plasmid to remain stable without any selective pressure. The 5-kb fragment and the PCR-amplified 2.2-kb fragment were subcloned into pKS450, forming the constructs pQR750 and pQR734. Both of these constructs were shown to remain segregationally stable over 120 h of nonselective growth. However, the construct pQR750 containing the 5-kb fragment produced more transketolase, 137 mg/mL, than the pQR734 construct (58 mg/mL) containing the smaller 2.2-kb insert (FIGURE 2). This was surprising as it was thought that the construct containing the *tkt* gene alone would express transketolase more efficiently.

ENZYME MODIFICATION

The X-ray crystallographic structure[23] has shown that the transketolase dimer forms two active sites, each of which is made up of residues from both of the transketolase subunits. Each active site forms a funnel-shaped cleft that leads out to the edge of the enzyme. The thiamine pyrophosphate (TPP) cofactor molecule is buried at the base of the active site cleft and the proposed donor/TPP intermediate adduct has been modeled into this structure.

We are attempting to generate new biocatalysts from *E. coli* transketolase that will perform carbon-carbon bond forming reactions using novel achiral, bulky, aromatic, or heterocyclic substrates. Using the X-ray crystallographic data and site-directed mutagenesis, we are trying to enlarge the opening to the active site cleft of transketolase to allow access for these novel bulky aldehyde acceptor substrates.

We have mutated an isoleucine residue (I189) that is positioned at the base of the funnel in a hydrophobic pocket above the TPP molecule, with its aliphatic side chain extending directly into the active site. This residue has been mutated to the smaller

hydrophobic alanine residue using one-sided overlap extension by PCR.[24] This is a two-reaction procedure requiring a single mutagenic primer and two flanking primers at the 5' and 3' ends of the gene. The mutagenic primer was designed to be 27 bases in length, incorporating two consecutive base changes in the middle of the primer. A 1-kb fragment containing the desired mutation was amplified using the mutagenic primer and one flanking primer. The product of this was then mixed with the other flanking primer and amplified in a second PCR reaction. This 2.2-kb PCR product containing the full-length *tkt* gene was cloned into pCR script SK(+) Stratagene to form the construct pQR739. The *tkt* gene was amplified to incorporate the *tkt* gene promoter to ensure that the mutant transketolase was expressed under the control of the strong constitutive *tkt* promoter. The mutation at position 189 was confirmed by DNA sequencing.

This construct was transformed into the *E. coli* strain JM107 and grown overnight in complex medium at 37 °C. JM107 pQR739 expressed high levels of the mutant enzyme, about 30% of the total cell protein, comparable to the wild-type enzyme in
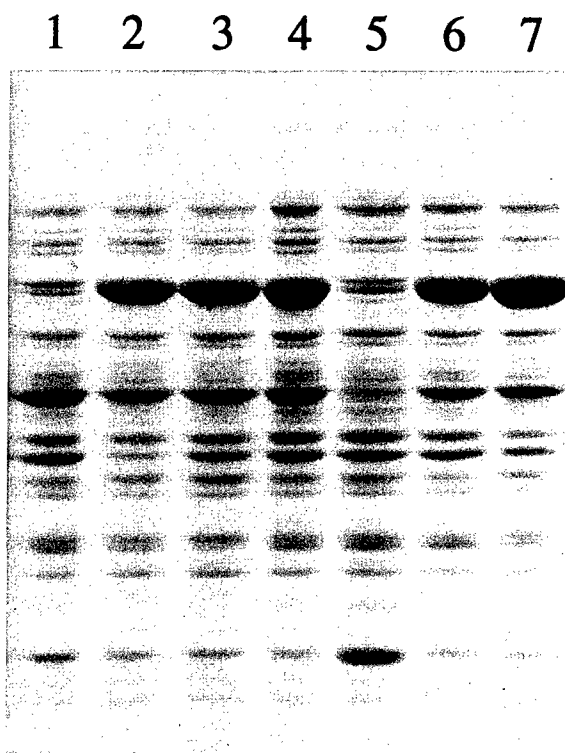
FIGURE 2. Gel: 10% SDS-PAGE of *E. coli* transketolase–expressing constructs. Cultures were grown overnight (18 h) at 37 °C in nutrient broth. One-mL cell pellets were sonicated and resuspended in 500 μL of 0.1 M glycylglycine buffer (pH 7.6). Track 1: JM107; track 2: JM107 pQR182; track 3: JM107 pQR700; track 4: JM107 pQR706; track 5: JM107 pQR728; track 6: JM107 pQR734; track 7: JM107 pQR750.
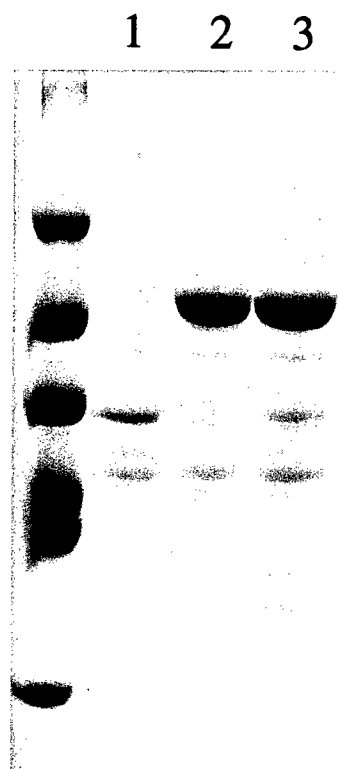
FIGURE 3. Gel: 10% SDS-PAGE of wild-type and mutant transketolase. Cultures were grown overnight (18 h) at 37 °C in nutrient broth. One-mL cell pellets were sonicated and resuspended in 500 μL of 0.1 M glycylglycine buffer (pH 7.6). Track 1: JM107; track 2: JM107 pQR706 (wild type); track 3: JM107 pQR739 (I189A).

construct pQR706 (FIGURE 3). Substitution of isoleucine 189 with alanine has a profound effect upon catalytic activity. This mutant retained only 20% of the wild-type catalytic activity with production of transketolase at 5 U/mL of culture in pQR706 (wild type) and at 1 U/mL of culture in pQR739 (I189A mutant). The affinity of the mutant for the cofactor TPP is about twofold greater than the wild-type enzyme, as can be seen from the binding constants (TABLE 2). The K_m value for the donor substrate D-xylulose-5-phosphate is similar to that of the wild-type enzyme, whereas the K_m for the acceptor substrate D-ribose-5-phosphate is about twofold lower than that of the wild-type enzyme.

TABLE 2. Kinetic Parameters for Wild-type and Mutant Transketolase[a]

Enzyme	Activity	K_m		
		TPP	Xyl-5-P	Rib-5-P
pQR706	100%	182 μM	155 μM	412 μM
pQR739	20%	244 μM	190 μM	250 μM

[a]The K_m parameters were determined for xylulose-5-phosphate as donor and ribose-5-phosphate as acceptor.

The wild-type *E. coli* transketolase K_m value for the donor substrate is very similar to that obtained for the yeast enzyme.[25] However, the K_m values for TPP (K_m of 1.82 μM) and D-ribose-5-phosphate (412 μM) are about threefold higher compared to the yeast enzyme (K_m of 0.5 μM and 146 μM, respectively).

These results imply that a mutation at residue 189 has little effect upon the affinity of the enzyme for the donor substrate, yet has some effect on the binding of the acceptor substrate and the TPP cofactor molecule. The isoleucine residue at position 189 seems to be involved in the catalytic mechanism. The exact role it plays in the mechanism, whether direct or indirect, is impossible to say at the present moment and further studies will be required. Nikkola *et al.*[26] suggested that the homologous yeast residue isoleucine 191 was involved in the hydrophobic binding of the thiazolium ring of the TPP molecule. This may be indicated by the change in the TPP binding constant seen in these experiments. The residue isoleucine 189 is at present being mutated to a valine residue.

These experiments, though, have been performed on impure enzyme from crude extracts that also contain endogenous transketolase protein from the host. However, the recombinant transketolase is expressed at such high levels that the endogenous enzyme would contribute little to the results. Still, the mutant form of transketolase I189A will need to be purified to homogeneity for more detailed kinetic studies.

ACKNOWLEDGMENTS

REFERENCES

1. BEDNARSKI, M. D., E. S. SIMON, N. BISCHOFBERGER, W-D. FESSNER, M-J. KIM, W. LEES, T. SAITO, H. WALDMANN & G. M. WHITESIDES. 1989. J. Am. Chem. Soc. **111**: 627.
2. STRAUB, A., F. EFFENBERGER & P. FISCHER. 1990. J. Org. Chem. **55**: 3926.
3. KOBORI, Y., D. C. MYLES & G. M. WHITESIDES. 1992. J. Org. Chem. **57**: 5899–5907.
4. EFFENBERGER, F., V. NULL & T. ZIEGLER. 1992. Tetrahedron Lett. **33**: 5157–5160.
5. DEMUYNCK, C., J. BOLTE, L. HECQUET & V. DALMAS. 1991. Tetrahedron Lett. **32**: 5085.
6. DALMAS, V. & C. DEMUYNCK. 1993. Tetrahedron Asymmetry **4**: 2383–2388.
7. HOBBS, G. R., M. D. LILLY, N. J. TURNER, J. M. WARD, A. J. WILLETTS & J. M. WOODLEY. 1993. J. Chem. Soc. Perkin Trans. **1**: 165–166.
8. SPRENGER, G. A., U. SCHORKEN, G. SPRENGER & H. SAHM. 1995. FEBS Eur. J. Biochem. In press.
9. HUMPHREY, A. J., N. J. TURNER, R. McCAGUE & S. J. C. TAYLOR. 1995. Chem. Commun. In press.
10. MYLES, D. C., P. J. ANDRULIS & G. M. WHITESIDES. 1991. Tetrahedron Lett. **32**: 4835–4838.
11. RACKER, E. 1961. *In* The Enzymes. Volume 5. P. D. Boyer, H. Lardy & K. Myrzback, Eds.: 397–406. Academic Press. New York.
12. DRATHS, K. M. & J. W. FROST. 1990. J. Am. Chem. Soc. **112**: 1657–1659.
13. SPRENGER, G. A. 1992. J. Bact. **174**: 1707–1708.
14. SPRENGER, G. A. 1993. Biochim. Biophys. Acta **1216**: 307–310.
15. SPRENGER, G. A. 1993. Biochim. Biophys. Acta **1158**: 103–106.
16. VIEIRA, J. & J. MESSING. 1982. Gene **19**: 259–268.

17. SPRATT, B. G., P. J. HEDGE, S. TEHEESEN, A. EDELMAN & J. K. BROOME-SMITH. 1986. Gene **41:** 337–342.
18. FRENCH, C. & J. M. WARD. 1995. Biotechnol. Lett. **17:** 247–252.
19. HOBBS, G. R., R. K. MITRA, R. CHAUHAN, J. M. WOODLEY & M. D. LILLY. 1995. J. Biotechnol. In press.
20. STEWART, G. S. A. B., S. LUBINSKY-MINK, C. G. JACKSON, A. CASSEL & J. KUHN. 1986. Plasmid **15:** 172–181.
21. SUMMERS, D. K. & D. J. SHERRATT. 1988. EMBO J. **7:** 851–858.
22. SUMMERS, D. K. & D. J. SHERRATT. 1984. Cell **36:** 1097–1103.
23. LITTLECHILD, J., N. J. TURNER, G. R. HOBBS, M. D. LILLY, A. RAWAS & H. WATSON. 1995. Acta Crystallogr. In press.
24. HORTON, R. M. & L. R. PEASE. 1991. *In* Directed Mutagenesis: A Practical Approach. M. J. McPherson, Ed.: 217–247. Oxford University Press. London/New York.
25. WIKNER, C., L. MESHALKINA, U. NILSSON, M. NIKKOLA, Y. LINDQVIST, M. SUNDSTROM & G. SCHNEIDER. 1994. J. Biol. Chem. **269:** 32144–32150.
26. NIKKOLA, M., Y. LINDQVIST & G. SCHNEIDER. 1994. J. Mol. Biol. **238:** 387–404.
27. HEINRICH, C. P., K. NOACK & O. WISS. 1972. Biochem. Biophys. Res. Commun. **49:** 1427–1432.

Transglycosylation by Wild Type and Mutants of a β-1,4-Glycosidase from *Cellulomonas fimi* (Cex) for Synthesis of Oligosaccharides[a]

P. V. NIKOLOVA,[b] S. DUFF,[c] A. MacLEOD,[d] AND
C. A. HAYNES[b,c]

[b]*Biotechnology Laboratory*
[c]*Department of Chemical Engineering*
and
Protein Engineering Network of Centers of Excellence
[d]*Department of Microbiology and Immunology*
University of British Columbia
Vancouver, British Columbia, Canada V6T 1Z3

INTRODUCTION

In contrast with glycosyl transferases, retaining glycosidases have received relatively little attention as potential catalysts for synthesis of oligosaccharide-based products. Retaining glycosidases hydrolyze with a net retention of anomeric configuration through formation of a covalent enzyme-glycosyl intermediate, which is then attacked by water to yield hydrolysis products.[1-4] Using the β-1,4-glycosidase Cex from *Cellulomonas fimi*, we are exploring solvent and reaction conditions where this intermediate may be intercepted by an alternative nucleophile, such as another sugar, to yield a transglycosylation product. Preliminary data indicate that natural sugars can serve as a donor in the transglycosylation reaction, but yields are low. In this work, we attempt to improve transglycosylation efficiencies through mutagenesis and the use of an activated donor sugar such as a nitrophenyl glycoside and high concentrations of a nonactivated acceptor sugar. When formed, transglycosylation product should accumulate provided the k_{cat}/K_m value for the transglycosylation reaction is significantly higher than that for the product of hydrolysis.

Addition of organic cosolvents is among the most efficient ways to shift relative rates of hydrolysis to transglycosylation. We have measured transglycosylation activities of Cex in buffer and in mixed acetonitrile/aqueous solvents to determine the sensitivity of transglycosylation reactions catalyzed by this retaining glycosidase system to water activity and solvent polarity. Finally, the conformational structure pattern and thermal stability of mutants of Cex have been assessed by transmission circular dichroism to confirm that mutations do not result in pronounced changes in structure (e.g., denaturation).

MATERIALS AND METHODS

Materials

Cellooligosaccharides (cellotriose through cellohexaose) used in this study were obtained from Yaizi Suisan Kagaku, distributed by Seikagaku Kogyo (Rockville, Maryland). Cellobiose, D-glucose, p-nitrophenyl β-D-cellobioside (pNPC), and p-nitrophenol were purchased from Sigma. All other reagents were analytical grade. Solvents were purchased from Aldrich Chemicals with the highest available purity and known water content.

Protein Production and Purification

Electrocompetent cells of *E. coli* (JM 101) were transformed with pUC 12-1.1-Cex (PTIS)[5] and then transferred into Lauria-Bertani (LB) and TYP media[6] supplemented with 100 μg/mL ampicillin at 30 °C. A 150-mL ($OD_{600nm} = 4.0$) shake-flask culture was used to inoculate a 20-L batch fermentor containing TYP media and 100 mg/L ampicillin. The culture ($OD_{600nm} = 5.6$) was induced for three hours by addition of isopropyl-β-D-thiogalactoside to 0.1 mM final concentration. The cells were harvested by centrifugation and lysed by homogenization, and the wild type or mutant Cex was purified as described previously.[7,8] The extinction coefficient at 280 nm for Cex and all Cex mutants is 1.61.[9]

Circular Dichroism Spectroscopy (CD)

Transmission CD measurements were made using a Jasco J-720 spectrophotometer controlled with J-700 software. Sample temperature was controlled with a Neslab Model RTE-110 water bath under computer control. Protein samples were equilibrated in 50 mM potassium phosphate buffer (pH 7.0). The change in ellipticity was monitored at 25 °C from 300 to 200 nm, at a scan speed of 100 nm/min. An average of six scans were recorded per sample. The change in ellipticity was also monitored at a fixed wavelength of 222 nm over the temperature range of 25 to 80 °C to determine the melting temperature, T_m. The thermal scan rate was 50 °C/h. Melting temperatures were determined from the first derivative of the resulting ellipticity versus temperature plots for the different samples.

Chromatography

HPLC analyses were performed using a μBondapak-NH$_2$/μPorasil Radial Pak Cartridge (8 mm $\times$ 100 mm) with an RCM cartridge holder and a μBondapak-NH$_2$ guard-pak insert (Waters). Substrates and cellosaccharide products were separated using a 70:30 acetonitrile:water mobile phase at a rate of 1.5 mL/min using a Waters model 610 RI detector. The injection volume was 50 μL. Prior to each run, the instrument was calibrated using a standard mixture of the components of interest and the resulting calibration curves were used for product concentrations.

Transglycosylation Kinetics

Reaction mixtures, with a 300-μL total reaction volume, were prepared by adding 100 μL of the substrate stock solution, 150 μL of acetonitrile, and 50 μL of enzyme solution (in 50 mM potassium phosphate buffer, pH 7.0), in that order. The substrate stock solution contained 100 mM pNPC in 50 mM potassium phosphate buffer (pH 7.0). The final ratio of water to acetonitrile was 50:50 (v/v). Controls, prepared in a similar way, contained only the substrate and the organic phase (150 μL of each phase). Reactions were carried out in 2-mL glass vials that were tightly closed with screw caps and placed in an incubator at 37 °C. Reaction progress was monitored by withdrawing samples for thin-layer chromatography (TLC) and/or HPLC analysis.

RESULTS AND DISCUSSION

Cellotetraose (G4) and higher order soluble cellosaccharides are potentially valuable products (e.g., natural nonmetabolized sweeteners) that cannot be easily synthesized. The retaining exoglucanase activity of Cex suggests that it could provide a useful route for cellotetraose production. Transglycosylation activities of wild-type (wt-)Cex were measured in water at 37 °C in the presence of an excess of natural sugars (glucose, cellobiose) and/or activated donor sugars (pNPC). In all cases, TLC indicates that equilibrium yields of G4 are low.

Changes in water activity by addition of acetonitrile were explored to improve G4 yields. In 50% acetonitrile at 37 °C, G4 accumulates to an equilibrium yield of 9.5% when an excess of pNPC serves as substrate, indicating that solvent properties can influence transglycosylation yields in the wt-Cex system.

Site mutations of residues involved in the hydrolytic function of Cex[7,9] were then investigated as a potential route to further improve transglycosylation activity in the mixed solvent system. The mutant proteins considered are listed in TABLE 1 along with their kinetic constants for pNP release in pure water and measured G4 yields in the 50:50 acetonitrile:water mixture at 37 °C. The native protein (~47 kDa) comprises two discrete domains, a catalytic domain (~35 kDa) and a cellulose-binding domain (~12 kDa), which are separated by a proline-threonine-rich linker peptide. Glutamic acid residues at positions 127 and 233 in the catalytic active site have been implicated as the acid-base catalyst[7] and the catalytic nucleophile,[9] respectively. For both residues, reduction of the lever arm for the reactive carboxylic group (E127D and E233D) and elimination of the carboxylic group (E127A and E233A) were evaluated for influence on kinetics and G4 yields (TABLE 1). Both mutations to E233 resulted in a drastic reduction in k_{cat} for (pNPC) hydrolysis in pure water, with little change in K_m, suggesting that they may improve transglycosylation yields. However, the substitutions at E233 (as well as the less interesting ones at E127) result in a total loss of transglycosylation activity, indicating that formation of the enzyme-glycosyl intermediate followed by efficient nucleophilic attack are required for transglycosylation activity.

Recent studies of the cellulose-binding domain of Cex indicate that its structure is predominantly β-sheet,[10] while X-ray crystallography data of the catalytic domain show that it is rich in α-helix structure and forms an α/β barrel.[11] Because it is

TABLE 1. Thermal Stability (T_m), Kinetic Constants for Hydrolysis of pNPC, and Relative Yields of Cellotetraose Product Formation via Transglycosylation when pNPC Was Used as Substrate[a]

Protein	T_m (°C)	K_m (mM)[b]	k_{cat} (min^{-1})[b]	k_{cat}/K_m (min^{-1}·mM^{-1})[b]	G4 Formation (%)[c]
wild type	59.6	0.60	948	1578	9.50
p-33	59.4	0.54	709	1373	10.00
Q87S	60.5	0.38	474	1247	12.81
E127A	55.8	0.025	2.3	92	0
E127D	NA	1.74	3.3	2	0
E233A	58.3	0.68	0.051	0.08	0
E233D	49.4	0.66	0.0038	0.006	0
Q87M	59.6	0.34	552	1624	12.5
Q87Y	57.6	2.27	276	122	0

[a]E127D and E127A: acid-base catalyst; E233A and E233D: catalytic nucleophile; p-33: catalytic domain only; NA: not available.

[b]Values are for hydrolysis of pNPC in 50 mM KP$_i$ buffer, pH 7.0.

[c]Relative values of transglycosylation product (G4, cellotetraose) formation as % of initial substrate concentration (pNPC).
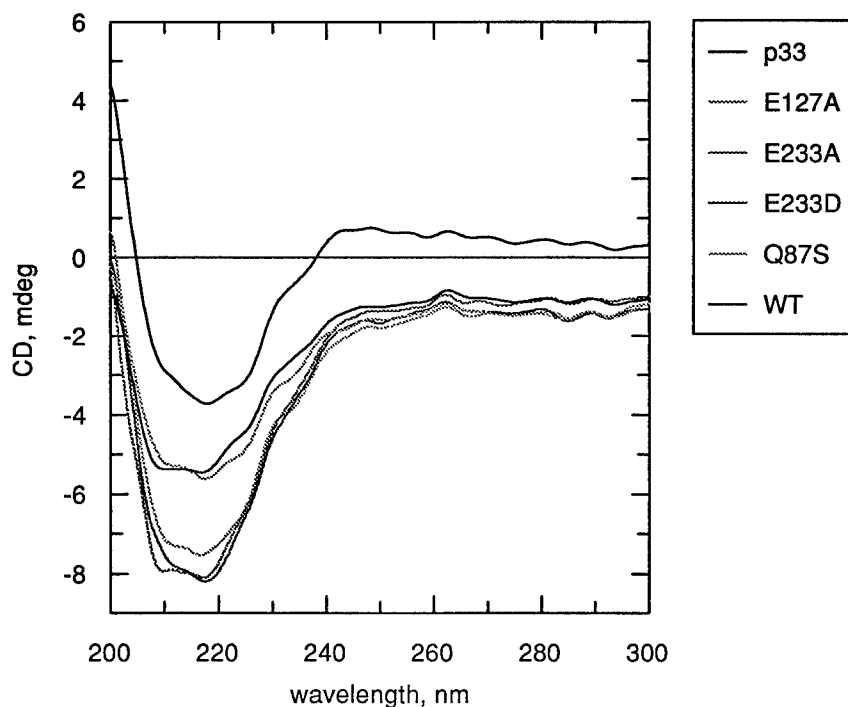
FIGURE 1. Far-UV CD spectra of wild type and mutants of Cex β-1,4-glycosidase from *Cellulomonas fimi* at 25 °C in 50 mM potassium phosphate buffer (pH 7.0).

primarily sensitive to α-helix content, CD should provide a specific probe of structural changes in the catalytic domain as a function of site mutation. As shown in FIGURE 1, the CD scan of each mutant exhibits a very similar conformational structure pattern to that of the wild-type enzyme, indicating that no gross conformational changes have resulted from the substitutions. Thermograms monitored by CD
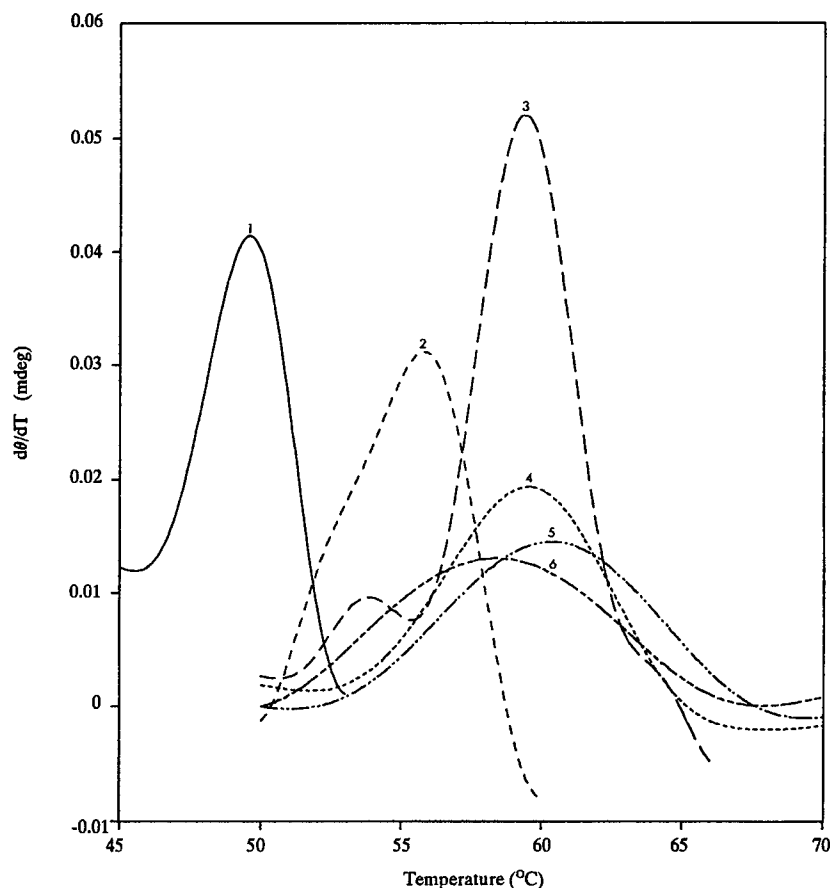
FIGURE 2. Thermal denaturation curves of wild type and mutants of Cex β-1,4-glycosidase from *Cellulomonas fimi* in 50 mM potassium phosphate buffer (pH 7.0) at 222 nm in the temperature interval of 25–80 °C. Key: (1) E233D, (2) E127A, (3) p-33, (4) wild type, (5) Q87S, and (6) E233A.

at 222 nm show that the melting temperatures (TABLE 1), as determined from the first derivatives of the denaturation curves (FIGURE 2), of most of the mutants do not differ significantly from that of wild-type Cex. However, T_m values for E127A and E233D are significantly lower than that for wild-type Cex, indicating that these mutations may result in some distortion of the active site.
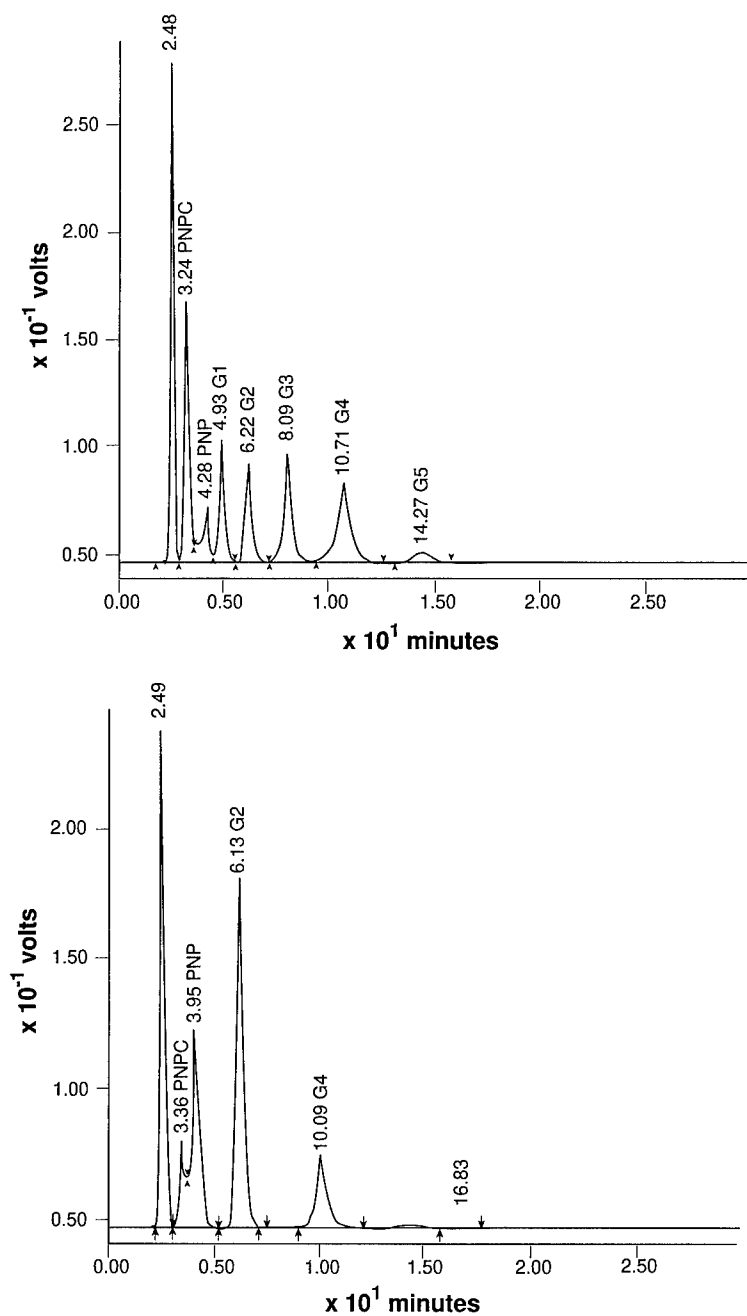
FIGURE 3. HPLC profile of standards (top) and a sample of the transglycosylation reaction carried out with the Q87S mutant of Cex β-1,4-glycosidase from *Cellulomonas fimi* in 50:50 (v/v) $CH_3CN:H_2O$ (50 mM potassium phosphate buffer, pH 7.0) (bottom).

Glutamine residue Q87, which appears to be involved in the binding interaction through the C_6-OH of the distal sugar ring of the substrate, was also replaced to determine the more subtle effects of perturbing bound substrate positioning on transglycosylation yields. The top and bottom panels of FIGURE 3 show the HPLC standard curve and chromatogram, respectively, of equilibrium products when the mutant Cex Q87S is incubated with an excess of pNPC in the mixed solvent system (pH 7) at 37 °C. A reproducible increase of approximately 20% in G4 yield is observed for Q87S compared to wild-type Cex (TABLE 1). More importantly, TLC results indicate that Q87S retains its transglycosylation activity in pure water. Similar increases in transglycosylation yield were found for Q87M (TABLE 1). However, not all mutations of Q87 result in an increase in transglycosylation activity, as evidenced by Q87Y, which shows no transglycosylation activity.

ACKNOWLEDGMENTS

REFERENCES

1. WITHERS, S. G., D. DOMBROSKI, L. O. BERVEN, D. G. KILBURN, R. C. MILLER, JR., R. A. J. WARREN & N. R. GILKES. 1986. Biochem. Biophys. Res. Commun. **139:** 487–494.
2. KOSHLAND, D. E. 1953. Biol. Rev. Camb. Philos. Soc. **28:** 416–436.
3. SINNOTT, M. L. 1990. Chem. Rev. **90:** 1171–1202.
4. DAVIES, G. & B. HENRISSAT. 1995. Structure **3:** 853–859.
5. O'NEILL, G., S. H. GOH, R. A. J. WARREN, R. C. MILLER, JR. & D. G. KILBURN. 1986. Gene **44:** 325–330.
6. NIKOLOVA, P. V., A. L. CREAGH, S. DUFF & C. A. HAYNES. 1996. To be submitted.
7. MACLEOD, A. M., T. LINDHORST, S. G. WITHERS & R. A. J. WARREN. 1994. Biochemistry **33:** 6371–6376.
8. GILKES, N. R., E. JERVIS, B. HENRISSAT, B. TEKANT, R. C. MILLER, JR., R. A. J. WARREN & D. G. KILBURN. 1992. J. Biol. Chem. **267:** 6743–6749.
9. TULL, D., S. G. WITHERS, N. R. GILKES, D. G. KILBURN, R. A. J. WARREN & R. AEBERSOLD. 1991. J. Biol. Chem. **266:** 15621–15625.
10. XU, G-Y., E. ONG, N. R. GILKES, D. G. KILBURN, D. R. MUHANDIRAM, M. H. BRANDTS, J. P. CARVER, L. E. KAY & T. S. HARVEY. 1995. Biochemistry **34:** 6993–7008.
11. WHITE, A., S. G. WITHERS, N. R. GILKES & D. ROSE. 1994. Biochemistry **33:** 487–494.

Catalytic Antibodies: The Rerouting of Chemical Reactions

Towards Electrophilic Aromatic Substitution by Carbon Dioxide[a]

JARI T. YLI-KAUHALUOMA[b] AND KIM D. JANDA[c,d]

[b]*Chemical Process Technology*
Technical Research Center of Finland
FIN-02150 Espoo, Finland

[c]*Departments of Molecular Biology and Chemistry*
Scripps Research Institute
La Jolla, California 92037

INTRODUCTION

The Kolbe-Schmitt (K-S) reaction belongs to a vast category of electrophilic aromatic substitution reactions. The basis of the reaction is the carboxylation of sodium phenolate with carbon dioxide.[1] Generally, the reaction affords *ortho*-substituted salicylic acids. The mechanism is not clearly understood, but apparently a complex is formed between the reactants, making the carbon atom of carbon dioxide more positive and thus putting it in a favorable position to attack the phenyl ring.

We and others have generated monoclonal antibody catalysts to various chemical reactions.[2] Our latest endeavor was to search the immunoglobulin repertoire for antibody catalysts to the K-S reaction. We engaged such a search based on the following considerations. The reaction requires remarkably drastic conditions to proceed, that is, high temperature (up to 200 °C), high pressure (up to 100 atm), and the use of a strong base (NaOH, Na_2CO_3). Consequently, the use of the K-S reaction is limited to only very stable phenols. A catalytic antibody with its ability to lower the energy of activation of a chemical reaction may allow the K-S reaction to be run under more ambient conditions.

The K-S reaction can produce compounds of biomedical relevance. One example is the class of compounds known as 4-aminosalicylic acids. These have been successfully used in the past as tuberculostatic agents. Our strategy was to raise antibodies against a transition-state analogue of the K-S reaction between 3-aminophenol and carbon dioxide (FIGURE 1).

26
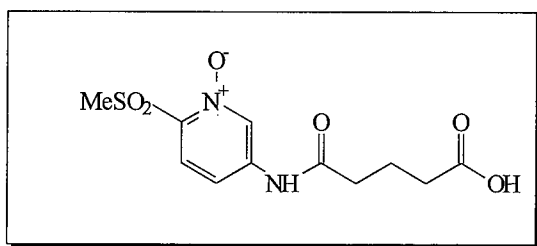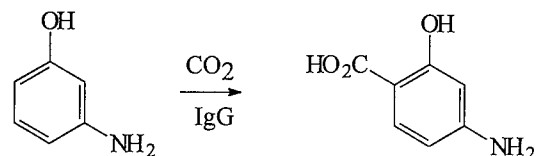
FIGURE 1. The K-S reaction and the structure of the pyridine *N*-oxide transition-state analogue.

RESULTS

The Preparation of Hapten

Thiomethylation of 2-chloro-5-nitropyridine was accomplished in two steps (92% yield) employing sodium sulfide in dimethylformamide (DMF)/H_2O and alkylating subsequently with iodomethane (FIGURE 2).[3] The sulfide was oxidized to the crystalline methylsulfone via traditional $KMnO_4$ treatment in an acetic acid/H_2O solution (87% yield).

2-Methylsulfonyl-5-nitropyridine was readily reduced to the corresponding aminopyridine in 99% yield (hydrogen, 5% palladium on carbon as the hydrogenation catalyst in ethanol). The aminopyridine was acylated with glutaric anhydride in the presence of *N,N*-diisopropylethylamine (91% yield). Oxidation of the unactivated pyridine nitrogen was accomplished by using the powerful and versatile oxidizer, dimethyldioxirane, in acetone at room temperature (76% yield).[4]
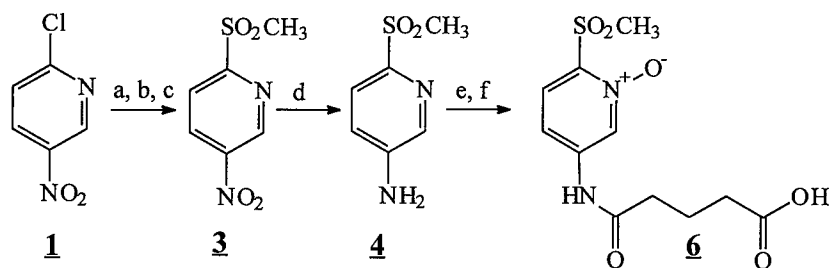
FIGURE 2. The preparation of immunoconjugate for carboxylation of phenolates: (a) Na_2S, DMF, H_2O, room temperature (rt), 30 min; (b) MeI, rt, 18 h, 92%; (c) $KMnO_4$, HOAc, H_2O, rt, 50 min, 87%; (d) H_2, 5% Pd/C, MeOH, 1 atm, rt, 4 h, 99%; (e) glutaric anhydride, EDIA, $CHCl_3$, +4 °C, 1 h, 91%; (f) dimethyldioxirane, acetone, rt, 5 h, 76%.

Activation, Coupling, and the Immunization

The hapten was activated for coupling with 1-(3-dimethylaminopropyl)-3-ethyl-carbodiimide and N-hydroxysuccinimide. The activated hapten was coupled to keyhole limpet hemocyanin and used to immunize 129GIX$^+$ mice for the production of monoclonal antibodies.[5] Twenty-four monoclonal antibodies against the hapten were shown by an ELISA to bind to the hapten conjugated to bovine serum albumin. All 24 hybridoma cell lines were cloned and injected into 129GIX$^+$ × BALB/c mice for production of ascites fluid. Monoclonal antibody from each sample was purified by ammonium sulfate precipitation, anion exchange, cation exchange, and affinity chromatography.

DISCUSSION

The transition-state analogue used as a hapten contains a methylsulfonyl moiety to mimic the CO_2 electrophile. Pyridine N-oxide mimics the negative charge of the phenoxide anion and the acylated 5-amino group resembles the *meta* substituent of the substrate. The effect of product inhibition can be expected to be negligible as the structure of the transition-state analogue does not resemble the structure of the expected product, 4-aminosalicylic acid.

We are currently screening the IgG antibodies for catalytic activity in bicarbonate buffer (100 mM, pH 9.0) at 37 °C and are attempting to employ supercritical carbon dioxide as the reaction medium for the monoclonal antibodies. Pressurized carbon dioxide should be an exceptionally advantageous reaction medium for the antibody-catalyzed K-S reaction. Carbon dioxide at supercritical stage ($T > 31$ °C, $p > 72.9$ bar) provides a reaction medium and reactant at liquidlike density, while maintaining gaslike diffusivity. Slightly above critical temperature and pressure, carbon dioxide is more compressible than ordinary solvents. Solvent properties, such as diffusivity, dielectricity constant, solubility parameters, and viscosity, are dependent on density and therefore on pressure. Changing the pressure of the reaction mixture is capable of altering the rates and selectivities of the reaction.

Proteins are insoluble and generally stable in supercritical carbon dioxide. A number of lipases and other enzymes retain their enzymatic activity in the nonaqueous, hydrophobic environment.[6] Analogously, catalytic antibodies are expected to retain their activity in supercritical carbon dioxide.

Further advantages of using supercritical carbon dioxide as reaction medium arise from its nontoxicity, nonflammability, and economical recycling. Reaction products may be separated, purified, and crystallized from the supercritical solvent by pressure reduction.

EXPERIMENTAL PROCEDURES

General Methods

Methanol and chloroform were continuously distilled from magnesium turnings and P_2O_5, respectively. All reagents were purchased from the Aldrich Chemical

Company. All solvents were obtained commercially and used without further purification.

The R_f values refer to the thin-layer chromatograms developed using 0.25-mm Merck silica gel 60 F-254 glass-supported plates visualized with ethanolic Ninhydrin (1%), phosphomolybdic acid (5%), or a UV lamp. Column chromatography was performed with silica gel 60 (230–400 mesh, E. Merck, Darmstadt, Germany). Yields are for unoptimized procedures and refer to chromatographically and spectroscopically (^{1}H NMR) homogeneous materials, unless otherwise noted.

All proton NMR spectra were obtained in DMSO-d_6 or DMF-d_7 at ambient temperature on a Bruker AM-300 instrument. Chemical shifts (δ) are reported in parts per million relative to the internal reference tetramethylsilane, and coupling constants (J) are given in Hz. Multiplicities are indicated by s (singlet), d (doublet), t (triplet), q (quartet), qn (quintet), and br (broad). Low resolution fast atom bombardment (FAB) mass spectra were provided by the TSRI Mass Spectrometry Facility.

Synthesis of the Hapten

2-Methylthio-5-nitropyridine (2)

To a stirred solution of 2-chloro-5-nitropyridine 1 (5.28 g, 33.3 mmol) in 30 mL of DMF, we added a solution of $Na_2S \cdot 9H_2O$ (10.0 g, 41.6 mmol) in 40 mL of DMF/H_2O (4:1). The solution was stirred at room temperature (rt) under N_2 atmosphere for 30 min. Iodomethane (3.1 mL, 50.0 mmol) was added and the mixture stirred at rt for 18 h, after which it was partitioned between EtOAc (300 mL) and H_2O (300 mL). The organic layer was dried with anhydrous $MgSO_4$, filtered, and evaporated *in vacuo*. Column chromatography on silica gel (EtOAc/hexane, 1:2) afforded 5.16 g of 2 as yellow crystals (91%, 30.3 mmol): ^{1}H NMR (DMSO-d_6) δ 9.18 (d, $^4J_{HH}$ = 2.8 Hz, 1 H), 8.34 (dd, $^3J_{HH}$ = 8.6 Hz, $^4J_{HH}$ = 2.8 Hz, 1 H), 7.52 (d, $^3J_{HH}$ = 8.6 Hz, 1 H), 2.60 (s, 3 H); FABLRMS (3-NBA/MeOH) m/e 171 [M + H]$^+$; R_f 0.75 (EtOAc/hexane, 2:1); melting point (mp) 114 °C (lit. 112 °C).[3]

2-Methylsulfonyl-5-nitropyridine (3)

A solution of $KMnO_4$ (7.95 g, 50.3 mmol) in 60 mL of water was added to a solution of 2 (4.28 g, 25.2 mmol) in 60 mL of glacial acetic acid at rt. The reaction mixture was stirred at rt for 50 min and quenched with 20 mL of saturated solution of $NaHSO_3$. Aqueous ammonia (25%, 50 mL) was added and the mixture was extracted with EtOAc (3 × 150 mL). The combined organic layers were washed with brine (100 mL), dried with anhydrous $MgSO_4$, filtered, and evaporated *in vacuo*. Recrystallization from EtOAc/hexane (2:1) gave 4.41 g (87%, 21.8 mmol) of 3 as large crystals: ^{1}H NMR (DMSO-d_6) δ 9.53 (d, $^4J_{HH}$ = 2.7 Hz, 1 H), 8.90 (dd, $^3J_{HH}$ = 8.7 Hz, $^4J_{HH}$ = 2.7 Hz, 1 H), 8.31 (d, $^3J_{HH}$ = 8.7 Hz, 1 H), 3.49 (s, 3 H); FABLRMS (3-NBA/CHCl$_3$) m/e 203 [M + H]$^+$; R_f 0.84 (EtOAc/hexane, 4:1; PMA); mp 117 °C (lit. 118 °C).[3]

2-Methylsulfonyl-5-aminopyridine (4)

To a solution of 3 (0.71 g, 3.51 mmol) in MeOH (30 mL), we added 5% palladium on activated carbon (0.40 g). The hydrogen balloon was attached to a stirred reaction vessel for 4 h. The mixture was filtered through Celite and evaporated to dryness to yield 0.60 g of 4 (99%, 3.47 mmol): ^{1}H NMR (DMSO-d_6) δ 7.99 (d, $^3J_{HH}$ = 8.6 Hz, 1 H), 7.65 (d, $^3J_{HH}$ = 8.6 Hz, 1 H), 7.03 (dd, $^3J_{HH}$ = 8.6 Hz, $^4J_{HH}$ = 2.7 Hz, 1 H), 6.32 (br s, 2 H), 3.08 (s, 3 H); FABLRMS (3-NBA/MeOH) m/e 173 [M + H]$^+$; R_f 0.26 (EtOAc/hexane, 2:1; Ninhydrin).

5-(5-[(2-Methylsulfonyl)pyridyl]amino)-5-oxopentanoic Acid (5)

A mixture of 4 (0.60 g, 3.47 mmol), glutaric anhydride (0.40 g, 3.47 mmol), and *N,N*-diisopropylethylamine (0.60 mL, 3.47 mmol) in CHCl$_3$ (15 mL) at +4 °C was stirred for 1 h and, after that, evaporated *in vacuo*. The crude product was chromatographed on Dowex 50W (H$^+$) ion exchange resin to give 0.72 g (91%) of 5 as off-white solid: ^{1}H NMR (DMSO-d_6) δ 10.5 (br s, 1 H), 8.86 (d, $^3J_{HH}$ = 8.7 Hz, 1 H), 8.39 (dd, $^3J_{HH}$ = 8.7 Hz, $^4J_{HH}$ = 2.6 Hz, 1 H), 8.06 (d, $^3J_{HH}$ = 8.7 Hz, 1 H), 3.25 (s, 3 H), 2.49 (t, $^3J_{HH}$ = 7.1 Hz, 2 H), 2.33 (t, $^3J_{HH}$ = 7.1 Hz, 2 H), 1.86 (qn, $^3J_{HH}$ = 7.1 Hz, 2 H); FABLRMS (3-NBA/MeOH) m/e 287 [M + H]$^+$.

5-(5-[(2-Methylsulfonyl)pyridyl]amino)-5-oxopentanoic Acid, N-Oxide (6)

A mixture of 5 (0.25 g, 0.87 mmol) and 0.92 M dimethyldioxirane in acetone (10 mL, 9.2 mmol) was stirred at rt for 5 h. Evaporation, trituration with diethyl ether, and drying *in vacuo* afforded 195 mg of 6 as light-brownish crystals (0.65 mmol, 76%): ^{1}H NMR (DMF-d_7) δ 10.3 (br s, 1 H), 8.99 ($^3J_{HH}$ = 8.6 Hz, 1 H), 8.48 (dd, $^3J_{HH}$ = 8.6 Hz, $^4J_{HH}$ = 2.8 Hz, 1 H), 8.04 (d, $^3J_{HH}$ = 8.6 Hz, 1 H), 3.29 (s, 3 H), 2.54 (t, $^3J_{HH}$ = 7.0 Hz, 2 H), 2.45 (t, $^3J_{HH}$ = 7.0 Hz, 2 H), 1.96 (qn, $^3J_{HH}$ = 7.0 Hz, 2 H); FABLRMS (3-NBA/MeOH) m/e 303 [M + H]$^+$.

ACKNOWLEDGMENTS

REFERENCES

1. LINDSEY, A. S. & H. JESKEY. 1957. Chem. Rev. **57:** 583–620.
2. JANDA, K. D. & Y. C-J. CHEN. 1994. Chemical and biological approaches to catalytic antibodies. *In* The Pharmacology of Monoclonal Antibodies: Handbook of Experimental Pharmacology. Volume 113. M. Rosenberg & G. P. Moore, Eds.: 209–237. Springer-Verlag. New York/Berlin.
3. BOURDAIS, J., P. DAUVILLIER, P. GAYRAL, M-C. RIGOTHIER, P. TIMON-DAVID, J. JULIEN, M.

GASQUET, F. DELMAS, J-C. JAMOULLE & C-L. LAPIERE. 1981. Eur. J. Med. Chem. **16**(3): 233–239.

4. MURRAY, R. W. & R. JEYARAMAN. 1985. J. Org. Chem. **50**(16): 2847–2853.
5. GODING, J. W. 1986. Monoclonal Antibodies: Principles and Practice. Academic Press. New York.
6. KAMAT, V. K., E. J. BECKMAN & A. J. RUSSELL. 1995. Crit. Rev. Biotechnol. **15**(1): 41–71.

Engineering of Novel Polyketides

Progress and Prospects

PETER J. KRAMER AND CHAITAN KHOSLA[a]

Department of Chemical Engineering
Stanford University
Stanford, California 94305-5025

IMPORTANCE OF POLYKETIDES

The term polyketide describes any member of a large family of natural products derived from the polymerization of organic acids through a series of decarboxylative condensations. Polyketides are produced by plants, fungi, marine animals, and the soil bacteria known as actinomycetes. This latter group, which includes the genus *Streptomyces*, has been the source of a large number of commercially valuable polyketides with a wide range of biological activities, including antibiotics, anticancer agents, and immunosuppressants.[1] Due to the large number of medically useful polyketides, there is much interest in understanding the chemistry and biology of the biosynthesis of these complex molecules. With a more complete understanding of the biosynthesis of these molecules, it is hoped that the enzymatic assemblies involved in polyketide biosynthesis might be harnessed via genetic engineering to produce an even greater diversity of novel molecules valuable to humans.

BIOSYNTHESIS OF POLYKETIDES

Although each polyketide has a unique final structure, all members of the polyketide family share a common chemistry of synthesis. As first suggested by Collie in 1907, the chemical synthesis of polyketides is centered around the reactive groups of the ketone and its adjacent α-methylene carbon.[2] The polyketide polymerization proceeds by a condensation between the methylene carbon of an extender unit and the nascent polyketide chain tethered to an acyl carrier protein (ACP) through a thioester linkage (FIGURE 1). The polymerization reaction is driven forward by the concurrent decarboxylation of the extender unit. Before continuing with the remaining details of polyketide biosynthesis, it should be noted that three opportunities for structural diversity—namely, the nature of the starter unit, the extender unit (R_1 and R_2 in FIGURE 1), and the stereochemistry resulting from their condensation—exist even at this early stage in the synthesis.

During the next step in polyketide biosynthesis, the keto group in the beta position can be reduced through a series of enzyme-catalyzed reactions to a hydroxyl (via ketoreductase), a double bond (via dehydratase), or a methylene group (via an enoyl reductase). This variable reduction at the beta carbonyl clearly distinguishes

[a]To whom all correspondence should be addressed.
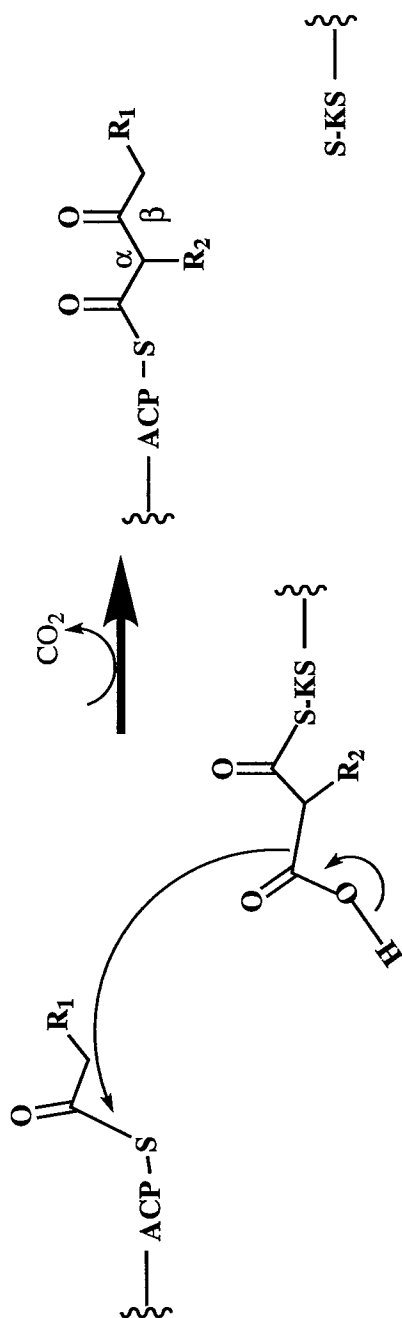
FIGURE 1. Illustration of the chain extension reaction via decarboxylative condensation, the central reaction of polyketide biosynthesis: α and β carbon positions on the newly formed polyketide chain are indicated. R_1 and R_2 are the pendant groups: H- for acetate extender units, $-CH_3$ for propionate extender units, etc.

polyketide biosynthesis from the similar decarboxylative condensation of acetate units seen in fatty acid biosynthesis[3] and is yet another source of molecular diversity. Although in the modular polyketide synthases (PKSs) the reductive reactions happen after each condensation[4,5] event,[6] there is evidence for delayed reduction of the extended chain in type II PKSs.[7-9] After the condensation and reduction events, the resulting thioester can itself be the subject of further nucleophilic attack at its thioester carbonyl, each time adding two carbons to the polyketide backbone, plus whichever pendant groups (R_2 in FIGURE 1) present on the extender unit. Because each condensation event results in a two-carbon, or acetate, addition to the growing backbone, the details of this synthetic mechanism are frequently referred to as the "acetate hypothesis", as articulated[10] and subsequently verified[11] by Birch in the early 1950s.

The polyketide polymerization reaction continues until the nascent polyketide chain reaches a chain length specific for each different polyketide. This variability in the degree of polymerization, or chain length, adds to the structural diversity of polyketides. Once the chain is formed and reduced, however, it folds and undergoes one or more intramolecular condensations; this cyclization pattern is specific to each polyketide. The cyclizations and subsequent aromatizations are both enzymatically controlled[9,12-14] and stochastic,[13,15] and represent another opportunity for structural diversity in the final product. At an as yet undetermined point in this pathway, the full-length polyketide chain is released via thiolysis or acyl transfer from the acyl carrier protein. Finally, the folded polyketide backbone can have hydroxyl, methyl, carbohydrate, or even other polyketide chains added in a series of tailoring reactions that produce the final product.[1] The location, stereochemistry, number, and nature of these added groups further diversify the polyketide structural repertoire.

POLYKETIDE SYNTHASES

Most of the biosynthetic steps of polyketide production are performed by an enzyme complex known as the polyketide synthase. Each synthetic activity, such as condensation, acyl-transfer, ketoreduction, dehydration, enol-reduction, or some cyclizations/aromatizations, is catalyzed by a separate active center in the polyketide synthase complex. These active centers are arranged on the polypeptides of the polyketide synthase complex in two different ways.

One architecture has all of the active sites for a complete round of synthesis (condensation through reduction) on a single polypeptide chain, with each domain separated by peptide linker regions (FIGURE 2).[6,16-21] One important feature of these synthases, called modular polyketide synthases (modular PKS), is that not only are the catalytic centers used only once per polyketide molecule, but in many cases they are also linearly organized along the peptide in the order in which they are used. In one noted exception, the proteins comprising the modular PKS involved in the synthesis of avermectin still have the active sites used in one condensation and reduction cycle in sequential order, but the synthase units for each different cycle are not colinear with their catalytic order.[19] Thus, in most, but not all, modular PKSs, knowledge of the protein sequence of the multienzyme is often sufficient to make realistic predictions of the catalytic sequence that generates the polyketide.[22] As
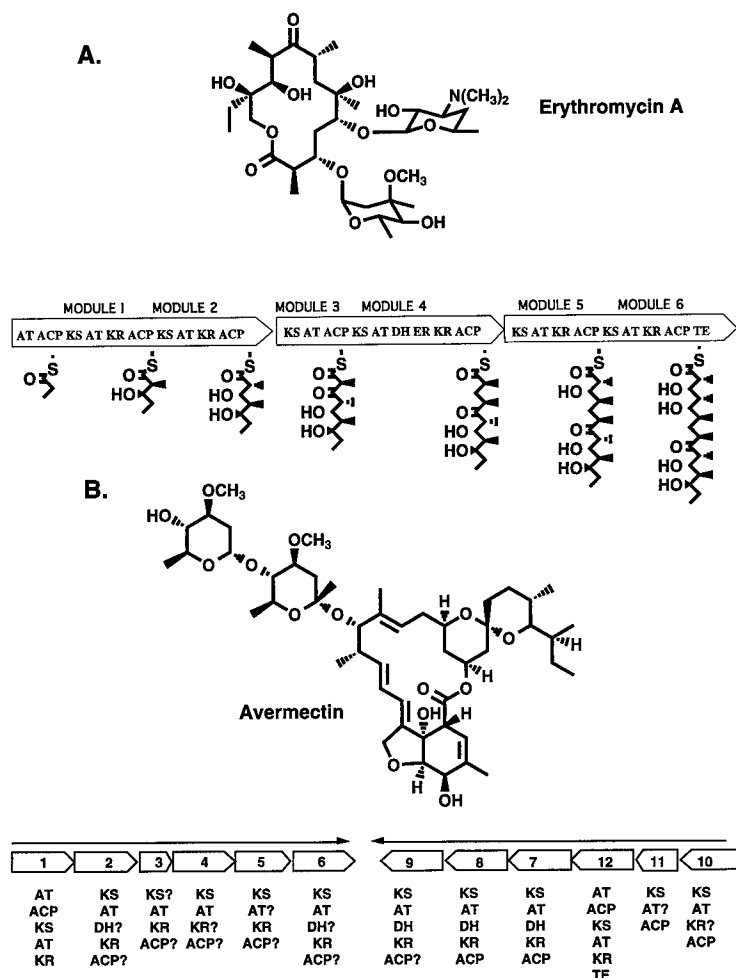
FIGURE 2. Two examples of modular polyketide synthases and the molecules they produce. (A) Erythromycin A structure and the colinear arrangement of the genes coding for the PKS components that assemble the polyketide chain in a stepwise manner, as indicated. (B) Avermectin structure, with the noncolinear arrangement of the genes coding for its PKS components, ultimately yielding the final structure. Long, thin black arrows indicate the direction of gene transcription, whereas numbered arrows represent the 12 separate PKS modules. Module organization is after MacNeil et al.,[19] with the numbering of the modules changed to reflect their order of action in assembling the final product.

evidence of the "modularity" of the modular PKS enzymes grows,[5,23,24] manipulation of the PKS proteins via genetic engineering seems quite likely to give rise to rationally designed novel polyketides.

The second commonly occurring architecture for polyketide synthesis is to have each of the catalytic centers on its own distinct polypeptide.[25-28] This arrangement of

catalytic centers requires that the individual polypeptides must associate in some as
yet unknown manner, forming a complex capable of performing the series of
synthetic reactions (FIGURE 3). Another important aspect of this group of PKSs is
that many catalytic centers must be used iteratively during the synthesis of a given
polyketide molecule.[27,29] This polypeptide complex, each with its own singular
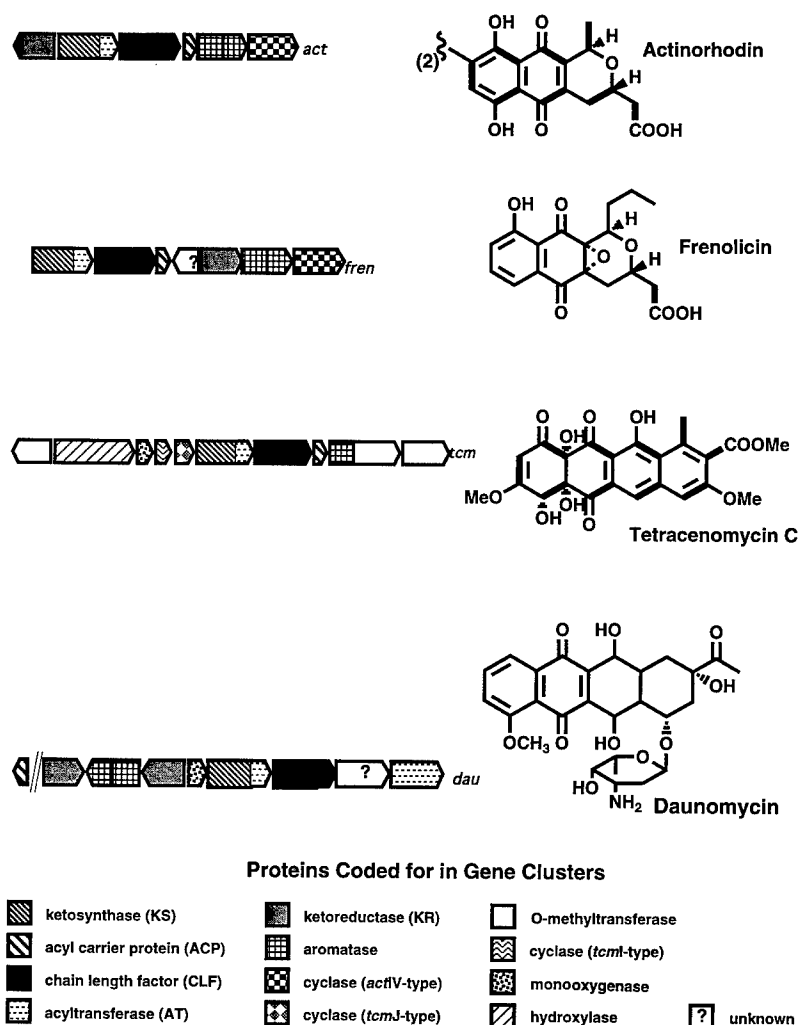
FIGURE 3. Four examples of type II polyketides, shown with a schematic depicting the
organization of the genes that code for the PKS complexes giving rise to each structure. Shaded
regions represent separate genes that code for the different proteins indicated in the key.
Native producers of the indicated polyketides: actinorhodin (*act*) from *S. coelicolor*; frenolicin
(*fren*) from *S. roseofulvus*; tetracenomycin (*tcm*) from *S. glaucescens*; and daunomycin (*dau*)
from *S. peucetius*.

function, is referred to as a type II PKS. The minimal type II PKS,[30] those proteins necessary for the complete round of condensation, reduction, and chain release, is composed of only three proteins:[7,14] the ketosynthase/acyltransferase, the "chain length determining factor", and an acyl carrier protein to which the nascent polyketide chain is attached.

The structure and function of the enzymes that comprise the PKS, and how this knowledge might be used to generate a diversity of potentially useful molecules, will be the subject of the rest of this study.

ENGINEERING POLYKETIDE DIVERSITY

Starter and Extender Units

The natural pool of type II polyketide starter units includes acetate,[31] propionate,[32] malonate,[33] butyrate, isobutyrate,[34] and others, whereas the pool of modular PKS starter units includes these and more, among them cyclohexanoate[20] and isovalarate.[34,35] Each of these starter units may function with their natural complement of biosynthetic proteins, but the degree of starter unit substitution allowed in polyketide synthesis has only recently been explored. Indeed, the biosynthetic machinery necessary to produce these novel precursors might well be absent in a heterologous host organism. Thus, the incorporation of new starter units will require direct feeding of the precursor to growing cells, switching the bacterial host, or cloning of the entire precursor biosynthetic pathway.[36] In the short term, the former is the most likely to demonstrate the feasibility of novel starter unit incorporation.

A precursor candidate fed to the bacteria must meet two obvious requirements. First, the novel starter unit must be capable of entering the cells and being loaded onto the PKS protein, or a hybrid PKS containing the relevant protein elements that carry the specificity for the novel starter unit must be functional. Second, the novel starter unit cannot interfere with further chain extension or other subsequent downstream reactions.

Examples of successes in the incorporation of novel starter units suggest that some PKSs may have the required relaxed downstream enzyme specificity to accommodate nonnative starter units. UV and chemically mutated strains containing the daunomycin type II PKS have been shown to use acetate, butyrate, isobutyrate, and acetoacetate starter units in place of the native propionate.[37] Fu *et al.* have shown that the oxytetracycline type II PKS, in the absence of the natural malonamyl primer, will use acetate as the starter unit.[38] Likewise, Meurer and Hutchinson have shown that the daunorubicin PKS will accept acetyl starter units in the absence of the native propionyl primer.[32] In each of these cases, the final molecule structure suggested that the novel starter units did not interfere with any of the downstream PKS enzymes. Some starter unit flexibility in the modular PKSs is implied by the incorporation of a variety of novel starter units[39,40] into the polyketide avermectin.

Whether the polyketide synthases are capable of incorporating novel extender units is still yet to be determined; however, support for the hypothesis is given in one report where erythromycin analogues incorporated malonate in place of methylmalonate.[6,41] If novel extender units are proved to be feasible, then any proposed extender unit should meet the same standards as a novel starter unit. Specifically, they must be

accessible to and capable of loading onto the condensing enzyme. Also, the down-stream processing enzymes must have sufficient relaxed specificity to process the unnatural polyketide chain. Separate studies on distinct PKSs suggest that rules regarding modular PKSs might not be applicable to type II PKSs.

Two experiments on the modular PKSs involved in the synthesis of the erythromy-cin precursor (6-deoxyerythronolide B, or DEB; FIGURE 2) suggest that these modular polyketides may be more forgiving of alterations in upstream enzyme activity. The first study by Donadio et al.[6] demonstrated that the elimination of an upstream ketoreductase activity did not affect the activity of downstream enzyme activity. Thus, the global structure of the novel polyketide was changed only by the substitution of an unreduced keto group for the hydroxyl found in the native structure. A related experiment[23] further demonstrated that the modular PKS governing the synthesis of DEB could tolerate the elimination of an enoyl reductase activity, giving rise to a double bond in the final structure. This suggests that each of the catalytic steps in this modular PKS acts independently. Although the experi-ments of Donadio et al. demonstrate that the modular PKSs will tolerate the removal of a catalytic activity, more experiments are needed to demonstrate if substitution or even insertion of catalytic modules is tolerated.

In contrast to the modular PKS studies, two studies on type II PKSs by McDaniel et al. suggest that downstream enzymes are significantly affected by alterations in the polyketide backbone. The first finding[13] was that, in hybrid PKS complexes, even proteins that cannot catalyze their designed reactions can alter the distribution of products generated by other enzymes in the complex. Thus, a cyclase specific to 16-carbon polyketide backbones was able to alter the product distribution of 20-carbon-producing PKS without ever catalyzing a reaction. The second study[9] demonstrated that an upstream ketoreductase specific to 16-carbon chains rendered a downstream 20-carbon-chain-specific cyclase/aromatase ineffective. These studies suggest that tinkering with the early stages of synthesis for type II PKSs leads to the production of polyketides with global structural changes, rather than exclusively specific local changes.

Backbone Chain Length

One of the most defining characteristics of the polyketide is the number of condensation events necessary for its synthesis. Although chain length is apparently defined by the number of active sites in the modular PKSs,[20,42] the chain length determination for type II PKSs is not as clear. McDaniel et al. have proposed that a heretofore uncharacterized protein product present in all of the known bacterial type II polyketide producers is the chain length determining factor (CLF).[30] As proof of the identity of the CLF, McDaniel et al. produced the CLF protein normally found in a complex catalyzing the formation of a 16-carbon chain with the ketosynthase from related PKSs that normally produce 18- and 20-carbon chains. The result of this study was that the polyketide produced had 16 carbons, consistent with the specificity of the CLF protein (see FIGURE 4). However, the fact that subsequent experiments with homologous CLF proteins from PKSs with chain length specificity other than 16 carbons all resulted in nonfunctional associations makes the identity of the CLF protein controversial.[43] Nevertheless, it is safe to say that the combination of the

ketosynthase and the CLF from a given PKS will consistently produce a polyketide of a given length.

The source of chain length specificity of the modular PKSs is more apparent than that for the type II PKSs. Because most modular PKS proteins are organized colinearly with the proposed synthetic pathway, reducing the chain length may be as simple as deleting a region of the protein that codes for one or more rounds of condensation. In fact, although DEB naturally occurs as a 14-membered lactone ring (FIGURE 2), truncated DEB precursors were properly cyclized by the PKS as a 6-membered ring[5,44] and, as long as the native thioesterase domain of the PKS was placed immediately after the point of truncation, as a 12-membered ring.[24] Although
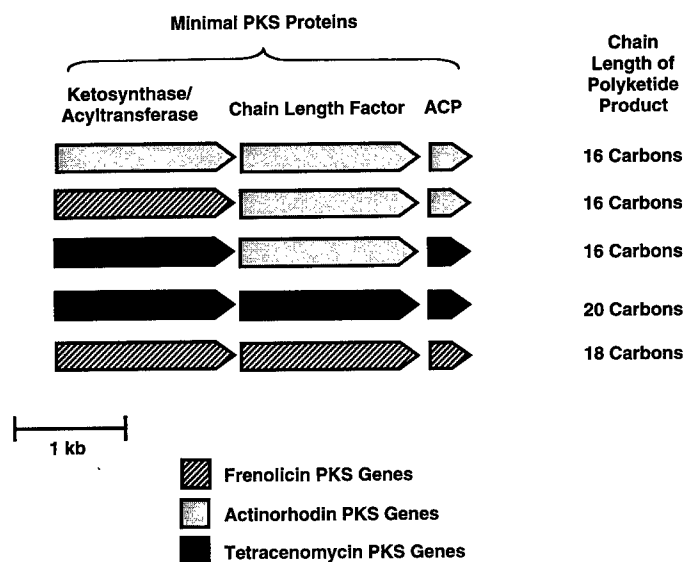
FIGURE 4. Experimental evidence of a chain length determining factor of the minimal polyketide synthases in type II PKSs.[8,30] Shaded regions represent protein products of the minimal PKS genes from the gene cluster indicated in the key. In all cases where a polyketide product is made, the chain length of that product corresponds to the chain length specificity of the chain length factor.

encouraging, the extent to which these results can be generalized to other modular PKSs awaits further experimentation.

Degree of Reduction

Another natural source of structural diversity is the degree of reduction of the β-keto group during biosynthesis of the polyketide chain. As mentioned above, introducing a novel reduction into a nascent 20-carbon polyketide chain from a type II PKS rendered downstream enzymes incapable of performing their natural func-

tions.[9] However, it is still significant that the ketoreductase with a natural substrate of 16 carbons could recognize and reduce the same ninth carbonyl from the carboxyl end of chains that are 18 and 20 carbons long.[7,45] Added structural diversity of type II polyketide ketoreduction was demonstrated by the variable reduction of the "minimal" 18-carbon polyketide at both the ninth and seventh carbon from the carboxyl end of the molecule[8] (carbon numbering scheme; FIGURE 5). The promise of more structural diversity lies in the fact that other ketoreductase domains have been identified by protein sequence alignment homology to the ketoreductase mentioned above,[29,46,47] but as yet no biochemical studies have verified the specificity of these homologues.

Experiments with the modular PKSs, outlined in the previous section, seem to suggest that the carbon backbone of the nascent polyketide in these synthases will proceed through all subsequent synthetic steps regardless of the degree of reduction
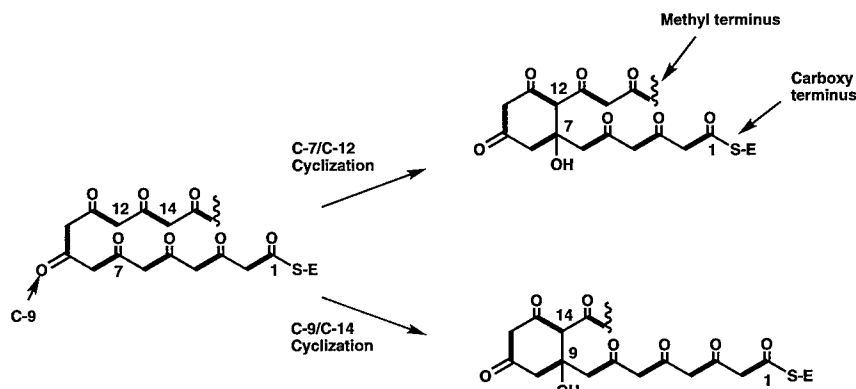
FIGURE 5. Two commonly observed regiospecificities of cyclization of the first ring in type II polyketide biosynthesis. The indicated C-9 is also the usual site of action of the actinorhodin ketoreductase, when it is present. The carboxyl terminus, as indicated, is designated carbon 1, after the fatty acid biosynthesis nomenclature.

of prior keto groups in the chain.[6,23] If these early results on the erythromycin-producing PKS prove generalizable to all modular PKSs, then variable polyketide chain reduction in this subset of polyketides could directly lead to rationally designed novel molecules.

Cyclization

Further structural diversity is programmed into the polyketides through the number, location along the backbone (regiospecificity), and aromatic nature of the carbon rings formed during the folding of the polyketide backbone. Modular PKSs and type II PKSs produce polyketides with significantly different cyclization patterns and have shown variable flexibility in the number and regiospecificity of cyclizations tolerated.

Type II PKSs generally produce polyketides with 6-membered rings and are often referred to as aromatic PKSs[1] (FIGURE 2). Which of the 6-membered rings are enzyme-catalyzed and which arise spontaneously has only recently been investigated in detail for a few type II PKSs.

Some "design" rules have emerged from these studies with regard to ring formation, and the rules have been verified by the production of two "rationally designed" novel polyketides.[48] The first of these rules is that the ketosynthase, CLF, and an ACP dictate the regiospecificity of the first cyclization in the absence of a specific cyclase enzyme, although the minimal PKS that generated a 20-carbon molecule showed mixed regiospecificity of the first cyclization.[13] The next rule is as follows: if a ketoreductase is included with the minimal PKS, then cyclization always occurs between the carbon three upstream and two downstream of the point of reduction (e.g., C-7/C-12 cyclization of a polyketide chain with a reduction at C-9, counting from the carboxyl end of the molecule; see FIGURE 5). If a specific cyclase is included with the minimal PKS, then the regiospecificity of the cyclization occurs one acyl condensation earlier in the chain synthesis (e.g., C-9/C-14 rather than C-7/C-12).[9] As mentioned above, this cyclase activity is eliminated in PKSs containing a ketoreductase.

Whether or not the first ring aromatizes is dictated by two more design rules. First, unreduced polyketides spontaneously aromatize the first ring. Second, in the presence of a ketoreductase, an aromatase gene with a chain length specificity equal to or greater than that of the nascent chain is needed. Thus, an aromatase that usually operates on a 20-carbon substrate could function with a polyketide chain of 20, 18, or 16 carbons; an 18-carbon-specific aromatase could operate on 18- or 16-carbon chains; etc.[13,48]

Cyclization of the second ring (C-5 to C-14) of aromatic PKSs has been shown to occur in reduced 16- and 18-carbon chains in the presence of a cyclase that has a natural 16-carbon chain specificity. A cyclase capable of catalyzing ring closure between C-5 and C-14 of a polyketide longer than 18 carbons has not yet been studied.

Subsequent cyclization reactions are most likely enzyme-catalyzed in nature, but engineered aromatic polyketides studied to date in the absence of these downstream enzymes have undergone spontaneous cyclizations governed by the relevant rules of chemistry. For example, if three ketide units remain on the methyl terminus of the polyketide, the chain will form a spontaneous benzene ring or a hemiketal if a convenient hydroxyl exists on the carbon located five carbons upstream of the condensing carbonyl. Similarly, the thioester-anchored end of the polyketide either can form a γ-pyrone via a carbonyl oxygen attack on the thioester carbonyl carbon or both ends of the polyketide could cocyclize through an aldol condensation. Alternatively, decarboxylation of the carboxyl end is frequently seen in free carboxylic acid moieties at this position.[48]

The rules governing the cyclization pattern of the large polyketide produced by modular PKSs are suggested by the final product structure. The macrolactones, a subgroup of the antibiotics produced by modular PKSs, all seem to cyclize by an attack by the hydroxyl of the starter unit on the terminal thioester carbonyl of the polyketide backbone.[49,50] That this lactonization occurs with relaxed specificity to chain length has been shown in two experiments by Kao *et al.*,[24,51] who demonstrated

that formation of 6-, 12-, and the native 14-membered lactone rings was catalyzed by the same thioesterase domain. Information about the cyclization flexibility of other polyketides synthesized by modular PKSs is still forthcoming.

Glycosylation and Methylation

The completely synthesized and cyclized polyketide backbone is modified further in most cases by a series of enzymes that can attach hydroxyl, methyl, glycosyl, or even acyl groups.[31] The number of enzymes involved in processing the aglycone polyketide chain is vast,[52] and the diversity of types and stereochemistries of the resulting pendant groups[53] expands the potential structural variability of novel polyketides extensively. Although early studies on the tailoring enzymes suggested a range of substrate flexibility, the specificity toward novel structures is still largely untested. However, two recent experiments are hopeful in this regard, demonstrating that tailoring enzymes can act on nonnative and novel polyketide substrates.[6,54]

IMPLICATIONS FOR ENGINEERING NOVEL POLYKETIDES

Each step in the biosynthesis of polyketides can be thought of as an opportunity to engineer novel structural elements as a way to expand nature's repertoire of polyketide natural products. The research reviewed above suggests that virtually all stages in the polyketide biosynthetic pathway tolerate some degree of manipulation. Also, because changes in the later-acting enzyme pathways will have a multiplying effect on alterations made earlier in the biosynthetic pathway, the potential number of novel structures produced through genetic manipulation is enormous. Due to the fact that new gene clusters coding for enzymes of new polyketide synthases are constantly being cloned, the biosynthetic repertoire available for manipulation continues to expand. Thus, the combination of genetics, molecular biology, and synthetic chemistry holds great promise for generating new molecules with biologically useful properties.

REFERENCES

1. O'HAGAN, D. 1991. The Polyketide Metabolites. Ellis Horwood. Chichester, United Kingdom.
2. COLLIE, J. N. 1907. Derivatives of the multiple ketene group. J. Chem. Soc. **91:** 1806–1813.
3. HOPWOOD, D. A. & D. H. SHERMAN. 1990. Molecular genetics of polyketides and its comparison to fatty acid biosynthesis. Annu. Rev. Genet. **24:** 37–66.
4. CANE, D. E. & C-C. YANG. 1987. Macrolide biosynthesis: 4. Intact incorporation of a chain elongation intermediate into erythromycin. J. Am. Chem. Soc. **109:** 1255–1257.
5. KAO, C. M., G. LUO, L. KATZ, D. E. CANE & C. KHOSLA. 1994. Engineered biosynthesis of a triketide lactone from an incomplete modular polyketide synthase. J. Am. Chem. Soc. **116**(25): 11612–11613.
6. DONADIO, S., M. J. STAVER, J. B. MCALPINE, S. J. SWANSON & L. KATZ. 1991. Modular organization of genes required for complex polyketide biosynthesis. Science **252:** 675–679.
7. BARTEL, P. L., C. B. ZHU, J. S. LAMPEL, D. C. DOSCH, N. C. CONNERS, W. R. STROHL, J. M. BEALE, JR. & H. G. FLOSS. 1990. Biosynthesis of anthraquinones by interspecies cloning

of actinorhodin biosynthesis genes in *Streptomyces*: clarification of actinorhodin gene functions. J. Bacteriol. **172**: 4816–4826.

8. McDANIEL, R., S. EBERT-KHOSLA, D. A. HOPWOOD & C. KHOSLA. 1993. Engineered biosynthesis of novel polyketides: manipulation and analysis of an aromatic polyketide synthase with unproven catalytic specificities. J. Am. Chem. Soc. **115**(25): 11671–11675.

9. McDANIEL, R., C. R. HUTCHINSON & C. KHOSLA. 1995. Engineered biosynthesis of novel polyketides: analysis of tcmN function in tetracenomycin biosynthesis. J. Am. Chem. Soc. **117**(26): 6805–6810.

10. BIRCH, A. J. & F. W. DONOVAN. 1953. Studies in relation to biosynthesis. Aust. J. Chem. **6**: 360–368.

11. BIRCH, A. J., R. A. MASSY-WESTROPP, R. W. RICKARDS & H. SWITH. 1958. Studies in relation to biosynthesis: Part XIII. Griseofulvin. J. Chem. Soc., p. 360–365.

12. McDANIEL, R., S. EBERT-KHOSLA, D. A. HOPWOOD & C. KHOSLA. 1994. Engineered biosynthesis of novel polyketides: *act*VII and *act*IV genes encode aromatase and cyclase enzymes, respectively. J. Am. Chem. Soc. **116**: 10855–10859.

13. McDANIEL, R., S. EBERT-KHOSLA, H. FU, D. A. HOPWOOD & C. KHOSLA. 1994. Engineered biosynthesis of novel polyketides: influence of a downstream enzyme on the catalytic specificity of a minimal aromatic polyketide synthase. Proc. Natl. Acad. Sci. U.S.A. **91**: 11542–11546.

14. SUMMERS, R. G., E. WENDT-PIENKOWSKI, H. MOTAMEDI & C. R. HUTCHINSON. 1992. Nucleotide sequence of the *tcmII–tcmIV* region of the tetracenomycin C biosynthetic gene cluster of *Streptomyces glaucescens* and evidence that the *tcmN* gene encodes a multifunctional cyclase–dehydratase–*O*-methyl transferase. J. Bacteriol. **174**(6): 1810–1820.

15. FU, H., D. A. HOPWOOD & C. KHOSLA. 1994. Engineered biosynthesis of novel polyketides: evidence for temporal, but not regiospecific, control of cyclization of an aromatic polyketide precursor. Chem. Biol. **1**(4): 205–210.

16. CORTÉS, J., S. F. HAYDOCK, G. A. ROBERTS, D. J. BEVITT & P. F. LEADLAY. 1990. An unusually large multifunctional polypeptide in the erythromycin-producing polyketide synthase of *Saccharopolyspora erythraea*. Nature **348**: 176–178.

17. LEADLAY, P. F., J. STAUNTON, J. F. APARICIO, D. J. BEVITT, P. CAFFREY, J. CORTÉS, A. MARSDEN & G. A. ROBERTS. 1993. The erythromycin-producing polyketide synthase. Biochem. Soc. Trans. **21**: 218–222.

18. CAFFREY, P., D. J. BEVITT, J. STAUNTON & P. F. LEADLAY. 1992. Identification of DEBS 1, DEBS 2, and DEBS 3, the multienzyme polypeptides of the erythromycin-producing polyketide synthase from *Saccharopolyspora erythraea*. FEBS **304**(2,3): 225–228.

19. MacNEIL, D. J., J. L. OCCI, K. M. GEWAIN, T. MacNEIL, P. H. GIBBONS, C. L. RUBY & S. J. DANIS. 1992. Complex organization of the *Streptomyces avermitilis* genes encoding the avermectin polyketide synthase. Gene **115**: 119–125.

20. SCHWECKE, T., J. F. APARICIO, I. MOLNAR, A. KÖNIG, L. E. KHAW, S. F. HAYDOCK, M. OLIYNYK, P. CAFFREY, J. CORTÉS, J. B. LESTER, G. A. BÖHM, J. STAUNTON & P. F. LEADLAY. 1995. The biosynthetic gene cluster for the polyketide immunosuppressant rapamycin. Proc. Natl. Acad. Sci. U.S.A. **92**: 7839–7843.

21. SWAN, D. G., A. M. RODRIGUEZ, C. VILCHES, C. MÉNDEZ & J. A. SALAS. 1994. Characterization of a *Streptomyces antibioticus* gene encoding a type I polyketide synthase which has an unusual coding sequence. Mol. Gen. Genet. **242**: 358–362.

22. DONADIO, S. & L. KATZ. 1992. Organization of the enzymatic domains in the multifunctional polyketide synthase involved in erythromycin formation in *Saccharopolyspora erythraea*. Gene **111**: 51–60.

23. DONADIO, S., J. B. McALPINE, P. J. SHELDON, M. JACKSON & L. KATZ. 1993. An erythromycin analog produced by reprogramming of polyketide synthesis. Proc. Natl. Acad. Sci. U.S.A. **90**: 7119–7123.

24. KAO, C. M., G. LUO, L. KATZ, D. E. CANE & C. KHOSLA. 1995. Manipulation of macrolide ring size by directed mutagenesis of a modular polyketide synthase. J. Am. Chem. Soc. **117**: 9105.

25. CABALLERO, J. L., E. MARTINEZ, F. MALPARTIDA & D. A. HOPWOOD. 1991. Organization

and functions of the *act*VA region of the actinorhodin biosynthetic gene cluster of *Streptomyces coelicolor*. Mol. Gen. Genet. **230:** 401–412.

26. HALLAM, S. E., F. MALPARTIDA & D. A. HOPWOOD. 1988. Nucleotide sequence, transcription, and deduced function of a gene involved in polyketide antibiotic synthesis in *Streptomyces coelicolor*. Gene **74:** 305–320.

27. FERNANDEZ-MORENO, M. A., E. MARTINEZ, L. BOTO, D. A. HOPWOOD & F. MALPARTIDA. 1992. Nucleotide sequence and deduced functions of a set of cotranscribed genes of *Streptomyces coelicolor* A3(2) including the polyketide synthase for the antibiotic actinorhodin. J. Biol. Chem. **267**(27): 19278–19290.

28. BIBB, M. J., S. BIRO, H. MOTAMEDI, J. F. COLLINS & C. R. HUTCHINSON. 1989. Analysis of the nucleotide sequence of the *Streptomyces glaucescens tcmI* genes provides key information about the enzymology of polyketide biosynthesis. EMBO J. **8**(9): 2727–2736.

29. SHERMAN, D. H., F. MALPARTIDA, H. M. KIESER, M. J. BIBB & D. A. HOPWOOD. 1989. Structure and deduced function of the granaticin-producing polyketide synthase gene cluster of *Streptomyces violaceoruber* Tü22. EMBO J. **8**(9): 2717–2725.

30. McDANIEL, R., S. EBERT-KHOSLA, D. A. HOPWOOD & C. KHOSLA. 1993. Engineered biosynthesis of novel polyketides. Science **262:** 1546–1550.

31. HOPWOOD, D. 1983. Actinomycete genetics and antibiotic production. *In* Biochemistry and Genetic Regulation of Commercially Important Antibiotics. Volume 2. L. C. Vining, Ed.: 1–21. Addison–Wesley. Reading, Massachusetts.

32. MEURER, G. & C. R. HUTCHINSON. 1995. The daunorubicin type II polyketide synthase enzymes DpsA and DpsB neither determine the choice of starter unit nor the folding pattern of aromatic polyketides. J. Am. Chem. Soc. In press.

33. JEFFS, P. W. & D. McWILLIAMS. 1981. Carbon-13 nuclear magnetic resonance study of the biosynthesis of cycloheximide: stereospecific incorporation of malonate into the glutarimide ring. J. Am. Chem. Soc. **103:** 6185–6192.

34. O'HAGAN, D. 1995. Biosynthesis of fatty acid and polyketide metabolites. Nat. Prod. Rep. **12:** 1–32.

35. O'HAGAN, D. 1992. Biosynthesis of polyketide metabolites. Nat. Prod. Rep. **9:** 447–479.

36. HOPWOOD, D. A. 1993. Genetic engineering of *Streptomyces* to create hybrid antibiotics. Curr. Opin. Biotechnol. **4:** 531–537.

37. OKI, T., Y. MATSUZAWA, K. KIYUOSHIMA & A. YOSHIMOTO. 1981. New anthracyclines, feudomycins, produced by the mutant from *Streptomyces coeruleorubisus* ME130-A4. J. Antibiot. **34**(7): 783–790.

38. FU, H., S. EBERT-KHOSLA, D. A. HOPWOOD & C. KHOSLA. 1994. Relaxed specificity of the oxytetracycline polyketide synthase for an acetate primer in the absence of a malonamyl primer. J. Am. Chem. Soc. **116**(14): 6443–6444.

39. DUTTON, C. J., S. P. GIBSON, A. C. GOUDIE, K. S. HOLDOM, M. S. PACEY, J. C. RUDDOCK, J. D. BU'LOCK & M. K. RICHARDS. 1991. Novel avermectins produced by mutational biosynthesis. J. Antibiot. **44**(3): 357–365.

40. HAFNER, E. W., B. W. HOLLEY, K. S. HOLDOM, S. E. LEE, R. G. WAX, D. BECK, H. A. I. McARTHUR & W. C. WERNAU. 1991. Branched-chain fatty acid requirement for avermectin production by a mutant of *Streptomyces avermitilis* lacking branched-chain 2-oxo acid dehydrogenase activity. J. Antibiot. **44**(3): 349–356.

41. McALPINE, J. B., J. S. TUAN, D. P. BROWN, K. D. GREBNER, D. N. WHITTERN, A. BUKO & L. KATZ. 1987. New antibiotics from genetically engineered actinomycetes: 2-noreryth-romycins, isolation, and structural determinations. J. Antibiot. **40**(8): 1115–1122.

42. DONADIO, S., M. J. STAVER, J. B. McALPINE, S. J. SWANSON & L. KATZ. 1992. Biosynthesis of the erythromycin macrolactone and a rational approach for producing hybrid macrolides. Gene **115:** 97–103.

43. HUTCHINSON, C. R. 1994. Drug synthesis by genetically engineered microorganisms. Bio/Technology **12:** 375–380.

44. CORTÉS, J., K. E. H. WIESMANN, G. A. ROBERTS, M. J. B. BROWN, J. STAUNTON & P. F. LEADLAY. 1995. Repositioning of a domain in a modular polyketide synthase to promote specific chain cleavage. Science **268:** 1487–1489.

45. FERNANDEZ-MORENO, M. A., E. MARTINEZ, J. L. CABALLERO, K. ICHINOSE, D. A.

HOPWOOD & F. MALPARTIDA. 1994. DNA sequence and functions of the *act*VI region of the actinorhodin biosynthetic gene cluster of *Streptomyces coelicolor* A3(2). J. Biol. Chem. **269**(40): 24854–24863.

46. YU, T-W., M. J. BIBB, P. W. REVILL & D. A. HOPWOOD. 1994. Cloning, sequencing, and analysis of the griseusin polyketide synthase gene cluster from *Streptomyces griseus*. J. Bacteriol. **176**(9): 2627–2634.

47. BIBB, M. J., D. H. SHERMAN, S. OMURA & D. A. HOPWOOD. 1994. Cloning, sequencing, and deduced functions of a cluster of *Streptomyces* genes probably encoding biosynthesis of the polyketide antibiotic frenolicin. Gene **142**: 31–39.

48. MCDANIEL, R., S. EBERT-KHOSLA, D. A. HOPWOOD & C. KHOSLA. 1995. Rational design of aromatic polyketide natural products by recombinant assembly of enzymatic subunits. Nature **375**: 549–554.

49. O'HAGAN, D., J. A. ROBINSON & D. L. TURNER. 1983. Biosynthesis of the macrolide antibiotic tylosin: origin of the oxygen atoms of tylactone. J. Chem. Soc. Commun., p. 1337–1340.

50. CANE, D. E., H. HASLER, P. B. TAYLOR & T-C. LIANG. 1983. Macrolide biosynthesis II: origin of the carbon skeleton and oxygen atoms of the erythromycins. Tetrahedron **39**(21): 3449–3455.

51. KAO, C. M., L. KATZ & C. KHOSLA. 1994. Engineered biosynthesis of a complete macrolactone in a heterologous host. Science **265**: 509–512.

52. HUTCHINSON, C. R. 1981. The biosynthesis of tetracycline and anthracycline antibiotics. *In* Antibiotics Volume IV: Biosynthesis. J. W. Corcoran, Ed.: 1–11. Springer-Verlag. Berlin/New York.

53. CORCORAN, J. W. 1981. Biochemical mechanisms in the biosynthesis of erythromycins. *In* Antibiotics Volume IV: Biosynthesis. J. W. Corcoran, Ed.: 132–174. Springer-Verlag. Berlin/New York.

54. NIEMI, J., K. YLIHONKO, J. HAKALA, R. PÄRSSINEN, A. KOPIO & P. MÄNTSÄLÄ. 1994. Hybrid anthracycline antibiotics: production of new anthracyclines by cloned genes from *Streptomyces purpurascens* in *Streptomyces galilaeus*. Microbiology **140**: 1351–1358.

Characterization of Polyclonal Antibody–catalyzed Hydrolysis

DONGZHOU LIU[a] AND YAOTING YU

Institute for Molecular Biology
Nankai University
Tianjin 300071, People's Republic of China

INTRODUCTION

Because of the versatility of the immune system to produce a diversity of antibodies, some antibodies, particularly those of monoclonal origins, have been developed to enhance the product formation in some chemical reactions.[1] These findings have prompted the search for more antibodies with unusual enzymatic properties that could be used as catalysts in chemical reactions, particularly in those where the corresponding natural enzymes are unavailable. In this communication, the simple and less time-consuming protocol of the production of catalytic polyclonal antibody (cat-PcAb) and its catalytic properties are reported.

MATERIALS AND METHODS

Materials

Esterase from porcine liver (PLE, EC3.1.1), keyhole-limpet hemocyanin (KLH), bovine serum albumin (BSA), and Freund's adjuvant were purchased from Sigma Chemical (St. Louis, Missouri). Protein A–Sepharose CL-4B gel was the product of Pharmacia Fine Chemicals (Uppsala, Sweden). The other chemicals (AR) and biochemicals were purchased from Aldrich Chemical (Milwaukee, Wisconsin) and GIBCO (Gaithersburg, Maryland).

Methods

Syntheses of Haptens and Immunogens

p-Nitrophenyl-di(p-nitrophenyl)phosphonopentanoate $\underline{1}$ was synthesized in five steps from triethyl phosphite and methyl-5-bromopentanoate.[2] The final hapten was purified by Merck-60 gel column separation and recrystallization from ether/ethane and was checked by 120 MHZ ^{1}H-NMR and ^{31}P-NMR. Then, the phosphonate hapten was coupled to KLH and BSA in 0.1 M sodium borate.[3] Quantitation of the

---

[a]Present address: Department of Chemistry, University of Louisville, Louisville, Kentucky 40292.

hapten/carrier ratio was determined by refluxing an aliquot of the protein conjugate in 2 M NaOH and measuring the OD value at 405 nm. The hapten densities of the conjugates were found to be 18 haptens per BSA and 45 haptens per KLH (for 100,000 MW). The conjugate of KLH-1 was used as the immunogen, whereas BSA-1 was employed as a coating antigen for evaluating the specificity of the prepared antisera in ELISA. (See FIGURE 1.)
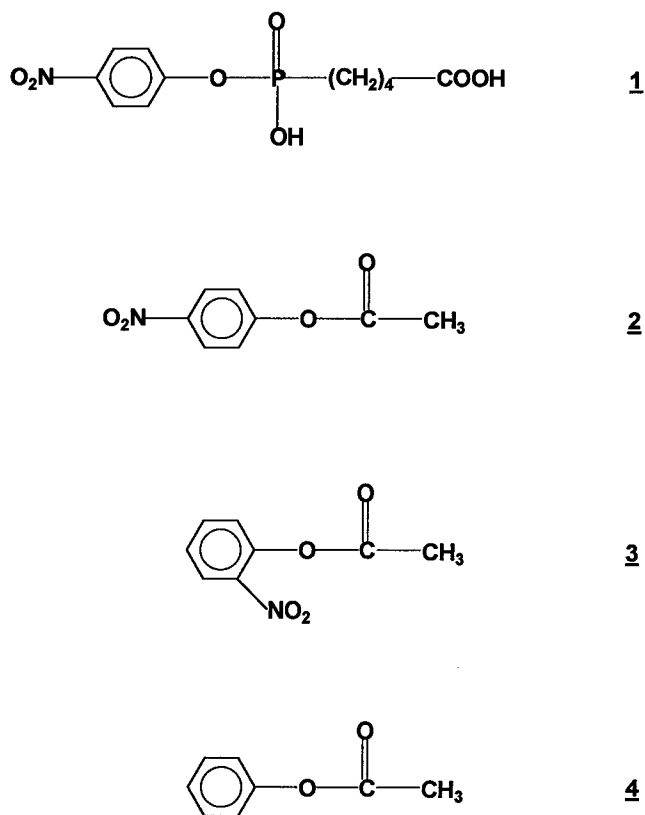
FIGURE 1. Chemical structure of hapten (1) and substrates 2, 3, and 4.

Antibody Production

Mature male New Zealand white rabbits were immunized with KLH-1 emulsified in Freund's adjuvant. When the titers of antisera were higher than 1:20,000, the whole antiserum was collected separately from each rabbit and stored at −20 °C. The cat-PcAb was purified from the antisera by repeated cycles of $(NH_4)_2SO_4$ precipitation and affinity chromatography on a protein A–Sepharose CL-4B column. Antibod-

ies were judged to be homogeneous by 7.5% SDS-PAGE, which yielded only heavy and light chains under reducing conditions, using Coomassie blue staining.

Kinetic and Thermodynamic Assay of the Hydrolysis

The initial rates of hydrolysis of *p*-nitrophenyl acetate $\underline{2}$, in the presence of 0.2 μM IgG from either an immunized (cat-PcAb) or control (nonimmunized, non-PcAb) rabbit, were determined for a range of substrate concentrations between 2 and 30 μM. The hydrolysis was followed in 25 mM Tris-HCl buffer, pH 8.0, containing 0.67% (v/v) acetonitrile at 30 °C, by monitoring an increase in A_{405nm} for the release of a *p*-nitrophenyl group ($\epsilon_{405} = 1.65 \times 10^3$ M$^{-1} \cdot$ cm^{-1}). The rate values were obtained by correcting the initial rates obtained in the presence of 0.2 μM cat-PcAb with those generated in the presence of 0.2 μM non-PcAb. The noncatalyzed rate was determined using analysis of initial rates and extrapolated to zero buffer concentration.

The hydrolyses of *o*-nitrophenyl acetate $\underline{3}$ and phenyl acetate $\underline{4}$ were studied in an analogous way, except that the hydrolyses were monitored at 415 nm ($\epsilon_{415} = 4.18 \times 10^3$ M$^{-1} \cdot$ cm^{-1}) and 270 nm ($\epsilon_{270} = 2.0 \times 10^3$ M$^{-1} \cdot$ cm^{-1}), respectively.

RESULTS AND DISCUSSION

The prepared cat-PcAb was found to catalyze the hydrolysis of *p*-nitrophenyl acetate $\underline{2}$, with the kinetics consistent with the Michaelis-Menten rate expression. Lineweaver-Burk analysis of the antibody-catalyzed hydrolysis afforded values of k_{cat} between 0.22 ± 0.02 min^{-1} and 22 ± 2 min^{-1}, depending upon the different efficient concentrations of cat-PcAb,[4] and the Michaelis constant K_m was found to be 13.1 ± 0.4. Despite the existence of structural heterogeneity in the PcAb, these investigations demonstrated that the catalytic properties of the active species of antibodies were sufficiently similar and the differences among them were not readily detected as deviations from the single-site saturation mode.

The specificity of the PcAb-catalyzed hydrolyses was also characterized. The prepared cat-PcAb could only accelerate the hydrolysis of substrate $\underline{2}$, which shared the same antigenic determinant group (*p*-nitrophenyl) with the immunogen KLH-$\underline{1}$, and did not catalyze the isomeric substrates $\underline{3}$ and $\underline{4}$. However, esterase from porcine liver, diluted 1:1000 in 25 mM Tris-HCl buffer, pH 8.0, could catalyze all the substrates $\underline{2}$, $\underline{3}$, and $\underline{4}$. Furthermore, the PcAb purified by the same procedures from the nonimmunized rabbit did not show any catalytic activity on the hydrolysis of substrate $\underline{2}$; in fact, its hydrolyzing rate was similar to that of noncatalyzed hydrolysis. These results indicate that the acceleration of the hydrolysis of $\underline{2}$ was due to the specific activity of cat-PcAb and not to the trace enzyme impurity contained in the PcAb preparation.

The pH dependence of the hydrolysis of $\underline{2}$ was examined in the presence of 0.2 μM cat-PcAb and 2 to 30 μM of $\underline{2}$ between pH 7.6 and 9.0 in 25 mM Tris-HCl at 30 °C. The k_{cat} of the PcAb-catalyzed reaction, which estimated that 10% of the total IgG was the catalytic antibody, exhibited a first-order dependence on [OH$^-$],

whereas K_m was relatively unaffected in this pH range: k_{cat} = 0.358 min^{-1}, K_m = 12.1 μM (pH 7.6); k_{cat} = 0.834 min^{-1}, K_m = 10.0 μM (pH 8.0); k_{cat} = 2.2 min^{-1}, K_m = 13.1 μM (pH 8.5); k_{cat} = 4.8 min^{-1}, K_m = 11.8 μM (pH 9.0). Consequently, a rational comparison between catalyzed and noncatalyzed reactions may be made by comparing the pH-corrected rate constants of $k_{cat}/[OH^-]$ = k'_{cat} and $k_{uncat}/[OH^-]$ = k'_{uncat}. It was found that the ratio of k'_{cat}/k'_{uncat}, which reflected the acceleration of the hydrolysis catalyzed by cat-PcAb, was in the range of 5.0 × 10^1 to 5.0 × 10^3.

The effect of the reaction temperature on the PcAb-catalyzed hydrolysis of $\underline{2}$ was studied in 25 mM Tris-HCl, pH 8.0. The activity of the antibody can be destroyed by heat denaturation at 80 °C and the optimal temperature for the catalysis was found to be 35 °C. According to the Arrhenius equation, the reaction activity energy (E_a) of the hydrolysis of $\underline{2}$ was determined in the presence of 0.22 μM cat-PcAb and 46 μM of $\underline{2}$ between the temperatures of 20 °C and 80 °C. As expected, the E_a of PcAb-catalyzed hydrolysis was lower than that of general base-catalyzed hydrolysis—at 20–50 °C: $E_{a,cat-PcAb}$ = 30.4 kJ/mol, $E_{a,general}$ = 42.3 kJ/mol; at 50–80 °C: $E_{a,cat-PcAb}$ = 24.3 kJ/mol, $E_{a,general}$ = 29.2 kJ/mol. These results indicate that the cat-PcAb could exhibit more potential catalytic activity at the lower temperature.

REFERENCES

1. LERNER, R. A., S. J. BENKOVIC & P. SCHULTZ. 1991. At the crossroads of chemistry and immunology: catalytic antibodies. Science **252**: 659–667.
2. JACOBS, J. W. & P. SCHULTZ. 1987. Catalytic antibodies. J. Am. Chem. Soc. **109**(7): 2174–2176.
3. TAWFIK, D. S., R. R. ZEMEL, R. ARAD-YELLIN, B. S. GREEN & Z. ESHHAR. 1990. Simple method for selecting catalytic monoclonal antibodies that exhibit turnover and specificity. Biochemistry **29**: 9916–9921.
4. GALLACHER, G., C. S. JACKSON & K. BROCKLEHURST. 1991. A polyclonal antibody preparation with Michaelian catalytic properties. Biochem. J. **279**: 871–881.

Preparation of Bifunctional Enzyme with Both Superoxide Dismutase and Glutathione Peroxidase Activities by Using Chemical Mutation[a]

GUIMIN LUO, WEIHUA LIU, QIAN SUN, LAN DING,
ZHENQI ZHU, GANGLIN YAN, AND TONGSHU YANG

National Laboratory of Enzyme Engineering
Jilin University
Changchun 130023, People's Republic of China

INTRODUCTION

Superoxide dismutase (SOD) has an important value in medicine, but H_2O_2 is produced when SOD dismutates superoxide anion ($O_2^{\cdot-}$). Recent studies have shown that H_2O_2 not only inhibits SOD activity,[1] but also damages its structure, resulting in its irreversible inactivation.[2] Moreover, H_2O_2 can be converted into hydroxyl free radical ($OH^{\cdot}$), which is more toxic to the organism, by way of the Fenton reaction.[3] Therefore, if the cumulated H_2O_2 could not be removed timely, SOD could not catalyze effectively and greater toxicity could be generated. In order to solve the problem, the Poznansky group[4] cross-linked SOD with catalase, which can scavenge H_2O_2, but the hybrid enzyme was not homogeneous and its molecular weight became high. Poznansky proposed that the molecular heterogeneity should be overcome by using gene fusion technology. However, the gene fusion technology is operatively complex and poor membrane permeability resulting from the high molecular weight still exists.

We proposed that glutathione peroxidase (GPX) activity, which scavenges H_2O_2, could be incorporated into the SOD molecule. There are 14 Ser residues in two subunits of SOD from pig blood.[5] The Ser can be converted into selenocysteine (SeCys),[6] which is the catalytic group of GPX.[7] Therefore, it is possible to prepare the bifunctional enzyme with both SOD and GPX activities. Because Ser residues are not essential for SOD catalysis, the SOD activity should not be changed greatly by the chemical mutation of serines. The molecular weight of mutated SOD should not be increased, and mutated SOD also has GPX activity, so it can scavenge active oxygen more effectively and prevent and cure various diseases caused by H_2O_2 and active oxygen: inflammation, cataract, and the diseases in heart, blood vessel, and brain.

MATERIALS AND METHODS

Chemicals

Cu,Zn-SOD from pig blood was purchased from Shichuan Biotechnology Development Company. Pyrogallol was a product from E. Merck. Reduced coenzyme II (NADPH) and phenyl methyl sulfonic fluoride (PMSF) were purchased from Sigma. Glutathione reductase was a product of Boehringer Mannheim. Bovine serum albumin (BSA) was a product of the Institute of Biochemistry, Academia Sinica. All other chemicals were of analytical grade.

Methods

Activity Determination for SOD and GPX

SOD activity was determined by using a modification of the reported method.[8] One unit of SOD activity was defined as the amount of enzyme required for the inhibition of auto-oxidation of pyrogallol by 50% under the assay conditions. GPX activity was determined according to reference 9. One unit of GPX activity was defined as the amount of enzyme required for oxidation of 1 μmol NADPH per minute at 37 °C.

Protein Assay

Protein concentration was determined by the Bradford method using BSA as a standard.[10]

Sulfhydryl (SH) and Selenosulfhydryl (SeH) Determination

SH and SeH amounts were determined by the DTNB method,[11] by amino acid analysis, and by the X-ray photoelectron energy spectrum.

Preparation of Bifunctional Enzyme

The Ser residues in SOD were activated by PMSF and then treated with H_2Se, resulting in the conversion of Ser into SeCys.[6] Three mg of SOD was dissolved in 0.05 mol/L (pH 7) phosphate buffer solution (PBS) containing 0.15 mol/L NaCl; then, 10 μL of PMSF (5 mg/mL in acetonitrile) was added and allowed to react for 1 h at room temperature; and the reaction mixture was saturated with H_2Se under protection of highly purified nitrogen. Finally, the mixture was incubated for 36 h at 40 °C and then centrifuged, dialyzed, and freeze-dried.
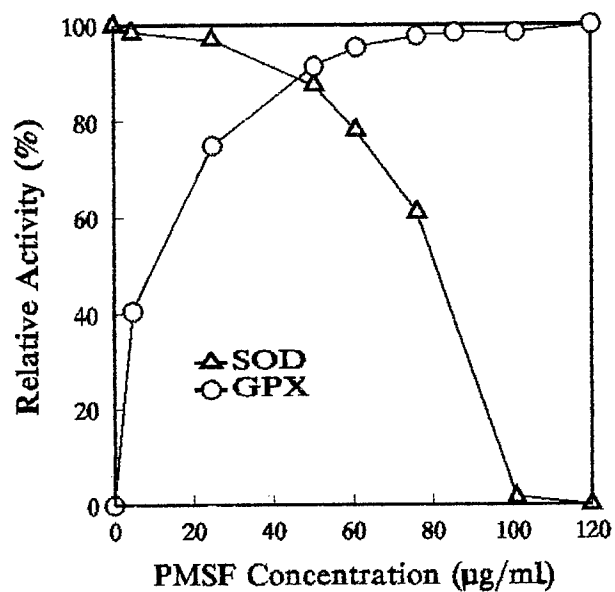
FIGURE 1. Effect of the concentration of PMSF on SOD and GPX activities of chemically mutated SOD. The concentration of SOD is 3 mg/mL.
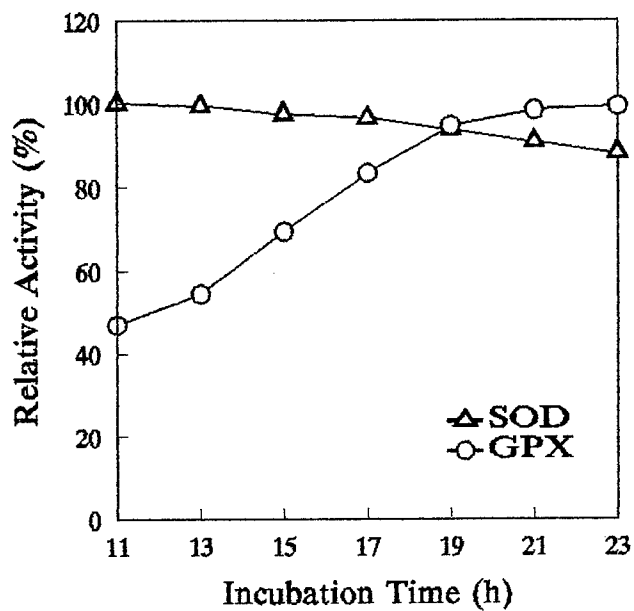
FIGURE 2. Effect of incubation time on SOD and GPX activities of chemically mutated SOD. The concentration of SOD is 3 mg/mL.
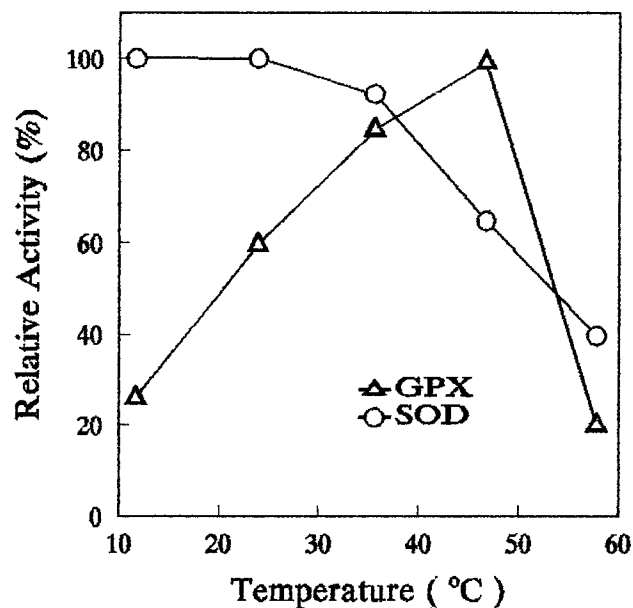
FIGURE 3. Effect of incubation temperature on SOD and GPX activities of chemically mutated SOD. The concentration of SOD is 3 mg/mL.

RESULTS AND DISCUSSION

Selection of Optimum Conditions for Preparing Bifunctional Enzyme

PMSF Amount Used

When other conditions were kept constant (pH 7.0, 40 °C, 36 h for H_2Se action) and only the PMSF amount used was changed, we obtained the results shown in FIGURE 1. When 50 µg/mL of PMSF was used, the mutated SOD retained up to more than 90% of its original SOD activity and possessed higher GPX activity.

Optimum Time of H_2Se Action

When other conditions were kept constant (pH 7.0, 50 µg/mL of PMSF, 40 °C) and only the time of H_2Se action was changed, we obtained the results shown in FIGURE 2. The optimum time of H_2Se action was obviously 20 h.

TABLE 1. Activities of the Mutated SOD

Sample	Activity of SOD (u/µmol)	Activity of GPX (u/µmol)
PZ51	0	0.99
SOD	6.94×10^5	0
mutated SOD	6.38×10^5	29

TABLE 2. K_m Comparison between the Bifunctional Enzyme and Native GPX

Enzyme	K_m (GSH) (mol/L)	K_m (H$_2$O$_2$) (mol/L)
bifunctional enzyme	3.7×10^{-4}	2.9×10^{-4}
native GPX	3.0×10^{-3}	1.0×10^{-5}

Optimum Temperature for H$_2$Se Action

When other conditions were kept constant (pH 7.0, 50 μg/mL of PMSF, 23 h) and only the temperature of H$_2$Se action was changed, we obtained the results shown in FIGURE 3. Obviously, 40 °C is optimum.

Activities of the Bifunctional Enzyme

The activities of the bifunctional enzyme obtained by using the optimum conditions mentioned above are shown in TABLE 1, in which PZ51 is the best GPX mimic known in the world and can treat many diseases resulting from active oxygen.[12] TABLE 1 shows that the mutated SOD retained 92% of its original SOD activity, and its GPX activity was 30 times greater than that of PZ51.

Properties of the Bifunctional Enzyme

Determination of Se Amount

The Se-3d binding energies of SeCys and the bifunctional enzyme were determined by the X-ray photoelectron spectrum using Al$_{k\alpha}$ as the target. The ratio of Se/N was experimentally determined to be 6.5/93.5 and the average N content in proteins was 16%, so the Se content of the bifunctional enzyme was calculated to be 4.5 mol Se/mol enzyme.

It was seen from amino acid analysis that the decrease of Ser residue number in native SOD was consistent with the increase of Cys in mutated SOD, indicating that the SeCys peak resulting from Ser overlapped the Cys peak in the amino acid elution diagram. Therefore, it was calculated that four Ser were converted into SeCys. The SH contents of the mutated and native SOD were determined by DTNB. Their difference should be the number of SeCys emerged, which was found to be six.

TABLE 3. Storage Stabilities of the Bifunctional Enzyme

Sample	Storage Conditions	Duration (months)	Relative Activity (%)	
			SOD	GPX
lyophilized powder	−20 °C	1	96	90
lyophilized powder	−20 °C	5	94	85
in solution[a]	4 °C	1	88	0
in solution[a]	4 °C	5	72	0

[a]Three mg of enzyme was dissolved in 0.05 M PBS (pH 7.0) containing 0.15 M NaCl.

TABLE 4. Storage Stabilities of the Bifunctional Enzyme

Sample[a]	Storage Conditions	Duration (days)	Relative Activity of GPX (%)
in solution	4 °C	1	90
in solution	4 °C	2	82
in solution	4 °C	3	75
in solution	4 °C	5	53

[a]Three mg of enzyme was dissolved in 0.05 M PBS (pH 7.0) containing 0.15 M NaCl.

Kinetic Behavior of the Bifunctional Enzyme

GPX has two substrates (GSH and H_2O_2). The concentration of one of them was fixed and the other was changed. The apparent K_m for each substrate should be obtained by a Lineweaver-Burk plot. The K_m comparison between bifunctional enzyme and native GPX is shown in TABLE 2.

It was shown from the K_m comparison that the affinity of bifunctional enzyme for GSH was greater than that of native GPX, but for H_2O_2 it was smaller.

Stabilities of the Bifunctional Enzyme

The stabilities of the bifunctional enzyme in solution and in the form of freeze-dried powder were also determined. The results are shown in TABLES 3 and 4.

It was shown from TABLES 3 and 4 that both the SOD and GPX stabilities of the bifunctional enzyme in the form of lyophilized powder were good enough at −20 °C, but in the solution the stability of the GPX activity was poor.

CONCLUSIONS

The experimental results show that the bifunctional enzyme with both SOD and GPX activities can be obtained by using chemical mutation of SOD. So far, there is no report in the literature on the preparation of the bifunctional enzyme using chemical mutation. Thus, we have developed a new strategy for preparing the bifunctional enzyme.

REFERENCES

1. ASADA, K. *et al.* 1975. J. Biol. Chem. **250:** 2801–2807.
2. LI, P. F. & Y. Z. FANG. 1993. Chin. Biochem. J. **9**(4): 411–416.
3. GUTTERIDGE, J. M. C. *et al.* 1985. FEBS Lett. **185:** 19–23.
4. MAO, G. D. *et al.* 1993. J. Biol. Chem. **268**(1): 416–420.
5. SCHININA, M. E. *et al.* 1985. FEBS Lett. **186:** 267–270.
6. WU, Z. P. *et al.* 1989. J. Am. Chem. Soc. **111:** 4513–4514.
7. FORSTROM, J. W. *et al.* 1978. Biochemistry **17:** 2639–2644.
8. LUO, G. M. *et al.* 1987. Chem. Pharm. Bull. **35:** 4229–4234.
9. WENDEL, A. 1981. Methods Enzymol. **77:** 325–333.
10. BRADFORD, M. M. 1976. Anal. Biochem. **72:** 248–254.
11. ELLMAN, G. L. 1959. Arch. Biochem. Biophys. **82:** 70–77.
12. SIES, H. 1993. Free Radical Biol. Med. **14:** 313–323.

Control of the Catalytic Mechanism
of an Enzyme by Amino Acid Substitution

KEIICHI MORIMOTO,[a] RYOTA KUROKI,[b]
AND BRIAN W. MATTHEWS[c]

[a]Research and Development Division
Kirin Brewery Company, Limited
Tokyo 150, Japan

[b]Central Laboratories for Key Technology
Kirin Brewery Company, Limited
Yokohama 236, Japan

[c]Institute of Molecular Biology
Howard Hughes Medical Institute
and
Department of Physics
University of Oregon
Eugene, Oregon 97403

INTRODUCTION

The glycosidases are important enzymes for utilizing sugar molecules as biomass. The design and creation of an enzyme having a new function is an important extension in the potential use of an enzyme in industry. Although many approaches have been used to investigate the catalytic mechanism of glycosidases,[1,2] the alteration of the catalytic mechanism of such enzymes has not yet been achieved. In the present work, we chose T4 phage lysozyme as a model because it is one of the most thoroughly investigated glycosidases and large amounts of structural information are available.[3,4] Recently, we found an inactive mutant (Thr-26 to Glu) that reacted with the substrate and formed a covalent enzyme-substrate adduct.[5] Determination of the tertiary structure of this mutant indicated that the glutamate newly introduced into the T4 lysozyme reacted with the saccharide instead of the catalytic water molecule seen in the wild-type structure. It was also suggested that control of the catalytic mechanism of T4 lysozyme might be possible by the mutation of the residue, Thr-26. Here, we extend these results and describe the successful alteration of the catalytic mechanism of an enzyme by amino acid replacement.

MATERIALS AND METHODS

Preparation of Mutant T4 Lysozymes

Several substitutions at the position of Thr-26 (T26 D, Q, and H), which is located at the α-side of the saccharide, were constructed and purified by standard procedures reported previously.[6,7]

Enzymatic Analysis

The enzymatic activity of the wild-type and mutant T4 lysozyme was determined by halo plate assay as reported previously.[8] Determination of the anomeric form of the product was performed by using HPLC with a reversed-phase column (μ-Bondasphere C18, 3.9 × 150 mm). For the determination of the anomeric form of the product, the saccharide substrate including peptide was prepared.[9] The substrate was designed to have a peptide suitable for both T4 lysozyme and HEWL. The reducing end of the substrate was further reduced to open the sugar ring, so identification of the anomeric form of the product was made easier. The analysis of product was performed after 5-min digestion at 25 °C using this substrate.

TABLE 1. Enzymatic Activities and the Result of Product Analysis of the Wild-type and Mutant T4 Lysozymes

Lysozymes	Halo Activity[a]	Product[b]
wild type	+ + + + +	α-anomer
T26D	+	n.d.[c]
T26E	−	covalent adduct[d]
T26Q	−	n.d.
T26H	+ + + +	β-anomer

[a]The halo activity gives a rough estimation of the enzymatic activity of T4 lysozymes.
[b]Product analysis was performed by using reversed-phase HPLC. See text for details.
[c]n.d. = not determined.
[d]Covalent adduct was determined by mass spectrometry and X-ray crystallography as reported previously.[5]

X-ray Crystallography

The mutants T26D, T26Q, and T26H were crystallized isomorphously under the same conditions as those of the wild type.[3] The tertiary structures were determined by X-ray crystallography based on the wild-type structure. The mutant structures were refined below 17% using the TNT refinement package.[10]

RESULTS AND DISCUSSION

The enzymatic activities of the wild-type and mutant T4 lysozymes are summarized in TABLE 1. Although the mutants T26E and T26Q were completely inactivated, the mutant T26D retained low activity. The mutant T26H was quite active, although slightly less than the wild type. The product analysis of the wild-type and T26H mutant T4 lysozymes using the saccharide substrate with a peptide is also summarized in TABLE 1. Whereas wild-type T4 lysozyme produces the α-anomer, the T26H mutant produces the β-anomer efficiently. This indicates that the direction of the water attacking in the T26H mutant is different from that in the wild type. The T26E mutant produced a covalent enzyme-substrate adduct as reported previously.[5]

The mutants T26D, T26Q, and T26H were crystallized with a space group of P3$_2$21, which is isomorphous to the wild type.[3] All structures were determined at 2.0-Å resolution or higher using X-ray crystallography. From the structure superposition of these mutants on to the wild type[3] and the T26E mutant with a covalent saccharide adduct,[5] it was found that these mutants had lost the water molecule bound between Asp-20 and Thr-26 in the wild-type T4 lysozyme structure (FIGURE 1). It was also found that the OE1 atom of Gln-26 (T26Q) and the Nε atom of the His-26 (T26H) were located at essentially the same position as the catalytic water molecule in the wild-type structure and the OE1 atom in Glu-26 (T26E). This strongly suggests that Glu-26 and His-26 in the mutants can directly attack the saccharide from the α-side. The facts that (i) the wild-type lysozyme produces the α-anomer, whereas the T26H mutant produces the β-anomer and (ii) the Nε atom of His-26 is located at the same position as that of the catalytic water molecule indicate that the catalytic mechanism of the wild type is different from that of the T26H mutant lysozyme. The catalytic mechanism of the wild-type enzyme proceeds through a single displacement mechanism in which a water molecule directly attacks the C1 carbon of the saccharide, as shown in FIGURE 2a. The catalytic mechanism of the T26H mutant proceeds through a double displacement mechanism in which His-26 first reacts with the saccharide and then a water molecule attacks the covalent intermediate formed between histidine and saccharide, leading to the products (FIGURE 2b). In this mechanism, Glu-11 may act again as a base to activate the catalytic water molecule.

This appears to be the first example in which genetic engineering has been used to alter the catalytic mechanism of an enzyme. It was found that only a small perturbation of the active site of the T4 phage lysozyme was enough to control the
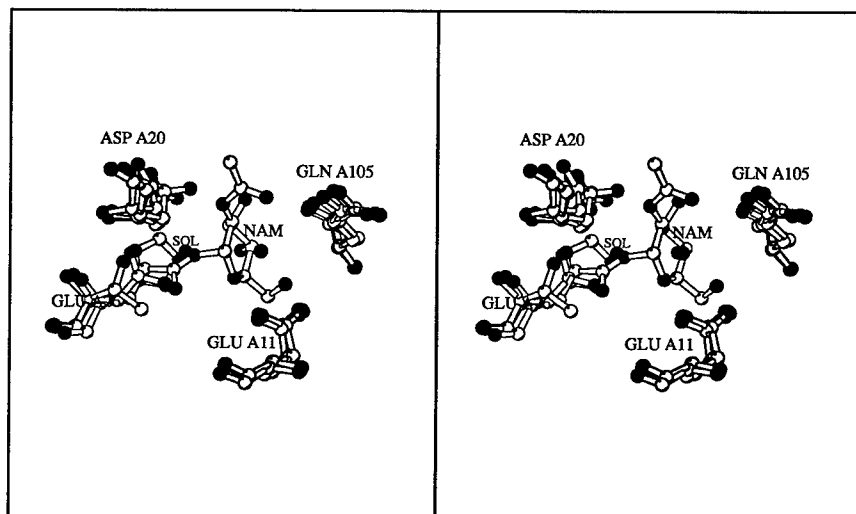
FIGURE 1. Superposition of the catalytic site residues of wild-type and mutant T4 lysozymes (T26D, T26E, and T26H). The saccharide is bound to the T26E mutant covalently.[5]
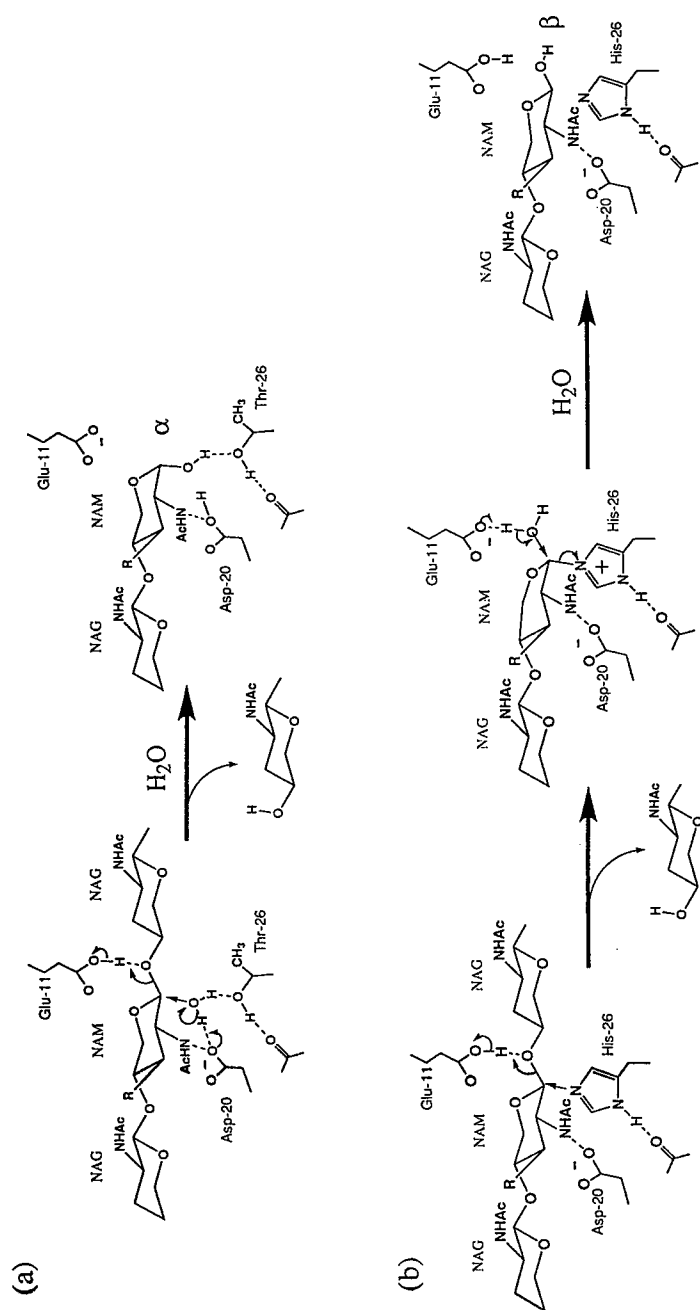
FIGURE 2. Proposed catalytic mechanism of the wild-type T4 lysozyme (a) and the T26H mutant lysozyme (b) based on final product analysis and tertiary structure analysis using X-ray crystallography.

catalytic mechanism with a predominant lytic activity. Although the active sites of the glycosidases have common features, several options of the catalytic residue at the α-side of the saccharide can be chosen for the hydrolysis of the saccharide chain. This variation may cause functional differences between the glycosidases and transglycosidases.

ACKNOWLEDGMENTS

We thank Larry H. Weaver for useful suggestions and technical assistance. We also thank Sheila Snow and Joan Wozniak for technical assistance.

REFERENCES

1. SINNOTT, M. L. 1990. Chem. Rev. **90:** 1171–1202.
2. SVENSSON, B. & M. SØGAARD. 1993. J. Biotechnol. **29:** 1–37.
3. WEAVER, L. H. & B. W. MATTHEWS. 1987. J. Mol. Biol. **193:** 189–199.
4. MATTHEWS, B. W. 1993. Annu. Rev. Biochem. **62:** 139–160.
5. KUROKI, R., L. H. WEAVER & B. W. MATTHEWS. 1993. Science **262:** 2030–2033.
6. MUCHMORE, D. C., L. P. MCINTOSH, C. B. RUSSEL, D. E. ANDERSON & F. W. DAHLQUIST. 1989. Methods Enzymol. **177:** 44–73.
7. POTEETE, A. R., S. DAO-PIN, H. NICHOLSON & B. W. MATTHEWS. 1991. Biochemistry **30:** 1425–1432.
8. STREISINGER, G., F. MUKAI, W. J. DREYER, B. MILLER & S. HORIUCHI. 1961. Cold Spring Harbor Symp. Quant. Biol. **26:** 25–30.
9. GLAUNER, B. 1988. Anal. Biochem. **172:** 451–464.
10. TRONRUD, D. E., L. F. TEN EYCK & B. W. MATTHEWS. 1987. Acta Crystallogr. **A43:** 489–503.

An Engineered Penicillin Acylase with Altered Surface Charge Is More Stable in Alkaline pH

GABRIEL DEL RÍO, AGUSTÍN LÓPEZ-MUNGUÍA,
AND XAVIER SOBERÓN

Instituto de Biotecnología
Universidad Nacional Autonoma de Mexico
Cuernavaca, Morelos 62271, Mexico

Protein engineering could be used for studying proteins and improving their attributes in many ways. One area where natural proteins are likely to be suboptimal for biocatalytic applications is pH optimum and pH-dependent instability. A general principle relates the surface charge of a protein with its isoelectric point (IP)[1] and it has been observed that proteins tend to be most stable near their IP.[2] The biocatalyst based on penicillin acylase, widely utilized for the production of semisynthetic penicillins, displays a diminished half-life at alkaline pH,[3] in a process that requires the constant addition of base in order to neutralize acid formed during the reaction.[4] Based on the amino acid sequence of *E. coli* penicillin acylase (PAC), we have utilized predictive methods to identify segments of the polypeptide potentially exposed at the surface and have targeted them for an oligonucleotide-directed mutagenesis regime that would cause an increase in the positively charged residues at those areas. The mutant library was screened by a filter assay to score bacterial colonies expressing PAC with enhanced half-life at alkaline pH. One sequenced mutant, in the large subunit, was shown to be a Trp for Arg replacement at position 431 (W431R) and it displayed a half-life twice as long at pH 8.5.[5] With the recently published crystallographic structure of PAC,[6] we can now understand the behavior of this mutant and can approach in a more rational way the design of new ones.

METHODS

The crystallographic coordinates of PAC were kindly provided by Peter Moody. For visual analysis, we employed Insight II Ver. 2.3 (Biosym Technologies); for electrostatic calculations, we employed DELPHI Ver. 2.0.

In order to represent the electrostatic potential on the surface of PAC, we used the focusing option in DELPHI. Three focusing calculations were carried out for each subunit and the dimer. The dielectric values for solvent and solute used were 80.0 and 2.0, respectively. The potential employed was from Amber,[7] and hydrogen atoms were added at pH 7.5 with an ionic strength of 0.145.
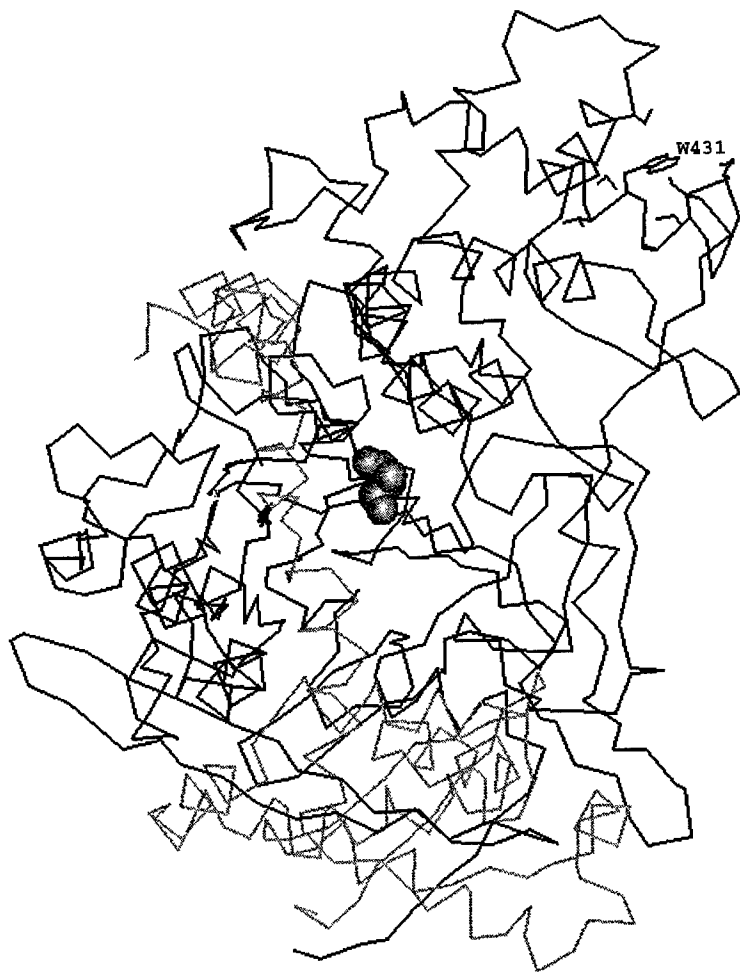
FIGURE 1. Penicillin acylase structure. The side chain of the amino acid residue mutated is shown. The catalytic serine is represented as a CPK model. The alpha-carbon tracings of the large and small subunits are shown in black and gray lines, respectively.

RESULTS AND DISCUSSION

An analysis of the surface charge of PAC reveals an overall negatively charged protein. Mature PAC is composed of two polypeptide chains as a result of proteolytic digestion of a connecting peptide;[8] both chains have a dominant negative charge on their surface. The interface between the large and the small subunits is extensive, and about 20% of this area comprises hydrophilic amino acids. Upon inspection of the electrostatic potential calculated with DELPHI, charge complementarity can be inferred in just a few places, with positively charged side chains on the small subunit

and extensive negatively charged ones on the large subunit. This charge distribution is consistent with the dependence of PAC refolding on pH, where productive yields occur only between pH 4 and 7. Lindsay and Pain[9] proposed that the pH dependence of assembly arises from a pH dependence of folding on the large subunit rather than association. The charge distribution observed is also consistent with the pH stability of the enzyme because its half-life is longer at acidic values of pH than at alkaline ones. A complementarity is frequently seen in electrostatic potential at intermolecular interfaces,[10] as the attractive forces would drive the molecular recognition events. It would be expected that PAC, devoid of such complementarity, requires a tighter interaction from other sources, mainly hydrophobic.[11]

Replacement W431R, which we recovered from a mutagenesis experiment targeted at the predicted surface of the protein, indeed turned out to be exposed at the end of an alpha-helix. Its location relative to the active site and the subunit interface is depicted in FIGURE 1. An Arg residue would be accommodated without trouble in place of the original Trp, with its guanidinium group fully exposed to the solvent, protruding from a neutral patch. The electrostatic potential perturbation, calculated with DELPHI, suggests that the stabilizing effect could involve an intrinsic stabilization of the large subunit at alkaline pH values rather than a tightening of the subunit association. The fact that the mutation is also relatively far away from the active site (32 angstroms) is consistent with our finding that the catalytic parameters of the mutant enzyme are very close to those of the wild-type enzyme.[5]

CONCLUSIONS

Our results confirm the expectation that engineering surface charge can affect the stability of an enzyme at specific pH conditions. The electrostatic calculations are consistent with the pH stability observed for this enzyme and it should be feasible to rationalize other experiments aimed at stabilizing this enzyme. The methods applied are sufficiently general for their consideration in other systems. Using the same procedures, we have isolated a second PAC mutant with enhanced stability at both acidic and alkaline pH. Its characterization should further improve our understanding of electrostatically dependent enzyme stability.

REFERENCES

1. RUSSELL, A. J. & A. R. FERSHT. 1987. Rational modification of enzyme catalysis by engineering surface charge. Nature **328:** 496–500.
2. DILL, K. A. 1990. Dominant forces in protein folding. Biochemistry **29:** 7133–7155.
3. OSPINA, S., A. LÓPEZ-MUNGUÍA, R. GONZALEZ & R. QUINTERO. 1992. Characterization and use of a penicillin acylase biocatalyst. J. Chem. Technol. Biotechnol. **53:** 205–214.
4. SHEWALE, J. G. & H. SIVARAMAN. 1987. Penicillin acylase: enzyme production and its applications in the manufacture of 6-APA. Process Biochem. **August:** 146–154.
5. DEL RÍO, G., M. A. RODRIGUEZ, M. A. MUNGUÍA, A. LÓPEZ-MUNGUÍA & X. SOBERÓN. 1995. Mutant *E. coli* penicillin acylase with enhanced stability at alkaline pH. Biotechnol. Bioeng. **48:** 141–148.
6. DUGGLEBY, H. J., S. P. TOLLEY, CH. P. HILL, E. J. DODSON, G. DODSON & P. C. E. MOODY. 1995. Penicillin acylase has a single-amino-acid catalytic center. Nature **373:** 264–268.

7. WEINER, S. J., P. A. KOLLMAN, D. A. CASE, U. C. SINGH, C. GHIO, G. ALAGONA, S. PROFETA, JR. & P. WEINER. 1984. A new force field for molecular mechanical simulation of nucleic acids and proteins. J. Am. Chem. Soc. **106:** 765–784.

8. SIZMANN, D., C. KEILMANN & A. BÖCK. 1990. Primary structure requirements for the maturation *in vivo* of penicillin acylase from *Escherichia coli* ATCC 11105. Eur. J. Biochem. **192:** 143–151.

9. LINDSAY, C. D. & R. H. PAIN. 1991. Refolding and assembly of penicillin acylase, an enzyme composed of two polypeptide chains that result from proteolytic activation. Biochemistry **30:** 9034–9040.

10. HONIG, B. & A. NICHOLLS. 1995. Classical electrostatics in biology and chemistry. Science **268:** 1144–1149.

11. LINDSAY, C. D. & R. H. PAIN. 1990. The folding and solution conformation of penicillin G acylase. Eur. J. Biochem. **192:** 133–141.

Modification of Alpha-Amylase Functions by Protein Engineering

MASAAKI TERASHIMA AND SHIGEO KATOH

Department of Synthetic Chemistry and Biological Chemistry
Kyoto University
Kyoto 606-01, Japan

INTRODUCTION

Modifications of enzyme functions by means of protein engineering are one of the objectives of new biotechnology. Although a few remarkable examples have been reported, the design principles for the enzyme modifications have not been established yet. Alpha-amylases, one of the most important enzyme types in industry, are excellent model enzymes to study the relationships between protein structures and reaction characteristics for the following reasons: (1) tertiary structures of the α-amylase family are well preserved regardless of their origin; (2) isozymes show a wide variety of reaction characteristics, despite their homologous structure; (3) the basic structure classified as (β/α) barrel structure is a common structure of typical enzymes.[1] Therefore, enzyme functions can be modified by a subtle change in the tertiary structure, and the principle obtained in α-amylase may be applicable to other enzymes.

Among the rice α-amylase family, two major isozymes, Amy1A and Amy3D, show distinct characteristics in thermostability, pH optimum, hydrolysis efficiencies in soluble starch, and oligosaccharide degradation in spite of their high homology in amino acid sequences.[2] One significant difference in their protein structures is that only Amy1A has an N-linked carbohydrate chain in the mature protein. Thus, a mutant enzyme ([N240Q]Amy1A) was created by site-directed mutagenesis to study the functional roles of the N-linked carbohydrate chain of Amy1A.[3] In this construction, an N-glycosylation site of Amy1A NGT was modified to QGT. Furthermore, a chimera enzyme (Amy1A/3D), which has 158 amino acid residues of the Amy1A N-terminus and 252 amino acid residues of the Amy3D C-terminus, was created to modify the characteristics of Amy1A.[4] Characteristics of these modified enzymes and effects of structural changes on the enzyme characteristics will be discussed in this article.

MATERIALS AND METHODS

Two cDNA clones of rice α-amylase isozymes Amy1A and Amy3D were kind gifts from R. Rodriguez (University of California, Davis). The construction and the protocol of a mutant gene (*[N240Q]Amy1A*) and a chimera gene (*Amy1A/3D*) were described elsewhere.[3,4] Enzymes, secreted into culture media from *Saccharomyces cerevisiae*, were purified with immunoaffinity chromatography using cross-reactive
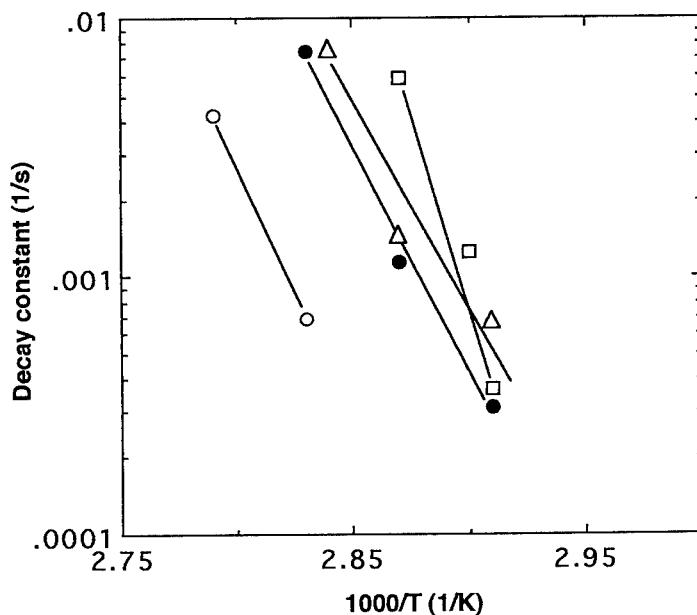
FIGURE 1. Temperature dependence of the first-order decay constant in heat inactivation: (○) Amy1A, (●) [N240Q]Amy1A, (□) Amy3D, and (△) Amy1A/3D.

antibarley α-amylase antibody or anti-C-terminal peptide antibody.[5-7] The purity of the enzymes was assayed by SDS-PAGE with silver staining.

The activities against soluble starch were determined by measuring the increase of the reducing ends formed by enzyme reactions. Maltose was used as a standard. One unit of activity was defined as the amount of enzyme required to liberate 1 μmol of maltose per minute.

The thermostabilities of the enzymes were determined by measuring the remaining activity against the soluble starch at 30 °C after treating the enzymes at predetermined temperatures for various time periods. First-order decay constants for heat inactivation were calculated from the slopes of the remaining activities versus treated time.[3]

The reactivities of the enzymes to oligosaccharide were determined with an HPLC system.[2] The enzyme reaction was initiated by adding 20 μL of enzyme solution to 180 μL of substrate solution at 30 °C, pH 5.0. At a predetermined time, 10 μL of the reaction mixture was injected to HPLC to determine the concentrations of the remaining substrate. One unit of the activity for maltoheptaose degradation was defined as the amount of enzyme required to degrade 1 μmol of maltoheptaose per minute.

RESULTS AND DISCUSSION

Temperature dependence of the first-order decay constants in heat inactivation is shown in FIGURE 1. Amy1A showed the highest thermostability among all the

enzymes. Because [N240Q]Amy1A showed almost identical thermostability to those of Amy3D and Amy1A/3D, the N-linked carbohydrate chain might have significant effects on the thermostability. It should also be noted that Amy3D and Amy1A/3D do not have the N-linked carbohydrate chain.

Temperature dependence of K_m and V_m, the kinetic parameters of the Michaelis-Menten equation, in soluble starch hydrolysis was determined by Lineweaver-Burk plots (FIGURES 2 and 3). The values of K_m and V_m for the genetically engineered enzymes, [N240Q]Amy1A and Amy1A/3D, were not significantly different from those for the wild-type enzymes, Amy1A and Amy3D, indicating that the tertiary structures of the genetically engineered enzymes were not drastically changed by these mutations. The K_m of Amy1A showed a strong temperature dependence (FIGURE 2), while those of other enzymes were constant in this temperature range. The values of V_m were in the order of Amy1A, Amy1A/3D, [N240Q]Amy1A, and Amy3D, as shown in FIGURE 3. From the comparisons of amino acid sequences between Amy1A and a barley α-amylase AMY2, the tertiary structure of Amy1A is almost identical to that of AMY2.[8] It was suggested from the AMY2 tertiary structure that the N-carbohydrate chain of Amy1A is likely attached to the protein surface close to the active cleft of the enzyme. Therefore, a direct interaction between the N-linked carbohydrate chain and the substrate (soluble starch) could cause a strong temperature dependence of the K_m, and the single amino acid
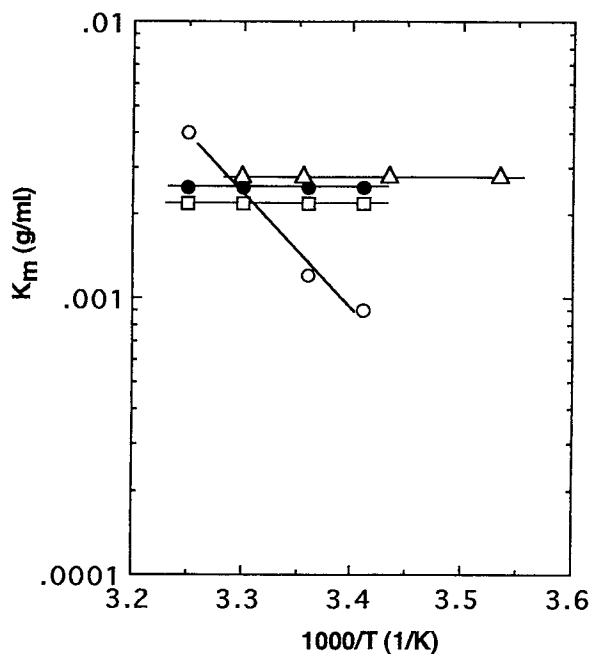
FIGURE 2. Temperature dependence of K_m for soluble starch degradation: (O) Amy1A, (●) [N240Q]Amy1A, (□) Amy3D, and (△) Amy1A/3D.
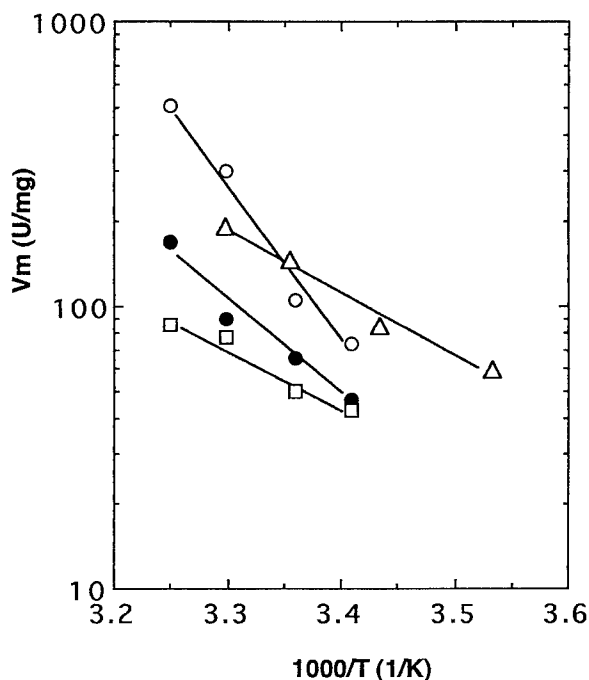
FIGURE 3. Temperature dependence of V_m for soluble starch degradation: (O) Amy1A, (●) [N240Q]Amy1A, (□) Amy3D, and (△) Amy1A/3D.

substitution from N to Q will cause a drastic change in the temperature dependence of K_m in [N240Q]Amy1A.

The specific activities in maltoheptaose hydrolysis of Amy1A, Amy3D, and Amy1A/3D are compared in TABLE 1. Amy3D and Amy1A/3D showed much higher activities than that of Amy1A. Because most of the amino acid residues of the active cleft are the same in Amy3D and Amy1A/3D, the tertiary structures of the active clefts might be adapted for the efficient oligosaccharide degradation. It should also be noted that Amy1A/3D showed higher activities in soluble starch hydrolysis (FIGURE 3). This may be due to the rigid structure in the N-terminal region derived from that of Amy1A. Three calcium-binding sites found in AMY2 are completely reserved in Amy1A, and the calcium binding helps to maintain the rigid active-site structure for efficient soluble starch hydrolysis.[9]

TABLE 1. Specific Activities of Enzymes in Maltoheptaose Degradation[a]

Enzyme	Activities (U/mg)
Amy1A	1.21
Amy3D	53.5
Amy1A/3D	42.0

[a]Specific activities of Amy1A, Amy3D, and Amy1A/3D were determined at 30 °C. Data taken from reference 4.

The present work has shown that the N-linked carbohydrate chain of rice α-amylase, positioned near the active cleft, has significant effects on thermostability and substrate recognition. The results on the chimera enzyme have shown that the suitable protein modules of highly homologous enzymes are interchangeable, and the preparation of chimera enzymes is one of the effective methods to create new enzymes with unique characteristics.

REFERENCES

1. FARBER, G. K. & G. A. PETSKO. 1990. The evolution of α/β barrel enzymes. Trends Biochem. Sci. 15(6): 228–234.
2. TERASHIMA, M., S. KATOH, B. R. THOMAS & R. L. RODRIGUEZ. 1995. Characterization of rice α-amylase isozymes expressed by Saccharomyces cerevisiae. Appl. Microbiol. Biotechnol. 43(6): 1050–1055.
3. TERASHIMA, M., A. KUBO, M. SUZAWA, Y. ITOH & S. KATOH. 1994. The roles of the N-linked carbohydrate chain of rice α-amylase in thermostability and enzyme kinetics. Eur. J. Biochem. 226(1): 249–254.
4. TERASHIMA, M., M. KAWAI, M. H. KUMAGAI, R. L. RODRIGUEZ & S. KATOH. 1995. Characteristics of a chimera enzyme engineered from two rice α-amylase isozymes. Appl. Microbiol. Biotechnol. In press.
5. KUMAGAI, M. H., M. SHAW, M. TERASHIMA, Z. VRKLJAN, J. R. WHITAKER & R. L. RODRIGUEZ. 1990. Expression and secretion of rice α-amylase by Saccharomyces cerevisiae. Gene 94: 209–216.
6. KATOH, S. & M. TERASHIMA. 1994. Purification of secreted α-amylases by immunoaffinity chromatography with cross-reactive antibody. Appl. Microbiol. Biotechnol. 42(1): 36–39.
7. KATOH, S., M. TERASHIMA & M. KOUNO. 1995. Purification of recombinant α-amylase by immunoaffinity chromatography with anti-peptide antibody. Appl. Microbiol. Biotechnol. 43(5): 871–876.
8. KADZIOLA, A., J. ABE, B. SVENSSON & R. HASER. 1994. Crystal and molecular structure of barley α-amylase. J. Mol. Biol. 239: 104–121.
9. BUSH, D. S., L. STICHER, R. HUYSTEE, D. WAGNER & R. L. JONES. 1989. The calcium requirements and enzymatic activity of two isoforms of barley aleurone α-amylase. J. Biol. Chem. 264(32): 19392–19398.

Site-directed Mutagenesis of Cysteinyl Residues in Aspartase of *Escherichia coli*

HSIU-HUI CHEN,[a] JIN-TANN CHEN,[b] AND HSIN TSAI[a,b]

aDepartment of Agricultural Chemistry
National Taiwan University
Taipei, Taiwan, Republic of China

bDevelopment Center for Biotechnology
Taipei, Taiwan, Republic of China

INTRODUCTION

Aspartase (L-aspartate ammonia-lyase, EC 4.3.1.1) catalyzes the reversible conversion of fumarate and ammonia to L-aspartate, and the reaction favors amination. The enzyme has been used as a biocatalyst for industrial production of L-aspartic acid.

The enzyme is composed of four identical subunits[1] and each subunit contains 11 cysteine residues.[2] Chemical modification studies showed that one of the cysteine residues of the enzyme was essential for catalytic activity.[3] Fluorescence-labeling studies further indicated that Cys^{140} or Cys^{430} might be involved in the catalytic reaction.[4]

One of the disadvantages of chemical modification is that the bulky chemical groups covalently attached to the amino acid side chains in the active site may block substrate binding, resulting in the loss of enzyme activity. Consequently, information of specific amino acid residues being involved in catalysis cannot be obtained. With site-directed mutagenesis, one can replace the specific amino acid residue with the desired one, and the catalytic function of the residue can be studied unequivocally.

We have cloned, sequenced, and expressed the aspartase gene (*asp*A) of *E. coli* B.[5] The high-level expression system enables us to obtain significant quantities of the wild-type and mutant enzymes for studying the structure-function relationships of aspartase.

Serine and cysteine have similar chemical structures, but their chemical properties are quite different. To study the functional role of the cysteine residues of aspartase, we have substituted each of the 11 cysteine residues with serine by site-directed mutagenesis.

MATERIALS AND METHODS

Synthetic Oligonucleotides

The mutagenic oligonucleotides made by Quality Systems (Taipei, Taiwan) were synthesized by phosphoramidite chemistry. Their sequences are shown in TABLE 1.

Mutation of aspA

The wild-type aspartase gene was subcloned into M13 bacteriophage RF DNA. The point mutation was introduced to the gene according to the method of Kunkel.[6] The mutant genes were screened and confirmed by DNA sequence analysis using Sanger's dideoxy-chain-termination method.[7]

TABLE 1. Oligonucleotides Used in Site-directed Mutagenesis

Oligonucleotide	Sequence (5′ → 3′)[a]
Ser-79	TTGCCGCAT*C̅TGATGAAGTCC[b]
Ser-88	AACGGAAAAT*C̅CATGGATCAG[b]
Ser-140	AACAAAT*C̅TCAGTCCACTAACGACGC*G̅TACCCG[b] _Mlu_ I
Ser-260	GGCTTCCCAT*C̅CGTACCGGCTG[b]
Ser-273	AGCGCCGG*A̅GTCAGAGGTCGC[c]
Ser-294	CCAAAATCT*C̅TAACGACCTGC[b]
Ser-339	TTTGAAG*G̅ATACCTGGTTAAC[c]
Ser-382	GCAGGTTGT*A̅GGAAGGGTTGG[c]
Ser-389	GATGCCGTTG[A*T̅GG*A̅T]TTTTCCAG[c] _Nsi_ I
Ser-400	GTAACCTTCG*G̅ACACTTCTTT[c]
Ser-430	ACCGGTTT*C̅CGC*G̅*G̅AGATTTTACC[c] _Sac_ II

[a]The asterisks mark the mismatched bases. The restriction sites (*Mlu* I and *Sac* II) created by mutation are underlined. The *Nsi* I site destroyed by mutation is boxed.
[b]The sequences are in the forward direction.
[c]The sequences are in the reverse direction.

Purification and Activity Assay of Aspartases

The wild-type and mutant aspartases were purified by aqueous two-phase extraction and ion exchange chromatography. The detailed procedures will be published elsewhere. The enzyme activity in the deamination reaction was measured spectrophotometrically by monitoring the increase in absorbance at 240 nm. Protein

concentration was determined by the method of Bradford.[8] The k_{cat} and K_m values were determined by the Lineweaver-Burk plot.

RESULTS

High Expression of aspA

The wild-type and mutant aspartase genes were subcloned into the pLB vector so that these genes were under the control of the PL promoter. All the genes cloned can be highly expressed in *E. coli* N4830. The cellular content of aspartase can reach to about 40% of total soluble proteins.

TABLE 2. Comparison of the Kinetic Parameters of Wild-type and Mutant Aspartases

Aspartase	k_{cat} (s^{-1})	k_{cat}/K_m (s^{-1}·M^{-1})	K_m (M)
wild-type	104	5.37×10^4	1.94×10^{-3}
Ser^{79}	103	5.00×10^4	2.06×10^{-3}
Ser^{88}	132	4.37×10^4	3.02×10^{-3}
Ser^{140}	90.9	3.61×10^4	2.52×10^{-3}
Ser^{260}	85.5	4.52×10^4	1.89×10^{-3}
Ser^{273}	99.3	2.71×10^4	3.67×10^{-3}
Ser^{294}	113	4.00×10^4	2.81×10^{-3}
Ser^{339}	76.3	3.25×10^4	2.35×10^{-3}
Ser^{382}	101	4.59×10^4	2.20×10^{-3}
Ser^{389}	72.4	3.13×10^4	2.31×10^{-3}
Ser^{400}	111	4.85×10^4	2.29×10^{-3}
Ser^{430}	107	4.23×10^4	2.53×10^{-3}

Kinetic Parameters for Aspartases

The activities of the purified wild-type and mutant aspartases were studied in the direction of L-aspartate deamination. The Lineweaver-Burk plot was used to obtain kinetic parameters. The k_{cat} and K_m values for the wild-type and mutant enzymes are shown in TABLE 2. All the mutant enzymes have essentially the same k_{cat} and K_m values as the wild-type enzyme.

DISCUSSION

The bell-shaped pH profile of aspartase activity[9] may be taken to indicate the presence of two functional groups on the enzyme, whose protonation states are critical to the reversible amination reaction. Chemical modification studies showed that the cysteine and histidine residues were essential for aspartase activity.[3,4,10] Genetic alteration of conserved amino acids of the fumarase-aspartase family showed that Cys^{389} and His^{123} had no significant effect on the activity of *E. coli*

aspartase, but Lys[326] appeared to be involved in substrate binding.[11] Recently, the X-ray crystallographic study of fumarase C of *E. coli* indicated that His[188] is probably located in the active site and may be involved in substrate binding.[12] Therefore, it is interesting to study whether the corresponding histidine residue in aspartase has similar function. As regards cysteine residues, we used site-directed mutagenesis and kinetic analysis to study whether any of them is involved in catalytic reaction.

The chemical properties of the sulfhydryl group of cysteine are different from those of the hydroxyl group of serine. The nucleophilicity of the former is known to be much better. The pK_a value of the sulfhydryl group is about 8.3, whereas that of the hydroxyl group is greater than 18. If cysteine is essential for catalysis, the replacement of Cys by Ser will affect the kinetic properties of aspartase. The fact that the kinetic parameters for Cys-to-Ser mutant aspartases are virtually the same as those for the wild-type enzyme (TABLE 2) indicates that none of the cysteine residues is essential for catalytic function.

REFERENCES

1. WATANABE, Y., M. IWAKURA, M. TOKUSHIGE & G. EGUCHI. 1981. Biochim. Biophys. Acta **661:** 261–266.
2. TAKAGI, J. S., N. IDA, M. TOKUSHIGE, H. SAKAMOTO & Y. SHIMURA. 1985. Nucleic Acids Res. **13:** 2063–2074.
3. MIZUTA, K. & M. TOKUSHIGE. 1975. Biochim. Biophys. Acta **403:** 221–231.
4. IDA, N. & M. TOKUSHIGE. 1985. J. Biochem. **98:** 793–797.
5. LIU, C. C., Y. HUNG, J-T. CHEN & H. TSAI. 1988. *In* Proceedings of the Seventh Federation of Asian and Oceanian Biochemists Symposium. Kuala Lumpur, Malaysia.
6. KUNKEL, T. A. 1985. Proc. Natl. Acad. Sci. U.S.A. **82:** 488–492.
7. SANGER, F., S. NICKLEN & A. R. COULSON. 1977. Proc. Natl. Acad. Sci. U.S.A. **74:** 5463–5467.
8. BRADFORD, M. M. 1976. Anal. Biochem. **72:** 248–254.
9. SUZUKI, S., J. YAMAGUCHI & M. TOKUSHIGE. 1973. Biochim. Biophys. Acta **321:** 369–381.
10. IDA, N. & M. TOKUSHIGE. 1984. J. Biochem. **96:** 1315–1321.
11. SARIBAS, A. S., J. F. SCHINDLER & R. E. VIOLA. 1994. J. Biol. Chem. **269:** 6313–6319.
12. WEAVER, T. M., D. G. LEVITT, M. I. DONNELLY, P. P. WILKENS-STEVENS & L. J. BANASZAK. 1995. Nature Struct. Biol. **1:** 654–662.

Protein Engineering of a Cephalosporin C Acylase

HISASHI YAMADA, YOSHINORI ISHII,
YUJI NOGUCHI, TOSHIKO MIURA,
THORU MORI, AND YOSHIMASA SAITO

Pharmacological Research Laboratories
Fujisawa Pharmaceutical Company, Limited
Osaka 532, Japan

INTRODUCTION

7-Aminocephalosporanic acid (7ACA), a key intermediate of cephem antibiotics, has been produced by chemical hydrolysis of cephalosporin C (CC). Recently, an enzymatic method using cephalosporin C acylase that catalyzes the hydrolysis of cephalosporin compounds to 7ACA has been preferred because it is simple to control and safe for the environment. A cephalosporin acylase isolated from *Pseudomonas* strain N176, designated as N176 acylase,[1,2] has high activity for glutaryl-7ACA (GL-7ACA) and is also effective for CC. However, its productivity from the original strain is low and the activity for CC is insufficient for a large-scale production of 7ACA. In order to apply the acylase for one-step enzymatic production of 7ACA from CC, (i) a high expression system of the wild-type N176 acylase in *E. coli* was established and (ii) a mutant acylase, in which Met[269] is changed to Tyr, with superior CC acylase activity was prepared by the use of protein engineering.[3,4] Next, we thought that mutation of every cysteine to serine should be interesting because the activity of the acylase was inhibited in the presence of PCMB (*p*-chloromercuribenzoic acid). In this report, we describe the kinetic analysis of the inhibition induced by PCMB, the mutation study of every cysteine in the acylase, and the characterization of a highly expressed mutant whose Cys[305] was altered to Ser. We also report the characterization and the application to bioreactor experiments of a new double mutant whose Cys[305] and Met[269] were changed to Ser and Tyr, respectively.

RESULTS AND DISCUSSION

Inactivation with PCMB

N176 cephalosporin C acylase was inactivated in the presence of PCMB.[2] Because PCMB is known to be an inhibitor of thiol enzymes, it seemed interesting to study the reaction of the acylase with PCMB (TABLE 1). When the acylase (40 μg/mL) was incubated with 100 nM PCMB at ambient temperature, the activity for GL-7ACA was reduced to 11.8% of that of the intact type. The reduction of the activity was prevented in the presence of Cys or β-mercaptoethanol. The reduction of acylase activity was dependent on the concentration of PCMB. The inhibition of

TABLE 1. Properties of Cysteine-to-Serine Mutants

	Activity (Percentage of Wild-type)[a]		
Mutant	CC (pH 8.7)	GL-7ACA (pH 7.5)	GL-7ACA (pH 8.7)
C102S	n.t.	109.0	91.2
C199S	82.0	85.5	91.0
C277S	83.8	79.4	84.5
C305S	83.8	124.0	92.4
C391S	89.5	47.2	84.2
C493S	n.t.	n.t.	~100[b]
C496S	90.2	67.4	76.3
C748S	n.t.	55.4	68.8

[a]Values for the wild-type acylase are 46.3 units/mg protein and 1.55 units/mg protein with GL-7ACA and CC, respectively; n.t., not tested.
[b]Assayed at pH 9.0.

the acylase by PCMB showed a typical competitive inhibition (K_i = 0.102 mM) from Lineweaver-Burk plot analysis (FIGURE 1). Therefore, PCMB seemed to interact with the enzyme, but not with the enzyme-substrate complex. The conformation of the acylase treated with PCMB was suggested to be unchanged as compared with that of the intact acylase from analysis of the tryptophan fluorescence absorbance. The acylase has 8 cysteine residues deduced from the DNA sequence.[2] The number of free SH groups was determined to be 7.6 from the reaction of the acylase with DTNB [5,5'-dithiobis(2-nitro)benzoic acid] in 8 M urea solution. Interestingly, no
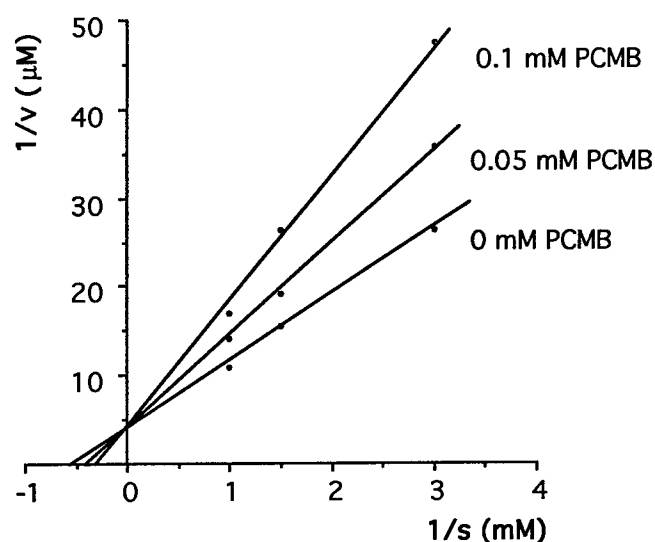
FIGURE 1. Inhibition of GL-7ACA acylase activity by PCMB. The K_i values were determined from the Lineweaver-Burk plot. N176 acylase (1.5 µg/mL) was incubated with GL-7ACA (0.33, 0.67, and 1.0 mM) in the presence of PCMB (0, 0.05, and 0.1 mM) at 37 °C in 0.1 M glycine buffer (pH 9.0). The amount of 7ACA formed was assayed by HPLC.

reaction was observed when DTNB was used in a Tris-HCl (pH 8.5) buffer (data not shown). These data indicate that all cysteines in the acylase have free SH groups and are located at hindered sites in the native form.

Cys-to-Ser Mutants

To investigate the role of cysteine in the acylase, each of the 8 cysteine residues was altered to Ser by site-directed point mutagenesis. The mutant acylases were produced in recombinant E. coli and purified by preparative HPLC. However, every mutant retained the acylase activities for GL-7ACA and CC (TABLE 1). These data indicate that any cysteines in the acylase are not essential for the acylase activity. Therefore, the inactivation caused by PCMB seems to be different from the case of thiol enzymes.

Among the mutants, expression of acylase activity with a mutant in which Cys[305] is changed to Ser, designated as C305S acylase, was increased by two (as CC acylase) to three times (as GL-7ACA acylase) as compared with the wild type (FIGURE 2). Expression of C305S acylase and the wild type at 20 °C and 30 °C was compared by SDS-PAGE analysis (FIGURE 3). In the case of C305S acylase, 25.4- and 58.2-kDa proteins, corresponding to the α and β chains of the acylase, are accumulated in the cellular soluble fraction at 20 °C (lanes 1 and 2). On the other hand, considerable
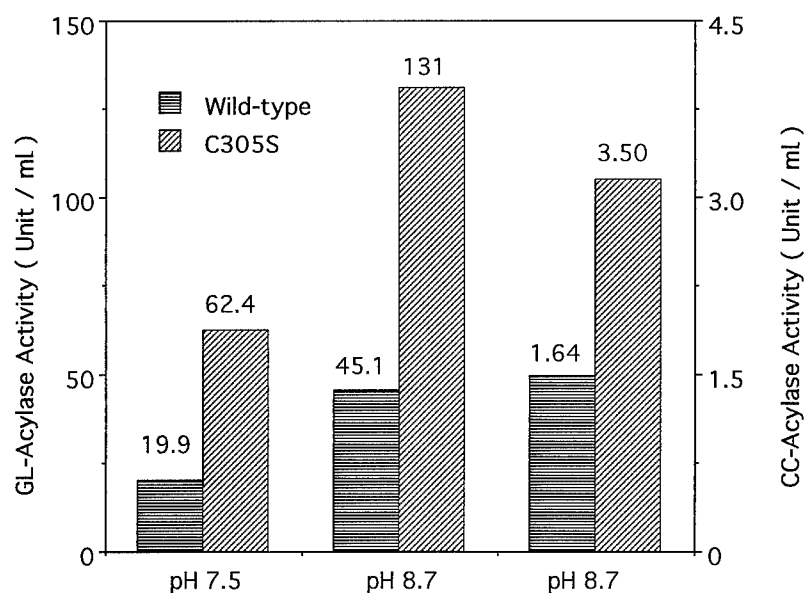
FIGURE 2. Expression level of the native and C305S mutant acylases. E. coli JM109 was used as the host strain. Cultivation was performed in 2% M9CA broth by induction with β-indole-acrylic acid. Cells were harvested by centrifugation and lysed by sonication. After centrifugation, the supernatant was used for the assay.
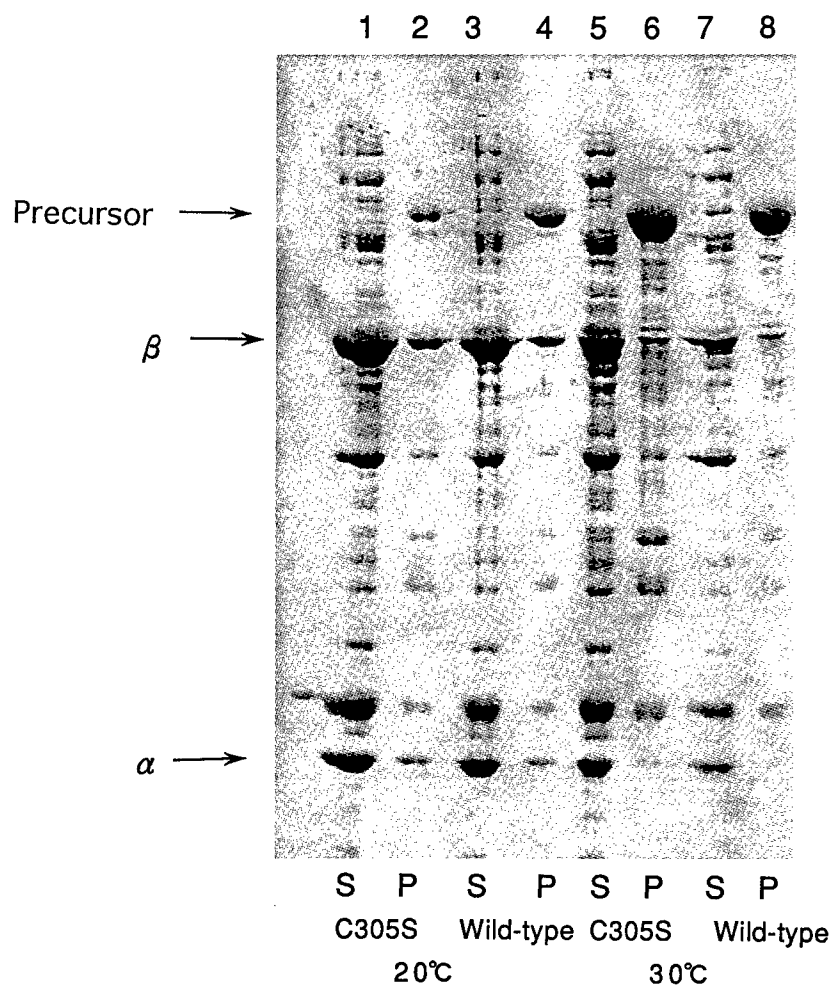
FIGURE 3. SDS-PAGE analysis of the expressed wild-type and C305S mutant acylases. Cultivation was performed in 2% M9CA broth by induction with β-indoleacrylic acid at 20 °C or 30 °C. Cells were harvested by centrifugation and lysed by sonication. The supernatant was recovered by centrifugation and the precipitates were dissolved in the buffer containing 8 M urea to obtain the precipitate fractions. Both fractions were analyzed by 12.5% SDS-PAGE. Lanes 1–4: at 20 °C; lanes 5–8: at 30 °C; lanes 1, 2, 5, and 6: C305S; lanes 3, 4, 7, and 8: wild-type; lanes 1, 3, 5, and 7: supernatant fractions; lanes 2, 4, 6, and 8: precipitate fractions. Arrows indicate the size of proteins corresponding to the α and β, respectively.

amounts of 83.6-kDa protein, corresponding to the precursor of the wild type, are found in the cellular insoluble fraction reextracted with 8 M urea, even at 20 °C (lanes 3 and 4). This trend is obvious when cultivation is performed at 30 °C (lanes 5–8) and consistent with the experiments reported by Schein and Noteborn.[5] These

TABLE 2. Activities of the Wild-type and Mutant Acylases

	Activity (Percentage of Wild-type)[a]	
Enzyme	GL-7ACA (pH 8.7)	CC (pH 8.7)
wild-type	100	100
C305S	101	108
M269Y/C305S	81	160

[a]Values for the wild-type acylase are 46.3 units/mg protein and 1.55 units/mg protein with GL-7ACA and CC, respectively.

data indicate that the high expression of C305S acylase is due to the facility of processing of the precursor protein expressed in *E. coli* cells and suggest that Cys^{305} is located near an important site involved in maturation of the enzyme.

A Hybrid Mutant Acylase, M269Y/C305S

We have reported that a mutant acylase whose Met^{269} is altered to Tyr, designated as M269Y acylase, showed higher CC acylase activity and was more efficient in converting CC to 7ACA in a bioreactor system.[3,4] Therefore, it seemed interesting to make a hybrid mutant by combination with M269Y and C305S. The hybrid mutant, designated as M269Y/C305S acylase, was prepared and compared with the wild-type
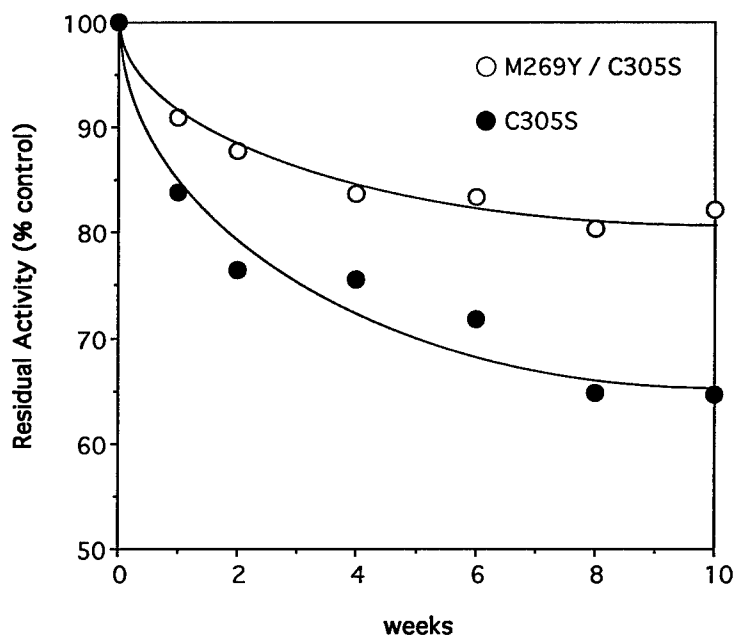
FIGURE 4. Stability of mutant acylases at 25 °C. Each activity for CC at the initial point is represented at 100%.

and C305S acylases (TABLE 2). It showed high CC acylase activity (160% as compared to the wild type), although the GL-7ACA acylase activity was reduced to about 80% of that of C305S acylase. The productivity in *E. coli* was almost equal to that of C305S acylase (data not shown). Furthermore, the stability of M269Y/C305S acylase at 25 °C was greatly improved as compared to C305S acylase (FIGURE 4). These results indicate that an additive effect was observed by the double mutation of Cys[305] to Ser and Met[269] to Tyr in N176 CC acylase.
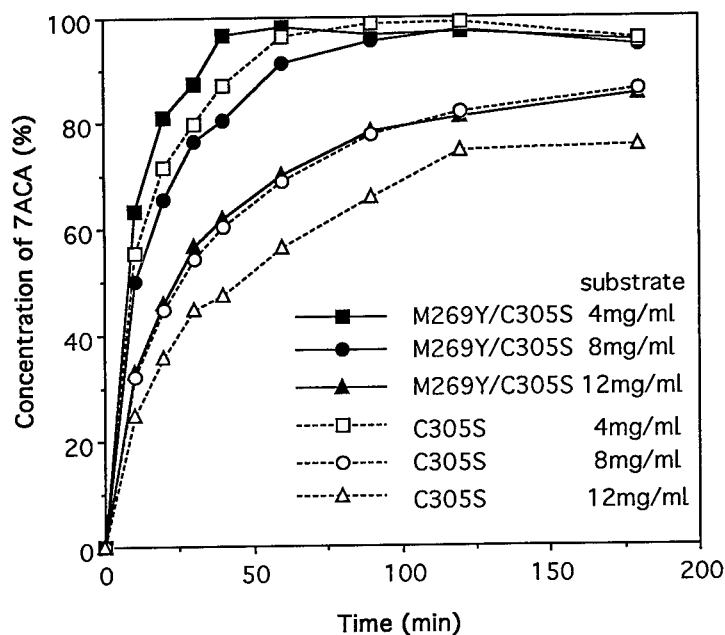
FIGURE 5. Conversion of CC to 7ACA in a bioreactor system. *E. coli* JM109 carrying p269Y305S (an expression vector for M269Y/C305S acylase) was cultivated in a 5-L jar fermentor in a similar manner as described before. The cells were suspended in TE buffer, lysed by a French press, and centrifuged. The supernatant was treated with 0.01% polymin P and purified by QAE-TOYOPEARL 650M column (Tosoh, Japan). Each enzyme (4 mg/mL) was incubated with CC (4, 8, and 12 mg/mL) at 25 °C in 0.15 M Tris-HCl, pH 9.0. At intervals, an aliquot of the reaction mixture was withdrawn and analyzed by HPLC to determine the 7ACA formed.

Reaction of M269Y/C305S Acylase in a Bioreactor System

To investigate the enzymatic capability of M269Y/C305S acylase, the reaction of the free enzyme (4 mg/mL) and CC (4, 8, and 12 mg/mL) was performed in a batch-type bioreactor system (FIGURE 5). The activity of M269Y/C305S acylase was twice as much as that of C305S acylase in the formation yield of 7ACA as well as in the reaction rate. The data are almost equal to those of M269Y mutant acylase.[3] Next, we tried to use M269Y/C305S acylase as an immobilized enzyme for the

Anion Exchange Resin (FE901) 10 mL

      ←   0.5 N NaOH

      ← H_2O

      ←   0.15 M Tris-HCl, pH9.0

      ←   M269Y/C305S mutant acylase

Stirring

Sup   Immobilized M269Y/C305S
       404 mg enzyme/10 mL resin
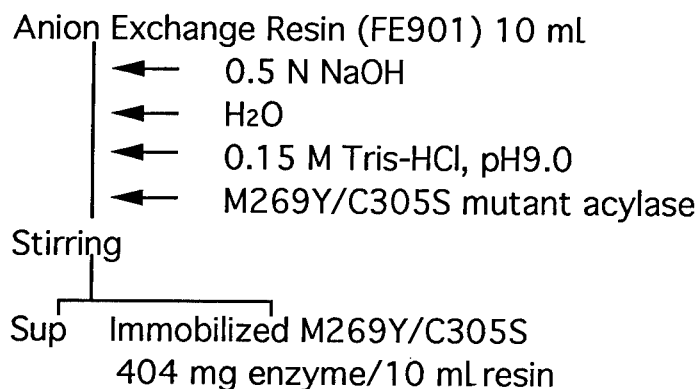
FIGURE 6. Preparation of immobilized M269Y/C305S.

industrial production of 7ACA. The enzyme was immobilized by adsorption to FE901 anion exchange resin (Organo, Japan) (FIGURE 6) and the immobilized enzyme (40 mg/mL resin) was used to produce 7ACA from CC in a simple bioreactor system, shown in FIGURE 7. In this reaction system, CC (125 mg/50 mL) was efficiently converted to 7ACA by circulation through the immobilized resin (400 mg/10 mL) at 25 °C for 120 min. The formation yields of 7ACA were more than 90% from the first to 55th cycles (FIGURE 8). Although the yields were lowered to about 80% from the 58th to 60th cycles, they were recovered by prolongation of the circulation time (150 min). The half-life of the immobilized enzyme was calculated to be about 55 cycles from the formation yields of 7ACA at the first (70%) and 55th (35%) cycles after 30-min reaction. These data indicate that the immobilized acylase
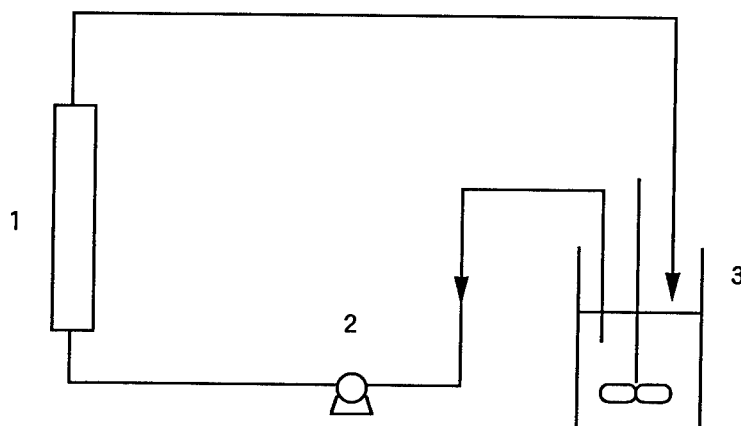
FIGURE 7. Schematic outline for production of 7ACA by the immobilized enzyme: (1) reaction column (400 mg enzyme/10 mL resin, 16 mm × 50 mm); (2) circulation pump for immobilized column (flow rate, 5 mL/min); (3) reservoir [CC: 125 mg in 50 mL of 0.14 M Tris-HCl (pH 9.0)].
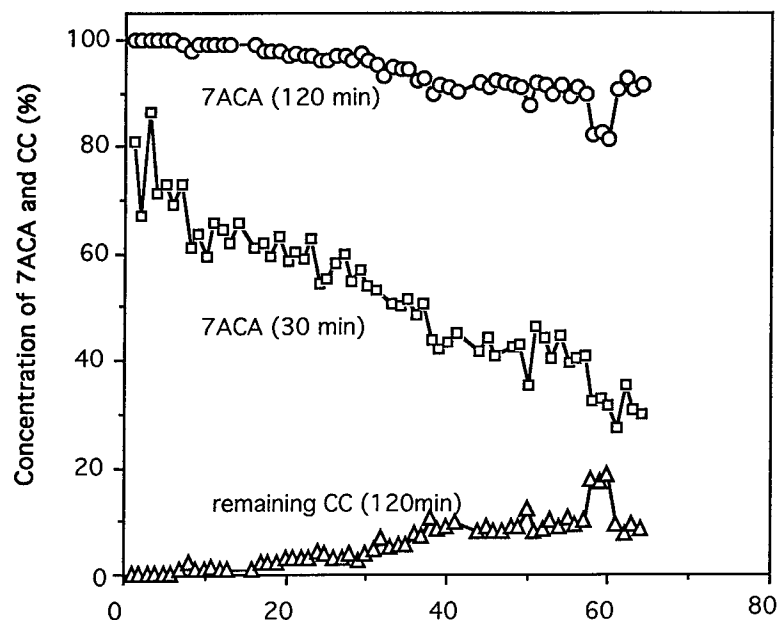
FIGURE 8. Conversion of CC to 7ACA with immobilized M269Y/C305S acylase. The remaining CC and 7ACA formed were assayed by reversed HPLC.

is effective in more than 60 cycles for the production of 7ACA. From these results, M269Y/C305S may be a promising enzyme in one-step enzymatic production of 7ACA from CC.

REFERENCES

1. ARAMORI, I., M. FUKAGAWA, M. TSUMURA, M. IWAMI, T. ISOGAI, H. ONO, Y. ISHITANI, H. KOJO, M. KOHSAKA, Y. UEDA & H. IMANAKA. 1991. Cloning and nucleotide sequencing of new glutaryl 7-ACA and cephalosporin C acylase genes from *Pseudomonas* strains. J. Ferment. Bioeng. **72:** 232–243.
2. ARAMORI, I., M. FUKAGAWA, M. TSUMURA, M. IWAMI, H. ONO, Y. ISHITANI, H. KOJO, M. KOHSAKA, Y. UEDA & H. IMANAKA. 1992. Comparative characterization of new glutaryl 7-ACA and cephalosporin C acylases. J. Ferment. Bioeng. **73:** 185–192.
3. ISHII, Y., Y. SAITO, T. FUJIMURA, H. SASAKI, Y. NOGUCHI, H. YAMADA, M. NIWA & K. SHIMOMURA. 1995. High-level production, chemical modification, and site-directed mutagenesis of a cephalosporin C acylase from *Pseudomonas* strain N176. Eur. J. Biochem. **230:** 773–778.
4. SAITO, Y., Y. ISHII, T. FUJIMURA, H. SASAKI, Y. NOGUCHI, H. YAMADA, M. NIWA & K. SHIMOMURA. 1996. Protein engineering of a cephalosporin acylase from *Pseudomonas* strain N176. Ann. N.Y. Acad. Sci. **782:** 226–240.
5. SCHEIN, C. H. & M. H. NOTEBORN. 1988. Formation of soluble proteins in *Escherichia coli* is favored by lower growth temperature. Biotechnology **6:** 291–294.

Thermal Stable Subtilisin with Oxidation-resistant Property

LIUQIN ZHU, YUFENG ZHAO, AND RUCHANG BI

Department of Protein Engineering
Institute of Biophysics
Academia Sinica
Beijing 100101, People's Republic of China

INTRODUCTION

Subtilisins are a family of alkaline serine endoproteases secreted by a wide variety of *Bacillus* species. They have been extensively investigated in regard to both basic and applied aspects as a promising target for protein engineering.

Wild-type subtilisins are not stable at high temperature and are not resistant to oxidation inactivation. To enhance the thermostability, disulfide bonds have been introduced into the protein by site-directed mutagenesis. Unfortunately, only a few of the mutants possessed higher thermostability than the wild type.[1]

Random mutagenesis is practical when coupled with an efficient screening of selection procedure to identify colonies expressing variant enzyme with the properties of interest, such as K_{cat}/K_m ratio, pH-activity profile, oxidation stability, heat stability, and substrate specificity.

RESULTS

Random mutagenesis was carried out on the subtilisin Ki2 (a subtilisin E–like enzyme) gene. A mutant that exhibited remarkable thermostability was obtained. Sequencing analysis revealed only an A-to-G substitution that converted the asparagine codon, AAT, to the serine codon, AGT (FIGURE 1).

To the heat-stable mutant gene, an M222A point mutation, which was an oxidation-resistant mutation,[2] was introduced by site-directed mutagenesis. Thus, a double mutant was obtained. The double mutant enzyme was purified and tested. The results indicate that the double mutant is both oxidation-resistant and heat-stable. The half-life of the double mutant was found to be five to six times longer than that of the wild-type enzyme (FIGURE 2). The double mutant was also as oxidation-resistant as the single mutant M222A of the subtilisin Ki2 (FIGURE 3).

DISCUSSION

Random mutagenesis by PCR was widely used in enzyme engineering. Many mutant subtilisins were obtained.[3] The N218S mutant of subtilisin E was found to be thermostable. This finding coincided with the prediction that reducing the Asn-Gly

mutant   wild type

A C G T A C G T

G
T
A
G
G
T
A
T
→G
A
C
A
A
C
T
T
T

G
T
A
G
G
T
A
T
A←
A
C
A
A
C
C
T
T
T
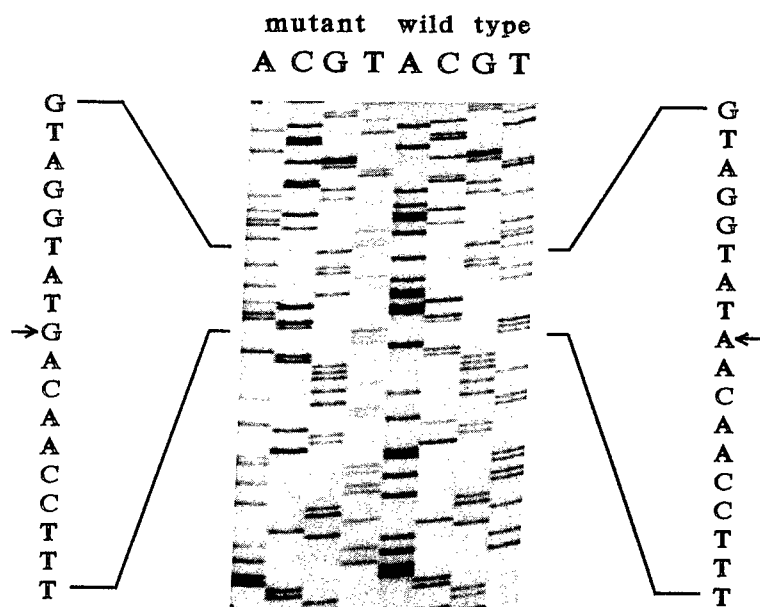
FIGURE 1. The sequence of subtilisin Ki2 and its mutant N118S around amino acid residue 118. The arrows show the difference between the two genes.
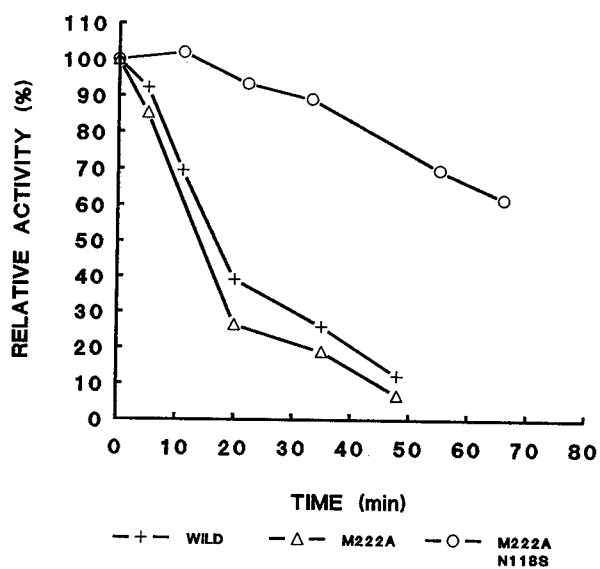
FIGURE 2. Thermostability of subtilisin Ki2 and its mutants. The enzyme was incubated at 65 °C for the time indicated. The residual amidase activities were measured on the substrate casein (1% in 25 mM borate buffer, pH 11) at 40 °C.
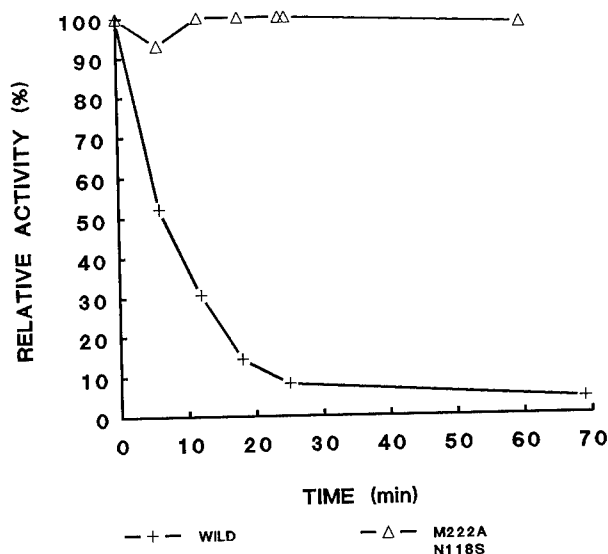
FIGURE 3. Effects of hydrogen peroxide on the activity of subtilisin Ki2 and its mutants. The enzyme was incubated at 37 °C for the time indicated. The residual initial activities were measured over time by mixing not more than 50 μL of the enzyme solution into 1.5 mL of N-Suc-AAPF-pNA substrate solution at 37 °C.

sequence will improve the heat stabilities (International patent no. w087/04461). In our case, Asn118 was followed by Met instead of Gly. Using computer simulation, we studied the thermostability of the mutant. The results of the energy calculation indicate that the increased thermostability of the mutant is due to an additional water molecule interacting with the Ser118 residue and its surrounding residues through hydrogen bonds.

REFERENCES

1. TAKAGI, H. 1993. Int. J. Biochem. **25**(3): 307–312.
2. ESTELL, D. A., T. P. GRAYCAR & J. A. WELLS. 1985. J. Biol. Chem. **260**(11): 6518–6521.
3. CHEN, K. & F. H. ARNOLD. 1991. Bio/Technology **9**: 1073–1077.

The Structural Effects of Solvent Engineering[a]

GREGORY K. FARBER

Department of Biochemistry and Molecular Biology
Pennsylvania State University
University Park, Pennsylvania 16802

INTRODUCTION

When the solvent environment around an enzyme is altered, a number of changes to enzyme reactivity have been observed.[1] Among the most interesting changes are alterations in substrate specificity. In addition to changes in enzyme reactivity, many enzymes exhibit enhanced thermostability when suspended in nonaqueous solvents.[2,3] Unfortunately, the activity of many enzymes is significantly lower when suspended in organic solvents than in aqueous solutions.[4] We have been interested in trying to discover the structural basis for these changes in enzyme function.

The tool that we have used in these studies is X-ray crystallography. We discovered that it was possible to grow protein crystals from the normal aqueous crystallization buffers and then transfer the crystals into a variety of different solvents.[5,6] The transfer process that we use resembles the protocol that is usually used to resuspend lyophilized proteins in organic solvents.[5] Crystals of turkey egg white lysozyme (TEWL) and of γ-chymotrypsin have been transferred into a wide range of solvents. The crystals behave in three different ways when placed in a neat organic solvent (TABLE 1).

In addition to transferring crystals directly into neat organic solvents, we have also transferred them into mixed solvents. These mixtures include aqueous solutions containing a denaturing agent (urea or a guanidinium salt), solutions either of water or of a nonaqueous solvent containing a weak binding ligand (a sugar or an alcohol), or aqueous solutions containing a high concentration of a polar solvent (50% dimethylformamide). These mixed solvents have differing effects on protein structure. A summary of these effects follows.

NONPOLAR SOLVENTS

As TABLE 1 indicates, protein crystals are stable in a number of different nonpolar solvents. We have solved the structure of γ-chymotrypsin in hexane[5] and this structure suggests an explanation for the altered substrate specificity of enzymes in organic solvents. The major effect that nonpolar solvents have on protein structure is a significant rearrangement of side chains that are on the surface of the protein. Such rearrangement had been predicted from molecular dynamics simulations.[7] The

TABLE 1. Results of Submerging TEWL Crystals in Organic Solvents

Class A Solvents—crystals are stable:
  (1) hexane
  (2) cyclohexane
  (3) toluene

Class B Solvents—many crystals crack, but some survive the transfer:
  (1) PEG 400
  (2) ethyl acetate
  (3) triton X-100
  (4) decylol
  (5) *t*-butyl acetate
  (6) triethyl amine
  (7) dimethyl malonate

Class C Solvents—crystals quickly develop hundreds of cracks:
  (1) acetone
  (2) tetrahydrofuran
  (3) diisopropylamine
  (4) methanol
  (5) octanol
  (6) glycerol

cause of the rearrangement is the change in solvent polarity. When placed in a nonpolar solvent, polar side chains that had been interacting with water molecules in the aqueous solution typically try to form new interactions in the interior of the protein. FIGURE 1 illustrates a typical example of such motion.

Such rearrangements occur throughout the surface of the protein. In cases of enzymes where the substrate binding site is large (proteases or glycosidases, for example), it is quite likely that some of these rearrangements will occur in the substrate binding site. Such rearrangements would alter the substrate specificity of the enzyme. In addition to the changes caused by the polarity of the solvent, we have observed strong binding sites for many different types of molecules near the surface of the protein. In the case of chymotrypsin in hexane, a total of seven hexanes were observed.[5] Two of these hexane molecules bind close to the active site. They may contribute to the altered binding of the substrate in the P4 subsite that is observed in this structure.

WEAK BINDING LIGANDS

A thermodynamic analysis of the effect of adding molecules like sugars or alcohols to the solvent around a protein suggests that the surface of a protein should be preferentially hydrated in the presence of these weak binding ligands.[8] When 4% isopropanol is added either to the aqueous crystallization buffer or to hexane around crystals of γ-chymotrypsin, the number of waters observable in the crystal structure doubles.[6] The new waters often occupy positions quite far from the protein surface. These waters interact with other water molecules in the second hydration sphere away from the protein.

By adding a weak binding ligand to the solution around a protein crystal, it is

possible to use this effect to regulate the effective concentration of water around the protein. This effect can be very useful in studying enzyme-bound intermediates where water is a substrate in the reaction. We have been able to shift the equilibrium between two enzyme-bound intermediates in the peptide hydrolysis reaction catalyzed by chymotrypsin by adding a weak binding ligand to the crystal.[6]

Weak binding ligands cause the water concentration in the crystal to increase. For those enzymes that use water as a substrate, it is possible to lower the water concentration in the crystal. We have shown that crystals of γ-chymotrypsin are active in the hydrolysis direction in hexane.[5] For every turnover, the concentration of water around the crystal decreases. By adding a known amount of substrate to a crystal, it is possible to obtain very low water concentrations in the crystal lattice. This experiment in combination with the addition of weak binding ligands provides
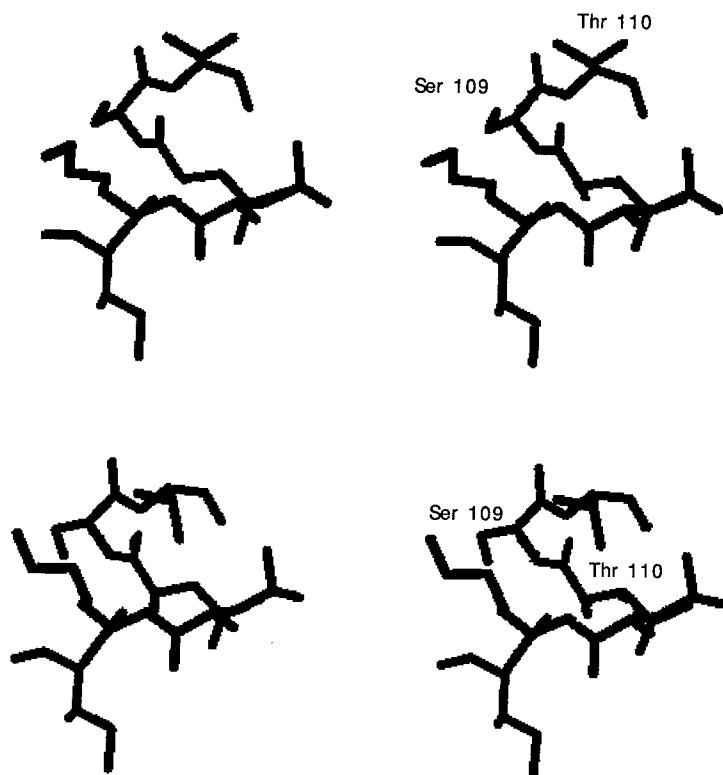
FIGURE 1. The top stereo pair shows residues 108–110 and 83–85 from the native structure of chymotrypsin in an aqueous solvent. Both of the side chains of Ser 109 and Thr 110 are pointed out into the solvent. The bottom stereo pair shows the same residues in the hexane structure. Thr 110 has rotated so that the side chain oxygen makes a good hydrogen bond with the backbone nitrogen of residue 84. The side chain of Ser 109 has also rotated to point away from the solvent. Such rearrangements are common for surface side chains in nonpolar solvents.

an experimental technique to directly observe the structural changes associated with changes in hydration.

DENATURANTS

Adding a weak binding ligand changes the water structure around a protein. Adding a denaturant changes the mobility of the protein atoms. When a denaturant is titrated into the solution around a protein crystal, the crystals shatter at a particular concentration.[9] Both dihydrofolate reductase (DHFR) in the presence of urea and ribonuclease in the presence of guanidinium chloride show such behavior.[9] We believe that the shattering is related to protein unfolding because crystals of mutants of DHFR that denature at lower urea concentrations than the wild-type enzyme also shatter at a correspondingly lower urea concentration.

Although the shattering of the crystals was not terribly surprising in the presence of a denaturant, the decreased flexibility of the resulting structure was. Motions in a protein crystal can be evaluated using the temperature factor (also known as the B-factor or the Debye-Waller factor). In both ribonuclease and dihydrofolate reductase, the addition of a denaturant resulted in a significant decrease in mobility.

The location of tight binding denaturant molecules in both structures offers an explanation for this effect. Many of the observed denaturants make multiple hydrogen bonds with parts of the protein that are not normally linked in any way. In effect, the denaturants act as noncovalent cross-linking agents. This cross-linking causes the native conformation of the protein to be less mobile in the presence of denaturants than in an aqueous solution. This loss of mobility was seen to a lesser extent with γ-chymotrypsin in hexane. In both cases, lower mobility is correlated with an increase in stability.

CONCLUSIONS

By altering the solvent around a protein crystal, it is possible to change the substrate conformation, to alter the number of bound waters, and to reduce the mobility of the protein. Different classes of solvents can be used to achieve each of these effects. Nonpolar solvents cause side-chain rearrangements that can result in changes in substrate specificity. The amount of water around a protein can be altered by adding a weak binding ligand. Protein mobility can be altered by adding a denaturant to the solution.

Preliminary work with subtilisin BPN in dimethylformamide (DMF) suggests that the changes due to polar solvents involve both changes in mobility and changes in solvent structure. However, unlike our other solvents, both of these effects appear to depend on the concentration of dimethylformamide. The structures that we have solved illustrate the usefulness of having a molecular basis for changes in protein function. In the case of subtilisin, the structures in DMF suggest a mechanism for the lower enzyme activity in this solvent. Site-directed mutants are now being designed that will significantly increase the activity of this enzyme in dimethylformamide.

REFERENCES

1. WESCOTT, C. R. & A. M. KLIBANOV. 1994. The solvent dependence of enzyme specificity. Biochim. Biophys. Acta 1206: 1–9 (and references herein).
2. ZAKS, A. & A. M. KLIBANOV. 1984. Enzymatic catalysis in organic media at 100 °C. Science 244: 1249–1251.
3. GARZA-RAMOS, G., A. DARSZON, M. TUENA DE GÓMEZ-PUYOU & A. GÓMEZ-PUYOU. 1990. Enzyme catalysis in organic solvents with low water content at high temperatures: the adenosinetriphosphatase of submitochondrial particles. Biochemistry 29: 751–757.
4. WONG, C-H., S-T. CHEN, W. J. HENNEN, J. A. BIBBS, Y-F. WANG, J. L-C. LIU, M. W. PANTOLIANO, M. WHITLOW & P. N. BRYAN. 1990. Enzymes in organic synthesis: use of subtilisin and a highly stable mutant derived from multiple site-specific mutations. J. Am. Chem. Soc. 112: 945–953.
5. YENNAWAR, N., H. P. YENNAWAR & G. K. FARBER. 1994. The structure of γ-chymotrypsin in hexane. Biochemistry 33: 7326–7336.
6. YENNAWAR, H. P., N. YENNAWAR & G. K. FARBER. 1995. A structural explanation for enzyme memory in nonaqueous solvents. J. Am. Chem. Soc. 117: 577–585.
7. HARTSOUGH, D. S. & K. M. MERZ. 1993. Protein dynamics and solvation in aqueous and nonaqueous environments. J. Am. Chem. Soc. 115: 6529–6537.
8. TIMASHEFF, S. N. 1993. The control of protein stability and association by weak interactions with water: how do these solvents affect these processes? Annu. Rev. Biophys. Biomol. Struct. 22: 67–97.
9. DUNBAR, J., H. P. YENNAWAR, S. BANERJEE, J. LUO & G. K. FARBER. 1996. The effect of denaturants on protein structure. Submitted.

The Use of a Novel Recombinant Heroin Esterase in the Development of an Illicit Drugs Biosensor[a]

DEBORAH A. RATHBONE, PETER-JOHN HOLT,
CHRISTOPHER R. LOWE, AND NEIL C. BRUCE[b]

Institute of Biotechnology
University of Cambridge
Cambridge CB2 1QT, United Kingdom

INTRODUCTION

The level of heroin abuse has risen dramatically over the past three decades, making it the most common drug of abuse at present in the United Kingdom. This upward trend has been mimicked by the number of deaths due to heroin overdoses or complications arising from prolonged use.[1] The social and economic impact of such drug abuse is of increasing concern, with drug-related offenses recorded at almost 50,000 in the United Kingdom in 1991 alone.[1] These worrying statistics are likely to increase as the boundaries within a united Europe become relaxed and customs inspections become more difficult or infrequent.

Current drug detection or identification methods include color tests,[2] high-performance liquid chromatography,[3] antibody-based tests,[4] and gas chromatography coupled with mass spectrometry.[5] As such, they are unsuitable for use by customs officers as on-the-spot detection systems. These techniques are largely laboratory-based, requiring use and time-consuming interpretation of results by skilled scientific personnel.

Biosensor technology provides the opportunity of allowing the rapid and sensitive detection of such compounds. Biosensors are self-contained systems whose specificities and sensitivities are provided by the biorecognition (enzymes/antibodies) and transducer components. The biological reaction that occurs between the target molecules and the biorecognition system is converted to a measurable output signal by the transduction and amplification components.

This report describes a novel biorecognition system for a heroin biosensor and the possible modifications that may be made to heroin esterase, one of the biorecognition components, in order to improve the system.

BIORECOGNITION ENZYMES

Two enzymes, heroin esterase and morphine dehydrogenase, have been coupled to form the biorecognition component of a biosensor for the detection of heroin (FIGURE 1).

[b]To whom all correspondence should be addressed.
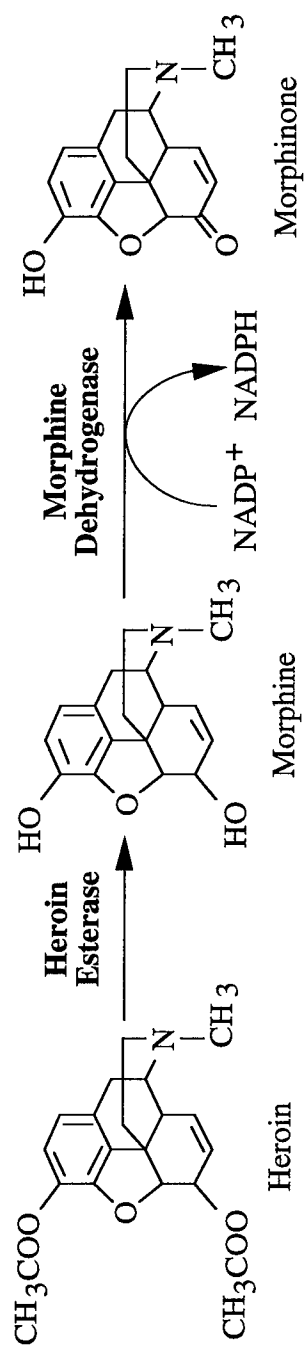
FIGURE 1. The coupled enzyme assay.

Morphine Dehydrogenase

Morphine dehydrogenase was identified in *Pseudomonas putida* M10, a member of a mixed culture isolated by selective enrichment of waste liquid taken from an opiate processing plant.[6,7] *P. putida* M10 was found to metabolize morphine, albeit slowly, and morphine dehydrogenase was determined as being the enzyme initiating this process. The structural gene for morphine dehydrogenase, *mor*A, was cloned and the recombinant protein overexpressed in *Escherichia coli*.[8] Specificity studies demonstrated that morphine dehydrogenase was suitable as a recognition component, being able to oxidize morphine and only a few related morphine alkaloids.[9] More importantly, morphine dehydrogenase required $NADP^+$ for activity; thus, the NADPH liberated in the reaction could be linked to various transduction systems.

Heroin Esterase

In order for morphine dehydrogenase to be used in the biosensor, heroin had first to be hydrolyzed to form morphine. A number of commercially available esterases were screened for activity towards heroin, but none proved useful, being able to hydrolyze only the C3 acetyl ester group, leaving the C6 group largely untouched. A novel esterase was identified in *Rhodococcus* sp. H1, isolated from garden soil by its ability to grow on heroin. This esterase was able to hydrolyze heroin to morphine.[10]

Heroin esterase was observed to be present in low levels in *Rhodococcus* sp. H1 and required induction by heroin during growth. It was thus necessary to clone the structural gene, *her*, to enable the high-level expression of recombinant heroin esterase in *E. coli* to assess its suitability as a biorecognition component.

The *her* gene was located on a 6.3-kb *Pst*I fragment of genomic DNA using an oligonucleotide probe mixture whose sequence was based on the N-terminal amino acid sequence of partially purified heroin esterase.[10,11] Analysis of the DNA sequence of the 5′ region of *her* revealed the absence of such regulatory motifs as promoter regions or ribosome binding sites that could be recognized by *E. coli*. It was not surprising, therefore, that recombinant heroin esterase was not expressed when the 6.3-kb clone was transformed into *E. coli*.[11,12] PCR was used to engineer a useful restriction site at the 5′ end of *her* to enable directional insertion into pT7-7, an expression vector carrying the T7 RNA polymerase promoter and an *E. coli* ribosome binding site.[11]

Characterization of Heroin Esterase

The purification of recombinant heroin esterase included ammonium sulfate precipitation, hydrophobic interaction chromatography (octyl-agarose 6XL), and Mono Q anion exchange chromatography.[11]

A combination of substrate and inhibitor studies and a comparison of the deduced amino acid sequence of *her* with other esterases (FIGURE 2) suggested that heroin esterase is a typical type-B serine active-site carboxylesterase. Recombinant heroin esterase exhibited a pH optimum of 8.5 and a temperature optimum of 30 °C

```
Strp.1            .......... .......... ..........
Strp.2            .......... .......... ..........
Rhod.             .......... .......... ..........
Morax.            MPILPVPALN ALLTKTIKTI KTGAAKNAHQ

                                                           26
Strp.1  .......... .......... .......... .......... ..........
Strp.2  .......... .......... .......... .......... ..........
Rhod.   .......... .......... .......... MTTFPTLDPE LAAALTMLPK ....VDFADL
Morax.  HHVLHHTLKG LDNLPAPVLE RINRRLKAST AEQYPLADAH LRLILAISNK LKRPLAIDKL

        27                                                           70
Strp.1  ...MASSELE LVRELIGLNW HTRNGDVEPR RVAYDRAQEA FGHLGLPPGE TVVIGDCSAE
Strp.2  ...MASPELE LVRELIELNW HTRNGEMEPR RIAYDRAQEA FGNLGVPPGD VVTVGHCTAE
Rhod.   PNARATYDAL IGAMLADLSF .......... .DGVSLRELS APGLDGDPEV KIRFV.....
Morax.  PKLRQKFGTD AVSLQAPSVW QQNADASGST ENAVSWQDKT IANADGG.DM TVRCYQKSTQ

        71             *  .**       *                  *  **     **     **    *  130
Strp.1  WVRPAQEDGR TLLYLHGGSY ALGSPQSHRH LSSALGAAAG AAVLALHYRR PPESPFPAAV
Strp.2  WVRPARQDGR TLLYLHGGSY ALGSPQSHRH LSSALGDAAG AAVLALHYRR PPESPFPAAV
Rhod.   TPDNTAGPVP VLLWIHGGGF AIGTAESSDP FCVEVARELG FAVANVEYRL APETTFPGPV
Morax.  NSERKSTDEA AMLFFHGGGF CIGDIDTHHE FCHTVCAQTG WAVVSVDYRM APEYPAPTAL

        131 •  **       |*    *  *    *  . **|  **       *              167
Strp.1  EDAVAAYRML RER...|GLP PGRITFAGDS AG|AGLAVAAL QVL....... ..........
Strp.2  EDAVAAYRML LEQ...|GCP PGRVTLAGDS AG|AGLAVAAL QAL....... ..........
Rhod.   NDCYAALLYI HAHAEEI|GID PSRIAVGGES AG|GGLAA... .......... ..........
Morax.  KDCLAAYAWL AEHSQSI|GAS PSRIVLSGDS AG|GCLAALVA QQVIKPIDAL WQDNNQAPAA

        168                       *  *      *   *              223
Strp.1  .......... RDAGDPLPAA AVCISPWADL ACEGASHVTR KEREILLDTE DLLR....MA
Strp.2  .......... RDAGTPLPAA AVCISPWADL ACEGASHTTR KAREILLDTA DLRR....MA
Rhod.   ....GTVLKA RDEGVVPVAF QFLEIPELDD RLEIVSMTNF VDTPLWHRPN AILSWKYYLG
Morax.  DKKVNDTFKN SLADLPRPLA QLPLYPVTDY EAEYPSWELY GEGLLLDHND AEVFNSAYTQ

        224               *  *  *  *     *  *        *  *  283
Strp.1  GRYLAGTDPR NPL..ASPAH GDLTGLPPLL IQVGSEEVLY DDARALEQAA LKAGVPVTFD
Strp.2  ERYLAGTDPR HPL..ASPAH GDLTGLPPLL IQVGSEEVLH DDARALEQAA LKAGTPVTFE
Rhod.   ESYSGPEDPD VSIYAAPSRA TDLTGLPPTY LSIMELDPLR DEGIEYALRL LQAGVSVELH
Morax.  HSGLPQSHPL ISV.....MH GDNTQLCPSY IVVAELDILR DEGLAYAELL QKEGVQVQTY

        284       *                      *              322
Strp.1  EWPEMFHVWH WYHPVLPEGR AAVETAGVFL RRATEEGER. .......... .
Strp.2  EWPEMFHVWH WYHPVLPEGR RAIEVAGAFL RTATGEGLK. .......... .
Rhod.   SFPGTFHGSA LVATAGVRER GAAKPHCDPE RVAFAVAVS* .......... .
Morax.  TVLGAPHG.. FINLMSVHQG LGNQTTYIIN EFACLVQNLL TSEGDKPNLR A
```

FIGURE 2. A comparison of the deduced amino acid sequence of *her* with other serine esterases. Strp 1: *Streptomyces viridochromogenes* N-acetylphosphinothricin-tripeptide deacetylase;[19] Strp 2: *S. hygroscopicus* acetyl hydrolase;[20] Rhod: *Rhodococcus* sp. H1 heroin esterase;[11] Morax: *Moraxella* sp. strain TA144 lipase/esterase.[14]

with heroin or 6-acetylmorphine as substrate. The apparent K_m and V_{max} values with 6-acetylmorphine as substrate were calculated as 0.72 ± 0.03 mM and 8.9 ± 0.33 µmol/min/mg, respectively.[11,13] Native heroin esterase was shown to have a tetrameric form of identical subunits of M_r 38,600 ± 700 and a native M_r of 137,000 ± 7100.[11]

DNA sequence analysis and comparisons with the sequences of other esterases would suggest that heroin esterase is a serine esterase containing the Ser-His-Asp catalytic triad involved in the charge transfer mechanism of such enzymes. His-86 in heroin esterase is conserved in other serine esterases (FIGURE 2). The fact that the region surrounding His-86 is conserved in other esterases is an indication that it may be a catalytically important residue. Furthermore, in site-directed mutagenesis of the lipase/esterase of *Moraxella* sp., this residue was changed to Gln, resulting in the loss of lipase/esterase activity, providing further evidence that this residue is a member of the catalytic triad.[14] Asp-132 is also part of a conserved region of sequence found in all four enzymes (FIGURE 2). The probable catalytic Ser residue in heroin esterase is Ser-160 as it is found as part of the typical serine active-site motif (boxed in FIGURE 2) common to serine esterases.

Recombinant heroin esterase was found to be irreversibly inhibited by copper sulfate, eserine, *p*-hydroxymercuribenzoate (*p*-HMB), and iodoacetamide.[11,13] Copper sulfate, *p*-HMB, and iodoacetamide are all thiol-modifying agents, suggesting that an essential thiol group is present at the active site of heroin esterase. Other serine carboxylesterases have been reported to be sensitive to sulfhydryl-modifying reagents.[15] If compared to studies of bovine esterase, where Cys-96 is adjacent to the catalytically important Asp-95,[16] Cys-133 in heroin esterase (next to the catalytic triad Asp-132) may be a possible candidate for this group.

THE LUMINESCENT HEROIN BIOSENSOR

FIGURE 3 illustrates the coupling of the two-enzyme system to luciferase from *Vibrio harveyi*. Unlike firefly luciferase, bacterial luciferase is not dependent on ATP, but instead uses an FMN:NADPH oxidoreductase and a long-chain aldehyde. Combined with the narrow substrate specificity of morphine dehydrogenase, the luminescent system allows the very specific and sensitive detection of heroin or morphine, with response times of seconds for morphine. Detection limits are typically 15 ng/mL morphine and 180 ng/mL heroin.[17] As the average heroin particle is 25–40 μm in size,[18] this detection limit equates to a single particle of heroin. If glucuronidase is also incorporated, the potential exists for the detection of morphine-3-glucuronide, the major heroin metabolite found in urine.

MODIFICATIONS OF HEROIN ESTERASE

It is possible to modify heroin esterase to enable its better incorporation into the biosensor system. Modifications may include the mutation of the three Cys residues to Ser or Ala, as in similar studies,[15] which may confer thermostability to the enzyme without otherwise affecting its catalytic ability. This would be desirable for an enzyme that is to be incorporated into a working biosensor. At present, heroin esterase is unstable at temperatures over 32 °C.

Knowledge of the three-dimensional crystal structure of recombinant heroin esterase would give an indication of the residues conferring surface charge. Site-directed mutagenesis may be employed to alter the surface charge of heroin esterase

and, thus, the pH optimum. Morphine dehydrogenase has a pH optimum of 9.5, so it would be desirable to raise the pH optimum of heroin esterase nearer to that of morphine dehydrogenase. Mutation of surface residues may influence the stability and solvent resistance of heroin esterase, which may prove beneficial in the fabrication of the biosensor. It would also be desirable to create mutants of heroin esterase that have improved kinetic properties, as heroin esterase is by far the limiting reaction of the system.
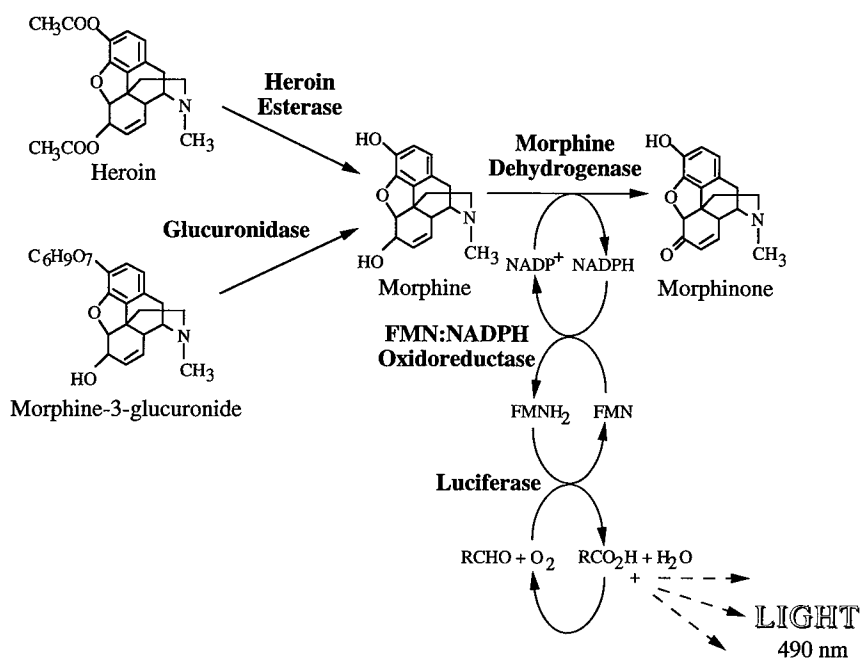
FIGURE 3. The bioluminescent heroin detection system.[17]

SUMMARY

Recombinant heroin esterase and morphine dehydrogenase have been coupled with bacterial luciferase to enable the sensitive and specific detection of heroin. Both enzymes have been purified and fully characterized; this knowledge has identified modifications that may be made to heroin esterase to improve the efficiency of the coupled reaction.

REFERENCES

1. CONCAR, D. & L. SPINNEY. 1994. New Sci. **1945:** 38–41.
2. MASOUD, A. N. 1975. J. Pharm. Sci. **64:** 841–844.
3. GOUGH, T. A. & P. B. BAKER. 1981. J. Chromatogr. Sci. **19:** 227–234.
4. SYVA COMPANY. Maidenhead, Berkshire, United Kingdom.

5. GOUGH, T. A., Ed. 1991. The Analysis of Drug Abuse. First edition. Wiley. New York.
6. BRUCE, N. C., C. J. WILMOT, K. N. JORDAN, L. D. GRAY STEPHENS & C. R. LOWE. 1990. Biochem. J. **274:** 875–880.
7. BRUCE, N. C., C. J. WILMOT, K. N. JORDAN, A. E. TREBILCOCK, L. D. GRAY STEPHENS & C. R. LOWE. 1990. Arch. Microbiol. **154:** 465–470.
8. WILLEY, D. L., D. A. CASWELL, C. R. LOWE & N. C. BRUCE. 1993. Biochem. J. **290:** 539–544.
9. BRUCE, N. C., D. A. CASWELL, C. E. FRENCH, A. M. HAILES, M. T. LONG & D. L. WILLEY. 1994. Ann. N.Y. Acad. Sci. **721:** 85–99.
10. CAMERON, G. W. W., K. N. JORDAN, P-J. HOLT, P. B. BAKER, C. R. LOWE & N. C. BRUCE. 1994. Appl. Environ. Microbiol. **60:** 3881–3883.
11. RATHBONE, D. A., P-J. HOLT, C. R. LOWE & N. C. BRUCE. 1995. Submitted.
12. RATHBONE, D. A., P-J. HOLT, N. C. BRUCE & C. R. LOWE. 1996. Ann. N.Y. Acad. Sci. **782:** 534–543.
13. HOLT, P-J. 1995. Ph.D. thesis. University of Cambridge.
14. FELLER, G., M. THIRY & C. GERDAY. 1991. DNA Cell Biol. **10:** 381–388.
15. AMAKI, Y., H. NAKANO & T. YAMANE. 1994. Appl. Microbiol. Biotechnol. **40:** 664–668.
16. DOCTOR, B. P., T. C. CHAPMAN, C. E. CHRISTNER, C. D. DEAL, D. M. DE LA HOZ, M. K. GENTRY, R. A. OGERT, R. S. RUSH, K. K. SMYTH & A. D. WOLFE. 1990. FEBS Lett. **266:** 123–127.
17. HOLT, P-J., N. C. BRUCE & C. R. LOWE. 1996. Anal. Chem. In press.
18. HOLT, P-J. 1996. Forensic Sci. Int. In press.
19. ALIJAH, R., D. HILLEMANN, B. NUSSBAUMER, S. PELZER & W. WOHLLBEN. 1991. Unpublished sequence data from EMBL.
20. RAIBAUD, A., M. ZALACAIN, T. G. HOLT, R. TIZARD & C. J. THOMPSON. 1991. J. Bacteriol. **173:** 4454–4463.

Morphinone Reductase

Characterization, Cloning, and Application to Biocatalytic Hydromorphone Production

C. E. FRENCH, A. M. HAILES,
D. A. RATHBONE,
AND N. C. BRUCE

Institute of Biotechnology
University of Cambridge
Cambridge CB2 1QT, United Kingdom

INTRODUCTION

A screening program to obtain enzymes suitable for use in an enzyme-based biosensor for the detection of illicit heroin led to the isolation of *Pseudomonas putida* M10 from opiate waste liquor.[1] *P. putida* M10 was found to transform morphine and codeine to hydromorphone and hydrocodone through the sequential action of an NADP^{+}-dependent morphine dehydrogenase and an NADH-dependent morphinone reductase[2] (FIGURE 1). Morphine dehydrogenase was found to be highly suitable for the detection of morphine and now forms the basis of a highly sensitive and specific assay for the detection of heroin and other opiates.[3]

Hydromorphone and hydrocodone are clinically useful and commercially important semisynthetic opiates. They are manufactured from the naturally occurring alkaloids, morphine, codeine, and thebaine, through chemical processes that require expensive catalysts and toxic reagents and, particularly in the case of hydromorphone, suffer from rather low yields. It was felt that a biotransformation process using morphine dehydrogenase and morphinone reductase might offer significant advantages. To this end, the properties of morphinone reductase were investigated.

CHARACTERIZATION OF MORPHINONE REDUCTASE

Morphinone reductase was purified by a single affinity chromatography step and the purified enzyme was characterized.[4] The subunit M_r was measured as 41,120 by electrospray mass spectrometry. The native M_r was estimated as 80,000 by gel filtration, indicating that the native protein is a homodimer. The visible absorption spectrum indicated that morphinone reductase was a flavoprotein. A flavin identified as FMN could be liberated by denaturation of the protein, showing that the flavin was not covalently bound. The deflavoenzyme was prepared by treatment with ammonium sulfate under acid conditions. Activity could be restored only by the addition of FMN. Titration with FMN showed that the enzyme binds one molecule of FMN per subunit. Steady-state kinetic analysis showed that morphinone reductase follows a ping-pong bi-bi mechanism typical of flavoproteins. Reduction of

R=H : morphine
R=CH$_3$: codeine

R=H : morphinone
R=CH$_3$: codeinone

R=H : dihydromorphine
R=CH$_3$: dihydrocodeine

R=H : hydromorphone
R=CH$_3$: hydrocodone
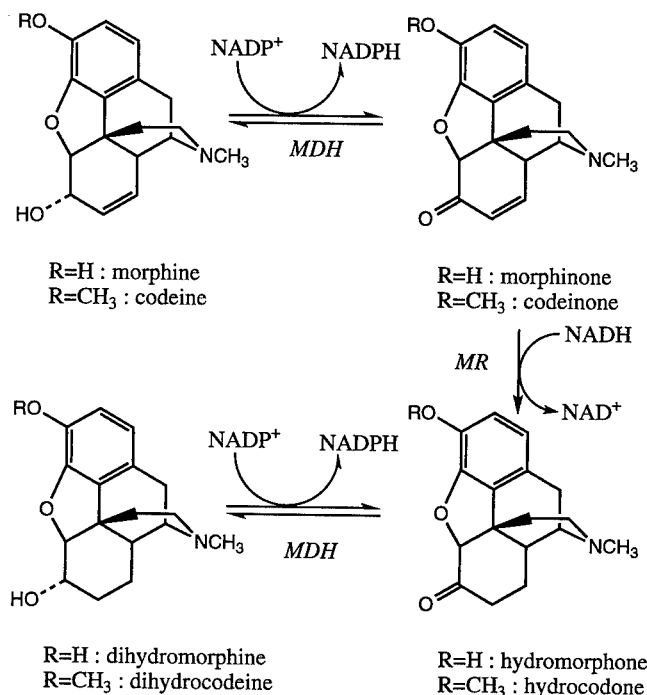
FIGURE 1. Initial transformations of morphine and codeine by *Pseudomonas putida* M10.

morphinone was competitively inhibited by steroids, suggesting that morphinone reductase might be derived from a steroid reductase.

CLONING OF *morB*

The structural gene encoding morphinone reductase, designated *morB*, was cloned by the use of degenerate oligonucleotide probes based on elements of the amino acid sequence of the purified enzyme.[5] The deduced amino acid sequence showed that morphinone reductase was a member of the α/β-barrel flavoprotein oxidoreductases, a group that includes the bacterial enzymes trimethylamine dehydrogenase of *Methylophilus methylotrophus*, bile acid–induced proteins C and H of *Eubacterium* sp., and an NADH oxidase of unknown function from *Thermoanaerobium brockii*, as well as the eukaryotic proteins Old Yellow Enzyme from yeasts of the genera *Saccharomyces* and *Kluyveromyces*, estrogen-binding protein from *Candida albicans*, and a number of putative plant proteins known only as expressed sequence tags. Curiously, morphinone reductase was more similar in structure, properties, and sequence to the fungal and putative plant proteins than to other bacterial members of this group. This may indicate that a gene ancestral to *morB* was acquired relatively recently from a eukaryotic source.

BIOTRANSFORMATION OF MORPHINE TO HYDROMORPHONE

Biotransformations for the production of hydromorphone and hydrocodone from morphine and codeine using morphine dehydrogenase and morphinone reductase were investigated. Two major problems were identified. First, the supply of stoichiometric quantities of the expensive cofactors $NADP^+$ and NADH would obviously not be economically viable. Second, the morphine dehydrogenase reaction is freely reversible and morphine dehydrogenase is also active, although with lower activity, against alkaloids possessing a saturated ring rather than the unsaturated ring of morphine and codeine. This leads to a buildup of dihydromorphine and dihydrocodeine (FIGURE 1), which are easily prepared chemically, and are therefore not of interest in a biotransformation process.

These problems might both be overcome by the cycling of cofactors between the two enzymes, so reduced cofactor produced by morphine dehydrogenase is reoxidized in the irreversible morphinone reductase reaction. This would allow the use of catalytic quantities of cofactor and would prevent the buildup of NADPH that drives the reduction of hydromorphone and hydrocodone to dihydromorphine and dihydrocodeine. To test this hypothesis, cell-free biotransformations were performed using purified morphine dehydrogenase and morphinone reductase together with mammalian glutamate dehydrogenase, which catalyzes the freely reversible oxidation of glutamate to α-ketoglutarate and ammonium ion and which can use either NAD(H) or NADP(H) as cofactor. It was hoped that mammalian glutamate dehydrogenase
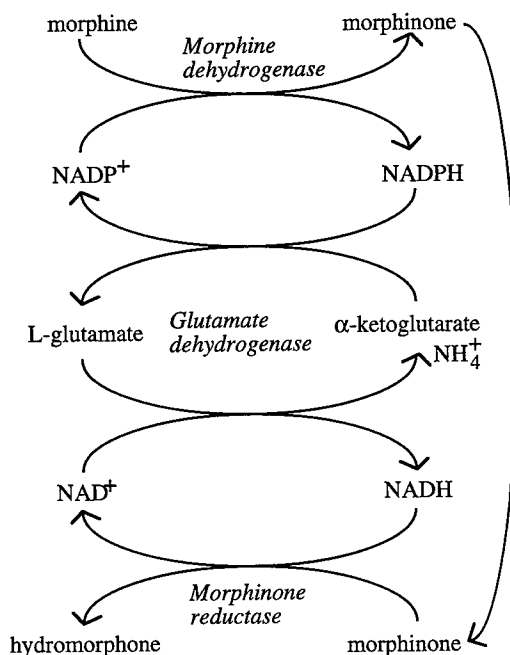
FIGURE 2. Cycling of cofactors using mammalian glutamate dehydrogenase.
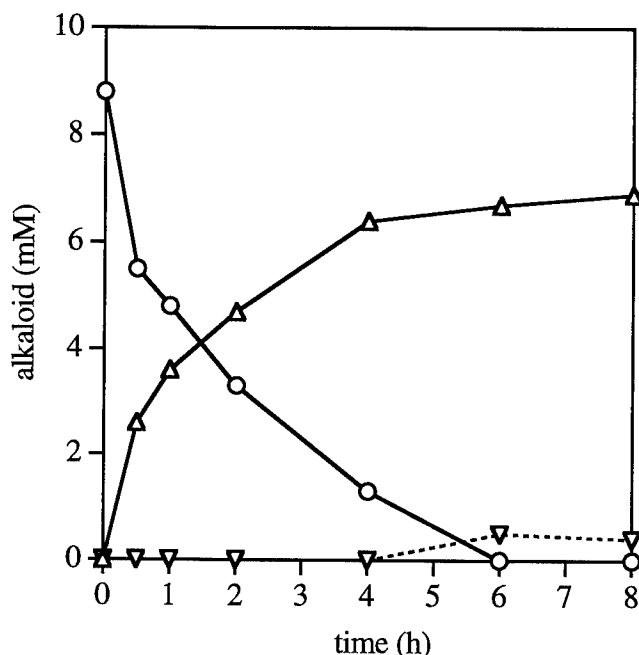
FIGURE 3. Biotransformation of morphine to hydromorphone. The reaction mixture contained 9 mM morphine, 0.5 mM $NADP^+$, 0.5 mM NADH, 1 mM L-glutamate, 1 mM α-ketoglutarate, 2 mM NH_4Cl, 9 U/mL morphine dehydrogenase, 0.7 U/mL morphinone reductase, and 2.6 mg/mL glutamate dehydrogenase in 50 mM phosphate buffer, pH 8.0. The reaction mixture was incubated at 4 °C. Samples were analyzed by HPLC.[2] Symbols: (○) morphine; (△) hydromorphone; (▽) dihydromorphine. Some alkaloid may have been lost due to spontaneous oxidation of the unstable intermediate, morphinone.

would permit the transfer of reducing equivalents from NADPH to NAD^+, thus enabling cofactor cycling (FIGURE 2). Using this system, morphine was converted to hydromorphone in high yield in the presence of low concentrations of cofactors, showing that cofactor cycling must be occurring (FIGURE 3). Very little dihydromorphine was produced, in contrast to systems without cofactor cycling, in which dihydromorphine typically predominated.

Biotransformation of morphine to hydromorphone and of codeine to hydrocodone is thus technically possible. Other approaches to cofactor cycling are also being investigated, specifically site-directed mutagenesis of morphine dehydrogenase to alter its cofactor specificity so that NAD^+ rather than $NADP^+$ becomes the preferred cofactor,[6] and the use as a biocatalyst of whole cells of recombinant *E. coli* expressing both morphine dehydrogenase and morphinone reductase.[7,8]

REFERENCES

1. BRUCE, N. C., C. J. WILMOT, K. N. JORDAN, A. E. TREBILCOCK, L. D. GRAY STEPHENS & C. R. LOWE. 1990. Microbial degradation of morphine alkaloids: identification of

morphinone as an intermediate in the metabolism of morphine by *Pseudomonas putida* M10. Arch. Microbiol. **154:** 465–470.

2. HAILES, A. M. & N. C. BRUCE. 1993. Biological synthesis of the analgesic hydromorphone, an intermediate in the metabolism of morphine, by *Pseudomonas putida* M10. Appl. Environ. Microbiol. **59:** 2166–2170.

3. HOLT, P-J., L. D. GRAY STEPHENS, N. C. BRUCE & C. R. LOWE. 1995. An amperometric opiate assay. Biosens. Bioelectronics **10:** 517–526.

4. FRENCH, C. E. & N. C. BRUCE. 1994. Purification and characterization of morphinone reductase from *Pseudomonas putida* M10. Biochem. J. **301:** 97–103.

5. FRENCH, C. E. & N. C. BRUCE. 1995. Bacterial morphinone reductase is related to Old Yellow Enzyme. Biochem. J. **312:** 671–678.

6. WALKER, E. H. & N. C. BRUCE. 1996. Towards engineering an improved morphine dehydrogenase. This volume.

7. FRENCH, C. E., A. M. HAILES, D. A. RATHBONE, M. T. LONG, D. L. WILLEY & N. C. BRUCE. 1995. Biological production of semisynthetic opiates using genetically engineered bacteria. Bio/Technology **13:** 674–676.

8. HAILES, A. M., C. E. FRENCH, D. A. RATHBONE & N. C. BRUCE. 1996. Engineering pathways in *Escherichia coli* for the synthesis of morphine alkaloid analgesics and antitussives. This volume.

New Approaches for the Verification of Kinetic Parameters of Immobilized Concanavalin A:Invertase Preparations Investigated by Flow Microcalorimetry[a]

PETER GEMEINER,[b] PETER DOČOLOMANSKÝ,[c]
JOZEF NAHÁLKA,[b] VLADIMÍR ŠTEFUCA,[d]
AND BENGT DANIELSSON[e]

[b]*Institute of Chemistry*
Slovak Academy of Sciences
SK-842 38 Bratislava, Slovakia

[c]*Institute of Molecular Physiology and Genetics*
Slovak Academy of Sciences
SK-833 34 Bratislava, Slovakia

[d]*Institut de Recherche et de Transfert sur les Lipides*
F-350 00 Rennes, France

[e]*Pure and Applied Biochemistry*
Chemical Center
University of Lund
S-221 00 Lund, Sweden

In our preceding paper,[1] we demonstrated a procedure based upon enzymic flow microcalorimetry using an enzyme thermistor (ET) to characterize the microkinetic properties of an immobilized enzyme (IME) and its further application in the screening of IMEs. In order to standardize the ET method (using the single ET unit called ET system 1 in FIGURE 1), it was necessary to show that the estimated relative kinetic parameter (ΔT_{max}) calorimetrically corresponds with the absolute value for the reaction rate within the whole measurement range. This report presents three experimental verification procedures. Two procedures are based on the adaptation of the flow-through ET-column to a mini-differential-reactor (DR) system with substrate recirculation and on post-ET-column methods for determination of the concentration change of the product (spectrophotometrically in ET system 2, FIGURE 2) or of the substrate (calorimetrically in ET system 3, FIGURE 3) with the IME-catalyzed enzymic hydrolysis. The third procedure is an independently operating DR system that spectrophotometrically estimates the concentration change of the product. The results obtained exhibited good correlation ($r = 0.921$) between the relative kinetic parameter ΔT_{max}, as determined calorimetrically by ET system 1, and the absolute value for the reaction rate (r_{max}), as determined by ET systems 2 and 3 (FIGURE 4).
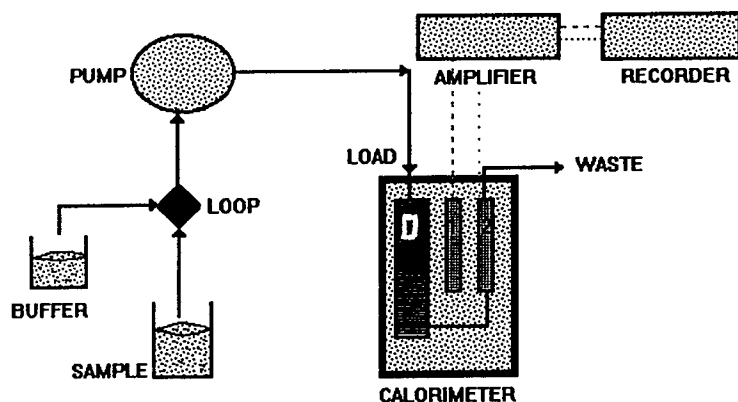
FIGURE 1. A standard ET unit (ET system 1). The main parts are the peristaltic pump (PUMP); the calorimeter with heat exchanger (I), standard reference column (1), and standard measurement column (2); the amplifier (with precision Wheatstone bridge); and the line recorder.

For the determination of r_{max}, the approaches proposed recently[2] have been extended. The new procedure is based on the adaptation of the mini-packed-bed-reactor (mPBR) configuration (ET-column in ET system 1) into a mini-differential-reactor (DR) system complemented by an appropriate post-ET-column enzymic analysis of the substrate or product. ET systems 2 and 3 are employed when monitoring of the concentration of the product or substrate (spectrophotometrically or calorimetrically, respectively) is required. Enzyme spectrophotometry constitutes
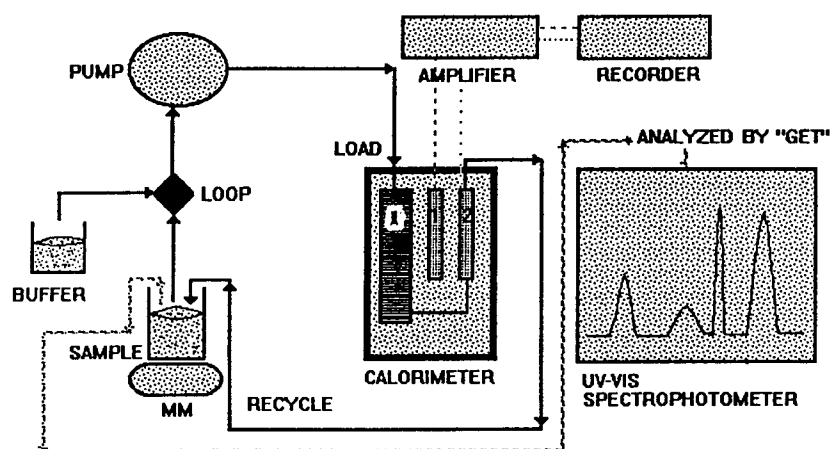
FIGURE 2. A standard ET unit adapted into a differential reactor system with recirculation of substrate solution combined with post-ET-column spectrophotometric analysis using the "glucose enzymatic" test (ET system 2). To the setup shown in FIGURE 1 were added a stirred reservoir (MM with magnetic stirrer) and a UV-VIS spectrophotometer.
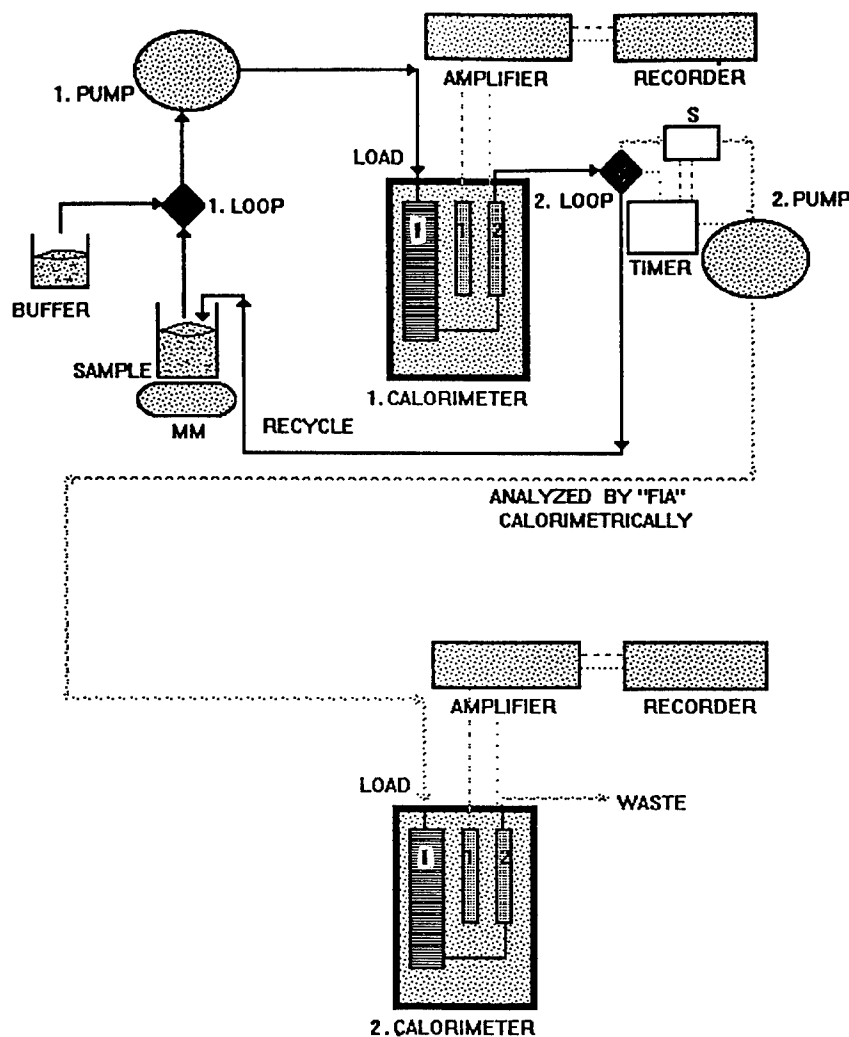
FIGURE 3. A standard ET unit adapted into a differential reactor system with recirculation of substrate solution combined with post-ET-column calorimetric flow-injection analysis (ET system 3). To the setup shown in FIGURE 1 were added a stirred reservoir (MM with magnetic stirrer), a time controller (TIMER), a sample collector (S), a second pulse-free pump, and a second ET unit.

a routine method for postcolumn analysis suitable for comparison with the calorimetric evaluation of the external differential reactor system[3] and the external stirred-batch reactor system[4] studied as reference systems. Absolute values for the maximum reaction rate, $r_{max(p)}$, of preparations with different amounts of IME (INV:Con A–cel Ia–e) determined using ET system 2 are listed in TABLE 1. (Note that INV = invertase,

Con A = concanavalin A, and cel = cellulose.) The calibration/correlation of the ΔT_{max} values (experimental data given in FIGURE 4B) with the $r_{max(p)}$ values (FIGURE 4A, TABLE 1) is shown in FIGURE 4C.

The $r_{max(s)}$ values were derived from experimental data (r_s, FIGURE 4D) obtained by flow microcalorimetry using a separate ET unit operating in FIA mode (ET system 3). The correlation of $r_{max(p)}$ and $r_{max(s)}$ values estimated with ET systems 2 and 3 is shown in FIGURE 4E.

From the data presented in FIGURES 4A–4C, it may be concluded that the screening of preparations with different amounts of IME (INV:Con A–cel I*a*–*e*) with the aid of either the relative kinetic parameter (norm ΔT_{max}) or the absolute value for the maximum reaction rate (r_{max}) provides comparable relative activities of the preparations (FIGURE 4C, $r = 0.921$). Consequently, the maximum response observed, ΔT_{max}, is a suitable parameter for use in the routine screening of IME
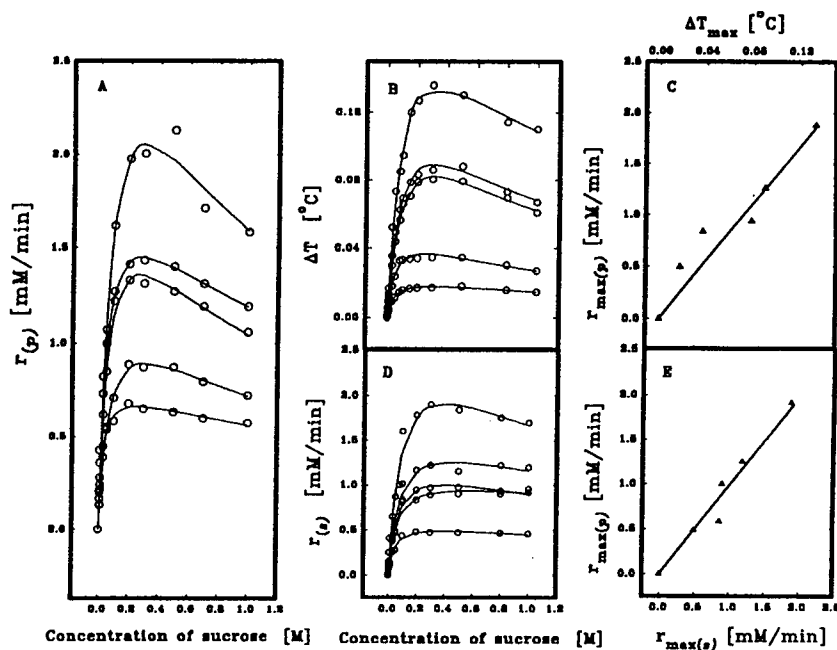
FIGURE 4. Two methods for the calibration of an ET demonstrated in the triads of panels A, B, C and A, D, E by the correlation between the norm ΔT_{max} (the maximum response value corresponding to each individual kinetic curve) and the absolute value for the reaction rate. The results presented on the first triad were measured using ET system 2 (FIGURE 2) and the results presented on the second triad were measured using ET system 3 (FIGURE 3). Panels A and D show the substrate concentration–dependent reaction rate responses, where the reaction rate *r* was estimated either by spectrophotometric post-ET-column analysis (A) or by calorimetric post-ET-column flow-injection analysis (D). Panel B represents the substrate concentration–dependent temperature responses, where the temperature signal ΔT was measured by the single ET unit (FIGURE 1). Preparations of INV:Con A–cel I*a*–*e* containing different amounts of adsorbed invertase and the same amounts of linked Con A (29.97 mg/g) were employed. Invertase concentrations (mg/g): 1.54, 3.64, 4.77, 6.18, and 7.44.

TABLE 1. Kinetic Constants of Preparations of INV:Con A–cel I[a]

Sample	$K_m \pm$ SE (mM)	$K_i \pm$ SE (mM)	ΔT_{max} (°C $\times$ 10^{-3})	r_{max} (mM/min)
I*a*	44.7 $\pm$ 3.18	2492.5 $\pm$ 262.7	0.018	0.66
I*b*	55.6 $\pm$ 6.03	1326.2 $\pm$ 207.4	0.036	0.86
I*c*	48.3 $\pm$ 3.94	1756.9 $\pm$ 131.1	0.037	0.89
I*d*	107.5 $\pm$ 8.02	872.5 $\pm$ 91.4	0.082	1.35
I*e*	101.1 $\pm$ 7.42	933.9 $\pm$ 107.7	0.089	2.05
I*f*	113.5 $\pm$ 11.66	1209.2 $\pm$ 168.2	0.133	—

[a]Preparations of INV:Con A–cel I*a*–*f* contained 29.97 mg Con A/g and different amounts of adsorbed invertase (mg/g: I*a* 1.54, I*b* 3.64, I*c* 4.77, I*d* 6.18, I*e* 7.44, and I*f* 11.81) and were described and defined in previous articles.[2,6] The kinetic constants were determined by equations 3 (K_m and K_i), 5 (r_{max}), and 6 (ΔT_{max}) from reference 6 and using ET systems 1 and 2.

preparations. Moreover, the reaction parameter, r_{max}, verified by two different techniques (ET systems 2 and 3), is a valuable measure of the absolute activities of IME preparations (FIGURE 4E, $k = 1.02, r = 0.934$).

The validity of the assumptions in the proposed model for the present ET unit was verified in our previous articles.[3,4] The nonideal adaptation of the flow-through column in the ET unit from a mini-packed-bed-reactor configuration (ET system 1) to a mini-recycling-DR system (ET systems 2 and 3) is probably one of the most important potential deviations from the model. To facilitate the analysis, intrinsic kinetic parameters were determined using the independent DR system coupled with postcolumn analysis of the glucose concentration. Using INV–cel I (invertase covalently linked to cel I) in the DR, the values of $K_m = 48.5$ mM and $K_i = 1752.0$ mM were calculated from the experimental results plotted in FIGURE 5A. These values were similar to those obtained for both free invertase, $K_m = 36.4$ mM and $K_i =$
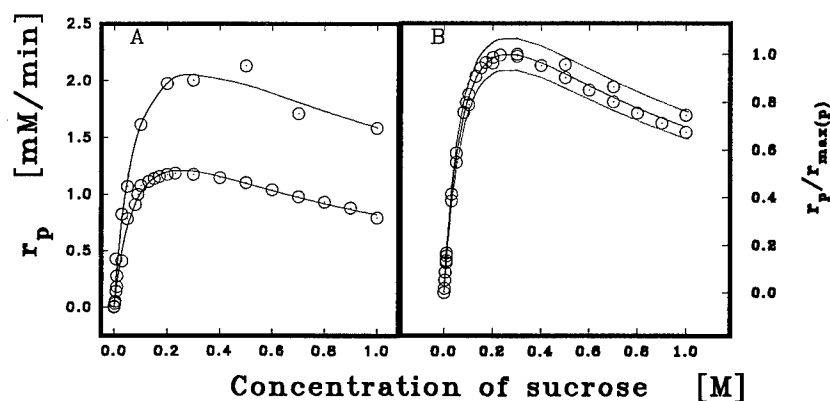
FIGURE 5. Substrate concentration–dependent temperature responses as measured by ET system 2 with preparation INV:Con A–cel I*c* (upper line) and by the DR system with preparation INV:Con A–cel I (bottom line). The validity of the kinetic model was verified by transforming the fitted lines (panel A) into normalized shape (panel B). Normalized lines were calculated from all experimental data shown in panel A and the dotted lines border the 95% interval of confidence of the mathematical model used.

1783 mM (corresponding satisfactorily with values published by Geankoplis *et al.*[5]), and immobilized invertase (INV:Con A–cel Ic; invertase biospecifically adsorbed to Con A–cel I), K_m = 48.3 mM and K_i = 1752.0 mM (FIGURE 5A). The finding that the adaptation of the mini-PBR to a mini-DR with recirculation of substrate (FIGURE 5B) does not result in any change of the compliance with the estimated K_m and K_i values for invertase immobilized in the mini-DR as calculated by a nonlinear regression (see equation 4 and Table II in reference 6) confirmed the proper choice of working conditions.

The demonstrated data proved that, within the whole experimental range applied in this study, the parameter T_{max} could be employed instead of the true reaction rate for IME screening. Moreover, the general detection principle and the standardized configuration of the ET favor the double use of enzyme thermistors (i.e., including ET systems 2 and 3) for normal screening of IMEs and as miniaturized DR systems allowing dual measurements of kinetic parameters.

REFERENCES

1. DOČOLOMANSKÝ, P., P. GEMEINER, D. MISLOVIČOVÁ, V. ŠTEFUCA & B. DANIELSSON. 1995. Ann. N.Y. Acad. Sci. **750:** 441–443.
2. DOČOLOMANSKÝ, P., P. GEMEINER, D. MISLOVIČOVÁ, V. ŠTEFUCA & B. DANIELSSON. 1994. Biotechnol. Bioeng. **43:** 286–292.
3. ŠTEFUCA, V., P. GEMEINER, L. KURILLOVÁ, B. DANIELSSON & V. BÁLEŠ. 1990. Enzyme Microb. Technol. **12:** 830–835.
4. WELWARDOVÁ, A., P. GEMEINER, E. MICHÁLKOVÁ, L. WELWARD & A. JAKUBOVÁ. 1993. Biotechnol. Tech. **7:** 809–814.
5. GEANKOPLIS, C. J., E. R. HAERING & M. C. HU. 1987. Ind. Eng. Chem. **26:** 1810–1817.
6. GEMEINER, P., P. DOČOLOMANSKÝ, J. NAHÁLKA, V. ŠTEFUCA & B. DANIELSSON. 1996. Biotechnol. Bioeng. **49:** 26–35.

The Effect of Water Content on the Thermostability of Solid-State Proteins

GUIDO GRECO, JR., DOMENICO PIROZZI,
GIUSEPPE TOSCANO, AND MICHELE MAREMONTI

Dipartimento di Ingegneria Chimica
Università degli Studi di Napoli "Federico II"
80125 Napoli, Italy

INTRODUCTION

To some extent, further progress in nonaqueous enzymology is restricted by the lack of fundamental understanding of solid-state enzyme deactivation. Recent studies[1–9] have elucidated some effects of the hydration level on both activity and stability of enzymes in dehydrated environments. Interactions between a protein molecule and the surrounding water lead to a greater conformational mobility of enzymes of critical significance for enzymatic activity. On the other hand, the thermostability of solid-state proteins is known to decrease as the amount of enzyme-bound water increases.[10,11] Consequently, the hydration level is a critical parameter to take into account in order to optimize industrial applications of nonaqueous enzymatic processes.

Three unrelated enzymes (α-chymotrypsin, EC 3.4.21.1, from bovine pancreas; acid phosphatase, EC 3.1.3.2, from potato; invertase, EC 3.2.1.26, from *Saccharomyces cerevisiae*) have been used as a model to study (i) the influence of the enzyme-bound water on long-term protein thermostability and (ii) the effect of nonaqueous reaction media on the deactivation dependence on the enzyme hydration level.

MATERIALS AND METHODS

The following enzymatic systems were used: (a) saccharose hydrolysis by invertase in 200 mM Na-acetate buffer, pH 4.65; (b) p-nitrophenyl phosphate (PNPP), disodium salt, hydrolysis by acid phosphatase in 200 mM Na-citrate buffer, pH 5.60; (c) n-succinyl-phenylalanine-p-nitroanilide (SUPHEPA) hydrolysis by α-chymotrypsin in 100 mM triethanolamine-HCl-NaOH buffer, pH 7.8.

Samples of enzyme solutions in the appropriate buffer were dried under vacuum in borosilicate-glass tubes at 20 °C, in the presence of silica gel, for at least seven days. In some runs, a subsequent, seven-day pretreatment was carried out in the presence of saturated K_2SO_4 solutions. The test tubes were then placed into a glycerol bath at the deactivation temperature. In some runs, 1 mL of n-hexadecane was added. Samples were withdrawn at predetermined time intervals and cooled down to 4 °C. The enzyme was then dissolved by adding 1 mL of buffer and by gently

stirring for 10 min. As regards the runs with hexadecane, the same procedure was followed and the enzyme was entirely recovered in the aqueous phase. The residual activity of the enzyme was subsequently assayed in aqueous solution.

Thermogravimetric analyses were also carried out (Du Pont 951 TGA) on solid-state enzyme samples dried in petri dishes according to the same general procedures described above.

RESULTS AND DISCUSSION

In previous works on enzyme deactivation kinetics,[12-15] we used an empirical model for correlative and heuristic purposes. The model is based on the straightfor-
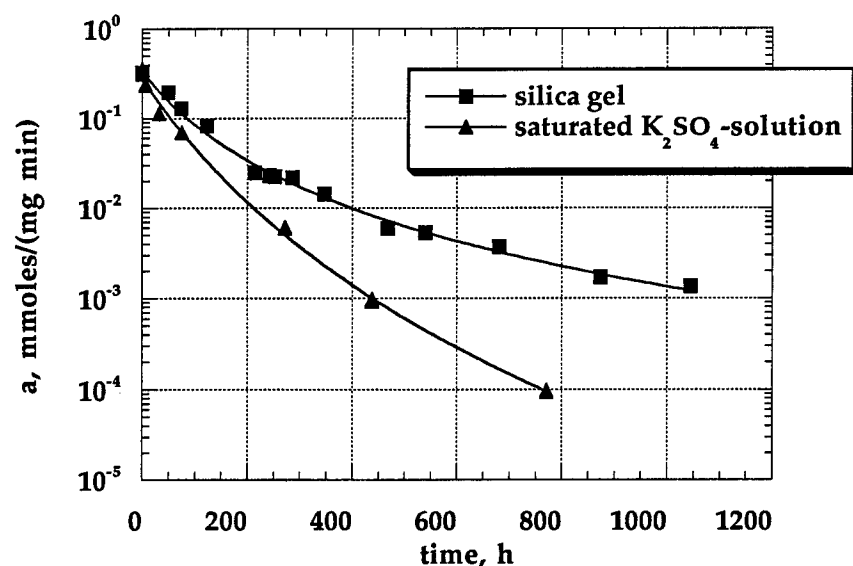
FIGURE 1. Thermal deactivation of solid-state invertase at 100 °C. Effect of initial water content.

ward transition from native enzyme N (specific activity a_N) to a partially deactivated enzyme D (specific activity a_∞) with irreversible, n-th order kinetics. Accordingly, the overall specific activity $a(t)$ obeys the following relationship:

$$a(t) = (a_N - a_\infty)(1 + kt)^{-n} + a_\infty$$

where k is a pseudo-first-order kinetic constant. All the experimental data discussed in the present work are interpolated by nonlinear regression curves based on this model. All curves clearly show departure from first-order kinetics. Nonzero activity levels are attained in sufficiently long experimental runs.

A first set of experiments were devoted to the determination of the effect of initial water amount on enzyme deactivation. In FIGURES 1–3, deactivation data pertaining to enzyme samples that were virtually anhydrous since the very beginning of the experiment are compared to those corresponding to pretreatment in the presence of saturated K_2SO_4 solutions. The results indicate that, whatever the enzyme system considered, the higher the initial amount of water bound to the enzyme, the faster is its deactivation.

In order to corroborate this result further, acid phosphatase (desiccated in the presence of saturated K_2SO_4 solutions) underwent an initial deactivation at 100 °C. After approximately 40 hours of exposure, the samples were withdrawn and reequili-
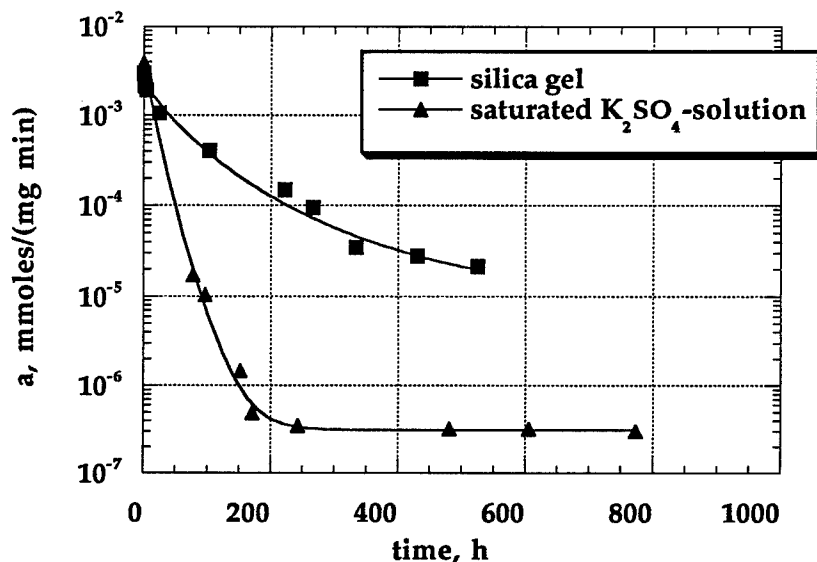
FIGURE 2. Thermal deactivation of solid-state acid phosphatase at 100 °C. Effect of initial water content.

brated in the presence of saturated K_2SO_4 solutions according to the usual procedure. Subsequently, the deactivation run was started again. Results are reported in FIGURE 4, together with a deactivation run with no intermediate reequilibration, for comparison purposes. It can be seen that increasing the amount of water increases considerably the rate of enzyme deactivation. Incidentally, it can be observed that the asymptotic activity value achieved does not depend on water content. This seems to indicate that the steady-state activity pertains to a totally dehydrated, stable enzyme structure.

FIGURE 5 shows the results of thermogravimetric analyses (TGA) performed on fragments of solid-state enzyme at 100 °C, in terms of residual water content. The residual specific activity was also determined for samples subjected to TGA. The
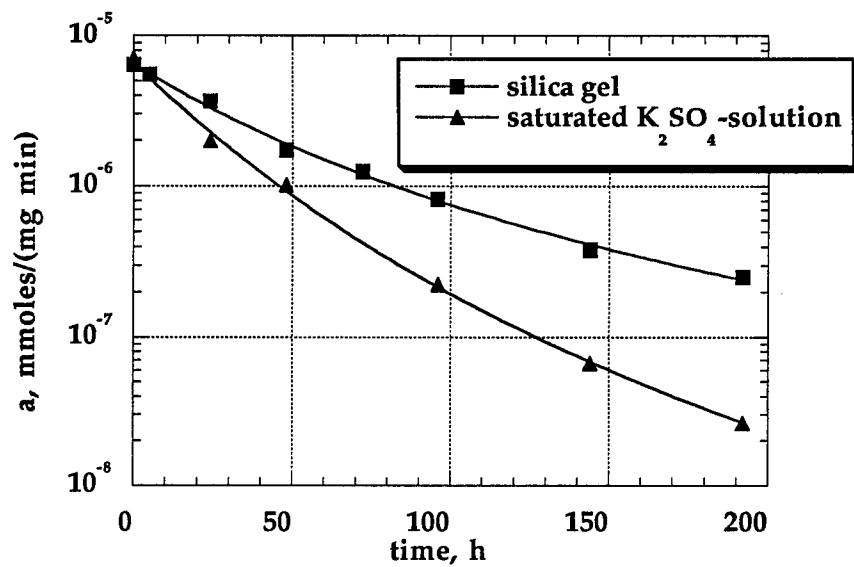
FIGURE 3. Thermal deactivation of solid-state α-chymotrypsin at 100 °C. Effect of initial water content.
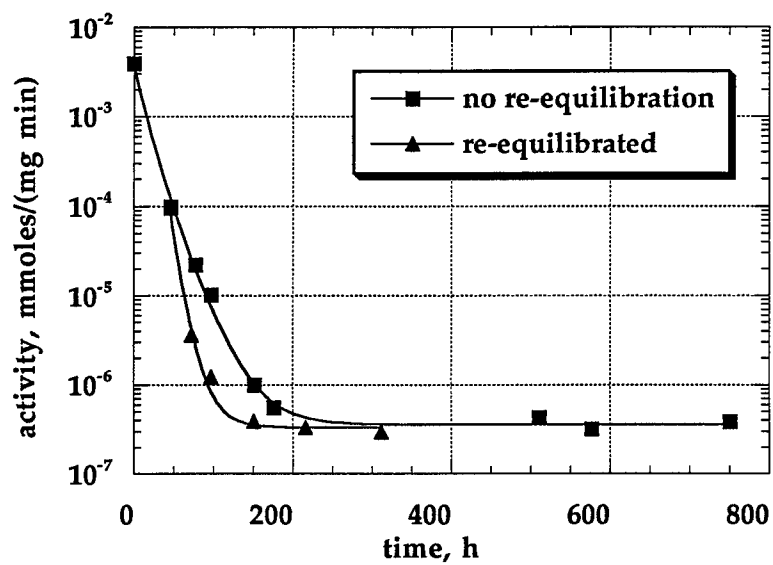
FIGURE 4. Thermal deactivation of solid-state acid phosphatase at 100 °C. Effect of intermediate reequilibration.
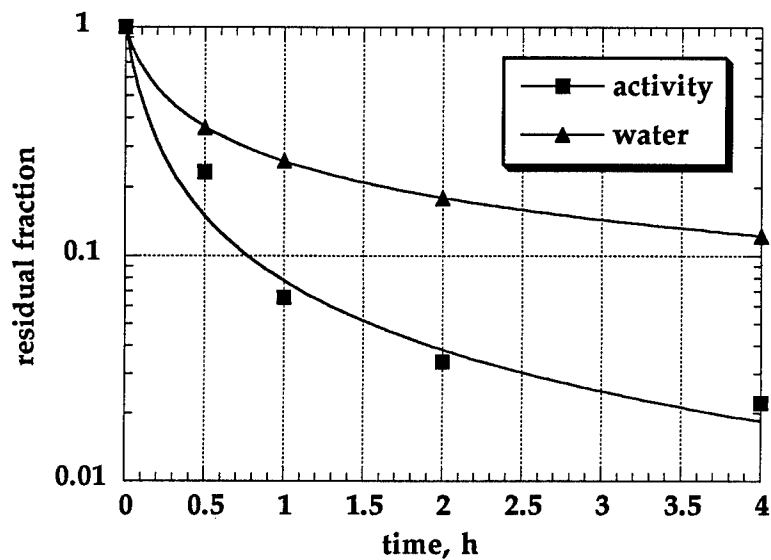
FIGURE 5. Thermal deactivation of solid-state α-chymotrypsin at 120 °C. Residual water content and residual activity as a function of time.
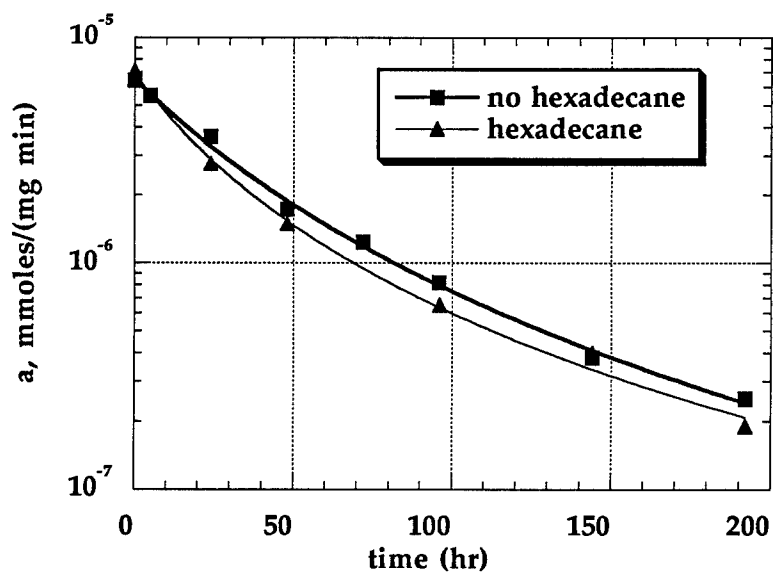
FIGURE 6. Thermal deactivation of solid-state α-chymotrypsin at 100 °C. Silica-gel equilibration. Effect of hydrophobic solvent.
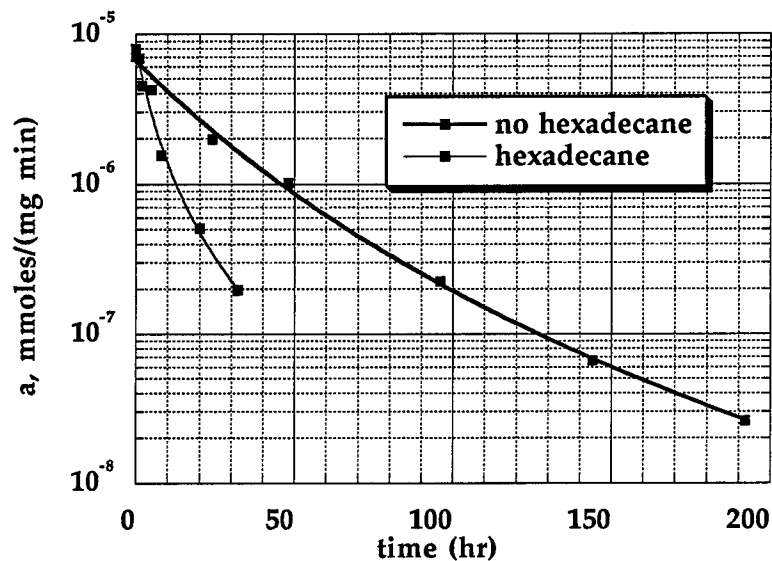
FIGURE 7. Thermal deactivation of solid-state α-chymotrypsin at 100 °C. Equilibration with saturated K_2SO_4 solution. Effect of hydrophobic solvent.

time-behavior of residual water and of residual activity is substantially the same, as indicated by the values of the model parameters used to correlate both data sets.

The effect of chymotrypsin exposure to *n*-hexadecane was analyzed as well. The virtually anhydrous, solid-state enzyme (FIGURE 6) is virtually unaffected. As regards the samples equilibrated with saturated K_2SO_4 solutions (FIGURE 7), the presence of a strongly hydrophobic layer "sealing" the protein determines a faster activity decay, as compared to that achieved in the absence of such a hindrance to water elimination.

CONCLUSIONS

The rate of deactivation of solid-state enzyme increases with increasing water content.

The kinetics of water elimination has a critical influence on the rate of deactivation. It could even be the overall rate-limiting step in solid-state enzyme deactivation.

The latter effect is confirmed indirectly by activity tests carried out in the presence of *n*-hexadecane. The hydrophobic solvent does not seem to affect the rate of deactivation per se to any significant extent. On the contrary, when water elimination becomes critical, the solvent accelerates enzyme deactivation, possibly by slowing down water elimination.

REFERENCES

1. ZAKS, A. & A. M. KLIBANOV. 1988. J. Biol. Chem. **263**(7): 3194–3201.
2. ZAKS, A. & A. M. KLIBANOV. 1988. J. Biol. Chem. **263**(17): 8017–8021.
3. YAMANE, T., Y. KOJIMA, T. ICHIRYU, M. NAGATA & S. SHIMIZU. 1989. Biotechnol. Bioeng. **34**: 838–843.
4. RUPLEY, J. A. & P. CARERI. 1991. Adv. Protein Chem. **41**: 37–72.
5. SCHULZE, B. & A. M. KLIBANOV. 1991. Biotechnol. Bioeng. **38**: 1001–1006.
6. DORDICK, J. S. 1992. Biotechnol. Prog. **8**: 259–267.
7. CLAPES, P., G. VALENCIA & P. ADLERCREUTZ. 1992. Enzyme Microb. Technol. **14**: 575–580.
8. LJUNGER, G., P. ADLERCREUTZ & B. MATTIASSON. 1994. Enzyme Microb. Technol. **16**: 751–755.
9. HALLING, P. J. 1994. Enzyme Microb. Technol. **16**: 178–206.
10. DORDICK, J. S. 1989. Enzyme Microb. Technol. **11**: 194–211.
11. VOLKIN, D. B., A. STAUBLI, R. LANGER & A. M. KLIBANOV. 1991. Biotechnol. Bioeng. **37**: 843–853.
12. GRECO, G., JR., D. PIROZZI, M. MAREMONTI, G. TOSCANO & L. GIANFREDA. 1993. The kinetics of enzyme inactivation. *In* Stability and Stabilization of Enzymes. W. J. J. Van den Tweel, A. Harder & R. M. Buitelaar, Eds. Elsevier. Amsterdam/New York.
13. TOSCANO, G., M. MAREMONTI, D. PIROZZI & G. GRECO, JR. 1994. Biocatalysis **11**: 321–327.
14. TOSCANO, G., D. PIROZZI, M. MAREMONTI & G. GRECO, JR. 1994. Biotechnol. Bioeng. **44**: 682–689.
15. TOSCANO, G., D. PIROZZI, M. MAREMONTI, L. GIANFREDA & G. GRECO, JR. 1994. Catal. Today **22**: 489–510.

The Use of Rational Mutagenesis to Modify the Chain Length Specificity of a *Rhizopus delemar* Lipase

MICHAEL J. HAAS, ROLF D. JOERGER, GREGORY KING,
AND ROBERT R. KLEIN

Eastern Regional Research Center
Agricultural Research Service
United States Department of Agriculture
Wyndmoor, Pennsylvania 19038

INTRODUCTION

Due to the occurrence of the carboxylic acid ester bond in numerous compounds of pharmaceutical, medical, and industrial importance, there is widespread interest in the characterization of lipases (triacylglycerol acylhydrolase, EC 3.1.1.3) and their use as applied catalysts. Within the past ten years, lipase-encoding genes from several organisms have been cloned. Some of these have been expressed in their new genetic backgrounds. Within the past six years, X-ray diffraction studies have produced models of the three-dimensional structures of several lipases. Also within this time frame, biochemical and molecular genetic data have been gathered that allow the identification, in some lipases, of those amino acids that play crucial roles in enzyme activity. These areas of research have converged to the extent that a coordinated approach, using computer-assisted molecular modeling and recombinant DNA technology, to examine structure-function relationships in these enzymes is now possible. Our laboratory has recently completed such a study[1] and the results of that study will form the basis of this review.

Lipases can be classified according to their abilities to hydrolyze the ester bonds of triglycerides. Two main groups of enzymes have been identified: (a) those hydrolyzing all three esters of the substrate and (b) those hydrolyzing only the terminal [1,3-] positions. Other groupings can also be made, for example, based on whether an enzyme displays specificity with regard to the degree of substitution of the glyceride or with regard to chain length or degree and location of unsaturation in the fatty acyl portions of the glyceride. It is axiomatic that the origins of these specificities lie in the amino acid sequences of the polypeptide chains of the enzymes. However, detailed information regarding the structural determinants of these selectivities is largely unknown.

The class of fungal lipases exhibiting 1,3-positional specificity toward the substrate contains enzymes from several organisms. These share varying degrees of genetic homology, often quite high, and have similar three-dimensional structures and active-site geometries. This group contains lipases from *Rhizomucor miehei* (Rm),[2] *Rhizopus delemar* (Rd),[3] *Rhizopus niveus*,[4] *Humicola lanuginosa* (Hl),[5] and *Penicillium camembertii* (Pc).[6] Several enzymes in this group are commercially available and are among the lipases most commonly used as applied catalysts. The

work of Derewenda and others has resulted in 3-D structures for a number of these enzymes[7-9] and in delineation of their probable active sites[7] and substrate-binding domains.[10]

The enzymes of this family are composed of single polypeptide chains, with molecular masses between 30,000 and 35,000, and all adopt a similar three-dimensional structure (FIGURE 1). It is likely that all members of the family are initially synthesized as preproenzymes, which then undergo proteolytic maturation. The catalytic center consists of a triad of amino acids: serine, histidine, and aspartic acid. The serine is responsible for a nucleophilic attack on the carbonyl carbon of the scissile ester bond. This serine lies within a consensus sequence, Gly-X-Ser-X-Gly, which is sufficiently conserved among lipases and esterases as to be diagnostic of this enzyme family. The catalytic triad is buried beneath the solvent-accessible surface of the protein. One loop of the peptide chain (the "lid") is capable of lying over the active-site cleft. The phenomenon of interfacial activation, whereby lipases become catalytically active only in the presence of a solvent-substrate interface, appears to result from a stabilization of the open-lid conformation, exposing the active site to substrate. Near the active site, there is a shallow surface trough that appears to accommodate the acyl chain of the scissile fatty acid (FIGURE 2). Based on insights provided by examinations of the three-dimensional structures of the *Rh. delemar* and *Rm. miehei* lipases, we have conducted directed mutagenesis of the gene for the *Rh. delemar* enzyme, focusing on sites near the active center, within the lid, and in the substrate-binding domains. We have then examined the effects of such mutagenesis on the activities and chain length specificities of the resulting enzymes.

MATERIALS AND METHODS

Molecular Modeling

Initial studies employed the crystal coordinates of the structure of the Rm lipase (generously provided by Z. Derewenda), which is highly homologous to the Rd enzyme[11] and for which crystallographic data indicate the site of binding of active-site-directed inhibitors.[10] Subsequent work utilized the coordinates of the Rd enzyme.[8] Molecular modeling was performed on an Indigo2 computer (Silicon Graphics, Incorporated, Mountain View, California) using Sybyl software (Tripos, Incorporated, St. Louis, Missouri).

The main experimental approach involved visual inspection of the models to identify those amino acid residues with apparent potential for physical interference with the fatty acyl chain of bound substrate. These residues were then subjected to site-directed mutagenesis. Other mutagenesis experiments involved changing amino acids that might play a role in enzyme activation or the catalytic event.

DNA Manipulations

Vector Construction

Plasmid pUC8.2-14 contains a cDNA encoding the entire preprolipase of *Rh. delemar* under the control of the lactose operon regulatory elements.[5] By introducing
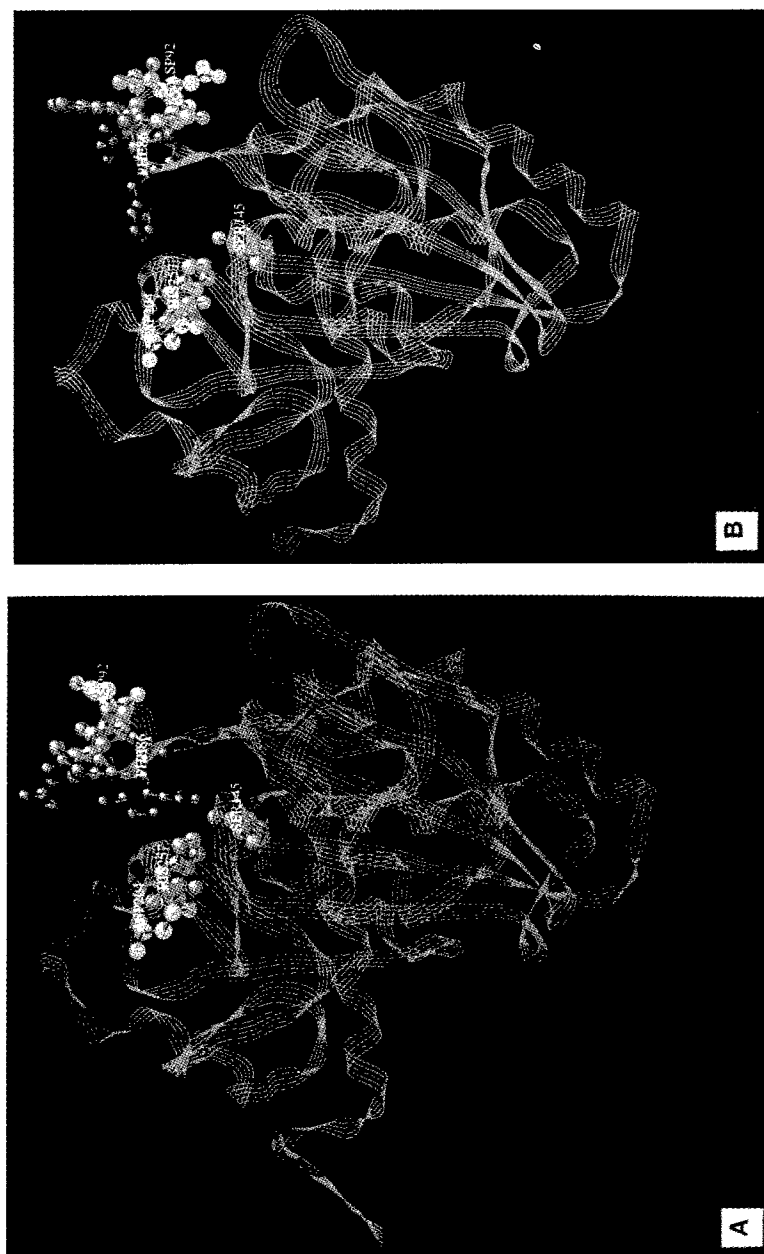
FIGURE 1. Three-dimensional structure of the *Rhizopus delemar* lipase, based on crystallographic coordinates.[8,9] In panel A, the "lid", residues 86–92, is in the closed conformation. In panel B, the lid is partially opened, exposing the active-site residues: ser145, asp204, and his257.
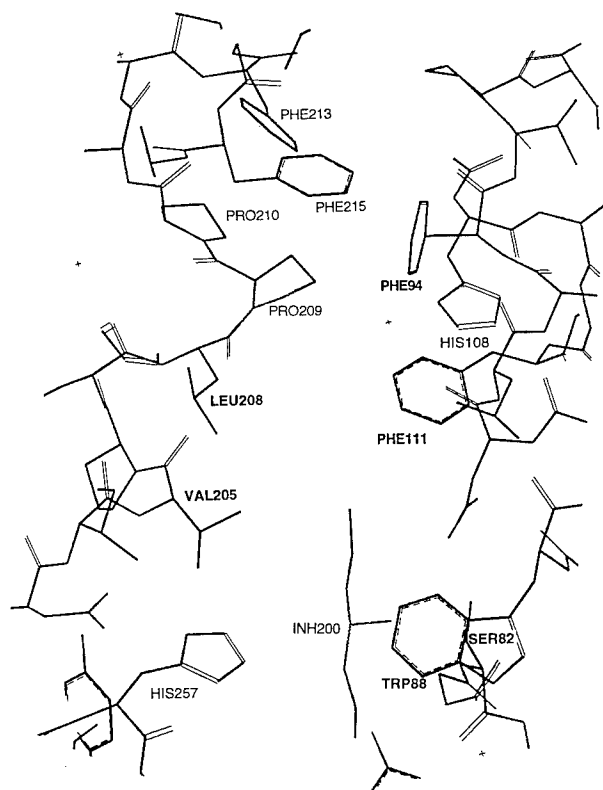
FIGURE 2. Structure of a portion of the *Rhizomucor miehei* (Rm) lipase with the inhibitor *n*-hexylphosphonate ethyl ester (INH200) bound in the active site and probable substrate-binding region (coordinates kindly provided by Z. Derewenda).[10] Residues that were the focus of the present study are visible. These include ser82 (thr83 in *Rhizopus delemar* lipase), which stabilizes the oxyanion catalytic intermediate; trp88 (ala89 in *Rh. delemar*), which is in the lid of the enzyme; and residues lining the substrate-binding region. The corresponding binding region residues in the *Rh. delemar* lipase are phe95 in place of Rm phe94, his109 (Rm his108), phe112 (phe111), val206 (val205), val209 (leu208), pro210 (pro209), pro211 (pro210), phe214 (phe213), and phe216 (phe215).

*Nco*I sites at appropriate locations in this plasmid, it was possible to isolate *Nco*I-*Bam*HI fragments encoding either the prolipase or the mature lipase. These were subcloned into plasmid pET11-d, creating plasmids pET11-d-431 (produces mature lipase) and pET11-d-1231s (produces prolipase), which were proficient at lipase production (FIGURE 3).[12] These vectors allowed the isolation of relatively large amounts of enzyme. For the experiments described here, the origin of phage f1 was introduced into these plasmids, producing pET11-d-f1-431 and pET11-d-f1-1231s.[1] This modification allowed the production of single-stranded circular DNA for use in site-directed mutagenesis without reducing the suitabilities of the plasmids for the production of enzyme.
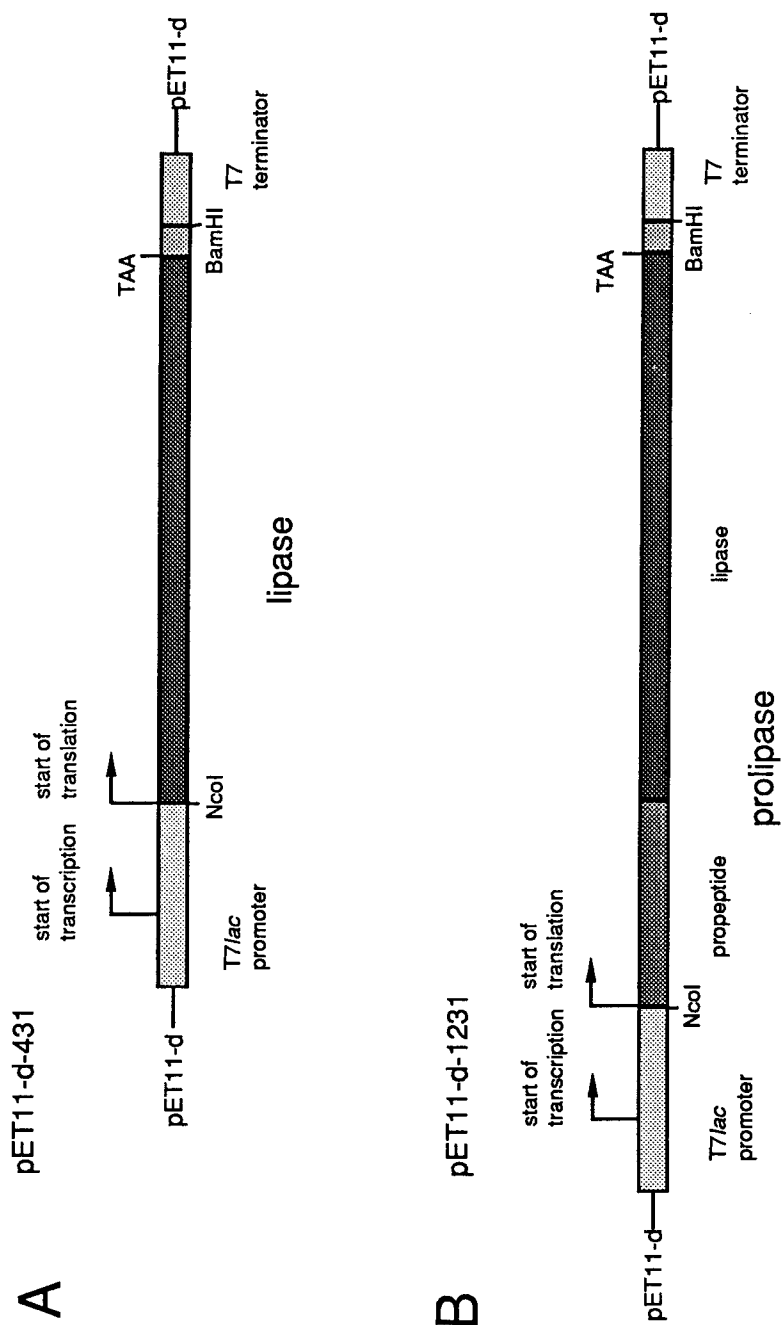
FIGURE 3. Schematic representation of the (A) lipase- and (B) prolipase-encoding DNA segments inserted into the expression plasmid pET11-d. These constructs[12] were the basis of those created here, by the insertion of the phage f1 origin of replication, for regulated lipase gene expression and the production of single-stranded circular DNAs. The termination codon for lipase and prolipase is indicated by the nucleotide triplet TAA.

Oligonucleotide-directed Mutagenesis

Single-stranded DNA for use in site-directed mutagenesis was obtained by infecting plasmid-containing *E. coli* JM101 cells with helper phage M13KO7 as described.[12] Mutagenesis was carried out by the method of Kunkel[13] using the Muta-Gene M13 *in vitro* Mutagenesis Kit (Bio-Rad Laboratories, Hercules, California). Mutagenic primers were designed to change both the amino acid sequence at a desired single site and the restriction enzyme fragmentation pattern of the DNA. This facilitated the detection of mutated plasmid DNA. Primers were so constructed that all possible amino acids were inserted at the site of interest.

DNA sequences were determined by the method of Sanger *et al.*[14] using the Sequenase Version 2.0 DNA Sequencing Kit (United States Biochemical, Cleveland, Ohio).

Mutant Screening

For the detection of modified prolipases produced from plasmid pET11-d-f1-1231s, screening relied on the ability of free fatty acids released from triglycerides by lipase to cause a distinctive change in the fluorescence spectrum and intensity of the dye rhodamine B included in solid growth medium containing single homogeneous triglycerides.[15] DNA sequencing was used to confirm the presence of the appropriate mutation in plasmids identified in this manner.

Such a phenotypic screening method could not be used to detect modified mature lipases because it was not possible to recover viable cells producing active mature enzyme. Therefore, to introduce mutations into the mature lipase, mutations created in the prolipase gene were transferred into the mature lipase gene by recombinant DNA techniques. DNA sequencing verified the acquisition of the mutations.

Enzyme Production

Late log phase cultures of *E. coli* BL21 (DE3) harboring wild-type or mutant plasmids were induced for lipase production by the addition of isopropyl-β-D-thiogalactoside and were harvested after 3 to 4 hours. Cells producing prolipase were broken by sonication. This lysate was used directly as the source of active prolipase.

All versions of the mature lipase, wild type and mutant, required refolding of the enzyme, initially present in inclusion bodies, before determination of enzyme activity.[11] To do this, the cells were broken by lysozyme-detergent treatment and their inclusion bodies were recovered by centrifugation. These were then solubilized in 8 M urea and the lipase within them was refolded by dilution in the presence of cystine and cysteine. Refolded mature lipase was purified to homogeneity by affinity and ion exchange chromatographies.

Enzyme Activity Measurements

Lipase activities were measured titrimetrically by a pH-stat method[16] at 25 °C and pH 7.5 using 0.1 N NaOH as the titrant. The substrates were 200 mM tributyrin (TB,

a triglyceride containing 4-carbon fatty acids), tricaprylin (TC, a homoglyceride containing 8-carbon fatty acids), or olive oil (OO, predominantly 18-carbon fatty acids) emulsified in aqueous 4.2% gum arabic solutions containing 14 mM $CaCl_2$. A unit (U) of activity released one micromole of fatty acid per minute.

Substrate selectivities were measured by incubation of the purified enzyme (in the case of the mature lipase) or total cell lysate (in the case of prolipase) at pH 7.5 for 2 h at 30 °C in solutions containing 0.4 M each of tributyrin, tricaprylin, and triolein. The degree of hydrolysis of each substrate was then determined by gas chromatography.

RESULTS AND DISCUSSION

Mutagenesis Experiments

In our experience, the production of active mature lipase is toxic to *E. coli*, whereas prolipase synthesis is tolerated. Therefore, when a phenotypic assay was to be used to assess the effects of site-directed mutagenesis on enzyme activity, the mutations were first created in the prolipase gene. This was then expressed in *E. coli*. After using rhodamine media to identify mutant prolipases of interest, these mutations were transferred into the mature lipase gene. This gene was expressed at high levels, leading to the accumulation of inclusion bodies containing inactive mutant mature lipases. These were isolated and the lipase within them was solubilized and renatured to yield active enzyme.

To examine the effects on activity of particular amino acid substitutions within the lid or active site of the lipase, the desired mutations were introduced into the gene for the mature enzyme. The mutated lipases encoded by these genes were then purified from inclusion bodies and characterized.

The introduction of the origin of replication of phage f1 into the lipase and prolipase expression plasmids, as first described for the transcription termination factor, rho,[17] created plasmids that could be used not only for lipase production, but also for production of the single-stranded DNAs required for site-directed mutagenesis.

Role of Threonine (thr) 83 in Facilitating Catalysis

In the Rm lipase, serine (ser) 82 lies very close to ser144, the active-site serine. It has been postulated that ser82 assists catalysis by stabilizing the tetrahedral oxyanion catalytic intermediate.[10] The analogous residue in the Rd lipase is a threonine (thr) located at position 83. The mutagenic conversion of thr83 to an alanine (ala) decreased the specific activity by almost three orders of magnitude (TABLE 1). When thr83 was mutagenically converted to a serine, the specific activities on various substrates were between one-fifth and one-half of that of the wild-type enzyme (TABLE 1). Alanine is unable to supply a hydroxyl group to stabilize the transition state intermediate, whereas it is feasible that serine could provide this stabilization. Thus, these data support the postulated role for ser82/thr83 in the catalytic event. Similar results have been reported for the *Penicillium camembertii* monoglyceride and diglyceride lipase.[18]

Relationship of Tryptophan in the Lid to Enzyme Activity

In this family of enzymes, a short stretch of the peptide chain (residues 86 to 92 in the Rd lipase) occludes the active site in the absence of substrate.[7] It has been postulated, and demonstrated using inhibitors,[10,19] that this lid is displaced when substrate analogues bind to the active site. This is thought to be the structural basis of the biochemical phenomenon termed "interfacial activation," the prerequisite that a substrate-water interface be present before a lipase will be catalytically active. Except for the Rd lipase, all known members of this family contain a trp in the lid, at a site corresponding to the alanine in position 89 of the Rd lipase. The presence of such a highly conserved residue suggests that the trp may play a crucial role in interfacial activation. To investigate this theory, ala89 in the Rd lipase was mutageni-cally converted to trp and the effects of this change on enzyme activity were determined. There was no increase in enzyme activity. Instead, there was a 22–42% reduction in specific activity relative to that of the purified wild-type enzyme (TABLE 1). However, compared to the wild-type enzyme, there were no profound changes in the relative activity toward various substrates tested (TABLE 1, FIGURE 4). Further work is required to precisely identify the importance and role of the trp in the lids of these enzymes.

Directed Mutagenesis of Sites within the Substrate-binding Groove

Studies with the Rm lipase employing the active-site-directed covalent inhibitor *n*-hexylphosphonate ethyl ester have identified a groove on the surface of the enzyme that appears to accommodate the fatty acyl chain of the scissile ester of the substrate (FIGURE 2).[10] Our goal was to determine whether alteration of residues within this groove would affect activity or substrate preference. In the Rd lipase, residues lying in positions 95 (phe), 112 (phe), 206 (val), and 209 (val) (corresponding to Rm residues 94, 111, 205, and 208, respectively) form part of this groove and are highly conserved in actuality or functionality in the Rd, Rm, Hl, and Pc enzymes.[9] These sites were individually subjected to site-directed mutagenesis using primers that would introduce all possible amino acid substitutions at these locations. The result-ing prolipase DNAs were introduced into bacteria by transformation or electropora-tion and expressed.

TABLE 1. Titrimetric Analysis (Single-Substrate Assay) of Lipolytic Activity of Refolded and Purified Recombinant Mature Lipases

Mutation[a]	Specific Activity (U/mL)[b]		
	Olive Oil	Tricaprylin	Tributyrin
wild type	3149	8539	2944
thr83 → ala	4	7	1
thr83 → ser	1664	3350	442
ala89 → trp	2106	6628	1702

[a]Amino acids numbered as in reference 5.
[b]Micromoles of fatty acid released per minute per mg of protein. The values are averages of two experimental determinations.
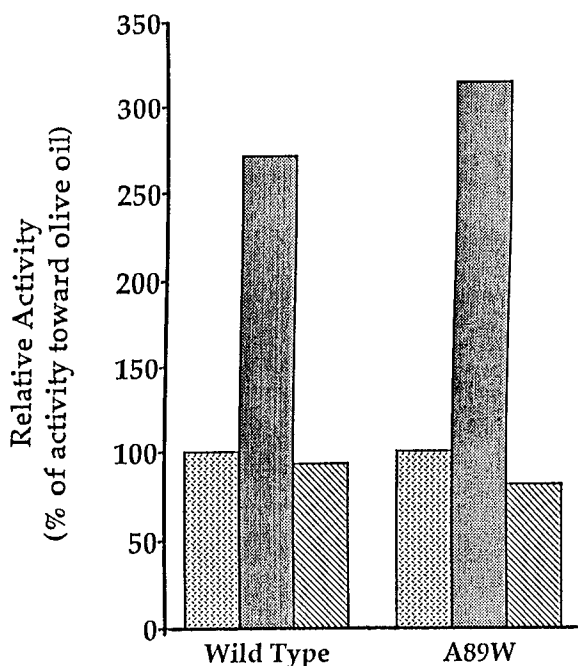
FIGURE 4. Relative activities calculated from the results of titrimetric assays of wild-type and mutant A89W lipase on olive oil (dotted bars), tricaprylin (dark bars), and tributyrin (hatched bars). Raw data are listed in TABLE 1. The activity on olive oil was set at 100%.

Mutated Prolipases

Bacteria bearing mutated prolipase DNAs were grown on rhodamine plates containing either olive oil or tricaprylin. This allowed visual identification of colonies that differed from wild type in their lipolytic activities toward these substrates. The majority of the cells showed no change in phenotype on these media, suggesting that, even though the residues at positions 95, 112, 206, and 209 of the Rd lipase are highly conserved, a number of replacements are tolerated without major changes in enzyme activity. There were also some mutants that exhibited a lipase-negative phenotype, presumably due to deficiencies in folding, substrate binding, or catalysis.

Five mutant prolipases were identified that exhibited altered activities on rhodamine media compared with the wild-type prolipase (TABLE 2). In these enzymes, chosen on the basis of an altered phenotype, there was no obvious pattern to the identity or type of amino acid introduced by mutation: in some cases, a large aromatic side chain was replaced by a small charged one (F95D); in others, a small nonpolar group was replaced by a large aromatic (V209W), a small polar (V206T), or a small nonpolar residue (V209G).

TABLE 2 shows the lipolytic activities of these enzymes toward the individual substrates OO, TC, and TB. In virtually all cases, there was a reduction in activity

TABLE 2. Lipolytic Activity (Single-Substrate Assay) in Lysates of
Prolipase-producing *E. coli* BL21 (DE3)

	Activity (U/mL)^a		
Mutation	Olive Oil	Tricaprylin	Tributyrin
wild type	158	270	65
phe95 → asp	35	198	29
phe112 → trp	100	59	65
val209 → trp	16	99	93
val206 → thr	64	234	41
val209 → gly	54	114	50

^{a}Micromoles of fatty acid released per minute per mg of protein. The values are averages of two experimental determinations.

compared with wild-type enzyme. In FIGURE 5A, these activities are expressed relative to a value of 100% for the activity toward triolein.

Another measure of the fatty acid specificity of an enzyme is gained by assaying it in the presence of a mixture of substrates and then determining the preference for the various fatty acids. These data are shown in TABLE 3 and FIGURE 5B.

The wild-type prolipase slightly prefers TC over OO, with TB being a somewhat poorer substrate than OO (FIGURE 5). For the mutant prolipases, an increase in the relative activity toward TC was the most common observation (four of the five isolates), with increases of as much as 3.6-fold in the assay of single substrates (FIGURE 5A). In mixed-substrate assays, this trait was much less pronounced, although still apparent (FIGURE 5B).

The replacement of phe95 with an aspartic acid caused a marked increase in the relative activity toward middle-chain-length substrates. This effect is most pronounced in the case of single substrates (TABLE 2, FIGURE 5A), but is also seen in mixed-substrate assays (TABLE 3, FIGURE 5B).

Replacement of phe112 by trp caused a nearly 3-fold reduction in the relative activity toward TC with both single and multiple substrates, changing C8 from the most to the least favored of the chain lengths examined (FIGURE 5). The relative activity against TB increased slightly in single-substrate assays and over 6-fold in mixed substrates (FIGURE 5). Thus, the mutagenic replacement of a large side chain by an even bulkier one reduced the relative activity toward medium-chain fatty acids and increased the activity toward short-chain ones.

A somewhat similar situation was seen in the activity toward mixed substrates when a bulky hydrophobic trp replaced val209, which lies across the substrate-binding trough from phe112. Compared with wild type, val209trp prolipase displayed a greatly increased (nearly 7-fold) relative activity toward short-chain substrates (TB) in the mixed-substrate assay (FIGURE 5B). Relative activity toward TC was also increased. In contrast to the F112W mutation, however, V209W retained its high relative activity toward TB, and its relative activity toward TC was even further enhanced, in single-substrate assays (FIGURE 5A).

The mutations V206T and V209G both yielded prolipases with increased relative activities toward middle-chain-length substrates (TC) in the single-substrate assay (FIGURE 5A). However, these did not persist in the mixed-substrate assay, where

these enzymes displayed activities very similar to wild-type prolipase (TABLE 3, FIGURE 5B). Perhaps the natures of the substrate emulsions are sufficiently different in the single- versus multiple-substrate cases to account for these differences in specificity.
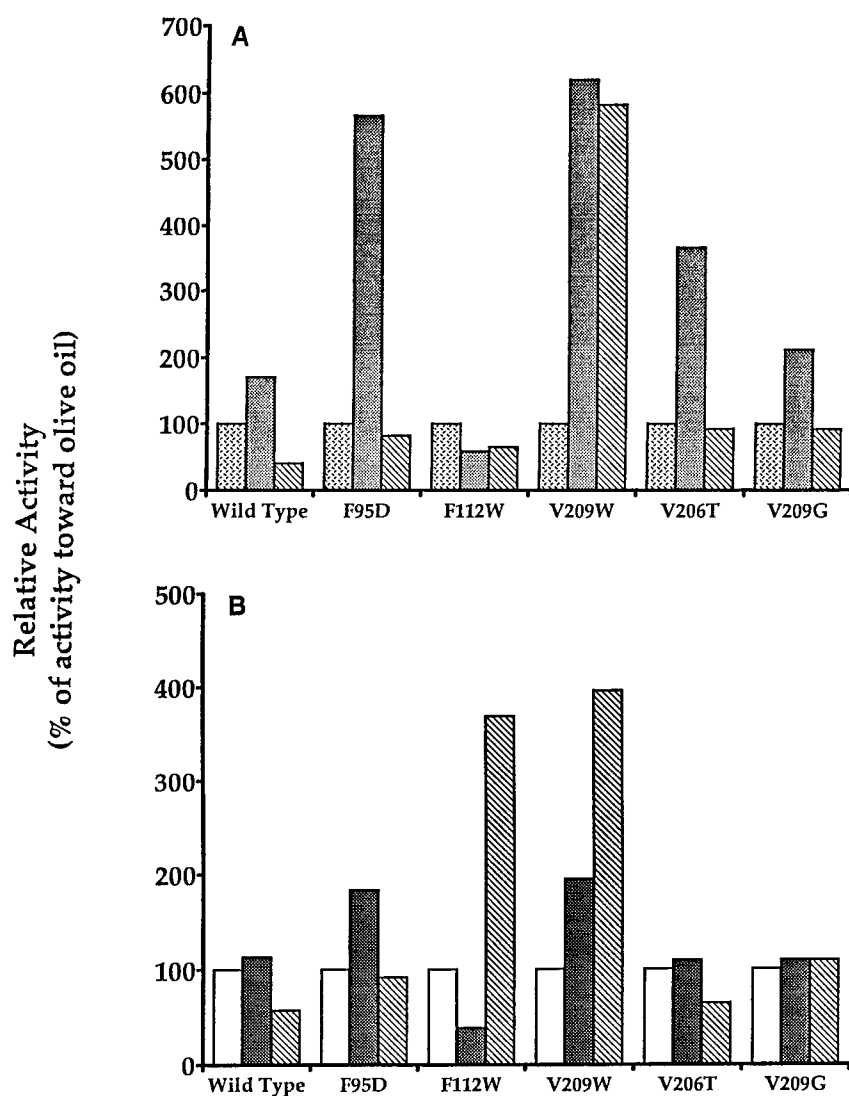
FIGURE 5. The relative lipolytic activities of crude wild-type and mutant *Rh. delemar* prolipases against (A) the single substrates olive oil (dotted bars, set at 100%), tricaprylin (dark bars), and tributyrin (hatched bars) and (B) mixtures of the substrates triolein (light bars, set at 100%), tricaprylin (dark bars), and tributyrin (hatched bars). Data are from TABLES 2 and 3.

TABLE 3. Hydrolysis of Equimolar Mixtures of Triolein, Tricaprylin, and Tributyrin by Prolipase in Cell Lysates

Mutation	% Hydrolysis		
	Triolein	Tricaprylin	Tributyrin
wild type	66.8	75.8	39.0
phe95 → asp	36.9	67.7	34.1
phe112 → trp	18.4	7.2	67.7
val209 → trp	18.2	35.4	72.0
val206 → thr	66.1	72.4	43.0
val209 → gly	54.8	60.0	60.0

TABLE 4. Titrimetric Analysis (Single Substrates) of Lipolytic Activity of Refolded, Purified Recombinant Mature Lipases

Mutation	Specific Activity (U/mL)[a]		
	Olive Oil	Tricaprylin	Tributyrin
wild type	3149	8539	2944
phe95 → asp	821	2978	404
phe112 → trp	1279	1127	1800
val209 → trp	281	1398	3896
val206 → thr	187	1079	281
val209 → gly	187	466	296

[a]Micromoles of fatty acid released per minute per mg of protein. The values are averages of two experimental determinations.

Mutated Mature Lipases

It is not possible to make conclusions about the effects of mutation on the specific activities of these proenzymes because these data were collected using crude lysates with unknown enzyme concentrations. To address this issue, the mutations introduced into the prolipase gene were transferred into the mature lipase gene by recombinant DNA techniques. The resulting mutant mature lipase genes were expressed; the lipases were recovered from inclusion bodies, refolded, and purified to homogeneity; and their activities were determined. The specific activities of these

TABLE 5. Hydrolysis of Equimolar Mixtures of Triolein, Tricaprylin, and Tributyrin by Purified, Refolded Mutant Mature Lipases

Mutation	% Hydrolysis[a]		
	Triolein	Tricaprylin	Tributyrin
wild type	80.1	83.9	42.4
phe95 → asp	59.3	79.5	55.3
phe112 → trp	40.3	32.1	58.7
val209 → trp	34.3	42.5	66.4
val206 → thr	15.6	21.3	8.9
val209 → gly	47.1	46.7	47.6

[a]Values are averages of two assays. Five μg of protein was added to each reaction tube, except for wild-type enzyme (2.5 μg assayed).
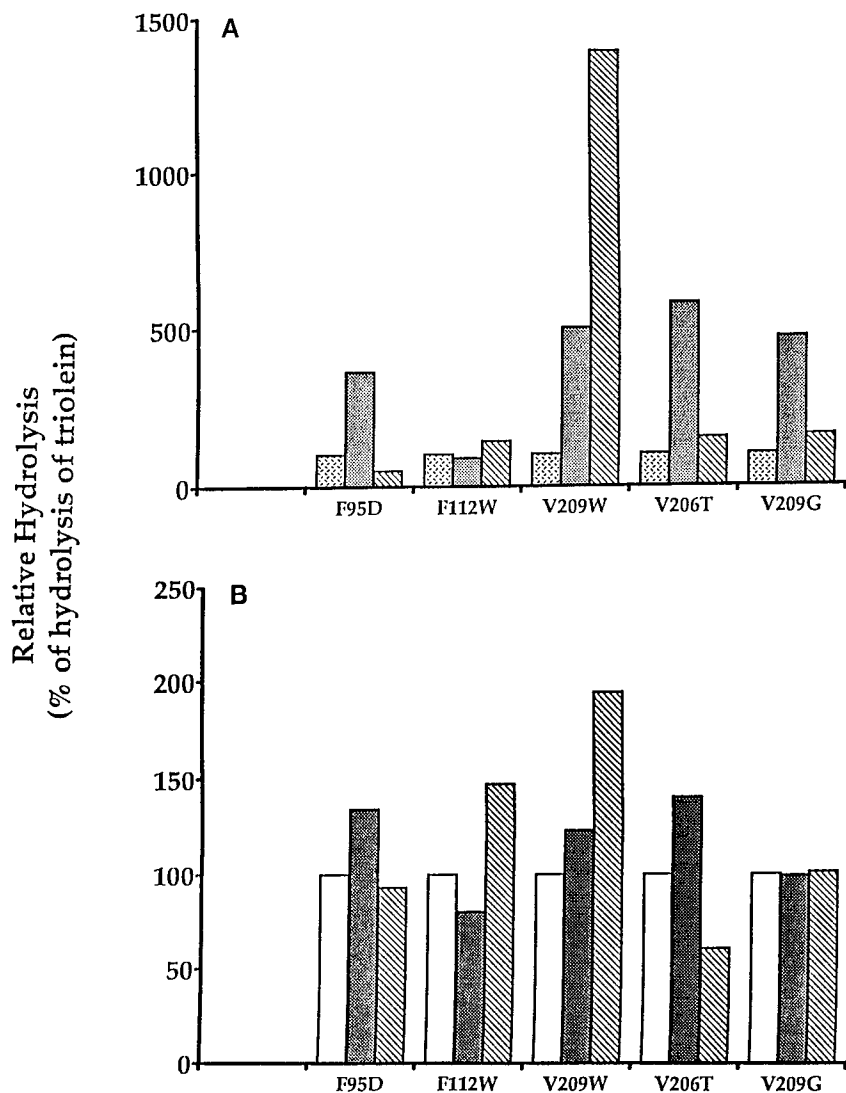
FIGURE 6. The relative lipolytic activities of purified mature wild-type and mutant *Rh. delemar* lipases: (A) single substrates olive oil (dotted bars, set at 100%), tricaprylin (dark bars), and tributyrin (hatched bars); (B) mixed substrates triolein (light bars, set at 100%), tricaprylin (dark bars), and tributyrin (hatched bars). Data are from TABLES 4 and 5.

enzymes against single (TABLE 4) and mixed (TABLE 5) substrates were determined and expressed relative to the activities toward oleic acid (FIGURE 6). It is notable that, relative to the wild-type lipase, all the mutations caused a substantial reduction in the specific activity of the resulting enzyme (TABLE 4), a phenomenon whose cause remains to be understood.

In general, the mutations caused the same phenotype in the mature enzymes as had been observed in the prolipases (above). [This validates the approach of expressing and screening mutant prolipases, which are produced in active forms, rather than focusing on the mature forms of the lipases, which require refolding before they can be assayed.] An exception to this is that the mature V209W lipase had more than twice the relative activity of its prolipase analogue toward TB (FIGURES 5 and 6). It is not known if this difference is due to an interaction of the propeptide portion of the enzyme with the substrate-binding region of the lipase or to the differences in purity between the prolipase and mature lipase preparations.

These studies have initiated an exploration of the relationship between structure and substrate specificity in this class of lipolytic enzymes. Additional work now under way seeks to further define the relationship between primary sequence and substrate specificity in the *Rhizopus delemar* lipase.

REFERENCES

1. JOERGER, R. D. & M. J. HAAS. 1994. Lipids **29:** 377–384.
2. BOEL, E., B. HUGE-JENSEN, M. CHRISTENSEN, L. THIM & N. P. FIIL. 1988. Lipids **23:** 701–706.
3. BOEL, E., B. HUGE-JENSEN, H. F. WOELDIKE, E. GORMSEN, M. CHRISTENSEN, F. ANDREASEN & L. THIM. 1991. *In* Lipases: Structure, Mechanism, and Genetic Engineering, p. 207–219. VCH Pub. New York.
4. YAMAGUCHI, S., T. MASE & K. TAKEUCHI. 1991. Gene **103:** 61–67.
5. HAAS, M. J., J. ALLEN & T. R. BERKA. 1991. Gene **109:** 107–113.
6. KUGIMIYA, W., Y. OHTANI, M. KOHNO & Y. HASHIMOTO. 1992. Biosci. Biotechnol. Biochem. **56:** 716–719.
7. BRADY, L., A. M. BRZOZOWSKI, Z. S. DEREWENDA, E. DODSON, G. DODSON, S. TOLLEY, J. TURKENBURG, L. CHRISTIANSEN, B. HUGE-JENSEN, L. NORSKOV, L. THIM & U. MENGE. 1990. Nature **343:** 767–770.
8. DEREWENDA, U., L. SWENSON, Y. WEI, R. GREEN, P. M. KOBOS, R. JOERGER, M. J. HAAS & Z. S. DEREWENDA. 1994. J. Lipid Res. **35:** 524–534.
9. DEREWENDA, U., L. SWENSON, R. GREEN, Y. WEI, S. YAMAGUCHI, R. JOERGER, M. J. HAAS & Z. S. DEREWENDA. 1994. Protein Eng. **7:** 551–557.
10. BRZOZOWSKI, A. M., U. DEREWENDA, Z. S. DEREWENDA, G. G. DODSON, D. M. LAWSON, J. TURKENBURG, F. BJORKLING, B. HUGE-JENSEN, S. A. PATKAR & L. THIM. 1991. Nature **351:** 491–494.
11. JOERGER, R. D. & M. J. HAAS. 1993. Lipids **28:** 81–88.
12. VIERA, J. & J. MESSING. 1987. Methods Enzymol. **153:** 3–11.
13. KUNKEL, T. A. 1985. Proc. Natl. Acad. Sci. U.S.A. **82:** 488–492.
14. SANGER, F., S. NICKLEN & A. R. COULSON. 1977. Proc. Natl. Acad. Sci. U.S.A. **74:** 5463–5467.
15. KOUKER, G. & K-E. JAEGER. 1987. Appl. Environ. Microbiol. **53:** 211–213.
16. HAAS, M. J., D. ESPOSITO & D. J. CICHOWICZ. 1995. J. Am. Oil Chem. Soc. **72:** 1405–1406.
17. RICHARDSON, L. V. & J. P. RICHARDSON. 1992. Gene **118:** 103–107.
18. YAMAGUCHI, S., T. MASE & K. TAKEUCHI. 1992. Biosci. Biotechnol. Biochem. **56:** 315–319.
19. DEREWENDA, Z. S., U. DEREWENDA & G. G. DODSON. 1992. J. Mol. Biol. **227:** 818–839.

Production, Characterization, and Molecular Modeling of Lipases for Esterification

SANNA JÄÄSKELÄINEN,[a,b] XIAO YAN WU,[a,b]
SUSAN LINKO,[a,b,c] YONGXIANG WANG,[a,d]
YU-YEN LINKO,[a] OLLE TELEMAN,[e] AND PEKKA LINKO[a]

*aLaboratory of Biotechnology and Food Engineering
Helsinki University of Technology
FIN-02150 Espoo, Finland*

*eVTT Biotechnology and Food Research
FIN-02044 VTT, Finland*

INTRODUCTION

Lipases (EC 3.1.1.3, triacylglycerol acyl hydrolases) are currently among the most studied enzymes owing to their great potential in a number of applications.[1,2] They catalyze a wide variety of hydrolysis, esterification, transesterification, and polyesterification reactions. The lipase from *Candida rugosa* (ex. *C. cylindracea*) Diddens and Lodder (ATCC 14830; CBS 6330) is one of the most investigated and cost-efficient.[3] Nevertheless, relatively little has been published on the production of *C. rugosa* lipase since the early work of the 1960s. *Rhizomucor miehei* lipase, on the other hand, has been shown to be an excellent biocatalyst in polyester synthesis largely because of the 3-D structure of its active center. The X-ray crystallographic structures of both lipases in "open" conformation have been recently determined,[4,5] which allows the investigation of lipase-catalyzed reactions by also molecular modeling. The present report discusses some strategies for the production and purification of *C. rugosa* lipase, the relationships between the hydrolytic and synthetic activities of lipases, and molecular modeling of the enzyme-substrate complexes of both *C. rugosa* and *R. miehei* lipases with implications to their performance as biocatalysts.

MATERIALS AND METHODS

Chemicals

Oleic acid (99%) and olive oil emulsion (50%) were purchased from Sigma (St. Louis, Missouri); 1-butanol (*p.a.*) was from E. Merck (Darmstadt, Germany); and yeast and meat extracts and peptone were from Difco (Detroit, Michigan). Refined,

low erucic acid rapeseed oil was obtained from the Raisio Group (Raisio, Finland) and 2-ethyl-1-hexanol was from Fluka (Buchs, Switzerland).

Enzymes

Commercial lipases from *Aspergillus niger* (3.4 U/mg), *Candida rugosa* (CrL; 88 U/mg), *Chromobacterium viscosum* (13.1 U/mg), *Pseudomonas fluorescens* (PfL; 13.8 U/mg), and *Rhizomucor miehei* (RmL; 6.1 U/mg) were obtained from Biocatalysts Limited (Wales, United Kingdom); porcine pancreatic lipase (PpL; 1.5 U/mg) was from Sigma; lipase OF (*Candida rugosa*; 15.0 U/mg) and lipase MY (*Candida rugosa*; 16.8 U/mg) were from Meito Sangyo Company (Tokyo, Japan); and lipase F-AP-15 (*Rhizopus* sp.; 23.3 U/mg) was from Amano Pharmaceutical Company (Nagoya, Japan). For most experiments, crude commercial lipases were used without further purification.

Microbial Strain

Candida rugosa ATCC 14830 was used in the lipase production experiments. Stock cultures were maintained on YM agar slants at +4 °C. The organism was screened for maximal lipase production using an agar plate assay method based on the dye Rhodamin B, modified from Kouker and Jaeger.[6] The Rhodamin B agar plates contained (per liter) 10 g olive oil, 3 g yeast extract, 3 g meat extract, 5 g peptone, 3 g KH_2PO_4, 1 g $MgSO_4 \cdot 7H_2O$, 15 g agar (sterilized separately), and 10 mL sterile filtered 1% Rhodamin B; pH was adjusted to 6.3 with 10% KH_2PO_4 before the addition of agar and olive oil. A clear orange fluorescent halo surrounding a colony under UV light after one to two days indicated lipase production.

Nutrient Media

The basal medium contained (per liter) 1 or 10 g glucose and/or 20 or 40 g olive oil (Sigma), 2.5 g peptone, 2.0 g urea, 1.5 g yeast extract, 1.5 g malt extract, 5 g KH_2PO_4, 1 g $MgSO_4 \cdot 7H_2O$, 10 mg $FeCl_3 \cdot 6H_2O$, 0.2 mg thiamine $\cdot$ HCl, 0.008 mg biotin, and 0.004 mg inositol.

Lipase Production and Purification

The *C. rugosa* inocula were grown in 500-mL conical flasks in shake cultures at 28 °C, 200 rpm, using 100 mL of medium through three to four transfers with a 5–10% inoculum each. The content of one flask was used to inoculate the fermentor. Lipase production was carried out in 3-L bioreactors (Biostat® MD; B. Braun Melsungen, Germany). Temperature was automatically controlled at 30 °C. Unless otherwise indicated, dissolved oxygen was controlled at about 20% of saturation (polarographic probe, W. Ingold) by regulating the stirrer speed and sterile airflow within set limits by sequential cascade control. In some fermentations, pure oxygen was supplied. The pH was allowed to change freely.

The BioPilot System from Pharmacia (Uppsala, Sweden) was used for CrL purification.[7] Crude lipase was suspended in 0.25 M sodium phosphate buffer (pH 7.0), stirred at 4 °C for 30 minutes, and then centrifuged. The supernatant was applied to a Phenyl Sepharose 6 Fast Flow (high sub.) column previously equilibrated with the buffer used for the pretreatment. Ethylene glycol in 1 mM sodium phosphate buffer (pH 7.0) was used for elution. The obtained main active component L1 was dialyzed against 50 mM sodium phosphate buffer (pH 7.0) and concentrated using a PM 10 ultrafiltration membrane (Amicon, cutoff MW of 10,000). The minor active component L2 obtained from HIC was applied to a Sephadex G-25 column for buffer changing. After that, fractions L1 and L2 were separately loaded onto a DEAE Sepharose Fast Flow column and eluted with a linear elution of 50 mM sodium phosphate buffer containing 0.5 M sodium chloride (pH 7.0). Finally, L1 and L2 were separately pooled, concentrated, desalted with ultrafiltration, and lyophilized for esterification.

Protein Characterization

The amount of protein in the sample was determined according to Lowry *et al.*,[8] using bovine serum albumin (Sigma) as standard.

Bio-Rad Mini-Protean II Dual Slab Cell was used for sodium dodecyl sulfate–polyacrylamide gel electrophoresis (SDS-PAGE) using Laemmli discontinuous polyacrylamide gel.[9] The separating gel contained 12% (w/v) polyacrylamide. Proteins were stained with Coomassie Brilliant Blue R-250 (Bio-Rad). Low-range-molecular-size prestained SDS-PAGE protein standards were from Bio-Rad Laboratories (Hercules, California).

Hydrolytic Activity

Hydrolytic activity was determined according to Sigma Bulletin No. 800, using 50% olive oil emulsion as substrate. The free fatty acids liberated were titrated with 0.05 M sodium hydroxide. One unit of lipase activity was defined as the amount of enzyme that catalyzes the release of one micromole of free acid per minute under the experimental conditions.

Esterification and Transesterification

Esterification of 1-butyl oleate synthesis was carried out with 0.77 mM 1-butanol and 0.7 mM oleic acid as substrates, except in the optimization of substrate ratio. In addition, the reaction mixtures contained varying amounts of deionized water and lipase, and mixing was performed at 200 rpm at 37 °C. Samples were taken at certain time intervals, a mixture of diethyl ether and ethanol (1:1, v/v) was added, and the residual free acid was titrated with 0.1 M sodium hydroxide. The conversion (%) in ester synthesis was based on the oleic acid consumed.

Transesterification for the synthesis of rapeseed oil 2-ethyl-1-hexyl ester was carried out with 0.227 mM rapeseed oil and 0.68 mM 2-ethyl-1-hexanol as substrates,

3.3% (w/w) of lipase as biocatalyst, and 3.0% of added water, at 37 °C, as described previously.[10] Samples were taken at certain time intervals. Qualitative analyses were carried out by TLC and quantitative analyses by reversed-phase HPLC. The conversion (%) was based on rapeseed oil consumed as determined by reversed-phase HPLC.

Molecular Modeling

The graphics program QUANTA 4.1.1 (Molecular Simulations Incorporated) was used to model the structures of two substrates, oleic acid and 1-butanol, and the interaction of the substrates with two lipases, RmL and CrL. The substrates were built and energy minimized with QUANTA. The CHARMm 23.1 (Molecular Simulations Incorporated)[11] program using a CHARMm force field was used for all other energy minimizations. Both programs were run on a Silicon Graphics Power Challenge workstation.

The crystallographic structures of the two lipases were obtained from Brookhaven Protein Data Bank. Oxygens of the water molecules, crystal disorder, calcium ions, sugars, and inhibitors were removed and all hydrogens were added by using either QUANTA or CHARMm. In all energy minimizations performed, a dielectric constant of 1 was used and the nonbonded interaction cutoff radius was set to 15.0 Å. Positions of the added hydrogens were optimized by energy minimizations. First, all α-carbons were kept fixed and, after the minimization using the Steepest Descent (SD) and the Conjugate Gradient (CG) algorithms, all atoms were allowed to move during the further minimization with the same algorithms.

The minimization of the two substrates, 1-butanol and oleic acid, was started with the SD algorithm and continued with the Adopted Basis Newton Raphson (ABNR) algorithm until a gradient tolerance of 0.01 was reached. In the minimization of the lipase-substrate complexes, α-carbons of the lipase structure were first fixed during the minimization with the SD and the CG algorithms. After that, all atoms were allowed to move and the minimization was started with the SD algorithm and continued with the CG algorithm until a gradient tolerance of 0.01 was reached.

RESULTS AND DISCUSSION

Lipase Production and Purification

Candida rugosa ATCC 14830 was selected for a detailed study on lipase production, owing to its general excellent characteristics in ester syntheses.[12] *C. rugosa* grew well on the simple, glucose-based maintenance medium YM recommended by ATCC, but no lipase was produced. A change of glucose to olive oil did not help either, unless certain salts and vitamins were included with the medium. Sufficient oxygen was important for lipase production, and supplying pure oxygen resulted in a marked improvement. With varying carbon and nitrogen source levels and combinations, the highest lipase activity of 7.60 U/mL was obtained with a combination of 40 g/L olive oil and 1 g/L glucose as the carbon source and by doubling the nitrogen sources in the basal medium. We should also stress that, under the process condi-

tions employed, lipase production was always more or less growth-associated. This agrees well with the observation of Valero *et al.*[13]

Two distinct lipase forms were obtained from CrL by Phenyl Sepharose hydrophobic interaction and DEAE Sepharose ion exchange chromatography: L1 at a 45% yield and L2 at a 4.7% yield. Both purified lipases were able to catalyze the esterification of 1-butanol and oleic acid and the transesterification of 2-ethyl-1-hexanol and rapeseed oil. Lipase L1 gave a 98% conversion for esterification in 12 h and a 99% conversion of rapeseed oil for transesterification in 24 h. The minor fraction L2 gave a 97% conversion for esterification in 30 h, but only a 79% conversion for transesterification over 24 h. The superiority of fraction L1, especially in transesterification, could also be clearly shown by thin-layer chromatography. Sodium deoxycholate treatment of the purified main lipase L1 considerably improved the initial rate in both esterification and transesterification.[7]

Synthetic versus Hydrolytic Lipase Activity

As lipases are increasingly used as biocatalysts in various synthetic reactions, but are sold on the basis of their hydrolytic activity, there is a clear need to relate the hydrolytic activities to synthetic performance. Therefore, we compared the hydrolytic activities of nine commercial lipases to their ester synthetic and transesterification activities.[14] It was concluded from the results that the hydrolytic activity of different lipases does not always give a good indication of the potential synthetic activity. For instance, hydrolytic activity of CrL was as high as 88 U/mg, with a conversion of oleic acid to butyl oleate of 92% obtained in 10 h and a conversion of rapeseed oil in transesterification with 2-ethyl-1-hexanol of nearly 100% obtained in 24 h. RmL, which showed a relatively low hydrolytic activity of 6.1 U/mg, had a very high synthetic activity, with conversions of about 93% in esterification and about 94% in transesterification in 24 h. The lipase from *Ch. viscosum* exhibited relatively high hydrolytic (13.1 U/mg) and transesterification (a conversion of 97% in 24 h) activities, but the esterification activity was low under the experimental conditions with a conversion of only 14% in 24 h.

Our aim was to find standard conditions for 1-butyl oleate biosynthesis as a method for synthetic lipase activity suitable for all lipases. Therefore, the ability of four lipases to catalyze 1-butyl oleate synthesis under different conditions was compared. First, the most suitable substrate ratio, water content, and lipase amount for each lipase were determined. The most suitable 1-butanol to oleic acid molar ratio varied from 0.7 mM/1.4 mM (RmL) to 1.4 mM/0.7 mM (PfL); water content varied from 3.2% (CrL, PfL) to 18.1% (w/w) (RmL); lipase amount varied from 45 U (PpL) to 704 U (CrL). Second, ester synthesis with four lipases was carried out with a 1-butanol to oleic acid molar ratio of 0.77/0.7 and a water content of 3.2% (w/w), with two different lipase amounts, the first containing 100 U of each lipase and the second 9 mg. Finally, the third experimental conditions contained the same substrate ratio as the two before, but the water content was raised to 7.0% (w/w) to enhance the ester synthetic activity of RmL. Lipase amount was kept at 100 U, except that a minimum of 4.0 mg was used.

Time courses of the ester syntheses with CrL and PpL at the "optimum" and three other experimental conditions are presented in FIGURE 1. It is seen that CrL
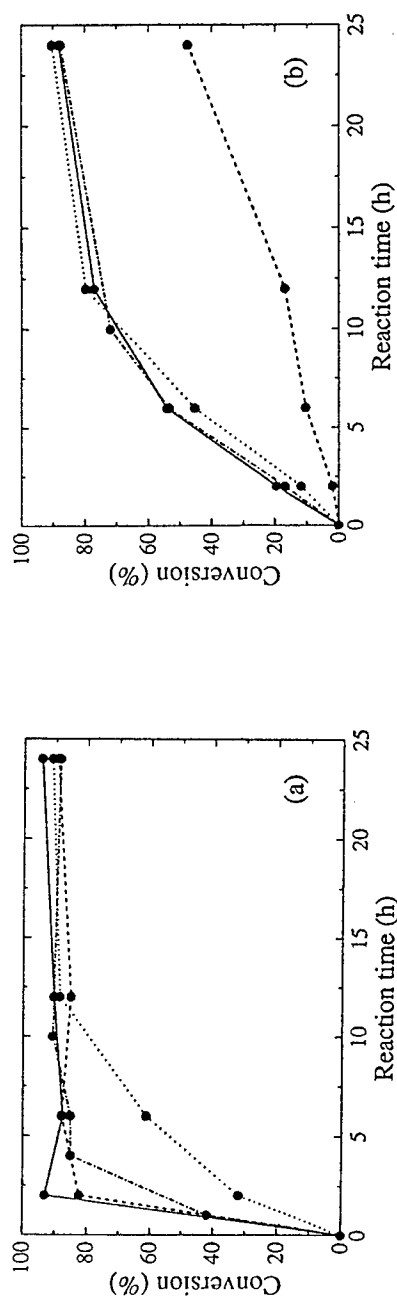
FIGURE 1. Conversion of oleic acid in esterification catalyzed by (a) *Candida rugosa* lipase and (b) porcine pancreatic lipase: (—) "optimum conditions"; (···) experiment 1; (- -) experiment 2; (-·-·-) experiment 3. Experiments 1–3 contained 0.7 mM oleic acid and 0.77 mM 1-butanol as substrates. Experiment 1 contained 3.2% (w/w) water and 100 U lipase, experiment 2 contained 3.2% (w/w) water and 9 mg lipase, and experiment 3 contained 7.0% (w/w) water and 100 U or a minimum of 4.0 mg lipase.

and PpL catalyzed ester synthesis under the third experimental conditions nearly as well as in "optimum" conditions. In conclusion, 1-butyl oleate ester synthesis would be an easy, relatively rapid, and accurate method for primary screening of the ester synthetic activity of lipase because the synthesis is carried out without any additional solvent or stabilizer and the conversion can be determined by a simple titration. Furthermore, the end point of the titration is very clear.

Molecular Modeling

RmL structure (PDB entry 4TGL) was determined by Derewenda *et al.*[4] at 2.65-Å resolution. The lipase consisted of one subunit with 269 amino acids, but the first 4 amino acids were not included in the structure. Furthermore, the PDB structure contained 239 oxygens from water molecules, 3 disulfide bonds, and a diethyl *p*-nitrophenyl phosphate inhibitor.

CrL structure (PDB entry 1LPP) was determined by Grochulski *et al.*[5] at 2.05-Å resolution. The structure contained 534 amino acids in one subunit, 296 oxygens from water molecules, 2 disulfide bonds, 2 calcium ions, 3 *n*-acetyl-*d*-glucosamines, and a hexadecanesulfonyl chloride inhibitor.

Minimization of RmL with Two Substrates

In the minimization of the RmL structure, overlapping of the added hydrogen atoms with other atoms was removed during the first 400 steps, which was seen from the total energy profile and rms deviations. After minimizing the lipase structure, the two substrates, 1-butanol and oleic acid, were added to the active site. Oleic acid was placed to the hydrophobic end and 1-butanol to the hydrophilic end of the active site on the basis of the crystallographic structures of RmL-inhibitor[15] and *Humicola lanuginosa* lipase (HlL)–inhibitor complexes.[16] In both complexes, the inhibitor occupied the binding site of the fatty acid cleaved off during the hydrolysis. It was clearly seen from the HlL-inhibitor complex that the fatty acid binding site is in the hydrophobic end of the active site. Because the active sites of the two homologous lipases resemble each other, it was concluded that the fatty acid points toward the hydrophobic end in the active site of RmL as well.

The final energy of the minimized RmL-substrate complex was −12,538 kcal/mol and that of the minimized lipase was −12,465 kcal/mol, indicating that some favorable contacts between the lipase and the substrates were formed during the minimization. The minimized RmL-substrate complex is presented in FIGURE 2a and active site amino acids are seen in FIGURE 3.

Minimization of CrL with Two Substrates

The active site of CrL is a narrow tunnel with separate binding sites for alcohol[17] and fatty acid,[5] whereas the active site of RmL is an "open" cleft at the surface of the molecule. The binding sites of the substrates were determined on the basis of the crystallographic structures of the two CrL-inhibitor complexes. As for RmL, the final
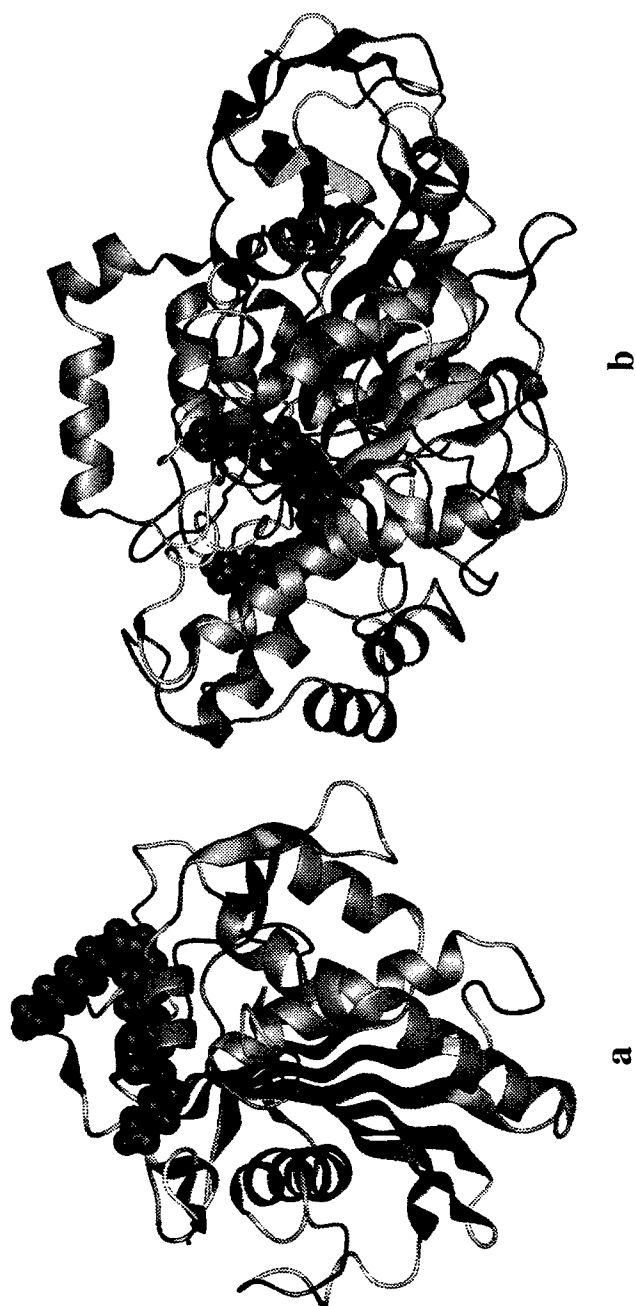
FIGURE 2. Lipases from (a) *Rhizomucor miehei* and (b) *Candida rugosa* complexed with 1-butanol and oleic acid after minimization. Secondary structures of lipases and van der Waals surfaces of substrates are shown.
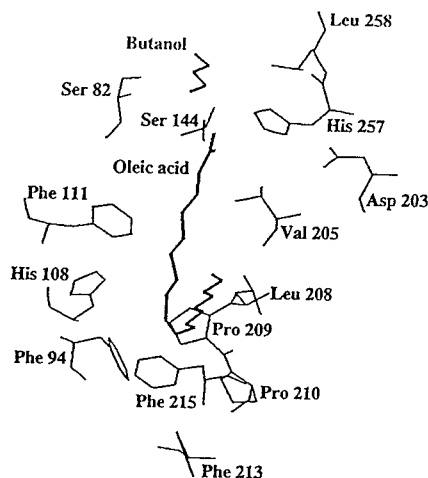
FIGURE 3. Oleic acid, 1-butanol, and amino acids of the active site of *Rhizomucor miehei* lipase after minimization. The catalytic amino-acid triad consists of Ser-144, Asp-203, and His-257.

energy of the minimized complex (−26,114 kcal/mol) was lower than the final energy of the minimized lipase (−26,039 kcal/mol). The minimized CrL-substrate complex is presented in FIGURE 2b.

Comparison of the Shapes of the Active Sites of RmL and CrL

We had previously shown that both RmL and CrL catalyze effectively 1-butyl oleate biosynthesis,[14] whereas RmL has a much better ability to catalyze high-molecular-mass polyesters, like poly(1,4-butyl sebacate).[18] In polyester synthesis, the "open" active site of RmL enables substrates to go in from one end and products to go out from the other end. The fatty acid binding site of CrL is open only from the other end close to the catalytic amino-acid triad. The alcohol rests in the alcohol binding site, separately from the fatty acid binding site.[17] Grochulski *et al.*[5] have given two different theories on how the fatty acyl chain enters the tunnel in hydrolysis, but nothing has been proven yet. However, in polyester synthesis, the forming polyester cannot go through the active site as in the case of RmL, which makes the reaction much more complicated to proceed.

A final point needs to be stressed: although the shapes of the active sites of these two lipases are different, both lipases have a "lid" (which opens in the presence of a water/oil interface), as well as a consensus pentapeptide Gly-X-Ser-X-Gly,[17] a common β-ε-Ser-α secondary structure motif,[19] and a common orientation of the catalytic amino-acid triad (Ser, His, and Glu or Asp).[17]

REFERENCES

1. BJÖRKLING, F., S. E. GODTFREDSEN & O. KIRK. 1991. The future impact of industrial lipases. Trends Biotechnol. **9:** 360–363.
2. VULFSON, E. N. 1994. Industrial applications of lipases. *In* Lipases: Their Structure,

Biochemistry, and Applications. P. Woolley & S. B. Petersen, Eds.: 271–288. Cambridge University Press. London/New York.

3. LINKO, Y.-Y., O. RANTANEN, H-C. YU & P. LINKO. 1992. Factors affecting lipase-catalyzed *n*-butyl oleate synthesis. *In* Progress in Biotechnology: Biocatalysis in Non-conventional Media. Volume 8. J. Tramper, M. H. Vermüe, H. H. Beeftink & U. von Stockar, Eds.: 601–608. Elsevier. Amsterdam/New York.

4. DEREWENDA, U., A. M. BRZOZOWSKI, D. M. LAWSON & Z. S. DEREWENDA. 1992. Catalysis at the interface: the anatomy of a conformational change in a triglyceride lipase. Biochemistry **31:** 1532–1541.

5. GROCHULSKI, P., F. BOUTHILLIER, R. J. KAZLAUSKAS, A. N. SERREQI, J. D. SCHRAG, E. ZIOMEK & M. CYGLER. 1994. Analogs of reaction intermediates identify a unique substrate binding site in *Candida rugosa* lipase. Biochemistry **33:** 3494–3500.

6. KOUKER, G. & K.-E. JAEGER. 1987. Specific and sensitive plate assay for bacterial lipases. Appl. Environ. Microbiol. **53:** 211–213.

7. LINKO, Y-Y. & X. Y. WU. 1996. Biocatalytic production of useful esters by two forms of lipase from *Candida rugosa.* J. Chem. Technol. Biotechnol. **65:** 163–170.

8. LOWRY, O. H., N. J. ROSEBROUGH, A. L. FARR & R. J. RANDALL. 1951. Protein measurements with the Folin phenol reagent. J. Biol. Chem. **193:** 265–275.

9. LAEMMLI, U. K. 1970. Cleavage of structural proteins during the assembly of the head of bacteriophage T4. Nature **227:** 680–685.

10. LINKO, Y-Y., M. LÄMSÄ, A. HUHTALA & P. LINKO. 1994. Lipase-catalyzed transesterification of rapeseed oil and 2-ethyl-1-hexanol. J. Am. Oil Chem. Soc. **71:** 1411–1414.

11. BROOKS, B. R., III, E. R. BRUCCOLERI, B. D. OLAFSON, D. J. STATES, S. SWAMINATHAN & M. KARPLUS. 1983. CHARMm: a program for macromolecular minimization and dynamics calculations. J. Comput. Chem. **4:** 187–217.

12. WANG, Y., J. LUOPA, T. RAJALAHTI & S. LINKO. 1995. Strategies for the production of lipase by *Candida rugosa:* neural estimation of biomass and lipase activity. Biotechnol. Lett. **9:** 741–746.

13. VALERO, F., J. L. DEL RIO, M. POCH & C. SOLA. 1991. Fermentation behavior of lipase production by *Candida rugosa* growing on different mixtures of glucose and olive oil. J. Ferment. Bioeng. **72:** 399–401.

14. WU, X. Y., S. JÄÄSKELÄINEN & Y-Y. LINKO. 1996. An investigation of crude lipases for hydrolysis, esterification, and transesterification. Enzyme Microb. Technol. In press.

15. BRZOZOWSKI, A. M., U. DEREWENDA, Z. S. DEREWENDA, G. G. DODSON, D. M. LAWSON, J. P. TURKENBURG, F. BJÖRKLING, B. HUGE-JENSEN, S. A. PATKAR & L. THIM. 1991. A model for interfacial activation in lipases from the structure of a fungal lipase-inhibitor complex. Nature **351:** 491–494.

16. LAWSON, D. M., A. M. BRZOZOWSKI, S. RETY, C. VERMA & G. G. DODSON. 1994. Probing the nature of substrate binding in *Humicola lanuginosa* lipase through X-ray crystallography and intuitive modelling. Protein Eng. **7:** 543–550.

17. CYGLER, M., P. GROCHULSKI, R. J. KAZLAUSKAS, J. D. SCHRAG, F. BOUTHILLIER, B. RUBIN, A. N. SERREQI & A. K. GUPTA. 1994. A structural basis for the chiral preferences of lipases. J. Am. Chem. Soc. **116:** 3180–3186.

18. LINKO, Y-Y., Z-L. WANG & J. SEPPÄLÄ. 1995. Lipase-catalyzed synthesis of poly(1,4-butyl sebacate) from sebacic acid or its derivatives with 1,4-butanediol. J. Biotechnol. **40:** 133–138.

19. GROCHULSKI, P., Y. LI, J. D. SCHRAG, F. BOUTHILLIER, P. SMITH, D. HARRISON, B. RUBIN & M. CYGLER. 1993. Insights into interfacial activation from an open structure of *Candida rugosa* lipase. J. Biol. Chem. **268:** 12843–12847.

Complicated Simplification of Dosage Regimen for Plasminogen Activators[a]

ALEXANDER V. MAKSIMENKO

Institute of Experimental Cardiology
Cardiology Research Center
Russian Academy of Medical Sciences
Moscow 121552, Russia

INTRODUCTION

The problem of enhancing thrombolytic therapy efficacy is associated with many factors; one of them is selection of an optimal dosing regimen. Different preparations used, various clinical cases, and emergency situations dictate a variance in dosing regimen. Selection of an inadequate route of administration has led to unfavorable results in the clinical study of new therapeutic agents. Therefore, it is very important to have a well-grounded administration regimen, but so far no generalized view on this problem has yet emerged in the published data. The present study considers this issue from the viewpoint of biochemical, pharmacokinetic, and therapeutic values of plasminogen activators, which are being studied and used in clinics. The present report aims to analyze current trends in the development of new schedules of plasminogen activator administration based on biomedical and clinical findings.

INTRAVASCULAR INFUSION OF PLASMINOGEN ACTIVATORS

The search for optimal doses of the preparations resulted in the development of a bolus-infusion schedule of administration, where one portion of the dose is administered as a bolus and the other as an infusion (FIGURE 1). This approach was conditional on the fact that active protein plasminogen activators exhibit a short half-life in blood flow and are administered as an infusion. However, although infusion provided a long-maintained elevated concentration of the preparation in blood flow, it failed to achieve quickly the therapeutic interval of concentrations. The latter is attained by means of bolus administration, but is short-term and dangerous due to hemorrhagic complications when being overdosaged. A combination of both methods yielded a bolus-infusion schedule of plasminogen activator administration, which is most widely used in clinics nowadays. Current clinical studies demonstrate that an urgent therapeutic aid to the patients with acute cardiovascular injuries is a crucial factor for a successful treatment.[1,2] This implies domiciliary administration of plasminogen activators. Intensive biomedical and clinical studies are being conducted now to put this method into practice.

BOLUS ADMINISTRATION OF PLASMINOGEN ACTIVATORS

Bolus administration of plasminogen activators has provided a prolonged thrombolytic activity (30–40 min), which notably increased their short half-life in blood flow (6–8 min).[3]

Comparison of bolus administration of tissue-type plasminogen activator (t-PA) with a 4-h t-PA infusion into rabbits with venous thrombosis demonstrated that the initial thrombolysis rate was important for achieving a more rapid reperfusion.[4] Bolus administration of plasminogen activator in equal doses appeared to provide a
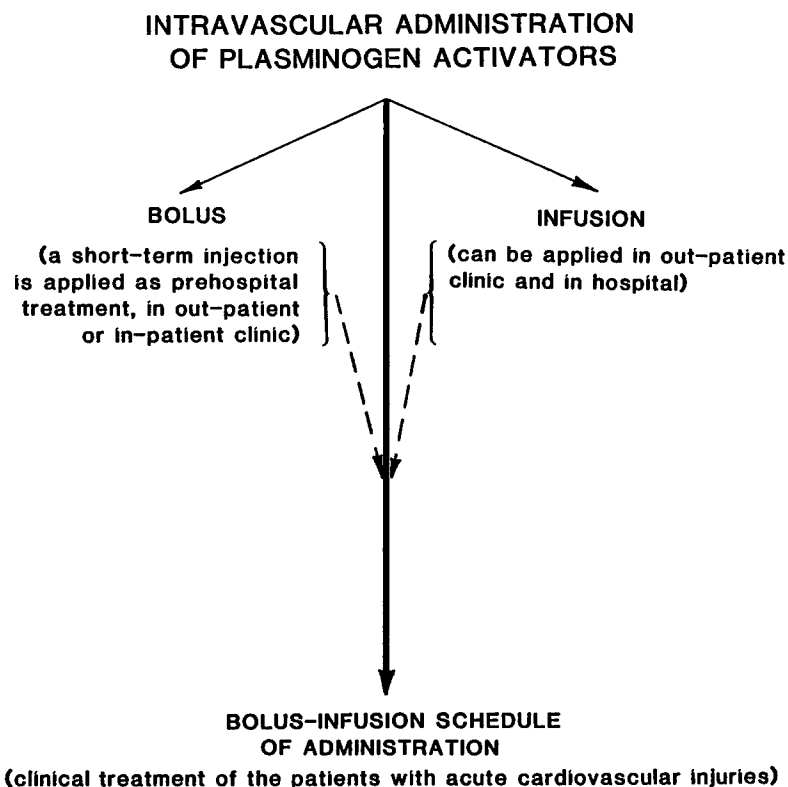
FIGURE 1. A schematic representation of the methods for intravascular administration of plasminogen activators.

higher rate of initial thrombolysis versus the infusion. Later stages of monitoring showed no differences in the size of thrombolysis depending on the route of administration.

Thus, the results of *in vivo* experiments demonstrated that bolus administration of plasminogen activators decreased the size of administered doses and provided an earlier reperfusion compared to the infusion at optimal concentration intervals of

preparations. These results, as well as some others, substantiated the testing of bolus administration of plasminogen activators in clinics.

Developments of plasminogen activators of new generations yielded mutant and hybrid (chimeric) forms of recombinant thrombolytics[5] and their modified derivatives.[6] Due to their properties, new plasminogen activators proved to be quite efficient after a bolus administration. YM 866, a mutant form of t-PA, demonstrated a preferable thrombolytic effect in arterial thrombosis in guinea pigs after bolus administration without a marked depletion of the fibrinolysis system compared to the wild form of t-PA.[7] Elevated thrombolytic activity of this derivative, as well as of E 6010, another mutant t-PA,[8] was attributed to the prolonged time of their half-life in blood flow acquired as the result of targeted mutagenesis. Clinical trials of E 6010 using the schedule of intravenous bolus administration into patients with acute myocardial infarction are being conducted nowadays in Japan.[9]

Efficacy of the thrombolytic action of BM 06.022, a mutant form of t-PA, after bolus administration appeared to be at least not lower than the values of standard thrombolytic therapy of the patients with acute myocardial infarction.[10] Bolus administration of plasminogen activators of new generations will probably be performed more often in the near future because clinical use of such agents allows an early recanalization of coronary vessels.[10]

Domiciliary administration of anistreplase accelerated the start of the treatment by more than two hours.[1] It improved therapy indexes versus the clinical therapy. Moreover, all advantages of domiciliary thrombolysis were observed in 61% of the patients when the treatment of myocardial infarction was initiated within two hours of symptom onset. The benefit of an early domiciliary thrombolysis is quite apparent. Total mortality rate in the group of domiciliary thrombolysis was half of that in the clinical group.[2] Thus, an early administration of plasminogen activators aids researchers in their efforts to improve schedules of bolus administration (probably by means of a repeated bolus of well-known thrombolytics), as well as to develop new forms of plasminogen activators with given properties.[5,6] Both trends appear to be quite laborious; however, such studies are being conducted rather intensively.

BOLUS-INFUSION ADMINISTRATION REGIMEN OF PLASMINOGEN ACTIVATORS

Results of biomedical studies emphasize the importance of reducing the term of plasminogen activator infusion in the bolus-infusion dosing regimen, as well as calling attention to the ratio between bolus and infusion doses. An optimal ratio is likely to provide improved clinical values of thrombolytic therapy.

A standard schedule (100 mg within 3 h) of t-PA administration into patients with acute myocardial infarction was compared to an accelerated dosing regimen (100 mg over 90 min) and the latter showed its advantage.[11] Accelerated administration of t-PA provided an earlier reperfusion without any notable changes in the safety of the treatment. These advantages make a good prognosis for the patients; however, additional trials are required. Data of multicenter clinical trials confirmed the high thrombolytic efficacy of accelerated t-PA administration, which was documented angiographically and by the retained contractile function of the myocar-

dium.[12] The proposed dosing schedule provided the highest rate of early reperfusions (angiographically documented 90 min after the start of the treatment) compared to three other strategies of thrombolytic intervention. Thus, accelerated administration of t-PA, or in other words "Neuhaus's method of front-loaded doses,"[13] showed prospects for clinical application.

Along with this, it is clear that the diversity of the cases of cardiovascular injuries cannot be limited to several concrete dosing regimens of plasminogen activator.[14] Necessity to achieve a complete reperfusion (TIMI grade 3), a multifactor development of pathology, and incidence of hemorrhagic and rethrombotic complications in thrombolysis directed the studies to combined applications of therapeutics.[15] The next stage of biomedical and clinical studies is just beginning.

CONJUNCTIVE ADMINISTRATION OF PLASMINOGEN ACTIVATORS

Combined application of plasminogen activators implies either administration of various plasminogen activators as a part of a single thrombolytic composition or conjunctive administration of plasminogen activators and the agent exhibiting another kind of therapeutic activity to maintain the therapeutic effect.[16]

Combined application of plasminogen activators with different mechanisms of action accelerated thrombolysis *in vivo*, decreased the doses of the preparations used,[17] and revealed a synergistic effect of thrombolytics.[18] Analysis of the compiled results of biomedical and clinical studies demonstrated that the combined administration of thrombolytics was more preferable than monotherapy; this was attributed to the acceleration of the onset of reperfusion and a decrease in the incidence of complications due to the change in the hemostatic protein level, rather than a synergistic effect (which may be hampered because of the narrow concentration interval of the components, where this effect can be manifested).[6,16]

Reperfusion of the occluded vessel, however, cannot guarantee the absence of complications of thrombolytic therapy.[16] New agents and methods of conjunctive thrombolytic therapy are being developed to eliminate such complications. Pharmacokinetic and other data[16] showed that a combination of bolus and infusion administration of plasminogen activator, a repeated bolus of plasminogen activator, and prolonged forms of plasminogen activators and agents of concomitant destination may promote a successful treatment. These approaches provide for the achievement of an efficient concentration of the preparation in blood flow (FIGURE 2) and in the injury locus. New forms of plasminogen activators[5,6] are being designed to increase their thrombospecificity by means of chemical and biological synthesis. Methods of conjunctive administration of plasminogen activators and agents of concomitant destination are currently being studied to reduce the incidence of complications in thrombolytic therapy.[16] These include thrombin inhibitors, antiplatelet agents, vasodilators, beta-blockers, and other preparations.

The task to develop optimal dosing regimens for thrombolytic therapy is quite a laborious one, which includes defining of the best time intervals and routes of administration (FIGURE 2), as well as establishing the interval of efficient doses. Taking into account that such investigations are to be conducted with caution,[19] much time will be required to solve the problem. However, these findings contribute

to the improvement of some stages of treatment for the variety of cases. Thus, a tailored thrombolytic therapy[14] is developed that aims to select an optimal dose regimen of treatment based on individual characteristics of the patient, risk factors, and time of therapy commencement.[20]
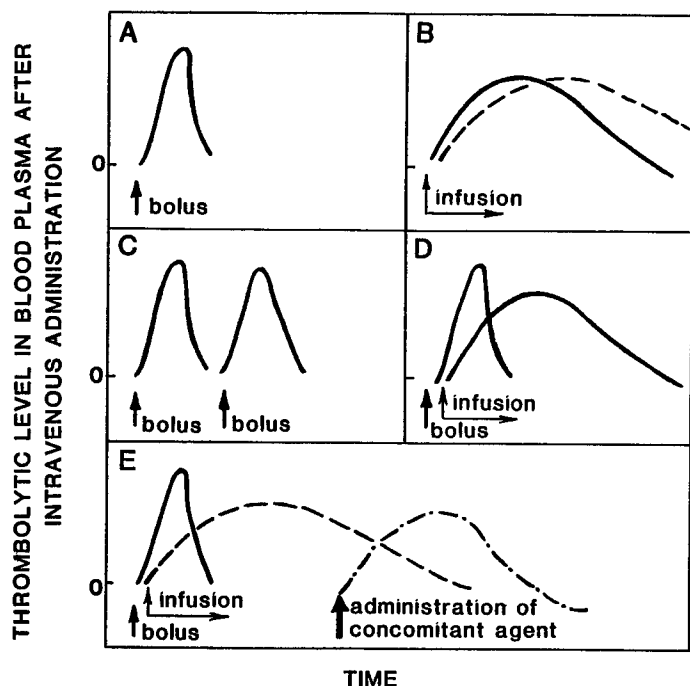
FIGURE 2. A schematic picture of alterations in plasminogen activator level in blood plasma after intravenous administration: (A) bolus; (B) infusion: —, native (wild or recombinant) plasminogen activator; ---, plasminogen activator with increased half-life in blood flow; (C) a repeated bolus; (D) a bolus-infusion schedule of plasminogen activator administration; (E) polytherapy by a bolus of thrombolysis trigger (t-PA or urokinase) with subsequent infusion of plasminogen activators with prolonged action and a later (-·--·-) administration of a concomitant agent of conjunctive action.

CONCLUSIONS

Administration schedules of plasminogen activators revealed a tendency for simplification. There is an apparent tendency to use a bolus administration and to reduce infusion terms. However, the observed simplification is attained at the expense of complicating the dosing regimen, the use of prolonged forms of plasmino-gen activators, and application of the agents exhibiting a conjunctive effect. Development of efficient thrombolytic compositions promises to simplify the dose schedules; however, the use of new preparations makes the study more complicated. In general,

such a "complicated simplification" presents one of the basic trends in the future study on the effects of thrombolytic therapy.

REFERENCES

1. GREAT GROUP. 1992. Feasibility, safety, and efficacy of domiciliary thrombolysis by general practitioners. Br. Med. J. **305:** 548–553.
2. RAWLES, J. M. (GREAT GROUP). 1994. Halving of mortality at 1 year by domiciliary thrombolysis in the Grampian Region Early Anistreplase Trial (GREAT). J. Am. Coll. Cardiol. **23:** 1–5.
3. BADYLAK, S. F., S. VOYTIKS, R. E. KLABUNDE, J. HENKIN & M. LESKI. 1988. Bolus dose-response characteristics of single-chain urokinase plasminogen activator and tissue plasminogen activator in a dog model of arterial thrombosis. Thromb. Res. **52:** 295–312.
4. CLOZEL, J-P., T. TSCHOPP, E. LUEDIN & P. HOLVOET. 1989. Time course of thrombolysis induced by intravenous bolus or infusion of tissue plasminogen activator in a rabbit jugular vein thrombosis model. Circulation **79:** 125–133.
5. MAKSIMENKO, A. V. 1994. Mutant and hybrid protein derivatives for experimental therapy using plasminogen activators. Khim. Farm. Zh. **28**(no. 5): 4–11 (in Russian; English translation, p. 293–302).
6. MAKSIMENKO, A. V. 1995. Molecular interaction during fibrinolysis: search for new plasminogen activators. Mol. Biol. **29:** 38–60 (in Russian; English translation, p. 20–31).
7. KAWASAKI, T., S. KAKU, T. TAKENAKA, K. YANAGI & N. OHSHIMA. 1994. Thrombolytic activity of YM 866, a novel modified tissue-type plasminogen activator in a photochemically induced platelet-rich thrombosis model. J. Cardiovasc. Pharmacol. **23:** 884–889.
8. SUZUKI, S., M. SAITO, N. SUZUKI, H. KATO, N. NAGAOKA, S. YOSHITAKE, Y. YUI & C. KAWAI. 1993. Intracoronary infusion of E 6010 has more potent thrombolytic activity than tissue plasminogen activator (t-PA) in dogs: a higher plasma level of E 6010 than t-PA causes potent thrombolytic activity. J. Cardiovasc. Pharmacol. **22:** 834–840.
9. KAWAI, C., S. HOSODA, T. MOTOMIYA, S. KIMATA, Y. YUI, K. KODAMA, R. MINAMINO, H. SATO & M. NOBUYOSHI. 1992. Multicenter trial of a novel modified t-PA, E 6010, by i.v. bolus injection in patients with acute myocardial infarction. Circulation **86:** I-409 (abstract no. 1630).
10. NEUHAUS, K. L., R. VON ESSEN, A. VOGT, U. TEBBE, J. RUSTIGE, H-J. WAGNER, K-F. APPEL, U. STIENEN, R. KONIG & W. MEYER-SABELLEK. 1994. Dose finding with a novel recombinant plasminogen activator (BM 06.022) in patients with acute myocardial infarction: results of the German Recombinant Plasminogen Activator Study. J. Am. Coll. Cardiol. **24:** 55–60.
11. CARNEY, R. J., G. A. MURPHY, T. R. BRANDT, P. J. DALEY, E. E. PICKERING, H. J. WHITE, T. J. MCDONOUGH, S. K. VERMILYA & S. L. TEICHMAN. 1992. Randomized angiographic trial of recombinant tissue-type plasminogen activator (alteplase) in myocardial infarction. J. Am. Coll. Cardiol. **20:** 17–23.
12. GUSTO ANGIOGRAPHIC INVESTIGATORS. 1993. The effect of tissue plasminogen activator, streptokinase, or both on coronary-artery patency, ventricular function, and survival after acute myocardial infarction. N. Engl. J. Med. **329:** 1615–1622.
13. NEUHAUS, K. L., W. FEUERER, S. JEEP-TEBBE, W. NIEDERER, A. VOGT & U. TEBBE. 1989. Improved thrombolysis with modified dose regimen of recombinant tissue-type plasminogen activator. J. Am. Coll. Cardiol. **14:** 1566–1569.
14. VAUGHAN, D. E. & E. BRAUNWALD. 1992. Front-loaded accelerated infusions of tissue plasminogen activator: putting a better foot forward. J. Am. Coll. Cardiol. **19:** 1076–1078.
15. PITT, B. 1992. Improved early infarct-related vessel patency after thrombolytic therapy. J. Am. Coll. Cardiol. **19:** 892–893.
16. MAKSIMENKO, A. V. 1994. Experimental combined thrombolytic therapy: current state and trends of development. Khim. Farm. Zh. **28**(no. 12): 3–13 (in Russian; English translation, in press).

17. ZISKIND, A. A., H. K. GOLD, T. YASUDA, M. KANKE, J. L. GUERRERO, J. T. FALLON, T. SAITO & D. COLLEN. 1989. Synergistic combinations of recombinant human tissue-type plasminogen activator and human single-chain urokinase–type plasminogen activator. Circulation **79:** 393–399.
18. COLLEN, D. 1988. Synergism of thrombolytic agents: investigational procedures and clinical potential. Circulation **77:** 731–735.
19. BASSAND, J. P. 1994. GUSTO (global utilization of streptokinase and tissue plasminogen activator in occluded arteries): logic wins at last. Eur. Heart J. **15:** 2–4.
20. SIMOONS, M. L. & A. E. R. ARNOLD. 1993. Tailored therapy: a perspective. Circulation **88:** 2556–2564.

Effective Enzyme Thrombolytic Composition on the Basis of Wild-type and Chemically Modified Plasminogen Activators[a]

ALEXANDER V. MAKSIMENKO, ELENA G. TISCHENKO,
ARTEM D. PETROV, AND MARINA L. PETROVA

Institute of Experimental Cardiology
Cardiology Research Center
Russian Academy of Medical Sciences
Moscow 121552, Russia

INTRODUCTION

Plasminogen activators play the role of biocatalyst in organisms, promoting the conversion of the plasma protein plasminogen to the enzyme plasmin.[1] The latter exhibits proteolytic activity, where fibrin serves as a substrate for the conversion. Proteolytic destruction of fibrin by plasmin is responsible for the thrombus dissolution.[2] Blood flow in the thrombosed vessel is restored and cardiovascular injuries become less crucial as a result of thrombolysis.

New preparations of plasminogen activators are being developed to enhance thrombolytic efficacy.[3] To this end, methods of chemical[4] and biological[5] synthesis are employed and the search for new plasminogen activators from other origins is pursued.[6] Earlier, we conjugated urokinase with fibrinogen.[7] This preparation of modified urokinase appeared to exhibit a pronounced and prolonged thrombolytic effect *in vivo*.[8] However, development of new preparations is not the sole approach to increasing thrombolysis efficacy.[6]

Conjunctive application of various plasminogen activator preparations can potentially enhance efficacy.[9] This conjunction is determined by different action mechanisms of plasminogen activators on the fibrin surface.[10] It is suggested that the combination of the trigger action of tissue-type plasminogen activator (which results in the exposure of new binding sites of the second type for plasminogen on the lysed fibrin clot[11]) and prolonged action of another activator, which sustains thrombolysis,[6,12] will provide substantial advantages for conjunctive thrombolytic therapy.[9]

The current work pursued an aim to test this approach on the model of venous thrombosis in dogs using tissue-type plasminogen activator (t-PA) as a trigger and the prolonged form of urokinase-fibrinogen (UK-Fbg) covalent conjugate as an agent of sustaining action for combined thrombolysis.

METHODS

The preparation of recombinant tissue-type plasminogen activator (Karl Thomae, Germany) and the urokinase-fibrinogen covalent conjugate obtained by the method described earlier[7] on the basis of commercial preparations of native urokinase (Japan Chemical Research Company, Japan) and human fibrinogen (Sigma) were used in the study.

Thrombolytic efficacy of the plasminogen activator preparations was assayed on the model of venous thrombosis in dogs described earlier.[13] Experiments were carried out on mongrel dogs with body weights of 10–21 kg (mean weight of 16 kg). Blood samples were taken to determine the initial level of blood radioactivity on a "Compugamma" counter (LKB, Sweden) in 5 min after removal of the ligature from the vein with the thrombus formed as a result of the ^{131}I-fibrinogen and blood

TABLE 1. Animal Groups

Animal Group No.	Administration Regime of Plasminogen Activators			Number of Dogs/Group (*n*)
	t-PA Administration			
	First Injection of t-PA (mg)	Two-Hour Infusion (mg)	Administration of UK-Fbg Conjugate (IU)[a]	
1	NaCl isotonic solution, 10 mL, control			4
2	—	—	25,000	4
3	2.5	—	—	3
4	1	1	25,000	4
5	1	4	25,000	4
6	1	1	250,000	4
7	—	—	250,000	3

[a]Administration of UK-Fbg conjugate intravenously as a bolus given 15 min after the first t-PA bolus.

fibrinogen interaction with thrombin. Blood samples were also taken 15, 30, 60, 90, 120, 150, 180, and 240 min after the initial administration of the thrombolytic to determine the radioactivity level. Changes in the level of blood radioactivity (% from the baseline level) indicated thrombolysis dynamics *in vivo*.[13] Each group included 3–4 dogs. The respective mode of administration and the doses of the preparations administered are listed in TABLE 1. The general scheme of the experiment is represented in FIGURE 1.

Results are given as mean values and standard deviations. Statistical analysis of the results was performed using the Kwikstat 2.11® package of statistical programs.[14] $P < 0.05$ was considered to indicate a statistical significance of differences.

RESULTS AND DISCUSSION

Intravenous bolus administration of 25,000 IU of UK-Fbg conjugate was reported[13] to prolong the thrombolytic effect of the preparation. We failed to observe any significant differences between the action of this dose and the action of t-PA

MONITORING OF BLOOD SAMPLES FOR 4 HOURS

| | 15 min | 30 min | 60 min | 90 min | 120 min | 150 min | 180 min | 240 min |

INITIATION OF THERAPY

2-hour intravenous infusion of t-PA

TERMINATION OF THERAPY

5 min

formation of venous thrombus

15 min

t-PA intravenous bolus

Intravenous bolus of UK-Fbg conjugate
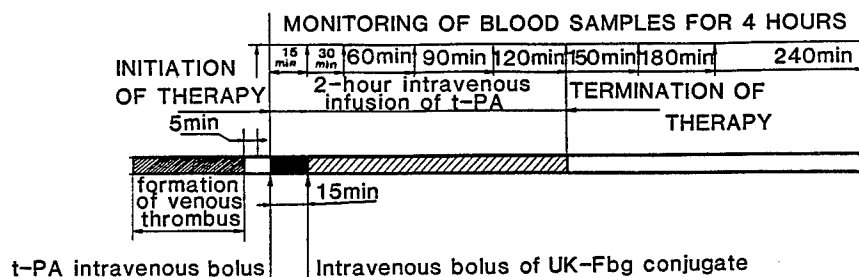
FIGURE 1. General scheme of the experiment. Conventional depiction of the tested dosage regime of t-PA and UK-Fbg covalent conjugate.

administered intravenously as a bolus in a dose of 2.5 mg (groups 2 and 3, TABLE 2). Conjunctive administration of t-PA and UK-Fbg covalent conjugate was used to enhance the thrombolytic effect. To this end, we performed a 2-h infusion of a given t-PA dose (in 50 mL saline) after bolus administration of 1 mg t-PA (in 10 mL saline) followed by a respective dose (in 10 mL saline) of UK-Fbg conjugate as an intravenous bolus given 15 min after the first bolus (TABLE 1). Different ratios of plasminogen activators were tested for this administration scheme (FIGURE 1, TABLE 1). Bolus-infusion administration in 1 mg t-PA and bolus administration of 25,000 IU of UK-Fbg showed virtually no significant differences compared with the action of similar doses of components (groups 4, 3, and 2; TABLE 2). Taking into account that the highest thrombolytic effect in dogs was achieved with a bolus-infusion scheme of

TABLE 2. Blood Sample Radioactivity in Dogs (% of Baseline Level) after Administration of Plasminogen Activators

Animal Group No.[a]	Blood Sample Radioactivity after the First Administration ($M \pm m$)							
	15 min	30 min	60 min	90 min	120 min	150 min	180 min	240 min
1	—	72 ± 18	62 ± 11	51 ± 16	46 ± 16	38 ± 6	32 ± 10	26 ± 13
2	—	76 ± 25	82 ± 10	79 ± 3	88 ± 26	75 ± 7	66 ± 14	81 ± 9
3	—	86 ± 21	89 ± 13	64 ± 22	60 ± 11	56 ± 16	64 ± 15	49 ± 9
4	—	68 ± 32	77 ± 14	85 ± 9	94 ± 18	73 ± 12	66 ± 16	81 ± 13
5	—	64 ± 22	67 ± 28	134 ± 36	128 ± 31	208 ± 20	224 ± 28	211 ± 19
6	128 ± 28	169 ± 9	243 ± 44	162 ± 23	167 ± 19	177 ± 31	189 ± 24	199 ± 16
7	95 ± 21	58 ± 28	119 ± 42	81 ± 15	90 ± 6	67 ± 19	72 ± 13	105 ± 11
P_{6-1}		*b	*	*	*	*	*	*
P_{6-3}		*	*	*	*	*	*	*
P_{6-7}		*	*	*	*	*	*	*
P_{6-5}		*	*		*	*	*	
P_{5-1}				*	*	*	*	*
P_{5-2}				*		*	*	*
P_{5-4}				*	*	*	*	*
P_{2-3}								*
P_{3-4}								*

[a]Designation of the animal groups according to TABLE 1.
[b]Asterisks indicate significant differences in the values of the compared groups, $P < 0.05$ (t test and ANOVA).

urokinase administration at a dose ratio of 1:3 (see reference 15) and the fact that t-PA has a short half-life in the blood flow,[2,3,6,10] we initiated a bolus administration of 1 mg t-PA and an infusion of 4 mg t-PA combined with 25,000 IU of UK-Fbg conjugate. Such a combination considerably increased thrombolysis, especially when t-PA infusion was discontinued (group 5, TABLE 2). However, the highest rate of thrombolysis was achieved with an increased dose of UK-Fbg conjugate of prolonged action. The bolus dose of UK-Fbg conjugate was raised to 250,000 IU during a bolus-infusion administration in 1 mg t-PA (group 6, TABLE 2), which provided a significantly faster action effect of the composition (FIGURE 2). Bolus administration
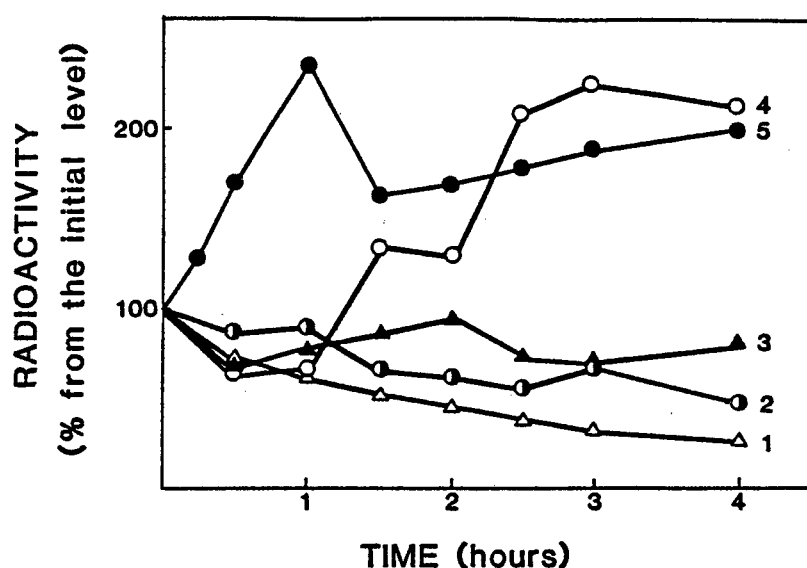
FIGURE 2. Dependence between the mean level of radioactivity of blood samples in dogs (% from the baseline level) and the time of taking blood samples after administration: (1) NaCl isotonic solution, a bolus of 10 mL/control; (2) 2.5 mg bolus of t-PA; (3) 1 mg bolus of t-PA, 1 mg infusion of t-PA, and 25,000 IU of UK-Fbg as a bolus; (4) 1 mg bolus of t-PA, 4 mg infusion of t-PA, and 25,000 IU of UK-Fbg as a bolus; (5) 1 mg bolus of t-PA, 1 mg infusion of t-PA, and 250,000 IU of UK-Fbg as a bolus.

of the UK-Fbg dose alone (group 7, TABLE 2) demonstrated a significant difference compared with the effect of the thrombolytic combination mentioned above (group 6, TABLE 2). This suggests that the thrombolytic potential of the UK-Fbg conjugate is revealed either in combination with mean t-PA doses infused (group 5, TABLE 2) or with the action of small t-PA doses combined with a bolus of large doses of UK-Fbg conjugate (group 6, TABLE 2). This dose regimen and dose ratio are likely to provide a significant trigger effect of t-PA, so a pronounced thrombolytic effect of UK-Fbg conjugate can be revealed. Conjunctive administration of the thrombolytics mentioned above is found to potentiate their thrombolytic action (FIGURE 2).

Conjunctive application of t-PA and UK-Fbg covalent conjugate appears to be promising for the development of efficient thrombolytic compositions for urgent therapy.

ACKNOWLEDGMENTS

REFERENCES

1. HENKIN, J., P. MARCOTTE & H. YANG. 1991. Prog. Cardiovasc. Dis. **34:** 135–164.
2. RUNGE, M. S., T. QUERTERMOUS & E. HABER. 1989. Circulation **79:** 217–224.
3. COLLEN, D., H. R. LIJNEN & H. K. GOLD. 1991. Prog. Cardiovasc. Dis. **34:** 101–112.
4. MAKSIMENKO, A. V. 1987. J. Chem. Soc. **32:** 541–547 (in Russian).
5. MAKSIMENKO, A. V. 1994. Khim. Farm. Zh. **28**(no. 5): 4–11 (in Russian; English translation, p. 293–302).
6. MAKSIMENKO, A. V. 1995. Mol. Biol. **29:** 38–60 (in Russian; English translation, p. 20–31).
7. MAKSIMENKO, A. V. & V. P. TORCHILIN. 1985. Thromb. Res. **38:** 289–295.
8. MAKSIMENKO, A. V., M. B. SAMARENKO, A. D. PETROV, E. G. TISCHENKO, M. YA. RUDA & V. P. TORCHILIN. 1990. Ann. N.Y. Acad. Sci. **613:** 479–482.
9. MAKSIMENKO, A. V. 1994. Khim. Farm. Zh. **28**(no. 12): 3–13 (in Russian; English translation, in press).
10. GUREVICH, V. 1989. Semin. Thromb. Hemostasis **15:** 123–128.
11. FLEURY, V., S. LOYAU, H. R. LIJNEN, W. NIEUWENHUISEN & E. ANGLES-CANO. 1993. Eur. J. Biochem. **216:** 549–556.
12. HOLVOET, P., M. DEWERCHIN, J. M. STASSEN, H. R. LIJNEN, T. TOLLENAERE, P. J. GAFFNEY & D. COLLEN. 1993. Circulation **87:** 1007–1016.
13. MAKSIMENKO, A. V., M. B. SAMARENKO, A. D. PETROV, E. G. TISCHENKO & V. V. ABRAMOVA. 1990. Khim. Farm. Zh. **24**(no. 2): 117–119 (in Russian).
14. ELLIOT, A. E. 1990. Statistical Data Analysis for IBM PC and Compatible Computers. Texasoft Mission Technologies. Houston, Texas.
15. KLAUBUNDE, R. E., C. C. HEMENWAY, J. HENKIN & S. F. BADYLAK. 1988. Thromb. Res. **50:** 857–864.

Primary Structure of Dextransucrase from *Leuconostoc mesenteroides* NRRL B-1299

Comparison with Dextransucrase from *Leuconostoc mesenteroides* NRRL B-512F[a]

VINCENT MONCHOIS, RENE-MARC WILLEMOT,
MAGALI REMAUD-SIMEON, CHRISTIAN CROUX,
PHILIPPE SOUCAILLE, AND PIERRE MONSAN

Centre de Bioingénierie Gilbert Durand
URA CNRS 544
INSA
Complexe Scientifique de Rangueil
31077 Toulouse Cedex, France

INTRODUCTION

Dextransucrase from *Leuconostoc mesenteroides* catalyzes the transfer of D-glucopyranosyl units from sucrose onto acceptor molecules. Two different products can be obtained: (i) a high-molecular-weight polysaccharide (dextran) and (ii) low-molecular-weight oligosaccharides when efficient acceptors, like maltose, are added to the reaction medium.[1]

The chemical structure of the dextran and oligosaccharides is dependent on the dextransucrase-producing strain: *Leuconostoc mesenteroides* NRRL B-512F produces a highly linear dextran molecule containing more than 95% $\alpha(1-6)$ osidic bonds, whereas NRRL B-1299 enzyme produces a highly branched dextran containing $\alpha(1-2)$ branchings. Both glucosyltransferases are used at an industrial scale.[2] Because the structure of the products is the essential key to their properties and their potential applications, we initiated a study of the structure/function relationship of these enzymes that should lead to the rational design of specific catalyzers for the synthesis of oligosaccharides.

With this in mind, we have cloned the gene coding for the dextransucrase from *L. mesenteroides* NRRL B-1299 and compared the sequence of the enzyme with the sequence already reported by Calgene on dextransucrase from *L. mesenteroides* NRRL B-512F.[3]

MATERIALS AND METHODS

The dextransucrase gene was reconstructed by screening *L. mesenteroides* NRRL B-1299 subgenomic DNA libraries with specific nucleotidic probes and cloned into pUC plasmid in the same or opposite direction relative to the lac-Z promoter (pGTF19 and pGTF18, respectively). DNA manipulations were carried out as described by Sambrook *et al.*[4] DNA sequencing was carried out via the dideoxy method in both directions by using custom-made primers. The primary structure of dextransucrase was compared with amino acid sequences of other glucosyltransferases using the FASTA programs. Enzyme activity was measured as described in reference 5.

Nucleotide sequence accession number: The dextransucrase gene sequence has been submitted to Genbank/EMBL and has been given accession number U38181.

RESULTS AND DISCUSSION

Expression of the Dextransucrase Gene in E. coli DH5α

The gene was expressed in *E. coli* DH5α as indicated by the release of reducing sugars from sucrose (FIGURE 1). The gene appeared to be expressed from its own promoter because addition of isopropyl β-thiogalactopyranoside (IPTG) to *E. coli* harboring pGTF19 did not increase enzyme activity. In addition, dextransucrase activity was still expressed when the gene was present on pGTF18 (FIGURE 1). These results suggest that the cloned fragment contains a promoter sequence recognized by the *E. coli* RNA polymerase. Oligosaccharides were detected by HPLC analysis of acceptor reaction products, indicating that the expressed enzyme was really a functional dextransucrase. However, because of the low expression level, it was impossible to detect the presence of dextran that is produced. In order to analyze this dextran, a fragment bearing the gene deleted from a 5′-end inverted repeated sequence, which probably blocked the RNA polymerase, was cloned in pUC19. With this new construction, the final activity ranging from 2 to 4 U/L was measured and was sufficient to synthesize dextran. The obtained polymer appeared to be insoluble.

Analysis of the Dextransucrase Gene Product

The dextransucrase gene covers 3870 bp and encodes a protein of 1290 amino acids with an M_r of 146,000, which is close to values found for the streptococcal glucosyltransferases (GTFs).[6] However, the ATG start codon is still presumptive, with the RBS (AGAG) being not very homologous to the Shine-Dalgarno consensus sequence AGGA. Amino acid sequencing of the N-terminal part of the protein will be necessary to confirm this view.

Homology with Glucosyltransferases/Dextransucrase of Known Sequence

The dextransucrase gene is very similar to *gtf* genes from streptococcal species and the dextransucrase gene from *L. mesenteroides* NRRL B-512F. The deduced

amino acid sequence displays 40% homology with the GTFs. The dextransucrase contains the two functional domains already described for other GTFs: an N-terminal catalytic domain responsible for the cleavage of sucrose and a C-terminal glucan-binding domain.

The N-terminal region, which corresponds to the catalytic region, also contains highly conserved domains. The sequence surrounding the aspartic acid at position 287, identified by Mooser and Iwaoka[7] in GTFs as a sucrose fixation site, is identical to that found in streptococcal GTFs. Thus, this aspartic acid residue identified as a covalently binding glucose site[7] should also be a sucrose-binding site for dextransu-crases (FIGURE 2). Site-directed mutagenesis experiments will be carried out to test
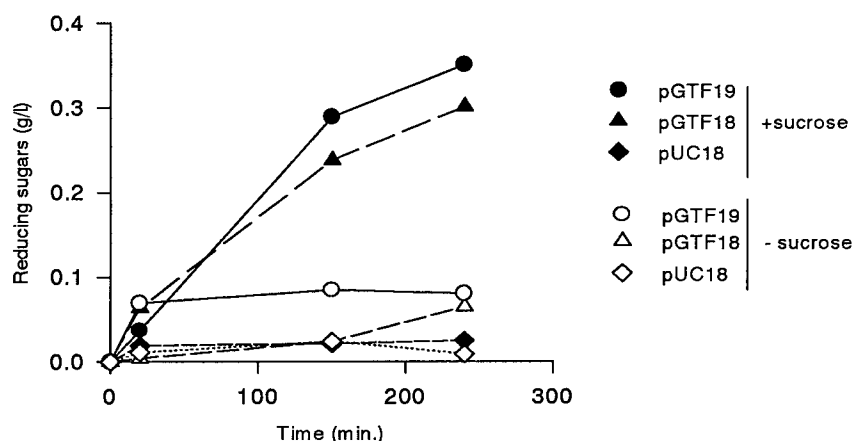
FIGURE 1. Dextransucrase activity of the *E. coli* DH5α-bearing dextransucrase gene. *E. coli* cells bear, respectively, pUC18, pGTF18, and pGTF19. IPTG (1 mM) was added in all cases and *E. coli* DH5α cells were cultured overnight at 30 °C in LB medium supplemented with 100 µg/mL ampicillin. Intracellular extracts were prepared by sonication. Activity was measured by determination of the reducing sugars released in the presence (solid symbols) or absence (open symbols) of 100 g/L sucrose.

this hypothesis. A sequence homologous to the site proposed by Funane *et al.*[8] as being the glucosyl-transfer site can be identified at position 244–256. In this se-quence, two aspartic residues located at position 246 and 248 could be proposed as potential sucrose-binding sites (FIGURE 2). A nonconserved threonine (position 401) was also identified on the *L. mesenteroides* NRRL B-1299 dextransucrase gene (FIGURE 2). Among the GTFs, it was shown that this residue greatly influenced the solubility of the glucan synthesized. Site-directed mutagenesis of the threonine residue at this position resulted in a streptococcal enzyme-synthesizing soluble glucan.[9] However, our results show that the threonine is not the key element determining the solubility of the synthesized dextran because the *L. mesenteroides* NRRL B-512F and B-1299 enzymes possess the threonine residue.

The carboxy-terminal domains of all streptococcal GTFs possess a series of glycine-rich repeats that are probably involved directly in glucan binding.[10] In the carboxy-terminal domain of the dextransucrase, five repeats homologous to the A

(I)

```
DS1299  282  DGYRVDAVDNVDADLL
DS512   544  DGIRVDAVDNVDADLL
GTFI    446  DSIRVDAVDNVDADLL
GTFS    430  DGVRVDAVDNVNADLL
```

(II)

```
DS1299  243  LANDVDNSNPVVQAEQLNWLHY
DS512   509  LANDVDNSNPVVQAEQLNWLYY
GTFI    411  LANDVDNSNPIVQAEQLNWLHY
GTFS    395  LANDVDNSNPVVQAEQLNHLHY
```

(III)

```
DS1299  385  AQPNYSFIRAHDSEVQTIIADII
DS512   649  AIPNYSFVRAHDSEVQTVIAQIV
GTFI    551  TVPSYSFARAHDSEVQDLIRDII
GTFS    535  PVPNYVFIRAHDSEVQTRIAKII
```

FIGURE 2. Comparison between conserved sites influencing the activity of GTFs. The sequences are deduced from *L. mesenteroides* NRRL B-1299 dextransucrase gene (DS1299), *L. mesenteroides* NRRL B-512F dextransucrase gene (DS512), and *S. downei* MFE28 *gtfI*[14] and *gtfS*[15] (GTFI, GTFS). The sucrose-binding site (I), the proposed glucosyl-transfer site (II), and the sequence with the nonconserved threonine (III) are represented in bold type.

repeats and three repeats homologous to the C repeats present in the glucan-binding protein of *Streptococcus mutans*[11] were identified (FIGURE 3). Other types of repeats, not previously described, have also been identified (FIGURE 3). This domain is also similar to the carboxy-terminal domain of the *C. difficile* toxin implicated in the binding with the carbohydrate part of antigens.[12] No direct correlation between the nature of the direct repeats and the glucan structure has been found yet.[13]

CONCLUSIONS AND PERSPECTIVES

Cloning and sequencing of the gene coding for the dextransucrase from *L. mesenteroides* NRRL B-1299 led to the first characterization of this enzyme. Comparison of the sequence of this glucosyltransferase with the sequences of dextransucrase from *L. mesenteroides* NRRL B-512F and GTFs from streptococcal species showed a good conservation of the overall structure and of the sites directly implicated in the enzyme mechanism. A higher level of enzyme expression will be necessary for the initiation of physicochemical investigations. Future site-directed mutagenesis experiments of the enzymatic sites (sucrose-binding and glucosyl-transfer sites) and

A repeats	C repeats	Other repeats
942WYYFDDKGKMVVGNQVINGINYYFLP	1159 GESRYY DPDSGNMITDRF	1006 HYFFEDGHMAQGIVTIIQSDG
1075WLYVDEKGNAVTGKQTINNQTVYFN	1223 GIMRYY DADTGELVRNRF	1053 HYF DG ASGNMLF KSWG
1117WLYLNNKGVAVTGEQIINGQTLYFGN	1286 GNQRYWMDKDSGEMKKITY	
1182WAYFGYDGVAVTGDRIIKGQNLYFNQN		
1246WVYFGQDGVPVTGVQVINGQTLYFD		

FIGURE 3. Amino acid sequences of A, C, and other repeats. These repeated units are located at the carboxyl end of the *L. mesenteroides* NRRL B-1299 dextransucrase. Residues are numbered from the start methionine. Conserved residues are in bold type.

detailed analysis of oligosaccharides and dextran produced by the mutants will give precious information on the structure/function relationships of such glucosyltransferases. The result of this study could lead to the elaboration of highly specific tools for the industrial synthesis of new osidic compounds.

REFERENCES

1. MONSAN, P. & F. PAUL. 1991. *In* Food Enzymology. Volume 2. P. F. Fox, Ed.: 69–81. Elsevier. Amsterdam/New York.
2. MONSAN, P., F. PAUL & D. AURIOL. 1995. Ann. N.Y. Acad. Sci. **750:** 357–363.
3. WINKLE DOUGLAS, M., J. T. PERCHOROROWICZ, C. M. HOUCH & B. R. THOMAS. 1989. United States patent no. WO89/12386.
4. SAMBROOK, J., E. F. FRITSCH & T. MANIATIS. 1989. *In* Molecular Cloning: A Laboratory Manual. Second edition. Cold Spring Harbor Laboratory Press. Cold Spring Harbor, New York.
5. REMAUD-SIMEON, M., A. LÓPEZ-MUNGUÍA, V. PELENC, F. PAUL & P. MONSAN. 1994. Appl. Biochem. Biotechnol. **44:** 101–117.
6. GIFFARD, P. M., C. L. SIMPSON, C. P. MILWARD & N. A. JACQUES. 1991. J. Gen. Microbiol. **137:** 2577–2593.
7. MOOSER, G. & K. R. IWAOKA. 1989. Biochemistry **28:** 443–449.
8. FUNANE, K., M. SHIRAIWA, K. HASHIMOTO, E. ICHISMA & M. KOBAYASHI. 1993. Biochemistry **32:** 13696–13702.
9. SHIMAMURA, A., Y. J. NAKANO, H. MUSAKA & H. K. KURAMITSU. 1994. J. Bacteriol. **176:** 4845–4850.
10. GIFFARD, P. M. & N. A. JACQUES. 1994. J. Dent. Res. **73:** 1133–1141.
11. BANAS, J. A., R. R. B. RUSSELL & J. J. FERRETTI. 1990. Infect. Immun. **58:** 667–673.
12. EICHEL-STREIBER, C., M. SAUERBORN & H. K. KURAMITSU. 1992. J. Bacteriol. **174:** 6707–6710.
13. NAKANO, Y. J. & H. K. KURAMITSU. 1992. J. Bacteriol. **174:** 5639–5646.
14. GILMORE, K. S., R. R. B. RUSSELL & J. J. FERRETTI. 1990. Infect. Immun. **58:** 2452–2458.
15. FERRETTI, J. J., M. L. GILPIN & R. R. B. RUSSELL. 1987. J. Bacteriol. **169:** 4271–4278.

Parameters Affecting Lipase Production
by HEMA-immobilized Bacteria

C. N. A. RAZAK, Z. ZAKARIA, A. B. SALLEH, K. AMPON,
W. M. Z. YUNUS, M. BASRI, AND D. MOHD

Enzyme and Microbial Research
Faculty of Science and Environmental Studies
Universiti Pertanian Malaysia
43400 UPM Serdang, Malaysia

INTRODUCTION

The immobilization of microbial cells has attracted the interest of industrial sectors due to its obvious practical advantages. Apart from catalyzing a single-step reaction, it is able to catalyze multistep reactions or biosynthesis and on a continuous basis. In addition, it elevates the tedious enzyme isolation and purification procedures. It also allows reactions to be carried out at a higher cell concentration and the products to be easily harvested.[1,2]
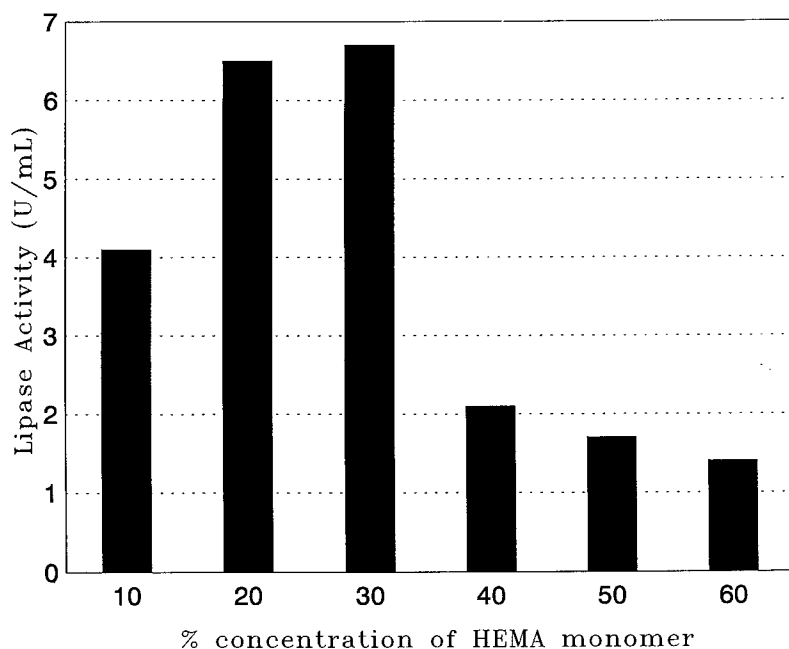
FIGURE 1. Effect of HEMA monomer concentration on lipase production: grown at 45 °C, 200 rpm, for 72 h.

To date, a wide range of microbial cells have been immobilized and are being used in various applications.[2] A variety of carrier materials, ranging from natural to artificial materials, each with their own merits and demerits, have been employed. 2-Hydroxyethyl methacrylate polymer (PHEMA) has been used by other workers to immobilize yeast and fungal cells.[3,4] It is a porous and swellable polymer prepared by radiation-induced polymerization of hydrophilic glass-forming monomers at temperatures below 0 °C. This report describes the application of PHEMA as the carrier material for the immobilization of a lipolytic *Pseudomonas* sp.
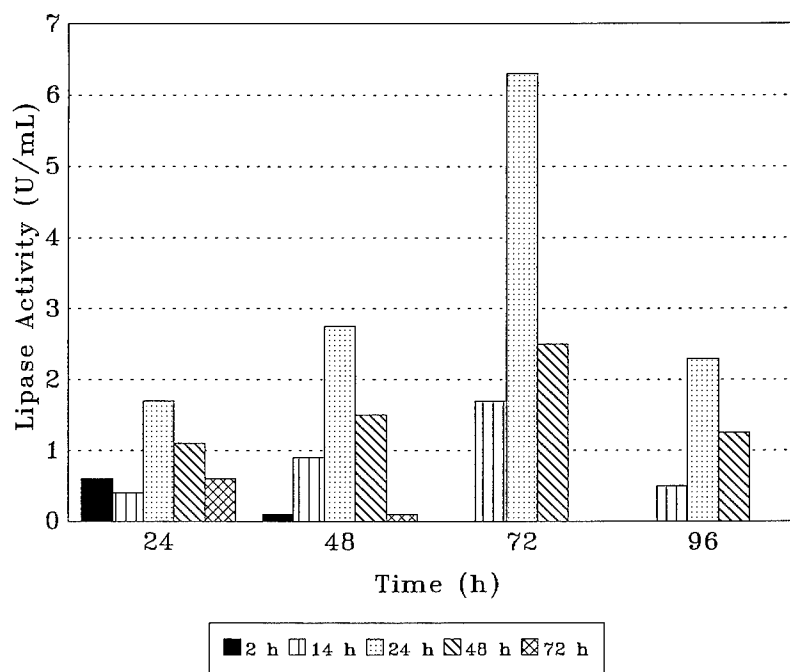
FIGURE 2. Effect of adsorption time on lipase production. PHEMA (20%, 1 g) was shaken together with bacteria (0.4 g) in 50 mL of nutrient for various time intervals.

MATERIALS AND METHODS

Preparation of PHEMA Using Gamma Radiation

Various concentrations of HEMA monomers:water (10%, 20%, 30%, 40%, 50%, and 60%, w/v) were irradiated at -78 °C with γ rays (1.5 Mrad) from a ^{60}Co source for 2 h. The resultant polymer carriers were cut into small cubes, soaked in water overnight, and sterilized by autoclaving at 121 °C for 15 min.
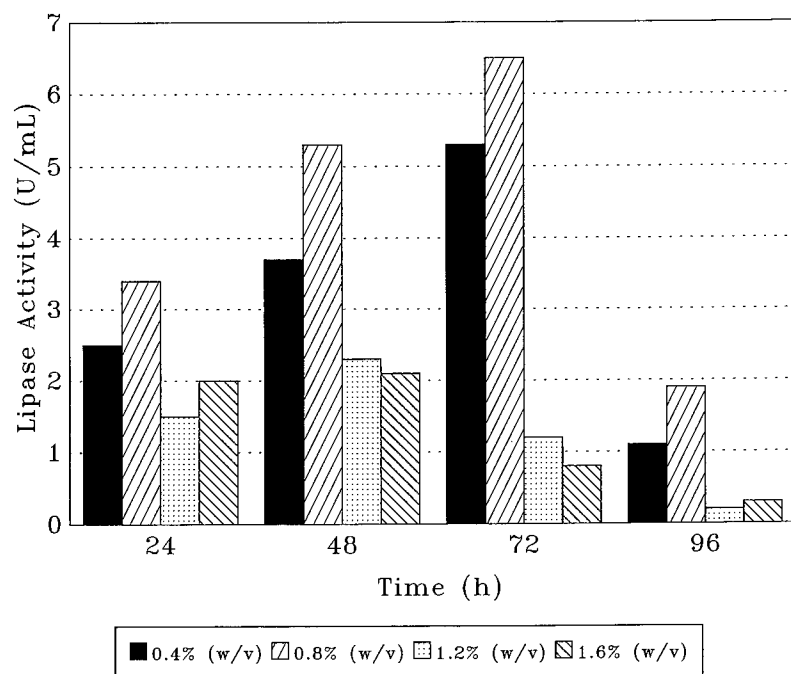
FIGURE 3. Effect of cell concentration on lipase production. PHEMA (20%, 1 g) was shaken with different concentrations of bacteria in 50 mL of nutrient for 24 h.

Immobilization of Cells

The cells (a lipolytic *Pseudomonas* sp. isolated from a palm oil mill effluent) were immobilized by a postpolymerization adsorption method. Bacterial cells (0.4 g) from an 18-h culture were cultured together with 1 g of PHEMA cubes in 50 mL nutrient broth at 37 °C for 24 h, under shaking conditions. The immobilized bacteria were decanted and washed twice with sterile nutrient broth.

Production of Lipase

Immobilized cells were inoculated into 50 mL medium containing 1% glycerol trioleate and 1% yeast extract, pH 7.0, in a 250-mL flask. The culture was shaken

TABLE 1. Effect of Polymer Size on Lipase Production

Size (mm) of PHEMA	Lipase Activity (U/mL)			
	24 h	48 h	72 h	96 h
2 × 2 × 2	3.8	4.0	6.0	0.3
4 × 4 × 2	3.2	3.7	6.8	2.1
6 × 6 × 2	0.7	2.7	2.3	1.3
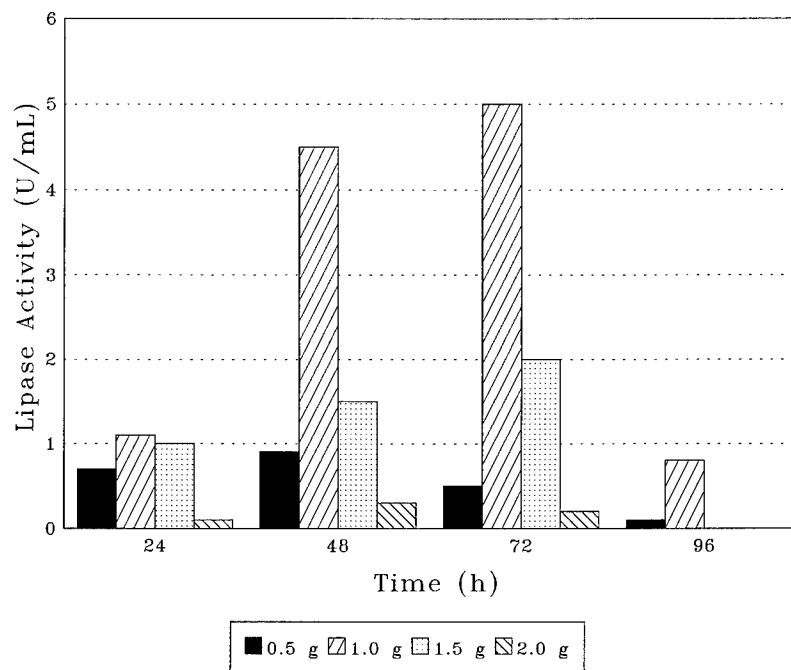
FIGURE 4. Effect of inoculum size on lipase production.

(200 rpm) at 45 °C in a water bath shaker. Lipase activity was assayed at 24-h intervals by the rate of olive oil hydrolysis.[5]

RESULTS AND DISCUSSION

Effect of HEMA Monomer Concentration

The highest lipase production was obtained when 20–30% monomer was used (FIGURE 1), similar to that reported by Yoshida and Kaetsu.[6] A monomer concentration of between 10% and 40% formed a white and porous polymer. At higher concentrations, the polymer was rigid and less porous.[6] Low production at higher concentrations could be attributed to fewer cells being adsorbed onto the polymer with few and smaller pores.

Effect of Adsorption Time

Lipase production increased with time up to 24 h. Increasing the adsorption time further resulted in decreased production (FIGURE 2). The decrease in production with longer adsorption time might be due to too many cells being adsorbed. The

nutrient and oxygen supply might become limited, especially to the cells on the inner layers.

Effect of Cell Concentration

Production of lipase was highest when a cell concentration of 0.8% (w/v) was used for the adsorption process (FIGURE 3). At lower concentrations, the production was reduced. With higher cell concentrations, the maximum productions were reached faster, but the yields were lower. This might be due to the polymer being overloaded with microorganisms, which reduced the rate of diffusion of the nutrient and oxygen, resulting in low productivity.

Effect of Polymer Size

TABLE 1 shows that production was highest when 4 × 4 × 2–mm polymer cubes were used. There was a marked decrease in production with 6 × 6 × 2–mm cubes. This might be due to inefficient nutrient transfer in bigger cubes. Hence, only cells on the outer surface are in their optimal condition.
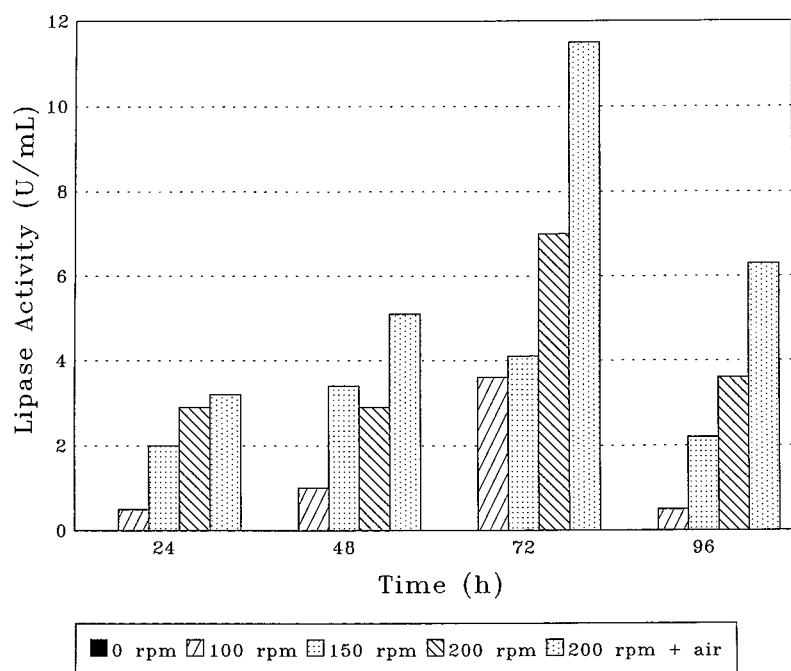
FIGURE 5. Effect of shaking and aeration on lipase production.

Effect of Inoculum Size

The optimum inoculum size was 1.0 g of PHEMA-immobilized bacteria in 50 mL medium (FIGURE 4). Increasing the inoculum size decreased the yield. A similar trend was observed with the alginate-immobilized cells, where an optimum inoculum size existed for a certain fixed volume of nutrient.[5] Use of excess immobilized cells reduced the cell activity.

Effect of Agitation

No lipase was produced under static conditions and the production increased with an increase in the shaking rate. Maximum yield was achieved when shaken at 200 rpm (FIGURE 5). Added aeration by means of bubbling sterile air into the culture
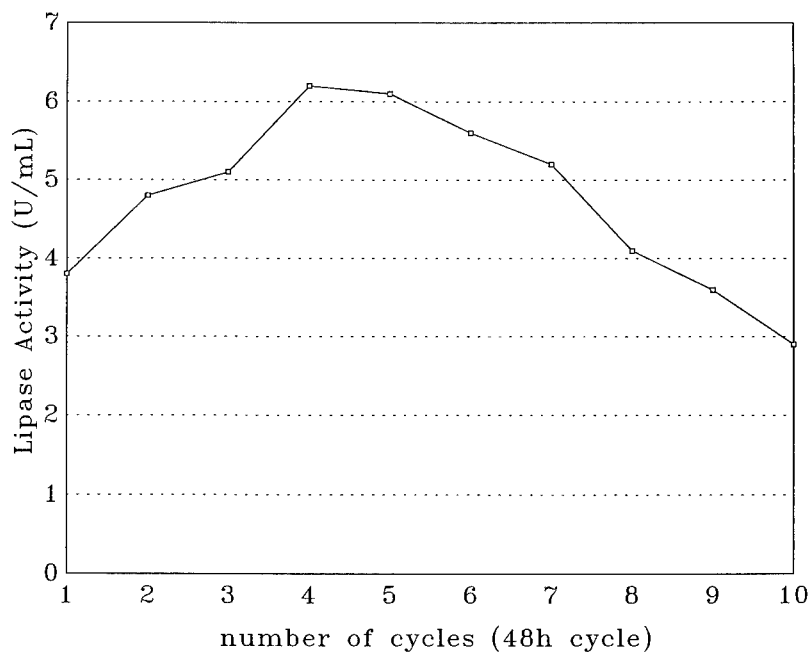
FIGURE 6. Effect of recycling on lipase production.

medium increased the production further. Agitation not only helped to mix the immobilized cells with the nutrient and facilitated the diffusion of air, but it also helped to prevent the accumulation of metabolites within the polymer.

Recycling

Lipase production by the immobilized cells continued to increase up to the fourth cycle (8 days) and slowly decreased (FIGURE 6). Similar behavior was also reported

by Kumakura *et al.*[7] The increase in production could be correlated to the maximum cell growth in that cycle. PHEMA, being porous, would swell to its maximum capacity in tandem with the growth of the cells. The immobilized cell system still retained 60% of its activity after the tenth cycle.

REFERENCES

1. SCOTT, C. D. 1987. Immobilized cells: a review of recent literature. Enzyme Microb. Technol. **9:** 66–73.
2. POWELL, W. L. 1990. *In* Microbial Enzymes and Biotechnology. Second edition. W. M. Forgaty & C. T. Kelly, Eds.: 369–394. Elsevier. Amsterdam/New York.
3. KAETSU, I., M. KUMAKURA, F. TAKASHI, N. KASAI & M. TAMADA. 1987. Immobilization of microbial cells and yeast cells and its application to biomass conversion using radiation techniques. Radiat. Phys. Chem. **29:** 191–193.
4. HIGA, O. Z., N. L. MASTRO & A. C. CASTAGNET. 1986. Immobilization of cellulase and cellobiose by radiation-induced polymerization. Radiat. Phys. Chem. **27:** 311–316.
5. ZAKARIA, Z., C. N. A. RAZAK, K. AMPON, M. BASRI, W. M. Z. YUNUS, Y. SHIRAI, A. B. SALLEH & K. HASHIMOTO. 1992. Optimum conditions for the production of lipase by alginate-immobilized bacteria. J. Gen. Appl. Microbiol. **38:** 429–438.
6. YOSHIDA, M. & I. KAETSU. 1981. Immobilization of glucoamylase on polymer surface by radiation-induced polymerization of glass-forming monomers at low temperatures. J. Appl. Polym. Sci. **26:** 687–700.
7. KUMAKURA, M., I. KAETSU & K. NISIZAWA. 1984. Cellulase production from immobilized growing cell composites prepared by radiation polymerization. Biotechnol. Bioeng. **26:** 17–21.

Automated Docking of Glucoamylase Substrates and Inhibitors

PEDRO M. COUTINHO,[a] MICHAEL K. DOWD,[b]
AND PETER J. REILLY[a,c]

[a]*Department of Chemical Engineering*
Iowa State University
Ames, Iowa 50011

[b]*Southern Regional Research Center*
United States Department of Agriculture
New Orleans, Louisiana 70179

INTRODUCTION

The *exo*-hydrolase glucoamylase (GA) in nature produces glucose from the nonreducing ends of starch and maltooligosaccharide molecules. It can cleave all α-linked bonds between two glucosyl residues, with rates decreasing in the order of α-(1 → 4) (maltose), α,β-(1 → 1) (α,β-trehalose), α-(1 → 6) (isomaltose), α-(1 → 3) (nigerose), and α-(1 → 2) (kojibiose).[1] At the high concentrations of partially hydrolyzed starch used as raw material in industry, GA produces appreciable amounts of all these disaccharides, but chiefly isomaltose,[2] and smaller amounts of oligosaccharides, reducing glucose yield to about 96% of theoretical. This is a serious problem, given the high tonnage of glucose produced as an intermediate in the high-fructose sweetener process.

Aspergillus awamori/niger GA is composed of two domains: catalytic (467 amino acid residues) and starch-binding (108 residues), separated by a 41-residue, highly glycosylated linker. The catalytic domain consists of 13 helices, 12 of them in an $(\alpha,\alpha)_6$-barrel.[3] The active site is in a funnel-shaped well, with Glu179 serving as the catalytic acid[4] and Glu400 as the catalytic base.[5] It holds maltose, its primary substrate, in a different mode than it holds isomaltose.[6]

We have been subjecting GA to site-directed mutagenesis to improve its selectivity toward glucose production (essentially to increase its ability to hydrolyze and synthesize maltose and/or decrease its ability to hydrolyze and synthesize isomaltose).[7] Automated docking of substrates and inhibitors in the active site helps in understanding the interaction of different substrates with GA and therefore in choosing suitable amino acid residues to mutate for improved selectivity. We have used this technique with a series of isomaltosides (FIGURE 1) of different hydrolysis kinetics and with a series of inhibitors (FIGURES 2 and 3) of very different strengths.

[c]To whom all correspondence should be addressed.
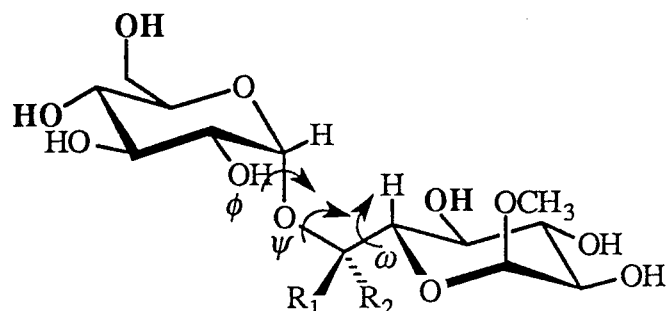
FIGURE 1. Methyl-α-isomaltoside (R$_1$ = H; R$_2$ = H), methyl-α-6R-C-methyl-α-isomaltoside (R$_1$ = CH$_3$; R$_2$ = H), and methyl-α-6S-C-methyl-α-isomaltoside (R$_1$ = H; R$_2$ = CH$_3$). The critical hydroxyl groups required for hydrolysis of isomaltose[18] are shown in bold.

COMPUTATIONAL TECHNIQUES

Structures of the molecules to be docked were optimized by the molecular mechanics algorithm MM3(92) (Quantum Chemistry Program Exchange, Blooming-ton, Indiana, or Technical Utilization Corporation, Powell, Ohio) as before.[8] All low-energy local minima of disaccharide substrates and inhibitors, but only the optimal monosaccharide structure, were used for docking.

Docking simulations were with AutoDock 2.1 (Scripps Research Institute, La Jolla, California)[9,10] using Monte Carlo–simulated annealing (the Metropolis method). The nonreducing-end ring of each ligand was superimposed on the crystal structure position of the corresponding ring of gluco-dihydroacarbose in the GA active site[11,12] to increase the number of successfully docked structures. Two rounds of docking simulations were made. After each round, cluster analysis of all structures generated for a single compound was performed. The best structures obtained for each ligand following the first round were redocked.
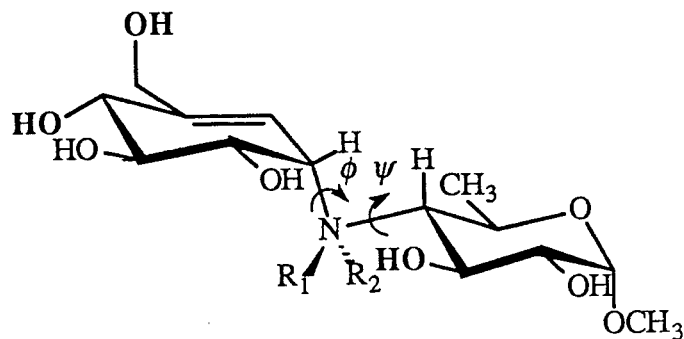
FIGURE 2. Methyl-α-R-acarviosinide (R$_1$ = H; R$_2$ = nothing) and methyl-α-S-acarviosinide (R$_1$ = nothing; R$_2$ = H). The critical hydroxyl groups required for hydrolysis of maltose[18] are shown in bold.
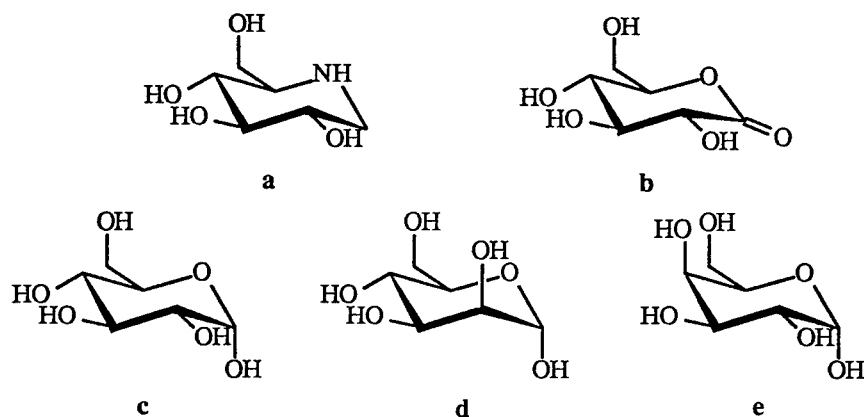
FIGURE 3. Structures: (a) 1-deoxynojirimycin, (b) glucono-1,5-lactone, (c) α-glucose, (d) α-mannose, and (e) α-galactose.

DOCKING OF INHIBITORS

Numerical results for the docked structures of 1-deoxynojirimycin, glucono-1,5-lactone, and α- and β-glucose are presented in TABLE 1, whereas those for methyl-α-R- and methyl-α-S-acarviosinide are found in TABLE 2. Actual docked and crystal structures of 1-deoxynojirimycin appear in FIGURE 4, whereas docked structures of methyl-α-R- and methyl-α-S-acarviosinide are compared with the crystal structure of acarbose in FIGURE 5.

TABLE 1. Docking of Monosaccharides and Analogues[a]

Substrate	Total Energy (kcal/mol)	Internal Energy (kcal/mol)	rmsd[b] (Å)	K_i (M^{-1})
1-deoxynojirimycin [327/400]	−72.03 (−67.75)	−1.46 (0.95)	0.257[c] (0.415)	3.3 × 10^4 [e]
glucono-1,5-lactone [144/200]	−65.40 (−61.37)	−2.48 (0.73)	0.335[c] (0.584)	6.3 × 10^2 [f,g]
α-glucose [144/200]	−71.95 (−66.52)	−1.41 (−0.99)	0.469[c] (0.638)	6.3[f]
β-glucose [299/400]	−74.01 (−66.51)	−2.73 (1.19)	0.390[d] (0.602[d])	

[a]Key—in brackets: number of structures in cluster/total number of simulations; in parentheses: cluster average results.
[b]rmsd: root-mean-square deviation.
[c]Using crystal structure of compound complexed with GA[5,12] as reference to determine rmsd.
[d]Using crystal structure of α-glucose complexed with GA as reference.
[e]Reference 13.
[f]Reference 14.
[g]Reference 15.

TABLE 2. Docking of Acarviosinides Compared to Acarbose in GA Complex[a]

Substrate	Total Energy (kcal/mol)	Internal Energy (kcal/mol)	Dihedral Angles (°)		rmsd[b] (Å)
			ϕ	ψ	
methyl-α-R-acarviosinide [11/100]	−104.77 (−103.55)	−4.62 (−5.96)	−19 (−14)	8 (4)	0.463[c] (0.450)
methyl-α-S-acarviosinide [93/100]	−102.22 (−96.52)	1.41 (1.45)	−20 (−20)	7 (7)	0.456[c] (0.494)
acarbose[c]			−16	6	

[a]Key—in brackets: number of structures in cluster/total number of simulations; in parentheses: cluster average results.
[b]rmsd: root-mean-square deviation.
[c]Using crystal structure of equivalent atoms of acarbose complexed with GA[16] as reference.
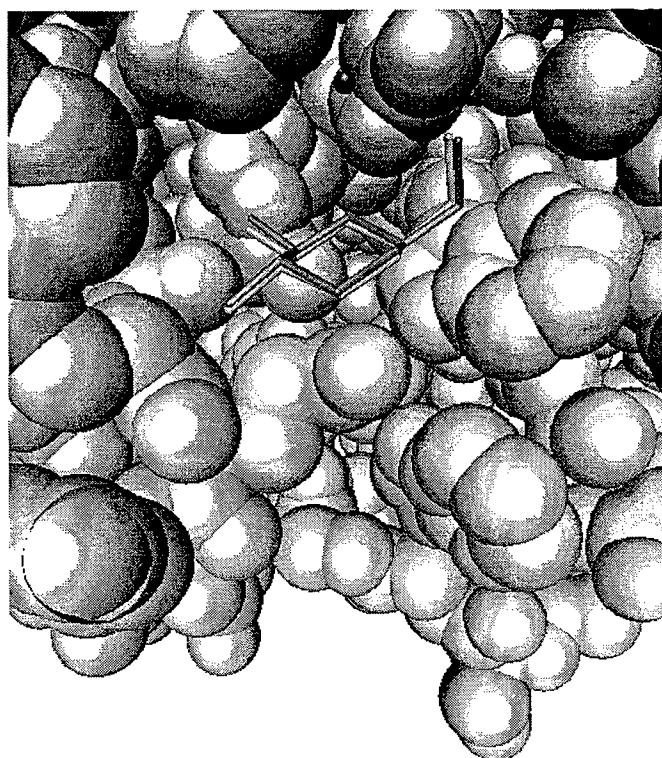
FIGURE 4. GA active site interacting with 1-deoxynojirimycin as obtained by docking simulation (dark gray) versus the crystal structure in GA complex (white). The catalytic water present in docking simulations is also shown.

Excellent fits were obtained for all four inhibitors compared to their crystal structures in the corresponding GA complex (TABLE 1). Interestingly, smaller deviations were found for β-glucose than for α-glucose when both were referenced to the α-glucose structure found in a GA complex.

The two acarviosinides are close to the equivalent residues of acarbose complexed in the GA active site,[16] as are their imino linkage dihedral angles (TABLE 2). Their very negative binding energies agree with their very high joint K_i (2.0×10^7 M^{-1}).[13]
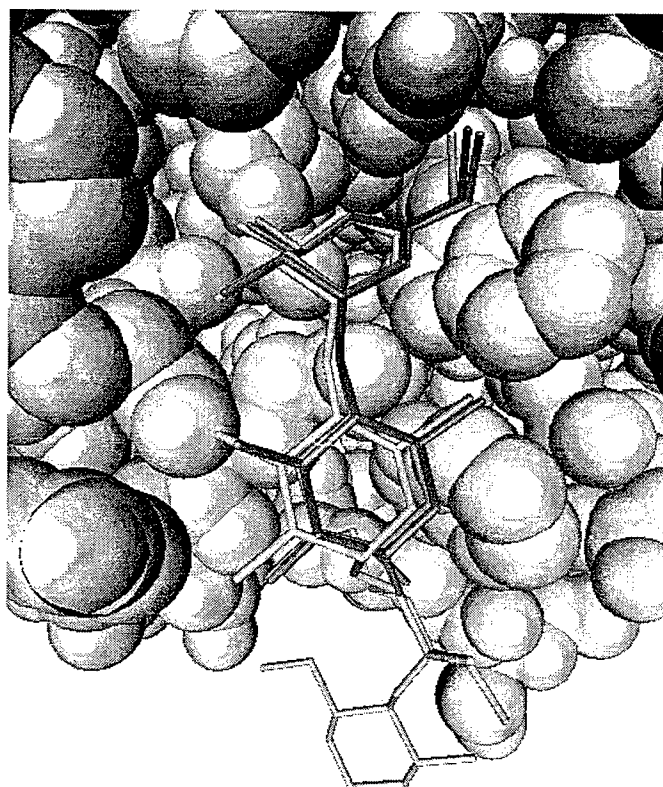
FIGURE 5. GA active site interacting with docked methyl-α-R-acarviosinide (dark gray) and methyl-α-S-acarviosinide (light gray) versus the crystal structure of acarbose in GA complex (white). The catalytic water present in docking simulations is also shown.

The docking simulations of monosaccharide substrates of GA that can be involved in condensation reactions are given in TABLE 3. Both anomeric forms of glucose, mannose, and galactose can dock in GA's active site, as found experimentally when the three monosaccharides were incubated with GA and disaccharides were formed.[17] Glucose binds better than the other monosaccharides and it reacts

TABLE 3. Docking of Monosaccharide Substrates

Substrate	Total Energy (kcal/mol)	Internal Energy (kcal/mol)	rmsd[a] (Å)
α-glucose	−71.95	−1.41	0.469
β-glucose	−74.01	−2.73	0.390
α-mannose	−69.21	−2.21	0.733
β-mannose	−69.07	−0.53	1.038
α-galactose	−67.24	−0.62	0.851
β-galactose	−70.32	−4.16	1.012

[a]Using crystal structure of α-glucose complexed with GA[12] as reference to determine root-mean-square deviation (rmsd).

faster. Binding of mannose is also observed in the first subsite, whereas that of galactose is only observed at the second subsite in the crystal structure.[12]

DOCKING OF ISOMALTOSIDES

Numerical results of the docking simulations of the isomaltosides are shown in TABLE 4, whereas their docked structures appear in FIGURE 6.

The total energy of interaction is lowest for the methyl-α-6R-C-methyl-α-isomaltoside, followed by methyl-α-isomaltoside and finally the 6S-C-compound. The results agree with the k_{cat}/K_M values obtained experimentally, even considering

TABLE 4. Final Docking Results for Isomaltosides in the Active Site[a]

Substrate	Total Energy (kcal/mol)	Internal Energy (kcal/mol)	Dihedral Angles (°) φ	ψ	ω	k_{cat}/K_M (mM^{-1}-s^{-1})
methyl-α-isomaltoside						
[136/300]	−97.48	0.50	−19	132	18	0.042[b]
	(−90.93)	(5.59)	(−18)	(137)	(9)	
[43/300]	−96.04	10.20	−20	146	4	
	(−91.92)	(11.09)	(−23)	(148)	(8)	
methyl-α-6R-C-methyl-α-isomaltoside						
[212/300]	−102.29	7.96	−27	137	16	0.96[b]
	(−96.52)	(1.45)	(−30)	(141)	(17)	
methyl-α-6S-C-methyl-α-isomaltoside						
[61/300]	−76.03	14.78	−41	127	36	0.012[b]
	(−70.91)	(15.35)	(43)	(126)	(34)	
[6/300]	−68.75	12.70	−48	146	53	
	(−67.33)	(12.82)	(−46)	(144)	(51)	
[86/300]	−67.94	20.53	5	−134	−27	
	(−59.10)	(20.49)	(14)	(−131)	(−30)	

[a]Key—in brackets: number of structures in cluster/total number of simulations; in parentheses: cluster average results.
[b]Reference 18.

that the position of the 6-OH in the first methyl-α-isomaltoside structure is such that binding may not lead to hydrolysis.

Methyl-6R-C-methyl-α-isomaltoside has a clear unique low-energy binding mode. The optimal productive structure of methyl-6S-C-methyl-α-isomaltoside has a relatively low energy of interaction compared to the other isomaltosides. This is partially due to the fact that the extra methyl group is found perpendicular to the plane formed by the two glycosyl rings; therefore, it makes bad steric contacts with the active-site wall in such a way that it cannot fully penetrate the active site. Of all the
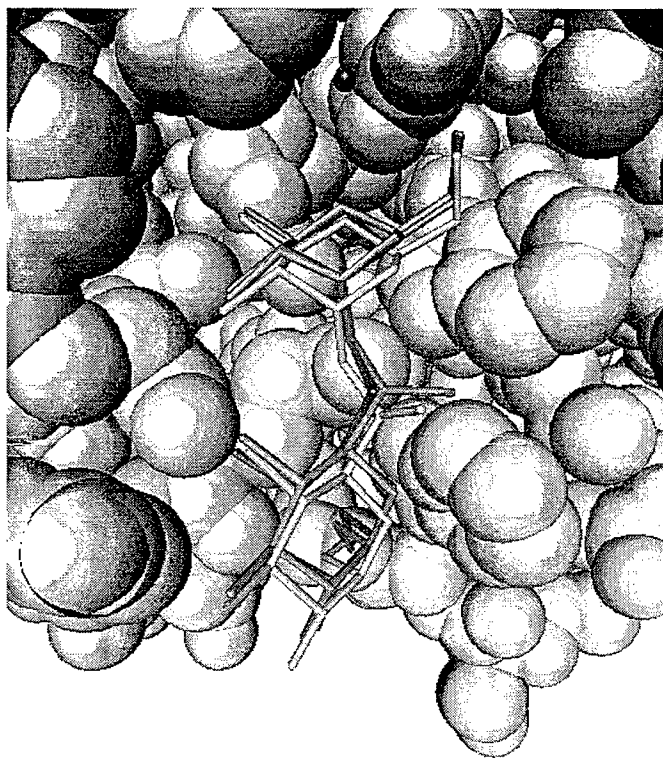
FIGURE 6. GA active site interacting with docked methyl-α-isomaltoside (dark gray) and with docked methyl-6R-C-methyl-α-isomaltoside (light gray) and its S-isomer (white). The catalytic water present in docking simulations is also shown.

isomaltosides, the 6S-C-compound had the highest internal energy—no surprise because MM3 modeling had already shown that it is the most conformationally restricted isomaltoside. As a result of these difficulties, other binding modes become accessible, such as the third cluster, which is completely nonproductive.

The binding energies from docking methyl-α-isomaltoside, methyl-6R-C-methyl-α-isomaltoside, and methyl-6S-C-methyl-α-isomaltoside agree with kinetic data. Furthermore, conformational and steric effects influence the binding of these

isomaltosides. The similarity of the docking results of simpler compounds with results obtained by crystallography validates the approach.

More generally, an effective docking procedure for monosaccharides and disaccharides has been developed to complement information obtained by X-ray crystallography and kinetic studies.

REFERENCES

1. MEAGHER, M. M. & P. J. REILLY. 1989. Biotechnol. Bioeng. **34:** 689–693.
2. NIKOLOV, Z. L., M. M. MEAGHER & P. J. REILLY. 1989. Biotechnol. Bioeng. **34:** 694–704.
3. ALESHIN, A., A. GOLUBEV, L. M. FIRSOV & R. B. HONZATKO. 1992. J. Biol. Chem. **267:** 19291–19298.
4. SIERKS, M. R., C. FORD, P. J. REILLY & B. SVENSSON. 1990. Protein Eng. **3:** 193–198.
5. HARRIS, E. M. S., A. E. ALESHIN, L. M. FIRSOV & R. B. HONZATKO. 1993. Biochemistry **32:** 1618–1626.
6. COUTINHO, P. M. & P. J. REILLY. 1994. Protein Eng. **7:** 393–400.
7. SIERKS, M. R., C. FORD, P. J. REILLY & B. SVENSSON. 1993. Protein Eng. **6:** 75–79.
8. DOWD, M. K., P. J. REILLY & A. D. FRENCH. 1994. Biopolymers **34:** 625–638.
9. GOODSELL, D. S. & A. J. OLSON. 1990. Proteins **8:** 195–202.
10. GOODSELL, D. S., H. LAUBLE, C. S. STOUT & A. J. OLSON. 1993. Proteins **17:** 1–10.
11. STOFFER, B., A. E. ALESHIN, L. M. FIRSOV, B. SVENSSON & R. B. HONZATKO. 1995. FEBS Lett. **358:** 57–61.
12. ALESHIN, A. E. 1995. Personal communication.
13. SIGURSKJOLD, B. W., B. SVENSSON, G. WILLIAMSON & H. DRIGUEZ. 1994. Eur. J. Biochem. **225:** 133–141.
14. LÁSZLO, E., J. HOLLÓ, A. HOSCHKE & G. SÁROSI. 1978. Carbohydr. Res. **61:** 387–394.
15. OHNISHI, H., H. KITAMURA, T. MINOWA, H. SAKAI & T. OHTA. 1992. Eur. J. Biochem. **207:** 413–418.
16. ALESHIN, A. E., L. M. FIRSOV & R. B. HONZATKO. 1994. J. Biol. Chem. **269:** 15631–15639.
17. PESTLIN, S., D. PRINZ, J. M. STARR & P. J. REILLY. 1996. Biotechnol. Bioeng. Submitted.
18. PALCIC, M. M., T. SKRYDSTRUP, K. BOCK, N. LE & R. U. LEMIEUX. 1993. Carbohydr. Res. **250:** 87–92.

Polyclonal Catalytic Anti-idiotypic Antibodies with a β-Lactamase Activity

BERANGERE AVALLE, DOMINIQUE MISTRO,
DANIEL THOMAS, AND ALAIN FRIBOULET

Laboratoire de Technologie Enzymatique
URA CNRS 1442
Université de Technologie de Compiègne
60206 Compiègne Cedex, France

INTRODUCTION

Since Niels Jerne's basic report in 1974 on the network theory of immune regulation,[1] the mimicry properties of anti-idiotypic antibodies, displaying an antigen functional "internal image," have been clearly demonstrated. From this concept arose the idea of the production of anti-idiotypic antibodies bearing catalytic skills, using an enzymatic active site as the antigen.[2,3] The first step consists of producing a monoclonal antibody Ab1 against the active site of the enzyme, thus exhibiting inhibition properties. This Ab1 is then used to elicit a second generation of antibodies Ab2, directed against the Ab1 hypervariable specific sequence, and thus potentially mimicking the enzymatic active site.

In the present work, β-lactamase (EC 3.5.2.6), a strictly bacterial amidase hydrolyzing the endocyclic amide bond of the β-lactam ring of antibiotics, was chosen as the model enzyme. This strictly bacterial activity offers the possibility to measure directly in serum the appearance of a catalytic activity, usually absent in mammalian systems.

PRODUCTION AND SCREENING OF MONOCLONAL ANTIBODIES AGAINST THE β-LACTAMASE ACTIVE SITE (Ab1)

Balb/c mice were immunized with 40 μg of purified β-lactamase from *Bacillus cereus*. After four injections at two-week intervals, mice were boosted three days before fusion. Three successive cell fusions with SP2/0 myeloma cells, under standard conditions,[4] have allowed the selection by ELISA test of 150 stable hybridoma cell lines secreting monoclonal IgG specific for the enzyme. Positive clones were then used to generate ascitic tumors in order to obtain sufficient quantities of monoclonal antibodies (mAbs) for inhibition studies. The inhibition of β-lactamase by specific mAbs purified on a protein A–agarose column was investigated by incubating each mAb at different concentrations with 5 nM β-lactamase, for 16 h at 4 °C, in 100 mM phosphate buffer, pH 7.4, containing 0.5% gelatin. The residual enzymatic activity was measured at 570 nm after adding the substrate, 12 μM PADAC [7-(thienyl-2-acetamido)-3-[2-(4-*N*,*N*-dimethylaminophenylazo) pyridinium-methyl]-3-cephem-4-carboxylic acid]. The residual enzyme activity decreases

up to 60% when the amount of one of the tested mAbs, 7AF9, increases from 10-fold to 200-fold, whereas it does not vary when incubated with other anti-β-lactamase antibodies (FIGURE 1). The mAb 7AF9 therefore displays an inhibitory action that is specific because, for example, mAb 110D9, which also tightly binds β-lactamase, has no significant effect on the enzymatic activity. In order to deepen the effect of mAb 7AF9 on the enzymatic activity, we have measured the inhibition kinetics with varying substrate concentration. We found that inhibition of β-lactamase by mAb 7AF9 follows a mixed-type inhibition. The inhibition constant was found to be 20
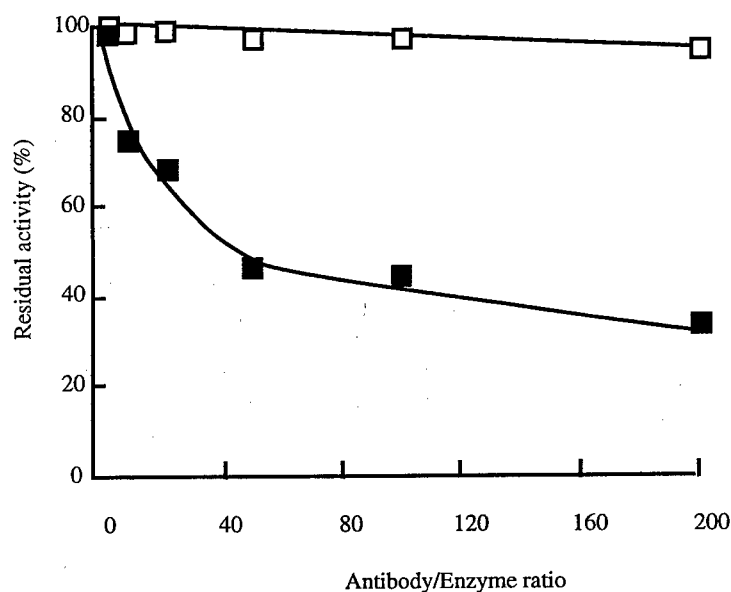
FIGURE 1. Inhibition of β-lactamase activity by Ab1. Measurement of residual activity was performed after incubation with mAbs that were first screened for binding to the enzyme. IgG 7AF9 (■) and IgG 110D9 (□) are shown as examples.

μM. On the other hand, mAb 7AF9 previously bound to β-lactamase coated in microtitration wells was displaced by increasing the concentration of benzylpenicillin, a substrate of the enzyme (data not shown). Thus, mAb 7AF9 competes with substrate for binding, at least in part, to the β-lactamase active site.

CATALYTIC ACTIVITY OF POLYCLONAL ANTISERA

IgG 7AF9 was therefore used to immunize Biozzi mice, which are highly responsive to weakly immunogenic antigens.[5] The ability of mice to produce antibodies to 7AF9 was evaluated on 200-fold diluted antisera, through an ELISA test where F(ab')$_2$ fragments of 7AF9 were coated on solid phase (FIGURE 2). All immunized Biozzi mice turned out to be sensitive to mAb 7AF9. The amount of IgG increases

with the immunization stage (named I1 to I4), whereas the IgM response follows a characteristic immunological profile.

The catalytic activity of polyclonal antibodies contained in the antiserum of immunized mice was then assayed by incubating 25-fold diluted antisera on plates previously coated with 2.5 μg/mL of goat anti-mouse Ig (H + L) antibodies. After washing with phosphate buffer saline (PBS)–0.1% Tween 20, PADAC was added at a final concentration of 25 μM. A weak, but significant and reproducible, catalytic activity was detected in antisera of immunized mice (FIGURE 2). This phenomenon is observed to be linked to the amount of specific antibodies, as displayed by the ELISA test. This result gives clear evidence for the presence in the polyclonal preparation of
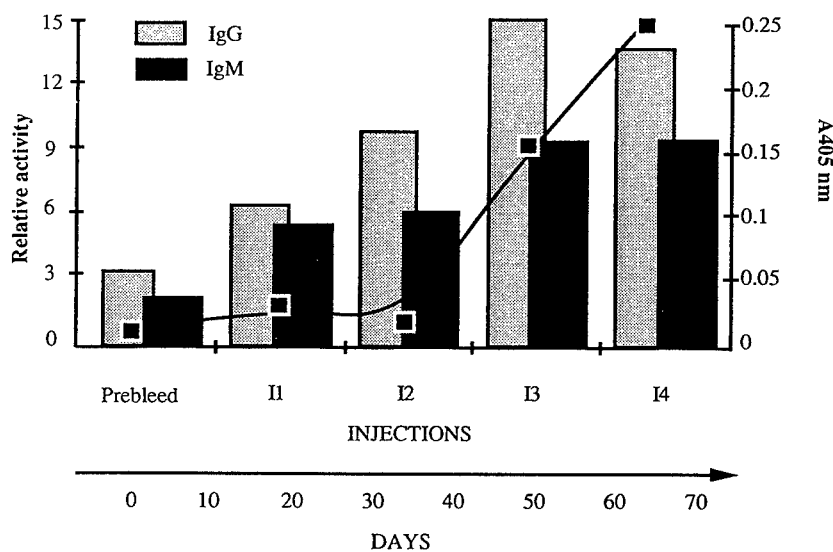
FIGURE 2. Immunological and catalytic activities of polyclonal antibodies (Ab2). IgG and IgM levels were measured at different steps of the immunization. β-Lactamase activity (■) was measured at each step in 25-fold diluted antisera.

an antibody fraction likely to catalyze the hydrolysis of the β-lactam substrate. These antibodies are clearly induced by the immunization with mAb 7AF9 because the catalytic ability of the polyclonal preparation follows the immunization regimen. This result is backed up by the fact that addition of increasing amounts of 7AF9 results in a proportional inhibition of the measured catalytic activity.

Hydrolysis of PADAC by polyclonal antibodies followed Michaelis-Menten kinetics, and the kinetic parameters were determined. The V_{max} and K_m values were calculated as $V_{max} = 1.3 \times 10^{-4}$ μM/min and $K_m = 3$ μM. The K_m value for PADAC hydrolysis by β-lactamase was found to be 10-fold higher. Low K_m values compared with the values obtained with corresponding enzymes or monoclonal antibodies have already been described.[6,7] These results might indicate that polyclonal preparations

allow the detection of good catalysts, in terms of affinity, that are not necessarily recovered after the fusion procedure to prepare monoclonal antibodies.

CONCLUSIONS

This report describes the experimental demonstration of the anti-idiotypic approach that allows the induction of the appearance of a catalytic activity beared by antibodies at a level sufficient to be directly measured in antisera. The next step of the present work consists of producing monoclonal catalytic antibodies in order to investigate the catalytic properties of a homogeneous preparation. However, these results open routes in the conception of vaccines eliciting catalytic antibodies—for example, with a specific protease activity against toxins or viral envelope proteins. On the other hand, many groups have shown that cephalosporins are highly versatile triggers in the construction of enzyme-activable prodrugs.[8] Catalytic antibodies with a β-lactamase activity could therefore allow the construction of bispecific antibodies or minibodies able to specifically bind to tumor cells and transform prodrugs into cytotoxic drugs.

REFERENCES

1. JERNE, N. K. 1974. Ann. Immunol. (Paris) **125:** 373–389.
2. JORON, L., L. IZADYAR, A. FRIBOULET, M. H. REMY, G. PANCINO, A. ROSETO & D. THOMAS. 1992. Ann. N.Y. Acad. Sci. **672:** 216–223.
3. IZADYAR, L., A. FRIBOULET, M. H. REMY, A. ROSETO & D. THOMAS. 1993. Proc. Natl. Acad. Sci. U.S.A. **90:** 8876–8880.
4. KÖHLER, G. & C. MILSTEIN. 1975. Nature **256:** 495–497.
5. FRIBOULET, A. & L. IZADYAR-DEMICHELE. 1995. Methods Mol. Biol. **51:** 211–222.
6. PAUL, S. 1994. Appl. Biochem. Biotechnol. **47:** 241–255.
7. GALLACHER, G., M. SEARCEY, C. S. JACKSON & K. BROCKLEHURST. 1992. Biochem. J. **284:** 675–680.
8. KERR, D. E., P. D. SENTER, W. V. BURNETT, D. L. HIRSCHEBERG, I. HELLSTROM & K. E. HELLSTROM. 1990. Cancer Immunol. Immunother. **31:** 202–206.

Localization of an Endoglucanase and a Xylanase from *Aspergillus niger* in Soybean by Immunogold-Cytochemical Labeling

T. VARZAKAS, D. L. PYLE, AND K. NIRANJAN

Biotechnology and Biochemical Engineering Laboratory
Department of Food Science and Technology
University of Reading
Reading RG6 6AP, United Kingdom

INTRODUCTION

Electron microscopy studies have been carried out to determine whether extracellular enzymes such as cellulases and hemicellulases from *A. niger* are freely diffusible or whether they are localized in the cell walls of soybean cells. The aim was to study soybean cell wall and cytoplasm ultrastructure during degradation, as well as to visualize the spatial distribution of enzymes and the soybean degradation by immunocytochemical labeling techniques. These enzymes were particularly chosen because they hydrolyze the structural polysaccharides of the soybean cell wall (cellulose, hemicellulose) and assist in extraction, with the immediate result of an increase in protein and oil yields.

TEM (transmission electron microscopy) has been used followed by immunogold labeling[1] to localize β-glucosidase within ultrathin sections of hyphae. Several recent studies have investigated the penetrability of wood-decay enzymes into the cell wall by the use of TEM and immunogold labeling.[2–4] It has been shown[5] that lignocellulolytic enzymes are located at the cell wall surfaces and cannot penetrate into the wood structure unless the wood cell wall has already been decayed by small molecules such as hydrogen peroxide or veratryl alcohol.

The aims of the study were as follows. The first aim was to localize the place of action of these two enzymes in half-soybean cotyledons. This place of action may be the site of synthesis, the site of storage of inactive precursor, or the site of activity. Half-soybean cotyledons were chosen because, by cutting small sections from them, it was easier to do our analysis and see the diffusion. The second aim was to see how the enzymes got into the protein and lipid bodies, whereas the third was to investigate why they ended up there and not in the cell wall and why the affinity for the cell wall was low. The hypothesis that needs to be tested is that cell wall–degrading enzymes should be localized in the cell walls and not in the storage bodies.

MATERIALS AND METHODS

Purification of β-Glucosidase and Production of Polyclonal Antibodies

β-Glucosidase was isolated[1] and purified from liquid cultures of *Coriolus versicolor* grown on CMC-Abrams medium. Antibodies were raised in rabbits in response

to three intramuscular injections of β-glucosidase at three-week intervals. The serum collected was given to us as a gift from C. Evans (University of Westminster, United Kingdom) for use in the immunogold-labeling experiment.

Specificity of Antibodies

The Ouchterlony double diffusion test[6] was carried out to test if the antibody was specific to the antigens added.

Experiments with Soybean Cotyledons

Soybean cotyledons were soaked and dehulled. Half-cotyledons were cooked at 100 °C to inactivate the endogenous enzymes present in the soybean. Then, they were imbibed with cellulase from *Aspergillus niger* (5 mg/mL in acetate buffer, pH 5) and hemicellulase from the same source (5 mg/mL in acetate buffer, pH 5.4), and incubated at 37 °C for two different periods of time, that is, 1 hour and 24 hours. A control involved half-soybean cotyledons inactivated by cooking at 100 °C for 15 minutes in order to kill the preexisting enzymes in the soybean. Following the experiment, both enzymes were washed off with acetate buffer and samples were ready for sectioning. Electron microscopy then followed, which involved fixation, dehydration, infiltration with resin, and examination under a Jeol 100S transmission electron microscope at 80 kV.

Immunocytochemical Labeling

Ultrathin sections of soybean embedded in LR White were collected on nickel grids with Formvar. Sections were quenched in a blocking solution for 30 minutes and were then incubated for 1 hour in antiserum to β-glucosidase diluted 1:50. The blocking solution and antiserum diluent was normal goat serum (Sera Lab, Crawley Down, Sussex, United Kingdom) given to us as a gift from C. Evans. This was diluted 1:30 in phosphate-buffered saline [PBS: 0.5 M NaCl, 10 mM KH_2PO_4 (pH 7.2), 0.02% NaN_3, and 0.5% (w/v) bovine serum albumin (BSA)]. Following this, sections were washed for 30 minutes in blocking solution and were then washed in PBS containing 0.1% BSA three times. The next step was incubation in GAR_{15} [Auro-Probe goat anti-rabbit IgG (H + L) G15] purchased from Cambio (Cambridge, United Kingdom). After three 10-minute washes in PBS containing 0.1% BSA, sections were rinsed in distilled water and stained in 2% (w/v) aqueous uranyl acetate for 1 hour and in 1% lead citrate for 10 minutes using the LKB 2168 Ultrastainer (Plant Sciences, University of Reading, United Kingdom).

A control was very important in the whole method. After killing of the enzymes in the control soybean tissue, sectioning, electron microscopy, and immunocytochemical labeling were carried out as described earlier.
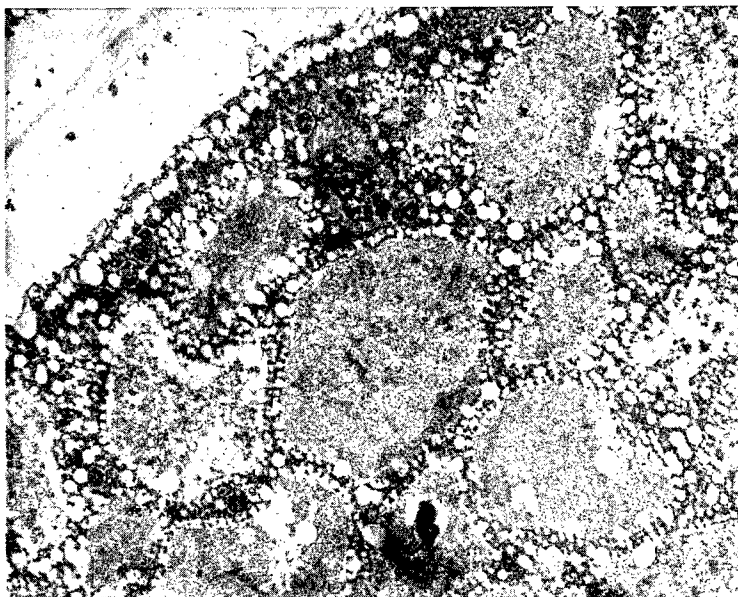
FIGURE 1. The control soybean tissue. There is very small nonspecific background labeling.

RESULTS AND DISCUSSION

The specificity of the antibodies was characterized by the immunodiffusion test. The antiserum to β-glucosidase caused smoothly fused precipitation lines around the antigens (the commercial preparations of cellulase and hemicellulase), forming cross-reactivity with them. The control was negative as no gold particles were observed under the TEM (FIGURE 1). Thus, we proceeded into the experiment described above. Immunogold labeling of soybean tissue with TEM was used to visualize endoglucanase and xylanase under different incubation times by treatment of all the sections with diluted antiserum to β-glucosidase in conjunction with a secondary antibody labeled with gold (see FIGURES 2–4).

There have been a lot of difficulties in interpreting the photos and this could be explained as follows. The labeling obtained was not strong, although the affinity was good, as observed from the Ouchterlony test. The nature of the resin seemed to affect the quality of labeling. We should also bear in mind the heterogeneity and impurities of the available substrates that make the specificity of cellulolytic and hemicellulolytic enzymes difficult to determine.

Enzymes appeared to have penetrated cell walls from the secondary to the primary layers including the middle lamella (FIGURES 2 and 4). However, little degradation seems to have occurred (FIGURE 2); the degradation was presumably the result of interactions between the cell wall and enzymes. The cell wall–degrading enzymes studied here mostly ended up in the cytoplasm of soybean cells (protein and

lipid bodies) after diffusing into it (FIGURE 3). There was more intensive labeling in the soybean cells (protein and lipid bodies) in comparison to the cell wall and the middle lamella. This seems to be in opposition to our hypothesis, which suggests that cell wall–degrading enzymes should be localized in the cell wall rather than in the storage bodies.

A quantitative evaluation of the labeling, expressed as the number of gold particles per μm^2 (area) of each cellular compartment, is presented in TABLE 1. This labeling corresponds to the enzymic activity of the specific enzyme. Areas and numbers of gold particles were determined with Image Analyzer (Plant Sciences, University of Reading) picture processing software. It is obvious that the most intensely labeled organelle is the cytoplasm of the soybean cells, including both the protein bodies and the lipid bodies. The labeling over the cell wall or the middle lamella appeared to be very low or nonexistent. However, the labeling experiment suggested that the endoglucanase after 24 hours of infiltration had intensive labeling over the middle lamella. Xylanase after 24 hours had more labeling compared to xylanase after 1 hour and to the rest of the samples for both protein and lipid bodies. Labeling of endoglucanase did not demonstrate any major differences between the samples of 1 hour and 24 hours.

Our micrographs have shown intense labeling over the protein bodies, but much less over the cell wall and the middle lamella. According to our theoretical calculations, there is more than enough enzyme for degradation to occur. We believe that
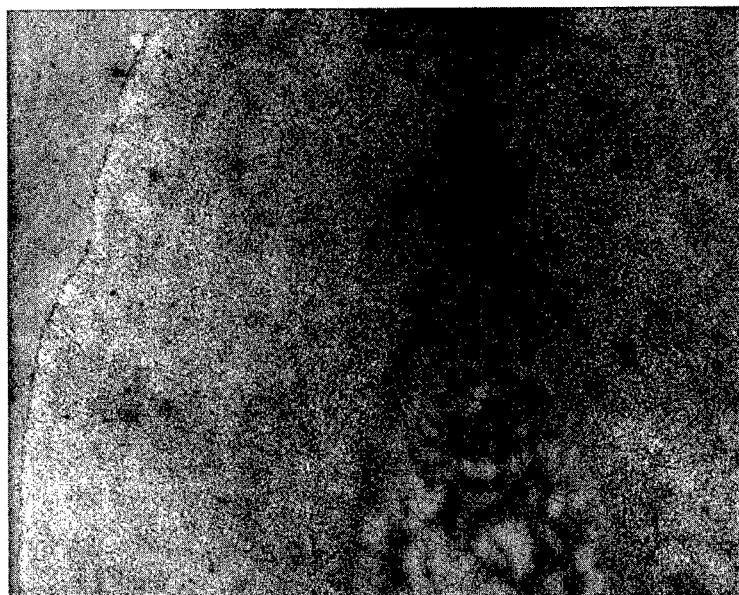
FIGURE 2. An area on the soybean cell wall with not very intense labeling. The sample was endoglucanase incubated for 1 hour.

the soybean pore size is just large enough to allow enzymes to pass through. These enzymes diffuse through, but do not stick to, the soybean cell wall as expected according to our hypothesis. Steric hindrance may have prevented the cell wall–degrading enzymes from sticking to the soybean cell walls. Various interferences also reduce the solute diffusivity. These might include the cytoplasmic membrane or plasmalemma; the cell wall; the tortuous nature of the air spaces, thereby increasing the diffusional path length; the adsorption of the solute to the solid matrix; and the release of high-molecular-weight polymers from the cytoplasm and from the solid matrix, increasing the viscosity of the imbibed liquid. Moreover, plant tissue may not be an optimal environment for enzyme activity.
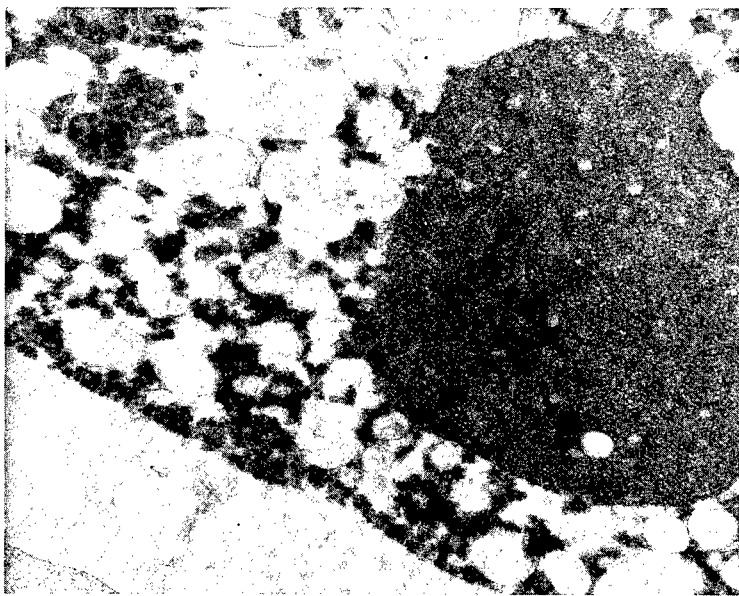
FIGURE 3. As in FIGURE 2, but with xylanase incubated for 1 hour: labeling mainly on the protein body.

It is important to stress that direct physical contact between cellulases and cellulose or between hemicellulases and hemicellulose can only be achieved if diffusion of these enzymes takes place at susceptible sites on the gross surfaces of the fiber or on the microfibrillar and molecular surfaces within the fiber wall. We should assume that it is necessary to have pores as large as or larger than the largest dimension of a given enzyme so that unimpeded accessibility occurs. This is because both rotational and translational modes of motion are assumed during diffusion of dissolved solute molecules.

FIGURE 4. As in FIGURE 2, but with xylanase incubated for 24 hours: not very intense labeling over the middle lamella.

CONCLUSIONS

Our results have shown that endoglucanase and xylanase are well localized in the cytoplasm of soybean cells, with not very intense labeling in the cell wall or middle lamella. Further investigation is required and these data need to be supported by measurements of pore sizes in the soybean. The results were not in accord with our hypothesis.

There have been a lot of difficulties in interpreting these results. Problems that

TABLE 1. Density of Labeling over the Cellular Compartments at Different Times[a]

	Cell Wall	Protein Body	Lipid Body	Middle Lamella
endoglucanase (1 h)	0.26 ± 0.25	2.77 ± 0.44	*	*
		2.47 ± 0.4		
endoglucanase (24 h)	*	2.41 ± 0.31	6.49 ± 1.99	4.56 ± 0.32
xylanase (1 h)	*	1.84 ± 0.53	1.29 ± 2.04	*
xylanase (24 h)	*	3.72 ± 0.36	10.63 ± 1.62	0.51 ± 2.68
		3.07 ± 1.09	7.87 ± 4.72	

[a]The values represent the number of gold particles per μm^2 ± SEM. An asterisk indicates that no activity was identified.

have been encountered involve the specificity of the primary antisera, the movement of the enzymes during fixation, and electron microscopy processing.

REFERENCES

1. EVANS, C. S. 1985. Properties of the β-D-glucosidase (cellobiase) from the wood-rotting fungus, *Coriolus versicolor.* Appl. Microbiol. Biotechnol. **22:** 128–131.
2. SREBOTNIK, E., K. MESSNER & R. FOISNER. 1988. Penetrability of white-rot wood by the lignin peroxidase of *Phanerochaete chrysosporium.* Appl. Environ. Microbiol. **54**(11): 2608–2614.
3. DANIEL, G., T. NILSSON & B. PETTERSSON. 1989. Intra- and extracellular localization of lignin peroxidase during the degradation of solid wood and wood fragments by *Phanerochaete chrysosporium* by using transmission electron microscopy and immunogold labeling. Appl. Environ. Microbiol. **55**(4): 871–881.
4. BLANCHETTE, R. A., A. R. ABAD, R. L. FARRELL & T. D. LEATHERS. 1989. Detection of lignin peroxidase and xylanase by immunocytochemical labeling in wood decayed by basidiomycetes. Appl. Environ. Microbiol. **55**(6): 1457–1465.
5. EVANS, C. S., M. V. DUTTON, F. GUILLEN & R. G. VENESS. 1994. Enzymes and small molecular mass agents involved with lignocellulose degradation. FEMS Microbiol. Rev. **13:** 235–240.
6. OUCHTERLONY, O. 1949. Antigen-antibody reactions in gels. Acta Pathol. Microbiol. Scand. **26:** 507–515.

Effect of Monovalent Cations (K⁺ and Na⁺) on Lactose Hydrolysis by *Kluyveromyces lactis* β-Galactosidase

A Kinetic Model[a]

MARÍA V. FLORES,[b] RODOLFO J. J. ERTOLA,[c]
AND CLAUDIO E. VOGET[c,d]

[b] *Grupo de Ingeniería Bioquímica*
Facultad de Ingeniería
Universidad Nacional de Mar del Plata
7600 Mar del Plata, Argentina

[c] *Centro de Investigación y Desarrollo en Fermentaciones Industriales*
(CINDEFI)
Facultad de Ciencias Exactas
Universidad Nacional de La Plata
1900 La Plata, Argentina

INTRODUCTION

Kinetic models are a prerequisite for the successful application of biocatalysts. In industrial practice, the difficulty lies in the kinetic complexity because the rates of enzymatically catalyzed reactions are influenced by almost every physical and chemical variable known. Enzymic lactose hydrolysis in milk and whey products is carried out with yeast- or fungal-derived β-galactosidases (β-gal, EC 3.2.1.23).[1] In previous studies, we have demonstrated the critical role of monovalent cations on the stability and activity of the *Kluyveromyces lactis* β-gal. The enzyme requires the presence of a monovalent cation, for example, K⁺, Na⁺, or NH₄⁺, to be active. Lactose hydrolysis is inhibited by Na⁺ in the presence of K⁺; thus, the inhibitory effect of Na⁺ is a function of the cation concentration ratio rather than a function of its absolute concentration.[2]

A simple model for lactose hydrolysis is described to explain the kinetic behavior of the *K. lactis* β-gal in the presence of the aforementioned cations. Considering that Na⁺ and K⁺ are the main monovalent cations present in natural substrates, the kinetic model will certainly have practical applications.

FORMULATION OF THE MODEL

It is assumed that Na⁺ and K⁺ activate the enzyme by binding to the same single specific receptor. The equilibrium reaction between the free cation and the free

[d] To whom all correspondence should be addressed.

enzyme can be expressed as follows:

$$E + Na \rightleftarrows ENa \qquad K_{Na} = [ENa]/[E][Na] \qquad (1)$$

$$E + K \rightleftarrows EK \qquad K_K = [EK]/[E][K] \qquad (2)$$
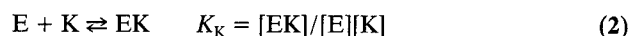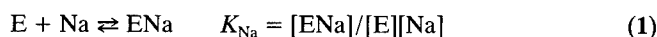
where K_{Na} and K_K are the equilibrium constants and ENa and EK are the cation-activated enzymes. Provided that K_K and K_{Na} are large and the cation concentration high, all of the enzyme will be cation-bound and therefore active. In practice, the initial rates of lactose hydrolysis are of zero order with respect to Na^+ or K^+ concentration in the range of 20–200 mM.[2] It should also be considered that the true cation concentration is $\gg E_0$ (total enzyme concentration) and therefore it is approximately equal to the amount of cation initially added.

When both cations are present, the receptors will be occupied by either Na^+ or K^+. The conservation equation for the total enzyme concentration is

$$E_0 \approx ENa + EK. \qquad (3)$$

Combining equations 1–3, the following expression is derived:

$$F_{Na} = \frac{1}{\left(1 + \dfrac{K_K[K]}{K_{Na}[Na]}\right)}. \qquad (4)$$

Equation 4 shows that F_{Na} (ENa/E_0), the fraction of the total amount of enzyme bound to Na^+, depends on both the equilibrium constant ratio and the cation concentration ratio. It is obvious that F_K (EK/E_0) is equal to $1 - F_{Na}$. Considering that the interaction of enzyme-substrate (or enzyme-product) does not interfere with the enzyme-cation equilibrium (equations 1 and 2) and that each enzyme fraction behaves as an independent enzyme system, the reaction rate in the presence of both cations can be described as a lineal combination of two terms:

$$V = V_K F_K + V_{Na} F_{Na} \qquad (5)$$

or

$$V = V_K(1 - F_{Na}) + V_{Na} F_{Na} \qquad (6)$$

where V is the reaction rate in the presence of both cations and V_K and V_{Na} are the intrinsic activities of the K^+- and Na^+-bound enzyme, respectively. The terms $V_{Na}F_{Na}$ and $V_K F_K$ represent the total activities exhibited by the fractions of Na^+- and K^+-bound enzyme, respectively. An important fact in equations 5 and 6 is that the reaction rate is expressed as a function of the cation concentration ratio, thus consistent with experimental observations.

Preliminary studies showed that the time course of lactose hydrolysis by *K. lactis* β-gal might be approximated by Michaelis-Menten kinetics, with a competitive inhibition by galactose. A general reaction model of lactose hydrolysis in the presence of Na^+ and K^+ could therefore be expressed as follows (steady-state

kinetics):

$$\frac{dX}{dt} = \frac{k_{2K}E_0(1 - X)}{K_{mK}\left(1 + \dfrac{XS_0}{K_{iK}}\right) + S_0(1 - X)}(1 - F_{Na}) + \frac{k_{2Na}E_0(1 - X)}{K_{mNa}\left(1 + \dfrac{XS_0}{K_{iNa}}\right) + S_0(1 - X)}F_{Na}$$

(7)

where $X = (S_0 - S)/S_0$ is the conversion and XS_0 is the concentration of the inhibitor galactose. The term k_2E_0 is V_m (maximum reaction rate), K_m is the Michaelis-Menten
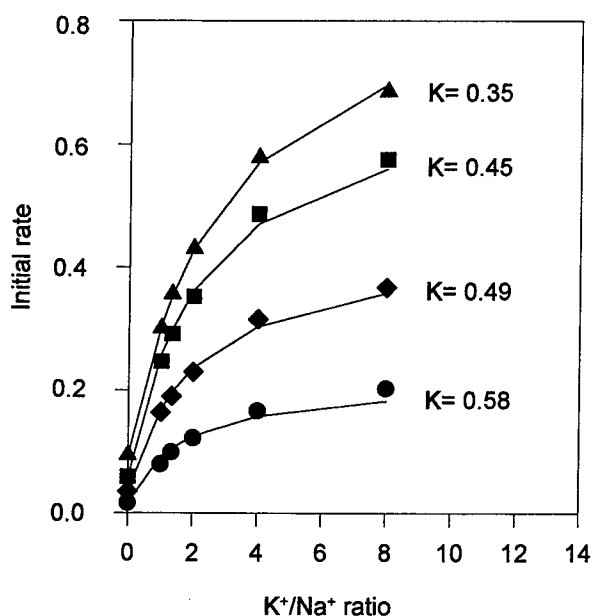
FIGURE 1. Initial rate of lactose hydrolysis in K^+/Na^+ mixtures. Assay system: 1.6×10^7 cells/mL in 20 mM K_2HPO_4-HCl, pH 6.6, containing 0.1 mM Mn^{+2}. Na^+ was added as NaCl. Initial lactose concentration was 139 mM. The reaction time was varied between 5 and 30 min depending on the incubation temperature. Experimental data—▲: 30 °C; ■: 25 °C; ◆: 15 °C; ●: 5 °C. Model data are shown by the solid line. K is the estimated value of the equilibrium constant ratio.

constant, and K_i is the competitive inhibition constant for galactose. F_{Na} does not depend on the conversion because the Na^+ and K^+ concentrations do not change during the time course of the reaction.

MATERIALS AND METHODS

A glutaraldehyde-stabilized whole cell biocatalyst was used as a source of β-gal. The biocatalyst was stored at 5 °C as a stock suspension containing 4×10^9 cells/mL (≈ 20 mg/mL of dried biocatalyst) in 50 mM K_2HPO_4-HCl (pH 6.6)/0.1 mM Mn^{+2},

with the addition of 0.1% methylparaben as a bacteriostatic agent. The preparation and properties of the whole cell biocatalyst have been reported elsewhere.[3] The kinetic parameters k_2 and K_m were determined from initial rate measurements employing lactose concentrations in the range from 7 to 139 mM. The constant K_i for galactose was estimated from the time course of lactose hydrolysis up to 80–85% conversion. In these experiments, an initial lactose concentration of 139 mM was utilized. Temperature effects were analyzed between 5 and 37 °C. Due to the instability of the enzyme in the presence of only Na$^+$,[2] the maximum temperature used to estimate K_i in the presence of this cation was 25 °C. The kinetic parameters were estimated using a Levenberg-Marquard nonlinear regression algorithm. Process simulations were carried out with ISIM (Interactive Simulation Language, Salsford University, United Kingdom).
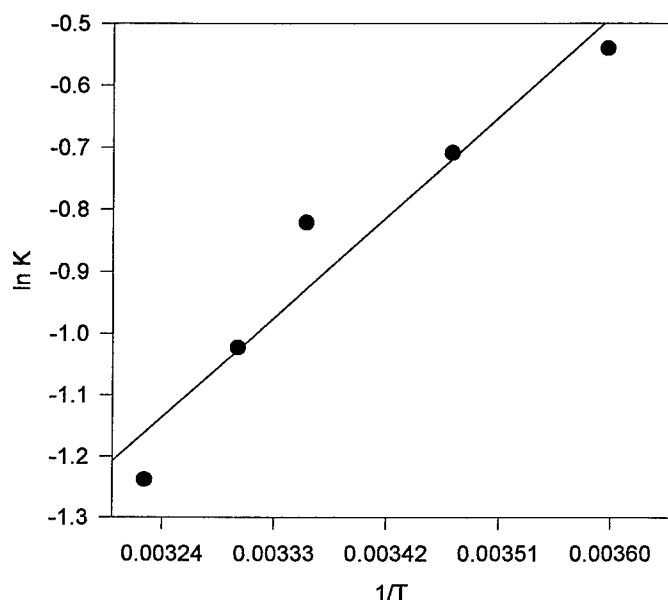
FIGURE 2. Arrhenius plot of the equilibrium constant ratio (K).

RESULTS AND DISCUSSION

Although the kinetic model includes the equilibrium constants of the cation-enzyme reaction, no attempt was done to determine these constants. To test the model, the ratio between the equilibrium constants (K_K/K_{Na}), hereafter the K parameter, was estimated by fitting initial velocity data using equations 4 and 6. The data used for the estimation of K were the initial reaction rates measured with different cation concentration ratios and V_K and V_{Na}, that is, the initial rates obtained in the presence of either Na$^+$ or K$^+$. Experimental data and the predicted values

TABLE 1. Estimated Kinetic Parameters for Hydrolysis of Lactose by Sodium- and Potassium-activated *K. lactis* β-Galactosidase[a]

	K^+	Na^+
k_2 (μmol/cell min)[b]	5.38×10^{-8}	4.33×10^{-9}
E_a	9.80	11.24
K_m (μmol/mL)[b]	33.10	10.82
E_a	—	5.24
K_i (μmol/mL)[b]	22.40	8.50
E_a	—	6.48

[a]Assay system: 20 mM K_2HPO_4-HCl or 20 mM Na_2HPO_4-HCl, pH 6.6, containing 0.1 mM Mn^{+2}. NaCl and KCl were added to the buffer solutions in order to obtain a cation concentration of 100 mM. E_a: Activation energy (kcal/mol) for the temperature dependence of the kinetic parameters in the range of 5 to 37 °C (estimated from the Arrhenius plot). The K_i of the Na^+-activated enzyme was determined over the range of 5 to 25 °C.

[b]Values of the kinetic parameters determined at 25 °C. Confidence intervals ($P < 0.05$) were ±5–10% of the estimated value.
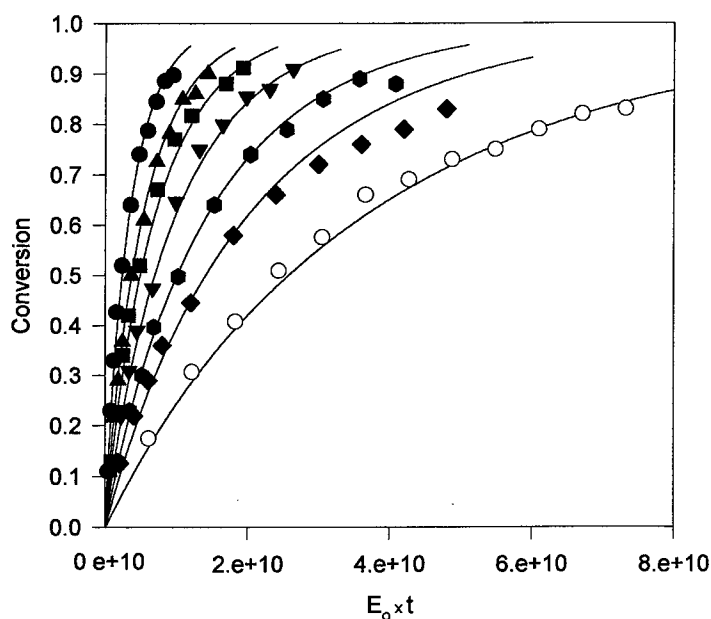
FIGURE 3. Comparison between model simulation and experimental data for the time course of lactose hydrolysis in K^+/Na^+ mixtures. Assay system: 20 mM K_2HPO_4-HCl, pH 6.6, containing 0.1 mM Mn^{+2}. Na^+ was added as NaCl. Reaction temperature: 25 °C; E_0: enzyme concentration (range: 7.9×10^7 to 4×10^8 cells/mL); *t*: reaction time (range: 5 to 150 min). Cation concentration (mM) of K^+/Na^+: experimental data— ●: 100/0; ▲: 40/10; ■: 40/20; ▼: 40/40; ⬤: 40/80; ◆: 40/160; ○: 0/100. Model data are shown by the solid line.
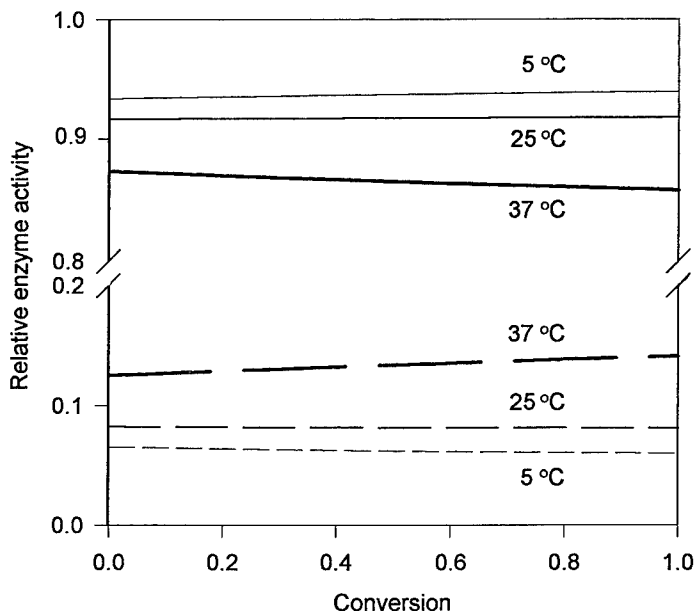
FIGURE 4. Contribution of the Na^+- and K^+-activated enzyme fraction to the total reaction rate. Simulations were carried out with a K^+/Na^+ ratio of 2. Fraction of the total activity: (– –) Na^+-bound enzyme; (—) K^+-bound enzyme.

based on the estimated K showed a good agreement (FIGURE 1). Lack-of-fit analysis ($P < 0.05$) showed that the kinetic model can be used for the adequate description of the ionic effect. The parameter K decreases as the temperature increases and it follows an Arrhenius-type temperature dependence (FIGURE 2). The outstanding result is that β-gal possesses a higher affinity for Na^+ than for K^+ (K values were < 1). With a K^+/Na^+ ratio of 2, typically found in natural substrates,[4] the calculated fractions of Na^+-bound enzyme (F_{Na}) were 0.46 and 0.61 at 5 and 37 °C, respectively.

The kinetic parameters included in the overall reaction rate expression (equation 7) for the Na^+- and K^+-activated enzymes are shown in TABLE 1. The most striking result corresponds to k_2 values. The maximum activity displayed by the Na^+-activated enzyme is around 10-fold lower than that of the K^+-activated enzyme, with the temperature dependence of k_2 similar in both cases. The Na^+-activated enzyme showed a slightly higher affinity towards lactose, thereby being more sensitive to the inhibitory effect of galactose. The K_m and K_i values of the K^+-bound enzyme were practically unaffected by the temperature. The kinetic parameters and K were used to predict conversion values over the time course of the hydrolytic reaction. A typical lactose hydrolysis experiment carried out at 25 °C in the presence of different cation concentration ratios is shown in FIGURE 3. Similar results were obtained at other temperatures (data not shown). The applicability of the model can be extended to the overall course of lactose hydrolysis, at least under the experimental conditions used.

The contribution of each enzyme fraction to the total reaction rate (with a $K^+/Na^+ = 2$) is shown in FIGURE 4. The activity from the Na^+-bound enzyme fraction ($V_{Na}F_{Na}$) only represents 10–15% of the total reaction rate (this behavior is mainly due to the low k_2 value of the Na^+-activated enzyme). Thus, the reaction is essentially performed by the K^+-activated enzyme. Under this condition, the Na^+ effect might be considered as a decrease in the effective concentration of the enzyme. Hence, we would expect the following: the higher the reaction temperature (higher F_{Na} values), the lower the productivity per mass unit of enzyme.

REFERENCES

1. GEKAS, V. & M. LÓPEZ-LEIVA. 1985. Hydrolysis of lactose: a literature review. Process Biochem. **2**: 2–12.
2. FLORES, M. V., R. J. J. ERTOLA & C. E. VOGET. 1996. Effect of monovalent cations on the stability and activity of *Kluyveromyces lactis* β-galactosidase. Lebensm. Wiss. Technol. In press.
3. FLORES, M. V., C. E. VOGET & R. J. J. ERTOLA. 1995. Stabilization of a cell biocatalyst with β-galactosidase activity by glutaraldehyde treatment. J. Chem. Technol. Biotechnol. **64**: 353–360.
4. IRVINE, D. M. & A. R. HILL. 1985. Cheese technology. *In* Comprehensive Biotechnology. Volume 3. M. Moo-Young, Ed.: 523–566. Academic Press. New York.

Structure-Function Studies on the Chitinolytic Enzymes of *Serratia marcescens* Chitinase and Chitobiase

C. E. VORGIAS, A. PERRAKIS, AND I. TEWS

European Molecular Biology Laboratory (EMBL)
22603 Hamburg, Germany

Chitin is the second most abundantly distributed biological polymer throughout nature. This homopolymer of N-acetyl-D-glucosamine is not only the major constituent of the fungal cell wall and the arthropod exoskeleton, but also it is an important nutrient source of carbon and nitrogen in the marine environment.

Our interest is the elucidation of the mechanism of chitin degradation by chitinolytic enzymes. These enzymes, chitinases (EC 3.2.1.14) and chitobiases (EC 3.2.1.30), are produced and secreted from chitinolytic bacteria. Chitinases have been classified into families 18 and 19 of glycosyl hydrolases.[1] They hydrolyze chitin to oligosaccharides, of which N,N'-diacetyl-glucosamine is the predominant product; this is the substrate for chitobiase (trivial name for N-acetyl-glucosaminidase), which is classified into family 20 of glycosyl hydrolases.[1]

As a first step on this project, we applied crystallographic techniques to investigate the molecular structure of these enzymes and gain information in order to elucidate the mechanism of chitin degradation on the molecular level.

THE STRUCTURE OF CHITINASE A

The X-ray structure of chitinase A from the chitinolytic bacterium *Serratia marcescens* has been solved by multiple isomorphous replacement (MIR) and refined at 2.3-Å resolution, resulting in a crystallographic R-factor of 16.2%.[2] The structure of chitinase A consists of three domains (see FIGURE 1). The amino-terminal domain (aa [amino acids] 24–137), which consists only of β-strands, connects through a hinge region (residues 138–158) to the main αβ barrel domain (residues 159–442 and 517–563). The third domain has an α + β fold and is formed by an insertion in the barrel motif (residues 443–516).

MODE OF ENZYMATIC DEGRADATION

To date, four structures of family 18 chitinase enzymes have been reported. These include hevamine, a plant defense protein with combined chitinase and lysozyme activity;[3] chitinase A from *Serratia marcescens*;[2] and endo-β-N-acetylglucosaminidases F1[4] and H.[5] In these four structures, the main and catalytic domain is

an αβ barrel, which establishes a common fold for all family 18 enzymes.[6] They possess a long groove for the binding of the substrate, on the C-terminal end of the αβ barrel. The hydrolysis of chitin by chitinases belongs to the general acid-base catalysis. From primary structure comparisons, mutagenesis, and structural data, it is clear that the proton donor is a glutamate residue (127 in hevamine, 315 in chitinase, and 132 in endo-β-N-acetylglucosaminidases F1 and H). The acidic character of this residue is further stabilized by a strong hydrogen bond of an aspartate in position n-2. The intermediate is likely stabilized by the N-acetyl group of the substrate itself.

THE STRUCTURE OF CHITOBIASE

The chitobiase gene encoding an 885-amino-acid protein was cloned and sequenced; the protein was produced in *Escherichia coli*, purified, characterized, and crystallized as described in reference 7. The 3D structure of chitobiase was solved by
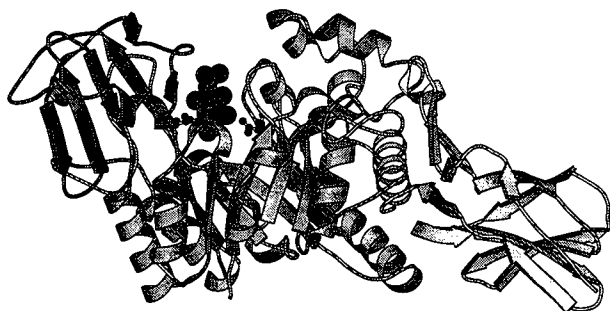
FIGURE 1. Ribbon diagram illustrating the structure of chitinase A, its three domains, and the groove of the active site where the sugar ring is bound.

MIR and refined to a resolution of 1.9 Å. Chitobiase has an eight-strand αβ-barrel structure (domain III, see FIGURE 2) with three additional domains. The N-terminal domain I, 154 aa, comprises two β-sheets. Domain II, 122 aa, has α + β topology. Domain III, 483 aa, an αβ-barrel motif, is the core of the structure, around which the other domains are organized. The active site is on the C-terminal end of the barrel, from where long loops interacting with domain I extend. The eight β-strands are surrounded by seven α-helices. Several deviations from the classical barrel motif have been identified. Domain IV, like domain I, comprises two β-sheets, but has only 67 aa. Overall dimensions of the protein are roughly 90 × 80 × 60 Å.

MODE OF ENZYMATIC ACTION OF CHITOBIASE

The enzymatic mechanism of N,N′-diacetyl-glucosamine degradation was determined from the crystal structure of several substrate/inhibitor complexes. The
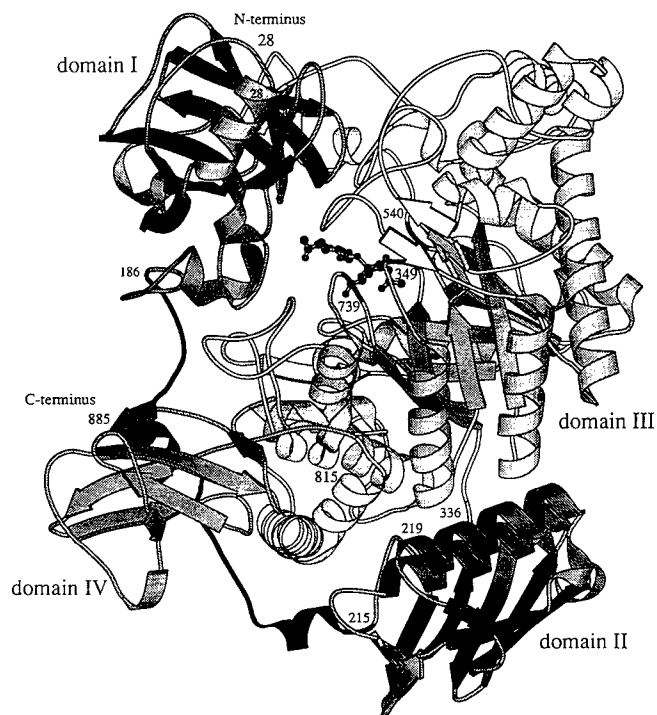
FIGURE 2. Schematic diagram illustrating the structure of chitobiase and its domains. The amino acid residue responsible for catalysis (glutamate 540) is shown in ball-stick symbols.

substrate lies in a pocket with the arginine 349 at its base, binding the nonreducing terminal sugar. There is only one protein carboxyl side chain as a catalytic group (glutamate 540), with the nucleophile being provided by the acetamido group of the substrate itself.

REFERENCES

1. HENRISSAT, B. & A. BAIROCH. 1993. Biochem. J. **293:** 781–788.
2. PERRAKIS, A. *et al.* 1994. Structure **2:** 1169–1180.
3. VAN SCHELTINGA, A. C. T. *et al.* 1994. Structure **2:** 1181–1189.
4. ROEY, P. V. *et al.* 1994. Biochemistry **33:** 13989–13996.
5. RAO, V., C. GUAN & P. V. ROEY. 1995. Structure **3:** 449–457.
6. DAVIES, G. & B. HENRISSAT. 1995. Structure **3:** 853–859.
7. TEWS, I. *et al.* 1995. Manuscript in preparation.

Effect of N-Linked Oligosaccharide on the Conformation and Properties of Glucoamylase from *Monascus rubiginosus*

ZHI YANG DONG, SHOU JUN YANG,[a] CHENG JIN,
AND SHU ZHENG ZHANG

Glycosylation Laboratory
Institute of Microbiology
Academia Sinica
Beijing 100080, People's Republic of China

Glucoamylase (EC 3.2.1.3) from *Monascus rubiginosus* was found to exist in multiple forms on PAGE (E_1 through E_5), in which E_3 and E_4 were the two major forms of glycoprotein (see FIGURE 1). Sugar content of E_3 and E_4 was 7% and 9%, respectively. We have reported a glycosylation-induced conformational difference between E_3 and E_4.[1-3]

In order to further investigate the effect of N-glycosylation on the conformation and properties of glucoamylase, we compared the conformation and properties of the natural glycoform and N-deglycosylated form of E_4 (see FIGURE 2). After the E_4 was treated with endo-N-acetylglucosiminidase H (endo-H), about 72% of the sugar content was removed. The N-deglycosylated form was designated as E'_4. The band of E'_4 on the PAGE moved closer to the E_3 position. Removal of N-linked sugar led to a significant thermostability decrease, whereas it had little effect on the catalytic activity. The results are summarized in TABLE 1.

The far-UV CD spectra of E'_4 displayed much higher molecular ellipticity than the E_4 (FIGURE 3). The α-helix contents for both forms were 18.9% and 14.5%, respectively, which indicated that the N-deglycosylated form has more compact conformation than the natural one. The fluorescence emission spectra of the two forms (FIGURE 4) showed the same peak at 335 nm, which is characteristic for tryptophan. However, the intensity of E'_4 was obviously higher than the E_4, which suggested that the removal of N-linked oligosaccharide from E_4 led to the moving of Trp to the more hydrophobic center. These results confirmed that the degree of N-glycosylation causes the conformational difference between the multiple forms of glucoamylase.

[a]To whom all correspondence should be addressed.

FIGURE 1. PAGE of the glucoamylase before and after the treatment by endo-H: (A) E_4; (B) E'_4; (C) E_3.
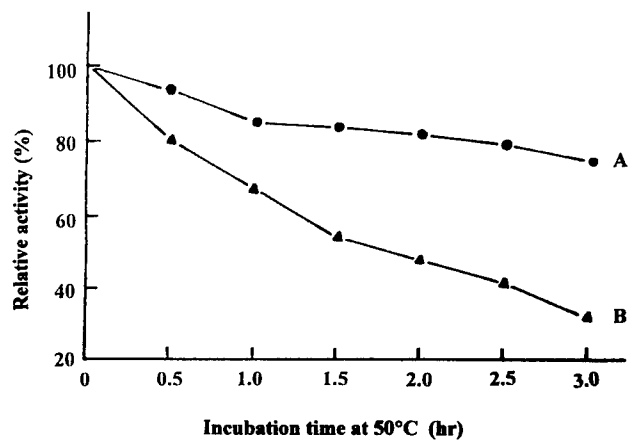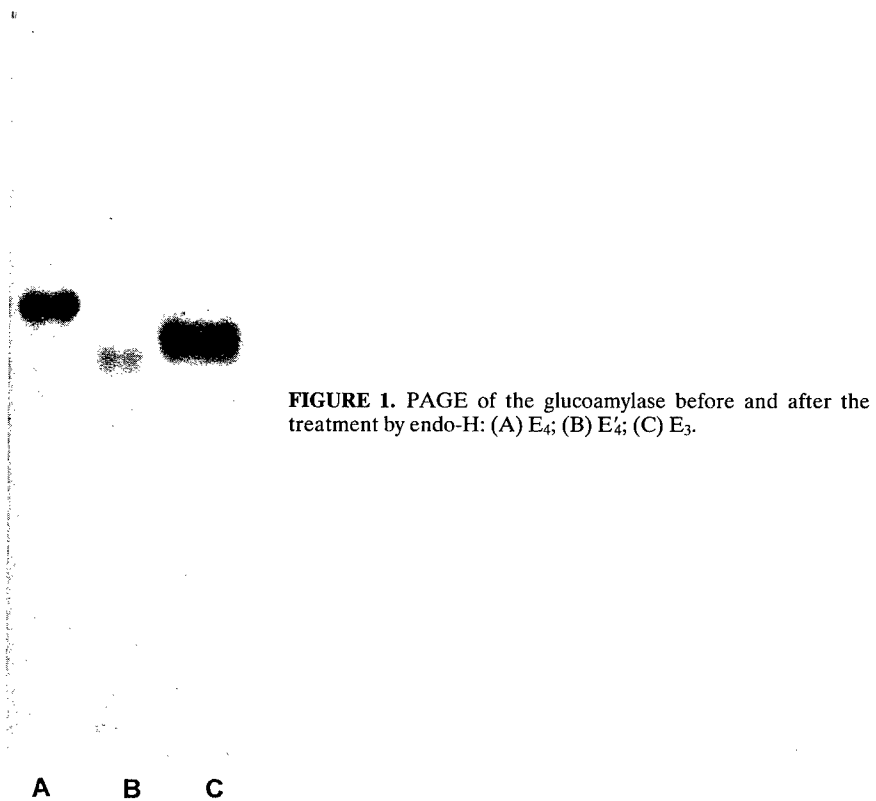
FIGURE 2. Thermostability of (A) E_4 and (B) E'_4.

TABLE 1. Some Properties of E_4 and E_4'

Glycoforms	K_m (g/mL)	V_{max} (mg/mg-h)	Sugar (%)	α-Helix (%)
E_3	3.5×10^{-3}	625	7.0	24.6
E_4	3.5×10^{-3}	555	9.56	14.5
E_4'	2.7×10^{-3}	578	2.68	18.91

FIGURE 3. The far-UV CD spectra of E_4 and E_4': (A) native glucoamylase (E_4); (B) N-deglycosylated glucoamylase (E_4').
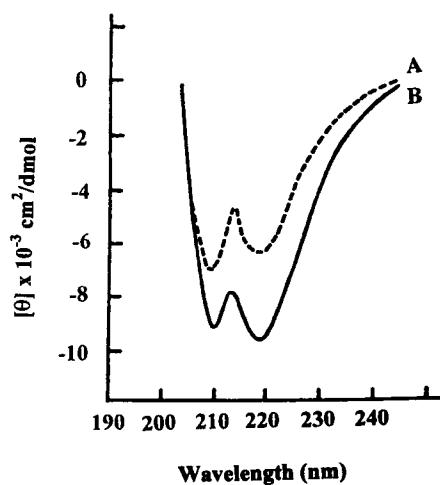
FIGURE 4. The fluorescence spectra of E_4 and E_4': (A) E_4; (B) E_4'.
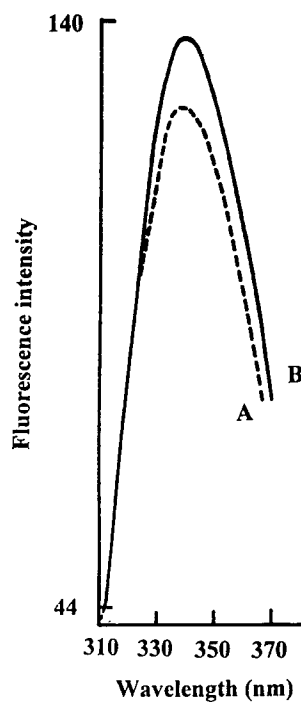
REFERENCES

1. YANG, S. J., S. G. GE, A. L. ZHANG & S. Z. ZHANG. 1984. Studies on the conformation of glucoamylase from *Monascus rubiginosus* Sato. Sci. Sin. **27**(9): 911–917.
2. GE, S. G., S. J. YANG & S. Z. ZHANG. 1994. *N*-Glycosylation-induced difference between multiple forms of glucoamylase. Chin. Sci. Bull. **39**(21): 1839–1842.
3. ZHANG, S. Z., S. G. GE, S. J. YANG, Z. Z. YAN, H. N. YU & W. T. WANG. 1995. Glycosylation-induced conformational difference between glycoforms of glucoamylase. Ann. N.Y. Acad. Sci. **750**: 344–348.

Immobilization of Enzymes for Use in Organic Media

PATRICK ADLERCREUTZ, RAÚL BARROS,
AND ERNST WEHTJE

Department of Biotechnology
Chemical Center
Lund University
S-221 00 Lund, Sweden

INTRODUCTION

During the last decade, the interest for enzymatic reactions in organic media has been intense. Many fundamental studies have been carried out and a few industrial processes have been developed. Because enzymes are insoluble in most organic media, heterogeneous systems are normally used. In the simplest case, an enzyme powder, obtained by lyophilization or other methods, is suspended in the medium. However, enzyme powders often tend to aggregate and attach to the walls of the reactor, especially when small amounts of water are added to increase the catalytic activity of the enzyme. These problems can be reduced by immobilizing the enzyme on a solid support. Furthermore, immobilization on a suitable support often increases the specific activity of the enzyme considerably. When the enzyme is insoluble in the reaction medium, simple immobilization methods such as adsorption or deposition are used. The properties of the support influence the catalytic activity of the enzyme in several ways. Both morphological and chemical characteristics are of importance (TABLE 1). This text will give a short overview of the importance of different support characteristics on enzyme activity.

INFLUENCE OF PARTICLE SIZE

When high catalytic activity is present in a porous particle, diffusion of the substrate through the pores to the enzyme may become rate-limiting. In a study of this effect, a lipase was immobilized on controlled pore glass supports with the same pore size, but different particle size. It was clearly shown that the reaction rate decreased with increasing particle size.[1] Although few other studies on this topic have been made in organic media, it is likely that internal mass transfer limitations will occur in other cases when high enzyme loadings and large particles are used.

INFLUENCE OF PORE SIZE

Few materials have pores of uniform size. In most supports used for enzyme immobilization, the pore diameter varies over a wide range.[2] This makes it difficult to

study the effects of pore size on enzyme activity. However, controlled pore glasses are ideally suited for this kind of study. When a lipase was immobilized by adsorption on controlled pore glass, it was found that the pore diameter should be at least 35 nm for the lipase to penetrate the pores and cover the available surface area.[1] The catalytic efficiency increased with increasing pore size up to about 100 nm. These requirements for large pores may seem surprising considering that the diameter of the lipase molecule is around 5 nm.

INFLUENCE OF SURFACE AREA

The surface area is often linked to the pore size. Materials having small pores can have quite large surface areas. In studies of the effect of enzyme loading on different porous supports, it was observed that the enzyme loading per unit surface area was of vital importance.[3] At high enzyme loadings, reductions in the specific activity of the enzyme were observed due to mass transfer limitations. At low enzyme loadings, even larger reductions in specific activity were observed. Using controlled pore glass

TABLE 1. Important Characteristics of a Support to Be Used for Enzymes in Organic Media

Morphological characteristics:
particle size
pore size
specific surface area
Chemical nature of the support surface:
water partition characteristics
substrate/product partition characteristics
direct effects of the support on the enzyme

supports, it was shown that in order to express full activity the enzyme should form at least a monolayer on the surface. At lower surface coverage, enzyme inactivation occurred. It was possible to replace part of the enzyme by another protein or a polymer, such as polyethylene glycol, and still get full specific activity.[3] Monolayer coverage corresponds to about 1 mg of protein per square-meter surface area. Celite is a useful support for many applications of enzymes in organic media. With this support, an enzyme loading of about 1 mg/g support was needed to obtain full specific activity of the enzyme. This indicates that Celite has an "effective surface area" of about 1 m^2/g. Measurements of the surface area accessible in pores with different size showed that a surface area of 1 m^2/g corresponds to pores down to 10 nm in diameter [F. Garcia and P. Adlercreutz, unpublished].

The reaction rates (mol of substrate converted per unit time and g of enzyme preparation) of chymotrypsin immobilized on different supports were measured. On Celite, the maximal rate was obtained at an enzyme loading of about 10 mg/g [Barros, Wehtje, and Adlercreutz, unpublished]. With the assumptions mentioned above, this corresponds to an average coverage of about 10 layers of enzyme molecules. Because pores down to 10 nm were considered in calculating the surface

area and the enzyme molecules have a diameter of about 5 nm, the enzyme cannot have been evenly spread on the surface. Instead, when maximal activity was obtained, it is likely that between 1 and 10–20 layers of enzyme molecules covered the surface. A further increase in the enzyme loading on the support did not cause any increase in reaction rate due to mass transfer limitations or blocking of the active sites of the enzyme molecules by protein-protein interactions.

INFLUENCE OF SURFACE CHEMISTRY

The surface chemistry of the support can influence the catalytic activity of the enzyme both directly and by indirect effects due to the partition of water and substrates in the reaction mixture.

Water Partition Effects

In the reaction mixture, water partitions between the enzyme, the support, and the reaction medium. The amount of water present on the enzyme plays an important role in determining its catalytic activity. At a fixed water concentration, there was thus a competition for water and the water-adsorbing capacity ("aquaphilicity") of the support was of vital importance.[4] Supports with high aquaphilicity caused dehydration of the enzyme and therefore low catalytic activity.

Substrate Partition Effects

The chemical nature of the support can influence the partition of substrates and products in the system and this can sometimes be of large importance for the reaction rate. This effect has been observed in a steroid conversion catalyzed by whole cells immobilized in polyurethanes with varying hydrophobicity.[5] The reaction rate increased with increasing hydrophobicity of the polyurethane. The increase in reaction rate correlated well with the increase in partition coefficient for the substrate between the polyurethane and the reaction medium. Thus, the high reaction rates were interpreted as being due to an enrichment of the hydrophobic substrate in the hydrophobic gel, thereby increasing the local substrate concentration.[5] It is quite possible that the most important aspect of the substrate enrichment was an increase in mass transfer of the substrate to the cells.

In cases where substrate inhibition occurs, it has been shown favorable to use a support that gives a low local substrate concentration.[6]

Direct Effects of the Support on the Enzyme

In order to study possible direct effects of the support on the enzyme, the indirect effects should be minimized. Water partition effects can be minimized by working at fixed water activity. In such a study, surprising effects were observed in a chymotrypsin-catalyzed alcoholysis reaction.[7] Large differences in the relative rates of the alcoholy-

sis reaction and the competing hydrolysis were observed depending on the support used. By using a polyamide support and a low water activity (0.33), it was possible to effectively suppress hydrolysis while still maintaining a high alcoholysis activity. At this low water activity, very low catalytic activity was detected on the other supports.

CONCLUSIONS

Enzymes immobilized on supports are useful catalysts for reactions in organic media. By using a porous support, the enzyme can be spread on a large surface area, thereby reducing mass transfer limitations. The morphological properties of the support are of vital importance for its performance. The surface area should be chosen to fit the desired enzyme loading. The enzyme should at least form a monolayer on the surface; otherwise, protecting proteins should be added. On the other hand, if the enzyme loading per unit surface area is too high, mass transfer limitations occur. The microenvironment of the enzyme on the support determines its catalytic activity. The support can affect the enzyme directly or via its influence on the partition of water and substrates in the reaction mixture. By choosing a proper support, the activity of the enzyme in different reactions (e.g., synthetic and hydrolytic) can be modulated. In conclusion, the immobilization of enzymes on supports gives many possibilities to influence enzyme catalysis and make useful enzyme catalysts. Especially for large-scale application, the use of enzymes on supports has proven highly beneficial.

REFERENCES

1. BOSLEY, J. A. & J. C. CLAYTON. 1994. Biotechnol. Bioeng. **43:** 934–938.
2. ISON, A. P., A. R. MACRAE, C. G. SMITH & J. BOSLEY. 1994. Biotechnol. Bioeng. **43:** 122–130.
3. WEHTJE, E., P. ADLERCREUTZ & B. MATTIASSON. 1993. Biotechnol. Bioeng. **41:** 171–178.
4. RESLOW, M., P. ADLERCREUTZ & B. MATTIASSON. 1988. Eur. J. Biochem. **172:** 573–578.
5. OMATA, T., T. IIDA, A. TANAKA & S. FUKUI. 1979. Eur. J. Appl. Microbiol. Biotechnol. **8:** 143–155.
6. KAWAKAMI, K., T. ABE & T. YOSHIDA. 1992. Enzyme Microb. Technol. **14:** 371–375.
7. ADLERCREUTZ, P. 1991. Eur. J. Biochem. **199:** 609–614.

Strategies for Enhancing Enzymatic Properties in Organic Solvent[a]

SHU-GUI CAO, HONG YANG, HUAN DONG,
NIAN-XIANG ZHANG, SI-PING HAN, SHI-DE LIU,
ZHAN-BIN LIU, AND TONG-SU YANG

State Key Laboratory of Enzyme Engineering
Jilin University
Changchun 130023, People's Republic of China

INTRODUCTION

Studies on biocatalysis in organic solvent have smashed the trammels of conventional enzymology. It is an important development in the biochemical field since the 1980s. It not only broadens the application of enzymes in the areas of chemical industry, material science, and medicine, but also provides a new method to reveal the structure and function of biocatalysts. Lipase as a type of biocatalyst is most important for the study of biocatalysis in organic solvent. Its high stereoselectivity to synthesize organic compounds indicates its potential in the resolution of racemic mixtures. However, lipase is not soluble in organic solvent. Its stereoselectivity and activity are not high enough. Therefore, the ability to enhance enzymatic properties in organic solvent is very important, not only as a basis of the application of enzyme catalysis in organic solvent, but also to provide new methods and information for the study of enzyme structure and function.

MATERIALS AND METHODS

Candida sp. lipase (CSL) was provided by the Institute of Microbiology, Academia Sinica, Beijing, China. *Penicillium expansum* lipase was purchased from the Nantong Biochemical Reagent Factory, Nantong, China. *Pseudomonas* sp. lipase (PSL) was purchased from Aldrich Chemical Company. Other reagents were of analytical grade.

Determination of the Substrate Conversion (%) and the Activity of Lipase in Organic Solvent

Determination of the substrate conversion (%) and the activity of lipase in organic solvent was done according to reference 1.

Measurement of Enantiomeric Excess

The enantiomeric excess (ee) of 2-octanol was determined by HPLC.[2] The enantiomeric excess of the obtained ester was calculated from the enantiomeric excess of the unreacted 2-octanol and the 2-octanol conversion, according to the formula $ee_P = ee_S/(C - ee_S)$.

RESULTS AND DISCUSSION

In this report, the following strategies for enhancing enzymatic properties in organic solvent have been studied.

Covalent Chemical Modification

Our earlier work showed that porcine pancreatic lipase modified with PEG can dissolve in benzene. Approximately 40% activity for porcine pancreatic lipase to catalyze the esterification of lauric acid and lauric alcohol can be retained by this method.

Noncovalent Chemical Modification

The effect of amphipathics (A, B, and C in FIGURE 1) on the esterification of lauric acid (0.45 mol/L) with lauric alcohol (0.45 mol/L) catalyzed by *Penicillium expansum* lipase (10 mg) in benzene (1 mL) was studied (TABLE 1). The results showed that amphipathics can increase the activity of *Penicillium expansum* lipase, with the ionic amphipathics especially having a stronger effect than nonionic amphipathics. This may be the reason that ionic amphipathics have a stronger interaction with the polar groups in the enzyme. Therefore, the dispersion of enzyme in organic solvent can be increased. The degree of dispersion of enzymes increased

A: $CH_3 (CH_2)$ n-O⟨ ⟩-O $(CH_2)_6 N_4 (CH_3)_3 Br$

B: meso-Zn^+tetra- (N, N -dimethylhexadecylaminophenyl) porphyrin bromide

C: $CH_3 (CH_2)$ n-O⟨ ⟩-OH
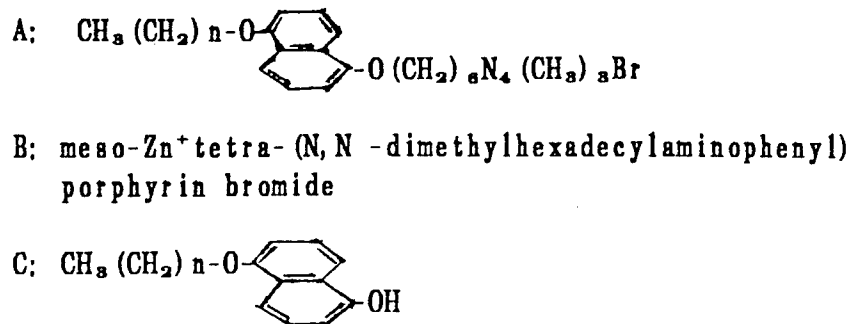
FIGURE 1. Chemical structure of amphipathic molecules.

TABLE 1. Effect of Amphipathics on the Esterification of *Penicillium expansum* Lipase

Amphipathics	Concentration of Amphipathics	Relative Activity
None	0	100%
Positively charged		
A	1.23×10^{-3} mg/mL	300%
B	1.16×10^{-3} mg/mL	300%
Nonionic		
C	$(2.8\text{--}4.6) \times 10^{-3}$ mg/mL	300%
Tween 20	5 mg/mL	120%
Triton X-100	0–100 mg/mL	100%
Negatively charged SDS	0.04 mg/mL	500%

because the hydrophobic tail of the amphipathics was dissolved in the organic phase and the reaction was evidently enhanced.

Our work[3] also showed that the enantioselectivity of *Candida* sp. lipase noncovalently modified by the amphipathic prepared by ourselves to catalyze the stereoselective esterification of (R, S)-2-octanol with octanoic acid in cyclohexane was enhanced 24-fold.

Immobilization of Enzyme

In earlier work,[4–6] we compared the activities of lipase immobilized on all kinds of carriers, including glass, acetone precipitated on porous glass, Al_2O_3, agar beads, and alginate gel coated with polyethylenimine or glutaraldehyde. The activity for lipase immobilized on the alginate gel coated with polyethylenimine or glutaraldehyde was increased 20-fold and 44-fold, respectively.

Solvent Engineering

The stereoselective esterification of (R,S)-2-octanol (0.28 mol/L) with dodecanoic acid (0.40 mol/L) was catalyzed by *Pseudomonas* sp. lipase (100 mg) (PSL) in 10 mL of different organic solvent. The results (TABLE 2) showed that the polarity (P) of the organic solvent had evident effect on the activity and stereoselectivity of PSL. In polar solvents, PSL had a very difficult time in showing its activity and stereoselectivity. In moderate solvents, PSL gave moderate activity and high stereoselectivity. PSL showed the highest stereoselectivity in toluene. In nonpolar solvents, PSL showed high activity and moderate stereoselectivity. In hexane, PSL showed the highest activity.

Water Activity

The stereoselective esterification of (R, S)-2-octanol (0.28 mol/L) with dodecanoic acid (0.40 mol/L) was catalyzed by *Pseudomonas* sp. lipase (100 mg) (PSL) in

TABLE 2. Effect of Solvent on the Stereoselective Esterification of (R, S)-2-Octanol with Dodecanoic Acid Catalyzed by PSL

Solvent[a]	log P	Reaction Time (h)	Alcohol Conversion (%)	Alcohol %ee (S)	Relative Activity (%)	X_R/X_S
DMF	−1.0	70	0	0	0	—
Methanol	−0.76	70	0	0	0	—
Acetone	−0.23	70	0	0	0	—
Acetonitrile	−0.33	70	33.5	5.2	11	1.2
Pyridine	0.71	70	0	0	0	—
THF	0.49	70	3.0	0	7	—
1,4-Dioxane	−1.1	70	3.0	2.0	7	4.7
CCL$_4$	3.0	70	21	37	17	—
Benzene	2.0	70	31	59	31	—
Toluene	2.5	58	47.5	78	57	13.5
Cyclohexane	3.2	46	56	73.5	76	3.7
Hexane	3.5	22	56	60	100[b]	2.8
Heptane	4.0	58	53	72	69	4.7
Isooctane	—	58	56	57	72	2.6
n-Dodecane	6.0	70	47	61	49	5.2

[a]DMF is N,N-dimethylformamide and THF is tetrahydrofuran.
[b]Note that 100% corresponds to the activity of 580 μmol/min–mg protein.

toluene containing different concentrations of water. The results (TABLE 3) showed that the stereoselectivity and activity of PSL depended on the water content in the system. When water was not put into the system, PSL showed no activity. This may be explained by the fact that a thin layer of water on the protein surface is necessary to retain the enzyme activity in organic solvent. When the water content in the reaction system was between 0.2% and 1.0%, the stereoselectivity and activity of PSL were high. With an increase of the water content in the system, PSL showed low stereoselectivity and activity. One reason for this effect may be that water affords a high conformation flexibility to PSL molecules. The protein with high conformation flexibility shows small steric constraints and its stereoselectivity decreases.

TABLE 3. Effect of Water Content in the Reaction System on the Stereoselective Esterification of (R,S)-2-Octanol with Dodecanoic Acid Catalyzed by PSL

Water Content (%)[a]	Relative Activity (%)	Alcohol Conversion (%)	Alcohol %ee (S)	X_R/X_S
0.0	7	4.1	3.8	1.67
0.2	92	53.4	73.7	4.59
0.4	100[b]	54.0	75.6	4.63
0.6	92	53.4	75.4	4.84
0.8	92	53.4	74.2	4.68
1.0	92	53.4	73.4	4.56
2.0	75	53.4	66.2	3.73

[a]Water addition after the enzyme and solvent are mixed.
[b]Note that 100% corresponds to the activity of 364 μmol/min–mg protein.

REFERENCES

1. CAO, S. G., Y. FENG & Z. B. LIU. 1991. Studies on catalysis of chemical modification and immobilized lipase in organic solvents. Chin. Biochem. J. **7**(6): 646.
2. HIRATA, H., T. YAMASHINA & I. IIDA. 1991. Determination of enantiomer content of secondary alkanol as diastereomeric *N*-[1-(1-naphthyl)ethyl]carbamate by normal phase HPLC. J. Jpn. Oil Chem. Soc. **40**(11): 9.
3. YANG, H., S. G. CAO *et al.* 1996. Enhancing the stereoselectivity and activity of *Candida* sp. lipase in organic solvent by noncovalent enzyme modification. This volume.
4. CAO, S. G., Y. FENG & Z. B. LIU. 1992. Esterification and transesterification with immobilized lipase in organic solvent. Appl. Biochem. Biotechnol. **32:** 1.
5. CAO, S. G., S. D. LIU *et al.* 1995. Studies on a new type of immobilized lipase fitting in organic solvents. Ann. N.Y. Acad. Sci. **750:** 222.
6. YANG, H., S. G. CAO & L. MA. 1994. A new kind of immobilized lipase in organic solvent and its structure model. Biochem. Biophys. Res. Commun. **200**(1): 83.

Enzymatic Catalysis in Nonconventional Media Using High Polar Molecules as Substrates

EDMUNDO CASTILLO, ALAIN MARTY,
J. STEPHANE CONDORET, AND DIDIER COMBES[a]

Département de Génie Biochimique et Alimentaire
Centre de Bioingénierie Gilbert Durand
INSA URA CNRS 544
Complexe Scientifique de Rangueil
31077 Toulouse Cedex, France

INTRODUCTION

Since the early 1980s, the use of enzymes in nonaqueous media as a tool in organic synthesis has been extensively studied.[1] With the advent of this enzymatic catalysis in nonconventional media, the synthesis of food emulsifiers with desired hydrophilic lipophilic balance (HLB) value using polyols as substrates gives very attractive results. These kinds of biosurfactants are widely used as nonionic emulsifiers and as synthetic intermediates in the food and pharmaceutical industry.[2,3] In theory, these tailor-made emulsifiers could be prepared from different polyols and fatty acids using regioselective lipases as catalysts in a near-anhydrous organic solvent. Because of the many possible sites to be attacked in the polyol molecule, products with different HLB could be obtained.

However, few types of reactions have been tested in those media. The main reason is the difficulty or even the inability to make polar compounds soluble at industrial scale using these kinds of solvents. This appears to be a great limitation for the application of enzymes in industrial organic synthesis because molecules of interest like polyols, alkaloids, carotenoids, amino acids, and sugars are very slightly soluble in very hydrophobic solvents. Some solutions have been proposed in the literature for dissolving polar solutes in organic solvents and making reactions with these kinds of substrates. Generally, the use of non-GRAS organic solvents such as pyridine or dimethylformamide has resulted in the best way to carry out these reactions.[4–6]

In 1972, Ferrier[7] reported the esterification of glucose in an organic phase by complexation of this sugar with phenylboronic acid (PBAC). With this method, he succeeded in chemical esterification of the free hydroxyl groups of sugars in benzene. Recently, reports have demonstrated the use of organoboronic acids to form carbohydrate-boronate complexes in order to produce soluble sugars and glycerol in nonpolar organic solvents and $SCCO_2$ (supercritical CO_2) for enzymatic reactions.[8–11] For these typical reactions, the main interest lies in a great selectivity of

---

[a] To whom all correspondence should be addressed.

reaction because of the protected positions of substrates obtained by complexation with PBAC. Thus, in this way, only monoesters of sugars or polyols are produced after recovery of PBAC by simple aqueous extraction.[7]

On a completely different principle is the method first described by Berger and Schneider in 1992.[12] In their work, they judiciously adsorbed nonsoluble solvent substrates onto a hydrophilic solid support to make the esterification reaction possible. For example, esterification of adsorbed glycerol with various free fatty acids, catalyzed by a lipase from *Rhizomucor miehei,* in *n*-hexane, diethyl ether, or *tert*-butyl-methyl ether was found to be very efficient in producing acylglycerols.[12]

In a previous paper,[11] we reported the preliminary results of the reactions using these two original methods to make high polar substrates soluble in nonpolar solvents. The feasibility of these kinds of reactions in SCCO$_2$ was reported.

In this work, we present the continuation of our previous work upon glycerol and we also present new successful reactions carried out with different polyhydroxylic compounds such as fructose and sucrose in supercritical CO$_2$ (SCCO$_2$) and in *n*-hexane.

MATERIALS AND METHODS

Enzymes and Chemicals

Commercial immobilized lipase from *Mucor miehei* Lipozyme™ was a gift from Novo Nordisk Industry (Bagsvaard, Denmark). All other chemicals were of >99% purity and were purchased from Sigma Chemical (U.S.A.). All solvents were purchased from PROLABO (France).

Bioconversions

Bioconversions using PBAC: Glycerol or D-fructose and PBAC were first incubated in *n*-hexane in magnetically stirred tubes. All reactions were started by addition of oleic acid and enzyme and were incubated at 40 °C during 24 h. All reactions in SCCO$_2$ were performed as previously described.[11] In the case of SCCO$_2$, in order to visualize the maximal solubilization of the produced complexes, a sapphire reaction vessel was used.

Bioconversions using silica gel: Sucrose and fructose were adsorbed on silica gel as previously described.[11] These adsorbed sugars were mixed with oleic acid and immobilized enzyme in *n*-hexane and SCCO$_2$ under the above-described conditions.

Analytical Methods

Analysis of sugar and glycerol ester synthesis was performed by HPLC using a Kontron 420 pump system equipped with a Varian R14 refractive index monitor (Varian Associates, U.S.A.) and a Nucleosil C18, 5µ column (250 × 4.6 mm) (Touzard et Matignon, France). Elution is conducted at 40 °C with methanol/acetic acid (99.7/0.3 v/v) and with a flow rate of 1 mL/min.

RESULTS AND DISCUSSION

PBAC as Solubilization Agent

First, by experiments that involve HPLC analysis and visual observations, we have established the optimal substrate/PBAC ratio to obtain the maximal solubilization of the polar substrates in n-hexane and $SCCO_2$. We have found an optimal ratio equal to 1 for the glycerol and an optimal ratio of 0.5 for the fructose in both solvents. The concentration of solubilized glycerol in n-hexane was more important than in $SCCO_2$. In the case of the fructose solubilizations, similar concentrations were found in both solvents. TABLE 1 presents the results of these solubilization tests.

In n-hexane, the maximal solubilizations were established at 45 °C; in $SCCO_2$, the solubilizations were tested at 14 MPa and 40 °C. Also, when performing reactions using these solubilized substrates, only around 80% of the substrate was available for the reaction (data not shown). We suspect from HPLC analysis the formation of soluble double-substrate complexes formed with two molecules of substrate (one -OH group for each molecule) and one molecule of PBAC, instead of two neighboring hydroxyls of each molecule of substrate. We suggest that this double-substrate complex formation restricts the availability of solubilized substrate for the reaction.

However, taking into account an "effective" maximal available concentration of soluble substrate, the reactions were carried out with stoichiometric quantities of glycerol or fructose, oleic acid, and immobilized enzyme using n-hexane and $SCCO_2$ as solvents. The kinetics of the esterification reaction of glycerol and oleic acid in n-hexane are shown in FIGURE 1.

In both reaction media, only one product in each case has been identified after the reactions. The products formed were monoolein in the case of reaction with glycerol and monooleyl-1-fructose in the case of reaction with fructose. The recovery of reaction products was easily made by liquid-liquid extraction with a slightly acidified solution of water. In the case of the reactions with glycerol, recovery of pure monoolein was possible with this method (90% of the total produced). In the case of fructose reactions, recuperation was carried out with a method reported by Schlotterbeck *et al.* in 1993[9] and 80% of pure fructose monoester was recovered.

It is interesting to mention that the conversion and profile of the products for the reactions in $SCCO_2$ lead to the same yields as those obtained in n-hexane for both reactions. However, to achieve these results, we have to be imperatively sure that the water activity in both systems was similar to the values established by Marty *et al.* in 1992.[13] This method implies the addition of a precise quantity of water according to the adsorption isotherm of water between the solvent and the enzymatic support.[13]

TABLE 1. Maximal Solubilization of Substrates in n-Hexane and $SCCO_2$

	n-Hexane		$SCCO_2$	
	Substrate/PBAC[a]	mM[b]	Substrate/PBAC[a]	mM[b]
glycerol	1	60	1	30
fructose	0.5	20	0.5	20

[a]Molar ratio of substrate to PBAC.
[b]Maximal concentration of solubilized substrate.
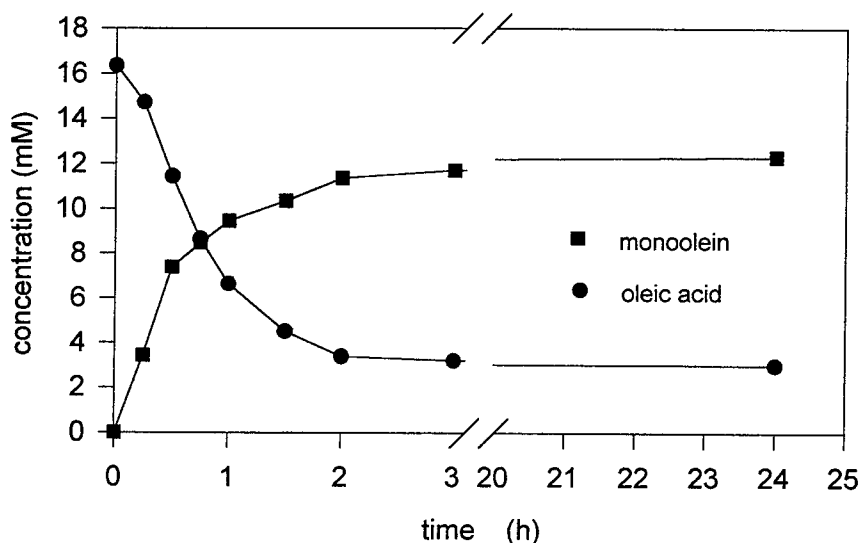
FIGURE 1. Time course of the synthesis of 1(3)-*rac*-monoolein. The reaction was performed with glycerol (20 mM), PBAC (20 mM), oleic acid (17 mM), and Lipozyme (50 mg) in a 15-mL reaction volume. Symbols: (●) oleic acid; (■) 1(3)-*rac*-monoolein.

Although the conversions reached in these reactions are high enough for industrial purposes, these kinds of reactions may result in a very expensive process because of the cost of PBAC. We are now developing a continuous process in $SCCO_2$ that considers, on the one hand, the continuous recuperation-reutilization of PBAC and, on the other, the recuperation of products in a continuous way using the potential advantages of the postreaction fractionation of the $SCCO_2$.

Immobilization of Substrates on Silica Gel

Adsorption of polyhydroxylated substrates on polar supports like silica gel seems to be a very attractive way to make possible esterification reactions with highly polar substrates in near-anhydrous solvents. First, in this work, we have found in agreement with Berger and Schneider[12] a ratio of glycerol/silica gel equal to 1 that allows the obtaining of high yields of products. Thus, we have tested the esterification reactions of adsorbed sucrose or fructose with oleic acid using *n*-hexane and $SCCO_2$ as solvents and using Lipozyme as the catalyst. For this purpose, both reactions were carried out using a sugar/silica gel ratio equal to 1. After 10 h of reaction, kinetic equilibria were achieved for both reactions, and conversions of substrate around 50% for fructose and 45% for sucrose were obtained. In control reactions carried out without silica gel, no conversion of substrate was observed. FIGURE 2 shows the main products detected after 12 h of reaction. These products were identified as a mixture of hydrophobic compounds, that is, monoesters, diesters, and triesters of sucrose and fructose. Traces of monoesters were only found in the reaction with sucrose.

High Pressure and Temperature

How to Deactivate Enzymes in Two Different Ways

DOMINIQUE CAVAILLE AND DIDIER COMBES

Centre de Bioingénierie Gilbert Durand
INSA
Complexe Scientifique de Rangueil
F-31077 Toulouse Cedex, France

INTRODUCTION

High hydrostatic pressure is an emerging physical parameter in biological studies and applications. The increasing interest of the food industry in the high pressure field[1] has brought about the need for fundamental studies on the behavior of biomolecular food constituents such as lipids, polysaccharides, and proteins.[2] Moreover, the knowledge of processes occurring in enzymes under extreme conditions of pressure or temperature is of immediate relevance in biochemistry.[3]

For this purpose, we have chosen two enzymes widely used in the food industry for their disaccharide hydrolysis catalysis: *Kluyveromyces lactis* β-D-galactoside galactohydrolase (EC 3.2.1.23) and *Saccharomyces cerevisiae* β-D-fructofuranoside fructohydrolase (EC 3.2.1.26). The effect of high pressure on the stability of these enzymes was studied. A similar study was realized after thermal treatment and the respective effects of the two physical parameters were compared.

MATERIALS AND METHODS

Enzymatic Solutions

Kluyveromyces lactis lactase, Maxilact LX-5000 (Gist Brocades), and *Saccharomyces cerevisiae* invertase (Sigma Chemical) were used without further purification. Enzymatic solutions were prepared in deionized water at concentrations respectively equal to 238.5 and 100 mg/L.

All the chemicals were of analytical grade.

Thermal Treatment at Atmospheric Pressure

Samples (1 mL) of enzymatic solutions in test tubes were heated in water baths at varying temperatures in the range of 40–70 °C. Aliquots were removed at intervals and rapidly cooled by immersion in an ice-water bath. The residual activity measurements were realized at 5 min to 24 h after the treatment.

Pressure Treatment at Controlled Room Temperature (25 ± 1 °C)

The apparatus for high hydrostatic pressure experiments consisted of a 700-MPa manual pump (Top Industrie) and a high pressure cell (2 mL internal volume). Pressure was controlled using a pressure gauge (Top Industrie). The pressurization liquid was the enzymatic solution. The pressure was increased within 1.5 min to the required value and was maintained for 0.5 min to 145 h. Subsequently, the pressure was released within 10 s. For each experiment, 2 mL of enzymatic solution was kept at atmospheric pressure throughout the treatment as a control. Activity measurements were carried out at 5 min to 24 h after the pressure release.

Enzyme Activity Assay

The lactase activity towards its artificial substrate, o-nitrophenyl-β-D-galactopyranoside (ONPG), was assayed at 37 °C. Two mL of ONPG (2 g/L) was added to 100 μL of lactase solution and the o-nitrophenyl production was measured for 2 min at 420 nm with a diode-array spectrophotometer (Hewlett Packard 8452A). Activities were calculated by linear regression of the absorbance versus reaction time.

Invertase activity was assayed by measuring its reaction with a sucrose solution. The reaction was started by addition of 100 μL of an invertase solution to 5 mL of a 0.4 M sucrose solution in 0.1 M sodium acetate buffer, pH 4.5. The variation in the concentration of reducing sugars resulting from the sucrose hydrolysis at 40 °C was measured using the 2,4-dinitrosalicylic acid method[4] as a function of time to determine the initial reaction rate. Equimolar mixtures of D-glucose and D-fructose were used as standard.

RESULTS AND DISCUSSION

Lactase and invertase were subjected to thermal or high pressure treatments and their respective activities were determined after the downshift of temperature or after pressure release. In all cases, the residual activity was monitored during a 24-h period to check for possible renaturation. The activity decreases that were measured were essentially irreversible, with less than 10% of activity being recovered after 24-h storage at room temperature and atmospheric pressure. The irreversible residual activities that were measured allow the half-lives ($t_{1/2}$) of the two enzymes to be obtained. FIGURE 1 presents the half-lives of lactase as a function of pressure or temperature. Lactase is very sensitive to both parameters under study, with half-lives of about 1.6 and 1.3 min, respectively, at 50 °C or 150 MPa. Moreover, the variation of the half-life with pressure or temperature is similar in the studied ranges, with a rapid decrease over a short range of pressure or temperature. This phenomenon is also observed for invertase. However, this last enzyme is less sensitive to thermal or hyperbaric treatment, as suggested by the values of the half-lives presented in TABLE 1. Indeed, whereas lactase is rapidly deactivated by thermal treatment at 45 °C ($t_{1/2}$ about 3.6 min), the half-life of invertase under the same conditions is almost 6 h. The
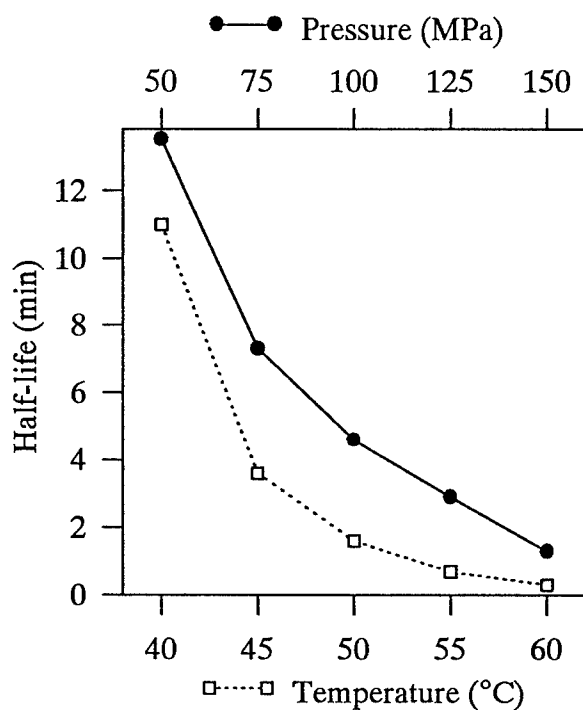
FIGURE 1. Effect of pressure (●) or temperature (□) on the half-life of *Kluyveromyces lactis* lactase.

same observation can be made under hyperbaric conditions, with the half-life of invertase being near 1 h at 650 MPa.

In addition, the denaturation curves can be described using the deactivation rate constant, k. This parameter is especially interesting because direct relations exist

TABLE 1. Half-lives of Lactase and Invertase as a Function of
Pressure or Temperature

T (°C)	$t_{1/2}$ (min)	P (MPa)	$t_{1/2}$ (min)
	Kluyveromyces lactis Lactase		
40	11.0	50	13.5
45	3.6	75	7.3
50	1.6	100	4.6
55	0.7	125	2.9
60	0.3	150	1.3
	Saccharomyces cerevisiae Invertase		
45	354	500	2088
50	51	550	584
55	39	600	370
60	15	650	55
70	1.2	—	—
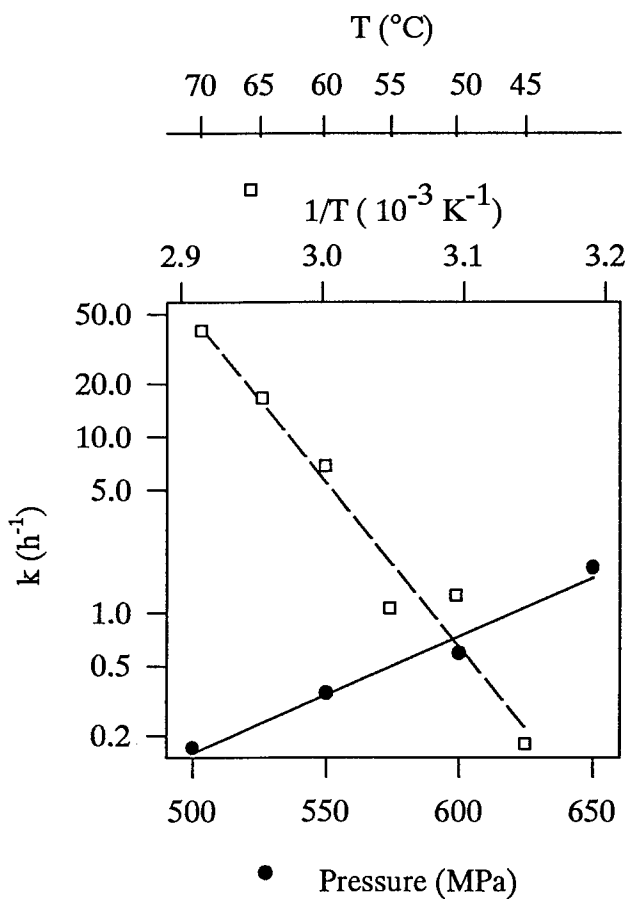
FIGURE 2. Effect of pressure (●) or temperature (□) on the deactivation rate constant of *Saccharomyces cerevisiae* invertase.

between either k and temperature (classical Arrhenius plot, equation 1) or k and pressure[3] (equation 2):

$$\ln k = -\frac{E_a}{R}\frac{1}{T} + a \qquad (1)$$

where E_a is the activation energy, T is the temperature, R is the gas constant, and a is a constant, and

$$\ln k = -\frac{P\Delta V}{RT} + b \qquad (2)$$

where ΔV is the volume variation, P is the pressure, and b is a constant.

According to these equations, the semilogarithmic plots of k versus, respectively, $1/T$ and P are linear. FIGURE 2 presents the plots obtained for invertase. The same

correlations can be obtained for lactase denaturation. It is obvious from this figure that invertase, as lactase, can be deactivated in two different ways: by increasing the pressure at room temperature or by increasing temperature at atmospheric pressure. Thus, pressure can be a useful alternative in order to avoid side reactions and by-products induced by heat. Moreover, it is possible to obtain a direct relation between temperature and pressure (FIGURE 3). As a matter of fact, from FIGURE 2, it appears that the same deactivation rate can be achieved by using either treatment.
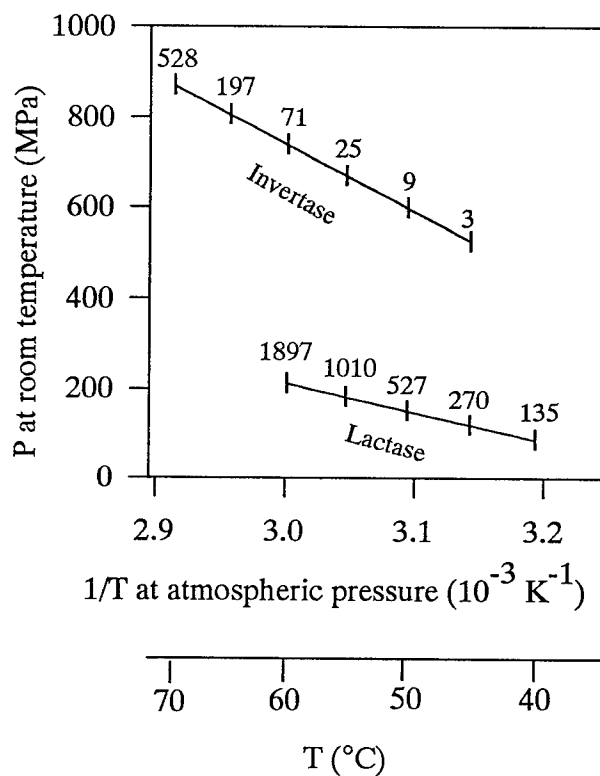
FIGURE 3. Correlation between thermal treatment at atmospheric pressure and hyperbaric treatment at room temperature. The numbers in the diagram are the values of the deactivation rate constant (k is expressed in units of 10^{-3} min^{-1}).

For example, in the case of invertase, either a thermal treatment (45 °C; 0.1 MPa) or a hyperbaric treatment (500 MPa; 25 °C) can lead to a k value of about 0.16 h^{-1}. This conclusion is not in contradiction with the ellipsoidal pressure-temperature diagram proposed by Hawley.[5] This investigator has studied the simultaneous effect of pressure and temperature on the reversible denaturation of chymotrypsinogen. In our case, the diagram in FIGURE 3 presents the correlation between various temperatures at atmospheric pressure and different pressures at room temperature.

This linear relation can be useful for finding a value of pressure leading to a stated deactivation rate constant.

In conclusion, according to the results obtained for lactase and invertase, it seems that an enzyme sensitive to thermal treatment is rapidly deactivated by high pressure too. This correlation between barostability and thermal stability is also true for lysozyme, the third enzyme studied in our group. Moreover, the high hydrostatic pressure can be a useful alternative in the deactivation of enzymes where heat can induce side reactions.

REFERENCES

1. CHEFTEL, J. C. 1992. Effects of high hydrostatic pressure on food constituents: an overview. *In* High Pressure and Biotechnology. Volume 224. C. Balny, R. Hayashi, K. Heremans & P. Masson, Eds.: 195–209. John Libbey Eurotext. London.
2. BALNY, C. & P. MASSON. 1993. Effects of high pressure on proteins. Food Rev. Int. **9:** 611–628.
3. MORILD, E. 1981. The theory of pressure effects on enzyme. Adv. Protein Chem. **34:** 93–166.
4. SUMNER, J. B. & S. F. HOWELL. 1935. A method for the determination of invertase activity. J. Biol. Chem. **108:** 51–54.
5. HAWLEY, S. A. 1971. Reversible pressure-temperature denaturation of chymotrypsinogen. Biochemistry **10:** 2436–2442.

Effects of Hydrostatic Pressure on Catalytic Activity and Stability of Two Alcohol Dehydrogenases

SANDRINE DALLET AND MARIE-DOMINIQUE LEGOY

Laboratoire de Génie Protéique et Cellulaire
Pôle Sciences et Technologies
Université de La Rochelle
17042 La Rochelle Cedex 1, France

We have investigated the effects of hydrostatic pressure on *Thermoanaerobium brockii* alcohol dehydrogenase (TBADH)[1] and yeast alcohol dehydrogenase (YADH)[2] in the range of 0.1 to 200 MPa in order to follow a possible modulation of the structure/activity without an irreversible denaturation process occurring (see TABLE 1). For each enzyme, catalysis is monitored under pressure from a novel high pressure bioreactor (FIGURE 1) and its structure is followed by HPLC (gel permeation).

EFFECTS OF HYDROSTATIC PRESSURE ON ENZYMES

Pressure, as well as temperature, organic solvents, or pH, is able to act as a modulator of biochemical processes.[3] Enzymes under pressure may provide us with new insights involving parameters such as activity/affinity, stability, and structure (subunit dissociation/structural reorganization).[4]

High pressure affects the structure/function of enzymes in a complex way, by altering both intramolecular and intermolecular interactions that are involved in maintaining protein stability.[5]

The pressure dependence of the reaction rate is calculated by the activation volume variation ($\Delta V^{\#}$) and the molar volume variation (ΔV).[6] An increase of pressure favors the protein conformation that occupies the lower volume in a system. As a consequence, a decrease of volume when pressure increases favors the reaction.[7]

In the case of catalytic reactions, it is possible to discriminate between the contribution of the binding phase (ΔV_b) and that of the catalytic phase (ΔV_{cat}) by monitoring changes to the activation volume. According to Morild,[8] the global activation volume change is

$$\Delta V^{\#} = -RT[\partial \ln(k_{cat}/K_m)/\partial P]_T.$$

The activation volume due to the catalytic phase is

$$\Delta V_{cat} = -RT(\partial \ln k_{cat}/\partial P)_T$$

TABLE 1. The Enzymes Used

Origin	Subunits	MW	Coenzyme	Specificity
YADH	4	150 kDa	NAD(H)	narrow for primary alcohols
TBADH	4	160 kDa	NADP(H)	broad, but secondary alcohols are preferred
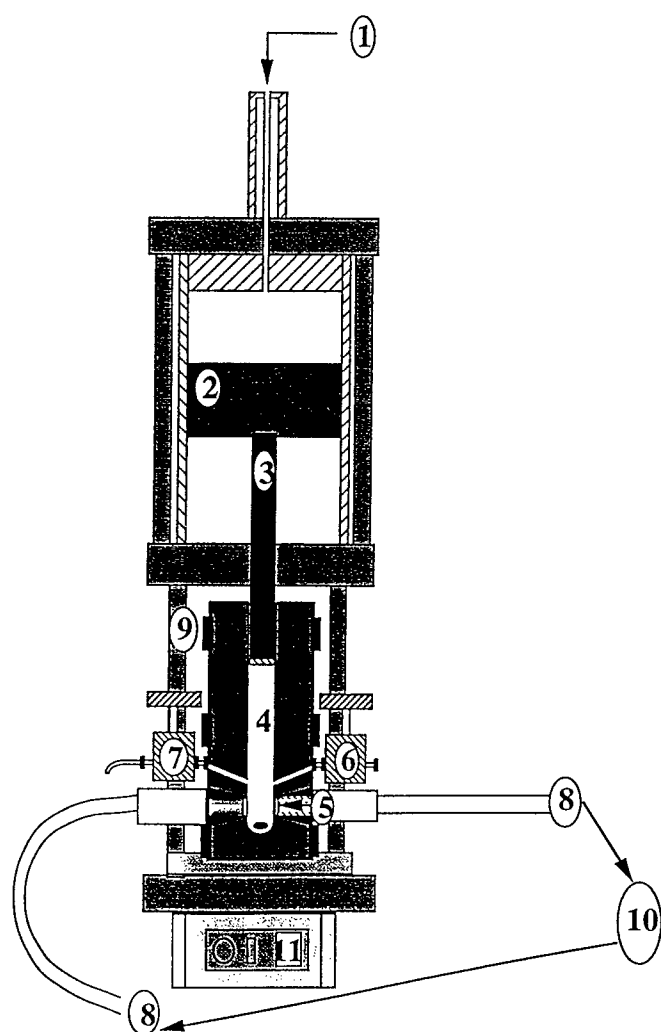
FIGURE 1. High pressure bioreactor. The bioreactor is made of stainless steel by Top Industrie (France). The maximal pressure reached is 250 MPa. Working temperature varied from ambient temperature up to 150 °C. The cell is equipped with two sapphire windows and connected to a photodiode array spectrophotometer [Otsuka MCPD 1000 (Braun Sciencetec)]. Kinetics are followed *in situ.* The sampling is possible through a high pressure valve without pressure release. Terms: (1) nitrogen gas inlet and control, (2) low pressure piston, (3) high pressure piston, (4) reaction cell, (5) sapphire windows, (6) high pressure injection valve, (7) high pressure sampling valve, (8) optical fibers, (9) heating ring, (10) photodiode array spectrophotometer, and (11) magnetic stirrer.
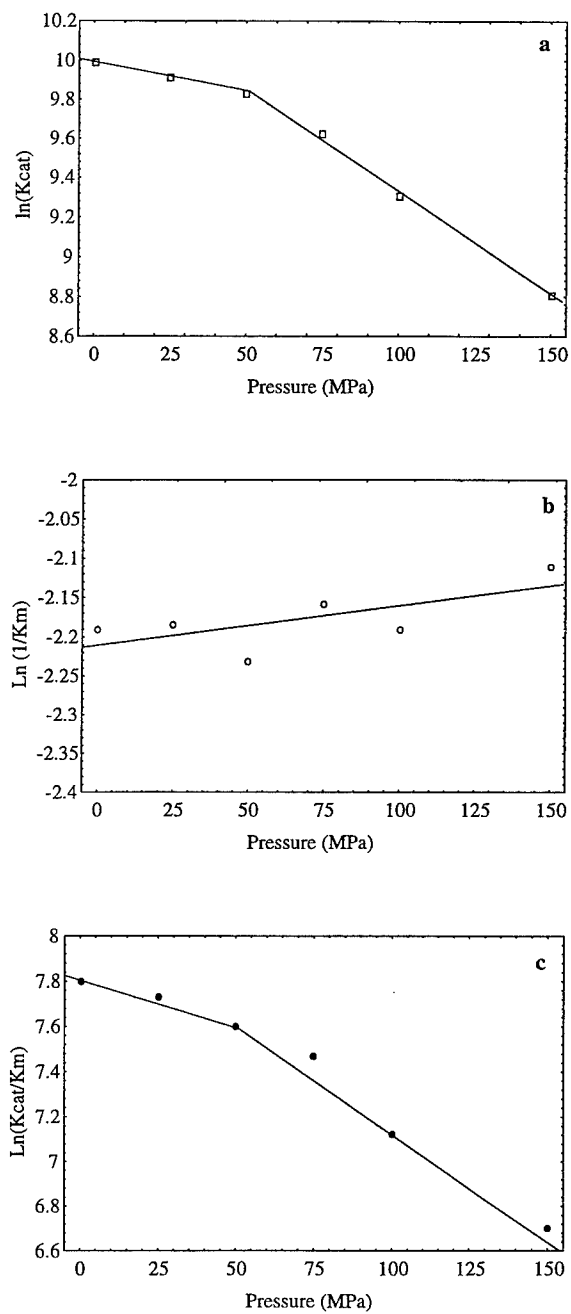
FIGURE 2. Pressure dependence of kinetic parameters of YADH (as a function of ethanol concentration): (a) $\ln(k_{cat})$, (b) $\ln(1/K_m)$, and (c) $\ln(k_{cat}/K_m)$.
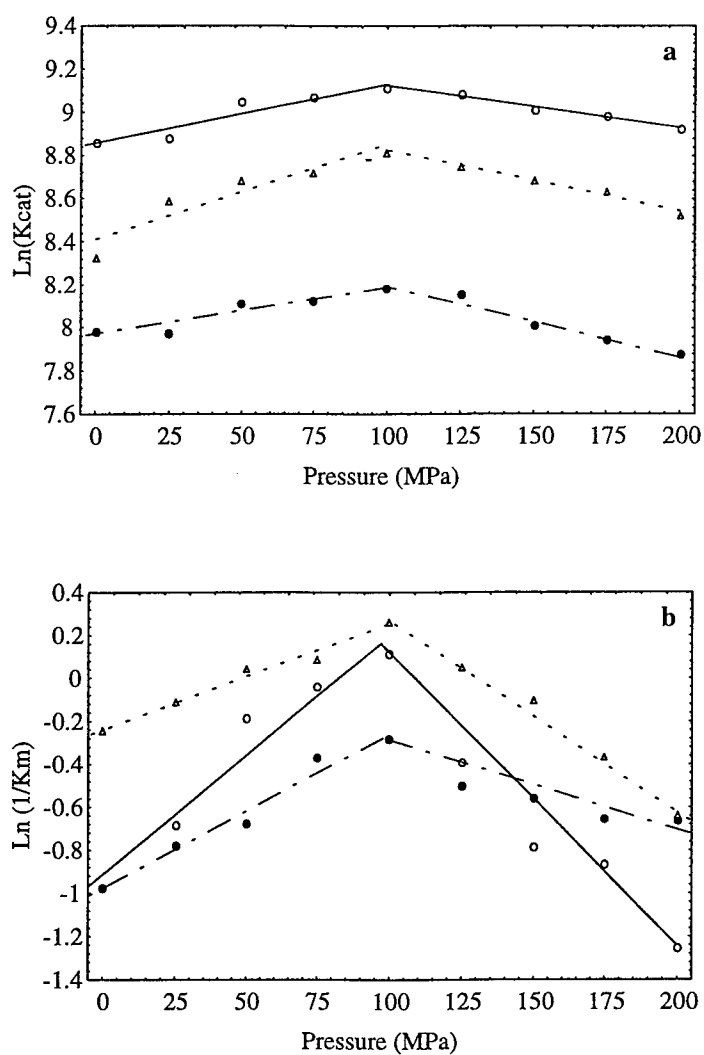
FIGURE 3. Pressure dependence of kinetic parameters of TBADH for alcohol oxidation (as a function of alcohol concentration): (a) $\ln(k_{cat})$ and (b) $\ln(1/K_m)$. The experiments were monitored in Tris-HCl buffer at pH 7.8, at 40 °C, with 0.7 mM NADP and alcohols as the variable substrates: (○) cyclopentanol, (●) 2-pentanol, and (△) 2-propanol.
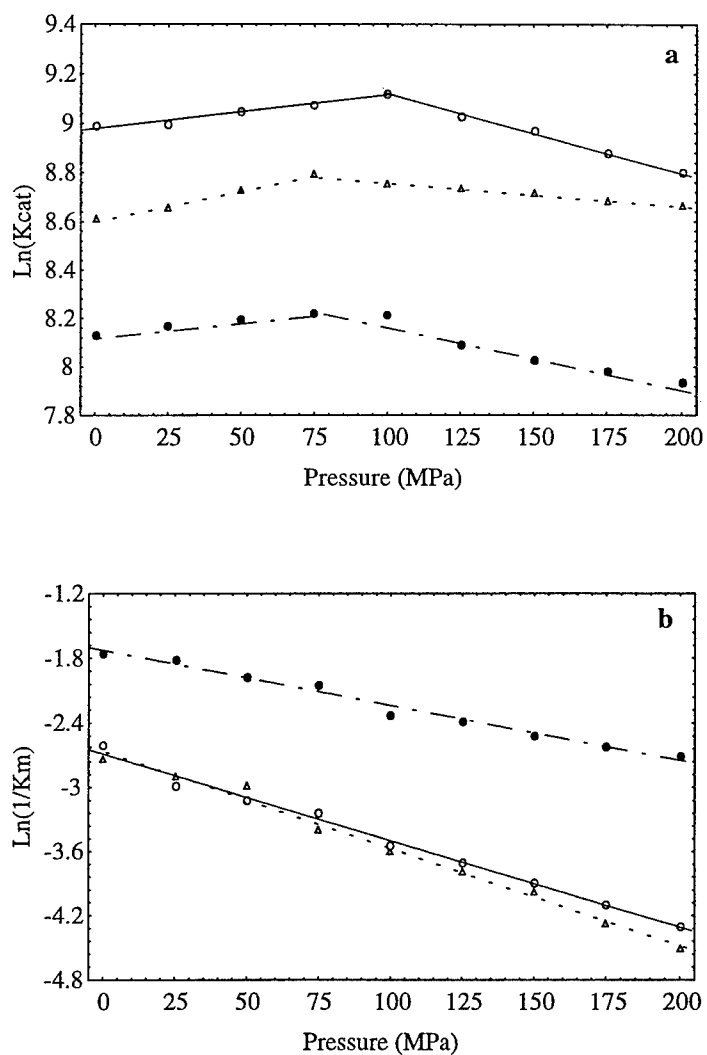
FIGURE 4. Pressure dependence of kinetic parameters of TBADH (as a function of NADP concentration): (a) $\ln(k_{cat})$ and (b) $\ln(1/K_m)$. The experiments were done in Tris-HCl buffer at pH 7.8, at 40 °C. The NADP concentration was the variable substrate (0.7 mM). Symbols: (○) 40 mM cyclopentanol, (●) 40 mM 2-pentanol, and (△) 40 mM 2-propanol.
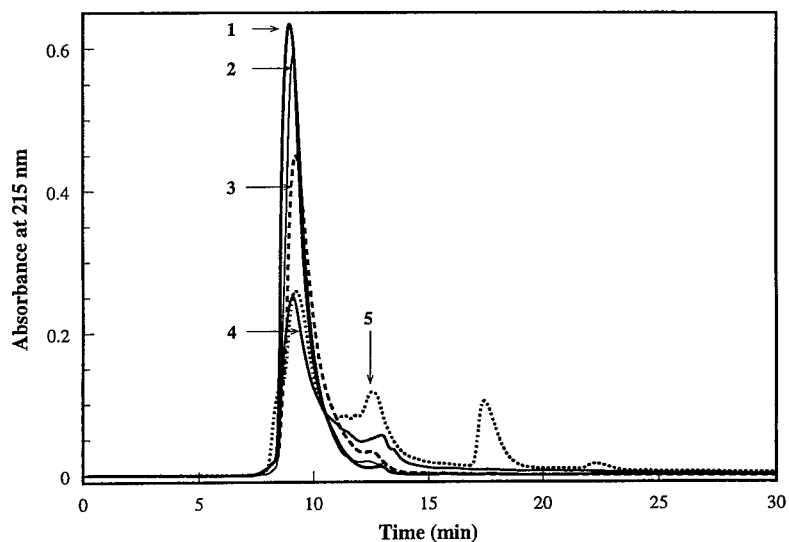
FIGURE 5. Evolution of the chromatographic profile of pressurized YADH: (1) YADH not pressurized, (2) 100 MPa, (3) 200 MPa, (4) 200 MPa for 3 h, and (5) denatured YADH in 8 M urea.
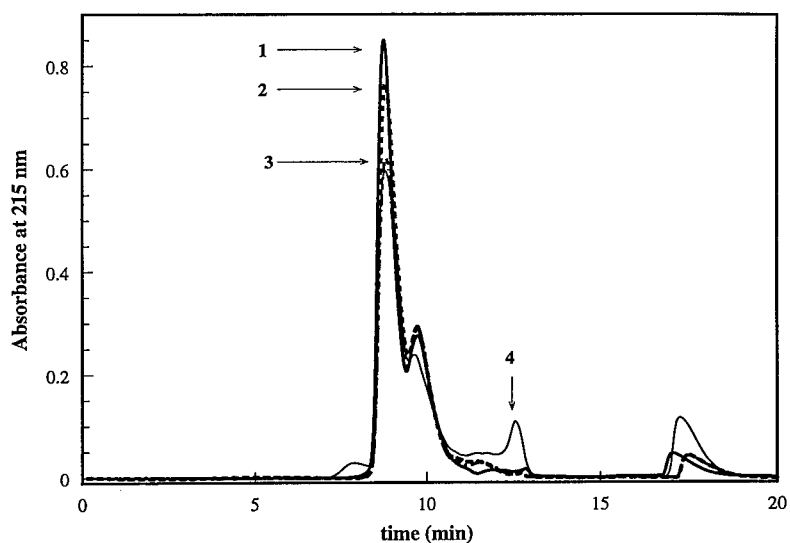
FIGURE 6. Evolution of the chromatographic profile of pressurized TBADH: (1) TBADH not pressurized, (2) 250 MPa for 1 h, (3) 250 MPa for 5 h, and (4) denatured TBADH in 8 M urea.

and the activation volume due to the binding phase is

$$\Delta V_b = -RT[\partial \ln(1/K_m)/\partial P]_T.$$

INACTIVATION OF YADH BY HIGH PRESSURE

Between 0.1 and 150 MPa, YADH lost 70% of its activity (FIGURE 2a). The catalytic efficiency also decreased in this range of pressure (FIGURE 2c). Nevertheless, pressure induces little effect on YADH affinity for ethanol (no more than 19% variation between 0.1 to 150 MPa) (FIGURE 2b).

It seems that the decrease of the activity is due to the catalytic step because the ΔV_{cat} absolute value is the most important factor. In other words, pressure slows down the complex enzyme-product dissociation. This effect may be due to a change of interaction between the substrates and the enzyme and to a reorganization of the surrounding water molecules.

ACTIVATION OF TBADH BY MODERATE PRESSURE

The results show that the pressure effect may be split into two parts: below and above 100 MPa. For an increase of pressure up to 100 MPa, the activity (FIGURES 3a and 4a) and the affinity for alcohol (FIGURE 3b) increased, and vice versa for pressure above 100 MPa. However, the activity and the affinity remain better up to 150 MPa than the activity at 0.1 MPa.

The affinity for NADP (FIGURE 4b) decreases for pressures in the range of 0.1 to 200 MPa. Nevertheless, for all pressures, the affinity for NADP is still better than the affinity for the alcohols.

CONFORMATION CHANGES INDUCED BY PRESSURE

FIGURE 5 displays HPLC chromatograms of YADH held at the desired pressure for 5 minutes, released to atmospheric pressure, and injected into a gel permeation column (TSK G3000). These chromatograms show that the decrease in activity of YADH is not correlated with subunit dissociation. The change in the retention time of the tetrameric enzyme tends to exhibit a molecular rearrangement that, in this case, results in a loss of activity and affinity.

In the same way, the chromatograms of FIGURE 6 bring to evidence that TBADH does not dissociate under pressure. This enzyme seems especially resistant to chemical denaturation: the presence of 8 M urea did not induce a total denaturation. In this case, the conformational change seems limited and favorable for the reaction.

Whereas the hypothesis was previously raised that oligomeric enzymes dissociate under moderate pressures (less than 200 MPa),[9] we evidenced that, in our case, moderate pressures did not induce subunit dissociation, but possibly conformational changes.

CONCLUSIONS

YADH is continuously inhibited by pressure, whereas TBADH activity is one of
the few cases at the present time where an enzyme can be activated by pressure, in
the range of 0.1 to 100 MPa. The comparisons of the two enzymes are in good
agreement with Fukuda and Kunugi:[10] barostability is linked to thermostability.
However, TBADH kinetic parameters display a complex behavior under pressure:
the pressure dependences of both the affinity and the catalytic constant are biphasic.
At 100 MPa, we observed a shift that is difficult to interpret. The monitoring of
oligomer dissociation by HPLC tends to show that YADH and TBADH do not
dissociate under pressure unless they reassociate very quickly at ambient pressure.

REFERENCES

1. LAMED, R. J. & J. G. ZEIKUS. 1981. Biochem. J. **195:** 183–190.
2. DICKINSON, F. M. & G. P. MONGER. 1973. Biochem. J. **131:** 261–270.
3. JAENICKE, R. 1991. Eur. J. Biochem. **202:** 715–728.
4. JAENICKE, R. 1981. Annu. Rev. Biophys. Bioeng. **10:** 1–67.
5. GROß, M. & R. JAENICKE. 1994. Eur. J. Biochem. **221:** 617–630.
6. HEREMANS, K. 1982. Annu. Rev. Biophys. Bioeng. **11:** 1–21.
7. BALNY, C., P. MASSON & F. TRAVERS. 1989. High Pressure Res. **2:** 1–28.
8. MORILD, E. 1981. *In* Advances in Protein Chemistry. Volume 34. C. B. Anfinsen, J. T.
    Edsall & F. M. Richards, Eds.: 93–166. Academic Press. New York.
9. GROß, M., G. AUERBACH & R. JAENICKE. 1993. FEBS Lett. **321:** 256–260.
10. FUKUDA, M. & S. KUNUGI. 1984. Eur. J. Biochem. **142:** 565–570.

Controlling Regioselectivity in Enzyme-catalyzed Acylation of Polyhydroxyl Compounds[a]

JOSEPH O. RICH[b] AND JONATHAN S. DORDICK[c]

Department of Chemical and Biochemical Engineering
and
Center for Biocatalysis and Bioprocessing
University of Iowa
Iowa City, Iowa 52242

INTRODUCTION

Enzymes suspended in anhydrous organic solvents are effective enantioselective, regioselective, and chemoselective catalysts for the derivatization of complex molecules.[1] Whereas enantioselectivity for a given functional group involves two possibilities (e.g., R or S), regioselectivity, particularly on complex molecules (e.g., carbohydrates), often involves multiple possibilities.

A case in point is the regioselective acylation of sugar hydroxyl groups. The selective chemical acylation of a given hydroxyl group requires extensive protecting/deprotecting methodologies.[2] Enzymes, however, are capable of the regioselective acylation of sugars.[3,4] Such synthetic steps have been used for the production of sweeteners, linear polymers, and hydrogels.

MATERIALS AND METHODS

Enzyme Preparation

Semipurified subtilisin BPN' (from *Bacillus amyloliquefaciens*) wild-type and mutant enzymes were generously provided by Thomas Graycar at Genencor International. Each enzyme was first purified by cation exchange chromatography, dialyzed against 20 mM sodium phosphate buffer (pH 7.8) for 24 h, and then lyophilized for 40 h.[5] Subtilisin Carlsberg (from *B. licheniformis*) was purchased from Sigma and used after lyophilization. Some enzymes were lyophilized in the presence of a twofold weight excess of an additive (sucrose or thymidine).

In the present work, we examine a simple, yet effective, methodology for controlling enzyme-catalyzed regioselectivity in the acylation of poly(hydroxy)-

226

containing compounds and for doing so at elevated catalytic efficiencies. This approach involves lyophilizing the enzyme in the presence of the substrate.

Transesterification Reaction Conditions

The transesterification of sucrose (50 mM) or thymidine (10 mM) with various vinyl esters (threefold molar excess) in anhydrous solvents was initiated upon addition of 1 mg of solid enzyme preparation in a 1-mL (sucrose) or 10-mL (thymidine) reaction volume and shaking at 250 rpm at 30 °C.

Analytical Conditions

Samples of the sucrose acylation reactions were precolumn-derivatized with 1,1,1,3,3,3-hexamethyldisilazane prior to analysis on a capillary (AT-1) GC column.[3] Thymidine reactions were followed on RP-HPLC (4.5 × 250 mm ODS-AQ, YMC) with an isocratic mobile phase of 60% water + 0.01% TFA and 40% acetonitrile and by UV detection at 254 nm. TLC and silica gel chromatography employed eluants of ethyl acetate:methanol:water (17:4:1 and 98:2:0 for sucrose and thymidine, respectively).

RESULTS AND DISCUSSION

The control of enzymic regioselectivity has been studied initially using the acylation of sucrose by vinyl esters in organic solvents (FIGURE 1A) as a model reaction.[3] Subtilisin BPN' preferentially acylates the 1'-hydroxyl of sucrose with some acylation at the 6-hydroxyl (1'-butyrate/6-butyrate = 6.2). The transesterification of sucrose with vinyl butyrate in anhydrous pyridine proceeded slowly with a $k_{cat}/K_m = 0.9$ M^{-1} s^{-1}. Simply lyophilizing the enzyme in the presence of sucrose increased the catalytic efficiency by 58-fold. The pretreatment with sucrose also yielded a more regioselective enzyme preparation (1'-butyrate/6-butyrate = 14.0). The preference for the 1'-position in sucrose acylation is strongly affected by the hydrophobicity of the solvent. For example, the ratio of acylation with vinyl butyrate at the 1'- to 6-hydroxyl groups (1'-butyrate/6-butyrate) dropped from 14 in pure pyridine to 4.1 in pyridine containing 40% hexane. Moreover, increasing the hydrophobicity of the reaction medium with hexane increased the overall k_{cat}/K_m from 52.4 M^{-1} s^{-1} to 218 M^{-1} s^{-1}. The chain length of the vinyl ester also affects both the catalytic efficiency and the regioselectivity of subtilisin-catalyzed sucrose acylation (FIGURE 2). Subtilisin lyophilized with sucrose had optimal activity with vinyl butyrate as the acyl donor. Acylation with vinyl acetate gave almost exclusively the 1'-acetate (1'-acetate/6-acetate ≥ 30). Increasing the chain length of the vinyl ester increased the relative rates of 6-acylation as compared to 1'-acylation (1'-caprylate/6-caprylate = 5.7). Similar results were observed for subtilisin Carlsberg. Indeed, the effect is more pronounced, resulting in a nearly complete loss of selectivity with vinyl caprylate (1'-caprylate/6-caprylate = 1.2). Molecular modeling studies revealed struc-

(A)

Sucrose

Subtilisin BPN'
Vinyl Ester
Organic Solvent
→

1'-monoester: R_1=OC(CH$_2$)$_n$CH$_3$; R_6=H
6-monoester: $R_{1'}$=H; R_6=OC(CH$_2$)$_n$CH$_3$
6,1'-diester: R_1=R_6=OC(CH$_2$)$_n$CH$_3$

(B)

Thymidine

Subtilisin BPN'
Vinyl Ester
Organic Solvent
→

5'-monoester: R_5=OC(CH$_2$)$_n$CH$_3$; R_3=H
3'-monoester: $R_{5'}$=H; $R_{3'}$=OC(CH$_2$)$_n$CH$_3$
5',3'-diester: R_5=R_3=OC(CH$_2$)$_n$CH$_3$
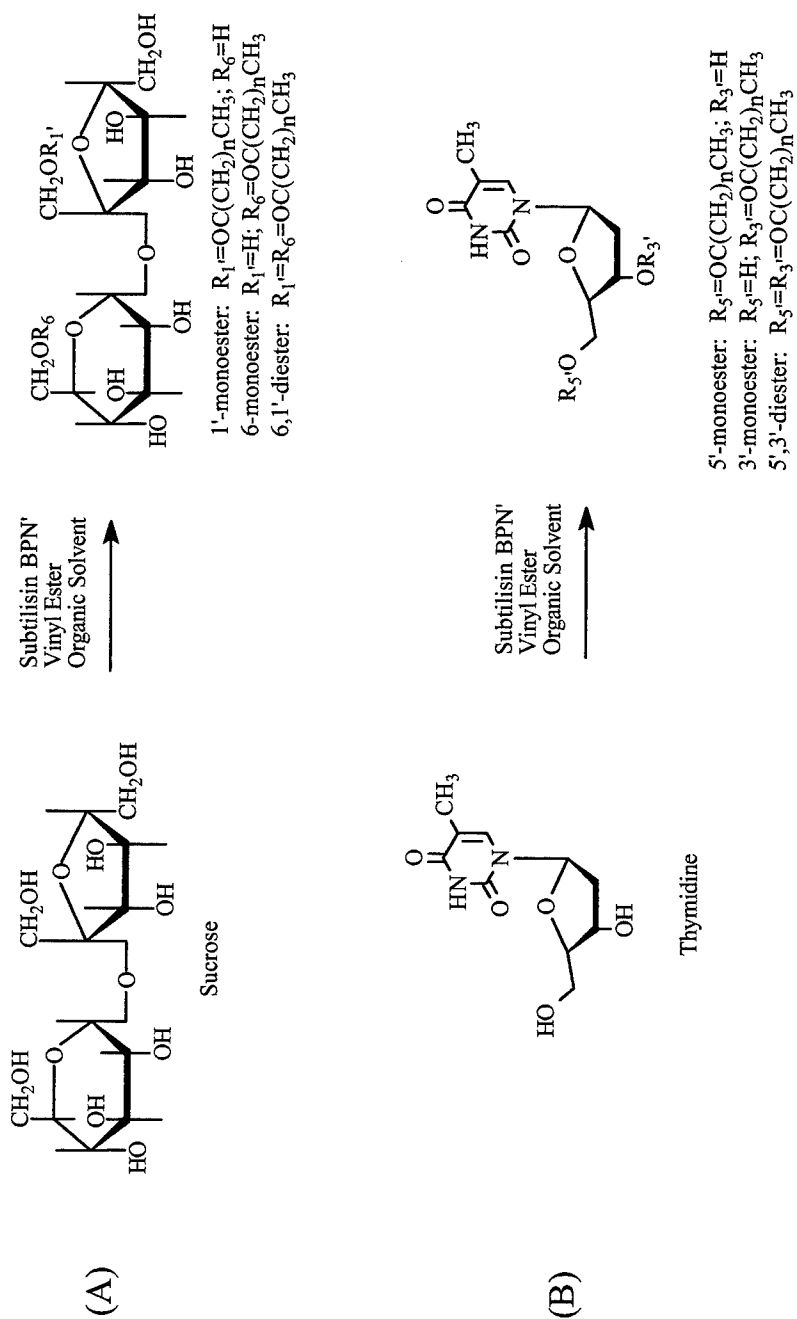
FIGURE 1. Reaction scheme for the subtilisin-catalyzed transesterification of sucrose (A) or thymidine (B) with a vinyl ester in an anhydrous organic solvent.

tural differences in the orientation of the 1'- and 6-sucrose tetrahedral intermediates in the S₁' pocket for different vinyl ester chain lengths.[3]

The computer-generated model of the sucrose–acyl-enzyme tetrahedral intermediate, as determined by nearest-neighbor calculations (i.e., determining the number of contacts of sucrose with enzyme residues closer than 2.5 Å), revealed that the 1'-OH (4 close contacts) is less sterically constrained than the 6-OH (22 close contacts).[3] Therefore, specific mutations in the active site of subtilisin should relieve the steric hindrance of the tetrahedral intermediates, thereby altering the regioselectivity. For example, the M222A mutation decreases the close contacts of both the 1'- (from 4 down to 3) and 6-butyrate intermediates (from 22 to 19). Because the change in unfavorable close contacts for the 6-OH was greater, the relative reactivity
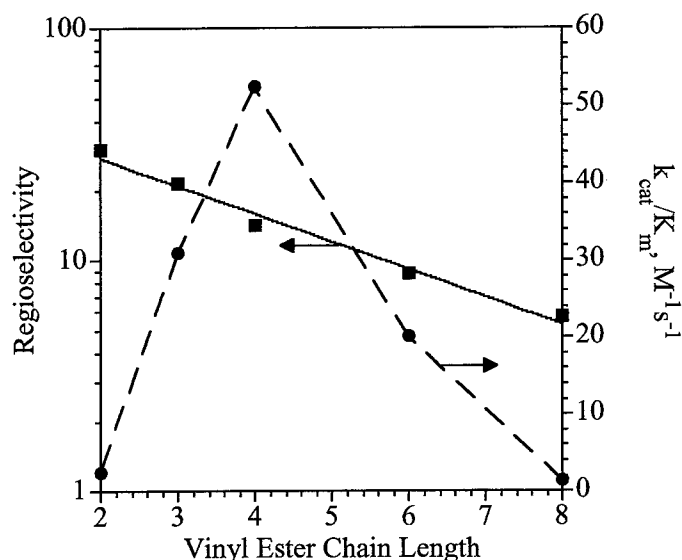
FIGURE 2. The effect of vinyl ester chain length on subtilisin BPN'–catalyzed acylation of sucrose in pyridine. The catalytic efficiency (●) and regioselectivity (■) are shown with broken and solid lines, respectively.

of the 6-OH should increase, thus decreasing 1'-butyrate/6-butyrate. Indeed, there was a nearly complete loss of regioselectivity (from 1'-butyrate/6-butyrate = 14.0 to 1.93) by replacing Met222 with Ala (FIGURE 3).

The subtilisin-catalyzed acylation of thymidine (FIGURE 1B) yields a mixture of the 5'- and 3'-monoesters with a slight preference for the 5'-ester. Several enzyme preparations were employed as catalysts for the butyrylation of thymidine. Although regioselectivity was not affected by the nature of the enzyme preparation, the activity of the enzyme was dramatically increased by lyophilizing the enzyme in the presence of thymidine. Specifically, subtilisin lyophilized in the presence of thymidine was about 60 times more active than the pH-adjusted enzyme preparation.

The reaction medium again had a dramatic effect on both the activity and regioselectivity of thymidine acylation. The overall k_{cat}/K_m ranged from about 500
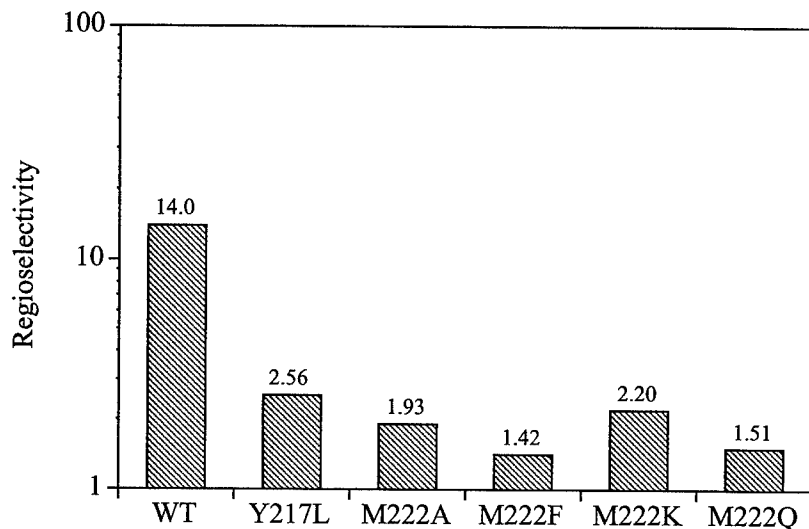
FIGURE 3. Decrease in regioselectivity by site-directed mutagenesis of the S_1' binding pocket of subtilisin BPN'. Notation for mutations: Y217L (Tyr217 → Leu), M222A (Met222 → Ala), M222F (Met222 → Phe), M222K (Met222 → Lys), and M222Q (Met222 → Gln).

$M^{-1}\,s^{-1}$ in dioxane, pyridine, and *tert*-amyl alcohol to about 10,000 $M^{-1}\,s^{-1}$ in THF containing 50% hexane. The regioselectivity (5'-butyrate/3'-butyrate) of both enzyme preparations was increased approximately 6-fold (from 2.5 to 14) by adding hexane to the THF reaction medium. The regioselectivity in thymidine acylation was not altered by mutations in the S_1' pocket. The catalytic activity, however, was increased by 540-fold by employing the M222F enzyme lyophilized with thymidine as the catalyst in the hexane/THF reaction medium.

CONCLUSIONS

Regioselective transformations of substrates with multiple functional groups are attainable using enzymes suspended in organic solvents. The activity and the regioselectivity of subtilisin-catalyzed sucrose acylation was controlled through the hydrophobicity of the reaction medium and the length of the acyl-donor side chain. Activity was also dramatically increased by lyophilizing the enzyme in the presence of the nucleophile.

REFERENCES

1. DORDICK, J. S. 1992. Biotechnol. Prog. **8:** 259–267.
2. HAINES, A. H. 1981. Adv. Carbohydr. Chem. Biochem. **39:** 13–70.
3. RICH, J. O., B. A. BEDELL & J. S. DORDICK. 1995. Biotechnol. Bioeng. **45:** 426–434.
4. RIVA, S., J. CHOPINEAU, A. P. G. KIEBOOM & A. M. KLIBANOV. 1988. J. Am. Chem. Soc. **110:** 584–589.
5. WANGIKAR, P. P., J. O. RICH, D. S. CLARK & J. S. DORDICK. 1995. Biochemistry **34:** 12302–12310.

Acyl Migration and Its Implications in Lipid Modifications

ANNA MILLQVIST FUREBY, PATRICK ADLERCREUTZ,
AND BO MATTIASSON

Department of Biotechnology
Chemical Center
Lund University
221 00 Lund, Sweden

INTRODUCTION

Selective modifications of lipids are conveniently carried out using 1,3-specific lipases. However, the selectivity is often not as good as anticipated due to acyl migration occurring concurrent with the lipase-catalyzed reaction. Acyl migration is the intramolecular transfer of one acyl moiety to an adjacent unoccupied hydroxyl group on the glycerol backbone; however, acyl migration is not restricted to glycerides, but occurs in all partial esterifications of polyols. This reaction is spontaneous, but is catalyzed by acids, bases, heat, and ion exchange resins.[1] Furthermore, the reaction conditions used are of great importance, for example, the choice of solvent, water activity (a_w), etc. Acyl migration has been studied in some detail for 2-mono-olein[2] and 1,2-dibutyrin.[3] The equilibrium composition of the isomers is for neat monoglycerides approximately 90% 1-monoglyceride and 10% 2-monoglyceride, and for neat diglycerides approximately 40% 1,2-diglyceride and 60% 1,3-diglyceride.[4] The equilibrium position varies only slightly depending on the solvent,[3] but the rate can be manipulated by changing the reaction conditions.

The effect of acyl migration in lipid modifications can be observed as low yields,[5-8] poor regioisomeric purity in partial glycerides,[8] trisaturated triglycerides in interesterification of triolein with stearic acid,[9] and triglyceride formation in synthesis of partial glycerides.[10-12] Because the purity is less than desired and an unwanted by-product is formed, purification of the product is more difficult. By choosing appropriate reaction conditions, acyl migration can be minimized.

MATERIALS AND METHODS

Acyl Migration Reactions

2-Monoolein (19 mM) was dissolved in an appropriate solvent, dry or adjusted to the desired a_w. Any additives were added and the mixture was incubated at 40 °C. Samples were analyzed by gas chromatography (GC).

Preparation of 2-Monopalmitin

Tripalmitin (12.5 mM) was dissolved in methyl *tert*-butyl ether (MTBE) or isooctane and adjusted to an a_w of 0.33. Ethanol was added to give a final concentration of 125 mM in alcoholysis reactions. Lipase from *Rhizopus arrhizus* immobilized on celite (0.1 g lipase powder/g carrier; 30 mg) was added to start the reaction. Samples were withdrawn at intervals and analyzed by GC.[7]

Preparation of 1,2-Dilaurin

Trilaurin (10 mM) was dissolved in diisopropyl ether (DIPE) or isooctane and adjusted to an a_w of 0.84. Ethanol was added to give a final concentration of 50 mM. Lipase from *Penicillium cyclopium* immobilized on porous polypropylene (1 g lipase powder/g carrier; 60 mg) was added to start the reaction. Samples were withdrawn at intervals and analyzed by GC.[8]

Synthesis of 1,3-Dicaprin

Ethyl caprate (5 mM) or capric acid (5 mM) was mixed with glycerol (0.46 g) containing 4% water (w/w) in an open container and then equilibrated to 40 °C. Lipase from *R. arrhizus* immobilized on porous polypropylene (1 g lipase powder/g carrier; 150 mg) was added to start the reaction. Samples were taken at intervals, diluted in MTBE, and analyzed by GC.[12]

RESULTS AND DISCUSSION

Acyl Migration in 2-Monoolein

The solvent has a major influence on the acyl migration rate: the rates in dry solvents were correlated with log P, E_T^N values, dipole moment, and several other polarity parameters for the solvents. None of the polarity parameters gave a satisfactory correlation with the results, but E_T^N values described the effect of the solvent on the acyl migration rate better than did any other parameter. The general conclusion that could be drawn was that aprotic, hydrophobic solvents and protic, hydrophilic solvents promote acyl migration, in particular water-miscible alcohols. The acyl migration rates were slow in solvents with intermediate E_T^N values (0.3–0.5), that is, aprotic, hydrophilic solvents such as ketones. Similar results were found for acyl migration in 1,2-dibutyrin.[3] The acyl migration in ethers showed a different behavior compared to all other solvents tested; during the first 48 to 72 hours, acyl migration was negligible, but then occurred at a significant rate after the initial lag-phase.

The water activity is an important reaction parameter that influences both the lipase activity and the reaction equilibrium.[13,14] Many lipases show good activity at low a_w, which is advantageous for synthetic purposes when hydrolysis has to be kept to a minimum and in triglyceride interesterification reactions. Acyl migration in
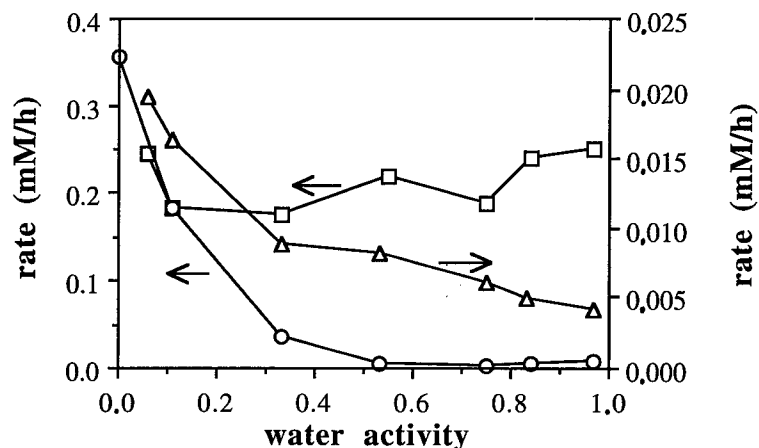
FIGURE 1. The influence of the water activity on the acyl migration rate: MTBE (O), isooctane (□), and MIBK (△).

isooctane was independent of a_w, whereas the acyl migration rates were high at low a_w in MTBE and MIBK (methyl isobutyl ketone) and then decreased at higher values of a_w (FIGURE 1). A possible reason for the decreased acyl migration rate at high a_w can be that the medium is more polar. The water activity is not important in isooctane because the water solubility is very low.

Lipases are often used as immobilized preparations and the effect of the support material on the acyl migration cannot be neglected. The acyl migration rates in the presence of various support materials in isooctane are given in TABLE 1. It is clear that the neutral supports had very little effect on the acyl migration rate, but acyl migration was catalyzed by the charged support materials. Duolite 568 is an anion exchange resin that is used for immobilization of Lipozyme-IM. This lipase preparation often acts as an unspecified lipase, despite the known 1,3-specificity of this lipase from *Mucor miehei*, but acyl migration is responsible for this behavior.[2,11] Celite deserves some extra attention: this commonly used material for enzyme immobilization catalyzes acyl migration, but after acid-wash of the celite it has no effect on acyl migration because the positive surface charges have been removed. Impregnation of

TABLE 1. Effect of Support Materials on the Acyl Migration Rate[a]

Support Material	Surface Character	Rate (mM/h)
celite	positive (?)	0.43
celite, acid-washed	neutral	0.16
Duolite 568	positive	1.8
silica	negative	6.0
silica, boric acid	negative	0.13
EP100	neutral	0.15
XAD-4	nonpolar	0.27
XAD-8	polar	1.7

[a]The reactions were carried out with 19 mM 2-monoolein in dry isooctane at 40 °C.

silica gel with boric acid has long been used to prevent acyl migration in chromato-graphic analyses of partial glycerides and it is clearly shown here that it is indeed the case. Acyl migration is inhibited because the boric acid forms a complex with the free hydroxyl groups on the glycerol backbone.

Implications in the Preparation of Partial Glycerides

The importance of the choice of solvent is shown in FIGURE 2 for alcoholysis of triglycerides for preparation of 2-monopalmitin and 1,3-dilaurin. The acyl migration rate is high in isooctane and, despite the higher initial reaction rate in this solvent, low yields are obtained because the products formed by acyl migration are rapidly alcoholized by the lipase.
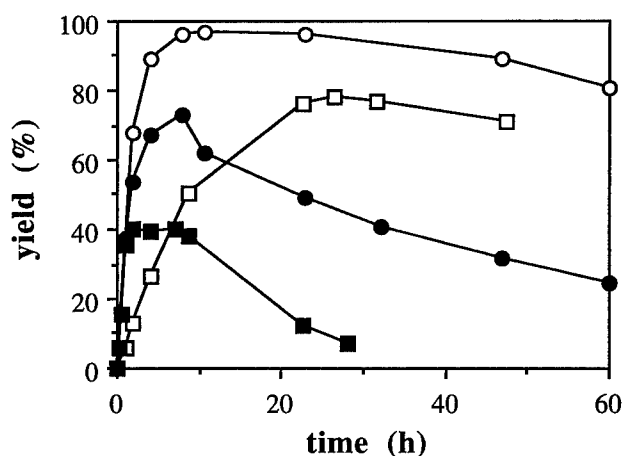
FIGURE 2. The effect of the solvent on the yields in alcoholysis of trilaurin for preparation of 2-monopalmitin and 1,2-dilaurin: MTBE and 2-monopalmitin (○), isooctane and 2-monopalmitin (●), DIPE and 1,2-dilaurin (□), and isooctane and 1,2-dilaurin (■).

The water activity is of vital importance for both the lipase activity and the reaction equilibrium: high yields are favored by high values of a_w because the reaction equilibrium is displaced in favor of the products and less acyl migration occurs. The remaining triglyceride and diglyceride at the end of the reactions was less than 10%, except for hydrolysis at the lowest a_w; thus, the low yield at low a_w is due to both acyl migration and an unfavorable equilibrium. In particular, in the case of 1,2-dilaurin preparation, the isomeric purity is improved at high values of a_w due to less acyl migration (FIGURE 3). In a separate experiment, no acyl migration was observed when 1,2-dilaurin was incubated in diisopropyl ether at $a_w = 0.84$. The change in isomeric purity could also be due to a change in the lipase specificity with the increased values of a_w. Addition of alcohol to the reaction medium had a positive effect on the yield as well as the purity of the product, with less formation of 1,3-dilaurin.
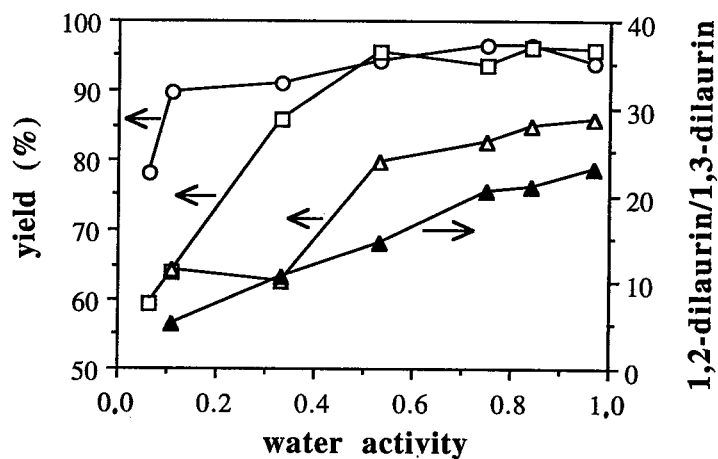
FIGURE 3. The influence of the water activity on the yields of 2-monopalmitin and dilaurin and the regioisomeric purity of dilaurin: 2-monopalmitin prepared by alcoholysis (○), 2-mono-palmitin prepared by hydrolysis (□), dilaurin prepared by alcoholysis (△), and the ratio of 1,2-dilaurin to 1,3-dilaurin (▲).

1,3-Diglycerides can be synthesized from glycerol and an acyl donor, using a 1,3-specific lipase.[12] In this reaction, acyl migration gives rise to the by-products, 1,2-diglyceride and triglyceride. The choice of acyl donor affected the acyl migration rate: when capric acid was used as the acyl donor, more tricaprin was formed at the same degree of substrate conversion than when ethyl caprate was used (FIGURE 4). This was presumably due to more acyl migration in the presence of the acid, which
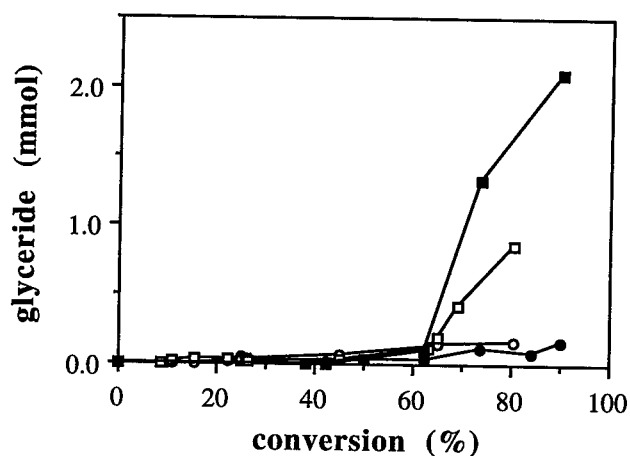
FIGURE 4. By-products formed due to acyl migration in synthesis of 1,3-dicaprin in a solvent-free system, starting from ethyl caprate and glycerol (open symbols) or capric acid and glycerol (filled symbols): 1,2-dicaprin (○, ●) and tricaprin (□, ■).

catalyzed the acyl migration. In the hydrophobic environment, the fraction of deprotonated fatty acid is probably very low, but evidently high enough to affect the acyl migration rate.

The reaction temperature had, as expected, an effect on the acyl migration rate, detected as increasing formation of tricaprin and 1,2-dicaprin at increasing temperature (TABLE 2). The yield of dicaprin was highest at low temperature, when the product precipitated from the reaction mixture, and the isomeric purity was also highest at this temperature because acyl migration is insignificant in the solid state.

CONCLUSIONS

Acyl migration has to be controlled in order to achieve good specificity and high yields in selective lipid modifications. The acyl migration rate is determined by the reaction conditions. Under the following conditions, acyl migration can be expected to be slow: (i) solvents with intermediate E_T^N values, for example, ketones, ethers, and toluene, (ii) water activity higher than 0.5, and (iii) neutral support for lipase immobilization. The acyl migration rate is further influenced by other components in the reaction medium and by the temperature.

TABLE 2. Effect of Temperature on Synthesis of 1,3-Dicaprin

Temperature (°C)	Dicaprin Yield (%)	Tricaprin Yield (%)	1,3-Dicaprin/1,2-Dicaprin
15	88	0.88	14
25	58	8.6	10
40	72	8.0	16
45	70	10.2	14
50	78	25	6

The effect of acyl migration was observed in various methods for the preparation of partial glycerides. In alcoholysis and hydrolysis of triglycerides for preparation of 2-monoglycerides and 1,2-diglycerides, the yield was low in isooctane, but high in ethers and ketones, and the yield was higher at high a_w levels. In particular, the isomeric purity of 1,2-diglycerides was improved at higher a_w levels due to less acyl migration. In synthesis of 1,3-diglycerides, the choice of acyl donor influenced the acyl migration, with ester giving less acyl migration than fatty acid. Furthermore, increasing temperature was shown to increase the acyl migration, detected both as impaired isomeric purity in the diglycerides and as formation of triglycerides.

REFERENCES

1. BLOOMER, S. 1992. Doctoral thesis. University of Lund.
2. MILLQVIST FUREBY, A., C. VIRTO, P. ADLERCREUTZ & B. MATTIASSON. 1996. Biocatalysis. In press.
3. SJURSNES, B. & T. ANTHONSEN. 1994. Biocatalysis 9: 285–297.
4. SERDAREVICH, B. 1967. J. Am. Oil Chem. Soc. 44: 381–393.
5. HOLMBERG, K. & E. ÖSTERBERG. 1988. J. Am. Oil Chem. Soc. 65: 1544–1548.

6. MAZUR, A. W., G. D. HILER & M. EL-NOKALY. 1991. *In* Microemulsions and Emulsions in Foods. Amer. Chem. Soc. Symposium Series. M. El-Nokaly & D. Cornell, Eds.: 51–61. Amer. Chem. Soc. Washington, District of Columbia.

7. MILLQVIST, A., P. ADLERCREUTZ & B. MATTIASSON. 1994. Enzyme Microb. Technol. **16:** 1042–1047.

8. MILLQVIST FUREBY, A., L. TIAN, P. ADLERCREUTZ & B. MATTIASSON. 1996. Enzyme Microb. Technol. In press.

9. BLOOMER, S., P. ADLERCREUTZ & B. MATTIASSON. 1991. Biocatalysis **5:** 145–162.

10. KIM, S. M. & J. S. RHEE. 1991. J. Am. Oil Chem. Soc. **68:** 499–503.

11. ERGAN, F., M. TRANI & G. ANDRÉ. 1990. J. Am. Oil Chem. Soc. **67:** 412–417.

12. MILLQVIST FUREBY, A., P. ADLERCREUTZ & B. MATTIASSON. 1996. J. Am. Oil Chem. Soc. In press.

13. VALIVETY, R. H., P. J. HALLING & A. R. MACRAE. 1992. Biochim. Biophys. Acta **1118:** 218–222.

14. WEHTJE, E., I. SVENSSON, P. ADLERCREUTZ & B. MATTIASSON. 1994. Biotechnol. Bioeng. **44:** 549–556.

Determination of Rate Constants in Lipase-catalyzed Esterification of Two Fatty Acids with Dodecanol

THOMAS GITLESEN, PATRICK ADLERCREUTZ,
AND BO MATTIASSON

Department of Biotechnology
Chemical Center
Lund University
S-221 00 Lund, Sweden

INTRODUCTION

The use of lipase in biomodification of fatty acid esters is of considerable interest in food applications. One advantageous property of lipases for these applications is the ability to distinguish between fatty acids of different fatty acid length. Fatty acid selectivity determination is often hindered by the complexity of the reaction mixture and reaction kinetics. Methods for evaluation of lipase selectivity include comparison of initial reaction rates[1,2] and determination of the V_{max}/K_m ratio.[3,4]

In this study, we deal with the determination of individual rate constants in the esterification of two fatty acids with dodecanol in organic solvent.

EXPERIMENTAL METHODS

Lipase from *Rhizopus arrhizus* was absorbed on EP-100 polypropylene powder as described.[5] Final enzyme loading was 0.3 g enzyme powder/g EP-100. To keep a constant water activity in all reaction vials, immobilized enzyme and substrate solutions were preequilibrated with the vapor of saturated salt solutions. The substrate solution contained decanoic and dodecanoic acid (0–800 mM) and 200 mM dodecanol in diisopropyl ether. The reactions were started by adding the enzyme preparation to 4 mL of substrate solution in capped glass vials. During the reaction, samples were removed and analyzed by gas chromatography (GC).

RESULTS AND DISCUSSION

Water is not only a product in the esterification reaction, but is also necessary for full enzyme activity. In water-immiscible solvents like diisopropyl ether, the addition of amphiphilic substrates can alter the water solubility of the reaction mixture.[5] It is therefore of vital importance to the interpretation of experimental data that the enzyme activity is not affected by the water content of the reaction mixture. A practical way to solve this problem is preincubation of enzyme and substrate in

closed vials containing saturated salt solutions with defined water activity. At equilibrium, water activity (a_w) is the same in all phases and water activity of the substrate solution will be that of the saturated salt solutions. To look for optimal enzyme working conditions, substrate solutions were preincubated at water activities ranging from 0.06 to 0.97 (FIGURE 1). The water activity profile showed an optimum at a_w equal to 0.33–0.54. Decanoic acid reacted faster than dodecanoic acid at all water activities. The ratio in initial activity between decanoic and dodecanoic acid did not change with water activity in the substrate solution. A water activity of 0.33 was chosen to ensure constant enzyme activity in all vials.

Lipase-catalyzed esterification has been shown to follow a ping-pong bi-bi mechanism (FIGURE 2). When acting on insoluble substrates, the kinetics of lipase-catalyzed reactions are rather complex. However, Michaelis-Menten kinetics have
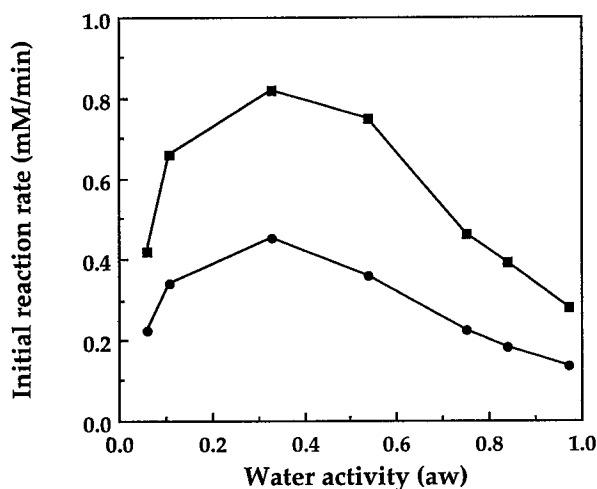
FIGURE 1. Effect of water activity on the initial reaction rate for decanoic acid (●) and dodecanoic acid (■). The reaction mixture contained 200 mM decanoic acid, 200 mM dodecanoic acid, and 200 mM dodecanol.

been obtained for lipase-catalyzed reactions in organic media.[6] If acylation of free enzyme reaction product and deacylation of acyl enzyme by water do not occur in the initial stage of conversion, the initial reaction rate can be represented by equations 1 and 2 under steady-state conditions (FIGURE 3).

The dissociation constants and the rate constants for acylation and deacylation of the acyl complex were determined by nonlinear least-square fitting of equations 1 and 2 to the experimental data. To get good convergence, the iteration procedure was dependent on a qualified guess for all the individual rate constants. To obtain the iteration start values, the apparent K_m and V_{max} were determined in the presence of varying concentrations of competing fatty acid using nonlinear least-square fitting of the experimental data to the Michaelis-Menten equation (see FIGURE 4). A plot of apparent K_m versus competing fatty acid concentration gave an estimate for equa-
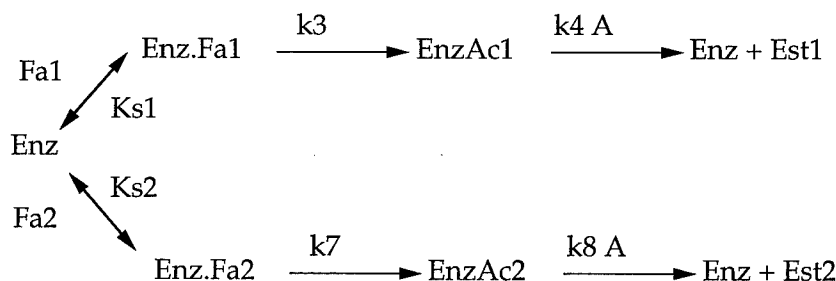
FIGURE 2. The kinetic scheme for the ping-pong bi-bi mechanism in the presence of competing fatty acid: Fa1, concentration of decanoic acid; Fa2, concentration of dodecanoic acid; Est1, concentration of dodecandecanoate; Est2, concentration of dodecandodecanoate; A, concentration of dodecanol.

tions 5 and 6 from the intercept with the x-axis and for equations 7 and 8 from the slope of the linear fit curve. At high concentrations of competing fatty acid, the apparent K_m became so large that the determination was not possible. Values that could not be properly determined were not included in the linear fit. The apparent V_{max} is not influenced by the competing fatty acid in this model. Because a good evaluation of V_{max} was possible only for reactions without competing fatty acid, this value was taken as the initial guess in equations 5 and 6. Equations 3–8 were solved for the individual rate constants and these were used as the start values in the search for the rate constants that could best describe the experimental data. An iteration function was written in MATLAB software. The regression function used the start values for the kinetic rate constants to generate a new data set. This was compared with the experimental values, and a new guess for the solution was made using the partial derivatives of the regression function. The iteration continued until the change in two sets of rate constants was less than 1%.

The regression values correspond well with the experimental data when simulated with equations 1 and 2 (see FIGURE 5). Good values for apparent K_m and V_{max} were only possible for single substrates. Addition of competing fatty acid caused a

$$\frac{V1}{Eo} = \frac{Vmax(fa1)\ Fa1}{Fa1 + Km(fa1) + Km(fa1fa2)\ Fa2} \quad (1)$$

$$\frac{V2}{Eo} = \frac{Vmax(fa2)\ Fa2}{Fa2 + Km(fa2) + Km(fa2fa1)\ Fa1} \quad (2)$$

$$Vmax(fa1) = \frac{k3\ k4\ A}{k3 + k4\ A} \quad (3)$$

$$Vmax(fa2) = \frac{k7\ k8\ A}{k7 + k8\ A} \quad (4)$$

$$Km(fa1) = Ks1\frac{k4\ A}{(k3 + k4\ A)} \quad (5)$$

$$Km(fa2) = Ks2\frac{k8\ A}{(k7 + k8\ A)} \quad (6)$$

$$Km(fa1fa2) = \frac{Ks1\ k3}{Ks2\ k8}\frac{(k7 + k8\ A)}{(k3 + k4\ A)} \quad (7)$$

$$Km(fa2fa1) = \frac{Ks2\ k7}{Ks1\ k4}\frac{(k3 + k4\ A)}{(k7 + k8\ A)} \quad (8)$$

FIGURE 3. Rate equations describing the kinetic scheme in FIGURE 2. Initial reaction rates are denoted by V and active-site concentration by E_0. All other symbols as in FIGURE 2.
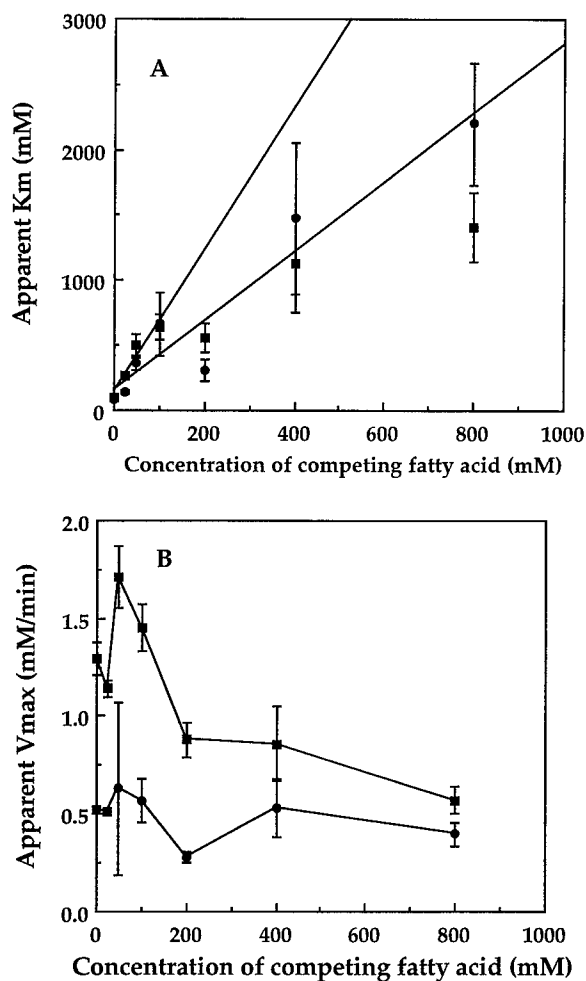
FIGURE 4. Effect of added competing fatty acid on apparent K_m and V_{max}: (■) decanoic acid; (●) dodecanoic acid. (A) Apparent K_m versus competing fatty acid concentration. Iteration start values for K_m (fa1), K_m (fa2), K_m (fa1fa2), and K_m (fa2fa1) were obtained from the slope and intercept of the linear regression curves. (B) V_{max} versus competing fatty acid concentration. Iteration start values for V_{max} (fa1) and V_{max} (fa2) were obtained from the y-axis intercept.

shift in the apparent K_m to substrate concentrations that were too high to be measured in this system. Nevertheless, by addition of competing fatty acid, individual rate constants were still obtainable.

The dissociation constants Ks1 and Ks2 were lower than those obtained for chymotrypsin[7] (TABLE 1). Lipases are adapted to work at interfaces and the hydrophobic environment of diisopropyl ether may offer binding conditions similar to those in emulsions.

The actual values of k3, k4, k7, and k8 will depend on the active-site concentra-

tion and must be treated with caution (TABLE 1). However, when considering the ratios of k3/k7 and k4/k8, all enzyme concentration effects cancel out, assuming the active-site concentration does not change by adding competing fatty acid. The constant ratio values for the acylation and deacylation step were 4.0 and 4.7, respectively, compared with a dissociation constant ratio close to 1. This indicates that the two related substrates bind to the lipase molecule with equal efficiency and
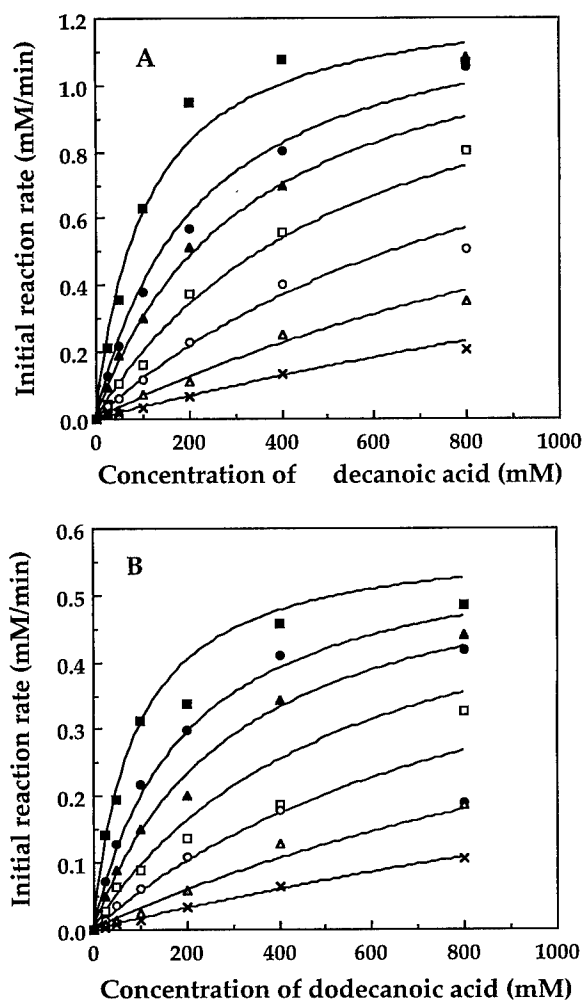
FIGURE 5. Simulation of fitted rate constants to the experimental data. (A) Initial reaction rate of decanoic acid. Added concentrations of dodecanoic acid were (■) 0 mM, (●) 25 mM, (▲) 50 mM, (□) 100 mM, (○) 200 mM, (△) 400 mM, and (×) 800 mM. Solid lines represent the best fit of the model. (B) Initial reaction rate of dodecanoic acid. Added concentrations of decanoic acid were (■) 0 mM, (●) 25 mM, (▲) 50 mM, (□) 100 mM, (○) 200 mM, (△) 400 mM, and (×) 800 mM. Solid lines represent the best fit of the model.

TABLE 1. Individual Kinetic Rate Constants for the Lipase-catalyzed Esterification of Decanoic Acid and Dodecanoic Acid with Decanol

	Decanoic Acid	Dodecanoic Acid	Ratio
Dissociation constant	552 mM	521 mM	1.1
Acylation constant	6.43 (min^{-1})	1.59 (min^{-1})	4.0
Deacylation constant	3.33 (min^{-1})	0.71 (min^{-1})	4.7

that the difference in reaction rates for these substrates is mainly governed by the acylation/deacylation of the acyl enzyme complex.

CONCLUSIONS

Lipase-catalyzed esterification of decanoic and dodecanoic acid with dodecanol in diisopropyl ether obeyed Michaelis-Menten kinetics reasonably well. Initial reaction rates were strongly dependent on the water activity in the reaction mixture, whereas the reaction rate ratio between decanoic acid and dodecanoic acid was not affected. By measuring the effect of added competing fatty acid, individual rate constants could be obtained. The dissociation constants are small compared with other enzymes in organic solvent. The rate constant ratios suggest that fatty acid selectivity is governed by conversion of enzyme-bound substrate rather than by the binding of substrate itself.

REFERENCES

1. MILLER, C., H. AUSTIN, L. POSORSKE & J. GONZIEZ. 1988. JAOCS **65:** 927–931.
2. WANG, C-S., A. KUKIS & F. MANGANARO. 1992. Studies on the substrate specificity of purified human milk lipoprotein lipase. Lipids **17:** 978.
3. BAILLARGEON, M. W., R. G. BRISTLINE & P. E. SONNET. 1989. Evaluation of strains of *Geotrichum candidum* for lipase production and fatty acid specificity. Appl. Microbiol. Biotechnol. **30:** 92–96.
4. RANGHEARD, S-M., G. LANGRAND, C. TRIANTAPHYLLIDES & J. BARATTI. 1989. Multicompetitive enzymatic reactions in organic media: a simple test for the determination of lipase fatty acid specificity. Biochim. Biophys. Acta **1004:** 20–28.
5. SVENSSON, I., E. WEHTJE, P. ADLERCREUTZ & B. MATTIASSON. 1994. Effects of water activity on reaction rates and equilibrium positions in enzymatic esterifications. Biotechnol. Bioeng. **44:** 549.
6. ZAKS, A. & A. M. KLIBANOV. 1985. Proc. Natl. Acad. Sci. U.S.A. **82:** 3192.
7. CHATTERJEE, S. & A. RUSSELL. 1992. Determination of equilibrium and individual rate constants for subtilisin-catalyzed transesterification in anhydrous environments. Biotechnol. Bioeng. **40:** 1069–1077.

The Effects of Cosolvent and Incubation Temperature on the Enantioselectivity of Aliphatic Ketone Reductions Catalyzed by Thermostable Secondary Alcohol Dehydrogenases

DANIEL L. GRAHAM, HELEN D. SIMPSON,
AND DONALD A. COWAN

Department of Biochemistry and Molecular Biology
University College London
London WC1E 6BT, England

INTRODUCTION

Alcohol NADP$^+$-dependent oxidoreductases (EC 1.1.1.2) (secondary alcohol dehydrogenases) are useful catalysts in the synthesis of novel chiral building blocks, particularly those that cannot be easily synthesized via chemical means. Secondary alcohol dehydrogenases (sec-ADHs) from the thermophilic glycolytic anaerobes such as *Thermoanaerobium* and *Thermoanaerobacterium* can reduce a broad range of aliphatic ketones to the corresponding secondary alcohols with excellent enantioselectivity.[1,2] The stereoselective reduction of diketones to diols has been demonstrated by a number of workers,[3–5] but the products are typically the homo-(S) isomers. Work performed within this laboratory and elsewhere has demonstrated that the addition of nonreactive cosolvents to thermostable sec-ADH-catalyzed transformations can have a marked effect on the stereoselectivity of the reaction and that this effect is temperature-dependent.[6,7] More recent studies have demonstrated that the addition of organic solvents provides a mechanism for controlling the enantioselectivity of such reactions.[8–10]

We have undertaken a study of the thermostable sec-ADH-catalyzed reduction of α- and β-diketones to chiral diols. The inherent stability of these enzymes has allowed us to apply a wide range of biotransformation temperature and solvent conditions. This, in addition to the use of diketone substituent groups, may provide us with a means of shifting the stereoselectivity of the reduction in favor of the desired diol product. This technology may then be applied to the biosynthesis of chiral intermediates or products with pharmaceutical importance.

EXPERIMENTAL METHODS

Growth of the Organism

Thermoanaerobacterium sp. Ket 4B1 was isolated from samples obtained from thermal areas in New Zealand. The organism was cultured anaerobically in 2-L bottles of complex glucose medium at 65 °C.[11]

Enzyme Purification

The sec-ADH from *Th.* sp. Ket 4B1 was purified according to the protocol previously described.[12]

Enzyme Assays

Alcohol dehydrogenase activity was routinely assayed between 40 and 70 °C in 20 mM glycine buffer, pH 7.8, containing 50 mM ketone and 0.25 mM NADPH. *Thermoanaerobium brockii* sec-ADH was obtained from Sigma Chemical (Poole, United Kingdom) as a purified, lyophilized powder containing 30–90 units of activity per mg protein. One unit of activity will oxidize 1 μmol of 2-propanol to acetone per min at pH 7.8 and at 40 °C in the presence of $NADP^+$.

TABLE 1. Percentage of Enzyme Activities of Two Thermostable sec-ADHs on a Series of Ketone Substrates at Different Incubation Temperatures[a]

Temperature (°C)	Butan-2-one	Pentan-2-one	Hexan-2-one	Heptan-2-one	Octan-2-one	Pentane-2,4-dione
Thermoanaerobium brockii sec-ADH						
40	40	36	31	9	8	37
50	43	52	46	20	16	42
60	68	75	57	25	24	20
70	100	106	82	44	30	0
Thermoanaerobacterium sp. Ket 4B1						
40	46	13	12	11	6	0
50	65	25	21	15	7	0
60	81	31	17	19	8	0
70	100	46	14	14	9	0

[a]The activities are quoted relative to the activity on butan-2-one at 70 °C.

Biotransformations

A range of biotransformations were performed using 10–30 units of enzyme, 10–50 mM ketone, and 0.5 mM NADPH with propan-2-ol as cosubstrate. The reaction mixtures were prepared in 20 mM glycine buffer, pH 7.8, and incubated at 40–60 °C for 24 h. Time-course samples (0.5 mL) were extracted with an equal volume of dichloromethane, which was dried with anhydrous magnesium sulfate prior to analysis by gas chromatography (GC).

ANALYTICAL METHODS

Spectrophotometric studies were performed at 340 nm on a Beckman DU7500. Chiral GC analysis was performed on a Shimadzu GC-14B using a derivatized cyclodextrin column (Lipodex-E 25 m × 0.25 mm, Camlab Limited) with helium as
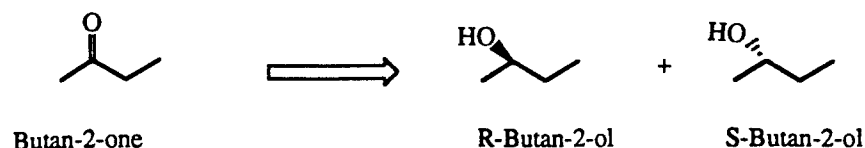
FIGURE 1. The sec-ADH-catalyzed reduction of butan-2-one.

the carrier gas and flame ionization detection. The samples were injected using a Shimadzu AOC17 autosampler and the chromatographic data were stored on a Shimadzu C-6RA integrator.

RESULTS

A comparison of the relative activities of *T. brockii* and *Th.* sp. Ket 4B1 sec-ADHs in the presence of a series of aliphatic ketones is shown in TABLE 1. The activity was measured via the drop in absorbance at 340 nm due to the oxidation of NADPH, over the temperature range of 40–70 °C, and the rates are quoted as a percentage relative to the optimal activity observed in the presence of butan-2-one at 70 °C. The data illustrate that the optimal activity of both enzymes for butan-2-one and pentan-2-one occurs at 70 °C or higher under the stated conditions. *T. brockii* sec-ADH seems to have broader substrate specificity for the ketone and diketone substrates studied. The gradual decrease in enzyme activity observed with increasing ketone alkyl chain length may be partly due to the decreasing aqueous solubility of the compounds. Similarly, the increase in activity observed with increasing temperature may be due in part to increased substrate solubility.

In a study of the reduction of butan-2-one by *Th.* sp. Ket 4B1 sec-ADH, the enantiomeric excess (ee) of the *R*-butan-2-ol product was found to vary according to the nature and quantity of cosolvent used in the biotransformation (see FIGURE 1 and TABLE 2). The %ee of the *R*-butan-2-ol was measured after 24-h incubation at 40 °C. The data show an increase in the %ee of the *R*-butan-2-ol product in the presence of a variety of cosolvents. In addition, a cosolvent concentration-dependent increase in enantioselectivity with all of the cosolvents used, with the exception of heptane, was observed.

TABLE 2. Enantiomeric Excess Figures (%) for the *R*-Butan-2-ol Product of *Thermoanaerobacterium* sp. Ket 4B1 sec-ADH Transformations with Butan-2-one in the Presence of Various Cosolvents at Different Concentrations[a]

[Solvent] % v/v	Acetonitrile	Methyl Propionate	Methanol	Dimethyl-formamide	Dimethyl Sulfoxide	Heptane
0	23	23	23	23	23	23
10	34	49	27	55	62	24
20	48	53	34	61	56	n.d.
40	65	64	49	n.d.	n.d.	n.d.

[a]n.d. indicates no alcohol detected due to high enzyme inhibition.
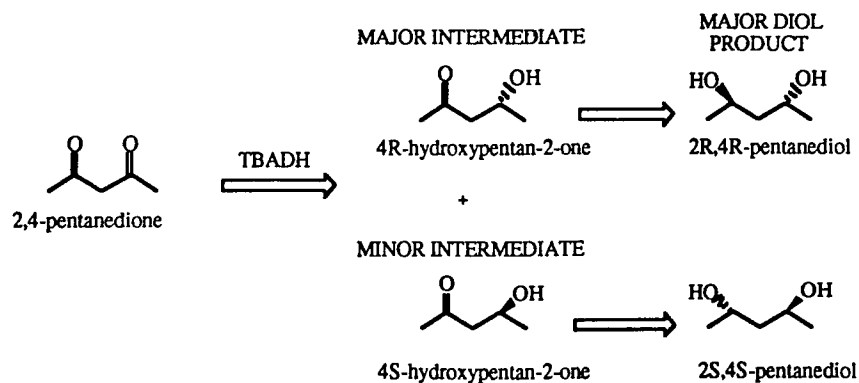
FIGURE 2. The proposed sec-ADH-catalyzed reduction of pentane-2,4-dione.

A similar effect was observed in experiments performed on the reduction of pentane-2,4-dione by *Thermoanaerobium brockii* sec-ADH. Biotransformations were performed at 40 °C and were sampled at 3 h and 24 h (FIGURE 2).

The %ee of the 4R-hydroxypentan-2-one intermediate (TABLE 3) was found to drop in the presence of cosolvent and a concentration-dependent decrease in enantioselectivity was observed. In the absence of cosolvent, the ee of this intermediate was found to be 83%; on the other hand, in the presence of 40% acetonitrile or ethanol, the ee was measured at 70%. Hence, the presence of 40% cosolvent had the effect of decreasing the yield of homo-(R)-diol. After 24-h incubation, the final yield of the homo-(R)-diol in the absence of cosolvent was 4%; in contrast, in the presence of 40% acetonitrile or ethanol, the final yield was 1.6%. The final yield of the homo-diol products will be further investigated in future experiments at lower substrate concentrations, which may proceed to complete conversion of the hydroxy-ketone (FIGURE 2).

The reduction of pentane-2,4-dione by *T. brockii* sec-ADH at different incubation temperatures indicated a temperature-dependent loss of enantioselectivity. Enzyme reactions were performed at 40, 50, and 60 °C in the absence of cosolvent (TABLE 4).

After 24 h at 40 °C, the ee of the 4R-hydroxypentan-2-one intermediate was 83%; on the other hand, at 60 °C, the ee was only 49–55%. This apparent decrease in

TABLE 3. Enantiomeric Excess Figures (%) for the 4R-Hydroxypentan-2-one Intermediate/Product of *Thermoanaerobium brockii* sec-ADH Transformations with Pentane-2,4-dione in the Presence of Various Cosolvents at Different Concentrations

[Solvent] % v/v	Acetonitrile		Toluene		Ethanol	
	3 h	24 h	3 h	24 h	3 h	24 h
0	83	83	83	84	83	83
10	80	78	81	82	78	77
20	77	76	78	78	76	75
40	70	70	76	75	71	70

selectivity toward the production of the R-hydroxyketone may be due to increased protein flexibility at the active site at elevated temperatures. Thus, incubation temperature may also be a crucial factor in the yield and enantiomeric purity of the homo-(R)-diol product.

DISCUSSION

Clearly, the nature of cosolvent, the cosolvent concentration, and the incubation temperature have an effect on the enantioselectivity observed in these biotransformations. In addition, the enzyme purity, the nature of the cosubstrate, the cosubstrate concentration, and the time of biotransformation may all affect enantioselectivity. *Thermoanaerobacterium* sp. Ket 4B1 has a growth temperature range of approximately 40–75 °C with an optimum at 65–70 °C. When the biotransformation of butan-2-one was carried out at 40 °C using whole cells of this organism, the ee of the resulting R-butan-2-ol product was only 5%, as opposed to 19% using a crude cell extract and 23% using the purified enzyme. The poor enantioselectivity of the whole cells may be due to the presence of other interfering enzyme activities, also present

TABLE 4. Enantiomeric Excess Figures (%) for the 4R-Hydroxypentan-2-one Intermediate/Product of *Thermoanaerobium brockii* sec-ADH Transformations with Pentane-2,4-dione at Different Incubation Temperatures

	%ee of 4R-Hydroxypentan-2-one in Biotransformation		
Temperature (°C)	1 h	3 h	24 h
40	83	83	83
50	81	77	63
60	74	66	49

to a lesser extent in the crude enzyme extract. Alternatively, the poor enantioselectivity may be a consequence of the reaction environment inside the cell, which may differ substantially from the *in vitro* system. The time of the biotransformation, whether whole cell or enzyme catalyzed, should not affect the overall enantioselectivity of the ketone reduction, but may affect the enantiomeric excess of the alcohol product as the reaction is reversible and the rates of R- and S-alcohol oxidation will be dependent on the reaction environment.

The effects of cosolvent and the cosolvent concentration are not clear. In general, solvents with lower log P values (and a higher dielectric constant), such as acetonitrile, seem to have a more significant influence on enantioselectivity, although in these experiments no clear correlation was observed. Solvents with high log P values, such as heptane, are only sparingly soluble in water and form a two-phase system when used as a cosolvent. Thus, the concentration of cosolvent at the protein active site becomes even more difficult to define. The effect of water-miscible solvents on enzyme structure has been investigated,[13] but as yet their effect on the enantioselectivity of a given reaction cannot be reliably predicted. The electron paramagnetic resonance spectrum of horse liver alcohol dehydrogenase indicated that the protein became more rigid as the dielectric constant of the solvent decreased. If a solvent has

the effect of making a protein more flexible, then it is likely to reduce enantioselectivity as the constraints placed on substrate structure at the active site are more relaxed.

Conversely, if the solvent has the effect of making the protein structure more rigid, then the interaction at the active site is likely to be more enantioselective. However, the situation is further complicated by the possible effects of the solvent on enzyme activity via specific interactions, in addition to its effect on protein conformation. In aqueous/organic mixtures and two-phase systems, there will come a point where the organic solvent concentration becomes deleterious toward enzyme activity as gross conformational changes bring about the denaturation of the protein. A simpler system for studying the role of solvent in enzyme enantioselectivity would be one in which an enzyme preparation was dried and subsequently resuspended in an anhydrous solvent, thus effectively eliminating the role of water concentration. Work in this area has already indicated that the activity of enzymes in such systems depends not only on the solvent in which the enzyme is resuspended, but also on the way in which the enzyme is dried and on stabilizing agents present during the drying process.[14] This preliminary study has indicated that the presence of a cosolvent may affect the enantioselectivity of aliphatic ketone reduction by thermostable sec-ADHs and that increasing the cosolvent concentration increases the effect. Consequently, the study of the activity of these enzymes in anhydrous organic solvent systems may reveal far more significant changes in enantioselectivity.

The effect of incubation temperature on the enantioselectivity of these enzymes may be explained via the changes in the flexibility of the protein. As the temperature is increased, the protein structure becomes more flexible and a reduction in enantioselectivity may be observed. However, thermostable enzymes are naturally more rigid at normal "mesophile" temperatures. Thus, the temperature at which the conformational state of the enzyme gives rise to maximal enantioselectivity may be elevated. In this case, there is an observed increase in enantioselectivity with increasing temperature. The enantioselectivity of *Thermoanaerobacterium* sp. Ket 4B1 sec-ADH was found to be temperature-dependent, as has been previously reported for *Thermoanaerobacter ethanolicus*[15] and *Thermoanaerobium brockii*.[16] The mechanistic basis of this dependence has been studied for the reverse reaction of *R*- and *S*-butan-2-ol to butan-2-one[12] and the enantioselectivity was found to depend on the enthalpy of activation and on the entropic state of each isomer. Thus, the effect of temperature on enantioselectivity depends on both the enzyme and substrate, for which there will be a racemic temperature and an optimal temperature under a given set of biotransformation conditions.

REFERENCES

1. KELLY, D. R. & J. D. LEWIS. 1991. J. Chem. Soc. Chem. Commun. **19:** 1330–1332.
2. SIMPSON, H. D. & D. A. COWAN. 1993. Ann. N.Y. Acad. Sci. **672:** 145–151.
3. FUGISAWA, Y. *et al.* 1987. Chem. Lett., p. 2227.
4. TAKESHITA, A. *et al.* 1989. Chem. Pharm. Bull., p. 1085.
5. VESCHAMBRE, R. *et al.* 1992. Biocatalysis **6:** 19.
6. PLANT, A. L. & D. A. COWAN. 1991. Abstr. Pap. Am. Chem. Soc. **201:** 99.
7. SIMPSON, H. D. & D. A. COWAN. 1995. Biocatalysis. Submitted.
8. SAKURAI, T., A. L. MARGOLIN, A. J. RUSSELL & A. M. KLIBANOV. 1988. J. Am. Chem. Soc. **110:** 7236–7237.

  9. TAWAKI, S. & A. M. KLIBANOV. 1992. J. Am. Chem. Soc. **114:** 1882–1884.
 10. CARREA, G., G. OTTOLINA & S. RIVA. 1995. Trends Biotechnol. **13:** 63–70.
 11. ZEIKUS, Z. G., P. W. HEGGE & M. A. ANDERSON. 1979. Arch. Microbiol. **122:** 41–48.
 12. SIMPSON, H. D. & D. A. COWAN. 1995. Protein Pept. Lett. **1:** 207–214.
 13. GUINN, R. M., P. S. SKERKER, P. KAVANAUGH & D. S. CLARK. 1991. Biotechnol. Bioeng.
          37: 303–308.
 14. PHAM, V. T., R. S. PHILLIPS & L. G. LJUNGDAHL. 1989. J. Am. Chem. Soc. **111:** 1935–1936.
 15. KEINAN, E., E. K. HAFELI, K. K. SETH & R. LAMED. 1986. J. Am. Chem. Soc. **108:** 162–169.
 16. PHAM, V. T. & R. S. PHILLIPS. 1990. J. Am. Chem. Soc. **112:** 3629–3632.

Control of Ionization State and Activity of Enzymes in Organic Media[a]

PETER J. HALLING, ANNE D. BLACKWOOD,
AND BARRY D. MOORE

*Departments of Bioscience and Biotechnology
and Pure and Applied Chemistry
University of Strathclyde
Glasgow G1 1XW, United Kingdom*

The activity, specificity, and stability of enzymes depend on the protonation of their ionizable groups. The initial protonation state of a low-water enzyme is set by the composition (especially pH) of the aqueous solution from which it is dried. Hence, this composition can affect subsequent biocatalyst behavior: the well-known "pH memory", first demonstrated by Zaks and Klibanov,[1] and recently explored in more detail by Yang *et al.*[2] An example of this phenomenon can be seen in FIGURE 1, with the activity of an immobilized subtilisin suspended in pentanone dependent on the pH of the last aqueous wash before drying.[3]

However, the ionization state of low-water enzymes can be altered subsequently by exposure to acidic or basic species. For example, these might be reactants or products, dissolved in a bulk organic phase. Such effects are less common than in aqueous media because uncharged acids and bases are effectively weaker, but can occur even with CH_3COOH.[4] The result may be inferior performance of the biocatalyst.

CONTROLLING THE IONIZATION STATE WITH "ORGANIC PHASE BUFFERS"

A mixture of a hydrophobic acid or base and its salt may be added deliberately as an "organic phase buffer".[3] Ideally, both the neutral and ion-pair form of the buffer should be sufficiently organic-soluble that they have no tendency to partition into an aqueous or polar phase. Such buffers are able to make an enzyme completely "forget" the previous aqueous pH (FIGURE 1, □ points). The ratio of the two forms controls ionization, as in aqueous media. By varying this ratio, we can also see a "pH profile" for activity of a low-water enzyme, with little effect of previous aqueous pH (FIGURE 2).

THE KEY ROLE OF COUNTERIONS

Unlike aqueous systems, the exchange of counterions must now be considered explicitly. FIGURE 3 shows the type of equilibria involved when an organic phase

251
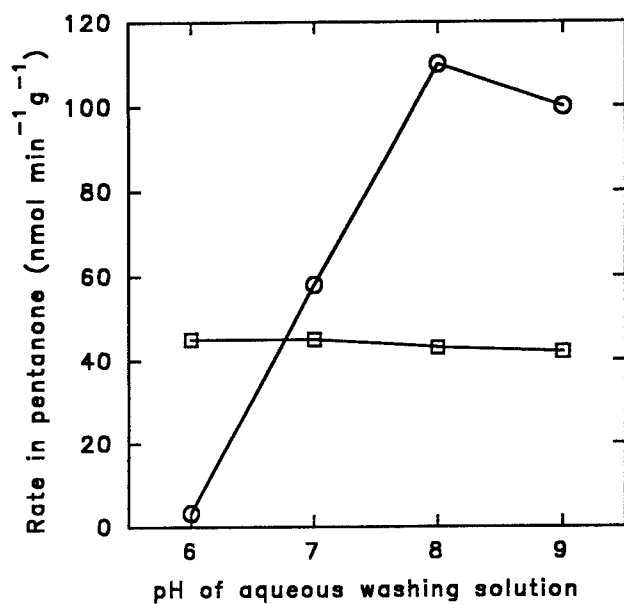
FIGURE 1. Effect of previous aqueous pH on subtilisin activity with and without organic phase buffers. Before drying, the immobilized enzyme was adjusted to the pH shown. Its activity in pentanone was then determined, with (□) or without (○) addition of 5 mM each of triphenylacetic acid and its Na+ salt.[3]
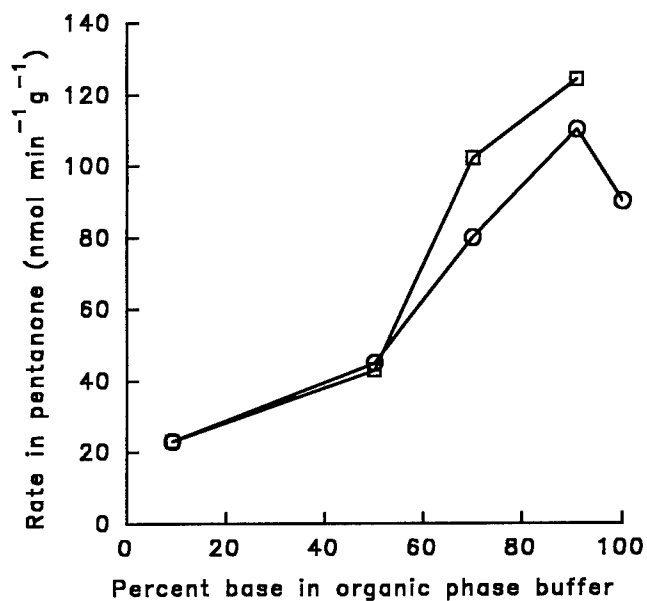
FIGURE 2. Effect of organic phase buffer ratio on subtilisin activity. Before drying, the immobilized enzyme was adjusted to pH 6 (○) or pH 8 (□). Triphenylacetic acid was the buffer in pentanone, with the percentage of Na+ salt shown.[3]
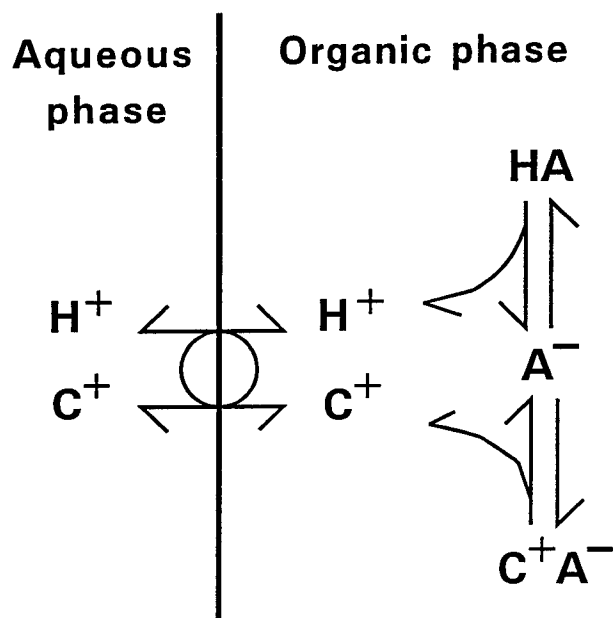
FIGURE 3. Equilibria involved in the equilibration of an organic phase buffer with an aqueous (or other polar) phase. This scheme is drawn for a buffer based on a neutral acid. An analogous scheme for a basic buffer would involve anions moving with the H^+.

buffer controls the pH of an aqueous phase or the ionization of a protein. TABLE 1 shows how the ratio of the organic phase buffer species controls the pH of an aqueous salt solution, at fixed counterion concentration.

Counterions to protein charges must also be considered. Electrical neutrality requires that counterions be provided whenever protein ionization is changed. In dilute aqueous solution, protonation is well described by pH alone. The nature and concentration of the counterions have little effect because they are far away. In low dielectric media, however, the counterions will tend to associate more closely with

TABLE 1. Control of Aqueous Phase pH by the Buffer Ratio in Equilibrated Organic Phase[a]

Organic Phase $[R_3N]/[R_3NH^+Cl^-]$	pH of Equilibrated Aqueous NaCl
0.053	3.03
0.2	3.54
1.0	4.44
5.0	5.35
19	5.83

[a]Tri-*iso*-octylamine and its hydrochloride (20 mM total) in pentanone were equilibrated with 0.1 M NaCl. The results are all reasonably consistent with a midpoint (pH + pCl) value of 6.5.[3]

the protein. Thus, protonation is affected by the availability of counterions, as well as of H^+. It is better to consider equilibria that explicitly include counterions (TABLE 2).

There are two different classes of equilibria, for acidic and basic groups. In each case, the ratio of buffer species controls a characteristic parameter, which in turn sets

TABLE 2. Protein and Buffer Ionization Equilibria and the Parameters Characterizing Them

Instead of simple protonation of protein groups like -NH$_2$ and -COO$^-$, we should consider two classes of equilibria, represented by:

1.

$$\text{Protein-NH}_2 + H^+ + Cl^- ==== \text{Protein-NH}_3^+\ Cl^-$$
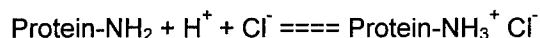
which can be controlled by a base buffer in the organic phase:

$$B\ \text{(organic phase)} + H^+ + Cl^- ==== BH^+\ Cl^-\ \text{(organic)}$$

2.

$$\text{Protein-COO}^-\ Na^+ + H^+ ==== \text{Protein-COOH} + Na^+$$
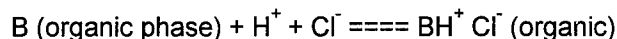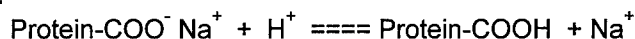
which can be controlled by acidic organic phase buffer:

$$A^-\ Na^+\ \text{(organic phase)} + H^+ ==== AH\ \text{(organic)} + Na^+$$
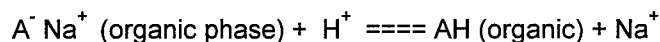
Parameters Characterizing These Equilibria

Equilibrium type (as above)	1	2
Thermodynamic activities	$a_{H^+} \cdot a_{Cl^-}$	a_{H^+}/a_{Na^+}
More familiar (?)[a]	(pH + pCl)	(pH − pNa)
Measure of:	availability of H^+ plus Cl^-	potential for exchange of H^+ for Na^+

[a]Note that the difference, (pH + pCl) − (pH − pNa) = (pCl + pNa), cannot be smaller than the solubility of NaCl.

the ionization state of the protein groups. This parameter may be viewed as a combination of thermodynamic activities or as a combination including pH (perhaps more familiar). However, each combination must be seen as a single parameter that cannot be separated into two terms. Although unfamiliar, these parameters are in

Aqueous pre-treatment

	pH 3	**pH 10**
Initial state	COOH −NH$_3^+$Cl$^-$ −COOH NH$_3^+$Cl$^-$	COO$^-$Na$^+$ −NH$_2$ −COO$^-$Na$^+$ NH$_3^+$Cl$^-$
Na-TPA buffer	COO$^-$Na$^+$ −NH$_3^+$Cl$^-$ −COO$^-$Na$^+$ NH$_3^+$Cl$^-$	COOH −NH$_2$ −COOH NH$_3^+$Cl$^-$
DBU-HCl buffer	COOH −NH$_2$ −COOH NH$_2$	COO$^-$Na$^+$ −NH$_3^+$Cl$^-$ −COO$^-$Na$^+$ NH$_3^+$Cl$^-$
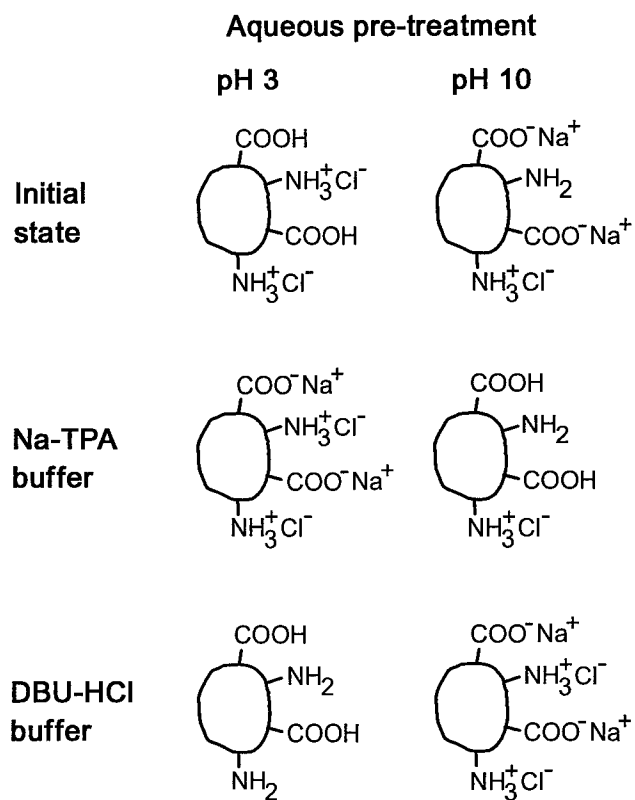
FIGURE 4. Diagrammatic representation of protein ionization states with different pretreatments and organic phase buffers.
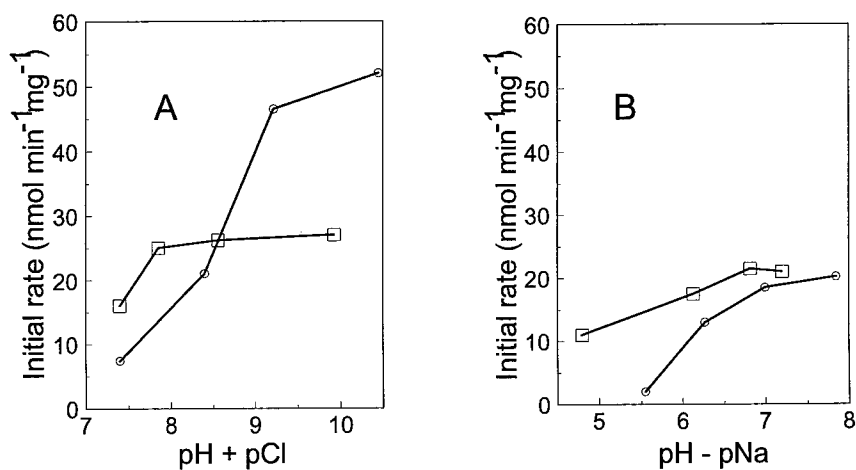
FIGURE 5. Activity of subtilisin pretreated to give different ionization states. Immobilized enzyme was prewashed at aqueous pH 3 (O) or pH 10 (□). After drying, its activity in pentanone was determined, using either (A) DBU/HCl to fix (pH + pCl) or (B) Na$^+$/TPA to fix (pH − pNa).[4]

one way simpler than pH. The definition of pH raises the issue of the thermodynamic activities of single ions, which cannot be measured without untestable assumptions.

TWO PARAMETERS THAT CAN BE MANIPULATED INDEPENDENTLY

The two parameters (pH + pCl) and (pH − pNa) can be manipulated independently and have different effects on the enzyme. FIGURE 4 shows how a combination of pretreatment and buffer selection can achieve this. FIGURE 5 shows the resulting catalytic activity of subtilisin under low-water conditions.[5] A form of the enzyme with particularly high activity is produced at high (pH + pCl) and low (pH − pNa). This form probably has coexisting free -NH$_2$ and -COOH groups. Such a form cannot be prepared in aqueous media because these groups would immediately exchange protons. This can be prevented under low-water conditions (for well-separated groups) by denying the counterions needed to allow charge separation in a low dielectric medium.

Full exploitation of this theoretical picture, and the related effects on the enzyme, requires a set of buffers and indicators comparable to those available for aqueous media. Our current work is aiming to make progress in this direction.

REFERENCES

1. ZAKS, A. & A. M. KLIBANOV. 1985. Proc. Natl. Acad. Sci. U.S.A. **82:** 3192–3196.
2. YANG, Z., D. ZACHERL & A. J. RUSSELL. 1993. J. Am. Chem. Soc. **115:** 12251–12257.
3. BLACKWOOD, A. D., L. J. CURRAN, B. D. MOORE & P. J. HALLING. 1994. Biochim. Biophys. Acta **1206:** 161–165.
4. VALIVETY, R. H., J. L. L. RAKELS, R. M. BLANCO, G. A. JOHNSTON, L. BROWN, C. J. SUCKLING & P. J. HALLING. 1990. Biotechnol. Lett. **12:** 475–480.
5. BLACKWOOD, A. D. 1995. Counter-ion and protein ionisation effects on the activity of subtilisin Carlsberg in organic media. Ph.D. thesis. University of Strathclyde, Glasgow, United Kingdom.

Substrate Specificity and Kinetics of
Candida rugosa Lipase in Organic Media[a]

ANJA E. M. JANSSEN,[b,c] ATUL M. VAIDYA,[d]
AND PETER J. HALLING[c]

[c]*Department of Bioscience and Biotechnology*
[d]*Department of Chemical Engineering*
University of Strathclyde
Glasgow G1 1XW, United Kingdom

INTRODUCTION

Substrate specificity of lipases in organic solvents is often based on measurements of the specificity constant, V_m/K_M, or an apparent K_M value. However, the apparent kinetic parameters can be very different from the true values, as was shown for a subtilisin-catalyzed transesterification.[1] For this reason, we have studied the fatty acid specificity of *Candida rugosa* lipase based on full kinetic measurements.

For comparison of the kinetic parameters in organic media, corrections for substrate solvation should be made. This can be done by using a transfer free-energy method,[2-4] by using activities instead of concentrations,[5] or by using partition coefficients.[6,7] These methods lead to corrected parameters that essentially are the same. However, this is only valid if the activity coefficients are constant values in the measured concentration range. For the determination of the kinetic parameters of reactions in organic solvents, high concentrations are often necessary to saturate the enzyme, and activity coefficients are no longer constant in the measured concentration range. In this case, it might be expected that the kinetic model would fit better in terms of substrate activity rather than substrate concentration.

EXPERIMENTAL METHODS

Candida rugosa lipase is immobilized by adsorption on Accurel EP100 macroporous polypropylene (loading 0.1 g crude lipase/g support). The organic phase, containing sulcatol [(±)6-methyl-5-hepten-2-ol], fatty acid, and toluene, and the immobilized lipase were preequilibrated to $a_w = 0.76$ using a saturated NaCl solution. The reaction mixture was shaken at 170 min^{-1} at 22 °C. Samples were analyzed by GLC measurements.

Usually eight data points were collected and the initial reaction rate was determined by linear regression. Twenty-four initial rate values were measured and

257

fitted according to the ping-pong model with competitive inhibition by the alcohol:

$$v = \frac{V_m}{1 + \dfrac{K_A}{[A]}\left(1 + \dfrac{[B]}{K_{IB}}\right) + \dfrac{K_B}{[B]}} \tag{1}$$

where v is the initial reaction rate, V_m is the maximum reaction rate, K_A and K_B are the ping-pong constants for the fatty acid (A) and alcohol (B), and K_{IB} is the inhibition constant of the alcohol.

For correction for solvation of the substrates, activity coefficients are required. We have used the UNIFAC group contribution method[8] to estimate the activity coefficients of the components in the reaction mixture.

RESULTS AND DISCUSSION

In order to determine the true kinetic constants, we have varied the fatty acid as well as the sulcatol concentrations in the initial rate measurements. An example of the experimental data is shown in FIGURE 1. We have used a ping-pong kinetic model with competitive alcohol inhibition to fit our data and we have obtained values for K_A, K_B, K_{IB}, and V_m.[9] In this paper, we only show the data of K_A and V_m/K_A (FIGURE 2). In FIGURE 2a, the increase in K_A with fatty acid chain length is obvious. This means that the binding of the short-chain fatty acids in toluene is much better than for the long-chain fatty acids. The absolute value of K_A for the long-chain fatty acids is uncertain because the initial rates were measured at concentrations far below
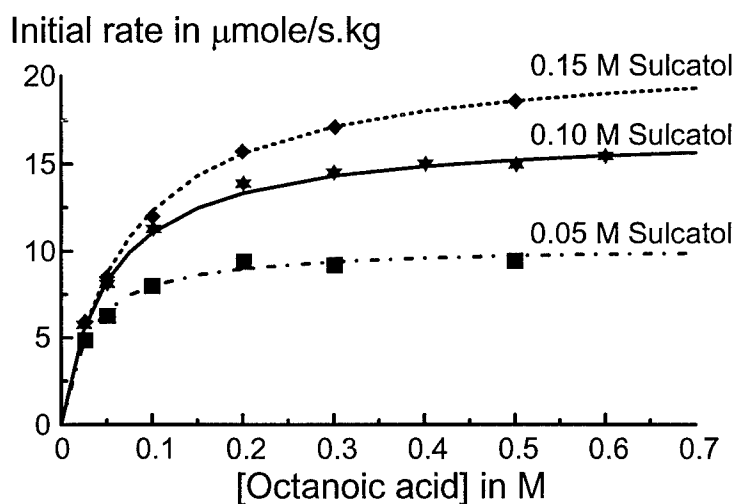
FIGURE 1. The initial reaction rates as functions of the octanoic acid concentration for the *Candida rugosa* lipase–catalyzed esterification in toluene at $a_w = 0.76$. The experimental data (symbols) are fitted to a ping-pong kinetic model with competitive alcohol inhibition. The reaction rates are expressed in μmol ester formed per s per kg immobilized enzyme.
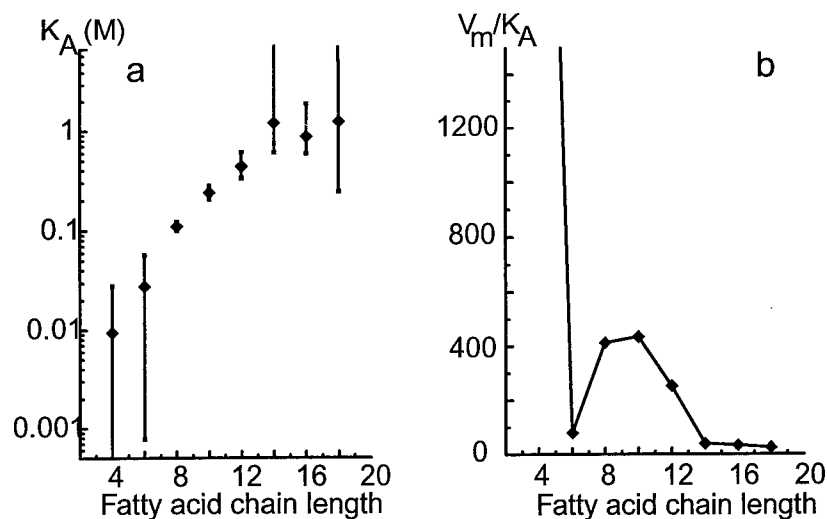
FIGURE 2. The ping-pong constant K_A (a) and the specificity constant V_m/K_A (b) as a function of the fatty acid chain length. The error bars represent 95% confidence intervals.

saturation conditions. In these cases, it is only possible to make good estimations of the specificity constant, V_m/K_A. The specificity constant, V_m/K_A (FIGURE 2b), shows a preference for C4, C8, C10, and C12 fatty acids. The low specificity for hexanoic acid is caused by the low value of V_m, indicating a slow conversion of the acyl-enzyme–alcohol complex to an ester-enzyme complex or a slow removal of the hexanoic acid ester rather than a poor binding of hexanoic acid.

For correction for solvation of the substrates, activity coefficients are required. We have used the UNIFAC group contribution method to estimate the activity coefficients of the components in the reaction mixture. The activity coefficients of the fatty acids are shown in FIGURE 3 for several substrate concentrations. The fatty acid activity coefficient decreases with increasing fatty acid concentration, as well as with increasing sulcatol concentration. This implies an improvement in fatty acid solvation by the fatty acid itself and by the sulcatol. Furthermore, the fatty acid activity coefficient decreases with chain length, which means that the long-chain fatty acids are better solvated than the short-chain fatty acids (if the pure liquid is chosen as the standard state). FIGURE 3 shows that the activity coefficients are not constant in the concentration range that we have measured. Therefore, we have used substrate activities, based on the pure liquid standard state, to fit to the kinetic model (equation 1). We have found that the sum of the squared residuals did not decrease by fitting activities rather than concentrations. In some cases, there was even a slight increase in the sum of squares. This could be due to inaccuracies in the estimation of the activity coefficients. Deviations in the UNIFAC calculations up to a factor of two have been reported before.[5] However, although UNIFAC activity coefficients may be wrong, the direction of deviation from ideality must be right (i.e., activity coefficients

Fatty acid activity coefficient

Fatty acid activity coefficient
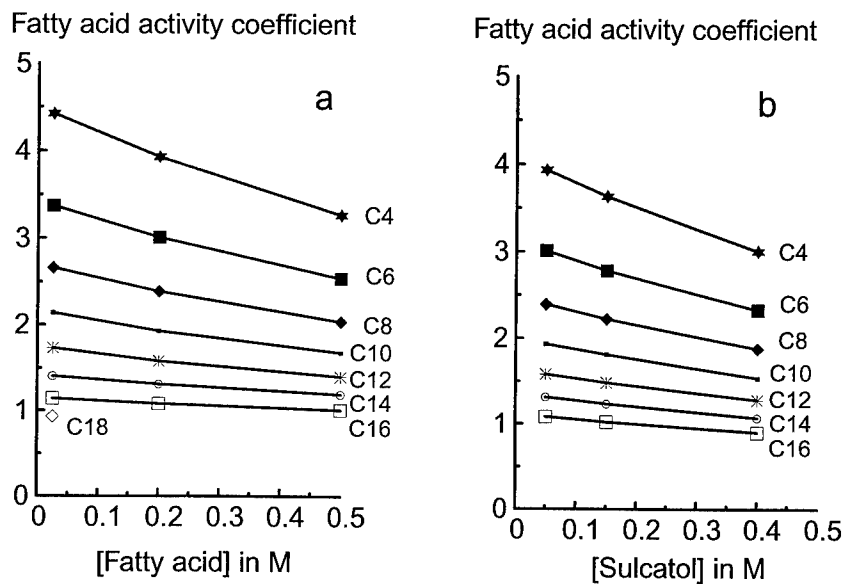
FIGURE 3. The fatty acid activity coefficients at various fatty acid and sulcatol concentrations. In part a, the sulcatol concentration is 0.05 M; in part b, the fatty acid concentration is 0.2 M. Activity coefficients are calculated with the UNIFAC group contribution method.
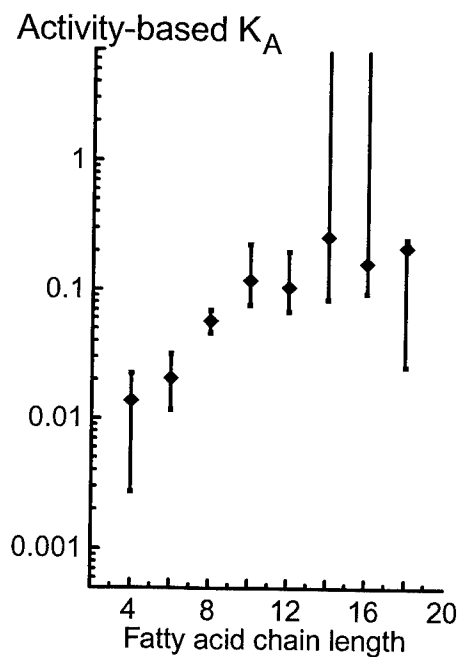
FIGURE 4. The activity-based ping-pong constant K_A as a function of the fatty acid chain length. The error bars represent 95% confidence intervals.

go down with increasing concentrations). The results suggest that enzyme kinetics may be better described by concentration than by activity.

The activity-based ping-pong constant, $K_A{}^{act}$, is shown in FIGURE 4. The increase in the activity-based $K_A{}^{act}$ with chain length is less than for the concentration-based K_A. If we had chosen to express the activity by using the gas phase or a dilute aqueous phase as a standard state, the $K_A{}^{act}$ would have decreased on increasing the fatty acid chain length. It was shown before that, when two or more substrates are compared, the "corrected specificity" becomes a function of the standard state.[4]

CONCLUSIONS

The esterification of saturated fatty acids and sulcatol in toluene, catalyzed by *Candida rugosa* lipase, has been studied and the true kinetic parameters were obtained by fitting the experimental data to a ping-pong kinetic model that includes alcohol inhibition. The binding of the fatty acid decreases with increasing fatty acid chain length and the lipase has a preference for C4, C8, C10, and C12 fatty acids. Corrections for solvation are made by using activities instead of concentrations to fit the kinetic parameters. This approach was used before for the comparison of kinetic parameters in different solvents. The activity coefficients in our experiments vary by over 25%; however, their use did not improve the fit of the data. This suggests that enzyme kinetics may be better described by concentration than by activity. This contrasts with what has been found in comparisons of different solvents, where the differences in activity coefficients are much larger.

REFERENCES

1. CHATTERJEE, S. & A. J. RUSSELL. 1992. Biotechnol. Bioeng. **40:** 1069–1077.
2. DORDICK, J. S. 1992. Biotechnol. Prog. **8:** 259–267.
3. WESCOTT, C. R. & A. M. KLIBANOV. 1993. J. Am. Chem. Soc. **115:** 1629–1631.
4. JANSSEN, A. E. M. & P. J. HALLING. 1994. J. Am. Chem. Soc. **116:** 9827–9830.
5. VAN TOL, J. B. A., R. M. M. STEVENS, W. J. VELDHUIZEN, J. A. JONGEJAN & J. A. DUINE. 1995. Biotechnol. Bioeng. **47:** 71–81.
6. HALLING, P. J. 1994. Enzyme Microb. Technol. **16:** 178–206.
7. REIMANN, A., D. A. ROBB & P. J. HALLING. 1994. Biotechnol. Bioeng. **43:** 1081–1086.
8. HANSEN, H. K., P. RASMUSSEN, A. FREDENSLUND, M. SCHILLER & J. GMEHLING. 1991. Ind. Eng. Chem. Res. **30:** 2355–2358.
9. JANSSEN, A. E. M., A. M. VAIDYA & P. J. HALLING. 1996. Enzyme Microb. Technol. **18:** 340–346.

Temperature Effects
on Protease-catalyzed Peptide
Synthesis in Organic Media

ÅSA JÖNSSON, ERNST WEHTJE,
PATRICK ADLERCREUTZ, AND BO MATTIASSON

Department of Biotechnology
Chemical Center
Lund University
S-221 00 Lund, Sweden

INTRODUCTION

The study of enzymatic reactions in organic media is a rapidly expanding research area.[1,2] One advantage of using organic solvent compared to water in protease-catalyzed peptide synthesis is that undesired hydrolytic side reactions can be suppressed and, consequently, higher peptide yields are obtained. Another way to increase the peptide yields is to decrease the reaction temperature. In the literature, there are a few reports of high peptide yields in organic media at low temperature.[3,4]

This study focuses on the effect of the reaction temperature on α-chymotrypsin-catalyzed dipeptide synthesis in both water-miscible and water-immiscible organic solvents. The effect of parameters such as the nature of the nucleophile, the organic solvent, water concentration, and water activity was studied. The influence of the reaction temperature is presented as the p value and the maximal peptide yields, that is, the yield obtained when all ester substrate is consumed.

EXPERIMENTAL METHODS

α-Chymotrypsin (EC 3.4.21.1) was immobilized on celite as previously described.[5] Immobilized enzyme and substrate solution were incubated separately overnight at the actual reaction temperature. The substrate solution contained organic solvent with a controlled amount of water, ester substrate, nucleophile (amino acid amides), and 1% of triethylamine (except when Leu-NH$_2$ was used as the nucleophile). The reaction was carried out in 4-mL stoppered glass bottles, which were placed in a cryostat at low temperatures (on a head-over-head incubator) and in a water bath with reciprocal shaking at high temperatures. Samples were taken at intervals and analyzed by HPLC.

The constant p describes the competition between the nucleophile and water for the acyl-enzyme.[6] The constant is defined as the nucleophile concentration at which the aminolysis and the hydrolysis rates are the same. The p value was determined as previously described.[5]

Water content in the organic phase was determined by Karl Fisher titration using a Metrohm KF coulometer.

RESULTS AND DISCUSSION

Temperature Effect on Peptide Yield

In peptide synthesis, it is of great importance to obtain high peptide yields, especially in the multistep synthesis of long peptides. When lowering the reaction temperature, the maximal peptide yield can be improved. The maximal yield was measured in four water-miscible organic solvents containing 10% of water (FIGURE 1). In all four solvents, the maximal peptide yield increased with decreasing temperature. The effect of the temperature was more pronounced in acetonitrile and tetrahydrofuran than in acetone and diglyme [bis-(2-methoxyethyl) ether]. The freezing point of the reaction medium is
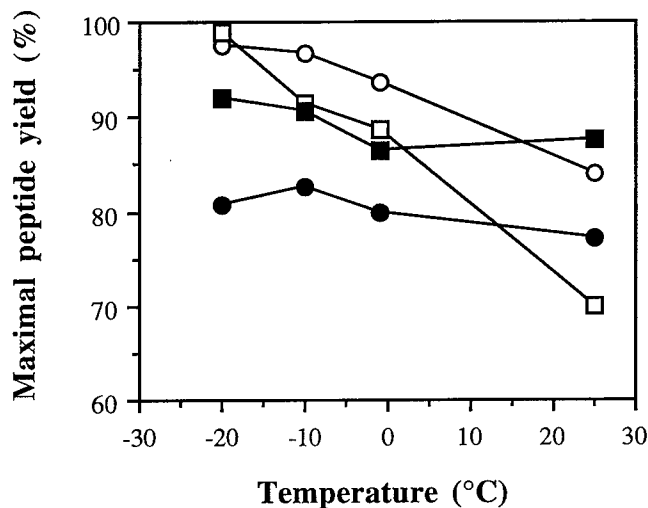
FIGURE 1. Effect of temperature on maximal peptide yield in different water-miscible solvents. The reaction mixture contained 20 mM Ac-PheOEt, 30 mM Ala-NH$_2$, 30 mM triethylamine, and 50 mg of immobilized chymotrypsin, and the water addition was 10%. Four solvents were studied: (O) acetonitrile, (●) acetone, (□) tetrahydrofuran, and (■) diglyme.

low, but in acetonitrile and tetrahydrofuran the ice formation started at −20 °C. In acetone and diglyme, no ice formation occurred at these temperatures.

The peptide yields were also studied for 11 different amino acid amides as nucleophiles and the maximal yields were obtained at two different temperatures, 25 °C and −10 °C (FIGURE 2). The reaction medium used was acetonitrile with a water content of 10%. All peptide yields were high for the nucleophiles tested, meaning that the substrate specificity for α-chymotrypsin is rather broad. Highest yields were obtained for the less hydrophobic nucleophiles, arginine amide and lysine amide. When decreasing the temperature to −10 °C, the general behavior was that the maximal peptide yield increased. For the best nucleophile, arginine amide, the increase was from 86% to 97%; for the least efficient one, D-alanine amide, the increase was from 33% to 50%.
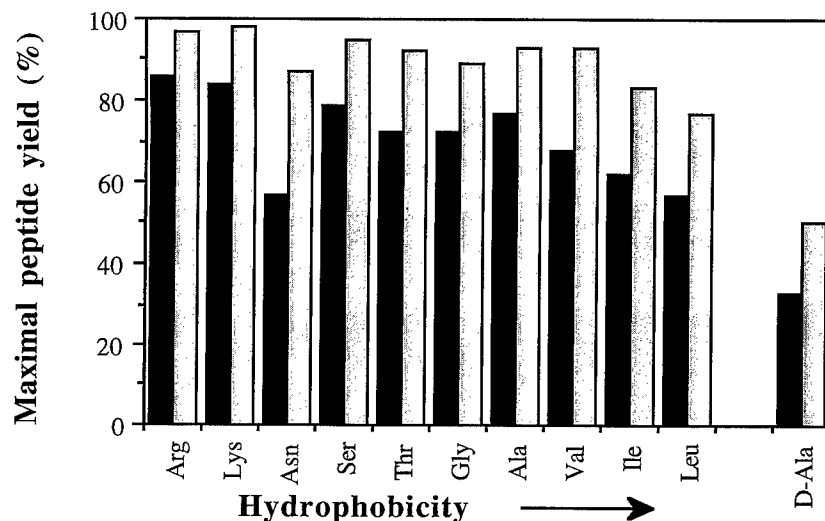
FIGURE 2. Effect of temperature on maximal peptide yield for different nucleophiles. The concentrations of substrates in acetonitrile with 10% water was 10 mM for Ac-PheOEt and 15 mM for the nucleophiles. The reaction was studied at 25 °C (black bars) and −10 °C (gray bars).

It is thus clear that the maximal peptide yield can be improved by lowering the reaction temperature. This effect seems to be general for different water-miscible solvents and for different nucleophiles. The synthetic activity of the enzyme at 25 °C was high for all nucleophiles tested. When changing the temperature from 25 to −10 °C, the activity was decreased by a factor of about seven (data not shown).

Temperature Effect on p Value

The influence of the temperature was determined as the p value, which is a measure of the efficiency of the nucleophile. The p value was determined in four water-miscible solvents containing 10% of water (FIGURE 3). The general tendency was as follows: when decreasing the reaction temperature, the p value decreased. This means that, at higher temperatures, a higher nucleophile concentration must be used to obtain the same product ratio as at lower temperatures. Thus, with a fixed nucleophile concentration, a higher peptide yield can be obtained at lower temperatures. This variation of the p value with the temperature results in the increasing peptide yields in FIGURES 1 and 2. The efficiency of the nucleophile compared to water became better in all four solvents, but it was more pronounced in acetonitrile and tetrahydrofuran.

Effect of Water Concentration / Water Activity on p Value

The amount of water dissolved in the organic solvent is an important parameter in enzyme-catalyzed reactions. The p value is affected by the water concentration in

the organic solvent. This effect was studied in one water-miscible and one water-immiscible solvent. In diglyme, the p value increases with increasing water concentration (FIGURE 4). These results in diglyme are what could be expected because water participates in the hydrolysis reaction. This trend was the same for all temperatures studied, but at lower temperatures the influence of the water concentration was less pronounced. In ethyl acetate, the effect of water concentration on the p value behaves in a more complex way (FIGURE 5). At high temperatures, 25 and 35 °C, the p value increases with increasing water concentration. When lowering the temperature, the p value shows an optimum at 1.75% for 5 °C and at 1.25% for −10 °C. The water content seems to affect the different steps in the reaction and the influence on the p value was not as expected. This has been shown for different substrates in water-immiscible solvent at fixed temperature in a previous report.[2] For both solvents, the p value is greatly influenced by the reaction temperature at high water concentrations and the effect decreases at low concentrations.

A better way to compare different water concentrations in organic solvents is to measure at controlled thermodynamic water activity.[6] The water activity is influenced by the water concentration in the medium and by the temperature. To pinpoint the effect of the temperature on the p value, the solvent (5-methyl-2-hexanone) was saturated with water (water activity = 1) at the actual reaction temperature. The water content in the reaction medium was measured and the p value was determined (FIGURE 6). The solubility of water decreased with decreasing temperature and the p value also decreased when the temperature was lowered. This means that the effect of decreasing p value with decreasing temperature is not due to the change in water activity with the temperature.
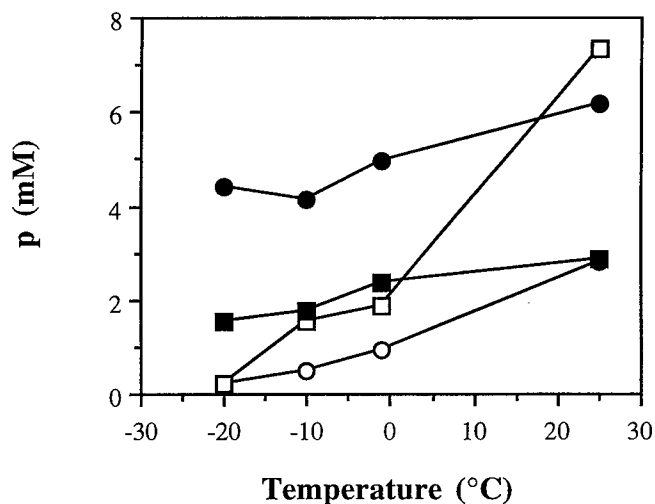
FIGURE 3. Effect of temperature on the p value in different water-miscible solvents. Reaction conditions as in FIGURE 1. Four solvents were studied: (O) acetonitrile, (●) acetone, (□) tetrahydrofuran, and (■) diglyme.
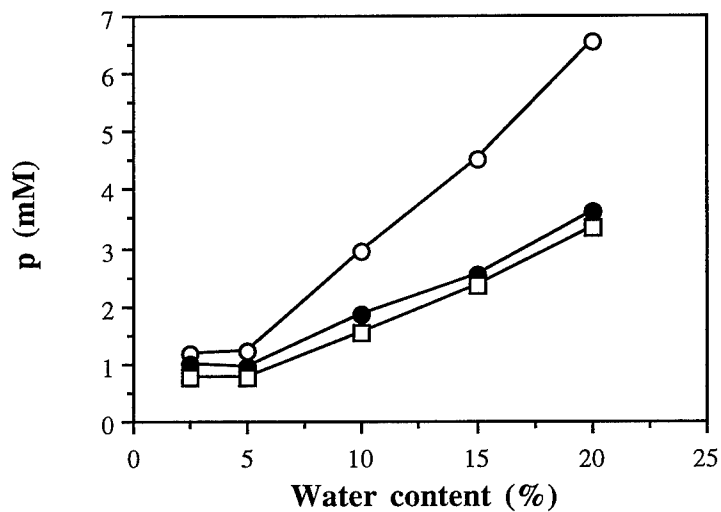
FIGURE 4. Effect of water content on the p value in water-miscible solvent. Diglyme was used as solvent and the reaction conditions used were as in FIGURE 1. Three temperatures were studied: (O) 25 °C, (●) −10 °C, and (□) −20 °C.
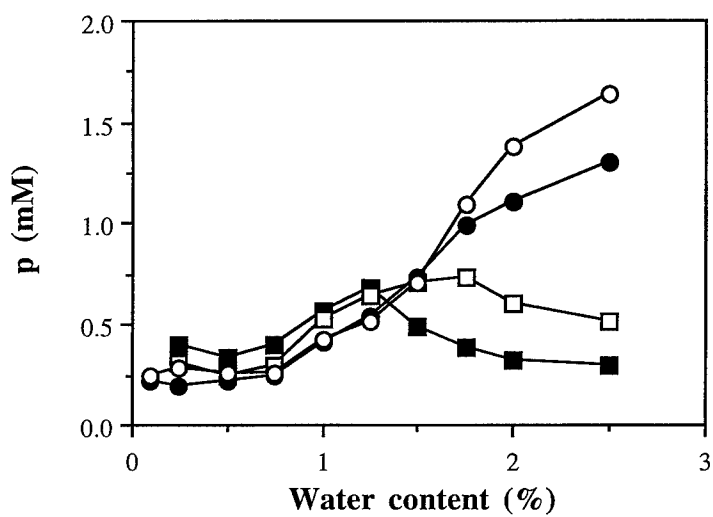
FIGURE 5. Effect of water content on the p value in water-immiscible solvent. The reaction mixture contained 10 mM Bz-TyrOEt, 15 mM Leu-NH₂, and 20 mg of immobilized chymotrypsin in ethyl acetate. Four temperatures were studied: (O) 35 °C, (●) 25 °C, (□) 5 °C, and (■) −10 °C.
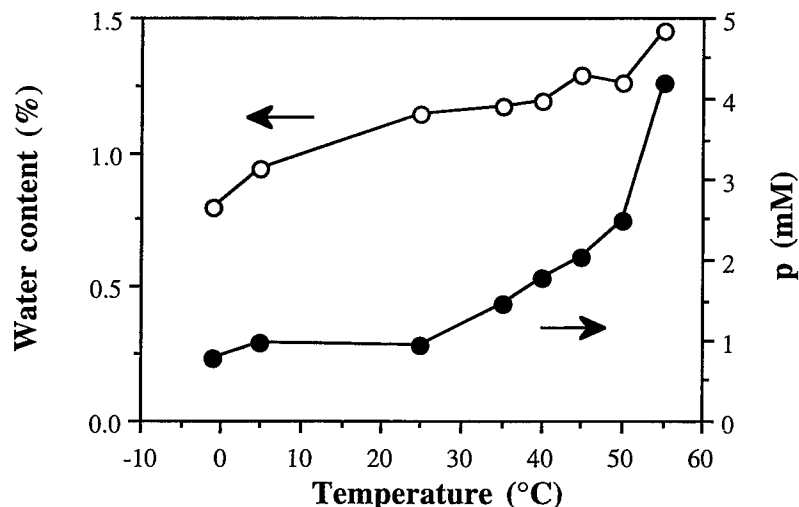
FIGURE 6. Effect of temperature on the *p* value at constant water activity. Reaction conditions as in FIGURE 5, except that water-saturated 5-methyl-2-hexanone was used as solvent. The water content (○) was measured and the *p* value (●) was determined.

CONCLUSIONS

The α-chymotrypsin-catalyzed reaction is positively affected by a decrease in temperature. The peptide yield is increased when the temperature is decreased. One reason for high peptide yields was the decrease in *p* values with decreasing temperature. The effect of water concentration (water activity) on the *p* value is more pronounced at high water activities than at low. At constant water activity, the *p* value decreased with decreasing temperature.

REFERENCES

1. KISE, H., K. FUJIMOTO & H. NORITOMI. 1988. Enzymatic reactions in aqueous-organic media. VI. Peptide synthesis by α-chymotrypsin in hydrophilic organic solvents. J. Biotechnol. **8:** 279–290.
2. CLAPÉS, P., G. VALENCIA & P. ADLERCREUTZ. 1992. Influence of solvent and water activity on kinetically controlled peptide synthesis. Enzyme Microb. Technol. **14:** 575–580.
3. CHEN, S-T., S-Y. CHEN, C-L. KAO & K-T. WANG. 1994. Improved yield by cryoeffect in kinetically controlled peptide synthesis catalyzed with alcalase. Biotechnol. Lett. **16:** 1075–1080.
4. JÖNSSON, Å., P. ADLERCREUTZ & B. MATTIASSON. 1995. Effect of subzero temperatures on the kinetics of protease-catalyzed dipeptide synthesis in organic media. Biotechnol. Bioeng. **46:** 429–436.
5. JAKUBKE, H-D. 1987. *In* The Peptides. S. Udenfriend & J. Meienhofer, Eds.: 103–106. Academic Press. New York/London.
6. VALIVETY, R. H., P. J. HALLING & A. R. MACRAE. 1992. Reaction rate with suspended lipase catalyst shows similar dependence on water activity in different organic solvents. Biochim. Biophys. Acta **1118:** 218–222.

Interesterification Biocatalysis of Purified Lipase Fractions from *Rhizopus niveus*[a]

S. KERMASHA AND M. SAFARI

Department of Food Science and Agricultural Chemistry
McGill University
Sainte Anne de Bellevue, Québec, Canada H9X 3V9

INTRODUCTION

Extracellular microbial lipases (glycerol ester hydrolases, EC 3.1.1.3) hydrolyze the triacylglycerol substrate.[1] However, the enzymatic reaction could also be reversible and these enzymes can catalyze the synthesis of ester bonds and the transesterification and interesterification of lipids in organic solvent media.[2]

Lipase from *Rhizopus niveus* has been shown to be useful in food applications.[3] The use of specific lipases to catalyze the interesterification reaction has received considerable attention because of certain advantages over chemical catalysts.[4,5] The positional specificity of 1,3-specific lipases from *Mucor miehei, Aspergillus niger,* and *Pseudomonas fluorescens* in isooctane,[6] in hexane,[7] and in the absence of a solvent[8] was investigated, using butterfat as substrate.

Milk fat contains appreciable amounts of oleic acid,[9] which is randomly distributed at the three possible positions on triacylglycerol molecules.[10] Hayes *et al.*[11] reported that the interchange of palmitic acid with oleic acid at the 2-position suppressed the cholesterol-raising potential of milk fat.

This study is a part of ongoing research[12–18] aimed at the optimization of interesterification of selected fatty acids in butterfat using organic solvent media. The objective of this work was too monitor the specificity of the purified enzyme fractions in terms of changes in the positional distribution of fatty acids on selected triacylglycerol molecules of butterfat.

MATERIALS AND METHODS

Lipase N (FI) obtained from Amano Pharmaceutical Company (Nagoya, Japan) by a unique fermentation process of a selected strain of *R. niveus* was partially purified by the addition of solid ammonium sulfate at 40–60% of saturation (FII). The enzymatic fraction (FII) was further purified by preparative ion-exchange chromatography on a Mono Q HR 10/10 column (FIII) followed by size-exclusion liquid chromatography on a Superdex 75 HR 10/30 column (FIV), using a fast-

268

protein liquid chromatography (FPLC) system (Pharmacia, LKB Biotechnology, Uppsala, Sweden).

Lipase assay was performed with butter oil emulsion according to a modification of the procedure described by Watanabe *et al.*[19] Interesterification of butterfat was carried out according to the procedure described previously.[14]

The preparation of free and bound fatty acid methyl esters was carried out according to the procedure described by Badings and De Jong.[20] Qualitative and quantitative analyses of free and bound fatty acids of interesterified butterfat were carried out according to the procedure described previously.[13]

The triacylglycerols of interesterified butterfat were separated according to the
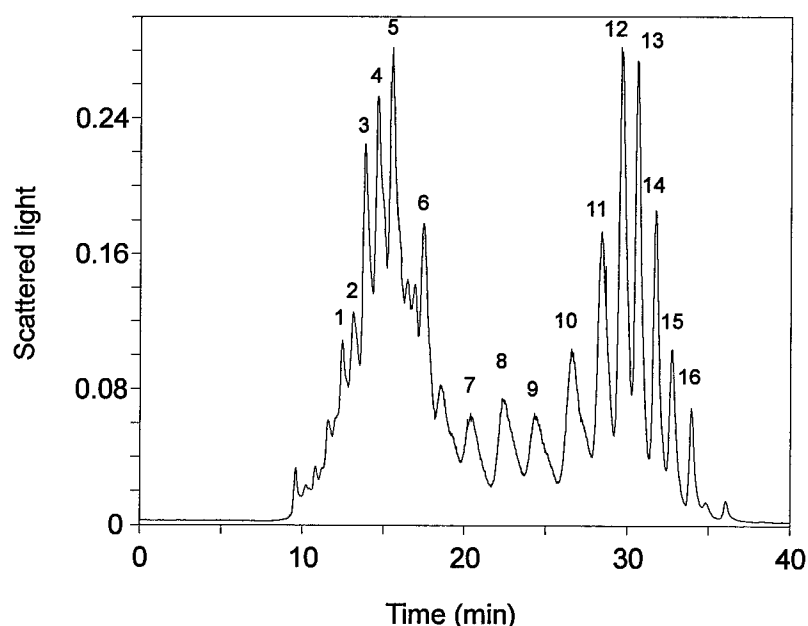
FIGURE 1. Chromatogram of the HPLC analyses of triacylglycerols of butterfat, using a Spherisorb-ODS-2 reverse-phase column (250 × 22 mm i.d., 5 μm pore size; Altech Associates, Deerfield, Illinois).

procedure described previously.[15] High-performance liquid chromatography (HPLC) analyses of triacylglycerols were performed according to the procedure described in reference 12. The separation of high-molecular-weight triacylglycerols, fraction numbers 8 to 16 (FIGURE 1), was carried out with a gradient elution and was demonstrated with a laser light-scattering detector (Varex Corporation, Burtonsville, Maryland).

Stereospecific analyses of selected triacylglycerol fractions from butter were performed for the determination of the positional distribution of fatty acids at *sn*-1, -2, and -3. The generation of *sn*-2 monoacylglycerols and *rac*-1,2-diacylglycerols was performed according to the procedure described by Skipsi *et al.*[21] The butterfat

triacylglycerols were subjected to Grignard's reaction, and the rac-1,2- and rac-1,3-diacylglycerols were resolubilized and recovered by preparative thin-layer chromatography according to the method of Mattson and Volpenhein.[22] The rac-phosphatidylcholines were synthesized by treating purified rac-1,2-diacylglycerols with phosphorus oxychloride and choline chloride, as described in reference 12. The hydrolyses of rac-phosphatidylcholines were performed according to the procedure described by Robertson and Lands.[23]

TABLE 1. Free Fatty Acid Composition of Interesterified Butterfats by Purified Enzymatic Extracts of Lipase N (Amano) Obtained from *Rhizopus niveus*

Carbon Number[b]	Relative Fatty Acid (mol %)[a]				
	Untreated Butter[c]	FI[d]	FII[e]	FIII[f]	FIV[g]
C4:0	7.9	9.0	9.9	9.2	11.1
C6:0	2.4	6.2	7.9	5.4	6.1
C8:0	1.6	5.5	7.0	4.4	3.5
C10:0	2.3	7.2	8.3	6.7	6.3
C12:0	2.5	6.0	7.2	9.0	11.6
C14:0	5.7	12.5	13.7	15.6	16.3
C14:1	0.6	1.0	1.5	2.0	1.6
C16:0	43.9	25.5	22.7	21.9	18.3
C16:1	0.7	0.8	1.3	1.8	1.6
C18:0	10.0	8.5	8.8	11.5	12.8
C18:1	21.0	17.0	11.4	11.1	10.8
C18:2	0.5	0.6	0.2	0.9	—
C18:3	0.3	0.2	0.1	0.5	—
C20:0	0.6	—	—	—	—

[a]Relative percent (mol) of free fatty acids liberated by the interesterification of butterfat by purified enzymatic extracts of lipase N (Amano). A dash indicates not detected.

[b]Carbon number of fatty acid methyl esters obtained from untreated and interesterified butterfats.

[c]Untreated butterfat fractionated by preparative HPLC column; fraction numbers 8 to 16 (FIGURE 1).

[d]Interesterified butterfat catalyzed by the lipase extract N.

[e]Interesterified butterfat catalyzed by partially purified extract of lipase N, obtained by ammonium sulfate precipitation at 40–60% of saturation.

[f]Interesterified butterfat catalyzed by purified extract of lipase N, obtained by ammonium sulfate precipitation, followed by preparative ion-exchange chromatography.

[g]Interesterified butterfat catalyzed by purified extract of lipase N, obtained by ammonium sulfate precipitation, followed by successive ion-exchange and size-exclusion liquid chromatographies.

RESULTS AND DISCUSSION

Changes in Free Fatty Acid Content of Interesterified Butterfat

TABLE 1 shows that the use of lipase extract (FI) for the interesterification of butterfat caused an increase in the total proportions of free small-chain fatty acids (C4–C10), C12:0, and C14:0 by 96%, 140%, and 119%, respectively, with a concomitant decrease in the proportions of C16:0 and C18:1 by 42% and 19%, respectively.

The data in TABLE 1 also demonstrate that the interesterification of butterfat by partially purified enzyme extract (FII) caused an increase in the proportions of free fatty acids C4–C10, C12:0, and C14:0 by 133%, 188%, and 140%, respectively, with a concomitant decrease in the proportions of C16:0 and C18:1 by 48% and 46%, respectively. In addition, the results indicate that the use of purified lipase fraction FIII, obtained by ion-exchange chromatography, for the interesterification of butterfat caused an increase in the amounts of free fatty acids C4–C10, C12:0, and C14:0 by 91%, 260%, and 173%, respectively, with a concomitant decrease in the proportions of C16:0 and C18:1 by 50% and 47%, respectively. The results also show that the use of purified lipase fraction FIV, obtained by size-exclusion chromatography, for the interesterification of butterfat caused an increase in the total proportions of free small-chain fatty acids (C4–C10), C12:0, and C14:0 by 90%, 364%, and 186%, respectively, with a concomitant decrease in the proportions of C16:0 and C18:1 by 58% and 49%, respectively.

These results (TABLE 1) suggest that the hydrolytic affinity of the purified lipases in the microemulsion system, used throughout this study, demonstrated an acyl-group specificity toward lower molecular weight fatty acids C4–C14:0. The results also indicate that this specificity was slightly increased by further purification of the lipase in the order of crude lipase (FI) > partially purified enzyme (FII) > ion-exchange chromatography fraction (FIII) > size-exclusion chromatography fraction (FIV).

Changes in the Positional Distributions of Selected Fatty Acids of Interesterified Butterfat

The results of TABLE 2 obtained from stereospecific analyses of butterfat triacylglycerols interesterified by lipase extract (FI) show that the proportions of relatively small chain fatty acids (C4–C10), C14:0, and C16:0, located at the sn-2 position of triacylglycerol molecules, decreased by 87%, 17%, and 20%, respectively, with a concomitant increase in the amounts of C18:0 and C18:1 by 20% and 46%, respectively. The results indicate that the interesterification also caused an increase in the proportions of relatively small chain fatty acids C4–C10 and those of C16:0, located at the sn-1 position, by 138% and 21%, respectively, with a concomitant decrease in the proportions of C18:1 and C12:0 by 42% and 25%, respectively, at the same position; however, there were no considerable changes in the amounts of C14:0 and C18:0 at the sn-1 position. The results further demonstrate that there was a decrease in the proportions of C16:0, C18:0, and C18:1 at the sn-3 position by 38%, 16%, and 11%, respectively, with a concomitant drastic increase (152%) in the amount of C14:0 at the same position.

The results of TABLE 2 obtained from stereospecific analyses of butterfat triacylglycerols interesterified by partially purified lipase (FII) show that there were 11%, 52%, and 13% increases in the total proportions of saturated small-chain fatty acids (C6–C10), C18:1, and C18:0, respectively, with concomitant decreases of 48% and 26% in the amounts of C16:0 and C14:0, respectively, at the sn-2 position. The results also demonstrate that the total proportions of fatty acids (C6–C10), C12:0, and C16:0, at the sn-1 position of triacylglycerols, increased by 69%, 11%, and 40%, respectively, with a concomitant decrease of 44% in the amount of C18:1 at the same position. The results indicate that the proportions of C14:0, C16:0, C18:0, and C18:1

TABLE 2. Stereospecific Analyses of Interesterified Butterfats by Purified Enzymatic Extracts of Lipase N (Amano) Obtained from *Rhizopus niveus*

Carbon Number[f]	Untreated Butter[a]			FI[b]			FII[c]			FIII[d]			FIV[e]		
	sn-1	sn-2	sn-3	sn-1	sn-2	sn-3	sn-1	sn-2	sn-3	sn-1	sn-2	sn-3	sn-1	sn-2	sn-3
C4:0	—[g]	—	—	—	—	—	—	—	—	—	—	—	—	—	—
C6:0	0.8	1.9	1.5	3.5	—	—	1.0	—	—	—	—	—	2.3	—	—
C8:0	0.5	1.5	1.2	1.8	—	—	1.7	0.2	—	0.5	—	—	1.0	2.1	6.0
C10:0	2.9	3.4	9.2	4.7	0.9	15.0	4.4	7.4	21.6	2.7	2.2	10.8	2.3	2.2	10.9
C12:0	4.7	3.7	11.9	3.5	5.1	11.3	5.2	7.6	12.7	4.5	6.8	21.9	6.8	5.1	17.6
C14:0	15.9	12.9	10.6	15.6	10.7	26.7	12.0	9.6	7.6	15.9	9.6	17.2	16.0	7.9	18.6
C16:0	28.0	33.1	34.4	33.8	26.5	21.4	39.1	17.1	19.3	41.2	17.0	14.9	34.7	16.6	22.5
C18:0	17.4	10.7	15.8	17.7	12.9	13.2	16.5	12.1	11.8	16.1	13.0	12.7	15.9	13.8	10.9
C18:1	27.7	28.7	9.0	16.1	42.0	8.0	15.5	43.7	7.2	16.4	44.5	8.3	14.7	45.9	10.8
C18:2	2.0	3.4	5.5	1.2	1.9	3.5	4.3	1.2	11.4	2.2	4.5	9.0	5.0	5.0	2.3
C20:0	0.1	0.7	0.9	2.1	—	0.9	0.3	1.1	8.4	0.5	2.4	5.2	1.3	1.4	0.4

[a]Untreated butterfat fractionated by preparative HPLC column; fraction numbers 8 to 16 (FIGURE 1).

[b]Interesterified butterfat catalyzed by the lipase extract N.

[c]Interesterified butterfat catalyzed by partially purified extract of lipase N, obtained by ammonium sulfate precipitation at 40–60% of saturation.

[d]Interesterified butterfat catalyzed by purified extract of lipase N, obtained by ammonium sulfate precipitation, followed by preparative ion-exchange chromatography (IEC).

[e]Interesterified butterfat catalyzed by purified extract of lipase N, obtained by ammonium sulfate precipitation, followed by successive IEC and size-exclusion liquid chromatographies.

[f]Carbon number of fatty acid methyl esters obtained from untreated and interesterified butterfats.

[g]Not detected.

decreased by 28%, 44%, 25%, and 20%, respectively, at the sn-3 position, with a concomitant increase in the proportions of relatively small chain fatty acids (C6:0–C10:0) and C12:0 by 81% and 7%, respectively.

The stereospecific analyses of interesterified butterfat catalyzed by lipase purified by ion-exchange chromatography (FIII) show (TABLE 2) that the proportions of C10:0, C14:0, and C16:0, at the sn-2 position, decreased by 35%, 26%, and 49%, respectively, whereas the amounts of C12:0, C18:0, and C18:1 increased by 84%, 21%, and 55%, respectively, at the same position. The results demonstrate that there was a reduction in the total proportions of C18:0 as well as of C18:1 located at the sn-1 position, by 7% and 41%, respectively, with a concomitant increase in the amount of C16:0 by 47% at the same position. The results also indicate that there was a drastic decrease (57%) in the proportion of C16:0, with a concomitant increase in the amounts of C12:0 and C14:0 by 84% and 62%, respectively, at the sn-3 position.

The stereospecific analyses of butterfat interesterified by lipase purified by size-exclusion chromatography (FIV) show (TABLE 2) that the proportions of C14:0 and C16:0, located at the sn-2 position, decreased by 39% and 50%, respectively, with a concomitant increase in the amounts of C18:0 and C18:1 by 29% and 60%, respectively. The results show that the interesterification also caused an increase in the proportions of relatively small chain fatty acids (C6–C10) and C16:0, located at the sn-1 position, by 34% and 24%, respectively, with a concomitant decrease in the proportions of C18:0 and C18:1 by 9% and 47%, respectively; however, there was no considerable change in the amount of C14:0 at the same position. The results also

demonstrate that there was an increase in the proportions of relatively small chain fatty acids (C6–C10), C12:0, and C14:0 at the *sn*-3 position by 42%, 48%, and 75%, respectively, with a concomitant decrease in the proportions of C16:0 and C18:0 by 35% and 31%, respectively. These results suggest that there was an acyl-exchange reaction among all three possible positions of triacylglycerol molecules, wherein C18:1 previously located mainly on the *sn*-1 position exchanged with C16:0 previously located on the *sn*-2 position. Overall, these findings indicated that the interesterification of butterfat catalyzed by purified lipase fraction FIV resulted in the obtaining of a product where the stereospecific analyses of positional distribution of selected fatty acids revealed the presence of mainly C18:1 fatty acid at the *sn*-2 position.

The results of TABLE 3 demonstrate that the interesterification of butterfat catalyzed by lipase N (Amano) caused a 39.3% increase in the hypocholesterolemic fatty acids (C18:0 and C18:1) at the *sn*-2 position, with a concomitant 14.9% decrease in the proportion of hypercholesterolemic fatty acids (C12:0, C14:0, and C16:0) at the same position. On the other hand, the interesterification of butterfat by purified enzymatic fraction FIV shows (TABLE 3) that the total amount of hypercholesterolemic fatty acids (C12:0, C14:0, and C16:0) at the *sn*-2 position decreased by 40.4%, with a concomitant increase of these fatty acids by 18.3% and 3.2% at the *sn*-1 and *sn*-3 positions, respectively. However, the results demonstrate that there was an important increase (51.5%) in the amount of hypocholesterolemic fatty acids (C18:0

TABLE 3. Changes in the Positional Distributions of Selected Fatty Acids in Triacylglycerols of Interesterified Butterfat

Carbon Number[d]	Relative Fatty Acid (%)[a]								
	Untreated Butter			Treated Butter[b]			Treated Butter[c]		
	sn-1	*sn*-2	*sn*-3	*sn*-1	*sn*-2	*sn*-3	*sn*-1	*sn*-2	*sn*-3
C12:0	4.7	3.7	11.9	3.5	5.1	11.3	6.8	5.1	17.6
C14:0	15.9	12.9	10.6	15.6	10.7	26.7	16.0	7.9	18.6
C16:0	28.0	33.1	34.4	33.8	26.5	21.4	34.7	16.6	22.5
C18:0	17.4	10.7	15.8	17.7	12.9	13.2	15.9	13.8	10.9
C18:1	27.7	28.7	9.0	16.1	42.0	8.0	14.7	45.9	10.8
C12:0–C16:0[e]	16.2	16.6	19.0	8.8[f]	14.9[g]	4.4[f]	18.3[f]	40.4[g]	3.2[f]
C18:0–C18:1[h]	22.5	19.7	12.4	25.0[g]	39.3[f]	14.5[g]	32.1[g]	51.5[f]	12.5[g]

[a]Relative percent (mol) of fatty acid composition of selected triacylglycerols of untreated and interesterified butterfats.

[b]Interesterified butterfat catalyzed by the commercial lipase N (Amano) obtained from *R. niveus*.

[c]Interesterified butterfat catalyzed by purified extract of lipase N, obtained by ammonium sulfate precipitation at 40–60% of saturation, followed by successive preparative ion-exchange and size-exclusion liquid chromatographies.

[d]Carbon number of fatty acid methyl esters obtained from untreated and interesterified butterfats.

[e]Changes in percentage of hypercholesterolemic fatty acids (C12:0, C14:0, and C16:0) at the *sn*-2 and *sn*-1,3 positions of selected triacylglycerols of interesterified butterfat.

[f]Relative percentage increase in the proportion of the selected fatty acids.

[g]Relative percentage decrease in the proportion of the selected fatty acids.

[h]Changes in percentage of hypocholesterolemic fatty acids (C18:0 and C18:1) at the *sn*-2 and *sn*-1,3 positions of selected triacylglycerols of interesterified butterfat.

and C18:1) at the *sn*-2 position, with a concomitant decrease in these fatty acids at the *sn*-1 and *sn*-3 positions by 32.1% and 12.5%, respectively. The results show that the purification procedure of lipase developed in our laboratory allowed an increase of the acyl-exchange reaction within triacylglycerol molecules of interesterified butterfat.

CONCLUSIONS

Although the lipase N (Amano) has a 1,3-specificity, the results gathered in this study indicated that the enzyme was able to exhibit different positional specificity under certain conditions. The partial purification and the successive ion-exchange and size-exclusion chromatographies of the lipase extract resulted in a well-purified monomeric enzyme fraction. In addition, the use of the purified enzymatic fraction for the interesterification of butterfat increased the acyl-exchange reactions of hypercholesterolemic fatty acids, located originally at the *sn*-2 position, by hypocholesterolemic fatty acids, located originally at the *sn*-1,3 positions.

REFERENCES

1. MACRAE, A. R. 1983. J. Am. Oil Chem. Soc. **60:** 291–294.
2. BELLO, M., D. THOMAS & M. D. LEGOY. 1987. Biochem. Biophys. Res. Commun. **146:** 361–367.
3. MATSUO, T., N. SAWAMURA, Y. HASHIMOTO & W. HASHIDA. 1980. United Kingdom patent no. GB 2035359 B.
4. THOMAS, K. C., B. MAGNUSON & A. R. McCURDY. 1988. Can. Inst. Food Sci. Technol. J. **21:** 167–173.
5. McDOUGALL, I. L. 1989. J. Soc. Dairy Technol. **42:** 40–41.
6. KALO, P., M. PERTILLA & A. KEMPPINEN. 1988. Meijeritiet. Aikak. **46:** 36–47.
7. KALO, P., H. HUOTARI & M. ANTILA. 1989. Meijeritiet. Aikak. **47:** 29–38.
8. KALO, P., H. HUOTARI & M. ANTILA. 1990. Milchwissenschaft **45:** 281–285.
9. ROBERTSON, D. S. 1987. *In* Food: Biochemistry and Nutritional Value. Longman/Wiley. New York.
10. NAWAR, W. W. 1985. *In* Food Chemistry. Second edition. O. R. Fenema, Ed.: 150. Dekker. New York.
11. HAYES, K. C., A. PRONCZUK, S. LINDSEY & D. DIERSON-SCHADE. 1991. Am. J. Clin. Nutr. **53:** 491–498.
12. KERMASHA, S., S. KUBOW, M. SAFARI & A. REID. 1993. J. Am. Oil Chem. Soc. **70:** 169–173.
13. SAFARI, M., S. KERMASHA & F. PABAI. 1993. Food Biotechnol. **7:** 265–273.
14. SAFARI, M., S. KERMASHA, F. PABAI & J. D. SHEPPARD. 1994. J. Food Lipids **1:** 247–263.
15. SAFARI, M., S. KERMASHA, L. LAMBOURSAIN & J. D. SHEPPARD. 1994. Biosci. Biotechnol. Biochem. **58:** 1553–1557.
16. SAFARI, M. & S. KERMASHA. 1994. J. Am. Oil Chem. Soc. **71:** 969–973.
17. KERMASHA, S., M. SAFARI & M. GOETGHEBEUR. 1995. Appl. Biochem. Biotechnol. **53:** 229–244.
18. PABAI, F., S. KERMASHA & A. MORIN. 1995. Appl. Microbiol. Biotechnol. **43:** 42–51.
19. WATANABE, N., Y. OTA, Y. MINODA & K. YAMADA. 1977. Agric. Biol. Chem. **41:** 1353–1358.
20. BADINGS, H. T. & C. DE JONG. 1983. J. Chromatogr. **270:** 493–506.
21. SKIPSI, V. P., R. F. PETERSON & M. BACLAY. 1964. J. Biochem. **90:** 374–378.
22. MATTSON, F. H. & R. A. VOLPENHEIN. 1961. J. Lipid Res. **2:** 58–62.
23. ROBERTSON, A. F. & W. E. M. LANDS. 1962. Biochemistry **1:** 804–810.

EPR Studies of Cutinase
in Microemulsions[a]

V. PAPADIMITRIOU,[b] A. XENAKIS,[b] C. T. CAZIANIS,[b]
H. STAMATIS,[c] M. EGMOND,[d] AND F. N. KOLISIS[c]

[b]Institute of Biological Research and Biotechnology
National Hellenic Research Foundation
11635 Athens, Greece

[c]Department of Chemical Engineering
Division IV
National Technical University of Athens
15700 Athens, Greece

[d]Unilever Research Laboratory
Vlaardingen, the Netherlands

INTRODUCTION

The structures of several lipases have been solved and it is well established that the interfacial activation is a key feature of lipolytic enzymes with an important lid. However, in order to better understand the mechanisms of lipolysis and esterifications catalyzed by lipase, it is important to clarify the role of water in substrate binding, conformational changes, and catalysis of lipase.

In this work, cutinase from *Fusarium solani* has been used as a model lipase. This enzyme hydrolyzes the insoluble polymer cutin, as well as triglycerides, as efficiently as true lipases. The structure of this enzyme has been solved, showing that it is a compact 20-kDa enzyme containing a small flap and an accessible active-site serine residue.[1] It is also known that cutinase is able to interact with lipid-water interfaces. A consequence of the association of the enzyme with the lipid phase is the modification of the water distribution and behavior at the interface and the active-site microenvironment. In our study, cutinase was encapsulated in microemulsions, where its catalytic behavior regarding the esterification of lauric acid with pentanol was related to the enzyme conformation followed by EPR spectroscopy. In these model systems, the size of the reverse micelles and thereby the amount of water can be controlled very accurately, thus allowing the study of a wide range of hydration levels, ranging from enzyme-containing large micelles to a situation where the enzyme is restricted in very poor water containing reverse micelles.

MATERIALS AND METHODS

Materials

Cutinase from *Fusarium solani pisi* was provided by the Unilever Research Laboratory (Vlaardingen, the Netherlands). The enzyme preparation had a specific

activity of 356 u/mg. One unit is defined as the amount of cutinase that catalytically hydrolyzes p-nitrophenylbutyrate (pNBP) to produce 1 μmol of p-nitrophenol per minute at 25 °C and pH 7.4. The spin label, 4-(ethoxyfluorophosphinyloxy)-2,2,6,6-tetramethylpiperidine-N-oxyl (EFP-TEMPO), was from Sigma. AOT [bis(2-ethylhexyl)-sulfosuccinate sodium salt], pNBP, and lauric acid were obtained from Sigma. Isooctane was purchased from Merck, whereas pentanol was from Ferak (Berlin, Germany). All chemicals were of the highest available degree of purity and twice-distilled water was used throughout this study.

Spin-labeling of Cutinase

The active-site serine residue of cutinase was spin-labeled by the phosphonylating spin label EFP-TEMPO in 0.1 M acetate buffer, pH 5.4, according to Kommareddi et al.[2] The reaction was followed by monitoring the cutinase activity as regards the hydrolysis of pNBP and was stopped after 3.5 hours. The unreacted spin label was removed by extensive dialysis against a 55 mM glycine/HCl (pH 3.5) solution. The spin-labeled enzyme solution was then removed from the dialysis bag and stored in a freezer. The concentration of the spin-labeled enzyme in the final solution was determined by measuring the absorbance at 280 nm.

Preparation of Microemulsions

Microemulsions were prepared by adding the appropriate amounts of the above-used glycine buffer solution in a 0.1 M solution of AOT in isooctane. The spin-labeled enzyme was solubilized in the water core of the reverse micelles by adding small aliquots of a concentrated stock solution in buffer. Solubilization was achieved by gentle shaking within less than 1 min. The total amount of water was adjusted to give the desired value of the molar ratio, $w_o = [H_2O]/[AOT]$. The water content of the initial stock solution, AOT/isooctane, was periodically checked by Karl Fischer titrations. The amount of water (in general, less than 1%) was taken into consideration in the calculation of the total water content. When the w_o values of the enzyme-containing reverse micelles were varied, the final concentration of spin-labeled enzymes in the aqueous phase was kept constant.

Activity Measurements

The reaction of the esterification of lauric acid by pentanol was carried out in 1-mL total volume of the microemulsion system at a temperature of 25 °C and an initial pH of the dispersed aqueous phase of 9. The initial reaction rates were determined spectrophotometrically, by measuring the depletion of fatty acid, as described elsewhere.[3]

Electron Paramagnetic Resonance (EPR) Measurements

EPR spectra were recorded at room temperature using a Bruker ER 200 D spectrometer operating at X-band. Spectra were accumulated and treated using the

DAT-200 software for PC (University of Lubeck, Germany). The samples were contained in an E-248 cell. Typical settings were as follows: field set, 3471 G; time constant, 1000 ms; scan time, 100 ms; microwave power, 7.5 mW; microwave frequency, 9.76 GHz; modulation amplitude, 2.5 G.

RESULTS AND DISCUSSION

Esterification Reactions in AOT Microemulsion Systems

Various parameters, such as pH, temperature, and w_o, are known to have a critical effect on cutinase activity in microemulsions. We have studied the effect of
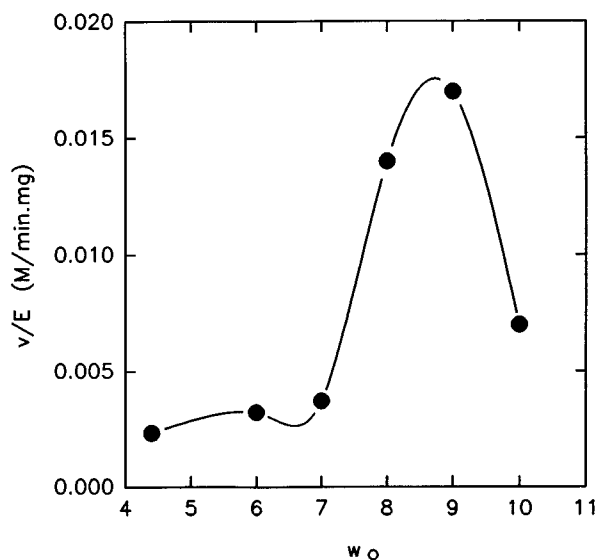
FIGURE 1. Esterification of lauric acid by 1-pentanol, catalyzed by cutinase, in AOT reverse micelles. Variation of the initial velocity of esterification as a function of $w_o = [H_2O]/[AOT]$; pH 9, $T = 25\ ^\circ C$.

the water content of the microemulsion, w_o, in a typical esterification reaction of lauric acid with pentanol in AOT/isooctane microemulsions catalyzed by cutinase. The reaction was carried out at 25 °C and pH 9, values corresponding to the optimum ones as determined by Sebastiao *et al.*[4] FIGURE 1 shows this effect, where the water content of the microemulsions is expressed in terms of the molar ratio w_o. It can be seen that cutinase activity follows a bell-shaped profile, presenting a maximum at $w_o = 9$ for the given microemulsion system. Structural studies on the AOT-based microemulsion systems have shown that the water-dispersed phase constitutes spherical droplets, surrounded by a monolayer of the surfactant molecules.[5] In small droplets (low w_o values), the restricted enzyme molecule cannot achieve its maximum activity. At w_o values around 10, the enzyme molecule has its optimal conformation,
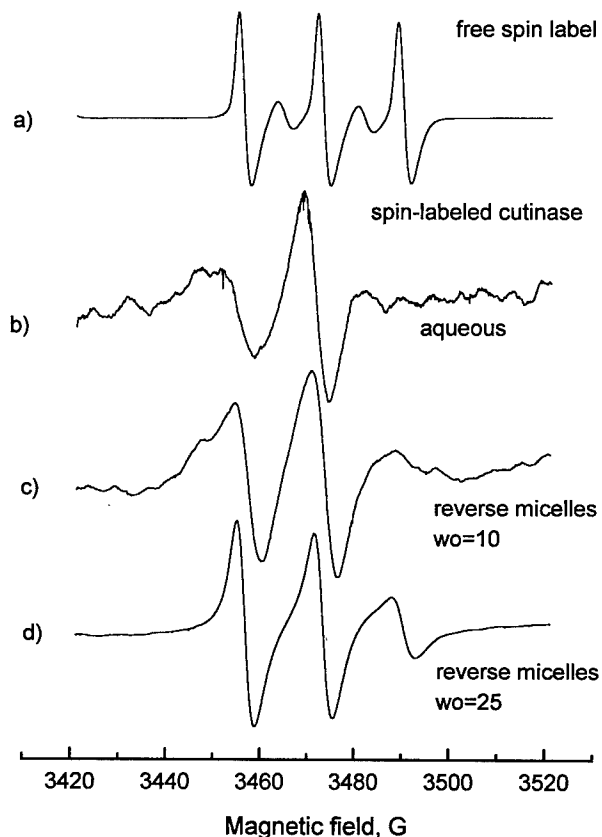
FIGURE 2. EPR spectra of free spin label (a) and of spin-labeled cutinase in aqueous solution (b) and reverse micellar solution (c, d).

being in close contact with the lipophilic substrate, and thus resulting in a maximum activity. At higher w_0 values, the size of the droplet is such that a quantity of free water appears in the water core of the droplet, creating a diffusional barrier.[6]

EPR Studies

In order to further elucidate the role that w_0 plays in the enzyme behavior, we have undertaken an EPR spectroscopic study. We have used EFP-TEMPO, an adequate spin-labeling probe known to selectively bind with the nucleophilic serine residue at the active site of seroproteases, such as chymotrypsin and trypsin.[7] The active site of cutinase consists of the same catalytic triad, Ser-His-Asp,[8] thus allowing the selective binding of the probe.

The EPR spectra were recorded in the above-described microemulsions with varying w_0 values. FIGURE 2 shows the free spin label spectrum (a), as well as the

spectra of the EFP-TEMPO-cutinase obtained in aqueous solution (b) and in reverse micelles (c, d). The shape of the bound-to-the-enzyme spin label spectra is considerably different from the free spin label one. The peaks are broadened and, in some cases, the high field peak almost disappears. These changes are indicative of hindered motion of the probe and depend on the medium in which the enzyme is solubilized: namely, in the aqueous solution the probe is quite immobilized, whereas in the microemulsions the mobility varies, depending on the ratio w_o. In microemulsions with small water content, low w_o, the spin-labeled enzyme is less mobile than in systems with high w_o values.

The effect of w_o on the mobility of the spin-labeled cutinase is illustrated in FIGURE 3, where the ratio h_{+1}/h_0 is plotted versus w_o. The ratio of the intensity of the low field line, h_{+1}, to the intensity of the center field line, h_0, is an empirical parameter expressing the mobility of the probe.[9] It is seen that the cutinase mobility constantly increases as w_o increases up to w_o = 10–15; however, after these values, the mobility remains nearly constant. In all microemulsions, the value of the ratio h_{+1}/h_0 of the spin-labeled enzyme is higher than in the aqueous solution.

From the structural crystallographic data of cutinase,[8] it is known that the active-site Ser-120 is in a crevice between two hydrophobic loops. These lipophilic side chains play the role of the "mini flap", interfering with interfaces and thus affecting the capability of the substrates to reach the active-site crevice. The immobilization of the spin label bound to the active site of cutinase observed above shows that, in aqueous solutions, the active-site region is rather rigid. In the case of microemulsions, the enzyme exhibits an increasing motional freedom as the w_o value
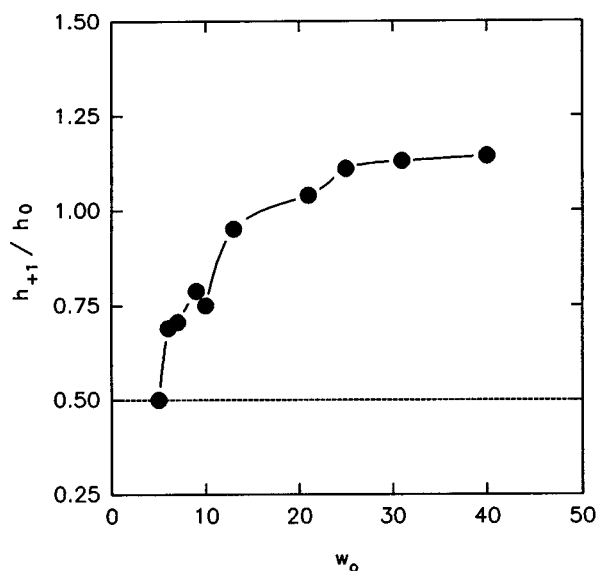
FIGURE 3. Variation of the ratio h_{+1}/h_0 of spin-labeled cutinase as a function of w_o in AOT reverse micelles. The dashed line presents the same ratio in aqueous solution.

increases. It seems that the enzyme is affected by the membrane of the reverse micelles that interact with the protecting lipophilic chains.

These observations are in accordance with the catalytic behavior of cutinase described above. At low w_0 values, the reverse micelles are too small to host the enzyme molecule in its optimal conformation, resulting in a low activity and a reduced mobility. At w_0 above the optimum-for-activity value, for example, 10–15, where the catalytic ability of cutinase drops, the interactions of the active site with the micellar membrane remain constant. Although the increased amount of water present in the large reverse micelles creates a diffusional barrier for the substrates, the active site of the enzyme is not affected anymore.

In conclusion, both the activity and the mobility of cutinase are affected when the enzyme is hosted in microemulsions. A major role is played by the water content parameter, w_0, which reflects the size of the reverse micelles. The active site of cutinase is more mobile for increasing w_0 values, whereas the ability of the enzyme to catalyze esterification reactions as a function of w_0 follows a bell-shaped pattern.

REFERENCES

1. MARTINEZ, C., A. NICOLAS, H. VAN TILBEURGH, P. M. EGLOFF, C. CUDREY, R. VERGER & C. CAMBILLAUD. 1994. Biochemistry 33: 83–89.
2. KOMMAREDDI, N. S., K. C. O'CONNOR & V. T. JOHN. 1994. Biotechnol. Bioeng. 43: 215–224.
3. STAMATIS, H., A. XENAKIS, M. PROVELEGIOU & F. N. KOLISIS. 1993. Biotechnol. Bioeng. 42: 103–110.
4. SEBASTIAO, M. J., J. M. S. CABRAL & M. R. AIRES-BARROS. 1993. Biotechnol. Bioeng. 42: 326–332.
5. ZULAUF, M. & H. F. EICKE. 1979. J. Phys. Chem. 83: 480–486.
6. STAMATIS, H., A. XENAKIS, E. DIMITRIADIS & F. N. KOLISIS. 1995. Biotechnol. Bioeng. 45: 33–41.
7. MORRISETT, J. D. 1976. In Spin Labeling: Theory and Applications, p. 273–338. Academic Press. New York.
8. MARTINEZ, C., P. DE GEUS, M. LAUWEREYS, G. MATTHYSSENS & C. CAMBILLAUD. 1992. Nature 356: 615–618.
9. SMITH, I. C. P. 1971. The spin label method. In Biological Application of Electron Spin Resonance, p. 483–539. Wiley-Interscience. New York.

Kinetics of Peptide Condensation in Aqueous-Organic Solvent

Progressive Inactivation and Catalytic Reaction

SHIGERU KUNUGI AND MASUMI YOSHIDA

Laboratory for Biopolymer Physics
Department of Polymer Science and Engineering
Kyoto Institute of Technology
Kyoto 606, Japan

INTRODUCTION

Peptide condensations from two-component amino acids or peptides are catalyzed by proteolytic enzymes through reverse reaction catalysis and facilitated by the presence of organic solvent because (1) the low fraction of water is thermodynamically favorable for the equilibrium, as well as for the equilibria of α-amino or α-carboxylate groups, and (2) the coexistence of good solvent is favorable for the solubilization of less polar substrates. Thus, many protease-catalyzed peptide syntheses have been successfully carried out in systems more or less containing organic solvents.

Recently, productions of solvent-resistant mutant enzymes by genetic manipulation have been started for proteases; however, fundamental investigations of the kinetic and thermodynamic aspects of the synthetic reactions have not been sufficiently performed, even with natural enzymes, compared with those efforts to elucidate the mechanisms of the hydrolytic catalysis.

In this report, we studied the effect of solvent on the condensation reaction from N-acyl-amino acid and amino acid amide—both the apparent equilibrium yield and the kinetics of the condensation—for the catalysis by thermolysin and carboxypeptidase (CPase) Y. In the system containing a substantial fraction of organic solvent, the simultaneous solvent-induced inactivation of the enzyme is to be considered for analysis of the actual rate profiles.

In the case of thermolysin, only the condensation reaction can provide peptide formation, but CPase Y can produce peptides either via the condensation reaction or via the acyl-transfer reaction. The kinetics of CPase Y–catalyzed hydrolysis of amino acid ester and peptide synthesis from N-acyl amino acid ester and amino acid amide in solvent systems were reported before,[1,2] but very little was examined on the condensation reaction. CPase Y has a carboxamidopeptidase activity on a peptide amide substrate with a small P'_1 amino acid following a large one, such as -Phe/GlyNH$_2$.[3] The reverse reaction of this hydrolysis has much simplified aspects because the ionization equilibria are concerned only with the bond-making groups. Thus, the present study analyzed the time profiles of the peptide condensation to obtain the initial velocity, taking into account the solvent-induced disactivation of the enzyme.

MATERIALS AND METHODS

Thermolysin was purchased from the Daiwa Kasei Company (Osaka, Japan; lot TIDC391). CPase Y was obtained from the Oriental Yeast Company (Osaka, Japan; lots 2100361 and 21003402). Their concentrations were determined spectrophotometrically.

Peptide condensation reactions were carried out with the A-component in excess of the C-component. In most of the cases, the buffering action was taken by the A-component: the aqueous solution of C-component and A-component was prioradjusted at desired pH with dilute acid (HCl) and then organic solvent was mixed.

The reaction mixture in a small test tube was incubated in a thermostated water bath (37 °C). Aliquots were taken out and analyzed by HPLC (Shimadzu LC10A–Cosmosil 5C18-P) after quenching by excess amount of dioxane/5% phosphoric acid mixture. The eluant contained MeCN [30–40% (v/v)], phosphoric acid (pH 3), and triethylamine (50 mM).

Inactivation of the enzyme was followed by adding an aliquot (of appropriate volume) from the incubated enzyme mixture to the standard medium containing the substrate (FuaGlyLeuNH$_2$ or BzTyrpNA). The absorbance change at 320–340 nm, due to the cleavage of this substrate at the Gly-Leu bond, was followed by a Union-SM401 spectrophotometer (Union Giken, Hirakata, Japan).

RESULTS AND DISCUSSION

Thermolysin

The effect of DMSO and MeCN was studied in homogeneous systems.[4,5] The rate dependence on the C-component concentration gave linear double-reciprocal plots, but that on the amine component at 70% MeCN or DMSO showed an apparent substrate inhibition profile. The analysis of the apparent K_m and k_{cat} parameters for both components at 40% MeCN indicated that the condensation reaction proceeded
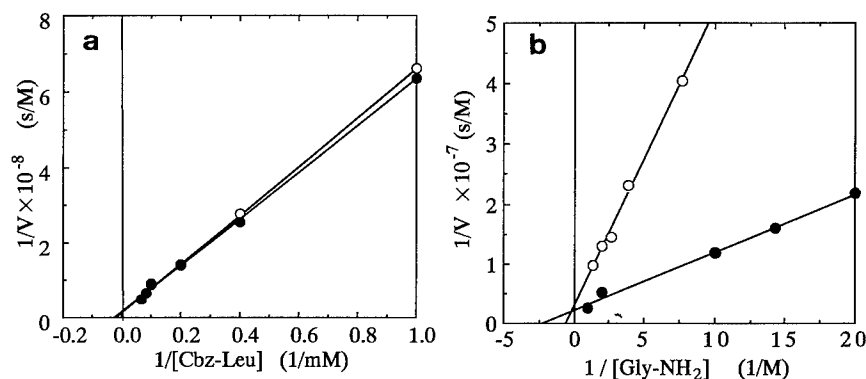
FIGURE 1. Lineweaver-Burk plot for the condensation reaction of Cbz-Leu or Cbz-Phe and GlyNH$_2$ catalyzed by CPase Y in 50% DMSO: 30 °C; pH 6.3; [CPase Y] = 1–2 μM. Panels: (a) [GlyNH$_2$] = 0.25 M (○) or 0.50 M (●); (b) [Cbz-Phe] = 2 mM (○) or 5 mM (●).

FIGURE 2. Cbz-Phe concentration dependence of the initial rate of the CPase Y–catalyzed condensation reaction of Cbz-Phe and GlyNH$_2$ in 50% DMSO: 30 °C; pH 6.3; [CPase Y] = 2 μM; [GlyNH$_2$] = 0.10 M (○) or 0.50 M (●).
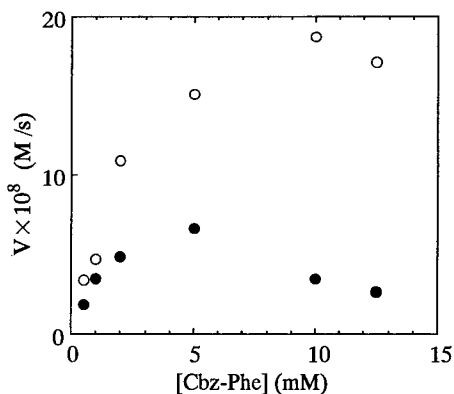
by a random bi-bi mechanism. The K_m values were estimated as 5.5 mM for Cbz-Phe and 110 mM for LeuNH$_2$, and k_{cat} was 4–5 s^{-1}. The K_m values for Cbz-Phe and LeuNH$_2$ were also evaluated at 70% MeCN to be 5 and 100–150 mM, respectively. This indicates that the catalytic property of this enzyme is not significantly influenced by the existence of a higher concentration of such organic solvents, except for the second nonproductive binding of the A-component.

CPase Y

In 50% DMSO, CPase Y activity decreased to 80% of the initial value after 20 min. Taking into account such disactivations, the time profiles of the peptide condensation were examined. At a fixed concentration of either component, the Lineweaver-Burk plot gave a linear reciprocal relation (FIGURE 1). When the concentration of Cbz-Leu was fixed, the reciprocal relation gave a certain crossing point and the condensation reaction by this enzyme did not seem to proceed by the ping-pong bi-bi mechanism, a typical one for the serine proteases.

With Cbz-Phe as the C-component, however, the condensation reaction rate did not give a simple saturation profile; instead, it showed an apparent substrate inhibition (FIGURE 2). Such a difference in the substrate (C-component) concentration dependence patterns between Cbz-Phe and Cbz-Leu might reflect the shape and size of the P$_1$ hydrophobic pocket of this enzyme.

REFERENCES

1. KUNUGI, S., T. KONDOH, H. HAYASHIDA & A. NOMURA. 1990. Biocatalysis **4:** 141–151.
2. KUNUGI, S., N. SUZUKI, M. YOKOYAMA & A. NOMURA. 1992. Ann. N.Y. Acad. Sci. **672:** 323–328.
3. KUNUGI, S., K. TANABE, K. YAMASHITA & M. FUKUDA. 1987. Bull. Chem. Soc. Jpn. **60:** 1399–1402.
4. KUNUGI, S., N. SUZUKI, A. SAKAMOTO & M. YOSHIDA. 1995. Bull. Chem. Soc. Jpn. **68:** 1019–1023.
5. KUNUGI, S. & M. YOSHIDA. 1996. Bull. Chem. Soc. Jpn. **69:** 805–809.

Xylanase Produced by *Bacillus thermoantarcticus*, a New Thermophilic Bacillus[a]

LICIA LAMA, BARBARA NICOLAUS,
VALERIA CALANDRELLI, ENRICO ESPOSITO,
AND AGATA GAMBACORTA

Istituto per la Chimica di Molecole di Interesse Biologico
CNR
80072 Arco Felice, Italy

INTRODUCTION

Xylan, a heteropolymer of (β1–4)-linked xylose, is the next most abundant natural polysaccharide after cellulose and accounts for 20% to 30% dry weight of agricultural residues. Its abundance indicates that xylanolytic enzymes can play an important role in bioconversion, in preparation of cellulose pulps, in fiber liberation technology, etc.[1,2] Generally, though, the processes are run at high temperatures and at extreme pH values. Therefore, enzymes tolerating high temperature and pH values are needed in order to make enzymatic processes technically and economically more feasible.

However, these xylan-degrading enzymes are limited to those from microorganisms that grow at ordinary temperatures, and the enzymes do not show thermostability at higher temperatures. There have been few reports about thermostable xylan-digesting enzymes.[3]

In this report, we describe the isolation and characterization of an extracellular thermostable xylanase from a novel thermophilic bacillus, *Bacillus thermoantarcticus*, isolated from a geothermal soil in Antarctica.[4]

MATERIALS AND METHODS

Culture Conditions

Bacillus thermoantarcticus was cultivated on a medium containing 0.6% yeast extract and 0.3% NaCl at 60 °C, pH 5.6, as previously described.[4]

Production of the enzyme was investigated on media containing 0.1% yeast extract, 0.3% NaCl, and 0.6% of a different carbon source: glucose, xylose, or xylan.

Preparation of Enzyme

Ammonium sulfate was added to the cell-free broth, obtained as previously described,[4] to 60–80% final concentration; after centrifugation, the dissolved pellet in 50 mM sodium acetate buffer, pH 5.6, was dialyzed against the same buffer.

Enzymatic Assay

Xylanase activity was assayed by using 2% birchwood xylan as the substrate, which was preliminarily suspended homogeneously in 50 mM sodium acetate buffer, pH 5.6. The mixture, containing 0.5 mL of enzyme solution and 0.5 mL of the substrate, was incubated at 80 °C for 10 min. The amount of reducing sugars liberated was determined by using 3,5-dinitrosalicylic acid (DNS method).[5] The reducing sugars of the reference samples (substrate solution incubated without enzyme and diluted enzyme solution in buffer) were deducted from the values of the test samples. One unit of enzymatic activity was defined as the amount of enzyme that releases 1 μmol of reducing sugars as an equivalent of xylose per minute under the above conditions.

The β-xylosidase activity was assayed by using 20 mM *p*-nitrophenyl-β-D-xylopyranoside as the substrate; 0.1 mL of the enzyme, 0.1 mL of the substrate, and 0.8 mL of sodium acetate buffer (pH 5.6) were incubated for 5 min at 70 °C. The reaction was stopped by adding 1 mL of 1 M potassium bicarbonate and 3 mL of H_2O. The liberated *p*-nitrophenol was measured at 420 nm.

Effect of Inhibitors

Various metal ions (1 mM) and other agents were added to the standard enzymatic reaction mixtures.

Protein Content

Protein content was determined by the method of Bradford[6] by using the BioRad protein assay with bovine albumin as a standard.

Effect of pH and Temperature on Xylanase Activity

The enzymatic reactions were carried out for 10 min at 70 °C in the following buffers (50 mM): glycine-HCl or NaOH (pH 3.0 or 9.0), sodium acetate (pH 4.0, 5.0, 5.6), and phosphate (pH 6.0, 8.0). The optimum temperature was determined by performing the standard reaction over the temperature range of 35 to 90 °C.

Thermostability was determined by incubating the enzyme solution at 60, 70, and 80 °C. At various times, the enzyme was removed and placed at 0 °C. The residual activity in each tube was determined by the standard assay.

TABLE 1. Production of Xylanase by *Bacillus thermoantarcticus* Grown in the Presence of Different Carbon Sources

Carbon Source (6 g/L)	Xylanase (U/mL)
xylan	1
xylose	0.12
glucose	0.1
yeast	0.09

Hydrolysis Experiments

These experiments were performed over the temperature range of 60 to 90 °C under standard assay conditions (reported above). The hydrolyses were assayed, at various time intervals, by the DNS method. The end products of hydrolysis were identified, both with thin-layer chromatography (TLC) and with HPAE-PAD Dionex using standard sugars. The solvent system for TLC (silica gel plates, 0.25-mm layers of silica gel F 254, Merck) was acetone:butanol:H_2O (8:1:1). Compounds were detected by spraying with α-naphthol, followed by heating at 150 °C for 5 min. Saccharides were eluted on Dionex, equipped with Carbo-Pac-PA-1 column using 100 mM NaOH as the solvent system.

RESULTS AND DISCUSSION

TABLE 1 shows the yield of β-xylanase by varying the carbon source in the culture medium. The production of xylanase by *Bacillus thermoantarcticus* was increased approximately 10 times when xylan was used as the growth substrate.
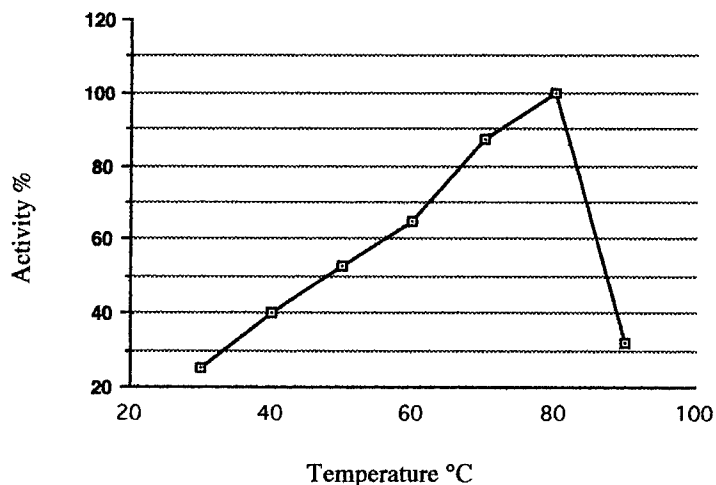
FIGURE 1. Effect of temperature on the activity of xylanase.

TABLE 2. Effect of Various Reagents on Xylanase Activity from *Bacillus thermoantarcticus*

Reagent (1 mM)	Relative Activity (%)
none	100
SDS	95
N-bromosuccinimide	59
p-hydroxymercuribenzoate	100
$CaCl_2$	100
$MgCl_2$	111
EDTA	100
$CuCl_2$	85
$FeSO_4$	61

In addition to xylanase, β-xylosidase was also produced by the strains grown on xylose and xylan (data not shown).

The temperature optimum of xylanase in the standard assay conditions was 80 °C (FIGURE 1) and the pH optimum was 5.6, retaining 43% of the maximum activity at pH 8.0 and 4.0. The enzyme was stable for 24 h at 60 °C, whereas at 70 °C about half of the initial activity remained after 24 h. At 80 °C, the half-life of the xylanase activity was 50 min.

We investigated the effect of metal ions and other agents on the activities of xylanase (TABLE 2). The activity was not influenced by Ca^{++} and Mg^{++}, whereas metals such as Cu^{++} and Fe^{++} and compounds such as SDS and *N*-bromosuccin-imide showed a partial inhibition. The addition of EDTA did not affect the activity, suggesting that no metals are needed for the enzymatic reaction.

Hydrolysis of Xylan

Hydrolysis experiments with birchwood xylan were carried out at different temperatures. The highest hydrolysis yield, evaluated by the DNS method, was obtained at 70 °C within 24 h. A relatively high yield was still obtained at 80 °C (TABLE 3). When xylanase and β-xylosidase concurrently reacted with the substrate, mainly xylose as the reaction product was found (70 °C, FIGURE 2). In contrast, at 80 °C, the amounts of xylobiose and xylotriose increased with respect to xylose, probably due to the lower thermophilicity of the β-xylosidase compared with endoxylanase (FIGURE 2).

TABLE 3. Hydrolysis of Birchwood Xylan with Xylanase from *Bacillus thermoantarcticus* at Different Temperatures

T (°C)	Reducing Sugars (% of Hydrolysis)		
	1 h	4 h	24 h
60	16	20	40
70	26	30	72
80	11	21	34
90	8	0	0
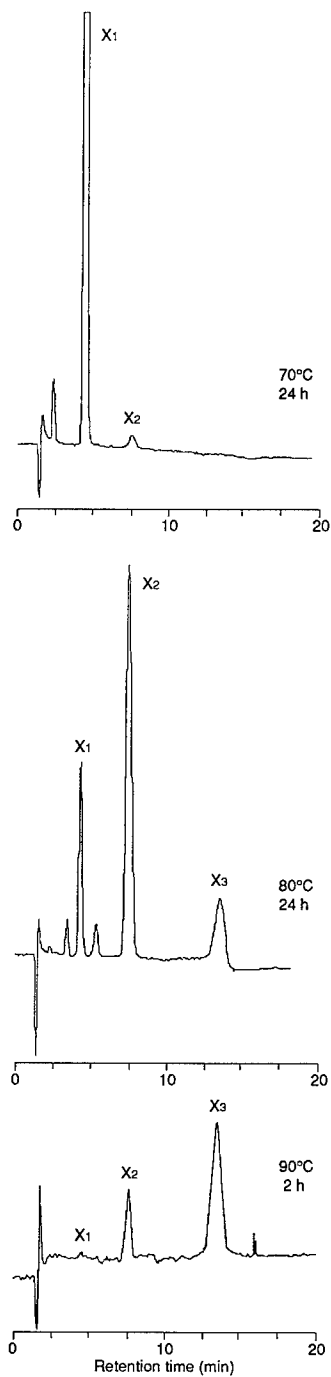
FIGURE 2. Hydrolysis of birchwood xylan at different temperatures. The analyses were carried out on HPAE-PAD Dionex, as reported in the text. Terms: x_1, xylose; x_2, xylobiose; x_3, xylotriose.

The extracellular activity levels produced by the strain were low. This is probably a reflection of the nature of the environment, in which secretion of large amounts of extracellular enzymes would be uneconomical for the organism.

The practical utilization of this strain for xylanase production would require genetic improvement of the microorganism to increase the xylanase production levels.

REFERENCES

1. BIELY, P. 1985. Trends Biotechnol. **3:** 286–290.
2. WONG, K. K. Y., L. U. L. TAN & J. N. SADDLER. 1988. Microbiol. Rev. **52:** 305–317.
3. NANMORI, T., T. WATANABE, R. SHINKE, A. KOHNO & Y. KAWAMURA. 1990. J. Bacteriol. **172:** 6669–6672.
4. NICOLAUS, B., L. LAMA, E. ESPOSITO, M. C. MANCA, G. DI PRISCO & A. GAMBACORTA. 1996. Polar Biol. **16:** 101–104.
5. BERNFELD, P. 1955. Amylases α and β. *In* Methods in Enzymology. Volume 1. S. I. Colowick & N. O. Kaplan, Eds.: 149–158. Academic Press. New York.
6. BRADFORD, M. M. 1976. Anal. Biochem. **72:** 248–254.

Influence of Environment Modifications on Enzyme Catalysis

Comparison of Macromolecular and Molecular Effects of Cosolvents on Lipoxygenase Reactions

HUGUES BERRY, CHRISTINE LAMBERT,
AND VÉRONIQUE LARRETA-GARDE[a]

Laboratoire de Technologie Enzymatique
University of Compiègne
60206 Compiègne Cedex, France

INTRODUCTION

With the emergence of biocatalysis in nonconventional media, it has been pointed out that enzymatic events are highly sensitive to modifications of the microenvironment and that the nature and state of the solvent greatly influence the reactivity of enzymatic proteins.[1] Cosolvent-containing media may thus be used to elucidate the relationship between the catalytic activity of the protein and the surrounding aqueous solution and may provide a possible model to approach *in vivo* catalysis.

Soybean lipoxygenase-1 had previously been studied in low-hydrated media with linoleic acid as a substrate and several significant differences were reported[2,3] in relation to changes of the reaction medium: either an amplification or decrease of the dioxygenation reaction, variations of specificity, and modifications of secondary reactions. Those results indicated a similar qualitative behavior of the enzyme regardless of the cosolvent used, whereas quantitative differences implied the identity of the additive. Both macroscopic and microscopic influences may be evoked: the former deals with a general effect of the additives on the structuration of the medium and its physicochemical and thermodynamical properties; the latter implies an effect of the cosolvents, at the molecular level, on the structure of reacting molecules.

The purpose of this work is to compare the effects of water-soluble cosolvents at molecular and macroscopic levels and to contribute to the determination of the relation between their presence in the reaction medium and the catalytic behavior of soybean lipoxygenase-1.

MATERIALS AND METHODS

Type-1 lipoxygenase was purified from soybean seeds as previously described.[4] Linoleic acid and arachidonic acid were purified and used at a final concentration of

[a]To whom all correspondence should be addressed.

300 μM. Dioxygenation activity was measured using a polarographic method convenient for lipoxygenase activity measurement in cosolvent-containing media.[5] Immobilization was performed with a co-cross-linking method using bovine serum albumin and glutaraldehyde at subzero temperature.

RESULTS

Macroscopic Effects

First, the consequences of the addition of water-soluble cosolvents (glycerol, sucrose, and salts) to the aqueous reaction medium were considered at a macroscopic level.

Water Activity

Water activity is a thermodynamical parameter that reports on the global effect of a compound on the availability of water. Lipoxygenase (LOX) was chosen as a model enzyme as it is very active ($k_{cat}/K_M = 5 \times 10^6$ $M^{-1} \cdot s^{-1}$) and does not use water as a reactant. Soybean lipoxygenase-1 activity was reported as a function of the reaction-medium water activity (FIGURE 1). When the additive concentration increases, the medium water activity decreases. The curves show a maximum, whereas an increasing function is usually observed. Moreover, the highest lipoxygenase activity was not obtained at a single water activity value, but the maximum depended on the identity of the additive. However, a high a_w (> 0.85) is required to observe a significant activity and a narrow range of high water activity (0.94 to 0.98) contained all the observed maxima. The same behavior was observed for linoleic and arachidonic acids, even though the two substrates differ in their carbon number and unsaturation.

Viscosity

The tested additives are viscosigens. Previous studies demonstrated that enzyme activity may be very sensitive to the medium viscosity. The limiting effect of viscosity on lipoxygenase activity was high for viscosity values $\geq$ 20 mPa·s (FIGURE 2). For lower values, the activity rate was not affected by viscosity, with activities even higher than in buffer being observed; the maxima lay between 2.5 and 9 mPa·s. The influence of viscosity was dependent on which substrate was used: the reaction was less affected by a viscosity increase with arachidonic acid than with linoleic acid.

pH and Ions

Type-1 soybean lipoxygenase is known to present a maximal activity with a single peak at pH 9.0, whereas other enzymes are more efficient at pH 7.0.[6] Moreover, using iron EPR, the sensitivity of the enzyme to ions has been demonstrated.[7] We tested the influence of pH without buffering the reaction medium by using diluted solutions
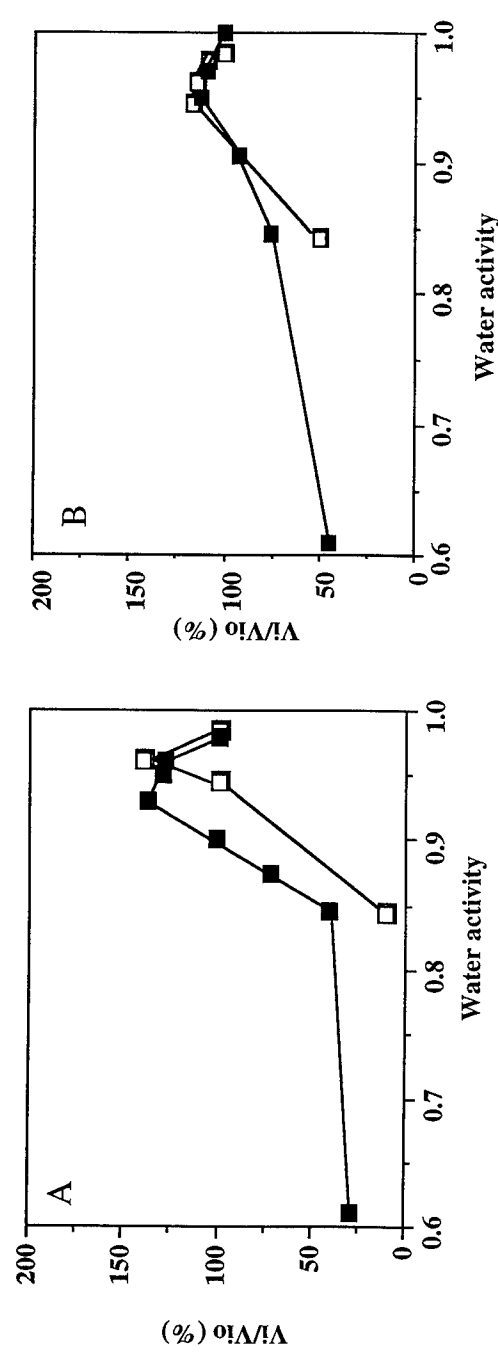
FIGURE 1. Relative activity of soybean lipoxygenase-1 as a function of water activity of the reaction medium containing glycerol (■) or sucrose (□). Substrate: (A) linoleic acid; (B) arachidonic acid. V_{i0} is the initial activity in the absence of cosolvent, equal to 120 μmol/min·mg LOX.
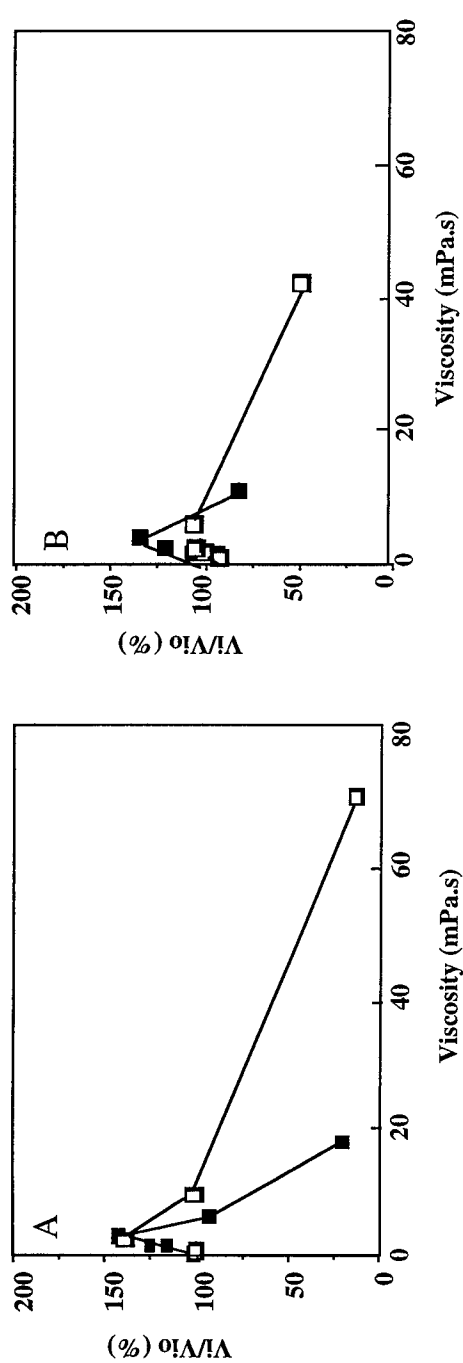
FIGURE 2. Relative activity of soybean lipoxygenase-1 as a function of viscosity of the reaction medium containing sorbitol (■) or sucrose (□). Substrate: (A) linoleic acid; (B) arachidonic acid. V_{i0} is the initial activity in the absence of cosolvent, equal to 120 μmol/min·mg LOX.
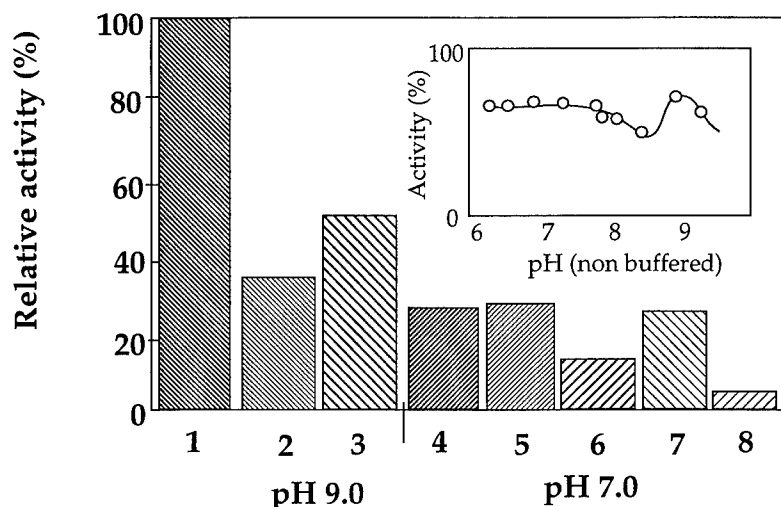
FIGURE 3. Lipoxygenase relative activity as a function of buffer at pH 9.0 for buffers 1, 2, and 3 and at pH 7.0 for buffers 4 to 8; 100% activity is equal to 120 μmol/min·mg LOX. Buffers—1: 0.1 M pyrophosphate buffer; 2 and 5: NaOH; 3 and 4: 0.04 M Veronal buffer; 6: 0.1 M Na-phosphate; 7: 0.1 M Tris-maleate; 8: 0.1 M K-phosphate. (Inset) Lipoxygenase activity as a function of reaction medium pH in nonbuffered media.

of NaOH and HCl; no pH variation is induced by the reaction itself. The usual pH dependence is not observed and maximal activity was measured at both pH 7.0 and pH 9.0. Several buffers were thus compared (FIGURE 3). The influence of ions is more important than the one of pH.

Although a macromolecular effect may drastically affect lipoxygenase catalysis for high cosolvent concentrations, a low salt, sugar, or polyol content may implicate a direct effect on the enzyme at the molecular level.

Effects at the Molecular Level

The influence of cosolvents on enzyme structure was considered. In a previous study,[3] slight differences in enzyme conformation induced by the addition of polyol to pyrophosphate buffer were evident. A modification of the position of aromatic residues was observed as well as an activation of the enzyme. Here, immobilization was used to further investigate the relationship between activity and microenvironment. It has been verified that immobilization restrains molecular movements. Lipoxygenase was immobilized in one buffer and used in another (TABLE 1). To exert a positive influence on lipoxygenase, pyrophosphate must be located in its microenvironment. As this influence is conserved after immobilization when used in another buffer, as previously observed for sorbitol,[2] we may suppose that it proceeds through similar slight variations in structure.

DISCUSSION

In order to evaluate the role of the reaction medium on the catalysis of lipoxygenase at a macroscopic level, the relation between various physicochemical parameters and enzyme activity was explored. Soybean lipoxygenase presented unusual dependences on these parameters; an optimal cosolvent concentration was observed for each substrate. The global parameters describing the reaction medium are not sufficient to totally control the catalytic behavior of the enzyme. However, by varying both the additive used to modify the environment and the substrate, this allowed for the determination of a critical range for each parameter corresponding to a maximal enzyme activity. The important point is not the actual value of these physicochemical parameters, but the fact that they are indicative of a particular organization of water around the enzyme, the substrate, the cosubstrate, and the cosolvent molecules. All the activity maxima correspond to a single range of additive concentration varying between 25 and 40 g of additive/100 g of solution.

For high concentrations of additives (above 40 g of additive/100 g of solution), reactant hydration and diffusion are not optimal—as indicated by water activity and viscosity measurements—which explains the decrease of enzyme activity. For low concentrations of additives (below 25 g of additive/100 g of solution), the media present almost the same water activity, viscosity, or surface tension regardless of the additive used. Thus, the quantitative differences observed in enzyme activity may implicate the identity of the used additives. The various effects of ions and pH are other illustrations of the limitation of global parameters to describe lipoxygenase behavior. The different cosolvents could exert different influences at the molecular level as already evoked.[2]

Using a spectroscopic method, it has been shown[3] that some slight structural modifications are induced by cosolvents, with the amplitude of the variation depending on the used additive. This observation is confirmed by fluorescence studies. Immobilization with covalent bonding was here used as a tool to "freeze" the enzyme

TABLE 1. Influence of 0.01 M Pyrophosphate on Lipoxygenase Activity in Various Conditions

Immobilization and Catalysis Conditions	Activity (μmol/min·mg LOX)	Relative Activity (%)
No immobilization; activity measured at pH 9.0 in 0.04 M Veronal buffer	87	100
No immobilization; activity measured at pH 9.0 in 0.01 M pyrophosphate buffer	123	140
LOX immobilized in 0.04 M Veronal buffer, pH 9.0; activity measured at pH 9.0 in 0.01 M pyrophosphate buffer	15	100
LOX immobilized at pH 9.0 in 0.01 M pyrophosphate buffer; activity measured at pH 9.0 in 0.04 M Veronal buffer	21	138

structure. These experiments have shown that the variations of enzyme structure are directly implicated in the activation of the enzyme and that ion-induced structural variations are additive to the ones produced by sugars and polyols.

Both macromolecular and molecular effects seem to be involved in the modification of lipoxygenase catalysis induced by the addition of water-soluble cosolvents to the reaction medium. It now appears unavoidable to consider that cosolvents exert two opposing effects on the enzyme:

(1) even at low concentrations, they induce slight conformational variations that may be favorable for enzyme activity;

(2) over a threshold of high additive concentration, the macroscopic influences are significant and they prevent the enzyme from expressing its activity normally.

The net influence of the additives on enzyme activity is thus dependent on the relative importance of these two antagonistic effects, directly related to the cosolvent chemical nature and concentration.

REFERENCES

1. TRAMPER, J., M. H. VERMUE, H. H. BEEFTINK & V. VON STOCKAR, Eds. 1992. Biocatalysis in Non-conventional Media. Prog. Biotechnol. Volume 8, p. 253–260. Elsevier. Amsterdam/New York.
2. LAMBERT, C., C. POURPLANCHE, M. BERJOT, J. C. MARX, A. J. P. ALIX & V. LARRETA-GARDE. 1995. Ann. N.Y. Acad. Sci. **750:** 44–50.
3. POURPLANCHE, C., C. LAMBERT, M. BERJOT, J. MARX, C. CHOPARD, A. J. P. ALIX & V. LARRETA-GARDE. 1994. J. Biol. Chem. **269**(50): 31585–31591.
4. GALEY, J. B., S. BOMBARD, C. CHOPARD, J. J. GIRERD, F. LEDERER, T. DO-CAO, H. N. N'GUYEN, D. MANSUY & J. C. CHOTTARD. 1988. Biochemistry **27:** 1058–1066.
5. POURPLANCHE, C., V. LARRETA-GARDE & D. THOMAS. 1991. Anal. Biochem. **198:** 160–164.
6. CHRISTOPHER, J., E. PISTORIUS & B. AXELROD. 1970. Biochim. Biophys. Acta **198:** 12–19.
7. GAFFNEY, B., D. MAVROPHILIPOS & K. DOCTOR. 1993. Biophys. J. **64:** 773–783.

Heat-proof Enzymes by Thin Film Technology[a]

C. NICOLINI

Institute of Biophysics
University of Genoa
and
ELBA Foundation
16153 Genoa, Italy

INTRODUCTION

Recent studies on heat-proof protein monolayers prepared by a modified Langmuir-Blodgett (LB) technique[1-3] appear to have the kind of implications that might lead the way to a new revolutionary protein-based nanotechnology, capable of capturing the immediate interest of a wide audience ranging from biotechnologists to electronic engineers and material scientists.[2,4] Typically, LB films of most organic compounds are formed in a Langmuir trough by spreading the solutions at the liquid-gas interface and transferring by a vertical-lift technique onto solid substrate. In our laboratories, protein monolayers are instead usually prepared with a horizontal-lift (Langmuir-Schaefer) (LS) technique properly modified to avoid protein denaturation due to high surface tension present at the air-water interface and then deposited on solid substrates over a wide range of surface pressure.[1,3,5] More recently, we have also utilized an ad hoc implemented adsorption trough.[6]

In order to outline the unique structural and functional properties and the biotechnological potential applications of this new nanotechnology to enzyme engineering, we summarize all the recent structural and functional assays on a few model enzymes both in solution and in thin films, underlining the still-open problems and the possible corresponding solutions. Nearly all the chosen enzymes have been well characterized in solution by X-ray crystallography and their three-dimensional structures are known at atomic resolution. In summary, as model systems, we have utilized three water-soluble enzymes for the LS-induced heat stability, namely, glutathione-S-transferase (GST), urease, and alkaline phosphatase (AP).

THIN ENZYME FILMS PRODUCED BY A NEWLY MODIFIED LANGMUIR-SCHAEFER TECHNOLOGY

To produce the film by classical LB technique, the solution of amphiphilic molecules consisting of hydrophilic groups interacting strongly with water and long

hydrocarbon chains is spread at the interface.[2,7] As proteins are not ordinary amphiphilic molecules suitable for the LB technique, several chemical (reverse micelles, derivatization) and biotechnological (site-specific mutagenesis, subphase) modifications need to be introduced in the standard LB technique to preserve the native protein structure and function at the air-water interface (for a comprehensive review, see references 2–4 and 7). All proteins were transferred by the LS technique (horizontal lift) as it is the most suitable to provide homogeneous reproducible coverage of the substrates with such type of monolayers. A new alternative approach implemented with an "in-house"-developed adsorption trough[6] is to close the substrate with the monolayer deposited by dipping down the latter with a plate located in the vicinity of the substrate. If then the substrate is removed together with the "closing" plate from the water subphase, water will be held between the plate and the substrate by capillary forces,[6] preventing any protein denaturation. The issue of protein monolayer formation at the air-water interface is critical for the preservation of native protein structure and function. The values of the forces are comparable with those of the surface tension. Thus, during the spreading of protein monolayers over the water surface, there is always a risk of denaturing the protein structure. There are some examples in the literature (e.g., cytochrome c) where such behavior really takes place and which can be overcome by utilizing reverse micelles[8] and protein derivatization.[2,7]

Nevertheless, all enzymes being deposited onto solid substrates by our LB method demonstrate a preservation of structural properties, as confirmed by numerous techniques (see FIGURES 1 and 2). The surface concentration of proteins, indirectly estimated from compression isotherm analysis, can be directly measured on solid substrates by a nanogravimetric technique. The subphase is typically a buffer solution of low ionic strength and with pH values around neutral. The total volume of the subphase is about 80 mL, with a protein solution in the same buffer deposited at a concentration of about 2.5×10^{-6} M. One or more layers can be quickly and successfully deposited and their thickness determination can be carried out by ellipsometry.[2] In order to assess the effect of film formation on the native protein structure, CD spectra have been recorded in solution and in LB films of GST at different surface pressures (FIGURE 1); by this and other (FIGURE 2) structural and functional probes, optimal conditions can be determined for the LB film assembly of all enzymes. This can be confirmed by the experimental evidence, where the average monolayer thickness assayed by ellipsometry increases towards its native protein value with increasing surface pressure, as the holes in the LB film tend to disappear.[9] The surface pressure strictly determines the orientation and subsequent monolayer thickness, in perfect agreement with the geometric features of the very same proteins independently determined by X-ray crystallography in solution.[2] With the only exceptions of cytochrome c and azurin, we can exclude in general the possibility of the presence of a denatured protein in the LB film on the water-surface interface and on the solid substrate; the dependence of the thickness on the number of layers as determined by means of nanogravimetry, ellipsometry, and interferometry represents indeed an unambiguous experimental proof of the absence of any denatured protein in the layer. Furthermore, usually prior to deposition on the activated substrate, the enzyme films are covalently bound to the surface, dried, and rinsed rather vigorously with water, a very important step in order to exclude the eventual

presence of any denatured sublayer. Everything that is not bound is washed out by the water jet.

ENZYMATIC ACTIVITY IN LB THIN FILMS

A significant residual functional activity is generally preserved in the LS films of all enzymes being so far studied, but to a quite different degree, as apparent in TABLE
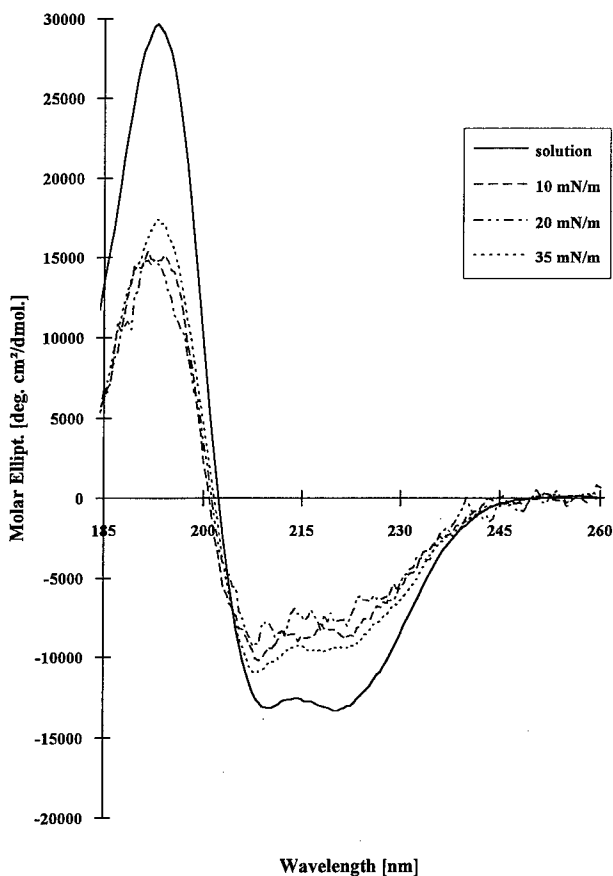
FIGURE 1. CD spectra of GST in solution and in LB monolayer versus surface pressure.

1. Despite occasional problems, the formation of LS film is successful even without micelles with all enzymes being tested so far (TABLE 1). The utilization of reverse micelles, which increases the protein yield recovered from the original solution, causes indeed a minor, but significant, reduction of the enzymatic activity (not shown). Each enzyme forms a stable LS monolayer up to a critical surface pressure, above which it collapses, as monitored in real time by Brewster microscopy (see
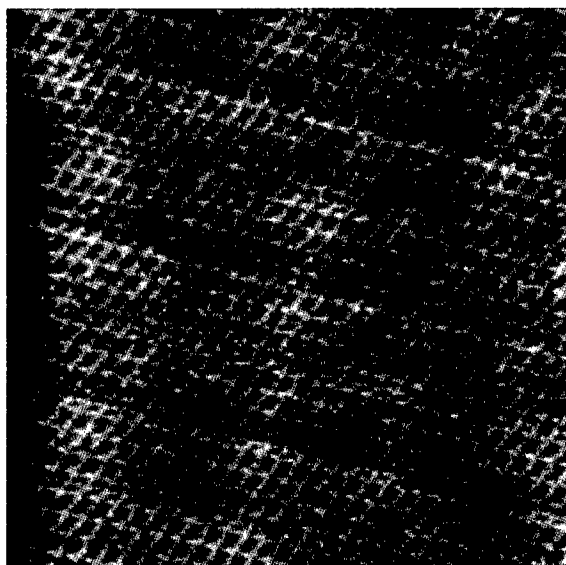
FIGURE 2. STM image of a monolayer of GST deposited by the modified LB technique on highly oriented pyrolytic graphite (HOPG). Image size: 750×900 Å; $V = 0.2$ volts (STM made by Asse-Z, Padua, Italy).

FIGURE 3 for the GST enzyme). Alkaline phosphatase (AP) has required the most extensive experimentation in order to optimize the film formation. The average activity of GST, urease, and AP LB film was observed and is summarized in TABLE 1, ranging between 2% and 9% of the solution value for the film deposited on nonsilanized silicon substrates, without micelles, for 30 minutes. It should be mentioned that the background spontaneous reactions in terms of the optical-density changes per unit time are approximately 44%, 8%, and 4% of the enzymatic activity in LS films for GST, AP, and urease, respectively. In a test case of GST, the film enzymatic activity was analyzed spectrophotometrically following the conjugation of glutathione (GSH) to 1-chloro-2,4-dinitrobenzene (CDNB) and the kinetics of product formation [1-glutathione-2,4-dinitrobenzene (GDNB)]. The kinetic constants of the Michaelis-Menten equation, that is, K_m and V_{max}, were estimated and compared to the solution values.

Thermal treatment of the samples was performed under "dry" conditions (i.e., in an oven up to 423 K) and the rather low residual activity (but significantly higher than the known background reaction) was evaluated.[10] GST is a member of a family of enzymes that play a physiological role in the detoxification of potential alkylating agents, including pharmacologically active compounds. These enzymes catalyze the nucleophilic addition of the thiol of GSH to electrophilic acceptors, such as aryl and alkyl halides, quinones, and organic peroxides. The analysis of the obtained data allowed for the selection of working conditions (such as subphase, speed of compression, deposition pressure, and pH) and helped to underline that the structure and the functional activity of the enzyme were preserved after its deposition.

Starting from these results, in a more recent work,[10] a kinetic study of GST in LB film deposited onto activated/inactivated silicon supports has been carried out. Long-range storage activity and thermal stability were also proven to last for over one year at an identical low level. The association constant was the same as in solution (see FIGURE 4) and the main difference was found to be the rather low value of the V_{max} constant (TABLE 2). In the monolayer assembled with our adsorption trough,[6] the enzymatic activity was significantly higher and quite close to the corresponding solution value for GST (FIGURE 4 and TABLE 1) and all other tested enzymes. The dramatic decrease of V_{max} for LS films with respect to that in solution could be explained by considering the combined effects of deposition and packing degree. In fact, the access to the active sites is prevented by the orientation and by the rigidity imposed by the surrounding enzyme molecules. GST is a dimeric enzyme of globular shape with each subunit being $53 \times 62 \times 56$ Å^3 and about 25 kDa. The enzyme contains two active sites and each subunit functions independently.[11] The active site is located in a deep cavity (19 Å), which is composed of three relatively mobile structural elements and is proposed to consist of a glutathione-binding region (the G-site) and a hydrophobic region (the H-site) to accommodate the electrophilic substrates.[11] Therefore, an unsuitable orientation could practically inactivate the enzyme in the film, as shown by the decreased activity with increasing surface pressure (TABLE 1). Moreover, as shown in a recent work,[12] an enzyme molecule is subjected to reversible conformational changes during its catalytic function that could be limited by the high film packing. The difference between the V_{max} constant of LS films immobilized and those not immobilized (TABLE 2 and FIGURE 3) was mainly due to the presence of epoxy groups on the surface that react with the GST

TABLE 1. Enzymatic Activity (mol/min of Product per mol of Enzyme) of Monolayers of GST and AP[a]

Sample	GST	AP
LS (20 mN/m)		
silanized	293 (370)	—
nonsilanized	160 (182)	—
LS (35 mN/m)		
silanized	—	700
nonsilanized	100 (182)	4210
LS (45 mN/m)	*	
silanized		1390
LS (55 mN/m)	*	
silanized		1900
Adsorbed monolayer	1418 (2394)	—
Solution	1820 (2820)	83,900 (97,900)
Spread	600 (855)	13,100 (25,900)

[a]These enzymes were either "adsorbed" by our newly developed trough or immobilized by the Lagmuir trough (LS) at different surface pressures onto silicon substrates (silanized or nonsilanized). The average value and the best value (in parentheses) of the enzyme activity were determined at 25 °C, after subtracting for the background due to spontaneous reactions among all added reagents in the absence of the corresponding enzyme. An asterisk indicates that the film is collapsed, as monitored in real time by Brewster microscopy.
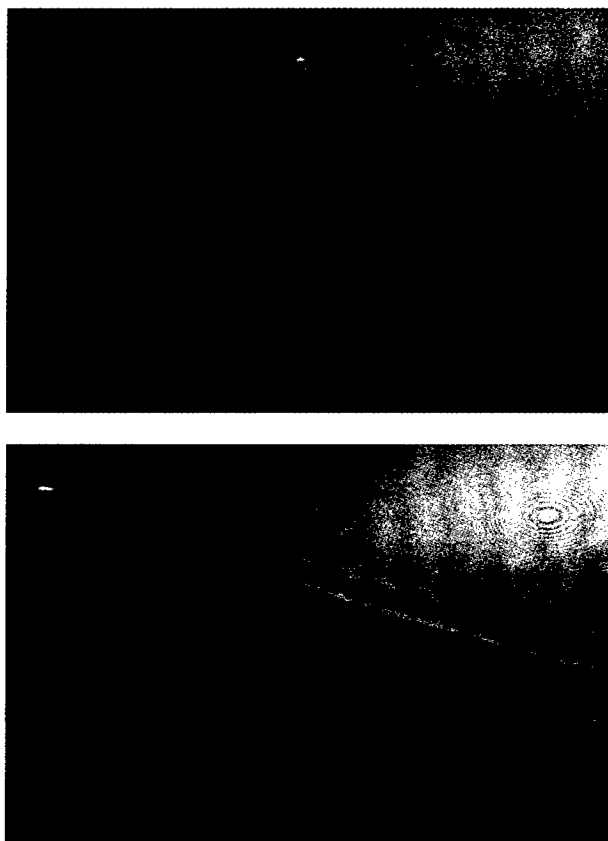
FIGURE 3. Brewster microscopy of the GST LS monolayer at (top) 25 and (bottom) 35 mN/m.

lysine residues.[10] In fact, the silanizing agent likely allows the maximization of the functional activity of the enzyme by increasing the order of the film.

Similar findings are obtained for the other two enzymes being tested, namely, alkaline phosphatase[13] and urease.[14] AP from calf intestine was bound to Hybond-N+ membranes by direct spreading and by the Langmuir-Schaefer deposition technique. Before use, 9 × 30–mm pieces of membrane were attached to glass slides to ensure a plane surface for the horizontal lift. The activity assays were performed by direct monitoring of the product formation by spectrophotometry with magnetic stirring inside the cuvette. Comfortingly, no detachment of enzyme was observed during the assay of membrane-bound LS films. Indeed, subsequent assays do not show a decrease of activity and no reaction was observed after removal of the membrane from the reaction volume.

Drying of the membrane at room temperature in a desiccator results in a sensible loss of activity for the spread, but not for the LS deposited enzyme. AP molecules are

very hydrophilic and it was impossible to obtain any noticeable amount of protein at the pure water surface. To form a stable AP monolayer, the effect of salting out of protein from aqueous solutions with high ionic force was used. A high surface pressure (up to 60 mN/m) was obtained on the 3 M solutions of NaCl and $(NH_4)_2SO_4$.
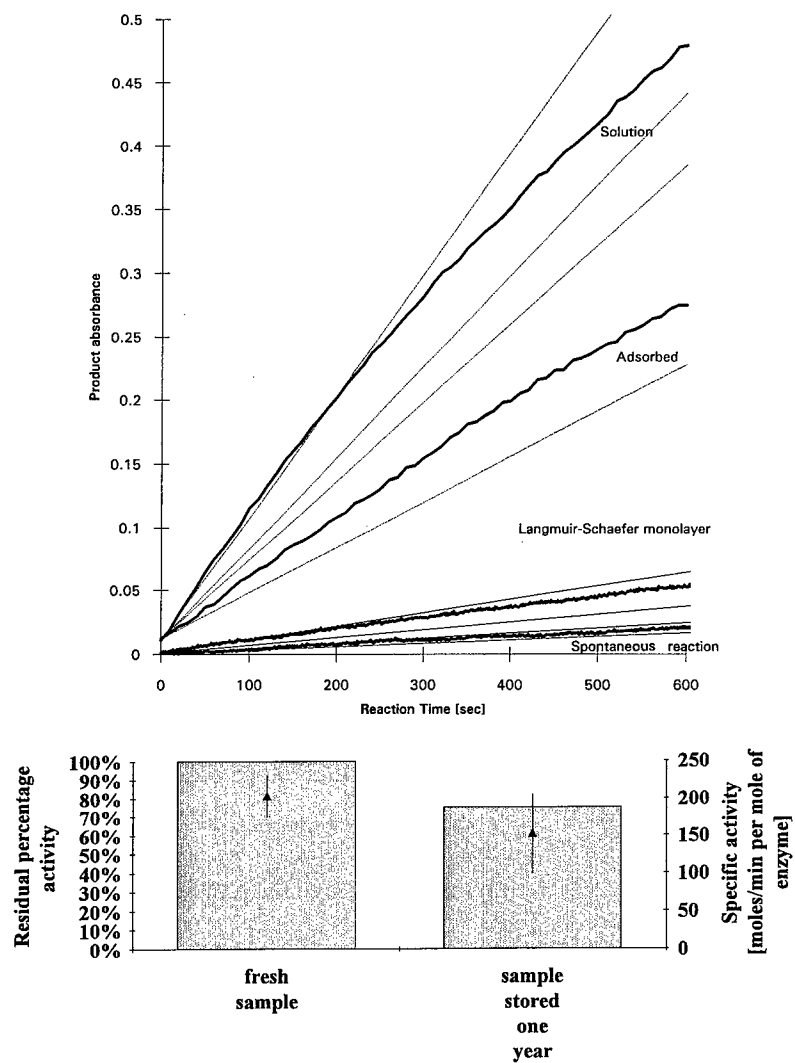
FIGURE 4. (Top) Enzymatic activity in absolute values (product absorbance per second) for GST in solution and in film made by either the LS or adsorption trough. (Bottom) Functional activity of fresh and of long-term (one-year) stored GST LS monolayers immobilized on a silanized silicon surface.

TABLE 2. Kinetic Parameters of GST in Solution and in LB Film

Kinetic Parameters	Solution	LB Film	Immobilized LB Film
K_m [mM]	0.13 ± 0.015	0.183 ± 0.054	0.16 ± 0.032
V_{max} [mol/min per mol of enzyme]	1820 ± 180	160 ± 50	293 ± 58

HEAT-PROOF PROTEINS IN LB THIN FILMS

One common feature of all of the protein LS films is the high thermal stability of the protein structure, both secondary and higher, and function as shown in several recent papers,[1,3,9,10,15] practically all demonstrating the preservation of the secondary structure up to 200 °C when organized into the film (TABLE 3). The first question that we addressed was about the generality of the preservation of the protein secondary structure in LS films under thermal treatment previously reported for membrane proteins. As summarized for the enzymes in TABLE 3, heat-proof protein structure up to now has been firmly established for LB films of RC,[1,16] GST,[9] AP,[13] bacterial[17] and bovine[18] rhodopsins, urease,[14] thioredoxins, cytochrome P450,[4] C551, and azurin metalloproteins. The circular dichroism data also confirm that, in all of the above cases, protein secondary structure is not affected by temperature. Furthermore, the enzymatic activity appears unaltered at three increasing temperatures (TABLES 3 and 4), confirming that even the enzyme function is "heat-proof" to a significant degree in LS films. This thermal stability was already found for other kinds of proteins, such as RC,[1,3,19] and for antibodies[3] and rhodopsins.[18] The "heat-proof" enzymatic activity was retained, even if significantly affected by the LS procedure, whereas the "heat-proof" functionality was completely lost when the enzyme was free in solution.[9,10] Interestingly, the enzyme activity is maximized when the deposition is carried out onto an activated surface (TABLE 1).

The enzymatic activity of immobilized GST films was also measured at room temperature on one-year-stored LS films (one monolayer thick and never utilized before) and after wet thermal treatment. It was found that enzyme films stored at 277 K will preserve their catalytic function and thermal stability, indicating that the silanizing agent and the storage itself do not affect the protein properties in the film (see bottom panel of FIGURE 4).

Similar data were obtained with AP deposited from 3 M NaCl, $(NH_4)_2SO_4$, and $CaCl_2$ subphases, which gave the best results in terms of surface pressure whenever silicon nitride and optical glass were used as substrates (TABLES 1, 3, and 5). In order to remove the salts from deposited films, substrates were washed with distilled water until optically transparent films were obtained.[13] Comfortingly, AP deposited from

TABLE 3. Functional and Structural Melting Temperatures (°C) of Proteins in Solution and in LS Thin Film

Protein	GST	AP	Urease
Solution structure	60 °C	60 °C	60 °C
LB film structure	> 150 °C	200 °C	190 °C
Solution functional activity	60 °C	60 °C	60 °C
LS film functional activity	> 150 °C	> 150 °C	> 150 °C

TABLE 4. Temperature-dependent Specific Activity[a] of the GST Enzyme in Solution and in LS Film (One Layer Thick)

Temperature	Solution	Spread	LB Film	LB Film Immobilized
298 K	$11.3 \cdot 10^{11}$	$2.8 \cdot 10^{10}$	$9.9 \cdot 10^{10} \pm 2.9 \cdot 10^{10}$	$2.2 \cdot 10^{11} \pm 4.4 \cdot 10^{10}$
353 K	0	$2.1 \cdot 10^{10}$	$8.2 \cdot 10^{10} \pm 2.4 \cdot 10^{10}$	$1.9 \cdot 10^{11} \pm 3.8 \cdot 10^{10}$
423 K	0	$1.6 \cdot 10^{10}$	$6.3 \cdot 10^{10} \pm 1.9 \cdot 10^{10}$	$1.6 \cdot 10^{11} \pm 3.2 \cdot 10^{10}$

[a]Given in terms of nmol/min per mol of enzyme.

the $CaCl_2$ subphase was fully inactive. Active AP films deposited from the NaCl and $(NH_4)_2SO_4$ subphases were studied by varying the surface pressure and monolayer number with good results (TABLE 1). The films were characterized by circular dichroism spectroscopy, ellipsometry, and microgravimetry. The measurements show that a sufficient anchoring can be achieved by covalent binding of the proteins to the silanized substrate because, only in this case, the film does not detach from the substrate during washing. Contrary to GST, the enzymatic activity of the films increases with the pressure of deposition, being proportional to the protein surface density (TABLE 1). Testing of the variations in secondary structure and enzymatic activity as a function of temperature shows that AP assembled in the film possesses a much higher thermostability than in solution. The activity and secondary structure of the protein remain unaltered after heating up to 150 °C and up to 45 mN/m (TABLE 5 and FIGURE 5).

AP is an enzyme widely used for hydrolysis of phosphate esters in various preparation techniques, for determination of theophylline, for antibody-enzyme coupling procedures, etc.[20] If we compare the thermal stability of AP in LB films with that in solution, the activity of the films decreases by two times on the average at 80 °C, whereas AP solution at the same temperature loses its activity completely. The secondary structure analysis also reveals a higher thermal stability in films. CD spectra of the films and solutions of AP are rather similar at room temperature (see FIGURE 5). The minor difference between the two spectra may be attributed to the orientation of the molecules. In the film, they most likely have some preferential direction, whereas the orientation in solution is random. The spectra change in quite a different way upon heating: the spectrum of the film remains almost unaffected up to 200 °C, whereas that of the solution changes drastically at 100 °C. The behaviors of the molecular ellipticities of the film and solution with temperature are compared in FIGURE 5. One can see that the secondary structure in the film is preserved at 200 °C, whereas in the solution it changes in the temperature range from 65 °C to 100 °C. These data agree with recently published results[15,21] on the thermal stability of

TABLE 5. Enzymatic Activity (absorbance/second) of AP and Urease LS Film Deposited on Silanized Silicon Substrate at Optimal Surface Pressures versus Temperature[a]

	25 °C	80 °C	150 °C
AP	0.00395	0.00197	0.0015
Urease	0.000067	0.000055	0.000052

[a]The activity was determined at 25 °C, 80 °C, and 150 °C.
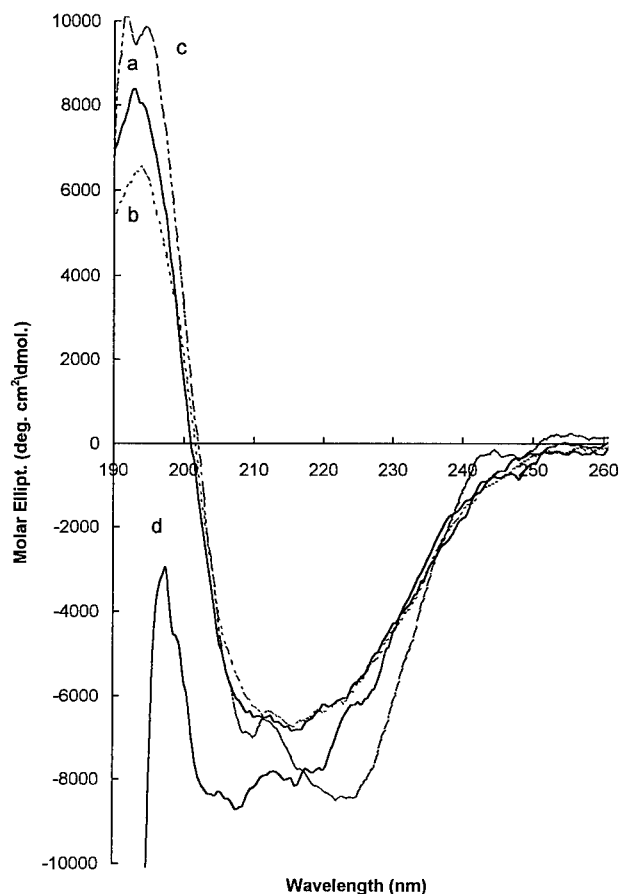
FIGURE 5. Molecular ellipticities of alkaline phosphatase in film (20 layers) at 25 °C (a) and 200 °C (b) and in solution (0.025 mg/mL, 2-mm optical path) at 25 °C (c) and 100 °C (d).

bovine rhodopsin, RC, and antibodies in LB films. The investigators observed the preservation of the structure and activity of the films up to 150 °C and proposed that molecular packing enhanced thermal stability. In view of our data, this effect seems to be general for enzyme films.[3]

BIOCATALYSIS

The application of biological materials to different branches of modern technology has expanded enormously during the recent period. Some of the applications that have already found their implementation are, for example, gene engineering–based production of biologically essential macromolecules, stereospecific biosynthesis with the utilization of specific enzymes (e.g., urease, ADH, AP, GST, and DNA

polymerase), and production of protein-based bioactuators. The recent discovery of the increased protein thermal stability in LS films opened new prospectives in the applications of protein films. One such application is the utilization of enzymes in biocatalysis. Nevertheless, one technical difficulty appears—enzyme films must be deposited onto small spheres in order to increase the number of enzyme molecules included in the process, thus providing a better performance of the reactor. In fact, an increased surface-to-volume ratio in the case of spheres will increase the number of enzyme molecules at fixed volume of the reactor. Moreover, as most of the enzymatic reactions are carried out in liquid phase, the molecules must be attached chemically to the sphere surface in order to prevent their detachment during functioning. A technique for deposition of the enzyme LS films over glass spheres was developed and adapted to enzyme-catalyzed processes (FIGURE 6). The sphere surface was activated by siloxane polymer. The activated spheres were distributed onto the enzyme preformed film (urease or GST) at the air-water interface. The
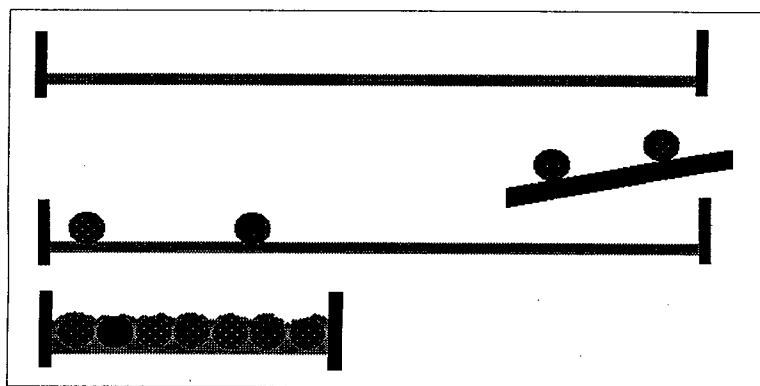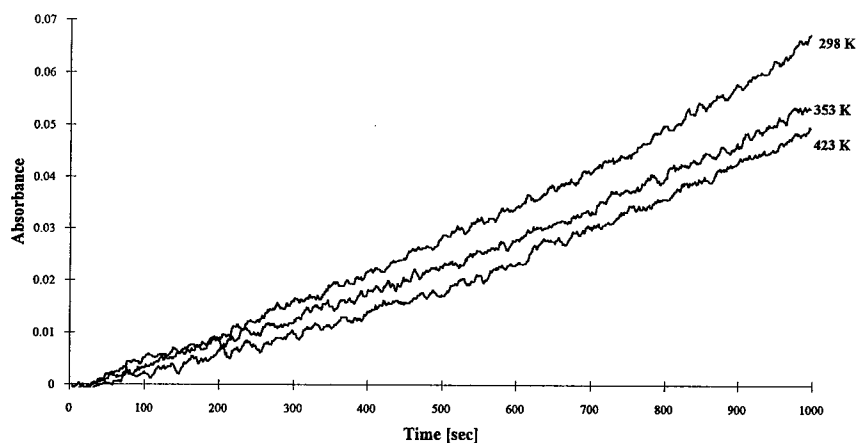
FIGURE 6. (Top) Activity test of urease in solution at 298 K and in LB film deposited on glass spheres at 298 K, 353 K, and 423 K. (Bottom) Scheme of the deposition procedure. In solution, the enzymatic activity of urease is consistently zero at 353 K and 423 K.

spheres covered with the enzyme layer were collected and dried.[22] The spectrophoto-metric measurements revealed that the activity of such enzyme films was preserved even after heating up to 150 °C (FIGURE 6). Thus, thermal stability enlarges the areas of application of protein films. In particular, one can suppose that it is possible to improve the yield of reactors based on enzymatic catalysis by increasing the tempera-ture of the reaction and using enzymes deposited by the LS technique. FIGURE 6 confirms the success of our technique to deposit enzyme LS films on the surface of small glass spheres, as shown by the presence of significant enzymatic activity of such samples before and after thermal treatment.

The experiments were done with two enzymes, urease (FIGURE 6) and GST. Both enzymes were chosen because their activity can be easily tested by spectrophotomet-ric measurements. Borosilicate glass spheres with a diameter of 1 mm were used as substrates for the deposition. The surface of the spheres was activated in the following way. Spheres were treated with boiling chloroform, rinsed on a glass filter, and dried under nitrogen. These spheres were silanized with 3-glycidoxypropyl trimethoxysilane in accordance with the technique proposed by Malmquist and Olofsson.[23] The silanization of the spheres was performed in nitrogen flux in order to prevent mutual attachment of the spheres and to activate their surface homoge-neously. The essential steps of the deposition procedure, which are the same for both enzymes, are illustrated in the bottom panel of FIGURE 6 and are described in detail in reference 22. The enzymatic activity of GST was evaluated as described previously. The GSH and CDNB concentrations were 2.5 mM and 0.5 mM, respectively. The diffusion effects were avoided by carrying out the measurements under continuous stirring using a magnetic microstirrer (Bioblock Scientific) at a speed of 600 rpm. The results of the activity test of GST are presented in reference 22 and those of urease are given in FIGURE 6 and reference 22. As in the previous case, both enzymes remain active in LS films up to high temperature, underlining once more that the molecular close packing in LS film appears to be the critical parameter responsible for this phenomenon.

CONCLUSIONS

The understanding and attainment of protein thermal stability is a very important goal, from both basic and applied points of view, as it requires a deep knowledge of all the parameters involved in the structural stabilization and as it is of fundamental importance in all those cases where proteins are used as functional elements for biodevices and bioreactors. Indeed, recently, proteins—mainly those involved in electron transport, in molecular recognition, and in catalytic processes—have under-gone increasing utilization in many technological applications, from biosensors and biotransistors to biocatalysis. However, several of these applications require operat-ing temperatures higher than 100 °C, a condition under which most of the proteins are known to denature, including those isolated from extreme thermophiles. The usual approach to this problem is protein engineering, which, in addition to its inherent limitations despite overemphasized claims, requires enormous efforts and needs a specific approach for each individual protein under study. Therefore, it was very amazing when we (in March 1993),[1] by forming highly packed 2D-ordered

protein films by the LB technique, were able to employ a general procedure for stabilizing protein structure up to 200 °C that was lost at 55 °C in solution and at 150 °C in dried smears (a kind of self-assembled film). The procedure turned out to be of general validity and was proved to be effective on both water-soluble (antibodies and cytochromes) and membrane proteins [Photosynthetic Reaction Centers (RC) from *Rhodobacter sphaeroides*], stabilizing not only the structure, but also the function to a certain extent. Comfortingly enough, these findings were confirmed by an X-ray study with synchrotron radiation only five months later by Shen *et al.*[24] for dry self-assembled films of bacteriorhodopsin and, more recently, by Miyake *et al.*[25] for dried photosynthetic membrane film. It is worth noting that the thermal behavior of the dry self-assembled smears of membrane proteins such as RC and water-soluble ones, for example, antibodies, displays a behavior that is intermediate between that of solution and of LB film.[3,16,26,27]

The number of applications using heat-proof enzymes already appears significant in the area of biotechnology and will continue to increase rapidly over the coming years as Technobiochip Manufacturing (Marciana, Italy) will introduce this LS- and adsorption-based film nanotechnology (the latter quite more effective in the preservation of enzymatic activity, but significantly less in terms of "heat stability") into the world market. To offer a possible explanation of the striking thermal stability induced by the LS film formation, a systematic comparative study was recently carried out on the same protein isolated from mesophilic versus thermophilic microorganisms, both in solution and in LS film.[28] It is well known indeed that proteins from thermophilic microorganisms can be very similar to mesophilic ones, except for their general stability to heat, organic solvents, detergents, common protein-denaturing agents, and proteolytic enzymes.

ACKNOWLEDGMENTS

REFERENCES

1. NICOLINI, C., V. EROKHIN, F. ANTOLINI, P. CATASTI & P. FACCI. 1993. Biochim. Biophys. Acta **1158**: 273–278.
2. NICOLINI, C. 1995. Biosens. Bioelectronics **10**: 105–127.
3. EROKHIN, V., P. FACCI & C. NICOLINI. 1995. Biosens. Bioelectronics **10**: 25–34.
4. NICOLINI, C. 1995. Molecular Bioelectronics. World Pub. London/Singapore. In press.
5. LANGMUIR, I. & V. J. SCHAEFER. 1938. J. Am. Chem. Soc. **60**: 1351–1360.
6. TROITSKY, V. I., T. S. BERZINA, A. PETRIGLIANO & C. NICOLINI. 1995. Thin Solid Films. In press.
7. NICOLINI, C. 1996. Molecular Manufacturing. ELBA Forum Series Volume 2. C. Nicolini, Ed. Plenum. New York.
8. EROKHIN, V., S. VAKULA & C. NICOLINI. 1994. Thin Solid Films **238**: 88–94.
9. ANTOLINI, F., S. PADDEU & C. NICOLINI. 1995. Langmuir **11**: 2719–2725.
10. PADDEU, S., F. ANTOLINI, T. DUBROVSKY & C. NICOLINI. 1995. Thin Solid Films. In press.
11. WANG, R. W., D. J. NEWTON, A. R. JOHNSON, C. B. PICKETT & A. Y. H. LU. 1993. J. Biol. Chem. **268**: 23981–23985.

12. RADMACHER, M., M. FRITZ, H. G. HANSMA & P. K. HANSMA. 1994. Science **265:** 1577–1579.
13. PETRIGLIANO, A., A. TRONIN & C. NICOLINI. 1995. Thin Solid Films. In press.
14. PADDEU, S., A. FANIGLIULO, M. LANZI, T. DUBROVSKY & C. NICOLINI. 1995. Sens. Actuators **25:** 876–882.
15. FACCI, P., V. EROKHIN, F. ANTOLINI & C. NICOLINI. 1994. Thin Solid Films **237:** 19–21.
16. FACCI, P., V. EROKHIN & C. NICOLINI. 1994. Thin Solid Films **243:** 403–406.
17. EROKHIN, V., P. FACCI, A. KONONENKO, G. RADICCHI & C. NICOLINI. 1995. Thin Solid Films. In press.
18. MAXIA, L., G. RADICCHI, I. M. PEPE & C. NICOLINI. 1995. Biophys. J. **69:** 1440–1446.
19. ANTOLINI, F., M. TROTTA & C. NICOLINI. 1995. Thin Solid Films **254:** 252–256.
20. BERGMEYER, H. U., M. GRASSL & H-E. WALTER. 1983. *In* Methods of Enzymatic Analysis. Third edition. Volume 2. H. U. Bergmeyer, Ed.: 269. Verlag Chemie. Weinheim.
21. TRONIN, A., T. DUBROVSKY & C. NICOLINI. 1995. Langmuir **11:** 385–389.
22. EROKHIN, V., P. FACCI, T. DUBROVSKY, S. VAKULA, S. PADDEU & C. NICOLINI. 1996. Thin Solid Films. In press.
23. MALMQUIST, A. & B. OLOFSSON. 1989. United States Patent No. 4,833,093.
24. SHEN, Y., C. R. SAFINYA, K. S. LIANG, A. F. RUPPERT & K. J. ROTHSCHILD. 1993. Nature **366:** 48–50.
25. MIYAKE, J., T. MAJIMA, K. NAMBA, M. HARA, Y. ASADA, H. SUGINO, S. AJIKI & H. TOYOTAMA. 1994. Mater. Sci. Eng. C1 **2:** 63–67.
26. DUBROVSKY, T., A. TRONIN, S. DUBROVSKAYA, S. VAKULA & C. NICOLINI. 1995. Sens. Actuators **23:** 1–7.
27. DUBROVSKY, T., A. TRONIN & C. NICOLINI. 1995. Thin Solid Films **257:** 130–133.
28. DE CHIARA, C., G. NICASTRO, M. ROSSI, L. FRANZONI, P. FACCI, G. MASCETTI & C. NICOLINI. 1996. Biochim. Biophys. Acta. In press.

An Organic Solvent–tolerant Bacterium and Its Organic Solvent–stable Protease

HIROYASU OGINO, KIYOSHI YASUI,
FUMITAKE WATANABE, AND HARUO ISHIKAWA

Department of Chemical Engineering
Osaka Prefecture University
Sakai, Osaka 593, Japan

INTRODUCTION

Recently, enzymatic reactions using protease have been studied extensively for the synthesis of peptides and esters. If organic solvents are used as media for enzymatic reactions, the equilibrium of the reactions catalyzed by hydrolytic enzymes can be shifted toward completion of the reverse reaction of hydrolysis, that is, the synthetic reaction. The main disadvantage of employing organic solvents as the media for enzymatic reactions is that enzymes are easily inactivated or denatured. Therefore, as reviewed by Khmelnitsky et al.,[1] several methods have been investigated for stabilizing enzymes in the presence of organic solvents. However, if there are proteases that are naturally stable in the presence of organic solvents, they would be very useful for synthetic reactions. In this report, we isolated an organic solvent–tolerant bacterium that produced proteolytic enzyme and investigated the organic solvent stability of the proteolytic enzyme.

MATERIALS AND METHODS

Isolation of Microorganisms That Produce Proteolytic Enzyme

A small amount of soil from natural sources was suspended in sterilized physiological saline, and 100-μL portions of the suspension were spread on wheat meal medium plates containing 0.5% (w/v) wheat meal, 0.5% (w/v) glucose, 0.1% (w/v) yeast extract, 0.5% (w/v) gelatin, 0.35% (w/v) K_2HPO_4, 0.1% (w/v) KH_2PO_4, 0.05% (w/v) $MgSO_4 \cdot 7H_2O$, and 1.5% (w/v) agar. The medium plates were incubated at 30 °C for 24 to 48 hours.

Selection of Organic Solvent–tolerant Microorganisms

Microorganisms that produced proteolytic enzymes were plated on nutrient medium plates (90 mm in diameter) containing 0.5% (w/v) glucose, 0.5% (w/v) polypeptone, 0.3% (w/v) yeast extract, 0.05% (w/v) $MgSO_4 \cdot 7H_2O$, 0.25% (w/v) NaCl, and 1.5% (w/v) agar adjusted to pH 7.5 with NaOH. The medium plates were overlaid with about 7 mL of cyclohexane and were incubated at 30 °C for 24 hours.

Assay of Proteolytic Activity

Proteolytic activity was determined by assaying the hydrolysis of casein as a substrate at pH 8.5 and 30 °C. One unit of proteolytic activity was defined as the amount of enzyme that produces the casein digest equivalent to 1 μmol of tyrosine per min.

Organic Solvent Tolerance of Microorganisms

The organic solvent tolerance of the selected microorganisms was tested by using the solidified and liquid nutrient media. In the first set of experiments, the cells were spread on the nutrient medium plates. After addition of 7 mL of cyclohexane, they were incubated at 30 °C for 24 hours. In the second set of experiments, the microorganisms were cultured in 500-mL baffled Erlenmeyer flasks containing 50 mL of the nutrient liquid medium and 15 mL of organic solvent at 30 °C. In this experiment, all the cultivation flasks were plugged with chloroprene-rubber stoppers. The cell growth was studied by measuring the dry cell weight.

Organic Solvent Stability of Enzyme

The microorganisms were cultured aerobically in the absence of organic solvent and were removed from medium by centrifugation at 12,000g and 4 °C for 5 min. Protease was purified from the culture supernatant. Then, 1.5 mL of organic solvent was added to 5 mL of the purified protease solutions in test tubes (16.5 mm in diameter) with screw caps and incubated at 30 °C with shaking at 160 oscillations per min. The remaining proteolytic activities were measured after 10 days.

RESULTS AND DISCUSSION

Isolation of Strain PST-01

To obtain proteases that are stable in the presence of organic solvents, we isolated microorganisms that produced proteolytic enzymes using wheat meal medium plates. Organic solvent–tolerant bacteria were selected using nutrient medium plates overlaid with cyclohexane. Strain PST-01 was selected as the most potent producer of proteolytic enzyme.

Characterization and Identification of Strain PST-01

The microbiological properties of strain PST-01 were investigated according to the methods described in *Bergey's Manual of Systematic Bacteriology*. TABLE 1 summarizes the morphological and biochemical characteristics of strain PST-01. According to these results, it was identified as a strain of *Pseudomonas aeruginosa*.

Organic Solvent Tolerance of Ps. aeruginosa PST-01

The growth of strain PST-01 in the liquid medium containing cyclohexane was compared with that in the liquid medium containing no organic solvent in FIGURE 1. The doubling time of strain PST-01 in the nutrient broth containing cyclohexane was about 50 min and was similar to that without the organic solvent, but the dry cell weight of the culture in the presence of cyclohexane after 12 hours of cultivation was about one-half of that in the absence of cyclohexane. The decrease in the dry cell

TABLE 1. Microbiological and Biochemical Characteristics of Strain PST-01

Morphological Characteristics		Voges-Proskauer test	−
		Methyl red test	−
Shape	rods	Hydrogen sulfide formation	+
Gram stain	negative	Citrate utilization	+
Cell length (μm)	0.5–0.8 ×	Indole production	−
	1.2–3.5	Hydrolysis of:	
Motility	+	gelatin	+
Flagellum	single, polar	starch	−
Culture Characteristics		poly-β-hydroxybutyrate	−
Aerobiosis	+	Carbon sources for growth	
Growth at:		L-arabinose	−
4 °C	−	D-xylose	+
41 °C	+	D-glucose	+
45 °C	−	D-mannose	−
		D-fructose	+
Biochemical Characteristics		D-galactose	−
Production of pigment		maltose	−
fluorescent	+	sucrose	−
pyocyanine	+	lactose	−
Arginine dihydrolase		trehalose	−
activity	+	D-sorbitol	−
Oxidase activity	+	D-mannitol	+
Catalase activity	+	m-inositol	−
Urease activity	−	glycerol	+
Denitrification	+		
Protocatechuate, ortho-			
cleavage	+		
Oxidation-fermentation			
test	oxidative		

weight that occurred when the medium contained cyclohexane was caused by the effect of cyclohexane on the bacterium.

The growth of strain PST-01 on the medium plates overlaid with organic solvents was observed. Observation showed that strain PST-01 grew well on the medium plates overlaid with n-hexadecane (log P = 8.8), n-tetradecane (log P = 7.6), n-dodecane (log P = 6.6), n-decane (log P = 5.6), n-octane (log P = 4.5), isooctane (log P = 4.5), 1-decanol (log P = 4.0), n-heptane (log P = 4.0), cyclohexane (log P = 3.2), or p-xylene (log P = 3.1). Strain PST-01 did not grow on the medium plates overlaid with organic solvents when the log P values were equal to or less than 2.5.
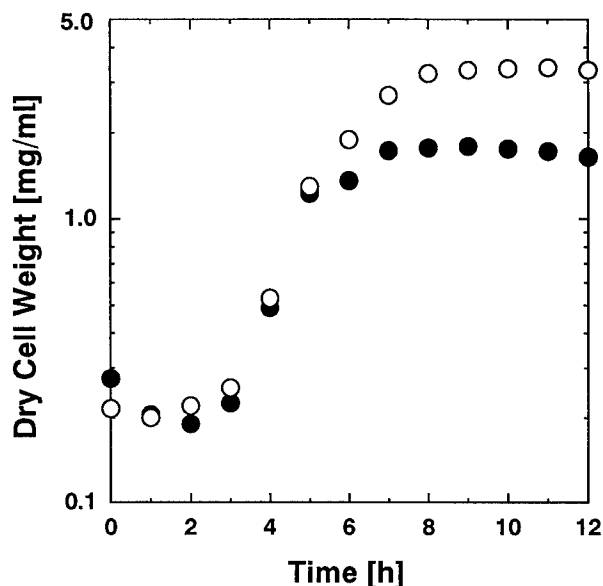
FIGURE 1. Time courses of the dry cell weights of strain PST-01. Strain PST-01 was cultivated using a 500-mL baffled Erlenmeyer flask containing 50 mL of the nutrient medium in the presence (●) or absence (○) of 15 mL of cyclohexane at 30 °C.

On the medium plates overlaid with n-hexane (log P = 3.5) or 1-octanol (log P = 2.9), the growth of strain PST-01 was poor.

The growth of the strain in the liquid media containing various organic solvents was also studied. FIGURE 2 shows the effect of the organic solvents on the dry cell weights of strain PST-01 after 24, 36, and 48 hours of cultivation. The dry cell weights of strain PST-01 grown in the media containing n-hexadecane, n-tetradecane, n-dodecane, n-decane, isooctane, n-octane, n-heptane, n-hexane, cyclohexane, or p-xylene exceeded 1.0 mg dry cell weight/mL medium.

The dry cell weights of strain PST-01 cultured in the presence of cyclohexane or p-xylene were compared with those of some standard strains and *Ps. aeruginosa* LST-03,[2] which grew well in the presence of organic solvents and produced lipolytic enzyme. As shown in FIGURE 3, strains LST-03 and PST-01 grew well in the presence of cyclohexane or p-xylene. However, the growth of the other reference strains was poor in the presence of p-xylene.

Purification of PST-01 Protease

The protease secreted by strain PST-01 was purified by precipitation with ammonium sulfate, hydrophobic interaction chromatography using Butyl-TOYOPEARL 650C and Butyl-TOYOPEARL 650M, and gel chromatography using Superdex 75. TABLE 2 summarizes the purification and shows that the enzyme was purified 203-fold with an overall yield of 73.5%. The purified enzyme gave a
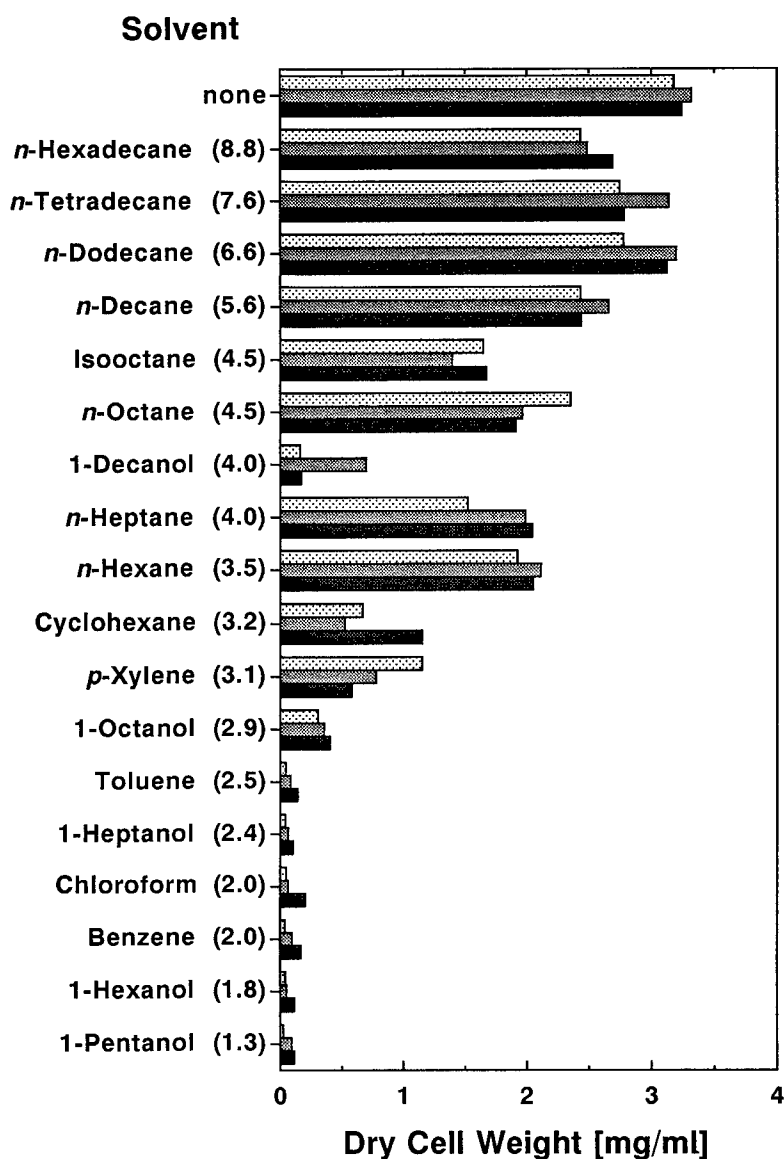
Solvent

FIGURE 2. The dry cell weights of strain PST-01 culture in the presence of organic solvent. Strain PST-01 was cultivated in a 500-mL baffled Erlenmeyer flask containing 50 mL of the nutrient medium in the presence or absence of 15 mL of organic solvent. All cultivation flasks were plugged with chloroprene-rubber stoppers. Results were obtained after 24 hours (light), 36 hours (gray), and 48 hours (dark) of cultivation. The numbers in parentheses show the log P values.
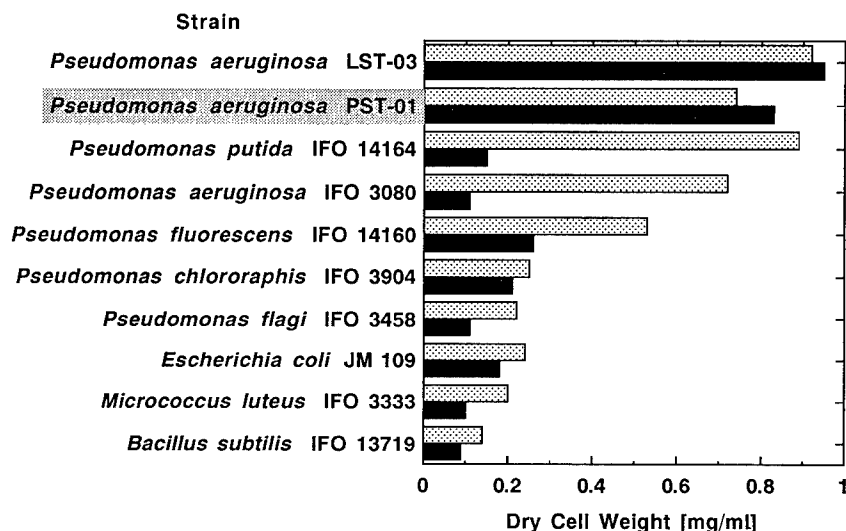
Strain

FIGURE 3. Growth of various strains in the presence of organic solvent. Cells were cultivated in 24$^\phi$ test tubes containing 10 mL of the nutrient medium in the presence of 3 mL of cyclohexane (light) or *p*-xylene (dark) at 30 °C for 36 hours. All test tubes were plugged with chloroprene-rubber stoppers.

single band on SDS-PAGE and its molecular weight was determined as 38,000. The optimum reaction temperature of the enzyme was 55 °C. Inactivation was not observed after the enzyme was incubated at 50 °C for 10 min. The optimum pH was 8.5.

Organic Solvent Stability of PST-01 Protease

The effect of various organic solvents on the stability of the purified PST-01 protease is shown in TABLE 3. The PST-01 protease is stable in the presence of several kinds of organic solvents. In particular, alcohol stabilized the enzyme.

TABLE 2. Summary of the Purification of PST-01 Protease[a]

Procedure	Total Volume (mL)	Total Activity (unit)	Specific Activity (unit/mg)	Purification (fold)	Yield (%)
Culture supernatant	1600	13.6×10^3	0.244	1	100
Ammonium sulfate	720	8.2×10^3	2.05	8.40	60.0
Butyl-TOYOPEARL 650C	223	11.1×10^3	20.2	83.1	81.3
Butyl-TOYOPEARL 650M	210	15.4×10^3	39.6	163	113
Superdex 75	5040	10.0×10^3	49.5	203	73.5

[a]Proteolytic activity was determined by assaying the hydrolysis of casein as a substrate at pH 8.5 and 30 °C. One unit of proteolytic activity was defined as the amount of enzyme that produces the casein digest equivalent to 1 μmol of tyrosine per min. Protein concentration was determined by measuring the absorbance at 280 nm using bovine serum albumin as a standard.

TABLE 3. Effect of Organic Solvents on the Stability of PST-01 Protease[a]

1-hexanol	1.68
ethanol	1.55
methanol	1.54
1-heptanol	1.52
dimethylsulfoxide	1.52
2-propanol	1.43
1-butanol	1.43
1-octanol	1.40
acetone	1.32
1-decanol	1.23
n-decane	0.98
toluene	0.96
p-xylene	0.88
n-octane	0.86
benzene	0.70
isooctane	0.68
n-dodecane	0.66
n-hexane	0.56
cyclohexane	0.54
n-heptane	0.46
none	1

[a]Five mL of the purified PST-01 protease solution was incubated at 30 °C with shaking in the presence of 1.5 mL of organic solvent for 10 days. The remaining activity was determined by assaying the hydrolysis of casein as a substrate at pH 8.5 and 30 °C. The remaining activity relative to the nonsolvent-containing control is shown.

Proteases are often used in nonaqueous media because these media can increase the solubility of substrates or products and can facilitate the product recovery. Moreover, they are favorable for peptide syntheses that are thermodynamically unfavorable in water. As shown above, the protease of strain PST-01 is stable in the presence of organic solvents and may prove valuable for synthesis in such environments.

REFERENCES

1. KHMELNITSKY, Y. L., A. V. LEVASHOV, N. L. KLYACHKO & K. MARTINEK. 1988. Engineering biocatalytic systems in organic media with low water content. Enzyme Microb. Technol. **10:** 710–724.
2. OGINO, H., K. MIYAMOTO & H. ISHIKAWA. 1994. Organic solvent–tolerant bacterium which secretes organic solvent–stable lipolytic enzyme. Appl. Environ. Microbiol. **60:** 3884–3886.

Medium and Biocatalyst Engineering as a Means to Affect Enzyme Activity and Stability in Organic Media

ANGELIKI ÖSTE-TRIANTAFYLLOU, ERNST WEHTJE,
PATRICK ADLERCREUTZ, AND BO MATTIASSON

Department of Biotechnology
Chemical Center
Lund University
S-221 00 Lund, Sweden

INTRODUCTION

Biocatalysts are being used in transformations in organic solvents.[1] The composition of the reaction medium is decisive with respect to the equilibrium position and the substrate specificity. The degree of hydration of the medium and the biocatalyst is acknowledged to be of extreme importance. The thermodynamic water activity (a_w) is used to describe the hydration level of these enzymatic systems. Minute amounts of water are necessary for the enzyme to maintain an active conformation. Further increase of the water content results in the enhancement of protein flexibility and enzymic activity.[2] Water is a good substrate for many enzymes, but it gives rise to undesirable side reactions. Therefore, in a previous work, we have attempted successfully to exchange the water in the organic medium with other compounds that were able to afford enhancement of synthetic rates.[3] These polar solvents that have small size and high dielectric constant are probably able to affect dielectric screening in a way similar to water, without being themselves substrates for the enzyme.

Engineering the biocatalyst itself has been used to improve catalytic rates in organic media, for example, by pretreatment of the protein with a substrate analogue, a competitive inhibitor, a polyhydroxyl alcohol, etc. Sorbitol had a positive effect on the activity of nonimmobilized and immobilized α-chymotrypsin.[4] One major problem associated with the rational use of enzymes in biocatalytic processes is their poor stability. The thermal stability of the protein molecule can be easily determined by differential scanning calorimetry (DSC), a technique that enables us to monitor conformational transitions of macromolecules.[5] In the present work, the temperature at which the transition of chymotrypsin takes place and the amount of energy involved provide an indication of the effect displayed by the additive on the thermal characteristics of the preparation. We consider as additives those compounds that constitute the microenvironment of the protein, that is, the water, the organic solvent, the sorbitol, and the buffer salts.

MATERIALS AND METHODS

The Effect of Water Activity and Sorbitol on Enzyme Activity

α-Chymotrypsin was lyophilized from a 20 mM sodium phosphate buffer, pH 7.8. Alternatively, sorbitol was dissolved in the buffer prior to the addition of the enzyme. Chymotrypsin activity was assayed under controlled water activity ($a_w = 0.08$ to 0.97). The transesterification reaction between AcPhOEt and 1-propanol in diisopropyl ether was monitored by HPLC (for details, see reference 4).

The Effect of the Microenvironment of the Enzyme on the Stability of α-Chymotrypsin Preparations

Chymotrypsin preparations containing various amounts of the additives were prepared by lyophilizing the enzyme from the appropriate solutions of either sorbitol or sodium phosphate buffer, pH 7.8, according to reference 6. The enzyme preparations, either in powder form or suspended in isooctane, were equilibrated against saturated salt solutions for water activity control ($a_w = 0.11$ to 0.97). Thermal analysis was performed using a DSC-2 differential scanning calorimeter (Perkin-Elmer). The temperature was increased from 310 to 383 K at a fixed rate of 5 K/min. The roles of the water, the organic solvent, the sorbitol, and the buffer salts on the thermal properties of the enzyme preparation were examined.

RESULTS AND DISCUSSION

For chymotrypsin-catalyzed reactions, high rates can be achieved at high water activities (FIGURE 1). Two major drawbacks, though, become apparent at high levels of hydration. Chymotrypsin expresses substantial hydrolytic activity because water is an excellent substrate for the protease.[4] Also, the lack of stability is striking. The denaturation temperature is decreasing continuously as the water activity increases because the majority of the enzyme inactivations observed in nonaqueous media are accelerated by water. Omission of the water in the system results in severe losses in catalytic activity. On the other hand, the stability of the dry enzyme is remarkable.

One way to afford changes on enzyme activity, and thus obtain high rates even at low hydration levels, is by modifying the biocatalyst preparation. For example, the addition of sorbitol to nonimmobilized and immobilized hydrolytic enzymes resulted in increased reaction rates and suppressed hydrolysis.[4] FIGURE 2 demonstrates that the catalytic activity of α-chymotrypsin is higher in the presence of sorbitol at any water activity. Sorbitol probably serves as a matrix for the enzyme and it provides the protein molecule with favorable interactions.

The addition of sorbitol to chymotrypsin caused the destabilization of the enzyme preparation against thermal inactivation, as determined by DSC (FIGURE 3). This observation differs from that reported for the aqueous solutions of proteins. A number of polyhydroxyl compounds have been shown to induce the enzyme stability in aqueous solutions. When the powder enzyme is considered, sorbitol acts as a
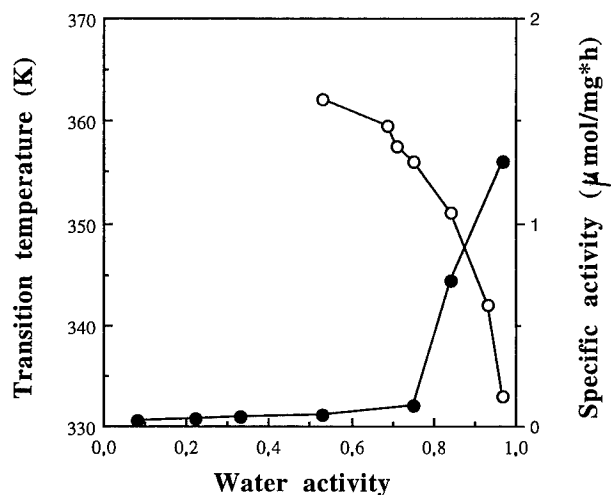
FIGURE 1. The transition temperature (○) and enzyme activity (●) as a function of the water activity for chymotrypsin.

molecular lubricant rather than as a stabilizer of the native structure of the protein, which is the aqueous case. FIGURE 3 also demonstrates that the destabilization of chymotrypsin is substantial for the various preparations, as the system tends to become water-saturated.

Markedly, equilibration through a nonpolar solvent, isooctane, resulted in high
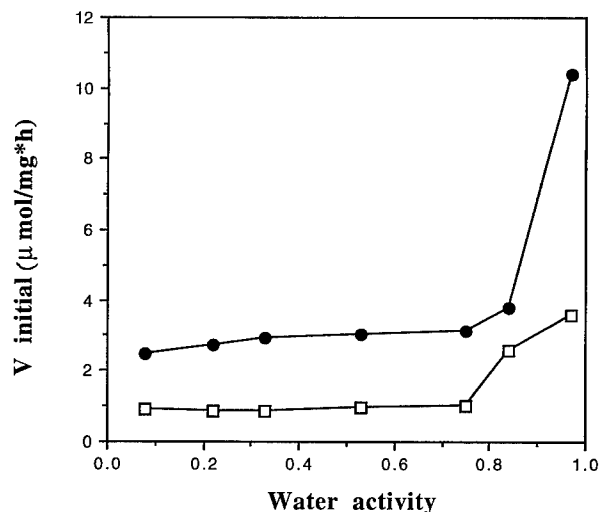
FIGURE 2. The activity of chymotrypsin as a function of the water activity: (□) native chymotrypsin; (●) sorbitol-chymotrypsin.
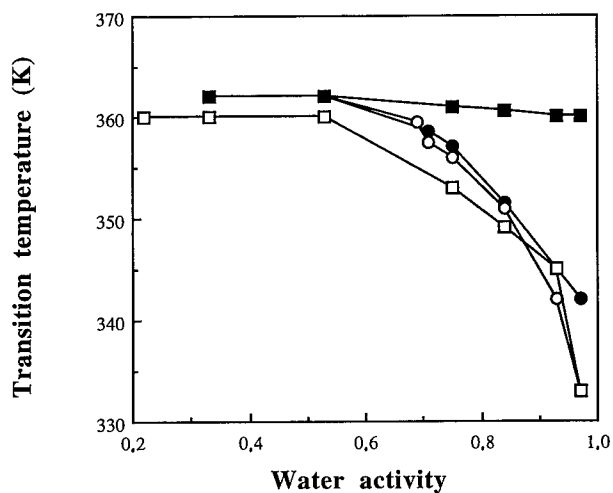
FIGURE 3. The denaturation temperature of chymotrypsin as a function of the water activity: (○) native chymotrypsin equilibrated through air; (●) native chymotrypsin equilibrated through solvent; (□) sorbitol-chymotrypsin equilibrated through air; (■) sorbitol-chymotrypsin equilibrated through solvent.

denaturation temperatures for the sorbitol-containing preparation at all water activities (FIGURE 3). In aqueous solutions, the water is mainly responsible for the hydrogen bonding and the electrostatic stabilization of the macromolecule. In the case of the suspension, the primary sources of electrostatic stabilization available to
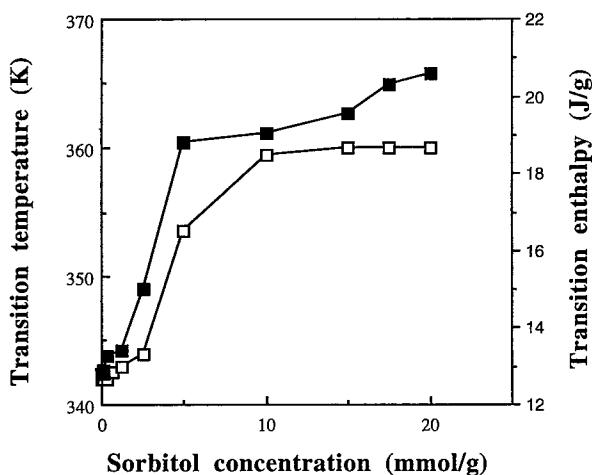
FIGURE 4. The transition temperature (□) and enthalpy (■) of chymotrypsin as a function of the concentration of sorbitol in the enzyme preparation. Equilibration through solvent at a_w = 0.97.

the charged side chains are the buffer species and other functional groups on the surface of the protein. When sorbitol is included in the suspension, the hydrogen bonding between groups of the protein and the sorbitol becomes prominent, in addition to the hydrogen bonding within the protein. Hence, the enzyme preparation gains in stability. A sorbitol concentration of 5 mmol/g of protein was a prerequisite to induce stabilization of the suspension at $a_w = 0.97$ (FIGURE 4). This concentration corresponds to 120 moles of sorbitol per mole of protein. The enthalpy of denaturation increases with increasing amounts of sorbitol. The excess energy could be explained in terms of increased hydrogen bonding as more sorbitol molecules combine with the protein molecule.

An important additive to the enzyme preparation is the buffer salts. The transition temperature increases with increasing amounts of sodium phosphate salts at $a_w = 0.97$ (FIGURE 5). Increasing the ionic strength seems to result in the
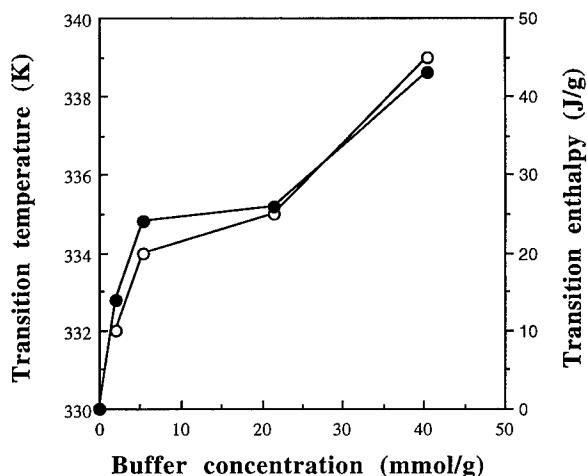
FIGURE 5. The transition temperature (O) and enthalpy (●) of chymotrypsin as a function of the concentration of buffer salts in the enzyme preparation. Equilibration through air at $a_w = 0.97$.

stabilization of the highly hydrated preparation. This stabilizing effect of the high ionic strength is often observed for dilute protein solutions, systems that are traditionally studied from the thermodynamic point of view. The counterions presumably prevent the molecule from clumping. FIGURE 5 also shows that the amount of energy that is demanded for this endothermic transition is dependent on the amount of the additive.

CONCLUSIONS

The application of differential scanning calorimetry on the "unusual" systems employed in bioorganic synthesis offers new perspectives for optimization of the processes. Great care should be taken in choosing the components of the catalytic

system. The solvent, the sorbitol, and the salts are able to affect the hydration of the enzyme and to interact directly with the protein. The experimental conditions should be designed so that high reaction rates are possible to achieve, but not at the expense of the stability of the biocatalyst. The present report illustrates that, when the biocatalyst is modified, the conditions that may favor high reaction rates also favor enzyme inactivation. Therefore, it might be necessary to compromise according to the actual goal.

REFERENCES

1. DORDICK, J. S. 1988. Biocatalysis in nonaqueous media. Appl. Biochem. Biotechnol. **19:** 103–112.
2. RUPLEY, J. A., E. GRATTON & G. CARERI. 1983. Water and globular proteins. Trends Biochem. Sci. **8:** 18–22.
3. ÖSTE-TRIANTAFYLLOU, A., P. ADLERCREUTZ & B. MATTIASSON. 1993. Influence of the reaction medium on enzyme activity in bio-organic synthesis: behavior of lipase from *Candida rugosa* in the presence of polar additives. Biotechnol. Appl. Biochem. **17:** 167–179.
4. ÖSTE-TRIANTAFYLLOU, A., E. WEHTJE, P. ADLERCREUTZ & B. MATTIASSON. 1995. Effects of sorbitol addition on the action of free and immobilized hydrolytic enzymes in organic media. Biotechnol. Bioeng. **45:** 406–414.
5. CHOWDHRY, B. Z. & S. C. COLE. 1989. Differential scanning calorimetry: applications in biotechnology. Trends Biotechnol. **7:** 11–18.
6. ÖSTE-TRIANTAFYLLOU, A., E. WEHTJE, P. ADLERCREUTZ & B. MATTIASSON. 1995. Calorimetric studies on α-chymotrypsin preparations in air and in organic media. Biochim. Biophys. Acta. In press.

Conformational Changes of Different Isolipases from *Candida rugosa* in Liquid Interfaces and after Their Contact with Low-Water-Content Media[a]

C. OTERO,[b] I. DEL-VAL,[b] L. ROBLEDO,[b] C. TORRES,[b]
J. A. ARCOS,[b] AND J. PÉREZ-GIL[c]

[b]*Unidad de Biocatálisis*
Instituto de Catálisis
Consejo Superior de Investigaciones Científicas
28049 Madrid, Spain

[c]*Departamento de Bioquímica y Biología Molecular I*
Facultad de Biología
Universidad Complutense
Madrid, Spain

INTRODUCTION

The interfacial activation of lipases is in general associated with the displacement of one or more lids that cover the active center. Their crystal structures give a static description of two conformations: an "inactive" (closed lid) and an "active" (fully opened lid) conformation. The active conformations of *Candida rugosa*[1] and *Rhizomucor miehei*[2] lipases were obtained from solutions of organic solvents and a question has been formulated: does a true lipid recognition site exist where the conformational transition is initiated? Furthermore, a more complex activation process than the model of a simple equilibrium between an "active" and "inactive" conformation has been suggested.[2]

In this work, the activation of lipases and their conformational changes after different activating treatments were studied. Treatment of solubilized lipases with a micellar interface was compared with treatment of solid suspensions of lipases with the solvent forming the continuous micellar phase. Two isolipases from *Candida rugosa,* which differ in their hydrophobicities and in their localization once solubilized in reverse micelles in spite of their high sequence homology,[3] were compared. The higher interaction of the more hydrophobic isolipase A with the micellar interface has been previously reported.[3] The influence of the protein hydrophobicity on the activation effect of the pretreatments has been considered. The existence of different lipase conformations from the "active" and "inactive" and of different activation processes has been studied using circular dichroism (CD) and fluorescence spectroscopy.

MATERIALS AND METHODS

Lipase from *Candida rugosa* type VII, sodium bis-(2-ethylhexyl)sulfosuccinate (AOT), and *p*-nitrophenyl butyrate (PNPB) were from Sigma Chemical (St. Louis, Missouri). Lipase purification was carried out as previously described.[4] The enzyme-catalyzed PNPB hydrolysis was used as a standard reaction for the activity assays. The reaction in sodium phosphate buffer was measured spectrophotometrically at 346 nm and 30 °C. The pretreatments were carried out for 5 minutes at 30 °C. The solid powder enzyme (4 mg) treated with *n*-heptane (1 mL, containing 1% v/v 0.1 M phosphate buffer at pH 7.0) was either filtered or extracted to a buffer solution (0.1 M phosphate, pH 7.0). Lipases solubilized in reverse micelles ([AOT] = 0.1 M; [H$_2$O]/[AOT] = 20) were extracted to a 0.5 M phosphate solution, pH 7.0. Proteins were quantified using the Peterson method.[5] Fluorescence and dichroism spectra of treated and untreated proteins, and estimations of the secondary structure from the CD spectra, were obtained as described elsewhere.[3,6]

TABLE 1. Hydrolytic Activities of Treated and Untreated Isolipases A and B from *Candida rugosa*

Isolipase	Pretreatment	Relative Activity (%)	Specific Activity (s^{-1})
A	—	100	279[a]
	heptane	121	337[a]
B	—	100	721[a]
	heptane	133	959[a]
A	—	100	84[b]
	micellar	333	280[b]
B	—	100	500[b]
	micellar	133	666[b]

[a]Specific activity in the hydrolysis of PNPB (1.66 mM) in 0.1 M phosphate buffer, pH 7.0, at 30 °C.

[b]Specific activity in the hydrolysis of PNPB (0.5 mM) in 0.1 M phosphate buffer, pH 7.0, at 30 °C.

RESULTS AND DISCUSSION

Two different treatments were applied to isolipases A and B from *Candida rugosa*. When the anionic reverse micelles of AOT were used for the lipase pretreatment, the proteins were solubilized into the nanodroplet during the pretreatment. The solid powders of lipases A and B were also treated in *n*-heptane.

TABLE 1 shows the activities of treated and untreated lipases in a buffer solution. TABLE 2 shows the change in the α-helix content of these lipases in buffer at 30 °C before and after each treatment. Isolipases A and B were activated after both types of pretreatments. These two pretreatments increased the α-helix content of the lipases. In the case of lipase A, the ellipticity variations indicated much higher α-helix content when AOT reverse micelles were used as the treatment medium than when the solid lipase powder was employed. In the case of lipase B, these two treatments induced similar relatively small increases of helicity. The activation (TABLE 1) and

TABLE 2. Secondary Structure of Treated and Untreated Isolipases A and B from *Candida rugosa*

Isolipase	Pretreatment	Medium	α-Helix (%)
A	—	aqueous	28
	heptane	aqueous	33
B	—	aqueous	24
	heptane	aqueous	29
A	—	aqueous	28
	micellar	micellar	49
	micellar	aqueous[a]	48
B	—	aqueous	24
	micellar	micellar	26
	micellar	aqueous[a]	30

[a]Lipase ellipticity after its treatment with reverse micelles and extraction to a buffer solution.

the conformational change (TABLE 2) obtained by the micellar contact were noticeably higher in the case of lipase A due to its higher interaction with the apolar side of the micellar interface.[3]

The crystallized lipase presents 5 Trp in the protein structure.[7] Possible variations in the Trp environment of lipases after these pretreatments were studied by fluorescence spectroscopy (TABLE 3). In the case of the micellar treatment of lipase A, the conformational reorganizations detected by CD (TABLE 2) modified the environment of Trp (blueshift of the emission peak).

The general conformational reorganizations detected in the protein molecule by CD and fluorescence spectroscopy also affected the active site and/or its environments, altering the hydrolytic activity. The modifications in the pocket of the active center obtained by pretreatments may be so important as to produce the increase of the enantioselectivity of lipase treated with 2-propanol.[8] The 2-propanol treatment also increased the hydrolytic activity up to 600%.[9]

These isoenzymes maintained their secondary structure (or slightly varied, TABLE 2) and kept the same Trp environment (TABLE 3) when they were extracted from the micellar medium to a water solution. The new conformations and activities (TABLES 1 and 2) were maintained in water for at least 2 hours at 30 °C. The

TABLE 3. Emission Fluorescence of Treated and Untreated Isolipases A and B from *Candida rugosa*

Isolipase	Pretreatment	Medium	λ_{max} (nm)
A	—	aqueous	336
	heptane	aqueous	336
	micellar	micellar	325
	micellar	aqueous[a]	325
B	—	aqueous	334
	heptane	aqueous	332
	micellar	micellar	333
	micellar	aqueous[a]	334

[a]The fluorescence spectra were obtained after the lipase treatment with reverse micelles and extraction to a buffer solution.

irreversibility of these new conformations in water may be explained by considering their stabilization by new internal interactions.

Higher activation of lipase A was obtained with the micellar contact, compared with pretreatment of its solid suspension. The activation by previous contact of solid protein dispersions in *n*-heptane did not increase using sonication during treatment. These two degrees of lipase A activation (also with different increments in the α-helix content) demonstrated that the activations of the lipases were not only due to the opening of their lids, but also to changes in their secondary structures.

The modification of the secondary structure of the protein and its reversibility were also considered. Our data for lipase A in micelles and after extraction to a buffer solution (TABLES 2 and 3) demonstrated the irreversibility of the conformational modification detected by CD and fluorescence spectroscopy. Although the activities of native lipases A and B in water are similar, lipase A is two orders of magnitude more active in reverse micelles than lipase B[3] and only three times more active than lipase B when they are pretreated and extracted to a water solution (TABLE 1). This may be consistent with the hypothesis of a partial reversibility of the lipase activation when it is solubilized in water (i.e., closing of the lid, but keeping the rest of the changes in the secondary structure) and with a model considering different activation degrees of the lipase. The irreversible modifications in the secondary structure could give rise to an active center with a wider entry. The lid could be closed when the treated lipase is again solubilized in water, but it would not block completely the entry to the active center of relatively small substrates in the new conformation. In agreement with this interpretation, it has been reported that 2-propanol and SDS pretreatments in water gave rise to enhancements of the activity of this "solubilized" lipase of four to six times in aqueous solution.[9] However, the pretreatment in water of this lipase with different amphiphiles increased the nonaqueous reaction rates of the "solid" enzyme by up to two orders of magnitude, which was explained as the molecular bioimprinting of the lipase.[10] In this case, the lid seems to remain open because cutinase (without lid) was not activated in this way.

REFERENCES

1. GROUCHULSKI, P., J. SCHRAG & M. CYGLER. 1992. *In* Proceedings of the American Crystallography Association: 1992 Annual Meeting, p. 122.
2. DEWERENDA, Z. S. 1994. Structure and function of lipases. *In* Advances in Protein Chemistry. Volume 45, p. 1–52.
3. OTERO, C., M. L. RÚA & L. ROBLEDO. 1995. FEBS Lett. **360:** 202–206.
4. RÚA, M. L., T. DIAZ-MAURIÑO, V. M. FERNANDEZ, C. OTERO & A. BALLESTEROS. 1993. Biochim. Biophys. Acta **1156:** 181–189.
5. PETERSON, G. L. 1977. Anal. Biochem. **83:** 346–356.
6. CRUZ, A., C. CASALS & J. PÉREZ-GIL. 1995. Biochim. Biophys. Acta **1255:** 68–76.
7. KAWAGUCHI, Y., H. HONDA, J. TANIGUCHI-MORIMURA & S. IWASAKI. 1989. Nature **341:** 164.
8. COLTON, I. J., S. N. AHMED & R. J. KASLAUSKAS. 1995. J. Org. Chem. **60:** 212–217.
9. KÖPF, A., T. SCHALKHAMMER, G. KIRCHNER & F. PITTNER. 1994. Biocatalysis **9:** 261–268.
10. MINGARRO, I., C. ABAD & L. BRACO. 1995. Proc. Natl. Acad. Sci. U.S.A. **92:** 3308–3312.

The Effect of Water Activity on Modified Lipase during Esterification[a]

A. B. SALLEH, M. TAIB, M. BASRI, K. AMPON,[b]
W. M. Z. YUNUS, AND C. N. A. RAZAK

Enzyme and Microbial Technology Research
Faculty of Science and Environmental Studies
Universiti Pertanian Malaysia
43400 UPM Serdang, Malaysia

INTRODUCTION

Water plays a key role in the structure and function of enzymes. A completely dehydrated enzyme is not catalytically active. Water increases the internal flexibility of the enzyme molecule, which is an essential requirement for enzyme function.[1] It can serve not only as a diffusion medium, but also as a reactant in many reactions.

The presence of water as such is very important for both the reaction rate and the equilibrium position.[2] To quantify the amount of water present in the reaction mixture, it is advantageous to use the thermodynamic water activity (a_w) instead of water content. The water activity governs the degree of hydration of enzymes and gives a direct indication of the mass action of water.[3]

To improve enzyme activity, especially in the microaqueous environment, several workers have presented reports on the use of modified enzymes.[4-6] Lipases modified with hydrophobic modifiers are known to enhance esterification activity and solubility in organic solvents. However, the attachment of these modifiers to the protein molecules may affect the water relationship of the catalyst.

EXPERIMENTAL PROCEDURES

Preparation of Modified Lipase

Lipase from *Candida rugosa* (Sigma, type IV) was partially purified as described in reference 6. Reductive alkylation was done essentially according to reference 5 using dodecyl aldehyde as the modifier. An increasing degree of modification was obtained by a stepwise increase of the aldehyde.

Activity Assay

The reaction mixture comprising oleic acid and propanol (1:4 molar ratio) and the enzyme were separately preequilibrated in a saturated salt hydrate environment

[b]Present address: School of Science and Technology, Universiti Malaysia Sabah, Kota Kinabalu, Sabah, Malaysia.

for at least 12 h. The salt hydrates used were LiCl (a_w = 0.12), MgCl$_2$ (a_w = 0.32), MgNO$_3$ (a_w = 0.55), KI (a_w = 0.68), and KNO$_3$ (a_w = 0.95).[3] The reaction was performed for 3 h at 37 °C with shaking. The activity was determined by titrating the unreacted free fatty acids using an ABU 91 autotitrator (Radiometer, Copenhagen, Denmark).
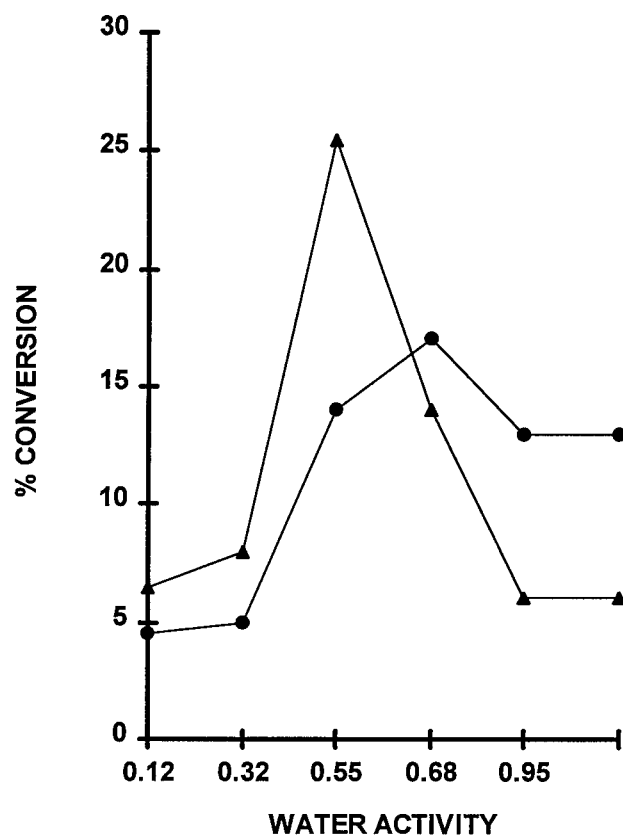
FIGURE 1. Activity of free lipase with (▲) and without (●) hexane.

RESULTS AND DISCUSSION

FIGURE 1 shows the esterification activity of unmodified lipase without and with hexane. The optimum activity shifts from a_w = 0.68 in the first instance to a_w = 0.55 in the presence of hexane. Bovara *et al.*[7] reported that the optimum V_{max} for free lipase (from *Pseudomonas cepacia*) was at a_w = 0.11–0.38, but this was in a transesterification reaction in toluene. The presence of solvent may enhance the solubility of the substrate, rendering it more assessible for the enzyme reaction; as
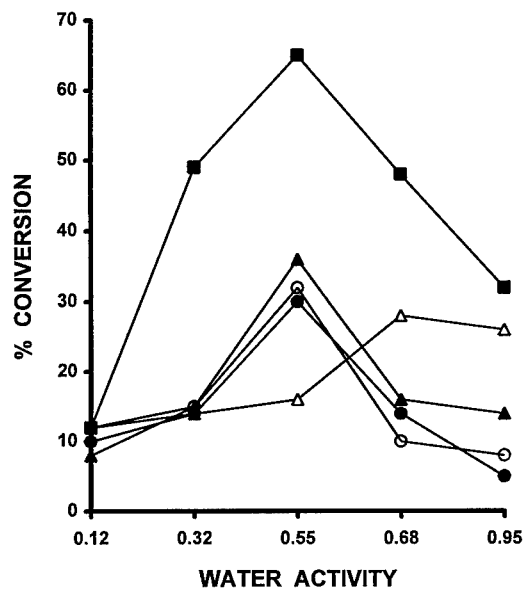
FIGURE 2. Activity of modified lipase in the absence of hexane. The lipase was modified to 20% ($\triangle$), 40% ($\blacksquare$), 65% ($\blacktriangle$), 75% ($\bullet$), and 90% ($\bigcirc$) with dodecyl aldehyde.

such, the reaction is optimal at lower water activity. The problem of protein aggregation, though, cannot be ignored when using free enzyme in organic solvents.

Using dodecyl-lipase in the absence of hexane, the optimum activity is at $a_w = 0.55$. This was true for all degrees of modification, except at the lowest degree of
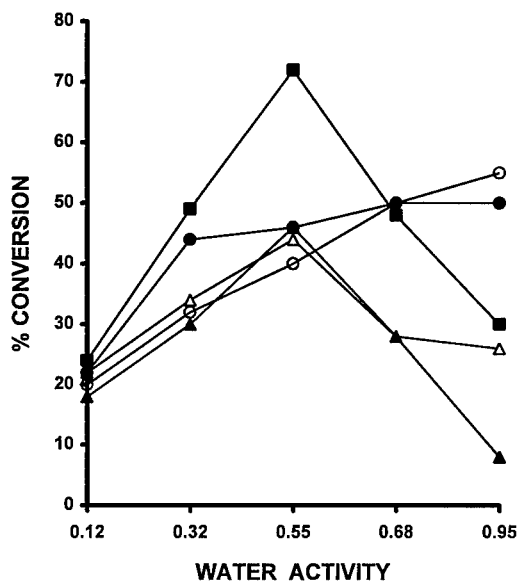
FIGURE 3. Activity of modified lipase in the presence of hexane. The lipase was modified to 20% ($\triangle$), 40% ($\blacksquare$), 65% ($\blacktriangle$), 75% ($\bullet$), and 90% ($\bigcirc$) with dodecyl aldehyde.

modification studied (20%). In this case, the optimum activity was at $a_w = 0.68$, a value similar to free lipase (FIGURE 2), indicating that the enzyme molecule is unaffected by the modification at this stage.

In the presence of hexane, similar results were obtained for the lower degrees of modification, indicating that the modification of the enzyme has masked any effect of the hexane. However, when the modification was increased further, the optimum activity was shifted to higher a_w values (FIGURE 3). Bovara *et al.*[7] also showed that the V_{max} of PEG-lipase was highest at the highest a_w studied (0.83), suggesting that the observed activity increased with increased hydration in a system where diffusion or aggregation played a minor role. As suggested in reference 5, lipase that was highly modified may be more soluble in the organic phase.

It was also observed that the optimum activity was obtained when the lipase was derivatized to 40% modification. As stated in reference 5, the optimum activity varied with different degrees of modification depending on the chain length of the aldehyde used, with the shorter chain aldehydes requiring higher degrees of modification to achieve the optimum reactivity and vice versa.

REFERENCES

1. RESLOW, M., P. ADLERCREUTZ & B. MATTIASSON. 1988. On the importance of support material for bioorganic synthesis: influence of water partition between solvents, enzyme, and solid support. Eur. J. Biochem. **172:** 573–578.
2. SVENSSON, I., E. WEHTJE, P. ADLERCREUTZ & B. MATTIASSON. 1994. Effect of water activity on reaction rates and equilibrium positions in enzymatic esterifications. Biotechnol. Bioeng. **44:** 549–556.
3. VALIVETY, R. H., P. J. HALLING & A. R. MACRAE. 1992. Reaction rates with suspended lipase-catalyst show similar dependence on water activity in different organic solvents. Biochim. Biophys. Acta **1122:** 143–146.
4. INADA, T., H. NISHIMURA, K. TAKAHASHI, T. YOSHIMOTO, A. R. SAHA & Y. SAITO. 1984. Ester synthesis catalyzed by polyethylene-modified lipase in benzene. Biochem. Biophys. Res. Commun. **122:** 845–850.
5. AMPON, K., A. B. SALLEH, F. SALAM, W. M. Z. YUNUS, C. N. A. RAZAK & M. BASRI. 1991. Reductive alkylation of lipase. Enzyme Microb. Technol. **13:** 597–601.
6. BASRI, M., K. AMPON, F. SALAM, W. M. Z. YUNUS, C. N. A. RAZAK & A. B. SALLEH. 1992. Amidation of lipase with hydrophobic imidoesters. J. Am. Oil Chem. Soc. **69:** 579–583.
7. BOVARA, R., G. CARREA, G. OTTOLINA & S. RIVA. 1993. Effect of water activity on V_{max} and K_m of lipase-catalyzed transesterification in organic media. Biotechnol. Lett. **15:** 937–942.

Alkaline and Thermophilic Amylases of Industrial Use

RYU SHINKE, KENJI AOKI, SHUICHIRO MURAKAMI,
TAKATO INOUE, AND TOMOYA BABA

Department of Biofunctional Chemistry
Faculty of Agriculture
Kobe University
Kobe 657, Japan

INTRODUCTION

Amylases have long been used for the hydrolysis of starch and related substances in fermentation, textile, and pharmaceutical industries.[1,2] Alkaline amylases have especially been desired as an additive to laundry washing mixtures because the washing mixtures are usually used in warm conditions. However, commercial amylases so far on the market have not necessarily been as thermostable as expected. Such a situation with alkaline and thermostable amylases has made us attempt to isolate microorganisms capable of producing industrially useful amylases.

This report deals with the isolation of thermophilic microorganisms grown at temperatures above 60 °C, the identification of isolates, the production of amylases, and the characterization of the alkaline and thermostable amylases purified.

ISOLATION AND IDENTIFICATION OF ALKALINE, THERMOPHILIC MICROORGANISMS

The composition of the media for screening alkaline and thermophilic microorganisms is shown in TABLE 1. Various soil samples from nature were suspended in a saline solution (3.0 mL) and allowed to stand for 2 min. Then, an aliquot of the supernatant was dropped on the agar plate medium and incubated at 30 °C for 1 to 3 days (first screening). The colonies that appeared on the plate were transferred to the second screening plate medium and incubated at 33 °C, to which Lugol's iodine solution was added to examine the formation of a halo showing amylase secretion around the colonies. The isolates obtained at the second screening were further transferred to a liquid medium with the same composition without agar as in TABLE 1 and were cultured at 33 °C for 24 h. Each culture filtrate was subjected to a measurement of the amylase activity at pH 10.0 at 30 °C or 60 °C. The amylase activity was measured by the 3,5-dinitrosalicylic acid method.[3] The isolates producing amylases with higher activity at 60 °C than at 30 °C were selected.

As a result, 27 strains were selected at the first screening among 110 isolates, and

332

TABLE 1. Screening Media for Amylase-producing Microorganisms

	Chemical Defined Medium	Polypepton Medium
soluble starch	2.0 g	2.0 g
yeast extract	0.05 g	0.3 g
Polypepton	—	0.5 g
NH_4NO_3	0.1 g	—
K_2HPO_4	0.1 g	0.1 g
$MgSO_4 \cdot 7H_2O$	0.02 g	0.02 g
NaCl	0.2 g	—
Na_2CO_3 (pH 10.0)	0.4 g	0.66 g
agar	1.5 g	1.5 g
H_2O	100 mL	100 mL

2 strains (A-5 and C-1) were selected at the second screening as the alkaline and thermostable amylase–producing microorganisms. Among these 2 strains, the A-5 strain was finally selected for the experiments.

As shown in FIGURE 1 and TABLE 2, a taxonomical investigation on the strain A-5
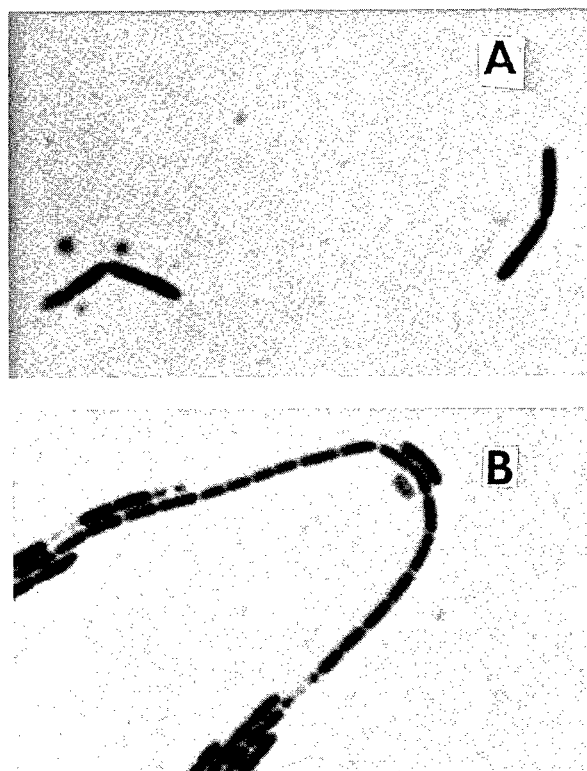
FIGURE 1. Microphotographs of newly isolated microorganisms: (A) negatively stained; (B) spore formed.

showed that the strain A-5 belongs to the *Bacillus* genus and is tentatively named *Bacillus* sp. A-5.

PRODUCTION AND PURIFICATION OF ALKALINE, THERMOSTABLE AMYLASES

The effects of carbon sources (TABLE 3), nitrogen sources (TABLE 4), metal salts (TABLE 5), and a casamino acid mixture (TABLE 6) on amylase production were examined using *Bacillus* sp. A-5. As a result, the bacterium was found to produce more amylases in the presence of casamino acid and metal salts in the culture media (TABLE 7).

The amylase fractions were isolated and purified from the culture media by salting out with ammonium sulfate, anion exchange chromatography and hydrophobic chromatography, gel filtration, etc. The results obtained are summarized in

TABLE 2. Morphological, Cultural, and Biochemical Properties of Strain No. A-5

(1) Morphological Characteristics	
Form	rods
Size	$0.7 \times 3\text{--}4.5\ \mu m$
Motility	motile
Gram stain	positive
Sporangia	slightly swollen
Spores	$0.5 \times 0.7\ \mu m$; oval; central
(2) Cultural Characteristics[a]	
Nutrient broth	+
Glucose-nutrient broth	+
Aerobic growth in glucose broth	+
Anaerobic growth in glucose broth	+
Production of acid from carbohydrate	
glucose	−
maltose	−
arabinose	−
lactose	−
mannitol	ND
Nutrient broth containing NaCl	
2.0%	+
5.0%	+
7.0%	+
10.0%	+
(3) Biochemical Characteristics	
Hydrolysis of gelatin	positive
Hydrolysis of casein	positive
Hydrolysis of starch	positive
Utilization of citrate	utilized
Voges-Proskauer test	negative
Catalase	positive
(4) pH and Temperature	
pH for growth in nutrient broth	6.0–12.0
Temperature for growth in nutrient broth (pH 10.0)	up to 50 °C

[a]Terms: +, normal growth at pH 10.0; −, no growth at pH 10.0; ND, not determined.

TABLE 3. Effects of Carbon Sources on Amylase Production

Carbon Sources	Units/mL	Protein (mg/mL)	Specific Activity (Units/mg)	OD$_{660nm}$
none	0.27	0.90	0.52	6.51
soluble starch	1.62	1.40	1.16	10.91
glucose	0.46	3.54	0.13	1.01
sucrose	0	3.58	0	1.93
maltose	0.25	2.53	0.10	6.52
dextrin	0.83	1.78	0.47	8.73

TABLE 4. Effects of Nitrogen Sources on Amylase Production

Nitrogen Sources	Units/mL	Protein (mg/mL)	Specific Activity (Units/mg)	OD$_{660nm}$
Polypepton	2.19	2.23	0.98	9.9
casamino acid	1.11	1.07	1.04	11.5
CSL	1.71	2.04	0.84	8.0
meat extract	1.02	1.59	0.64	10.7

TABLE 5. Composition of Metal Salt Solutions A, B, and C[a]

Solution A	Nitrilotriacetic acid	1.00 g
	$CaSO_4 \cdot 2H_2O$	0.60 g
	$MgSO_4 \cdot 7H_2O$	1.00 g
	NaCl	0.08 g
	KNO_3	1.03 g
	$NaNO_3$	6.89 g
	Na_2HPO_4	1.11 g
	H_2O	1000 mL
Solution B	$FeCl_3$	0.40 g
	H_2O	1000 mL
Solution C	H_2SO_4	0.50 mL
	$MnSO_4 \cdot 5H_2O$	3.16 g
	$ZnSO_4 \cdot 7H_2O$	0.50 g
	H_3BO_3	0.50 g
	$CuSO_4 \cdot 5H_2O$	0.025 g
	$Na_2MoO_4 \cdot 2H_2O$	0.025 g
	$CoCl_2 \cdot 6H_2O$	0.046 g
	H_2O	1000 mL

[a]Each 10 mL of solution B or C was added to 1000 mL of solution A.

TABLE 8. Finally, two enzyme fractions (fractions A and B) were obtained by polyacrylamide gel electrophoresis.

SOME PROPERTIES OF PURIFIED AMYLASES

The molecular weights of purified enzymes were measured by gel filtration on a Toyopearl HW-55 (Superfine) column and also by SDS-polyacrylamide gel electrophoresis (FIGURE 2). The molecular weight of fraction A was estimated to be 110,000 and that of fraction B was estimated to be 90,000.

TABLE 6. Composition of Casamino Acid Solution

soluble starch	2.0 g
casamino acid	0.5 g
yeast extract	0.3 g
K_2HPO_4	0.1 g
$MgSO_4 \cdot 7H_2O$	0.02 g
Na_2CO_3 (pH 10.0)	0.35 g
metal salt solution	5.0 mL
H_2O	95.0 mL

TABLE 7. Effects of Metal and Casamino Acid Solutions

Medium		Activity (U/mL)	Protein (mg/mL)	Specific Activity (U/mg)
Polypepton	metal (−)	2.40	2.19	1.10
	metal (+)	2.69	2.23	1.21
Casamino acid	metal (−)	1.11	1.07	1.04
	metal (+)	2.14	1.04	2.06

TABLE 8. Summary of the Purification of Amylase from Alkalophilic *Bacillus* sp. A-5

Purification Step	Volume (mL)	Total Activity (U)	Total Protein (mg/mL)	Specific Activity (U/mg)	Recovery (%)
Culture supernatant	960	1240	112	1.1	100
Salting out (ammonium sulfate)	82.0	730	44.7	16.3	59.0
Chromatography DEAE-cellulose (DE-52)	85.6	614	6.30	98.5	49.5
phenyl-Toyopearl 650M	60.0	332	0.80	416	26.7
Toyopearl HW-55 650M	13.2	174	0.53	330	14.0
PAGE					
A band	4.25	123	0.47	261	10.2
B band	3.60	14.8	0.057	260	1.19

The optimum pH and the optimum temperature for the enzyme reaction were 10.5 and 65 °C, respectively (FIGURES 3 and 4). The pH stability and the thermostability of both enzyme fractions were almost the same, namely, pH 6.0 to 11.0 and 65 °C, respectively, in the presence of 2 mM calcium chloride (FIGURES 5 and 6).

RAW STARCH DIGESTIBILITY OF ALKALINE AND THERMOSTABLE AMYLASES

The amylases purified from *Bacillus* sp. A-5 culture media were found to hydrolyze both raw and heat-treated starches of wheat and potato. The main
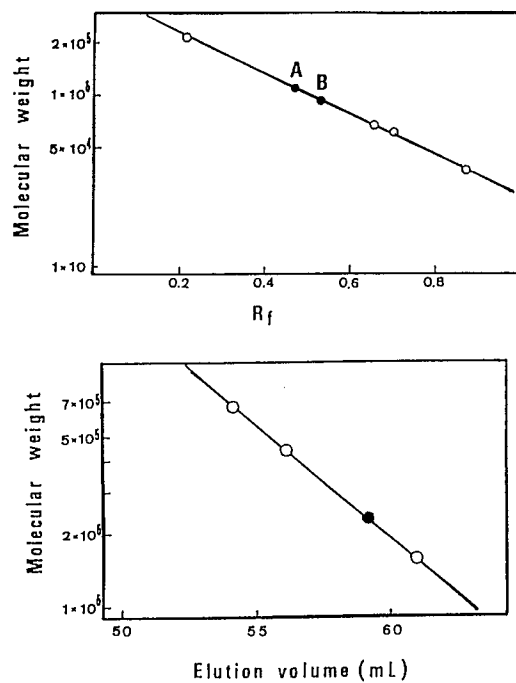
FIGURE 2. Estimation of the molecular weight of purified amylase from *Bacillus* sp. A-5: (top) SDS-PAGE; (bottom) gel filtration on Toyopearl HW-55 (Superfine) column.
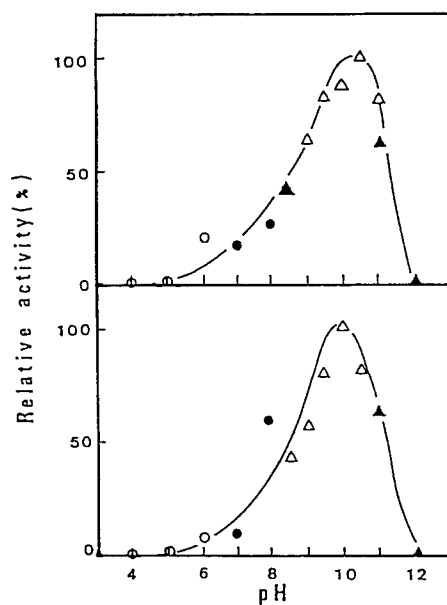
FIGURE 3. Optimum pH of purified amylases: (top) purified enzyme A; (bottom) purified enzyme B. Symbols: (O) pH 3–6, 0.1 M acetate buffer; (●) pH 7–8.5, 0.1 M Tris-HCl buffer; (△) pH 8.5–11.0, 0.1 M glycine-NaCl-NaOH buffer; (▲) pH 11.0–12.0, 0.1 M phosphate buffer.
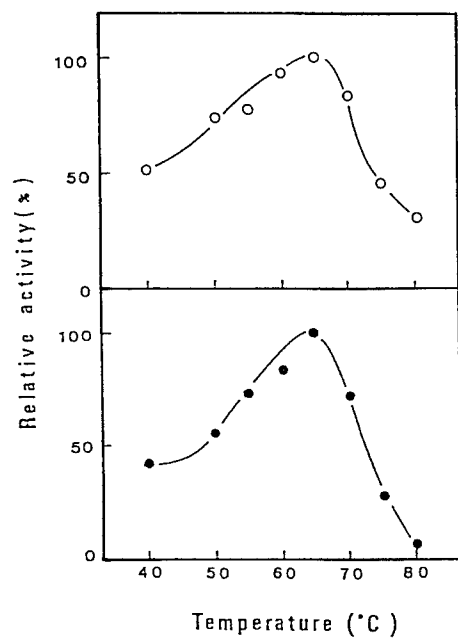
FIGURE 4. Optimum temperature of purified amylases: (top) purified enzyme A; (bottom) purified enzyme B.
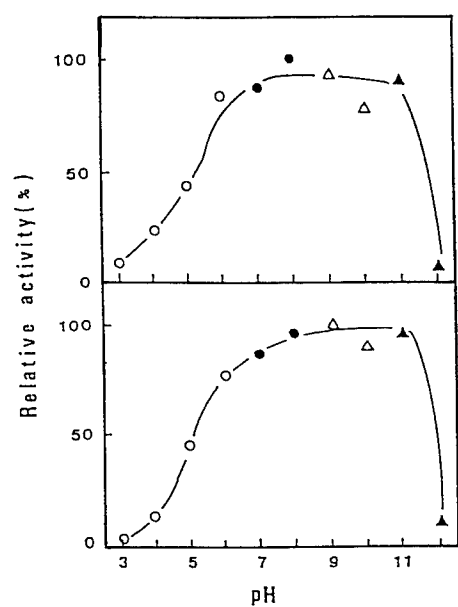
FIGURE 5. pH stability of purified amylases: (top) purified enzyme A; (bottom) purified enzyme B. Same symbols as in FIGURE 3.

FIGURE 6. Thermostability of purified amylases: (top) purified enzyme A; (bottom) purified enzyme B. Concentration of CaCl$_2$: 2 mM.
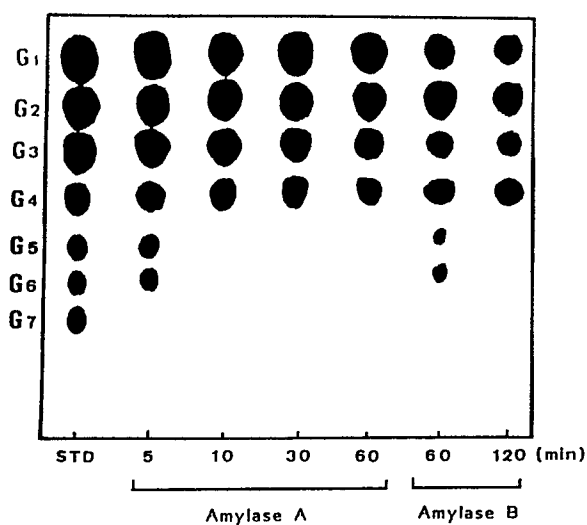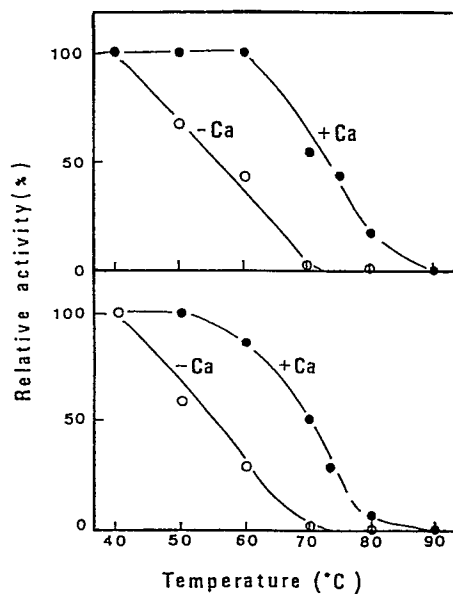
FIGURE 7. Paper chromatography of reaction products by purified amylases. Terms—G$_1$: glucose; G$_2$: maltose; G$_3$: maltotriose; G$_4$: maltotetraose; G$_5$: maltopentaose; G$_6$: maltohexaose; G$_7$: maltoheptaose; STD: standard maltooligosaccharide mixture.

products of the enzyme reactions were G_1, G_2, G_3, and G_4, with by-products of G_5 and G_6 (FIGURE 7).

These reaction products show that amylases A and B belong to α-amylase. It is also noted that *Bacillus* sp. A-5 is the first isolate capable of producing both alkaline and thermostable amylases and that the amylases are very useful for not only cleaning residual carbohydrates on dishes in automatic dishwashers, but also for industrial devices that will be widely used in the future.[2]

REFERENCES

1. SHINKE, R. 1988. Plant beta-amylases. *In* Handbook of Amylases and Related Enzymes, p. 81–86. Pergamon. Elmsford, New York.
2. SHINKE, R. 1995. Molecular biology of amylases and related enzymes. *In* Enzyme Chemistry and Molecular Biology of Amylases and Related Enzymes, p. 166–196. CRC Press. Boca Raton, Florida.
3. NANMORI, T., R. SHINKE, Y. NAKANO, S. KITAOKA & H. NISHIRA. 1985. Immunological studies on beta-amylase of *Bacillus cereus*. Appl. Microbiol. Biotechnol. **21:** 383–389.

Characterization of Thermostability
of *Clostridium stercorarium* Xylanase

KAZUO SAKKA,[a] MASAYUKI FUKUMURA,[a]
AKIYOSHI TANAKA,[b] AND KUNIO OHMIYA[a]

[a]*Faculty of Bioresources*
[b]*Faculty of Education*
Mie University
Tsu 514, Japan

Xylan is a major component of hemicellulose in plant cell walls and the most abundant form of biomass second to cellulose. In recent years, thermostable xylanases have received considerable attention for potential applications in biomass conversion strategies and in biobleaching of pulp. Study of the molecular events that take place in proteins on heating should be of great practical interest.

The *xynB* gene encoding a xylanase XynB was cloned from a thermophilic bacterium *Clostridium stercorarium* F-9 in *Escherichia coli* and sequenced.[1] The deduced amino acid sequence of XynB showed that the protein consisted of 387 amino acids, containing no cysteine residue, with a molecular weight of 44,377 and was classified into family F.[2] XynB purified from a recombinant *E. coli* showed both cellulolytic and xylanolytic activities in the same manner as the enzymes in family F.[1] In this paper, we report the characterization of the thermostability of XynB and discuss the process of the thermal denaturation of XynB.

XynB was purified from a total cell-free extract by ammonium sulfate precipitation and DEAE-Toyopearl 650S (Tosoh Company, Tokyo, Japan), Butyl-Toyopearl 650S (Tosoh), and TSK-gel G3000SW (Tosoh) column chromatographies. The purest preparation, the homogeneity of which was confirmed by SDS-polyacrylamide gel electrophoresis and by isoelectric focusing gel electrophoresis, was used for study of the thermostability of XynB.

The "remaining activity" was determined as follows. XynB solutions (500 μL, 13 μg/mL) at pH 5.5 and 7.0 dispensed in microfuge tubes were incubated at 100 °C for various periods and quickly chilled on ice, and then the enzyme activity ("remaining activity") was measured at 60 °C with PNPC as a substrate. As shown in FIGURES 1A and 1B, XynB showed a remaining activity of about 60% even after incubation at 100 °C and pH 7.0 for 10 min, but no activity at pH 5.5, whereas at both pH values it was maximally active at 80 °C and not active at 100 °C. FIGURE 1C shows differential scanning calorimetry (DSC) traces of XynB obtained at pH 5.5 and 7.0. The shape of the DSC trace did not depend on pH. A fairly large excess specific heat due to the unfolding reaction of XynB was observed between 80 °C and 90 °C. Maximum value of the excess specific heat was 7.9 J/K-g, and the enthalpy change of the unfolding reaction was estimated to be 26 J/g at 85 °C. These results indicate that XynB begins to denature at around 80 °C and is completely denatured at 100 °C and that the remaining activity detected at 60 °C after incubation at pH 7.0 and 100 °C is due to
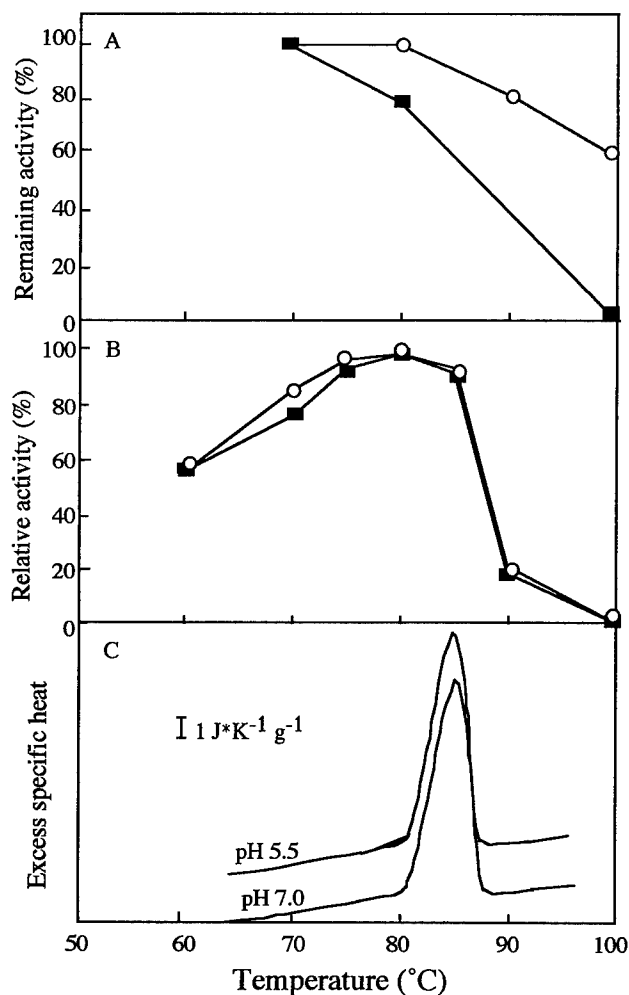
FIGURE 1. Effects of temperature on XynB. (A) Effects of temperature on the stability of XynB. The remaining activity was measured at 60 °C, after XynB was kept at the indicated temperatures and at pH 5.5 (■) and 7.0 (○) for 10 min. (B) Effects of temperature on the activity of XynB. The enzyme reaction was done at pH 5.5 (■) and 7.0 (○), at given temperatures for 10 min using PNPC as a substrate. (C) DSC curves observed with XynB (1.1 mg/mL) at pH 7.0 and 5.5. DSC was done with an adiabatic scanning microcalorimeter, DASM-4 (Biopribor, Moscow, Russia), with an NEC personal computer, at a scan rate of 1.0 K/min.

the activity of the enzyme that recovered its native structure by correct protein refolding from the denatured state during chilling on ice.

When the XynB solution (0.4 mg/mL) of pH 5.5 was kept at 100 °C for 5 min, a large quantity of precipitate without any activity was formed. After centrifugation at

4000*g* for 10 min, no XynB was detected in the supernatant by protein assay. The aggregated XynB was dissolved in various concentrations of urea and guanidine-HCl (GdnHCl), diluted 30-fold with PC buffer, and then the enzyme activity was measured. This activity was defined as the "recovered activity." As shown in FIGURE 2, up to 50% of the enzyme activity was recovered by the urea or GdnHCl treatment. The effect of urea was dependent on pH, whereas that of GdnHCl was independent of pH. When the aggregated XynB was dissolved in 8 M urea solution, it showed no activity, but then recovered its activity immediately after the dilution of urea. The far-UV CD spectra of native XynB and the enzyme that was thermally aggregated and dissolved in 8 M urea solution showed that the structure of XynB in 8 M urea solution is far from the native structure; that is, the aggregated XynB is disentangled and dissolved by urea treatment. These results indicate that its native structure is restored by rapid refolding after dilution of urea.

XynB solution was kept at 100 °C in the solutions of pH 7.0 and 5.5 for various periods and the remaining activity and the recovered activity of XynB were determined, respectively (FIGURE 3). At pH 7.0, the remaining activity decreased gradually with two phases as the reaction time of the thermal denaturation became longer. The enzyme aggregated at pH 5.5 was collected and treated with 8 M urea to be dissolved, and the recovered enzyme activity was measured. The recovered activity also gradually diminished as the incubation time at 100 °C became longer. This course of the recovered activity is similar to that of the remaining activity observed at pH 7.0. These results indicate that the rate of the irreversible loss of XynB activity was not affected by aggregate formation; that is, the irreversible denaturation of the protein is caused by the same mechanism in solution and in aggregates. For the XynB that was kept at 100 °C and pH 5.5 for various periods and then treated with 8 M urea, K_m and V_{max} values were measured. V_{max} values decreased gradually from 67 to 19 nmol/μg-min in proportion to the incubation period at 100 °C, while the K_m was
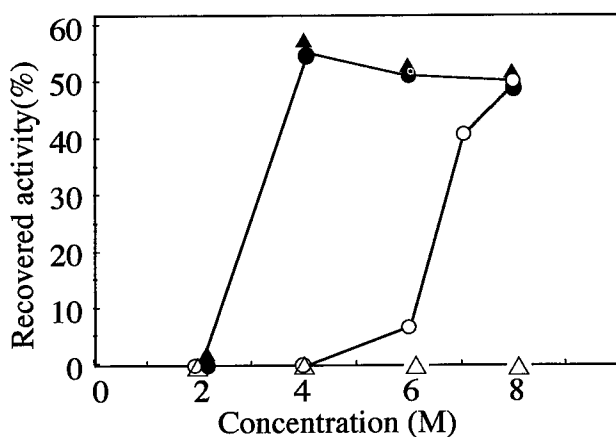
FIGURE 2. Effects of denaturants on the recovery activity of the thermally aggregated XynB. Aggregates formed by heating for 5 min at 100 °C and pH 5.5 were dissolved with GdnHCl and urea. The solution was diluted 30-fold to measure the recovered activity. Denaturant used: GdnHCl at pH 6.4 (●) and 5.5 (▲); urea at pH 6.4 (○) and 5.5 (△).
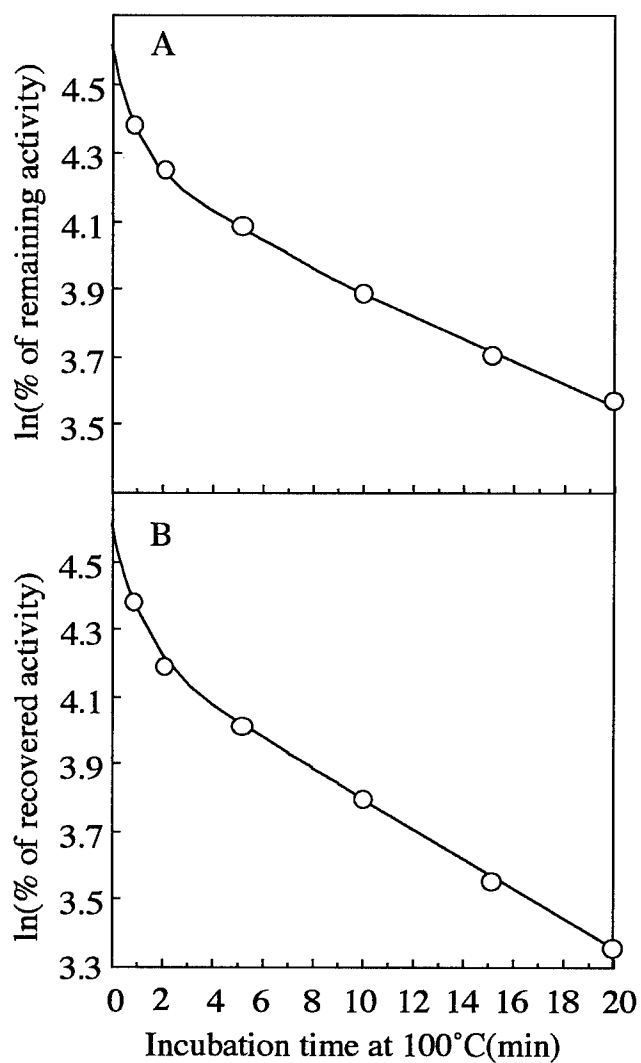
FIGURE 3. Time course of the remaining activity and the recovered activity of XynB at pH 7.0 and 5.5. (A) Semilogarithmic plot of the remaining activity of XynB at pH 7.0 versus the reaction time of the thermal denaturation. XynB (13 μg/mL) was incubated at 100 °C. Samples were periodically withdrawn and chilled on ice. Remaining activity was assayed at 60 °C using PNPC as a substrate. The solid line is a theoretical curve based on equation 1. (B) Semilogarithmic plot of the recovered activity versus the reaction time of the thermal denaturation. XynB (0.4 mg/mL) aggregated at 100 °C and pH 5.5 was dissolved in 8 M urea solution (pH 6.4) for 24 h and diluted 30-fold with PC buffer (pH 6.3). The recovered enzyme activity was measured at 60 °C using PNPC as a substrate. The solid line is a theoretical curve based on equation 1.

constant, suggesting that the structure of the renatured enzyme by the urea treatment is the same as that of the native enzyme. From FIGURE 3B, the apparent rate constant of the first faster phase, $k_{(fast)app}$, was evaluated to be 0.90 min^{-1} and that of the second slower phase, $k_{(slow)app}$, was evaluated to be 0.0425 min^{-1}. A minimum and possible mechanism that can explain the result shown in FIGURE 3B is as follows (at 100 °C):

$$N \xrightarrow{k_1} D1 \underset{k_{-2}}{\overset{k_2}{\rightleftharpoons}} D2 \xrightarrow{k_3} D3 \tag{1}$$

where N is the native enzyme; D1 is a denatured state of the enzyme that is formed rapidly after the thermal denaturation starts and that can be renatured by the urea treatment; D2 and D3 are denatured states of the enzyme that cannot be renatured by the urea treatment; and k_1, k_2, k_{-2}, and k_3 are the indicated rate constants. In this model, the remaining activity at pH 5.5 corresponds to the relative amount of N, and the recovered activity corresponds to the amount of D1. Because the remaining activity at an incubation time of 0.5 min is less than 0.01%, the value of k_1 is greater than 9.2 min^{-1}. The values of three rate constants, k_2, k_{-2}, and k_3, were evaluated by the least squares method to be 0.33, 0.57, and 0.13 min^{-1}, respectively, by assuming that the first step in equation 1 is sufficiently faster than the other steps. Equation 1 is also valid for the denaturation mechanism at pH 7.0, by regarding D1 as the enzyme species that is denatured and inactive at 100 °C, but is easily renatured by lowering the temperature. Assuming again that the first step is sufficiently faster than the second or the third step, the values of k_2, k_{-2}, and k_3 for the thermal denaturation at pH 7.0 can be evaluated by the least squares method to be 0.42, 1.01, and 0.13 min^{-1}, respectively.

REFERENCES

1. FUKUMURA, M., K. SAKKA, K. SHIMADA & K. OHMIYA. 1995. Nucleotide sequence of the *Clostridium stercorarium* xynB gene encoding an extremely thermostable xylanase and characterization of the translated product. Biosci. Biotechnol. Biochem. **59:** 40–46.
2. SHIMADA, K., S. KARITA, K. SAKKA & K. OHMIYA. 1994. Cellulases, xylanases, and their genes from bacteria. *In* Recombinant Microbes for Industrial and Agricultural Applications. Y. Murooka & T. Imanaka, Eds.: 395–429. Dekker. New York.

Ammonolysis of Carboxylic Esters Catalyzed by Lipases

Synthesis of Fatty Acid Amides

M. C. DE ZOETE, A. C. KOCK–VAN DALEN,
F. VAN RANTWIJK, AND R. A. SHELDON

Laboratory of Organic Chemistry and Catalysis
Delft University of Technology
2628 BL Delft, the Netherlands

INTRODUCTION

Lipases (triacyl glycerol hydrolase, EC 3.1.1.3) are stable and rugged enzymes that act, often enantioselectively, on a wide variety of nonnatural reactants. The exploitation of their characteristic features has become an essential part of the synthetic repertoire.[1] We[2] and others[3] recently reported that ammonia acts as an unnatural acyl acceptor (ammonolysis). Carboxylic esters are converted to the corresponding carboxylic amides in essentially quantitative yield in an exothermic and, hence, irreversible reaction. The lipase from *Candida antarctica*[4] (B type, Novozym 435) emerged from the initial investigations[2] as the catalyst of choice.

We wished to extend lipase-catalyzed ammonolysis to the synthesis of fatty acid amides; these are now industrially produced from the fatty acids by a reaction with anhydrous ammonia at approximately 200 °C and 345–690 kPa and are primarily used for their lubricating and surfactant properties.[5] A low-temperature enzymatic process would seem advantageous for the synthesis of pure fatty acid amides, particularly the thermally unstable unsaturated ones that, *inter alia*, dominate the market for refined fatty acid amides. In the present paper, we report the synthesis of fatty acid amides from lipids as well as from the fatty acids by a one-pot procedure.

MATERIALS AND METHODS

Chemicals and Enzymes

All solvents and reagents were of reagent grade and were dried on molecular sieves before use. Novozym 435 (*Candida antarctica* B lipase on a proprietary carrier, activity of 7550 PLU/g), SP525 (a lyophilized lipase-preparation from *Candida antarctica* B), SP523 (a lyophilized lipase-preparation from *Humicola*), and Novozym IM20 (*Rhizomucor miehei* lipase on anionic resin, activity of 29 BIU/g) were kindly donated by Novo-Nordisk. Lipomax, a lyophilized lipase-preparation from *Pseudomonas alcaligenes*, was kindly donated by Gist-brocades.

SP525, SP523, and lipase from *P. alcaligenes* were immobilized on Accurel EP100 according to a published procedure.[6] The activities of the resulting preparations

were as follows—SP525: 12.4 kLU/g; SP523: 14.3 kLU/g; Lipomax: 7.5 kLU/g [1 kLU (kilo–Lipase Unit) will liberate 1 mmol of butyric acid from tributyrin at 25 °C and pH 7.2 in 1 min].

Ammonolysis of Lipids

Tributyrin (10 g, 34 mmol), trilaurin (5 g, 7.8 mmol), triolein (5 g, 5.6 mmol), or jojoba wax (5 g, approximately 8.1 mmol) was dissolved in *t*-butyl alcohol (50 mL) that had been saturated with ammonia (2.5 M). Novozym 435 (250 mg) was added and the reaction mixture was shaken at 60 °C until the reaction was judged to be complete by GC (tributyrin) or TLC (other lipids). The reaction products were isolated by standard workup procedures. Full experimental details will be published elsewhere.

Ammonolysis of Butyl Octanoate

Lipase (50 mg) was added to a solution of butyl octanoate (0.5 mL) and diethyleneglycol dibutyl ether (50 μL, internal standard) in ammonia-saturated *t*-butyl alcohol/*n*-butyl alcohol mixtures (5 mL). The reaction mixture was shaken at 40 °C and the course of the reaction was monitored by HPLC. Results are given later in this report.

One-Pot Ammonolysis of Carboxylic Acids

Lipase SP525 on Accurel EP100 (250 mg) was added to a solution of octanoic acid (5 g, 35 mmol) or oleic acid (5 g, 17.7 mmol) and *n*-butyl alcohol (6 g, 81 mmol) in *t*-amyl alcohol (50 mL). The reaction mixture was stirred for 24 h under reflux at 50 °C *in vacuo*; the refluxing *t*-amyl alcohol was dried over molecular sieves (HPLC yield of butyl octanoate, 98%). The reaction mixture was subsequently saturated with ammonia and stirred at 40 °C until the reaction was judged to be complete by HPLC (168 h). The amides were isolated by standard workup procedures. Full experimental details will be published elsewhere.

RESULTS AND DISCUSSION

Ammonolysis of Lipids

Initial experiments were performed with tributyrin and trilaurin, which were smoothly converted by Novozym 435 into the corresponding amides; in the absence of enzyme, no reaction took place. As an example of long-chain triglycerides, we performed the ammonolysis of olive oil, which consists mainly (approximately 85%) of triolein, because oleamide is one of the most interesting fatty acid amides (see FIGURE 1). The reaction proceeded somewhat sluggishly (72 h at 60 °C for the complete reaction), as might be expected because oleic acid is known to react rather slowly with *C. antarctica* lipase as well as with other lipases.[7] Nearly pure oleamide
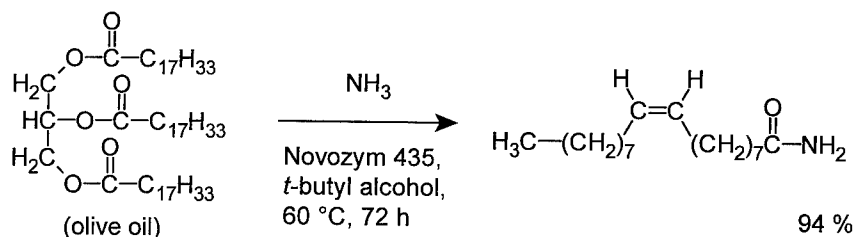
FIGURE 1. Ammonolysis of triolein.

was isolated in about 90% yield; recrystallization afforded pure oleamide in a yield of 82%.

Jojoba wax ester, which is a mixture of long-chain esters (see TABLE 1), is known to resist chemical ammonolysis at the usual conditions of 200 °C and 300–600 kPa.[8] Ammonolysis of jojoba wax by Novozym 435 resulted in a mixture of fatty acid amides and fatty alcohols after 72 h at 60 °C. Crystallization from hexane afforded the amides (mainly cis-11-eicosenamide) in approximately 90% yield. The alcohols, which account for almost 50% of the starting material, were isolated by short-path-length distillation as a 1:1 mixture of cis-11-eicosenol and cis-13-docosenol.

One-Pot Procedure

Because it is often convenient to start from the carboxylic acid, we have developed a one-pot procedure for the esterification and ammonolysis in the same reaction medium. Octanoic acid was used as a model reactant for the long-chain fatty acids (see FIGURE 2).

The esterification step was straightforward, although removal of water (reflux over 4-Å molecular sieves under reduced pressure) was required for complete conversion. Because a one-component medium would be advantageous in large-scale applications, we first used n-butyl alcohol as the reactant and solvent. Ammonolysis was quite sluggish, though, because n-butyl alcohol strongly inhibited[9] Novozym 435 in the ammonolysis step (on the basis of the heats of formation of the reactants and products, ammonolysis would be expected to proceed to completion). The inhibitive effect of n-butyl alcohol was further investigated by ammonolysis of butyl octanoate using a number of lipases (see TABLE 2).

TABLE 1. Composition of Jojoba Wax:[8]
cis,cis-$CH_3(CH_2)_7CH{=}CH(CH_2)_mCOO(CH_2)_nCH{=}CH(CH_2)_7CH_3$

	m				n			
m, n	7	9	11	13	8	10	12	14
av. comp. (%)	11	71	14	1	1	45	44	9
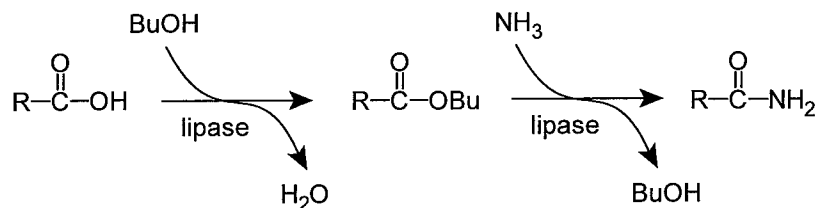
FIGURE 2. One-pot conversion of a carboxylic acid into the amide.

Inhibition of Novozym 435 by *n*-butyl alcohol was avoided by using one equivalent of *n*-butyl alcohol in *t*-amyl alcohol as solvent. Again, water was removed by reflux at diminished pressure over molecular sieves. Butyl octanoate was readily formed (98% in 20 h), but the subsequent ammonolysis was accompanied by 10% hydrolysis to octanoic acid. The problem was traced to the hydrophilic carrier of Novozym 435; this accumulated traces of water in the esterification step, which were released upon saturation of the reaction mixture with ammonia. Accordingly, we next used lipase SP525 (*Candida antarctica* B) immobilized on Accurel EP100 because this very apolar support (polypropene) would not absorb water. Esterification (using two equivalents of *n*-butyl alcohol) was carried out as before (98% ester in 24 h). Subsequent ammonolysis yielded a 97% yield of octanamide, and only traces of octanoic acid could be detected. After normal workup procedures, octanamide was isolated in 93% yield. By a similar procedure, oleic acid was transformed into oleamide, which was isolated in 90% yield.

ACKNOWLEDGMENTS

TABLE 2. Ammonolysis of Butyl Octanoate[a]

	Conversion (% in 24 h): *n*-Butyl Alcohol (% v/v in *t*-Butyl Alcohol)		
Lipase Source	0	50	100
Candida antarctica SP525	99	42	13
C. antarctica Novozym 435[b]	77	9	5
Humicola SP523	41	27	8
Pseudomonas alcaligenes	80	23	11
Rhizomucor miehei[b]	15	0	0

[a]Butyl octanoate (0.5 mL), NH_3 (2.5 M), lipase (immobilized on Accurel EP100 unless noted otherwise, 50 mg), solvent (5 mL), 40 °C, and 24 h.
[b]Immobilized on a proprietary carrier.

REFERENCES

1. For a review, see: DE ZOETE, M. C., F. VAN RANTWIJK & R. A. SHELDON. 1994. Catal. Today **22:** 563–590.
2. DE ZOETE, M. C., A. C. KOCK–VAN DALEN, F. VAN RANTWIJK & R. A. SHELDON. 1993. J. Chem. Soc. Chem. Commun., p. 1831–1832; DE ZOETE, M. C., A. C. KOCK–VAN DALEN, F. VAN RANTWIJK & R. A. SHELDON. 1994. Biocatalysis **10:** 307–316; DE ZOETE, M. C., F. VAN RANTWIJK & R. A. SHELDON. 1995. PCT Int. Appl. WO 95/07359.
3. GARCIA, M. J., F. REBOLLEDO & V. GOTOR. 1993. Tetrahedron Lett. **34:** 6141–6142; CHEN, S-T., M-K. JANG & K-T. WANG. 1993. Synthesis, p. 858–860.
4. ISHII, M. (Novo Industri A/S). 1988. PCT Int. Appl. WO 88/02775; HELDT-HANSEN, H. P., M. ISHII, S. A. PATKAR, T. T. HANSEN & P. EIGTVED. 1989. *In* Biocatalysis in Agricultural Biotechnology. Chapter 11. ACS Symposium Series Volume 389. J. R. Witaker & P. E. Sonnet, Eds.: 158–172. Amer. Chem. Soc. Washington, District of Columbia.
5. OPSAHL, R. 1992. *In* Kirk-Othmer Encyclopedia of Chemical Technology. Fourth edition. Volume 2. J. I. Koschwitz & M. Howe-Grant, Eds.: 346–356. Wiley. New York.
6. PEDERSEN, S. & P. EIGTVED (Novo-Nordisk A/S). 1990. PCT Int. Appl. WO 90/15868.
7. KIRK, O., F. BJÖRKLING, S. E. GODTFREDSEN & T. O. LARSEN. 1992. Biocatalysis **6:** 127–134.
8. SHANI, A. 1995. Chemtech **52**(5): 49–54.
9. CHULALAKSANANUKUL, W., J. S. CONDORET, P. DELORME & R. M. WILLEMOT. 1990. FEBS Lett. **276:** 181–184; RIZZI, M., P. STYLOS, A. RIEK & M. REUSS. 1992. Enzyme Microb. Technol. **14:** 709–714; MAXIMO, M. F. & J. P. VAN DER LUGT. 1994. Biocatalysis **8:** 321–335; ÖHRNER, N., M. MARTINELLE, A. MATTSON, T. NORIN & K. HULT. 1994. Biocatalysis **9:** 105–114; DE GOEDE, A. T. J. W., M. VAN OOSTEROM, M. P. J. VAN DEURZEN, R. A. SHELDON, H. VAN BEKKUM & F. VAN RANTWIJK. 1994. Biocatalysis **9:** 145–155; BERGLUND, P., M. HOLMQUIST, K. HULT & H.-E. HÖGBERG. 1995. Biotechnol. Lett. **17:** 55–60.

Control of Water Activity
in Organic Medium

ERNST WEHTJE,[a] JASMEDH KAUR,[b]
INGEMAR SVENSSON,[a] PATRICK ADLERCREUTZ,[a]
AND BO MATTIASSON[a]

[a]Department of Biotechnology
Chemical Center
Lund University
S-221 00 Lund, Sweden

[b]IIT Delhi
New Delhi, India

INTRODUCTION

The water activity (a_w) is a key parameter in enzyme catalysis in organic media. In most cases, the enzymatic activity increases with increasing water activity. However, for some lipases, the enzyme activity is optimal at a certain water activity.[1,2] Furthermore, during the course of the esterification or hydrolysis reactions, the water activity changes due to production/consumption of water. The reaction yield will depend on the water concentration at equilibrium. In order to be able to optimize both reaction rate and yield, it is therefore extremely important to adjust and control the water activity.

The water activity can initially be adjusted by equilibration of the reaction medium in containers of saturated salt solutions.[3] This technique has been further developed and can be used in a continuous system by circulating a salt solution inside a silicone tubing that is submerged into the medium.[4] Water vapor can be transported through the tubing wall into the solvent. This technique has been used in lipase-catalyzed esterifications in order to study the effect of water activity on reaction rates and equilibrium positions.[2]

EXPERIMENTAL PROCEDURES

The lipase-catalyzed reaction studied was the esterification of 200 mM decanoic acid and 200 mM dodecanol, unless stated otherwise. The enzyme preparations used were either preimmobilized Lipozyme from Novo Nordisk (Bagsværd, Denmark) or *Rhizopus arrhizus* lipase (Amano, Japan) immobilized on EP-100 (Akzo, Obernburg). Silicone tubing of various dimensions was obtained from Leewood Marketing. Water contents were analyzed by titrations using a Karl Fischer coulometer from Metrohm. Reaction yields were measured by packed column gas chromatography using a Supelco SP-216-PS column.

RESULTS AND DISCUSSION

Water Transportation

Transportation of water was achieved by pumping saturated salt solutions inside a silicone tubing, which was submerged into the organic solvent (FIGURE 1). The transport of water through the tubing was studied by using the same a_w difference across the tubing, but in different directions; that is, the solvent was preequilibrated at $a_w = 0.33$ and a salt solution of $a_w = 0.97$ was used inside the tubing and vice versa. The rate of water removal and supply was similar. This indicates that the direction of transport does not affect the rate and that the difference across the tubing and not the absolute values of initial or final a_w influence the rate.

The rate of water transport through tubings of different dimensions, such as diameter and thickness, was studied by using different saturated salt solutions and dehydrated solvents. The flux of water, F (mol/s), was different for the different tubings (TABLE 1). Thinner tubings (2010 and 3020) and tubings with large outer surface area (3020) promoted the transport. The specific transportation of water, J (mol/m$^2 \cdot$ s), through the cylindrical membrane was calculated by integrating the

Enzyme reactor   Salt container
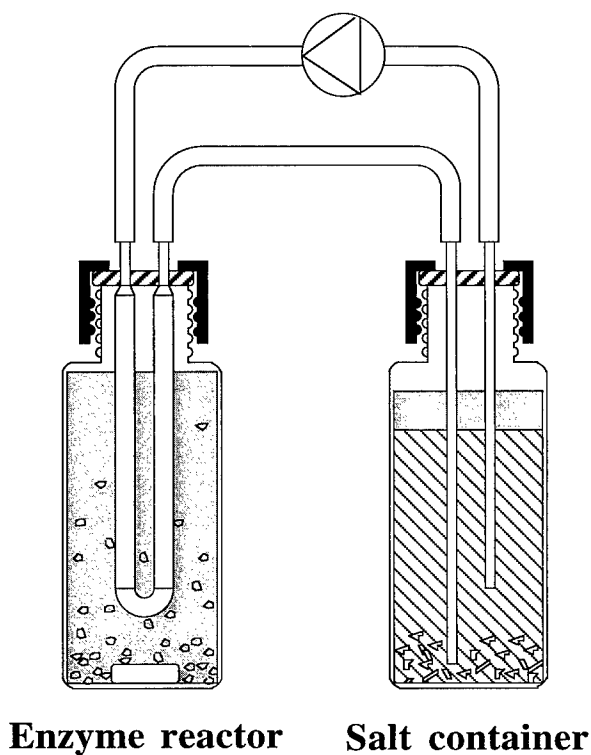
FIGURE 1. Water activity control system (from reference 4).

TABLE 1. Water Transport into 5-Methyl-2-hexanone Using Different Saturated Salt Solutions (Water Activity: 0.33, 0.53, and 0.75)

Tubing	Flux of Water $\times 10^7$ (mol/s)			Diffusion (a_w) of Water $\times 10^7$ (mol/m $\cdot$ s)			Diffusion (Concentration) of Water $\times 10^{10}$ (m^2/s)		
	0.33	0.53	0.75	0.33	0.53	0.75	0.33	0.53	0.75
HTT 2010	1.66	2.53	3.85	3.52	3.35	3.60	7.45	6.95	6.31
HTT 3010	1.36	2.26	3.07	3.22	3.31	3.17	7.31	6.75	5.81
HTT 3015	1.83	3.07	4.40	3.29	3.41	3.44	7.45	6.95	6.31
HTT 3020	2.42	4.06	5.63	2.80	2.92	2.86	6.35	5.96	5.25
TT 2010	1.83	2.97	4.35	3.23	3.25	3.37	7.31	6.63	6.18
TT 3010	1.69	2.55	3.57	3.50	3.29	3.26	7.94	6.71	5.97
TT 3020	2.42	3.96	5.54	3.00	3.07	3.03	6.80	6.26	5.55
Average				3.22	3.23	3.23	7.23	6.60	5.91

transport by using the mean log area, $2\pi L[(X_o - X_i)/\ln(X_o - X_i)]$. From these results, the diffusion coefficient, D (mol/m $\cdot$ s or m^2/s), could be calculated by using either the a_w or water concentration difference. It was shown that all tubings tested, regardless of their actual dimensions, gave similar D values and thus functioned in a similar way concerning the mass transfer of water. The driving force for the transportation was shown to be the a_w difference, $(\partial a_w/\partial x)$, and not the water concentration difference, $(\partial c/\partial x)$; note the difference in average values of D in TABLE 1. This was confirmed by studying the transport into pure solvent and solvent that contained 400 mM substrates. The water solubility in the latter is approximately 90% higher, but the transport rate is similar to the one in pure solvent. Therefore, the driving force for the transport must be the water activity and not the water concentration difference. The transport was measured in different solvents: diisopropyl ether, methyl isoamyl ketone, butyl acetate, and ethyl acetate. The transportation (diffusion) coefficients were 1.67, 3.23, 3.91, and 6.86 mol/m $\cdot$ s, respectively. These coefficients seem to depend on the solubility of water and on the swelling behavior in the different solvents. Swelling of the tubing promoted the transport and increased solubility of water gave higher transportation coefficients.

In order to study the water transport further, a continuous, large-scale (250-mL) system was designed, which could be used to simulate water production. After preequilibration, a tank reactor containing butyl acetate and 2.5 m of HTT 2010 tubing (at $a_w = 0.33$) was continuously fed with water-saturated solvent and the water content was monitored in the reactor. The concentration of water increased and this created an a_w difference across the tubing that facilitated the transport of water through the tubing. When the rate of water removal matched the feed of water, a constant level of water was obtained. This steady-state concentration of water increased as the flow rate of water-saturated solvent increased. The diffusion coefficient based on the a_w difference was independent of the flow rate (FIGURE 2).

Batch Reactions

Lipase-catalyzed reactions were performed in order to study the effect and efficiency of the water transport during biocatalysis. The water control system was
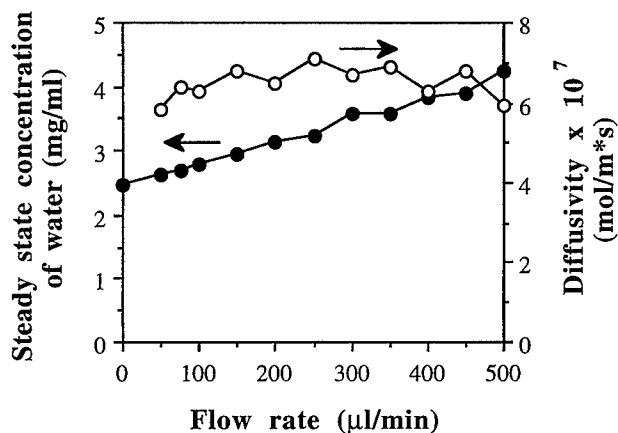
FIGURE 2. Continuous water activity control at a_w = 0.33 using a tank reactor containing 250 mL of butyl acetate and 2.5 m of HTT 2010 silicone tubing: water concentration (●) and the diffusion coefficient based on water activity (○) at different flow rates of water-saturated solvent.

studied in the esterification of decanoic acid and dodecanol and in the hydrolysis of the corresponding ester (FIGURE 3). The uncontrolled esterification and hydrolysis reactions stopped at lower conversions than the controls, which both reached the same equilibrium, that is, 67% ester at a_w = 0.33. This shows that the system works equally well in removing water as in supplying water.

The progress curves for the controlled and uncontrolled reactions are initially similar; see FIGURE 3. After some reaction time, the ester yield differs in the two reactions. The water content in a controlled esterification reaction increases initially in order to reach a steady state and eventually starts to decrease (FIGURE 4). The increase is due to the necessity to create an a_w difference across the silicone tubing in order to speed up the water transport. The steady state represents a situation where
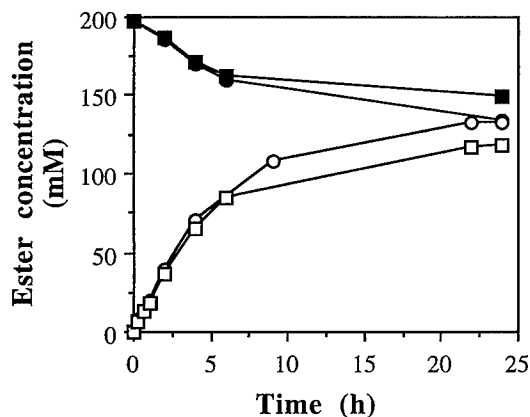
FIGURE 3. Concentration of ester in esterification (○, □) and hydrolysis (●, ■) reactions in di-isopropyl ether using immobilized lipase from *Rhizopus arrhizus*. Initial water activity was 0.33 and reactions were performed with continuous water activity control (○, ●) or without control (□, ■).

the water production is equal to the water removal. Higher reaction rates give larger a_w differences. When the reaction rate declines, the water level decreases and, at the end, the final water concentration is lower than the initial one due to decreased solubility of water in the product mixture compared to the substrate solution.

The water activity control system worked even in reactions performed in neat substrate solution (equimolar mixture of acid and alcohol). The yield of ester increased from 90.6% in the uncontrolled reaction to 94.6% in the reaction performed at constant a_w = 0.33. The water concentration at equilibrium was four times lower in the controlled reaction.

Continuous Reactions

Lipase-catalyzed esterification was studied in a packed-bed reactor with continuous water activity control. The enzyme preparation (Lipozyme) was packed in a silicone tubing (HTT 3020) and the reaction medium was pumped through the
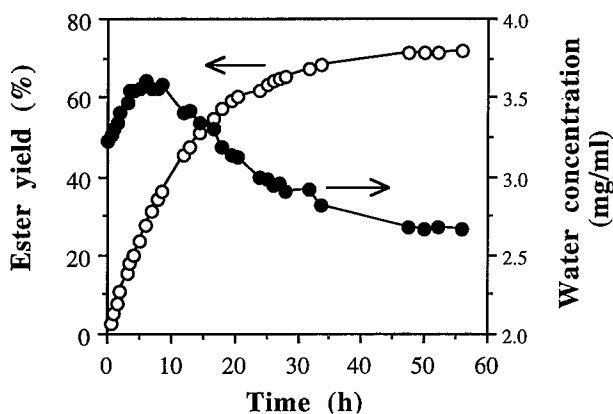
FIGURE 4. Ester yield (○) and water content (●) in the Lipozyme (1 g)–catalyzed esterification reaction in 5-methyl-2-hexanone (250 mL) at a constant water activity of 0.33.

enzyme reactor. In order to control the water activity, the tubing (containing the enzyme preparation) was submerged in a saturated salt solution (a_w = 0.33). The yield of ester at the outlet was dependent on the flow rate. At low flow rates (0.02 mL/min), the reaction reached equilibrium and the yield of ester was 74% (FIGURE 5). When the flow rate was increased, the yield decreased and, at rates higher than 0.2 mL/min, the reaction was under kinetic control, giving a constant productivity. In all cases, the water transportation seems to be efficient and the water transport rate was not rate-limiting. The esterification reaction was studied for two months, without any significant decrease in ester yield at low flow rate (FIGURE 6). However, if the yield was measured at 1 mL/min, the yield was shown to decrease by almost 50%. To increase the ester yield further, the outlet from the reactor was led into a second reactor containing lipase from *Candida antarctica* and molecular sieves. The ester
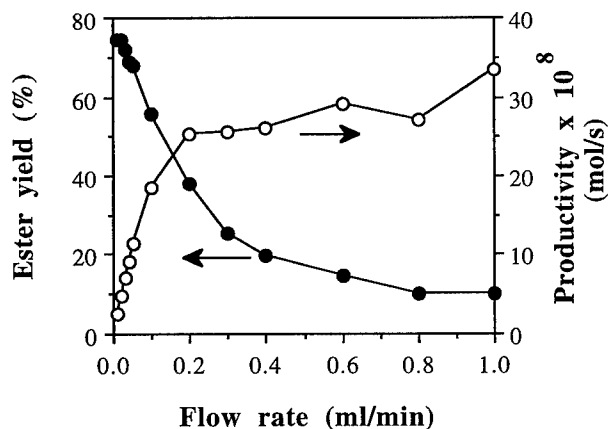
FIGURE 5. Ester yield (●) and productivity (○) of the packed-bed reactor (400 mg Lipozyme, packed in HTT 3020 silicone tubing) at different flow rates of substrate in 5-methyl-2-hexanone.

yield increased to 85% due to the removal of water and the subsequent reduction in water activity. This additional reaction was studied for two weeks.

CONCLUSIONS

- Water transportation can be achieved by the use of salt solutions and silicone tubings. The system functions in both removing and supplying water to a reaction.
- The transportation rate can be predicted by taking into account the dimensions of the tubing and the water activity difference across the tubing.
- The system can be used in batch as well as continuous modes, as exemplified by lipase-catalyzed esterifications.
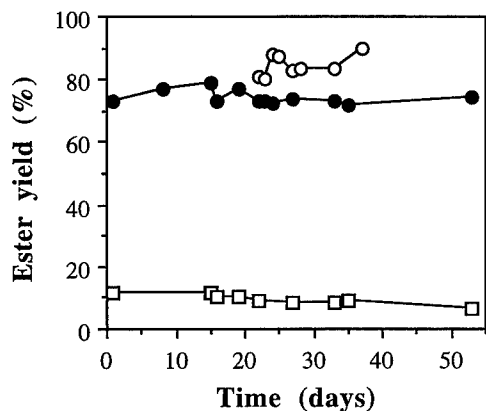
FIGURE 6. Yield of ester in 5-methyl-2-hexanone of the packed-bed reactor at 0.01 mL/min (●) and 1 mL/min (□), and yield from the additional enzyme reactor (○).

REFERENCES

1. VALIVETY, R. H., P. J. HALLING & A. R. MACRAE. 1992. Reaction rate with suspended lipase catalysts shows similar dependence on water activity in different solvents. Biochim. Biophys. Acta **1118:** 218–222.
2. SVENSSON, I., E. WEHTJE, P. ADLERCREUTZ & B. MATTIASSON. 1994. Effects of water activity on reaction rates and equilibrium positions in enzymatic esterification. Biotechnol. Bioeng. **44:** 549–556.
3. GODERIS, H., G. AMPE, M. FEYTEN, B. FOUWÉ, W. GUFFENS, S. V. CAUWENBERGH & P. TOBBACK. 1987. Lipase-catalyzed ester exchange reactions in organic media with controlled humidity. Biotechnol. Bioeng. **30:** 258.
4. WEHTJE, E., I. SVENSSON, P. ADLERCREUTZ & B. MATTIASSON. 1993. Continuous control of water activity during biocatalysis in organic media. Biotechnol. Lett. **7:** 873–878.

Enhancing the Stereoselectivity and Activity of *Candida* Species Lipase in Organic Solvent by Noncovalent Enzyme Modification[a]

HONG YANG,[b] SHU-GUI CAO,[b] SI-PING HAN,[b]
NI-NI GUO,[b] XIU-GONG GAO,[b] ZHONG-LI HUANG,[b]
HUAN DONG,[b] NIAN-XIANG ZHANG,[b]
TONG-SU YANG,[b] YING CHU,[c] AND JIA-LI XU[d]

[b]*State Key Laboratory of Enzyme Engineering*
Jilin University
Changchun 130023, People's Republic of China

[c]*Department of Chemistry*
Teachers Training College of Dongbei
Changchun 130021, People's Republic of China

[d]*Institute of Microbiology*
Academia Sinica
Beijing 100080, People's Republic of China

INTRODUCTION

Chiral 2-octanol is not only an important chiral building block, but also a material applied in liquid crystals with high dielectric constants.[1] Often, the enantiomeric purity of 2-octanol is of crucial importance for its application. It is easier to make chiral amine and chiral carboxylic acid through a chemical process,[1] but it is difficult to obtain chiral alcohol in the same way. Therefore, it is very important to develop an effective strategy to produce chiral alcohol with high enantiomeric purity.

In recent years, increasing attention has been focused on the potential of the stereoselectivity of enzymes in organic solvent in resolution of (*R,S*)-2-octanol. Although the enantiomeric purity of 2-octanol obtained by enzyme catalysis is higher than that obtained by chemical methods, it is not high enough. Most biocatalytic reactions are only partially stereoselective. Besides the insufficient enantiomeric purity, the reaction time for the enzyme to catalyze in organic solvent is long.[2] How to increase the stereoselectivity and activity of enzyme in organic solvent is very important to produce ideal chiral 2-octanol.

In this paper, we have not only enhanced the stereoselectivity of *Candida* species lipase (CSL), but also increased its activity by noncovalent enzyme modification with amphipathics. A simple and effective strategy for the production of ideal chiral 2-octanol is thus provided.

MATERIALS AND METHODS

Candida species lipase (CSL) was provided by the Institute of Microbiology, Academia Sinica, Beijing, People's Republic of China. (R)-$(-)$- and (S)-$(+)$-1-(1-naphthyl)ethyl isocyanates (R-NEI and S-NEI) were purchased from Aldrich Chemical. (R,S)-2-Octanol and other reagents were all of analytical grade.

Stereoselective Esterification of (R,S)-2-Octanol with Octanoic Acid Catalyzed by CSL in Organic Solvent

(R,S)-2-Octanol (2.5 mL of 0.56 mol/L) and octanoic acid (2.5 mL of 0.8 mol/L) were mixed together in cyclohexane; then, 20 mg of CSL and 0.4% (v/v) water were added into the above mixture and incubated with shaking (120 strokes per min) at 37 °C. The reaction was terminated by removing the enzyme.

Determination of the Substrate Conversion (Percent) and the Esterification Activity of Lipase

Octanoic acid in the reaction system was titrated with methanol containing 0.025 N NaOH in a benzene-methanol (4:1 v/v) mixture in the presence of methanol containing 0.3% thymol blue. The substrate conversion (percent) and the esterification activity of lipase were calculated from the decrease of the amount of octanoic acid.

Measurement of Enantiomeric Excess

The enantiomeric excess (ee) of 2-octanol was determined by HPLC.[3] The enantiomeric excess of the obtained ester was calculated from the enantiomeric excess of the unreacted 2-octanol and the 2-octanol conversion, according to the formula $ee_p = ee_s/(C - ee_s)$.

Determination of the Stereoselectivity of Lipase

The stereoselectivity of lipase was calculated according to the ratio V_{OR}/V_{OS}.

Preparation of CSL Powders with Different pH

Crude CSL powders were dissolved in 0.02 mol/L phosphate buffer with different pH values and centrifuged at 6000 rpm for 15 minutes. The supernatants were ultrafiltrated with PM30 film in 0.02 mol/L phosphate buffer with different pH values and then the concentrated solutions were lyophilized into CSL powders.

RESULTS AND DISCUSSION

In this paper, racemic 2-octanol was resolved by CSL-catalyzed stereoselective esterification of (R,S)-2-octanol with octanoic acid in cyclohexane. Our earlier work[4]

ANNALS NEW YORK ACADEMY OF SCIENCES

showed that this stereoselective esterification was only partially stereoselective and that the enantiomeric excess of the prepared chiral 2-octanol was only 75.9%. Moreover, the esterification activity of CSL was poor. In order to enhance the activity and the stereoselectivity of lipase in organic solvent, amphipathics with different chain length and different electric charge, such as amphipathic A, CTAB (cetyltri-methylammonium bromide), and Triton X-100 (FIGURE 1), were put into the reaction system according to the characteristics of enzyme catalysis in organic solvent. We performed various studies (see below).
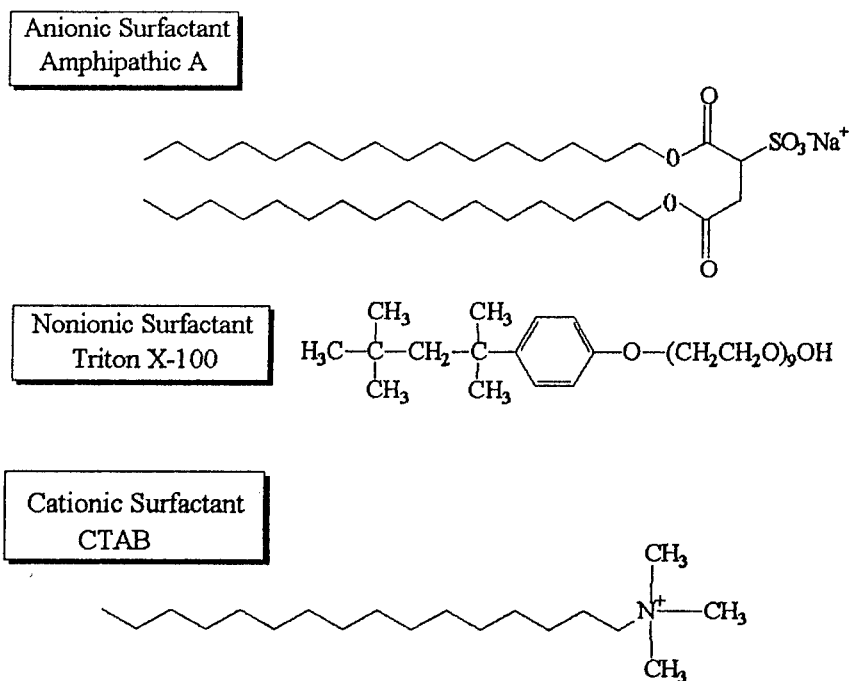
FIGURE 1. The chemical structure of amphiphilic molecules.

Effect of Amphipathic A, Triton X-100, and CTAB on the Stereoselective Esterification of (R,S)-2-Octanol

The stereoselective esterification of (R,S)-2-octanol (0.28 mol/L) with octanoic acid (0.40 mol/L) was catalyzed by CSL (20 mg) in cyclohexane (5 mL) containing different concentrations of amphipathic A, Triton X-100, or CTAB. The results demonstrated that the positively charged CTAB (details not shown) and the neutral Triton X-100 (details not shown) had no evident effect on the activity and stereoselectivity of CSL, but the negatively charged amphipathic A (TABLE 1) made the stereoselectivity of CSL increase greatly. The stereoselectivity of CSL was dependent

TABLE 1. Effect of Amphipathic A on the Stereoselective Esterification of
(R, S)-2-Octanol with Octanoic Acid Catalyzed by CSL Powder[a]

Concentration of Amphipathic A (mg/mL)	Reaction Time (h)	Alcohol Conversion (%)	Unreacted (S)-Alcohol ee (%)	(R)-Ester ee (%)	V_{OR}	V_{OS}	V_{OR}/V_{OS}	Relative Activity (%)
0	90	45.0	52.2	63.8	9.2	1.80	5.1	100
0.11	90	47.8	71.2	77.8	10.6	0.63	16.9	102
0.25	90	45.2	71.2	86.3	10.7	0.38	28.2	101
0.50	90	43.9	75.2	96.1	10.8	0.18	61.0	100
1.00	90	51.5	98.0	92.3	12.2	0.10	122.8	105
1.50	90	47.9	86.1	93.6	11.0	0.10	110.5	101
2.00	90	44.9	79.6	97.7	10.9	0.10	108.0	96
3.00	90	43.8	74.6	95.0	10.6	0.10	105.9	94

[a]The water content in the reaction system was 0.4%.

on the concentration of amphipathic A. CSL showed the highest stereoselectivity when the concentration of amphipathic A was 1.00 mg/mL. Under optimal conditions, the ratio of V_{OR}/V_{OS} was enhanced 24-fold. (S)-2-Octanol with 98.0% ee and (R)-2-octyl octanoate with 97.7% ee were prepared. The esterification activity of CSL was not affected greatly by amphipathic A. These results revealed that amphipathic A enabled (R)-2-octanol to react with octanoic acid more easily, but amphipathic A prevented (S)-2-octanol from reacting with octanoic acid.

Effect of AOT on the Stereoselective Esterification of (R,S)-2-Octanol

In order to investigate the pattern of the effect of amphipathics on the activity and stereoselectivity of lipase, we studied the effect of [sulfosuccinic acid bis(2-ethyl-hexyl) ester]sodium salt (AOT) (FIGURE 2) on the stereoselective esterification of (R,S)-2-octanol because AOT had the same amount of electric charge and the same functional groups as amphipathic A. The results (TABLE 2) showed that AOT had no evident effect on the stereoselectivity of CSL, but it enhanced the activity of CSL by 20%. Why did amphipathic A and AOT, which had the same amount of electric charge and the same functional groups, have different effects on this reaction? This may be explained by the facts that the hydrophobic chain length of AOT is much shorter than that of amphipathic A and that AOT has smaller steric hindrance than amphipathic A. Therefore, AOT cannot prevent (S)-2-octanol from reacting with
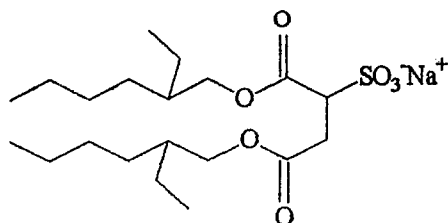
FIGURE 2. The chemical structure of the anionic surfactant AOT.

TABLE 2. Effect of AOT on the Stereoselective Esterification of (R, S)-2-Octanol with Octanoic Acid Catalyzed by CSL Powder[a]

Concentration of AOT (mg/mL)	Reaction Time (h)	Alcohol Conversion (%)	Unreacted (S)-Alcohol ee (%)	(R)-Ester ee (%)	V_{OR}	V_{OS}	V_{OR}/V_{OS}	Relative Activity (%)
0	90	45.0	52.2	63.8	9.2	1.80	5.1	100
0.20	90	48.2	55.1	59.2	10.5	1.86	5.6	112
0.60	90	48.3	55.9	59.8	10.2	1.89	5.4	110
1.00	90	50.1	58.7	58.5	11.3	2.02	5.6	121
1.50	90	49.6	51.2	52.0	10.9	2.18	5.0	119
2.00	90	49.9	52.8	53.0	11.1	2.13	5.1	120

[a]Other reaction conditions were the same as those in TABLE 1.

octanoic acid. On the contrary, AOT made the reactions of both (R)-2-octanol and (S)-2-octanol fast.

Effect of pH on the Stereoselective Esterification of (R,S)-2-Octanol in the Presence of Amphipathic A

The stereoselective esterification of (R,S)-2-octanol (0.28 mol/L) with octanoic acid (0.40 mol/L) was catalyzed by CSL powders (20 mg) with different pH values in cyclohexane (5 mL) in the presence of amphipathic A (1.00 mg/mL). The results (TABLE 3) showed that the pH value of CSL had an effect on the activity and stereoselectivity of CSL in the presence of amphipathic A. When the pH value of CSL was 6.6, CSL showed the highest activity. The higher that the pH value was, the lower the stereoselectivity of the lipase. When there was no amphipathic A in the reaction system, the pH value had no evident effect on the stereoselectivity of the lipase.[4] These results revealed that the effects of the amphipathics on the stereoselective esterification were dependent on the electric charge of the enzyme. This may be explained by the fact that the positive charge of CSL decreases as the pH value of CSL increases. Therefore, the negatively charged amphipathic A is hindered in making contact with the enzyme molecules.

TABLE 3. Effect of pH of the CSL Powder on the Stereoselective Esterification of (R, S)-2-Octanol with Octanoic Acid in the Presence of Amphipathic A[a]

pH	Reaction Time (h)	Alcohol Conversion (%)	(S)-Alcohol ee (%)	(R)-Ester ee (%)	V_{OR}	V_{OS}	V_{OR}/V_{OS}	Relative Activity (%)
4.4	90	41.2	69.5	99.0	8.5	0.08	110	78
4.9	90	47.8	87.8	95.9	10.5	0.10	109	96
5.3	90	45.9	80.2	94.5	9.8	0.09	106	90
6.0	90	46.1	79.1	92.5	10.0	0.11	91	92
6.6	90	49.8	81.5	82.2	10.9	0.12	91	100
7.8	90	42.1	68.5	93.8	8.8	0.10	89	81

[a]The concentration of amphipathic A in the reaction system was 1.0 mg/mL. Other reaction conditions were the same as those in TABLE 1.

CONCLUSIONS

In conclusion, the activity and the stereoselectivity of CSL were dependent not only on the electric charge of the amphipathics and lipase, but also on the structure of the amphipathics. Amphipathic A can enhance the stereoselectivity of CSL evidently (24-fold). AOT can make the activity of CSL increase by 20%. (S)-2-Octanol with 98.0% ee and (R)-2-octyl octanoate with 97.7% ee were prepared by one procedure reaction.

REFERENCES

1. OKAHATA, Y. & K. IJIRO. 1990. Kagaku To Kogyo **43**(8): 1242.
2. JANSSEN, A. J. M. & B. ZWANENBURG. 1991. Tetrahedron **47**: 7645.
3. HIRATA, H., T. YAMASHINA & I. IIDA. 1991. Determination of enantiomer content of secondary alkanol as diastereomeric N-[1-(1-naphthyl)ethyl]-carbamate by normal phase HPLC. J. Jpn. Oil Chem. Soc. **40**(11): 9.
4. YANG, H., S-G. CAO *et al.* 1995. Optical resolution of (R,S)-2-octanol with lipases in organic solvent. Ann. N.Y. Acad. Sci. **750**: 250.

Stopped-Flow, Pre-Steady-State Kinetic Study of Horseradish Peroxidase Catalysis in Nonaqueous Media

SHUNGUANG WANG,[a] WEI LIU,[b] XINSONG JI,[a]
LIN MA,[c] TIEJIN LI,[b] AND ZHONGYI YUAN[a]

[a] Shanghai Institute of Biochemistry
Academia Sinica
Shanghai 200031, People's Republic of China

[b] Department of Chemistry
[c] National Laboratory of Enzyme Engineering
Jilin University
Changchun 130023, People's Republic of China

INTRODUCTION

In recent years, nonaqueous enzymology has witnessed rapid progress and has become a hot topic in the field of classical enzymology.[1,2] Upon placing an enzyme in a nonaqueous medium, the biocatalyst is subjected to a number of factors that can alter its native aqueous-based structure and function. Because substantial differences have been noted between the reaction rate, maximal velocity (V_{max}), specific activity (κ_{cat}),[3,4] substrate affinity (K_m), specificity constant (κ_{cat}/K_m),[5,6] and enantioselectivity (E)[7,8] determined in water and in various organic solvents, it has been attempted to demonstrate the mechanism by which organic solvents can affect the enzymatic reaction and the relationship between enzyme performance and the physical properties of those media.

Comparison of enzyme activities in different solvents and the development of predictive models relating enzyme activity to solvent structure will depend on a detailed understanding of the effect of the solvent on the mechanism and the rates of the individual steps during catalysis. However, all of the studies to date use steady-state kinetic methods to study the catalytic behavior. The enzyme is regarded as a catalyst in steady-state kinetics; therefore, it is difficult to directly investigate the solvent effects on the enzyme molecule itself and hence on the overall reaction. On the other hand, the enzyme can be treated as a reactant directly involved in the elementary steps in pre-steady-state kinetics, thereby allowing us to follow the changes occurring in the enzyme molecule itself.[9] However, such a method has never been applied in the field of nonaqueous enzymology due to the stringent requirements, such as the preparation of stable intermediate and the homogeny of the reaction media by this method. Most of the enzymes can only retain their activity in the solid state in nonpolar organic solvents with low water content; water-miscible polar solvents or even high water concentration would inactivate them,[10] thus making it impossible to study their catalytic behavior using pre-steady-state kinetics.[11] Fortunately, horseradish peroxidase (HRP) is catalytically active in water-miscible

364

organic solvents with high water concentration[3,5] and has a wide specificity with substrates that are highly soluble in nonaqueous media. Furthermore, detailed information concerning the elementary steps during the catalytic cycle in aqueous solution is available,[12] which is beneficial for the study of the catalytic behavior in nonaqueous media using pre-steady-state kinetics.

The catalytic cycle of horseradish peroxidase has been well established as a result of the early pre-steady-state kinetic studies by Chance.[13-15] Resting enzyme (Fe^{3+}) reacts with H_2O_2 to give a green intermediate, compound I. The heme iron in compound I is in the oxyferryl ($Fe^{4+} = 0$) state and an electron has been removed from the heme porphyrin ring to produce π cation radical species, resulting in an overall oxidation state of +5 for the heme prosthetic group, which is two oxidizing equivalents higher than that of the resting enzyme. Compound I is reduced by the reducing substrate AH_2 to the resting enzyme in two sequential one-electron steps via a second intermediate, compound II. Compound II also contains an oxyferryl center in which the π cation radical of compound I has been reduced. Reduction of compound II to the resting enzyme or dissociation of the radical product (AH˙) from compound II is normally rate-limiting.

Horseradish peroxidase is an ideal model with which to carry out the pre-steady-state kinetic study. The two intermediates formed during the catalytic cycle have their characteristic absorption spectra. There also exist different isosbestic points among three forms of the enzyme. Furthermore, the enzyme is very stable and is commercially available in large amounts of the pure protein form. Taking advantage of all these properties, we select HRP as a model to study the solvent effects on the elementary steps of the enzymatic reaction using stopped-flow, pre-steady-state kinetics.

MATERIALS AND METHODS

Materials

Horseradish peroxidase (type II) was purchased from Sigma Chemical (St. Louis, Missouri) and used without further purification. Hydrogen peroxide was commercially obtained from local markets as 30% solution, whose concentration was determined by the method of Ovenston and Rees.[16] The solvents and substrates used in this work were purchased from different suppliers and were of the highest quality commercially available. All solvents were bidistilled prior to use, and 1,4-dioxane and tetrahydrofuran were further purified to remove any trace organic peroxides. All substrates were recrystallized or bidistilled prior to use. The double-distilled water was deionized by an ion-exchange column and then was distilled over alkaline potassium permanganate. The buffer used in this study was 10 mM phosphate solution at pH 7.0.

Methods

Preparation of Enzyme Solution

The enzyme stock solution (10 mM) was prepared by dissolving the required amount of enzyme powder in a given volume of 10 mM phosphate buffer, pH 7.0. The

concentration was spectrophotometrically determined by recording the absorbance of the diluted sample at 403 nm ($\epsilon = 1.02 \times 10^5$ M^{-1}-cm^{-1}). The stock solution was stored at 4 °C and diluted prior to use.

Stopped-Flow, Pre-Steady-State Kinetic Measurements

Stopped-flow, pre-steady-state kinetic measurements were carried out in a UNION GIKEN RA401 stopped-flow spectrophotometer. The reaction cell was thermostatically maintained at 25 ± 0.5 °C. Measurements ($n = 8$–11) were made under pseudo-first-order reaction conditions at each substrate concentration. The apparent first-order rate constant was calculated by using Guggenheim's method. When plotting the apparent first-order rate constants versus their corresponding substrate concentrations, the slope of the weighted least-squares regression line represents the real second-order constant of the elementary steps.

Considering that the HRP structure undergoes few, if any, changes upon the transition from aqueous solution to nonaqueous media,[3] the monitoring wavelength of each elementary step was set by reference to that of the same reaction in aqueous solution. For example, for the single turnover experiment of the formation of compound I, it was imperative to ensure that no compound II was present. This was accomplished by monitoring the reaction in the vicinity of 395 nm on the stopped-flow apparatus prior to each set of experiments. A narrow band-pass was obtained by using a slit width of < 0.7 nm. Because HRP I and HRP II are isosbestic in this wavelength region, no change in absorbance should be observed. Therefore, compound I formation was monitored at 395 nm. Similarly, compound II formation from compound I was monitored at 412 nm, and the disappearance of compound II was monitored at 425 nm. The final concentration of enzyme was generally about 1 μM.

Compound II was made by first mixing equal volumes of enzyme (2.0 μM) and H_2O_2 (2.1 μM) and then mixing with an equal volume of p-cresol (1 μM). This intermediate is fairly stable in nonaqueous media. By contrast, compound I is very difficult to prepare due to its high reactivity and photosensitivity. Furthermore, other unknown potential trace reductants present in the reaction media may also act as hydrogen donors to reduce this intermediate to compound II. In the present study, the reduction of compound I is monitored by the method of Dunford and Hasinoff,[17] with the native HRP (2 μM) in one syringe of the stopped-flow apparatus and H_2O_2 (2 mM) and reducing substrate in the other. The formation of compound I is essentially complete within the dead time of the instrument and the subsequent reduction of compound I is readily followed. By setting the monochromator at 411 nm, an isosbestic point for HRP I and HRP II, any competition of HRP II, formed from the HRP I reduction, for the excess of substrate is eliminated as a source of error.

Measurements of Activity Coefficients

The activity coefficient of the enzyme was determined by measuring its saturation solubility in various media. The enzyme powder was added to 0.2 mL of buffer and aqueous organic solvents until saturation. The saturation solubility in various media was obtained by measuring the absorbance of the supernatants at 403 nm.

The activity coefficients of H_2O_2 in water/propanol, water/ethanol, water/acetonitrile, and water/methanol solutions were calculated by measuring the partition coefficients from the aqueous/organic mixture into isooctane (isooctane is immiscible with water, propanol, methanol, ethanol, and acetonitrile). The activity coefficient of H_2O_2 in an organic solvent relative to that in water is then given by equation 1:

$$\frac{\gamma_S}{\gamma_W} = \frac{P_W}{P_S} \qquad (1)$$

where γ_W and γ_S represent the activity coefficients of H_2O_2 in water and in an aqueous/organic mixture and where P_W and P_S are the partition coefficients of H_2O_2 between water and isooctane and between the solvent mixture and isooctane, respectively. In a typical experiment, the average values of the partition coefficients were measured by adding 200 μL of 30% H_2O_2 solution to 2 mL of water or a water/organic mixture and then contacting the resulting solution with 2 mL of isooctane. The solutions were shaken for 24 h at 300 rpm at 25 °C. The concentration of H_2O_2 in each phase was determined by recording the absorbance at 240 nm. Thermodynamic estimations of the activity coefficients of the substrates in the water/solvent mixture were performed using the UNIFAC model as developed by Fredenslund, Rasmussen, and Gmehling.[18]

RESULTS AND DISCUSSION

Effect of Organic Solvents on Elementary Steps of the HRP-catalyzed Reaction

In the present study, we have measured the second-order rate constants of the three elementary steps of the HRP-catalyzed oxidation of *p*-cresol in seven organic solvents with different amounts of water. These solvents included methanol, ethanol, acetone, dioxane, 1-propanol, tetrahydrofuran (THF), and acetonitrile. FIGURE 1 shows that the pseudo-first-order rate constants are linear with the substrate concentrations and that the second-order rate constants are determined by the slope of these lines; the values are given in TABLE 1.

It should be pointed out that the constants contained in TABLE 1 are apparent values; hence, it is not easy to find out the relationship between the change of the rate constants and the physical properties of the solvents at first sight. Nevertheless, one can note that the rate constants of κ_1, the formation of compound I from the resting enzyme, remain almost constant in organic media; however, the rate constants of compound II formation decrease as much as one order of magnitude in organic solvents. For example, the rate constant in THF is 30 times or so lower than that in buffer. Very dramatic changes occur in κ_3, the rate constant of the HRP II disappearance, which are one to two orders of magnitude lower in solvents than in buffer. For example, κ_3 is 130 times lower in 70% methanol. The above data indicate that the three elementary steps respond differently to the effects of organic solvents, which may be relevant to the fact that the enzyme and its intermediates are in different states and to the different catalytic mechanism of each elementary reaction.

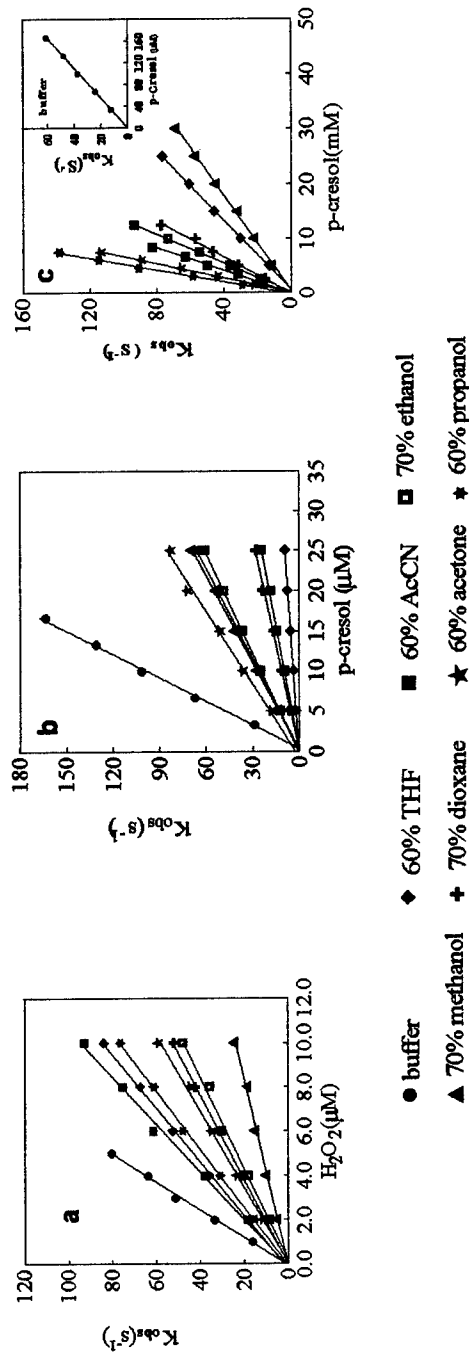In a particular solvent, the rate constant of each elementary step decreases as the

FIGURE 1. Plots of the pseudo-first-order rate constant for the reaction of the formation of (a) HRP I, (b) HRP II, and (c) HRP in aqueous and various nonaqueous media.

TABLE 1. Pre-Steady-State Kinetic Data Obtained with *p*-Cresol as Substrate in Various Solvents

Solvent	κ_1 (M^{-1}·s^{-1}) ($\times 10^6$)	κ_2 (M^{-1}·s^{-1}) ($\times 10^6$)	κ_3 (M^{-1}·s^{-1}) ($\times 10^3$)
water	15.8 ± 0.49	9.97 ± 0.28	0.364 ± 0.006
acetone (50%)	5.80 ± 0.20	3.30 ± 0.16	15.2 ± 0.24
acetonitrile (60%)	9.30 ± 0.45	0.97 ± 0.04	10.1 ± 0.23
dioxane (70%)	5.22 ± 0.07	1.12 ± 0.04	5.99 ± 0.30
ethanol (70%)	4.83 ± 0.28	2.41 ± 0.02	7.51 ± 0.09
methanol (60%)	2.36 ± 0.28	2.75 ± 0.06	2.31 ± 0.05
propanol (60%)	7.61 ± 0.16	2.66 ± 0.09	18.4 ± 0.72
THF (60%)	8.24 ± 0.19	0.35 ± 0.01	3.16 ± 0.04

mole fraction of water-miscible organic solvents (e.g., dioxane) increases. For example, TABLE 2 shows the rate constants of the three elementary steps determined in water/dioxane media with different amounts of dioxane aqueous solution. It indicates that the rate constants decrease as the dioxane concentration increases.

In conclusion, all of the above-mentioned data demonstrate that the rate constant of each elementary step decreases in organic solvent as compared to that in buffer. The disappearance of HRP II is most sensitive to the effects of organic solvents.

Transfer Free Energy Analysis of the HRP-catalyzed Reaction in Nonaqueous Media

A number of factors may contribute to the observed solvent effects on the HRP-catalyzed reaction in nonaqueous media, such as substrate solvation and direct interactions of the solvents with the enzyme.[19,20] In some cases, substrate solvation may be able to explain completely the observed effects of changing solvents.[21] However, even if this does not hold, different solvents must affect the enzyme behavior by this mechanism. Hence, this influence should be discounted before seeking explanations for the residual effects in terms of intrinsic effects on the enzyme molecule itself.[22] To that end, a free energy analysis of the elementary steps in the HRP-catalyzed reaction is commenced. Using the transfer free energy, it is possible to elucidate the solvent effects on the free energies of the ground state and transition state of each elementary step. Such a method may be able to shed some light on the intrinsic effects of organic solvents on the reactions, as demonstrated by Ryu and Dordick[3] and by Wescott and Klibanov.[23,24]

FIGURE 2 depicts a simplified kinetic and thermodynamic model for each elementary step of the HRP-catalyzed reaction in both water and organic solvents.

TABLE 2. Pre-Steady-State Kinetic Data Obtained with *p*-Cresol as Substrate in Aqueous Solution with Different Amounts of Dioxane

Dioxane (v/v, %)	κ_1 (M^{-1}·s^{-1}) ($\times 10^6$)	κ_2 (M^{-1}·s^{-1}) ($\times 10^6$)	κ_3 (M^{-1}·s^{-1}) ($\times 10^3$)
0	15.8 ± 0.49	9.97 ± 0.28	0.364 ± 0.006
36	7.93 ± 0.31	7.46 ± 0.27	61.6 ± 0.98
50	6.80 ± 0.37	3.37 ± 0.12	21.3 ± 0.16
70	5.22 ± 0.07	1.12 ± 0.04	5.99 ± 0.30

Water   HRP + H2O2 $\xrightarrow{\Delta G_1^W}$ $[\text{HRP}\cdot \text{H}_2\text{O}_2]^{\ddagger}$

$\Delta G_{E(O)}^{tr}$ $\Delta G_{H_2O_2}^{tr}$ $\Delta G_{[E(O)\cdot S]^{\ddagger}}^{tr}$

Solvent   HRP + H2O2 $\xrightarrow{\Delta G_1^S}$ $[\text{HRP}\cdot \text{H}_2\text{O}_2]^{\ddagger}$

Water   HRP(I) + S $\xrightarrow{\Delta G_2^W}$ $[\text{HRP(I)}\cdot \text{S}]^{\ddagger}$

$\Delta G_{E(I)}^{tr}$ ΔG_S^{tr} $\Delta G_{[E(I)\cdot S]^{\ddagger}}^{tr}$

Solvent   HRP(I) + S $\xrightarrow{\Delta G_2^S}$ $[\text{HRP(I)}\cdot \text{S}]^{\ddagger}$

Water   HRP(II) + S $\xrightarrow{\Delta G_3^W}$ $[\text{HRP(II)}\cdot \text{S}]^{\ddagger}$

$\Delta G_{E(II)}^{tr}$ ΔG_S^{tr} $\Delta G_{[E(II)\cdot S]^{\ddagger}}^{tr}$

Solvent   HRP(II) + S $\xrightarrow{\Delta G_3^S}$ $[\text{HRP(II)}\cdot \text{S}]^{\ddagger}$
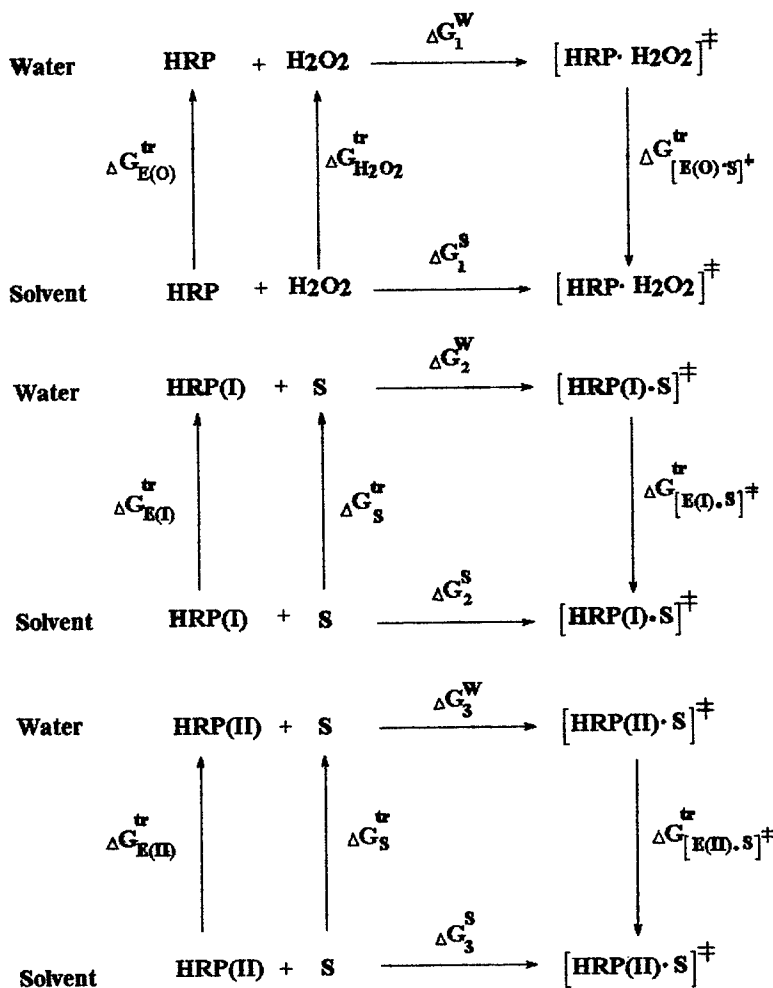
FIGURE 2. Transfer free energies between aqueous and nonaqueous media. Free energy symbols are as described in the text. Note that the transfer free energies for the reactants (including enzyme and substrate) stand for the change of the free energies during the transferring from solvent to water, whereas those for the transition-state complex stand for the change from water to solvent.

Transfer free energies (ΔG^{tr}) represent the differences in free energies between water and an organic solvent for the resting enzyme, HRP I, HRP II, the substrate, and the enzyme-substrate transition-state complex, where subscripts S and W represent the organic solvent and water, respectively.

The ground-state energy of the reactant can be easily calculated by the following equation:

$$\Delta G = RT \ln \left(\frac{\gamma}{\gamma^0}\right) \tag{2}$$

where γ refers to the activity coefficient of the reactant in a given solvent and γ^0 is the activity coefficient of an arbitrary standard state. Therefore, the energies of HRP in water and organic solvent are given by equations 3 and 4:

$$\Delta G_E^S = RT \ln \left(\frac{\gamma^S}{\gamma^0} \right),$$ (3)

$$\Delta G_E^W = RT \ln \left(\frac{\gamma^W}{\gamma^0} \right).$$ (4)

The transfer free energy of HRP is given by equation 5:

$$\Delta G_E^{tr} = \Delta G_E^W - \Delta G_E^S = RT \ln \left(\frac{S_E^S}{S_E^W} \right)$$ (5)

where S_E^S and S_E^W represent the saturation solubilities of HRP in organic solvent and in water, respectively. Similarly, the transfer free energy of the substrate can be obtained, as shown by equation 6:

$$\Delta G_S^{tr} = RT \ln \left(\frac{\gamma_S^W}{\gamma_S^S} \right) = RT \ln \left(\frac{P_S^S}{P_S^W} \right)$$ (6)

where P_S^W and P_S^S refer to the partition coefficients of the substrate between water and isooctane and between solvent and isooctane, respectively.

The activation energies of the same elementary reaction occurring in water and solvent are related to the rate constants (e.g., κ_1^W and κ_1^S) according to equations 7 and 8:

$$\Delta G_1^S = -RT \ln \left(\frac{\kappa_1^S h}{\kappa_B T} \right),$$ (7)

$$\Delta G_1^W = -RT \ln \left(\frac{\kappa_1^W h}{\kappa_B T} \right).$$ (8)

Here, h is Planck's constant, κ_B is Boltzmann's constant, and T is the absolute temperature.

Expressing ΔG_1^S as the sum of the energetic terms of alternate paths yields

$$\Delta G_1^S = \Delta G_E^{tr} + \Delta G_S^{tr} + \Delta G_1^W + \Delta G_{(ES^\ddagger)}^{tr}$$ (9)

where $\Delta G_{(ES^\ddagger)}^{tr}$ represents the transfer free energy of the transition-state complex from water to organic solvent, which gives the intrinsic difference in the transition-state free energies for a given elementary reaction between organic solvent and water. Substituting equations 5–8 into equation 9 and rearranging, one obtains

$$\Delta G_{(ES^\ddagger)}^{tr} = RT \ln \left(\frac{\kappa_1^W}{\kappa_1^S} \right) + RT \ln \left(\frac{S_E^W}{S_E^S} \right) + RT \ln \left(\frac{P_S^W}{P_S^S} \right)$$ (10)

where the transfer free energies of the substrate can be easily calculated from the thermodynamic relationships using the ratio of the activity coefficients in a solvent relative to water. The ratio of the activity coefficients of the resting enzyme is

TABLE 3. Thermodynamic Activity Coefficient of p-Cresol in Various
Nonaqueous Media

Solvent	Activity Coefficient
acetone (50%)	1.30
acetonitrile (60%)	0.72
dioxane (70%)	1.63
ethanol (70%)	1.30
methanol (70%)	1.50
propanol (60%)	0.83
THF (60%)	1.01

calculated by measuring its saturation solubility in organic solvent and water. It is
assumed that the three forms of the enzyme, that is, resting enzyme, compound I,
and compound II, have similar solubilities in the same media. The activity coeffi-
cients of H_2O_2 are calculated by measuring the partition coefficients between
aqueous organic solvents and isooctane. Thermodynamic estimations of the activity
coefficients in various media are performed using the UNIFAC model. TABLE 3
contains the calculated γ values of p-cresol in various nonaqueous media.

All values in equations 5, 6, and 9 can now be calculated. The resultant values of
the transfer free energies of enzyme, H_2O_2, substrate (p-cresol), and transition-state
complex upon the transition from water to organic solution are shown in TABLE 4.
This table indicates that the transferring of the enzyme from water to organic media
is an energy-consuming process. Because the transfer free energies are positive, this
demonstrates that the enzyme molecules have higher free energies and are destabi-
lized in organic solvents, whereas the substrates, that is, H_2O_2 and p-cresol, are
stabilized in the organic phase. The net effect is that the free energies of the ground
state of the reactants (enzyme and substrate) increase in going from water to
nonaqueous media. Therefore, the ground state of each elementary reaction is
destabilized by organic solvents. The data contained in TABLE 4 also show that the
free energies of the transition-state complex are improved in organic phases,
resulting in the destabilization of the transition state of the enzymatic reaction. The
intrinsic effects of the solvents on the destabilization of both the ground state and the
transition state of each elementary step are schematized in FIGURE 3. Although the
increase in free energy of the reactants (ground state) is favorable to the reaction,

TABLE 4. Transfer Free Energy (kcal/mol) for Enzyme, Substrate, and
Transition-State Complex between Water and Various Aqueous Organic
Solvent Mixtures[a]

Solvent	ΔG^{tr}_E	$\Delta G^{tr}_{H_2O_2}$	ΔG^{tr}_S	$\Delta G^{tr}_{[E \cdot H_2O_2]\ddagger}$	$\Delta G^{tr}_{[E(I) \cdot S]\ddagger}$	$\Delta G^{tr}_{[E(II) \cdot S]\ddagger}$
propanol	4.932	−0.786	−2.363	3.705	3.352	4.501
ethanol	4.476	−1.007	−2.075	4.172	3.243	4.423
acetonitrile	4.843	−0.686	−2.425	4.471	3.812	4.548
methanol	2.312	−1.227	−1.190	2.213	1.086	3.322
dioxane	3.513	N.D.	−1.943	N.D.	2.864	4.025
acetone	4.867	N.D.	−2.075	N.D.	3.448	4.681
THF	3.534	N.D.	−2.252	N.D.	3.272	4.217

[a]N.D. = not determined.

the destabilization of the transition complex is greater than that of the ground state of the reaction, which gives rise to the increase of the activation energy of the reaction. Consequently, many of the observed solvent effects on the decrease in the rate constants of each elementary step can be accounted for by such a destabilization of the transition state. The intrinsic effect in going from water to nonaqueous media, then, is to disturb the transition state of the enzymatic reaction.

Ryu and coworkers have carried out transfer free energy analyses of the HRP-catalyzed oxidation of a phenolic substrate in nonaqueous media such as 70% dioxane, based on steady-state kinetic data. They claim that the decreased catalytic efficiency in organic solvent results from the ground-state stabilization of phenolic substrates, whereas the enzyme-substrate complex is insensitive to solvent and substrate hydrophobicity.[3] In addition, although they have drawn out the equation to calculate the transfer free energy of the transition complex, they did not investigate
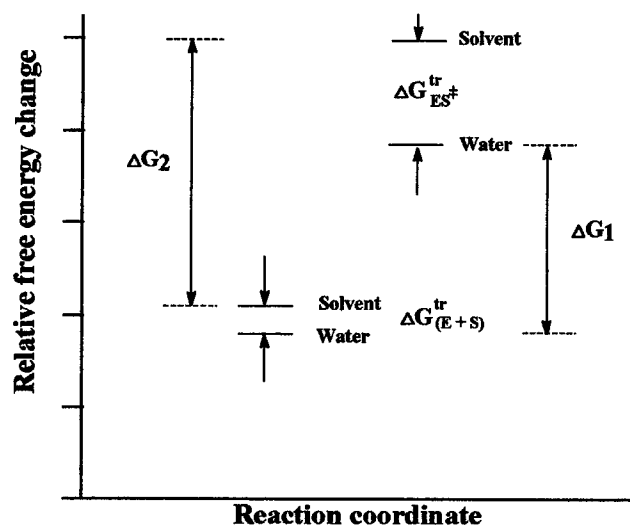

FIGURE 3. Free energy diagrams for the HRP-catalyzed oxidation of substituted phenols and anilines (comparison between aqueous and nonaqueous media).

the changes in the free energies of this complex. When using a series of substrates with systematic structural variations, it is assumed that the effects of the changes in substrate hydrophobicity on the transfer free energies of the enzyme-substrate complex and the transition state could be calculated in a single solvent without knowing the values of the enzyme activity coefficients. In fact, because the enzyme is soluble in aqueous organic solvents such as 70% methanol, 70% dioxane, 70% ethanol, and 60% 1-propanol, its free energy changes and hence the contribution to the reaction cannot be neglected. The results of our transfer free energy analysis based on pre-steady-state kinetic data strongly suggest that it is the destabilization of

the transition-state complex rather than the ground-state stabilization of substrates that is mainly responsible for the decreased reaction rate in organic solvents in comparison with that in water.

CONCLUSIONS

In the present study, stopped-flow, pre-steady-state kinetics are used to study the catalytic behavior of horseradish peroxidase in nonaqueous media. To our knowledge, such a method has never been employed by others in the field of nonaqueous enzymology. It demonstrates that the main effect of organic solvents on enzyme is to destabilize the charged transition state. The three elementary reactions respond differently to changing solvents, showing that the effect of organic solvent on the transition state is strongly dependent on the structure of the transition complex.

ACKNOWLEDGMENTS

REFERENCES

1. KLIBANOV, A. M. 1989. Enzymatic catalysis in anhydrous organic solvents. TIBS **14:** 141–144.
2. WESCOTT, C. R. & A. M. KLIBANOV. 1994. The solvent dependence of enzyme specificity. Biochim. Biophys. Acta **1206:** 1–9.
3. RYU, K. & J. S. DORDICK. 1992. How do organic solvents affect peroxidase structure and function? Biochemistry **31:** 2588–2598.
4. ZAKS, A. & A. M. KLIBANOV. 1985. Enzymatic catalysis in organic media at 100 °C. Science **224:** 1249–1251.
5. RYU, K. & J. S. DORDICK. 1989. Free energy relationships of substrate and solvent hydrophobicities with enzymatic catalysis in organic media. J. Am. Chem. Soc. **111:** 8026–8027.
6. ZAKS, A. & A. M. KLIBANOV. 1986. Substrate specificity of enzymes in organic solvents vs. water is reversed. J. Am. Chem. Soc. **108:** 2767–2768.
7. SAKURAI, T., A. L. MARGOLIN, A. J. RUSSELL & A. M. KLIBANOV. 1988. Control of enzyme enantioselectivity by the reaction medium. J. Am. Chem. Soc. **110:** 7236–7237.
8. PARIDA, S. & J. S. DORDICK. 1993. Tailoring lipase specificity by solvent and substrate chemistries. J. Org. Chem. **58:** 3238–3244.
9. FERSHT, A. R. 1985. Enzyme Structure and Mechanism. Second edition. Freeman. San Francisco.
10. GUPTA, N. N. 1992. Enzyme function in organic solvents. Eur. J. Biochem. **203:** 25–32.
11. CHATTERJEE, S. & A. J. RUSSELL. 1993. Kinetic analysis of the mechanism for subtilisin in essentially anhydrous organic solvents. Enzyme Microb. Technol. **15:** 1022–1029.
12. DUNFORD, H. B. 1990. Horseradish peroxidase: structure and kinetic properties. *In* Peroxidases in Chemistry and Biology. J. Everse, K. E. Everse & H. B. Grisham, Eds.: 1–23. CRC Press. Boca Raton, Florida.
13. CHANCE, B. 1949. The properties of the enzyme-substrate compound of peroxidase and peroxides: I. The structure of the primary and secondary complexes. Arch. Biochem. **21:** 416–430.

14. CHANCE, B. 1950. The enzyme-substrate compounds of horseradish peroxidase and peroxides: II. Kinetics of formation and decomposition of the primary and secondary complexes. Arch. Biochem. **22:** 225–252.

15. CHANCE, B. 1952. The spectra of the enzyme-substrate complexes of catalase and peroxidase. Arch. Biochem. Biophys. **41:** 404–430.

16. OVENSTON, T. C. J. & W. T. REES. 1950. The spectrophotometric determination of small amounts of hydrogen peroxidase in aqueous solution. Analyst **75:** 204–208.

17. HASINOFF, B. B. & H. B. DUNFORD. 1970. Kinetics of the oxidation of ferrocyanide by horseradish peroxidase compounds I and II. Biochemistry **9:** 4930–4939.

18. FREDENSLUND, A., J. GMEHLING & P. RASMUSSEN. 1977. Vapor-Liquid Equilibria Using UNIFAC. Elsevier. Amsterdam/New York.

19. YANG, Z. & D. A. ROBB. 1994. Partition coefficients of substrate and products and solvent selection for biocatalysis under nearly anhydrous conditions. Biotechnol. Bioeng. **43:** 365–370.

20. REIMANN, A., D. A. ROBB & P. J. HALLING. 1994. Solvation of CBZ-amino acid nitrophenyl esters in organic media and the kinetics of their transesterification by subtilisin. Biotechnol. Bioeng. **43:** 1081–1086.

21. VAN TOL, J. B. A., R. M. M. STEVENS, W. J. VELDHUIZEN, J. A. JONGEJAN & J. A. DUINE. 1995. Do organic solvents affect the catalytic properties of intrinsic kinetic parameters of lipase in ester hydrolysis and formation in various organic solvents? Biotechnol. Bioeng. **47:** 71–81.

22. HALLING, P. J. 1994. Thermodynamic predictions for biocatalysis in nonconventional media: theory, tests, and recommendations for experimental design and analysis. Enzyme Microb. Technol. **16:** 178–206.

23. WESCOTT, C. R. & A. M. KLIBANOV. 1993. Solvent variation inverts substrate specificity of an enzyme. J. Am. Chem. Soc. **115:** 1629–1631.

24. WESCOTT, C. R. & A. M. KLIBANOV. 1993. Predicting the solvent dependence of enzymatic substrate specificity using semiempirical thermodynamic calculations. J. Am. Chem. Soc. **115:** 10362–10363.

Fusion Proteins

Expression and Function[a]

LEIF BÜLOW AND KLAUS MOSBACH

*Department of Pure and Applied Biochemistry*
Chemical Center
Lund University
S-221 00 Lund, Sweden

INTRODUCTION

Enzyme technology is frequently preoccupied with the characterization of single enzymes after carefully removing all contaminating proteins. The goal of these studies is obvious: to elucidate how a given enzyme works without interference of other enzymes or proteins. However, most biochemical reactions *in vivo* are organized into multistep pathways where several enzymes are involved. The enzymes are often sequentially operating in a reaction path or part of a metabolic pathway. The product of the first enzyme (E_1) will hence serve as a substrate for the second, whose product will serve as the substrate for the subsequent enzyme, and so forth:

$$A \xrightarrow{E_1} B \xrightarrow{E_2} C \xrightarrow{E_3} P.$$
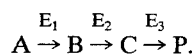
Physical arrangements among enzymes in these pathways are less pronounced in lower organisms such as prokaryotes, but in eukaryotic cells many proteins of different metabolic pathways are complexed in ordered or, at least, in nonrandom arrangements. Such organization of enzymes can be seen as a progression of increasing complexity extending from separate enzymes consisting of separate polypeptide chains, through oligomeric enzymes, which may show allosteric interactions between subunits, and eventually to multienzyme proteins. The existence of enzymes capable of catalyzing several separate enzymatic steps has been verified and characterized either as multienzyme complexes with low dissociation constants or as multifunctional enzymes. A multifunctional protein is composed of monomers or oligomers of polypeptide chain(s) with covalently linked active sites. During evolution, as the living cell became more complex with more enzyme molecules and larger cell volume, the need for fine regulation rose. The creation of proximity between metabolically related enzymes to varying extents most probably fulfilled these requirements.

The arrangement of sequentially operating enzymes into multienzyme complexes and multifunctional enzymes offers several catalytic advantages. Integration of consecutively operating enzymes brings their active sites together and provides for

the facilitated transfer of intermediate substrates between them. In addition, the existence of interdomain contacts allows interaction between the enzymes during catalysis. The proximity also allows the enzymes to be sensitive to fine regulatory signals with coordinated changes of different activities for the regulation of cell metabolism.

PREPARATION OF ARTIFICIAL BIFUNCTIONAL ENZYMES

The hybrid proteins to be constructed in the laboratory can be considered to be architecturally analogous to the naturally occurring bifunctional enzymes. When preparing a bifunctional enzyme by genetic engineering, fusions can be made to either the amino or carboxyl terminal region. The gene of interest is most often isolated by the polymerase chain reaction (PCR) from a genome or a vector by the use of two specific primers that will promote the amplification of the gene by a DNA polymerase (preferentially using a polymerase that gives as few misincorporations as possible; e.g., the *Pfu* polymerase). Additionally, special properties of the linker spacing the enzyme moieties can be designed by the selection of a certain oligonucleotide sequence. The choice of linker region may be very important for the stability, function, and production of the fusion protein. We have thus observed that the correct folding of fusion enzymes can depend on the length and the primary structure of the linker, especially if the enzymes are oligomeric. For instance, to examine the role of the connecting region in the artificial bifunctional enzyme β-galactosidase/galactose dehydrogenase, linkers of different length were inserted between the catalytic units. The specific activity of the galactose dehydrogenase part of the complex was increased when longer linkers (9 and 13 amino acids) were used as connectors. These bifunctional enzymes were predominantly found to comprise hexamers, but complexes of higher molecular weight were also formed. Furthermore, the sequential reaction was carried out more efficiently using hybrid enzymes with the longer linkers, as demonstrated both *in vitro* using purified protein preparations (FIGURE 1) as well as *in vivo* by determining the growth rates of recombinant *E. coli* cells on a minimal medium containing lactose.

Over the years, we and others have prepared a series of various artificial consecutive bifunctional enzymes. These include β-galactosidase/galactokinase,[1,2] galactose dehydrogenase/β-galactosidase,[3,4] galactose dehydrogenase/β-galactosidase/galactokinase,[5] galactose dehydrogenase/bacterial luciferase,[6] malate dehydrogenase/citrate synthase,[7,8] γ-glutamyl kinase/glutamic-γ-semialdehyde dehydrogenase, and lactate dehydrogenase/galactose dehydrogenase.

One of the most important aspects in our work has been to evaluate the importance of proximity. We have in many instances demonstrated that a fused enzyme system is more effective in transferring the intermediate substrate to the second enzyme than a corresponding wild-type system. For instance, the transient time is hence frequently substantially reduced (cf. FIGURE 1). In this context, the kinetic parameters K_m and k_{cat} must also be considered. Most often, we only observe small changes in these values, particularly if we compare k_{cat}/K_m values.
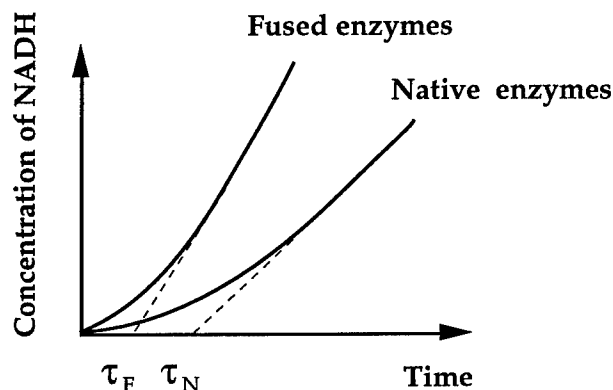
FIGURE 1. Schematic representation of the formation of NADH in the coupled reaction from lactose by β-galactosidase/galactose dehydrogenase and in an identical system with the corresponding separate native enzymes.

ENGINEERING OF CELL METABOLISM USING BIFUNCTIONAL ENZYMES

The intracellular metabolic setup that has been naturally evolved is not always the best. To get the highest possible biotechnological yield of a desired metabolite, genetic modifications of the cells may therefore be demanded. Recombinant DNA technology has provided the possibility to alter the phenotypes in specific and desired directions. The introduction of a fusion enzyme in a reaction sequence in living cells such as microbial and plant cells to effectively regulate the production of a certain metabolite is thus most valuable. For instance, by fusing two enzymes at a metabolic branch point, the intermediate substrates could be efficiently "channeled" to the desired pathway. Moreover, the problem of feedback regulation of a synthesizing pathway could possibly be solved because the intermediate substrate will be transferred between the enzymes and will appear free in solution only to a minor extent compared to if the enzymes were separate. In this paper, we will discuss a few specific examples from our own laboratory that demonstrate the potential of using bifunctional enzymes to engineer cell metabolism.

β-Galactosidase/Galactokinase

The fusion proteins β-galactosidase/galactokinase in combination with galactose dehydrogenase have been used as model systems to evaluate the importance of proximity at an artificial metabolic branch point. The product of galactose dehydrogenase, that is, galactono-lactone, represents a metabolic end product in *E. coli* (FIGURE 2). When *E. coli* cells harboring these enzymes were grown on lactose as the sole carbon source, a faster growth rate was observed in the fused enzyme system compared to a wild-type one with three separate enzymes, indicating an efficient transfer of the intermediate galactose to the kinase moiety.[2] The linker region proved to be critical. The shortest linker resulted in the shortest generation times. Such

"substrate channeling" was also verified *in vitro* using purified enzymes. Similar studies have been performed with galactose dehydrogenase/β-galactosidase.

Malate Dehydrogenase/Citrate Synthase

Metabolic studies of genetically fused enzymes have also been shown to be applicable in yeast. In these experiments, we have prepared malate dehydrogenase/citrate synthase (MDH/CS) fusion proteins and have expressed them in the mitochondria of the transgenic cells. The use of the noninvasive NMR technique to determine the pools of intermediates proved extremely useful and we could demonstrate substrate channeling between malate dehydrogenase and citrate synthase.[7,8] For instance, [3-^{13}C]propionate was used to study the citric acid metabolism in recombinant yeast cells carrying CS/MDH fusion proteins. This substrate is metabolized to [2-^{13}C]succinyl-CoA before it enters the citric acid cycle in the mitochondria. This metabolite is then further oxidized to succinate and fumarate and, if there is free diffusion of these intermediates, the ^{13}C-label should be equally distributed in the C2 and C3 positions of malate and oxaloacetate and in metabolites derived from these, such as alanine. By determining the ratio of C2/C3 of the formed alanine, we could hence determine the degree of free rotation or tumbling. If allowed to rotate freely, this ratio will be equal to 1, corresponding to 100% tumbling. Using this methodology, we could estimate that the tumbling in our fusion enzyme was only 12%, leaving 88% of the intermediates to be transferred in a conserved fashion.

Proline

Many organisms adapt to osmotic stress by increasing the intracellular concentration of osmotically active compounds (osmolytes). The most commonly occurring osmolytes are amino acids, polyols, sugar alcohols, and methylamines.[9] These compounds balance the osmotic strength of the cytosol with that of the environment without being toxic to the cell. Proline has been found to accumulate in microorganisms,[10,11] in algae, and in higher plants under physiologically extreme conditions with low water activity and high salinity. In bacteria, proline is synthesized from L-
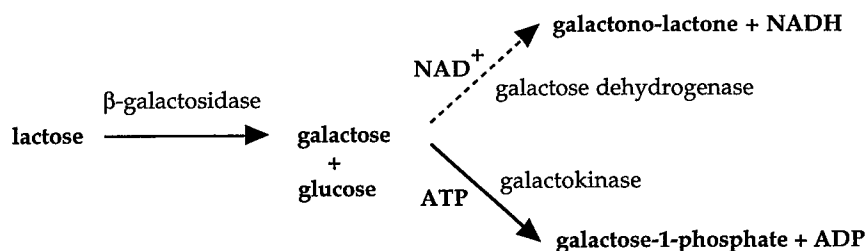

FIGURE 2. Reaction scheme for the hydrolysis of lactose to galactose and glucose followed by either phosphorylation or oxidation of galactose. Galactose dehydrogenase was used as a scavenging enzyme to the galactokinase part of the β-galactosidase/galactokinase fusion enzyme.

glutamate, via γ-glutamyl phosphate, γ-glutamic semialdehyde, and Δ'-pyrroline-5-carboxylate (FIGURE 3). The product of glutamyl kinase (GK) and the substrate of glutamyl phosphate reductase (GPR), namely, γ-glutamyl phosphate, is extremely labile. The fusion of proteins GK/GPR could stabilize the labile intermediate by substrate channeling and could thereby increase the overall proline production. Interestingly, this strategy with the enzyme activities of GK and GPR on the same bifunctional enzyme has been observed in certain plants[12] that accumulate proline during water stress.

The genes of the proline biosynthetic pathway in *E. coli* are located on the same operon. We have produced an artificial bifunctional enzyme GK/GPR by removing the stop codon from the *proB* gene and fusing the genes *proB* and *proA* in frame using PCR-mediated mutagenesis. The bifunctional enzyme was expressed in a proline auxotroph *E. coli* strain, JM 83, and grown in salt containing minimal (M9) media to
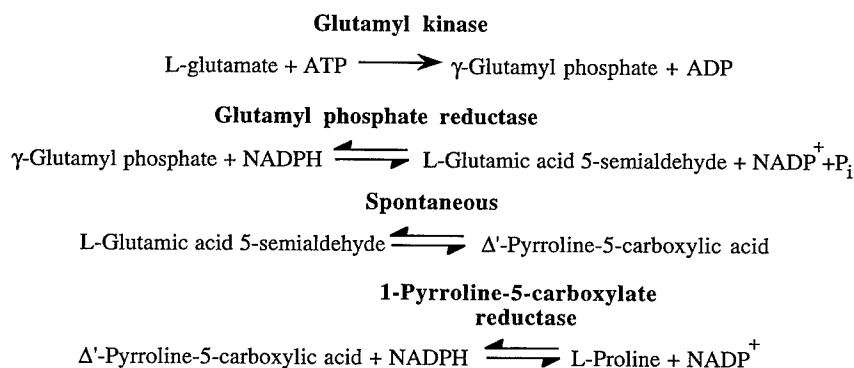
Glutamyl kinase

L-glutamate + ATP $\longrightarrow$ γ-Glutamyl phosphate + ADP

Glutamyl phosphate reductase

γ-Glutamyl phosphate + NADPH $\rightleftharpoons$ L-Glutamic acid 5-semialdehyde + NADP$^+$+P$_i$

Spontaneous

L-Glutamic acid 5-semialdehyde $\rightleftharpoons$ Δ'-Pyrroline-5-carboxylic acid

1-Pyrroline-5-carboxylate reductase

Δ'-Pyrroline-5-carboxylic acid + NADPH $\rightleftharpoons$ L-Proline + NADP$^+$

FIGURE 3. Biosynthesis of L-proline from L-glutamate in *E. coli*.

assess the osmoprotecting properties. In order to determine if the artificial bifunctional enzyme GK/GPR is more effective than the two separate wild-type enzymes, the intracellular proline concentration was measured, assuming that the constructs are expressed at the same level. The proline levels at low external salt concentrations were in the same range, whereas at 0.5 M NaCl the GK/GPR enzyme fusion produced twice as much proline as the enzymes apart. Higher proline concentration also had a positive effect on the osmotolerance. The generation times of *E. coli* JM 83 expressing the enzyme fusion are considerably shorter at elevated salt concentrations.

Glycine Betaine

The quaternary ammonium compound, glycine betaine, is another very effective osmolyte and accumulates during water stress induced primarily by high salinity, but also by drought and low temperatures,[13] in bacteria, cyanobacteria, and certain higher plants. However, several commercially important crops, such as potato, rice,

tomato, and tobacco, lack the ability to accumulate glycine betaine. This has motivated us to introduce a glycine betaine biosynthetic pathway in such species to increase their stress tolerance and crop yield.

Glycine betaine is derived from a two-step oxidation of choline to glycine betaine via the unstable intermediate, betaine aldehyde.[14] Bacterial CDH is a most useful enzyme for introducing this pathway into new species because it is able to catalyze not only the oxidation of choline to betaine aldehyde, but also the second step to glycine betaine. In this study, we have therefore chosen to introduce the *E. coli betA* gene, encoding CDH, into tobacco (*Nicotiana tabacum* cv. SR1) in order to evaluate the possibilities of enhancing the stress tolerance by intracellular accumulation of glycine betaine. Indeed, by introducing this enzyme into tobacco, there was an 80% difference in salt tolerance between the transgenic plants and the wild-type line at 300 mM NaCl as measured by the dry weights.[15]

Cold stress induces the accumulation of glycine betaine in different organisms. In initial experiments, 10 transgenic and 10 wild-type plants were exposed to −5 °C for 6 h and then placed at 20 °C for 7 days before visually evaluating the damages. The transgenic plants were substantially less affected compared with the wild-type plants, indicating that the accumulation of glycine betaine can reduce the effects caused by freezing in plants expressing CDH.

PERSPECTIVES

The introduction of artificial enzymelike proteins, bifunctional enzymes, or other proteins that cross normal cell borders into suitable host cells will no doubt be most valuable to improve our understanding of cell metabolism. The potential of modifying or introducing completely novel internal pathways using such enzyme systems is extremely interesting. Besides evaluating conventional metabolic pathways such as glycolysis and the citric acid cycle, we intend to introduce, for example, novel carbon dioxide fixation enzyme systems into animal and plant cells. In addition, the destruction or accumulation of harmful pollutants will be important targets for our research. It is also of importance to predict metabolic responses that are induced by genetic or environmental changes when planning such metabolic engineering experiments. In order to relate the flux in a metabolic pathway to the kinetic properties of the enzymes, mathematical treatment of the metabolic events will therefore be essential in our further studies.

REFERENCES

1. BÜLOW, L. 1987. Characterization of an artificial bifunctional enzyme, β-galactosidase/ galactokinase, prepared by gene fusion. Eur. J. Biochem. **163:** 443–448.
2. CARLSSON, H., P. LJUNGCRANTZ, L. BÜLOW & K. MOSBACH. 1992. Engineering of lactose metabolism in *E. coli* by introducing β-galactosidase/galactokinase fusion enzymes. Biotechnol. Lett. **14:** 439–444.
3. LJUNGCRANTZ, P., H. CARLSSON, M-O. MÅNSSON, P. BUCKEL, K. MOSBACH & L. BÜLOW. 1989. Construction of an artificial bifunctional enzyme, β-galactosidase/galactose dehydrogenase, exhibiting efficient galactose channeling. Biochemistry **28:** 8786–8792.
4. CARLSSON, H., P. LJUNGCRANTZ, C. LINDBLADH, M. PERSSON & L. BÜLOW. 1994. Use of

genetically prepared enzyme conjugates in lactose and galactose analyses. Anal. Biochem. **218:** 278–283.

5. LJUNGCRANTZ, P., L. BÜLOW & K. MOSBACH. 1990. Construction and characterization of a recombinant tripartite enzyme, galactose dehydrogenase/β-galactosidase/galactoki-nase. FEBS Lett. **275:** 91–94.

6. LINDBLADH, C., M. PERSSON, L. BÜLOW & K. MOSBACH. 1992. Characterization of a recombinant bifunctional enzyme, galactose dehydrogenase/bacterial luciferase, display-ing an improved bioluminescence in a three-enzyme system. Eur. J. Biochem. **204:** 241–247.

7. LINDBLADH, C., C. HÄGGLUND, W. C. SMALL, M. RAULT, K. MOSBACH, L. BÜLOW, C. EVANS & P. A. SRERE. 1994. Preparation and characterization of a fusion protein of yeast mitochondrial citrate synthase and malate dehydrogenase. Biochemistry **33:** 11692–11698.

8. LINDBLADH, C., R. D. BRODEUR, G. LILIUS, L. BÜLOW, K. MOSBACH & P. A. SRERE. 1994. Metabolic studies on *S. cerevisiae* containing fused citrate synthase/malate dehydroge-nase. Biochemistry **33:** 11684–11691.

9. YANCEY, P. H., M. E. CLARK, S. C. HAND, R. D. BOWLUS & G. N. SOMERO. 1983. Living with water stress: evolution of osmolyte systems. Science **217:** 1214–1222.

10. CSONKA, L. 1991. Prokaryotic osmoregulation: genetics and physiology. Annu. Rev. Microbiol. **45:** 569–606.

11. BÜLOW, L. & K. MOSBACH. 1991. The oligopeptide gly-pro-gly-pro-ala-gly-pro-gly-pro increases the internal proline level and improves osmotolerance when expressed in *E. coli.* Gene **109:** 125–129.

12. HU, C., A. J. DELAUNEY & D. VERMA. 1992. A bifunctional enzyme (D1-pyrroline-5-carboxylate synthetase) catalyzes the first two steps in the proline biosynthesis in plants. Proc. Natl. Acad. Sci. U.S.A. **89:** 9354–9358.

13. MCCUE, K. & A. D. HANSON. 1990. Drought and salt tolerance: towards understanding and application. TIBTECH **8:** 358–362.

14. LAMARK, T., I. KAASEN, M. W. ESHOO, P. FALKENBERG, J. MCDOUGALL & A. R. STRÖM. 1991. DNA sequence and analysis of the *bet* genes encoding the osmoregulatory choline–glycine betaine pathway of *Escherichia coli.* Mol. Microbiol. **5:** 1049–1064.

15. LILIUS, G., N. HOLMBERG & L. BÜLOW. 1996. Enhanced NaCl stress tolerance in transgenic tobacco expressing bacterial choline dehydrogenase. Submitted.

Molecular Engineering of Streptavidin[a]

TAKESHI SANO, SANDOR VAJDA, GABRIEL O. REZNIK,
CASSANDRA L. SMITH, AND CHARLES R. CANTOR

Center for Advanced Biotechnology
and
Departments of Biomedical Engineering, Pharmacology, and Physics
Boston University
Boston, Massachusetts 02215

INTRODUCTION

Streptavidin is a tetrameric protein produced by the bacterium *Streptomyces avidinii*; it has great similarity to the chicken protein avidin.[1-4] These proteins bind the vitamin biotin with an extremely high affinity. The dissociation constant of streptavidin-biotin and avidin-biotin complexes is estimated at around 10^{-15} M;[3,4] this is one of the tightest noncovalent interactions found in biological systems. Streptavidin and avidin are among the most stable proteins known; these proteins are resistant to, for example, high temperatures, extremes of pH, organic denaturants, and proteolytic enzymes. These characteristics generate considerable protein chemical interest, making streptavidin and avidin unique models in studying high-affinity macromolecule-ligand interactions and the structural stability of proteins in general. For example, one may ask why the interaction between these proteins and biotin is so tight and why these proteins are structurally so stable. The tetrameric nature of these proteins provides additional structural interest.

We have been doing rational structural and functional studies to answer such questions about streptavidin. Streptavidin has neither cysteine residue nor carbohydrate moieties, whereas avidin has one disulfide bridge and one *N*-linked oligosaccharide chain per subunit.[3,4] These differences make streptavidin a more easily manipulated target using recombinant DNA technology, thereby facilitating systematic studies.

STRUCTURES OF STREPTAVIDIN AND ITS BIOTIN-BINDING SITE

The three-dimensional structure of streptavidin, obtained by X-ray crystallography[5,6] (FIGURE 1), has helped enormously to understand the structural characteristics of this protein. Each streptavidin subunit consists of eight β-strands, forming a very stable β-barrel structure with a simple antiparallel topology. Four subunits are positioned in dihedral D_2 symmetry to form a tetramer, which can be viewed as a dimer of a stable subunit dimer. A pair of subunits is associated very tightly to form a stable dimer, in which the subunit barrel surfaces have complementary curvatures,

making numerous intersubunit van der Waals interactions. A tetramer is formed by two stable dimers that are associated relatively weakly via a small intersubunit contact area that contains hydrogen bonds and van der Waals interactions. Thus, each streptavidin molecule has two different subunit interfaces; one is the strong interface between subunits in a stable dimer and the other is the weak interface between two stable dimers (dimer-dimer interface). The biotin-binding site is located at one end of each β-barrel near the dimer-dimer interface.

A number of amino acid residues make contact with biotin, providing the extremely high stability of the streptavidin-biotin complex. The biotin-binding pocket is exquisitely positioned to provide a precise fit to biotin both geometrically and electrostatically. The amino acid residues that make hydrogen bonds or strong van der Waals contacts with biotin are shown schematically in FIGURE 2, and the interaction energies between these residues and biotin are listed in TABLE 1. Eight amino acid residues make hydrogen bonds with different parts of the biotin. The residues that form hydrogen bonds are Asn-23, Ser-27, and Tyr-43 with the ureido oxygen of biotin; Ser-45 and Asp-128 with each of the ureido amino groups; Thr-90 with the thiophene sulfur; and Asn-49 and Ser-88 with the carboxyl oxygens. Four tryptophan residues, Trp-79, -92, -108, and -120, together with Leu-25, Val-47, and Leu-110, form hydrophobic parts of the biotin-binding pocket, which interact with the thiophene ring and the alkyl chain of biotin through van der Waals forces. Interestingly, one of these residues, Trp-120, is not derived from the subunit binding to biotin, but instead is from an adjacent subunit through the dimer-dimer interface.
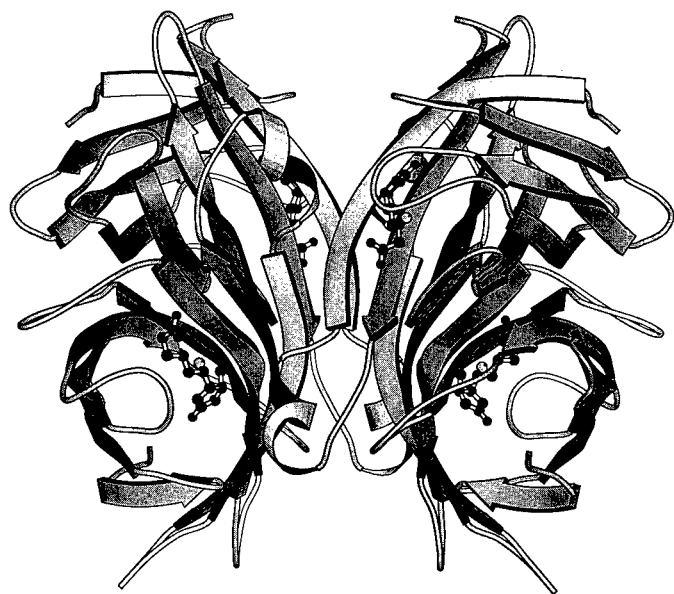

FIGURE 1. Schematic illustration of tetrameric streptavidin with four bound biotins. This picture is drawn based on the known three-dimensional structure of the natural core streptavidin-selenobiotin complex, obtained by X-ray crystallography.[6]
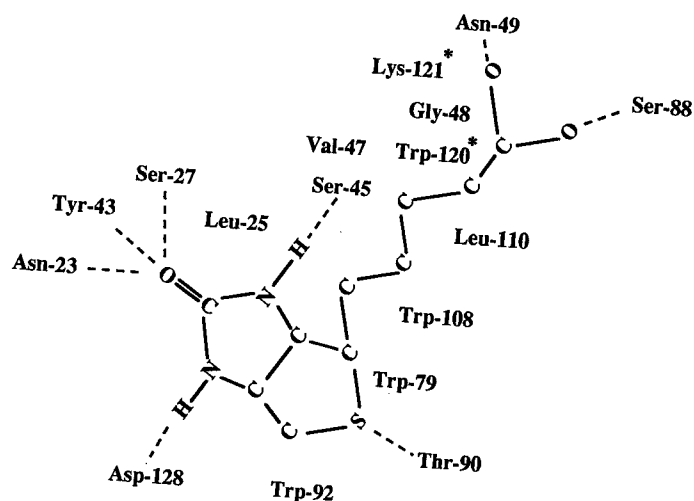
FIGURE 2. Schematic illustration of biotin and the biotin-binding site of streptavidin. Hydrogen bonds between biotin and amino acid residues of streptavidin are shown by dashed lines. Trp-120 and Lys-121, marked with asterisks, are derived from an adjacent subunit through the dimer-dimer interface. Modified from reference 7 with permission.

Similarly, Lys-121, which makes electrostatic interaction with the carboxyl group of biotin, is also provided by an adjacent subunit. These intersubunit contacts play key roles in the extremely tight biotin binding by this tetrameric protein. Another interesting structural feature is that a loop consisting of the sequence from Ser-45 to Ala-50 is likely to be relatively flexible,[5] but it is ordered upon biotin binding, whereupon Val-47, Gly-48, and Asn-49 on the loop make strong electrostatic and van der Waals interactions with biotin.

CLONING AND EXPRESSION OF THE STREPTAVIDIN GENE

Several years ago, we cloned the gene for streptavidin in *Escherichia coli*.[8] Then, attempts were made to express the cloned streptavidin gene by using bacterial expression systems. Active streptavidin is extremely toxic to any cell in which it is expressed because it tightly binds cellular biotin, which is essential for cell growth and viability. Thus, many expression systems showed very low expression efficiencies or, in some cases, host cells could not even maintain expression plasmids carrying the streptavidin gene stably. However, by using the bacteriophage T7 expression system, which has very tight control in expressing target genes,[9] a cloned streptavidin gene was expressed very efficiently in *E. coli*, and expressed streptavidin accounted for greater than 25% of the total cell protein.[10]

Expressed streptavidin formed inclusion bodies, as seen in many bacterial overexpression systems. However, solubilization of the inclusion body fraction, followed by renaturation, generated tetrameric streptavidin with full biotin-binding

ability.[10] The establishment of efficient expression and purification systems for streptavidin allowed us to modify, systematically, the structure of streptavidin by genetic engineering to fully understand the structural and functional characteristics of this protein.

DESIGN OF STREPTAVIDIN MUTANTS

The known three-dimensional structure of streptavidin[5,6] is of great assistance in designing streptavidin mutants. In addition, the use of computational molecular modeling methods, based on the known three-dimensional structure, allows rational

TABLE 1. Electrostatic, van der Waals, and Total Interaction Energies between Biotin and Amino Acid Residues of Streptavidin[a]

| Residue | Interaction Energy (kcal/mol) | | |
	Electrostatic	van der Waals	Total
Asn-23	−1.14	−0.92	−2.07
Leu-25	−0.10	−1.60	−1.70
Ser-27	−2.19	−0.55	−2.74
Ser-45	−0.94	−2.17	−3.11
Val-47	0.12	−2.52	−2.40
Gly-48	−0.91	−1.54	−2.46
Asn-49	−1.78	−2.23	−4.01
Trp-79	0.05	−4.51	−4.46
Ser-88	−2.68	−0.84	−3.52
Thr-90	−0.00	−1.23	−1.23
Trp-92	0.17	−1.69	−1.52
Trp-108	−0.03	−2.34	−2.37
Leu-110	−0.02	−2.42	−2.45
Trp-120[b]	−0.01	−1.61	−1.62
Lys-121[b]	−1.20	−0.27	−1.47
Asp-128	−1.26	−1.14	−2.40

[a]The electrostatic and van der Waals interaction energies between biotin and each amino acid residue were calculated using the X-ray structure of the streptavidin-selenobiotin complex[6] and the CHARMm molecular mechanics program with the CHARMm-19 parameter set. A distance-dependent dielectric of $4r$ was used in the calculation. Nonpolar hydrogen atoms were added to the structure using the HBUILD option of CHARMm. The resulting streptavidin tetramer with four bound biotins was subjected to 200 steps of Newton-Raphson minimization in order to eliminate possible steric overlaps.
[b]Trp-120 and Lys-121 are derived from an adjacent subunit through the dimer-dimer interface.

design of streptavidin mutants. In almost all cases, streptavidin mutants, which were predicted to be stable and active after the change of one or more amino acid residues, behaved as predicted. Here, we describe a few streptavidin mutants, which were recently designed, and the structural and thermodynamic considerations behind the design of these mutants.

A Minimum-sized Core Streptavidin

When streptavidin is produced by *S. avidinii*, it is secreted as a precursor and then its signal peptide is removed. The resulting mature protein is extremely susceptible to proteolysis and thus both the N- and C-termini are readily truncated to yield so-called core streptavidin.[11,12] However, natural core streptavidin preparations are often heterogeneous and such structural heterogeneity can be observed even within single tetrameric molecules. Thus, it would be desirable to make structurally homogeneous streptavidin for systematic studies on this protein. In particular, we were interested in designing a minimum-sized core streptavidin that might have enhanced properties because of the removal of any nonfunctional terminal sequences that are located on the surface of the molecule.

Most natural core streptavidin molecules consist of the sequences from around Ala-13 to around Ser-139, but the identity of the terminal residues varies. The sequences of natural core streptavidins are not necessarily those that are structurally most favorable; instead, they may merely indicate that the sequences around amino acids Ala-13 and Ser-139 are particularly susceptible to proteolysis. In fact, the X-ray crystallographic studies on natural core streptavidin were able to refine the structure only from Ala-13 or Glu-14 to Val-133 without the terminal regions,[5,6] which corresponds almost perfectly to the stable β-barrel structure consisting of the sequence from Gly-19 to Val-133. This indicates that the terminal regions, present in core streptavidin, are rather disordered,[5] which suggests that they have little contribution to the fundamental properties of streptavidin, such as biotin binding, formation of the β-barrel structure, and subunit association. This prediction encouraged us to remove all of the terminal sequences, which have no apparent function, to design a minimum-sized core streptavidin. The recombinant core streptavidin that we designed has the amino acid sequence from Gly-16 to Val-133[13] and thus consists of almost only the β-barrel structure characteristic of streptavidin.

This minimum-sized core streptavidin is tetrameric and binds one biotin per subunit, as does natural streptavidin. The truncation of the terminal residues had no appreciable effects on the solubility characteristics of the protein, unlike those present in mature, full-length streptavidin, which cause the formation of higher-order aggregates. However, this minimum-sized core streptavidin showed enhanced stability against denaturation by strong organic denaturants. For example, this molecule retained greater than 80% of its biotin-binding ability in the presence of 6 M guanidine hydrochloride at pH 1.5, under which conditions natural core streptavidin lost almost all of its biotin-binding ability. In addition, this core streptavidin had higher biotinylated DNA-binding ability than natural core streptavidin. These results suggest that the terminal regions, present on the surface of natural core streptavidin, reduce the overall stability of streptavidin and prevent biotinylated macromolecules from approaching the biotin-binding sites.

A Streptavidin Mutant with a Reduced Biotin-binding Affinity

Trp-120 makes intersubunit hydrophobic contacts to biotin bound by an adjacent subunit through the dimer-dimer interface. This intersubunit contact is likely to make a key contribution to the high biotin-binding affinity of streptavidin because

dissociated subunits have much lower affinity for biotin as seen by electrophoretic analysis of natural streptavidin[14] and because immobilized monomeric avidin is known to release biotin under relatively mild conditions.[15] Interaction energy calculations (TABLE 1) also show that this residue makes relatively strong van der Waals interactions with biotin. To understand the role of the intersubunit contacts made by Trp-120 to biotin in the properties of streptavidin, we designed a streptavidin mutant, in which Trp-120 is replaced with phenylalanine.[16]

This W120F streptavidin mutant can still bind biotin tightly enough to fully retain it even in the presence of high concentrations of urea at neutral pH or in a wide pH range. However, its biotin-binding ability was reduced to the point where bound and free biotins show facile exchange under physiological conditions. The biotin-binding affinity of this mutant was estimated to be $1-3 \times 10^8 \ M^{-1}$, indicating the significant contribution of the intersubunit contacts made by Trp-120 to biotin binding.

Biotin binding by natural streptavidin strengthens the dimer-dimer association by approximately 5 kcal/mol. Electrophoretic analysis of the W120F mutant in the presence of sodium dodecyl sulfate indicates that its subunit association is not tightened significantly upon biotin binding, unlike natural streptavidin. The reduced effect of biotin binding on the subunit association of this mutant is apparently caused by the lack of the intersubunit contacts made by Trp-120 to biotin through the weak dimer-dimer interface.

Cross-linked Streptavidins with Tighter Subunit Association

Tetrameric streptavidin has two subunit interfaces—the strong interface between subunits in a stable dimer and the weak dimer-dimer interface. If the subunit association, particularly at the weak dimer-dimer interface, could be tightened, the resulting streptavidin might retain bound biotin more stably even under relatively harsh conditions because the maintenance of the tetrameric structure, particularly the dimer-dimer interface, is essential for the intersubunit contacts made by Trp-120 and Lys-121 to biotin. To enhance the subunit association of streptavidin, specific covalent cross-links were introduced into pairs of subunits through the dimer-dimer interface.[17]

In natural streptavidin, His-127 residues from two adjacent subunits are in close proximity across the weak dimer-dimer interface of the tetramer.[5,6] Replacing His-127 with cysteine (H127C) generated a fully active, tetrameric protein that can spontaneously form two disulfide bonds through the weak dimer-dimer interface under mild oxidizing conditions. The two pairs of adjacent cysteine residues can also be cross-linked irreversibly by a sulfhydryl-specific bifunctional cross-linker. The successful cross-linking of Cys-127 residues through the dimer-dimer interface without disturbing the biotin-binding ability indicates that two Cys-127 residues are located in close proximity, suggesting that no significant changes in local structure occurred by the H127C mutation or by cross-linking between Cys-127 residues.

Another cross-linked mutant was made by first assembling a heterotetramer consisting of two species of subunits in a 1:1 ratio; one has lysine at position 127 and the other has aspartic acid. These tetramers apparently formed predominantly with Lys-127 and Asp-127 apposed across the weak dimer-dimer interface; this configuration should be electrostatically more favorable than those having the same amino

acid residues facing each other at the interface. This proposal has been confirmed by successful, almost quantitative, cross-linking of the amino group of Lys-127 and the carboxyl group of Asp-127 by a zero-length cross-linker, a water-soluble carbodi-imide. The resulting cross-linked molecule was essentially fully active.

These cross-linked streptavidins showed enhanced resistance to various denatur-ing conditions. For example, these streptavidins remained mostly tetrameric after heat treatment at 80 °C in the absence of biotin, under which conditions natural core streptavidin dissociated completely into subunits. The cross-linked molecules re-tained bound biotin more stably than their counterparts without cross-links or natural core streptavidin in the presence of high concentrations of guanidine hydrochloride at very acidic pH. These results demonstrate that the introduction of covalent bonds between adjacent subunits through the weak dimer-dimer interface enhances the overall stability of streptavidin. They also reveal the importance of the intersubunit contacts made by Trp-120 and Lys-121 to biotin through the dimer-dimer interface in biotin binding by streptavidin, which is consistent with the results seen with the W120F mutant with a reduced biotin-binding affinity.

PERSPECTIVES

Several streptavidin mutants have been described that were designed to under-stand the structural and functional characteristics of streptavidin. Because of the unusual properties of streptavidin, such as the extremely tight ligand-binding ability and very high structural stability, further, more extensive studies on this protein should not only provide deeper understanding of this attractive protein, but should also offer useful insights into the structural characteristics of high-affinity macromol-ecule-ligand interactions and the stability of proteins in general. In addition, many of the streptavidin variants produced will also be very useful as biological tools in biotechnological applications of the streptavidin-biotin system.

REFERENCES

1. CHAIET, L., T. W. MILLER, F. TAUSING & F. J. WOLF. 1963. Antimicrob. Agents Chemother. **3**: 28–32.
2. CHAIET, L. & F. J. WOLF. 1964. Arch. Biochem. Biophys. **106**: 1–5.
3. GREEN, N. M. 1975. Adv. Protein Chem. **29**: 85–133.
4. GREEN, N. M. 1990. Methods Enzymol. **184**: 51–67.
5. WEBER, P. C., D. H. OHLENDORF, J. J. WENDROSKI & F. R. SALEMME. 1989. Science **243**: 85–88.
6. HENDRICKSON, W. A., A. PÄHLER, J. L. SMITH, Y. SATOW, E. A. MERRITT & R. P. PHIZACKERLEY. 1989. Proc. Natl. Acad. Sci. U.S.A. **86**: 2190–2194.
7. VAJDA, S., Z. WENG, R. ROSENFELD & C. DELISI. 1994. Biochemistry **33**: 13977–13988.
8. ARGARAÑA, C. E., I. D. KUNZ, S. BIRKEN, R. AXEL & C. R. CANTOR. 1986. Nucleic Acids Res. **14**: 1871–1881.
9. STUDIER, F. W., A. H. ROSENBERG, J. J. DUNN & J. W. DUBENDORFF. 1990. Methods Enzymol. **185**: 60–89.
10. SANO, T. & C. R. CANTOR. 1990. Proc. Natl. Acad. Sci. U.S.A. **87**: 142–146.
11. PÄHLER, A., W. A. HENDRICKSON, M. A. G. KOLKS, C. E. ARGARAÑA & C. R. CANTOR. 1987. J. Biol. Chem. **262**: 13933–13937.
12. BAYER, E. A., H. BEN-HUR, Y. HILLER & M. WILCHEK. 1989. Biochem. J. **259**: 369–376.

13. SANO, T., M. W. PANDORI, X. CHEN, C. L. SMITH & C. R. CANTOR. 1996. J. Biol. Chem.
         270: 28204–28209.
14. SANO, T., M. W. PANDORI, C. L. SMITH & C. R. CANTOR. 1994. *In* Advances in
         Biomagnetic Separation. M. Uhlén, E. Hornes & Ø. Olsvik, Eds.: 21–29. Eaton Pub.
         Natick, Massachusetts.
15. GREEN, N. M. & E. J. TOMS. 1973. Biochem. J. **133:** 687–700.
16. SANO, T. & C. R. CANTOR. 1995. Proc. Natl. Acad. Sci. U.S.A. **92:** 3180–3184.
17. REZNIK, G. O., S. VAJDA, C. L. SMITH, C. R. CANTOR & T. SANO. 1995. Nat. Biotechnol. In
         press.

Engineering Pathways in *Escherichia coli* for the Synthesis of Morphine Alkaloid Analgesics and Antitussives

ANNE M. HAILES, CHRISTOPHER E. FRENCH,
DEBORAH A. RATHBONE, AND NEIL C. BRUCE[a]

Institute of Biotechnology
University of Cambridge
Cambridge CB2 1QT, United Kingdom

INTRODUCTION

The morphine alkaloids are an important group of structurally complex compounds and have long been exploited for their significant pharmacological properties.[1] The high value of these natural therapeutic products has resulted in the synthesis of a vast number of semisynthetic morphine derivatives. Hydromorphone is an example of a semisynthetic opiate drug that is a powerful analgesic, some seven times more potent than the parent compound, morphine.[2] Chemical synthesis of hydromorphone involves the catalytic hydrogenation of morphine followed by an Oppenaur oxidation using metal-*t*-butoxide and a suitable ketone.[3] This method is not ideal, in that it is necessary to protect certain functional groups, and it is inefficient, resulting in low yields. Similarly, methods for the chemical synthesis of the antitussive, hydrocodone, are also unsatisfactory. Semisynthetic opiates such as hydromorphone and hydrocodone are therefore attractive targets for a biotransformation process.

Microorganisms possess an enormous variety of catabolic enzymes that have potential applications in biotransformation systems. Selective enrichments with waste liquors from an opiate processing site led to the isolation of a strain of *Pseudomonas putida*, designated strain M10, which was capable of metabolizing morphine.[4] The steps initiating the transformation of morphine by *P. putida* M10 were shown to proceed via morphinone and hydromorphone (FIGURE 1). Oxidation of the C-6 hydroxy group of morphine was shown to be catalyzed by an NADP+-dependent morphine dehydrogenase, whereas the second reaction was shown to involve saturation of the 7,8-olefin bond of morphinone to give hydromorphone.[5] Both morphine dehydrogenase and morphinone reductase have been purified to homogeneity and fully characterized.[6,7] Similar reactions were also observed with codeine as the substrate, yielding codeinone and hydrocodone (FIGURE 1). Morphine dehydrogenase and morphinone reductase require expensive pyridine nucleotide cofactors and it is therefore unlikely that a cell-free system would be feasible on a commercial scale. The number of unwanted side reactions observed with *P. putida*

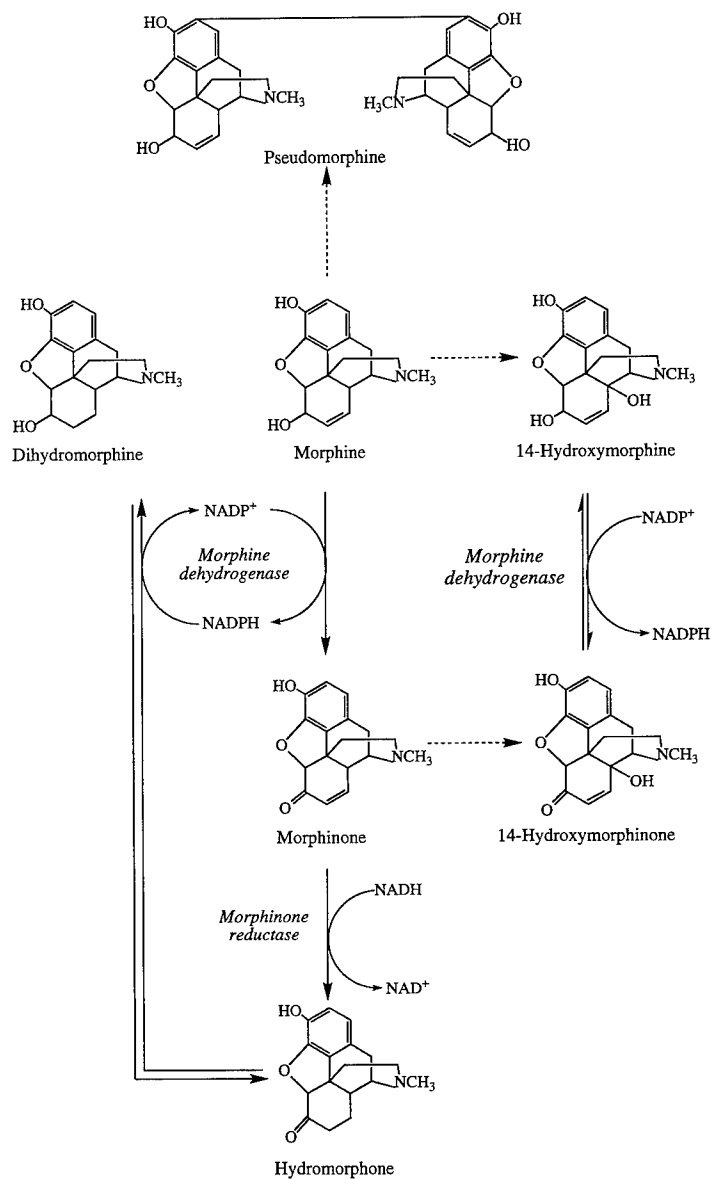[a]To whom all correspondence should be addressed.

FIGURE 1. Biotransformations of morphine in *Pseudomonas putida* M10. Dashed arrows indicate reactions where an enzyme activity has not been identified.

M10 meant that this organism would be unsuitable for a biotransformation process.[5,8] Here, we describe the use of recombinant DNA technology to construct a route in *Escherichia coli* that addresses these problems and enables, in high yields, the conversion of morphine to hydromorphone and codeine to hydrocodone.[9,10]

RESULTS AND DISCUSSION

Plasmid curing and Southern hybridization experiments revealed that the structural gene for morphine dehydrogenase, *mor*A, was located on a large natural plasmid of approximately 165 kb in *P. putida* M10.[11] Oligonucleotide probes based on the N-terminal amino acid sequence of morphine dehydrogenase were used to probe the plasmid DNA. The structural gene, *mor*A, together with its promoter and ribosome binding site motifs, was found to be located within a 1.7-kb *Sph*I fragment. Oligonucleotide probes based on three regions of the morphinone reductase amino acid sequence revealed that *mor*B was located on the chromosome of *P. putida* M10 and not on the same megaplasmid as *mor*A.[12] Subcloning experiments led to the isolation of a 4.0-kb *Cla*I fragment, containing the structural gene (*mor*B), the native promoter, and the ribosome binding site. The DNA fragments containing *mor*A and *mor*B were inserted into either pBluescript SK+ (Stratagene) or the low copy number plasmid, ps1EMBL,[13] together with their native promoters. A number of plasmid constructs were prepared: pMORA4, carrying *mor*A only; pMORB3, carrying *mor*B only; and pMORAB5, carrying both *mor*A and *mor*B (FIGURE 2).[12] Each construct directed the constitutive expression of morphine dehydrogenase and/or morphinone reductase when transformed into *E. coli* JM109. The relative enzyme activities in two of the recombinant strains were found to be quite different: *E. coli* JM109 pMORAB5 exhibited almost tenfold more morphine dehydrogenase than morphinone reductase; in contrast, in *E. coli* JM109 pMORA4/pMORB3, the levels of morphinone reductase were slightly higher than morphine dehydrogenase.[10]
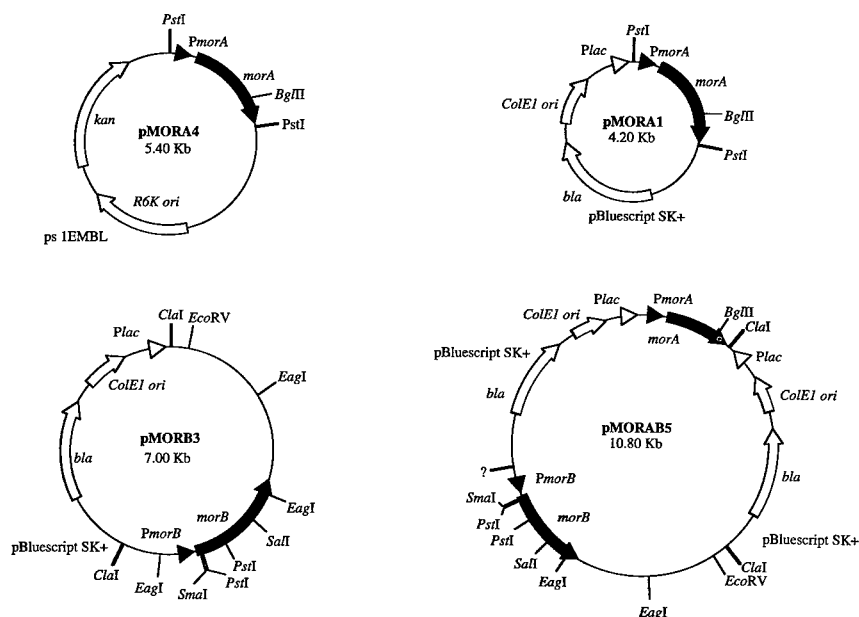

FIGURE 2. Recombinant plasmid constructs: *ori* = origin of replication; *bla* = β-lactamase; *kan* = kanamycin resistance determinant; ? = the undetermined restriction site of pMORAB5; P = the promoter regions of *mor*A or *mor*B.[14]

Whole cells of *E. coli* JM109 pMORAB5 and *E. coli* JM109 pMORA4/pMORB3 were tested extensively for their ability to transform morphine and codeine. Cultures of recombinant *E. coli* were grown under selective pressure in 200-mL rich medium (20 g tryptone, 5 g yeast extract, 0.5 g NaCl, and 0.25 g KCl, all added per liter) and were harvested in late log phase. Cells were washed in 50 mM phosphate buffer, pH 7.0, and resuspended in the same buffer at a concentration of 0.5 g/mL. Whole cell incubations (3 mL) at 37 °C typically contained the cell suspension (0.5 mL) and 10 mM substrate in 50 mM phosphate buffer, pH 7.0. Samples (300 μL) were taken at intervals and analyzed by HPLC.

Analysis of the supernatants from whole cell incubations containing *E. coli* JM109 pMORAB5 and 10 mM morphine revealed the disappearance of morphine coincident with the accumulation of two compounds, with retention times of 4.2 min and 5.0 min, corresponding to authentic dihydromorphine and hydromorphone. Complete transformation of morphine was observed after 6.5 h, yielding 50% hydromorphone and 25% dihydromorphine (FIGURE 3). Dihydromorphine accumulated because hydromorphone was observed to be a substrate, albeit a poor one, for morphine dehydrogenase.[8,14] The conversion of hydromorphone to dihydromorphine is probably facilitated by the high levels of NADPH accumulating in the cells. Low levels of a number of other compounds with characteristic morphine alkaloid UV spectra were also observed, which accounts for the incomplete conversion of morphine to hydromorphone and dihydromorphine; these are presumably products of morphinone degradation as morphinone has been reported to be extremely unstable.[15] Whole cell incubations where morphine was replaced with codeine as the
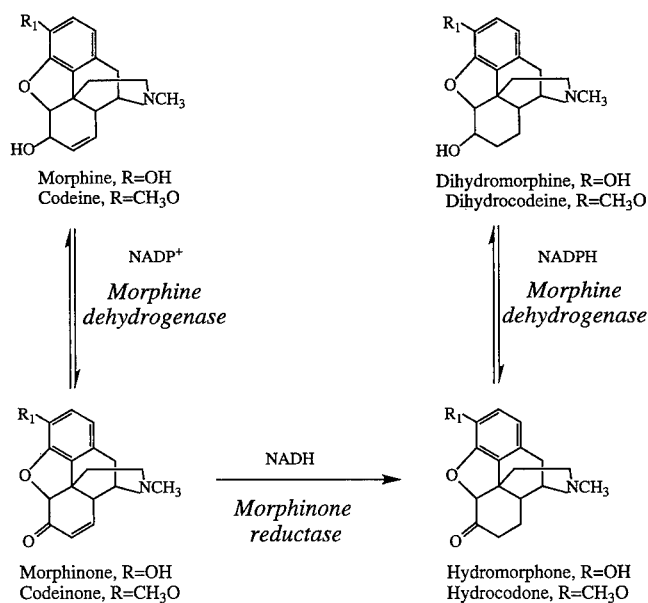

FIGURE 3. A route for the biological synthesis of hydromorphone and hydrocodone in recombinant *Escherichia coli*.
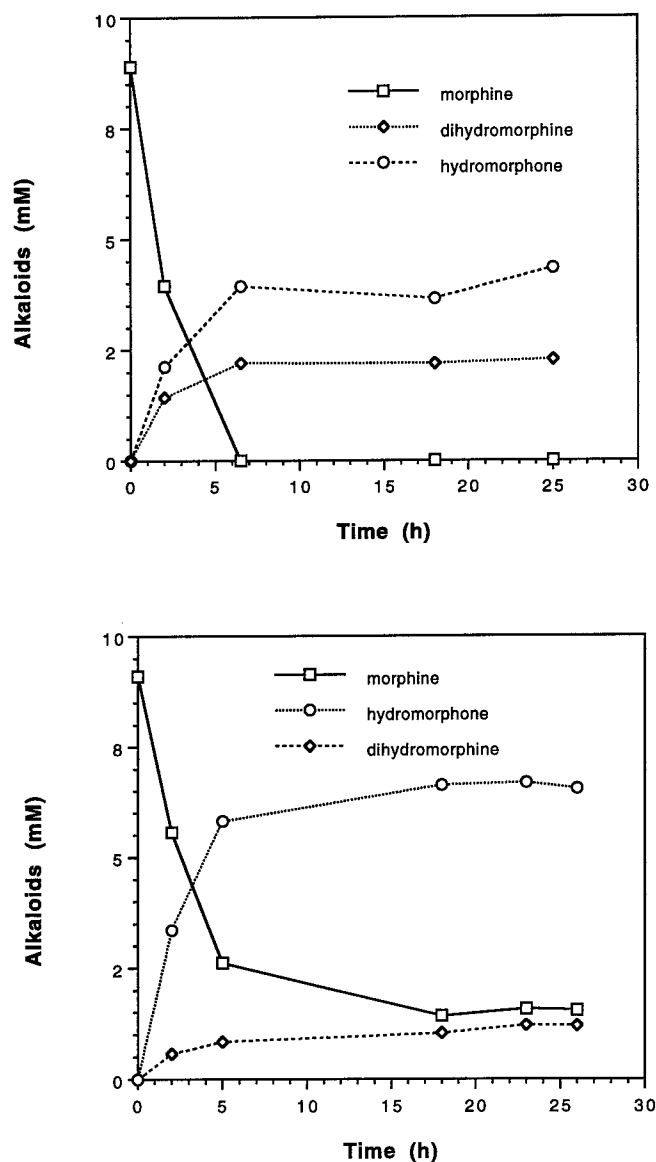
FIGURE 4. Biotransformations of 10 mM morphine by whole cells of (top) *E. coli* JM109 pMORAB5 and (bottom) *E. coli* JM109 pMORA4/pMORB3.

substrate resulted in the production of hydrocodone and dihydrocodeine (data not shown).

The levels of dihydromorphine were found to be reduced considerably when transformations were performed with the recombinant strain, *E. coli* JM109

pMORA4/pMORB3; this recombinant strain carried *mor*A on a low copy number plasmid, derived from ps1EMBL, and *mor*B on a higher copy number plasmid, derived from pBluescript SK+, resulting in significantly higher levels of morphinone reductase activity. Consequently, increased yields of hydromorphone (72%) were observed in whole cell incubations with *E. coli* JM109 pMORA4/pMORB3.

These results demonstrate the capability of recombinant cells of *E. coli* to convert morphine to hydromorphone and codeine to hydrocodone (FIGURE 4). Dihydromorphine is easily prepared by chemical methods and is therefore not of particular interest for a biotransformation process. We have shown that the levels of dihydromorphine can be significantly reduced by raising the levels of morphinone reductase activity. This biotransformation system has not, as yet, been optimized and problems regarding cofactor cycling are currently being addressed.

REFERENCES

1. PELLETIER, S. W. 1983. *In* Alkaloids: Chemical and Biological Perspectives. S. W. Pelletier, Ed.: 1–31. Wiley. New York.
2. MELMON, K. L. & H. F. MORRELLI. 1972. Clinical Pharmacology: Basic Principles in Therapeutics. Macmillan Co. New York.
3. RAPOPORT, H., D. R. BAKER & H. N. REIST. 1957. J. Org. Chem. **15:** 1489–1492.
4. BRUCE, N. C., C. J. WILMOT, K. N. JORDAN, A. E. TREBILCOCK, L. D. GRAY-STEPHENS & C. R. LOWE. 1990. Arch. Microbiol. **154:** 465–470.
5. HAILES, A. M. & N. C. BRUCE. 1993. Appl. Environ. Microbiol. **59:** 2166–2170.
6. BRUCE, N. C., C. J. WILMOT, K. N. JORDAN, L. D. GRAY-STEPHENS & C. R. LOWE. 1991. Biochem. J. **274:** 875–880.
7. FRENCH, C. E. & N. C. BRUCE. 1994. Biochem. J. **301:** 97–103.
8. LONG, M. T., A. M. HAILES, G. W. KIRBY & N. C. BRUCE. 1995. Appl. Environ. Microbiol. **61:** 3645–3649.
9. BRUCE, N. C., C. E. FRENCH, A. M. HAILES, M. T. LONG & D. A. RATHBONE. 1995. TIBTECH **13:** 200–205.
10. FRENCH, C. E., A. M. HAILES, D. A. RATHBONE, M. T. LONG, D. L. WILLEY & N. C. BRUCE. 1995. Bio/Technology **13:** 674–676.
11. WILLEY, D. L., D. A. CASWELL, C. R. LOWE & N. C. BRUCE. 1993. Biochem. J. **290:** 539–544.
12. FRENCH, C. E. & N. C. BRUCE. 1995. Biochem. J. **312:** 671–678.
13. POUSTKA, A., H-R. RACKWITZ, A. M. FRISCHAUF, B. HOHN & H. LEHRACH. 1984. Proc. Natl. Acad. Sci. U.S.A. **81:** 4129–4133.
14. BRUCE, N. C., D. A. CASWELL, C. E. FRENCH, A. M. HAILES, M. T. LONG & D. L. WILLEY. 1994. Ann. N.Y. Acad. Sci. **721:** 85–99.
15. BENTLEY, K. W. 1954. The Chemistry of the Morphine Alkaloids. Oxford University Press (Clarendon). London/New York.

Engineering Factor X Fusions
for Expression in *Pichia pastoris*[a]

M. M. GUARNA,[b] H. C. F. CÔTÉ,[c] E. A. AMANDORON,[d]
R. T. A. MacGILLIVRAY,[c] R. A. J. WARREN,[d]
AND D. G. KILBURN[b,d]

[b]*Biotechnology Laboratory*
[c]*Department of Biochemistry*
[d]*Department of Microbiology and Immunology*
University of British Columbia
Vancouver, British Columbia, Canada V6T 1Z3

INTRODUCTION

Affinity tags linked to polypeptides expressed as fusion proteins facilitate their purification. If the native form of the protein is desired, the affinity tag must be removed precisely. This can be accomplished with highly specific proteases such as factor Xa (FXa). Factor Xa offers the advantage of high specificity, but not of affordability. In this study, two FX constructs were expressed in the methylotropic yeast, *Pichia pastoris*. *P. pastoris* was chosen as a host because it produces recombinant proteins at high levels in a simple, well-defined, and inexpensive medium. It can be easily grown to high-cell densities by fed-batch fermentation and, unlike *S. cerevisiae*, usually does not hyperglycosylate recombinant proteins.

FX is a vitamin K–dependent glycoprotein that is synthesized in the liver and circulates in plasma as a two-chain zymogen. It is composed of a light chain and a heavy chain, held together by a disulfide bond. Whereas the heavy chain comprises the catalytic domain of the protein, the light chain contains a Gla domain and two epidermal growth factor–like (EGF) domains. Prior to secretion into the plasma, the single chain precursor undergoes several cotranslational and posttranslational modifications, including the γ-carboxylation of 11 glutamic acid residues located in the Gla domain. Although the Gla domain is essential for biological activity of FX, it is not required for protease activity of FXa. Because γ-carboxylation of glutamic acid residues is a posttranslational modification not performed by yeast, a deletion variant encoding only the second epidermal growth factor–like domain and the catalytic domain of the molecule (E2FX, FIGURE 1) was expressed. The second EGF domain was included in the construct because it has been shown to make contacts with the catalytic domain[1] and may be essential for correct folding.

The recombinant proteins carried an affinity tag to facilitate their purification and immobilization. Immobilization of FXa prior to cleavage circumvents the problem of contamination of the target protein with the processing enzyme. Alternatively, after performing the cleavage in solution, the enzyme can be removed from the
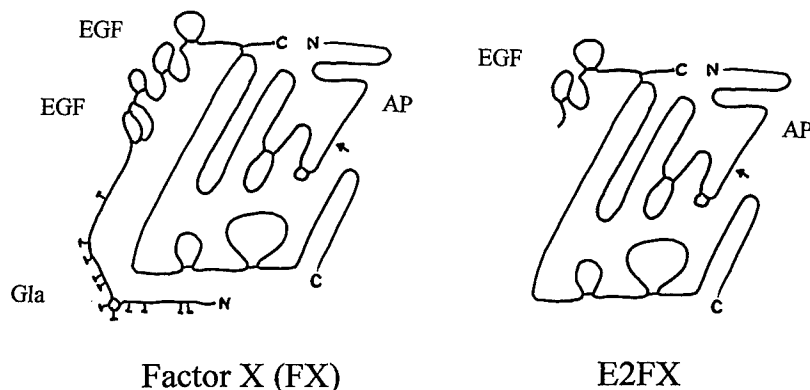
FIGURE 1. Schematic representation of factor X (modified from reference 7) and the deletion variant E2FX, lacking the domain containing the glutamic acid residues that are γ-carboxylated (Gla) and the N-terminal epidermal growth factor (EGF) domain. An arrow identifies the site of cleavage when the zymogen is activated.

processing mixture by means of its affinity tag.[2] Two affinity tags were used in this study: a polyhistidine tail (H6) and the cellulose binding domain (CBD). The CBD of the exoglucanase Cex from *Cellulomonas fimi* was fused at the C-terminus of E2FX; in a second construct, the CBD of the endoglucanase CenA, also from *C. fimi*, was fused at the N-terminus of E2FX. CBD fusions are particularly attractive for immobilization because, under appropriate conditions, binding to cellulose is virtually irreversible and cellulose is a versatile, inexpensive, and inert matrix. The expression, binding, and activity of the tagged E2FX variants were investigated.

RESULTS AND DISCUSSION

The E2FX constructs were cloned into the yeast expression vector pPIC9K that carries the *Tn903 kan^r* gene, allowing selection of high-copy-number clones using Geneticin[3] (G418). In this system, copy number has been shown to correlate positively with expression level.[3–5] The cDNA is cloned in frame with the alpha-factor signal sequence and expression is driven by the methanol-inducible alcohol oxidase (AOX1) promoter. Either *Bgl*II or *Sac*I was used to digest the DNA prior to electroporation to facilitate chromosomal integration. The frequency of transformation was 3-fold higher using *Sac*I-digested DNA rather than *Bgl*II-digested DNA (TABLE 1). This result is consistent with those of Scorer *et al.*[3] and Boraston *et al.* (personal communication), who reported an even greater (20-fold) difference in the transformation efficiency depending on the restriction enzyme used.

In *P. pastoris*, there are two alcohol oxidase genes, AOX1 and AOX2. The AOX1 is responsible for the vast majority of alcohol oxidase activities in the cell. Transformation of *P. pastoris* with pPIC9K-derived vectors can disrupt the AOX1 gene, resulting in a slow methanol utilization phenotype (Mut^S). Disruption of the AOX1

gene is dependent on the type of integration. When $BglII$ is used to digest the vector prior to transformation, one of the two DNA fragments produced is targeted to transplace into the AOX1 gene, resulting in a Mut^S phenotype. Of the clones tested, however, 85% of the clones derived from a transformation using $BglII$-digested vectors showed a Mut$^+$ phenotype (TABLE 1). Molecular mechanisms to explain this observation have been proposed by Clare *et al.*[4] The frequency of Mut$^+$ transformants was even higher when the DNA used for transformation was linearized with $SacI$ instead of $BglII$. This is consistent with a linear $SacI$-digested vector being more likely to integrate by a single crossover event without disruption of the AOX1 gene.

Clones resistant to up to 4 mg/mL of G418 were isolated and tested for production. Secretion of the recombinant proteins was detected by Western blot analysis of the culture supernatants with a polyclonal anti-FX antibody. Clones secreting the highest levels of FX antigen were further characterized. The secreted proteins were tested for activity following the binding to cellulose (Avicel) or to Nickel (Ni)–agarose. The results showed that the affinity tags in the case of E2FX-H6 and E2FX-CBDcex were functional and the binding was specific. The bound protein was then activated by reaction with Russell's Viper Venom (RVV), and FXa proteolytic activity toward small chromogenic substrates was demonstrated with the immobilized enzymes (FIGURE 2).

To our knowledge, this is the first time that recombinant proteins with factor X activity have been produced in yeast. However, the recombinant FX fusion proteins produced by *P. pastoris* were heterogeneous in molecular weight. This heterogeneity might be a result of (a) the presence of fortuitous polyadenylation sites in the DNA that may give rise to truncated mRNAs,[6] (b) nonnative glycosylation of the recombinant proteins, and/or (c) proteolytic degradation of the proteins produced. We are currently investigating these effects in order to develop strategies for high-level production of these FX fusion proteins.

TABLE 1. Transformation of *Pichia pastoris* Strain GS115 with pPIC9K Containing the E2FX Constructs[a]

Construct in Vector pPIC9K	$SacI$-digested DNA		$BglII$-digested DNA	
	Number of Transformants per Plate	Fraction of Transformants Displaying Mut$^+$ Phenotype	Number of Transformants per Plate	Fraction of Transformants Displaying Mut$^+$ Phenotype
no insert	18	NA	11	NA
E2FX	65	1.00	19	0.60
E2FX-H6	33	0.92	5	0.80
CBD-E2FX	103	1.00	26	1.00
CBD-E2FX-H6	23	1.00	25	1.00
total no./average fraction	242	0.98	86	0.85

[a]For each construct, both the number of transformants per plate and the fraction of Mut$^+$ transformants isolated after electroporation with either $SacI$- or $BglII$-digested DNA are shown. NA = not available.
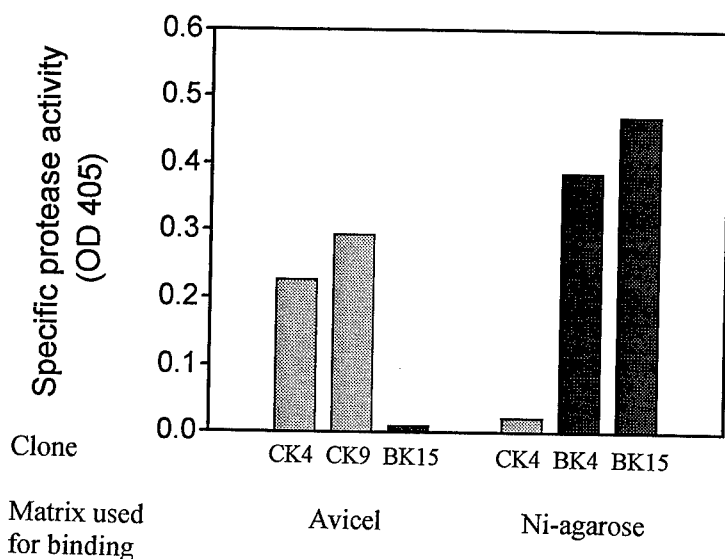
FIGURE 2. Activity assay of FX derivatives. *Pichia pastoris* GS115 was transformed with derivatives of the vector pPIC9K. Proteins from culture supernatants were bound to Avicel or Ni-agarose. The immobilized enzymes were activated with RVV and activity was tested with a chromogenic substrate. Clones CK4 and CK9 express E2FX-CBD and clones BK4 and BK15 express E2FX-H6.

ACKNOWLEDGMENTS

REFERENCES

1. PADMANABHAN, K., K. P. PADMANABHAN & A. TULINSKY. 1993. J. Mol. Biol. **232:** 947–966.
2. ASSOULINE, Z., H. SHEN, D. G. KILBURN & R. A. J. WARREN. 1994. Protein Eng. **7:** 787–792.
3. SCORER, C. A., J. J. CLARE, W. R. McCOMBIE, M. A. ROMANOS & K. SREEKRISHNA. 1994. Bio/Technology **12:** 181–184.
4. CLARE, J. J., F. B. RAYMENT, S. P. BALLANTINE, K. SREEKRISHNA & M. A. ROMANOS. 1991. Bio/Technology **9:** 455–460.
5. CLARE, J. J., M. A. ROMANOS, F. B. RAYMENT, J. E. ROWEDDER, M. A. SMITH, M. M. PAYNE, K. SREEKRISHNA & C. A. HENWOOD. 1991. Gene **105:** 205–212.
6. ROMANOS, M. A., A. J. MAKOFF, N. F. FAIRWEATHER, K. M. BEESLEY, D. E. SLATER, F. B. RAYMENT, M. M. PAYNE & J. J. CLARE. 1991. Nucleic Acids Res. **19:** 1461–1467.
7. DAVIE, E. W., K. FUJIKAWA & W. KIESEL. 1991. Biochemistry **30:** 10363–10370.

Cloning and Overexpression of Thermostable D-Hydantoinase from Thermophile in *E. coli* and Its Application to the Synthesis of Optically Active D-Amino Acids

DONG-CHEOL LEE,[a] SEUNG-GOO LEE,[a]
SEUNG-PYO HONG,[b] MOON-HEE SUNG,[b]
AND HAK-SUNG KIM[a]

[a]*Department of Biotechnology*
Korea Advanced Institute of Science and Technology
Yusung-Gu, Taejon 305-701, Korea

[b]*Applied Microbiology Research Group*
Genetic Engineering Research Institute
KIST
Yusung-Gu, Taejon 305-701, Korea

INTRODUCTION

In the 1980s, a simple chemoenzymatic method for the production of various D-amino acids including D-*p*-hydroxyphenylglycine (D-HPG) was developed by employing asymmetric biotransformation.[1,2] In this process, a chemically synthesized racemic hydantoin derivative is asymmetrically hydrolyzed to the *N*-carbamoyl-D-amino acid by D-stereospecific hydantoinase. The resulting *N*-carbamoyl-D-amino acid is further converted to the corresponding D-amino acid by nitrous acid treatment or carbamoylase. The residual L-form substrate is spontaneously racemized to the D-form under alkaline conditions, leading to 100% theoretical yield.

From a practical standpoint, several problems have been found in the production process of D-HPG from 5-(4-hydroxyphenyl)hydantoin (HPH). One of them is that the substrate is slightly soluble in water at room temperature, which might be a barrier to a high production rate. Thus, the enzyme reaction at high temperature is more advantageous because the enzyme activity and substrate solubility increase, given that the enzyme is stable at elevated temperature. In this context, the use of a thermostable enzyme is highly required.

Recently, we isolated *Bacillus stearothermophilus* SD-1 from soil that produces a thermostable D-hydantoinase.[3] The enzyme was purified to homogeneity and its biochemical properties were investigated.[4] Here, we report the cloning and overexpression of the thermostable D-hydantoinase in *E. coli*. Culture conditions of recombinant *E. coli* for the production of the thermostable enzyme were optimized, and the synthesis of optically active D-HPG using free or immobilized enzyme was conducted.

CLONING OF THE THERMOSTABLE D-HYDANTOINASE GENE
INTO *E. COLI*

Chromosomal DNA of *Bacillus stearothermophilus* SD-1 was partially digested with Sau3AI. The chromosomal DNA fragments were ligated with the dephosphorylated pBR322 linearized by BamHI digestion, and the ligate was used to transform *E. coli* DH5α. The transformant grown on agar plates containing ampicillin was transferred onto 1% hydantoin-LB plates containing 0.005% phenol red to primarily screen the hydantoinase-positive colonies. D-Hydantoinase-expressing strains were detected with bright yellow color on the plates. The strains were assayed for hydantoinase activity and one of them was isolated as a hydantoinase-producing *E. coli*. The recombinant plasmid having the hydantoinase gene was designated pHBR5. In order to enhance the expression level of the enzyme, the size of the inserted gene encoding D-hydantoinase was reduced to 3.1 kb from 10.5 kb, and the resulting gene was reinserted into the pUC18 vector (FIGURE 1). The plasmid constructed was named pHU183 and was transformed into different *E. coli* strains. The D-hydantoinase produced by the recombinant *E. coli* was confirmed to be identical with that of *B. stearothermophilus* SD-1 by the analyses on both SDS-PAGE and Western blotting with polyclonal antibody for the enzyme.

OVEREXPRESSION OF THE ENZYME IN *E. COLI*

The thermostable D-hydantoinase from *B. stearothermophilus* SD-1 was overexpressed in the *E. coli* strain containing plasmid pHU183. The D-hydantoinase-encoding gene was located at 1 kb downstream from the *lac* promoter on the pUC18 plasmid. The expression level of the enzyme was much higher by its own promoter than by IPTG; thus, constitutive expression was conducted in this work. It is very practical to express the enzyme constitutively because the use of a common inducer such as IPTG is not economical for the production of bulk enzyme on an industrial scale due to its expensive price.

The expression level of the protein in different *E. coli* strains is shown in TABLE 1, and XL1-Blue was observed to be most suitable as a host strain in semisynthetic media for large-scale cultivation. The enzyme was expressed in its soluble form, and the enzyme content was up to 20% of the total intracellular protein in *E. coli*. The specific activity of the recombinant *E. coli* was 30 times higher than that of the original strain, *B. stearothermophilus* SD-1. FIGURE 2 shows the plasmid stability, and the plasmid was maintained stably for more than 80 generations even without selection pressure.

The large-scale cultivation of the recombinant was conducted in semisynthetic media containing glycerol as the sole carbon source with pH control using ammonia water. The effect of pH on the cultivation was negligible in the range of 6 ~ 8, but the expression level of enzyme was significantly affected by the culture temperature. The specific activity at 37 °C was about two times higher than that at 30 °C. Plasmid
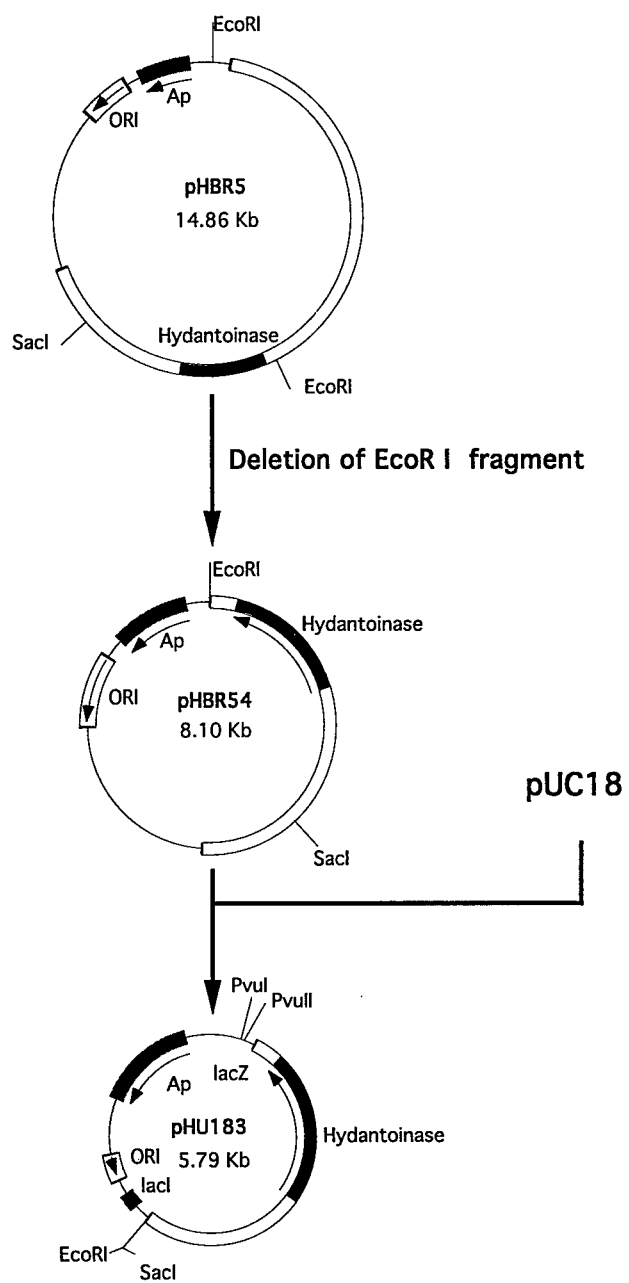
FIGURE 1. Map of the constructed plasmid pHU183.

TABLE 1. Specific Activity of D-Hydantoinase Expressed in Different *E. coli* Strains[a]

Culture Medium	Host Strain			
	DH5α	XL1-Blue	JM105	HB101
Luria-Bertani	20.1	20.9	22.9	22.5
Minimal	1.3	15.3	3.5	1.9

[a]Specific activity of enzyme: units/mg–dry cell weight.

content and the level of expressed enzyme within the recombinant at 37 °C were observed to be higher than those at 30 °C. The cell concentration reached up to 25 g-DCW/L in 30-L batch fermentation and the specific activity was the same as that observed previously (FIGURE 3).

APPLICATION TO THE SYNTHESIS OF D-AMINO ACID

Cultivated cells were disrupted using a homogenizer, and heat treatment was conducted at 60 °C. The cell debris and the aggregates of heat-labile proteins were removed by centrifugation. The free enzyme was applied to the production of *N*-carbamoyl-D-*p*-hydroxyphenylglycine (NCHPG) from HPH in distilled water. The optimal temperature and pH were determined to be 55 °C and 9.0, respectively. The concentrations of HPH and enzyme were 100 g/L and 20,000 units/L, respectively, and the pH was controlled at 9.0. As a result, the conversion yield reached about 80% in 3 h.
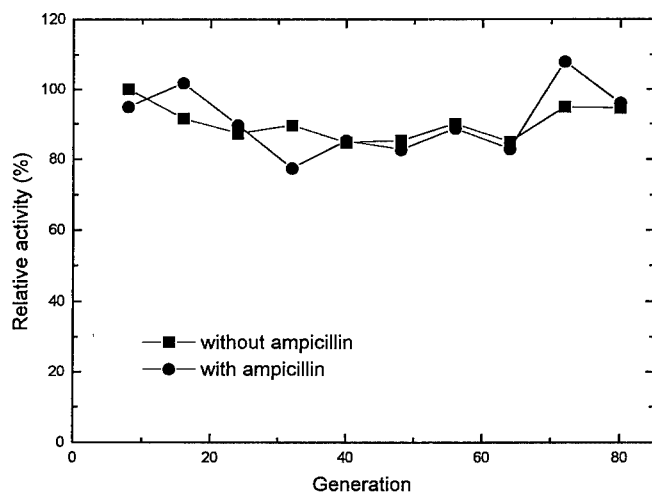
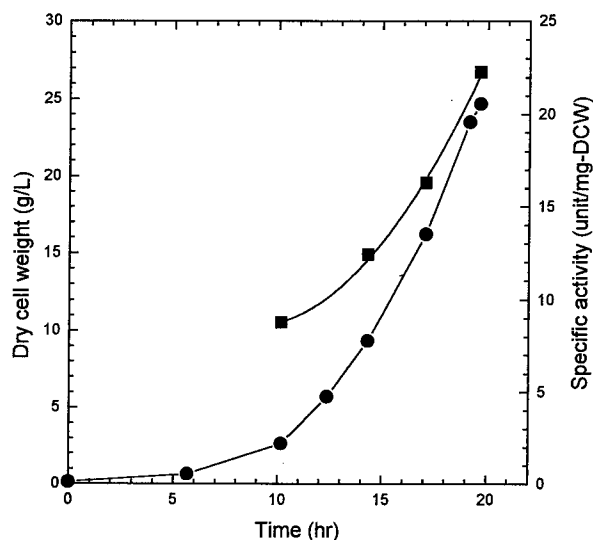FIGURE 2. Stability of the plasmid containing the D-hydantoinase-encoding gene in XL1-Blue.

FIGURE 3. Batch cultivation of recombinant *E. coli* harboring the pHU183 plasmid: dry cell weight (DCW) (●); specific activity of the enzyme (■).

SUMMARY

We cloned the thermostable D-hydantoinase gene from *B. stearothermophilus* SD-1 into *E. coli*. The cloned gene was constitutively expressed by its own promoter, and the enzyme was produced in its soluble form. The specific activity of the recombinant *E. coli* was 30 times higher than that of *B. stearothermophilus* SD-1. The cultivation conditions were investigated for the overproduction of the enzyme, and the temperature was found to affect the plasmid content and the expression level of the enzyme. Recombinant *E. coli* was cultivated in 30-L batch fermentation, the cell concentration reached 25 g-DCW/L, and the specific activity was about 20,000 units/g-DCW. D-Hydantoinase produced from the recombinant *E. coli* could be successfully applied to the synthesis of *N*-carbamoyl-D-amino acid from the 5-monosubstituted hydantoin derivative.

REFERENCES

1. YAMADA, H., S. TAKAHASHI, Y. KII & H. KUMAGAI. 1978. Distribution of hydantoin-hydrolyzing activity in microorganisms. J. Ferment. Technol. **56:** 484–491.
2. TAKAHASHI, S., T. OHASHI, Y. KII, H. KUMAGAI & H. YAMADA. 1979. Microbial transformation of hydantoins to *N*-carbamoyl-D-amino acids. J. Ferment. Technol. **57:** 328–332.
3. LEE, S-G., D-C. LEE, M-H. SUNG & H-S. KIM. 1994. Isolation of thermostable D-hydantoinase-producing thermophilic *Bacillus stearothermophilus* SD-1. Biotechnol. Lett. **16:** 461–466.
4. LEE, S-G., D-C. LEE, S-P. HONG, M-H. SUNG & H-S. KIM. 1995. Thermostable D-hydantoinase from *Bacillus stearothermophilus* SD-1: characteristics of purified enzyme. Appl. Microbiol. Biotechnol. **43:** 270–276.

Recent Advances in Cell-free Protein Synthesis towards a Protein Biosynthesizer[a]

HIDEO NAKANO, YASUAKI KAWARASAKI,
AND TSUNEO YAMANE

Laboratory of Molecular Biotechnology
Department of Applied Biological Sciences
Faculty of Agriculture
*Nagoya University*
Nagoya 464-01, Japan

INTRODUCTION

Recently, a cell-free protein synthesis system has received considerable attention as a novel laboratory-scale method for the preparation of protein from a cloned or synthesized DNA template, particularly since the development of a continuous-flow cell-free protein synthesis system, called CFCF, by Spirin and coworkers in 1988.[1] This system allowed a constant rate of protein synthesis for more than 20 hours. However, it needs a special apparatus consisting of a reaction chamber with an ultrafiltration membrane, a pump, and an incubator to control its temperature. Although the total amount of product is significantly improved by the CFCF system as compared with a conventional cell-free system, the reported value is usually 100 to 200 μg per mL of reaction mixture, and its protein synthesis rate is typically 5 μg/mL-h, which is almost the same as that of a conventional batch system.[1-5] In addition, the final concentration of the product eluted through a membrane in the CFCF system is very low. Because the flow rate of the feeding solution is about 1.5 mL/h, the concentration of the product in the eluant is roughly 3 μg/mL. Therefore, it is preferable to prolong the reaction period in a batch reaction without particular instruments and necessary to increase both the protein synthesis rate and the concentration of the final product for the application of the cell-free system to the preparation of proteins from template DNA.

In this study, we have succeeded in prolonging the translational reaction in a conventional batch system from 1 hour to 10 hours by improving the reaction conditions such as temperature, creatine phosphate, etc., without any particular devices. In addition, condensing translational extract by polyethylene glycol (PEG) precipitation has been able to increase the initial protein synthesis rate by about 10-fold. Moreover, when Cu^{2+} was added to the reaction mixture, the high protein synthesis rate was sustained for a longer time, resulting in a higher amount of product. Nishimura and coworkers recently reported that Cu^{2+} depressed the

TABLE 1. Typical Reaction Conditions for Cell-free Protein Synthesis Reactions Using Condensed and Uncondensed Wheat Germ Extract

HEPES-TMA (pH 7.6) or	
HEPES-KOH (pH 7.6)	60 mM
Dithiothreitol	4 mM
ATP	1 mM
	3 mM for condensed extract
GTP	0.1 mM
Amino acids	0.16 mM
RNase inhibitor	1000 U/mL
Spermidine	0.3 mM
Magnesium acetate	0.5 mM
Creatine phosphate	40 mM
Creatine kinase	40 μg/mL
Wheat germ tRNA	100 μg/mL
mRNA (*in vitro* transcript from	7.6 μg/mL
plasmid pTEV-DHFR[7])	23 μg/mL for condensed extract
Wheat germ extract (preparation	20% (v/v)
described elsewhere[8,9])	30% for condensed extract
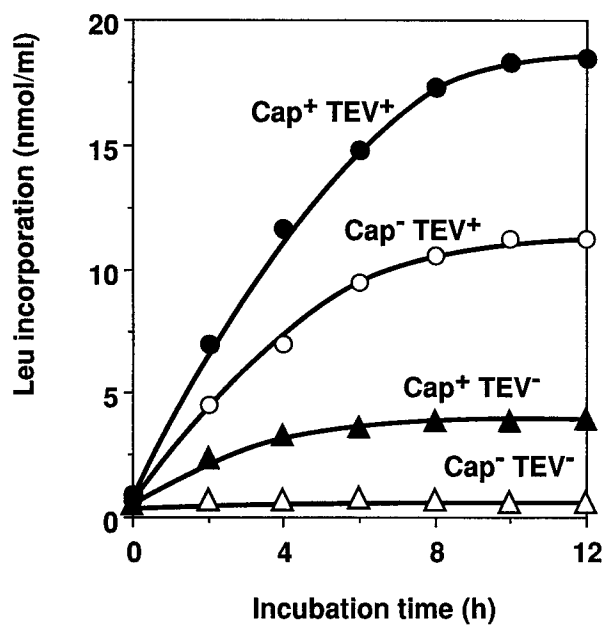
FIGURE 1. Effect of the 5′-untranslated sequence on the translation of *dhfr* mRNA. Reaction mixtures containing 7.5 μg/mL of capped TEV-*dhfr* mRNA (●), 7.5 μg/mL of capped *dhfr* mRNA (▲), 30 μg/mL of uncapped TEV-*dhfr* mRNA (○), or 30 μg/mL of uncapped *dhfr* mRNA without the TEV sequence (△) were incubated at 26 °C.

degradation of mRNA in *Escherichia coli* cell extract.[6] Our results show that Cu^{2+} depressed not only the degradation of mRNA, but also the degradation of ATP in wheat germ extract. The results suggest the importance of reducing both mRNA and ATP degradations to realize a "protein biosynthesizer".

RESULTS AND DISCUSSION

Prolonged Cell-free Protein Synthesis

To prolong the protein synthesis reaction, we optimized the reaction conditions as summarized in TABLE 1. The most important points for extending the protein synthesis reaction were to keep the ATP level by the ATP regeneration system and to supplement tRNA. When 8 mM creatine phosphate was used, 4 hours of reaction was possible. When 40 mM creatine phosphate was used, the reaction continued for up to 10 hours. Wheat germ extract contains endogenous tRNA, but it was not enough for such a long cell-free protein synthesis. Without supplementary tRNA, the protein synthesis stopped at an earlier time, even if creatine phosphate was high enough.

FIGURE 1 presents the time-course profiles of protein synthesis. As a result of these modifications of the reaction conditions, we could obtain 30 μg of DHFR protein in 1 mL of reaction mixture after 10 hours of incubation, which is comparable
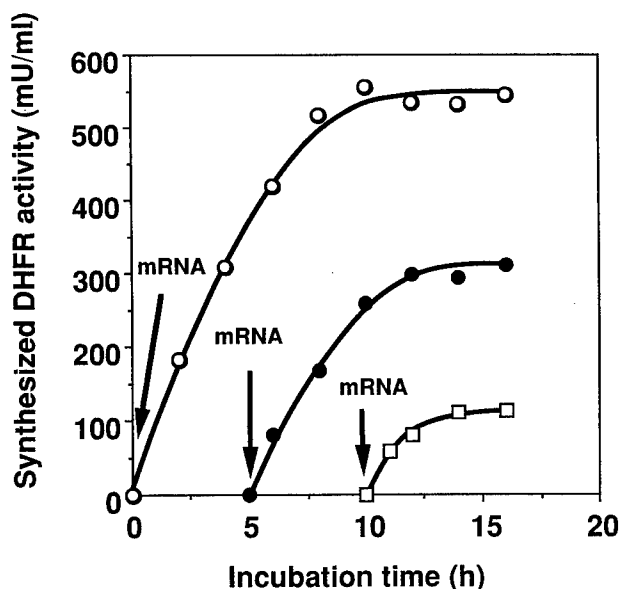

FIGURE 2. A reaction mixture without mRNA was incubated at 26 °C for the period indicated; the reaction was started by adding 7.5 μg/mL (final concentration) of capped TEV-*dhfr* mRNA. Protein synthesis was initiated by adding the mRNA to a reaction mixture after 0 (○), 5 (●), and 10 (□) hours of preincubation.
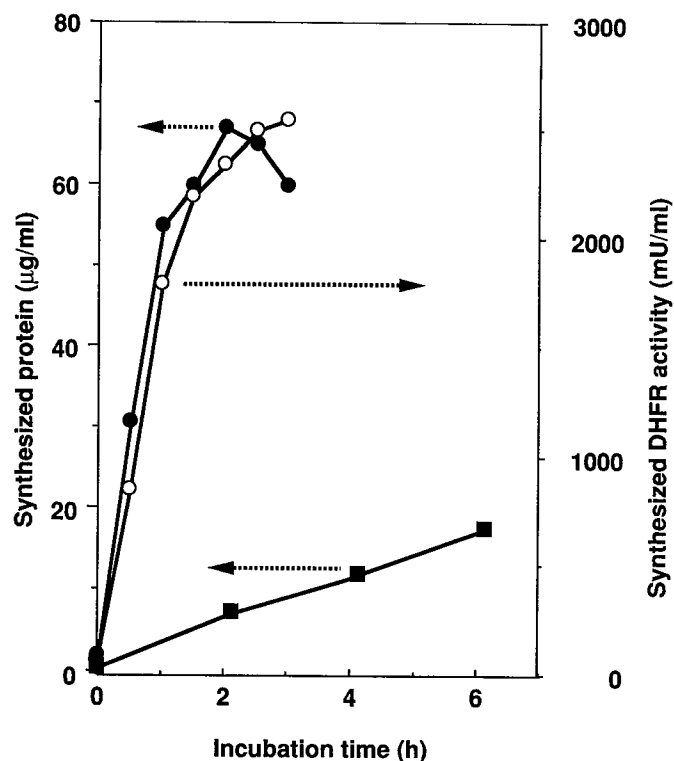
FIGURE 3. Time course of protein synthesis using condensed extract. The reaction mixture with the condensed extract containing 14.7 mCi/mmol [^{14}C]-leucine was incubated for the specified time; then, the incorporated radioactivity into the trichloroacetic acid insoluble fraction (●) and the generated DHFR activity (○) were simultaneously measured. For comparison, a typical protein synthesis using uncondensed extract is also shown by the incorporation of [^{14}C]-leucine (■).

to the CFCF system. Moreover, uncapped mRNA was also translated for the same period. This mRNA contains a 5'-untranslated (5'-UTR) sequence functioning as a ribosome entry site from tobacco etch virus (TEV). The uncapped TEV-*dhfr* mRNA needed a fourfold higher concentration than that of capped TEV mRNA; however, 18.5 μg of DHFR protein per mL of reaction mixture was synthesized after 12 hours of incubation. Without the TEV 5'-UTR sequence, uncapped mRNA was poorly translated. The amount of protein synthesized from this uncapped mRNA was 30–40 times smaller than that using the same amount of uncapped TEV mRNA.

Is it possible to prolong the reaction period more? To answer this question, protein synthesis was initiated by adding mRNA into a preincubated reaction mixture after 0, 5, and 10 hours. As seen in FIGURE 2, the protein synthesis of the reaction initiated without preincubation ceased completely at 10 hours. However, the addition of mRNA after 10 hours of preincubation could initiate protein synthesis. This suggests that the degradation of mRNA is one of the reasons for the
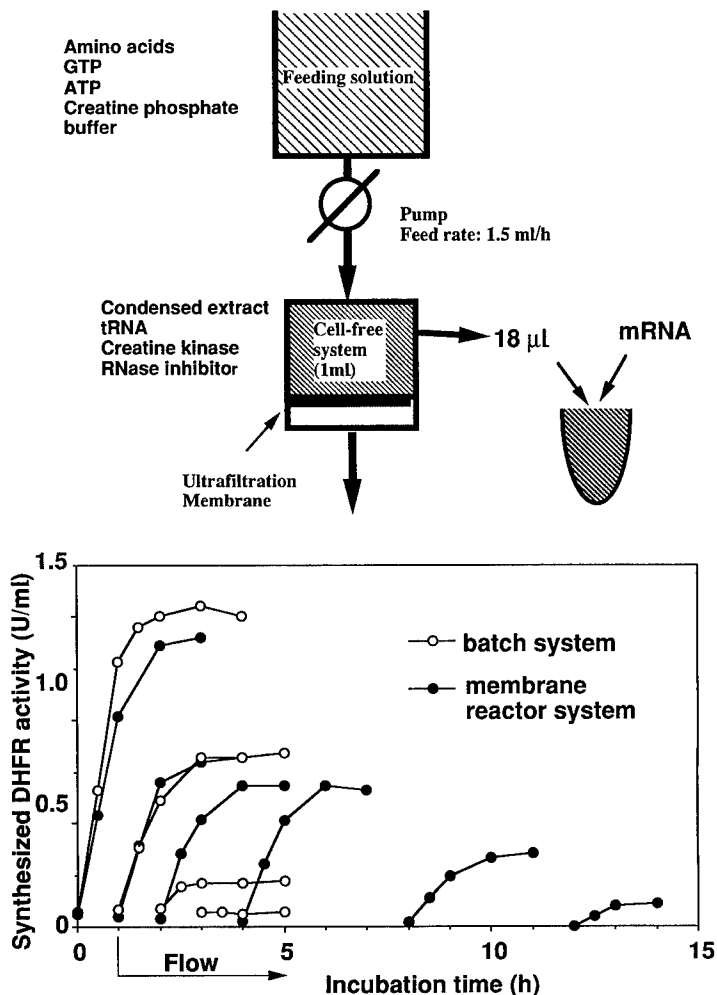
FIGURE 4. Translational activity of the condensed extract system confined by a membrane reactor with a continuous supply of buffer solution containing every low-molecular-weight component. The cell-free protein synthesis mixture without mRNA was held in a membrane reactor using an ultrafiltration XM 50 membrane. Feeding solution containing every low-molecular-weight substrate was continuously supplied to the reactor. A small portion (18 µL) of the reaction mixture was withdrawn from the reactor at the indicated incubation times, and its translational activity was measured by adding fresh mRNA (●). As a control experiment, after various incubation times without feeding, the translational reaction was started by adding mRNA to the mixture (○).

stopping of protein synthesis in our system. In addition, all of these reactions stopped completely at 14 hours of incubation, even if the reaction started after 10 hours of preincubation. This suggests that there may be other factors to stop protein synthesis, such as inactivation of translation machinery.

High Rate of Protein Synthesis Using Condensed Extract

In our previous report, wheat germ extract condensed by ultrafiltration was able to synthesize protein at a higher rate.[8] To increase the condensation rate, extract was concentrated by polyethylene glycol (PEG) precipitation. The PEG-condensed extract needed some modifications of the reaction conditions for maximal productivity, as listed in TABLE 1.

FIGURE 3 shows the time course of protein synthesis measured simultaneously by synthesized DHFR activity and leucine incorporation. It indicates that the initial protein synthesis rate was 55 μg/mL-h, which was about 10 times higher than that of uncondensed extract. Although an extremely high initial protein synthesis rate was obtained, the durability of this reaction, about 2 hours, was 5 times shorter than our prolonged batch system of about 10 hours. To obtain a higher yield, a longer reaction period is needed.

There are at least two limiting factors for the reaction. One is the increased phosphatase activity in the extract. After 2 hours of incubation, ATP and GTP concentrations began to decrease rapidly (data not shown). Another possibility is mRNA degradation because the reaction mixture sustained in the membrane reactor as illustrated in FIGURE 4 did have a translational activity if fresh mRNA was added. This figure also indicates the importance of maintaining the ATP level because a reaction mixture incubated in a batch manner lost its translational activity from freshly added mRNA.
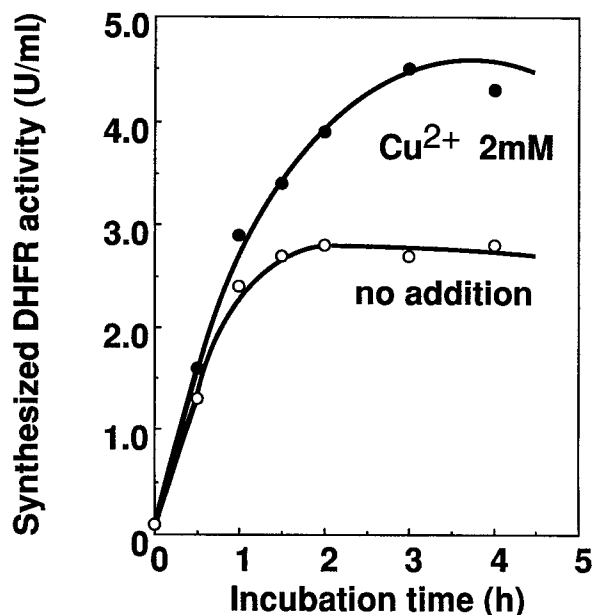

FIGURE 5. Effects of Cu^{2+} on the cell-free protein synthesis using the condensed extract. Protein synthesis with or without 2 mM $Cu(OAc)_2$ using the condensed extract is shown.

Therefore, both ATP and mRNA degradations are limiting in cell-free protein synthesis using a condensed extract. The use of an inhibitor for each degradation activity can be effective. Fortunately, Cu^{2+} was able to reduce both of these activities, resulting in a longer reaction period, although its suppressing effects on each activity were not perfect. The addition of Cu^{2+} prolonged the reaction period of our condensed system (FIGURE 5), resulting in an increased amount of product per reaction volume (120 μg/mL). In fact, it was comparable to that of the CFCF system. In addition, it should be emphasized that the protein was produced in only 3 hours in the system, as opposed to 20 hours in the CFCF system. Therefore, the overall productivity was roughly 6 times higher than that of the CFCF system. Moreover, the final concentration of the product was about 40 times higher than that obtained in the eluant of the CFCF system.

CONCLUSIONS

We have studied the cell-free protein synthesis using wheat germ extract in the conventional batch reaction focusing on both a higher protein synthesis rate and a longer synthesis period. The following points were improved with considerable success:

(1) Optimization of the reaction conditions of cell-free protein synthesis enabled a longer protein synthesis, up to 10 hours, even in a batch system.

(2) Condensation of wheat germ extract by precipitation with polyethylene glycol increased the initial protein synthesis rate by about 10 times; moreover, the amount of product reached 0.12 mg/mL in only 3 hours with the use of Cu^{2+}, a possible inhibitor against RNase and phosphatase.

ACKNOWLEDGMENTS

REFERENCES

1. SPIRIN, A. S., V. I. BARANOV, L. A. RYABOVA, S. Y. OVODOV & Y. B. ALAKHOV. 1988. Science **242**: 1162–1164.
2. ENDO, Y., S. OTSUZUKI, K. ITO & K. MIURA. 1992. J. Biotechnol. **25**: 221–230.
3. KIGAWA, T. & S. YOKOYAMA. 1991. J. Biochem. **110**: 166–168.
4. KUDLICKI, W., G. KRAMER & B. HARDESTY. 1992. Anal. Biochem. **206**: 389–393.
5. TULIN, E. E., K. TSUTSUMI & S. EJIRI. 1995. Biotechnol. Bioeng. **45**: 511–516.
6. NISHIMURA, N., Y. KITAOKA & M. NIWANO. 1994. J. Ferment. Bioeng. **78**: 130–133.
7. KAWARASAKI, Y., T. KAWAI, H. NAKANO & T. YAMANE. 1995. Anal. Biochem. **226**: 320–324.
8. NAKANO, H., T. TANAKA, Y. KAWARASAKI & T. YAMANE. 1994. Biosci. Biotechnol. Biochem. **58**: 631–634.
9. NAKANO, H., T. TANAKA, Y. KAWARASAKI & T. YAMANE. 1996. J. Biotechnol. In press.

Distance Mapping as a Tool in Protein Modification

V. NAGARAJAN,[a] VASANTHA PATTABHI,[a]
AND P. V. SUNDARAM[b,c]

[a]*Department of Crystallography and Biophysics*
University of Madras
Madras 600 025, India

[b]*Center for Protein Engineering and Biomedical Research*
The Voluntary Health Services
Madras 600 113, India

INTRODUCTION

The three-dimensional structure of proteins, essential for catalytic activity, is maintained to a large extent by noncovalent linkages such as H-bonds, salt bridges, and disulfide bonds. Covalent bonding that is energetically favorable helps to reinforce the active conformation and helps to stabilize proteins. Introduction of covalent bonds may increase the stability of the proteins, which may be desirable in unnatural environments provided by organic solvents, increased temperatures, and extremes of pH. Introduction of additional linkages using cross-linkers is one of the methods available to us. We have been successful in increasing the stability of proteases like trypsin, α-chymotrypsin, and papain using various cross-linkers without much loss in activity. In the course of this study, we found that a knowledge of intergroup (NH_2 and $COOH$) distances is useful in the choice of cross-linkers.

METHODS

When a protein reacts with a double-headed molecule like glutaraldehyde, both ends react independently with suitable amino acids on the protein. This leads to intrachain cross-link formation and the length of this link depends on the length of the cross-linker used. A knowledge of the reactive groups on the protein that may be cross-linked, as well as the chain lengths of the cross-linking reagents, would be helpful to predict the number of potential cross-links possible. Sometimes, however, single amino groups may be blocked by the modifying agent and amino group estimation by the TNBS method does not necessarily indicate cross-linking. Distance mapping also helps in estimating the heterogeneity of the products that may be formed. For example, if the following lysine pairs, Lys 1..Lys 2, Lys 1..Lys 3, Lys 4..Lys 5, and Lys 45..Lys 70, are within the stipulated distance in a protein structure, then we can anticipate two types of modified molecules, one with Lys 1..Lys 2 linkage and the other with Lys 1..Lys 3 linkage, whereas other interactions remain the same.

[c]To whom all correspondence should be addressed.

TABLE 1. Classification of Lysine Pairs Based on Distances between Them

Protein	Source	Total No. of Residues	Total No. of Lysines	Lysine-Lysine Distance		
				<7 Å	7–10 Å	10–15 Å
trypsin	bovine	223	14	2	2	8
chymotrypsin	cow	245	14	1	4	9
papain	papaya	212	10	1	1	5
lysozyme	hen egg white	129	6	—	—	1
RNase T1	aspergillus	104	2	—	—	—

Distances between the reactive groups on proteins were calculated using the PDB coordinates[1] and a table was prepared giving the distance ranges. In the present study, glutaraldehyde was the linker and hence the distances between the ϵ-NH$_2$ groups of lysine were tabulated for various proteins of interest (TABLE 1).

Glutaraldehyde has a free rotation about the C=C bond and it can adopt two extreme limit conformations (FIGURE 1B) with cross-linker lengths varying from 5 to 8 Å. Hence, lysines with separations of the order of 5 to 8 Å are likely to be cross-linked.

Similar distance mapping was done for linkers that interact with carboxyl groups, that is, aspartic acid and glutamic acid. In this case, the O...O distances of both O$_1$ and O$_2$ were done with O$_3$ and O$_4$ (FIGURE 1A) and the least of the four contacts is given in TABLE 2.
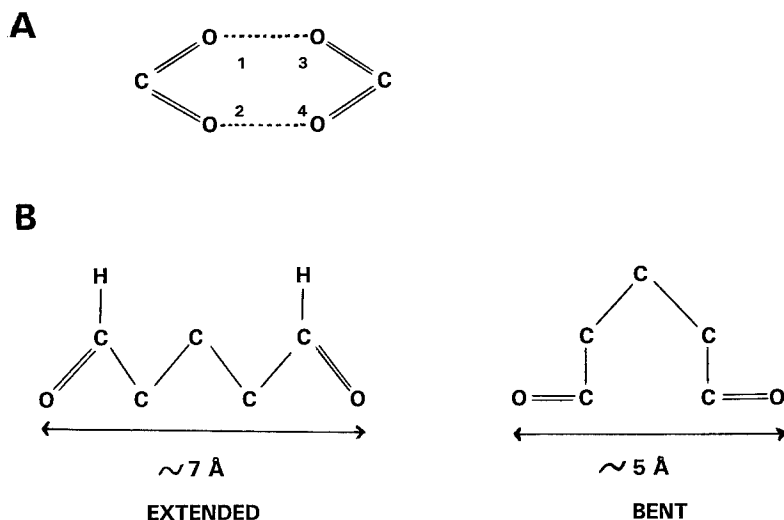

FIGURE 1. (A) The numbering of the oxygens in the carboxyl group of aspartic or glutamic acid. (B) The extreme limit conformations of glutaraldehyde.

TABLE 2. Distance Mapping of Carboxyl Groups[a]

Protein	Total Residues	No. of Terminal COOH Groups	Distance between COOH Groups		
			<5 Å	5–10 Å	10–15 Å
trypsin	223	10	2	7	7
lysozyme	129	9	—	6	4
RNase S	124	10	—	2	4
RNase T1	104	12	2	5	4

[a]When two potential pairs of COOH groups are activated by condensing agents such as carbodiimide, the bridge distance linking the COOH groups will depend on the diamines chosen.

Energy Calculation

Theoretical energy calculations can be utilized in order to study the effect of chemical modification on protein structure and its activity. A model calculation using the program AMBER 3.0 Revision A[2,3] was carried out on the protein papain. Although the difference in energy between the native protein and the chemically modified one (cross-linked) is expected to be small, the movement of the active site residues can throw light on the effect of the modification at the active site and hence
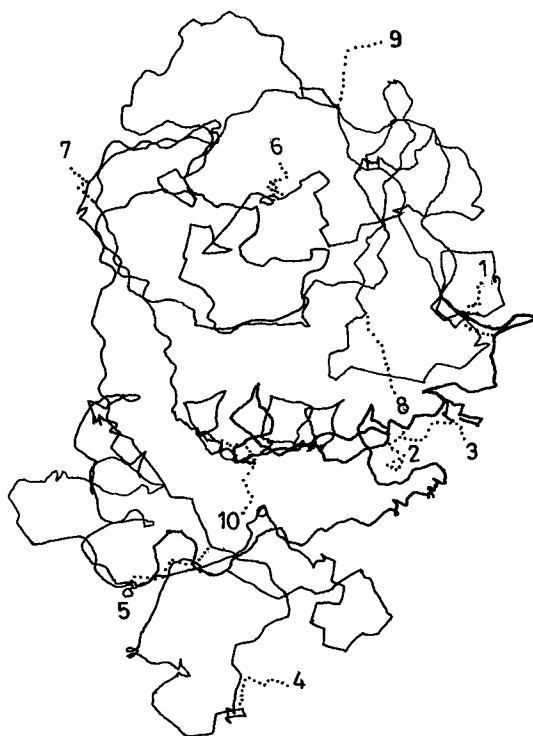
FIGURE 2. Three-dimensional structure of papain showing the lysine residues (dotted lines). The numbering of the lysines is from the N-terminal to the C-terminal, but does not refer to the actual sequence number.

on its activity. The glutaraldehyde model was built using computer graphics in the two extreme limit conformations and was minimized.

Papain has 212 amino acids, out of which 10 are lysines. FIGURE 2 shows the positions of the lysines in papain. Lys 17 and Lys 174 were cross-linked using glutaraldehyde and the model was minimized. During minimization, the atoms beyond a 10-Å radius from lysines 17 and 174 were frozen; however, the active site groups were excluded from this criterion, that is, they were free to move. The minimization followed the steepest descent method for the first 50 cycles and was switched over to the conjugate gradient method thereafter. The results are tabulated in TABLE 3. The backbone of the native enzyme was overlapped on the modified enzyme to see the movement of the backbone in the neighborhood of the cross-linked lysines and at the active site, as shown in FIGURE 3.

RESULTS

This study shows that the movement of the active site residues in the bent (~ 5 Å length) conformation is slightly more than in the extended conformation. On the other hand, the movement of lysines in the extended model is greater because the distance of separation between Lys 17 and Lys 174 is 4.5 Å, which is less than the cross-linker length of 7 Å. Energetically, cross-linking with the bent glutaraldehyde conformation is more favorable.

CONCLUSIONS

A good cross-linker is one that is equal to or slightly shorter than the distance separating the two reactive groups. If its length is longer, then it fails to impose the desired rigidity and hence stability.

TABLE 3. Energy Minimization of Papain Cross-linked with Glutaraldehyde

|	
Energy of the native protein	-2.07822×10^3 kcal/mol
Energy of the modified protein:	
(i) extended glutaraldehyde conformation	-1.920454×10^3 kcal/mol
(ii) bent glutaraldehyde conformation	-1.977829×10^3 kcal/mol
(slight increase in energy from the native is due to the restricted minimization)	
Deviations after minimization (glutaraldehyde extended):	
at the active site	Cys 25 (max): Sγ, 0.7 Å
	His 159 (max): Cδ2, 0.537 Å
in cross-linked lysines	Lys 17 (max): Cϵ, 3.822 Å
	Lys 174 (max): Nζ, 3.005 Å
Deviations after minimization (glutaraldehyde bent):	
at the active site	Cys 25 (max): Sγ, 1.038 Å
	His 159 (max): Cδ2, 0.896 Å
in cross-linked lysines	Lys 17 (max): Nζ, 2.421 Å
	Lys 174 (max): Nζ, 1.000 Å
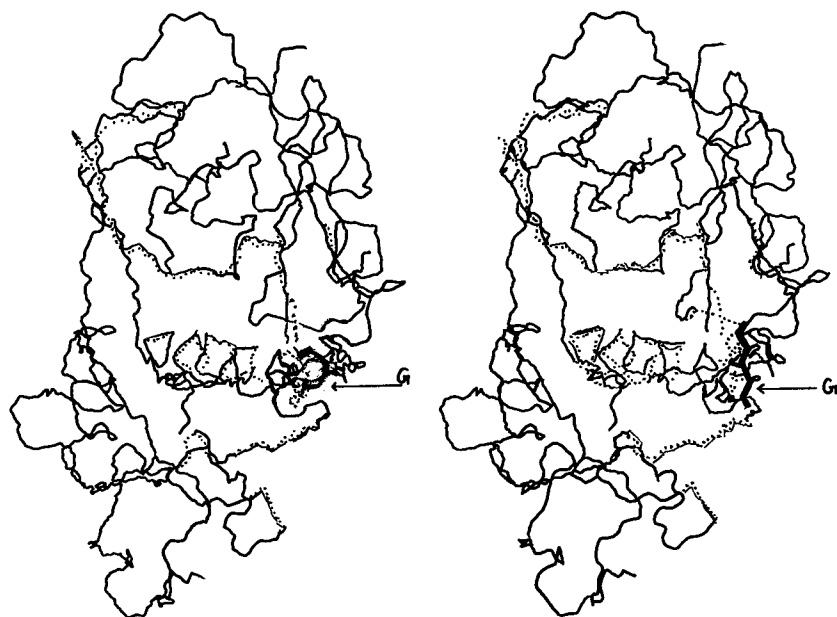
FIGURE 3. Overlap diagram of native and chemically modified papain (energy-minimized). Dotted lines show the regions where a small deviation from the native is seen. The thick line (G) is the glutaraldehyde cross-linked (between Lys 17 and Lys 174) and before minimization: (left) glutaraldehyde bent; (right) glutaraldehyde extended.

Distance mapping of the reactive groups on proteins would therefore help to select an ideal cross-linker and thereby produce a stable protein.

REFERENCES

1. BERNSTEIN, F. C., T. F. KOETZLE, G. J. B. WILLIAMS, E. F. MEYER, JR., M. D. BRICE, J. R. RODGERS, O. KENNARD, T. SHIMANOUCHI & M. TASUMI. 1977. J. Mol. Biol. **112:** 535–542.
2. SINGH, U. C., F. K. BROWN, P. A. BASH & P. A. KOLLMAN. 1987. J. Am. Chem. Soc. **109:** 1607–1614.
3. WEINER, S. J., P. A. KOLLMAN, D. A. CASE, U. C. SINGH, C. GHIO, G. ALAGONA, S. PROFETA & P. WEINER. 1984. J. Am. Chem. Soc. **106:** 765–784.

Cellulose-binding Domains

Versatile Affinity Tags for Inexpensive Large-Scale Purification, Concentration, and Immobilization of Fusion Proteins

P. TOMME,[a,b,c] N. R. GILKES,[b,c] M. M. GUARNA,[a]
C. A. HAYNES,[a,d] D. HASENWINKLE,[a,c] E. JERVIS,[a,d]
P. JOHNSON,[c,e] L. McINTOSH,[c,e] R. A. J. WARREN,[b,c]
AND D. G. KILBURN[a,c]

[a]Biotechnology Laboratory
[b]Department of Microbiology and Immunology
[c]Protein Engineering Network Centers of Excellence
[d]Department of Chemical Engineering
[e]Departments of Chemistry, Biochemistry, and Molecular Biology
University of British Columbia
Vancouver, British Columbia, Canada V6T 1Z3

INTRODUCTION

When grown in the presence of cellulose, most cellulolytic (micro)organisms produce a multitude of polypeptides, many of which display a strong affinity for the insoluble cellulosic matrix. The number and identity of the various components depend upon the substrate used to maintain growth of the organism and probably reflect the structural heterogeneity of the cellulosic materials. Since 1982, when the first cellulase gene was sequenced,[1] almost 300 cellulase and xylanase sequences have become available. Analysis of the polypeptides revealed that many of these enzymes have a modular organization typically composed of at least a catalytic domain (CD) for hydrolysis of the substrate and a carbohydrate-binding domain or cellulose-binding domain (CBD) for binding to the insoluble matrix.[2]

The presence of two distinct domains was first demonstrated by limited proteolysis of cellulases from *Trichoderma reesei* and *Cellulomonas fimi*.[3,4] The individual domains were released as discrete functional units because of the proteolytic susceptibility of the connecting linker sequences. Subsequently, the domain structure of many glycosyl hydrolases has been probed by biochemical and genetic analyses, and the gene fragments encoding individual domains have been successfully cloned and expressed in heterologous hosts such as *E. coli*.[5,6] The cellulose-binding domains, either alone or as a fusion partner, retain their strong and specific binding for cellulose, a property useful in various biotechnological applications.

This paper describes the different properties of CBDs derived from *C. fimi* glucanases. A rationale for the use of these CBDs in the purification, concentration, and immobilization of fusion proteins containing the CBD as a fusion partner is also discussed. Finally, several examples of these applications with enzymes constructed in our laboratory are described in detail.

CELLULOSE-BINDING DOMAINS FROM *CELLULOMONAS*
FIMI GLUCANASES

We have cloned seven cellulases/xylanases from the bacterium *C. fimi* and characterized their corresponding products. All are modular enzymes containing two or more domains, at least one of which is a cellulose-binding domain (FIGURE 1). CBDs share considerable sequence similarity and are located at either the N- or C-terminal end of the enzymes (FIGURE 1). The tandem repeated CBD (N1N2) at the N-terminus of endoglucanase C (CenC) is only distantly related to the other *C. fimi* CBDs.[7]
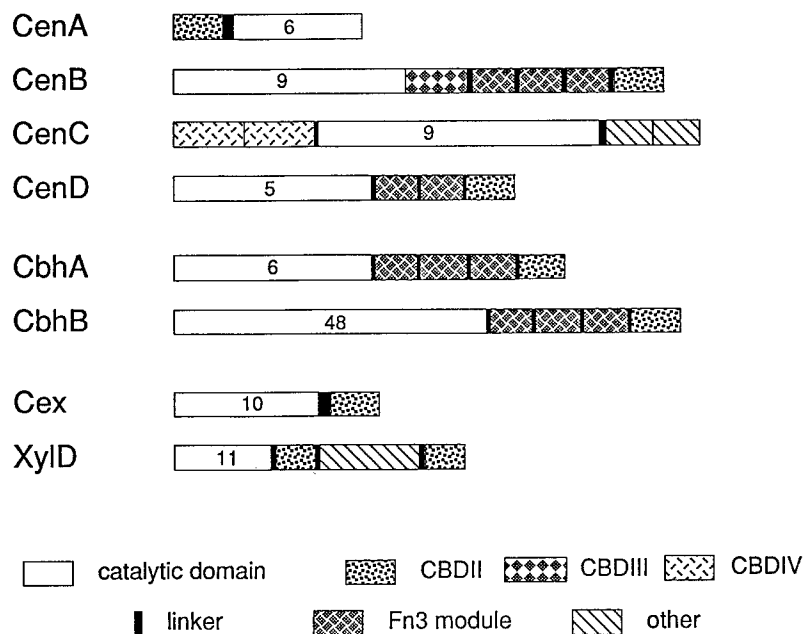
FIGURE 1. Domain structure of the *Cellulomonas fimi* cellulases and xylanases. Each enzyme is represented as a linear map showing the arrangements of the various structural and functional domains. CenA, CenB, CenC, and CenD are endo-β-1,4-glucanases. CbhA and CbhB are cellobiohydrolases, Cex is a mixed β-1,4-xylanase/β-1,4-glucanase, and XylD is a β-1,4-xylanase. CBDII, CBDIII, and CBDIV refer to the family II, III, and IV cellulose-binding domains, respectively. The CBDIV of CenC (two copies) corresponds with the tandem repeat N1N2. Fn3 indicates a fibronectin type III–like module.

Cellulose-binding domains can be classified in ten families (I–X) of structurally related proteins based on their amino acid sequences.[7] The majority of *C. fimi* CBDs (e.g., CBD_{Cex}) belong to family II, whereas the CBD_{CenC} has been classified in family IV.[7,8] CBDs from different families appear to have different properties, whereas it remains unclear if functional differences exist between CBDs of the same family.

CBD_{Cex}, produced in *E. coli*, has been characterized in detail (see below) and its structure in solution was recently solved by 2D NMR analysis.[9] Both the tandem repeat (N1N2) and one of the individual repeats (N1) of CBD_{CenC} have been hyperexpressed in *E. coli* and are under continuing study. The elucidation of the N1 structure in solution is also currently under way. CBD_{Cex} and CBD_{CenC} (N1) are the focus of this paper.

INTERACTION OF CBDs WITH CELLULOSIC POLYMERS

CBD_{Cex} and CBD_{CenC} have distinctively different specificities and binding affinities for cellulose. Whereas CBD_{Cex} has high affinity (K_r of 20.8 ± 0.4 L/g) for ordered, H-bonded cellulose such as bacterial microcrystalline cellulose (BMCC),[5] CBD_{CenC} does not bind crystalline cellulosic matrices.[10] Binding of CBD_{Cex} to BMCC is stable over a wide pH range (3.0–9.0) and at elevated temperatures (50 °C).[5] Both CBD_{Cex} (K_r of 1.5 ± 0.2 L/g) and CBD_{CenC} bind to amorphous, phosphoric acid–swollen cellulose (PASC) and to Avicel, a microcrystalline cellulose containing both crystalline and amorphous regions. However, whereas CBD_{CenC} can be eluted from Avicel with distilled water,[10] elution of CBD_{Cex} requires more drastic conditions such as 4 M guanidinium hydrochloride.[5] It is of particular interest that CBD_{CenC} (N1N2 or N1) binds to soluble cellulosic polymers such as hydroxyethylcellulose (HEC) (see below), a unique property not shared by CBD_{Cex} or any of the many CBDs reported in the literature.

THERMODYNAMIC ANALYSIS OF BINDING

The thermodynamics for binding of CBD_{Cex} to insoluble BMCC and CBD_{CenC} to soluble HEC were investigated by isothermal titration calorimetry (ITC). Analysis of the ITC binding for CBD_{Cex} (FIGURE 2) against three putative binding models indicated two energetically different, independent classes of binding sites on the BMCC surface.[11] The high-affinity sites are characterized by an association constant K_a of 6.3 (± 1.4) × 10^7 M^{-1} and the low-affinity sites by a K_a of 1.1 (± 0.6) × 10^6 M^{-1}. The binding of CBD_{Cex} to either type of site is slightly exothermic, but is largely entropically driven ($T\Delta S° = 30.6$ kJ/mol, $\Delta H° = -5.8$ kJ/mol). The large and negative differential heat capacity change ($\Delta C_p° = -2.5$ to -1.5 kJ/mol-K) associated with binding indicates that the dehydration effects of sorbent and protein make a significant contribution to the driving force for binding.[11]

In contrast, the binding of N1 to soluble HEC (FIGURE 3) is driven by a large exothermic standard enthalpy change [$\Delta H° = -30.1$ (± 0.5) kJ/mol] with a slightly unfavorable entropic contribution ($T\Delta S° = -2.1$ kJ/mol). The small, but negative, differential heat capacity change [$\Delta C_p° = -430$ (± 33.4) J/mol-K] and the thermodynamic data indicate that H-bonding and dispersion forces (van der Waals interactions) are the main driving forces for binding of the sugar to the polypeptide. With a K_a of 6.7 (± 0.4) × 10^4 M^{-1}, interaction between CBD_{CenC} (N1) and HEC is weaker than that between CBD_{Cex} and BMCC, but is still fairly strong for binding of a soluble sugar.
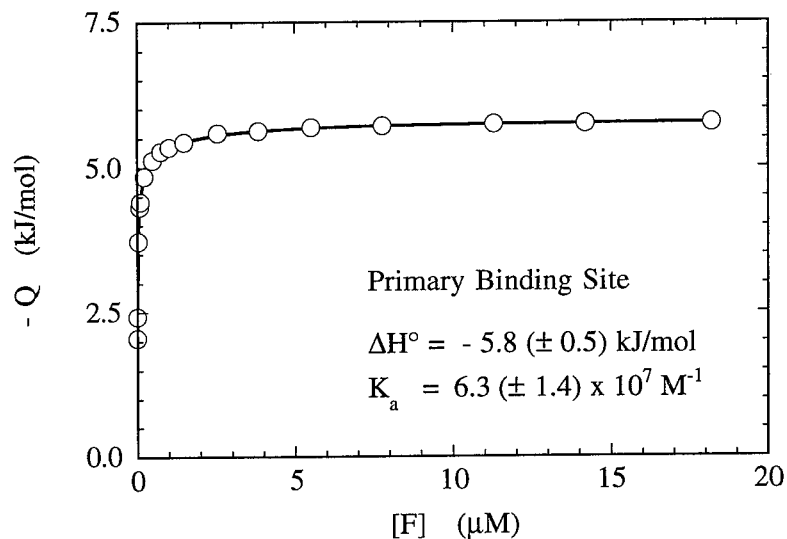
FIGURE 2. Cumulative calorimetric heat for binding of CBD_{Cex} (F) to BMCC in 50 mM potassium phosphate buffer at pH 7.0 and 30 °C.
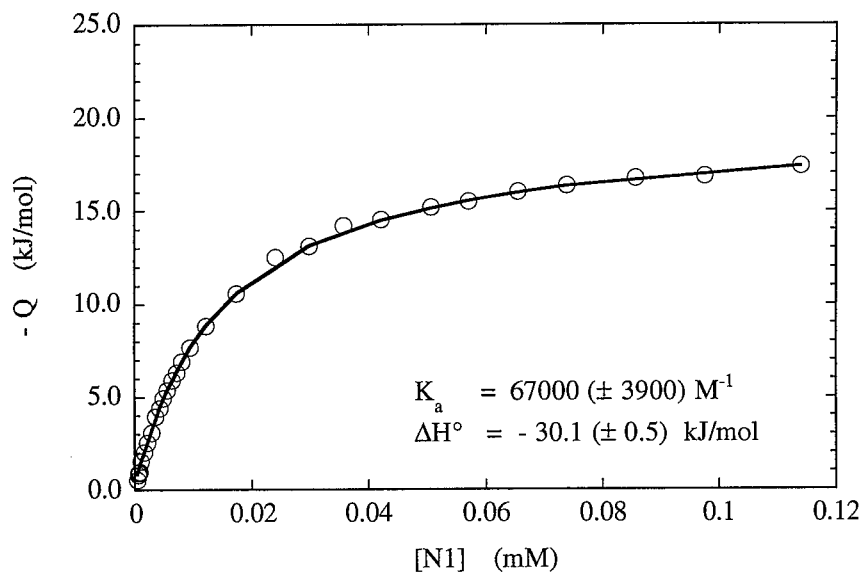

FIGURE 3. Cumulative calorimetric heat for binding of CBD_{CenC} (N1) to HEC in 50 mM potassium phosphate buffer at pH 7.0 and 35 °C.

CBDs IN ENZYME ENGINEERING AND BIOTECHNOLOGY

CBD_{Cex} and Conventional Affinity Chromatography

Protein recovery and purification are important aspects of biotechnology and are a major economic consideration in the design of fermentation processes. Biospecific affinity purification holds an important place in the repertoire of protein purification techniques. Current affinity matrices are usually complex and expensive, requiring covalent attachment of the ligand to the solid support. Cellulose, on the other hand, is relatively cheap and available in a variety of forms: papers (filters), membranes, powders, beads, and cotton. Cellulose-binding domains (e.g., CBD_{Cex}) bind specifically to cellulose and can be eluted under mild conditions. Specific reagents and modifications of the matrix are not required. Under appropriate conditions, binding is essentially irreversible, ideal for enzyme immobilization.[12] Fusion proteins containing the CBD "affinity tag" can be constructed and expressed as heterologous proteins in hosts such as *E. coli* or *Pichia pastoris*. The CBD can be placed at either the N- or C-terminal end of the fusion partner or, if desired, between two target proteins,[13] making the system extremely versatile. Furthermore, an Ile-Glu-Gly-Arg site for cleavage with factor Xa can be engineered between the N-terminal tag and the protein of interest.[14] After purification on cellulose, the fusion proteins can be cleaved with factor Xa, the CBD can be removed by passage through a second cellulose column, and the target protein can be obtained in pure form in the flow-through. We have tested and demonstrated the feasibility of these systems

TABLE 1. Cellulose-binding Domain Fusion Proteins

| CBD	Fusion	Partner	Expression System
CenA	CBD_{CenA}-PhoA	alkaline phosphatase	*E. coli*
CenA	CBD_{CenA}-IL2	human interleukin 2	mammalian cells
			Pichia
			Streptomyces
CenA	CBD_{CenA}-IL3	human interleukin 3	*E. coli*
			mammalian cells
CenA	CBD_{CenA}-Benzonase™	endonuclease	*E. coli*
CenA	CBD_{CenA}-RGD	adhesion peptide	*E. coli*
CenA	XynA-CBD_{CenA}-CD_{CenA}	xylanase	*E. coli*
Cex	Abg-CBD_{Cex}	β-glucosidase	*E. coli*
Cex	Cbg-CBD_{Cex}	β-glucosidase (thermostable)	*E. coli*
Cex	Glu oxidase–CBD_{Cex}	glucose oxidase	(chemically linked)
Cex	Prot A–CBD_{Cex}	protein A	*E. coli*
Cex	Avid-CBD_{Cex}	streptavidin	*E. coli*
Cex	factor X–CBD_{Cex}	factor X	*Pichia*
			mammalian cells
Cex	*E. coli* cells–CBD_{Cex}	Lpp-OmpA	*E. coli*
Cex	XylA-CBD_{Cex}	xylanase	*E. coli*
CenB	SF-CBD_{CenB}	stem cell factor	*E. coli*
CenC	CBD_{CenC} (N1)–CD_{CenA}	CenA catalytic domain	*E. coli*
CenC	CBD_{CenC}-PhoA	alkaline phosphatase	*E. coli*
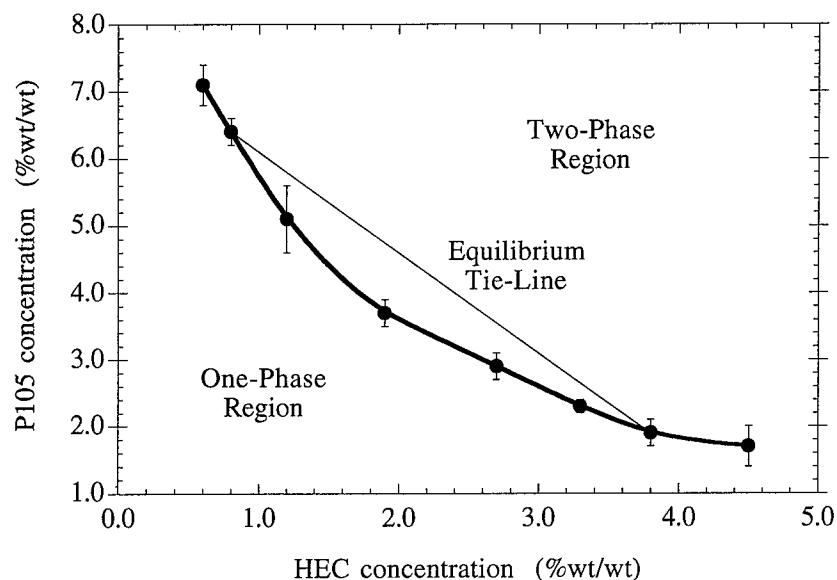
FIGURE 4. Phase-equilibrium data for mixtures of hydroxyethylcellulose (HEC) and Pluronic P105 in 50 mM potassium phosphate buffer at pH 7.0 and 35 °C.

extensively with a variety of fusion proteins using different CBDs and fusion partners (TABLE 1).

CBD_CenC and Aqueous Two-Phase Affinity Partitioning

Whereas the traditional means of protein purification are widely used in biotechnology, aqueous two-phase extraction systems have recently received considerable industrial interest as a continuous process for large-scale purification of protein products, including high-dose therapeutics such as insulin, and of industrial proteins such as 3-oxosteroid isomerase and phosphofructokinase. Two-phase systems offer unique advantages over traditional methods, including high activity yield, fast approach to equilibrium, easy scale-up, and continuous processing. Although a wide variety of aqueous two-phase systems are available, the relatively low partition coefficients and the lack of selectivity in the conventional partitioning systems have motivated the development of affinity partition systems. However, most affinity systems are limited by the high expense of the chemistry needed to produce the polymer-ligand conjugates and by their low capacity and low resolving power. The unique affinity and exquisitely selective binding of CBD_{CenC} (N1) for water-soluble cellulosic polymers such as HEC offers the possibility to develop a cost-effective, highly flexible, and high-capacity affinity partitioning system.

Aqueous two-phase systems can be formed by combining almost any water-soluble carbohydrate with an appropriate poly(oxy-ether). FIGURE 4 shows the phase diagram obtained using the procedures of Haynes *et al.*[15] for mixtures of HEC and

Pluronic P105 [a poly(ethylene glycol)–poly(propylene glycol) copolymer] in 50 mM potassium phosphate buffer at pH 7.0 and 37 °C. A stable two-phase partition system is formed at any total polymer concentration above approximately 3% (wt/wt) Pluronic P105 and 2% HEC, giving a fairly large range of two-phase compositions and equilibrium tie-line lengths useful for affinity partitioning. Fusion proteins (e.g., CBD_{CenC}-hirudin) containing CBD_{CenC} (N1) as an N-terminal affinity tag can thus be purified using the HEC/Pluronic partitioning system. Factor Xa cleavage sites can be engineered into the fusion proteins for recovery of the target protein (e.g., hirudin).

CONCLUSIONS

The specific affinity of cellulose-binding domains for insoluble or soluble cellulosic materials offers great possibilities. Conventional affinity purification methods using CBDs as affinity tags are useful for one-step, small- to medium-scale purifications of high-value proteins or pharmaceuticals. Aqueous two-phase affinity partitioning systems are especially well suited for the large-scale concentration and purification of bulk proteins. Both systems can be used for immobilization of various fusion proteins. Molecular genetic techniques facilitate the coupling of the CBDs to almost any target protein, either at the N- or C-terminal end, an important point if the presence of the CBD on one of the termini might inactivate the protein. The use of appropriate cleavage sites can further facilitate the recovery of the target protein.

REFERENCES

1. WHITTLE, D. J., D. G. KILBURN, R. A. J. WARREN & R. C. MILLER, JR. 1982. Gene 17: 139–145.
2. TOMME, P., R. A. J. WARREN & N. R. GILKES. 1995. Adv. Microbiol. Physiol. 37: 1–81.
3. GILKES, N. R., R. A. J. WARREN, R. C. MILLER, JR. & D. G. KILBURN. 1988. J. Biol. Chem. 263: 10401–10407.
4. TOMME, P., H. VAN TILBEURGH, G. PETTERSSON, J. VAN DAMME, J. VANDERKERCKHOVE, J. KNOWLES, T. TEERI & M. CLAEYSSENS. 1988. Eur. J. Biochem. 170: 575–581.
5. ONG, E., N. R. GILKES, R. C. MILLER, JR., R. A. J. WARREN & D. G. KILBURN. 1993. Biotechnol. Bioeng. 42: 401–409.
6. DIN, N., I. FORSYTHE, L. D. BURTNICK, N. R. GILKES, R. C. MILLER, JR., R. A. J. WARREN & D. G. KILBURN. 1994. Mol. Microbiol. 11: 747–755.
7. TOMME, P., R. A. J. WARREN, R. C. MILLER, JR., D. G. KILBURN & N. R. GILKES. 1995. In Enzymatic Degradation of Insoluble Polysaccharides. ACS Symposium Series. J. N. Saddler & M. Penner, Eds.: 142–161. Amer. Chem. Soc. Washington, District of Columbia.
8. BÉGUIN, P. & J-P. AUBERT. 1994. FEMS Microbiol. Rev. 13: 25–58.
9. XU, G. Y., E. ONG, N. R. GILKES, D. G. KILBURN, D. R. MUHANDIRAM, M. BRANDEIS, J. P. CARVER, L. E. KAY & T. S. HARVEY. 1995. Biochemistry 34: 6993–7009.
10. COUTINHO, J. B., N. R. GILKES, R. A. J. WARREN, D. G. KILBURN & R. C. MILLER, JR. 1992. Mol. Microbiol. 6: 1243–1252.
11. CREAGH, L., E. ONG, E. JERVIS, D. G. KILBURN & C. A. HAYNES. 1995. Proc. Natl. Acad. Sci. U.S.A. Submitted.
12. ONG, E., N. R. GILKES, R. C. MILLER, JR., R. A. J. WARREN & D. G. KILBURN. 1991. Enzyme Microb. Technol. 13: 59–65.
13. TOMME, P., N. R. GILKES, R. C. MILLER, JR., R. A. J. WARREN & D. G. KILBURN. 1994. Protein Eng. 7: 117–123.
14. ASSOULINE, Z., H. SHEN, D. G. KILBURN & R. A. J. WARREN. 1993. Protein Eng. 6: 787–792.
15. HAYNES, C. A., F. J. BENITEZ, H. W. BLANCH & J. M. PRANSNITZ. 1993. AIChE J. 39: 1539–1557.

Purification and Properties of Cyclodextrinase from *Bacillus stearothermophilus* HY-1

SHOU JUN YANG, ZHONG WANG,
AND SHU ZHENG ZHANG

State Key Laboratory of Microbial Resources
Institute of Microbiology
Academia Sinica
Beijing 100080, People's Republic of China

Cyclodextrinase (EC 3.2.1.54) catalyzes the hydrolysis of cyclodextrins to form the corresponding linear oligosaccharides of α-1,4-linkages. Cyclodextrinase has been isolated from some organisms.[1-5] Recently, we isolated a *Bacillus stearothermophilus* HY-1 from soil in South China that produced cyclodextrinase. The enzyme was purified to homogeneity. Some physicochemical and enzymatic properties of the enzyme were determined. The results are summarized in TABLE 1. PAGE of cyclodextrinase is shown in FIGURE 1.

The enzyme hydrolyzes α-, β-, and γ-cyclodextrins and linear maltooligosaccharides to produce oligosaccharides in which maltose is the main component. It could also hydrolyze pullulan to panose. See FIGURE 2 and TABLE 2 for further details.

When the enzyme was incubated with 10 mM diethylprocarbonate (DEPC) in 0.1 M phosphate buffer (pH 6.0) and with 1.0 mM N-bromosuccinimide (NBS) in 10 mM

TABLE 1. Physicochemical and Enzymatic Properties of Cyclodextrinase

optimum temperature	55 °C
optimum pH	6.2
K_m for α-CD	1.79 (mg/mL)
V_{max} for α-CD	336 (μmol/mg-min)
molecular weight	61,000 by SDS-PAGE
pI	pH 5.0
inhibitor (mM, relative activity %)	Zn^{2+} (1.5); Hg^{2+} (1.6); Cu^{2+} (1.6); Fe^{3+} (33)

TABLE 2. Substrate Specificity of α-Cyclodextrinase

Substrate	Relative Activity (%)
α-CD	100
β-CD	56.6
γ-CD	62.3
soluble starch	10.0
amylose	15.7
amylopectin	10.8
pullulan	10.0
glycogen	0
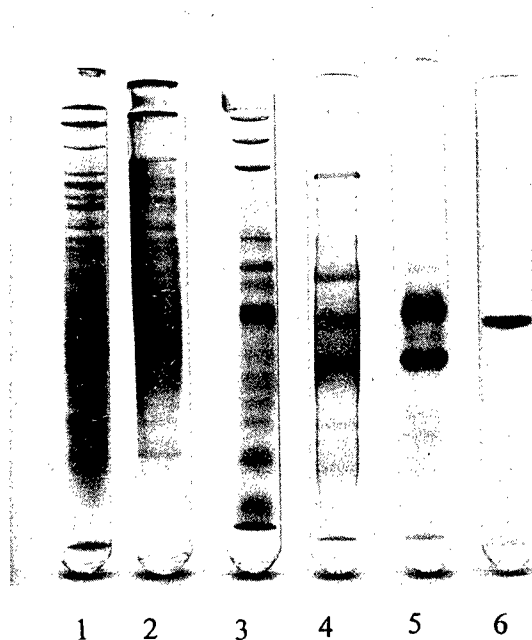
FIGURE 1. PAGE of cyclodextrinase: (1) cell-free extract; (2) ammonium sulfate fractionation; (3) DEAE-cellulose; (4) hydroxyapatite; (5) Sephadex G150; (6) α-CD-AH-Sepharose 4B.
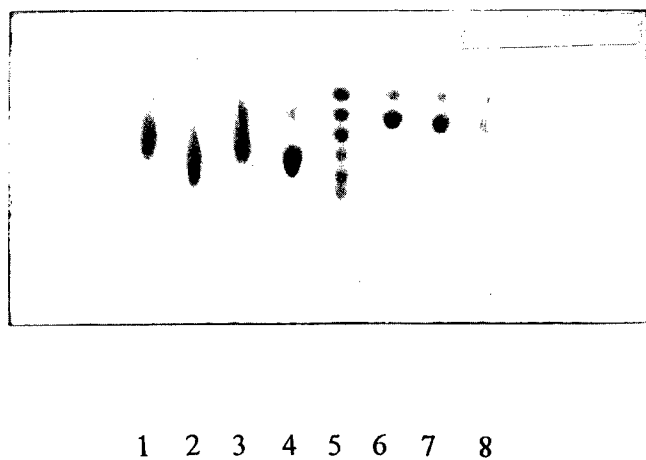

FIGURE 2. Product analysis of the enzyme on various substrates by silica thin-layer chromatography: (1) soluble starch; (2) amylose; (3) amylopectin; (4) pullulan; (5) G1–G6; (6) α-CD; (7) β-CD; (8) γ-CD.

TABLE 3. Effect of Chemical Modification Reagents on Activity

Reagents[a]	Concentration (mM)	Buffer	pH	Relative Activity (%)
none	—			100
NEM	10	phosphate buffer	7.0	92.6
IAA	1.0		7.0	95.0
NAI	1.0		8.0	107
DEPC	1.0		6.0	83.6
	10			2.3
NBS	0.01	acetate buffer	4.6	100
	0.1			8
	1.0			4.6

[a]Abbreviations—NEM: *N*-ethylmaleimide; IAA: iodoacetamide; NAI: *N*-acetylimidazole; DEPC: diethylprocarbonate; NBS: *N*-bromosuccinimide.

acetate buffer (pH 4.6), the enzyme activity was almost completely lost (see TABLE 3). After the inactivated enzyme was treated with hydroxylamine chloride, the enzyme recovered to 52% of its original activity, which suggested that the histidyl residue(s) is essential for the activity. Various concentrations of α-cyclodextrin (α-CD) were added to the enzyme solution at 3 min prior to the adding of NBS and
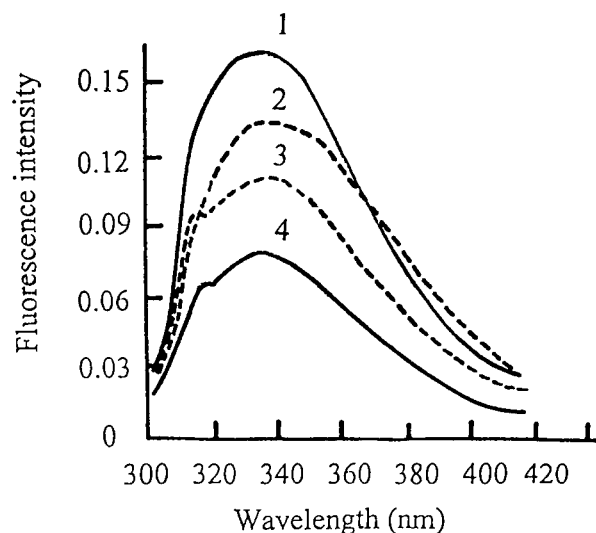
FIGURE 3. Fluorescence emission spectra of α-cyclodextrinase after NBS treatment and α-CD protection:

No.	NBS (mM)	Substrate Concentration (%)
1	0	0
2	10	0.8
3	10	0.2
4	10	0

the enzyme activity was protected by the substrate. The fluorescence emission spectra of the enzyme showed a peak at 335 nm, which is characteristic for tryptophan (see FIGURE 3). The intensity of the modified enzyme was obviously less than the native enzyme; the protected enzyme was also present. These results prove that the tryptophyl residue(s) is located on or near the active site of the enzyme.

REFERENCES

1. DEPINTO, J. & L. L. CAMPBALL. 1969. Purification and properties of cyclodextrinase of *Bacillus macerans.* Biochemistry **7:** 121–125.
2. KITAHATA, S., M. TANIGUCHI, S. D. BELTRAN, T. SUGIMOTO & S. OKADA. 1983. Purification and some properties of cyclodextrinase from *Bacillus coagulans.* Agric. Biol. Chem. **47:** 1441–1447.
3. OGUMA, T., M. KIKUCHI & K. MIZUSAWA. 1990. Purification and some properties of cyclodextrin-hydrolyzing enzyme from *Bacillus sphaericus.* Biochim. Biophys. Acta **1036:** 1–5.
4. YOSHIDA, A., Y. IWASAKI, T. AKIBA & K. HORIKOSHI. 1991. Purification and properties of cyclodextrinase from alkalophilic *Bacillus* sp. J. Ferment. Bioeng. **71:** 226–229.
5. SAHA, B. C. & J. G. ZEIKUS. 1990. Characterization of thermostable cyclodextrinase from *Clostridium thermohydrosulfuricum* 39E. Appl. Environ. Microbiol. **56:** 2941–2943.

Purification of L-Aspartase
by Gene Fusion

HONGYING ZHANG, XIAOPING WANG, JIN ZHANG,
JUN LU, AND WENYUAN DU

State Key Laboratory of Enzyme Engineering
Jilin University
Changchun 130023, People's Republic of China

INTRODUCTION

Screening is a very important step in the process of gene engineering and protein engineering. Usually, nutritional deficient strains are needed to act as the receptor for cloning recombinant plasmids in order to ensure that the products are the desired ones and not just mixtures with those from the receptor. A new gene fusion system[1] was developed, which allows for rapid and efficient purification of recombinant proteins expressed in bacteria. The expression of polypeptides in frame with glutathione S-transferase (GST) (EC 2.5.1.18, MW = 26 kDa) allows for the purification of the fusion protein from crude bacterial extracts under nondenaturing conditions by affinity chromatography on glutathione agarose. The vector expression system has also incorporated specific protease cleavage sites to facilitate proteolysis of the bacterial fusion protein. This system can also be employed even if there is no suitable nutritional deficient strains at hand. In this study, L-aspartase with four identical subunits was employed as a test protein. The active L-aspartase (a tetramer) was obtained.

MATERIALS AND METHODS

Strains, Plasmids, Enzymes, and Chemicals

The strain *E. coli* J$_2$ with the plasmid carrying the gene of aspartase was stored in our laboratory. *E. coli* JM101 was purchased from Huamei Company. The vector pGEX-2T was purchased from Pharmacia LKB. Glutathione and glutathione agarose (attached through the sulfur) were obtained from Wako (Osaka, Japan). The other chemicals used were of analytical or biochemical reagent grade.

Construction of the Fusion Plasmid of pGEX-2T-aspA

An approximately 1.5-kb fragment containing the aspartase gene (aspA) was obtained by PCR, phosphorylated and inserted into plasmid, and cut with SalI. This produced an approximately 6.4-kb plasmid, pGEX-2T-aspA.

Growth and Induction

An overnight culture of *E. coli* JM101 transformed with parental or recombinant pGEX-2T-aspA plasmids was diluted as 1:10 in fresh complex medium supplemented with 50 μg/mL ampicillin. The cells were grown at 37 °C to midlog phase (A_{600} = 0.6–1.0).

The expression of the fusion proteins was induced by adding isopropyl-β-D-thiogalactoside (IPTG) to a final concentration of 1.0 mM. Growth of cells was allowed for an additional 3–5 hours at 37 °C.

Preparation of Cell Extracts

The cells were pelleted by centrifugation and resuspended in 1/100 to 1/50 volumes of PBS + 1% Triton X-100 (PBS: 150 mM NaCl, 16 mM NaH_2PO_4, 4 mM Na_2HPO_4, pH 7.3). The lysis of cells was carried out by mild sonication. The crude extracts were centrifuged at 10,000 rpm for 5 min at 4 °C. The supernatant was now ready for subsequent purification of the fusion protein using glutathione Sepharose 4B column.

Purification and Cleavage of the Fusion Protein

These two procedures were performed according to Guan and Dixon.[2]

RESULTS AND DISCUSSION

Transformation and Identification of Recombinant Plasmids with pGEX-2T-aspA

The recombinant plasmids pGEX-2T-aspA (FIGURE 1) were transformed into *E. coli* JA221 cells and were purified again from the transformed cells for identification, which was carried out on 0.7% agarose (FIGURE 2).

Purification of L-Aspartase from the Fusion Protein

The fusion protein was purified first. Then, a specific cleavage was made at the junction of GST-aspartase. The digested mixture was then put through the affinity column again. The pure aspartase could thus be obtained (FIGURE 3).

Recovery of Aspartase Activity

L-Aspartase is a tetramer enzyme. In fact, inactive enzymes were found first, which means that the aspartase polypeptide chains of the fusion protein could not fold correctly because of the existence of the GST polypeptide chain and the fixation of its N-terminus at the junction of this fusion protein. The interaction of its subunits cleaved from the fusion protein must happen in order to form active enzymes.
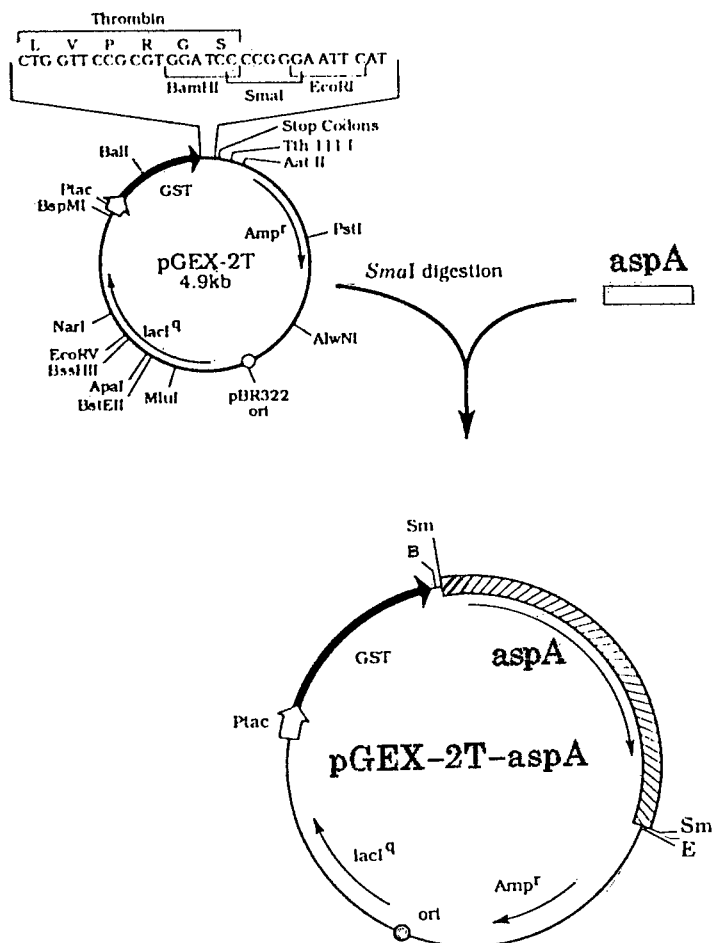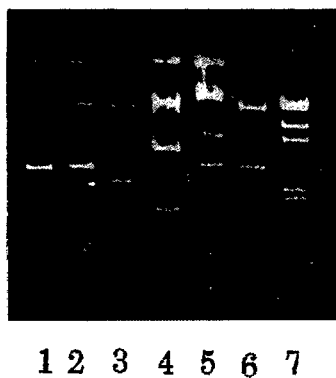
FIGURE 1. The construction of the recombinant plasmid pGEX-2T-aspA.

FIGURE 2. Identification of the recombinant plasmid pGEX-2T-aspA: (1, 2) recombinant pGEX-2T-aspA; (3) pGEX-2T; (4) digested by BamHI; (5) digested by EcoRI; (6) digested by SmalI; (7) marker (λDNA/HindIII).
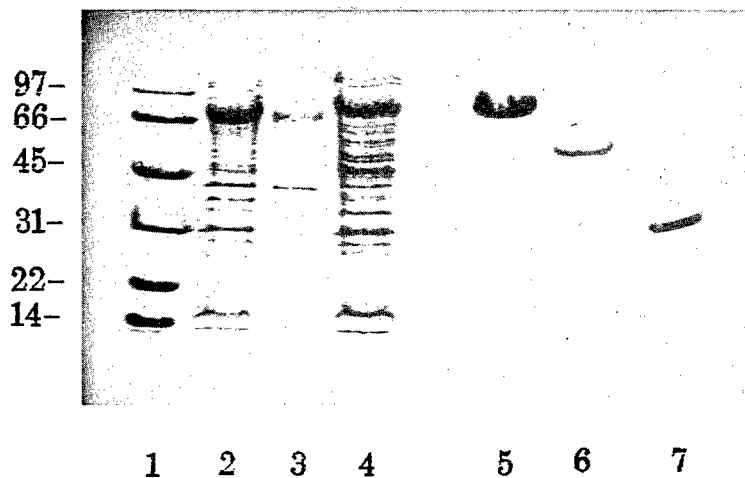
97–
66–
45–
31–
22–
14–

1 2 3 4 5 6 7

FIGURE 3. The SDS-PAGE of the fusion protein: (1) marker; (2) total proteins; (3) pellet; (4) supernatant; (5) the fusion protein GST-aspartase after affinity column; (6) aspartase after cleavage of the fusion protein; (7) GST protein after cleavage of the fusion protein.

Therefore, denaturation of the enzymes by 8 M urea was done at 4 °C. Then, the enzymes underwent renaturation by dialysis against 50 mM Tris-HCl buffer (pH 8.0) at the same temperature for two days. The activity of aspartase was gradually recovered (FIGURE 4). This result indicated that the N-terminus of aspartase is
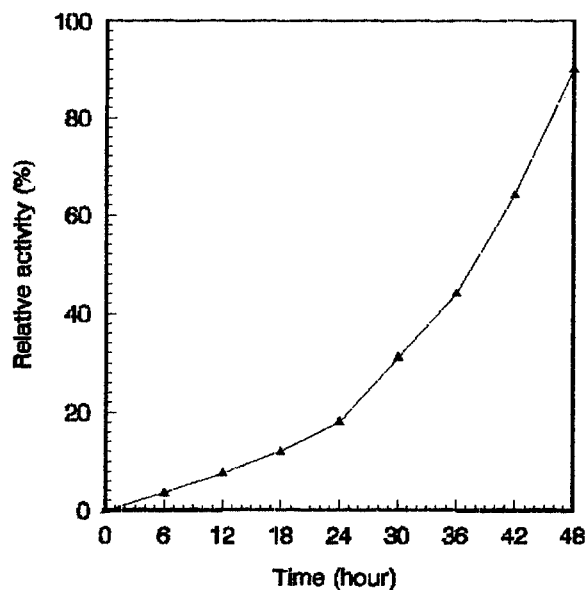
FIGURE 4. The recovery of renatured aspartases.

important for its folding. It might not be located at the surface of the enzyme and it might not exist in the form of a random coil.

This result also indicated that the fusion protein system could be used for purification of active enzymes not only with monomers, but also polymers, especially for obtaining engineered enzymes from cloned cells under the condition of no nutritional deficient strains.

REFERENCES

1. SMITH, D. B. & K. S. JOHNSON. 1988. Gene **67:** 31–40.
2. GUAN, K. L. & J. E. DIXON. 1991. Anal. Biochem. **192:** 262–267.

Carbon-Carbon Bond Synthesis

Reactor Design and Operation for Transketolase-catalyzed Biotransformations[a]

JOHN M. WOODLEY, ROBIN K. MITRA,
AND MALCOLM D. LILLY

Advanced Center for Biochemical Engineering
Department of Chemical and Biochemical Engineering
University College London
London WC1E 7JE, United Kingdom

INTRODUCTION

The use of isolated enzymes, immobilized enzymes, or intact microbial cells to effect organic chemistry is now finding widespread application as reflected by the papers in these proceedings. The reaction-specific, regiospecific, and stereospecific properties of the enzymes are particularly advantageous to complement conventional chemistry for the production of chiral intermediates of use as building blocks for high-value agrochemical and pharmaceutical products. In the laboratory, a large number of new enzymatic activities of potential synthetic use have been found in recent years, but only a limited number of types of biotransformation (e.g., hydrolysis, esterification) have reached commercial exploitation.[1] One reason for this is the lack of an established basis for translating laboratory biotransformations into large-scale processes. The lack of design data and no clear precedent in many instances mean that new biotransformations are frequently developed on a case-by-case basis, leading to long development times. Therefore, reducing the time to scale up a biotransformation is an important aim of the underpinning engineering in order to exploit the full power of enzyme-based catalysis.

With this objective in mind, we have recently adopted a philosophy to design that exploits a structured decision-making procedure.[2] This enables design decisions to be made at the earliest possible opportunity (initially eliminating poor designs and later targeting good ones). The procedure is outlined in FIGURE 1 and is initially based on the characterization of the reaction components [reactant(s) and product(s)], the reaction, the biocatalyst, and the interactions between them. The characterization requires experimental tools to collect the appropriate data. At this stage, only data essential for design are required (e.g., to date, we have identified experimental tools for two-liquid-phase biocatalytic processes[3,4]). The characteristic data collected are then used to set constraints based on guidelines. These constraints on the biocatalyst production process, the choice of biocatalyst form, the reactor environment (i.e., reactor choice and operating strategy), and the product recovery

434

process are then used to eliminate those designs that are inappropriate. This enables the engineer to focus on the selection, integration, and operation of a process that takes advantage of the good features of a specific biotransformation, while minimizing those that are disadvantageous. Some guidelines for process selection and design are now available (specifically for operation of two-liquid-phase biocatalytic processes[4] and selection of *in situ* product removal techniques in biotransformation[5]). However, there remains a need to validate the structured approach; hence, in this paper, this issue is addressed, employing carbon-carbon bond synthesis using the enzyme transketolase as an example.
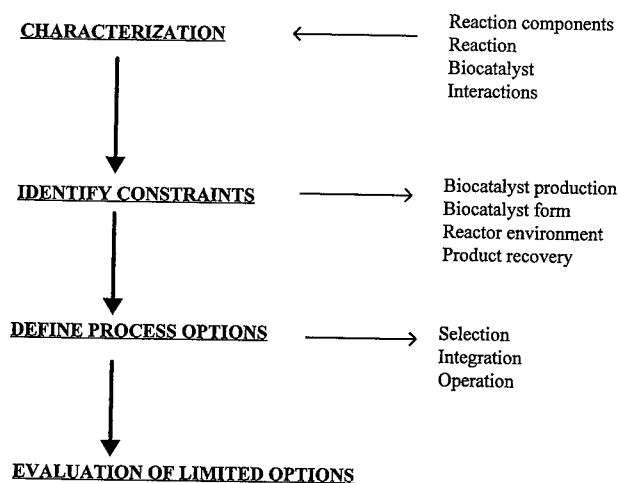
FIGURE 1. Structured design philosophy.

TRANSKETOLASE-CATALYZED CARBON-CARBON BOND SYNTHESIS

Transketolase (TK) (EC 2.2.1.1) catalyzes the transfer of a two-carbon ketol group from a ketose to an aldose. In this way, it may be used catalytically to synthesize carbon-carbon bonds, complementing the established stoichiometric chemical syntheses.[6] This reaction is of key importance in the synthesis of a wide range of molecules, and the ability to carry out the reaction stereospecifically means that this biotransformation is of particular commercial interest. Although the enzyme requires thiamine pyrophosphate (TPP) and magnesium (II) ions (Mg^{2+}) to function, it does not need these to be recycled and does not necessarily require phosphorylated compounds (as the enzyme in its natural environment) to work. Thus, it will catalyze a wide range of aldehyde acceptors by the general scheme shown in FIGURE 2A. Until recently, the predominant source of the enzyme was from spinach and yeast,[6] but to ensure its large-scale production we have now cloned and overexpressed TK in *Escherichia coli*.[7] Using this host, we have grown the organism to 20 g dry cell weight (dcw)/L, producing 4 kg of enzyme from a 1000-L glycerol-fed fermentation.[8–10] The

A

ketol donor   aldehyde acceptor

B

β-Hydroxypyruvate   Glycolaldehyde   L-Erythrulose
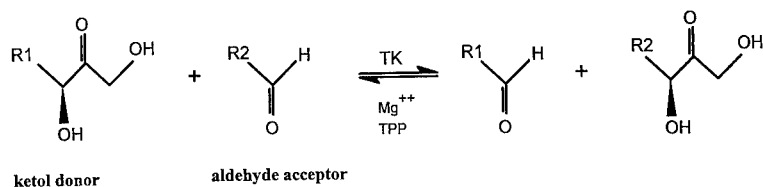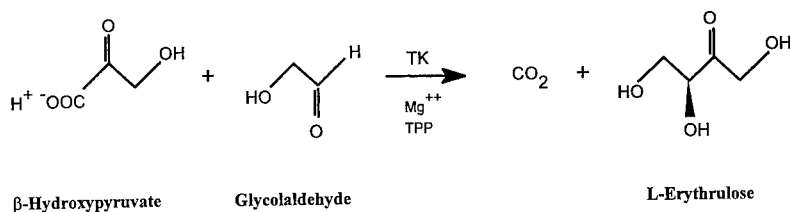
FIGURE 2. General (A) and model (B) transketolase-catalyzed biotransformations for carbon-carbon bond synthesis.

TK represents around 35% of the intracellular protein expressed by the cell. A second approach to improving the large-scale application of TK has been to render the reaction irreversible through the use of β-hydroxypyruvate as the ketol donor, giving the by-product carbon dioxide.[11,12] Using this ketol donor, a wide range of aldehydes, both water-soluble and poorly water-soluble, have been converted.[12-14] The simplest aldehyde to be converted is glycolaldehyde; using this as the acceptor, along with β-hydroxypyruvate as the ketol donor, yields L-erythrulose.[14] This reaction is shown in FIGURE 2B. Using an HPLC-based assay,[15] we have studied this model reaction in detail as the basis for kinetic measurements,[16] reaction characterization,[17] reactor operations, enzyme immobilization,[18] and product recovery.[19,20]

Characteristics of the Model TK Reaction

Initial characterization was of the reactants and products of the reaction. Although the biocatalyst also needed to be characterized, the properties of the catalyst could be altered (through choice or modification via genetic or protein engineering). However, the properties of the reactants and products are constant (set by the target product molecule of interest). Using these data,[17] we have identified constraints for reactor selection and, subsequently, operational strategy.

REACTOR SELECTION

The use of design data characteristic to a specific biotransformation can be used to guide the selection of an appropriate reactor. Such guidance is focused on eliminating inappropriate choices rather than restricting design to one specific reactor type. This procedure is based on qualitative judgments on past precedent. The process synthesis approach[21] parallels that used in the chemical industry and is a powerful tool for targeting the design. This is particularly well illustrated with the transketolase-catalyzed conversion of β-hydroxypyruvate and glycolaldehyde into L-erythrulose. TABLE 1 summarizes those characteristics of the biotransformation that are key to providing constraints for selection or operation of the reactor. The pH lability of the reactants and product, together with the net consumption of acid in the reaction and the production of a gas (by-product carbon dioxide), eliminates the use of a plug flow reactor (packed bed). Likewise, glycolaldehyde is toxic to the enzyme and this eliminates the use of either a plug flow or batch stirred tank reactor. In this reaction, the product (erythrulose) can itself act as a ketol donor, thus providing competitive inhibition.[22] In this way, a high product concentration would be exposed to the enzyme in the continuous stirred tank reactor, eliminating this choice. Hence, by default, this leaves the fed-batch stirred tank reactor for consideration with pH-stat operation at 7.0 and 25 °C, maintaining a low glycolaldehyde concentration (by feeding) and a low L-erythrulose concentration (potentially by *in situ* product removal). This illustrates well the use of characterization data to guide reactor selection. The use of the data to guide operational strategy will be discussed in the remainder of this paper using the control of pH and glycolaldehyde concentration in a fed-batch stirred tank reactor as an example.

TABLE 1. Characteristics and Constraints for Reactor Selection and Operation

| Characteristics | Constraints on Reactor[a] | | | | Operation |
| | Selection | | | | |
	FBSTR[b]	BSTR[c]	CSTR[d]	PFR[e]	
Reactants/products					
pH lability				●	pH = 7
T lability					*T* = 25 °C
Reaction					
acid consumption				●	pH stat
gas production				●	
Interactions					
substrate toxicity		●		●	low [Ga[f]]
product inhibition			●		low [E[g]]

[a]● = limitation on selection of this type of reactor.
[b]Fed-batch stirred tank reactor.
[c]Batch stirred tank reactor.
[d]Continuous stirred tank reactor.
[e]Plug flow reactor.
[f]Glycolaldehyde.
[g]L-Erythrulose.

TABLE 2. Effect of pH on Reactants and Product Stability at 0.5 M after Incubation for 6 h at 25 °C

pH	% Component Remaining after Incubation		
	Hydroxypyruvate	Glycolaldehyde	L-Erythrulose
6.5	97	97	98
7.0	97	96	98
7.5	96	95	96
8.0	91	89	93
8.5	77	74	80
9.0	51	46	58

REACTOR OPERATION TO MAINTAIN THE OPTIMAL ENVIRONMENT

pH Control

The need for pH control in the reactor arises first from the pH lability of the reactants and product. The stability of the ketol donor (lithium hydroxypyruvate), acceptor (glycolaldehyde), and product (L-erythrulose) at pH values from 6.5 to 9.0 over 6 hours of incubation at 25 °C is shown in TABLE 2. Degradation over the 6-hour period of incubation was significant at alkaline pH values. This was more pronounced at 35 °C.[17] Experiments were carried out at concentrations of reactants and product up to 0.5 M in order to assess the stability of the components at realistic process (rather than laboratory) concentrations. As predicted, the rate of degradation was autocatalytic,[23] being a function of the initial concentration. At an initial concentration of 0.5 M, up to 60% of the components had degraded after 6 hours at pH 9.0 compared to 20% at an initial concentration of 0.1 M.[17] These results clearly indicate the need to operate at pH values less than 8.0. The pH lability of the enzyme is not as restrictive, being stable over the range from 6.5 to 9.0. However, a significant loss of initial enzyme activity is observed at pH values less than 6.0 and greater than 9.5.[17] This provides a secondary need for pH control. However, these restrictions on the operational pH are not in themselves a requirement for control. This arises from the net change in pH during the reaction.

FIGURE 3 shows a batch reaction profile for the conversion of 0.5 M hydroxypyruvate and 0.5 M glycolaldehyde to L-erythrulose at 25 °C with 25 U/mL of TK. As a result of the consumption of hydroxypyruvate (supplied as the lithium salt), the pH of the reaction mixture increased. This was in part offset by the production of carbon dioxide (with water in equilibrium with carbonic acid). The dissociation of carbonic acid to bicarbonate and carbonate is itself a function of pH. Hence, at alkaline pH values the change in overall pH in the reaction is negligible, whereas at neutral pH there is a net requirement for acid and at acidic pH values a still greater requirement for acid. The batch reaction shown in FIGURE 3 was operated initially at pH 7 based on the observations of the loss of hydroxypyruvate, glycolaldehyde, and L-erythrulose at high pH values and of TK activity at lower pH values. Over the course of the reaction, a 1.5-pH-unit increase was observed. This led over the 2-hour period of reaction to a slight decrease in TK activity (making for inefficient use of the enzyme) and to a loss of reactants and product. After 2 hours of reaction, no reactants remained. However, more significant was the low final concentration of erythrulose,

0.38 M, indicating only a 76% conversion despite operating with hydroxypyruvate to ensure that the equilibrium was in favor of synthesis. The low conversion was a result of the accumulated losses and indicated the need to operate with pH control as previously discussed.

In contrast, FIGURE 4 shows a batch reaction profile for the conversion of 0.5 M hydroxypyruvate and 0.5 M glycolaldehyde to erythrulose at 25 °C with 25 U/mL of TK, now operated with addition of 1.0 M HCl as required to maintain the pH at 7.0. This reflects large-scale operation where the use of buffers would lead to buffer salts in the product stream, and be prohibitively expensive, but more significantly would lead to the breakdown of reactants.[15] Operation in this way gave complete conversion of the hydroxypyruvate and glycolaldehyde to L-erythrulose as predicted due to the production of by-product carbon dioxide.

Substrate Feeding Strategies

The synthetic potential of transketolase is in part due to the wide variety of aldehydes that can be used as ketol acceptors. However, it is well known that protein in the presence of aldehydes can form an imine (Schiff's base) via the terminal amine. Hence, it is expected that the use of an aldehyde as a ketol acceptor will be toxic to the transketolase activity. Potentially, the least toxic aldehyde would be predicted as glycolaldehyde.[24,25] Nevertheless, there is a substantial toxic effect of this substrate on transketolase as shown in TABLE 3. These measurements were made under the most favorable conditions for the enzyme in the presence of cofactors (0.9 mM Mg^{2+} and 2.4 mM TPP) and a reducing agent[17] (10 mM
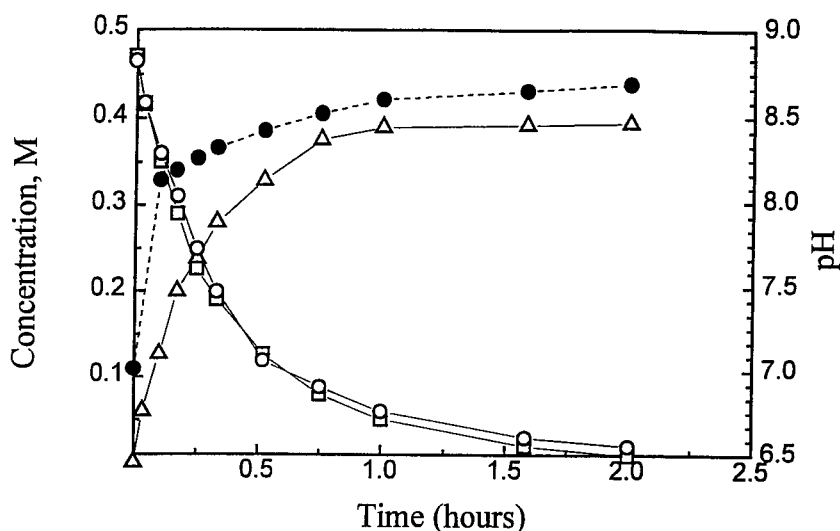
FIGURE 3. Batch biotransformation profile at 25 °C (initial TK concentration of 25 U/mL, 0.5 M hydroxypyruvate, and 0.5 M glycolaldehyde): pH (●) and adjusted concentrations of hydroxypyruvate (□), glycolaldehyde (○), and L-erythrulose (△) with time.
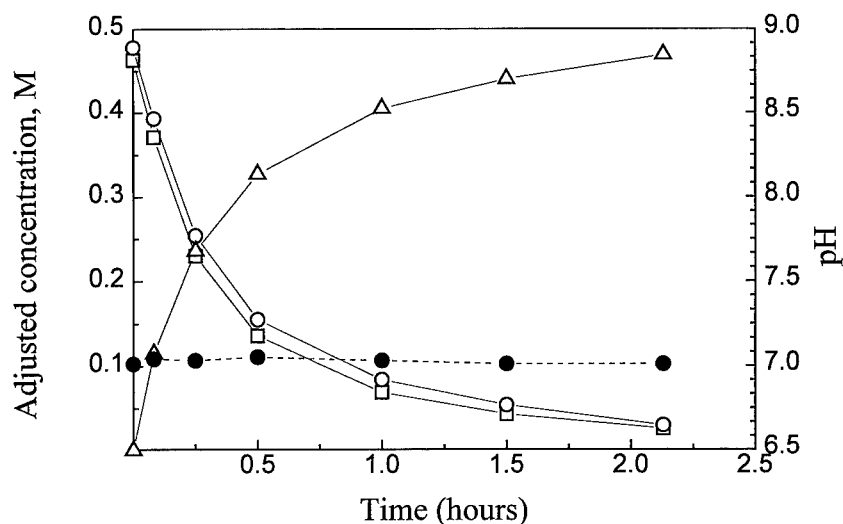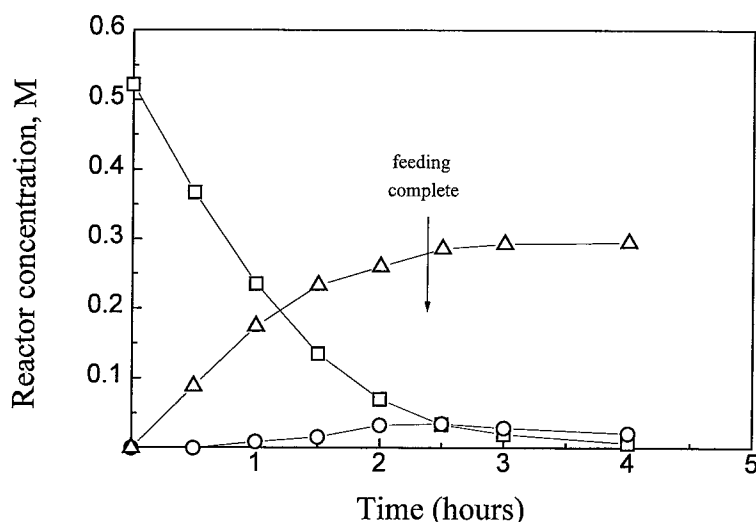
FIGURE 4. Batch biotransformation profile at 25 °C (initial TK concentration of 25 U/mL, 0.5 M hydroxypyruvate, and 0.5 M glycolaldehyde) and pH controlled to 7.0 with 1.0 M HCl: pH (●) and adjusted concentrations of hydroxypyruvate (□), glycolaldehyde (○), and L-erythrulose (△) with time.

mercaptoethanol) to prevent oxidative damage to the protein. At a glycolaldehyde concentration of 0.5 M, around 80% of the TK activity was lost in 6 hours. These results clearly indicate the need to maintain a low (<50 mM) concentration of glycolaldehyde within the reactor. Because the substrate is water-soluble, this can best be achieved by feeding to the reactor. Feeding an acidified substrate (pH 3.0) stream further reduces the dilution effect of HCl as a titrant. FIGURE 5 illustrates the reaction profile for a fed-batch biotransformation using a 1.25 M (pH 3.0) glycolaldehyde feed at 0.17 volume/initial volume/hour. In this way, the glycolaldehyde was maintained at a reactor concentration of less than 50 mM while yielding complete conversion to erythrulose. The figure gives the reactor concentration (i.e., diluted by titrant and feed). Using this strategy, the toxic effects of the glycolaldehyde may be avoided. However, the final concentration of product is still limited by the aqueous saturation concentration of the hydroxypyruvate (0.7 M). Given the dilution effect, this does not argue for feeding glycolaldehyde alone. Feeding of lithium hydroxypy-

TABLE 3. Effect of Glycolaldehyde Concentration on Transketolase Stability at 25 °C and pH 7.0 (in the Presence of 10 mM Mercaptoethanol)

Glycolaldehyde Concentration (mM)	Residual TK Activity after 6-h Incubation (%)
0	102
50	94
100	78
250	54
500	25

ruvate will be limited by aqueous solubility, but use of the free acid can overcome this constraint. This has the additional benefit of reduced salt formation due to a reduction in titrant and an absence of lithium ions. (The potassium salt has also been used, but the aqueous solubility is similar to that of the lithium salt.) FIGURE 6 illustrates the reaction profile for a hydroxypyruvate fed-batch reaction. Again, complete conversion was obtained. A further advantage of this approach is the ability that it gives to apply nonselective *in situ* product removal techniques. The separation *in situ* of hydroxypyruvate and erythrulose is particularly difficult, but feeding hydroxypyruvate eliminates this problem.

FIGURE 5. Fed-batch biotransformation profile at 25 °C (initial TK concentration of 25 U/mL, 0.5 M hydroxypyruvate) and pH controlled to 7.0 with 1.0 M HCl, fed at 0.17 vol/initial vol/h with 1.25 M (pH 3.0) glycolaldehyde: reactor concentrations of hydroxypyruvate (□), glycolaldehyde (○), and L-erythrulose (△) with time.

Feeding of the free hydroxypyruvic acid on demand as a titrant can also be used to exclude the use of HCl and may afford still higher product concentrations on account of reduced dilution. Consequently, feeding both substrates has clear advantages and a summary of the possible strategies to substrate feeding is given in TABLE 4.

DISCUSSION

In this paper, we have illustrated the use of a structured approach to design for reactor selection and operation for transketolase-catalyzed carbon-carbon bond synthesis. Qualitative judgments based on design data provided a clear logic for operation in a fed-batch stirred tank reactor, thus avoiding unnecessary research evaluating other reactor options.
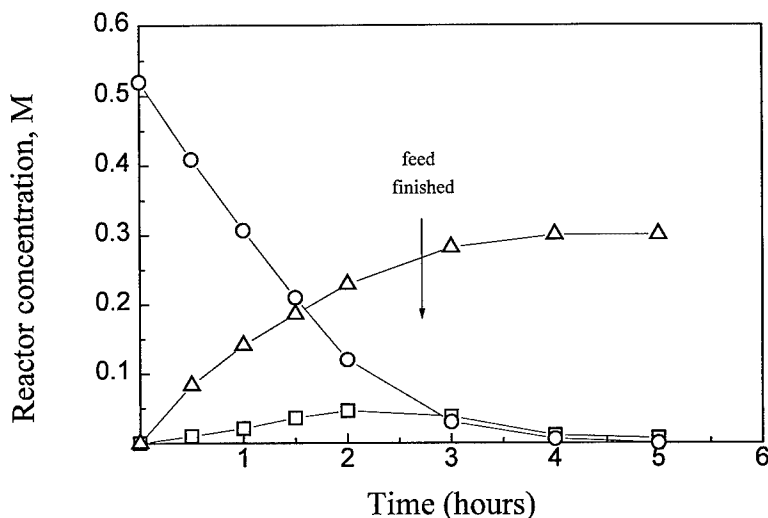
FIGURE 6. Fed-batch biotransformation profile at 25 °C (initial TK concentration of 22 U/mL, 0.5 M glycolaldehyde) and pH controlled to 7.0 with 1.0 M HCl, fed at 0.14 vol/initial vol/h with 1.25 M (pH 3.0) hydroxypyruvic acid: reactor concentrations of hydroxypyruvate (□), glycolaldehyde (○), and L-erythrulose (△) with time.

Characterization also provided data that set constraints for operation. Those that are biocatalyst-dependent will be common to all TK-catalyzed biotransformations. In addition, although the narrow operational pH is frequently quoted as a limitation of biocatalysis, in the case of the reaction example presented here it is the pH lability of both reactants and the product that provides an upper limit to operational pH. This limitation is a function of the concentration of the components as discussed and

TABLE 4. Limitations to Substrate Feeding to the Stirred Tank Reactor

Limiting Feature	Feeding Strategy[a]			
	No Feed (Batch)	One Feed		Two Feeds
		GA[b]	HPA[c]	
toxicity[d]	●		●	
solubility[e]	●	●		
titrant volume[f]	●	○	○	○
salt[g]	●	○	○	○
selective ISPR[h]	●	●		

[a]● = limitation for this strategy; ○ = partial limitation for this strategy.
[b]Glycolaldehyde (pH 3.0).
[c]Hydroxypyruvic acid (pH 3.0).
[d]Glycolaldehyde toxicity to TK.
[e]Solubility of hydroxypyruvate in solution.
[f]Volume of acid titrant to be added to maintain pH 7.0.
[g]Salt formation via the use of lithium hydroxypyruvate and HCl as titrant.
[h]In situ product removal.

is illustrated on the operational window of reactor aldehyde concentration versus reaction pH in FIGURE 7. The upper limits to aldehyde concentration and pH are both dependent on the specific reaction. This therefore provides a powerful tool to indicate the minimum data necessary for a new reaction system. This is particularly valuable where data on the enzyme and generic reaction features have already been assessed. The need to feed substrates is clear, but the optimization of feed rates, and indeed the feeding strategy, requires further evaluation and is the focus of current research. Many of the most useful aldehydes are poorly water-soluble and this also raises the possibility of feeding from a second, organic, phase. Such an approach has proved particularly successful in the conversion of toluene to toluene-*cis*-glycol by a blocked mutant of *P. putida*[26,27] alongside a fed-batch approach.[28]
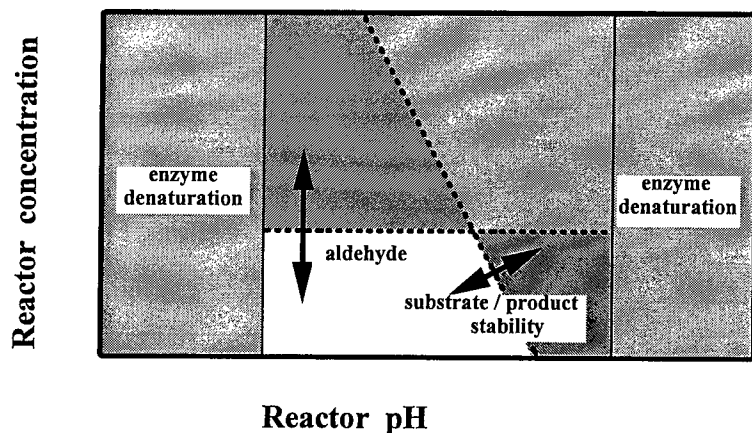
Reactor pH

FIGURE 7. Schematic reactor operational window giving guidance for aldehyde feeding and pH control.

CONCLUDING REMARKS

In this paper, the value of a structured approach to guide reactor selection and operation has been shown; the use of windows of operation[29] (FIGURE 7) to guide operational strategy has also been illustrated. There is a clear need for further improvement in reactor efficiency by optimization of feeding, enzyme immobilization, and the use of *in situ* product removal. This work is part of a larger program investigating the large-scale application of transketolase by extending the range of reactions catalyzed and looking for improvement in the biocatalyst via the use of X-ray structural knowledge and rDNA technology.[14]

REFERENCES

1. CHEETHAM, P. S. J. 1994. Case studies in applied biocatalysis—from ideas to products. *In* Applied Biocatalysis. J. M. S. Cabral, D. Best, L. Boross & J. Tramper, Eds.: 47–108. Harwood Academic. Chur, Switzerland.

2. WOODLEY, J. M. & M. D. LILLY. 1994. Biotransformation reactor selection and operation. *In* Applied Biocatalysis. J. M. S. Cabral, D. Best, L. Boross & J. Tramper, Eds.: 371–393. Harwood Academic. Chur, Switzerland.

3. WOODLEY, J. M., A. J. BRAZIER & M. D. LILLY. 1991. Lewis cell studies to determine reactor design data for two-liquid-phase bacterial and enzymic reactions. Biotechnol. Bioeng. **37:** 133–140.

4. WOODLEY, J. M. & M. D. LILLY. 1992. Process engineering of two-liquid-phase biocatalysis. *In* Biocatalysis in Non-conventional Media. J. Tramper, M. H. Vermue, H. H. Beeftink & U. von Stockar, Eds.: 147–154. Elsevier. Amsterdam/New York.

5. FREEMAN, A., J. M. WOODLEY & M. D. LILLY. 1993. *In-situ* product removal as a tool for bioprocessing. Bio/Technology **11:** 1007–1012.

6. RACKER, E. 1961. Transketolase. *In* The Enzymes. P. D. Boyer, H. Lardy & K. Myrboch, Eds.: 397–406. Academic Press. New York.

7. FRENCH, C. & J. M. WARD. 1995. Improved production and stability of *E. coli* recombinants expressing transketolase for large-scale biotransformation. Biotechnol. Lett. **17:** 247–252.

8. HOBBS, G. R., M. D. LILLY, N. J. TURNER, J. M. WARD & J. M. WOODLEY. 1994. Transketolase production for use as a catalyst for carbon-carbon bond formation. *In* Proceedings of the 1994 IChE Research Event, Rugby, p. 289–291.

9. HOBBS, G. R., M. D. LILLY, N. J. TURNER, J. M. WARD & J. M. WOODLEY. 1994. Development of transketolase as a catalyst for carbon-carbon bond formation. Prog. Biotechnol. **9:** 463–466.

10. HOBBS, G. R., R. K. MITRA, R. P. CHAUHAN, J. M. WOODLEY & M. D. LILLY. 1996. Enzyme-catalyzed carbon-carbon bond formation: large-scale production of *Escherichia coli* transketolase. J. Biotechnol. **45:** 173–179.

11. SRERE, P. A., J. R. COOPER, M. TABACHNICK & E. RACKER. 1958. The oxidation pentose phosphate cycle. I. Preparation of substrates and enzymes. Arch. Biochem. Biophys. **74:** 295–305.

12. HOBBS, G. R., M. D. LILLY, N. J. TURNER, J. M. WARD, A. J. WILLETTS & J. M. WOODLEY. 1993. Enzyme-catalysed carbon-carbon bond formation: use of transketolase from *Escherichia coli*. J. Chem. Soc. Perkin Trans. **I:** 165–166.

13. HOBBS, G. R., C. FRENCH, M. GYAMERAH, G. MORRIS, M. D. LILLY, N. J. TURNER, J. M. WARD, A. J. WILLETTS & J. M. WOODLEY. 1994. Development of a process for transketolase-catalysed carbon-carbon bond formation. *In* Proceedings of the 1994 IChE Research Event, Rugby, p. 247–249.

14. LILLY, M. D., R. CHAUHAN, C. FRENCH, M. GYAMERAH, G. R. HOBBS, A. HUMPHREY, M. ISUPOV, J. A. LITTLECHILD, R. K. MITRA, K. G. MORRIS, M. RUPPRECHT, N. J. TURNER, J. M. WARD, A. J. WILLETTS & J. M. WOODLEY. 1996. Carbon-carbon bond synthesis: the impact of rDNA technology on the production and use of *E. coli* transketolase. Ann. N.Y. Acad. Sci. **782:** 513–525.

15. MITRA, R. K. & J. M. WOODLEY. 1996. A useful assay for transketolase in asymmetric syntheses. Biotechnol. Tech. **10:** 167–172.

16. GYAMERAH, M., R. K. MITRA & A. J. WILLETTS. 1995 (September). Kinetics of overexpressed transketolase from *Escherichia coli* JM107/pQR700. Poster presentation at Biotrans '95, University of Warwick, United Kingdom.

17. MITRA, R. K., J. M. WOODLEY & M. D. LILLY. 1996. Transketolase-catalyzed carbon-carbon bond formation: biotransformation characterization for process evaluation and selection. Enzyme Microb. Technol. Submitted.

18. BROCKLEBANK, S. P., R. K. MITRA, J. M. WOODLEY & M. D. LILLY. 1996. Carbon-carbon bond synthesis: preparation and use of immobilized transketolase. This volume.

19. CHAUHAN, R. P., J. M. WOODLEY & L. W. POWELL. 1996. *In situ* product removal from *E. coli* transketolase-catalyzed biotransformations. This volume.

20. CHAUHAN, R. P., L. W. POWELL & J. M. WOODLEY. 1996. *In-situ* recovery of L-erythrulose from a transketolase-catalyzed reaction: evaluation of boron-based separations. Biotechnol. Bioeng. Submitted.

21. RUDD, D. F., G. J. POWERS & J. J. SIIROLA. 1973. Process Synthesis. Prentice–Hall. Englewood Cliffs, New Jersey.

22. HOBBS, G. R. 1994. The production and use of transketolase as a catalyst for carbon-carbon bond formation. Ph.D. thesis, University of London.

23. HEDRICK, J. L. & H. J. SALLACH. 1961. The metabolism of hydroxypyruvate: I. The nonenzymatic decarboxylation and autoxidation of hydroxypyruvate. J. Biol. Chem. **236:** 1867–1871.

24. DEMUYNCK, C., J. BOLTE, L. HECQUET & V. DALMAS. 1991. Enzyme-catalyzed synthesis of carbohydrates: synthetic potential of transketolase. Tetrahedron Lett. **32:** 5085–5088.

25. DALMAS, V. & C. DEMUYNCK. 1993. Study on the specificity of a spinach transketolase on achiral substrates. Tetrahedron Asymmetry **4:** 2383–2388.

26. BALLARD, D. G. H., A. J. BLACKER, J. M. WOODLEY & S. C. TAYLOR. 1994. Poly-phenylenes from biosynthetic *cis*-dihydroxycyclohexadiene. *In* Plastics from Microbes: Microbial Synthesis of Polymers and Polymer Precursors. D. P. Mobley, Ed.: 139–168. Hanser Pub. Munich/Vienna/New York.

27. COLLINS, A. M., J. M. WOODLEY & J. M. LIDDELL. 1995. Determination of reactor operation for the microbial hydroxylation of toluene in a two-liquid-phase process. J. Ind. Microbiol. **14:** 382–388.

28. HACK, C. J. 1992. Biochemical engineering studies of *cis*-glycol production. Ph.D. thesis, University of London.

29. WOODLEY, J. M. & N. J. TITCHENER-HOOKER. 1996. The use of windows of operation as a bioprocess design tool. Bioprocess Eng. **14:** 263–268.

Solubilization of Enzymes in Apolar Solvents via Noncovalent Complex Formation with Soluble Polymers[a]

BO MATTIASSON, MARINA OTAMIRI,
AND PATRICK ADLERCREUTZ

Department of Biotechnology
Center for Chemistry and Chemical Engineering
Lund University
S-221 00 Lund, Sweden

Operating enzyme catalysis in apolar organic solvents is associated with certain constraints. Good control of water activity in such systems has been demonstrated to be essential.[1,2] Several measures to control water activity (A_w) have been presented.[3-5] However, it may also be possible to make the system more robust against small variations in A_w. Hydrophilic substances added to the reaction medium have proven useful as buffering agents. They either can get involved with the catalyst phase[6,7] or are added to the reaction medium.[8] In a previous study, we demonstrated the versatility of adding ethyl cellulose (EC) to a solvent phase when carrying out catalysis with solid-phase catalysts.[8] From FIGURE 1, it is seen that the EC-containing system is substantially more tolerant towards variations in water content. Thus, the enzyme activity is stabilized as compared to when operating without ethyl cellulose. Heterogeneous catalysis is often characterized by mass-transfer problems and also by the properties of the support affecting the catalytic process.[9,10] It would therefore be of interest to evaluate the possibility to combine the EC presence in the reaction solvent with elimination of the solid support. Such a soluble enzyme system has earlier been reported when covalently modifying enzyme with PEG.[11,12] However, such a covalent modification is always associated with a loss of enzyme functionality and sometimes also activity. The idea of forming noncovalent complexes between a protein and a polymer is in essence similar to depositing a protein on a solid support for later use in apolar organic solvents. Aggregation between the proteins and polymer chains will be energetically favorable as the polymer will shield the polar proteins from direct contact with the apolar solvent. The ability of a solvent to dissolve a polymer can be seen from the solubility parameters (TABLE 1). It is empirically found that a difference between the polymer and a solvent in solubility parameter of max 3.5–4 is acceptable; otherwise, the polymer will not dissolve.[13] Therefore, many of the polymers listed are not compatible with water, but are compatible with other solvents, including ethanol (see TABLE 1).
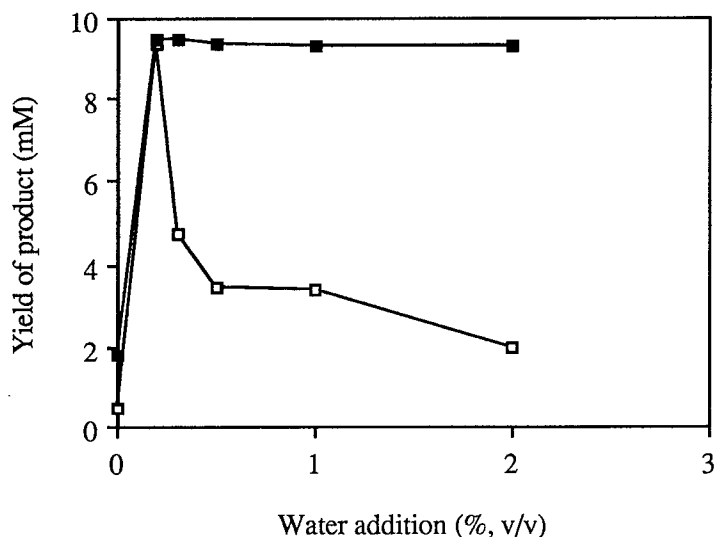
446

FIGURE 1. Yield of product after 24 h of reaction time with various water additions using chymotrypsin immobilized on celite in ester synthesis: (■) in toluene containing 4% (w/w) EC; (□) in toluene.

PREPARATION AND CHARACTERIZATION
OF NONCOVALENT COMPLEXES

EC was preswollen in ethanol and then added to an aqueous solution of chymotrypsin (CT). The buffer strength of the solution was shown to be of importance for the outcome of the process. More stable and active complexes were formed by using solutions with higher buffer salt content. After proper mixing, the water was

TABLE 1. Solubility Parameters of Solvents and Polymers

Solvents	δ^a	Polymers	δ^b
1,1,1-Trichloroethane	8.63	Polyvinyl butyral (PVB)	8.14
Toluene	9.09	Ethyl cellulose (EC)	9.05
Chloroform	9.26	Polystyrene (PS)	9.59
Benzene	9.29	Polyethylene glycol (PEG)	10.64
2-Butanone	9.55	Polyvinyl methyl ketone (PVMK)	11.31
Ethyl acetate	9.64	Polymethyl methacrylate (PMM)	12.70
Ethanol	12.47		
Water	23.43		

[a]Values were calculated from the expression, $\delta = [d(\Delta H_v - RT)/M]^{0.5}$ (cal-cm^{-3})$^{0.5}$, where d is the density, ΔH_v is the molar heat of vaporization, and M is the molecular weight, which were taken from the *Handbook of Chemistry and Physics (65th edition)*; $R = 1.99$ cal/(K-mol) and $T = 298$ K.

[b]Values were calculated using Small's expression, $\delta = d\Sigma G/M$ (cal-cm^{-3})$^{0.5}$. G and M are the molar attraction constant and the molecular weight of monomer groups, respectively. The values of G were taken from the *Handbook of Chemistry and Physics (65th edition)*.

removed by lyophilization. The lyophilized powder obtained was soluble in the apolar organic solvents (chloroform, toluene, benzene, etc.), yielding optically clear solutions. Filtration of mixtures consisting of EC and protein (^{14}C-labeled albumin) was carried out using a Durapore membrane with pores of diameters of 5 μm. When EC was not present, the dispersion of the protein was not stable and with time the protein aggregated into large complexes that precipitated. In the presence of EC, EC-albumin complexes that were small enough to pass the membrane were formed. It is thus obvious that EC helps to keep the protein in solution. Further studies in this direction using light scattering gave similar results, demonstrating that complexes were being formed.[14] When only EC was present, no such complexes were observed; when only chymotrypsin was present, big lumps were found as described above. It can thus be concluded that CT-EC, when lyophilized from an aqueous buffer solution, generates complexes that are soluble in apolar organic solvents.

STABILITY OF COMPLEXES

The molecular stability was investigated using differential scanning calorimetry (DSC).[15] When pure CT was added to toluene, it was not possible to detect any transition by raising the temperature to almost 100 °C. On addition of water, 1% and 2% (v/v), transition peaks were observed at 75 °C and 59 °C, respectively. The greater the amount of water that was added, the lower was the transition temperature. With the addition of CT to a 10% (w/w) EC solution in toluene containing 2% (v/v) water, a stabilization of $\Delta T_d = 15$ °C compared to the system without EC was obtained. The preformed complexes showed an even higher stabilization. TABLE 2 shows the temperature of denaturation for enzyme in native and complexed forms in different media. Complex formation between an enzyme and a soluble polymer was mainly studied with respect to chymotrypsin.[16] The studies, however, have been expanded to also cover horse liver alcohol dehydrogenase and lipases. The trends are the same: a better performance for the soluble enzyme complexes as compared to that of both immobilized/deposited enzymes and solid enzyme particles dispersed in the medium.

TABLE 2. Temperature of Denaturation (T_d) of Native and Complexed CT in Different Media and of Native Enzyme in Toluene Containing Different Amounts of EC

Medium	T_d (°C)
Water	54
Water containing 20% (w/w) PEG	62
Toluene containing 2% (v/v) water	59
Toluene containing 2% (v/v) water and 4% (w/w) EC	66
Toluene containing 2% (v/v) water and 10% (w/w) EC	76
Toluene containing 2% (v/v) water and 20% (w/w) EC	82
EC-CT containing 5% (w/w) EC in toluene with 2% (v/v) water	82

TABLE 3. Comparison of Activities of Native CT and CT-EC Complex in Ester Synthesis in Toluene

	Initial Reaction Rate (μmol-mg^{-1}-min^{-1})		
	Water Addition (% v/v)		
System	0.2	0.5	1.0
CT in toluene	0.004	0.002	0.000
CT in EC/toluene	0.009	0.014	0.008
CT-EC in toluene	0.019	0.021	0.026

ACTIVITY OF COMPLEXES

Catalytic properties of the preparations were evaluated and compared to systems without EC or to a system where EC was directly dissolved and the enzyme was added afterwards. The initial reaction rates are shown in TABLE 3. The kinetic behavior of these systems has been adequately described elsewhere.[14] The solubility parameter turned out to be a useful parameter when evaluating the suitability of a certain polymer for carrying out biocatalysis. FIGURES 2a and 2b show the relation between the initial reaction rate and the solubility parameter of different organic solvents and different polymers used as complexing agents to CT in chloroform, respectively. Besides demonstrating the usefulness of the solubility parameter, the figures also indicate that polymers other than EC may be used. There are, however, differences in the ability of the polymers to interact with the proteins. Consequently, it may be stated that both less-polar solvents and polymers are needed to enhance the activity of enzymes. When using a mixture of polymers, for example, EC and PS, it was shown that the enzyme preferred EC-phase, even if CT-PS complexes were formed prior to the addition to EC–organic solvent solution.[13]

POLYMER TWO-PHASE SYSTEMS AND RECOVERY
OF PRODUCT AND ENZYME

When dissolving two polymers in a common organic solvent, incompatibility may occur and, above certain concentrations, phase separation leads to formation of a polymer-polymer two-phase system.[17] FIGURE 3 shows a phase diagram for polystyrene–ethyl cellulose in chloroform. The diagram is constructed using the continuous dilution method,[18] which gives the two conditions when phase separation starts to form until a completely turbid solution is obtained. From similar studies involving bioconversions in aqueous two-phase systems, it is demonstrated that the use of such systems is especially attractive when substrate or product inhibition is prevalent.[19] In the systems studied here, substrate inhibition was observed (see TABLE 4) and it is also well known that when dealing with reversal of hydrolytic processes it is always advantageous to remove the product *in situ*. TABLE 5 lists the partition constants for substrate and product for a PS-PVB system. The favorable factor from the results shown in the table is the extreme partitioning of the components. Substrate and product are partitioning close to 1 and, in order to influence the extraction of
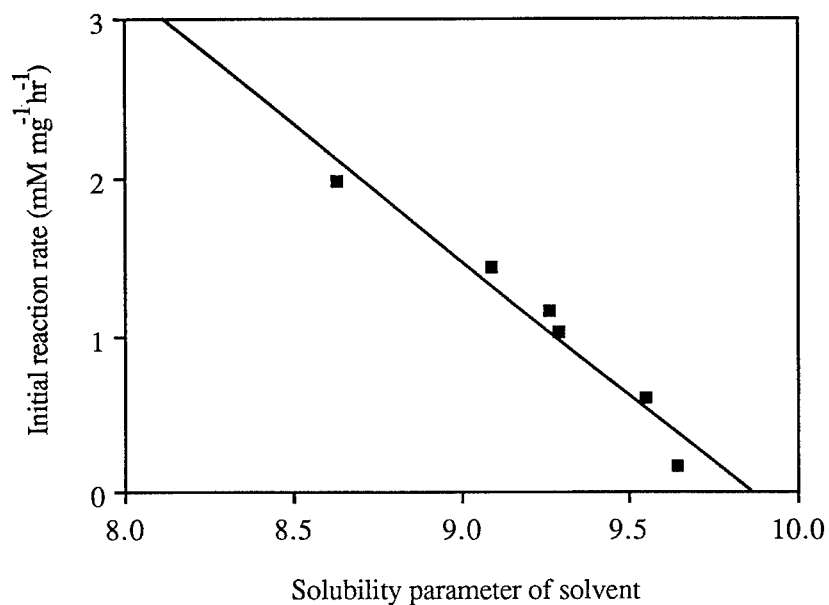
FIGURE 2a. Dependence of the reaction rate for the EC-CT complex on the solubility parameter of different solvents.
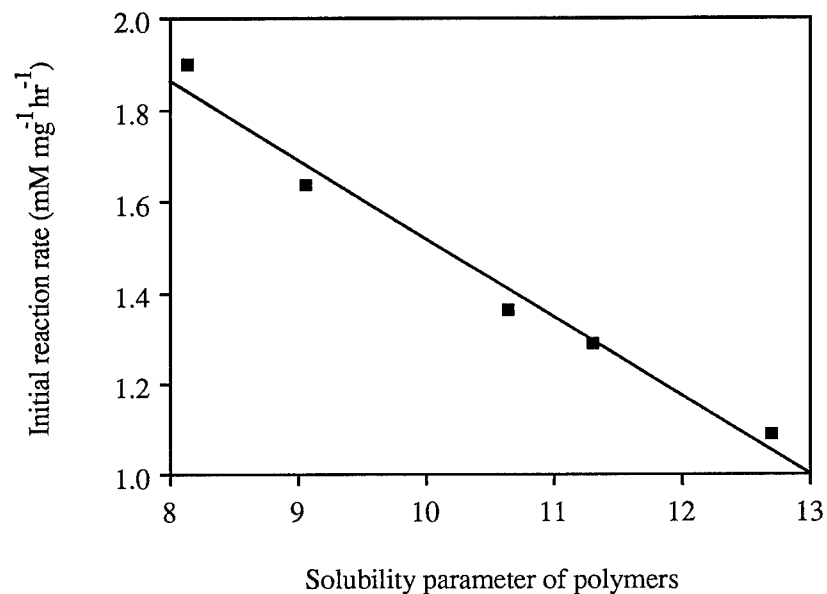

FIGURE 2b. Dependence of the reaction rate for polymer-CT complexes in chloroform on the solubility parameter of different polymers (PVB, EC, PEG, PVMK, and PMM) used for the preparation of complexes.
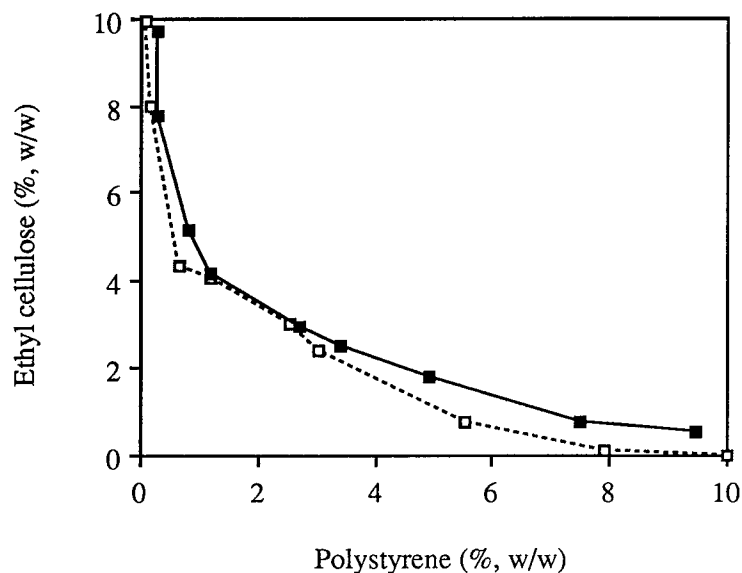
FIGURE 3. Phase diagram for the PS-EC two-phase system in chloroform with the beginning (□) and end (■) of the transition from a one- to two-phase system.

product, one has to manipulate the phase-volume ratios. By doing so, it is possible to extract most of the product formed from the biocatalytic phase (see TABLE 5).

It has been argued that operating with soluble enzymes in organic solvents may solve some problems; however, more are created, such as separation problems, contamination of the product stream, etc. The two-phase concept keeps the enzyme in one phase to >99.5% and processing of the other phase turns out to be quite straightforward. Dilution in three volumes of methanol caused an almost quantitative precipitation of the polymer, and the product was recovered from the supernatant in good yields. Recovery of the enzyme from the biocatalyst-rich phase is also accomplished by addition of a volume of buffer that causes formation of a separate

TABLE 4. Activity at Substrate Concentrations of 20 mM and 100 mM for Native CT in Chloroform and for Complexed CT in Different Polymer Two-Phase Systems in Chloroform

	Initial Reaction Rate (μmol·mg^{-1}·min^{-1})		
	Substrate Concentration (mM)		Inhibition Constant
System	20	100	(K_I) (mM)
Chloroform	0.009	0.003	71
PVMK-PS/chloroform	0.034	0.022	117
PVB-PS/chloroform	0.042	0.030	281
PMM-PS/chloroform	0.071	0.053	256
EC-PS/chloroform	0.073	0.048	167
PEG-PS/chloroform	0.071	0.042	106

TABLE 5. Partition of Product and Substrate in PVB-PS Two-Phase Systems in Chloroform

PS:PVB	V_t/V_b		$K_p{}^a$		X^b (% w/w)	
(%:% w/w)	Product	Substrate	Product	Substrate	Product	Substrate
5:5	0.8	—	0.80	—	37	—
8:2	2.5	—	0.79	—	67	—
9:1	7.4	9.8	0.86	0.31	86	76
9.2:0.8	15.8	—	0.99	—	94	—

^{a}Partition coefficient (K_p) expressed as C_t/C_b (t = top; b = bottom).
^{b}Amount of compound in the PS-rich top phase expressed as $X = 100(C_tV_t)/(C_tV_t + C_bV_b)$.

phase where the protein partitions, but not the polymer. Studies have indicated >99% recovery in this step based on protein content and almost equally efficient recovery of the enzymatic activity.[14]

It can be concluded that the formation of noncovalent complexes between enzymes and soluble polymers seems to offer interesting possibilities with regard to molecular properties of the biocatalyst as well as from a bioprocess engineering point of view.

REFERENCES

1. HALLING, P. J. 1984. Effects of water on equilibria catalyzed by hydrolytic enzymes in biphasic reaction systems. Enzyme Microb. Technol. **6:** 513–516.
2. SVENSSON, I., E. WEHTJE, P. ADLERCREUTZ & B. MATTIASSON. 1994. Effects of water activity on reaction rates and equilibrium positions in enzymatic esterifications. Biotechnol. Bioeng. **44:** 549–556.
3. CASSELS, J. & P. J. HALLING. 1988. Effect of thermodynamic water activity on thermolysin-catalyzed peptide synthesis in organic two-phase systems. Enzyme Microb. Technol. **10:** 486–491.
4. KUHL, P. & P. HALLING. 1991. Salt hydrates buffer water activity during chymotrypsin-catalyzed peptide synthesis. Biochim. Biophys. Acta **1078:** 326–328.
5. WEHTJE, E., I. SVENSSON, P. ADLERCREUTZ & B. MATTIASSON. 1993. Continuous control of water activity during biocatalysis in organic media. Biotechnol. Tech. **7:** 873–878.
6. ÖSTE-TRIANTAFYLLOU, A., E. WEHTJE, P. ADLERCREUTZ & B. MATTIASSON. 1995. Effects of sorbitol addition on the action of free and immobilized hydrolytic enzymes in organic media. Biotechnol. Bioeng. **45:** 406–414.
7. WEHTJE, E., P. ADLERCREUTZ & B. MATTIASSON. 1993. Improved activity retention of enzymes deposited on solid supports. Biotechnol. Bioeng. **41:** 171–178.
8. OTAMIRI, M., P. ADLERCREUTZ & B. MATTIASSON. 1991. Effects on ester synthesis in toluene by immobilized chymotrypsin by addition of polymers to reaction medium. Biotechnol. Appl. Biochem. **13:** 54–64.
9. RESLOW, M., P. ADLERCREUTZ & B. MATTIASSON. 1988. On the importance of the support material for bioorganic synthesis: influence of water partition between solvent, enzyme, and solid support in water-poor media. Eur. J. Biochem. **172:** 573–578.
10. ADLERCREUTZ, P. 1991. On the importance of the support material for enzymatic reactions in organic media. Eur. J. Biochem. **199:** 609–614.
11. MATSUSHIMA, A., M. OKADA & Y. INADA. 1984. Chymotrypsin modified with polyethylene glycol catalyzed peptide synthesis in benzene. FEBS Lett. **178:** 275–277.
12. LJUNGER, G., P. ADLERCREUTZ & B. MATTIASSON. 1993. Reaction catalyzed by PEG-modified α-chymotrypsin in organic solvents: influence of water content and degree of modification. Biocatalysis **7:** 279–288.

13. OTAMIRI, M. 1994. Application of polymers in enzyme catalysis in organic solvents. Ph.D. thesis, University of Lund.
14. OTAMIRI, M., P. ADLERCREUTZ & B. MATTIASSON. 1992. Complex formation between chymotrypsin and ethyl cellulose and its reactivity in ester synthesis in toluene. Biocatalysis **6:** 291–305.
15. OTAMIRI, M., P. ADLERCREUTZ & B. MATTIASSON. 1994. A differential scanning calorimetric study of chymotrypsin in the presence of added polymers. Biotechnol. Bioeng. **44:** 73–78.
16. VIRTO, C., I. SVENSSON, P. ADLERCREUTZ & B. MATTIASSON. 1995. Catalytic activity of noncovalent complexes of horse liver alcohol dehydrogenase, NAD^+, and polymers, dissolved or suspended in organic solvents. Biotechnol. Lett. **17:** 877–882.
17. OTAMIRI, M., P. ADLERCREUTZ & B. MATTIASSON. 1994. Polymer-polymer organic two-phase systems—a new type of reaction media for bioorganic synthesis. Biotechnol. Bioeng. **43:** 987–994.
18. LARSSON, M. & B. MATTIASSON. 1988. Characterization of aqueous two-phase systems based on polydisperse phase–forming polymers: enzymatic hydrolysis of starch in a PEG-starch aqueous two-phase system. Biotechnol. Bioeng. **31:** 979–983.
19. HAHN-HÄGERDAL, B., B. MATTIASSON, E. ANDERSSON & P-Å. ALBERTSSON. 1982. Soluble temporarily immobilized biocatalysts. J. Chem. Technol. Biotechnol. **32:** 157–161.

Purification of Urokinase by Affinity Cross-flow Filtration Using a Water-soluble Macroligand[a]

XUE JUN CAO,[b] JIA WEN ZHU,[b] DA WEI WANG,[b]
XING YAN WU,[c] AND GAN CE DAI[b,d]

[b]Chemical Engineering Research Center
[c]Department of Biochemical Engineering
East China University of Science and Technology
Shanghai 200237, People's Republic of China

INTRODUCTION

As a newly developed bioseparation technique, affinity cross-flow filtration combines affinity interaction and membrane separation, having the advantages of high selectivity and high throughput inherent to the respective individual processes. Within the last decade, a number of related papers have been published.[1-14] In some cases, dextran was used as the soluble macroligand to purify the target protein, but no satisfactory results were obtained.[12-14] We synthesized water-soluble macroligand using dextran T2000 as matrix, epichlorohydrin as activator and cross-linker, and p-aminobenzamidine (p-AB) as ligand to purify urokinase (UK), yielding good results. The preparation strategy was as follows: dextran was activated by epichlorohydrin and reacted with ammonia solution, forming a terminal primary amine; the latter reacted with succinic anhydride, creating new carboxyl terminals; finally, it was coupled with p-AB in the presence of N-ethyl-N'-(3-dimethylaminopropyl)-carbodiimide hydrochloride (EDC), forming the macroligand (FIGURE 1).

EXPERIMENTAL PROCEDURES

Materials

Glu-Gly-Arg 7-amido-4-methylcoumarin (GGA-MCA) and p-AB were purchased from Sigma; EDC was from Merck; dextran T2000 was from Pharmacia; UK standard was from the National Institute of Control for Pharmaceutical and Biological Products, Beijing; and crude urokinase was from the Biochemical Laboratory at the Shanghai Institute of Pharmaceutical Industry. Epichlorohydrin, succinic anhydride, and other chemicals were of analytical reagent grade.

[d]To whom all correspondence should be addressed.

Equipment

The fluorospectrophotometer (model F950) was made by the Shanghai No. 3 Analytical Instruments Factory. The UV-vis spectrophotometer (model M750) was made by the Tai-Zhou Radio-Instruments Factory in Jiangsu province. The hollow-fiber ultrafilter with 100,000-MWCO membrane was made by the Tianjin Institute of Textile Industry. The pellicon cassette system (with 5000-MWCO membrane) was kindly provided by the Millipore Corporation.

Assay Methods

UK activity was determined by the fluorometric method.[15] Protein concentration was determined by UV absorbancy at 280 nm. The *p*-AB ligand density of the macrocarrier was determined by measuring the absorbancy at 292 nm before and

FIGURE 1. Reaction sequence for the preparation of the affinity macroligand.
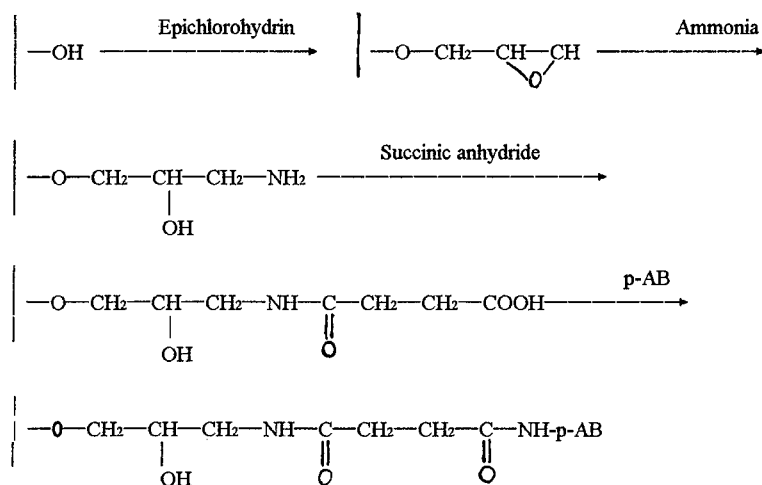
after the coupling reaction (*p*-AB exhibits a strong absorption at this wavelength with $E_{1cm}^{1\%} = 800$).[13] The complete conversion of the amino group to a carboxyl group during the succinic anhydride step was checked by the ninhydrin test.[16] Dextran T2000 concentration was determined by the polarimetric method ($[\alpha]_D^{25} = +199°$).

Preparation of Affinity Macroligand

First, 2.0 g dextran T2000 and 0.8 g NaOH were dissolved in 50 mL of water, to which 2.0 mL of epichlorohydrin was added. The solution was kept at 40 °C with mixing for 2 h. The epoxy-activated dextran was precipitated out by ethanol addition. The precipitate was dissolved in concentrated ammonia solution and kept at 40 °C

with mixing for 3 h. The residual ammonia was removed by heating. After cooling to room temperature, 2.5 g succinic anhydride was added gradually, with the pH maintained at 6.0 by adding solid NaOH. Then, the solution was allowed to stand for 5 h and the residual low-molecular-weight reagent was ultrafiltrated off. The retentate solution was added with 100 mg p-AB and 150 mg EDC, maintained at room temperature with the pH adjusted in the range of 4.0–4.5 for 12 h, and finally ultrafiltrated to remove residual reagents.

Determination of the Optimum Adsorption Conditions

First, 200 mL of 0.25% (w/v) affinity macroligand solution was added with phosphates, NaCl, and crude urokinase, resulting in 0.05 M phosphate, 0.4 M NaCl, and 5000 IU/mL UK. The solution was adjusted to pH 7.0 and ultrafiltrated with the hollow-fiber system under total recycling condition. When equilibrium was attained, the UK concentration in the permeate was measured. The experiment was repeated at other pH values: 7.2, 7.5, 7.8, and 8.0.

Second, salt concentration experiments were conducted in a similar way, with the exception that the pH was kept constant at 7.5, with varied NaCl concentrations of 0.1, 0.2, 0.3, 0.4, and 0.5 M.

Measurement of Rejection

First, a 200-mL solution containing either 0.5 g dextran T2000 or 0.5 g affinity macroligand was ultrafiltrated by the hollow-fiber system under total recycling condition. The concentrations of the permeate and retentate were then separately measured.

Second, a 200-mL enzyme solution of 2000 IU/mL urokinase at pH 7.5 containing 0.05 M phosphate and 0.4 M NaCl was likewise ultrafiltrated. Then, the enzyme concentrations both in the permeate and in the retentate were measured.

Affinity Ultrafiltration for Purification of Urokinase

A similar urokinase solution, but with a concentration of 4000 IU/mL, was ultrafiltered until equilibrium was reached. It was then diafiltrated with the same buffer until the A_{280} dropped to zero. Then, a 0.1 M acetate buffer (containing 0.5 M NaCl) at pH 4.0 was added to elute the UK. The eluate was concentrated by the pellicon cassette system. Enzyme and protein concentrations in the retentate were determined.

RESULTS AND DISCUSSION

Affinity Macroligand

The epichlorohydrin-activated dextran can be directly coupled with p-AB, but the reactivity is low, requiring an excess amount of p-AB. To overcome this

disadvantage, we separated the activated dextran by ethanol precipitation and via amination, succinic anhydride carboxylation, and p-AB coupling to get the affinity macroligand. Because many steps were involved, the yield was inevitably low, about 50%. The ligand density of the macroligand was determined as 1.2 μmol/mg dextran, implying roughly one molecule of p-AB for every ten molecules of glucose. The density might be too high, leading to steric hindrance.
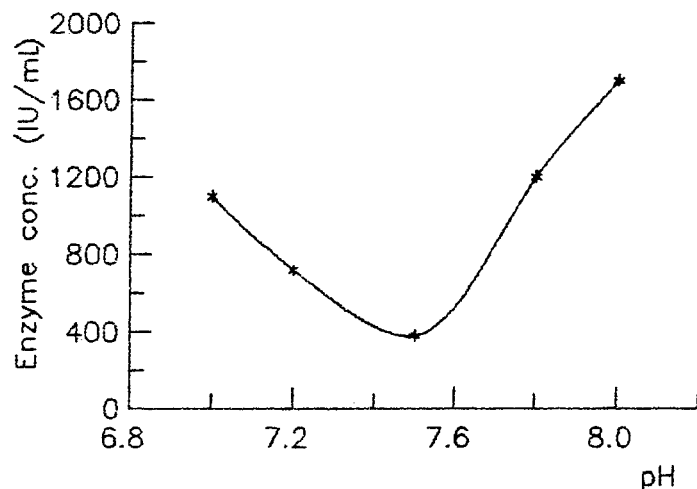
FIGURE 2. Comparison of the adsorption at different pH values. The ordinate denotes the residual enzyme concentration in the permeate in equilibrium.

Optimum Conditions for Adsorption

FIGURE 2 shows the remaining urokinase concentration versus pH, indicating an optimum pH at 7.5. Likewise, FIGURE 3 shows that the optimum NaCl concentration was 0.4 M.

Rejection Characteristic of 100,000-MWCO Membrane

TABLE 1 shows the rejection coefficients of dextran, p-AB–dextran, and urokinase. Dextran T2000, having a nominal molecular weight of 2×10^6, that is, 20 times greater than the membrane MWCO, still could pass the membrane in some degree due to its linear structure. With extensive diafiltration washing, all of the dextran might be lost. Epichlorohydrin, as a bifunctional reagent, when reacting with dextran could cause some cross-linking in addition to activation. Consequently, the rejection coefficient of the affinity macroligand increased to over 99.5%, indicating the salient advantage of epichlorohydrin activation. TABLE 1 also shows no rejection to urokinase, verifying the applicability of the membrane.
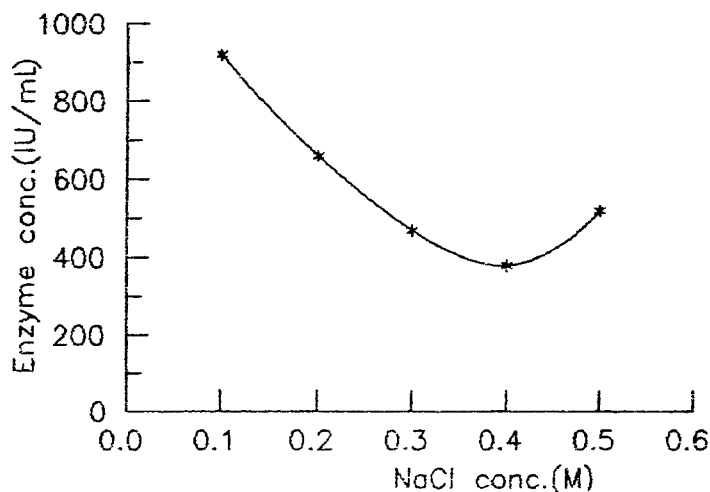
FIGURE 3. Comparison of the adsorption at different NaCl concentrations. The ordinate denotes the residual enzyme concentration in the permeate in equilibrium.

Affinity Ultrafiltration for Purification of Urokinase

The purification results are shown in TABLE 2. The yield is somewhat lower because, during diafiltration, a greater volume of washing buffer was used as compared with conventional chromatography. The purification factor reached as high as 112, indicating that the macroligand selectivity for urokinase was quite good. This was in contradiction to the prevailing view that dextran is not suitable for affinity matrix due to its high nonspecific adsorption. Moreover, dextran is widely used as a plasma expander for humans and therefore can be safely used in the purification of drugs.

CONCLUSIONS

The dextran-based water-soluble macroligand is most suitable for cross-flow ultrafiltration, with unexpected lower nonspecific adsorption. Activation of dextran with epichlorohydrin had the advantage of a simultaneous cross-linking effect, allowing the dextran-based macroligand to be almost completely retained by the membrane and being especially useful in the production of drugs due to its biocompatibility.

The proposed method is feasible for urokinase purification, with an 82% yield and a purification factor of 112.

TABLE 1. Rejection Characteristics of 100,000-MWCO Membrane

	Dextran T2000	p-AB–Dextran T2000	Urokinase
Rejection (%)	87.8	99.5	0

TABLE 2. Affinity Ultrafiltration Purification of Urokinase

Macroligand	Purification Factor	Recovery (%)	Specific Activity (IU/A_{280})
p-AB–Dextran T2000	112	82	56,000

ACKNOWLEDGMENTS

REFERENCES

1. MATTIASSON, B. & M. RAMSTORP. 1984. Ultrafiltration affinity purification isolation of concanavalin A from seeds of *Canavalia ensiformis*. J. Chromatogr. **283:** 323–330.
2. MATTIASSON, B. & G. I. L. TORBJORN. 1986. Ultrafiltration affinity purification. *In* Membrane Separations in Biotechnology. W. C. McGregor, Ed.: 99–114. Dekker. New York.
3. NOUBAR, B. A., F. G. NEAL & L. C. CHARLES. 1989. Mathematical modelling of the continuous affinity-recycle extraction purification technique. J. Chromatogr. **478:** 1–19.
4. HERAK, D. C. & E. M. MERRIL. 1990. Affinity cross-flow filtration: some new aspects. Biotechnol. Prog. **6:** 33–40.
5. POWERS, J. D., P. K. KILPATRICK & R. G. B. CARBONELL. 1989. Biotechnol. Bioeng. **33:** 173–182.
6. LING, T. G. I. & B. MATTIASSON. 1989. Membrane filtration affinity purification (MFAP) of dehydrogenases using Cibacron Blue. Biotechnol. Bioeng. **34:** 1321–1325.
7. MALE, K. B., J. H. T. LUONG & A. L. NGUYEN. 1987. Studies on the application of a newly synthesized polymer for trypsin purification. Enzyme Microb. Technol. **9**(6): 374–378.
8. LUONG, J. H. T., K. B. MALE & A. L. NGUYEN. 1988. Syntheses and characterization of a water-soluble affinity polymer for trypsin purification. Biotechnol. Bioeng. **31:** 439–446.
9. LUONG, J. H. T., K. B. MALE & A. L. NGUYEN. 1988. A continuous affinity ultrafiltration process for trypsin purification. Biotechnol. Bioeng. **31:** 516–520.
10. MALE, K. B., A. L. NGUYEN & J. H. T. LUONG. 1990. Isolation of urokinase by affinity ultrafiltration. Biotechnol. Bioeng. **35:** 87–93.
11. FISHER, R. R., B. MACHIELS, K. C. KYRIACOU & J. E. MORRIS. 1989. Affinity ultrafiltration and affinity precipitation using a water-soluble complex of poly(vinyl alcohol) and Cibacron Blue F3GA. *In* Protein-Dye Interactions: Developments and Applications. M. A. Vijayalakshmi & O. Bertrand, Eds.: 190–196. Elsevier. Amsterdam/New York.
12. HUBERT, P. & E. DELLACHERIE. 1980. Use of water-soluble biospecific polymers for the purification of proteins. J. Chromatogr. **184:** 325–333.
13. DOMINIQUE, A. M., Q. T. NGUYEN & E. DELLACHERIE. 1981. Biospecific ultrafiltration: a promising purification technique for proteins? J. Membr. Sci. **9:** 337–342.
14. CHOE, T. B., P. MASSE & A. VERDIER. 1986. Separation of trypsin from trypsin/α-chymotrypsin mixture by affinity ultrafiltration. Biotechnol. Lett. **8:** 163–168.
15. MORITA, T., H. KATO, S. IWANAGA, K. TAKADA, T. KIMURA & S. SAKAKIBARA. 1977. New fluorogenic substrates for α-thrombin, factor Xa, kallikreins, and urokinase. J. Biochem. **82:** 1495–1498.
16. MEI, J. S. 1992. Ninhydrin test. *In* Organic and Analytical Chemistry. Higher Educational Publisher. Beijing.

Odor Removal from Amerhold DR-25
by Hydrolysis of Ethyl Propionate
Using Enzyme Catalysts

KEVIN A. DiGREGORIO

Union Carbide Corporation
Technical Center
South Charleston, West Virginia 25303

INTRODUCTION

Union Carbide Corporation and its subsidiary, Amerchol Corporation, have developed a water-based, latex resin (Amerhold DR-25) for aqueous hair spray formulations.[1] Current commercial formulations contain ethanol as a carrier, but replacing ethanol with water provides significant environmental, safety, and economic advantages. However, most latexes and similar materials contain residual monomers, some benign and some that impart an unpleasant odor. Amerhold DR-25 contains 70–120 ppm ethyl propionate (EP), the source of a residual odor. EP contamination comes from ethyl acrylate (EA), a monomer used to make the latex, and EP levels must be reduced to <20 ppm and preferably to 0 ppm for personal-care use.

We can use enzymes to hydrolyze EP, either by pretreating the feed (EA) or by posttreating the latex, and can effectively remove the odor. Pretreatment requires enzyme-catalyzed hydrolysis in an organic phase (EA), whereas posttreatment is carried out in an aqueous phase (the latex particles are suspended in water). The chemistry, showing the desired selective hydrolysis of EP in bulk EA, is given in FIGURE 1. The resulting propionic acid and ethanol are benign.

To posttreat the latex, we need highly active, but not highly selective, enzymes. To pretreat EA, we also need high selectivity for EP over EA. Several investigators have shown high selectivity in similar situations for compounds having only slight structural differences using enzymes in hydrolyses, esterifications, and transesterifications.[2–6] For example, Miller *et al.*[5] observed large differences in reaction rates among saturated and unsaturated C_6 acids esterified with octanol, and Imperial Chemicals[6] published a patent application that discloses the removal of unsaturated monomers (alkyl acrylates and methacrylates) from polymer dispersions using enzyme-catalyzed hydrolysis.

Thus, we screened 43 enzymes for the hydrolysis of EP either in bulk EA or in the water-based latex. We then used the best enzymes to develop a commercial process to hydrolyze and remove EP—and the residual odor—from Amerhold DR-25.

RESULTS AND DISCUSSION

The 43 enzyme catalysts screened for EP hydrolysis in either EA or the latex are listed in TABLE 1. After the screening, the best enzymes were used to pretreat the

feed in biphasic mixtures or to posttreat the latex using continuous and batch reactors.

Pretreating the Feedstock

Enzyme Screening

We screened 38 enzymes using mixtures of 9:1 EA:EP (by weight) saturated with H_2O (~ 1 wt%). To compare activity, we measured the production of propionic acid and acrylic acid (from EA hydrolysis). To compare selectivity for EP over EA hydrolysis, we determined the relative yield of propionic versus acrylic acid. Enzymes showing moderate to very good activity are listed in TABLE 2. L-1754, Lipozyme, AY-30, and CCE showed the best combination of activity and selectivity. They were 32–89 times more selective for EP and hydrolyzed 20–30% of EP in 6 h. This was promising, but not good enough for commercial use. Enzymes CE, MAP-10, and 62305 were the most selective catalysts, and Novozym 435, PS-30, and Lipolase were the most active. Lipolase was the only enzyme of 38 tested that selectively hydrolyzed EA over EP. Enzymes showing very low to no activity are listed in TABLE 3.
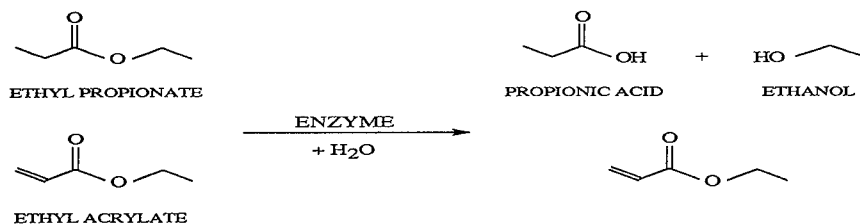
FIGURE 1. The chemistry of the desired selective hydrolysis of EP in bulk EA.

Biphasic Mixtures with Lipozyme

To increase EP hydrolysis and overcome equilibrium constraints imposed by water-saturated EA (only 1 wt% water), we used our best immobilized enzyme, Lipozyme, in two-phase aqueous-organic mixtures. Nonimmobilized enzymes were also used, but were partitioned into the water phase. We increased the overall hydrolysis of EP by adding 50% water, but actually decreased the rate (FIGURE 2). These were mixed in an incubator-shaker, where poor mixing between the phases and between Lipozyme and the reactants slowed EP hydrolysis. In fact, Lipozyme pooled in the bottom water layer. Still, the 50% water system provided a constant supply of water, continually driving EP hydrolysis.

To improve mixing, we used an overhead impeller in a larger reactor and significantly increased EP hydrolysis. Using a 50:50 aqueous:organic mixture in the shaker, the EP concentration decreased 49% in 23 h (FIGURE 2); with the impeller, it decreased 80% in 26 h (FIGURE 3). We further increased EP hydrolysis by raising the water content to 90 vol%, thereby decreasing the EP concentration by 97% in 23 h

TABLE 1. Enzymes Examined for the Hydrolysis of ppm Quantities of Ethyl Propionate in Bulk Ethyl Acrylate or in Amerhold DR-25 (Water-based Latex)

Enzyme	Type	Source or Common Name	Other Information	Company
L-1754	Lipase	*Candida rugosa*		Sigma
L-1150	Lipase	*Candida rugosa*	Immobilized on acrylic beads	Sigma
L-3001	Lipase	Wheat germ		Sigma
L-3126	Lipase	Porcine pancreas		Sigma
P-5380	Protease	Subtilisin Carlsberg		Sigma
P-1512	Protease	Thermolysin		Sigma
P-4032	Protease	*Aspergillus oryzae*		Sigma
P-4630	Protease	Bovine pancreas		Sigma
P-4755	Protease	*Aspergillus oryzae*		Sigma
P-0384	Protease	*Streptomyces caespitosus*		Sigma
P-6141	Protease	*Bacillus polymyxa*		Sigma
P-5147	Protease	*Streptomyces griseus*		Sigma
P-5027	Protease	*Rhizopus* species	Newlase	Sigma
P-7026	Protease	*Aspergillus sojae*		Sigma
P-3375	Protease	Papain		Sigma
P-7545	Protease	Porcine pancreas	Pancreatin	Sigma
C-4129	Protease	Bovine pancreas	Chymotrypsin	Sigma
62305	Lipase	*Rhizopus arrhizus*		Fluka
ChiroCLEC CR	Lipase	*Candida rugosa*	Cross-linked enzyme crystals	Altus Biologics
CCL	Lipase	*Candida rugosa*		Altus Biologics
CCE	Esterase	*Candida rugosa*		Altus Biologics
D-L-1754	Lipase	L-1754 (*Candida rugosa*)	Freeze-dried with sucrose	J. Dordick (University of Iowa)
Novozym 435	Lipase	*Candida antarctica*	Immobilized on acrylic resin	Novo
Novozym 525	Lipase	*Candida antarctica*		Novo
Lipozyme 10,000 L	Lipase	*Mucor miehei*	Liquid	Novo
Lipozyme IM 60	Lipase	*Mucor miehei*		Novo
Lipolase 100 T	Lipase	Fungal origin		Novo
Esperase 6.0 T	Protease	*Bacillus* species		Novo
Neutrase 1.5 MG	Protease	*Bacillus subtilis*		Novo
Alcalase 3.0 T	Protease	*Bacillus licheniformis*		Novo
Savinase 6.0 T	Protease	*Bacillus* species		Novo
Termamyl 60 T	Amylase	*Bacillus licheniformis*		Novo
Lipase AK	Lipase	*Pseudomonas* species		Amano
Lipase PS-30	Lipase	*Pseudomonas* species		Amano
Lipase AY-30	Lipase	*Candida rugosa*		Amano
AY-L	Lipase	*Candida rugosa*	Liquid	Amano
Proleather	Protease	*Bacillus subtilis*		Amano
L-10	Lipase	*Candida lipolytica*		Amano
CE	Lipase	*Humicola langinosa*		Amano
CES	Lipase	*Pseudomonas* species		Amano
MAP-10	Lipase	*Mucor javanicus*		Amano
Protease N	Protease	*Bacillus subtilis*		Amano
Prozyme 6	Protease	*Aspergillus oryzae*		Amano

TABLE 2. Enzymes Showing Moderate to Very Good Activity for the
Enzyme-catalyzed Hydrolysis of Ethyl Propionate in Ethyl Acrylate[a]

Enzyme	Reaction Time (h)	Propionic Acid (wt%)	Acrylic Acid (wt%)	Relative Yield (Propionic Acid/ Acrylic Acid)[b]
None (control)	240	0.0	0.0	—
L-1754	4	1.8	0.3	50.3
Lipozyme IM 60	5	1.8	0.2	88.9
Lipase AY-30	5	1.2	0.4	31.8
CCE	6	1.2	0.2	62.4
CE	5	0.3	0.02	118.2
MAP-10	4	0.3	0.0	∞
62305	6	0.1	0.0	∞
L-3126	5	0.4	0.6	5.3
Lipase AK	4	0.3	0.8	3.5
Lipase PS-30	5	1.0	4.2	2.2
P-7545	7	0.2	0.3	6.0
Novozym 435	2	1.2	4.2	2.7
Protease N	3	0.01	0.02	4.4
D-L-1754	4	0.02	0.03	6.9
CCL	5	1.2	1.6	6.4
Lipolase 100 T	6	0.5	4.5	0.9

[a]Activity measured by propionic and acrylic acid production and selectivity measured by relative yield. Reaction conditions: 100 mg/mL enzyme, 9:1 ethyl acrylate:ethyl propionate by weight, saturated with water (~ 1 wt%), 30 °C, shaking speed of 200 rpm (incubator-shaker).
[b]Relative yield = propionic acid yield/acrylic acid yield

$$= \frac{\text{(moles propionic acid produced/initial moles ethyl propionate)}}{\text{(moles acrylic acid produced/initial moles ethyl acrylate)}}.$$

(FIGURE 3). Importantly, the EA concentration remained fairly constant, decreasing only 0.16% in 23 h with the 90:10 aqueous-organic mixture.

Posttreating the Latex

Enzyme Screening

We screened 15 enzymes—11 of the best from the previous screening and 4 additional—to find the most active for EP hydrolysis in Amerhold DR-25. We also hydrolyzed EA, although more slowly, and measured the disappearance of EP and EA to evaluate activity (TABLE 4). Novozym 435 was by far the most active and was used in further studies in batch reactors and in a continuous tube to evaluate its commercial potential.

Continuous Reactor with Novozym

We hydrolyzed EP from Amerhold DR-25 using 1 g of Novozym 435 in a continuous, packed-bed tubular reactor (FIGURE 4). We also hydrolyzed residual EA, but to a smaller extent. We made three runs with fresh catalyst. In the first, Novozym 435 maintained activity at 30 °C for 653 h (FIGURE 5), but quickly

TABLE 3. Enzymes Showing Very Low to No Activity for the Enzyme-catalyzed
Hydrolysis of Ethyl Propionate in Ethyl Acrylate [a]

Enzyme	Reaction Time (h)	Propionic Acid (wt%)	Acrylic Acid (wt%)
P-4032	192	0.3	0.05
P-5380	96	0.1	0.04
Savinase 6.0 T	144	0.1	0
P-3375	26	0.03	0.0
CES	48	0.2	0.8
Prozyme 6	24	0.03	0.0
L-3001	25	0.0	0.0
P-1512	96	0.0	0.0
Proleather	144	0.0	0.0
P-5147	25	0.0	0.0
C-4129	26	0.0	0.0
Neutrase 1.5 MG	25	0.0	0.0
Alcalase 3.0 T	26	0.0	0.0
Esperase 6.0 T	27	0.0	0.0
L-10	26	0.0	0.0
P-4630	20	0.0	0.0
P-4755	21	0.0	0.0
P-0384	22	0.0	0.0
P-6141	21	0.0	0.0
P-5027	22	0.0	0.0
P-7026	23	0.0	0.0
Termamyl 60 T	24	0.0	0.0

[a]Activity measured by propionic and acrylic acid production. Reaction conditions: 100 mg/mL enzyme, 9:1 ethyl acrylate:ethyl propionate by weight, saturated with water (~ 1 wt%), 30 °C, shaking speed of 200 rpm (incubator-shaker).
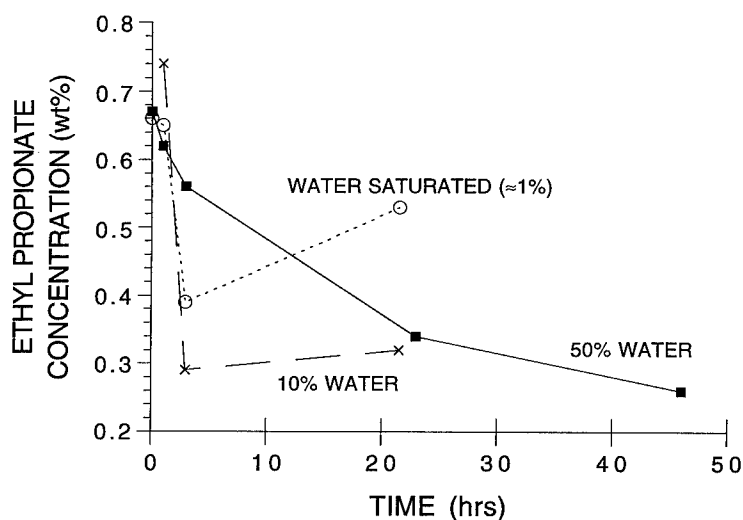
FIGURE 2. Ethyl propionate concentration versus time for the Lipozyme-catalyzed hydrolysis of ethyl propionate in $\sim 99:1$ ethyl acrylate:ethyl propionate with various amounts of added water (100 mg/mL enzyme on water-free basis, 30 °C, batch reactor in incubator-shaker).

deactivated at 50 °C (FIGURE 6). Using fresh catalyst at 60 °C and a 50 mL/h latex flow rate, we saw higher initial activity, but quick deactivation (FIGURE 7). In the last run, we saw deactivation throughout the run, but still good activity (FIGURE 8). We do not know why the catalyst slowly deactivated in this run, but not in the first (FIGURE 5), although the inlet EP concentration was higher in this last run.
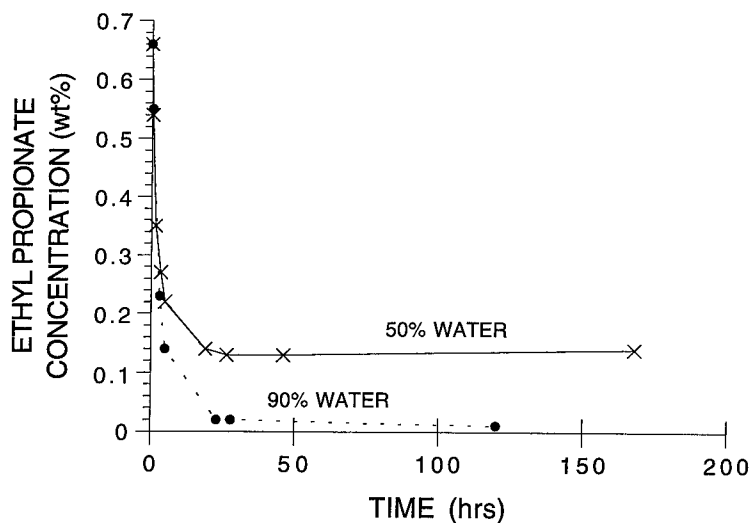
FIGURE 3. Ethyl propionate concentration versus time for the Lipozyme-catalyzed hydrolysis of ethyl propionate in biphasic mixtures of ~ 99:1 ethyl acrylate:ethyl propionate with 50% or 90% water (100 mg/mL enzyme on water-free basis, 30 °C, batch reactor with overhead impeller for stirring).

Batch Reactor with Novozym

We used Novozym 435 to hydrolyze EP from Amerhold DR-25 in a batch reactor at three different concentrations (FIGURE 9). We can easily remove all EP within 1 h. However, because of high catalyst cost, the lowest enzyme concentration, 0.01 wt%, is more cost-effective for commercial use.

Commercialization

Posttreating the latex is favored over pretreating the feedstock. Hydrolysis in water-based latex requires less enzyme, less reaction time, and no liquid separation of phases, and produces no added waste. Similarly, a batch process is favored to treat the latex over a continuous process because the continuous process requires significant capital investment, whereas the batch process can be retrofit into existing facilities. Thus, we successfully scaled up the batch process for treating the latex, using a 100-gal pilot plant facility and a 3000-gal commercial facility for several experimental trial runs.

TABLE 4. Concentrations of Ethyl Propionate and Ethyl Acrylate in the Enzyme-catalyzed Hydrolysis of Ethyl Propionate and Ethyl Acrylate in Amerhold DR-25 (Water-based Latex)[a]

Enzyme	Enzyme Concentration (wt%)	Reaction Time (h)	Ethyl Propionate (ppm)	Ethyl Acrylate (ppm)
None (control)	—	0	91	139
		24	93	140
Novozym 435	0.09	0	117	200
		4	0	121
Lipozyme IM 60	0.9	0	91	139
		4	27	132
PS-30	0.9	0	114	196
		4	34	141
ChiroCLEC CR	0.09	0	109	171
		4	28	146
L-1754	0.9	0	91	139
		24	33	125
62305	0.9	0	97	145
		24	30	156
AY-30	0.9	0	112	112
		24	27	159
Lipolase 100 T	0.9	0	114	196
		24	25	141
L-3126	0.9	0	92	178
		24	9	97
Lipozyme 10,000 L	0.9	0	92	178
		24	15	155
CE	0.9	0	97	149
		24	62	129
MAP-10	0.9	0	97	149
		24	79	151
CCE	0.9	0	112	112
		24	76	181
L-1150	0.9	0	114	196
		24	94	186
AY-L	0.9	0	92	178
		24	53	172

[a]Reaction conditions: 30 °C, shaking speed of 200 rpm (incubator-shaker).

Finally, although recycling Novozym 435 may reduce catalyst cost significantly, it is difficult and labor-intensive in small-scale batch facilities. Thus, we may not need an immobilized enzyme and can use a more concentrated, nonimmobilized, and ultimately cheaper form of Novozym 435 at tenfold or lower concentrations. Comparison of that catalyst, Novozym 525, with its immobilized form, Novozym 435, is shown in FIGURE 10. Importantly, we also can add Novozym 525 to the latex and can let it
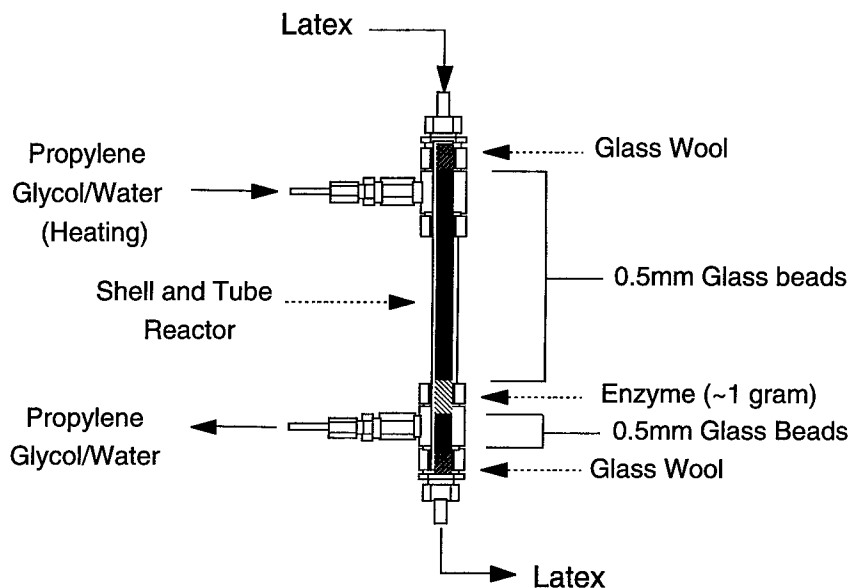
FIGURE 4. Continuous tubular reactor used for the Novozym 435–catalyzed, continuous hydrolysis of ethyl propionate in Amerhold DR-25.
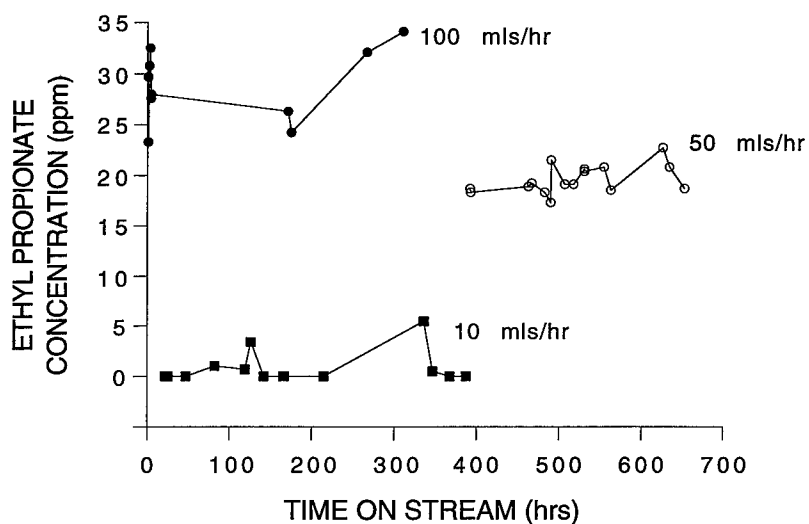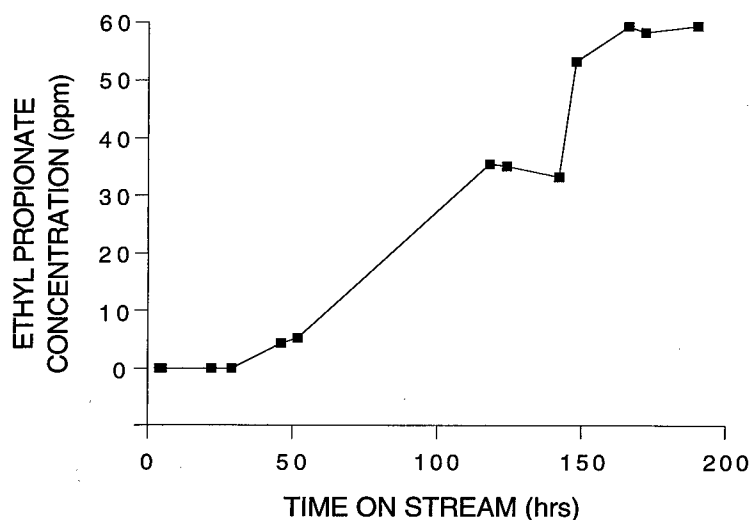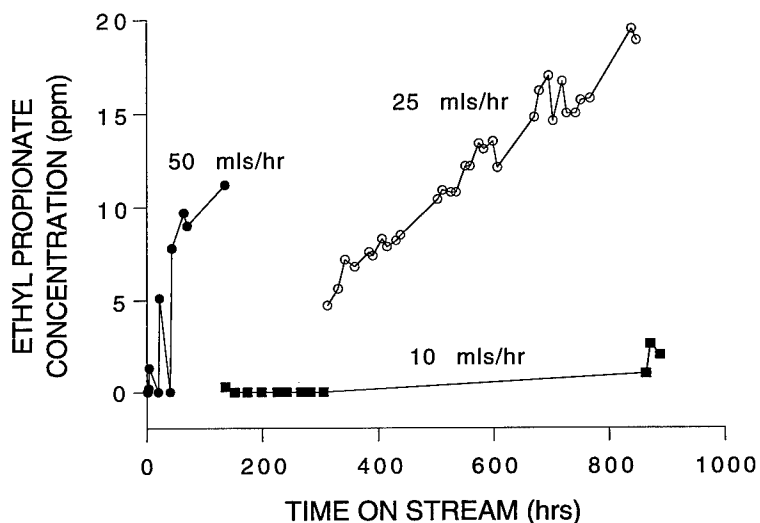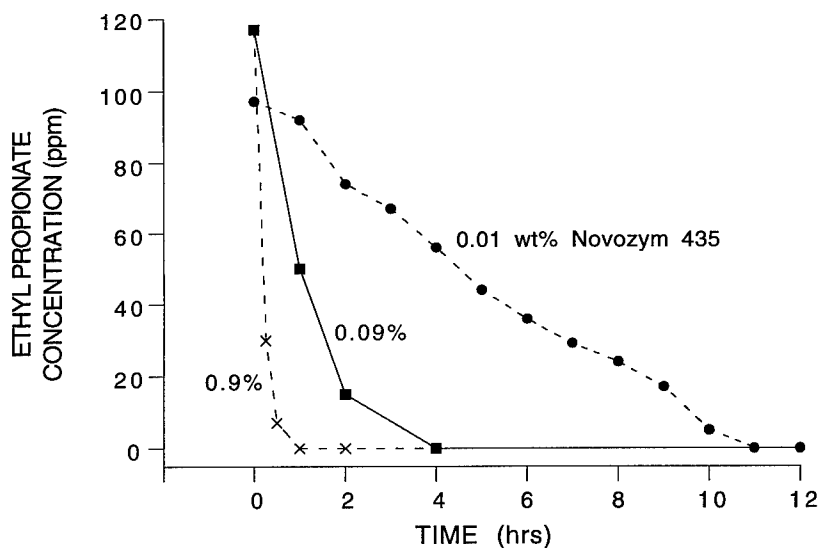

FIGURE 5. Ethyl propionate concentration versus time for the Novozym 435–catalyzed hydrolysis of ethyl propionate in Amerhold DR-25 in a continuous tubular reactor at various flow rates (1 g enzyme, 75–85 ppm ethyl propionate in feed, 30 °C, all data from the same run, first charge of fresh Novozym 435 to continuous reactor).
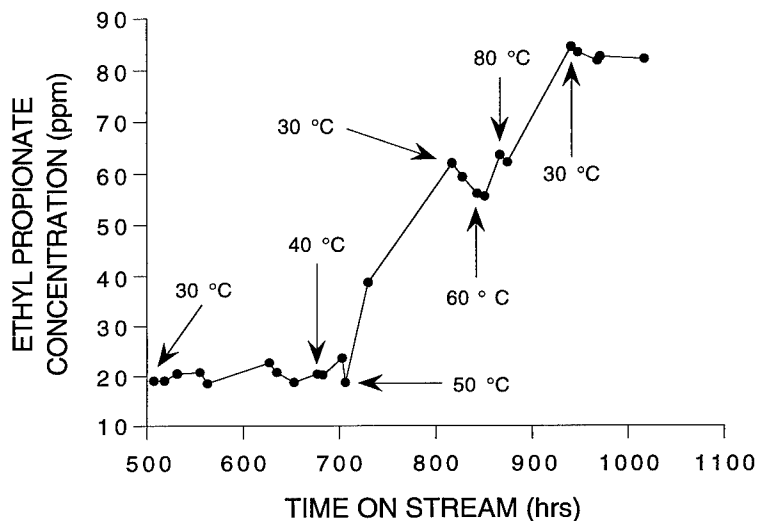
FIGURE 6. Ethyl propionate concentration versus time for the Novozym 435–catalyzed hydrolysis of ethyl propionate in Amerhold DR-25 in a continuous tubular reactor at various temperatures (1 g enzyme, 75–85 ppm ethyl propionate in feed, 50 mL/h feed rate for Amerhold DR-25, first charge of fresh Novozym 435 to continuous reactor; continuation of run shown in FIGURE 5).

hydrolyze EP during shipment, rather than using valuable reactor time in plant facilities.

EXPERIMENTAL METHODS

We purchased enzymes from Sigma Chemical and Fluka or received free samples from Amano International Enzyme Company, Novo Nordisk BioChem North America, and Altus Biologics. We also received one enzyme (L-1754) freeze-dried with sucrose from Jonathan Dordick of the University of Iowa. We used enzymes without further purification or other changes.

Pretreating the Feedstock

For catalyst screening, we added 4 mL of fresh 9:1 (by weight) EA:EP to 10-mL glass flasks with 400 mg of enzyme. For water-saturated mixtures, we presaturated the EA:EP mixture with 10 vol% water in a sonic bath. For two-phase mixtures, we added 10, 50, or 90 vol% water directly to the reaction flasks. Flasks were placed in a New Brunswick Innova 4000 Incubator-Shaker (200 rpm, 30 °C). For larger-scale experiments using biphasic solutions, we added either 35 or 7 mL of 99:1 EA:EP to a 200-mL round-bottom flask with either 3500 or 700 mg of enzyme (100 mg/mL on water-free basis) and then added either 35 or 63 mL of water (for 50% and 90%

water solutions). We used a side-arm, overhead impeller at 250 rpm and controlled the temperature (30 °C) with a heating mantle.

Posttreating the Latex

For screening, we typically added the appropriate amount of enzyme to 20 mL of Amerhold DR-25 and placed the reaction flasks in the incubator-shaker (200 rpm, 30 °C). For larger-scale reactions, we added enzyme catalyst to 400 mL or more of latex and used an overhead stirrer (300 rpm) and heating mantle (30 °C).

For continuous reactor studies, we fed Amerhold DR-25 into the top of a tubular reactor packed with glass beads (preheater) and 1 g of Novozym 435. We controlled the flow rate using a Gilson Model 302 pump and the reactor temperature using an outer jacket (tube). We fed a mixture of propylene glycol and water to the jacket from a temperature-controlled circulating bath. For sampling, we collected 2.5 mL of fresh sample directly from the reactor outlet rather than from the product collector.

Analytical Methods

We analyzed reaction mixtures by gas chromatography (1 μL, manual injection) using an HP 5890 equipped with an FID on a 30-m DB-WAX column. We used toluene as an internal standard and acetone to solubilize latex particles.

FIGURE 7. Ethyl propionate concentration versus time for the Novozym 435–catalyzed hydrolysis of ethyl propionate in Amerhold DR-25 in a continuous tubular reactor starting with fresh enzyme at 60 °C (1 g enzyme, 69–74 ppm ethyl propionate in feed, 50 mL/h feed rate for Amerhold DR-25, second charge of fresh Novozym 435 to continuous reactor).

FIGURE 8. Ethyl propionate concentration versus time for the Novozym 435–catalyzed hydrolysis of ethyl propionate in Amerhold DR-25 in a continuous tubular reactor at various flow rates (1 g enzyme, 30 °C, 73–106 ppm ethyl propionate in feed, all data from the same run, third charge of fresh Novozym 435 to continuous reactor).

FIGURE 9. Ethyl propionate concentration versus time for the Novozym 435–catalyzed hydrolysis of ethyl propionate in Amerhold DR-25 in a batch reactor with 0.01, 0.09, and 0.9 wt% Novozym 435 (30 °C, batch reactor with overhead impeller, catalyst amount based on the total weight of Amerhold DR-25).
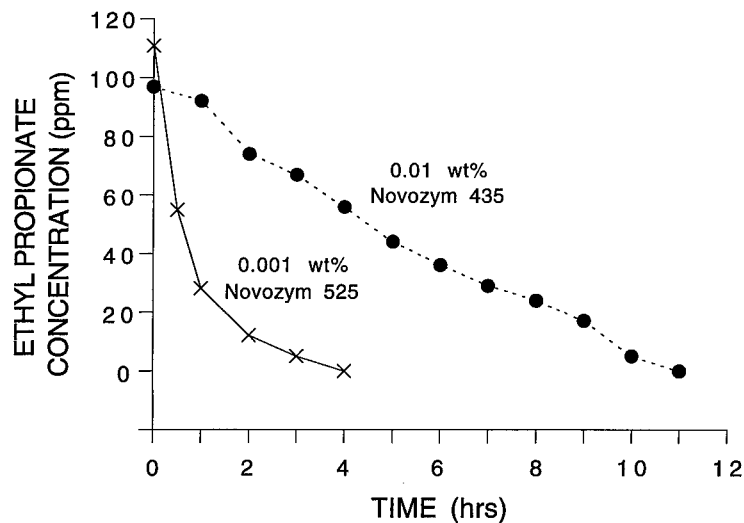
FIGURE 10. Ethyl propionate concentration versus time for the Novozym 435 (immobilized)–catalyzed and Novozym 525 (water-soluble)–catalyzed hydrolysis of ethyl propionate in Amerhold DR-25 in a batch reactor (30 °C, batch reactor with overhead impeller, catalyst amount based on the total weight of Amerhold DR-25).

REFERENCES

1. AMERCHOL CORPORATION. 1995. United States Patent No. 5,413,775.
2. CARTA, G., J. L. GAINER & M. E. GIBSON. 1992. Synthesis of esters using a nylon-immobilized lipase in batch and continuous reactors. Enzyme Microb. Technol. **14:** 904–910.
3. GHOGARE, A. & G. S. KUMAR. 1989. Oxime esters as novel irreversible acyl transfer agents for lipase catalysis in organic media. J. Chem. Soc. Chem. Commun. **20:** 1533–1535.
4. CESTI, P., A. ZAKS & A. M. KLIBANOV. 1985. Preparative regioselective acylation of glycols by enzymatic transesterification in organic solvents. Appl. Biochem. Biotechnol. **11:** 401–407.
5. MILLER, C., H. AUSTIN, L. POSORSKE & J. GONZALEZ. 1985. Characteristics of an immobilized lipase for the commercial synthesis of esters. J. Am. Chem. Soc. **65:** 927–931.
6. IMPERIAL CHEMICAL INDUSTRIES. 1991. WO Patent Application No. 91/15520.

Stability of Immobilized Penicillin Acylase under Reactive Conditions[a]

ANDRES ILLANES, CLAUDIA ALTAMIRANO,
AND ANDREA RUIZ

School of Biochemical Engineering
Universidad Católica de Valparaíso
Valparaíso, Chile

INTRODUCTION

Thermal inactivation is a limiting factor for prolonged use of an enzyme in an industrial process, but inactivation in the presence of substrate and products has received little attention, with most studies being conducted under nonreactive conditions.

Enzyme inactivation, evaluated in terms of decay constants determined in the absence of substrate and products, may overestimate or underestimate its catalytic potential. The purpose of this work is to evaluate the decay parameters in the presence of substrate and products and to determine their modulation effects. Penicillin acylase (PA) (EC 3.5.1.11) was chosen as a case study, with its complex kinetic behavior being adequate to the purpose of this work.[1]

THEORETICAL BACKGROUND

One-stage first-order kinetics is the simplest and most popular model to describe enzyme inactivation, but in most cases it hardly represents experimental data nor the heterogeneous nature of immobilized enzymes. Enzyme decay is usually a multistage process, which can be adequately represented by a series mechanism considering transition from a fully active stage to progressively less-active stages.[2] A series mechanism in which one enzyme species (E_1) undergoes inactivation through an intermediate stage (E_2) to a final inactive stage (E_3) is represented by equation 1, where subscript o refers to the initial condition; k_1 and k_2 are the first-order transition rate constants to the intermediate and final enzyme stages, respectively; a is the molar specific activity; and e is the global volumetric activity:

$$\frac{e}{e_o} = \left[1 + \frac{a_2}{a_1} \cdot \frac{k_1}{k_2 - k_1} \right] \cdot \exp(-k_1 t) - \left[\frac{a_2}{a_1} \cdot \frac{k_1}{k_2 - k_1} \right] \cdot \exp(-k_2 t). \tag{1}$$

A scheme for the reaction kinetics and inactivation of IPA (immobilized penicillin acylase) is presented in FIGURE 1 for a series-type mechanism. Based on the proposed hypothesis, different inactivation rates will be produced for each of the enzyme species (E, ES, EP_1, EP_2, EP_1P_2, EP_2S). Considering different first-order

transition rate constants (k_i) for all possible enzyme species (EZ),

$$-\frac{d[EZ]}{dt} = k_i \cdot [EZ], \tag{2}$$

$$k_i = k \cdot (1 - n_i), \tag{3}$$

where the n_i terms represent the effector modulation factors and k represents the constant for the free enzyme.

For a series-type mechanism, considering one intermediate and one final inactive form, first-order transition rates can be determined for each of the enzyme species by fitting experimental data to equation 1. Corresponding modulation factors are calculated from equation 3.
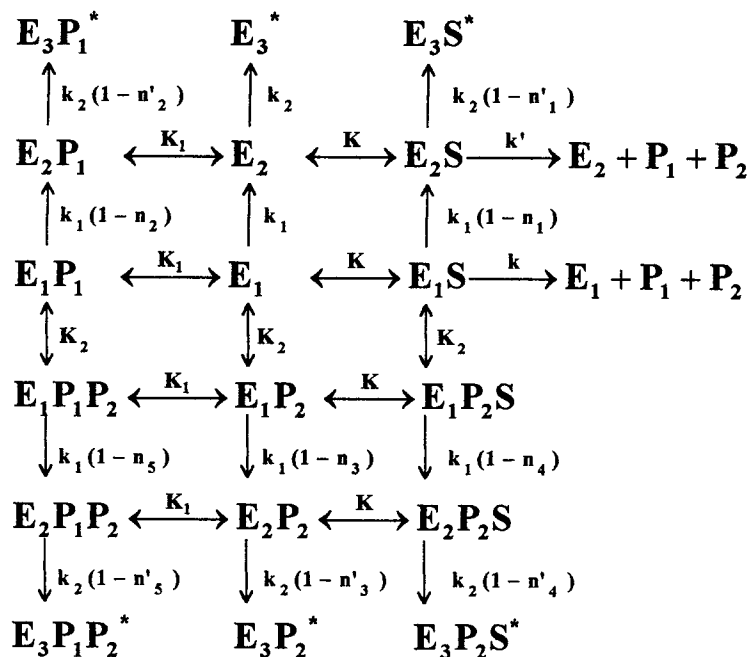
FIGURE 1. Scheme for reaction kinetics and enzyme inactivation in the conversion of PG (S) into PAA (P_1) and 6APA (P_2), according to a series-type mechanism.

MATERIALS AND METHODS

Escherichia coli PA immobilized in polyacrylamide gel (IPA), 400–450 IU/g, was kindly supplied by SINQUISA (Síntesis Química, Lima, Peru). IPA activity was assayed by measuring the initial rate of PG (penicillin G) hydrolysis. One international unit (IU) of IPA is the amount of enzyme that hydrolyzes 1 μmol of PG per min at 37 °C, pH 7.8, and 50 g/L of PG. Thermal stability of IPA in the absence of effectors and in the presence of products was studied in a batch reactor with

automatic pH and temperature control and with a bottom filter for medium replacement. In the presence of substrate, experiments were conducted in a continuous stirred-tank reactor at pseudo-steady-state condition. The time for each experiment to approach enzyme half-life was determined. First-order transition rate constants in equation 1 were determined by nonlinear regression. Experiments were conducted at constant effector concentrations (5 K_i and 12 K_m), which can be considered adequate to displace the equilibrium to the corresponding enzyme complex (see FIGURE 1).

RESULTS AND DISCUSSION

Kinetic experiments of thermal inactivation of IPA were conducted at pH 7.8 and 40 °C. Experimental results were in all cases in good agreement with equation 1, and transition rate constants were determined by nonlinear regression for the enzyme in the absence of effectors and in the presence of substrate and products. Their values are given in TABLE 1, together with modulation factors (n_i, n'_i), half-lives ($t_{1/2}$), and correlation coefficients (r).

TABLE 1. Transition Rate Constants and Modulation Factors of IPA in the Absence and Presence of Effectors[a]

	E	ES (1)	EP$_1$ (2)	EP$_2$ (3)	EP$_2$S (4)	EP$_1$P$_2$ (5)
$k_1 \cdot 10^2$ [h^{-1}]	4.004	0.148	13.210	0.104	0.139	5.079
$k_2 \cdot 10^3$ [h^{-1}]	2.105	8.603	6.795	5.485	6.182	2.955
a_2/a_1	0.75	0.75	0.75	0.75	0.75	0.75
n_i		0.96	−2.31	0.98	0.97	−0.27
n'_i		−3.10	−2.25	−1.61	−1.94	−0.40
$t_{1/2}$ [h]	218	560	67	800	620	155
r	0.99	0.97	0.99	0.92	0.97	0.98

[a]Based on a series-type mechanism. The numbers in the parentheses represent the i values of the complexes.

PAA (phenylacetic acid) increased the inactivation rate of IPA, as reflected by negative values of the modulation factors, in both stages, for the secondary complex EP$_1$ and for the tertiary complex EP$_1$P$_2$. On the other hand, 6APA (6-aminopenicillanic acid) and PG had a strong protection effect on the first stage of inactivation, as shown by positive values of the modulation factors for the secondary complexes ES and EP$_2$ and for the tertiary complex EP$_2$S. However, all effectors increased transition rates from the intermediate to the final inactive stage, therefore increasing the inactivation rate in that stage. Global effect can be better appreciated when examining enzyme half-life, which was significantly higher in the presence of 6APA and PG and lower in the presence of PAA. IPA half-life at saturating concentrations of 6APA and PG increased to 26 days. There are no data available to compare this figure properly, but it is similar to that determined from the data of Ospina *et al.*[3] and is higher than that reported by Sauber[4] for *E. coli* IPAs under variable reactive conditions.

Positive modulation has been explained in terms of favoring a rigid configuration and a hydrophobic microenvironment,[5] which might be a sound explanation for the protection effect of PG and 6APA. There is no such explanation for PAA increasing

the inactivation rate. However, it has been reported for other effectors in a few cases and explained in terms of (i) the promotion of dissociation of the quaternary structure[6] and (ii) active-site oxidation and autoinactivation.[7] The former explanation cannot be ruled out in the case of *E. coli* PA, which has a quaternary structure composed of two different subunits whose dissociation reduces activity. As shown elsewhere,[8] modulation factors have a strong impact on enzyme performance in a reactor and are therefore useful parameters for proper assessment.

CONCLUSIONS

- 6APA and PG stabilized IPA against thermal inactivation, whereas PAA increased the inactivation rate.
- IPA inactivation was a multistage process in the absence and presence of effectors, which was modeled according to a series-type mechanism. The secondary complex EP_2 was the most stable enzyme form, followed by the tertiary complex EP_2S and the secondary complex ES, with all being significantly more stable than the free enzyme E; in contrast, the tertiary complex EP_1P_2 and the secondary complex EP_1 were less stable than the free enzyme.
- A model for IPA inactivation has been validated for operation times close to the enzyme half-life. However, industrial practice and optimization of catalyst use make it advisable to validate the model up to two or even three half-lives.

ACKNOWLEDGMENTS

REFERENCES

1. LEE, S. B. & D. Y. RYU. 1982. Reaction kinetics and mechanisms of penicillin acylase: a comparative study by computer simulation. Enzyme Microb. Technol. **4:** 35–38.
2. HENLEY, J. P. & A. SADANA. 1986. Deactivation theory. Biotechnol. Bioeng. **28:** 1277–1285.
3. OSPINA, S., A. LÓPEZ-MUNGUÍA, R. L. GONZÁLEZ & R. QUINTERO. 1992. Characterization and use of a penicillin acylase biocatalyst. J. Chem. Technol. Biotechnol. **53:** 205–214.
4. SAUBER, K. 1993. Lessons from industry. *In* Stability and Stabilization of Enzymes. W. J. van den Tweel, A. Harder & R. M. Buitelaar, Eds.: 145–151. Elsevier. Amsterdam/New York.
5. BICKERSTAFF, G. 1984. Applications of immobilized enzymes to fundamental studies on enzyme structure and function. *In* Topics in Enzyme and Fermentation Biotechnology. Volume 9. A. Wiseman, Ed.: 162–201. Ellis Horwood. Chichester.
6. MISSET, O. 1993. Stability of industrial enzymes. *In* Stability and Stabilization of Enzymes. W. J. van den Tweel, A. Harder & R. M. Buitelaar, Eds.: 111–131. Elsevier. Amsterdam/New York.
7. BOURDILLON, C., C. HERVAGAULT & D. THOMAS. 1985. Increase in operational stability of immobilized glucose oxidase by the use of an artificial cosubstrate. Biotechnol. Bioeng. **27:** 1619–1622.
8. ILLANES, A., C. ALTAMIRANO & O. CARTAGENA. 1994. Enzyme reactor performance under thermal inactivation. *In* Advances in Bioprocess Engineering. E. Galindo & O. T. Ramírez, Eds.: 467–472. Kluwer. Dordrecht.

Application of Microbial Enzymes in Diagnostic Analysis

GAOXIANG LI,[a] JIANGUO LIU,[a] MING YIN,[a] JIAN GUO,[b]
AND SHUNZHEN XIE[a]

[a]Institute of Microbiology
Academia Sinica
Beijing 100080, People's Republic of China

[b]National Center for Clinical Laboratory
Beijing 100730, People's Republic of China

INTRODUCTION

Many enzymes, froma variety of sources, are used as diagnostic reagents in clinical chemistry for determination of metabolites in blood or urine. Such metabolites as uric acid, bilirubin, aspartate-aminotransferase, and glucose are measured in many clinical laboratories. Enzymes are becoming increasingly popular as analytical reagents because of their sensitivity, high degree of specificity, and rapidity. Enzymes are employed in analytical systems based on widely differing presentations. In many respects, microorganisms are a more practical source of enzymes for clinical uses than animal tissue. There has been a rapid growth in the application of microbial enzymes for diagnosis in the area of clinical chemistry.

We have successfully developed the microbial enzymes for application in diagnostic analysis. We describe here the properties of some purified microbial enzymes and their application in clinical analysis.

MATERIALS AND METHODS

All strains were obtained from the Institute of Microbiology, Academia Sinica. Coenzymes were purchased from Boehringer Mannheim. Carrier ampholytes for isoelectric focusing–pharmalyte were purchased from Pharmacia Chemicals. The other chemicals were of analytical grade. Equipment for enzyme purification was purchased from Pharmacia-LKB.

RESULTS AND DISCUSSION

A Thermostable Lactate Dehydrogenase (LDH)

A strain, *Lactobacillus* sp. L15, was found to produce thermostable intracellular D-LDH. The thermostable LDH retained 40% of its initial activity after it was

476

TABLE 1. Purification and Properties of LDH from *Lactobacillus* sp. L15

| Fermentative Unit (IU/mL) | Purification | | | Properties | | | |
	Specific Activity (IU/mg)	Recovery (%)	Purified-fold	Optimum pH	pH Stability	Thermal Stability	K_m Value
5	279	60	80	7.0–7.8	6.2–7.5	Retained 40% activity, 95 °C, 10 min	2.3×10^{-1} mM (pyruvate) 5.9×10^{-2} mM (NADH)

incubated at 95 °C for 10 minutes, but the LDH from pig heart was completely inactivated at 65 °C for 10 minutes. The LDH was partially purified by ammonium sulfate fractionation and DEAE–Sephadex A-50 column chromatography. The preparation showed an approximately 80-fold increase in specific activity, with a recovery of 60% of its original activity. The purified LDH had a specific activity of 280 IU/mg protein. TABLE 1 shows some properties of the purified LDH.

LDH is a useful enzyme for clinical analysis that catalyzes the interconversion of pyruvate and lactate. Thus, this enzyme has been used for measuring the activity of L-alanine-aminotransferase (ALT/GPT, EC 2.6.1.2) to diagnose liver disease, as follows:

$$\alpha\text{-oxoglutarate} + \text{L-alanine} \xrightarrow{\text{ALT/GPT}} \text{L-glutamate} + \text{pyruvate}$$

$$\text{pyruvate} + \text{NADH} + \text{H}^+ \xrightarrow{\text{LDH}} \text{lactate} + \text{NAD}^+.$$
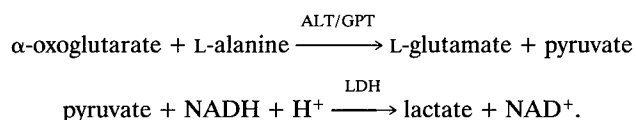
The enzyme reagent kit is used for the serum ALT/GPT determination. The results of experiments are shown in TABLE 2. A good correlation was observed between the values obtained by our ALT kit and Boehringer, Sclavo, and Baker kits for ALT determination. The correlation coefficients were 0.998, 0.995, and 0.997, respectively.

A Thermostable L-Malate Dehydrogenase (MDH)

A strain, *Bacillus stearothermophilus* AS 605, was found to produce thermostable intracellular L-malate dehydrogenase (EC 1.1.1.37). The thermostable MDH was

TABLE 2. Application of LDH in ALT/GPT Analysis

Linear Range (ALT)	CV (%)	SD	Correlation and Regression Line	Stability at 4 °C
0–800 IU/L	3.8	4.2	$Y = 0.95X - 5.90$ $r = 0.998$ X = Boehringer kit	Retained ~100% activity for 10 months

TABLE 3. Purification and Properties of MDH from *Bacillus stearothermophilus* AS 605

| Fermentative Unit (IU/mL) | Purification | | | Properties | | | |
	Specific Activity (IU/mg)	Recovery (%)	Purified-fold	Optimum pH	pH Stability	Half-life	K_m
2.75	200	35	93	7.0	6.5–7.7	10 h, 50 °C	2.96×10^{-5} M oxaloacetate

partially purified by ammonium sulfate fractionation, DEAE-cellulose column chromatography, and gel filtration with Sephadex G-150. The thermostable MDH retained 50% of its initial activity after it was incubated at 50 °C for 10 h, but the MDH from pig heart was completely inactivated at 50 °C for 10 min. TABLE 3 shows some properties of the purified MDH. The K_m value is similar to that of the MDH from pig heart and *Bacillus subtilis*.[1] By SDS-polyacrylamide gel electrophoresis and gel filtration, the molecular weight of the purified enzyme was determined as 152,000, consisting of four homologous subunits of 38,000 each. The MDH powder kept at 4 °C was stable for 10 months and the enzyme retained about 90% of its original activity.

MDH is a useful enzyme for clinical analysis that catalyzes the interconversion of oxaloacetate and malate. Thus, this enzyme has been used for measuring the activity of aspartate-aminotransferase (EC 2.6.1.1, AST/GOT) to diagnose heart disease and liver illness, as follows:

$$\text{L-aspartate} + \alpha\text{-ketoglutarate} \xrightarrow{\text{AST/GOT}} \text{oxaloacetate} + \text{L-glutamate}$$

$$\text{oxaloacetate} + \text{NADH} + \text{H}^+ \xrightarrow{\text{MDH}} \text{L-malate} + \text{NAD}^+.$$
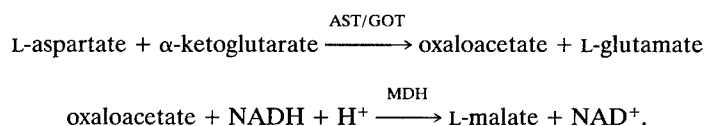
The enzyme reagent kit is used for the serum AST/GOT determination. The results of experiments are shown in TABLE 4. A comparison experiment was carried out in 65 serum samples from patients, in which both our AST kit and the Japanese AST kit were used for AST determination. The correlation between the results obtained from the two AST kits is given in TABLE 4 and can be summarized as follows: $Y = 2.926 + 1.092X$ and $r = 0.9997$ (Y, our kit; X, Japanese kit). A good

TABLE 4. Application of MDH in AST/GOT Analysis

| Linear Range (AST) | | Imprecision | | Correlation and Regression Line | Stability at 4–8 °C |
		CV (%)	SD		
0–1680 IU/L	Within:	0.31–1.31	0.90–1.12	$Y = 1.09X + 2.92$	Retained ~90%
	Between:	0.94–1.25	0.93–1.30	$r = 0.999$	activity for 10
				X = Japanese kit	months

TABLE 5. Purification and Properties of BOX from *Myrothecium verrucaria* Mv.2.1089

	Purification				Properties				
Fermentative Unit (IU/mL)	Specific Activity (U/mg)	Recovery (%)	Purified-fold	Optimum pH	Optimum Temperature (°C)	pH Stability	Thermal Stability (°C)	K_m (M)	pI
3–4	40–50	40–50	14	7.5	50	9–9.5	<50	9.4×10^{-5}	4.4

correlation was also observed between the values obtained by our AST kit and the Baker Company Encore AST kit ($Y = 0.991X + 3.724$ and $r = 0.9925$). The AST reagent kit with MDH from thermophilic bacteria is in accord with the demands of medical laboratory technology.

Bilirubin Oxidase (BOX)

Bilirubin oxidase (EC 1.3.3.5) has been obtained from *Myrothecium verrucaria*, as Murao and Tanaka have reported.[2,3] Recently, we have succeeded in the isolation of a rich BOX-producing strain from several strains of *Myrothecium verrucaria*. BOX was purified from a culture filtrate of strain Mv.2.1089 by DEAE-cellulose and Sephadex G-100 column chromatographies. The purified enzyme had a specific activity of 40–50 U/mg protein and showed a single band on polyacrylamide gel electrophoresis. Some of the general properties of this bilirubin oxidase were as follows: the optimum pH for the enzyme reaction was 7.5 and the optimum temperature was 50 °C. The enzyme was stable at pH values ranging from 9.0 to 9.5. The molecular weight was calculated to be 61,900–62,700 by SDS-PAGE and gel-filtration techniques. The apparent K_m value of the bilirubin oxidase was calculated to be 9.4×10^{-5} mol/L. The enzyme activity was greatly reduced by incubation of BOX with Fe^{2+}, Hg^+, NaN_3, NH_4^+, and Zn^{2+}. The enzyme reaction was inhibited in the presence of Ca^{2+}, Zn^{2+}, Fe^{2+}, and BSA (TABLE 5).

The enzyme reagent kit is used for determination of the total serum bilirubin and conjugated bilirubin levels. The results of experiments are shown in TABLE 6. The percentage of recovery of the method ranged from 92.4% to 101.6% for the total bilirubin assay. A comparison experiment with both our BOX kit method (Y) and the Backman kit method (X) was carried out in 30 serum samples from patients for the

TABLE 6. Application of BOX in Total Bilirubin (TBIL) and Conjugated Bilirubin (CBIL) Analysis

	Linear Range (mg/dL)		CV (%)	SD	Correlation and Regression Line		Stability of BOX at 4–8 °C
TBIL	0–25	Within:	1.58–1.92	0.02–0.08	$Y = 0.985X - 0.04$	$Y = 1.06X - 0.21$	Half-life
		Between:	1.20–4.90	0.09–0.16	$r = 0.9904$	$r = 0.998$	of 6–9
CBIL	0–13	Within:	0.57–8.28	0.46–0.53	$n = 30$	$n = 50$	months
		Between:	4.48–7.32	0.03–4.48	$X = $ Backman kit method	$X = $ Caffeine method	

TABLE 7. Purification and Properties of α-Glucosidase from *Saccharomyces* sp. 39

	Purification			Properties				
Fermentative Unit (IU/mL)	Specific Activity (U/mg)	Recovery (%)	Purified-fold	Optimum pH	Optimum Temperature (°C)	pH Stability	Thermal Stability (°C)	K_m
7–9	50–54	33–36	15–17	6.8	40	6.8–7.5	<35	3.1×10^{-4} M

total bilirubin assay. A good correlation for the two methods was obtained as follows: $Y = 0.985X - 0.04$ and $r = 0.9904$ (TABLE 6).

α-Glucosidase

α-Glucosidase (EC 3.2.1.20) was produced[4] by *Saccharomyces* sp. 39 and purified by ammonium sulfate fractionation and DEAE-cellulose column chromatography. The purified enzyme had a specific activity of 52.2 U/mg protein. The optimum pH for the enzyme reaction was 6.8 and the optimum temperature was 40 °C. The K_m values of α-glucosidase for the substrates, p-nitrophenyl-α-D-glucopyranoside and maltose, were found to be 3.1×10^{-4} mol/L and 1.25×10^{-2} mol/L, respectively. The corresponding V_{max} for p-nitrophenyl-α-D-glucopyranoside was 44 μmol/min-mg and that for maltose was 6.9 μmol/min-mg. The enzyme could not hydrolyze the p-nitrophenyl-α-D-maltopentaoside and p-nitrophenyl-α-D-maltoheptaoside. Some properties are shown in TABLE 7.

The α-glucosidase has been used for determination of the serum α-amylase activity to diagnose pancreatitis, as follows:

$$3\,p\text{-nitrophenylmaltoheptaoside} + 3\,H_2O \xrightarrow{\alpha\text{-amylase}} 2\,p\text{-nitrophenylmaltotetraoside}$$

$$+ 2\,\text{maltotriose} + p\text{-nitrophenylmaltotrioside} + \text{maltotetraose}$$

$$p\text{-nitrophenylmaltotrioside} + 3\,H_2O \xrightarrow{\alpha\text{-glucosidase}} p\text{-nitrophenol} + 3\,\text{glucose}.$$
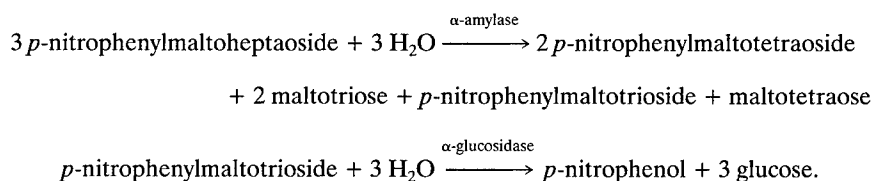
A good linear calibration curve was obtained over the range of 35–435 units/L of α-amylase activity. The results of experiments are shown in TABLE 8.

In a word, the development of microbial enzyme technology points to an exciting future in the field of diagnostic reagents.

TABLE 8. Application of α-Glucosidase in Determination of Serum α-Amylase Activity

	Linear Range (U/L)		CV (%)	SD	Correlation and Regression Line
PNPM$_7$[a]	35–435	Within:	0.56–1.08	0.28–1.59	$Y = 0.3087X + 4.396$
		Between:	2.30–2.70	1.88–4.41	$r = 0.9897$
					$X = $ Aus. Bros. Kit

[a]p-Nitrophenylmaltoheptaoside (substrate).

REFERENCES

1. YOSHDA, A. 1965. Enzymic properties of malate dehydrogenase of *Bacillus subtilis.* J. Biol. Chem. **240**(3): 1118–1124.
2. MURAO, S. & N. TANAKA. 1981. A new enzyme "bilirubin oxidase" produced by *Myrothecium verrucaria* MT-1. Agric. Biol. Chem. **45**(10): 2383–2384.
3. MURAO, S. & N. TANAKA. 1982. Isolation and identification of a microorganism producing bilirubin oxidase. Agric. Biol. Chem. **46**(8): 2031–2034.
4. NEEDLEMAN, R. B., H. J. FEDEROFF, T. R. ECELESHALL, B. BUCHFERER & J. MARMUR. 1978. Purification and characterization of an α-glucosidase from *Saccharomyces carlsbergensis.* Biochemistry **17**(22): 4657–4661.

The Effect on the Response to L-Lactate and H₂O₂ of a Carbon Paste Electrode Modified with Lactate Oxidase and Peroxidases Also Containing Different Additives and Solvents[a]

D. NARASAIAH,[b] U. SPOHN,[c] AND L. GORTON[b]

[b]Department of Analytical Chemistry
University of Lund
S-221 00 Lund, Sweden

[c]Institute of Biotechnology
Department of Biochemistry/Biotechnology
University of Halle
D-06120 Halle, Germany

INTRODUCTION

The influence of nonaqueous solvents on enzyme behavior is an increasingly interesting phenomenon in modern enzymology.[1-3] We have selected various organic pasting liquids in preparation of enzyme-modified carbon paste electrodes (EMCPE). Rice et al.[4] investigated the influence of the pasting liquids on the response of unmodified carbon paste and found slightly decreasing electron transfer rates for hexacyanoferrate II with an increasing chain length of investigated paraffins. The influence of additives as promoters and on the stability of the enzymes is of interest in fundamental investigations of the direct electron transfer between oxidoreductases and the electrode material,[5,6] in stabilization of sensor enzymes,[7-10] and in improving the performance of EMCPEs.[11-14]

Peroxidases are generally small, often glycosylated, redox enzymes with protoporphyrin IX as the strongly bound cofactor. They are all active for the reduction of hydrogen peroxides. In the reaction with peroxide, the native form of the enzyme becomes oxidized in a single two-electron step into a state usually denoted compound I. The rereduction back to the native form occurs in two single one-electron steps with an intermediate form denoted compound II.[15] The different peroxidases, for example, horseradish peroxidase (HRP),[16-24] fungal peroxidase (ARP),[12,22,23,25,26] lactoperoxidase (LRP),[22,27] chloroperoxidase (CRP),[28] catalase (CAT),[27] cytochrome-c-peroxidase,[29] and heme-containing peptides MP-9 (microperoxidase-9)[25,30] and MP-11,[31-33] catalyze the reduction of H₂O₂ in different electrode materials.

482
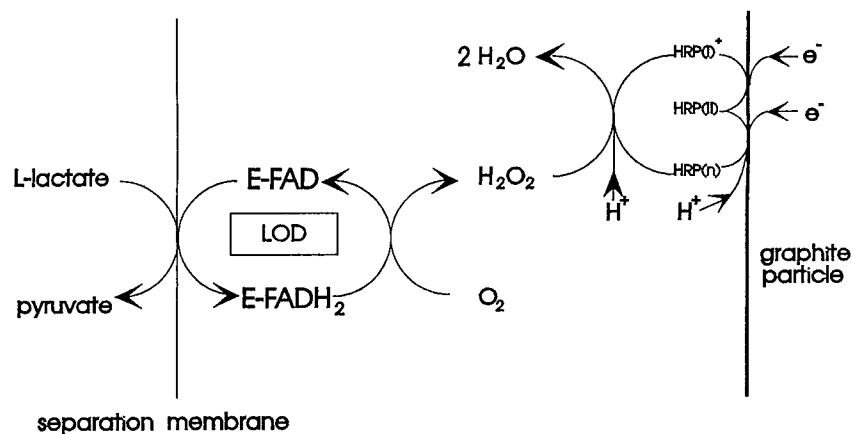
FIGURE 1. Reaction sequence for the L-lactate sensor based on coimmobilized LOD and HRP in carbon paste.

Experimental details and measuring setup were described elsewhere.[16,17] The flow-injection (FI) setup and reaction sequence are shown diagrammatically in FIGURES 1 and 2.

PREPARATION OF CARBON PASTE ELECTRODES

The carbon powders (CPs) were heated for 15 seconds at 700 °C in a muffle furnace and cooled to ambient temperature. To prepare enzyme-modified carbon pastes (EMCP), 100 mg of CP was suspended in 400 μL of solution prepared by
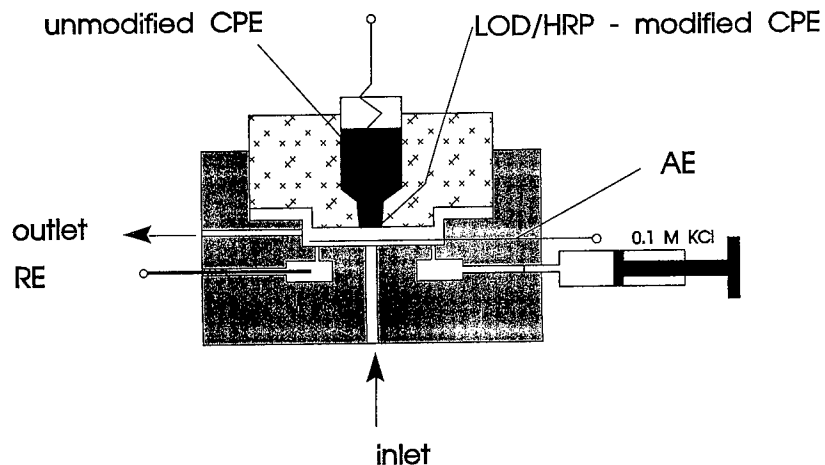
FIGURE 2. Schematic diagram of the flow-injection cell.

mixing 200 μL of enzyme solution containing 1 mg of lactate oxidase (LOD) and 1 mg of HRP/other peroxidases in 0.1 M sodium phosphate buffer and 200 μL of aqueous solution of the corresponding additives. The mixture was stored for 16 h at 4 °C in all cases and dried under water-jet vacuum for 4.5 h. The carbon paste was prepared by mixing 100 mg of the unmodified CP with 40 μL of silicone oil and filled into plastic syringe holders, leaving 3–4 mm empty in the tip to be filled with the enzyme-modified carbon paste.

RESULTS AND DISCUSSION

FIGURE 3 shows the dependencies of the electrode FI response to H_2O_2 and L-lactate, as well as the continuously measured background current on the electrode potential. As can be seen, lactate could be detected both cathodically and anodically. Because of the much better signal-to-background ratio, the cathodic detection
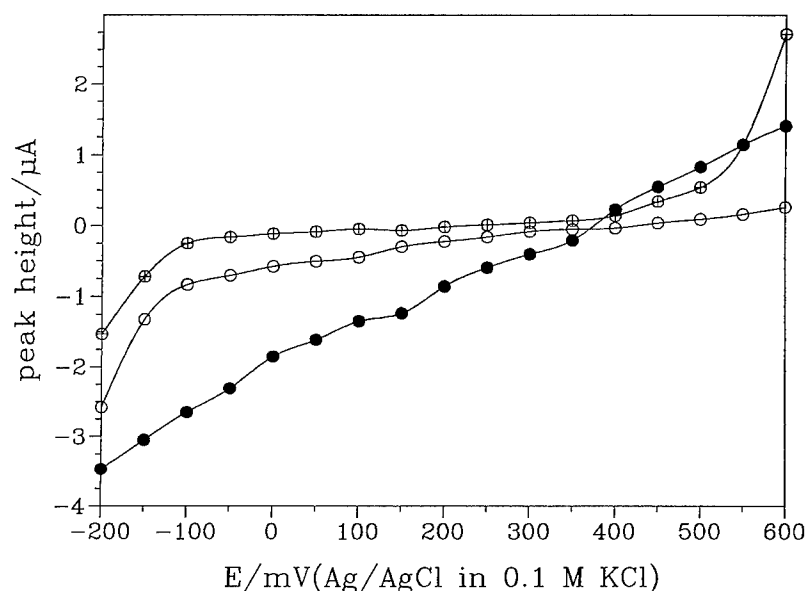
FIGURE 3. Dependencies of the electrode responses on the electrode potential at pH 7.0, 25 °C, measured in 0.1 M KPi; flow rate of 0.58 mL/min and injection volume of 50 μL. Symbols: (⊕) residual, (○) 0.50 mM H_2O_2, and (●) 5 mM L-lactate.

should be preferred and is possible in the potential range between +350 and −200 mV with higher sensitivity. The optimum potential range lies between −50 and +200 mV because the residual current lies around 0.

FIGURE 4 shows the double-logarithmic calibration graphs for the H_2O_2 and lactate detection recorded under FI conditions. The bienzyme electrode shows an almost linear behavior for the H_2O_2 detection between 0.01 and 0.2 mM. The lactate plot is also linear in the concentration range between 0.05 and 2 mM. The detection
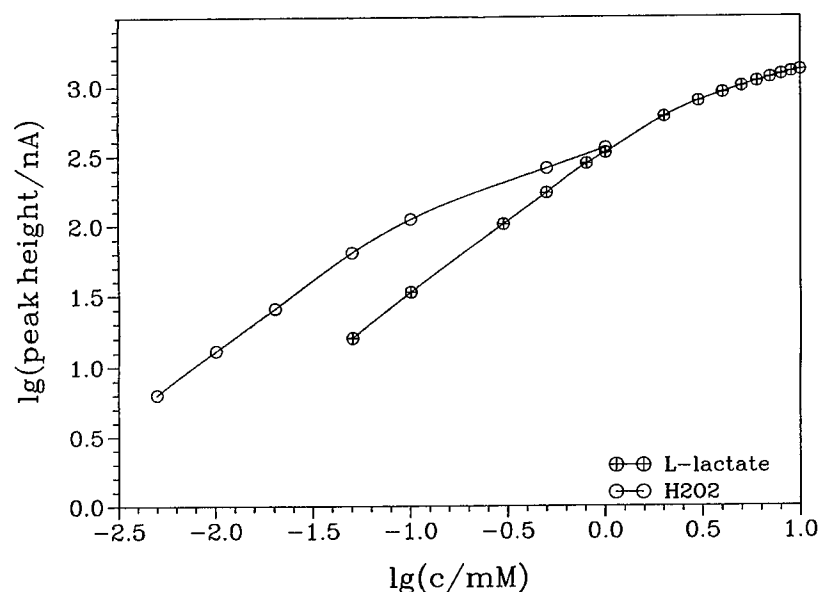
FIGURE 4. Double-logarithmic calibration graphs for H_2O_2 and L-lactate recorded at pH 7.0 with the sensor prepared by adsorptive coimmobilization in the presence of PEI.

limit lies between 0.5 and 2 μM for H_2O_2 and between 1 and 5 μM for L-lactate. TABLE 1 summarizes the kinetic constants characterizing the response.

Different experiments with various amounts of enzymes (FIGURE 5) show that the 1:1 mass ratio of LOD to HRP results in the highest sensitivity for both hydrogen peroxide and L-lactate.

Polyethylenimine (PEI) was previously shown in many instances to increase the sensitivity of enzyme-modified electrodes when added to the paste.[12–14] Here, the sensitivities for lactate and hydrogen peroxide detection were almost linearly increasing with PEI added to the paste. In part, this can be explained by an increase of the

TABLE 1. Kinetic Parameters of H_2O_2 and Lactate Detection for Different Additives[a]

	H_2O_2		Lactate	
Additives	I_{max} (nA)	K_m (app) (μM)	I_{max} (nA)	K_m (app) (μM)
p-L-lysine	1186 ± 137	721 ± 91	976 ± 10	2234 ± 108
p-L-arginine	880 ± 109	423 ± 191	798 ± 61	2673 ± 565
spermidine	1435 ± 320	427 ± 215	835 ± 62	2271 ± 545
spermine	1070 ± 157	460 ± 178	336 ± 30	2054 ± 656
PEI: 0.64 mg, pH 9.0	290 ± 66	624 ± 347	319 ± 50	3947 ± 2787
PEI: 4.00 mg, pH 7.0	752 ± 147	593 ± 188	466 ± 73	3949 ± 1308

[a]Calculated from electrochemical Hanes plots; confidence limit $\alpha = 0.05, n = 4$.

electrochemical microsurface.[34] However, the noise level is also increasing with the amount of PEI taken to the paste.

Positively charged poly-L-amino acids when added to the paste cause an essential increase in the sensitivity compared to PEI. By comparing the effect of PEI and poly-L-amino acids, it may be concluded that there is an additional effect besides the simple increase in the electrochemical surface. Highest H_2O_2 sensitivity is found after the addition of spermidine and spermine and, for L-lactate, by addition of poly-L-lysine followed by spermidine and poly-L-arginine (see FIGURES 6 and 7). HRP and LOD (TABLE 1) are influenced in a different manner by the additives. A strong electrostatic interaction between the positively charged additives and LOD can be postulated, which can cause an encaging of the LOD by the high molecular cationic polyelectrolytes, PEI, poly-L-lysine, and poly-L-arginine. The same reason
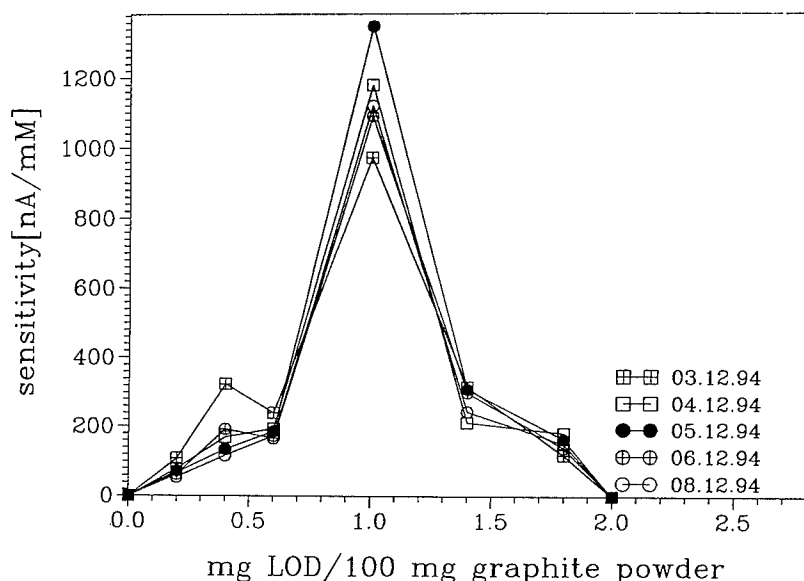
FIGURE 5. Dependence of the lactate sensitivity on the ratio of the taken amounts of LOD to HRP; all values are recorded from three electrodes; three injections per concentration point.

cannot be explained in the case of HRP-additive spermidine. It may be assumed especially that the spermidine acts as a promoter for the electron transfer between HRP and the carboneous material. Spermine and spermidine have been previously shown to promote a direct electron transfer reaction between redox enzymes and electrodes.[35]

The highest degree of stabilization (FIGURE 8) can be achieved by the addition of poly-L-arginine to the carbon paste. It is not unreasonable to assume symplex formation of LOD with the cationic polyelectrolytes, together with a considerably decreased solubility of the enzyme in the aqueous electrolyte and an increased thermal stability, as postulated by Gibson et al.[10]
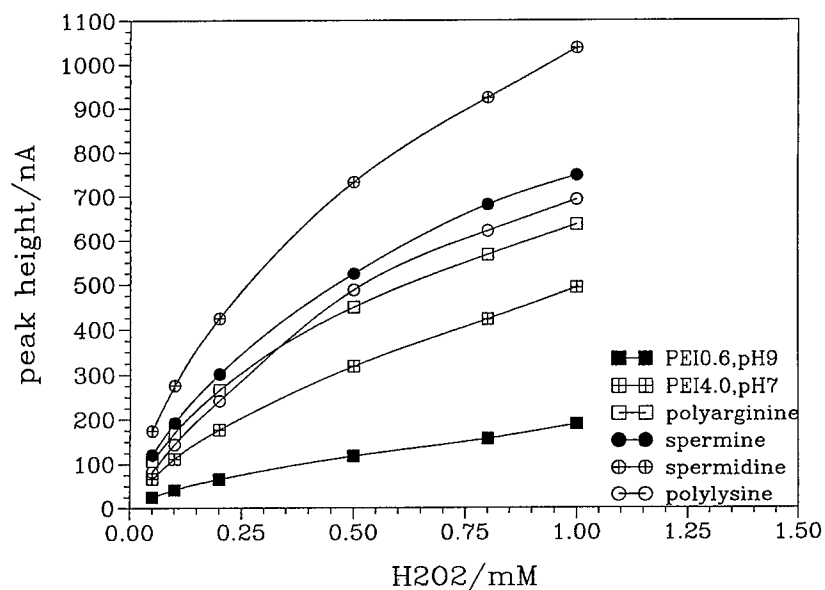
FIGURE 6. Calibration plots for H_2O_2 determination recorded for different additives and measuring conditions as in FIGURE 3.
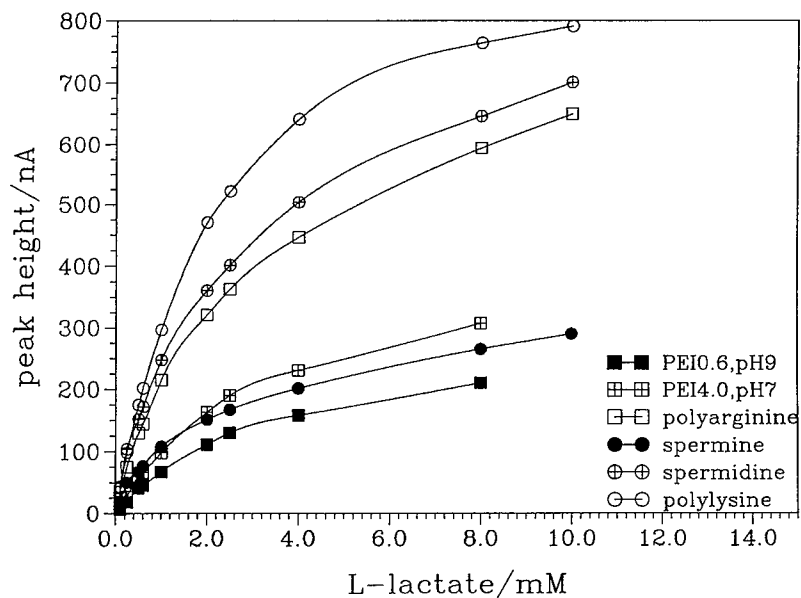
FIGURE 7. Calibration plots for lactate determination recorded for different additives and measuring conditions as in FIGURE 3.
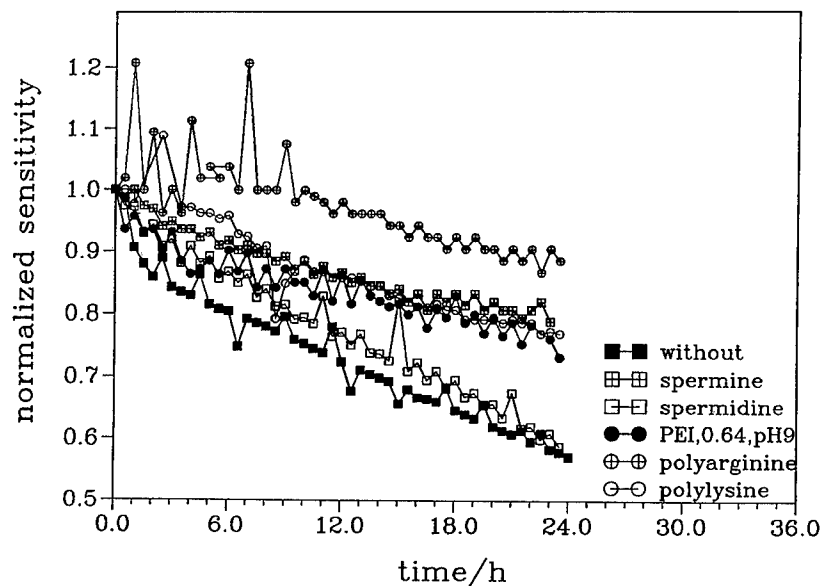
FIGURE 8. Long-term stability of HRP/LOD-modified CPEs presented as the normalized sensitivities versus measuring time; one injection per 30 minutes; measuring conditions as in FIGURE 3.
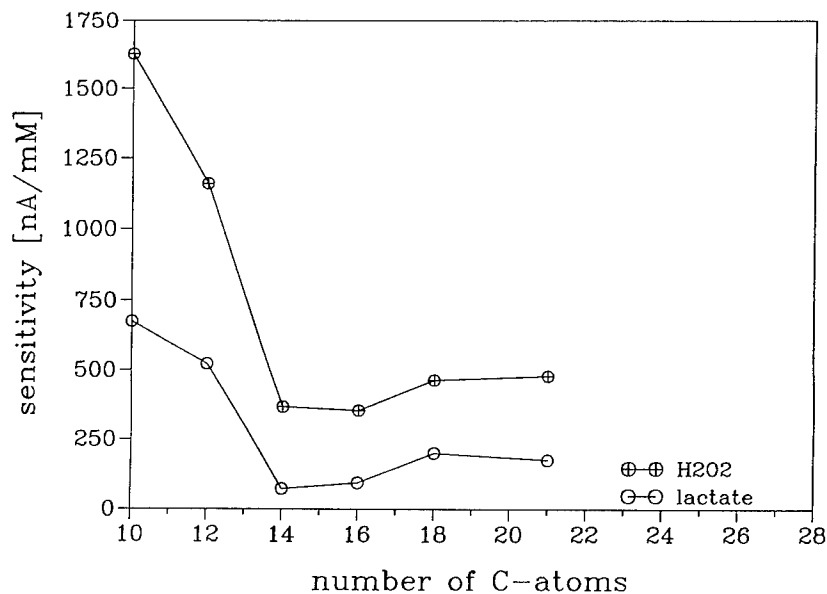
FIGURE 9. Dependencies of H_2O_2 and lactate sensitivity on the number of C-atoms in the n-paraffins used for the EMCPE preparation; measuring conditions as in FIGURE 3.

The sensitivity of the biosensor is decreasing with the increase of C-number up to C16 as a pasting liquid (FIGURE 9, TABLE 2). However, by using the solid octadecane, a considerable increase in the sensitivity was obtained. Thus, octadecane is an attractive pasting medium to prepare solid-state HRP/LOD-modified electrodes. The use of higher paraffins is limited by the increasing melting point and otherwise by the necessary use of a fluidizing solvent that must be evaporated after mixing of the carboneous powder and the paste binder.

The highest lactate sensitivities were found by using silicone oil and paraffin oil followed by octadecane, but the highest H_2O_2 sensitivity was found by using naphthene. However, in this case, n-hexane was used to dissolve the naphthene before adding the enzyme-modified graphite powder.

PEROXIDASES

Although several peroxidases were selected initially, only a few of them showed good electrocatalytic response to H_2O_2. FIGURE 10 shows some hydrodynamic

TABLE 2. Kinetic Parameters of H_2O_2 and Lactate Detection for Different Organic Liquids and Solids[a]

Pasting Medium	H_2O_2		Lactate	
	I_{max} (nA)	K_m (app) (μM)	I_{max} (nA)	K_m (app) (μM)
silicone oil	1052 ± 357	619 ± 391	1285 ± 140	3023 ± 879
C14	295 ± 45	343 ± 172	419 ± 34	1912 ± 528
C16	317 ± 47	484 ± 187	532 ± 64	3927 ± 1165
C18	749 ± 166	832 ± 380	1248 ± 322	5273 ± 2822
C21	572 ± 143	571 ± 189	653 ± 74	2661 ± 577
paraffin oil	1019 ± 151	762 ± 227	1305 ± 124	3589 ± 853
dinonyl-phthalate	450 ± 47	568 ± 131	670 ± 23	2656 ± 256
naphthene	1562 ± 187	467 ± 143	692 ± 41	1019 ± 159
stearyl-amine	27 ± 2	302 ± 57	22 ± 3	1074 ± 500

[a]Calculated from electrochemical Hanes plots; $\alpha = 0.05, n = 4$.

voltammograms recorded during repeated injections of L-lactate. The following peroxidases, ARP, HRP, MP-8, and MP-11, were selected because only those electrodes prepared with these peroxidases can provide an acceptable L-lactate sensitivity. It can be seen that L-lactate can be detected at electrode potentials in the optimal potential window between −50 and +200 mV versus Ag/AgCl. ARP and HRP showed a very similar behavior in this case. FIGURE 11 shows calibration graphs for the H_2O_2 detection for carbon paste electrodes (CPEs) prepared by modification with the selected peroxidases. With the exception of MP-11-modified CPEs, all CPEs show an excellent sensitivity with respect to H_2O_2. MP-8- and MP-11-modified CPEs show a higher degree of linearity in the selected concentration range, which may be explained by the higher number of electrocatalytically active centers on the electrode surface. The consequence would be greater apparent K_m values. ARP-modified CPEs show the highest H_2O_2 sensitivity.
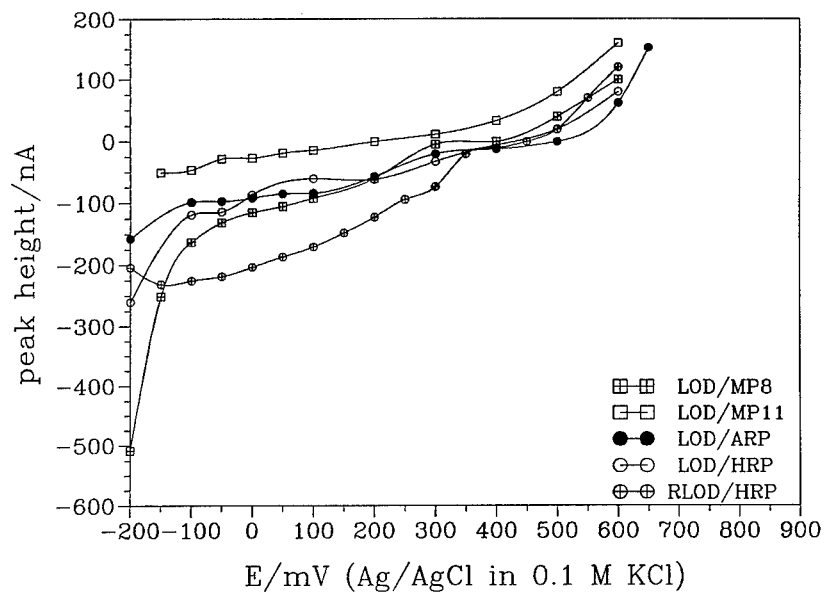
FIGURE 10. Hydrodynamic voltammograms recorded for 1 mM L-lactate; measuring conditions as in FIGURE 3.
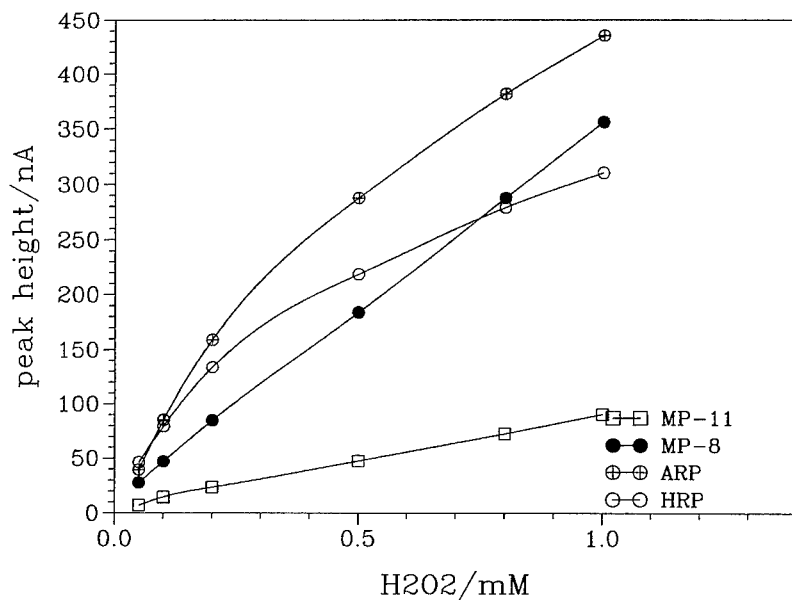
FIGURE 11. H_2O_2 calibration curves recorded with LOD/peroxidase-modified CPEs and at -50 mV versus Ag/AgCl; measuring conditions as in FIGURE 3.
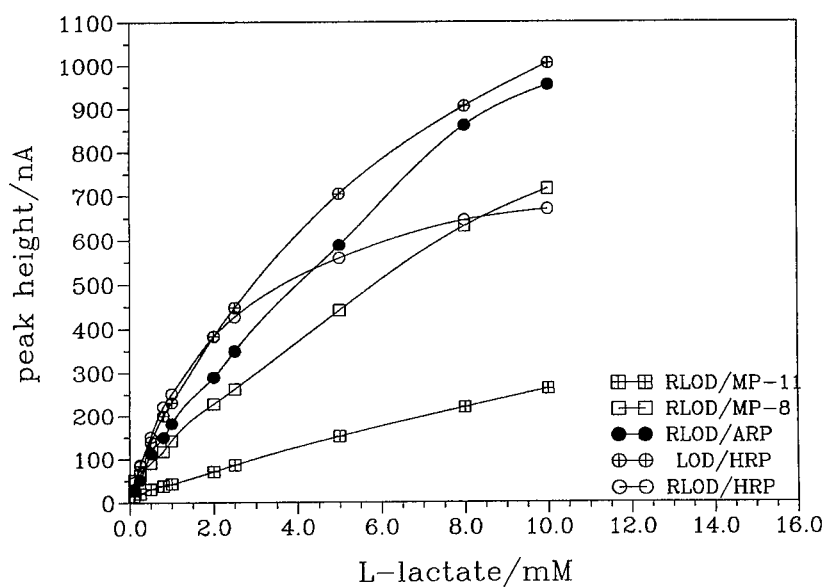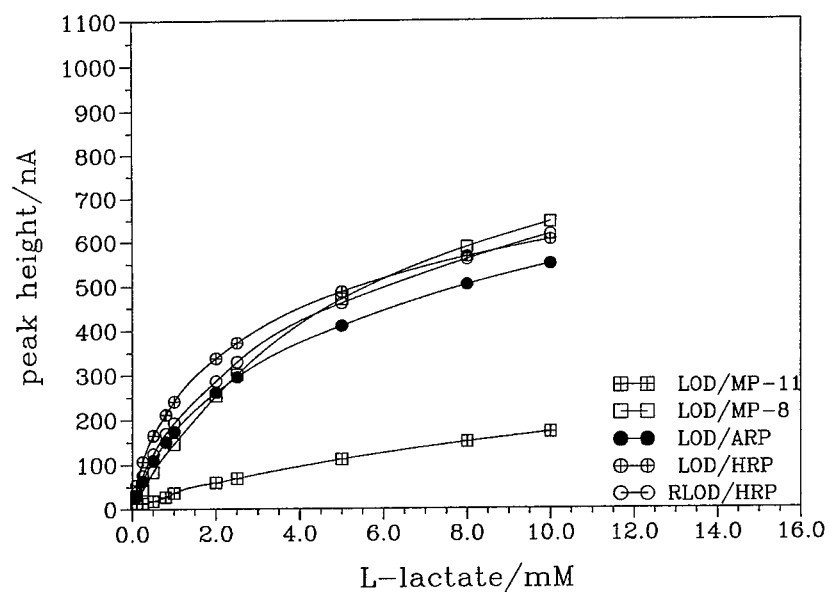
FIGURE 12. Lactate calibration curves recorded with (top) LOD/peroxidase- and (bottom) RLOD/peroxidase-modified CPEs; measuring conditions as in FIGURE 3.

FIGURE 12 shows calibration graphs for the lactate detection recorded with LOD- and RLOD-modified CPEs (note that the "R" stands for recombinant). No essential differences between the lactate sensitivities of the LOD-modified CPEs containing ARP, HRP, and MP-8 were found. The situation was similar for the corresponding RLOD-modified CPEs, although the differences between the ARP-, HRP-, and MP-8-modified CPEs were greater. In both series of experiments, the MP-11-modified CPEs showed the lowest sensitivity. Because the lactate sensitivities in both the RLOD- and the LOD-modified electrode series are not essentially influenced by three of the selected peroxidases (MP-8, HRP, and ARP), it can be concluded that the response is dominated by the corresponding lactate oxidase. Because both the LOD/MP-11- and the RLOD/MP-11-modified CPEs show a significantly higher degree of linearity compared to the other CPEs, the H_2O_2 detection catalyzed by MP-11 seems to be dominating.

ACKNOWLEDGMENTS

REFERENCES

1. DORDICK, J. S. 1989. Enzymatic catalysis in monophasic organic solvents. Enzyme Microb. Technol. **11:** 194–211.
2. ZAKS, A. & A. M. KLIBANOV. 1985. Enzyme-catalyzed processes in organic solvents. Proc. Natl. Acad. Sci. U.S.A. **82:** 3192–3196.
3. DABULISK, K. & A. M. KLIBANOV. 1993. Dramatic enhancement of enzymatic activity in organic solvents by lyoprotectants. Biotechnol. Bioeng. **41:** 566–571.
4. RICE, M. E., Z. GALUZ & R. N. ADAMS. 1989. Graphite paste electrodes: effect of paste composition and surface states on electron-transfer rates. J. Electroanal. Chem. **143:** 89–102.
5. ARMSTRONG, F. A., H. A. O. HILL & N. J. WALTON. 1988. Direct electrochemistry of redox proteins. Acc. Chem. Res. **21:** 407–413.
6. McNEIL, C. J., D. ATHEY & W. O. HO. 1995. Direct electron-transfer bioelectronic interfaces—application to clinical analysis. Biosens. Bioelectronics **10:** 75–83.
7. GIBSON, T. & J. R. WOODWARD. 1992. Protein stabilization in a biosensor system. *In* Biosensors and Chemical Sensors. ACS Symposium Series. Volume 487. P. G. Edelman & J. Wang, Eds.: 40–55.
8. GIBSON, T., I. J. HIGGINS & J. R. WOODWARD. 1992. Stabilization of analytical enzymes using a novel polymer-carbohydrate system and the production of a stabilized single reagent for alcohol analysis. Analyst **117:** 1293–1297.
9. GIBSON, T., J. N. HULBERT, S. M. PARKER, J. R. WOODWARD & I. J. HIGGINS. 1992. Extended shelf life of enzyme-based biosensors using a novel stabilization system. Biosens. Bioelectronics **7:** 701–708.
10. GIBSON, T., J. N. HULBERT & J. R. WOODWARD. 1993. Preservation of shelf life of enzyme-based analytical systems using a combination of sugars, sugar alcohols, and cationic polymers or zinc ions. Anal. Chim. Acta **279:** 185–192.
11. POPESCU, I. C., G. ZETTERBERG & L. GORTON. 1995. Influence of graphite powder, additives, and enzyme immobilization procedures on a mediatorless HRP-modified carbon paste electrode for amperometric flow-injection detection of H_2O_2. Biosens. Bioelectronics **10:** 443–461.
12. JOHANSSON, E., G. MARKO-VARGA & L. GORTON. 1993. Study of a reagent and mediatorless biosensor for D-amino acids based on co-immobilization of D-amino acid oxidase and peroxidase in carbon paste electrodes. J. Biomater. Appl. **8:** 146–173.
13. KACANICLIC, V., K. JOHNSSON, G. MARKO-VARGA, L. GORTON, G. JONSSON-PETTERSSON & E. CSOREGI. 1994. Amperometric biosensors for detection of L- and D-amino acids

based on co-immobilized peroxidase and L- and D-amino acid oxidases in carbon paste electrodes. Electroanalysis **6:** 381–390.

14. DOMINGUEZ, E., H. L. LANS, Y. OKAMOTO, P. D. HALE, T. A. SKOTHEIM, L. GORTON & B. HAHN-HAGERDAHL. 1993. A carbon paste electrode chemically modified with a phenothiazine polymer derivative and yeast alcohol dehydrogenase for the analysis. Biosens. Bioelectronics **8:** 229–237.

15. GORTON, L. 1995. Carbon paste electrodes modified with enzymes, tissues, and cells. Electroanalysis **7:** 23–45.

16. SPOHN, U., D. NARASAIAH & L. GORTON. 1995. A bienzyme carbon paste electrode for the amperometric detection of L-lactate at low potentials. Anal. Chim. Acta. In press.

17. NARASAIAH, D., U. SPOHN & L. GORTON. 1995. Simultaneous determination of D- and L-lactate by enzyme-modified carbon paste electrodes. Anal. Lett. In press.

18. JOHANSSON, G. & L. GORTON. 1989. An electrochemical sensor for hydrogen peroxide based on peroxidase adsorbed on a spectrographic graphite electrode. Electroanalysis **1:** 465–468.

19. WOLLENBERGER, U., V. BOGDANOVSKAYA, S. BOBRIN, F. SCHELLER & M. TARASEVICH. 1990. Enzyme electrodes using bioelectrocatalytic reduction of hydrogen peroxide. Anal. Lett. **23:** 1795–1808.

20. JONSSON-PETTERSSON, G. 1991. Reagentless hydrogen peroxide and glucose sensors based on peroxidase immobilized on graphite electrodes. Electroanalysis **3:** 741–750.

21. NARASAIAH, D. 1994. An enzyme electrode for hydrogen peroxide based on peroxidase immobilized on glassy carbon electrodes. Biosens. Bioelectronics **9:** 415–422.

22. CSOREGI, E., G. JONSSON-PETTERSSON & L. GORTON. 1993. Mediatorless electrocatalytic reduction of hydrogen peroxide at graphite electrodes chemically modified with peroxidases. J. Biotechnol. **30:** 315–337.

23. CSOREGI, E., L. GORTON, G. MARKO-VARGA, A. TUDOS & W. KOK. 1994. Peroxidase-modified carbon-fiber microelectrodes in flow-through detection of hydrogen peroxide and organic peroxides. Anal. Chem. **66:** 3604–3610.

24. HO, W. O., D. ATHEY, C. MCNEIL, H. HAGEN, G. EVANS & W. MULLEN. 1993. Mediatorless horseradish-peroxidase enzyme electrodes based on activated carbon: potential application to specific binding assay. J. Electroanal. Chem. **351:** 185–197.

25. TATSUMA, T., M. GONDAIRA & T. WATANABE. 1992. Peroxidase incorporated polypyrrole membrane electrodes. Anal. Chem. **64:** 1183–1187.

26. KULYS, J. & R. D. SCHMID. 1990. Mediatorless peroxidase electrode and preparation of bienzyme sensors. Bioelectrochem. Bioenerg. **24:** 305–311.

27. TATSUMA, T., K. ARIYAMA & N. OYAMA. 1995. Electron-transfer from a polythiophene derivative to compound-I and compound-II. Anal. Chem. **67:** 283–287.

28. RUZGAS, T., L. GORTON, J. EMNEUS & G. MARKO-VARGA. 1995. Direct bioelectrocatalytic reduction of hydrogen peroxide at a chloroperoxidase-modified graphite electrode. Anal. Proc. **6:** 207–208.

29. ARMSTRONG, F. & A. LANNON. 1988. Towards macromolecular recognition at electrodes: fast interfacial electron transfer to cytochrome c peroxidase at graphite electrodes is promoted by amino glycosides. Biochem. Soc. Trans. **16:** 842–843.

30. TATSUMA, T. & T. WATANABE. 1991. Peroxidase model electrodes: heme peptide–modified electrodes as reagentless sensors for hydrogen peroxide. Anal. Chem. **63:** 1580–1585.

31. RAZUMAS, V., J. KAZLAUSKAITE, T. RUZGAS & J. KULYS. 1992. Bioelectrochemistry of microperoxidases. Bioelectrochem. Bioenerg. **28:** 159–176.

32. LOTZBEYER, T., W. SCHUHMANN, E. KATZ, J. FALTER & H. SCHMIDT. 1994. Direct electron transfer between the covalently immobilized enzyme microperoxidase MP-11 and a cystamine-modified gold electrode. J. Electroanal. Chem. **377:** 291–294.

33. MABROUK, P. A. 1995. First direct interfacial electron transfer between a biomolecule and a solid electrode in non-aqueous media: direct electrochemistry of microperoxidase-11 at a glassy carbon in dimethyl sulfoxide solution. Anal. Chim. Acta **307:** 245–251.

34. KULYS, J., L. GORTON, E. DOMINGUEZ, J. EMNEUS & H. JARSKOG. 1994. Electrochemical characterization of carbon pastes modified with proteins and polycations. J. Electroanal. Chem. **372:** 49–55.

35. HILL, H. A. O. & N. I. HUNT. 1993. Direct and indirect electrochemical investigations of metalloenzymes. *In* Methods in Enzymology. Volume 227. J. F. Riordan & B. L. Vallee, Eds.: 501–522. Academic Press. New York.

Optimization of Glucose-1-Phosphate Production Employing Glucan-Phosphorylases in Continuous Enzyme Membrane Reactors

RICHARD GRIESSLER, ANDREAS WEINHÄUSEL,
DIETMAR HALTRICH, KLAUS D. KULBE,
AND BERND NIDETZKY[a]

Division of Biochemical Engineering
Institute of Food Technology
Universität für Bodenkultur Wien
1190 Vienna, Austria

INTRODUCTION

The use of soluble enzymes in continuous biocatalytic processes has been proven to be a valuable approach, especially when high productivities and space-time yields have to be achieved.[1,2] The ultrafiltration membrane reactor is the corresponding tool with regard to process technology to perform the continuous enzymatic conversion reactions. The particular advantages of a soluble enzyme reactor include the application of high volumetric activities of the biocatalyst, the bioconversion in homogeneous solutions with a concomitant easy process control, and the absence of intrinsic mass-transfer limitations for multicomponent reactions.[1-5] With the sufficiently stable enzyme fully retained by an ultrafiltration membrane, many cycles of substrate conversion can be accomplished with only an initial dosage of biocatalyst being required, whose synthetic potential is thus efficiently exploited.

In view of an enzymatic synthesis of glucose-1-phosphate (Glc-1-P), a number of α-glucan-phosphorylases from bacteria and plants have been studied in our laboratory with regard to their suitability in continuous process development.[6-8] Glc-1-P is a compound with various possible applications, especially medically oriented.[9] The phosphorylases, in turn, are capable of catalyzing the degradation and the synthesis of α-glucans (starch, glycogen, maltodextrins) according to equation 1:

$$(\alpha\text{-1,4-D-glucoside})_n + P_i \Leftrightarrow (\alpha\text{-1,4-D-glucoside})_{n-1} + \alpha\text{-D-Glc-1-}P. \qquad (1)$$
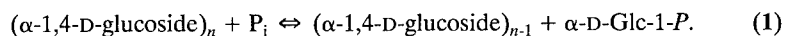
Although *in vivo* the role of glucan-phosphorylases is the mobilization of storage α-glucan in the form of Glc-1-P, the thermodynamics of the reaction in equation 1 point to a nonfavorable equilibrium constant with regard to Glc-1-P production.[6,7] Despite this fact, we were interested in optimizing the reaction conditions for the phosphorylase-catalyzed synthesis of Glc-1-P, aiming at improving the attainable

---

[a]To whom all correspondence should be addressed.

degrees of phosphate conversion and at identifying important factors that govern the productivity of a continuous α-glucan-phosphorylase enzyme reactor. The enzyme used was a recently isolated phosphorylase from *Corynebacterium callunae.*[6,8]

RESULTS AND DISCUSSION

Optimized Reaction Conditions

During the enzymatic synthesis of Glc-1-*P*, the maximum attainable product concentration will be limited either by phosphate or by the glucan substrate (equation 1). Therefore, studies on the reaction equilibrium have usually been carried out in the presence of a large surplus of degradable glucan, whereas the maximum degradability of the glucan has been assayed at nonlimiting phosphate concentration such that the final degree of phosphate conversion was in the range of 10%. TABLE 1 clearly demonstrates that the concentration of maltodextrin has no influence on the equilibrated fraction of phosphate converted in Glc-1-*P*.

At a given reaction temperature of 30 °C and a pH of 7.5, approximately 18% of the initial phosphate is converted in the reaction equilibrium. When a substrate like maltodextrin is considered, the maximum degree of conversion in Glc-1-*P* may be hampered not only by the limit dextrin of the phosphorylase (maltotetraose or

TABLE 1. Equilibrium of the Phosphorolytic Reaction (Glc-1-*P*/Initial Phosphate) in 300 mM Phosphate Buffer, pH 7.5 and 30 °C, at Different Concentrations of Maltodextrin

Maltodextrin [mg/mL]	70	148
Glc-1-*P* [mM]	50.62	51.09
Equilibrium [G-1-*P*/P$_i$]	0.179	0.177

maltopentaose), but also by glycosidic linkages present in maltodextrin other than of the α-1,4 type. Even after exhaustive incubation with phosphorylase, a maximum of approximately 40% glucan could be degraded. Simultaneous or sequential treatment of the substrate with pullulanase (120 units/g glucan; 12 h) is only moderately effective (+10% in conversion). In fact, as judged from an analysis by thin-layer chromatography of the resulting reaction mixture, no uniform end product is obtained upon phosphorylase action on the pretreated substrate.

Because glucose-1-phosphate not only represents the product of the phosphorolysis reaction, but also is the substrate in the reverse direction of reaction (glucan synthesis in equation 1), its possible inhibitory effect on phosphorolysis is very difficult to quantify. Assays in the presence of low concentrations of Glc-1-*P* seem to support the hypothesis of inhibition by Glc-1-*P* (FIGURE 1). In addition, the time courses of Glc-1-*P* synthesis have been monitored at various initial concentrations of maltodextrin and phosphate. Their analysis revealed at least biphasic kinetics with respect to the incubation time. Although the reaction apparently proceeds close to the expected initial rate up to approximately 15–20 mM Glc-1-*P*, a significantly
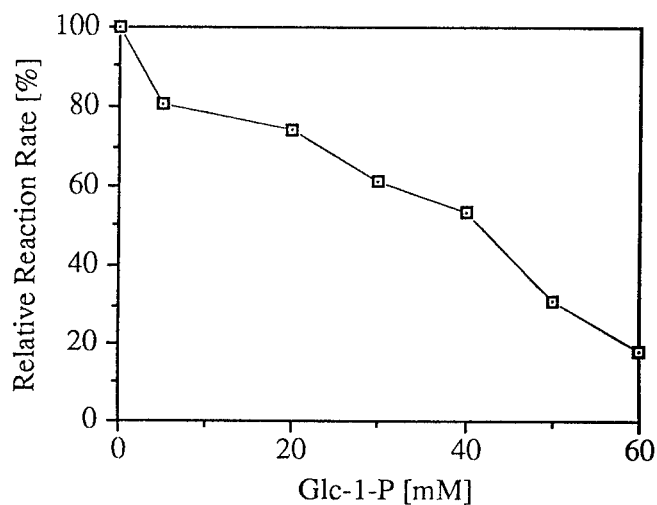
FIGURE 1. Inhibitory effect of Glc-1-*P* on phosphorylase action in 300 mM phosphate buffer, pH 7.5 and 30 °C, in the direction of phosphorolysis.

reduced reaction rate is seen above this concentration, even at very incomplete degrees of conversion, that is, less than 10% of phosphate and less than 10% of maltodextrin converted (FIGURE 2). It is especially clear from the data in FIGURE 3 that the equilibrium concentrations of Glc-1-*P* are attained in an extremely slow manner, no matter which concentration of maltodextrin is chosen. We conclude from
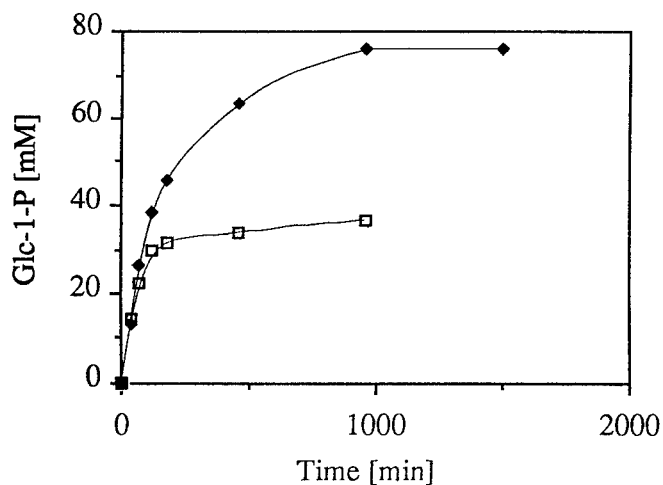
FIGURE 2. Conversion of 95 g/L maltodextrin by 0.3 U/mL phosphorylase in 300 mM (□) and 600 mM (◆) phosphate buffer, pH 7.5 and 30 °C.

these results that a continuous conversion process must not operate at conditions close to this equilibrium, which in turn would lead to extremely low productivities.

Continuous Conversions

Two different reactor systems were used throughout this study. A membrane reactor with a flat membrane configuration (dead-end filtration, DE, 80-mL volume) and a recirculating reactor system with an external ultrafiltration membrane module (cross-flow filtration, CF, 120-mL volume) were employed. A schematic representa-
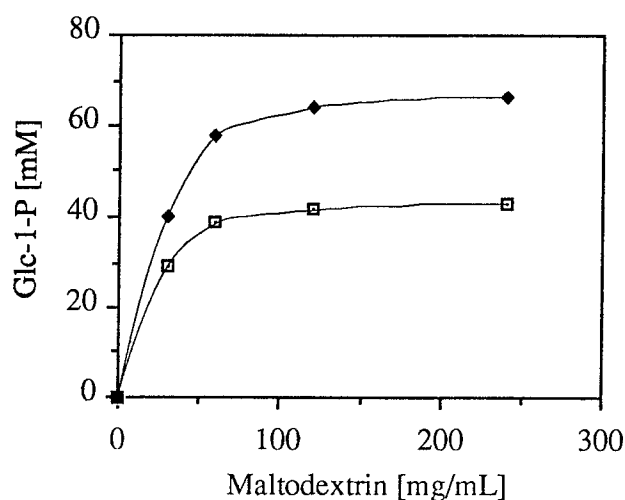
FIGURE 3. Conversion by 0.8 U/mL phosphorylase in 600 mM phosphate buffer, pH 7.5 and 30 °C, at different maltodextrin concentrations after 90 min (□) and 240 min (◆) of incubation time.

tion of the experimental onset is shown in FIGURE 4. The continuous conversion studies have been carried out with the aim of identifying the operational stability of the glucan-phosphorylase in the recirculating reactor system and comparing the productivities in the two membrane reactors. Data of a typical continuous conversion experiment in the DE reactor are given in FIGURE 5 and illustrate the effect of varying dilution rates on the production of Glc-1-*P* using phosphate-limited reaction conditions. The reactor productivities were evaluated at the corresponding dilution rates and indications for a roughly linear relation of productivity and dilution rate are found. Aiming at identifying an optimal operational point of the continuous reactor, the dilution rate was increased in a stepwise manner and the concentration of Glc-1-*P* was measured over a period of 3–5 reactor cycles. In fact, even when a 30-kDa ultrafiltration membrane was employed, maltodextrin started to accumulate due to significant retention at dilution rates higher than 0.25 h^{-1}, probably as a result of membrane fouling.
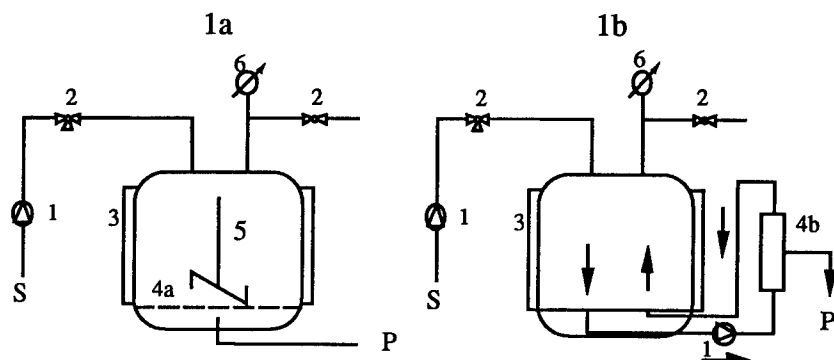
FIGURE 4. Setup for experiments in a continuous stirred-tank reactor with a flat membrane (1a) and an external filtration module (1b). Terms: S, substrate feed; P, product stream; 1, pump; 2, valve; 3, cooling jacket; 4a, flat membrane; 4b, cross-flow membrane; 5, magnet stirrer; 6, pressure gauge.

We have thus used a CF reactor for further experiments. Results of the phosphorylase action in the continuous CF reactor are graphically represented in FIGURE 6. Although productivities are definitely improved even under not-yet-optimized conditions in this reaction system when comparison is made with the DE reactor (TABLE 2) and also no apparent membrane fouling occurred, the operational stability of the phosphorylase is almost threefold reduced. The decreased half-life of the enzyme is most probably due to its sensitivity to shear stress, a behavior that we
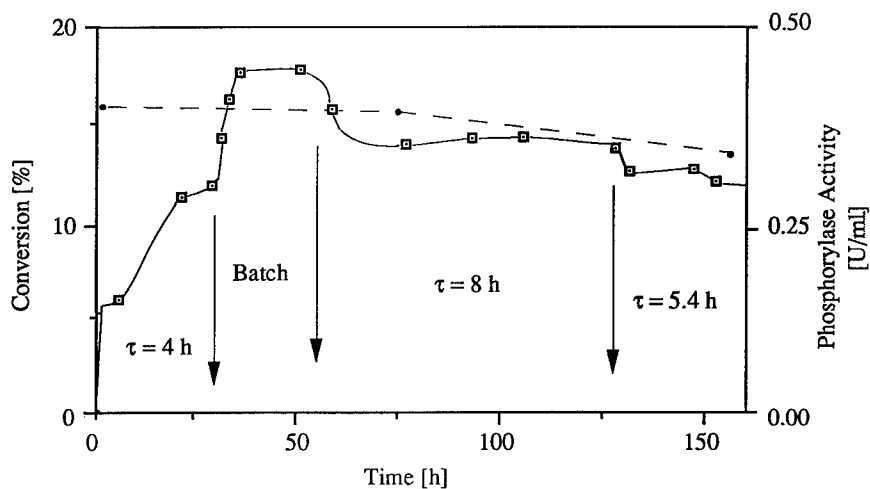
FIGURE 5. Continuous conversion of 60 g/L maltodextrin in 300 mM phosphate buffer, pH 7.5 and 30 °C, by *C. callunae* phosphorylase (□, % conversion of phosphate; ●, enzyme activity). τ is the average residence time.
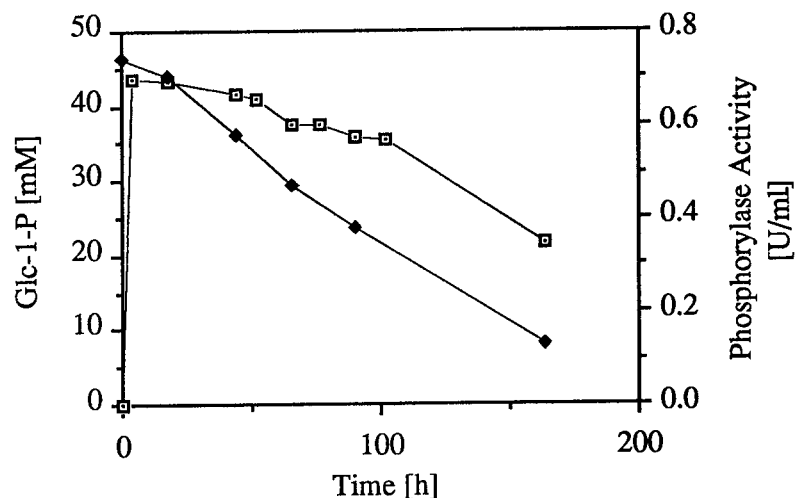
FIGURE 6. Continuous conversion of 60 g/L maltodextrin in 500 mM phosphate buffer, pH 7.5, at 30 °C by *C. callunae* phosphorylase in a continuous stirred-tank reactor with an external cross-flow filtration module (□, Glc-1-*P*; ◆, enzyme activity). Dilution rate = 0.33 h⁻¹; recirculation rate = 2.5 min⁻¹.

have noticed for other glucan-phosphorylases as well (Eis, Griessler, and Nidetzky; unpublished). Addition of BSA to reduce the amount of phosphorylase nonspecifically bound to the ultrafiltration membrane or the reactor vessel had only minor effects on the phosphorylase activity and stability. If Glc-1-*P* was to be produced by the phosphorolytic conversion of α-glucans, efficient means for phosphate recovery and for the separation of the product and phosphate would have to be developed. Current methods available from the literature employing column chromatographic separation techniques do not seem adequate for a large-scale isolation of Glc-1-*P* from dilute product mixtures.[10] Therefore, at least at present, the use of sucrose phosphorylase for the conversion of sucrose in fructose and Glc-1-*P* appears superior to an α-glucan-phosphorylase-catalyzed synthesis, especially with regard to the reaction equilibrium.[11]

TABLE 2. Process Performance of *C. callunae* Phosphorylase at 30 °C in Two Different Reactor Types

	Phosphate [mM]	Initial Enzyme Activity [U/mL]	Half-life [days]	Dilution Rate [h⁻¹]	Productivity[a] [mmol Glc-1-*P*/(L·h)]
DE reactor	300	0.70	14	0.25	7.4
CF reactor	500	0.70	5	0.33	15.3

[a]Approximately 10% conversion of phosphate.

REFERENCES

1. PRAZERES, D. M. F. & J. M. S. CABRAL. 1994. Enzymatic membrane bioreactors and their applications. Enzyme Microb. Technol. **16:** 738–750.
2. KULA, M. R. & C. WANDREY. 1987. Continuous enzymatic transformation in an enzyme membrane reactor with simultaneous NADH regeneration. Methods Enzymol. **136:** 9–21.
3. WICHMANN, R., C. WANDREY, A. F. BÜCKMANN & M. R. KULA. 1981. Continuous enzymatic transformation in an enzyme membrane reactor with simultaneous NAD(H) regeneration. Biotechnol. Bioeng. **23:** 2789–2802.
4. HOWALDT, M., A. GOTTLOB, K. D. KULBE & H. CHMIEL. 1988. Simultaneous conversion of glucose/fructose mixtures in a membrane reactor. Ann. N.Y. Acad. Sci. **542:** 400–405.
5. HOWALDT, M., K. D. KULBE & H. CHMIEL. 1987. Minimizing enzyme requirement by choice of appropriate reactor type. Ann. N.Y. Acad. Sci. **506:** 669–675.
6. WEINHÄUSEL, A., B. NIDETZKY, M. ROHRBACH, B. BLAUENSTEINER & K. D. KULBE. 1994. A new maltodextrin phosphorylase from *Corynebacterium callunae* for the production of glucose-1-phosphate. Appl. Microbiol. Biotechnol. **41:** 510–516.
7. WEINHÄUSEL, A., B. NIDETZKY, C. KYSELA & K. D. KULBE. 1995. Application of *Escherichia coli* maltodextrin-phosphorylase for the continuous production of glucose-1-phosphate. Enzyme Microb. Technol. **17:** 140–146.
8. NIDETZKY, B., A. WEINHÄUSEL, R. GRIESSLER & K. D. KULBE. 1995. Enzymatic synthesis of α-glucose-1-phosphate: a study employing a new maltodextrin phosphorylase from *Corynebacterium callunae*. J. Carbohydr. Chem. **14:** 1017–1028.
9. VANDAMME, E., J. VAN LOO, L. MACHTELINCKX & A. DE LAPORTE. 1987. Microbial sucrose phosphorylase: fermentation, process properties, and biotechnical applications. Adv. Appl. Microbiol. **32:** 163–201.
10. HOKSE, H. 1983. Purification of α-glucose-1-phosphate. Stärke/Starch **353:** 101–102.
11. GUIBERT, A. & P. MONSAN. 1988. Production and purification of sucrose phosphorylase from *Leuconostoc mesenteroides*. Ann. N.Y. Acad. Sci. **542:** 307–311.

Real-Time Biomolecular Interaction Studies Based on Peroxidase Label and Chemiluminescent Flow-Injection System

ALEXANDER P. OSIPOV, NATALIYA V. ZAITSEVA,
AND ALEXEY M. EGOROV

Department of Chemical Enzymology
Faculty of Chemistry
M. V. Lomonosov Moscow State University
Moscow 119899, Russia

INTRODUCTION

The study of biomolecular interactions is essential for exploring the structure-function relationships of biomolecules. The characterization of the kinetics and thermodynamics of such interactions is very important for understanding processes of molecular recognition and biological functions. Real-time Biomolecular Interaction Analysis (BIA) represents a new technology for studying biomolecular interactions in real time, without labeling any of the interactants. Recently, several instrumental approaches were proposed for the continuous detection of such interactions.[1] There are now three instruments on the market for label-free, real-time monitoring of intermolecular interactions: BIOS-1 from Artificial Sensor Instruments (ASI; Zurich, Switzerland), IAsys from Fisons Applied Sensor Technology (Fisons; Cambridge, United Kingdom), and BIAcore from Pharmacia Biosensor (Biosensor; Uppsala, Sweden/Piscataway, New Jersey).[2] These instruments also allow the possibility of measuring the quantity of immunocomplexes on the surface of the active part of the biosensors in a real-time regime. However, one of the reasons limiting a wide application of these instruments is their high cost.

The flow-injection method proposed earlier in our laboratory based on the thin-layer flow cell and on the reaction of enhanced chemiluminescence for detection of peroxidase label has made it possible to follow the biomolecular interaction in a real-time mode.[3] This paper reports on our determination of the kinetic rate constants for some processes of biomolecular interactions on the boundary liquid–solid phase (sensor surface) by use of this technique.

MATERIALS AND METHODS

Chemicals/substrates for horseradish peroxidase (HRP) were supplied by Sigma. HRP (RZ $\approx$ 3.1) was obtained from Agrotecnika (Kiev, Ukraine). Acids and salts of analytical grade were supplied by Reakhim (Moscow). Luminol and p-iodophenol were recrystallized. All solutions were prepared with water purified with a Milli-Q system (Millipore). Monoclonal antibodies against peroxidase, simazine, and 2,4-

dichlorophenoxyacetic acid (2,4-D) and their conjugates with peroxidase were supplied by Immunotek (Moscow).

Immobilization Procedures

A polystyrene cover of standard microplate (Nunc Immunoplates, MaxiSorp) was cut into pieces (0.7 × 0.7 cm). The pieces were incubated for different periods of time in a solution of peroxidase-labeled monoclonal antibodies against 2,4-D (1 μg/mL). After washing with PBST (0.1 M phosphate buffer, 0.14 M NaCl, 0.05% Triton X-100), a piece was placed in a cuvette of a luminometer containing the substrate mixture (5×10^{-5} M luminol and p-iodophenol and 1 mM H_2O_2 in Tris-HCl buffer, pH 8.6). The cuvette was then placed in the measuring chamber of a luminometer and the maximum light intensity was recorded in 1 minute.

To study the kinetics of immobilization of antibodies in the flow cell, the solution of monoclonal antibodies against 2,4-D (1 μg/mL) was pumped through the cell for different time periods (flow rate was 0.35 mL/min). After washing with PBST, the substrate mixture (5×10^{-5} M luminol and p-iodophenol and 1 mM H_2O_2 in Tris-HCl buffer, pH 8.6) was pumped through the cell and the maximum light intensity was recorded.

Instrumentation

A Tecator FIA 5020 instrument (Sweden) equipped with three additional peristaltic pumps and a double-injection valve was used. An LKB 1250 luminometer was used to detect the chemiluminescent reaction.

RESULTS

The schematic of the thin-layer flow-through cell is shown in FIGURE 1. It consists of two transparent pieces of polystyrene cover as immunoassay microplates with an outlet and inlet. The membrane spacer creates a 0.5-cm-wide, 0.01-cm-thick, and 2-cm-long flow channel. The two polystyrene plates were clutched between two steel plates (one of them had an oval hole for passing the light from the wall to a photomultiplier tube) and were tightly held together by screws. This cell was directly mounted into the chamber of the luminometer in front of the photomultiplier window. If the substrate solution moves through the cell, the reaction of enhanced chemiluminescence catalyzed by peroxidase bound in a complex on the inner parts of the cell takes place. The intensity of the chemiluminescence is proportional to the quantity of peroxidase label on the cuvette walls.

First, we studied the kinetics of the adsorption of peroxidase-labeled antibodies on the inner walls of the flow-through cell and on the pieces of polystyrene plates in static conditions. In both cases, equal concentrations of labeled antibodies and surface squares for adsorption were used. The results of comparative experiments are shown in FIGURES 2A and 2B.

The time for achieving equilibrium conditions in the case of the flow-through cell is considerably shorter than in static conditions and equals several minutes. We also showed that the kinetics of the interaction of the peroxidase-labeled model antigen simazine with specific monoclonal antibodies immobilized on the inner walls of the flow cell had the same pattern (FIGURE 3). The reason for this acceleration may be the following. The reaction of the adsorption or interaction of the antigen with immobilized antibodies is controlled by a diffusion of reactants through the unstirred fluid layer adjoined to a surface of the solid phase. The thickness of the diffusion boundary layer is on the order of approximately 100 μm. In an ultranarrow cell, its thickness is comparable with the thickness of the unstirred layer. In the flow regime, due to displacement of a fluid in the channel, the thickness of the unstirred layer becomes smaller, the diffusion distance between reactants is reduced, and the rate of reaction is increased.
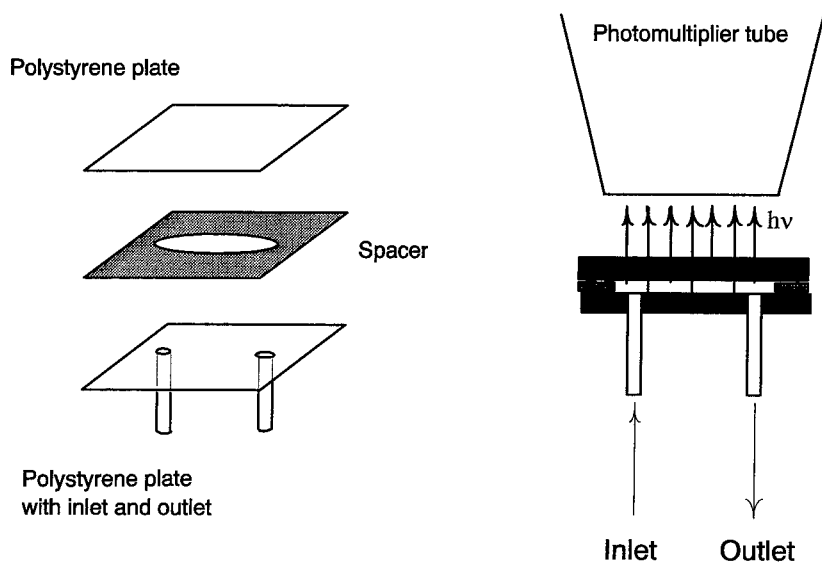
FIGURE 1. Schematic of the thin-layer flow cell with chemiluminescent detection.

A general idea of an experimental setup for intermolecular interaction measurements using our method is very similar to the above-mentioned optical biosensor systems. One partner of a reaction pair (for instance, antibody) is immobilized on the sensor surface, whereas the other reaction partner (peroxidase-labeled antigen) is in a free flow along the surface. Under the conditions of a flow-through experiment, constant replenishment of the antigen in a solution takes place and its concentration in the bulk phase is constant at any given time. The association and dissociation processes run continuously. By replacing the reagent solution with a solution of substrates, one can measure the kinetics of binding the labeled reagent with the immobilized component on the cell surface as a function of time. As a result,
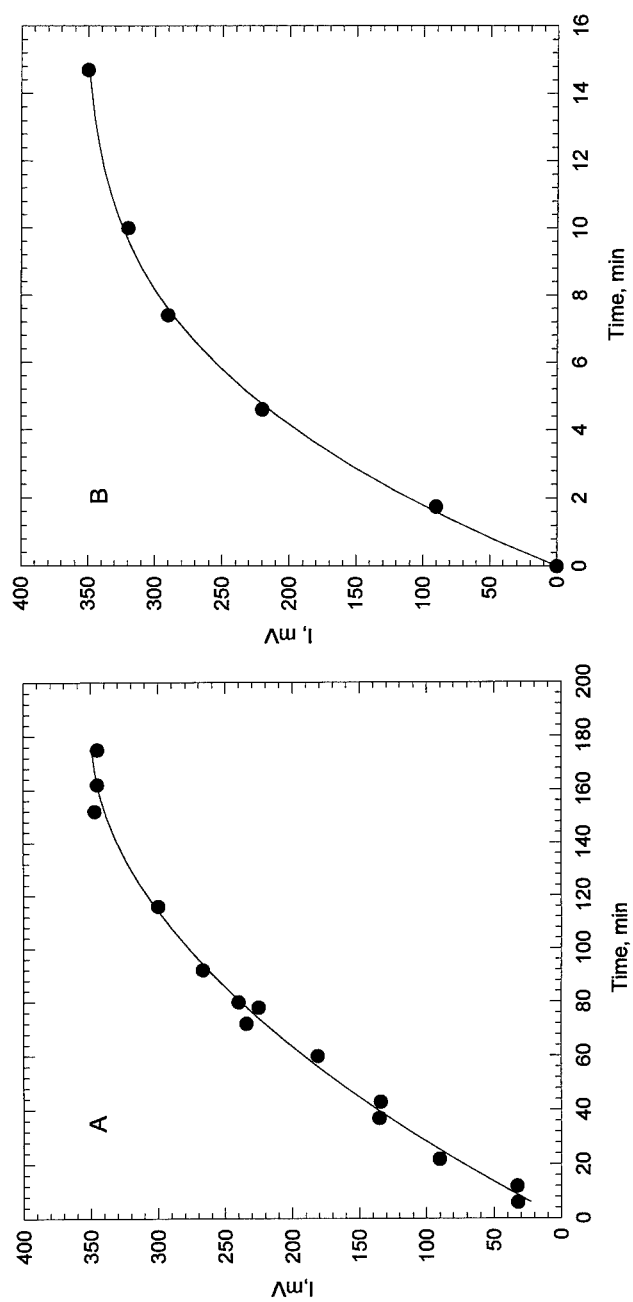
FIGURE 2. Kinetics of the adsorption of peroxidase-labeled antibodies on a polystyrene plate in static (A) and flow (B) conditions.

sensograms as pictured in FIGURE 3 are obtained. They look like the usual sensograms characterized, for instance, for BIAcore binding data.

The kinetic constants for the reversible interaction of peroxidase-labeled antigen Ag* (in this case, simazine as the model antigen) with immobilized antibodies in the flow-through cell may be obtained by the linear transformation of the sensograms according to earlier data on surface plasmon resonance[4] in the coordinates of equations 1 and 2:

$$dI/dt = k_1[Ag^*]_0 I_{max} - (k_1[Ag^*]_0 + k_{-1})I, \tag{1}$$

$$k_{app} = k_1[Ag^*]_0 + k_{-1}, \tag{2}$$
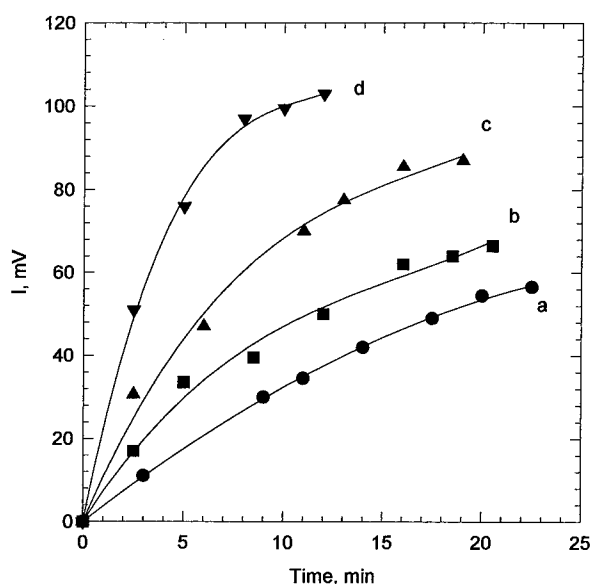
FIGURE 3. Kinetics of the binding of peroxidase-labeled simazine with monoclonal antibodies against simazine immobilized on the walls of the flow-through cell at different concentrations of labeled antigen: 0.68 μM (a), 1.0 μM (b), 2.3 μM (c), and 3.4 μM (d).

where k_1 is the association rate constant, k_{-1} is the dissociation rate constant, $[Ag^*]_0$ is the concentration of labeled antigen in solution, I is the observed signal of chemiluminescence intensity, and I_{max} is the maximum signal of chemiluminescence.

Determination of k_{app} at a number of ligate concentrations of $[Ag^*]_0$ allows one to plot k_{app} versus $[Ag^*]_0$, from which single values for k_1, the slope, and k_{-1}, the y-intercept, are obtained.

FIGURES 4A and 4B represent the linearization data for the process of the interaction between the peroxidase-labeled model antigen simazine and monoclonal antibodies against simazine in the coordinates of equations 1 and 2 (in other experiments, we used the peroxidase-labeled small haptens—progesterone, 2,4-dichlorophenoxyacetic acid, and atrazine). The kinetic constants calculated from
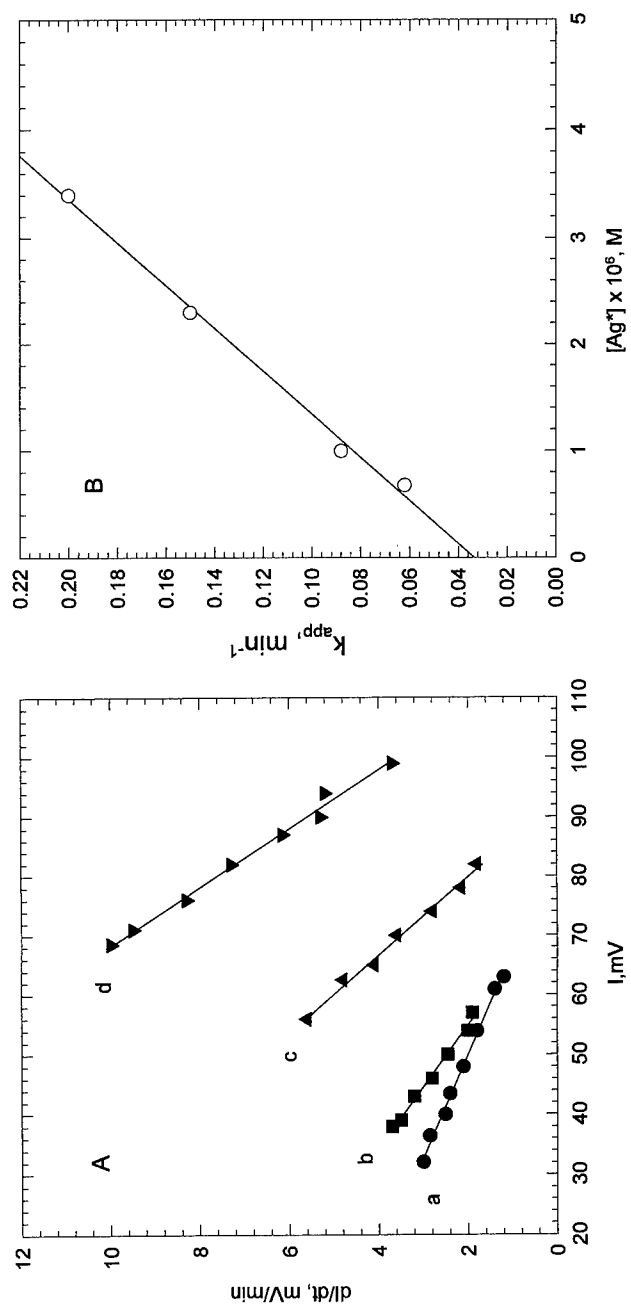
FIGURE 4. Determination of the individual rate constants in the coordinates of equations 1 (A) and 2 (B) according to the primary data of FIGURE 3. The letter terms in part A are those used in FIGURE 3.

these primary data were $k_{-1} = 3.4 \times 10^{-2}$ min^{-1} and $k_1 = 5.0 \times 10^4$ M^{-1}-min^{-1}. The overall affinity constant (k_1/k_{-1}) was therefore calculated to be approximately 1.5×10^6 M^{-1}.

Regeneration of the flow-through cell may be reached by a consecutive pumping of the solutions of acid, buffer, and specific antibodies.

CONCLUSIONS

The simple system based on the thin-layer flow-through cell and the chemiluminescent detection of the peroxidase label may be successfully used for molecular recognition studies and for analyzing the kinetics of biomolecular interactions.

REFERENCES

1. LUKOSZ, W. 1991. Principles and sensitivities of integrated optical and surface plasmon sensors for direct affinity sensing. Biosens. Bioelectronics **6**: 215–225.
2. HODGSON, J. 1994. Light, angles, action: instruments for label-free, real-time monitoring of intermolecular interactions. Biotechnology **12**: 31–35.
3. EGOROV, A. M., A. P. OSIPOV & E. V. VLASOV. 1994. Flow-injection thin-layer cell immunosensor with chemiluminescent detection of peroxidase label (abstract). *In* The Third World Congress on Biosensors, 1–3 June 1994, New Orleans, p. 3.15.
4. O'SHANNESSY, D. J., M. BRIGHAM-BURKE, K. K. SONESON, P. HENSLEY & I. BROOKS. 1993. Determination of rate and equilibrium binding constants for macromolecular interactions using surface plasmon resonance: use of nonlinear least squares analysis methods. Anal. Biochem. **212**: 457–468.

Amperometric Enzyme-channeling Immunosensor[a]

J. RISHPON AND D. IVNITSKI

Department of Molecular Microbiology and Biotechnology
Tel Aviv University
Ramat Aviv, 69978 Israel

Enzyme immunoassays (EIA) are important in clinical diagnostics, veterinary medicine, environmental control, and bioprocess analysis because their high selectivity and sensitivity enable the detection of a broad spectrum of analytes in complex samples.[1,2] Decentralizing quantitative immunoassays from hospital laboratories, where complex instrumentation and highly qualified technical staff are required, can be accomplished by combining immunoenzymatic systems with electrodes to create immunoelectrochemical sensors that provide immediate "on-the-spot" results.[3,4] In this paper, we present a novel, rapid, one-step, separation-free immunosensor that is based on an enzyme-channeling immunoassay (ECIA), where the product of one enzyme is the substrate for the second enzyme. The binding interaction catalyzes the conversion of the initial substrate to a final detectable electroactive product. Cyclic regeneration of the substrate, accumulation of a redox mediator, and control of the hydrodynamic conditions at the sensor/solution interface enable direct preferential measurement of surface-bound enzyme label with high sensitivity and do not require a separation step to remove excess free label from the bulk solution. The immunoassay is complete in 5 to 30 min, depending on the complexity of the system.

EXPERIMENTAL WORK

Electrodes

Disposable cylindrical graphite electrodes were made from pencil lead (HB, 0.5-mm diameter). Polyethylene imine (PEI) from a methanolic solution was adsorbed onto the graphite electrode surface, onto which a glucose oxidase (GOD)–antibody conjugate was covalently immobilized using a glutaraldehyde linker.[5] The PEI graphite electrode was modified with an avidin-GOD conjugate for a competition assay using a biotin sensor. The remaining sites were blocked with 1% BSA (w/w) for 60 min at 20 °C. Amperometric measurements were monitored at a fixed electrode potential (0.0 V versus SCE) by an EG&G PAR 273 potentiostat interfaced to a 486 PC system equipped with PAR M270 software. The system consists of a three-electrode cell with a rotating graphite antibody working electrode, a platinum counter, and saturated calomel reference (SCE) electrodes, using acetate buffer (0.1 M, pH 5.6) containing 0.15 M NaCl and 3 mM KI. The working electrode

was inserted into a holder attached to a Pine Instruments rotator with an MSRS speed controller, and the electrode base (5 mm) was exposed to the test solution.

Amperometric Enzyme-channeling Immunoassay

The principle of ECIA is as follows (see FIGURE 1): The GOD-antibody (avidin)–coated electrode is dipped into a solution containing glucose, iodide ions, and the appropriate analyte, which in turn is bound to a peroxidase-labeled antibody (biotin) conjugate. On the electrode surface, the GOD catalyzes the oxidization of glucose to H_2O_2, and the iodine produced in the peroxidase-catalyzed H_2O_2/iodide
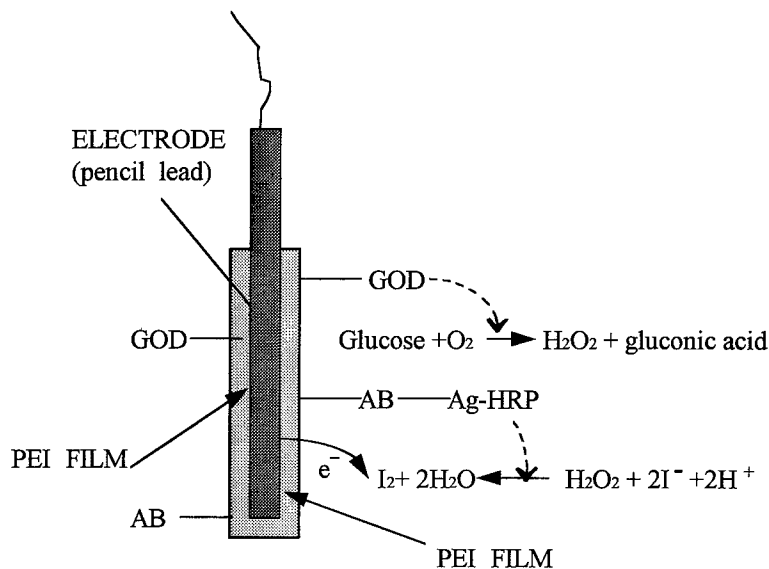
FIGURE 1. Schematic illustration of the separation-free, amperometric enzyme-channeling immunoassay with immobilized antibody and glucose oxidase on the PEI-modified electrode surface.

redox system is monitored amperometrically by the electrochemical reduction of iodine back to iodide.[6]

The corresponding *Staphylococcus aureus* assay was based on a second-antibody, "sandwich" protocol. An electrode coated with immobilized GOD and rabbit immunoglobulin G (RbIgG) was placed in a cell containing different concentrations of *S. aureus*, rotated at 500 rpm, and then incubated for 30 min at room temperature. During the final 10 min of incubation, the mixture was labeled by adding 5 μL of a RbIgG-horseradish peroxidase (HRP) conjugate (diluted 1:400). The background signal was measured and stabilized for 2 min, 10 μL of glucose (0.16 M) was added, and the catalytic current was monitored continuously for 1 min.
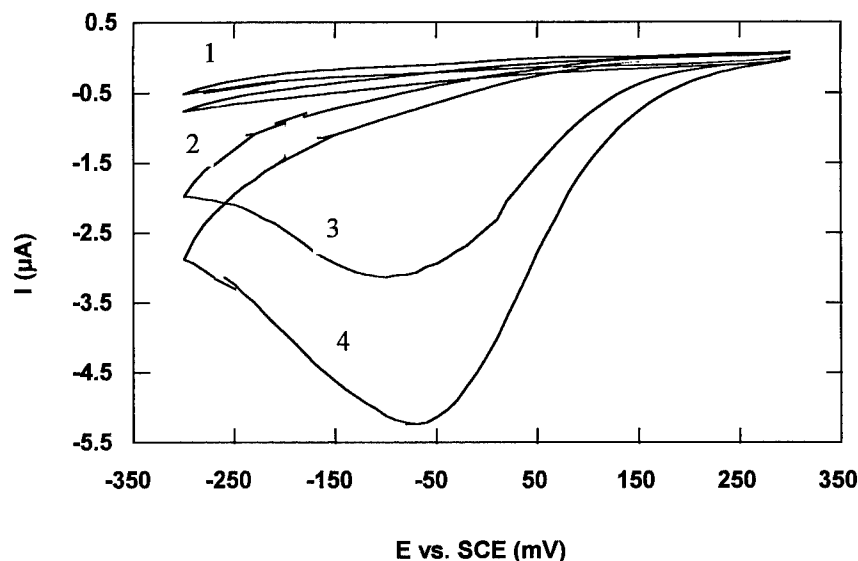
FIGURE 2. Cyclic voltammograms of BSA-GOD (curves 1 & 2) and RbIgG-GOD (curves 3 & 4) electrodes in 0.1 M acetate buffer (pH 5.6) with 0.15 M NaCl, 3 mM KI, and 160 ng/mL αRbIgG-HRP. [Glucose]: curves 1 & 3, 5 mM; curves 2 & 4, 20 mM. Electrode rotation speed = 1000 rpm; scan rate = 10 mV/s.

RESULTS AND DISCUSSION

The limiting factor in the development of a sensitive, separation-free immunoassay is the high background level of signal, which was obtained by free peroxidase label (the conjugate) in the bulk solution. Resolution between surface-bound and free conjugate could be realized if the mediation efficiency of the conjugate on the electrode surface is higher than that in the bulk solution. We found that accumulation of a redox mediator, cyclic regeneration of the substrate, and control of the hydrodynamic conditions at the sensor/solution interface allow the solving of this problem. Cyclic voltammograms at different glucose concentrations for control of the BSA-GOD electrodes (FIGURE 2, curves 1 and 2) and the RbIgG-GOD electrodes (curves 3 and 4) showed that a large catalytic current occurred at the RbIgG-modified electrodes, reflecting the preferential measurement of surface-bound peroxidase-labeled antibody (or antigen) over the free enzyme–labeled reagent in the bulk solution. An analogous effect occurred in peroxidase-antibody and avidin-biotin systems. Typical dynamic amperometric responses (current versus time curves) were significant with anti-HRP-modified electrodes and insignificant with BSA-modified electrodes (FIGURE 3). The analytical signal was obtained 10 seconds after adding the glucose. The avidin-GOD-modified PEI graphite electrode gave a sigmoid calibration curve for biotin (FIGURE 4). Higher concentrations of biotin (> 200 ng/mL) elicited no change in the current upon addition of glucose, indicating insignificant nonspecific binding of the conjugate. The blank signal in the absence of
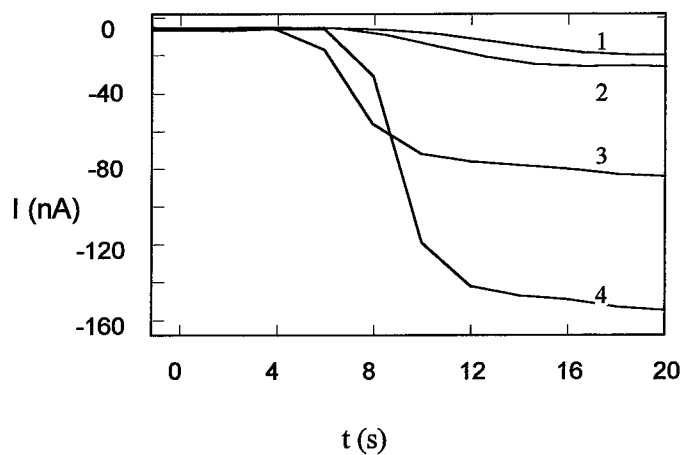
FIGURE 3. The amperometric responses of BSA (curves 1 & 2) and anti-HRP (curves 3 & 4) electrodes to the addition of peroxidase (curves 1 & 3, 8.6 ng/mL; curves 2 & 4, 17.2 ng/mL). The electrodes are poised at 0.0 V versus SCE at 500 rpm. Other conditions are described in FIGURE 2.
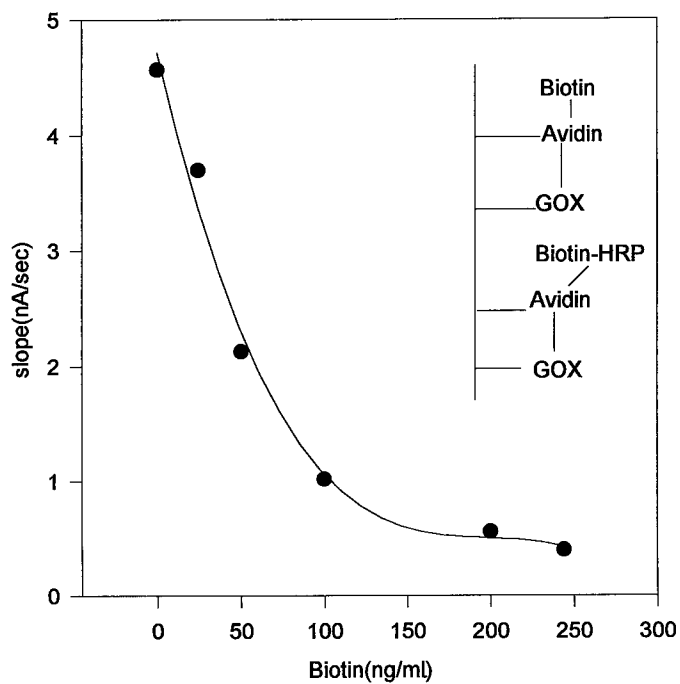
FIGURE 4. Calibration curve for biotin determination in a separation-free, competitive enzyme immunoassay, using avidin-GOD electrodes in acetate buffer containing 5 mM glucose and 212 ng/mL biotin-HRP. Electrode rotation speed = 500 rpm; other conditions are described in FIGURE 2.

the biotin-HRP conjugate is equivalent to the signal for 220 ng/mL biotin in the assay. To detect the major cell wall component of *S. aureus*, that is, protein A, bacterial cells were bound to an IgG-modified electrode surface. FIGURE 5 shows that the changing current reflects different concentrations of *S. aureus*, ranging from 1.0×10^3 to 4.0×10^4 cells/mL. Nonspecific binding of the RbIgG-peroxidase conjugate to the electrode surface was low.

CONCLUSIONS

We have developed a new amperometric enzyme-channeling immunosensor for rapid, separation-free, quantitative EIA of different compounds without a washing step. The key factor in generating amplified enzymatic signals is limiting the enzymatic reactions to the membrane/electrode interface by localizing the antibody,
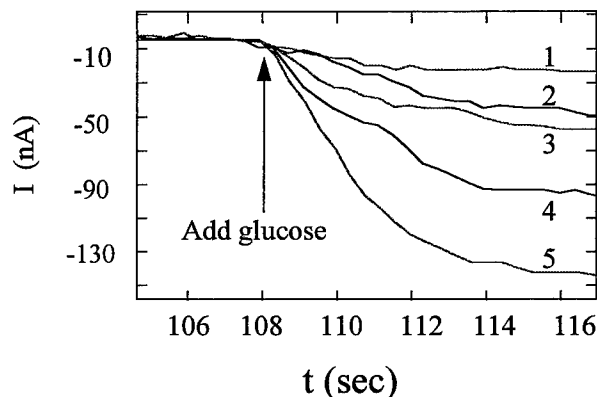
FIGURE 5. The response curves generated by the amperometric immunosensor specific for protein A in the presence and absence of *S. aureus* cells.

the GOD, and the antigen-peroxidase at the electrode surface. The PEI film blocks the electrode interactions with positively charged species, whereas negative ions are incorporated onto the membrane. Iodide ions are useful as mediators in amperometric ECIAs because the iodine-iodide system is reversible, noncarcinogenic, and stable with time, and the background current is low (<0.01 μA).[7] The analytical signal originating at the electrode surface relative to the signal originating from the bulk solution is 10–20 times enhanced. The immunosensor should be useful for characterizing the binding reactions via the estimation of affinity constants and dissociation rate constants from slopes that are associated with current changes. Further developments, using automated, multielectrode systems for the simultaneous detection of different samples, are now in progress.

REFERENCES

1. HAGE, D. S. 1993. Anal. Chem. **65:** 420R–424R.
2. MCNEIL, C. J., D. ATHEY & W. O. HO. 1995. Biosens. Bioelectronics **10:** 75–83.
3. RISHPON, J., Y. GEZUNDHAJT, L. SOUSSAN, I. ROSEN-MARGALIT & E. HADAS. 1992. *In* Biosensor Design and Application. Chapter 6. P. R. Mathewson & J. W. Finley, Eds.: 56–72. Amer. Chem. Soc. Washington, District of Columbia.
4. RISHPON, J., L. SOUSSAN, I. ROSEN-MARGALIT & E. HADAS. 1992. J. Immunoassay **13:** 231–252.
5. GUILBAULT, G. G., B. HOCK & R. SCHMID. 1992. Biosens. Bioelectronics **7:** 411–419.
6. IVNITSKI, D., R. A. SITDIKOV & V. E. KUROCHKIN. 1992. Anal. Chim. Acta **261:** 45–52.
7. IVNITSKI, D. & J. RISHPON. 1996. A one-step, separation-free amperometric enzyme immunosensor. Biosens. Bioelectronics **11:** 45–51.

Performance of the Apoenzyme-Membrane Sensors for Microdetermination of Heavy Metal Ions

IKUO SATOH

Department of Chemical Technology
Faculty of Engineering
Kanagawa Institute of Technology
Kanagawa-ken 243-02, Japan

INTRODUCTION

In a series of studies on the apoenzyme (cofactor-free enzyme) reactivation microassay for heavy metal ions with use of immobilized metalloenzymes as recognition elements, my colleagues and I have demonstrated their generality and usefulness of novel bioanalytical methods.[1–13] The details of the assay principle and procedure were also reported earlier. Currently, we are presenting unique microdetermination methods of heavy metal ions using apoenzyme-membrane sensors. Use of the apoenzyme membrane[14–16] in the proposed methods enabled more rapid assays for copper(II), zinc(II), and cobalt(II) ions than did apoenzyme beads.

In this paper, ascorbate oxidase and alkaline phosphatase coimmobilized onto a porous polymer membrane were used as a recognition element for copper(II), zinc(II), and cobalt(II) ions in combination with flow-injection amperometry. Then, the performance of the proposed biosensing system was investigated.

EXPERIMENTAL WORK

Ascorbate oxidase (ASOD; EC 1.10.3.3, from cucumber; 85 U/mg of powder), alkaline phosphatase (ALP; EC 3.1.3.1, from *Escherichia coli*; 55 U/mg of powder), and partially aminated polyacrylonitrile membrane from the Asahi Chemical Industry Company (previously the Toyo Jozo Company; Ohito-cho, Shizuoka-ken, Japan) and L-ascorbic acid-2-phosphate from the Kyowa Hakko Kogyo Company (Tokyo) were kindly provided. Other reagents were all commercially available and used without further purification. Doubly deionized water (≥ 17.0 megohm-cm resistivity) purified with a Millipore Milli-Q system (Nihon Millipore Limited, Tokyo) was used in all procedures.

Both enzymes, that is, ASOD and ALP, were coimmobilized onto the membrane (1 cm $\times$ 1 cm) by modifying the procedure (the amounts of the enzymes applied to the coupling reaction were 1667 units for ASOD and 333 units for ALP, respectively) as previously described.[15] The preparation was tightly secured with a rubber O-ring on the sensing part of a polarographic oxygen electrode (type BO-P, Able Company, Tokyo). This enzyme-membrane electrode was mounted into a flow-through cell

514

(Able Company) and then used as the sensor for monitoring the amount of dissolved oxygen enzymatically consumed.

The flow-injection sensing system based on amperometry was the same as previously reported.[15] Temperature-controlled water was successively circulated around the enzyme-membrane sensor to maintain the reaction temperature (303 ± 0.1 K). A constant voltage of -0.7 V (versus Ag/AgCl) was applied to the platinum cathode with a potentiostat (model HA-301, Hokuto Denko Company, Tokyo). The potentiostat was connected with an ammeter (model HE-104, Hokuto Denko Company) and the current output was displayed on a pen recorder (model R-62M3, Rikadenki Kogyo Company, Tokyo). A capacitor (1 μF) was connected between the input terminals of the recorder to reduce noise in the signal.

Buffer solutions (0.1 M Tris-HCl, pH 8.0, containing 1 M NaCl) were pumped continuously through the system (1.0 mL/min). Sample solutions were injected as short pulses via a rotary injection valve with a sample loop (type 5020, Rheodyne Incorporated, Cotati, California). N,N-Diethyl dithiocarbamate solution (5 mM, pH 8.0) and 2,6-pyridine dicarboxylate solution (20 mM, pH 6.0) were used as the cofactor-complexing agent for removing copper(II) ions from the catalytic site of ASOD and zinc(II) and cobalt(II) ions from that of ALP, respectively.

RESULTS AND DISCUSSION

Biosensing of Copper(II) Ions

Ascorbate oxidase catalyzes the oxidation of L-ascorbate to dehydroascorbate as follows:

$$2 \text{ L-ascorbate} + O_2 \xrightarrow{\text{ASOD}} 2 \text{ dehydroascorbate} + 2 \text{ H}_2\text{O}. \tag{1}$$
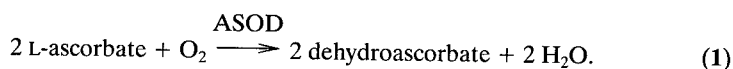
The enzyme activity can be amperometrically monitored by detecting the variation in oxygen tension attributable to the enzymatic oxidation with the oxygen electrode as previously reported.[14] Injections of 0.1 mL of L-ascorbate solution with various concentrations, containing an equimolar amount of ethylenediaminetetraacetate (EDTA), to the enzyme membrane resulted in significant consumption of dissolved oxygen; sharp peaks from a stable baseline were observed on a recording chart. The assay took 2.5 min for the injection. The calibration graph for the substrate in the concentration range of 0.02–2.0 mM was sigmoidal versus the variation in oxygen uptake; at higher concentrations, the plots almost flattened. Thus, the enzyme activity was monitored as oxygen uptake by injecting 0.1 mL of 10 mM L-ascorbate. The relative standard deviation (rsd) of 40 repeated measurements of 10 mM L-ascorbate was 0.9%.

Exposing the cofactor-bound enzymes, that is, holoenzymes [copper(II) ions as the cofactor], on the membrane to 5.0 mM N,N-diethyl dithiocarbamate solution (pH 8.0) as the cofactor-complexing agent extremely decreased the oxygen uptake resulting from the enzyme-catalyzed oxidation. The apoenzyme could be virtually regenerated by injecting at least 2.5 mL of the chelator.

Adding 0.25 mL of 1.0 mM copper(II) ions to the system reversibly reactivated

the apoenzyme immobilized on the membrane. The responses attributable to the partial reactivation of the apoenzymes were obtained as a function of the concentration of copper(II) ions added. Thus, copper(II) ions could be amperometrically determined in the range of 0.05–1.0 mM. Consequently, it was confirmed that ascorbate oxidase coimmobilized with ALP on the porous membrane could serve as the recognition element for copper(II) ions, as well as ASOD separately fixed.[14]

Biosensing of Zinc(II) Ions

Alkaline phosphatase can catalyze the hydrolysis of orthophosphoric monoesters to form an alcohol and orthophosphate. Therefore, the phosphatase activity can be amperometrically determined provided that L-ascorbic acid-2-phosphate as the substrate for ALP, as indicated in equation 2 below, is introduced into the membrane:

$$\text{L-ascorbic acid-2-phosphate} + H_2O \xrightarrow{\text{ALP}} \text{L-ascorbate} + \text{orthophosphate.} \quad (2)$$
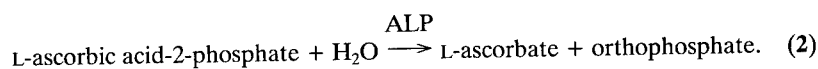
Application of the enzyme coupling method[17] to the amperometric monitoring of ALP activity may be readily realized because the L-ascorbate to be formed by the enzymatic hydrolysis of L-ascorbic acid-2-phosphate may be sequentially oxidized by ASOD coexisting on the same membrane.

Introduction of 0.1 mL of L-ascorbic acid-2-phosphate with various concentrations, containing an equimolar amount of EDTA, to the enzyme membrane also caused marked consumption of oxygen. The calibration graph for L-ascorbic acid-2-phosphate in the range of 0.1–10 mM showed a sigmoidal curve. This means that ASOD coimmobilized on the membrane could serve as an indicator enzyme in the coupled enzyme reactions. The current output exhibited an almost constant level of response with L-ascorbic acid-2-phosphate higher than 10 mM. Thus, APL activity on the membrane was monitored by injecting 0.1 mL of 20 mM L-ascorbic acid-2-phosphate. The precision of the assay (rsd) was 1.3% ($n = 40$).

The oxygen uptake resulting from the coupled reactions manifested a minimal value by exposing the holoenzyme membrane, that is, the zinc-bound enzymes, to 20 mM 2,6-pyridine dicarboxylate solution (pH 6.0) as the chelating agent with regeneration volumes of 2.5 mL or higher. Regeneration of zinc-free ALP could thus be virtually achieved by loading the chelator. The phosphatase activity of the zinc-free enzyme membrane could be satisfactorily recovered by subsequently injecting 0.25 mL of zinc(II) ions. Amperometric determination of zinc(II) ions in the range of 1.0–100 μM could be realized in a similar manner as mentioned above. The hydrolytic activity of ALP slightly suffered from the other chelator (*N,N*-diethyl dithiocarbamate solution), whereas ASOD coimmobilized on the membrane was not susceptible to deactivation resulting from exposure to the 2,6-pyridine dicarboxylate solution.

The effect of pH in 50 μM zinc(II) solution on the apoenzyme membrane was also investigated (from 4.0 to 8.0 in steps of 1.0). No noticeable difference in

reactivation was observed at each pH. This feature of the proposed bioanalysis for zinc(II) ions may be quite favorable for practical applications because it makes a pretreatment of precise pH-adjustment unnecessary.

Biosensing of Cobalt(II) Ions

The reactivation phenomena of the immobilized apoenzymes regenerated from ALP attributable to injection of cobalt(II) ions were previously observed.[11,12,16] An amperometric flow-injection determination of cobalt(II) ions using the membrane coimmobilized with ASOD and ALP was then tested. The membrane with the cobalt-substituted phosphatase could be readily obtained through the regeneration-reactivation process. The employment of the cobalt-enzyme membrane provided a sigmoidal calibration for L-ascorbic acid-2-phosphate, as did the zinc-enzyme mem-
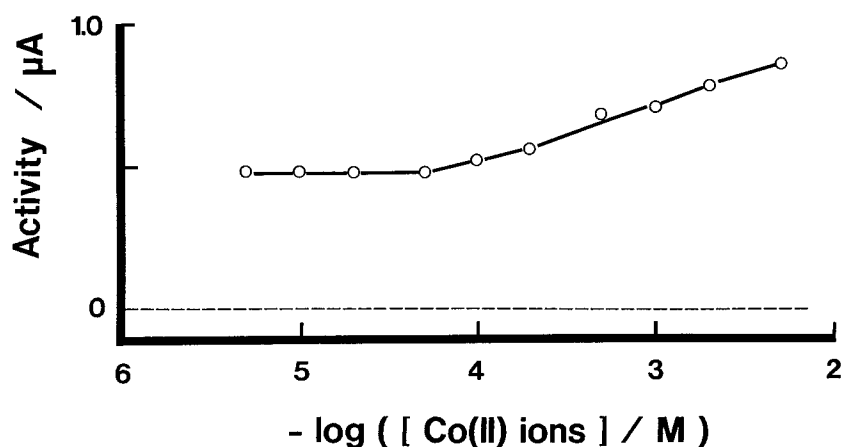
FIGURE 1. Calibration curve for cobalt(II) ions (sample volume: 0.25 mL, pH 6.0).

brane. However, the sigmoidal curve shifted toward a higher concentration range of cobalt(II) ions. In subsequent experiments, 200 mM L-ascorbic acid-2-phosphate, sufficient to obtain a high response, was used for monitoring the phosphatase activity. The regeneration and reactivation profiles for the cobalt-enzymes were almost similar to those for the apoenzymes from the zinc-enzymes. Cobalt(II) ions could be amperometrically determined in the range of 0.02–5.0 mM as shown in FIGURE 1. Slight responses in lower concentration regions of the standards are due to the ASOD-catalyzed oxidation of L-ascorbate, coexisting in L-ascorbic acid-2-phosphate substrate as an impurity.

Further studies are currently in progress toward establishing a microassay for calcium and lanthanide ions based on the apoenzyme reactivation method.

ACKNOWLEDGMENT

REFERENCES

1. SATOH, I., T. KASAHARA & N. GOI. 1990. Amperometric biosensing of copper(II) ions with an immobilized apoenzyme reactor. Sens. Actuators **B1:** 499–503.
2. SATOH, I. & T. MASUMURA. 1990. Flow-injection biosensing of zinc(II) ions with use of an immobilized alkaline phosphatase reactor. *In* Technical Digest of the Ninth Sensor Symposium (Tokyo), p. 197–200. Institute of Electrical Engineers of Japan. Tokyo.
3. SATOH, I. 1990. Apoenzyme reactivation microassay for zinc(II) ions in combination with flow-through transducers. *In* Proceedings of the Third International Meeting on Chemical Sensors (Cleveland), p. 106–107. Organizing Committee of the Third International Meeting on Chemical Sensors. Cleveland.
4. SATOH, I. & Y. AOKI. 1990. Biosensing of zinc(II) ions using an apoenzyme reactor and an ISFET detector in flow streams. Denki Kagaku **58**(12): 1114–1118.
5. SATOH, I. 1990. Calorimetric biosensing of heavy metal ions with the reactors containing the immobilized apoenzymes. Ann. N.Y. Acad. Sci. **613:** 401–404.
6. SATOH, I. 1991. Flow-injection calorimetry of heavy metal ions using apoenzyme-reactors. Netsusokutei (Calorimetry Therm. Anal.) **18**(2): 89–96 (in Japanese).
7. SATOH, I. & T. NAMBU. 1991. Flow-injection photometric biosensing of copper(II) ions with use of an immobilized ascorbate oxidase column. *In* Technical Digest of the Tenth Sensor Symposium (Tokyo), p. 77–80. Institute of Electrical Engineers of Japan. Tokyo.
8. SATOH, I. & Y. YAMADA. 1991. Flow-injection biosensing of cobalt(II) ions with use of an immobilized alkaline phosphatase reactor. *In* Digest of Technical Papers of the Sixth International Conference on Solid-State Sensors and Actuators (Transducers '91) (San Francisco), p. 699–702. IEEE. New York.
9. SATOH, I. 1991. An apoenzyme thermistor microanalysis for zinc(II) ions with use of an immobilized alkaline phosphatase reactor in a flow system. Biosens. Bioelectronics **6**(4): 375–379.
10. SATOH, I. 1991. Flow-injection microdetermination of heavy metal ions using a column packed with immobilized apoenzyme beads. J. Flow Injection Anal. **8**(2): 111–126.
11. SATOH, I. 1992. Use of immobilized alkaline phosphatase as an analytical tool for flow-injection biosensing of zinc(II) and cobalt(II) ions. Ann. N.Y. Acad. Sci. **672:** 240–244.
12. SATOH, I., Y. TOKORO, K. SUZUKI & Y. YAMADA. 1993. Long-term use of the immobilized alkaline phosphatase column as a recognition element for heavy metal ions. *In* Proceedings of the East Asia Conference on Chemical Sensors (Fukuoka, Japan), p. 235–238. Organizing Committee of the East Asia Conference on Chemical Sensors. Fukuoka, Japan.
13. SATOH, I. 1994. Flow-injection calorimetry using a column packed with carboxypeptidase A–immobilized beads. Trans. Mater. Res. Soc. Jpn. **15A:** 425–428.
14. SATOH, I., H. ITOH & H. ANZAI. 1992. Flow-injection amperometric biosensing of copper(II) ions using a contact-type of an apoenzyme sensor. *In* Proceedings of the Second World Congress on Biosensors (Geneva, Switzerland), p. 183–190. Elsevier/Mayfield House. Amsterdam/New York/London.
15. SATOH, I. 1993. Amperometric biosensing of heavy metal ions using a hybrid type of apoenzyme membrane in flow streams. Sens. Actuators **B13–14:** 162–165.
16. SATOH, I. 1995. Multi-ion biosensor with use of a hybrid-enzyme membrane. Sens. Actuators **B24–25:** 103–106.
17. HOLM, D. J. & H. PECK. 1983. Analytical Biochemistry, p. 280–282. Longmans, Green. New York.

Amplifying Bienzyme Cycle–linked Immunoassays for Determination of 2,4-Dichlorophenoxyacetic Acid[a]

FRANK F. BIER, EVA EHRENTREICH-FÖRSTER,
AND FRIEDER W. SCHELLER[b]

Institute of Biochemistry and Molecular Physiology
Faculty of Analytical Biochemistry
University of Potsdam
Potsdam, Germany

INTRODUCTION

Signal processing in the living cell is a multistep process that combines recognition (e.g., a hormone binding to a receptor) with enzymatic activity (e.g., production of energy and/or metabolites).

The combination of biochemical modules like receptors and amplifiers *in vitro* leads to new types of biochemical machines not originally designed by nature. A very common example of this type is the enzyme immunoassay. Another example is the bienzyme cycle developed to enhance the analytical performance of enzyme-based sensors,[1–4] for example, for epinephrine.[5]

In this report, we demonstrate the combination of a bienzyme amplifier with antibody-hapten binding for the example of the determination of the pesticide 2,4-dichlorophenoxyacetic acid (2,4-D). Two different methods of combination were investigated:

(1) The straightforward method is the use of a suitable enzyme-label, which produces a substrate of the cycle.
(2) A homogeneous immunoassay for haptens is achieved by introducing a bifunctional reagent, which is a shuttle molecule for the bienzyme cycle at one end and a competitor for the hapten to be assayed at the other end. Such a molecule is named a redox-label.

EXPERIMENTAL WORK

The enzyme cycle consists of tyrosinase (EC 1.14.18.1, TYR), which is capable of oxidizing a broad range of phenol derivatives and short polypeptides containing tyrosine, and oligosaccharide dehydrogenase (ODH). ODH is an NADH-independent dehydrogenase, capable of reducing some of the tyrosinase products. A

[b]Address all correspondence to F. W. Scheller at the Max-Delbrück-Center of Molecular Medicine, D-13125 Berlin, Germany.

selection of substrates of the cycle is given in FIGURE 1 and compared to the action of tyrosinase alone. The cycling system is schematically shown in the lower part of FIGURE 2. The main substrates of ODH are maltose and glucose. Glucose was given in excess (25 mM) throughout all experiments, with the exception of control
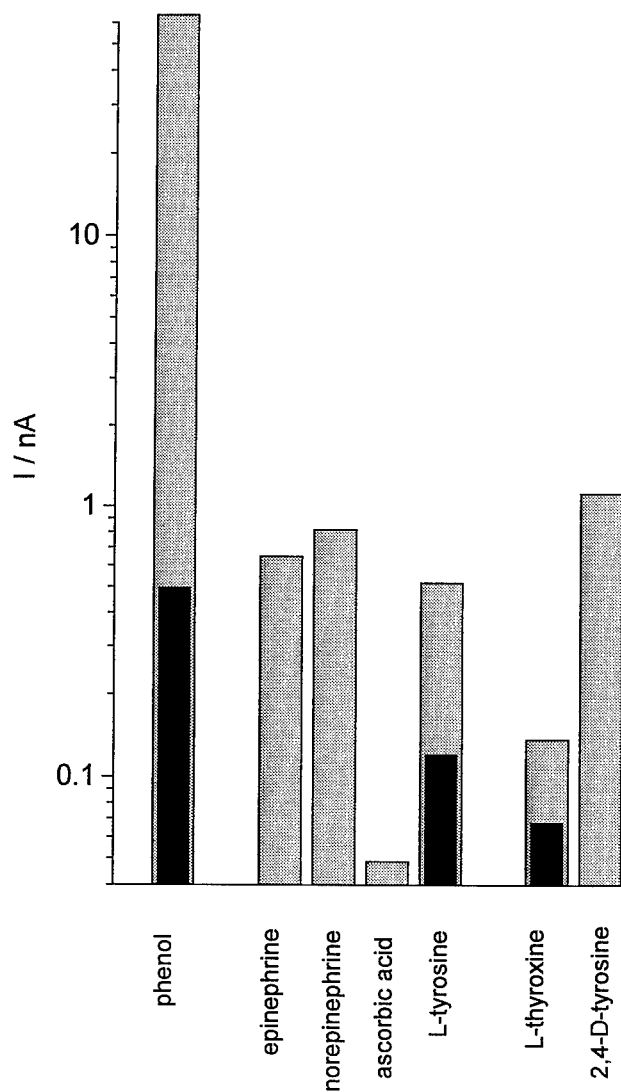
FIGURE 1. Comparison of the electrode response to various substrates for tyrosinase alone (dark) and the amplifier bienzyme electrode ODH/TYR (gray). The gain factor for phenol is 150; for tyrosine it is 3.5; and for 2,4-D-tyrosine it is 6. The response of the sensor is given in nA/μM of substrate and is shown in logarithmic scale.
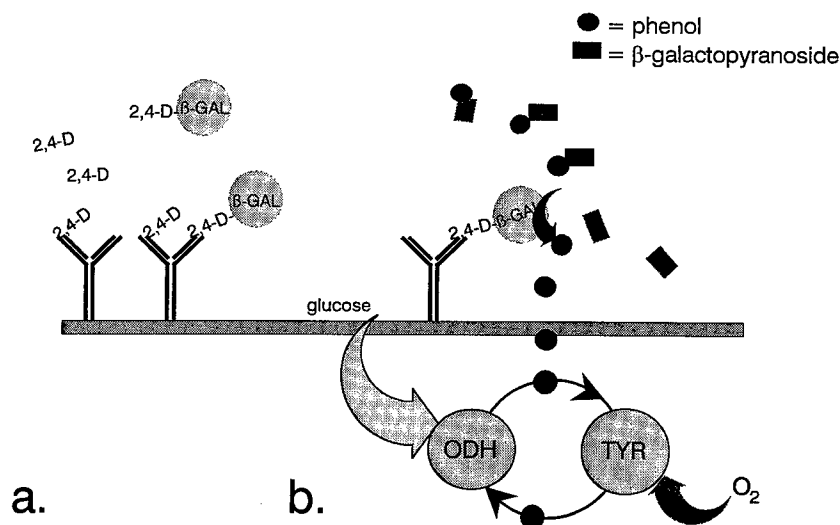
FIGURE 2. Scheme of a direct competitive immunoassay (bound antibody) (a), connected to the bienzyme cycling system constituted by oligosaccharide dehydrogenase (ODH) and tyrosinase (TYR) (b).

experiments with tyrosinase alone, which were performed without glucose. Oxygen consumption was measured with a Clark-electrode (-600 mV versus Ag/AgCl) in a stirred cell (1 mL) and the enzymes were coentrapped in gelatin (as described by Pfeiffer and Wollenberger[6]) containing 400 U/cm² ODH and 300 U/cm² TYR.

The monoclonal 2,4-D-antibody was a kind gift from M. Fránek (Brno).[7] The redox-label 2,4-D-tyrosine was synthesized by R. Dölling (BioTeZ, Berlin).

RESULTS

First, combining an immunoassay with the bienzyme amplifier by an enzyme-label was successfully applied to 2,4-D determination using β-galactosidase (β-GAL) as the label and phenyl-β-galactopyranoside (p-gal) as the substrate.

The assay was performed by coating a microtiter plate with the monoclonal anti-2,4-D antibody. 2,4-D competes against the 2,4-D–β-galactosidase conjugate as depicted in the left part of the scheme in FIGURE 2a. Only one step in the immunoassay was necessary. FIGURE 3 shows the calibration curve for 2,4-D.

The c_{50} value was found at 0.4 ng/L; the detection limit [(S/R) > 3] was at 10 pg/L, that is, 50 fM or correspondingly 10 amol in the measuring volume of 200 μL. The electrode response was within 3 min; however, because no stopping of the enzyme-label reaction on p-gal was done, the incubation time was watched carefully to be fixed at 30 min. Also shown in FIGURE 3 is the assay curve for a similar system containing laccase (EC 1.10.3.2) instead of tyrosinase;[5,8] the substrate for the cycle ODH/laccase is *p*-aminophenol and, correspondingly, the label substrate in the linked immunoassay is *p*-aminophenyl-β-galactopyranoside.

Second, in our example, a redox-label was constructed by coupling 2,4-D with tyrosine via a peptide bond. The antibodies were immobilized at the top of the enzyme layer and saturated with the redox-label, as is schematically shown in FIGURE 4; if this sensor was presented to a 2,4-D-contaminated solution, a positive signal occurred from the release of the redox-label, as is shown in FIGURE 5.

DISCUSSION AND CONCLUSIONS

A bienzyme-membrane electrode based on ODH/TYR has been combined with a competitive immunoassay using β-galactosidase as the label enzyme and phenyl-β-
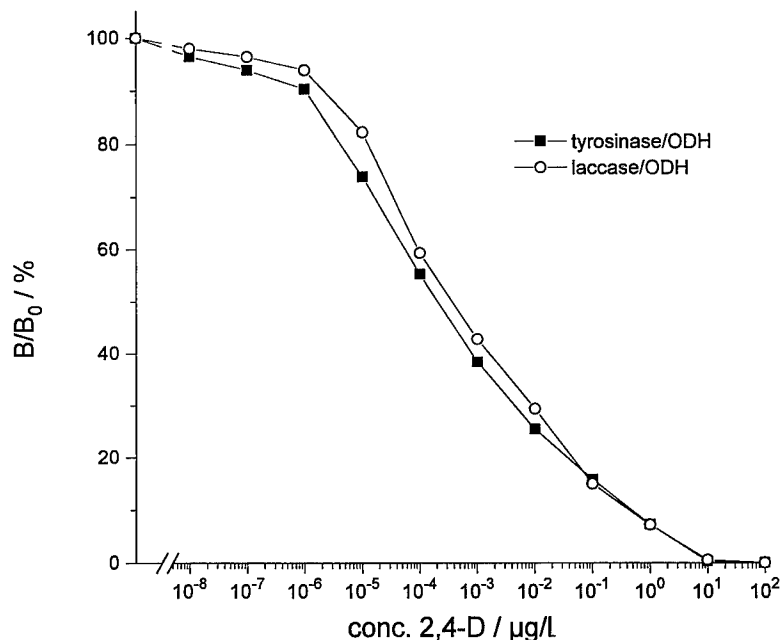
FIGURE 3. Direct competitive immunoassay using a monoclonal antibody with bienzyme electrode detection. Calibration curves for 2,4-dichlorophenoxyacetic acid (2,4-D) using β-galactosidase (β-GAL) as the enzyme-label are shown for two types of bienzyme cycles, ODH/TYR and ODH/laccase.

D-galactopyranoside as the label substrate. With the example of the 2,4-D competitive assay, we showed a linear range of four decades from 1 to 1000 ng/L and a detection limit of 10 pg/L for a monoclonal antibody. Such low concentrations are not only of interest for, for example, environmental monitoring, but also for clinical diagnostics and forensic studies.

Furthermore, it has been demonstrated that the construction of a homogeneous immunoassay for haptens is possible using bienzyme cycles and redox-labels; how-
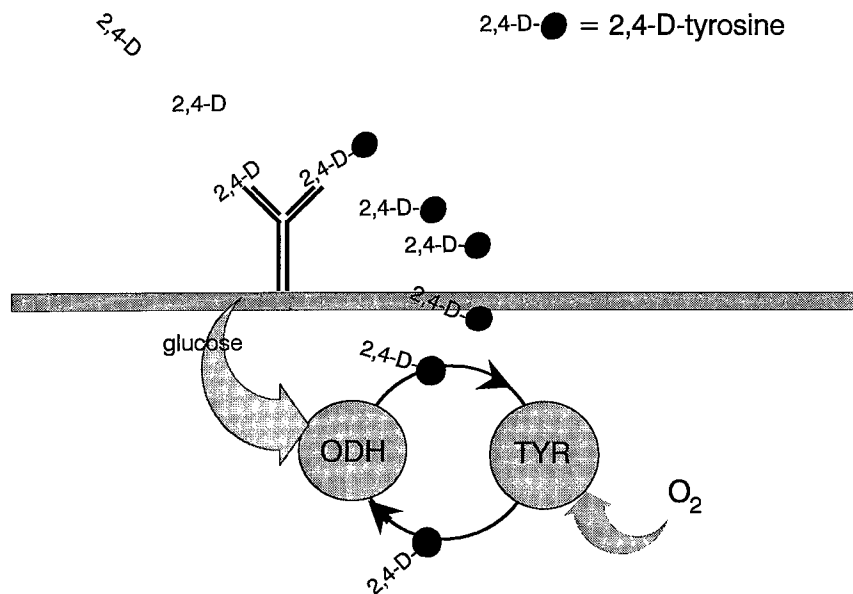
FIGURE 4. Scheme of the redox-label immunoelectrode for the example of 2,4-D.
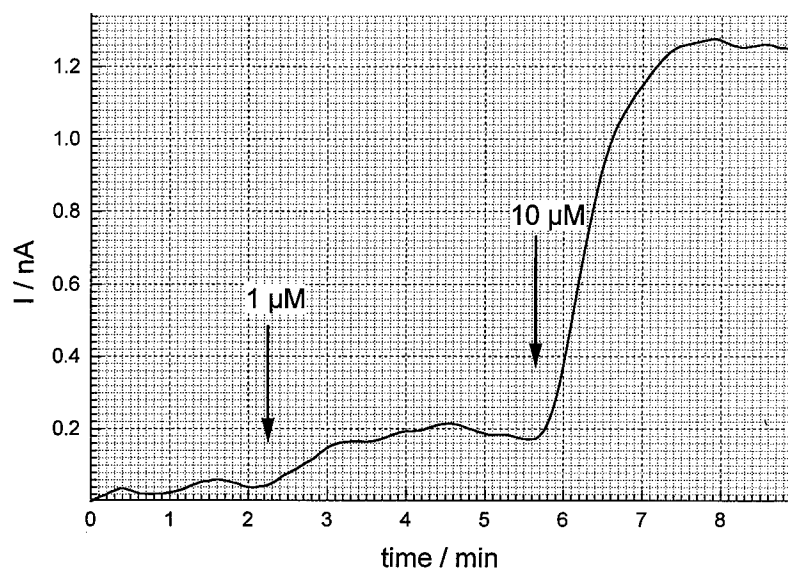
FIGURE 5. Response of the redox-label immunoelectrode to 2,4-D.

ever, optimization has to be done especially regarding the chemistry of the redox-label to achieve higher sensitivities.

Further technical progress will be achieved by fusion of the antibodies with the enzymes of the bienzyme cycle.

ACKNOWLEDGMENTS

REFERENCES

1. MIZUTANI, F., T. YAMANAKA, Y. TANABE & K. TSUDA. 1985. Anal. Chim. Acta **177:** 153.
2. SCHELLER, F., N. SIEGBAHN, D. DANIELSON & K. MOSBACH. 1985. Anal. Chem. **57:** 1740–1743.
3. SCHELLER, F. W., R. RENNEBERG & F. SCHUBERT. 1988. Methods Enzymol. **137:** 29–43.
4. WOLLENBERGER, U., F. SCHUBERT, D. PFEIFFER & F. W. SCHELLER. 1993. Trends Biotechnol. **11:** 255–262.
5. GHINDILIS, A. L., A. MAKOWER, C. G. BAUER, F. F. BIER & F. W. SCHELLER. 1995. Anal. Chim. Acta **304:** 25–31.
6. PFEIFFER, D. & U. WOLLENBERGER. 1993. Biosens. Bioelectronics **8**(2): xix–xx.
7. FRÁNEK, M., V. KOLAR, M. GRANATOVA & Z. NEVORANKOVA. 1994. J. Agric. Food Chem. **42:** 1369–1374.
8. BIER, F. F., E. EHRENTREICH-FÖRSTER & F. W. SCHELLER. 1996. Fresenius J. Anal. Chem. **354:** 861–865.

Laccase

A Marker Enzyme for Solvent-modified Immunoassays[a]

W. F. M. STÖCKLEIN[b] AND F. W. SCHELLER[b]

Institute of Biochemistry and Molecular Physiology
University of Potsdam
Potsdam, Germany

INTRODUCTION

Immunoassays depend on the high affinity between antibody and antigen (or hapten), on the specificity of antibodies, and [for flow-injection immunoanalysis (FIIA)] on the regenerability of binding sites. Among the factors influencing these key properties of immunoanalytical systems, organic solvents have been poorly investigated, despite their large potential for enzymatic synthesis of organic compounds[1] and for enzyme sensors.[2] The first notable description of antibody-antigen binding in organic solvents was published by Russell *et al.*[3] The aim of our study was to modify enzyme immunoassays based on FIIA[4] by the use of organic solvents. The acid stability of laccase allowed the setup of a model FIIA system for the screening of solvent effects on hapten and conjugate elution from immobilized antibodies.[5] Here, the influence of solvent-water mixtures on the unmodified marker enzymes, laccase and horseradish peroxidase (HRP), and on chemically modified laccase is described.

EXPERIMENTAL WORK

The enzyme assays and immunoassays were performed as described in reference 5.

Chemical Modification of Laccase

Two different methods were applied:

(a) Hydrophilization with pyromellitic acid dianhydride and the determination of amino groups with trinitrobenzene sulfonic acid were performed according to Mozhaev *et al.*[6] The protein content was determined with the bicinchonic acid method (Pierce; Rockford, Illinois).

(b) Hydrophobization with palmitic acid *N*-hydroxysuccinimide ester (PA-NHS) was based on the method described by Melik-Nubarov *et al.*[7] in reversed micelles. The following substances were added to 910 μL of 0.1 M aerosol-OT in octane: 1.4 μmol PA-NHS in 50 μL of ethyl acetate, 14 nmol

[b]Address for correspondence: Max-Delbrück-Center for Molecular Medicine, 13122 Berlin, Germany.

laccase in 13 μL, and 27 μL of 10 mM phosphate (pH 7). The (optically transparent) mixture was shaken overnight at room temperature. The modified enzyme remained in the glass tube after removal of the solvent and was resuspended in 0.1 M phosphate (pH 7). In the control without PA-NHS, the enzyme could be recovered by extraction with buffer.

RESULTS AND DISCUSSION

Influence of Water-miscible Organic Solvents on Enzyme Activity

In the activity assay with ABTS as substrate, laccase was less influenced by water-miscible organic solvents than peroxidase (TABLE 1). However, the sensitivity of peroxidase towards these solvents depended strongly on the substrate. Whereas the solvent sensitivity was in the same range for the luminescence and fluorescence reactions with ABTS, a considerably higher resistance against ethanol was observed with tetramethylbenzidine (TMB). For laccase, the solvent resistance becomes lower in TMB compared to ABTS. The different results for the two enzymes in ABTS and TMB reflect the substrate preference, with TMB being the better substrate for HRP and with ABTS being the better for laccase in terms of the measured absorbance changes at 370 nm (TMB) and 420 nm (ABTS).

When the enzymes were preincubated for 15 h at room temperature in ethanol-water and before their activity was measured in buffer, peroxidase turned out to be more solvent-resistant than laccase. Therefore, the sensitivity of peroxidase to ethanol, when present in the assay mix, is not due to a solvent effect on enzyme stability. Both enzymes are stabilized by 20% ethanol. The stabilizing effect could be caused, at least partially, by a protection against microbial or proteolytic attack. The residual laccase activity was 85% after preincubation in buffer under the same conditions. At water concentrations below 20%, distinct activity maxima were found with laccase in ethanol and n-butanol consistent with published observations for many enzymes. This concentration range, however, has not yet been considered to be of interest for flow immunoassays in organic solvents.

TABLE 1. Activity of Laccase and Horseradish Peroxidase (HRP) in the Presence of Ethanol[a]

		Solvent (v/v) for 50% Inhibition of:		
Solvent	Substrate	Laccase	HRP	
ethanol	ABTS	44%	12%	absorbance
	TMB	34%	28%	absorbance
	luminol	—	14%	luminescence
	HPPA	—	9%	fluorescence
DMF	ABTS	23%	14%	absorbance
	TMB	19%	33%	absorbance
acetonitrile	HPPA	—	5%	fluorescence

[a]Assay conditions were as described in reference 5. ABTS: 2,2'-azino-di-[3-ethyl-benzthiazoline-sulfonate(6)]; DMF: dimethylformamide; HPPA: 3-(4-hydroxyphenyl)propionic acid; TMB: 3,3',5,5'-tetramethylbenzidine.

TABLE 2. Stability of Unmodified and Modified Laccases in Organic Solvent[a]

Solvent	% Activity		
	Laccase	L-Py	L-Pa
buffer	95	85	103
THF	39	48	61
acetone	2	8	32
ethanol	1	0	13
acetonitrile	37	27	14

[a]Enzymes were incubated for 60 min in 95% solvent at room temperature and assayed at 1/100 dilutions in assay mixtures; THF: tetrahydrofuran.

Stability of Modified Laccases in Ethanol-Water

Hydrophilization with pyromellitic acid was chosen because stabilization in solvents was described for other enzymes modified in this way.[6] The stabilizing effect is assumed to be due to "shielding" of hydrophobic clusters on the protein surface. Modification with palmitic acid was chosen because the solubility (or dispersibility) of enzymes can be increased by hydrophobization and thus the modified enzymes are less prone to denaturation by solvents.

The denaturation kinetics of modified laccases in 50% and 95% solvent were determined over 60 min (TABLE 2, FIGURE 1). In the palmitic acid–modified enzyme (L-Pa), 78% of the amino groups were modified, with the residual activity after modification being 62%. The pyromellitic acid–modified enzyme (L-Py) had 83% modification of amino groups and 99% residual activity. A significant increase in solvent stability was found for L-Pa, whereas L-Py showed only a slight increase in stability. An exception among the solvents tested is acetonitrile. The sensitivity of modified laccases against this solvent is increased. Obviously, another mode of solvent action on the enzymes is found for acetonitrile.

Laccase as a Marker for Enzyme Immunoassays

Flow-injection immunoanalysis of haptens, for example, pesticides, involves regeneration of the immobilized immunoreactants, which are often antibodies. In competitive or sequential saturation immunoassays, elution of the hapten and enzyme conjugate is preceded by an enzyme detection step. With laccase as the marker enzyme, elution and enzyme detection could be combined, as laccase is active and rather stable at pH 2.[5] A special advantage of laccase for this type of immunoassay is that hydrogen peroxide (which is toxic for proteins) is not needed, in contrast to HRP. The low pH is in many cases sufficient for efficient elution. However, the stability of immobilized antibodies in the range of pH 2 is often a problem. Therefore, organic solvents should be applicable to replace the strongly acidic conditions. With the described FIIA for the detection of coumarin, it could be shown that 10% ethanol in 0.1 M glycine at pH 2.2 had the same eluting effect as buffer at pH 2 without ethanol. When pH 2 buffer was used with ethanol contents up to 30%, the elution peaks became increasingly sharp.
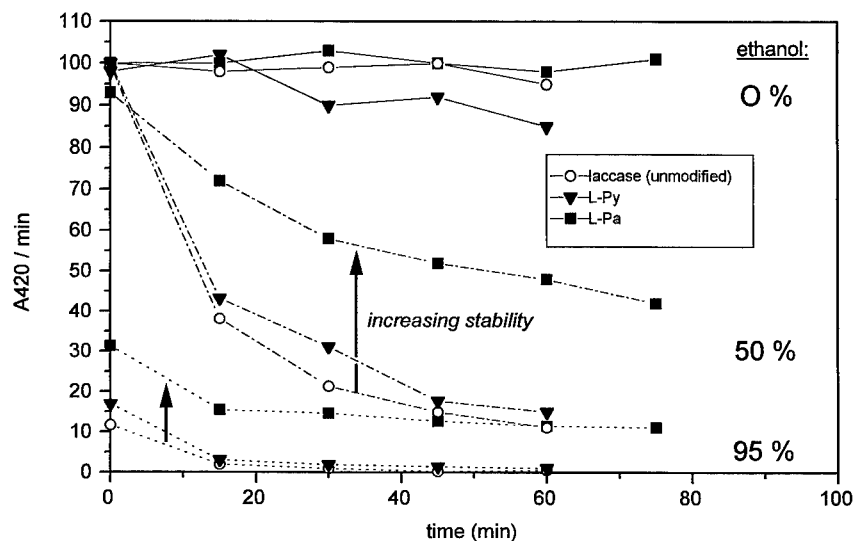
FIGURE 1. Stability of unmodified and modified laccases in ethanol/water. Enzymes were incubated in water with 0%, 50%, or 95% ethanol at room temperature and aliquots were diluted 1/100 for assay every 15 min.

Organic solvents as elution modifiers can also be useful for the concentration or purification of acid-unstable antigens/haptens on antibody-columns and to achieve complete elution. Immobilized antibodies have been found to resist even pure ethanol for 1 hour.[5] The stability may be even increased, as outlined above for enzymes in 20% ethanol.

At present, the investigations are continuing with conjugates of modified laccase and atrazine, using higher ethanol concentrations for elution/detection. Further experiments include the manipulation of antibody specificity for the differentiation of cross-reacting haptens, for example, different triazine herbicides.

REFERENCES

1. DORDICK, J. S. 1989. Enzyme Microb. Technol. **11:** 194–211.
2. SAINI, S., G. F. HALL, M. E. A. DOWNS & A. P. F. TURNER. 1991. Anal. Chim. Acta **249:** 1–15.
3. RUSSELL, A. J., L. J. TRUDEL, P. L. SKIPPER, J. D. GROOPMAN, S. R. TANNENBAUM & A. M. KLIBANOV. 1989. Biochem. Biophys. Res. Commun. **158:** 80–85.
4. WITTMANN, C. & R. D. SCHMID. 1994. J. Agric. Food Chem. **42:** 1041–1047.
5. STÖCKLEIN, W. F. M., F. W. SCHELLER & R. ABUKNESHA. 1995. Sens. Actuators **B24–25:** 80–84.
6. MOZHAEV, V. V., V. A. ŠIKŠNIS, N. S. MELIK-NUBAROV, N. Z. GALKANTAITE, G. J. DENIS, E. P. BUTKUS, B. Y. ZASLAVSKY, N. M. MESTECHKINA & K. MARTINEK. 1988. Eur. J. Biochem. **173:** 147–154.
7. MELIK-NUBAROV, N. S., Y. G. SUZDALTSEVA, E. L. PRISS, V. I. SLEPNEV, A. V. KABANOV, O. P. ZHIRNOV, P. G. SVESHNIKOV & E. S. SEVERIN. 1993. Biochem. Mol. Biol. Int. **29**(5): 939–947.

Activity of Nisin Immobilized in a Hollow-Fiber Reactor[a]

ANNA LANTE, GABRIELLA PASINI,
ANTONELLA CRAPISI, PAOLO SCALABRINI,
AND PAOLO SPETTOLI[b]

Dipartimento di Biotecnologie Agrarie
Università di Padova
35131 Padova, Italy

INTRODUCTION

Semipermeable membrane devices have been used increasingly in the food industry. These systems have also been suggested for the nonfood industry, for example, continuous biological conversions with immobilized enzymes and proteins. A basic advantage of this confinement process is the nonchemical nature of the immobilization procedure and the subsequent lack of chemical modification of the immobilized compounds.[1]

Although a slow, and anyway small, leakage of loaded substances through the membrane could represent a limitation to the use of the technique,[2] the slow release can be exploited to control the content of additives in foods, including those classified as GRAS (generally recognized as safe).[3]

The objective of this research was to confine commercial nisin, a food preservative active against food-spoilage bacteria,[4] in a hollow-fiber device and to evaluate its antimicrobial activity on the indicator strain *Lactobacillus delbrueckeii* subspecies *bulgaricus* 1489 in broth medium.

MATERIALS AND METHODS

Chemicals

Nisin (37×10^6 U/g) was obtained from Aplin and Barret, Limited (Dorset, United Kingdom). Hollow-fiber cartridge PM 2 was purchased from Romicon (Woburn, Massachusetts). MRS medium and Bacto-agar were from Difco Laboratories (Detroit, Michigan).

Bacterial Culture and Counts

Lactobacillus delbrueckeii var. *bulgaricus* 1489, chosen as the indicator strain, was from stock collections of the Istituto Lattiero Caseario e di Biotecnologie Agroalimen-

[b]To whom all correspondence should be addressed.

tari (Thiene, Italy) and was grown in MRS medium. The total numbers of viable cells of the indicator strain (standardized overnight culture) were expressed as colony forming units (CFU)/mL.

Nisin Loading in a Hollow-Fiber Cartridge

Nisin (0.5–20 mg) was dissolved in 25 mL of MRS medium and time by time confined in the lumen-side inlet of the hollow fibers because these polysulfone ultrafiltration fibers have an inner volume of 25 mL. Then, 225 mL of MRS medium inoculated with 0.5% standardized overnight indicator strain culture was pumped in the outer-shell space and recycled through the bioreactor at 40 mL/min for 2 hours at 25 °C.

Assay for Nisin Activity

Aliquots of 100 μL of MRS inoculated solution were taken from the reservoir of the cartridge at regular time intervals (T_{0h}, T_{1h}, T_{2h}). Nisin activity was evaluated as CFU/mL of indicator strain determined using the pour plate method on MRS medium solidified with 1.8% Bacto-agar.

One control was carried out by dissolving the same amounts of free nisin in 225 mL of MRS medium inoculated with 0.5% standardized overnight indicator strain culture and by repeating the same procedure as previously reported.

Protein was determined by a spectrophotometric assay at 335 nm as proposed by Habeeb.[5]

RESULTS AND DISCUSSION

The biological activity of the substances loaded in hollow fiber can be affected by the contact with the polysulfone material fibers.[2] Five mg of commercial nisin was dissolved in 225 mL of MRS medium, pumped in the outer-shell-space hollow fibers, and recycled through the bioreactor for 6 hours; the nisin retains its antimicrobial activity, expressed as the formation of inhibition halos.[6] This indicates that polysulfone does not affect the protein action on the indicator strain.

In order to evaluate the lowest amount of nisin that carries on antimicrobial activity against the indicator strain, six trials were performed with 0.50, 1.00, 2.00, 5.00, 10.0, and 20.0 mg of nisin, respectively, loaded in a hollow-fiber cartridge. As shown in FIGURE 1, *Lactobacillus delbrueckeii* var. *bulgaricus* 1489 remains viable in the case of 0.50 mg of nisin employed. This could be due to adsorption phenomena that might occur in polysulfone hollow fiber.[7] In all other cases, the cells are inhibited and the protein stability in the hollow-fiber bioreactor increases in proportion to the loaded amounts. As a matter of fact, the best operational stability was obtained at 20 mg of protein with about 16 cycles of reuse. Recent studies[8] have demonstrated that nisin must adhere to the microorganism to show its inhibitory activity. In this respect, after the load of nisin into a Romicon PM 2 cartridge, MRS medium pumped in the outer-shell space was assayed for protein determination. About 5% of the protein passed through the fibers during the experimental operation in all trials with nisin

ranging from 1.00 to 20.0 mg. Although polysulfone fibers have a nominal molecular-weight cutoff of 2 Da, it appears that some of the fiber pores are sufficiently large to allow nisin (molecular weight = 3.4 Da) to pass through them, as observed by Patkar *et al.*[7] Our data confirm that nisin must come into tight contact with microbial cells in order to explicate its antimicrobial activity, which is in agreement with Daeschel *et al.*[9] and with our previous research.[10]
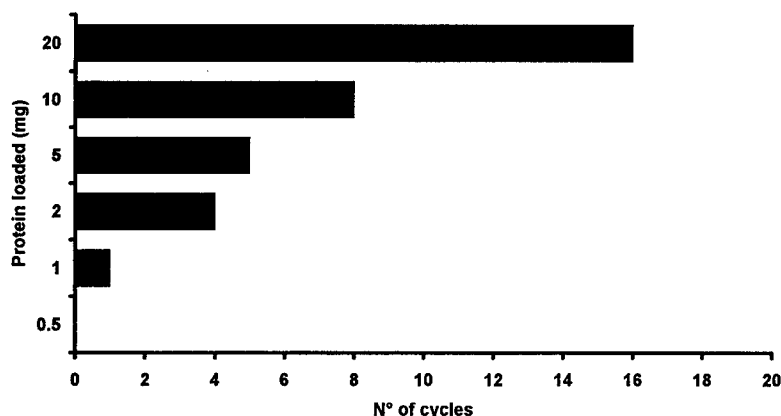
FIGURE 1. Operational stability of nisin as a function of the loaded amounts.

CONCLUSIONS

The obtained results show that nisin can be confined within polysulfone semipermeable membranes without getting the protein inactivation due to the contact with the fibers. Nisin is released slowly from the hollow-fiber system and only in such a state can it display its antimicrobial activity. Nevertheless, the containment of nisin within a hollow-fiber cartridge could represent a convenient tool to modulate the presence of preservative in a medium with respect to the overall amount normally used. The approach described could be the basis of a technology for the inhibition of undesirable microorganisms in liquid foodstuffs.

ACKNOWLEDGMENTS

REFERENCES

1. ZABORSKY, O. 1973. Immobilized Enzymes. CRC Press. Boca Raton, Florida.
2. KORUS, R. A. & A. C. OLSON. 1977. Use of glucose isomerase in hollow-fiber reactors. J. Food Sci. **42:** 258–260.

3. CERUTTI, G. 1992. Il Rischio Alimentare. Tecniche Nuove. Milan.
4. DELVES-BROUGHTON, J. 1990. Nisin and its uses as a food preservative. Food Technol.
    44: 100–117.
5. HABEEB, T. 1966. Determination of free amino groups in proteins by trinitrobenzenesul-
    fonic acid. Anal. Biochem. **14:** 328–336.
6. TRAMER, J. & G. G. FOWLER. 1964. Estimation of nisin in foods. J. Sci. Food Agric.
    15: 522–528.
7. PATKAR, A. Y., B. D. BOWEN & J. M. PIRET. 1990. Protein adsorption in polysulfone
    hollow-fiber bioreactors used for serum-free mammalian cell culture. Biotechnol.
    Bioeng. **42:** 1099–1106.
8. PIARD, J. C. & M. DESMAZEAUD. 1992. Inhibiting factors produced by lactic acid bacteria:
    2. Bacteriocins and other antibacterial substances. Lait **72:** 113–142.
9. DAESCHEL, M. A., J. MCGUIRE & H. AL-MAKHLAFI. 1992. Antimicrobial activity of nisin
    adsorbed to hydrophilic and hydrophobic silicone surfaces. J. Food Prot. **55:** 731–735.
10. LANTE, A., A. CRAPISI, G. PASINI & P. SCALABRINI. 1994. Nisin released from immobiliza-
    tion matrices as antimicrobial agent. Biotechnol. Lett. **16:** 293–298.

Immobilization of Aminoacylase on an Anion Exchange Column to Be Used as a Chromatographic Reactor

M. L. JANSEN,[a] E. VAN ZESSEN,[a] A. J. J. STRAATHOF,[a,b]
L. A. M. VAN DER WIELEN,[a] K. CH. A. M. LUYBEN,[a]
AND W. J. J. VAN DEN TWEEL[c]

[a]Department of Biochemical Engineering
Delft University of Technology
2628 BC Delft, the Netherlands

[c]DSM Research
6160 MD Geleen, the Netherlands

INTRODUCTION

Chromatographic reactors are plug-flow reactors where the substrate is introduced pulsewise and, while being converted, is spatially separated from the potentially inhibiting product(s) due to the chromatographic action of the column.[1] The substrate conversion may exceed the equilibrium and the products may be collected sequentially at the column exit. This type of integration of reaction and separation may be attractive for efficient and compact processing of enzymatic reactions.

We are studying the potential of the chromatographic reactor using the aminoacylase-catalyzed hydrolysis of N-acetyl-D,L-methionine as a model reaction. Because the enzyme is L-specific, a mixture of L-methionine, acetate, and unconverted N-acetyl-D-methionine is obtained, which requires chromatographic separation.

The aim of the research presented in this paper is to find a simple and efficient method to immobilize aminoacylase on a carrier for application in a chromatographic reactor and to identify conditions where immobilized aminoacylase is active and stable on the column. These conditions should be compatible with the conditions required for chromatographic separation of the substrate and products.

The chromatographic separation (in the absence of reaction) has been achieved using an anion exchange column. It critically depends on the pH in the range of 4–7.[2] Therefore, the kinetics and stability of aminoacylase will be studied in this pH range. Also, immobilization of aminoacylase by adsorption on anion exchange resin is studied. This is being applied in an industrial aminoacylase process.[3] Thus, the stationary phase for the chromatography will also be used as the immobilization matrix.

[b]To whom all correspondence should be addressed.

EXPERIMENTAL WORK

Materials

The anion exchange resin (Macro-Prep® Q, Bio-Rad, chloride form) has been described and characterized previously.[2,4] The amino acids and derivatives were from Sigma (St. Louis, Missouri), as was the aminoacylase (N-acylamino acid amidohydrolase; EC 3.5.1.14). This was Acylase I grade I lyophilized powder from porcine kidney, containing 75% protein with a specific activity of 0.56–0.83 kat/kg protein at 25 °C. At 37 °C (our assay conditions, see below), we found 0.65 kat/kg crude enzyme. The aminoacylase content is low because it can be purified 20-fold.[5]

Enzyme Activity Assay

Kinetic experiments, unless stated otherwise, were carried out with a 100-mL aqueous solution of 100 mmol/L N-acetyl-D,L-methionine, 0.5 mmol/L $CoCl_2$, and 0.02% (m/m) NaN_3 at 37 °C. The pH was maintained at 7 by addition of 0.1 mol/L NaOH using a Metrohm pH-stat system. The reaction was initiated by the addition of an amount of enzyme solution equivalent to 0.1 mg of protein. Initial reaction rates were determined from 500-µL samples at 0, 2, 4, 6, 8, and 10 min. Each sample was mixed with 1 mL of a 15 mmol/L 1,10-phenanthroline solution in order to stop the reaction. Subsequently, methionine was determined colorimetrically. The procedure of Hazra et al.[6] was modified by using 119 µL of 1 M aqueous TNBS instead of crystalline TNBS, and methionine was analyzed in 100 µL of aqueous solution, diluted to a maximum concentration of 0.6 mM, instead of as dry matter.

Enzyme Immobilization

Macro-Prep Q (12.5 g) was washed five times with 100 mL of water to remove the storage solution and equilibrated by washing eight times with 100 mL of a 10 mmol/L potassium phosphate buffer at pH 7. Resin (3 g) was suspended in flasks filled to 50 mL with potassium phosphate buffer at pH 7 and 0.94, 1.88, 3.76, and 7.52 g/L enzyme. The flasks were shaken for 24 h at 10 °C and 200 rpm. After incubation, the resin was filtered and washed with 10 mmol/L potassium phosphate buffer to remove the surplus enzyme.

For column experiments, a 50-mL solution was prepared containing 14.4 mg of crude aminoacylase, 10 mM NaCl, and 0.1 mM $CoCl_2$ at pH 6. Macro-Prep Q (14.4 g, Cl^--form) was added and a small amount of HCl was added to retain pH 6. The suspension was shaken 1 h at 25 °C and subsequently centrifuged.

Continuous Conversion in Column

Column experiments were performed at 25 °C using 15-mm-diameter columns that were packed with immobilized enzyme (13.4 g, 85-mm bed height). After elution

with 10 mM NaCl at 3 mL/min for 30 min, the steady-state conversion experiment was started by switching the feed to 25 mmol/L N-acetyl-D,L-methionine. For the pulse experiment, a flow of 6.6 mL/min of the NaCl solution was intermitted by pulses of 0.9 mL of the D,L-substrate solution.

RESULTS AND DISCUSSION

Conversion of D-Substrate

The literature value of K_m^L is 0.9 mmol/L.[5,7] Initial rate studies were performed at concentrations strongly exceeding K_m^L with pure L-substrate or D,L-substrate and gave identical maximum rates for both substrates. For the D-substrate, it was found that $K_m^D = 14$ mmol/L and $k_{cat}^D = 0.017$ mol/(kat-s). Because $k_{cat}^L \equiv 1$ mol/(kat-s), the enantiomeric ratio,[8] $(k_{cat}^L/K_m^L)/(k_{cat}^D/K_m^D)$, thus calculated is 900, which is considerably lower than the value of 8000 calculated from the data of Birnbaum *et al.*[9] Nevertheless, either value indicates that conversion of D-substrate may be neglected when L-substrate is present. In addition, the K_m values indicate that inhibition by D-substrate plays no role in any of the experiments described below.

Reversibility

When the amount of D,L-substrate is below 0.1 mol/L, the equilibrium conversion exceeds 98% (of the L-enantiomer) at pH 7.[7] For other pH values, the equilibrium conversion will be higher. Therefore, the reaction was assumed to be irreversible at the conditions applied in this paper.

Substrate and Product Inhibition

At pH 7, Wandrey and Flaschel[7] found inhibition constants of 12 mmol/L for L-methionine, 3.74 mmol/L for acetate, and 1566 mmol/L for D,L-substrate. When reaction rates are calculated using these values, it can be shown that substrate inhibition is below 6% up to 0.1 mol/L racemic substrate, which was confirmed by our experiments. However, product inhibition retards the reaction when the extent of conversion exceeds 7%. In the range of 0–7% conversion, the substrate concentration is much higher than the Michaelis constant. Thus, a simple zeroth-order model may be used up to 7 mmol/L product from 0.1 mol/L N-acetyl-D,L-methionine at pH 7. It was assumed that this situation would not change with changing pH.

Diffusion Limitation

For most experiments, zeroth-order kinetics apply. Then, calculation of the efficiency for spherical particles,[10] using the radius $R_P = 25$ μm, the bulk substrate concentration $c_S \leq 0.1$ mol/L, and the substrate diffusion coefficient $D \approx 10^{-10}$ m²/s,

shows that no diffusion limitation occurs when $V_{max} \leq 0.096$ mol/(L-s). This condition was easily fulfilled in the experiments. Diffusion limitation due to product accumulation is neglected because diffusion coefficients of the products are larger than that of the substrate.[2]

For low substrate concentrations, first-order kinetics apply. Then, an efficiency of $>95\%$ will be obtained when $V_{max} < 1.35$ mmol/(L-s).

pH Optimum

Aminoacylase has been shown[5,7] to be optimally active around pH 7 and extrapolation of literature data suggests hardly any activity below pH 6. However, at our assay conditions, the maximum is around pH 6 and considerable activity is present down to pH 5 (see FIGURE 1). High activities at low pH may be caused by the buffer type[5] because, for pH $<$ 6.5, we switched from triethanolamine to citrate in these experiments. However, it is beyond the scope of this paper to study and explain such effects.

The storage stability of aminoacylase was studied at 4 °C. The results (FIGURE 2) indicate that the enzyme is stable at pH 6–7, but a relatively rapid inactivation occurs at pH 4–5. Nevertheless, a reasonable activity level remains at pH 5. At higher temperatures, this inactivation will be faster, but it was assumed that conversion experiments would be possible even at pH 5.
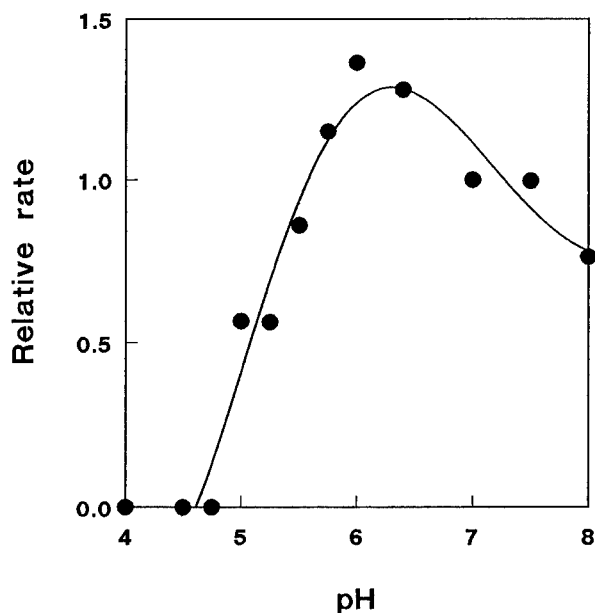
FIGURE 1. Activity of aminoacylase as a function of pH.
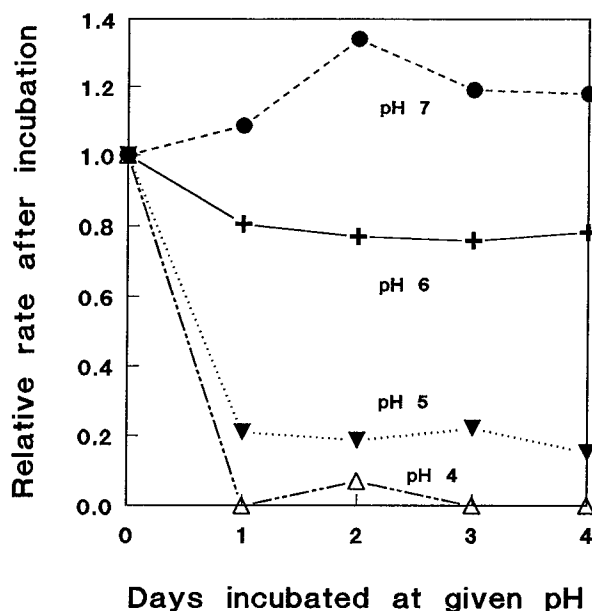
FIGURE 2. Activity of aminoacylase at assay conditions (pH 7, 37 °C) after incubation at several pH values (4 °C).

Course of pH and Ionic Strength due to Conversion

Above pH 6.9, the reaction produces H^+; below pH 6.9, it consumes H^+.[7] If the reaction is unbuffered and when no pH control is applied, the pH will approach 6.9 and pH gradients will appear in a column of aminoacylase. It can be calculated that the pH of 0.4 mol/L substrate may rise from 6 at 0% conversion to 6.5 at 50% conversion.[7] However, in our experiments, either the extent of conversion or the substrate concentration was much lower, so no significant pH gradients occurred.

The ionic strength determines the adsorption/desorption of the enzyme, as will be explained below. The ionic strength of the reaction mixture increases linearly with increasing initial substrate concentration, from about 5 mmol/L in the absence of substrate to about 105 mmol/L in the presence of 100 mmol/L substrate. The ionic strength is neither dependent on the extent of conversion (assuming that zwitterionic methionine does not contribute) nor on the pH in the range of 6–7. Below pH 6, there is a slight decrease in ionic strength due to the protonation of the acetate ion.

Batch Adsorption of the Enzyme

When the enzyme was adsorbed batchwise on the resin either at pH 6 in the presence of 10 mM NaCl or at pH 7 in the presence of 10 mM phosphate, virtually no activity remained in the solution. Between 65% and 100% was found back in the

immobilized enzyme and, for a typical experiment at pH 7, about 5×10^{-3} percent of the enzyme activity was found back in the solution by extending the assay time to several hours.

Adsorption, Desorption, and Conversion on a Column

On columns containing 1.77 g of resin, about 0.82 mg of crude enzyme was adsorbed from 0.1 mol/L D,L-substrate at pH 7. No breakthrough of the column was observed during loading. The amount of enzyme adsorbed was calculated to be sufficient for a significant extent of conversion of the 0.1 M D,L-substrate that was eluted for several days at pH 5.2, 6.0, and 7.1. However, FIGURE 3 shows that a very
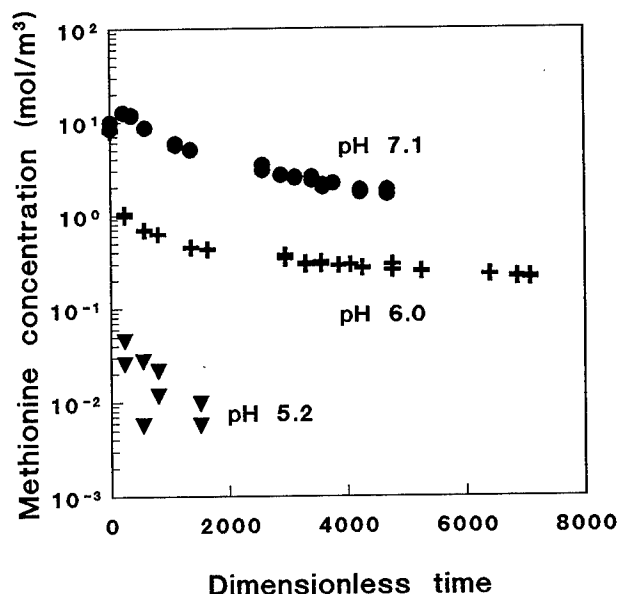
FIGURE 3. Long-term course of the conversion rate of 0.1 M D,L-substrate when eluted through columns of immobilized aminoacylase. A dimensionless residence time of 6000 corresponds to about 40 h.

rapid loss of activity occurs at pH 5.2 and 6.0. At pH 7.1, the initial loss in activity is large as well, but the activity loss rate for both pH 6.0 and 7.1 declines after 3000 dimensionless residence times. Then, steady-state experiments are possible. The steady-state methionine concentration in the effluent of such a column was measured for residence times between 2 and 20 min. A linear increase with increasing residence time confirmed the zeroth-order model.

Desorption of enzyme from the column was clearly dependent on the pH and ionic strength of the desorbing buffer applied. Because the isoelectric point of aminoacylase is 5.2, adsorption of the enzyme should increase above this pH. High

ionic strengths increase desorption. However, the desorption could not be quantitatively predicted using equilibrium models that relate the ionic strength of the buffer and the charge of the enzyme to the adsorption equilibrium position. It was assumed that the pH-dependent protein diffusion rates also determine the adsorption/desorption phenomena.

Conditions for Operation of a Chromatographic Column

The operation of a chromatographic column requires pH $\leq$ 6 for the chromatographic separation of substrate and products,[2] whereas the enzyme requires pH > 5 for sufficient activity and operational stability. In order to allow complete conversion of L-substrate, the amount of active enzyme that remains adsorbed on the column should remain sufficiently high for several days. This requires a relatively low substrate concentration (with a low ionic strength) and a high pH.

The compromise that we studied was 25 mM D,L-substrate of pH 6. During a steady-state column operation of 70 h, virtually 100% conversion of the L-enantiomer was observed. However, this does not imply a stable enzyme activity on the column because excess enzyme seemed to be present on the column. In order to study activity losses that occur at these specific concentrations of both enzyme and substrate and flow rate, a new method was used. Pulses of substrate were applied to the column and the retention time of the (unretained) L-methionine peak that left the column was monitored. This retention is mainly determined by the length of the (initial) part of the column where the conversion occurs and the substrate is retained by the resin (cf. reference 11). During five consecutive pulses, the methionine retention gradually increased. Assuming that the peak concentrations are mainly in the zeroth-order range, the enzyme activity can be calculated. A decrease to about 80% of the original value was observed. This calculation procedure should be refined because the concentrations at the sides of the peaks are in the first-order range and because product inhibition may become significant. However, the stability seems to be sufficient for further designing of the chromatographic reactor, which will be dealt with in a subsequent publication.

CONCLUSIONS

The behavior of aminoacylase on the ion exchange column is complicated by a large number of phenomena that mutually influence each other via the pH, the substrate or product concentration, and the enzyme activity. Many phenomena are understood and can be accounted for, but the adsorption/desorption equilibrium and the stability of the enzyme cannot be described properly yet. However, a simple immobilization procedure has been developed and an enzyme column with sufficient activity and stability for further development of the chromatographic reactor has been obtained.

ACKNOWLEDGMENTS

REFERENCES

1. VAN DER WIELEN, L. A. M., A. J. J. STRAATHOF & K. CH. A. M. LUYBEN. 1993. *In* Precision Process Technology. M. P. C. Weijnen & A. A. H. Drinkenburg, Eds.: 353–379. Kluwer. Dordrecht.
2. JANSEN, M. L., G. W. HOFLAND, J. HOUWERS, A. J. J. STRAATHOF, L. A. M. VAN DER WIELEN, K. CH. A. M. LUYBEN & W. J. J. VAN DEN TWEEL. 1996. To be published.
3. CHIBATA, I., T. TOSA, T. SATO & T. MORI. 1976. Methods Enzymol. **44:** 746–759.
4. JANSEN, M. L., A. J. J. STRAATHOF, L. A. M. VAN DER WIELEN, K. CH. A. M. LUYBEN & W. J. J. VAN DEN TWEEL. 1996. AIChE J. In press.
5. HENSELING, J. & K-H. RÖHM. 1988. Biochim. Biophys. Acta **959:** 370–377.
6. HAZRA, A. K., S. P. CHOCK & R. W. ALBERS. 1984. Anal. Biochem. **137:** 437–443.
7. WANDREY, C. & E. FLASCHEL. 1979. Adv. Biochem. Eng. **12:** 147–218.
8. CHEN, C-S., Y. FUJIMOTO, G. GIRDAUKAS & C. J. SIH. 1982. J. Am. Chem. Soc. **104:** 7294–7299.
9. BIRNBAUM, S. M., L. LEVINTOW, R. B. KINGSLEY & J. P. GREENSTEIN. 1952. J. Biol. Chem. **194:** 455–470.
10. VAN 'T RIET, K. & J. TRAMPER. 1991. Basic Bioreactor Design. Dekker. New York.
11. ADACHI, S., K. HASHIMOTO, R. MATSUNO, K. NAKANISHI & T. KAMIKUBO. 1980. Biotechnol. Bioeng. **22:** 779–797.

Biomolecular Modules for Creatinine Determination[a]

AXEL WARSINKE,[b,c] ALEXANDER BENKERT,[b]
WERNER SCHÖSSLER,[d] AND FRIEDER SCHELLER[b]

[b]Institute of Biochemistry and Molecular Physiology
University of Potsdam
Potsdam, Germany

[d]IMTEC Immundiagnostika GmbH
Zepernick, Germany

INTRODUCTION

Creatinine is one of the most important parameters in clinical diagnostics. Because the concentration in serum (2–100 μmol/L) and the urinary excretion (80–200 μmol/day-kg) are less influenced by dietary changes such as high intake of protein or creatine-free diet, creatinine is a much more reliable index of the renal glomerular filtration rate and function than urea.

Besides chemical (Jaffé reaction)[1] and chromatographic (e.g., HPLC)[2] methods, enzymatic methods for the determination of creatinine have been established in the past. These methods are based on multienzyme sequences with often more than three enzymes. The final product of the sequence is indicated by fluorimetric,[3] photometric,[4] amperometric,[5] or potentiometric[6] methods.

All these methods are in general laborious, not applicable to creatinine concentrations below 50 μmol/L, and susceptible to interference by various metabolites (e.g., endogenous creatine or ammonia) present in high concentrations in body fluids (creatine: 10–100 μmol/L).

In this study, we have used a modified principle of Albert et al.[7] to overcome these problems. Catalytic-active and binding modules have been developed and combined, converting creatinine to products, which are bound by the binding module and determined subsequently. The concentration of the bound product, which has been determined by enzyme immunoassay, reflects directly the creatinine concentration in the sample. The catalytic module is based on the enzyme creatinine deiminase, whereas the binding modules are based on antibodies to 1-methylhydantoin (FIG-URE 1).

[c]Address for correspondence: Max-Delbrueck-Center for Molecular Medicine, 13122 Berlin, Germany.

MATERIALS AND METHODS

1-Methylhydantoin derivatives have been synthesized with a propionic acid spacer (or an acetic acid spacer) in position 5 according to Hausdörfer[8] and with a butyric acid spacer in position 3 according to Albert et al.[7] The coupling of the derivatives to BSA and KLH has been performed by a standard carbodiimide coupling procedure. The 1-methylhydantoin-KLH conjugate was used for immunization of rabbits; in contrast, for the development of an indirect competitive 1-methylhydantoin-ELISA, the 1-methylhydantoin-BSA derivative was used for the coating of microtiter plates (Maxisorp, Nunc). Polyclonal antibodies (sheep) to 1-methylhydantoin were a kind gift of Boehringer Mannheim. Peroxidase-labeled anti-rabbit antibodies and anti-sheep antibodies were purchased from BioGenes (Berlin, Germany) and Sigma, respectively. For the development of a direct competitive 1-methylhydantoin-ELISA, the synthesized 1-methylhydantoin derivatives were coupled to alkaline phosphatase by a standard carbodiimide method. Creatinine deiminase (EC
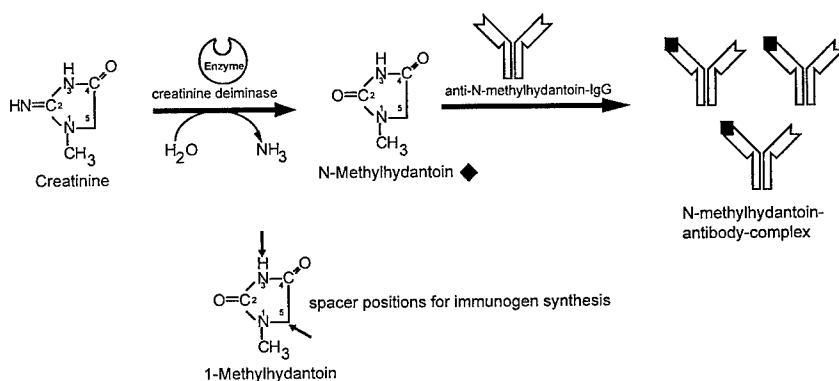
FIGURE 1. Principle of creatinine determination by combination of catalytic-active and binding modules.

3.5.4.21) with 12 U/mg was obtained from ICN. For creatinine determination, the enzyme was used directly within the microtiter plate wells coated with BSA-1-methylhydantoin conjugates. After addition of creatinine and antibodies to 1-methylhydantoin, the plates were incubated for 15 min. After washing the remaining solid phase, bound antibodies were determined with the peroxidase-labeled antibodies.

RESULTS AND DISCUSSION

For the determination of 1-methylhydantoin with an ELISA, different assay configurations have been tested with the produced antibodies and BSA conjugates. Best results were obtained with an indirect competitive configuration. The 1-methylhydantoin-BSA conjugate with the propionic acid spacer in position 5 for coating worked best in combination with polyclonal antibodies from sheep. For 1-methylhydantoin, the lower detection limit (0.95 B/B_0) was 0.013 µg/mL (0.115 µmol/L) and
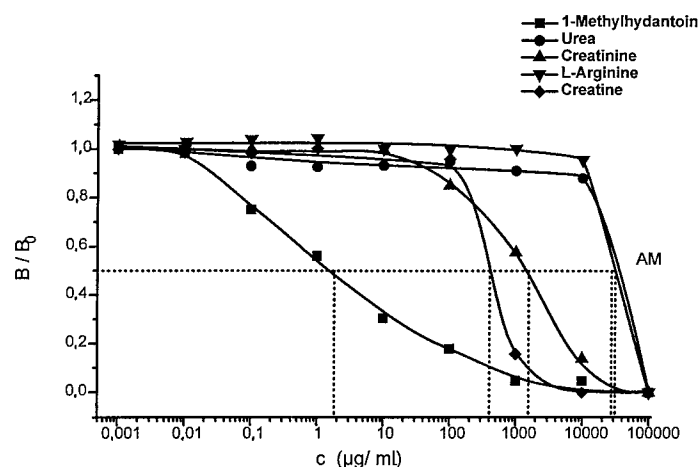
FIGURE 2. Calibration curves for 1-methylhydantoin and cross-reactive substances in the indirect competitive 1-methylhydantoin-ELISA. Coating: 10 µg/mL BSA-1-methylhydantoin in PBS; 100 µL/well; 2 h; wash: 3× PBS. Blocking: 1% casein/PBS; 200 µL/well; 1 h; wash: 3× PBS. Analyte: 0.001–100,000 µg/mL in 1% casein/PBS; 50 µL/well. Anti-1-methylhydantoin (sheep): 1/20,000 in 1% casein/PBS; 50 µL/well; 15 min; wash: 3× PBS. Anti-sheep-POD: 1/1000 in 1% casein/PBS; 100 µL/well; 3 h; wash: 3× PBS/Tween, 3× PBS. Substrate: TMB + H_2O_2 in 0.1 M acetate buffer, pH 5.0; 200 µL/well; 30 min. Stop: 4 N H_2SO_4; 100 µL/well. Read: 450/650 nm.

the upper detection limit (0.05 B/B_0) was 0.9 mg/mL (8 mmol/L). A typical calibration curve for 1-methylhydantoin is shown in FIGURE 2.

For the specificity of an immunoassay, the high cross-reactivity of polyclonal antibodies, which is often observed for low-molecular-weight antigens, can be
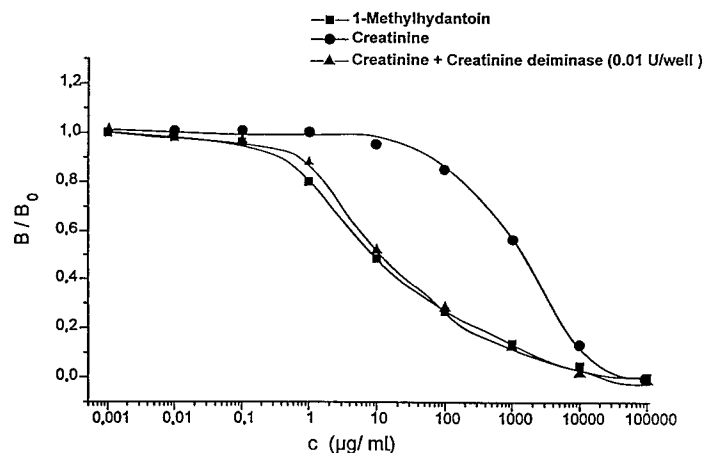
FIGURE 3. Calibration curves for creatinine (with and without creatinine deiminase) and 1-methylhydantoin in the 1-methylhydantoin-ELISA.

tremendous. For this reason, we have tested various substances that are present in body fluids and that have similar structure elements like 1-methylhydantoin.

As shown in FIGURE 2, the antibodies exhibit CR-50% values of 0.44% for creatine, 0.11% for creatinine, 0.0063% for urea, and 0.0057% for arginine.

The combination of the creatinine deiminase reaction with the 1-methylhydantoin-ELISA was performed within the microtiter plate. Different amounts of the enzyme and different preincubation times of the enzyme with the substrate have been tested to optimize the assay. Here, 0.01 U/well was sufficient to obtain nearly 100% conversion (FIGURE 3). A preincubation step was not necessary. The lower detection limit for creatinine was 0.9 μg/mL (8 μmol/L) and the upper detection limit was 2 mg/mL (18 mmol/L). In comparison to the 1-methylhydantoin-ELISA, the measuring range was shifted to higher concentrations. The reason for this could be the higher pH of the incubation buffer (pH 8.0) that is necessary for the enzyme.

CONCLUSIONS

If it is difficult to obtain appropriate enzymes or antibodies for an analyte, the combination of catalytic-active and binding modules is a useful alternative to a pure enzymatic or pure immunochemical test. With the described principle, creatinine has been determined to be <50 μM, but for real samples (urine, serum) further improvements are necessary. The production of monoclonal antibodies will increase the specificity. Furthermore, a site-directed coupling of the catalytic and recognition modules (e.g., recombinant or catalytic antibodies, high affinity peptides, aptameres or aptazymes, imprinting material) can be used in direct assay configurations.

REFERENCES

1. JAFFÉ, M. 1886. Über den Niederschlag, welchen Pikrinsäure in normalen Harn erzeugt und über eine neue Reaktion des Kreatinins. Hoppe-Seyler's Z. Physiol. Chem. **10:** 391.
2. SOLDIN, S. J. & J. G. HILL. 1978. Micromethod for determination of creatinine in biological fluids by high performance liquid chromatography. Clin. Chem. **24:** 747.
3. KINOSHITA, T. & Y. HIGARA. 1980. A fluorimetric determination of serum creatinine and creatine using a creatinineamidohydrolase-creatinamidinohydrolase-sarcosine oxidase-peroxidase system and diacetyldichlorofluorescein. Chem. Pharm. Bull. **28:** 3501.
4. FOSSATI, P., L. PRENCIPE & G. BERTI. 1983. Enzymatic creatinine assay: a new calorimetric method based on hydrogen peroxide measurement. Clin. Chem. **29:** 1494.
5. RUI, C. S., K. SONOMOTO, H. I. OGAWA & Y. KATO. 1993. A flow-injection biosensor system for the amperometric determination of creatinine: simultaneous compensation of endogenous interferents. Anal. Biochem. **210:** 163.
6. WINQUIST, F. & I. LUNDSTRÖM. 1986. Determination of creatinine by an ammonia-sensitive semiconductor structure and immobilized enzymes. Anal. Chem. **58:** 145.
7. ALBERT, W., J. ZIEGENHORN, J. SIEDEL, H. G. BATZ, H. LENZ & B. PAUTZ. 1983. Verfahren und Reagenz zur Bestimmung von Creatinin. Ger. Offen. No. DE 3150878A1.
8. HAUSDÖRFER, A. 1898. Über Diphenyl α-γ- u. α-δ- diacipiperazin. Ber. Dtsch. Chem. Ges. **22:** 1799.

In Situ Product Removal from E. coli Transketolase-catalyzed Biotransformations[a]

RASHMI P. CHAUHAN,[b] JOHN M. WOODLEY,[b]
AND LAWSON W. POWELL[c]

[b]Advanced Center for Biochemical Engineering
Department of Chemical and Biochemical Engineering
University College London
London WC1E 7JE, United Kingdom

[c]SmithKline Beecham Pharmaceuticals
Worthing, West Sussex BN14 8QH, United Kingdom

INTRODUCTION

Transketolase (TK) is an enzyme that catalyzes the transfer of a two-carbon ketol group from a ketose to an aldose to form a stereospecific carbon-carbon bond. The active form of the enzyme comprises two 73-kDa subunits in association with the cofactors thiamine pyrophosphate (TPP) and magnesium (II) ions (Mg^{2+}).[1] TK is found at high levels in spinach and yeast[2] and has also been produced in recombinant E. coli.[3,4] It is this form of the enzyme that has been used in studies to effect a variety of biotransformation reactions[5,6] as part of larger organic syntheses of high-value compounds.

Here, we briefly describe studies conducted to establish a recovery method for the product of a model E. coli TK-catalyzed biotransformation. The philosophy behind using in situ product removal (ISPR) is also addressed and discussed with regard to formulating a rational approach to product recovery from biotransformations.

Two approaches exist to remove a product molecule from a biotransformation: at the completion of the reaction and while it is still in progress. If the latter option is taken, the separation may be termed in situ product removal (ISPR).[7] A number of characteristics of the system need to be defined to determine the feasibility of a specific product recovery method. In particular, it is important to characterize the various compounds present in the system, including the product molecule.[7] This provides the basis to identify which distinguishing feature of the product molecule should be used to remove it from the other associated compounds in the environ-

545

ment. Categories have been suggested to systematically characterize a compound with respect to choosing a particular product recovery method.[7] These comprise physical and chemical characteristics of the molecule, such as molecular weight, volatility, hydrophobicity, charge, and specific elements.

IN SITU PRODUCT REMOVAL (ISPR)

A product may interfere with the productivity of a particular bioprocess in several ways. It may exhibit inhibitory or toxic behavior toward the biocatalyst, confer physicochemical effects on the system, or react with other components present in the system. ISPR can reduce the loss of product incurred from these interactions and hence can improve the productivity of the process.[7,8] In some cases, this approach has proved very successful.

Numerous studies on the theoretical aspects of integrating bioprocesses with subsequent downstream operations have been reported, including some that express the importance of merging fermentation with product recovery.[9–11] Others refer to the effect of ISPR on both fermentations and biotransformations, with examples.[12–14] The approaches used to establish the best means of ISPR, with emphasis on the need to characterize the product molecule, are also covered.[10,12,15]

The production of a particular component from a fermentation usually involves the use of simple compounds undergoing several chemical steps catalyzed by a number of enzymes to produce a distinctly different compound, for example, in the production of secondary metabolites. In contrast, the formation of a product from a biotransformation often involves only one enzyme to perform a single chemical change, resulting in a compound only slightly different than its substrates. This places a burden on the specificity of the product removal method to be used.

In spite of the amount of literature available, a systematic approach for the correct selection of ISPR methods does not exist. Here, we address this issue using reactions catalyzed by *E. coli* transketolase as examples.

E. COLI TK-CATALYZED REACTIONS

The general type of TK-catalyzed reaction is shown in FIGURE 1A. The enzyme catalyzes the transfer of a two-carbon ketol group from a ketose (1) to an aldehyde acceptor (2), to give a new aldose (3) and ketose (4). This reaction is reversible, whereby the newly formed products are readily converted back to the starting reactants to comply to the established equilibrium. The potential applications of this enzyme for the production of novel 2-ketoses have been discussed in the literature.[16–19]

β-Hydroxypyruvate can also be used as a ketol donor in TK-catalyzed reactions, rendering the reaction irreversible via the production of carbon dioxide as one of the products.[3] This is shown in FIGURE 1B, that is, the reaction used as a model system. β-Hydroxypyruvate (5) reacts with glycolaldehyde (6) (the simplest α-hydroxylated aldehyde) to give L-erythrulose (7) and carbon dioxide.

L-Erythrulose, the product of the model reaction, is a competitive inhibitor of *E.*

A

B
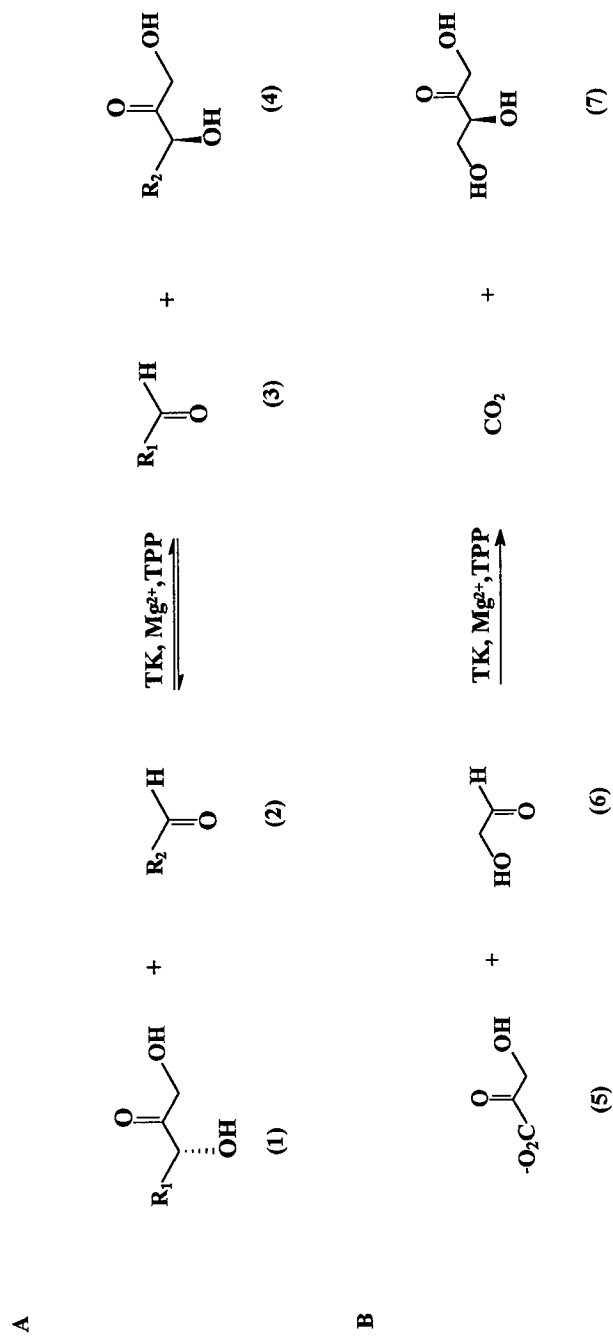
FIGURE 1. *E. coli* transketolase-catalyzed reaction: (A) generalized form; (B) model reaction.

coli TK, with an inhibition constant of approximately 146 mM (M. Gyamerah, unpublished results). It is suggested that L-erythrulose can act as a ketol donor, resulting in a futile TK-catalyzed reaction with glycolaldehyde.[5,6] This ketose may therefore compete with β-hydroxypyruvate for the active site of the enzyme. ISPR would reduce this effect, thus increasing the efficiency of the reaction, and hence this is an excellent model for the study of ISPR.

Other strategies exist to improve the biotransformation and to lessen the demand on ISPR. Feeding substrates to a biotransformation can reduce any toxic or inhibitory effects that they might have on the enzyme, such as the destabilizing effect of glycolaldehyde on *E. coli* TK.[20] Substrate feeding can also maintain certain conditions of the biotransformation. Feeding the free acid form of β-hydroxypyruvate can be used to maintain the pH of the reaction.[21] The use of β-hydroxypyruvate as a ketol donor results in an irreversible reaction. Alternative ketol donors result in reversible reactions, creating more complex systems from which to perform product recovery.

ISPR OF TK-CATALYZED REACTIONS

Although for the model system it appears that the only requirement for ISPR is to overcome inhibition of TK by L-erythrulose and to prevent it from interacting any further with glycolaldehyde, the importance of ISPR will be greater for other transketolase-catalyzed reactions. TABLE 1 shows four types of reactions that TK can catalyze. Depending on the types of substrates used and whether feeding strategies are employed, ISPR may prove particularly useful. Reactions involving feeding of both substrates and the use of β-hydroxypyruvate as the ketol donor result in only the product component being present in the reaction mixture, easing separation to a maximum level. The most difficult situation is when alternative ketol donors are used without feeding strategies, where there are a total of four compounds present in the reaction medium.

ISPR for the Model Reaction

In accordance with the characterization recommended to choose a suitable product recovery method, the compounds of the model *E. coli* TK-catalyzed biotrans-

TABLE 1. The Effect of Using Different Substrates in TK-catalyzed Reactions on the Need for and Ease of ISPR

Substrates		Products		Benefits from ISPR		Number of Compounds in System	
Ketol Donor	Aldehyde Acceptor	Main Product	Coproduct	Product Inhibition	Shifts Equilibrium	Batch	Fed-Batch
fructose-6-phosphate	glycolaldehyde	L-erythrulose	erythrose-4-phosphate	✓	✓	4	2
fructose-6-phosphate	3-*O*-benzyl-D-glyceraldehyde	5-*O*-benzyl-D-xylulose	erythrose-4-phosphate	✓	✓	4	2
β-hydroxypyruvate	glycolaldehyde	L-erythrulose	carbon dioxide	✓		3	1
β-hydroxypyruvate	3-*O*-benzyl-D-glyceraldehyde	5-*O*-benzyl-D-xylulose	carbon dioxide	✓		3	1

TABLE 2. Characterization of Substrates and Product of the *E. coli*
Transketolase-catalyzed Model Reaction[a]

Component Characteristic	Substrates		Product
	β-Hydroxypyruvate (5)	Glycolaldehyde (6)	L-Erythrulose (7)
Molecular weight	low (MW = 110)	low (MW = 60.1)	low (MW = 120.1)
Hydrophobicity[b]	hydrophilic (log P = −3.85)	hydrophilic (log P = −2.12)	hydrophilic (log P = −4.68)
Volatility	nonvolatile	nonvolatile	nonvolatile
Charge	negative	neutral	neutral
Functional groups[c]			
aldol	×	✓	×
ketol	✓	×	✓
hydroxyl	✓	✓	✓[d]
carboxyl	✓	×	×
carbonyl	✓	✓	✓

[a]Based on reference 7.
[b]Defined by reference 22.
[c]Symbols: ✓ and × represent the presence and absence of functional groups, respectively.
[d]Three hydroxyl groups.

formation were evaluated. For ISPR, it is desirable for the product molecule to differ in a distinct manner from the other compounds in the biotransformation. As shown in TABLE 2, there did not appear to be any useful differences between L-erythrulose and the two substrates: they are all nonvolatile, hydrophilic, and polar small molecules.

The uses of ion exchange resins, phenylboric acid, and immobilized phenylboronates were investigated as potential product removal methods. Ion exchangers were not considered suitable for the *in situ* removal of L-erythrulose. The more-anionic substrate molecules bound to anion exchangers more readily than the product. The use of cation exchangers were discounted as the binding of L-erythrulose was too weak for use as an efficient removal method.

In addition to those initial characteristics of L-erythrulose, glycolaldehyde, and β-hydroxypyruvate outlined, it was noted that L-erythrulose alone contains three hydroxyl groups within its structure, with two in the vicinal diol configuration. It has been well documented that phenylboric acid forms complexes with compounds containing vicinal diols or 1,3-diols, and extensive information into the theory and uses of this chemistry is available.[23–27] It was noted that contacting L-erythrulose and phenylboric acid resulted in a water-insoluble complex. This increased in quantity with the use of alkali solutions. This was not observed with mixtures containing the model substrates and phenylboric acid.

Although the use of free phenylboric acid offers a relatively cheap and selective means of L-erythrulose removal, the complex formation process requires alkali pH, which decreases the stability of all three reaction compounds and creates process implications for ISPR. The highly reversible nature of the reaction in aqueous conditions means that the potential amount of L-erythrulose recoverable from this

method is greatly decreased. The complexation process requires concentrated solutions of L-erythrulose, which creates problems if ISPR is to be considered because the product stream will then be dilute.

To overcome the associated problems of using phenylboric acid for the ISPR of L-erythrulose, the use of immobilized phenylboronates was studied. Numerous reviews and theoretical papers discuss the use of various types of immobilized boronate resins.[28-31] These have most commonly been agarose or polyacrylamide-based supports with phenylboronate ligands covalently attached. FIGURE 2 shows the interaction between a phenylboronate ligand and a *cis*-diol.

Studies Using Immobilized Boronates

To quantify the degree of L-erythrulose binding, a frontal uptake analysis experiment was performed.[32] The resin used was Affi-Gel® 601 gel (Bio-Rad Laboratories, Hemel Hempstead, England). Fifty mL of a 20 mM solution of L-erythrulose (Fluka Chemicals, Gillingham, England) was prepared in 40 mM barbital buffer, pH 9.5. One g of Affi-Gel® 601 gel was preswollen in buffer and packed into a 120 mm × 15 mm EconoPac® column (Bio-Rad Laboratories) to give a bed volume of 6 mL. Columns were also prepared for each compound as a control, where the L-erythrulose solution was prepared and the washing and swelling of the resin was performed using pure water. For both the control and the experimental columns, 1-mL aliquots of each solution were applied to each respective column and the effluent fractions were collected for analysis using an HPLC assay developed by Mitra.[33]

This experiment produced a frontal uptake profile, shown in FIGURE 3, which was used to obtain a value for the binding capacity of the resin for L-erythrulose of 50 μmol per mL of resin.

DISCUSSION

Of all the options examined, it appears that the greatest potential for selective removal of L-erythrulose from the model *E. coli* TK-catalyzed reaction lies in the application of immobilized boronate resins. The use of immobilized systems eliminates the problem of complex removal and hydrolysis due to the covalent linkage of the phenylboronate ligand to the matrix. Less extreme pH values are required for binding and elution than those for chemical complexation. The use of immobilized phenylboronates is also easier to apply as an ISPR process by using and regenerating two columns alternately. A schematic showing a possible type of ISPR rig used to perform the recovery of L-erythrulose from the model reaction is given in FIGURE 4.

However, the separation process is dependent on increasing pH, which creates process and compound stability implications. Separation is also less efficient with dilute product streams. The manufacturers of immobilized boronates advise the use of small concentrated solutions of the target molecule to achieve good binding,[32] which is not applicable to the ISPR of TK-catalyzed processes.

The binding capacity of Affi-Gel 601® of 50 μmol per mL for L-erythrulose
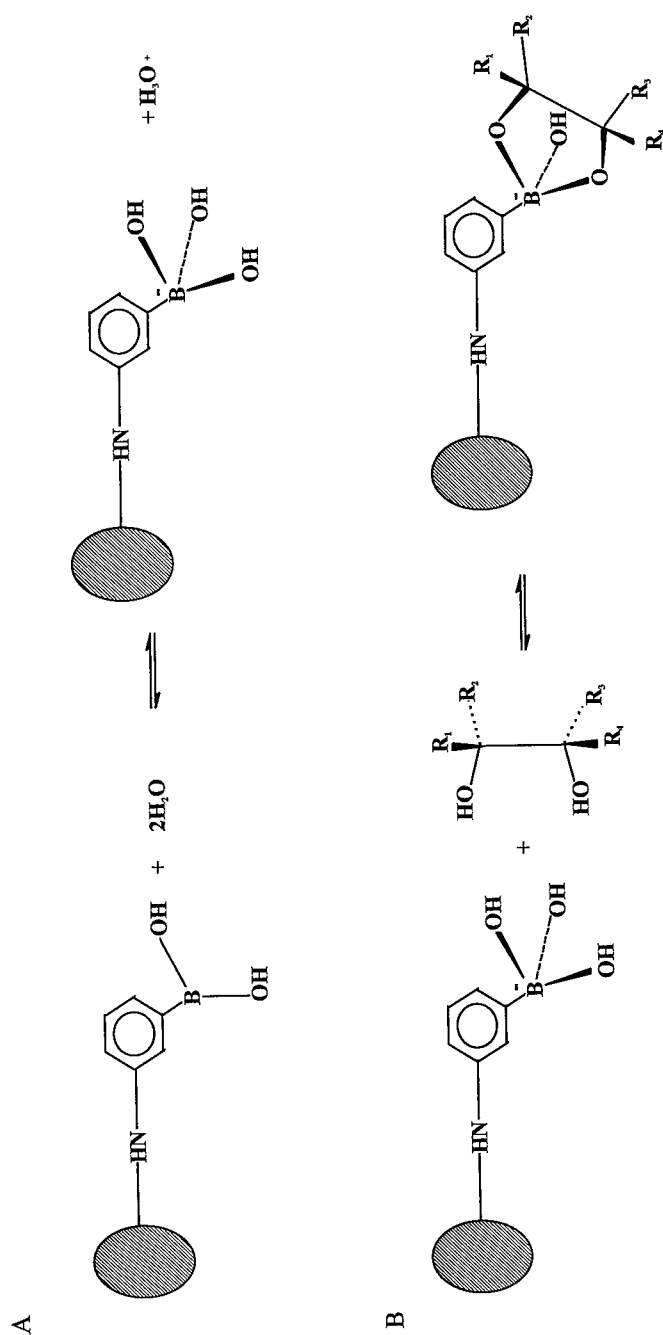
FIGURE 2. (A) Ionization of immobilized phenylboric acid from coplanar to anionic tetrahedral form. (B) Proposed reaction of phenylboronate ligand with a *cis*-diol (based on reference 32).
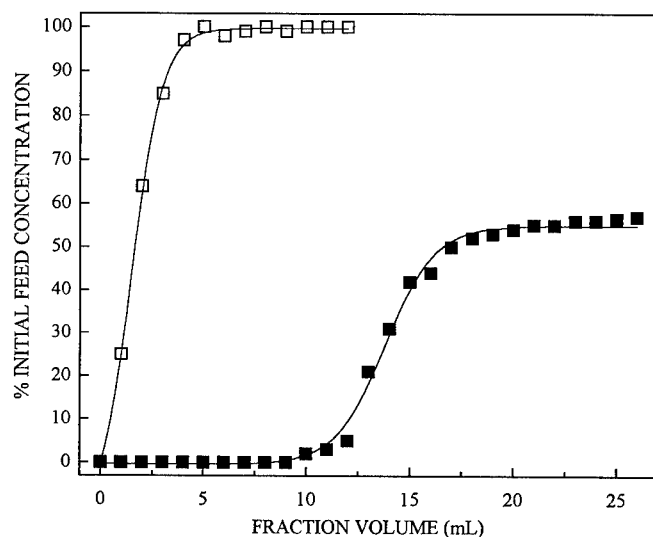
FIGURE 3. Frontal uptake profile of L-erythrulose using Affi-Gel® 601 gel: (■) pH 9.5; (□) pH 7.

equates to only 40% utilization of the total ligand concentration of the gel. In addition, the use of polyacrylamide resins is associated with a considerable degree of swelling and shrinkage with change in pH. This provides a variety of problems, particularly with the use of packed columns. There is also a degree of nonspecific binding that occurs, whereby glycolaldehyde and β-hydroxypyruvate bind to the resin, creating problems for ISPR.
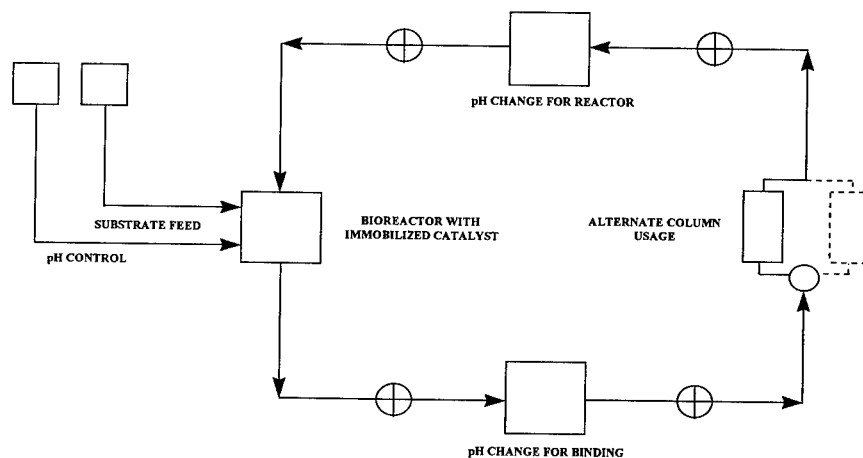
FIGURE 4. Possible ISPR system for *E. coli* transketolase-catalyzed reactions.

If one or both substrates were fed into the reaction at an appropriate rate, then their concentrations in the reaction volume would be minimal. The number of components in the system from which to remove L-erythrulose would be reduced and the choice of potential ISPR methods would be more extensive. For example, ion exchange adsorption may be a possible ISPR method or the use of other adsorptive materials could be investigated.

The use of immobilized boronate resins can be applied for the ISPR of other *E. coli* TK-catalyzed reactions. Immobilized boronates can be potentially used to recover products of TK-catalyzed reactions, providing the product contains *cis*-diol groups. If α-hydroxylated aldehyde acceptors are used as substrates, then the product will always contain *cis*-diol groups within its structure. However, other considerations must be made in such cases where the use of immobilized boronates would not be practical. For example, substrates such as fructose-6-phosphate also contain *cis*-diols within their structure and could compete with the product for binding sites on the boronate resins. It is also important to establish whether the coproducts of TK-catalyzed reactions possess this structural feature—for example, when fructose-6-phosphate is used as a ketol donor, the diol containing erythrose-4-phosphate is produced as a coproduct of the reaction.

Future studies into the ISPR of TK-catalyzed reactions will continue with the implementation of immobilized boronates with the model reaction and comparisons will be made with other TK-catalyzed reactions, different reactor operating modes, and different ISPR techniques.

REFERENCES

1. RACKER, E., G. DE LA HABA & I. G. LEDER. 1953. Thiamine pyrophosphate, a coenzyme of transketolase. J. Am. Chem. Soc. **75:** 1010–1011.
2. RACKER, E. 1961. Transketolase. *In* The Enzymes. P. D. Boyer, H. Lardy & K. Myrboch, Eds.: 397–406. Academic Press. New York.
3. DRATHS, K. M. & J. W. FROST. 1990. Synthesis using plasmid-based biocatalysis: plasmid assembly and 3-deoxy-D-arabino-heptulosonate production. J. Am. Chem. Soc. **112:** 1657–1659.
4. FRENCH, C. & J. M. WARD. 1995. Improved production and stability of *E. coli* recombinants expressing transketolase for large-scale biotransformation. Biotechnol. Lett. **17:** 247–252.
5. HOBBS, G. R., M. D. LILLY, N. J. TURNER, J. M. WARD, A. J. WILLETTS & J. M. WOODLEY. 1993. Enzyme-catalysed carbon-carbon bond formation: use of transketolase from *Escherichia coli.* J. Chem. Soc. Perkin Trans. **1:** 165–166.
6. HOBBS, G. R. 1994. The production and use of transketolase as a catalyst for carbon-carbon bond synthesis. Ph.D. thesis, University of London.
7. FREEMAN, A., J. M. WOODLEY & M. D. LILLY. 1993. *In situ* product removal as a tool for bioprocessing. Bio/Technology **11:** 1007–1012.
8. MATTIASSON, B. & O. HOLST. 1991. Objectives for extractive bioconversion. *In* Extractive Bioconversions. B. Mattiasson & O. Holst, Eds.: 1–11. Dekker. New York.
9. WANG, H. Y. 1983. Integrating biochemical separation and purification steps in fermentation processes. Ann. N.Y. Acad. Sci. **413:** 313–321.
10. SZATHMARY, S. & P. GRANDICS. 1990. Bioreactor integration with downstream processing. Bio/Technology **8:** 924–925.
11. ROFFLER, S. R., H. W. BLANCH & C. R. WILKE. 1984. *In-situ* recovery of fermentation products. Trends Biotechnol. **2:** 129–136.
12. DAUGULIS, A. J. 1988. Integrated reaction and product recovery in bioreactor systems. Biotechnol. Prog. **4:** 113–121.

13. HOLST, O., R. KAUL, M. LARSSON & B. MATTIASSON. 1987. Integration of bioconversions and downstream processing. Ann. N.Y. Acad. Sci. **506:** 468–477.
14. KOBAYASHI, T. 1990. Integration of reaction with product recovery in bioreactor systems. Ann. N.Y. Acad. Sci. **613:** 248–254.
15. BIEDERMANN, K. 1994. Integrated bioprocessing. *In* ECB6: Proceedings of the Sixth European Congress on Biotechnology. L. Alberghina, L. Frontali & P. Sensi, Eds.: 897–904. Elsevier. Amsterdam/New York.
16. KOBORI, Y., D. C. MYLES & G. M. WHITESIDES. 1992. Substrate specificity and carbohydrate synthesis using transketolase. J. Org. Chem. **57:** 5899–5907.
17. EFFENBERGER, F., V. NULL & T. ZIEGLER. 1992. Preparation of optically pure L-2-hydroxyaldehydes with yeast transketolase. Tetrahedron Lett. **33**(36): 5157–5160.
18. HECQUET, L., M. LEMAIRE, J. BOLTE & C. DEMUYNCK. 1994. Chemo-enzymatic synthesis of precursors of fagomine and 1,4-dideoxy-1,4-imino-D-arabinitol. Tetrahedron **35**(47): 8791–8794.
19. MYLES, D. C., D. J. ANDRULIS III & G. M. WHITESIDES. 1991. A transketolase-based synthesis of (+)-exo-brevicomin. Tetrahedron Lett. **32**(37): 4835–4838.
20. MITRA, R. K., J. M. WOODLEY & M. D. LILLY. 1995. Transketolase-catalyzed carbon-carbon bond formation: biotransformation characterization for process evaluation and selection. Enzyme Microb. Technol. In press.
21. WOODLEY, J. M., R. K. MITRA & M. D. LILLY. 1996. Carbon-carbon bond synthesis: reactor design and operation for transketolase-catalyzed biotransformations. This volume.
22. LAANE, C., S. BOEREN, R. HILHORST & C. VEEGER. 1987. Optimization of biocatalysis in organic media. *In* Biocatalysis in Organic Media. C. Laane, J. Tramper & M. D. Lilly, Eds.: 65–84. Elsevier. Amsterdam/New York.
23. BERGOLD, A. & W. H. SCOUTEN. 1983. Borate chromatography. *In* Solid-Phase Biochemistry: Analytical and Synthetic Aspects. W. H. Scouten, Ed.: 149–187. Wiley. New York.
24. EVANS, W. J., E. J. McCOURTNEY & W. B. CARNEY. 1979. A comparative analysis of the interaction of borate ion with various polyols. Anal. Biochem. **95:** 383–386.
25. FERRIER, R. J. 1978. Carbohydrate boronates. Adv. Carbohydr. Chem. Biochem. **35:** 31–80.
26. LORAND, J. P. & J. O. EDWARDS. 1959. Polyol complexes and structure of the benzeneboronate ion. J. Chem. Soc. **24:** 769–774.
27. ZITTLE, C. A. 1951. Reaction of borate with substances of biological interest. Adv. Enzymol. Relat. Areas Mol. Biol. **12:** 493–527.
28. ADAMEK, V., X. LIU, Y. ZHANG, K. ADAMKOVA & W. H. SCOUTEN. 1992. New aliphatic boronate ligands for affinity chromatography. J. Chromatogr. **625:** 91–99.
29. BENEŠ, M. J., A. ŠTAMBERGOVA & W. H. SCOUTEN. 1993. Affinity chromatography with immobilized benzeneboronates. *In* Molecular Interactions in Bioseparations. T. T. Ngo, Ed.: 313–322. Plenum. New York.
30. DEAN, P. D. G., F. A. MIDDLE, C. LONGSTAFF, A. BANNISTER & J. J. DEMBINSKI. 1983. Applications of immobilized boronic acids. *In* Affinity Chromatography and Biological Recognition. I. M. Chaiken, M. Wilchek & I. Parikh, Eds.: 433–443. Academic Press. New York.
31. MAZZEO, J. R. & I. S. KRULL. 1989. Immobilized boronates for the isolation and separation of bioanalytes. Biochromatography **4:** 124–130.
32. FULTON, S. 1981. Boronate Ligands in Biochemical Separations. Amicon Corporation. Danvers, Massachusetts.
33. MITRA, R. K. & J. M. WOODLEY. 1996. A useful assay for transketolase in asymmetric syntheses. Biotechnol. Tech. **10**(3): 167–172.

Use of Enzyme Technology to Convert Waste Lactose into Valuable Products

DAVID E. STEVENSON, ROGER A. STANLEY,
AND RICHARD H. FURNEAUX

New Zealand Institute for Industrial Research and Development
Lower Hutt, New Zealand

A sizable part of the New Zealand economy is based on the processing of food and there is a considerable demand for new ways to upgrade the lower-value by-products obtained into added-value products. One such by-product is lactose, produced in large quantities by New Zealand's cheese-making industry. We have been investigating the use of β-galactosidase (β-D-galactoside galactohydrolase, EC 3.2.1.23) to convert lactose into more valuable galactosides (β-D-galactopyranosides) and oligosaccharides. The latter are of interest as bifidobacteria factors in human nutrition.

The normal reaction of glycosidase enzymes involves the cleavage of the glycosidic bond to form a glycosyl enzyme complex, with the liberation of the aglycone.[1] The complex subsequently reacts with water to liberate a monosaccharide. The complex, however, can be intercepted by an (acceptor) alcohol to give transglycosylation products. Transglycosylation has been used extensively to prepare oligosaccharides and glycosides.[2] Lactose is one of the most useful glycosyl donors due to its low cost.

There are four main factors that influence the yield of galactoside that can be obtained from a transgalactosylation reaction: donor concentration, acceptor alcohol concentration, reaction time, and the properties of the enzyme (including its operational stability). We initially carried out a systematic variation of the reaction conditions aiming to optimize yields.[3] The highest possible donor concentration usually increases the yield, but in practice the concentration is limited by the solubility of lactose. A high acceptor concentration is also very beneficial, but again there are limitations. Acceptor solubility may be limited, especially if it is a hydrophobic solid; the presence of organic cosolvents can help to a limited extent. Even if the donor is highly water-soluble, for example, ethanol, limits are imposed by reductions in enzyme stability and lactose solubility. The ideal situation is when both donor and acceptor are present at high concentrations. This is not practical, however, unless the donor and acceptor are the same molecule, that is, in lactooligosaccharide synthesis when enzymic treatment of high concentrations of lactose results in extensive transfer of galactose onto lactose molecules to give trisaccharides and tetrasaccharides.[4]

Because the product is normally also a substrate for the enzyme, reaction time is an important parameter. The galactoside concentration rises rapidly at first; however, once most of the lactose has been hydrolyzed, the products start to compete with it for binding to the enzyme active site and the product concentration starts to fall.[3] Determination of the reaction time course is one of the best ways to optimize reaction yields.

Evaluation of two commercially available β-galactosidases, those from *Kluyvero-myces lactis* and *K. fragilis*, revealed their practical limitations, that is, susceptibility to inactivation by organic solvents and elevated temperature, and their ability to hydrolyze the reaction products. We were then able to define the characteristics of an ideal transglycosylation biocatalyst.[3] These were high operational stability and a strong preference for hydrolysis of lactose over galactosides. A comparative study of oligosaccharide and galactoside synthesis from lactose using β-galactosidases from *Aspergillus oryzae* and *Caldocellum saccharolyticum* revealed a nearly ideal enzyme.[4] The latter organism is a thermophile, so the resistance of its enzyme to inactivation by heat and organic solvents came as no surprise. Completely unexpected, however, was its very low activity for hydrolysis of alkyl galactosides. Not only did the enzyme produce high yields of galactoside from, for example, ethanol, but it also did not detectably degrade the product once the yield had reached its maximum, meaning that reaction time was relatively unimportant. In lactooligosaccharide synthesis, this enzyme was able to hydrolyze the products, but the optimized yield was still much higher (42%) compared with that from the *A. oryzae* enzyme, used for this purpose industrially (31%).[5] Further study led us to an even better enzyme, that from *Streptococcus thermophilus*, which was relatively stable in organic solvents (TABLE 1). Moreover, although it could hydrolyze galactosides, it had a relatively stronger preference for lactose, giving even higher yields of product.[6]

A critical factor to be addressed in moving towards commercialization of this synthetic method is the efficient isolation of the galactosidic products from the free sugar by-products that result from it. These comprise unreacted lactose, glucose and galactose from hydrolyzed lactose, and an equivalent amount of glucose to the galactoside produced. The only method used in the past was chromatography on silica gel, often after peracetylation of the reaction products, which was a relatively inefficient procedure due to the low selectivity of silica between the product and by-products. Two more efficient methods, however, are now available.[3] For galacto-sides with a sufficiently hydrophobic aglycone, preparative reversed-phase chroma-tography results in the glycosidic products and the acceptor alcohol binding to the column, while all the other materials elute in the void volume. The desired products can then be eluted with aqueous 2-propanol. Galactosides with more polar aglycones can be purified by chromatography on a strong anion exchange resin in the free base form. Only the free sugars bind to the column, due to the relative acidity of their anomeric hydroxyl group; the glycosidic products, having no comparable group, are

TABLE 1. Characteristics of β-Galactosidases Used in Oligosaccharide and β-Galactopyranoside Synthesis

Source of Enzyme (Reference)	pH Optimum	Maximum Usable Alcohol Concentration	Maximum Operating Temperature	Hydrolysis of Alkyl Galactosides
K. lactis (3)	6.8	3 M (ethanol)	40 °C	yes
K. fragilis (3)	6.8	3 M (ethanol)	40 °C	yes
A. oryzae (4)	4.8	4 M (ethanol)	50 °C	yes
C. saccharolyticum (4)[a]	6.3	5 M (ethanol)	65 °C	no
S. thermophilus (6)	7.0	6 M (2-fluoroethanol)	50 °C	yes

[a]This enzyme also has β-glucosidase, β-fucosidase, and β-xylosidase activities.

TABLE 2. Examples of β-Galactoside Synthesis on a Preparative Scale

Aglycone	Acceptor Concentration (M)	Lactose Concentration (M)	Enzyme	Yield (%)[a]	Reference
Hexanediol	1.5	0.75	*K. lactis*	49[c]	3
Butanediol	2.0	1.0	*K. lactis*	40[c]	3
Glycerol	3.0	1.0	*K. lactis*	60[d]	3
Benzyl alcohol	0.5[b]	1.0	*K. lactis*	6	3
Ethanol	4	1.0	*K. lactis*	36	3
2-Fluoroethanol	0.5	2.0	*K. lactis*	19	7
2-Fluoroethanol	0.5	2.0	*C. saccharolyticum*	26	4
2-Fluoroethanol	0.277	5.0	*S. thermophilus*	54	6
Allyl alcohol	0.277	3.0	*S. thermophilus*	38.5	9

[a]Yields are expressed relative to the limiting reactant. Values are isolated yields from preparative-scale reactions.
[b]30% v/v ethane-1,2-diol dimethyl ether as cosolvent.
[c]Yield of monogalactosides.
[d]88:12 mixture of isomers with galactosyl moiety on position-1 and -2 of glycerol.

not bound. With both of these methods, silica chromatography of the underivatized galactosides can be used for final cleanup, a relatively efficient procedure in the absence of free sugars.

We have prepared a number of galactosides on the gram scale (TABLE 2) to test the practicality of the synthesis; two in particular are potentially useful. New Zealand has a serious problem with introduced mammalian pests (e.g., rabbits, opossums), which breed prolifically and cause serious environmental damage. Poisoning programs, using baits containing sodium cyanide or sodium monofluoroacetate, are used to control numbers, but are hampered by "bait shyness." This problem is thought to be caused by animals smelling the volatile free acids formed from the toxins in decaying baits. Fluoroethyl galactoside is odorless and can be readily converted to free fluoroethanol in the digestive tract of the target animal. The fluoroethanol is then converted into fluoroacetate in the liver. We have been able to produce a crude preparation containing as much as 38% of the desired toxin.[6] The galactoside is being evaluated as an alternative bait toxin by pest control researchers.[7] It is also undergoing trials in molecular biology as a means of selecting plasmid-transformed cells with intact β-galactosidase genes from those with β-galactosidase genes that have a gene of interest inserted in them and are therefore inactive (J. Lederburg, personal communication).

Allyl galactoside is a useful synthetic intermediate in carbohydrate synthesis and is of interest as a monomer for the synthesis of novel hydrophilic polymers.[8] Allyl alcohol appears to have a strong inactivating effect on β-galactosidases, but the *S. thermophilus* β-galactosidase can synthesize its galactoside in much higher yield than even the *A. oryzae* enzyme.[9]

REFERENCES

1. SINNOTT, M. L. 1990. Catalytic mechanisms of glycosyl transfer. Chem. Rev. **90:** 1171–1202.

2. TOONE, E. J., E. S. SIMON, M. D. BEDNARSKI & G. M. WHITESIDES. 1989. Enzyme-catalyzed synthesis of carbohydrates. Tetrahedron **45:** 5365–5422.
3. STEVENSON, D. E., R. A. STANLEY & R. H. FURNEAUX. 1993. Optimization of alkyl β-D-galactopyranoside synthesis from lactose using commercially available β-galactosidases. Biotechnol. Bioeng. **42:** 657–666.
4. STEVENSON, D. E., R. A. STANLEY & R. H. FURNEAUX. 1996. Oligosaccharide and alkyl β-galactopyranoside synthesis from lactose with *Caldocellum saccharolyticum* β-glycosidase. Enzyme Microb. Technol. In press.
5. KAN, T. & Y. KOBAYASHI. 1987. Method for producing oligosaccharides. European patent no. 0266177.
6. STEVENSON, D. E. & R. H. FURNEAUX. 1996. High yield synthesis of ethyl and 2-fluoroethyl β-D-galactopyranosides using *Streptococcus thermophilus* β-galactosidase. Enzyme Microb. Technol. **18:** 513–518.
7. STEVENSON, D. E., A. D. WOOLHOUSE, R. H. FURNEAUX, D. BATCHELOR & C. T. EASON. 1994. Synthesis of 2-fluoroethyl β-D-galactopyranoside and 2-fluoroethyl 6-*O*-(β-D-galactopyranosyl)-β-D-galactopyranoside from lactose using β-galactosidase. Carbohydr. Res. **256:** 185–188.
8. DORDICK, J. S. 1992. Enzymatic and chemoenzymatic approaches to polymer synthesis. Trends Biotechnol. **10:** 287–293.
9. STEVENSON, D. E. & R. H. FURNEAUX. 1996. Synthesis of allyl β-D-galactopyranoside from lactose using *Streptococcus thermophilus* β-galactosidase. Carbohydr. Res. **284:** 279–283.

Development of a Pilot-Plant
Fermentation Process for the Production
of Yeast Lactase[a]

F. ACEVEDO, J. C. GENTINA, N. BOJORGE, I. REYES,
AND A. TORRES

School of Biochemical Engineering
Universidad Católica de Valparaíso
Valparaíso, Chile

INTRODUCTION

Yeast lactase has an increasing application in dairy products and digestive preparations. In Chile, the market of dairy products that use lactase has increased from 58,800 to 124,000 tons/year in the last ten years.

This work is part of a major project that includes the study of the fermentation, solid-liquid separation, cell disruption, debris separation, enzyme purification, and formulation of the product. Results on the fermentation stage are presented related to optimization of the medium, agitation, aeration, and feeding strategy in a 180-liter fermentor.

MATERIALS AND METHODS

Kluyveromyces fragilis was used throughout this study. It was kept in agar slants with lactose, salts, and yeast extract. Whey permeate, supplied by Dos Alamos S.A.C.I., contained (per liter) 43.5 g lactose, 51.0 g total solids, and 3.5 g protein.

A 20-L fermentor was used for laboratory studies and for inocula propagation for the pilot runs. In the fed-batch runs, concentrated whey permeate (180 g lactose/L), also supplied by Dos Alamos S.A.C.I., was fed through a computer programmable peristaltic pump. All fermentations were run at 30 °C and pH 4.2.

Cell concentration was determined by 650-nm absorbance and dry weight,[1] ethanol by gas chromatography, and lactose by the dinitrosalicylic method.[2] Lactase activity was assayed with isoamyl alcohol–permeabilized cells and ONPG as substrate. One international activity unit was defined as the amount of enzyme that catalyzes the reaction of one micromole of substrate per minute, at the assay conditions.

TABLE 1. Results of Shake-Flask and Laboratory Fermentor Experiments[a]

	Flasks	20-L Fermentor	
	A	A	B
Medium	A	A	B
Specific growth rate (h^{-1})	0.34	0.35	0.52
$Y_{x/s}$ (g cells/g lactose)	0.37	0.43	0.24
$Y_{e/s}$ (g ethanol/g lactose)	na	0.21	0.35
Specific activity (IU/g cells)	6120	5500	6130

[a]Terms—A: medium with 8 g lactose/L; B: medium with 40 g lactose/L; na: not assayed.

RESULTS AND DISCUSSION

Shake-Flask Experiments

Optimum temperature and pH were determined in shake flasks (30 °C, pH 4.2). A basal medium was designed considering the elemental compositions of the permeate and the biomass. The composition of the medium was then optimized. To avoid oxygen limitation, the permeate was diluted five times. No significant differences were detected when using vitamins and food-grade yeast extract, so the latter was chosen for its lower price. The optimized medium contained (per liter) 8.0 g lactose (supplied by the diluted permeate), 0.6 g $(NH_4)_2SO_4$, 0.4 g K_2HPO_4, and 1.0 g yeast extract.

Laboratory Fermentor Cultures

The diluted optimized medium was first validated in a 20-L fermentor operated at 450 rpm and 1.1 vvm. Then, a medium containing full-concentration permeate (all components present in concentrations five times higher) was tested. The results (TABLE 1) are satisfactory in terms of specific growth rate and specific activity. However, the low cell yield and the high ethanol yield of the run with full-concentration medium suggest a partially fermentative metabolism.

Next, experiments were performed to investigate the effect of aeration and agitation. Batch cultures were run in four conditions: 450 rpm, 2.0 vvm (condition I); 250 rpm, 0.0 vvm (II); 300 to 600 rpm, 0.3 to 1.8 vvm, so the dissolved oxygen concentration was at all times over 20% saturation (III); and 300 to 700 rpm, 0.4 to 2.6 vvm, so the oxygen concentration was over 35% saturation (IV).

Results shown in TABLE 2 confirm that, as noted by other authors,[3] lactase-

TABLE 2. Effect of Aeration and Agitation Rates in the 20-L Laboratory Fermentor[a]

	I	II	III	IV
Specific growth rate (h^{-1})	0.59	0.16	0.38	0.52
$Y_{x/s}$ (g cells/g lactose)	0.26	0.06	0.18	0.28
$Y_{e/s}$ (g ethanol/g lactose)	0.16	0.46	0.25	0.13
Specific activity (IU/g cells)	5560	6320	6050	4880
Volumetric activity (IU/L)	60,080	13,007	42,047	57,340

[a]Conditions—I: 450 rpm, 2.0 vvm; II: 250 rpm, 0.0 vvm; III: 300–600 rpm, 0.3–1.8 vvm, >20% saturation; IV: 300–700 rpm, 0.4–2.6 vvm, >35% saturation.

specific activities are higher at low or nil aerations (II and III). Nevertheless, because of the differences in cell yields, the total activity per batch, represented by the volumetric activity, is higher under aerated conditions (I and IV). These results led to the selection of condition I to scale up the process to the pilot fermentor.

Pilot Fermentor Cultures

Agitation and aeration determined in the laboratory were scaled up to the pilot equipment. Constant agitator tip speed and constant k_La criteria were used, resulting in 285 rpm and 1.4 vvm.

Specific growth rates of 0.46 h^{-1} and activities over 57,000 IU/L were obtained in batch cultures. Growth was exponential during the first 6 to 8 hours, a period in which the lactose was consumed, the dissolved oxygen was depleted, and the specific activity reached a maximum. From that moment on, the previously excreted ethanol was metabolized and the lactase activity decayed. The same behavior was found in the laboratory-scale experiments.

TABLE 3. Pilot-Plant Fed-Batch Fermentations

Final cell concentration (g/L)	25.6
Specific growth rate (h^{-1})	0.15
Specific activity (IU/g cells)	> 5000
Volumetric activity (IU/L)	128,100
$Y_{x/s}$ overall (g cells/g lactose)	0.31
$Y_{x/s}$ fed period (g cells/g lactose)	0.34
$Y_{e/s}$ (g ethanol/g lactose)^a	0.11

^{a}Calculated at the time of maximum ethanol concentration.

The effect of agitation and aeration on the oxygen transfer coefficient, k_La, in the pilot fermentor was studied and the following correlation was established:

$$k_La = 0.0054(\text{vvm})^{0.78}(\text{rpm})^{1.75} \quad (\text{h}^{-1}).$$

Cultures run at equal oxygen transfer coefficient values, but at different agitation and aeration rates, resulted in different specific activities. Higher activities were obtained with 450 rpm and 2.0 vvm.

To overcome the decay in lactase activity after lactose depletion, fed-batch experiments were performed. The exponential feed rate was set to obtain a constant growth rate of 0.15 h^{-1}. Initial volumes were 80 to 83 L, and 40 L of 180 g lactose/L concentrated permeate was fed in 6 to 7 hours. TABLE 3 shows typical results of the fed-batch experiments. The specific activities of 5000 to 5500 IU/g of cells are considered satisfactory.

CONCLUSIONS

A suitable technology was developed for the production of yeast lactase in a pilot-scale fermentor. The whey permeate–based medium was optimized, the influ-

ence of the operational variables was determined, and a satisfactory feeding strategy was established.

REFERENCES

1. COONEY, C. L. 1981. Growth of microorganisms. *In* Biotechnology. Volume 1. H. J. Rehm, Ed.: 73–112. Verlag Chemie. Weinheim.
2. MILLER, G. 1959. Use of dinitrosalicylic acid reagent for the determination of reducing sugars. Anal. Chem. **31:** 426–429.
3. GARCÍA-GARIBAY, M., J. TORRES, A. LÓPEZ-MUNGUÍA & L. T. CASAS. 1987. Influence of oxygen transfer rate on β-galactosidase production from *Kluyveromyces marxianus*. Biotechnol. Lett. **9:** 417–420.

Kinetic Studies of *Fusarium solani* Cutinase in a Gas/Solid System

S. LAMARE AND M. D. LEGOY

Laboratoire de Génie Protéique et Cellulaire
Pôle Science
Université de La Rochelle
17042 La Rochelle Cedex, France

INTRODUCTION

The effects of solvation/hydration on the kinetics of transesterification and hydrolysis reactions have been studied, using a recombinant cutinase from *Fusarium solani*, adsorbed onto Chromosorb P, in a gas/solid system. The experimental setup was a continuous gas/solid bioreactor, in which nitrogen, vaporized substrates, and products, constituting the gaseous phase, were percolating a packed-bed reactor containing the adsorbed biocatalyst. Results exhibited a noncommon behavior, for which an explanation should be based on the modification of the polarity of the active site. Such a model is proposed, in good correlation with the results for the two types of reaction.

MATERIALS AND METHODS

Fusarium solani cutinase cloned and expressed in *E. coli* was a kind gift of Corvas (Ghent, Belgium). The purity of the preparation was higher than 95% and was checked by SDS electrophoresis. Enzyme adsorption was performed onto Chromosorb P (Rhône Poulenc, France, mesh 30/60). Fifty mg dissolved in 3 mL of a 20 mM phosphate buffer at pH 7.5 was deposited onto 1.5 g of dry Chromosorb. After vigorous shaking, the preparation was placed overnight under vacuum. Loaded Chromosorb was then stored at 4 °C. All the substrates were purchased from Aldrich and were of the highest available purity (99% minimum).

EXPERIMENTAL SETUP

The bioreactor is composed of saturation flasks containing the substrates and water. By bubbling a carrier gas (nitrogen) inside, it is possible to obtain a saturated gas with a known compound vapor pressure. By mixing different gas lines and by controlling precisely the carrier flows, temperature, and total pressure, it is then possible to realize a gas for which the composition is defined by the thermodynamic activity of each vaporized compound. Thus, we used the experimental setup depicted in FIGURE 1 for experiments of transesterification between propionic acid methyl ester and *n*-propanol and for hydrolysis of propionic acid methyl, ethyl, and propyl

esters. A more complete description of the experimental setup has been previously published.[1]

TRANSESTERIFICATION REACTION BETWEEN PROPIONIC ACID METHYL ESTER AND n-PROPANOL

The effect of the hydration state of the biocatalyst on the kinetic behavior was studied at 60 °C as a function of the thermodynamic activity of water and substrates. Previous results[2] highlighted the need to take into account the thermodynamic activity for defining the substrate availability in this system. During the whole set of
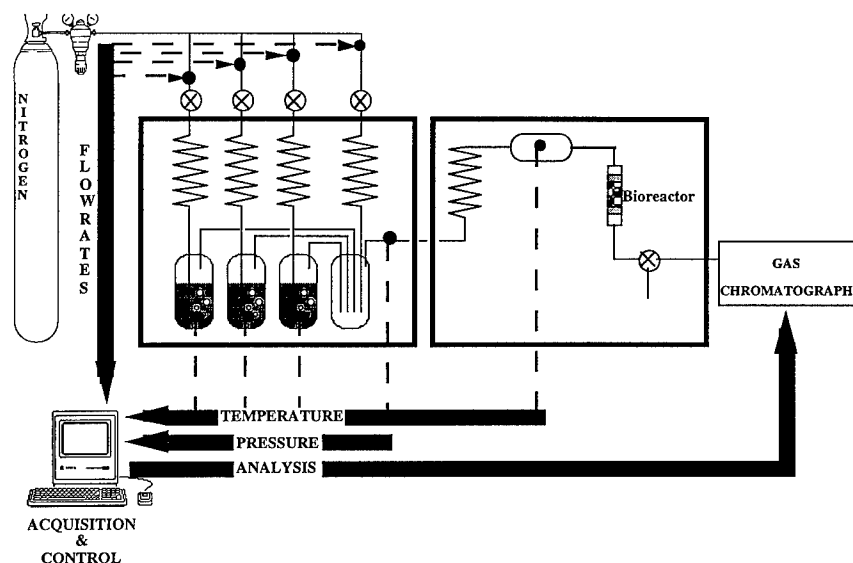
FIGURE 1. Experimental setup.

experiments, the total flow was set at 500 μmol/min, giving a volumetric flow of 12.5 mL/min and a residence time close to 0.4 s. Care was taken so that the conversion never exceeded 1% in order to maintain the correct thermodynamic activities of the substrate and water throughout the reactor. Three degrees of hydration have been tested, corresponding to a_w values equal to 0.2, 0.4, and 0.6. Results are presented in FIGURES 2, 3, and 4, respectively. Results exhibited sigmoidal curves when varying the a_{ester} at fixed $a_{alcohol}$ and an enhancing effect by the alcohol when the enzymatic preparation was not fully hydrated (i.e., $a_w < 0.6$).

The mechanism of reaction cannot be asserted yet. Nevertheless, assuming a ping-pong model,[3–5] some hypothesis, based on the hydration/solvation of the active site, can be formulated in order to explain this kinetic behavior.

For low hydration conditions ($a_w = 0.2$), the alcohol acts as an effector when it is
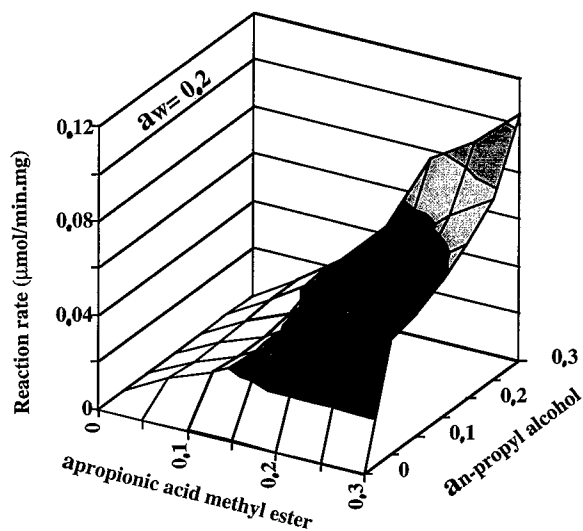
FIGURE 2. Transesterification between propionic acid methyl ester and n-propanol at 60 °C and $a_w = 0.2$.

present at high activity. This effect can be detected for $a_{alcohol}$ higher than 0.15. The effect of the alcohol is double.

It may, under low hydration conditions, solvate some nonhydrated polar sites onto the protein, leading to a more flexible protein by replacing some water molecules acting as a plasticizer.[6,7]
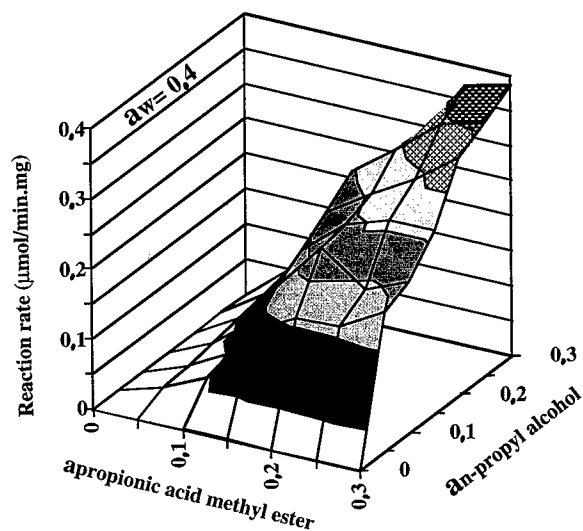
FIGURE 3. Transesterification between propionic acid methyl ester and n-propanol at 60 °C and $a_w = 0.4$.
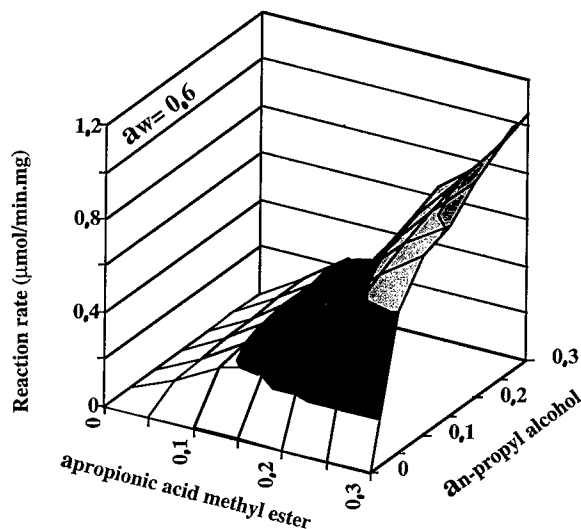
FIGURE 4. Transesterification between propionic acid methyl ester and n-propanol at 60 °C and $a_w = 0.6$.

Furthermore, a major solvation of the active site by the alcohol generates hydrophobic interactions implicated in the binding[8] of the most apolar substrate, the ester. When a_{ester} increases, it creates some competition for the solvation, and the catalytic efficiency is related to the ratio between the substrates. An exclusion of the alcohol by the ester may explain the sigmoidal pattern observed when varying the a_{ester}.

For higher hydration conditions ($a_w = 0.4$), the activator role of the alcohol is minimized and its action is mainly due to its distribution in the active site as described before. In the same way, the ester can compete with the alcohol, and sigmoid curves are still observed when varying the a_{ester}. Once the enzyme is fully hydrated ($a_w = 0.6$), the exclusion phenomena of the alcohol by the ester are minimized by a correct hydration of the active site. The activity versus the a_{ester} is then more linear and the activity versus the $a_{alcohol}$ presents rapidly a plateau. This also produces a very high K_M for the ester and a lower one for the alcohol.

Hydrolytic experiments were necessary in order to validate this model.

HYDROLYSIS OF PROPIONIC ACID ALKYL ESTERS
FOR TWO HYDRATION CONDITIONS

If the proposed model is valuable, the hydrolysis of different polar substrates may highlight two phenomena:

1. A low hydration state of the enzyme must lead to a less-reactive apolar substrate. Hydrolysis can occur for high a_{ester} values as a_w decreases.

2. The use of a high a_w must lead to a greater availability of and a higher reactivity for apolar substrates. The apparent K_M for the apolar substrates must be lower than for the polar ones.

In this set of experiments, a temperature of 50 °C was used in order to obtain higher a_{ester} values. The effect of a 10 °C modification has been previously described.[8] The results presented are in good correlation with the model proposed:

1. As expected, for low water activity, the more polar the substrate, the lower its reactivity. Using $a_w = 0.2$, hydrolysis of the methyl ester is possible when $a_{ester} > 0.6$, whereas the ethyl ester can be hydrolyzed when $a_{ester} > 0.7$. No hydrolysis of the propyl ester can be detected for $a_{ester} < 0.8$ (see FIGURE 5).
2. For high a_w (0.6), the more apolar the substrate, the lower its apparent K_M, as reported by the a_{ester} required to obtain the saturation and a constant reaction rate (see FIGURE 6).

CONCLUSIONS

These results appear rather complex, but they highlight some topics that have to be developed in the near future. First, it now seems that the hydration/solvation of a protein must be considered carefully, and the interactions between the enzyme and the chemical species present in its microenvironment must be understood precisely, as well as the interactions existing between the chemical species themselves. The concept of thermodynamic activity also shows its own limitations. Even if the thermodynamic activity appears to be the better way for defining the hydration/solvation state, we now have to understand precisely the distribution of the different molecules onto the different domains of the protein.
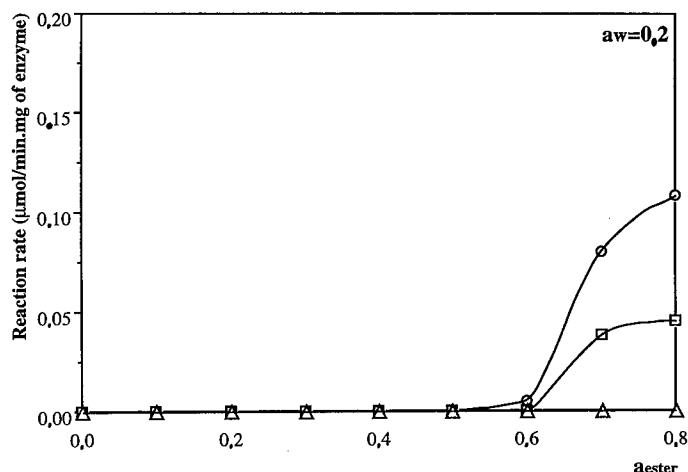
FIGURE 5. Hydrolysis of propionic acid methyl (○), ethyl (□), and propyl (△) esters at 50 °C and $a_w = 0.2$.
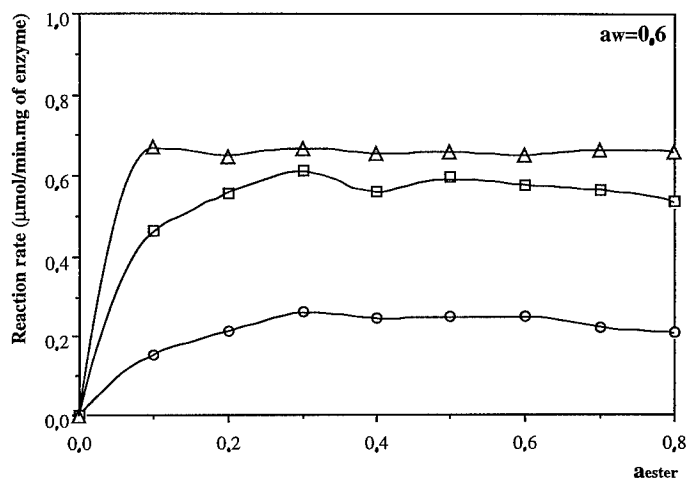
FIGURE 6. Hydrolysis of propionic acid methyl (○), ethyl (□), and propyl (△) esters at 50 °C and $a_w = 0.6$.

Second, this system is very singular. Considering the 150-μL bioreactor that we used, loaded with 1 or 2 mg of pure protein, it corresponds to 10^{-7} moles of enzyme. The 150 μL of gas at 60 °C represents about 6×10^{-6} moles. Working with a partial pressure of substrates in the range of 0.020 to 0.200 atm implies that the ratio between the enzyme molecules and the substrates and products will differ by one or two orders of magnitude. It appears then as a very good experimental tool suited for the studies concerning molecular modeling of the enzyme/substrate/water interactions. Full results will be released soon in the literature.

REFERENCES

1. LAMARE, S. & M. D. LEGOY. 1995. Biotechnol. Bioeng. **45:** 387–397.
2. LAMARE, S. & M. D. LEGOY. 1995. Biotechnol. Tech. **9:** 127–132.
3. CHULALAKSANANUKUL, W. *et al.* 1990. FEBS Lett. **276:** 181–184.
4. MARTY, A. *et al.* 1992. Biotechnol. Bioeng. **39:** 273–280.
5. RIZZI, M. *et al.* 1992. Enzyme Microb. Technol. **14:** 709–714.
6. GORMAN, L. & J. DORDICK. 1992. Biotechnol. Bioeng. **39:** 392–397.
7. HALLING, P. 1989. Trends Biochem. Sci. **7:** 50–51.
8. KLIBANOV, A. 1989. Trends Biochem. Sci. **14:** 141–144.

A Stable Cholesterol Esterase[a]

R. VENKATESH AND P. V. SUNDARAM[b]

Center for Protein Engineering and Biomedical Research
The Voluntary Health Services
Madras 600 113, India

INTRODUCTION

The use of esterases as biocatalysts for industrial biosynthetic processes has received much attention recently. However, their intrinsic low stability needs to be overcome for their successful application. Cholesterol esterase (CE) is one such enzyme that is currently in demand for use in routine clinical analysis, although it may be used in synthesis as well.

In this study, we have covalently modified cholesterol esterase isolated from *Pseudomonas* sp. and have studied its stability and kinetics of inactivation.

MATERIALS AND METHODS

Cholesterol esterase was modified with bifunctional and polyfunctional aldehydes such as monomeric glutaraldehyde (MGA) and polyglutaraldehyde (PGA) and a high-molecular-weight oxidized polymer of sucrose (OSP) at pH 8 in phosphate buffer (0.05 M). The covalent modification follows the reductive deamination method that engages the ϵ-NH$_2$ groups in the protein. The degree of modification of the protein was followed using the trinitrobenzene sulfonic acid procedure.

The enzyme was assayed using *p*-nitrophenyl acetate (PNPA) as the substrate at pH 6.5 in phosphate buffer (0.01 M). The final concentration of PNPA was 0.88 mM and the enzyme taken for each assay was 10 μg. The assay was run at room temperature for one minute.

RESULTS AND DISCUSSION

Covalent coupling of cholesterol esterase to bifunctional, multifunctional, and polyfunctional aldehydes resulted in the modification of 75–80% of the surface lysine residues (TABLE 1). Thermal inactivation measured between 30 and 85 °C was rather steep for the native enzyme, whereas the modified enzymes were destabilized after longer periods of time. The half-life of modified cholesterol esterase was severalfold higher (TABLE 2) than that of the native enzyme. The free energy of inactivation ($\Delta G\ddagger$) increased by 2.24 kcal/mol for MGA-CE, by 2.4 kcal/mol for PGA-CE, and by 2.82 kcal/mol for OSP-CE. The modified enzymes also displayed a higher activation

[b]To whom all correspondence should be addressed.

TABLE 1. Conditions for Modification

Enzyme	Modifier Concentration	Modification Time	% Amino Group Modified	% Activity Retained
Native	—	—	—	100
OSP-CE	14 mg	18 h	75	117
MGA-CE	50 μmol	4 h	80	103
PGA-CE	12 mg	4 h	80	96

TABLE 2. Temperature Effects on Native and Modified Cholesterol Esterase[a]

	$\Delta G\ddagger$ (kcal/mol)	$\Delta H\ddagger$ (kcal/mol)	$\Delta S\ddagger$ (cal/mol/K)	$t_{1/2}$ (h)	T_{50} (°C)	ΔT_{50}
Native CE	27	31.56	16.2	0.923	55	—
MGA-CE	29.24	42.51	38.6	115	77	22
PGA-CE	29.4	43.4	43.84	115	79	24
OSP-CE	29.82	42.9	38.1	295	85	30

[a]Terms—$\Delta G\ddagger$: activation free energy of inactivation; $\Delta H\ddagger$: activation enthalpy of inactivation; $\Delta S\ddagger$: activation entropy of inactivation; $t_{1/2}$: half-life of thermal inactivation; T_{50}: temperature where 50% activity is retained; ΔT_{50}: the temperature difference between modified and native enzyme. The $\Delta G\ddagger$ and $t_{1/2}$ values at 343 K are given here.

energy of inactivation (E_i), a higher activation enthalpy of inactivation ($\Delta H\ddagger$), and a twofold to threefold increase in the activation entropy of inactivation ($\Delta S\ddagger$).

Urea inactivation studies showed that, after 2 h at 40 °C in 8 M urea, the native enzyme retained only 30% activity, whereas MGA-CE retained 63.5%, PGA-CE retained 79%, and OSP-CE retained 98.5% activity. The relative stability of native and modified CE in 80% v/v polar organic solvents indicated that modified enzymes are extremely stable, retaining 90% of the activity, whereas the native enzyme is more prone to inactivation.

The trend in the stabilization is OSP-CE > PGA-CE > MGA-CE > native. This shows that an increase in the molecular weight of the aldehyde used for modification results in increased stability. Multifunctional and polyfunctional aldehydes protect enzymes presumably by forming covalent bonds around the enzyme molecule to produce a "cage"-like effect.

Rigid Proteases Are More Stable[a]

R. VENKATESH,[b] N. RAJALAKSHMI,[b] J. SIVAKUMAR,[b]
PETER SELLERS,[c] AND P. V. SUNDARAM[b,d]

[b]Center for Protein Engineering and Biomedical Research
The Voluntary Health Services
Madras 600 113, India

[c]Department of Physical Chemistry
Chemical Center
University of Lund
S-221 00 Lund, Sweden

INTRODUCTION

Proteases from microbial, plant, and animal sources are versatile in their specificity, often high in their activity, and reasonably stable within a defined range of temperature and pH. However, currently, there is a drive to stretch their stability and applicability to levels beyond what nature intended.

It is our aim to convert a naturally occurring biocatalyst to an ideal one by manipulating its structure chemically. Our efforts are directed to develop simple methods of modification of proteases and at the same time to converge on their properties that may be amenable to change through these modifications. Because proteases are subject to autocatalysis, it becomes a bigger challenge to modify them and yet retain enough activity and stability. Studies on inactivation kinetics and catalytic properties indicate that trypsin, α-chymotrypsin, and papain[1,2] may be modified to achieve these objectives and at the same time prevent autocatalysis.

METHODS

Trypsin, α-chymotrypsin (CT), and papain were covalently coupled to soluble oxidized polymeric sucrose (PS; mol. wt. = 400 kDa). The adducts were characterized and their kinetics of inactivation were studied under the influence of urea and temperature. Papain and trypsin were assayed with BAPNA and CT with ATEE as substrates.

Kinetic measurements of thermal inactivation were performed over a 24-h period and the first-order rate constant (k_i) of inactivation was used to calculate the half-life

[d]To whom all correspondence should be addressed.

571

of the enzyme and the activation energy of inactivation (E_i). Unfolding of enzymes was monitored by fluorescence emission spectroscopy.

RESULTS AND DISCUSSION

During the covalent coupling of an oxidized polymer of sucrose to the proteases, papain, trypsin, and CT, retention of catalytic activity depended on the proportion of enzyme to polymer, as well as on the coupling time. The relationship was hyperbolic and passed through an optimum depending on the number of amino groups modified. The best proportion of PS:enzyme was 1:2 for all three proteases. Whereas trypsin retained full activity on modification, papain showed a 20% decrease in specific activity and CT retained only 66% activity. Similarly, the affinity of the enzymes to their substrates was also altered by modification. Although the K_m for papain was the same for both native papain and PS-papain, the k_{cat}/K_m value was lower for the modified enzyme, showing a decrease in turnover on coupling to a large polymer. In the case of trypsin, the affinity for BAPNA increased, whereas that for BAEE decreased. The changes in K_m and k_{cat}/K_m are not appreciable and indicate that the gross tertiary structure of the protein is not changed significantly on modification.

Although the pH optima were not altered, the behaviors of the modified enzymes at high temperatures and in the presence of urea were dramatically different from their native counterparts. The optimal temperature for PS-papain was 11 °C higher than that for the native enzyme (TABLE 1), whereas PS-trypsin showed an increase of 29 °C. Thermal stability measured between 30 and 90 °C indicates that the modified enzymes have acquired a high degree of thermotolerance. This is reflected by the higher T_{50} values (temperature where 50% activity is retained) for the modified proteases and is indeed convincing of stabilization. The thermogram obtained by DSC again indicates that PS-trypsin (FIGURE 1) is more thermotolerant.

The modified proteases were also highly resistant to inactivation by urea. PS-papain was in fact activated by urea (FIGURE 2) and their $t_{1/2}$ values (time for 50% inactivation) could not be determined. The native counterparts, however, showed a short half-life (10 min for trypsin, 15 min for CT, and 33 min for papain).

TABLE 1. Temperature Effects on Native and Modified Proteases[a]

	T_{opt} (°C)	T_{50} (°C)	$\Delta H\ddagger$ (kJ/mol)	$\Delta S\ddagger$ (J/mol-K)
papain	62.6	68	162	152
PS-papain	73.6	78	240	355
trypsin	45	54	155	148
PS-trypsin	74	74	250	388
CT	ND	50	182	236
PS-CT	ND	64	337	677

[a]Terms—T_{opt}: optimum temperature for activity; T_{50}: temperature where 50% activity is retained; enzymes were incubated for 30 min at various temperatures in the range from 30 to 90 °C; they were then cooled and residual activity was measured at 30 °C; $\Delta H\ddagger$: activation enthalpy of inactivation; $\Delta S\ddagger$: activation entropy of inactivation; ND: not determined.
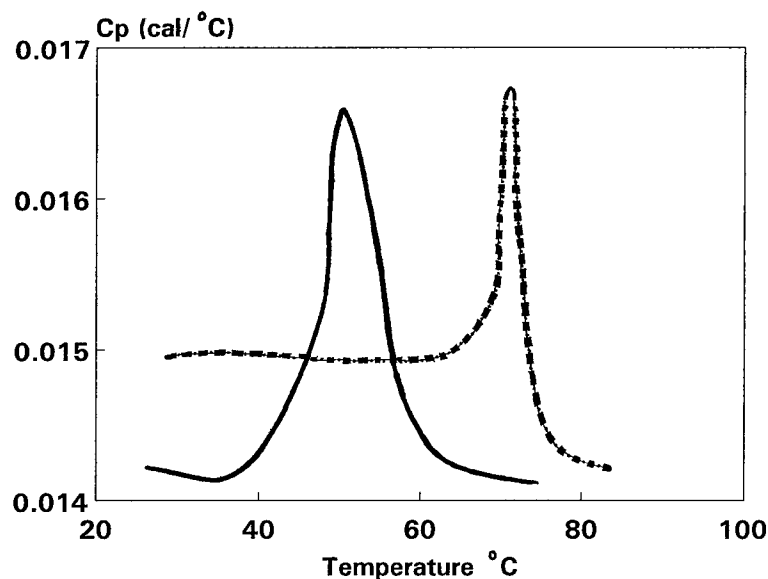
FIGURE 1. DSC thermogram of trypsin (—) and PS-trypsin (–·–). DSC was performed in a Microcal Differential Scanning Calorimeter at a heating rate of 1 °C/min.

The fluorescence emission spectrum of trypsin (FIGURE 3) was maximal at 340 nm, which shifted to 356 nm for the native enzyme and only to 341 nm for PS-trypsin when the samples were heated to 60 °C. CT and papain also showed a similar behavior. The redshift in emission maximum when the protein is heated at high temperature indicates that the tryptophan residues are solvent-exposed.[3] The reduced redshift shows how the modified enzymes resist unfolding more than the native proteins.

Thermal inactivation measured between 30 and 90 °C was rather steep for the native enzymes, whereas their modified counterparts were destabilized after longer periods of time as well as at higher temperatures. The inactivation of all three proteases followed a two-step series-type mechanism, but we have taken only the first-order rate into consideration. The main aim of this study was to compare the performance of proteases with the enzymes covalently modified using a large polymer. The rate constant of thermoinactivation (k_i) increased logarithmically with temperature. The half-life of inactivation ($t_{1/2}$) increased severalfold for the modified enzymes (FIGURE 4). Similarly, the energy of inactivation (E_i) was also much higher, implying that more energy is required to inactivate the protein.

The activation free energy ($\Delta G\ddagger$), the activation enthalpy ($\Delta H\ddagger$), and the activation entropy ($\Delta S\ddagger$) calculated from k_i were much higher for the modified enzymes (TABLES 1 and 2) than those for their native counterparts. Whereas trypsin and CT were better stabilized at 50 °C, papain showed optimal stabilization at 70 °C. The $\Delta(\Delta G\ddagger)$ values of 10 kJ/mol for papain, 11.3 kJ/mol for CT, and 16.7 kJ/mol for

% Activity Retained
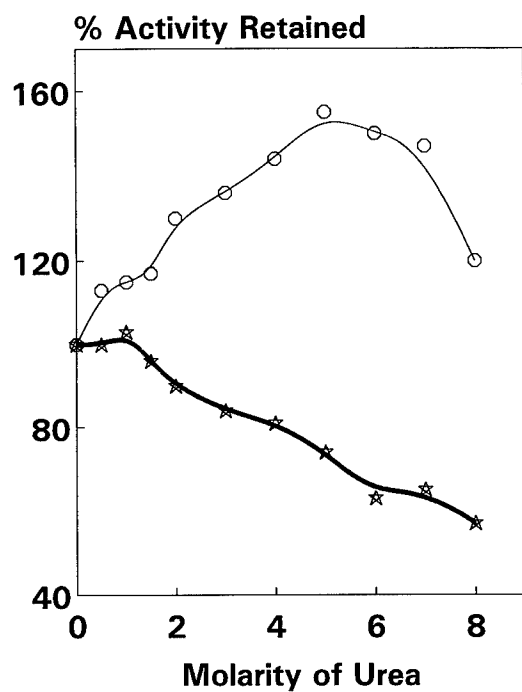
FIGURE 2. Stability to inactivation by urea of papain (☆) and PS-papain (○). Enzymes were inactivated at 37 °C for 1 h and residual activity was measured after 6-fold dilution.
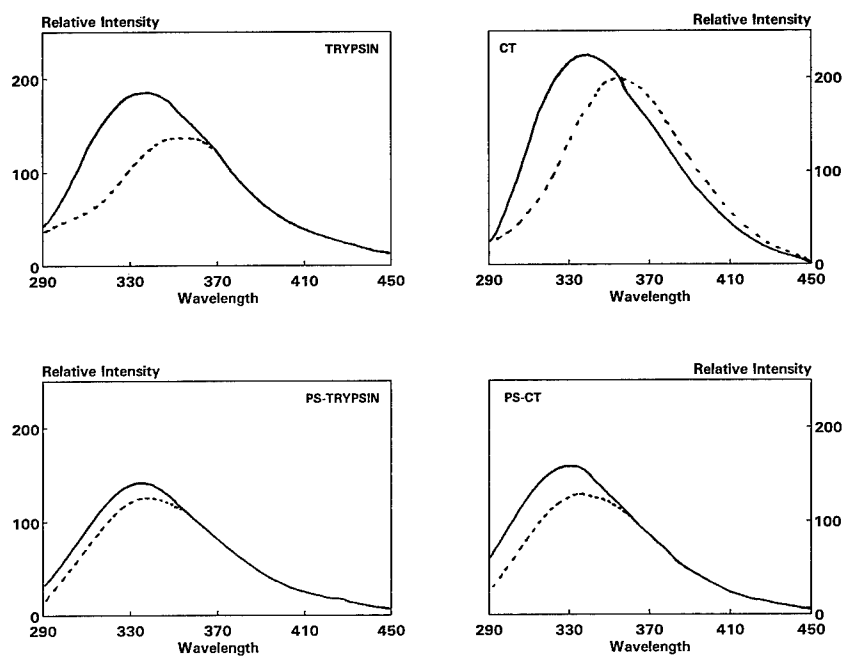
FIGURE 3. Fluorescence emission spectra of trypsin and CT incubated at 30 °C (—) or 60 °C (- - -) for 60 min. Excitation wavelength: 280 nm.
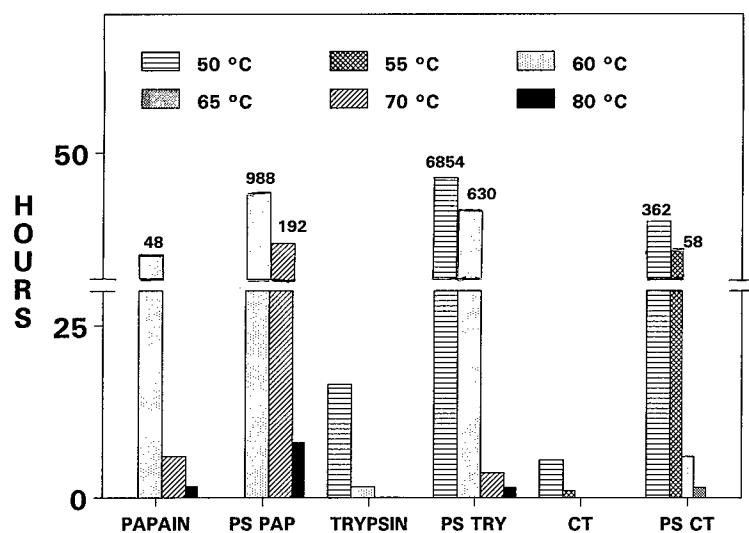
FIGURE 4. The influence of temperature on the half-life of native and modified proteases.

trypsin represent good stabilization of these proteases. Although $\Delta H\ddagger$ increased by 1.5- to 2-fold for modified proteases, their $\Delta S\ddagger$ values were higher by 2- to 3-fold.

The results indicate that the phenomenon of trapping the enzyme in a "cage", as it were, induces a selective "rigidity" to the protein.[4,5] Rigidity leads to some loss in activity, but a gain in stability and tolerance towards temperature and denaturants. An increase in entropic value for modified enzymes resembles the situation in thermophilic enzymes.[6] Entropy values are a measure of the state of the whole protein. Enzymes that are modified become rigid and more stable due to the stronger covalent bonds between the polymer and the protein; the active site core has less freedom to wobble out of the natural conformation, whereas the outside of the protein is free to unfold, thereby accounting for the increase in entropy.

TABLE 2. Free Energy of Thermoinactivation[a] for Native and Modified Proteases

	Temperature (°C)					
	50	55	60	65	70	80
papain	—	—	114	—	110	108
PS-papain	—	—	122	—	120	113
$\Delta(\Delta G\ddagger)$	—	—	8	—	10	5
trypsin	110	—	107	—	100	102
PS-trypsin	126	—	123	—	112	113
$\Delta(\Delta G\ddagger)$	16	—	16	—	12	11
CT	107	104	—	—	—	—
PS-CT	118	115	110	108	—	—
$\Delta(\Delta G\ddagger)$	11	11	—	—	—	—

[a]$\Delta G\ddagger$: kJ/mol, obtained from the rate of thermal inactivation using the relationship, $k_i = (k_B T/h) \cdot \exp(-\Delta G/RT)$.

REFERENCES

1. RAJALAKSHMI, N. & P. V. SUNDARAM. 1995. Stability of native and covalently modified papain. Protein Eng. **8:** 1039–1047.
2. SUNDARAM, P. V., R. VENKATESH, N. RAJALAKSHMI & L. SUBRAMANIAN. 1995. Kinetics of inactivation of enzymes stabilized by chemical modification with carbohydrate polymers. *In* Perspectives in Protein Engineering. R. Epton, Ed. Mayflower Worldwide. Nottingham, United Kingdom.
3. CHO, Y., G. WEI, S. WATKIME, S-P. LEE, T. R. KIM, J. W. BRADY & C. A. BATT. 1994. Thermostable variants of bovine β-lactoglobulin. Protein Eng. **7:** 263–270.
4. VENKATESH, R., S. WARRIER, S. SHUBHADA & P. V. SUNDARAM. 1992. Mono-, di-, and polyaldehyde-mediated chemical modification of urease. Ann. N.Y. Acad. Sci. **672:** 580–582.
5. VENKATESH, R., S. ARUN, N. RAJALAKSHMI, L. SUBRAMANIAN, V. MEENAKSHI, K. VENUGOPALAN & P. V. SUNDARAM. 1995. General strategies in the stabilization of enzymes by structural modification. Ann. N.Y. Acad. Sci. **750:** 130–133.
6. NUMATA, K., M. MURO, N. AKUTSU, Y. NOSOH, A. YAMAGISHI & T. OSHIMA. 1995. Thermal stability of chimeric isopropylmalate dehydrogenase genes constructed from a thermophile and a mesophile. Protein Eng. **8:** 39–43.

Reaction Engineering Aspects
of Activated Sugar Production

CMP-Neu5Ac as an Example

UDO KRAGL,[a] TERESA KLEIN,[a] DJURDA VASIC-RACKI,[b]
MATTHIAS KITTELMANN,[c] ORESTE GHISALBA,[c]
AND CHRISTIAN WANDREY[a]

[a] Institut für Biotechnologie
Forschungszentrum Jülich GmbH
D-52425 Jülich, Germany

[b] Faculty of Chemical Engineering
University of Zagreb
HR-41000 Zagreb, Croatia

[c] Pharmaceutical Division
Ciba Geigy Limited
CH-4002 Basel, Switzerland

INTRODUCTION

Cytidine 5'-monophospho-*N*-acetylneuraminic acid (CMP-Neu5Ac) is one of the key components for enzymatic synthesis of oligosaccharides (e.g., sialyl Lewis^x). The role of these compounds and of glycotechnology in general has been reviewed recently.[1-3] The biosynthesis and also the *in vitro* synthesis of biologically active glycoconjugates require the activated form of Neu5Ac, CMP-Neu5Ac, as substrate for various sialyltransferases. CMP-Neu5Ac can be synthesized chemically[4] or enzymatically by means of a CMP-Neu5Ac synthetase [EC 2.7.7.43].[5-7] Both methods have advantages and disadvantages; for example, when nonnatural derivatives of Neu5Ac shall be activated, chemical methods may be advantageous.

It is evident that all compounds required, including necessary enzymes, must be available in large quantities at reasonable costs in order to make progress possible in glycotechnology. Under this premise, we have been working on the production of various building blocks, such as of Neu5Ac,[8] *N*-acetyllactosamine,[9] β1,4-galactosyl-transferase,[10,11] or α2,6-sialyltransferase.[12] Recently, we described the large-scale production of CMP-Neu5Ac synthetase from a nonrecombinant strain, *Escherichia coli* K-235/CS1.[13] The enzymatic synthesis of CMP-Neu5Ac is depicted in FIGURE 1. The formed pyrophosphate is converted to phosphate by means of an inorganic pyrophosphatase [EC 3.6.1.1] in order to overcome its product inhibition. The main problem is the chemical hydrolysis of the product CMP-Neu5Ac itself, as well as (to a smaller extent) the hydrolysis of CTP. In this paper, we present some preliminary

CTP + Neu5Ac $\xrightarrow[\text{V}_1]{\text{synthetase}}$ CMP-Neu5Ac + PPi

V_2 | chemical hydrolysis V_3 | pyrophosphatase

CMP + Neu5Ac   2 Pi

enzymes:
• CMP-Neu5Ac synthetase
  E. coli K235/CS1, non recombinant
• inorganic pyrophosphatase
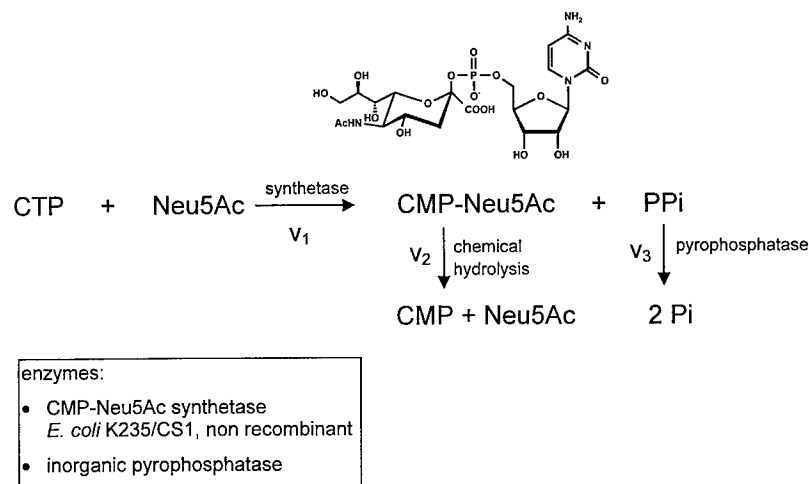
FIGURE 1. Reaction scheme for the synthesis of CMP-Neu5Ac.

kinetic studies on the CMP-Neu5Ac synthetase and some first approaches for a scale-up of the reaction.

MATERIALS AND METHODS

CMP-Neu5Ac synthetase was obtained and purified as described elsewhere.[13] For large-scale synthesis, a simplified purification protocol employing an aqueous two-phase system has been used.[14] Inorganic pyrophosphatase was obtained from Sigma (Deisenhofen, Germany). Neu5Ac was produced in house as described elsewhere.[8] CTP was obtained from Sigma as well. All other chemicals were from Fluka (Buchs, Switzerland).

CMP-Neu5Ac, CTP, CDP, CMP, and cytidine were analyzed on an HPLC column (Alltech Carbohydrate, 10 μm; Unterhaching, Germany) using a kalium phosphate/acetonitrile gradient and UV detection at 270 nm. Kinetic parameters were estimated from initial rate measurements using Scientist for Windows (Micro-Math, Salt Lake City, Utah). The same software was used for simulation of concentration-time curves in batch and continuously operated reactors.

Kinetic measurements were performed using 100 mM Tris-buffer, pH 8.0. During production runs, the pH was kept constant by automatic titration using a Dosimat 665 (Metrohm, Filderstadt, Germany).

For synthesis in a continuously operated stirred-tank reactor (CSTR), an enzyme membrane reactor (EMR) was used as described elsewhere.[15,16]

Tests and characterization of nanofiltration membranes were done using a P 28 test module (Celfa, Seewen, Switzerland). The most suitable membrane was found to be a nanofiltration membrane, ROM 365, from Amafilter (Langenhagen, Germany). The same setup was used for the concentrating and desalinating of CMP-Neu5Ac.

RESULTS AND DISCUSSION

Kinetics of the Reaction System

The set of equations together with the estimated kinetic parameters are given in FIGURE 2. The synthesis of CMP-Neu5Ac can be sufficiently described by multiplication of two Michaelis-Menten equations, together with a competitive inhibition by pyrophosphate and a substrate-surplus inhibition by CTP.[17] A product inhibition by CMP-Neu5Ac could not be detected in the concentration range investigated. For the enzymatic hydrolysis of pyrophosphate as well as for the chemical hydrolysis of CMP-Neu5Ac, a first-order rate equation was used. In the first case, the enzyme concentration has to be regarded as well, which is the reason for different units for the rate constants. The standard deviation shows a good accuracy of the estimated parameters.

To validate the model, simulations of various syntheses in batch and continuously operated reactors have been verified experimentally. Two examples are shown in FIGURES 3 and 4. There is a good agreement between the predicted and observed concentration-time curves. The continuously operated enzyme membrane reactor could be operated for about 40 hours before the precipitated phosphate required a shutdown. However, with the conditions as given in FIGURE 4, an overall conversion of 0.78, a selectivity of 0.82, and a space-time yield of 254 g/(L · day) were reached. Despite the fact that the continuously operated membrane reactor is advantageous in reactions showing a substrate-surplus inhibition, its use cannot be favored in cases with strong product inhibition. In the latter case, a batch or plug-flow reactor would be better.

FIGURE 5 shows a comparison between a batch reactor and a CSTR for the synthesis of CMP-Neu5Ac. Obviously, the product inhibition is much more dominat-

$$v_1 = \frac{[E_1] \cdot V_{max} \cdot [CTP]}{K_M^{CTP} \cdot \left(1 + \frac{[PPi]}{K_i^{PPi}}\right) + [CTP] + \frac{[CTP]^2}{K_i^{CTP}}} \cdot \frac{[Neu5Ac]}{K_M^{Neu5Ac} + [Neu5Ac]}$$

$$v_2 = [E_2] \cdot k_{PPi} \cdot [PPi]$$

$$v_3 = k \cdot [CMP - Neu5Ac]$$

FIGURE 2. Kinetic equations and the derived kinetic constants.
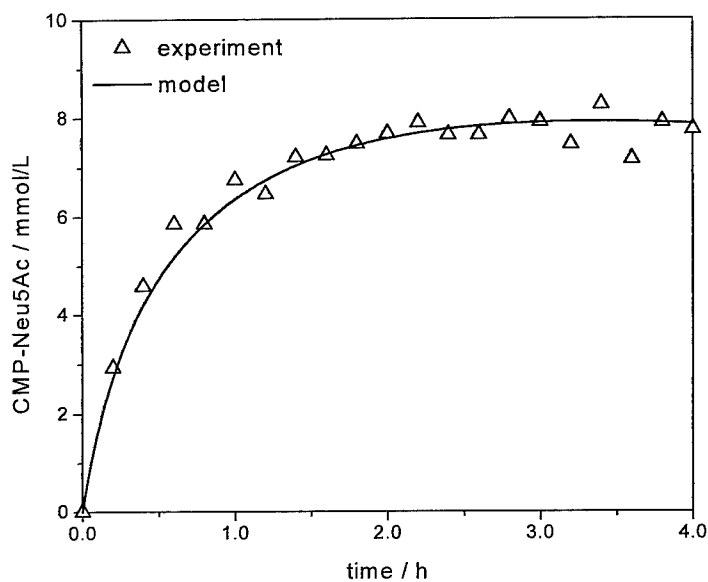
FIGURE 3. Batch synthesis of CMP-Neu5Ac. Conditions: 11 mM CTP, 11 mM Neu5Ac, 2.3 U/mL CMP-synthetase, no pyrophosphatase, pH 8.0, 30 °C.
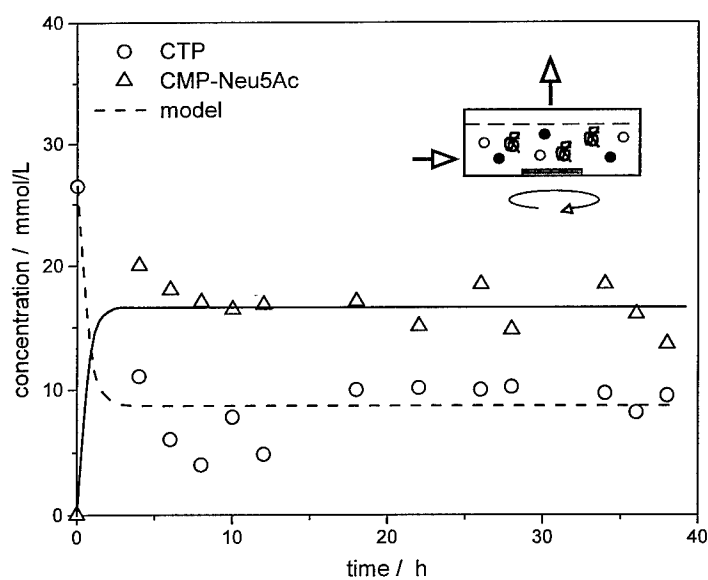
FIGURE 4. Continuous synthesis of CMP-Neu5Ac. Conditions: 27 mM CTP, 27 mM Neu5Ac, 3.0 U/mL CMP-synthetase, 5.6 U/mL pyrophosphatase, residence time = 1 h, pH 8.0, 30 °C.
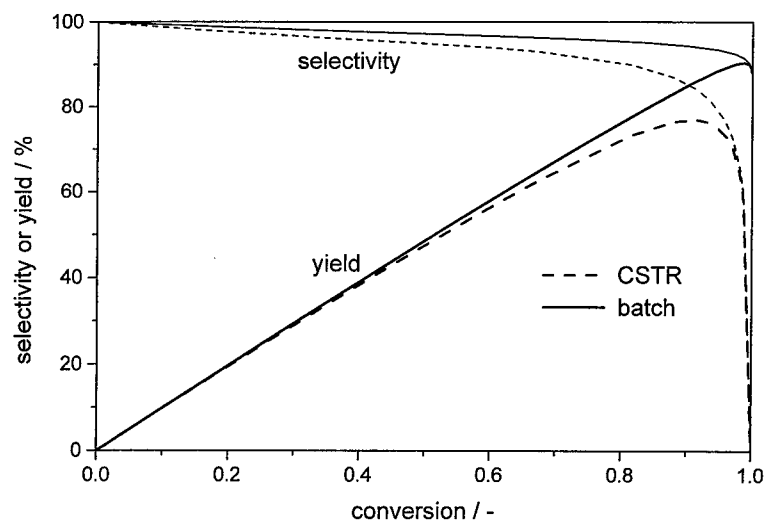
FIGURE 5. Comparison of the batch and the continuous process for the synthesis of CMP-Neu5Ac. Conditions: 50 mM CTP, 50 mM Neu5Ac, 5.0 U/mL CMP-synthetase, 5.0 U/mL pyrophosphatase, pH 8.0, 30 °C.

ing, favoring a batchwise production of CMP-Neu5Ac. In this case, the precipitated phosphate is only influencing the recovery of the enzymes. In order to compensate for the substrate-surplus inhibition by CTP, a fed-batch technique was employed. The feeding strategy was optimized using simulation as well (data not shown).

Multigram Production

Based on the results as discussed above, the large-scale synthesis has been performed in a fed-batch reactor. In order to overcome product hydrolysis, short reaction times (less than 8 hours) were employed. Typical reaction conditions as well as the results are summarized in TABLE 1. Simulations show that the selectivity of 75% is caused mainly by the chemical hydrolysis of CMP-Neu5Ac.

Besides the production itself, the product isolation is also an important issue when scaling up is considered. CMP-Neu5Ac is sensitive towards heat and acidic or

TABLE 1. Conditions and Results for Fed-Batch Synthesis of CMP-Neu5Ac

CTP	4×5 mM
Neu5Ac	20 mM
$MgCl_2$	80 mM
inorganic pyrophosphatase	1.75 U/mL
CMP-Neu5Ac synthetase	0.2 U/mL
pH	8.0
temperature	30 °C
scale	450 mL
yield	60%

basic conditions. In the literature, the use of volatile buffers for anion exchange chromatography has been described.[6,18,19] In addition, desalting using gel filtration after chromatography can be used.[7] However, both methods proved to be too tedious for large-scale synthesis. Alternatively, a method was developed employing nanofiltration for concentrating and desalinating CMP-Neu5Ac before and after anion exchange chromatography using a sodium formate gradient. Among the membranes tested, a nanofiltration membrane, type ROM 365, has proven to be the most suitable one. For CMP-Neu5Ac, it shows a retention of >99%; in contrast, for sodium formate, retention is only 27%. This means that diafiltration with 20 volumes of water is sufficient for complete desalination. The basic steps are summarized in TABLE 2. A more detailed description will be published elsewhere.[20] The same membrane could also be used for retention of cofactors such as NAD(P)H in continuously operated membrane reactors.[21]

TABLE 2. Steps for Isolation of CMP-Neu5Ac

Step	Remark
centrifugation	
filtration	0.1 μM, 2000 Da
concentration by nanofiltration	ROM 365 membrane
anion exchange chromatography; gradient elution with Na-formate	Dowex 1 × 2
concentration by nanofiltration	ROM 365 membrane
diafiltration	ROM 365 membrane, 20 volumes of water
lyophilization	

CONCLUSIONS

The enzymatic synthesis of CMP-Neu5Ac seems to be a feasible method for large-scale production. Based on kinetic studies, a fed-batch reactor has proven to be advantageous. For product isolation, a classical chromatographic step employing gradient elution with a filtration using recently developed nanofiltration membranes could be combined advantageously. With the results presented here, large amounts of CMP-Neu5Ac may now become available for synthesis of sialylated oligosaccharides. Thus, the use of stoichiometric amounts[22] may become economically attractive compared to the use of multienzyme cycles for *in situ* generation and regeneration of CMP-Neu5Ac.[23]

REFERENCES

1. GIJSEN, H. J. M., L. QUIAO, W. FITZ & C-H. WONG. 1996. Chem. Rev. **96:** 443–473.
2. FUKUDA, M. & O. HINDSGAUL, Eds. 1994. Molecular Glycobiology. Oxford University Press. London/New York.
3. MONTREUIL, J., J. F. G. VLIEGENTHART & H. SCHACHTER, Eds. 1995. Glycoproteins. Elsevier. Amsterdam/New York.
4. MARTIN, T. J. & R. R. SCHMIDT. 1993. Tetrahedron Lett. **34:** 1765–1768.
5. SCHAUER, R., M. WEMBER & C. FERREIRA DO AMARAL. 1972. Hoppe-Seyler's Z. Physiol. Chem. **353:** 883–886.

6. HIGA, H. H. & J. C. PAULSON. 1985. J. Biol. Chem. **260:** 8838–8849.
7. GROSS, H-J., A. BÜNSCH, J. C. PAULSON & R. BROSSMER. 1987. Eur. J. Biochem. **168:** 595–602.
8. KRAGL, U., M. KITTELMANN, O. GHISALBA & C. WANDREY. 1995. Ann. N.Y. Acad. Sci. **750:** 300–305.
9. HERRMANN, G. F., U. KRAGL & C. WANDREY. 1993. Angew. Chem. Int. Ed. Engl. **32:** 1342–1343.
10. HERRMANN, G. F., C. KREZDORN, M. MALISSARD, R. KLEENE, H. PASCHOLD, D. WEUSTER-BOTZ, U. KRAGL, E. G. BERGER & C. WANDREY. 1995. Protein Expression Purif. **6:** 72–78.
11. MALISSARD, M., L. BORSIG, S. DI MARCO, M. G. GRÜTTER, U. KRAGL, C. WANDREY & E. G. BERGER. 1996. Biochemistry. In press.
12. BORSIG, L., S. X. IVANOV, G. F. HERRMANN, U. KRAGL, C. WANDREY & E. G. BERGER. 1995. Biochem. Biophys. Res. Commun. **210:** 14–20.
13. KITTELMANN, M., T. KLEIN, U. KRAGL, C. WANDREY & O. GHISALBA. 1995. Appl. Microbiol. Biotechnol. **44:** 59–67.
14. VERNAU, J. & M-R. KULA. 1990. Biotechnol. Appl. Biochem. **12:** 397–404.
15. KULA, M-R. & C. WANDREY. 1987. Methods Enzymol. **136:** 9–21.
16. KRAGL, U., D. GYGAX, O. GHISALBA & C. WANDREY. 1991. Angew. Chem. Int. Ed. Engl. **30:** 827–828.
17. BISELLI, M., U. KRAGL & C. WANDREY. 1995. Reaction engineering for enzyme-catalyzed biotransformations. *In* Handbook of Enzyme Catalysis in Organic Synthesis. K. Drauz & H. Waldmann, Eds.: 89–155. Verlag Chemie. Weinheim.
18. SHEN, G-J., J. L-C. LIU & C-H. WONG. 1992. Biocatalysis **6:** 31–42.
19. SIMON, E. S., M. D. BEDNARSKI & G. M. WHITESIDES. 1988. J. Am. Chem. Soc. **110:** 7159–7163.
20. KRAGL, U., L. HASBACH & C. WANDREY. 1994. Nanofiltration and reverse osmosis for downstream processing and purification of fine chemicals. Poster presented at the Seventh International Symposium on Synthetic Membranes in Science and Industry, Tübingen, Germany.
21. SEELBACH, K. & U. KRAGL. 1996. Enzyme Microb. Technol. Accepted.
22. UNVERZAGT, C., S. KELM & J. PAULSON. 1994. Carbohydr. Res. **251:** 285–301.
23. LIU, J. L-C., G-J. SHEN, Y. ICHIKAWA, J. F. RUTAN, G. ZAPATA, W. F. VANN & C-H. WONG. 1992. J. Am. Chem. Soc. **114:** 3901–3910.

Enzymatically Modified Alginates
as Useful Biopolymers

DONAL F. DAY

Audubon Sugar Institute
Louisiana State University
Baton Rouge, Louisiana 70803

The properties of alginates are determined by their primary structures. Seaweed alginates have M/G (mannuronic/guluronic) ratios between 0.45 and 1.85. In contrast, the ratios for bacterial alginates are significantly higher, up to 4.0.[1] Polymers with a high percentage of guluronic acid (low M/G ratio) have greater strand-to-strand binding than the high mannuronic acid counterparts. Alginates with low M/G ratios produce strong, yet brittle, gels that do not respond to water.[2] Most bacterial alginates have high M/G ratios and form more elastic gels. Increasing the length of the homopolymeric blocks, especially the polyguluronic blocks, increases the gel strength. Alternating mannuronic acid and guluronic acid monomers decrease the number of cross-linkages and decrease the gel strength. Generally, as the polymeric chain increases in length, the polymer becomes less elastic. The molecular weight of the alginate from *Macrocystis pyrifera* averages about 47 kDa, compared to *Pseudomonas syringae pv. phaseolicola* alginate with a molecular weight of 127 kDa.[3] Yet, this higher molecular weight does not greatly alter the gel elasticity of the bacterial alginates because of acetylation. Unlike the seaweed polymers, the mannuronic acid residues of the bacterial polymers are *O*-acetylated on the C-2 and C-3 carbons.[4] The degree of acetylation, expressed as acetyl group per monomer, usually ranges from 0.1 to 1.0. The effects of acetylation on the properties of seaweed alginates are detailed in this study.

The weight-average molecular weight (M_w) was determined for acetylated and deacetylated alginates. Acetylated alginates were between 7% and 11% larger than their deacetylated counterparts (TABLE 1). All test polymers had polydispersity indices of approximately 3.0, indicating a wide variation of molecular sizes. Acetylation linearly altered the flow dynamics of alginate solutions (FIGURE 1). It increased the solution viscosity of bacterial alginate by 16% and that of seaweed alginate by 8% at 50% acetylation. The viscosity for each alginate solution was independent of temperature up to 52 °C. Above 52 °C, the viscosities of the solutions decreased linearly. Between 52 °C and 85 °C, the viscosities of the acetylated and deacetylated seaweed alginates decreased at the same rate, 3.4% per °C, whereas the acetylated and deacetylated bacterial alginate viscosities decreased at different rates, 9.2% and 6.5% per °C, respectively. At 85 °C, the comparative viscosities of all the alginate solutions were identical (FIGURE 2).

The abilities of cations to precipitate the various alginates were compared via $P_{1/2}$ values. The $P_{1/2}$ is defined as the concentration of cation, in mM, required to precipitate 50% of the polymer from 400 mg/mL alginate solution. The relative

TABLE 1. Size and Composition of Test Alginates

Alginate Sample	Acetyl/Uronic Acid (mol/mol) (%)[a]	$M_w{}^b$ ($\times 10^4$)	$M_w/M_n{}^c$	M/G Ratio
Seaweed	0	4.7	3.36	60:40
Acetylated seaweed	30	5.2	3.25	60:40
Bacterial	100	12.7	2.95	82:18
Deacetylated bacterial	0	11.9	3.13	82:18

[a]Acetylation was measured according to the method described by McComb and McCready.[5]
[b]Weight-average molecular weight.
[c]Polydispersity: alginate sizes and polydispersity indices were determined from gel-permeation chromatography by measurement of multiangle light-scattering intensities using a DAWN-Photometer (Wyatt Technology, Santa Barbara, California).
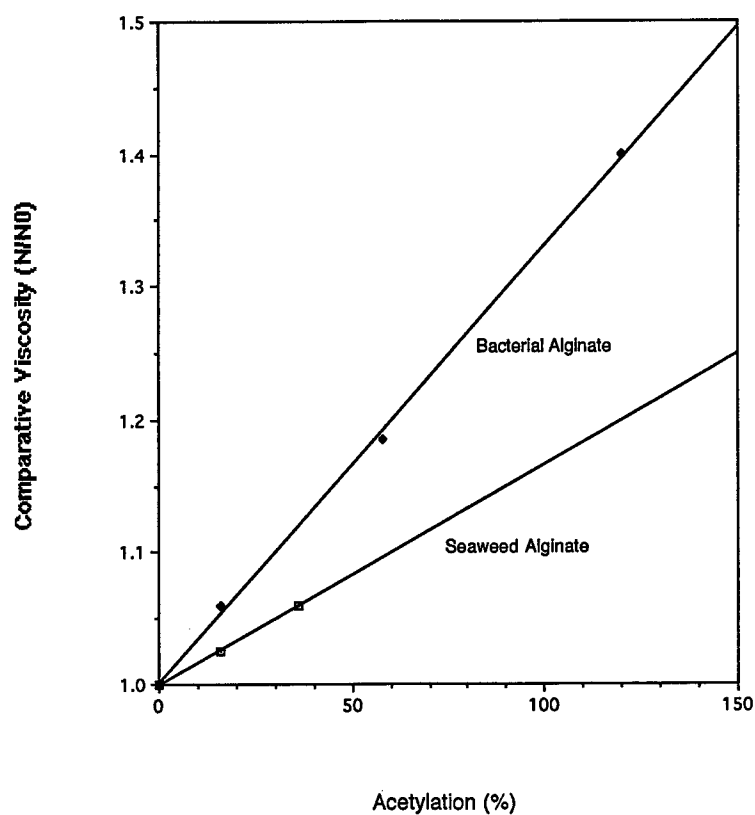
FIGURE 1. The effect of acetylation on the solution viscosities of alginates (determined by the method of Allison and Matthews[6]) expressed as comparative viscosity (N/N_0, where N is the time elapsed for the alginate solutions to fall a fixed distance and N_0 is the time for deionized water to fall that same distance).

order of precipitation of seaweed and bacterial alginate by these ions is as follows:

$$Pb^{2+} > U^{6+} > Fe^{3+}, Sr^{2+} > Ca^{2+} > Co^{2+} > Mg^{2+}, Cs^{1+}, Rb^{1+}.$$
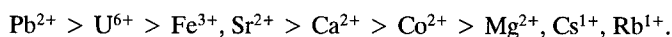
Acetylation of the alginate reversed the binding order for only two ions, Fe^{3+} and Pb^{2+}. It significantly increased the $P_{1/2}$ for Co^{2+}, Ca^{2+}, and Sr^{2+} (TABLE 2). Determination of the breakthrough point of Fe^{3+} on a known amount of alginate showed only a 2% difference in the amount of Fe^{3+} bound between acetylated and nonacetylated samples. This confirmed the difference in affinities between the two polymers, but also highlighted the small magnitude of the change that acetylation made to the binding of this ion.

Both the acetylation and the M/G ratio influence an alginate's ability to bind cations.[7] An increased affinity for ions reflects an increased number of cross-links. Increased cross-linkages produce gels with less elasticity and stronger, more-rigid structures. Generally, acetylation decreased the affinity for cations, especially calcium. The exception was an increase in the affinity for ferric ions. Whether or not the alterations in cation binding due to acetylation of the polymer are of commercial
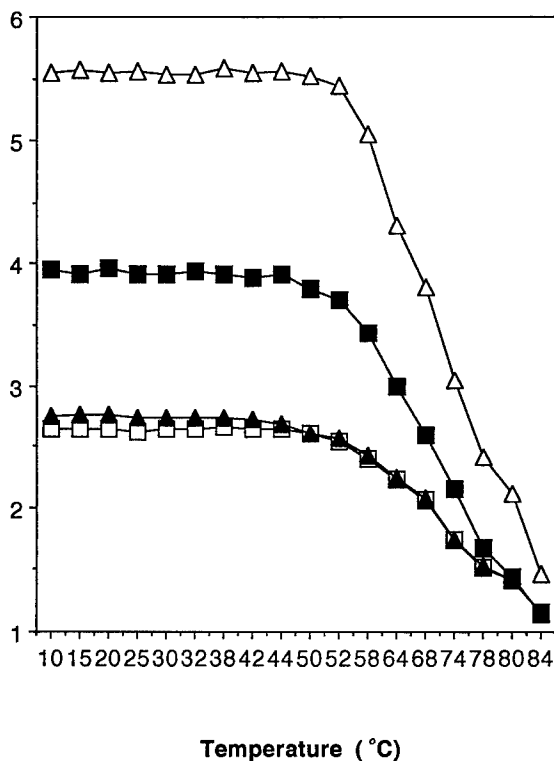
Temperature (°C)

FIGURE 2. Comparative viscosities (N/N_0) of seaweed alginate (▲), acetylated seaweed alginate (□), bacterial alginate (△), and deacetylated bacterial alginate (■) as a function of temperature. Alginate solutions were 400 mg/mL (w/v).

TABLE 2. Alginate Precipitation as a Function of Cation

Ions	Fold-Change in $P_{1/2}$[a]	
	Alginate ($P_{1/2}$)	Acetylated Alginate ($P_{1/2}$)
Cs^{1+}, Rb^{1+}, Mg^{2+}	no affinity[b]	no affinity
Ca^{2+}	3.1	3.8
Sr^{2+}	1.8	1.9
Fe^{3+}	1.8	−0.7
Co^{2+}	9.6	4.3
Pb^{2+}	0.5	2.3
U^{6+}	0.9	0.3

[a]$P_{1/2}$ is the concentration of metal ions (mM) required to precipitate 50% (w/v) of the alginate from 400 mg/mL (w/v) alginate solutions. Values expressed are the fold-difference from $P_{1/2}$ of seaweed alginate (positive values = less precipitation; negative values = greater precipitation).
[b]"No affinity" signifies that the ion did not precipitate 50% of the alginate sample up to 100 mM ion concentration.

value remains unknown. Acetylation of this polymer does offer the potential for creating gels with varying viscosity, strength, and water-holding capability. With a commodity product such as alginate, the ability to differentiate product lines and to format new product applications is an advantage.

SPECIFIC METHODS

Acetylation/Deacetylation of Alginates

A bioreactor containing immobilized *P. syringae* was used for the continuous acetylation of *Macrocystis pyrifera* alginate according to the method reported in reference 8. Alginates were deacetylated by treatment with 0.25 N NaOH.[9]

Precipitation of Alginates by Metal Ions

The relative precipitations by cations of the various alginates were compared using the procedure reported by Ashby.[9]

REFERENCES

1. ZELLER, S. G. & G. R. GRAY. 1992. Carbohydr. Res. 226: 313.
2. HAUG, A. & B. LARSEN. 1971. Carbohydr. Res. 17: 29.
3. FETT, W. F., S. F. OSMAN, M. L. FISHMAN & T. S. SIEBLES. 1986. Appl. Environ. Microbiol. 52: 466.
4. NARBAD, A., M. J. E. HEWLINS, P. GACESA & N. J. RUSSELL. 1990. Biochem. J. 267: 579.
5. McCOMB, E. A. & R. M. McCREADY. 1957. Anal. Chem. 29: 819.
6. ALLISON, D. G. & M. J. MATTHEWS. 1992. J. Appl. Bacteriol. 73: 484.
7. HAUG, A. 1961. Acta Chem. Scand. 15: 1794.
8. LEE, J. W. & D. F. DAY. 1995. Appl. Environ. Microbiol. 61: 650.
9. ASHBY, R. 1994. Ph.D. dissertation. Louisiana State University.

Lipase-catalyzed Synthesis of Lactone and Biodegradable Polyester in Organic Solvent[a]

HUAN DONG, SHU-GUI CAO, HONG-DA WANG,
SI-PING HAN, NIAN-XIANG ZHANG, AND HONG YANG

State Key Laboratory of Enzyme Engineering
Jilin University
Changchun 130023, People's Republic of China

INTRODUCTION

During the last decade, theories of nonaqueous catalysis have been deeply developed.[1] Recently, studies and applications of enzymatic organic solvent synthesis have become very popular.

Lactone, as a special kind of ester, plays an important role in research and application. Some short-chain lactones are important intermediates of useful materials, such as intermediates for synthesizing macromolecular polyesters.

Synthesis of biodegradable macromolecules, such as aliphatic polyesters, has been paid more attention by many countries because of the pollution of nonbiodegradable materials in our daily lives. There are many reports about the synthesis of biodegradable polyesters, but most work has been done with chemical methods. Reports with enzymatic methods are very rare.[2]

In this paper, a new route for synthesizing aliphatic polyester is introduced. The route included two steps: (1) lipase-catalyzed hydroxyester to synthesize lactone; (2) lipase-catalyzed lactone ring-opening polymerization to form polyester. All steps were done in nonaqueous systems.

In this study, ethyl 6-hydroxycaproate was chosen as the substrate. The effect of the sources of the lipase on lactonization and polymerization was studied. The influence of water concentration and reaction time on the molecular weight (Mw) of the polyester was also discussed. Lastly, a possible mechanism of enzymatic ring-opening polymerization was given.

MATERIALS AND METHODS

Lipase

Porcine pancreatic lipase (PPL) was purchased from Sigma Chemical. *Candida cylindracea* AY (AYL) and *Pseudomonas* S.P. I (PSLI) were purchased from Teino Pharmaceutical (Japan). Expansion *Penicillium* lipase (PEL) was purchased from Nantong Biochemical Pharmaceutical Factory (Nantong, China). *Pseudomonas* S.P.

II (PSLII), *Camalica* lipolytic lipase (CLL), and *Candida cylindracea* lipase (CCL) were provided by the Institute of Microbiology, Academia Sinica (Beijing, China).

Substrate

ε-Caprolactone was obtained from Aldrich Chemical and ethyl 6-hydroxycaproate was synthesized according to the published method.[3] Other reagents were of analytical grade.

Determination of Lactonization Activity of Lipase

To a tube, lipase powder (50 mg) was added to the solution of 0.02 mmol ethyl 6-hydroxycaproate in 1.0 mL benzene. After sealing the tube, the mixture was shaken on a rotatory shaker at 120 rpm at 37 °C. The reaction was terminated and benzene was removed *in vacuo*. One mL of 40% methanol (methanol:water = 4:6, v/v) was added, gently stirred, and filtrated. The clear solution was assayed with HPLC (Waters), which was equipped with a 4.0 mm (φ) × 150 mm NovaPak C_{18} column (Millipore) and an R401 refractometer (Millipore). Samples were eluted with 40% methanol at a flow rate of 1.0 mL/min. External standard was ε-caprolactone.

Determination of Polymerization Activity of Lipase

First, 0.1 mL ε-caprolactone and 50 mg lipase were mixed; then, they were incubated at 60 °C. The reaction was terminated by adding 3.0 mL dichloromethane and filtrating out the lipase. The organic solution was divided into two parts. One part (1.0 mL) was for determining the polymerization activity on HPLC. The other (2.0 mL) was for determining the molecular weight of the polymer on GPC. To the first part, after removing dichloromethane, 1.0 mL of HPLC flow phase (40% methanol) was added; then, the solid was filtrated and the clear solution was assayed by HPLC to determine the unconsumed ε-caprolactone. The analytic method was the same as above.

Determination of the Molecular Weight of Polyester

According to the above part, the sample for GPC was *in vacuo* to remove dichloromethane. The remainder was precipitated by methanol. The cloudy solution was centrifuged to obtain a white solid, namely, polyester. The white solid was dried and dissolved in tetrahydrofuran (THF) (GPC flow phase) for GPC assay. GPC analysis was performed by a Shimadzu LC-4A (Japan) with a refractive index (RI) detector (RID-2As). Two columns (Model JU1010, Jilin University, China) were contacted and the flow rate was 1.0 mL/min. Calibration curves for GPC analysis were made with polystyrene as the standard.

Determination of the Structure of Polyester

The structure of polyester was determined by ^{1}H- and ^{13}C-NMR spectra (400 MHz, Unity-400, Varian).

Determination of the System Water Concentration

Water concentration of the system was determined with a Karl-Fischer moisture meter (Model KF-1, Shanghai Chemical Industry Research Institute, China).

RESULTS AND DISCUSSION

Selection of the Optimal Sources of Lipase for Synthesis of ε-Caprolactone

TABLE 1 shows that the ability of lactonization by lipase was greatly dependent on the source of the lipase. CCL and PPL were more easily lactonized than other sources of lipase. For CCL and PPL, the conversions of synthesis of caprolactone were 60% and 82%, respectively. In the meantime, the system water concentration for CCL and PPL was 0.20%, which also was the optimal system water concentration. Because of the different structures of the different lipases, the optimal system water concentrations varied. From TABLE 1, PPL and CCL were selected as the ideal enzymes for lactonization of ethyl 6-hydroxycaproate.

Selection of the Optimal Sources of Lipase for Enzymatic Polymerization

TABLE 2 shows that, by taking molecular weight and molecular weight distribution (MwD) as the standard, the abilities to synthesize polycaprolactone by different sources of lipase were of varied character. After 30 days, the reaction reached equilibrium (the equilibrium refers to the time when Mw is not changed). The results show that PSLI and CCL were suitable enzymes for polymerization because high-molecular-weight polyesters were obtained, which were 13,200 and 8700 daltons, respectively. On the other hand, AYL and CLL were the poorest enzymes because

TABLE 1. Optimal Water Concentration and Conversion Synthesizing ε-Caprolactone Catalyzed by Different Sources of Lipase in Benzene[a]

Lipase	Optimal Water Concentration (%)	Conversion (%)
PPL	0.20	82
AYL	0.50	27
CCL	0.20	60
PSLI	0.60	40
PSLII	0.40	56
PEL	0.40	10
CLL	0.30	24

[a]The reaction conditions were the same as described in the text. The reaction time was 144 hours.

TABLE 2. The Polymerization of ε-Caprolactone Catalyzed by Different Sources of Lipase[a]

Lipase	Polymerization		Conversion (%)
	Mw ($\times 10^3$)	MwD	
PSLI	8.7	2.25	97.2
PSLII	5.6	1.69	97.8
AYL	5.3	1.40	98.3
PEL	6.3	1.86	98.6
CCL	13.2	2.20	98.6
PPL	7.8	2.36	98.5
CLL	5.6	1.93	97.7

[a]The reaction conditions were the same as described in the text. The reaction time was 30 days.

their polyesters had molecular weights of 5300 and 5600 daltons, respectively. We selected PSLI for further studies because it was easily obtained.

Relation between Polymerization Course and Reaction Time

FIGURE 1a shows the relation between reaction time and molecular weight. The results indicate that, during the reaction course, the molecular weight increased gradually until equilibrium (about 30 days).

FIGURE 1b shows that the molecular weight distribution increased slowly with an increase of reaction time.

FIGURE 1c reveals the relationship between conversion and time course. At half of the reaction time (about 15 days), conversion of ε-caprolactone had been nearly 100%, but the reaction still did not reach equilibrium. The curve shape was different from FIGURES 1a and 1b. All of this inferred that the increases of conversion and molecular weight did not concur. This may be relevant to the mechanism of polymerization.

Effect of Water Concentration on Enzymatic Polymerization

The system water concentrations were in the realm of 0.1% to 20%. The relationships among molecular weight, molecular weight distribution, and water concentration were studied.

We discovered that the relation curve of molecular weight and system water concentration resembled a bell (FIGURE 2a). The bell's peak was the optimal water concentration, which was 3.8%. This value was obviously higher than the normal optimal water concentration for lipase catalysis in organic solvent (no more than 1.0%).

FIGURE 2b shows another bell-shape curve for the relationship of system water concentration and molecular weight distribution.

FIGURE 2c reveals the relationship of conversion and system water concentration. This curve was different from FIGURES 2a and 2b. At 3.8% water concentration, the
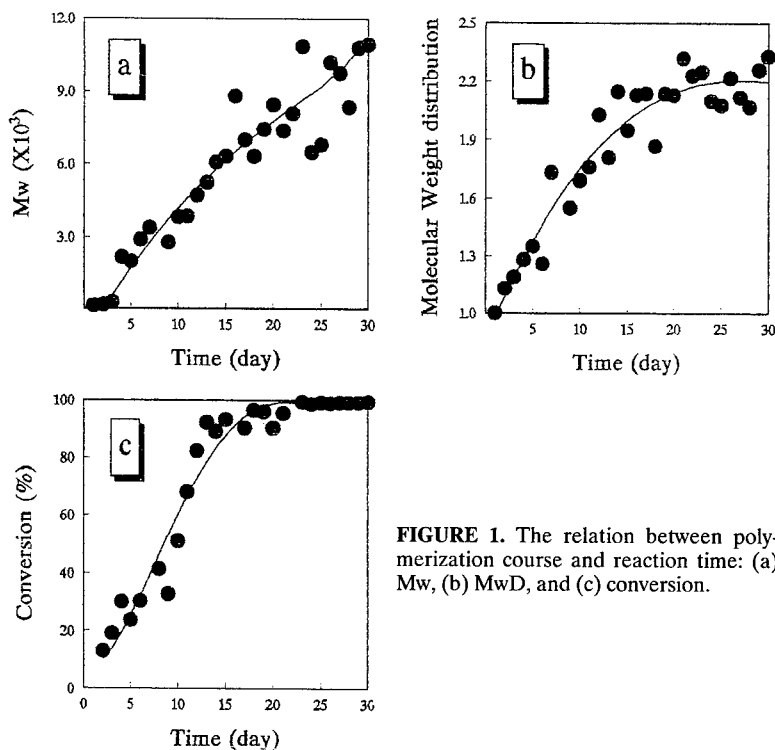
FIGURE 1. The relation between polymerization course and reaction time: (a) Mw, (b) MwD, and (c) conversion.

conversion did not change, although the system water concentration increased. All of this may be relevant to the mechanism of polymerization as well.

Determination of the Structure of Polyester

The structure of polyester was determined by ^{1}H- and ^{13}C-NMR spectra.

In the ^{1}H-NMR spectrum, we observed four big peaks. The multiplet peak at 1.40 ppm was ascribed to four methylene protons (-CO-CH$_2$CH$_2$CH$_2$CH$_2$CH$_2$O-). At 1.65 ppm, a pentaplet peak was due to two methylene protons of -CH$_2$CH$_2$O-. At 2.30 ppm, the large triplet peak was contributed by two methylene protons of -CO-CH$_2$-. At 4.02 ppm, another larger triplet peak was observed, which was due to two methylene protons of -CH$_2$O-. Noticeably, at 3.65 ppm, very small triplet peaks were observed, which were ascribed to the split of two methylene protons attached to the terminal hydroxyl group.

The ^{13}C-NMR spectrum for polyester was very simple. Six large single peaks represented the chemical shift of six carbon atoms in the repeat unit. Furthermore, on enlarged spectroscopy near 175 ppm, there were two peaks, which were due to the chemical shift of two kinds of carbonyl carbon atoms. The larger one at 173.353 ppm was ascribed to the carbonyl carbon atom in the repeat unit; the smaller one at 176.441 ppm was the signal of the terminal carboxyl group.

Therefore, the polyester's structure was as follows: one terminal was the hydroxyl group, the other was the carboxyl group, and the middle consisted of repeat units of the ring-opening ε-caprolactone unit.

Mechanism of Enzymatic Polymerization

From all the above results and discussions, we can offer the following possible mechanism of enzymatic polymerization: At the beginning of the polymerization, the amount of monomer ε-caprolactone is very large. The polymerization is mainly concerned with the monomer's ring-opening, and the product is an oligomer. The molecular weight of the polyester is low. This process needs participation of water molecules (FIGURE 2). This may be the reason for a higher optimal water concentration than normal. With the reaction going, the amount of monomer becomes less and less; however, the amount of oligomer is now more than that at the beginning. When the conversion of monomer is nearly 100%, the polymerization mainly deals with the oligomer, which is called linear-polymerization. This results in an increase of the molecular weight and the molecular weight distribution. This process produces water molecules, which may be the reason that high water concentration (above 3.8%) can inhibit the polymerization, thereby making the equilibrium reverse to hydrolysis.
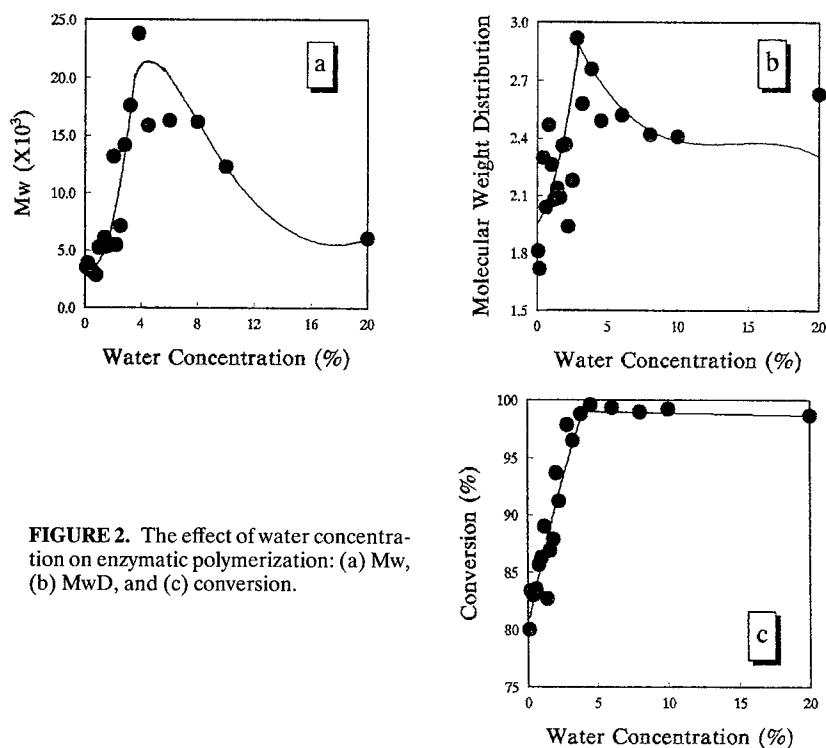
FIGURE 2. The effect of water concentration on enzymatic polymerization: (a) Mw, (b) MwD, and (c) conversion.

Thus, too-high water concentrations make the molecular weight low (FIGURE 2). Furthermore, from FIGURE 1, the disaccord of the conversion curve and the molecular weight curve also proves this two-step mechanism.

CONCLUSIONS

In this study, we suggested a new route for enzymatic synthesis of polyester and discussed every link of this route. PPL and PSLI were selected as optimal sources of lipase. Optimal water concentration for this route was also determined. We also gave a possible mechanism for polymerization. This study provides a substantial basis for further studies, such as copolymerization with other substrates and the biodegradable qualities of polyester.

REFERENCES

1. ZAKS, A. & A. M. KLIBANOV. 1984. Science **224:** 1249–1251.
2. UYAMA, H. & S. KOBAYASHI. 1993. Chem. Lett., p. 1149–1150.
3. BROUN, H. C. & K. A. KEBLYS. 1966. J. Org. Chem. **31:** 485.

Enzymatic Regioselective Transesterification of Sugar Alcohols and Aromatic Esters in Organic Solvents[a]

HYUN GYU PARK,[b] HO NAM CHANG,[b] AND
JONATHAN S. DORDICK[c]

[b]Bioprocess Engineering Research Center
and
Department of Chemical Engineering
Korea Advanced Institute of Science and Technology
Taeduk Science Town
Taejon 305-701, Korea

[c]Department of Chemical and Biochemical Engineering
University of Iowa
Iowa City, Iowa 52242

INTRODUCTION

Esters of monosaccharides and disaccharides have a number of interesting and potentially useful properties, including surface activity, antitumor activity, and plant growth–inhibiting activity. This potential has not been fully explored because production of oligoesters (e.g., di-, tri-, and tetra-) of sugars is a difficult problem in organic chemistry due to the abundance of hydroxyl groups in sugar molecules and their similar reactivities.[1] Even preferential acylation of primary over secondary hydroxyl groups can only rarely be carried out with free sugars; this usually requires protected sugars, thereby necessitating cumbersome protection and deprotection steps. Enzymatic regioselective acylation of sugars offers an alternative to the poor selectivity of chemical synthesis and, recently, there have been many reports on the enzymatic synthesis of sugar esters using lipases or proteases in organic media.[2]

Very recently, we investigated the catalytic potential of the commercially available crude protease from *Bacillus licheniformis*, suspended in organic solvents, toward aromatic compounds.[3,4] Our previous success in developing enzymatic synthesis of aromatic polyester is extended to regioselective transesterification of sugar alcohols and aromatic esters. In the present work, we report that enzymatic acylations were carried out for disaccharides, mainly sucrose, with an activated ester of terephthalic acid in pyridine by employing the same enzyme.

MATERIALS AND METHODS

Materials

Protease from *Bacillus licheniformis* (Optimase M-440) was obtained from Solvay Enzyme (Elkhart, Indiana), and Sigma Sil-A was obtained from Sigma Chemical (St. Louis, Missouri) and used for the preparation of TMS derivatives of sugars. Bis(2,2,2-trifluoroethyl)terephthalate was synthesized from terephthaloyl chloride and 2,2,2-trifluoroethanol following the general methodology[5] and had the same characteristics as previously described.[3] All other chemicals and solvents used in this work were of analytical grade.

Analytical Methods

All sugar derivatives in this work were determined by gas chromatography using a 10-m Alltech AT-1 capillary column packed with polydimethylsiloxane and all reaction mixtures were subjected to precolumn derivatization with 1,1,1,3,3,3-hexamethyldisilazane according to the general methodology.[6] The positions of acylation in all enzymatically prepared compounds were established by ^{13}C-NMR (Brüker AMX 500).

Reactions

Our acylation strategy was to use enzyme-catalyzed transesterification of sugars with an activated ester donor [bis(2,2,2-trifluoroethyl)terephthalate; TFE-te] in anhydrous pyridine. The initial concentrations of TFE-te and sucrose were 0.1 and 0.4 M, respectively. The reaction was initiated by the addition of 100 mg/mL of Optimase M-440, and the suspension was magnetically stirred at 250 rpm. The reaction was terminated by filtering out the enzyme and evaporating the pyridine. The sucrose esters were purified by using silica gel chromatography with an eluant consisting of ethyl acetate/methanol/water (18:1.25:1).

RESULTS AND DISCUSSION

Comparison of the Reactivities for Various Disaccharides and TFE-te

The enzymatic transesterification experiments were carried out for various disaccharides: maltose, lactose, and sucrose. Cellobiose was excluded from the experiments due to its too-low solubility in pyridine. In all cases, the reaction readily took place and in no case was any appreciable conversion detected without enzyme. The data in TABLE 1 indicate that sucrose was the best substrate for the enzymatic transesterification with TFE-te. Furthermore, the low cost and ready availability of pure sucrose make this disaccharide a highly desirable starting material for the preparation of new, commercially significant products and materials.

TABLE 1. Acylation of Various Disaccharides with TFE-te Catalyzed by Optimase M-440 in Anhydrous Pyridine[a]

Disaccharide	Conversion after 24 h (%)[b]
maltose	19.5
lactose	20.8
sucrose	52.2

[a]Conditions: 0.025 M disaccharides; 0.1 M TFE-te; Optimase M-440, 100 mg/mL; pyridine, 1 mL; 37 °C.

[b]Determined by gas chromatography on the basis of the disappearance of the substrate disaccharide.

Effect of Reaction Temperature on Enzymatic Acylation of Sucrose

The rate of the enzymatic transesterification between sucrose and TFE-te and the enzyme inactivation rate were studied in pyridine in the range from 27 °C to 50 °C. The enzymatic acylation of sucrose in pyridine accelerated upon an increase of the temperature (from 27 °C to 50 °C) as depicted in FIGURE 1. However, the inactivation rate also increased as the reaction temperature increased. After 1 day, there was no significant decrease in the enzyme activity at 30 °C (less than 10%), whereas the residual activity was only 50.1% at 50 °C. Comparison of the top and
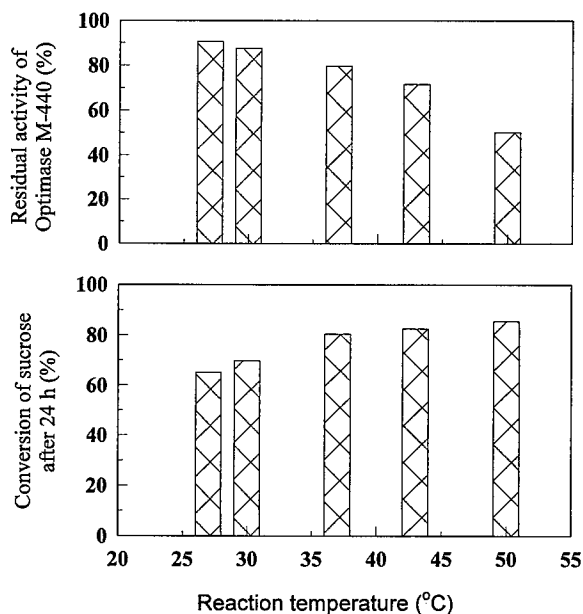
FIGURE 1. Effects of temperature on the acylation rate of sucrose (bottom) and on the inactivation of Optimase M-440 suspended in anhydrous pyridine (top). Crude enzyme (100 mg) was added to the solution (1 mL) in different vials and the suspensions were shaken at different temperatures. After 24 hours, pyridine was decanted and the residual activity was analyzed by GC with the same substrates at 37 °C.

bottom panels of FIGURE 1 reveals that the temperature had the opposite effects on the enzyme in organic solvent. Whereas the reaction rate increased as the temperature increased, the inactivation was much faster at high temperature.

Sucrose Ester Synthesis

In order to preparatively synthesize the sucrose esters, we scaled up the enzymatic process. Sucrose (0.1 M) and TFE-te (0.4 M) were dissolved in 100 mL of pyridine and the reaction was carried out at 37 °C. After 20 days, the reaction was terminated by filtering out the enzyme and evaporating the organic solvent. The residual solids were loaded onto a silica column (see MATERIALS AND METHODS), and sucrose esters were separated into monoester and diester. No triester was ever formed, as evidenced by TLC and GC.

To determine the site of sucrose acylation, ^{13}C-NMR analysis of the sucrose ester products was carried out. Following the general strategy developed by Yoshimoto *et al.*,[7] acylation at position 1' of sucrose should result in a downfield shift of the peak at C1' and in an upfield shift of the peak at C2'. Acylation at position 6 of sucrose should result in a downfield shift of the peak at C6 and in an upfield shift in the peak at C5. The chemical shifts in TABLE 2 enable us to assign structures to the monoester and diester products, with the sucrose monoester identified as sucrose 1'-terephthalate and the diester product identified as sucrose 6,1'-diterephthalate. Hence, sucrose was acylated at the 1' position followed by acylation at the 6 position (FIGURE 2).

The solubility of the sucrose ester products was tested in a variety of solvents. The monoester and diester were soluble in a variety of polar organic solvents, including DMSO, DMF, methanol, ethanol, acetone, tetrahydrofuran, and pyridine. The diester was insoluble in water, whereas the monoester was soluble, indicating that a monoester and diester mixture could be separated by simple extraction using water.

To summarize, protease has been employed in the present study for the regioselective acylation of sugars with activated terephthalate in pyridine. This work leads

TABLE 2. Chemical Shifts (ppm) of Sucrose Terephthalate and Sucrose Diterephthalate in DMSO

Carbon Number	Sucrose	Sucrose Monoterephthalate	Sucrose Diterephthalate
2'	104.0	102.2	102.2
1	91.7	92.2	92.1
5'	82.6	82.9	83.0
3'	77.1	76.7	76.72
4'	74.3	73.4	73.61
3	72.9	73.0	72.55
5	72.8	72.65	70.13
2	71.6	71.43	71.23
4	69.9	69.63	69.77
1'	62.0	63.74	65.17
6'	62.1	62.05	62.41
6	60.5	60.51	63.58
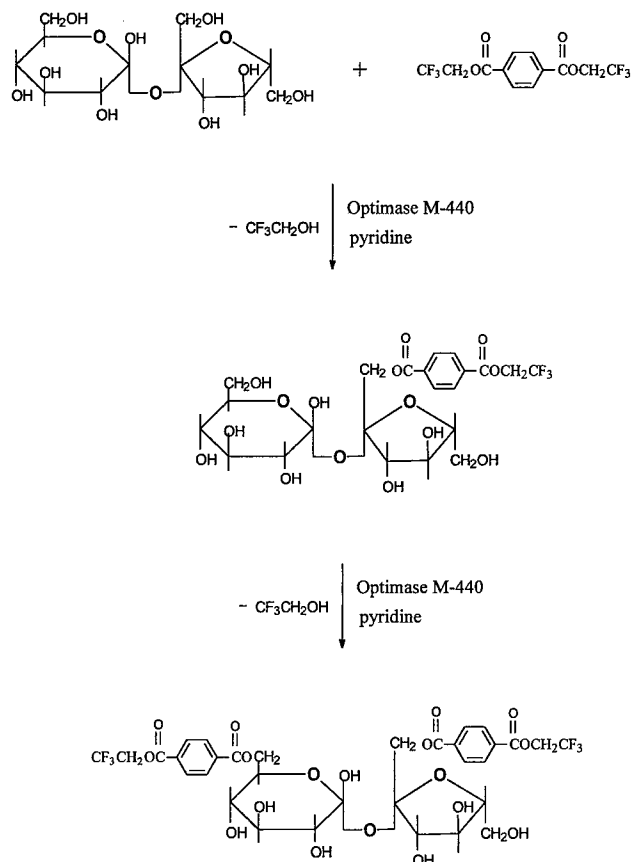
FIGURE 2. Scheme of sucrose acylation in anhydrous pyridine catalyzed by Optimase M-440.

to a straightforward synthetic methodology for the preparative production of aromatic monoesters and diesters of sugars.

REFERENCES

1. SHAW, J. & A. M. KLIBANOV. 1987. Preparation of various glucose esters via lipase-catalyzed hydrolysis of glucose pentaacetate. Biotechnol. Bioeng. **29:** 648–651.
2. PATIL, D. R., D. G. RETHWISCH & J. S. DORDICK. 1991. Chemoenzymatic synthesis of novel sucrose-containing polymers. Macromolecules **24:** 3462–3463.
3. PARK, H. G., H. N. CHANG & J. S. DORDICK. 1994. Enzymatic synthesis of various aromatic polyesters in anhydrous organic solvents. Biocatalysis **11:** 263–271.
4. PARK, H. G., H. N. CHANG & J. S. DORDICK. 1995. Enzymatic polytransesterification of aromatic diols in organic solvents. Biotechnol. Lett. **17**(10): 1085–1090.
5. STEGLICH, W. & G. HOFFE. 1969. *N,N*-Dimethyl-4-pyridinamine, a very effective acylation catalyst. Angew. Chem. Int. Ed. Engl. **8:** 981.

6. SWEELY, C. C., R. BENTLY, M. MAKITA & W. W. WELLS. 1963. Gas-liquid chromatography
     of trimethylsilyl derivatives of sugars and related substances. J. Am. Chem. Soc. **85:** 2497.
7. YOSHIMOTO, K., Y. ITATANI & Y. TSUDA. 1980. ^{13}C-Nuclear magnetic resonance spectra of
     O-acylglucoses: additivity of shift parameters and its application to structure elucida-
     tions. Chem. Pharm. Bull. **28:** 2065–2074.

Production of Levan, a Fructose Polymer, Using an Overexpressed Recombinant Levansucrase

KI-BANG SONG, HAFEDH BELGHITH, AND
SANG-KI RHEE[a]

Applied Microbiology Research Group
Korea Research Institute of Bioscience and Biotechnology
KIST
Yusong, Taejon 305-600, Korea

INTRODUCTION

In nature, two kinds of fructan, classified by the type of linkage, are found. One is inulin, which is generally found in plants and has a β-2,1 linkage composed of several hundred fructose monomers.[1,2] Levan, a β-2,6-linked polyfructan, is another fructan that is produced mainly by microorganisms: *Bacillus subtilis*,[3] *Zymomonas mobilis*,[4] *Bacillus polymyxa*,[5] *Aerobacter levanicum*,[6] *Erwinia herbicola*,[7] *Rhenella aquatilis*,[8] etc. Due to the different length of polymeric structure and the degree of branching, some properties of the levan produced by each microorganism differ from each other.[5,9] Levan is generally much larger in molecular weight than inulin, which is composed of up to 3 million fructose residues.

Although the characteristics of levan formation by levansucrase were investigated partly using a *Bacillus* levansucrase system,[1,3] the levan formation mechanism and some characteristics have not been fully understood due to the extremely low expression of levansucrase in wild-type microorganisms. Attempts for the production of levan have remained mainly in the stage of screening and characterization of levan-producing enzyme. Consequently, the production and utilization of levan in the industrial field have been strictly limited, and only a few papers have reported the production of levan using fermentation techniques.[2,7,10,11] Recently, great interest in this fructan has been renewed to discover applications for levan as a new industrial gum in the fields of cosmetics, foods, and pharmaceutical goods.[5]

Previously, we cloned and sequenced the levansucrase gene (*levU*) of *Z. mobilis*.[12] In this study, levansucrase gene was overexpressed in *E. coli,* and some optimal conditions of levan formation using the native and genetically modified levansucrases were investigated.

MATERIALS AND METHODS

Bacterial Strains, Plasmids, and Gene Manipulations

E. coli BL21 (DE3, F⁻ *ompT* r^-_B m^-_B)[13] was used as a cloning host for levansucrase expression. A shuttle vector, pET3d, was used for the overexpression of

the *levU* gene in *E. coli*. The plasmid pZL8 was used[12] as a source of the *levU* gene. *E. coli* was routinely grown at 37 °C in LB medium for gene manipulation and in M9ZB medium[13] for overexpression. All restriction enzymes, T4 DNA ligase, and DNA-modifying enzymes were purchased from Boehringer Mannheim (Germany) and KOSCO (Korea). DNA manipulation and transformation of *E. coli* were accomplished according to the methods described by Maniatis *et al.*[14]

Preparation and Purification of Levansucrase Enzyme

E. coli BL21 containing the plasmids, pEL 12 and pEL 13, were grown aerobically at 37 °C. After IPTG induction, the harvested cells were resuspended in 100 mM Tris buffer (pH 6.8) and then disrupted by ultrasonication with a SONIFIER (Branson) at 4 °C for 3 min. The cell debris was removed by centrifugation and the supernatant was used as the cell-free extract. The purification of modified levansucrase from *E. coli* lysate was done using Ni-NTA resin, which was purchased from QIAGEN.

Enzyme Assay

Levansucrase activity was indicated as sucrose hydrolysis activity, and it was determined by the method of O'Mullan *et al.*[15] One unit (U) of enzyme activity was defined as the amount of enzyme releasing one micromole of glucose per minute.

Analytical Methods

The protein concentration was determined by the Bradford method. Quantitative determinations of glucose, fructose, sucrose, oligosaccharides, and levan were conducted by HPLC (Beckman) with a refractive index detector and a Shodex Ionpack KS-802 column (Showa Denko Company, Japan). Deionized water was used as a mobile phase at a flow rate of 0.4 mL/min.

RESULTS AND DISCUSSION

The genes encoding levansucrase were obtained from PCR reaction using pZL8 plasmid as a template. The gene encoding a native enzyme was obtained using two synthetic primers, P1 (5'-CGCCGGATCCACATGTTGAATAAAGCAGGC-3') and P2 (5'-CGCGGATCCACATGTGCATTATCAGAAACGTC-3'). To simplify the purification of levansucrase from cleared *E. coli* lysate, a genetically modified levansucrase gene, which contained His-affinity tag, was constructed by the attachment of an amino-acid sequence of six histidine residues in the C-terminal region of the levansucrase gene (*levU*) by PCR reaction using two synthetic primers, P3 (5'-CGCCGGATCCACATGTTGAATAAAGCAGGC-3') and P4 (5'-CGTCATGT-TAGTGATGGTGATGGTGATGTAAAGACAGGGCTG-3'). Two PCR products were digested with AflIII and subcloned into the NcoI site of pET3d. The resulting

plasmids, pEL 12 containing a native gene and pEL 13 containing a modified gene, were transformed to *E. coli* BL21. When the *E. coli* transformants were grown at 37 °C, enzyme activities in both cases were detected after 4 h of IPTG induction in the soluble fractions of cell lysate. By a prolonged incubation, the ratio of insoluble aggregates (inclusion body formation) against soluble fraction was markedly increased, and the enzyme activities were not detected in soluble fractions after 16 h of incubation (FIGURE 1). Under the control of the T7 promoter, both levansucrases were produced up to 30–40% in the total cell protein of *E. coli.*
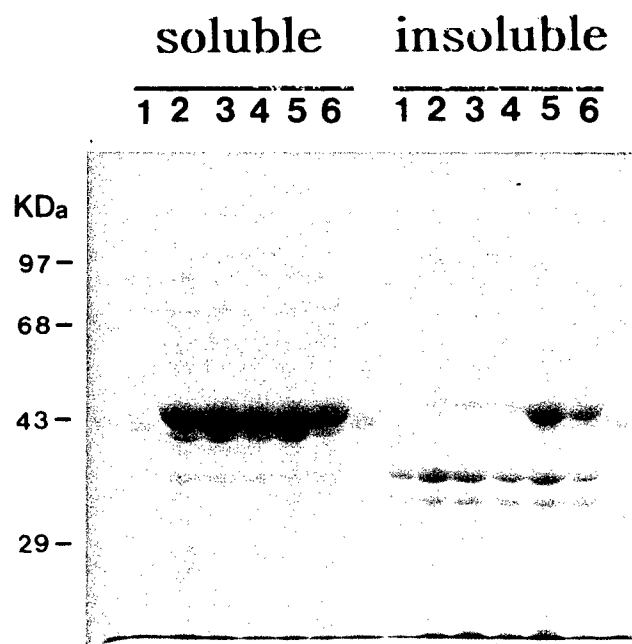
FIGURE 1. SDS-PAGE analysis of levansucrase overproduced in *E. coli* carrying pEL 12. Protein standards are indicated on the left. Terms: 1, sample before induction; 2–6, samples after 2, 4, 6, 8, and 16 h of induction.

The purification of the modified levansucrase from *E. coli* carrying the plasmid pEL 13 was done. After disruption of cells, this protein was purified by one step using Ni-NTA resin column chromatography. By use of this affinity chromatography, a modified protein showing more than 95% homogeneity in SDS-PAGE analysis was obtained. End products formed by native and genetically modified proteins from sucrose were compared by HPLC analysis (FIGURE 2). In both cases, a highly polymerized product, that is, levan, and glucose were formed as major reaction products. A small amount of kestose and a trace amount of nystose were also detected.
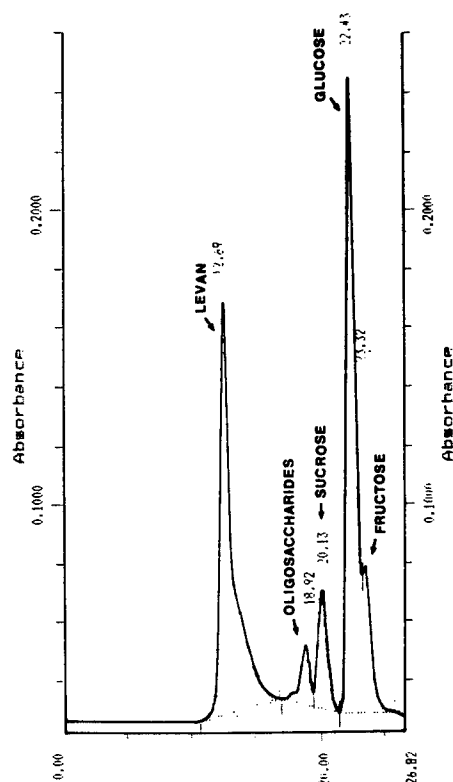
FIGURE 2. A typical HPLC chromatogram showing the products of the transfructosylation reaction with sucrose by levansucrase overexpressed in *E. coli*.

TABLE 1. Effect of Temperature on the Transfructosylation Reaction of Levansucrases

	Native Levansucrase[a]			Modified Levansucrase[b]		
Temperature (°C)	Fructose Liberated (%)	Oligosaccharide Formed[c] (%)	Levan Formed (%)	Fructose Liberated (%)	Oligosaccharide Formed[c] (%)	Levan Formed (%)
10	15.4	11.8	46.4	12.2	0.49	37.5
20	21.4	12.0	37.3	14.2	0.75	32.5
30	58.0	17.0	24.8	43.3	2.06	23.6
40	74.0	22.0	13.0	—[d]	—	—

[a]Levan content was calculated based on the amount of fructose liberated.

[b]Levan content was calculated by standard calibration using authentic levan (produced by *A. levanicum* from Sigma).

[c]Converted into raffinose.

[d]Not determined.

TABLE 2. Effect of Temperature on the Formation of Levan (g/L)

Temperature (°C)	Time (h)					
	4	10	27	46	78	167
−3	7.3	10.5	20.5	30.0	34.5	30.5
0	10.1	15.7	29.5	36.5	37.2	32.3
5	11.3	22.2	33.2	36.4	38.4	33.0
10	15.2	29.3	34.9	36.7	37.5	29.7

As has been shown already, the most interesting feature of levansucrase was its low-temperature-activated levan formation.[16] In this study, the effect of temperature on levan formation by the two enzymes was investigated. The reaction mixtures containing 10% sucrose in a 50 mM acetate buffer were incubated at different temperatures. As shown in TABLE 1, the synthesis of levan in both cases was greater at lower temperatures and the conversion yield of available fructose to levan was around 40%. The amount of oligosaccharides and free fructose in the reaction mixture tended to increase with the increase of the reaction temperature. These results showed that no enzymatic alteration for levan formation occurred by the C-terminal modification of this enzyme. Subsequently, the effect of temperature on levan formation by the modified enzyme was investigated in more detail at different low temperatures by incubating reaction mixtures containing 10% sucrose and 2.08 units of enzyme in a 50 mM acetate buffer. As shown in TABLE 2, more levan was formed at lower temperatures. The initial rate of levan formation was enhanced by the increase of the reaction temperature. After 20 h of incubation, the levan formation in each reaction, except the −3 °C reaction, was saturated, and the levan content formed was slightly decreased with the increase of incubation time. This phenomenon could be explained by the disproportionate reaction of this enzyme.[16] Under these conditions, the optimum temperature for levan formation was 0 °C, whereas a considerably lower amount of levan was formed during incubation at −3 °C.

The effect of pH on levan formation was investigated at various pH values using the modified levansucrase. A 5-mL reaction mixture, containing 10% sucrose and 0.42 units of enzyme in 50 mM acetate buffer, was incubated at 10 °C. The levan formation was tested by measuring the amount of levan produced at different times. Levan formation under acidic conditions was more significant than the formation at pH 6 and above (TABLE 3). No levan formation was observed at pH values above 9. The optimum pH was found to be 5. Similarly, the optimum pH for native levansucrase of *Z. mobilis* was reported to be pH 4–6.[17]

TABLE 3. Effect of pH on the Formation of Levan (g/L)

Time (h)	pH									
	3.0	3.5	4.0	4.5	5.0	5.5	6.0	6.5	7.0	7.5
5	6.6	8.0	9.3	10.0	10.5	9.2	7.0	5.5	4.3	3.0
48	26.7	30.0	32.9	35.2	35.9	31.1	28.0	27.5	22.1	17.1

TABLE 4. Effect of Enzyme Concentration on the Formation of Levan (g/L)

Enzyme Concentration (Units)	Time (h)				
	4	12	48	96	144
0.42	2.5	4.0	21.7	35.7	39.0
1.05	4.9	12.9	34.9	48.5	42.2
2.08	24.9	44.9	49.0	49.2	46.2

To investigate the effect of enzyme concentration on levan formation by the modified levansucrase, different amounts of enzyme (0.42, 1.05, and 2.08 units of enzyme per mL each) were added to a 5-mL reaction mixture, containing 10% sucrose in 50 mM acetate buffer (pH 5), and were incubated at 10 °C. As shown in TABLE 4, the amount and rate of levan formation were enhanced by the increase of enzyme concentrations. After 70 h of incubation, the total amounts of levan formed in the three enzyme reactions were similar. After 70 h of incubation at 0 °C, however, the amounts of levan formed at the concentrations of 0.42 and 1.05 U were only 83% and 45% of that formed at the concentration of 2.08 U, respectively (data not shown). Overall, the optimum enzyme concentration was 1.05 U/mL.

The effect of substrate concentrations (5%, 10%, 20%, 30%, and 40% of sucrose each) on levan formation was also investigated. A 10-mL reaction mixture, containing 1.05 units of enzyme per mL in 50 mM acetate buffer (pH 5), was incubated at 10 °C. As TABLE 5 shows, the resulting amounts of levan formed were increased with the increase of substrate concentration. Due to the oligosaccharide formation at the high concentration of substrate, the yield of levan formed from sucrose decreased according to the increase of substrate concentration. When calculated as a conversion yield, the optimum substrate concentration for levan production was 20%.

In conclusion, the optimum temperature for the production of levan using the modified levansucrase was 0 °C and the optimum pH was 5. A high velocity of levan formation was achieved with the enzyme concentration of 1.05 U/mL. The optimum concentration of sucrose as a substrate for levan production was 20%. Under these optimum conditions, high-molecular-weight levan was produced, but only low concentrations of fructose and oligosaccharide were liberated.

TABLE 5. Effect of Substrate Concentration on the Formation of Levan (g/L)

Substrate Concentration (%)	Time (h)					
	2	11	18	25	36	59
5	12.1	19.0	21.8	21.6	21.4	20.8
10	14.8	38.2	36.7	39.1	34.2	34.9
20	14.1	51.4	56.7	52.9	51.4	52.0
30	14.6	52.4	71.1	66.9	69.8	59.4
40	11.5	39.1	59.8	58.8	60.0	56.4

REFERENCES

1. SUZUKI, M. & N. J. CHATTERTON. 1993. Science and Technology of Fructans. CRC Press. Boca Raton, Florida.
2. HAN, Y. W. 1989. J. Ind. Microbiol. **4:** 447–452.
3. TANAKA, T., S. OI, M. IIZUKA & T. YAMAMOTO. 1978. Agric. Biol. Chem. **42:** 323–326.
4. DAWES, E. A. & D. W. RIBBONS. 1966. Biochem. J. **98:** 804–812.
5. HAN, Y. W. & M. A. CLARKE. 1990. J. Agric. Food Chem. **38:** 393–397.
6. EVANS, T. H. & H. HIBBERT. 1946. Adv. Carbohydr. Chem. **2:** 253–277.
7. KEITH, K., B. WILEY, D. BALL, S. ARCIDIACONO, D. ZORFASS, J. MAYER & D. KAPLAN. 1991. Biotechnol. Bioeng. **38:** 557–560.
8. OHTSUKA, K., S. HINO, T. FUKUSHIMA, O. OZAWA, T. KANEMATSU & T. UCHIDA. 1992. Biosci. Biotechnol. Biochem. **56:** 1373–1377.
9. EBSKAMP, M. J. M., I. M. VAN DER MEER, B. A. SPRONK, P. J. WEISBEEK & S. C. M. SMEEKENS. 1994. Bio/Technology **12:** 272–275.
10. YOSHIDA, Y., R. SUZUKI & Y. YAGI. 1990. J. Ferment. Bioeng. **70:** 269–271.
11. REISS, M. & H. HARTMEIER. 1989. Chem. Mikrobiol. Technol. Lebensm. **12:** 1–7.
12. SONG, K. B., H. K. JOO & S. K. RHEE. 1993. Biochim. Biophys. Acta **1171:** 320–324.
13. STUDIER, F. W., A. H. ROSENBERG, J. J. DUNN & J. W. DUBENDORFF. 1990. Methods Enzymol. **185:** 60–89.
14. MANIATIS, T., E. F. FRITSCH & J. SAMBROOK. 1982. Molecular Cloning: A Laboratory Manual. Second edition. Cold Spring Harbor Laboratory. Cold Spring Harbor, New York.
15. O'MULLAN, P. J., T. CHASE, JR. & D. E. EVELEIGH. 1991. Biotechnol. Lett. **13:** 137–142.
16. TANAKA, T., S. OI & T. YAMAMOTO. 1979. J. Biochem. **85:** 287–293.
17. YANASE, H., M. IWATA, R. NAKAHIGASHI, K. KITA, N. KATO & K. TONOMURA. 1992. Biosci. Biotechnol. Biochem. **56:** 1335–1337.

The Optimization and Semicontinuous Synthesis of Oligosaccharides

N. K. SMITH, S. G. GILMOUR, AND R. A. RASTALL

Biotechnology and Biochemical Engineering Group
Department of Food Science and Technology
and
Department of Applied Statistics
University of Reading
Reading RG6 6AP, United Kingdom

INTRODUCTION

In recent years, it has been recognized that carbohydrates play an important role in many diverse living systems. In order to try and understand these roles further, it is first necessary to synthesize these oligosaccharide structures on a suitable scale, probably in kg quantities. At present, there are no methods available for the synthesis of many of these types of sugars on such a scale; many of them are just economically unfeasible. Many workers are now looking towards using enzymes, specifically the glycosidases, for synthesis of these molecules. The major drawback of this method is the relatively low yields of products due to the kinetics of the enzyme. In order to obtain the highest possible yields, it is essential that the various parameters, such as total sugar and acceptor concentrations, be optimized.[1]

METHODS

Each reaction mixture was prepared in 0.1 M acetate buffer and adjusted to the relevant pH. The buffer for the α-mannosidase reactions also contained 1 mM zinc sulfate to maintain the activity. The appropriate sugars were added to each reaction vessel and dissolved prior to the addition of the enzyme. The reaction mixtures were incubated at 55 °C for 72 hours. Analysis was carried out using HPLC, and a 3 μ spherisorb amino column (4 × 250 mm) was used with refractive index detection and with 80% acetonitrile as the eluant.

Experiments were set up according to a three-factor central composite design and results were fitted to a quadratic model by SAS statistical software.

RESULTS

Synthesis could be described by the following model:

$$\ln(\text{yield} + 1) = \beta_0 + \beta_1 pH + \beta_2 S + \beta_3 A$$
$$+ \beta_{11} pH^2 + \beta_{22} S^2 + \beta_{33} A^2$$
$$+ \beta_{12} pH \cdot S + \beta_{13} pH \cdot A + \beta_{23} S \cdot A$$
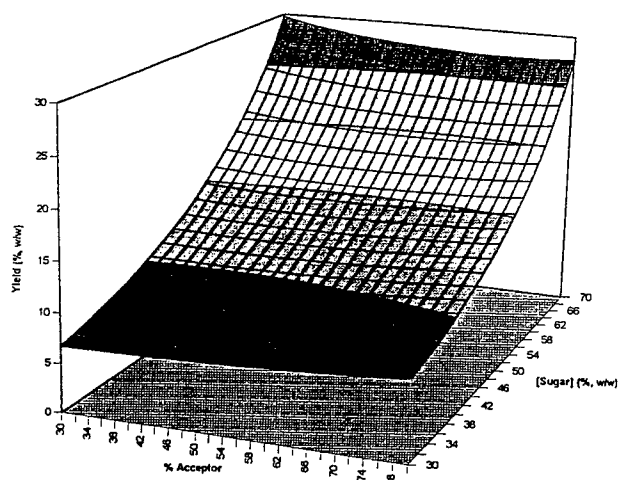
FIGURE 1. Response surface for α-mannosidase (mannosyl-trehalose).
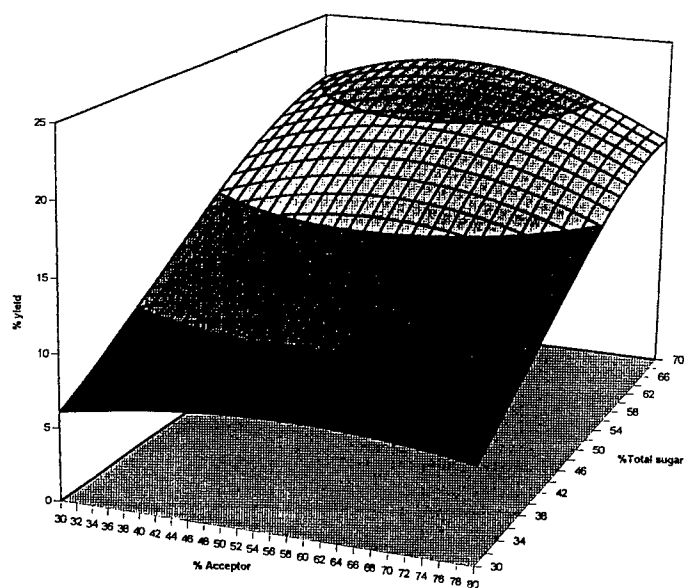
FIGURE 2. Response surface for α-mannosidase (mannosyl-sucrose).

where S = sugar and A = acceptor. For the example of glucoamylase for the synthesis of glucosyl-trehalose (with R^2 = 0.9363), we have

$$\ln(\text{yield} + 1) = -9.221 + (2.106 \times pH) + (0.0132 \times \text{sugar}) + (0.0622 \times \text{acceptor})$$
$$+ (-0.145 \times pH^2) + (-0.000554 \times \text{sugar}^2)$$
$$+ (-0.000839 \times \text{acceptor}^2) + (-0.0129 \times pH \times \text{sugar})$$
$$+ (0.00266 \times pH \times \text{acceptor}) + (0.00048 \times \text{sugar} \times \text{acceptor}).$$

FIGURES 1, 2, 3, and 4 illustrate the response surfaces for the synthesis of mannosyl-trehalose and mannosyl-sucrose by α-mannosidase, galactosyl-trehalose by β-galactosidase, and glucosyl-trehalose by glucoamylase, respectively.

DISCUSSION

Using statistical analysis and response surface methodology, it has been possible to optimize pH, [acceptor], and [total sugar] with respect to product yields. It is interesting to note that the acceptor concentration plays a much more significant role for glucoamylase when compared with the other glycosidases investigated. Another interesting point to note is that, for α-mannosidase, 55% sucrose is the optimum when being used as an acceptor, whereas it is as low as 30% when trehalose is used.

The type of experiment outlined here provides a basis from which further developments could be made to improve yields. One such development could be that of a semicontinuous bioreactor (currently being undertaken). In such a bioreactor is immobilized glycosidase, donor, and acceptor. By continuously feeding in substrates,
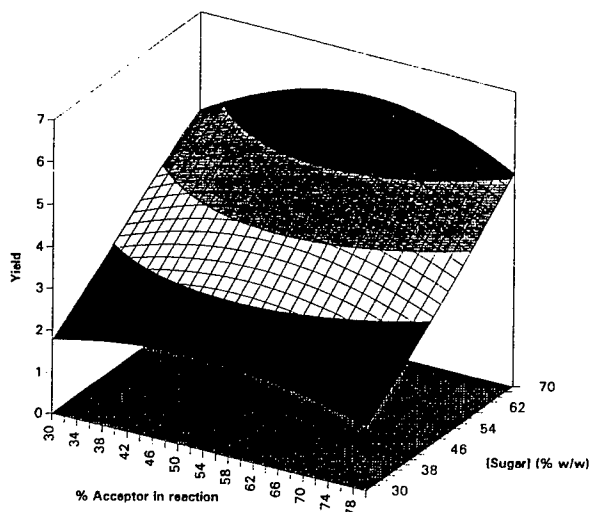
FIGURE 3. Response surface for β-galactosidase.
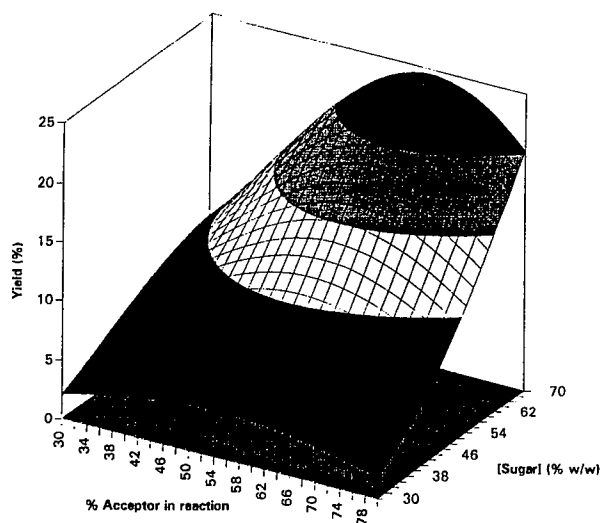
FIGURE 4. Response surface for glucoamylase.

removing products, purifying, and recycling unused substrates, it should be possible to synthesize large quantities of product. It is important that the new parameters in such a system be optimized, such as enzyme immobilization, impeller-type stirrer speed, and temperature, as it is vital to maximize the flow throughput of substrates and the removal of the product stream in order to maximize oligosaccharide production with regard to time.

REFERENCE

1. RASTALL, R. A. & C. BUCKE. 1992. Biotechnol. Genet. Eng. Rev. **10:** 253–281.

The Application of Asymmetric Bioreductions to the Production of Chiral Pharmaceutical Drugs

MICHEL CHARTRAIN, JOSEPH ARMSTRONG,
LORRAINE KATZ, STEVEN KING, JAYANTHI REDDY,
YAO-JUN SHI, DAVID TSCHAEN,
AND RANDOLPH GREASHAM

Merck Research Laboratories
Rahway, New Jersey 07065

INTRODUCTION

Studies in the past few years have witnessed a tremendous growth in the understanding of the pharmacokinetics and metabolisms of pharmaceutical drugs.[1] These studies have revealed that, often, only one of the enantiomers of a racemic drug is actually the active form of that drug. Although very often the other enantiomer is just referred to as "isomeric ballast", its presence can in some instances be detrimental.[1] Due to these insights and to the probability of novel regulatory trends, the development of chiral pharmaceutical drugs has greatly expanded.[2,3]

Chiral chemistry has many powerful tools at its disposal; however, in some instances, the synthesis of chiral intermediates still proves to be difficult or even impossible. Under these circumstances, the use of asymmetric biocatalysis, employing either whole cells or isolated enzymes, can be an attractive alternative.[3] Chiral alcohols are widely used precursors in chemical syntheses, and their production by asymmetric bioreduction of their ketone precursors has been demonstrated in many instances.[4-9]

We have applied asymmetric biocatalysis as a tool for the production of chiral precursors for the production of novel pharmaceutical drugs.[10-12] This report describes the approaches used in the development of several successful processes that supported the production of highly optically pure chiral alcohol precursors at the preparative scale.

RESULTS

General Approach

The implementation of asymmetric biocatalyses in the manufacture of experimental drugs begins with the identification of a suitable step in chemical syntheses where the use of chiral chemical catalysis is not practical or, in some extreme cases, impossible. This is achieved by frequently reviewing the synthesis of new experimen-

tal drugs in close collaboration with development chemists. The feasibility of implementing an asymmetric biocatalytic step is considered based on previous internal and external knowledge and experience. Once the conceptualization is completed, a microbial screening program followed by the rapid development of a small-scale process capable of supporting the production of preparative amounts of the desired chiral intermediate are then rapidly implemented.

Microbial Screening

The selection of the microbes tested in our screen is based on our internal experience and on published information. The screening takes advantage of micro-

Ketosulfone   Trans-Hydroxysulfone
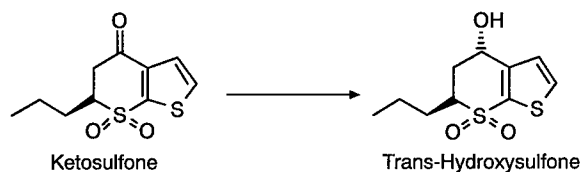
Microorganism	Conversion (%)	Diastereoisomer	Diastereomeric Excess (%)
Rhodotorula rubra (MY 2169)	100	Trans	91
Rhodotorula pilimanae (ATCC 32762)	100	Trans	91
Saccharomyces bayanus (MY 1930)	97	Cis	92
Yarrowia lipolytica (ATCC 48436)	69	Trans	85
Geotrichum candidum (MF 2916)	17	Cis	60
Candida apicola (MY 1793)	8	Trans	60
Pichia vini (MY 1622)	95	Cis	50
Saccharomyces cerevisiae (MY 1423)	20	Cis	66
Pichia nakasei (MY 1497)	2	Trans	33

FIGURE 1. Asymmetric bioreduction of a ketosulfone precursor to a carbonic anhydrase inhibitor.

bial diversity as much as possible by evaluating a broad range of microbial species (yeasts, bacteria, and fungi) that have been isolated from very diverse environments. For practical purposes, whole microbial cells are used in order to take advantage of their cofactor recycling ability.[9] Screenings are usually performed at the shake-flask scale (250 mL), employing standard cultivation media.[10-12] Unless it presents some toxicity to the microorganisms, the molecule to be bioconverted is usually added upon inoculation. In many instances, a biocompatible solvent such as ethanol or DMSO is used to facilitate the addition of water-insoluble molecules. The following examples present the results obtained when screening for suitable microorganisms for the biocatalysis of several asymmetric bioreductions.

FIGURE 1 shows the results obtained when searching for a microbe capable of

asymmetrically bioreducing a ketosulfone to its corresponding *trans*-hydroxysulfone. This *trans*-hydroxysulfone is a precursor to the carbonic anhydrase inhibitor, L 685,393, an experimental drug targeted for the treatment of ocular glaucoma.[13] Biocatalysis was evaluated here because, although chemical production of the *cis*-diastereoisomer was simple, the production of the *trans*-diastereoisomer proved to be far more complicated. All of the 9 yeast species evaluated in this screen were able to produce hydroxysulfone, and 2 of them, both *Rhodotorula* species, produced the desired *trans*-hydroxysulfone with elevated diastereomeric excess (de = 91%). FIGURE 2 summarizes the search for a microbe capable of catalyzing the formation of (*S*)-tetralol by asymmetric bioreduction of the tetralone precursor. This (*S*)-tetralol is a precursor for MK-0499, an experimental drug targeted for the treatment of cardiac arrhythmias.[14] The highest (*S*)-tetralol enantiomeric excesses achieved by

β-Tetralone   (S)β-Tetralol
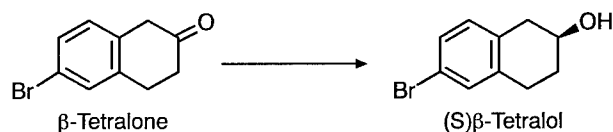
Strains Tested: 80

Microorganism	"ee" (%)
Yarrowia lipolytica (ATCC 48436)	0
Pichia strasburgensis (MY1614)	50 (S)
Candida kruisii (MY 1807)	50 (R)
Candida milleri (MY 1826)	0
Candida citrus (MY 1818)	33 (S)
Trichosporon capitatum (MY 1890)	71 (S)
Rhodotorula rubra (M1)	0
Candida famata (MY 1888)	0
Hansenula fabianii (MY 1496)	0

FIGURE 2. Asymmetric bioreduction of a β-tetralone to (*S*)-β-tetralol.

chiral chemistry were about 20% and made biocatalysis an attractive approach.[15] After evaluating about 80 microbial species, we found that about 8 of them were able to carry the desired reaction, with only 1, *Trichosporon capitatum*, supporting the formation of (*S*)-tetralol with an enantiomeric excess of 71%. FIGURE 3 shows the results of a more difficult screening effort. The desired reaction was the asymmetric reduction of a β-ketoester to its corresponding (*R*)-hydroxyester. This (*R*)-hydroxyester is a precursor in the synthesis of the wide-spectrum β-lactam antibiotic, BO 2727.[16–18] It was only after the evaluation of about 260 microbial strains that *Mortierella alpina* MF 5534 was found to catalyze the desired asymmetric bioreduction. The diastereomeric excess of the (*R*)-hydroxyester produced was greater than 98%.
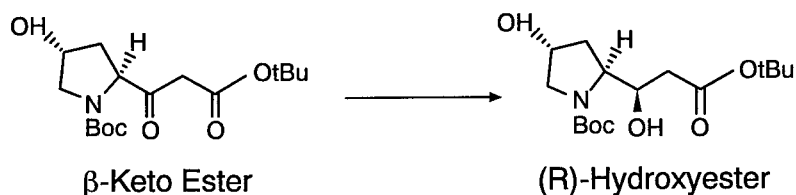
Mortierella alpina MF 5534

FIGURE 3. Asymmetric bioreduction of a β-ketoester to (R)-hydroxyester.

Preparative-Scale Process Development

Once the identification of the appropriate biocatalyst is completed, the next challenge is the development of a process capable of supporting the production of preparative quantities (100-g scale) of the desired chiral intermediate.

Mortierella alpina MF 5534 was identified as a desirable biocatalyst for the asymmetric bioreduction of a ketoester to its corresponding (R)-hydroxyester (FIGURE 3) with a diastereomeric excess greater than 98%. When evaluating the effect of various media compositions and environmental conditions on the optical purity of the (R)-hydroxyester produced, it was found that the diastereomeric excess remained greater than 98% at all times.[10] The major challenge was the process scale-up in laboratory bioreactors (23-L scale). FIGURE 4 shows that an (R)-hydroxyester concentration of about 550 mg/L was achieved after about 250 hours of cultivation.
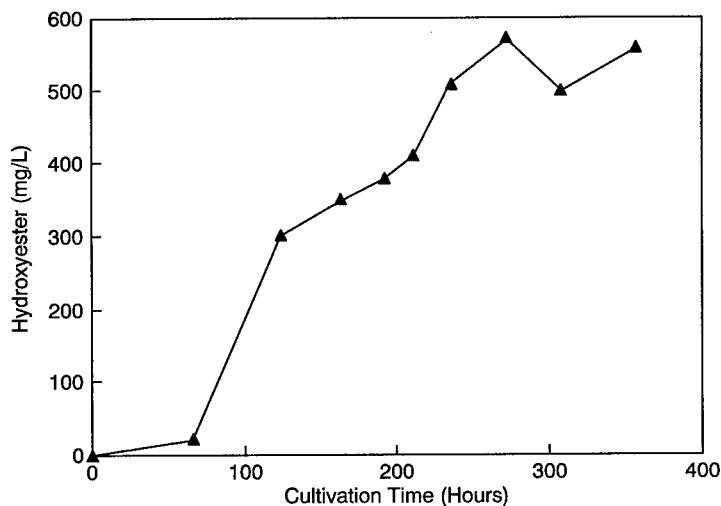
FIGURE 4. Asymmetric bioreduction of a β-ketoester to (R)-hydroxyester by *Mortierella alpina* MF 5534.

This process supported the production of gram quantities of (S)-hydroxyester with a diastereomeric excess greater than 98%.[10]

Rhodotorula rubra MY 2169 catalyzes the asymmetric bioreduction of ketosulfone to trans-hydroxysulfone (FIGURE 1). The diastereomeric excess observed of about 91% fell short of the required purity of 95% or greater. The evaluation of several process parameters showed that the diastereomeric excess of the trans-hydroxysulfone at harvest remained around 90–91%,[11] although the bioconversion rate and yield greatly improved. However, the analyses of several bioreductions revealed that the trans-hydroxysulfone diastereomeric excess was greater than 98% during the early part of the bioconversion and that it quickly dropped to about 90% by the end of the process. This decrease in optical purity was found to be very reproducible and to occur only when the initial ketosulfone concentration dropped
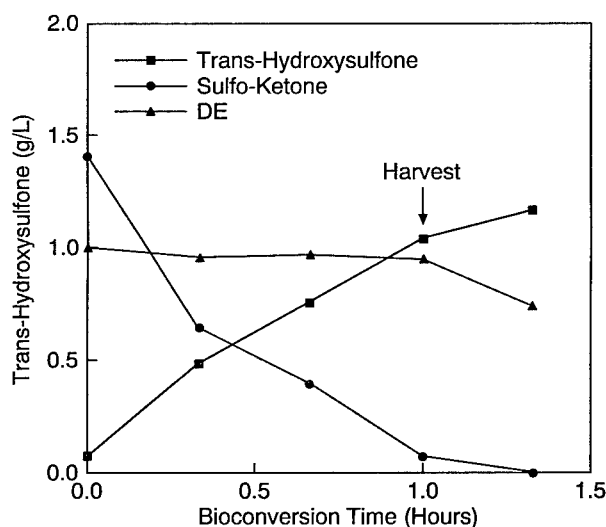
FIGURE 5. Asymmetric bioreduction of a ketosulfone to trans-hydroxysulfone by Rhodotorula rubra MY 2169.

below 0.1 g/L.[11] By exploiting this observation, a process where the bioreduction was harvested before the ketosulfone concentration dropped below 0.1–0.2 g/L was designed. This process routinely achieved the production of trans-hydroxysulfone with a diastereomeric excess at harvest of greater than 95%. FIGURE 5 presents a typical asymmetric bioreduction kinetic time course. This process easily supported the production of gram quantities of the desired trans-hydroxysulfone that were used in the subsequent synthetic steps of the drug candidate L 685,393.

Finally, Trichosporon capitatum MF 1890 was identified as a potential catalyst for the asymmetric bioreduction of a tetralone to its corresponding (S)-tetralol (FIGURE 2). The 71% (S)-tetralol enantiomeric excess (ee) achieved was quite far from the final goal of 98% ee. The evaluation of several process parameters revealed that the (S)-tetralol enantiomeric excess was controlled by the physiological stage of the
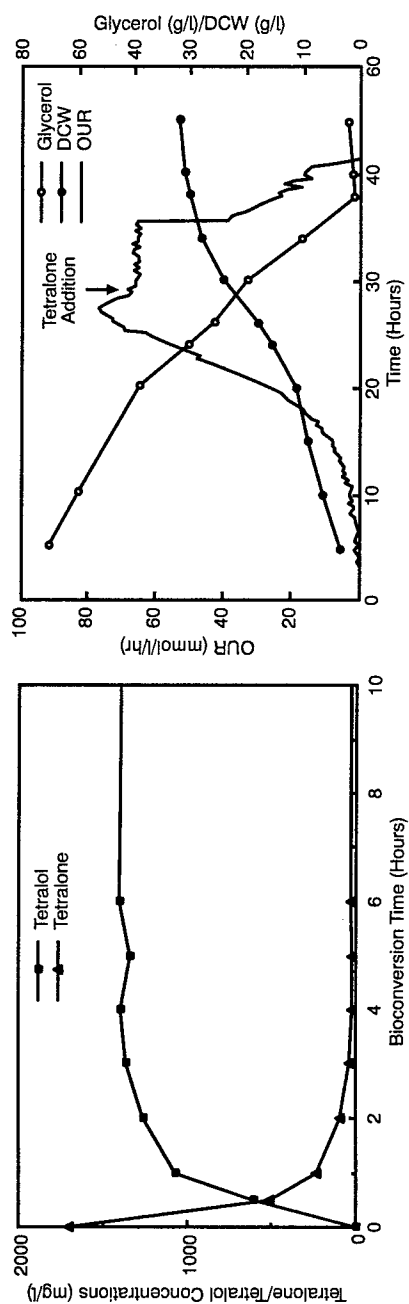
FIGURE 6. Asymmetric bioreduction of a β-tetralone to (*S*)-β-tetralol by *Trichosporon capitatum* MY 1890. OUR = oxygen uptake rate.

biocatalyst. An elevated optical purity of greater than 95% ee was achieved when employing cells that had not initiated the catabolism of glucose.[12] Upon development of a cultivation medium in which glucose had been replaced with glycerol, the production of (S)-tetralol with an enantiomeric excess greater than 99% was routinely achieved. This asymmetric bioreduction process was scaled up in laboratory bioreactors, yielding gram quantities of optically pure (S)-tetralol (ee > 99%) (FIGURE 6).

CONCLUSIONS

The application of asymmetric bioreduction for the production of precursors to novel pharmaceutical drugs proved to be an extremely valuable tool. In situations where chiral chemistry is not practical or not feasible, asymmetric bioreduction processes are able to meet the demand for preparative quantities of optically pure synthons. The key to a successful operation is a rapid turnaround time from project conception to the delivery of preparative amounts of purified chiral intermediate.

Microbial screening was able to supply suitable biocatalysts for the respective desired asymmetric bioreductions investigated here. The key to the success of the screening effort was the use of a well-diversified microbial library (broad range of species from well-diversified ecosystems) coupled with an efficient screening methodology. Interestingly, during most of these screening efforts, it was possible to identify microbial strains capable of carrying out the enantiocomplementary reaction.

As expected, process development studies yielded improvements in the rate and yield of bioreductions. It was also observed that the optical purity of the reduced compound could be dramatically influenced by the environmental conditions or by the physiological stage of the microbes. However, good understanding and control of the processes yielded products with elevated optical purity. Chemical evaluation of the chiral synthons produced by these asymmetric bioreduction processes demonstrated that these processes can be both practical and successful.

REFERENCES

1. ARIENS, E. 1993. Nonchiral, homochiral, and composite chiral drugs. TIBS **14:** 68–76.
2. RAUWS, A. & K. GROEN. 1994. Current regulatory (draft) guidance on chiral medicinal products: Canada, EEC, Japan, United States. Chirality **6:** 72–75.
3. STINSON, S. 1994. Chiral drugs. Chem. Eng. News **September:** 38–72.
4. JONES, B. 1986. Enzymes in organic synthesis. Tetrahedron **42:** 3351–3403.
5. KIESLICH, K. 1991. Biotransformations of industrial use. Acta Biotechnol. **11:** 559–570.
6. LILLY, M. 1994. Advances in biotransformation processes. Chem. Eng. Sci. **49:** 151–159.
7. CSUK, R. & B. GLANZER. 1991. Baker's yeast mediated transformations in organic chemistry. Chem. Rev. **91:** 49–97.
8. NAKAMURA, K., Y. KAWAI, T. KITAYAMA, T. MIYAI, M. OGAWA, Y. MIKATA, M. HIGAKI & A. OHNO. 1989. Asymmetric reduction of ketones with microbes. Bull. Inst. Chem. Res. Kyoto Univ. **67:** 157–168.
9. SERVI, S. 1990. Baker's yeast as a reagent in organic synthesis. Synthesis **1:** 1–25.
10. CHARTRAIN, M., J. ARMSTRONG, L. KATZ, J. KELLER, D. MATHRE & R. GREASHAM. 1995. Asymmetric bioreduction of a β-ketoester to (R)-hydroxyester by the fungus *Mortierella alpina* MF 5534. J. Ferment. Bioeng. **80:** 176–179.
11. KATZ, L., S. KING, R. GREASHAM & M. CHARTRAIN. 1995. Asymmetric bioreduction of a

ketosulfone to the corresponding _trans_-hydroxysulfone by the yeast _Rhodotorula rubra_ MY 2169. Enzyme Microb. Technol. In press.

12. REDDY, J., D. TSCHAEN, Y. J. SHI, V. PECORE, L. KATZ, R. GREASHAM & M. CHARTRAIN. 1996. Asymmetric bioreduction of a β-tetralone to its corresponding (_S_)-alcohol by the yeast _Trichosporon capitatum_ MY 1890. J. Ferment. Bioeng. **81:** 304–309.

13. BALDWIN, J., G. PONTICELLO & M. CHRISRY. 1989. Thieno thiopyran sulfamide derivatives: pharmaceutical composition and use. United States patent no. 4,797,413.

14. LYNCH, J., A. WALLACE, R. STUPIENSKI, E. BASKIN, C. BEARE, S. APPLEBY, J. SALATA, N. JURKIEWICZ, M. SANGUINETTI, R. STEIN, J. GEHRET, T. KOTHSTEIN, D. CLAREMON, J. ELLIOTT, J. BUTCHER, D. REMY & J. BALDWIN. 1994. Cardiac electrophysiologic and antiarrhythmic actions of two long-acting spirobenzopyran piperidine class-III agents, L-702,958 and L-706,000 [MK-499]. J. Pharmacol. Exp. Ther. **269:** 541–554.

15. TSCHAEN, D., L. ABRAMSON, D. CAI, R. DESMOND, U. DOLLING, L. FREY, S. KARADY, Y. J. SHI & T. VERHOEVEN. 1995. Asymmetric synthesis of MK-0499. J. Org. Chem. **60:** 4324–4330.

16. NAKAGAWA, S., T. HASHIZUME, K. MATSUDA, M. SANADA, O. OKAMOTO, H. FUKATSU & N. TANAKA. 1993. _In vitro_ activity of a new carbapenem antibiotic, BO 2727, with potent antipseudomonal activity. Antimicrob. Agents Chemother. **37:** 2756–2759.

17. HUNT, J., A. CARTER, J. MURRELL, H. DALTON, K. HALLINAN, D. CROUT, R. HOLT & J. CROSBY. 1995. Yeast-catalyzed reduction of β-ketoesters: (1) factors affecting whole-cell catalytic activity and stereoselectivity. Biocatal. Biotransform. **12:** 159–178.

18. USHIO, K., K. INOUYE, K. NAKAMURA, S. OKA & A. OHNO. 1986. Stereochemical control in microbial reduction: (4) effect of cultivation conditions on the reduction of β-keto esters by methylotrophic yeasts. Tetrahedron Lett. **27:** 2657–2660.

Practical Enzymatic Resolution of Racemic Alcohols and Amines in Organic Solvents[a]

ARIE L. GUTMAN, ELEONORA SHKOLNIK,
ELAZAR MEYER, FELIX POLYAK, DOV BRENNER,
AND AVIV BOLTANSKI

Department of Chemistry
Israel Institute of Technology
Technion City
Haifa 32,000, Israel

INTRODUCTION

One of the most important properties of enzymes is their ability to catalyze reactions in a stereoselective manner. This has been used for many years by organic chemists, who have exploited enzymes as catalysts in asymmetric synthesis and resolution for the preparation of optically pure compounds.[1] It is now well established that hydrolytic enzymes such as lipases, esterases, and proteases are highly stable in organic solvents and can be used for certain types of transformations that are difficult or impossible to carry out in water.[2] The most common reactions are lipase-catalyzed stereoselective esterifications and transesterifications, which have been extensively used for preparative kinetic resolutions of chiral acids and alcohols,[3] as well as for the synthesis of chiral lactones[4] and polyesters.[5] It has also been reported that some lipases and proteases are effective in catalyzing the reaction between carboxylic esters and amines in anhydrous organic solvents,[6] and these reactions have been recently used in intermolecular or intramolecular fashion for kinetic resolution of racemic amines[7] and for the synthesis of lactams.[8] In the present paper, we wish to report on novel applications of enzymes in organic solvents for the synthesis of chiral alcohols and amines with an emphasis on the development of large-scale processes useful for industrial production.

ENZYMATIC SYNTHESIS OF CHIRAL ALCOHOLS VIA ACYLATION IN ORGANIC SOLVENTS

Chiral secondary alcohols are common as intermediates and as valuable chiral auxiliaries in organic synthesis and are of great synthetic utility for the pharmaceutical and the fine-chemical industries. Unlike the chiral acids or amines, which can be resolved via diastereomeric crystallization of appropriate salts, alcohols do not form salts. Hence, chiral alcohols cannot be obtained easily by this direct method. It is

therefore not surprising that much effort has been devoted to the kinetic resolution of racemic secondary alcohols via enzymatic acylation in organic solvents. The acylating agents included carboxylic acids, various activated and enol esters, or acyclic aliphatic acid anhydrides, and the enzymatic reactions amounted to conversion of one enantiomer of the alcohol (1) into an ester (2) with the other one remaining as the unreactive alcohol (3) (SCHEME 1). Separation of the unreacted alcohol (3) from the ester (2) (followed by hydrolysis of the latter) enabled the resolution of racemic mixtures into their enantiomers.

A major problem with this approach is the difficulty of separating the ester from the unreacted alcohol. In many cases, both have similar boiling points, making it impossible to separate them by distillation, and tedious chromatographic separation becomes necessary. This makes the procedure impractical for large-scale preparation.

We developed a principal solution to this problem by using succinic anhydride as an acylating agent.[9] The reaction depicted in SCHEME 2 was shown to be highly stereospecific with a whole range of secondary alcohols (4a–4e) using several commercially available lipase preparations. Particularly productive from the point of
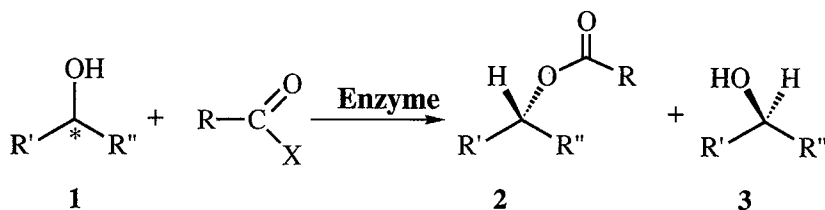
Scheme 1

view of enzyme efficiency and stereospecificity were the reactions with succinic anhydride catalyzed by the lipases, Amano P, Amano PS, and Amano Sam 2, in *tert*-butyl methyl ether. This enabled us to convert the (*R*)-enantiomer of the alcohol into the half-acid, which could be separated from the unreacted (*S*)-alcohol by simple extraction with aqueous base. The unreacted (*S*)-alcohol was recovered by evaporating the organic solution, whereas the (*R*)-enantiomer was obtained in quantitative yield by straightforward hydrolysis of the half-acid. This method was shown to be effective for the preparation of several pharmaceutically important alcohol intermediates with higher than 98% optical purity on a multikilo scale.

Reactions catalyzed by lipase Amano Sam 2 required only small quantities of enzyme and, in preparative experiments, we worked with a substrate:enzyme ratio of 100:3. Because the price of this enzyme is less than $1/gram, $30 worth of enzyme enabled us to carry out a reaction on 1 kg of *sec*-phenethyl alcohol (4e) to obtain 280 grams and 420 grams of the optically pure (*R*)- and (*S*)-enantiomers, respectively (see EXPERIMENTAL WORK below). This high substrate-to-enzyme ratio coupled with the extreme ease of separation between the reacted and unreacted enantiomers
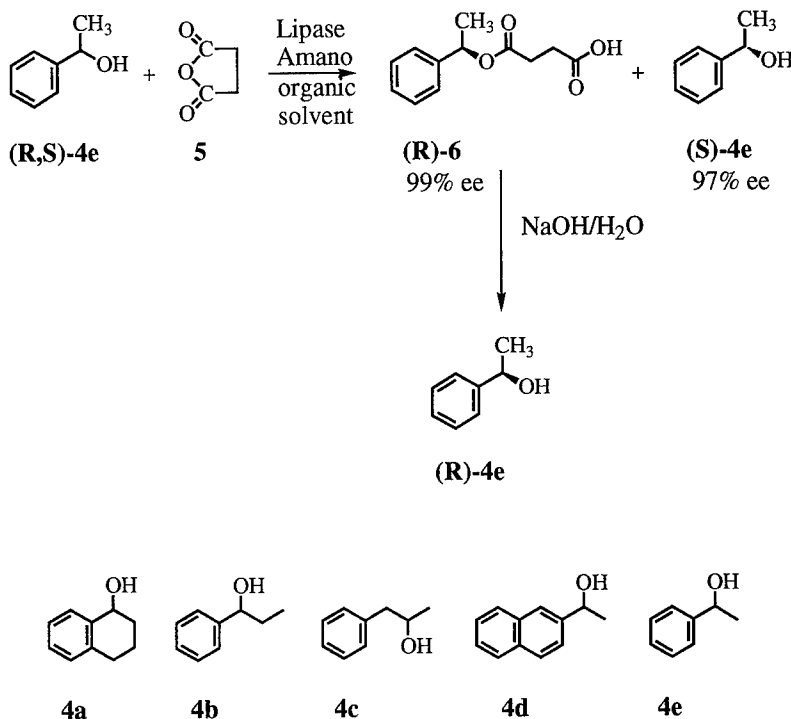
Scheme 2

make the economics of the process plausible for industrial preparation of various optically pure phenyl-alkyl and naphthyl-alkyl secondary alcohols.

Although this approach was useful for the preparation of several chiral secondary alcohols, it cannot apply to highly sterically hindered alcohols, such as 2,2,2-trifluoro-1-(9-anthryl)ethanol (7), which remained unreactive under all enzymatic acylation conditions tried. The inefficiency of enzymatic acylation of this alcohol can be explained by steric and electronic considerations affecting the mechanism of the enzymatic process. In the first step, an acyl-enzyme intermediate is formed between the enzyme and the acylating agent (step I, SCHEME 3). In the second (critical) step, the carbonyl of this intermediate has to undergo a nucleophilic attack by the alcohol oxygen of (7), which is accompanied by the breakup of the acyl-enzyme link, resulting in the release of the free enzyme and the formation of the desired ester. It is at this second stage, which is critical from the point of view of enantiodiscrimination, that the steric hindrance around the hydroxyl group plays a crucial role by blocking the approach of the nucleophile to the carbonyl that is positioned deep inside the enzyme pocket (SCHEME 3). The electronic effect of the CF$_3$ group, which strongly

reduces the nucleophilicity of the alcohol oxygen, is also responsible for the ineffi-ciency of step II.

To resolve this problem, we developed an alcoholysis approach, according to which the easily prepared racemic butyrate ester (8) is enzymatically reacted with butanol. In this case, enantiodiscrimination is exercised during the first enzymatic step and the reacting ester (and hence the released alcohol) is one enantiomer, whereas the other one is left behind as the unreactive ester. The second step along this route simply involves the breakup of the acyl-enzyme intermediate by an achiral nucleophile (butanol) and is of no stereochemical interest. According to this approach, the electron-withdrawing effect of the CF_3 group should help as it creates a better leaving group (SCHEME 4).

We exploited this approach for preparative purposes. Using crude porcine pancreatic lipase (PPL) immobilized on aluminum oxide in *n*-butanol, it was possible to conveniently carry out this reaction on a large scale and to obtain in one laboratory batch hundreds of grams of the (*R*)-alcohol and of the unreacted (*S*)-butyrate ester (SCHEME 5). After a facile separation procedure between the (*R*)-alcohol and the unreacted (*S*)-ester, the latter was hydrolyzed and both enantiomers of the alcohol were obtained.

The very high cost of the enantiomerically pure isomers of (7) ($33 for 100 mg from Aldrich Chemical) and its important analytical applications as chiral shift reagents and as key ingredients of stationary phases for chiral chromatography columns emphasize the practical usefulness of this enzymatic process. Furthermore, it was shown that the stability of PPL and the rate of the enzymatic reaction could be
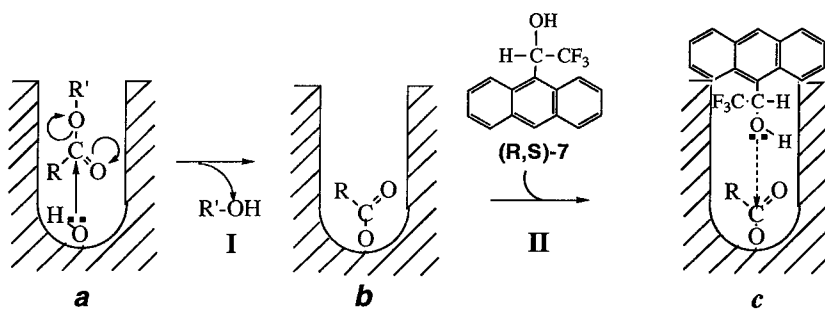
a - *formation of acyl-enzyme intermediate via nucleophilic attack of serine oxygen on the acylating agent;*
b - *acyl-enzyme intermediate;*
c - *sterically hindered interaction between acyl-enzyme and racemic alcohol.*

Scheme 3

(R,S) - 7

(R)-7

a - free enzyme;
b - acyl-enzyme intermediate.
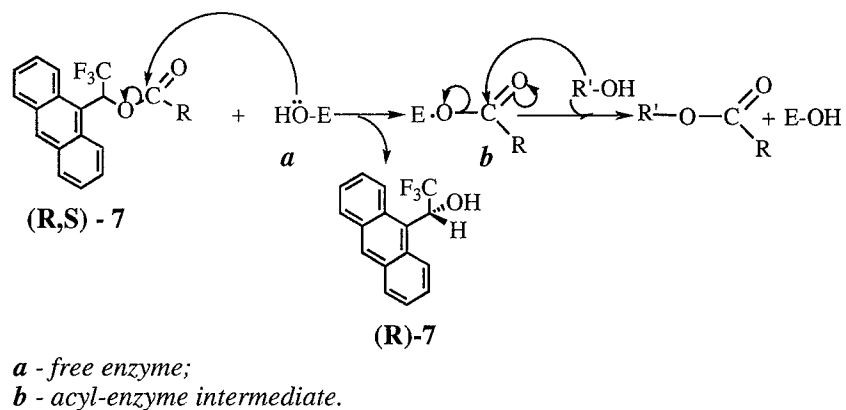
Scheme 4

enhanced considerably by simple dispersion of the enzyme on neutral aluminum oxide. The combination of an inexpensive and stable enzyme and of a relatively efficient reaction makes the economics of the process feasible for the practical preparation of this and other sterically hindered alcohols. Work in our laboratory is

(R,S) -8

(S)-8   **(R)-7**

(S)-7
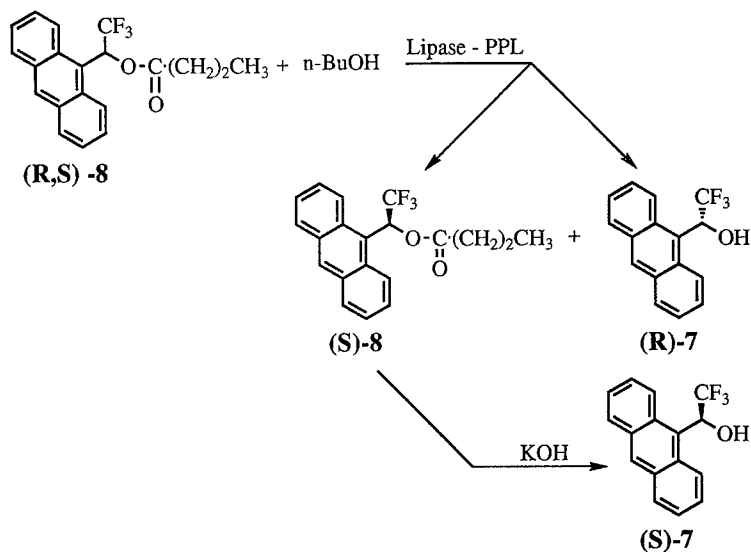
Scheme 5

currently under way to determine the generality of this approach to other sterically hindered alcohols.[10]

RESOLUTION OF RACEMIC AMINES VIA ENZYMATIC AMINOLYSIS IN ORGANIC SOLVENTS

Practical methods for the synthesis of chiral amines usually involve multistep transformations starting from chiral natural amino acids, or resolution of racemic mixtures via reaction with a chiral acid to form a diastereomeric mixture of salts, followed by consecutive fractional crystallizations and recovery of the amine. As an efficient alternative to these classical methods, we developed a facile large-scale continuous process for enzyme-catalyzed aminolysis in organic solvents that enabled us to prepare a whole range of optically active amines. We also addressed several technological aspects pertaining to enzyme immobilization and to development of a continuous enzymatic reactor.

(R)-9   **(R)-10**
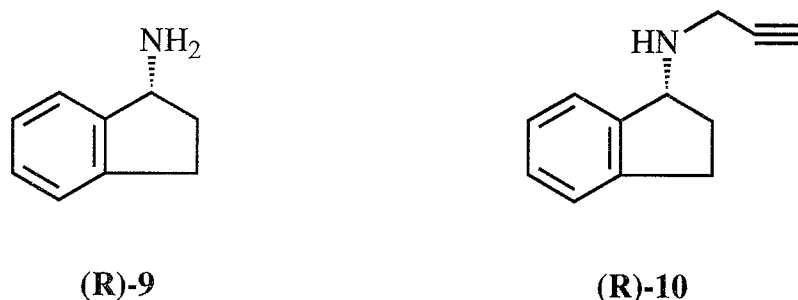
FIGURE 1. Structures (*R*-9) and (*R*-10).

Our target chiral amines included the pharmaceutically important intermediate, (*R*)-1-aminoindan (*R*-9) (see FIGURE 1). The latter is an immediate synthetic precursor of the heretofore unknown (*R*)-*N*-propargyl-1-aminoindan (PAI) (*R*-10) (see FIGURE 1), which was shown to be a potent irreversible inhibitor of the B form of monoamine oxidase and could therefore be used in the treatment of Parkinson's disease, memory disorders, dementia of the Alzheimer type, depression, and the hyperactive syndrome.[11] Recently, very considerable differences in MAO-B-inhibiting activity have been reported between the two enantiomers of PAI: it was shown that the (*R*)-(+) enantiomer is nearly four orders of magnitude more active than the (*S*)-(−) enantiomer.[12]

We found that certain enzymes catalyzed the stereoselective aminolysis reaction of the racemic 1-aminoindan (9) with esters, in particular, with the active ester 2,2,2-trifluoroethyl butyrate, in various organic solvents. The (*S*)-enantiomer of
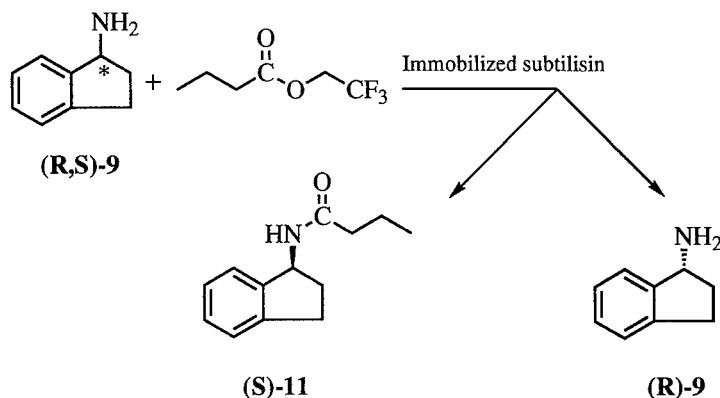
Scheme 6

1-aminoindan reacted in preference to give the corresponding amide (12), whereas the (R)-enantiomer remained as a free amine (SCHEME 6).

Unfortunately, the desired stereospecific enzymatic reaction was accompanied by a significant nonenzymatic reaction between the active ester and amine. Because the latter reaction undermined the stereospecificity of the enzymatic reaction, it was important to slow it down. This could be done by an appropriate choice of solvent and by shortening the time of contact between the amine and active ester. When *tert*-amyl alcohol or 3-methyl-3-pentanol was used as solvent, the nonenzymatic reaction is slowest. Furthermore, we succeeded in reducing the time of contact between the reaction components by performing the reaction in a continuous flow reactor with noncovalently immobilized enzyme (FIGURE 2).[13]

A slurry of the immobilized enzyme in 3-methyl-3-pentanol was packed onto a gravitational column equipped with a water jacket for temperature control. Solutions of 1-aminoindan and of 2,2,2-trifluoroethyl butyrate in 3-methyl-3-pentanol were delivered to the mouth of the column in parallel, through separate channels of a dual-piston pump, and the mixing took place just before loading onto the column. The enzymatic aminolysis reaction took place on the column and the eluant was allowed to drip directly into a solution of aqueous hydrochloric acid; this immediately converted the unreacted (R)-1-aminoindan to its hydrochloride and thus prevented any possibility of further nonenzymatic reaction between the chiral (9) and the remaining active ester.

The extent of the enzymatic reaction and of the optical purity of the desired (R)-aminoindan is a function of several parameters: (a) the flow rate through the column, which determines the time of contact between the reactants and the enzyme; (b) concentrations of the reactants, 1-aminoindan and 2,2,2-trifluoroethyl butyrate; (c) temperature; and (d) the content of water in the solvent. All these parameters are easily controlled and they were modified while periodically monitoring the optical purity of the eluting amine by HPLC on a chiral column. At steady-state operating conditions, a column constructed with 3.7 g of subtilisin on 370 g of glass beads

operated continuously for 95 hours at 36 °C to elute 330 g of racemic (9) and to give, in 40% yield, (R)-1-aminoindan of optical purity higher than 98%. In this continuous flow procedure, the enzyme-to-substrate ratio was 1:90. Furthermore, it is important to note that at the end of the process the immobilized enzyme was "clean" of any contaminants and its activity was only very slightly lower than at the beginning. Clearly, it could be used to resolve further quantities of 1-aminoindan. To check the lifetime of the immobilized subtilisin in a packed column, a small column was constructed and used approximately once a month over a period of 10 months to resolve a small quantity of the reactants. After each experiment, the column was washed with 3-methyl-3-pentanol and left "wet" with solvent at room temperature until the next run. The performance of this column was assessed on the basis of optical purity of the eluting (R)-1-aminoindan, and it was revealed that no detectable loss of enzymatic activity occurred on the column after 10 months of such intermittent operation and storage.

The enzymatic process described in this work may be used as a general method for the resolution of chiral primary amines. It can be readily scaled up for industrial application because it is highly efficient, yields optically pure (R)-amines, and withstands long-term operation. The high substrate-to-enzyme ratios and the possibility for efficient recycling of the solvent and active ester make the economics of the process plausible. The method, therefore, represents a valid alternative to the classical chemical resolutions of amines and it should be particularly useful in cases where resolution via diastereomeric crystallizations is not readily accomplished.
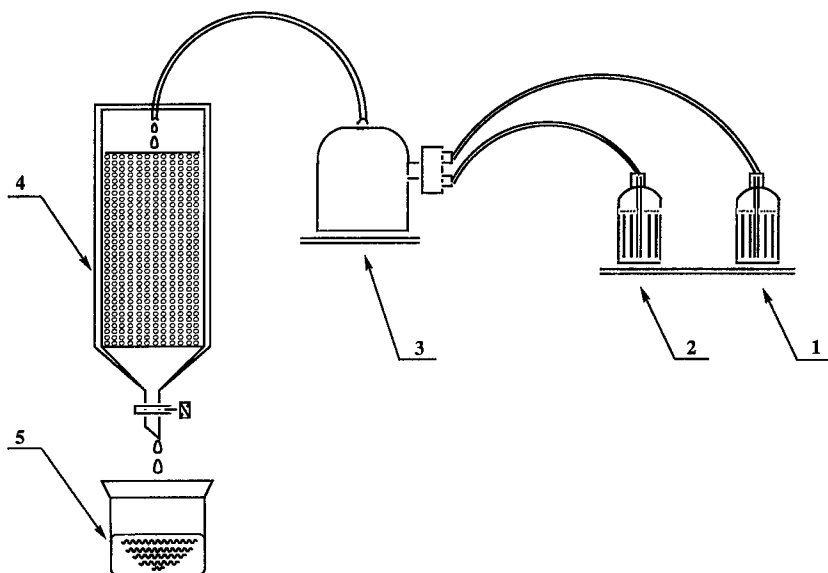
FIGURE 2. Continuous enzymatic reactor: (1) solution of active ester; (2) solution of amine; (3) dual-piston pump; (4) column-packed subtilisin immobilized on glass beads; (5) stirred solution of aqueous hydrochloric acid.

EXPERIMENTAL WORK

General Methods

^{1}H-NMR spectra were recorded on a Bruker AM 200-MHz spectrometer in CdCl$_3$. All chemical shifts were reported in ppm with tetramethylsilane as the internal standard. Enantiomeric excess (ee) for the chiral alcohols was determined by Merck Hitachi HPLC on a chiral column (Chiralcel OJ, Daicel) with a mixture of hexane and 2-propanol (95:5) as the mobile phase at a flow rate of 0.9 mL/min, using detection at 258 nm. Enantiomeric excess for the chiral amines was determined on a chiral column [Crownpak CR(+), 4 × 150 mm (Daicel)] eluting with a mixture of 15% methanol and 85% perchloric acid (pH 2) at a flow rate of 1.3 mL/min, with detection at 222 nm. Optical rotations were determined on a JASCO digital polarimeter, DIP-370. Column chromatography and "filtration through silica" were performed on silica gel kieselgel 40, 0.063–0.200 mm (E. Merck). Solvent extracts of aqueous solutions were dried over anhydrous Na$_2$SO$_4$. Solutions were concentrated under reduced pressure on a rotary evaporator. Chemical purity of substrates and products was determined either by HPLC as described above or by HP 5890 Series II GC on a DB-210 column. Freeze-drying was performed on a 1-L LYPH-LOCK Labconco lyophilizer. Determinations of water in organic solvents and in immobilized enzyme preparations were performed using the Karl-Fischer method on a Metrohm titration instrument consisting of dosimat Model 665 and processor Model 678 EP/KF.

The lipases, Amano PS and Amano Sam 2, were purchased from Amano Pharmaceutical. Porcine pancreatic lipase (PPL) was purchased from Sigma Chemical. Subtilisin A (batch A-4008-75) was kindly provided by Novo Nordisk, A/S Denmark. Aluminum oxide (Al$_2$O$_3$) used for enzyme dispersion was Aluminum oxide 90 active neutral (E. Merck). Glass beads were acid-washed (<106 μm) and purchased from Sigma Chemical (G-4649). Unless otherwise stated, all solvents and other chemicals were obtained from commercial suppliers and were used without further purification.

Preparative Resolution of sec-Phenethyl Alcohol (4e)

One liter (1.01 kg) of sec-phenethyl alcohol (4e) in 5 liters of t-butyl methyl ether (TBME) was placed in a polyethylene wide-mouth bottle equipped with a powerful magnetic stirrer. To the solution were added 0.994 kg of succinic anhydride and 30 g of lipase SAM 2. A suspension was formed because succinic anhydride is poorly soluble in TBME and the enzyme is insoluble in this or other organic solvents. The suspension was stirred at room temperature and progress of the reaction was followed by NMR: (4e) has a quartet at 4.77 ppm corresponding to the benzylic hydrogen, whereas the quartet of this hydrogen in the product (6) appears at 5.90 ppm. Accurate integration of the appropriate signals enabled us to determine the ratio between starting material and product and thus determine the degree of conversion. After 38 hours, the enzymatic reaction reached 30.4% conversion and was stopped by filtering off the solids, which were washed with TBME, dried at room temperature in the air, and kept aside (to reuse the enzyme). The filtrates were

extracted with a 1 M solution of sodium carbonate (3 × 1 L) and with 1 L of water. The aqueous phase containing (6) was washed with TBME (2 × 600 mL) and then hydrolyzed by adding 300 g of sodium hydroxide and stirring for 6 hours at room temperature. Then, the basic aqueous solution was extracted with 3 × 500 mL dichloromethane; the organic phase was washed with water (500 mL), dried over Na_2SO_4, and evaporated; and the residue was distilled (98 °C/20 mmHg) to give 280 g of *R*-(+)-*sec*-phenethyl alcohol, $[\alpha]_D^{20} = +40.8°$ (neat). The ee of this alcohol was determined to be 98% by HPLC on a chiral column. The combined organic phases (which contained the unreacted *S*-enriched alcohol) were poured into the 10-L polyethylene wide-mouth bottle; the enzyme and the succinic anhydride recovered from the previous experiment, together with 15 g of fresh enzyme and 50 g of succinic anhydride, were added; and the suspension was stirred at room temperature. Periodically, aliquots were withdrawn and the increase in optical purity of the unreacted (*S*)-enantiomer was monitored by HPLC on the chiral column. The reaction was continued for 3 days until the complete disappearance of (*R*)-alcohol. The insoluble enzyme and succinic anhydride were then filtered off, the organic solution was washed with 1 M sodium carbonate (3 × 1 L), and the organic solvent was removed under reduced pressure. The residue was distilled (98 °C/20 mmHg) to give 420 g of (*S*)-(−)-*sec*-phenethyl alcohol, $[\alpha]_D^{20} = −42.7°$ (neat). The ee of this alcohol was determined to be 99.6%.

Preparation of Dispersed Porcine Pancreatic Lipase (PPL)

PPL (370 g) was added to neutral aluminum oxide (370 g) and thoroughly mixed in a stoppered Erlenmeyer flask by gentle inversions of the flask for about 15 minutes. The resultant homogeneous white powder was stored in the cold and used in the preparative enzymatic resolution experiments.

Preparative Resolution of (R,S)-2,2,2-Trifluoromethyl-1-(9-anthryl)ethanol (7) by Enzymatic Alcoholysis

(*R,S*)-2,2,2-Trifluoromethyl-1-(9-anthryl)ethyl butyrate (8) (370 g, 1.03 mol) was dissolved in 2.5 L of boiled *n*-butanol in a 5-L flat-bottom flask equipped with a powerful magnetic stirrer. The solution was cooled to 40 °C and 400 g of the dispersed PPL preparation (containing 200 g PPL) was added. The resultant suspension was vigorously stirred at 40 °C and the reaction progress was followed by periodically examining aliquots of the suspension by HPLC on the chiral column. Integration of the appropriate HPLC signals enabled us to determine the ratio between starting material and product, as well as their optical purity. Thus, both the reaction rate and the ee values of the remaining ester and formed alcohol were followed simultaneously during the course of the reaction. On the fourth day of the reaction, an additional 340 g of the dispersed enzyme and 500 mL of butanol were added and the reaction was continued for another 6 days (altogether 10 days). After 9 days, it was observed that the reaction came to a virtual standstill at 47% conversion, at which point the remaining (*S*)-ester had an enantiomeric excess value of ee = 98.3% and the resultant alcohol had ee = 96.5%. The butanol solution was

filtered off, the solid dispersed PPL was washed with 5 L of hot acetone, and the combined filtrates were evaporated at reduced pressure to remove most of the acetone. To the remaining butanol solution, hexane (350 mL) was added and evaporated to remove azeotropically part of the butanol. This operation was repeated four times and most of the butanol was removed in this way. An additional 500 mL of hexane was then added to the remaining butanol solution, and the new solution was left overnight at -15 °C. Crystallization occurred and the precipitate was filtered off and washed with hexane to give the crystalline alcohol (R-7) (55 g, 39%), with ee = 100%. The mother liquor was evaporated to dryness to give 281 g of light-brown oily residue containing the ester (S-8) and the alcohol (R-7) at a ratio of approximately 2.5:1. This was mixed with 250 g of silica gel in 400 mL of hexane and partially evaporated until a thick brown slurry was obtained. The slurry was placed onto a 300-g silica gel column and eluted with hexane. TLC and HPLC examination indicated that the eluant (7 L) contained only the ester (S-8). After all the ester was eluted, the column was washed with diethyl ether (1.5 L) to remove the alcohol (R-7). Evaporation of the hexane fractions resulted in the crude ester (S-8), which was crystallized from ethanol to give (S)-2,2,2-trifluoromethyl-1-(9-anthryl)ethyl butyrate (S-8) (171 g, 92%), as white crystalline powder. The ee of the ester as determined by HPLC was 99.2%. Evaporation of the ether fractions resulted in the crude alcohol (R-7), which was washed with hexane to give (R)-2,2,2-trifluoromethyl-1-(9-anthryl)ethanol (R-7) (62 g, 43%). Together with the first crop, 117 g of alcohol (R-7) was obtained (yield of 82%) with an optical purity of ee = 99.4% by HPLC, $[\alpha]_D^{20} = -32°$ (c = 6, CHCl$_3$).

Hydrolysis of (S-8)

To a solution of the ester (S-8) (171 g, 0.475 mol) in 600 mL of methanol was added KOH (27 g, 0.49 mol) in 60 mL of water and the mixture was stirred at room temperature for 1 h. Water (400 mL) was then added, forming a white suspension that was stirred for another 1 h and filtered to afford white precipitate, which was dried and washed with hexane to give a white crystalline powder of (S-7) (130 g, 99%). Optical purity of ee = 99% was obtained by HPLC, $[\alpha]_D^{20} = +32.5°$ (c = 6, CHCl$_3$).

Preparation of Immobilized Subtilisin and Packing of the Column

First, 3.7 g of subtilisin A was dissolved in 130 mL of 0.1 M phosphate buffer (pH 7.8) and the solution was mixed with 370 g of glass beads (Sigma, G-4649, acid-washed, <106 microns). The slurry was then gently stirred and freeze-dried to constant weight during 24 h. The resultant solid material was crushed to a thin powder, which was suspended in 3-methyl-3-pentanol to a thin slurry, and that slurry was loaded onto a gravitational column (3.8 cm × 56 cm) equipped with a jacket for maintenance of the desired temperature. When the slurry settled down, the packed support had a density of 1.25 g/mL and its dimensions were 26 × 3.8 cm (occupying volume of approximately 300 mL). In another experiment, 5.7 g of subtilisin immobilized on 570 g of glass beads was packed on the same reactor. In that case, the

volume of the support material was 450 mL and the dimensions of the packed reactor were 40 × 3.8 cm. The immobilized enzyme could be kept on the column with 3-methyl-3-pentanol for at least 10 months without any detectable deterioration.

Enzymatic Aminolysis of 1-Aminoindan (9)

The solution of 1-aminoindan (9) was prepared by mixing 318 mL (330 g, 2.5 mol) of the amine (*R,S*)-9 with 3174 mL of 3-methyl-3-pentanol (solution A). The solution of 2,2,2-trifluoroethyl butyrate was prepared by mixing 1330 mL (1443 g, 8.5 mol) of the active ester with 2160 mL of 3-methyl-3-pentanol (solution B). Solutions A and B were placed in glass bottles and each was connected with the top of the column (26 × 3.8 cm) (containing 3.7 g of subtilisin on 370 g of glass beads) by Teflon tubing through separate channels of a dual-piston pump, Gearmotor type NYC-1303, purchased from Bodine Electric (Chicago). The column was fitted with a water jacket for temperature control at 36 °C. The two solutions were fed into the column in parallel, each at a rate of 35 mL/h. The rate of outflow from the column was controlled by a valve at the bottom adjusted to maintain the outflow at about 70 mL/h, thus keeping the layer of the solution above the packed bed at levels not higher than 2–5 cm. This was intended to minimize the time of contact between the reactants before elution through the column. After 95 hours of continuous operation, the column was washed for a period of 10 hours with 3-methyl-3-pentanol at a flow rate of 70 mL/h. All the eluant from the column (approximately 7.5 L) was dripping into a reservoir containing a total of 2.5 L of 1 M hydrochloric acid, which was vigorously stirred to immediately convert the unreacted free (*R*)-amine (*R*-9) into the hydrochloride salt and to prevent any nonenzymatic reaction with remaining active ester after passage through the column. The acidic aqueous layer contained (*R*)-1-aminoindan hydrochloride. The layers were separated and the organic layer was distilled to leave a "cakelike" residue containing the amide (11) and some of the (*R*)-amine hydrochloride, which was moderately soluble in 3-methyl-3-pentanol. This "cake" was dissolved in a mixture of dichloromethane (1 L) and water (1 L) and the layers were separated. The dichloromethane layer was evaporated to give (*S*)-(−)-*N*-butyrylindanamide (11) (247 g, 49%). The aqueous layer containing the amine hydrochloride was combined with the original acidic aqueous layer and its HPLC on a chiral column showed an ee > 98%. To recover the free (*R*-9), water was evaporated, the hydrochloride salt was suspended in dichloromethane, and the suspension was treated with a solution of ammonia in dichloromethane. Ammonium chloride was filtered off and washed with dichloromethane, the solvent was evaporated, and the residue was distilled at 80 °C and 3 mmHg to give (*R*-9) (132 g, 40%).

CONCLUSIONS

This paper exemplified some applications of enzymatic catalysis to the preparative synthesis of chiral alcohols and amines required and used as pharmaceutical intermediates and chiral auxiliaries. It is clear that the methods can be scaled up and applied to commercial production of a wide variety of these and other chiral compounds.

REFERENCES

1. WONG, C-H. & G. M. WHITESIDES. 1994. Enzymes in Synthetic Organic Chemistry. First edition. Tetrahedron Organic Chemistry Series. Volume 12. Pergamon. Elmsford, New York.
2. (a) CHEN, C-S. & C. J. SIH. 1989. General aspects and optimization of enantioselective biocatalysis in organic solvents: the use of lipases. Angew. Chem. Int. Ed. Engl. **28:** 695–707; (b) KLIBANOV, A. M. 1990. Asymmetric transformations catalyzed by enzymes in organic solvents. Acc. Chem. Res. **23:** 114–120; (c) GUTMAN, A. L. & M. SHAPIRA. 1995. Synthetic applications of enzymatic reactions in organic solvents. *In* Advances in Biochemical Engineering/Biotechnology. Volume 52. Springer-Verlag. Berlin/New York.
3. (a) KIRCHNER, G., M. P. SCOLLAR & A. M. KLIBANOV. 1985. Resolution of racemic mixtures via lipase catalysis in organic solvents. J. Am. Chem. Soc. **107:** 7072–7076; (b) for recent reviews, also see reference 2c above.
4. (a) GUTMAN, A. L., K. ZUOBI & A. BOLTANSKI. 1987. Enzymatic lactonization of γ-hydroxyesters in organic solvents: synthesis of optically pure γ-methylbutyrolactone and γ-phenylbutyrolactone. Tetrahedron Lett. **28:** 3861–3864; (b) MAKITA, A., T. NIHIRA & Y. YAMADA. 1987. Lipase-catalyzed synthesis of macrocyclic lactones in organic solvents. Tetrahedron Lett. **28:** 805–808; (c) GUO, Z-W. & C. J. SIH. 1988. Enzymatic synthesis of macrocyclic lactones. J. Am. Chem. Soc. **110:** 1999–2001; (d) GUO, Z-W., T. K. NGOOI, A. SCILIMATI, G. FULLING & C. J. SIH. 1988. Macrocyclic lactones via biocatalysis in non-aqueous media. Tetrahedron Lett. **29:** 5583–5586; (e) GUTMAN, A. L. & T. BRAVDO. 1989. Enzyme-catalyzed enantioconvergent lactonization of γ-hydroxy diesters in organic solvents. J. Org. Chem. **54:** 4263–4265; (f) GUTMAN, A. L., K. ZUOBI & T. BRAVDO. 1990. Lipase-catalyzed preparation of optically active γ-butyrolactones in organic solvents. J. Org. Chem. **55:** 3546–3552.
5. (a) GUTMAN, A. L., D. OREN, A. BOLTANSKI & T. BRAVDO. 1987. Enzymatic oligomerization versus lactonization of ω-hydroxyesters. Tetrahedron Lett. **28:** 5367–5368; (b) MARGOLIN, A. L., J-Y. CRENNE & A. M. KLIBANOV. 1987. Stereoselective oligomerizations catalyzed by lipases in organic solvents. Tetrahedron Lett. **28:** 1607–1610; (c) WALLACE, J. S. & C. J. MORROW. 1989. Biocatalytic synthesis of polymers: synthesis of an optically active, epoxy-substituted polyester by lipase-catalyzed polymerization. J. Polym. Sci. Part A **27:** 2553–2567; (d) GUTMAN, A. L. & T. BRAVDO. 1989. Enzyme-catalyzed enantioconvergent polymerization of β-hydroxyglutarate in organic solvents. J. Org. Chem. **54:** 5645–5646; (e) KNANI, D., A. L. GUTMAN & D. KOHN. 1993. Enzymatic polyesterification in organic media: enzyme-catalyzed synthesis of linear polyesters. J. Polym. Sci. Part A **31:** 1221–1232.
6. ZAKS, A. & A. M. KLIBANOV. 1985. Enzyme-catalyzed processes in organic solvents. Proc. Natl. Acad. Sci. U.S.A. **82:** 3192–3196.
7. KITAGUCHI, H., P. A. FITZPATRICK, J. E. HUBER & A. M. KLIBANOV. 1989. Enzymatic resolution of racemic amines: crucial role of the solvent. J. Am. Chem. Soc. **111:** 3094–3095.
8. GUTMAN, A. L., E. MEYER, X. YUE & C. ABELL. 1992. Enzymatic formation of lactams in organic solvents. Tetrahedron Lett. **33:** 3943–3946.
9. GUTMAN, A. L., D. BRENNER & A. BOLTANSKI. 1993. Convenient practical resolution of racemic alkyl-aryl alcohols via enzymatic acylation with succinic anhydride in organic solvents. Tetrahedron Asymmetry **4:** 839–844.
10. SHKOLNIK, E. & A. L. GUTMAN. 1994. Resolution of racemic sterically hindered secondary alcohols via enzymatic alcoholysis of their esters: the first enzymatic preparation of optically pure 2,2,2-trifluoro-1-(9-anthryl)ethanol. J. Bioorg. Med. Chem. **2:** 567–572.
11. YOUDIM, M. B. H., J. P. FINBERG & K. F. TIPTON. 1988. Monoiminooxidases. *In* Handbook of Experimental Pharmacology. Volume 90/I, chapter 3, p. 121–197. Springer-Verlag. Berlin/New York.
12. YOUDIM, M. B. H., J. P. M. FINBERG, R. LEVY, J. STERLING, D. LERNER & T. BERGER-PASKIN. 1991. European patent application no. 91100081.8.
13. GUTMAN, A. L., E. MEYER, E. KALERIN, F. POLYAK & J. STERLING. 1992. Enzymatic resolution of racemic amines in a continuous reactor in organic solvents. Biotechnol. Bioeng. **40:** 760–767.

Enzymatic Production
of α-Butylglucoside and Its Fatty
Acid Esters

PIERRE F. MONSAN,[a,b] FRANÇOIS PAUL,[b,c]
VINCENT PELENC,[b] AND EMMANUEL BOURES[d]

aCentre de Bioingénierie Gilbert Durand
UMR 5504–LA INRA
Institut National des Sciences Appliquées de Toulouse
Complexe Scientifique de Rangueil
31077 Toulouse Cedex, France

bBioEurope
31031 Toulouse Cedex, France

dULICE (Groupe Limagrain)
63204 Riom Cedex, France

INTRODUCTION

Due to environmental concern, the interest of biodegradable surfactants has importantly increased during the past years. This has resulted in the industrial development of new processes for surfactant production. Particularly, corn starch, which is a renewable raw material, can be used as a source of hydrophilic moieties to synthesize alkyl polyglucoside surfactants by reaction with fatty alcohols.[1,2] This chemical synthesis allows the production of a variety of surfactants of interest for application in the detergent industry.[3,4]

The synthesis of alkylglycosides can also be obtained using enzymes as catalysts through transglucosylation or reverse-hydrolysis reactions involving alcohols as acceptors.[5–9] The obtention of β-alkylglucosides, for example, is catalyzed by almond β-glucosidase operated in nonconventional conditions.[7–9]

In addition, the enzyme-catalyzed esterification of chemically synthesized alkyl-glucosides allows one to obtain a variety of nonionic surfactants of controlled hydrophilic/lipophilic balance (HLB).[10–15] As such nonionic surfactants are of interest for cosmetic and personal-care applications,[16] it is worth developing a totally enzymatic process for the production of this type of surfactant.

For this purpose, we have developed a two-step enzymatic process[17] consisting of (i) the enzymatic synthesis of α-butylglucoside (α-BG) from a starch hydrolysate catalyzed by the α-transglucosidase from *Aspergillus* sp. operated in a two-phase system and (ii) the lipase-catalyzed esterification of α-BG to obtain a mixture of monoester and diester derivatives (FIGURE 1).

cPresent address: Centre Européen de Bioprospective, Centre de Bioingénierie Gilbert Durand 3, I.N.S.A. Complexe Scientifique de Rangueil, 31077 Toulouse Cedex, France.

MATERIALS AND METHODS

Enzymes and Substrates

α-Transglucosidase was purchased from Amano (Japan). The enzymatic activity of the commercial liquid preparation, Transglucosidase L, is 2000 units/mL. One unit corresponds to the production of one micromole of glucose per hour at 40 °C and pH 5.0 from 50 g/L maltose (assayed by HPLC analysis). Glucosyl donors were maltodextrins (Glucidex® 12) and a maltose-rich glucose syrup (Flolys D 5780 S), both from Roquette Freres (France). *n*-Butanol was purchased from Docks Des Alcools (France).

Lipases were from Novo Nordisk Bioindustrie (Denmark). Two immobilized preparations were used: Novozym 435, lipase from *C. antarctica*; and Lipozyme®, lipase from *M. miehei*. Capric acid (Prifrac® 2906) was from Unichema France (France) and coconut fatty acids (cosmetic grade) were from Stearinerie Dubois Fils (France).
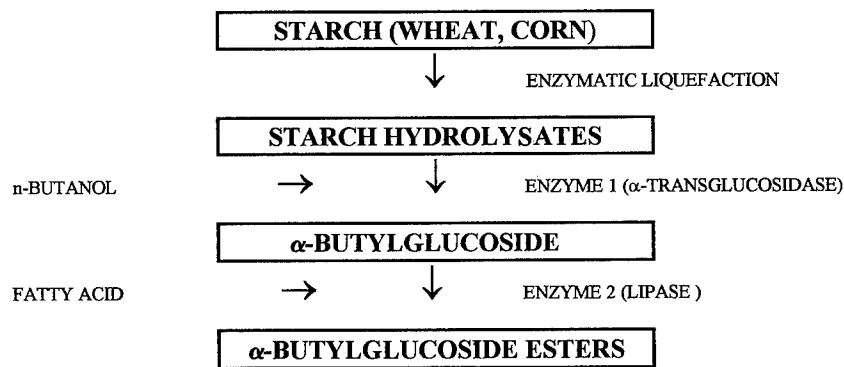
FIGURE 1. Scheme of the enzymatic process for the synthesis of α-BG esters.

α-BG Synthesis: Batch Assays

The influence of the organic phase volume on the α-BG synthesis yield was studied under the following conditions:

- aqueous phase—volume: 10 mL; maltodextrins: 2 g; *n*-butanol: 0.9 mL (7%, w/w); transglucosidase activity was gradually increased with increased organic phase volume/aqueous phase volume ratio: ratio 0 and ratio 1, 10 U/mL; ratio 5, 50 U/mL; ratio 7.5, 75 U/mL; ratio 10, 100 U/mL; ratio 15, 150 U/mL; reaction mixtures were incubated at 40 °C and pH 5.0 under continuous stirring during 72 hours;
- organic phase—*n*-butanol saturated with water at 40 °C before addition to the aqueous phase.

α-BG analysis of both phases was performed by HPLC [column: Polypore H$^+$ (ALLTECH, France); eluant: 0.01 N sulfuric acid; flow rate: 0.5 mL/min; detection: refractive index].

α-BG Synthesis: Continuous Biphasic Reactor

The aqueous phase containing the α-transglucosidase enzyme (200 U/mL) saturated with *n*-butanol (6%, w/w) and the maltose-rich syrup [dry matter: 30% (w/w)] was essentially absorbed into calcium alginate beads (average bead diameter: 3 mm). This phase was put in a tubular reactor (final volume: 100 L). The organic phase [*n*-butanol containing 12% water (v/v)] was continuously pumped into the reactor at a flow rate of 15 L/hour. The outlet α-BG and glucose concentrations in the organic phase were 20 g/L and 8 g/L, respectively (corresponding to a mixture of 70% α-BG and 30% glucose). Operational temperature was 40 °C and pH was 5.0.

Ester Synthesis in Melted Reaction Mixtures

Ester synthesis catalyzed by Novozym 435—coconut fatty acids: 216 g; α-BG containing 4% glucose: 260 g (molar ratio of fatty acids/α-BG: 1.1); immobilized enzyme: 6% (w/w); reaction mixture was continuously stirred in an evaporator at 68 °C under a reduced pressure of 30 mbar.

Ester synthesis catalyzed by Lipozyme®—capric acid: 34 g; α-BG: 37 g (molar ratio of capric acid/α-BG: 1.3); immobilized enzyme: 5% (w/w); reaction mixture was continuously stirred in an evaporator at 65 °C under a reduced pressure of 30 mbar.

The reaction mixtures were analyzed by HPLC [gel filtration column: Jordy Gel 100 Å (ALLTECH, France); eluant: tetrahydrofuran; flow rate: 1.0 mL/min; detection: refractive index].

RESULTS AND DISCUSSION

Enzymatic Production of α-Butylglucoside (α-BG)

The synthesis of α-BG is catalyzed by the α-transglucosidase enzyme from *Aspergillus* sp. (EC 2.4.1.24) using maltose as the D-glucosyl donor and *n*-butanol as the acceptor:

$$\text{maltose} + n\text{-butanol} \xrightarrow{\text{α-transglucosidase}} \text{α-D-butylglucoside} + \text{glucose.}$$
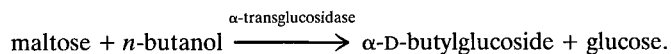
The α-transglucosidase activity was detected in extracts from *A. oryzae*[18] and *A. niger*.[19] It accepts a wide variety of D-glucosyl donors—starch hydrolysates, maltose, and (to some degree) α-alkylglucosides—and can be used to prepare glucosyl-oligosaccharides with various glucosidic linkages.[20] D-Glucose cannot be used as a donor in the reaction. Short aliphatic chain alcohols are acceptors,[21] as well as polyols[22] and steroidal alcohols.[21]

The reaction catalyzed with α-transglucosidase stereospecifically yields the α-anomer of butyl-D-glucoside without any significant presence of the β-anomer. This is a key feature of the enzymatic reaction, as chemical butanolysis of starch gives a mixture of α- and β-anomers. The chemical synthesis of pure α-BG is possible, but can be obtained only by an α-transglucosylation reaction using α-methylglucoside as the starting material.[23]

As α-BG is also a substrate for the α-transglucosidase enzyme, the reaction rapidly reaches an equilibrium position when operated in a monophasic aqueous system. The corresponding conversion yield is only 5%. In view of operating an efficient synthesis process, it is thus necessary to remove the α-BG from the reaction medium. For this purpose, it is possible to continuously extract α-BG in a butanol-rich phase, as butanol is only slightly soluble in water, and a biphasic system is obtained above 9% (v/v) butanol added to the reaction mixture.

As the nonmiscible butanol phase is saturated with water, a partition coefficient $K_{\alpha BG}$ (defined as the ratio of the α-BG concentration in the organic phase to the α-BG concentration in the aqueous phase) equal to 1.05 at 40 °C is obtained. D-Glucose is only slightly soluble in the butanol phase ($K_{glucose} = 0.025$), whereas higher oligosaccharides are not soluble at all.

In fact, increasing the ratio of the butanol phase to the aqueous phase results in a linear increase of the efficiency of the reaction (FIGURE 2). It can thus be envisaged to operate the α-transglucosidase enzyme in a continuous biphasic reactor.

At this level, the stability of the enzyme is a key problem. It can be seen from FIGURE 3 that an aqueous phase containing sugars [Flolys D 5780 S: 30% (w/w)] and
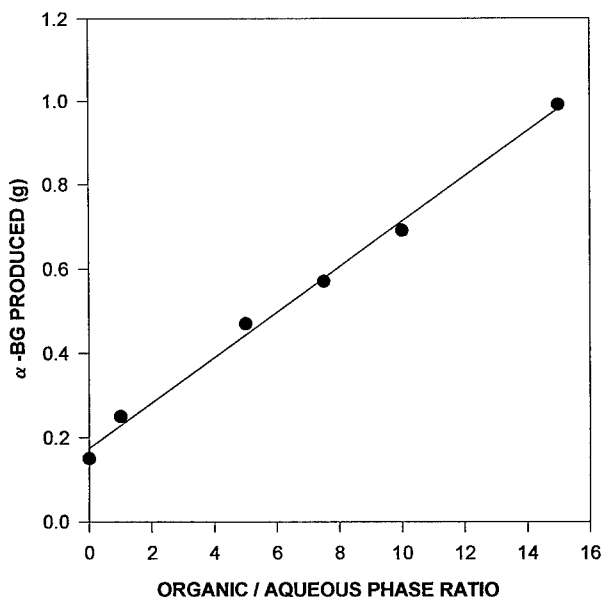
FIGURE 2. Influence of the organic phase volume on the α-BG synthesis yield. Experimental conditions are described in the text.
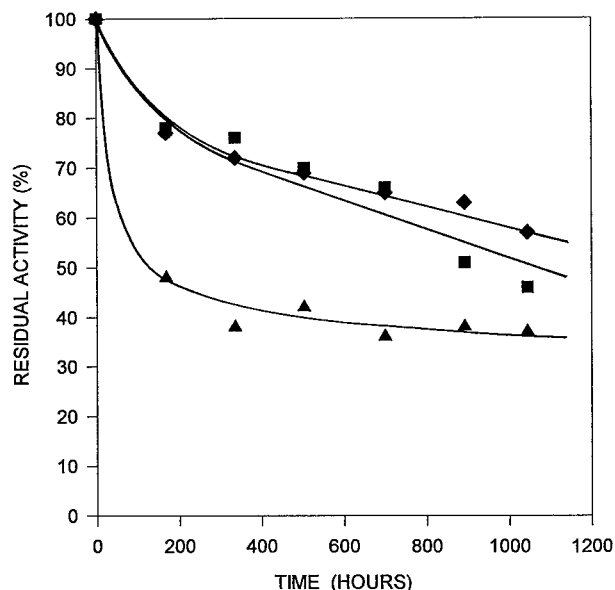
FIGURE 3. Long-term stability of the α-transglucosidase from *Aspergillus* sp. in the presence of butanol at 40 °C: ◆, reaction mixture without butanol (control); ■, aqueous reaction mixture saturated with dissolved butanol; ▲, biphasic continuous reactor.

saturated with *n*-butanol has only a slightly increased denaturating effect on the α-transglucosidase, when compared to the same aqueous phase without *n*-butanol. On the contrary, the presence of a butanol/water interface, particularly important during the reactor preparation, results in an initial rapid inactivation of the enzyme (FIGURE 3). This phenomenon has been already well documented.[24]

This interfacial denaturation can be limited by entrapping the enzymatic aqueous phase into calcium alginate beads, which significantly stabilizes the enzyme during the reactor operation (FIGURE 3).

We have thus operated a continuous biphasic packed-bed reactor consisting of a calcium alginate–entrapped stationary aqueous phase and a mobile butanol organic phase circulated upwards through the aqueous phase. In addition, the calcium alginate beads allow a homogeneous distribution of the butanol phase in the reactor. This results in an efficient extraction of the α-BG from the aqueous phase into the butanol phase. In such operation conditions, the half-life of the enzyme is equal to 75 days at 40 °C. The reactor productivity is 1 g α-BG/h-L.

The D-glucose fraction present in the butanol phase at the reactor outlet is removed by continuous liquid-liquid extraction with demineralized water. A pilot-scale reactor has been developed with a 100-L enzyme reactor. The complete operation scheme is given in FIGURE 4, showing the recycling of butanol and glucose in the reactor. The final purity of the α-BG is above 95% (w/w). This product presents the very original characteristic of being highly soluble in water [up to 50% (w/w) at 25 °C] as well as in polar organic solvents [70% (w/w) in ethanol at 25 °C].

As a consequence, α-BG is an interesting D-glucosyl derivative for further chemical or enzymatic transformation in nonaqueous media. For example, α-BG is miscible with melted fatty acids above its melting point (64 °C), which has been used to synthesize its ester derivatives.

Enzymatic Production of α-BG Esters

FIGURES 5 and 6 illustrate the kinetics of ester synthesis from α-BG and various fatty acids in melted reaction mixtures (65 °C) under reduced pressure for the
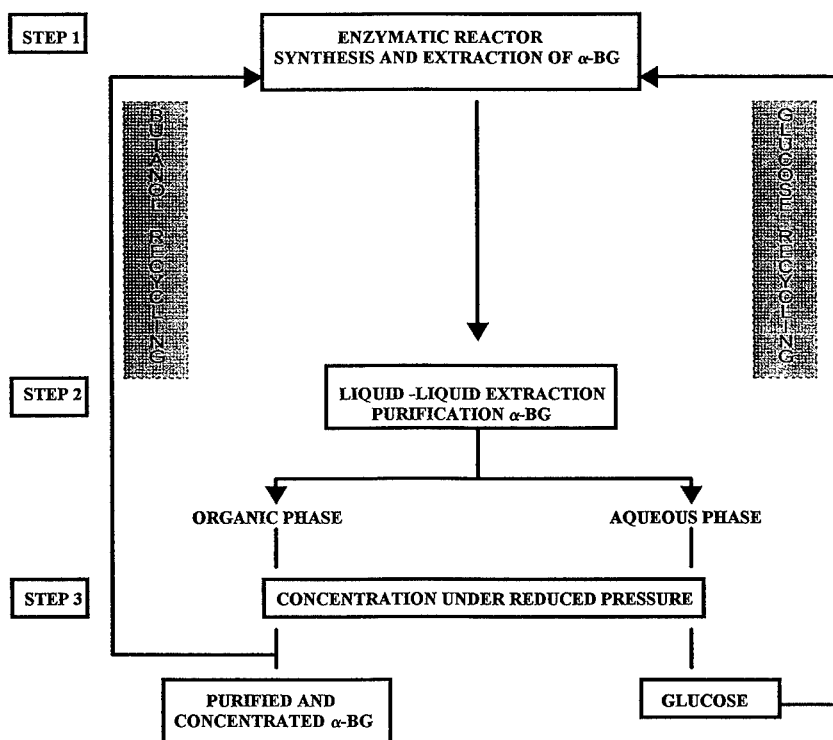
FIGURE 4. Scheme of the enzymatic production and purification of α-BG.

elimination of water produced. Two preparations of immobilized lipases were used: Novozym 435, lipase from *C. antarctica*, catalyzes only the synthesis of monoester (6-*O*-acylbutylglucoside); and Lipozyme®, lipase from *M. miehei*, catalyzes the synthesis of a mixture of monoester and diester (6-*O*-acylbutylglucoside and 2,6-*O*-diacylbutylglucoside). An ester synthesis yield above 80% can be obtained in these conditions after a 48-h incubation time.
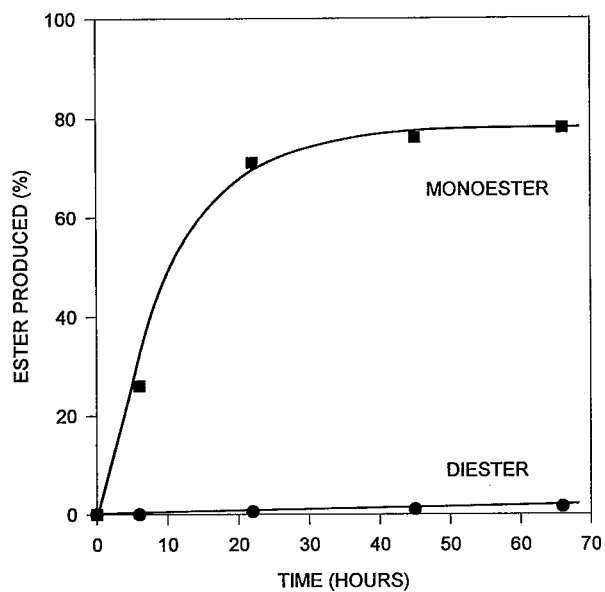
FIGURE 5. Kinetics of α-BG ester synthesis by the immobilized lipase from *C. antarctica* (Novozym 435): ■, monoesters; ●, diesters. Experimental conditions are described in the text.
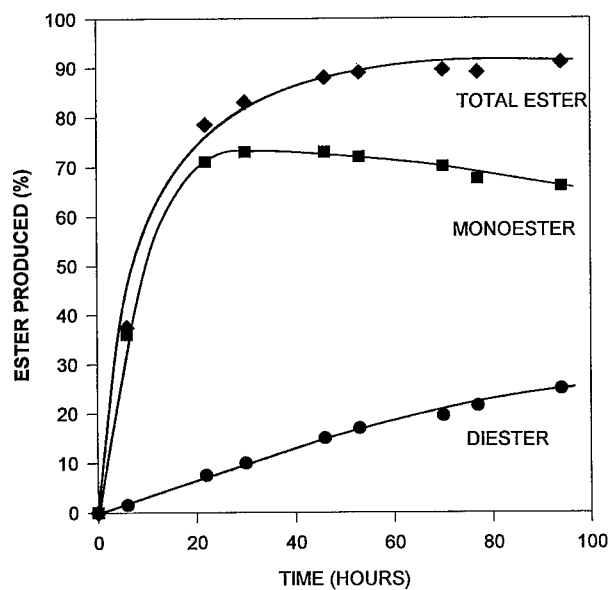
FIGURE 6. Kinetics of α-BG ester synthesis by the immobilized lipase from *M. miehei* (Lipozyme®): ◆, total esters; ■, monoesters; ●, diesters. Experimental conditions are described in the text.

By varying the type of fatty acids and the molar ratio between fatty acids and α-BG, a range of esters of various HLB is obtained, from 4.5 [mixture of monoester (75%) and diester (25%) of palmitic acid] up to 10 (monoester of capric acid). α-BG esters are currently under evaluation in the cosmetic field as a new category of mild, highly biodegradable nonionic emulsifiers.

CONCLUSIONS

The operation of fungal α-transglucosidase in a continuous biphasic reactor results in an efficient stereoselective synthesis of α-butylglucoside from maltose-rich starch hydrolysate and n-butanol. Butanol acts both as a substrate and as a solvent for the continuous extraction of α-butylglucoside, which allows for the dramatic increase of the reaction yield.

Due to its specific solubility both in water and in polar organic solvents, α-butylglucoside has proved to be a very interesting intermediate for further chemical or enzymatic modification. Particularly, its miscibility with fatty acids in melted reaction mixtures makes possible its efficient esterification catalyzed with immobilized lipases. The corresponding ester derivatives are under industrial development as biodegradable cosmetic emulsifiers, in particular, for nanoemulsion stabilization and liquid crystal formation.

REFERENCES

1. PUTNIK, C. F. & N. F. BORYS. 1986. Alkyl polyglycosides. Soap Cosmet. Chem. Spec. **6:** 34–37.
2. SCHULZ, P. 1992. Chemistry and technology of alkylglycosides. Chim. Oggi **8/9:** 33–38.
3. SALKA, B. 1993. Alkyl polyglycosides: properties and applications. Cosmet. Toilet. **108**(3): 89–94.
4. KNAUT, J. & G. KREIENFELD. 1993. Alkyl polyglycosides: a new surfactant class based on renewable raw material. Chim. Oggi **9:** 41–46.
5. SUGAWARA, S., Y. NAKAMURA & T. SHIMOMURA. 1960. Transglucosidation action of crystalline mold maltase. Part I. Transfer of glucose from α-heteroside to alcohols and sugars. Bull. Agric. Chem. Soc. Jpn. **24**(3): 278–280.
6. PAZUR, J. H. & T. ANDO. 1961. The isolation and the mode of action of a fungal transglucosylase. Arch. Biochem. Biophys. **93:** 43–49.
7. VULFSON, E. N., R. PATEL & B. A. LAW. 1990. Alkyl-β-glucoside synthesis in a water-organic two-phase system. Biotechnol. Lett. **12**(6): 397–402.
8. VIC, G. & D. THOMAS. 1992. Enzyme-catalyzed synthesis of alkyl β-D-glucosides in organic media. Tetrahedron Lett. **33**(32): 4567–4570.
9. LJUNGER, G., P. ADLERCREUTZ & B. MATTIASSON. 1994. Enzymatic synthesis of octyl-β-glucoside in octanol at controlled water activity. Enzyme Microb. Technol. **16:** 751–755.
10. BJÖRKLING, F., S. E. GODTFREDSEN & O. KIRK. 1989. A highly selective enzyme-catalyzed esterification of simple glucosides. J. Chem. Soc. Chem. Commun., p. 934–935.
11. KIRK, O., F. BJÖRKLING & S. E. GODTFREDSEN. 1989. Esters of glycosides and a process for enzymatic preparation thereof. International Patent Application No. WO 89/01480.
12. DAVID, M-H. L., H. O. J. LEMMENS, H. GÜNTHER & H. W. RÖPER. 1989. Surface active compounds and a process for their preparation. European Patent Application No. 0,334,498.
13. HILLS, G. A., A. R. MACRAE & R. R. POULINA. 1990. Ester preparation. European Patent Application No. 0,383,405.

14. PHILIPPE, M. 1992. Procédé de préparation par voie enzymatique de monoesters en position 6 du glucopyranoside de méthyle. French Patent Application No. 92/03811.

15. DE GOEDE, A. T. J. W., M. WOUDENBERG–VAN OOSTEROM & F. VAN RANTWIJK. 1994. Selective lipase-catalyzed esterification of carbohydrates. Carbohydr. Eur. **10:** 18–20.

16. SEKIGUCHI, S., T. YASUMASU, H. MIYAKE & Y. ENDO. 1992. Nonionic surface active agent. United States Patent No. 5,109,127.

17. PELENC, V., F. PAUL & P. MONSAN. 1993. Enzymatic stereospecific production of α-glucosides from starch by reaction with alcohol in the presence of α-transglucosidase and optionally conversion to α-butylglucoside ester using a lipase. International Patent Application No. WO 93/04185.

18. PAZUR, J. H. & D. FRENCH. 1951. The transglucosidase of *Aspergillus oryzae*. J. Am. Chem. Soc. **73:** 3536.

19. PAN, S. C., L. W. NICHOLSON & P. KOLACHOV. 1951. Isolation of a crystalline trisaccharide from the unfermentable carbohydrate produced enzymically from maltose. J. Am. Chem. Soc. **73:** 2547–2550.

20. CHIANG, J. P. C. & O. J. LANTERO. 1986. Method of preparing novel thermostable transglucosidase. European Patent Application No. 0,219,673.

21. PAN, S. C. 1970. Synthesis of estriol 16α-(α-D-glucoside) by enzymic transglucosylation. Biochemistry **9**(8): 1833–1838.

22. FOGARTY, W. M. & C. P. BENSON. 1982. Measurement of glucose transfer to glycerol by *Aspergillus niger* transglucosidase. Biotechnol. Lett. **4**(1): 61–64.

23. PIGMAN, W. & R. O. LAFFRE. 1951. The preparation of *n*-butyl α-D-glucoside. J. Am. Chem. Soc. **73:** 4994–4995.

24. GHATORAE, A. S., G. BELL & P. J. HALLING. 1994. Inactivation of enzymes by organic solvents: new technique with well-defined interfacial area. Biotechnol. Bioeng. **43:** 331–336.

Synthetic Applications of NAD(P)(H)-dependent Enzymes

GIACOMO CARREA, GIANLUCA OTTOLINA,
PIERO PASTA, AND SERGIO RIVA

Istituto di Chimica degli Ormoni
C.N.R.
20131 Milano, Italy

INTRODUCTION

In the frame of our general research on the synthetic applications of enzymes, our group has been studying the behavior of NAD(P)(H)-dependent enzymes, specifically dehydrogenases and monooxygenases, since the beginning of the eighties. Here, we report an overview of the results obtained so far.

DEHYDROGENASES

The dehydrogenases catalyze, in the presence of NAD(P) or NAD(P)H, the regiospecific and stereospecific oxidoreduction of a variety of hydroxyl and carbonyl compounds. The *in situ* regeneration of NAD(P)(H) can be effectively obtained by coupled enzymatic reactions, which allow the use of catalytic amounts of coenzyme (FIGURE 1).[1] TABLE 1 shows the enzymes that have been investigated in our studies.

Hydroxysteroid dehydrogenases (HSDH) catalyze the reversible oxidoreduction of the hydroxyl-keto groups of steroids with high regiospecificity and stereospecificity. We have studied the usefulness of HSDHs for bile acid synthesis in aqueous buffers. As an example, FIGURE 2 shows the different regiospecific and stereospecific

$$R_2CHOH + NAD(P) \xrightarrow[\text{DEHYDROGENASE}]{} R_2CO + NAD(P)H + H^+$$
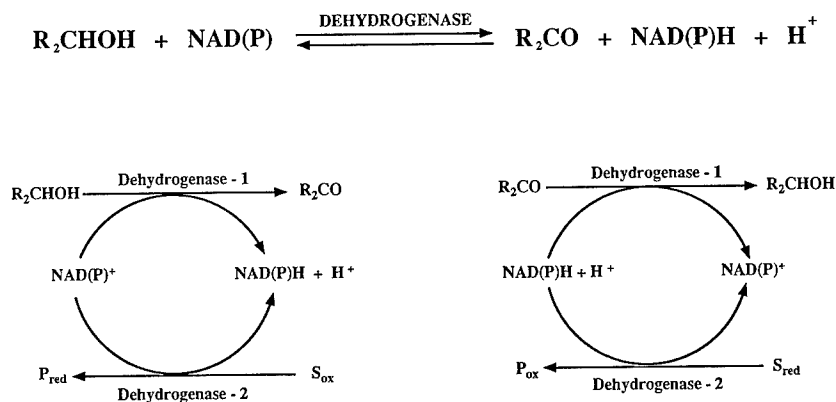
FIGURE 1. Enzymatic *in situ* regeneration of NAD(P) and NAD(P)H.

TABLE 1. Dehydrogenases Investigated in Our Studies

Enzyme	Source	Cofactor
alcohol DH	horse liver	NAD
alcohol DH	baker's yeast	NAD
alcohol DH	*Thermoanaerobium brockii*	NADP
3α-hydroxysteroid DH	*Pseudomonas testosteroni*	NAD
3β-hydroxysteroid DH	*Pseudomonas testosteroni*	NAD
7α-hydroxysteroid DH	*Escherichia coli*	NAD
7α-hydroxysteroid DH	*Clostridium absonum*	NADP
7β-hydroxysteroid DH	*Clostridium absonum*	NADP
12α-hydroxysteroid DH	*Clostridium P*	NADP

reductions of dehydrocholic acid (**1**).[2] The products were obtained quantitatively and, by using a suitable deuterated substrate donor for cofactor regeneration, it was also possible to prepare selectively deuterated steroids.[3]

As a more general approach, we also studied the potential of these enzymatic processes to perform specific chemical transformations, namely the hydroxyl α/β inversion at positions 3 and 7 of the steroid skeleton (FIGURE 3).[4,5]

Hydroxysteroid dehydrogenases can also be used to transform neutral steroids. In this case, two-phase systems have been used and the reaction conditions have been optimized with several steroids belonging to the androstane and pregnane classes.[6] Finally, it has to be mentioned that HSDH can also transform nonsteroidic compounds, as has been shown by us, for instance, in the preparation of the eight isomeric muscarines.[7]

FIGURE 4 shows the chemical route for the transformation of cholic acid (**2**) into ursodeoxycholic acid (**3**), a compound that is widely used for the dissolution of cholesterol gallstones. The compound in the box, 12-chetochenodeoxycholic acid (**4**),
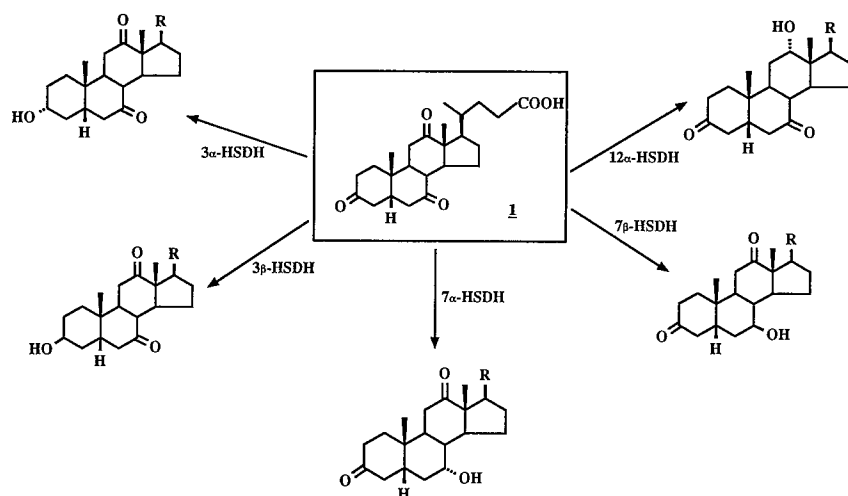
FIGURE 2. Regiospecific and stereospecific reduction of dehydrocholic acid (**1**) catalyzed by different hydroxysteroid dehydrogenases.[2]
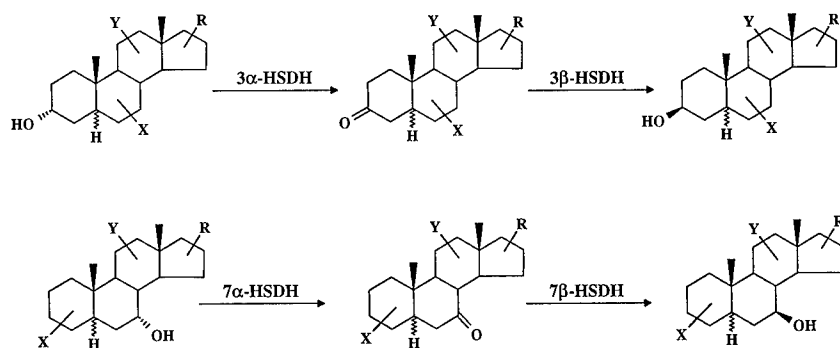
FIGURE 3. 3α/3β and 7α/7β inversions catalyzed by HSDHs.[4,5]

is a key intermediate and can be enzymatically prepared in one step by using 12α-HSDH.[8] Following optimization of the reaction conditions, compound **4** was obtained on a multikilogram scale in a membrane reactor containing an initial 4% solution of cholic acid. Free 12α-HSDH and glutamate dehydrogenase (the enzyme used to regenerate NADP by reduction of α-ketoglutarate to glutamate) were retained inside the reactor and reused for several cycles (up to 50) with satisfactory retention of their catalytic activity.

Alternative chemoenzymatic routes to compound **3** were also investigated. FIGURE 5 shows a three-step sequence that involves two chemical transformations and one enzymatic transformation. Preparation of 12-cheto-ursodeoxycholic acid (**5**) from dehydrocholic acid was obtained in one step by using in the same reactor
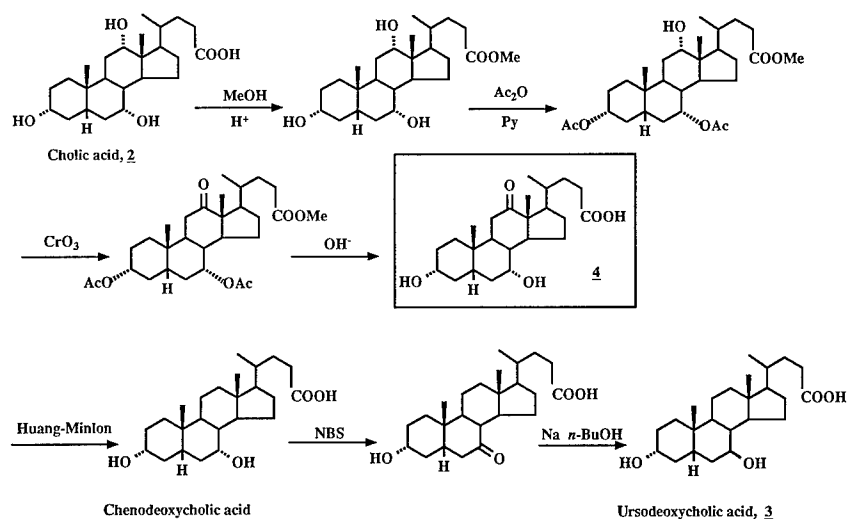
FIGURE 4. Chemical synthesis of ursodeoxycholic acid (**3**) from cholic acid (**2**).
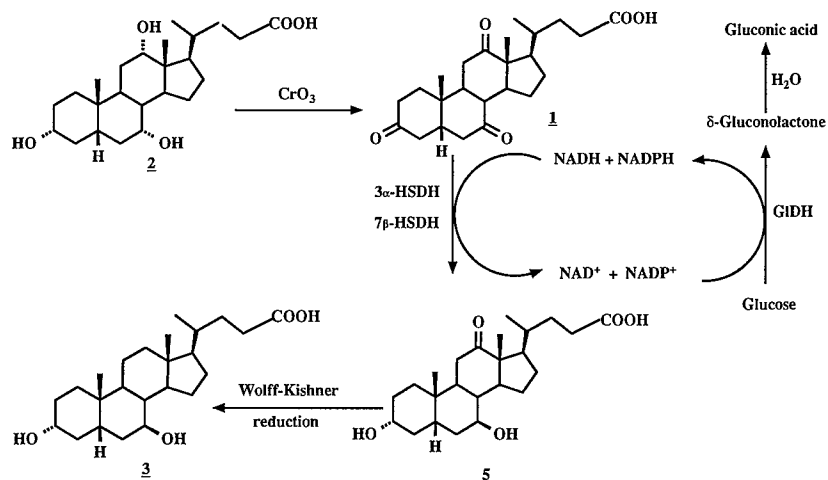
FIGURE 5. Alternative three-step chemoenzymatic route to ursodeoxycholic acid.[9]

3α-HSDH (NAD-dependent), 7β-HSDH (NADP-dependent), and glucose dehydrogenase (to regenerate both NADH and NADPH).[9]

FIGURE 6 shows an alternative three-step sequence. In this case, compound 3 was obtained by a chemical reduction of **5**, prepared from cholic acid through two consecutive enzymatic steps.[10]

The scaling up of dehydrogenase-catalyzed reactions can theoretically be performed in different kinds of reactors, using free or immobilized enzymes, neutral or charged membranes, and native or modified nicotinamide cofactors. The general goal is obviously to recycle the enzymes (that are retained inside the reactor) and, if possible, the expensive coenzyme.

Together with A. F. Buckmann (GBF, Braunschweig, Germany), we synthesized several macromolecular coenzymes and studied their properties (FIGURE 7).[11,12]
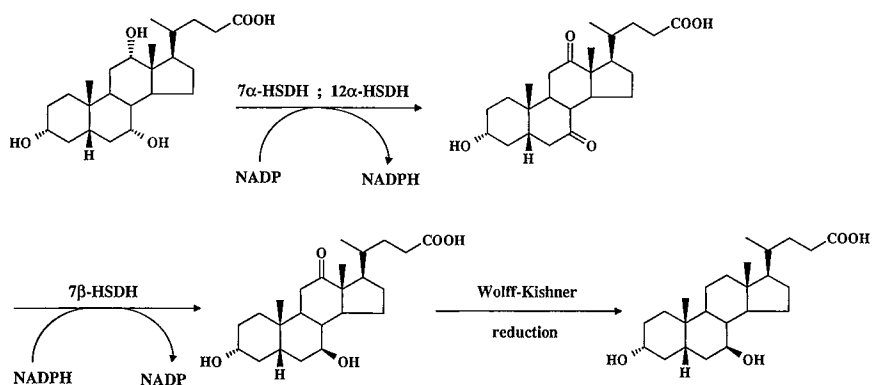
FIGURE 6. Alternative three-step chemoenzymatic route to ursodeoxycholic acid.[10]

PEG-N(1)-(2-aminoethyl)-NAD

PEG-C(8)-(6-aminohexyl)amino-NAD

PEG-N⁶-(2-aminoethyl)-NAD

PEI-N⁶-carboxymethyl-NAD

PAA-N⁶-(2-aminoethyl)-NAD
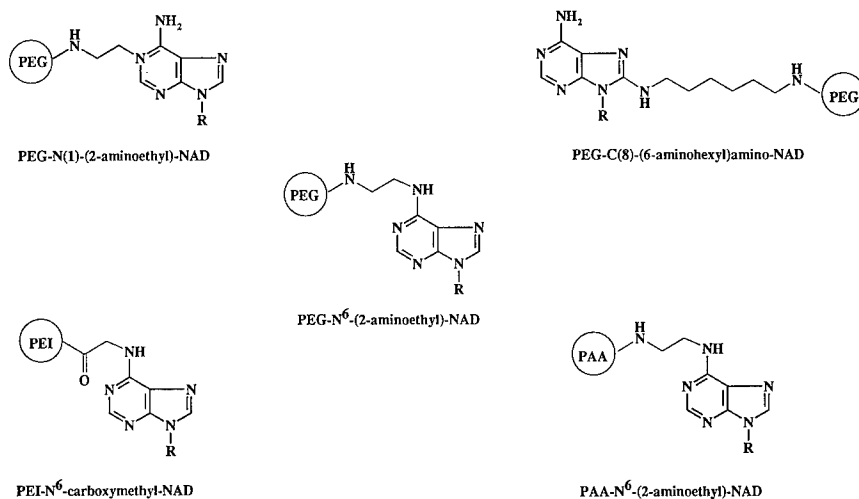
FIGURE 7. Examples of macromolecular NAD.[11]

Although we found that some enzymes do accept the modified NAD(P) molecules quite well in terms of both k_{cat} and K_m (i.e., alcohol DH from *Thermoanaerobium brockii*, glutamate DH from *Proteus* species, malic enzyme from chicken liver), other dehydrogenases are sensitive to any small modification of the coenzyme molecule and do not show satisfactory catalytic activity (i.e., glucose DH, 12α-HSDH).

MONOOXYGENASE

Cyclohexanone monooxygenase (CMO) has a great synthetic potential because it catalyzes, sometimes with remarkable stereoselectivity, the conversion of ketones into esters or lactones (Baeyer-Villiger reaction) and the oxygenation of hetero-atoms.[13] As shown in FIGURE 8, the oxidation reactions require NADPH that, as usual, is regenerated *in situ* by a coupled enzymatic reaction.

A   **B**   **C**

$$R\text{-}S\text{-}R' + NADPH + O_2 + H^+ \xrightarrow{\ CMO\ } R\text{-}SO\text{-}R' + NADP^+ + H_2O$$

$$D\text{-glucose-6P} + NADP^+ \xrightarrow{\ G6P\text{-}DH\ } D\text{-gluconate-6P} + NADPH + H^+$$
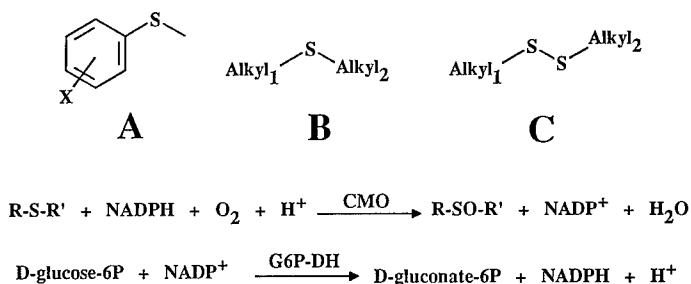
FIGURE 8. Oxidation of sulfides to sulfoxides catalyzed by CMO.[14]

A

2-propanol + PEG-NADP$^+$ $\xrightarrow{\text{ADHTB}}$ acetone + PEG-NADPH + H$^+$

B
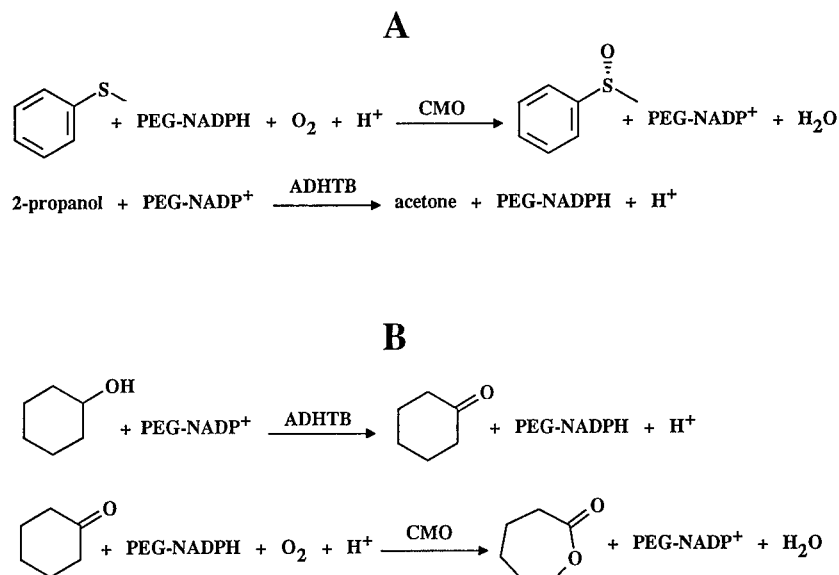
FIGURE 9. Reactions catalyzed by CMO using PEG-NADPH.[15]

We have systematically investigated the oxidation of sulfides to sulfoxides by CMO from *Acinetobacter* NCIB 9871, considering alkyl aryl sulfides (**A**), dialkyl sulfides (**B**), and dialkyl disulfides (**C**).[14]

CMO does accept macromolecular NADPH, specifically NADPH linked to polyethylene glycol (PEG-NADPH); therefore, it was possible to perform the enzymatic oxidation inside a membrane reactor using alcohol DH from *T. brockii* (ADHTB) to regenerate PEG-NADPH (FIGURE 9).[15] TABLE 2 compares the kinetic constants of CMO and ADHTB for NADP(H) and PEG-NADP(H), showing the high affinity of both enzymes for the enlarged cofactor. The main drawback to the exploitation of this approach appeared to be the limited stability of CMO, especially in the purified form that is necessary to perform Baeyer-Villiger reactions.

Using a "cubic space" approach,[16] an active site model to explain and predict the

TABLE 2. Kinetic Constants of CMO and ADHTB for NADP(H) and PEG-NADP(H)

Enzyme	Coenzyme	V_{max} (relative)	K_m (μM)
CMO	NADPH		<5
	PEG-NADPH[a]	88[c]	33
	PEG-NADPH[b]	62[c]	15
ADHTB	NADP		13
	PEG-NADP	84[c]	28

[a]With cyclohexanone (0.6 mM) as the substrate.
[b]With methyl phenyl sulfide (0.6 mM) as the substrate.
[c]Relative to the value obtained with native NADP(H) taken as 100.
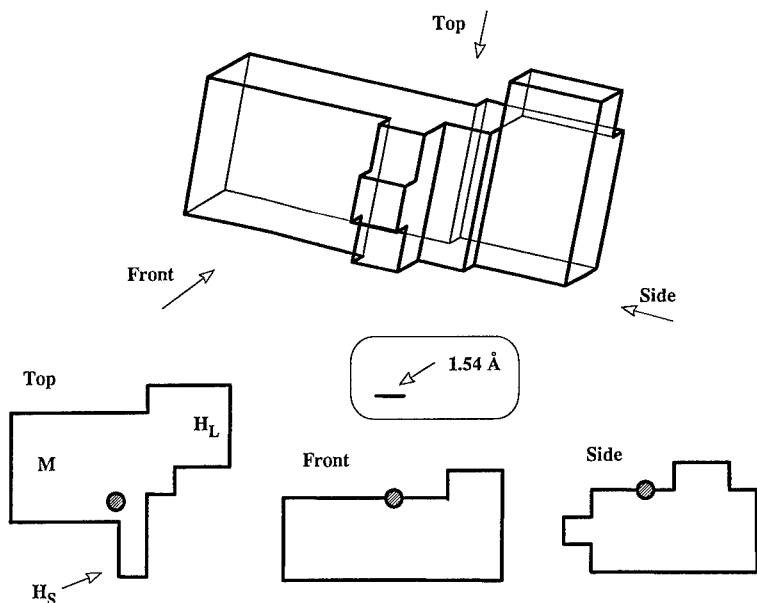
FIGURE 10. Active site model of CMO. The catalytically essential region (oxygen) is encircled. The top, front, and side views are also shown, together with the scale. In the top view, the main (M), the hydrophobic large (H_L), and the hydrophobic small (H_S) pockets are depicted.[17]

stereoselectivity of the sulfoxidation of sulfides to optically active sulfoxides was proposed (FIGURE 10).[17] The model was derived from the results experimentally obtained with over 30 different sulfides and appeared to be suitable for explaining the stereoselectivity of CMO-catalyzed Baeyer-Villiger reactions.[18]

ACKNOWLEDGMENTS

REFERENCES

1. CHENAULT, H. K. & G. M. WHITESIDES. 1987. Appl. Biochem. Biotechnol. **14:** 147–197.
2. RIVA, S., R. BOVARA, P. PASTA & G. CARREA. 1986. J. Org. Chem. **51:** 2902–2906.
3. RIVA, S., G. OTTOLINA, G. CARREA & B. DANIELI. 1989. J. Chem. Soc. Perkin Trans. **I:** 2073–2074.
4. RIVA, S., R. BOVARA, L. ZETTA, P. PASTA, G. OTTOLINA & G. CARREA. 1988. J. Org. Chem. **53:** 88–92.
5. BOVARA, R., E. CANZI, G. CARREA, A. PILOTTI & S. RIVA. 1993. J. Org. Chem. **58:** 499–501.
6. CARREA, G., S. RIVA, R. BOVARA & P. PASTA. 1988. Enzyme Microb. Technol. **10:** 333–340.

7. DeAmici, M., C. DeMicheli, G. Molteni, D. Pitré, G. Carrea, S. Riva, S. Spezia & L. Zetta. 1991. J. Org. Chem. **56:** 67–72.

8. Carrea, G., R. Bovara, R. Longhi & S. Riva. 1985. Enzyme Microb. Technol. **7:** 597–600.

9. Carrea, G., A. Pilotti, S. Riva, E. Canzi & A. Ferrari. 1992. Biotechnol. Lett. **14:** 1131–1135.

10. Bovara, R., G. Carrea, S. Riva & F. Secundo. 1996. Biotechnol. Lett. **18:** 305–308.

11. Riva, S., G. Carrea, F. M. Veronese & A. F. Buckmann. 1986. Enzyme Microb. Technol. **9:** 556–560.

12. Ottolina, G., G. Carrea, S. Riva & A. F. Buckmann. 1990. Enzyme Microb. Technol. **12:** 596–602.

13. Walsh, C. T. & Y. C. J. Chen. 1988. Angew. Chem. Int. Ed. Engl. **27:** 333–343.

14. Carrea, G., B. Redigolo, S. Riva, S. Colonna, N. Gaggero, E. Battistel & D. Bianchi. 1992. Tetrahedron Asymmetry **3:** 1063–1068.

15. Secundo, F., G. Carrea, S. Riva, E. Battistel & D. Bianchi. 1993. Biotechnol. Lett. **15:** 865–870.

16. Jones, J. B. 1990. Pure Appl. Chem. **62:** 1445–1448.

17. Ottolina, G., P. Pasta, G. Carrea, S. Colonna, S. Dallavalle & H. L. Holland. 1995. Tetrahedron Asymmetry **6:** 1375–1386.

18. Ottolina, G., G. Carrea, S. Colonna & A. Ruckemann. 1996. Tetrahedron Asymmetry **7:** 1123–1136.

Optical Resolution of Pantolactone by a Novel Fungal Enzyme, Lactonohydrolase

SAKAYU SHIMIZU AND MICHIHIKO KATAOKA

Department of Agricultural Chemistry
Kyoto University
Kitashirakawa, Sakyo-ku
Kyoto 606-01, Japan

INTRODUCTION

Calcium D-pantothenic acid is mainly used as an additive for animal feeds and for various pharmaceutical products. Several derivatives of D-pantothenate, such as panthenyl alcohol, pantetheine, 4'-phosphopantetheine-S-sulfonate, coenzyme A, and so on, are also used for pharmaceutical products, as additives for infant formulae, and as chemical reagents. The current world production of calcium D-pantothenate is about 4000 tons per year. At present, the commercial production of D-pantothenate depends exclusively on chemical synthesis. The chemical synthesis process involves reactions yielding racemic pantolactone from isobutyraldehyde, formaldehyde, and cyanide; optical resolution of the racemic pantolactone to D-pantolactone; and condensation of the D-pantolactone with β-alanine. Drawbacks of this chemical process are the troublesome resolution of the racemic pantolactone and racemization of the remaining L-isomer. In this resolution step, the use of an expensive alkaloid as a resolving agent is unavoidable. To avoid or simplify this troublesome resolution step, various microbial enzymatic reactions—such as stereo-specific reduction of ketopantolactone,[1-3] ketopantoate,[4] or 2'-ketopantothenate derivatives,[5,6] stereoselective inversion of L-pantolactone in a racemic mixture to D-pantolactone,[7-9] and stereoselective hydrolysis of esterified pantolactone[10,11]— have been tried. Recently, we found that several filamentous fungi, such as *Fusarium*, *Gibberella*, and *Cylindrocarpon*, produce a novel enzyme that catalyzes the reversible hydrolysis of pantolactone. The reaction is stereospecific and only the D-enantiomer in the racemic mixture is hydrolyzed (or lactonized if the acid form is the substrate). Therefore, the enzyme is a promising catalyst for the optical resolution of pantolactone as shown in FIGURE 1.

Here, we report the results of our recent work on the enzymatic resolution of racemic pantolactone, which includes the characterization of the lactonohydrolase of *Fusarium oxysporum* as the catalyst, the evaluation of hydrolysis and lactonization reactions for the optical resolution, and the determination of reaction conditions for practical large-scale resolution of pantolactone.

A NOVEL LACTONOHYDROLASE OF *F. OXYSPORUM*

A novel lactonohydrolase was isolated from the cells of *F. oxysporum* AKU 3702 and crystallized.[12] The relative molecular mass of the native enzyme is 125 kDa and

the subunit molecular mass is 60 kDa. The enzyme hydrolyzes aldonate lactones, such as D-galactono-γ-lactone and L-mannono-γ-lactone, stereospecifically. All the substrate lactones, which can be hydrolyzed by the enzyme, have a downward hydroxyl group at the 2-position, when the lactone rings are drawn according to Howarth's system (TABLE 1), but the corresponding enantiomers are not hydrolyzed at all. Some of them are competitive inhibitors. The enzyme can also catalyze the asymmetric hydrolysis of D-pantolactone. These reactions are reversible, and the reaction equilibrium at pH 6.0 is nearly 1:1 as to the molar concentrations of D-pantolactone and D-pantoate (FIGURE 2). The enzyme also irreversibly hydrolyzes several aromatic lactones, such as dihydrocoumarin and homogentisic acid lactone (see TABLE 1). The enzyme contains about 1 mol of calcium per subunit and 15.4% (w/w) glucose equivalent of carbohydrate. Calcium seems to be necessary for both enzyme activity and stability. The enzyme carries three kinds of N-linked high-mannose-type sugar chains (FIGURE 3) at the 28th, 106th, 179th, and 277th Asn residues. The carbohydrate moiety is an essential participant in the stabilization of the enzyme. TABLE 2 summarizes the properties of the enzyme.
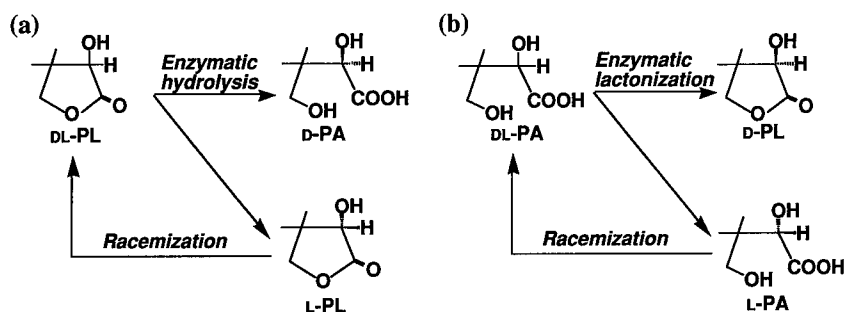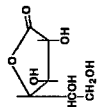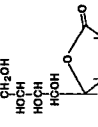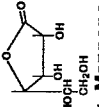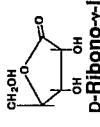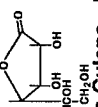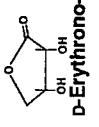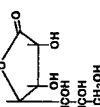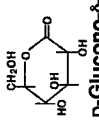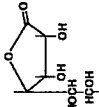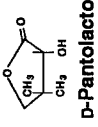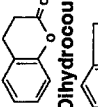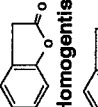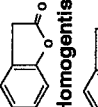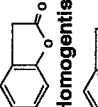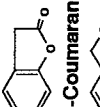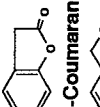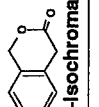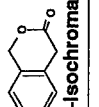
FIGURE 1. Schematic representation of the enzymatic resolution of D,L-pantolactone (a) and D,L-pantoate (b). Terms: PL, pantolactone; PA, pantoate.

OPTICAL RESOLUTION OF RACEMIC PANTOLACTONE
WITH LACTONOHYDROLASE

If racemic pantolactone is used as a substrate for the hydrolysis reaction by the lactonohydrolase of *F. oxysporum*, only the D-pantolactone might be converted to D-pantoate and the L-enantiomer might remain intact. Consequently, the racemic mixture could be resolved into D-pantoate and L-pantolactone as shown in FIGURE 1a. After the removal of L-pantolactone from this reaction mixture with solvent extraction, etc., D-pantoate remaining could be easily converted to D-pantolactone by heating under acidic conditions. The reverse reaction, that is, lactonization of D-pantoate, might also be possible for the resolution. In this case, D-pantoate in a racemic mixture of pantoate is specifically lactonized into D-pantolactone as shown in FIGURE 1b.

TABLE 1. Substrate Specificity of Lactonohydrolase from *F. oxysporum*

Substrate (150 mM)	Relative hydrolyzing activity (%)	Km (mM)
D-Galactono-γ-lactone	100	3.6
L-Mannono-γ-lactone	128	23
D-Gulono-γ-lactone	167	29
D-glycero-D-gulo-Heptono-γ-lactone	59.4	118
D-glycero-L-manno-Heptono-γ-lactone	132	167

Substrate (150 mM)	Relative hydrolyzing activity (%)	Km (mM)
α,β-Glucooctanoic γ-lactone	16.4	-
D-Ribono-γ-lactone	39.0	2.5
D-Erythrono-γ-lactone	117	377
D-Glucono-δ-lactone	107	-
D-Pantolactone	48.3	120

Substrate (2.5 mM)	Relative hydrolyzing activity (%)	Km (mM)
Dihydrocoumarin	100	6.3
Homogentisic acid lactone	16.6	2.5
2-Coumaranone	16.4	8.7
3-Isochromanone	0.58	4.4

FIGURE 2. Effect of pH on the reaction equilibrium of *Fusarium* lactonohydrolase. The hydrolysis of D-pantolactone (a) and the lactonization of D-pantoate (b) were carried out. The enzyme was incubated with 150 mM D-pantolactone (D-PL) (a) or 150 mM D-pantoate (b) at 30 °C under the indicated pH conditions. See reference 12 for details.

Hydrolysis of D- or L-Pantolactone with F. oxysporum Cells

When *F. oxysporum* cells were incubated with D-pantolactone, the lactone substrate was immediately hydrolyzed to pantoate; however, if L-pantolactone, in place of D-pantolactone, was incubated under the same conditions, the formation of
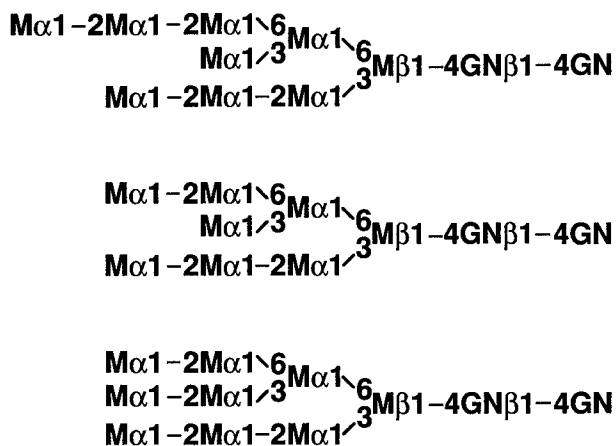
FIGURE 3. Carbohydrate structures of the lactonohydrolase of *F. oxysporum*. Terms: M, mannose; GN, *N*-acetylglucosamine.

TABLE 2. Properties of Lactonohydrolase from *F. oxysporum*

Native M_r	
TSK G-3000SW	125,000
Asahipak GS-520	120,000
Subunit M_r (SDS-PAGE)	60,000
Number of subunits	2
E (1 mg/mL, 280 nm, 1-cm light path)	0.784
p*I*	4.7
N-terminal amino acid	Ala
Metal content (Ca)	2.40 mol/mol
Sugar content (as glucose)	15.4% (w/w)
K_m & V_{max}	
Hydrolysis (pH 7.0)	
D-galactono-γ-lactone	3.6 mM, 1440 units/mg
L-mannono-γ-lactone	23 mM, 1300 units/mg
D-gulono-γ-lactone	29 mM, 1120 units/mg
D-pantolactone	120 mM, 653 units/mg
Lactonization (pH 6.0)	
D-galactononate	52.6 mM, 216 units/mg
L-mannononate	38.5 mM, 113 units/mg
D-gulononate	20.8 mM, 59.0 units/mg
D-pantoate	9.1 mM, 193 units/mg
Optimum pH	hydrolysis: 7–7.5
	lactonization: 6.0
Optimum temperature	50 °C
pH stability (30 °C, 30 min)	2–11.5
Thermal stability (pH 7.0, 20 min)	50 °C
Stabilizer	Ca^{2+} + D-PL + D-PA
Inhibitor	
L-pantolactone (competitive inhibition,	
K_i = 79 mM), chelating reagents, Mn^{2+}, Zn^{2+},	
Fe^{2+}, Cu^{2+}	
Reaction	

D-Galactono-γ-lactone   D-Galactononate
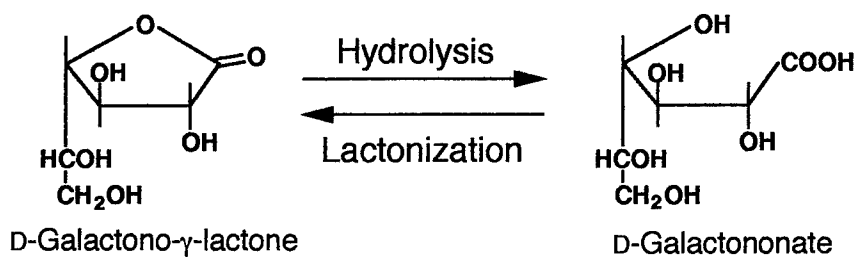
pantoate was essentially negligible. These results suggested that *F. oxysporum* cells as well as the purified lactonohydrolase could catalyze the enantioselective hydrolysis of pantolactone. During the hydrolysis of D-pantolactone, the pH of the reaction mixture became acidic, reaching an equilibrium between hydrolysis and lactonization. FIGURE 4 shows the effect of pH on the hydrolysis of pantolactone. At pH values between 5.5 and 7.0, the rate of hydrolysis of D-pantolactone increased in proportion to the pH of the reaction mixture, whereas no enzymatic hydrolysis of the L-enantiomer was observed. The maximum D-pantolactone hydrolysis activity was

observed at pH 7.5; however, both D- and L-pantolactone were hydrolyzed spontaneously above pH 7.0. The spontaneous hydrolysis of L-pantolactone would cause a decrease in the optical purity of the D-pantoate formed. The results suggest that a suitable pH for the asymmetric enzymatic hydrolysis of racemic pantolactone might be around pH 7.0, giving both a high hydrolysis rate and a high optical purity of D-pantoate.[13]

Stereoselective Hydrolysis of D-Pantolactone and Lactonization of D-Pantoate with F. oxysporum Cells

As mentioned above, both hydrolysis and lactonization reactions might be used for the optical resolution. Thus, stereoselective hydrolysis of D-pantolactone and lactonization of D-pantoate with *F. oxysporum* cells were investigated. From the results of the optimization of culture conditions, the cells cultivated in 3% glycerol, 0.5% Polypepton, 0.5% yeast extract, and 0.5% corn steep liquor, pH 6.0, were used as the catalyst for the reaction.

As shown in FIGURE 5, D-pantolactone was stereospecifically hydrolyzed to D-pantoate with 5380 mM (700 mg/mL) D,L-pantolactone as the substrate, with automatic controlling of the pH of the reaction mixture at 7.0 with 15 M NH_4OH. The formation of L-pantoate was barely detected. After 24 h, the concentration of
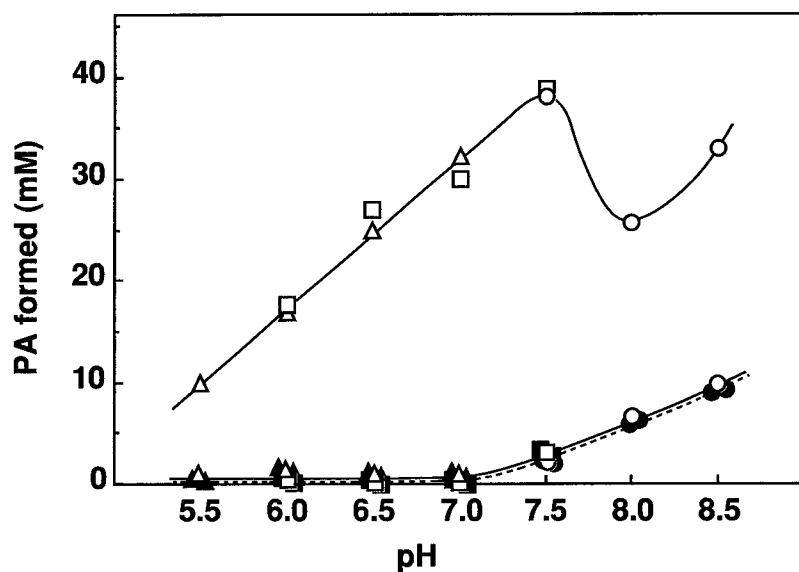
FIGURE 4. Effect of pH on the hydrolysis of D- or L-pantolactone with or without cells of *F. oxysporum*. Here, 154 mM (20 mg/mL) D-pantolactone (□, △, ○) or L-pantolactone (■, ▲, ●) was incubated with (—) or without (---) 10 mg of washed cells in 2 mL of 450 mM buffer of various pH at 30 °C for 1 h with reciprocal shaking. Symbols: (△, ▲) MES/NaOH; (□, ■) PIPES/NaOH; (○, ●) Tris/HCl. PA = pantoate. See reference 13 for details.

ANNALS NEW YORK ACADEMY OF SCIENCES

the pantolactone hydrolyzed in the reaction mixture reached 2480 mM (322 mg/mL) with an optical purity of 96% ee for D-pantoate.[14]

When 385 mM D,L-pantoate (50 mg/mL as D,L-pantolactone) was incubated with washed cells of *F. oxysporum* at 30 °C for 14 h with automatic controlling of the pH of the reaction mixture at 5.0 with acetate, 40% of the pantoate was lactonized with an enantioselectivity of 83% ee for the D-isomer. In an organic solvent–water two-phase system, in which an aqueous solution of 1540 mM D,L-pantoate (200 mg/mL as D,L-pantolactone) containing 50 mM $CaCl_2$ and cells was incubated with ethyl acetate at 30 °C for 20 h at pH 5.0, D-pantoate in the racemic mixture was almost stoichiometrically lactonized to D-pantolactone (90% ee). This improvement was suggested to be due to a shift of the reaction equilibrium during the lactonization on extraction of the reaction product, that is, D-pantolactone, into the organic phase.[15]

LARGE-SCALE RESOLUTION OF RACEMIC PANTOLACTONE WITH IMMOBILIZED CELLS OF *F. OXYSPORUM*

Practical hydrolysis of the D-isomer in a racemic mixture is carried out using immobilized mycelia of *F. oxysporum* as the catalyst. Stable catalyst with high hydrolytic activity can be prepared by entrapping the fungal mycelia into calcium alginate gels. When the immobilized mycelia were incubated in a reaction mixture
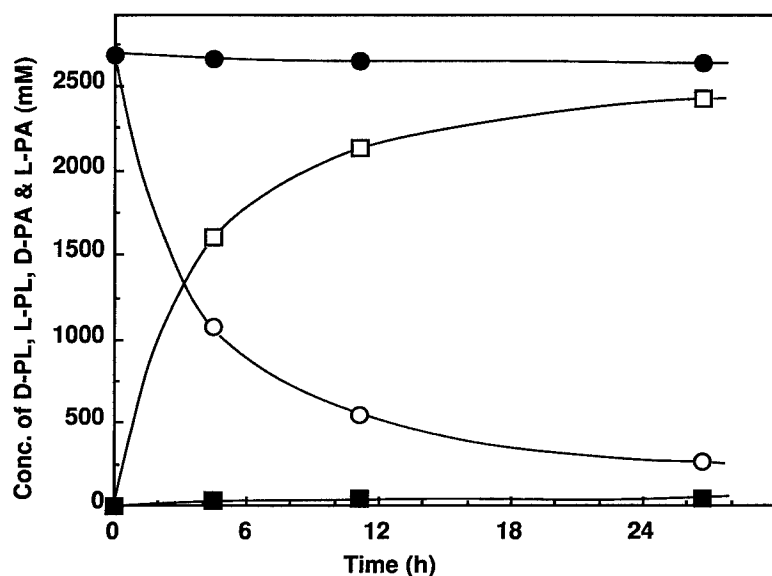
FIGURE 5. Optical resolution of racemic pantolactone with *F. oxysporum*. Ten g of washed cells were incubated with 50 mL of aqueous D,L-pantolactone solution (700 mg/mL) at 30 °C for 24 h with gentle stirring (300 rpm). The pH of the mixture was automatically controlled at 6.8–7.3 with 15 M NH_4OH. Symbols: O, D-pantolactone (D-PL); ●, L-pantolactone (L-PL); □, D-pantoate (D-PA); ■, L-pantoate (L-PA). See reference 14 for details.
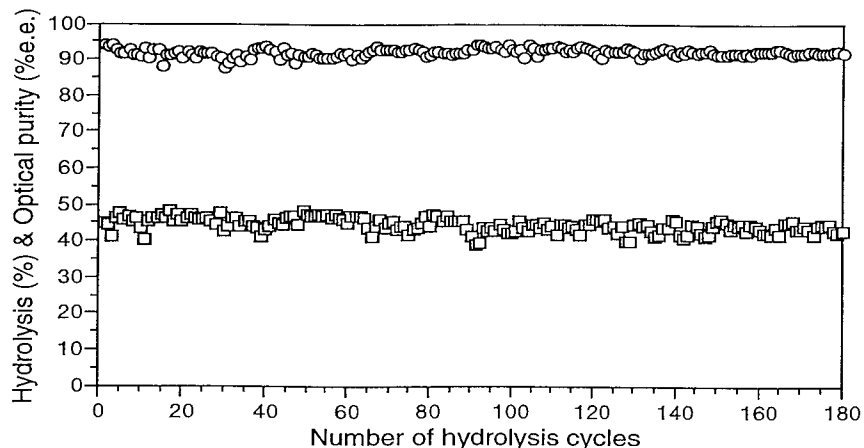
FIGURE 6. Stereospecific hydrolysis of pantolactone by *F. oxysporum* mycelia entrapped in calcium alginate gels. Here, 280 L of immobilized mycelia (containing 15.2 kg of wet cells) was incubated with 350 L of aqueous D,L-pantolactone solution (350 g/L) at 30 °C for 21 h. The pH of the mixture was automatically controlled at 6.8–7.2 with 15 M NH_4OH. All the immobilized mycelia filtrated from the reaction mixtures were used for the subsequent reactions. The hydrolysis reactions were carried out 180 times. Symbols: O, optical purity for D-pantoate; □, hydrolysis rate.

containing 350 g/L of D,L-pantolactone for 21 h at 30 °C under the conditions of automatic pH control (pH 6.8–7.2), 90–95% of the D-enantiomer was hydrolyzed (optical purity, 90–97% ee). After repeated reactions for 180 times (i.e., 180 days), the immobilized mycelia retained more than 90% of their initial activity (FIGURE 6).

There have been several reports of the application of enzymatic asymmetric hydrolysis to the optical resolution of pantolactone.[10,11] In these cases, esterified substrates, such as *O*-acetyl or *O*-formyl pantolactone, and lipases were used as the starting materials and catalysts, respectively. Because the lactonohydrolase of *F. oxysporum* hydrolyzes the intramolecular ester bond of pantolactone, it is not necessary to modify the substrate, pantolactone, before the hydrolysis reaction. Therefore, the process presented here is an advantageous and promising one for the practical production of D-pantolactone.

REFERENCES

1. HATA, H., S. SHIMIZU & H. YAMADA. 1987. Enzymatic production of D-(−)-pantoyl lactone from ketopantoyl lactone. Agric. Biol. Chem. **51:** 3011–3016.
2. SHIMIZU, S., H. HATA & H. YAMADA. 1984. Reduction of ketopantoyl lactone to D-(−)-pantoyl lactone by microorganisms. Agric. Biol. Chem. **48:** 2285–2291.
3. SHIMIZU, S., H. YAMADA, H. HATA, T. MORISHITA, S. AKUTSU & M. KAWAMURA. 1987. Novel chemoenzymatic synthesis of D-(−)-pantoyl lactone. Agric. Biol. Chem. **51:** 289–290.
4. KATAOKA, M., S. SHIMIZU & H. YAMADA. 1990. Novel enzymatic production of D-(−)-pantoyl lactone through the stereospecific reduction of ketopantoic acid. Agric. Biol. Chem. **54:** 177–182.

5. KATAOKA, M., S. SHIMIZU, Y. DOI, K. SAKAMOTO & H. YAMADA. 1990. Stereospecific reduction of ethyl 2'-ketopantothenate to ethyl D-(+)-pantothenate with microbial cells as a catalyst. Appl. Environ. Microbiol. **56:** 3595–3597.

6. KATAOKA, M., S. SHIMIZU, Y. DOI, K. SAKAMOTO & H. YAMADA. 1990. Microbial production of chiral pantothenonitrile through stereospecific reduction of 2'-ketopantothenonitrile. Biotechnol. Lett. **12:** 357–360.

7. SHIMIZU, S., S. HATTORI, H. HATA & H. YAMADA. 1987. One-step microbial conversion of a racemic mixture of pantoyl lactone to optically active D-(−)-pantoyl lactone. Appl. Environ. Microbiol. **53:** 519–522.

8. SHIMIZU, S., S. HATTORI, H. HATA & H. YAMADA. 1987. Stereoselective enzymatic oxidation and reduction system for the production of D-(−)-pantoyl lactone from a racemic mixture of pantoyl lactone. Enzyme Microb. Technol. **9:** 411–416.

9. KATAOKA, M., S. SHIMIZU & H. YAMADA. 1991. Stereospecific conversion of a racemic pantoyl lactone to D-(−)-pantoyl lactone through microbial oxidation and reduction reactions. Recl. Trav. Chim. Pays-Bas Belg. **110:** 155–157.

10. GLANZER, B. I., K. FABER & H. GRIENGL. 1988. Microbial resolution of O-acetyl pantoyl lactone. Enzyme Microb. Technol. **10:** 689–690.

11. BEVINAKATTI, H. S. & R. V. NEWADKAR. 1989. Lipase catalysis in organic solvents: transesterification of O-formyl esters of secondary alcohols. Biotechnol. Lett. **11:** 785–788.

12. SHIMIZU, S., M. KATAOKA, K. SHIMIZU, M. HIRAKATA, K. SAKAMOTO & H. YAMADA. 1992. Purification and characterization of a novel lactonohydrolase, catalyzing the hydrolysis of aldonate lactones and aromatic lactones, from *Fusarium oxysporum*. Eur. J. Biochem. **209:** 383–390.

13. KATAOKA, M., K. SHIMIZU, K. SAKAMOTO, H. YAMADA & S. SHIMIZU. 1995. Optical resolution of racemic pantolactone with a novel fungal enzyme, lactonohydrolase. Appl. Microbiol. Biotechnol. **43:** 974–977.

14. KATAOKA, M., K. SHIMIZU, K. SAKAMOTO, H. YAMADA & S. SHIMIZU. 1995. Lactonohydrolase-catalyzed optical resolution of pantoyl lactone: selection of a potent enzyme producer and optimization of culture and reaction conditions for practical resolution. Appl. Microbiol. Biotechnol. **44:** 333–338.

15. KATAOKA, M., M. HIRAKATA, K. SAKAMOTO, H. YAMADA & S. SHIMIZU. 1996. Optical resolution of racemic pantoic acid through microbial stereoselective lactonization in an inorganic solvent/water two-phase system. Enzyme Microb. Technol. **18:** in press.

Enantioselective Penicillin Acylase–catalyzed Reactions

Factors Governing Substrate and Stereospecificity of the Enzyme

V. K. ŠVEDAS, M. V. SAVCHENKO, A. I. BELTSER,
AND D. F. GURANDA

A. N. Belozersky Institute of Physicochemical Biology
Moscow State University
000958 Moscow, Russia

For many years, penicillin acylase from *Escherichia coli* has been considered first of all as a practically important enzyme of industrial use for modification of β-lactam antibiotics.[1-3] During the last years, penicillin acylase has become a subject of new attentive interest from both fundamental and practical points of view.[4] The crystal structure of penicillin acylase at 1.9-Å resolution has been reported and, principally, a new mechanism to endow the enzyme with its catalytic properties has been suggested.[5] Penicillin acylase has been used for deprotection of the amino groups in amino acid derivatives,[6,7] for enzymatic resolution of enantiomers of fluoro-substituted α-amino acids,[8] secondary alcohols, and α-substituted phenylacetic acids,[9-11] and for enantioselective acylation during synthesis of loracarbef.[12] In contrast to all other acylases, penicillin acylase has been shown to be an effective biocatalyst for resolution of enantiomers of aminoalkylphosphonic acids,[13] aminoalkylphosphonous acids,[14] and β-amino acids[15,16] (FIGURE 1). One can thus see that penicillin acylase is an enzyme of wide substrate specificity. Nevertheless, the reported studies on the substrate specificity of penicillin acylase have been done so far mainly on a semiquantitative level or only for a very limited number of substrates.[17-20] Benzylpenicillin, which is often claimed as the preferred substrate of penicillin acylase from *E. coli*,[1-3] is not, for example, one of the five most reactive substrates characterized so far (TABLE 1). Stereospecificity of this enzyme in practice was not studied.

Let us consider the specificity of penicillin acylase to the substrate of the general formula (FIGURE 2). The following problems have been studied: capacity of acyl group binding pocket ρ1; specificity of ρ2 and ρ3 subsites; and chiral discrimination of the substrate in the penicillin acylase active center.

ACYL GROUP BINDING POCKET

Topography of the acyl group binding pocket (subsite ρ1) was studied by the bifunctional inhibitors, alkylboronic acids, with a changing length of the alkyl chain;[21] penicillin acylase specificity to the acyl group of the substrate was also investigated for the series of *N*-acylated glycines[22] (FIGURE 3). There is a remarkable increase of inhibition with a growing alkyl radical, but the capacity of the binding pocket is
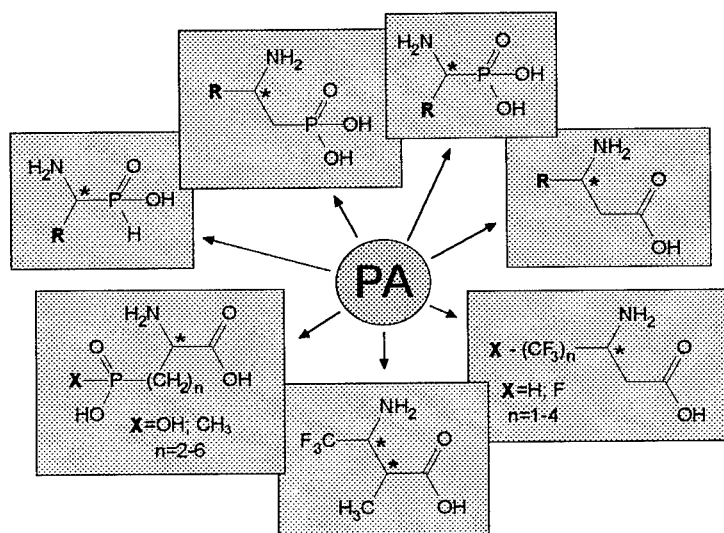
FIGURE 1. Structures of the organoelement analogues of natural amino acids and nonconventional amino acids prepared in optically pure form using penicillin acylase (PA).

limited by the amyl radical (the length of the amyl radical most closely corresponds to the length of the benzyl radical, as in the best substrates of penicillin acylase). Further increase of the alkyl chain leads to the distinguished decrease of the inhibition. Practically, the same kind of dependence is observed in the case of penicillin acylase–catalyzed hydrolysis of *N*-acylglycines. The important similarity between these two dependencies is that the slope of the dependencies is close to a value of two; thus, the binding of the alkyl chain is not just a simple extraction of the alkyl chain from water to the hydrophobic pocket of the enzyme, but also an elimination of some thermodynamically unfavorable contacts with water in the enzyme active center—or, in other words, an expulsion of some water molecules from the binding pocket. As an illustration, a model "knife-scabbard" can be used.

TABLE 1. The Most Reactive Substrates of Penicillin Acylase

Substrate	k_{cat}/K_M ($M^{-1} \cdot s^{-1}$)	%
Phenylacetyl-Abu[a]	$4.6 \cdot 10^7$	100
Phenylacetyl-Phe	$3.7 \cdot 10^7$	80
Phenylacetyl-Ala	$2.1 \cdot 10^7$	46
Phenylacetyl-Ala^{PH}	$2.0 \cdot 10^7$	43
Phenylacetyl-Gly	$2.0 \cdot 10^7$	43
Benzylpenicillin	$1.7 \cdot 10^7$	37
Phenylacetyl-Gly-Val	$1.5 \cdot 10^7$	33
Phenylacetyl-Gly-Leu	$1.1 \cdot 10^7$	24
Phenylacetyl-Gly-Phe	$0.9 \cdot 10^7$	20
Phenylacetyl-Ala^P	$0.64 \cdot 10^7$	14

[a]Abu = alpha-aminobutyric acid.
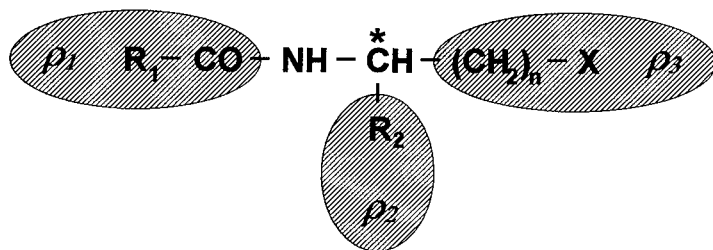
FIGURE 2. Schematic representation of the penicillin acylase substrate and location of its structural fragments in the corresponding subsites of the enzyme active center.
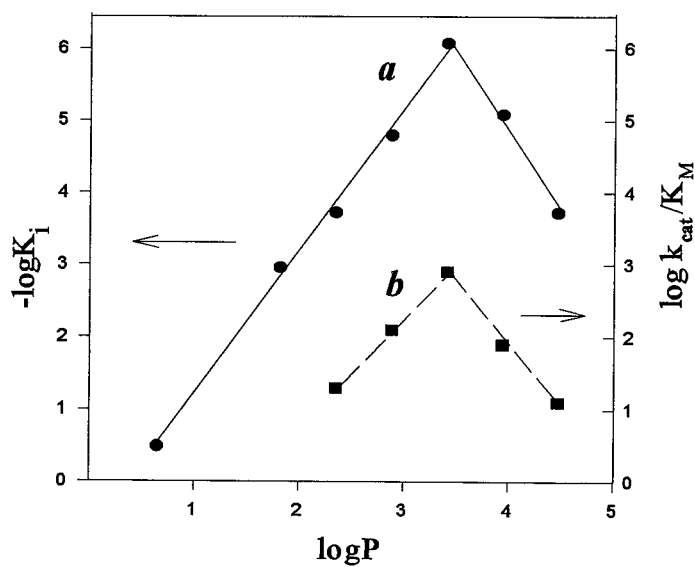
FIGURE 3. Penicillin acylase inhibition by alkylboronic acids (*a*) and penicillin acylase–catalyzed hydrolysis of *N*-acylated glycines (*b*): dependencies of the inhibition constants (*a*) and of the second-order rate constants of the hydrolysis (*b*) on the hydrophobicity of the alkyl radical.
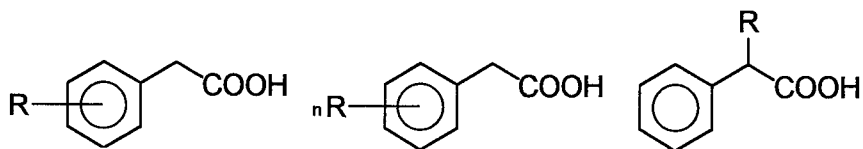
where R= H, OH, F, Cl, Br, NH₂, NO₂, OCH₃

FIGURE 4. Structures of penicillin acylase inhibitors—phenylacetic acid derivatives.
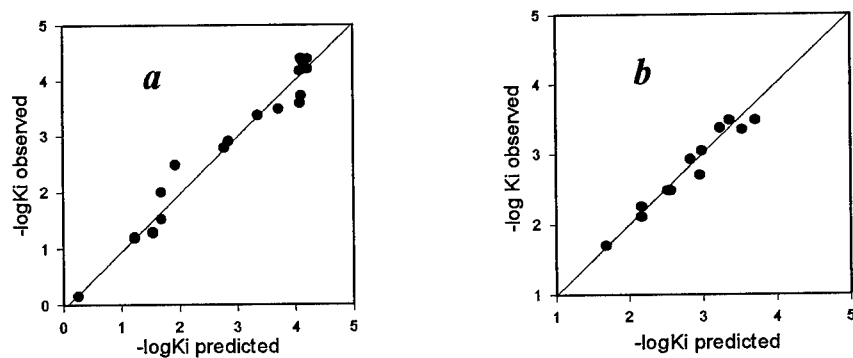
FIGURE 5. Penicillin acylase inhibition by phenylacetic acid derivatives: two-parameter correlations of the inhibition constants with the hydrophobicity and molecular volume of the inhibitor—(a) for p- and m-substituted PAA derivatives (equation 1); (b) for o- and α-substituted PAA derivatives (equation 2).

TABLE 2. Specificity of Penicillin Acylase to N-Phenylacetyl-α-Amino Acids

R[a]	$k_{cat}/K_M \ (\mathrm{M^{-1} \cdot s^{-1}})$
H	$1.9 \cdot 10^7$
CH_3	$2.1 \cdot 10^7$
C_2H_5	$4.6 \cdot 10^7$
$i\text{-}C_3H_7$	$5 \cdot 10^5$
$i\text{-}C_4H_9$	$3.8 \cdot 10^5$
C_4H_9	$2 \cdot 10^6$
Ph	$4.7 \cdot 10^6$
$Ph\text{-}CH_2$	$3.7 \cdot 10^7$
$NH_2\text{-}(CH_2)_4$	$2 \cdot 10^6$
$PO(OH)(CH_3)\text{-}(CH_2)_3$	$3.1 \cdot 10^6$
$HOOC\text{-}CH_2$	$1.7 \cdot 10^6$
$H_2N\text{-}CO\text{-}CH_2$	$1.2 \cdot 10^4$

[a]R in $RCH(NHCOCH_2Ph)COOH$.

TABLE 3. Specificity of Penicillin Acylase to N-Phenylacetyl-β-Amino Acids

R[a]	$k_{cat}/K_M \ (\mathrm{M^{-1} \cdot s^{-1}})$
CF_3	$3.1 \cdot 10^5$
CH_3	$2.8 \cdot 10^6$
C_3H_7	$1.3 \cdot 10^5$
$i\text{-}C_3H_7$	740
$i\text{-}C_4H_9$	$3 \cdot 10^4$
Ph	$1.1 \cdot 10^6$
4-F-Ph	$9 \cdot 10^5$
$3,4,5\text{-}(MeO)_3\text{-}Ph$	$1 \cdot 10^6$

[a]R in $RCH(NHCOCH_2Ph)CH_2COOH$.

TABLE 4. Stereospecificity of Penicillin Acylase to α-Amino Acid Derivatives

Substrate	$\dfrac{(k_{cat}/K_M)^L}{(k_{cat}/K_M)^D}$
Phenylacetyl-Ala[P]	58,000
Phenylacetyl-Ala[PH]	1400
Phenylacetyl-Ala	1000
Phenylacetyl-AlaOMe	280
Phenylacetyl-Ala-D-Ala	65

X-ray structures of the penicillin acylase modified by phenylmethylsulfonylfluoride and of the enzyme complex with phenylacetic acid, published recently, confirmed this observation.[5]

For a more detailed characterization of the acyl group binding subsite ρ1, penicillin acylase inhibition by 30 substituted phenylacetic acid (PAA) derivatives was studied (FIGURE 4). The competitive inhibition was found in all cases.

The best inhibitors were PAA and their derivatives with hydrophobic substituents (Cl-, Br-, etc.) in the *m*-position. The specificity was as follows: *m*-PAA > *p*-PAA > *o*-PAA. The derivatives of PAA with the polar substituents (-OH, -NH$_2$) in the α-position showed the lowest inhibition effect. No significant stereospecificity to the α-substituted derivatives (with an asymmetric α-carbon) was detected. A two-parameter correlation of the inhibition constants with the hydrophobicity (log P) and molecular volume (MolVol) of the inhibitor was shown. Two correlation series with different roles of the hydrophobicity were obtained: (i) for *p*- and *m*-substituted derivatives (FIGURE 5a),

$$-\log K_i = 1.2(\pm 0.1) \cdot \log P - 5.4(\pm 0.9) \cdot 10^4 \cdot \text{MolVol} + 6.5(\pm 0.8); \qquad (1)$$

(ii) for *o*- and α-substituted inhibitors (FIGURE 5b),

$$-\log K_i = -0.4(\pm 0.04) \cdot \log P - 3.3(\pm 0.2) \cdot 10^4 \cdot \text{MolVol} + 8.0(\pm 0.3). \qquad (2)$$

The *p*-OH and *m*-NO$_2$ derivatives did not fit the correlation. The following conclusions can thus be made based on the correlations obtained: despite the strongly limited capacity of the hydrophobic pocket ρ1 in the penicillin acylase active center (FIGURE 2), there is a possibility of additional hydrophobic interactions at the *m*-position of the benzyl radical and of H-bond formation at the *p*-position (≈ 6 kJ/mol); also, the hydrophobic pocket is covered by the polar narrow crack, which is not wider than 1.4–1.8 Å.

TABLE 5. Stereospecificity of Penicillin Acylase to Lysine Derivatives

Substrate	$(k_{cat}/K_M)^L$	$(k_{cat}/K_M)^D$	$\dfrac{(k_{cat}/K_M)^L}{(k_{cat}/K_M)^D}$
α-*N*-Phac-Lys	$2.0 \cdot 10^6$	13	150,000
di-α,ε-*N*,*N*-Phac-Lys	$5.9 \cdot 10^6$	$2.4 \cdot 10^3$	25
ε-*N*-Phac-Lys	$6.7 \cdot 10^6$	$4.6 \cdot 10^4$	1.5

TABLE 6. Stereospecificity of Penicillin Acylase for Different Substrate Series: $RCH(NHCOCH_2Ph)X$

R	X	$\dfrac{(k_{cat}/K_M)^L}{(k_{cat}/K_M)^D}$	X	R	$\dfrac{(k_{cat}/K_M)^L}{(k_{cat}/K_M)^D}$	X	R	$\dfrac{(k_{cat}/K_M)^L}{(k_{cat}/K_M)^D}$
CH_3	CH_2COOH	220	COOH	C_4H_9	400	CH_2COOH	CH_3	220
	$COOCH_3$	280		$i\text{-}C_3H_7$	780		CF_3	500
	$PO(OH)(OCH_3)$	520		$i\text{-}C_4H_9$	950		$i\text{-}C_4H_9$	940
	COOH	1000		CH_3	1000		$p\text{-Br-Ph}$	6600
	PO_2H_2	1400		$p\text{-F-Ph}$	2600		$p\text{-}CH_3O\text{-Ph}$	7900
	$PO(O\text{-}i\text{-}C_3H_7)_2$	1800		$o\text{-F-Ph}$	2800		$p\text{-Cl-Ph}$	9300
	$PO(OCH_3)_2$	2300		Ph	4300		$3,4,5\text{-}(CH_3O)_3\text{-Ph}$	12,500
	$PO(OH)_2$	58,000		$PO(OH)(CH_3)(CH_2)_3$	5300		$p\text{-F-Ph}$	13,000
Ph	$PO(OH)_2$	300		$Ph\text{-}CH_2$	5700		Ph	14,000
	COOH	4300		$NH_2\text{-}(CH_2)_4$	150,000			
	CH_2COOH	14,000						

Phac-D,L-p-F-Phg

[PA]

L-p-F-Phg + **Phac-D-p-F-Phg**

ee>98% *170x[PA]* *acid hydrolysis*

D-p-F-Phg **D-p-F-Phg**

ee>98% *ee 80%*

FIGURE 6. Biocatalytic preparation of D-*p*-fluorophenylglycine.

SPECIFICITY OF THE SUBSITE ρ2

Penicillin acylase has a wide substrate specificity to the α-amino acid side chain (TABLE 2). *N*-Phenylacetyl-β-amino acid derivatives (TABLE 3) are much less reactive substrates in comparison with the corresponding α-amino acid derivatives. The most remarkable decrease in the penicillin acylase catalytic activity is observed in the case of α- and β-amino acids with a branched alkyl side chain. Thus, sterically

(2R*,3R*) **(2R*,3S*)**
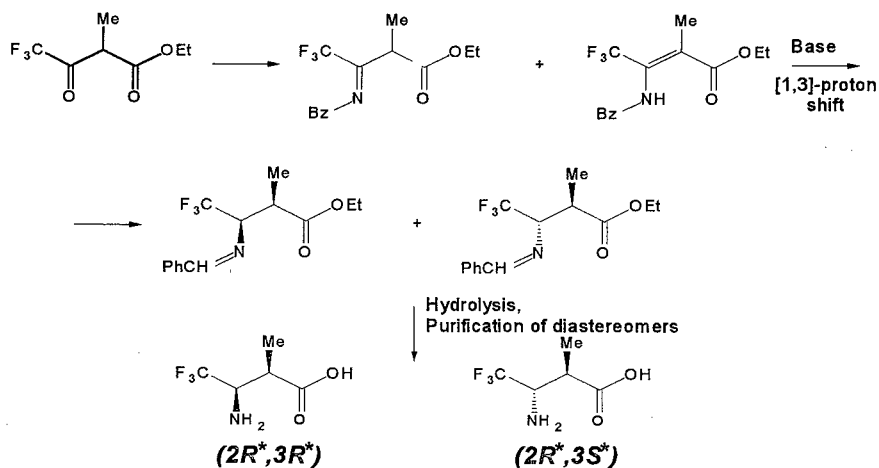
FIGURE 7. Scheme of the stereoselective synthesis of diastereomers of α-methyl-β-trifluoromethyl-β-alanine.
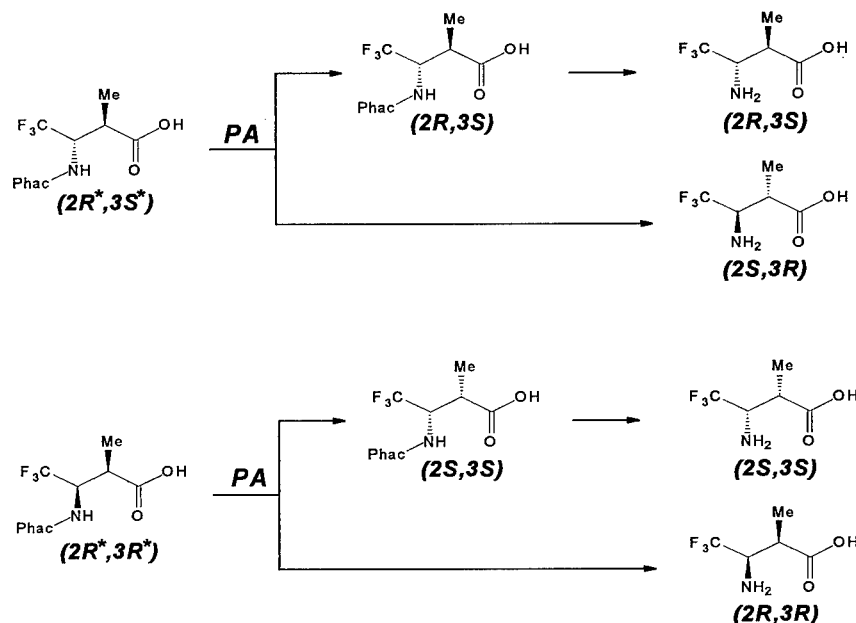
FIGURE 8. Scheme of the penicillin acylase–catalyzed preparation of the four isomers of α-methyl-β-trifluoromethyl-β-alanine.

controlled interactions are the most important factor governing substrate specificity at subsite ρ2.

INTERACTIONS AT SUBSITE ρ3

Interaction of the negative charge of the substrate at subsite ρ3 is the most important factor for chiral discrimination in the penicillin acylase active center (TABLE 4). The highest stereospecificity, equal to 58,000, is observed in the case of 1-N-phenylacetylaminoethylphosphonic acid (phosphonic analogue of alanine); hydrolysis of 1-N-phenylacetylaminophosphonous acid (phosphonous analogue of alanine) is characterized by about the same stereospecificity as for N-phenylacetylalanine hydrolysis. However, when the negatively charged group of the substrate is blocked, the penicillin acylase stereospecificity is remarkably decreased. Thus, it is reasonable to suggest the presence of a positively charged group in the subsite ρ3 that is responsible for a rather effective electrostatic interaction with the negatively charged group of the substrate. Experimental data on the hydrolysis of the different N-phenylacetylated derivatives of lysine strongly support this suggestion (TABLE 5). Penicillin acylase–catalyzed hydrolysis of α-N-phenylacetyl-L-lysine (the positively charged side chain group is located in subsite ρ2 and the carboxy group is in subsite ρ3) proceeds with the same second-order rate constant, $2 \cdot 10^6$ M^{-1}·s^{-1}, as N-phenylacetyl-L-norleucine hydrolysis. Therefore, the positive charge in this case does

not have any significant influence on the catalytic properties of the enzyme. In the case of the D-enantiomers (where the side chain should be located at subsite ρ3 and the carboxy group at subsite ρ2), hydrolysis of α-N-phenylacetyl-D-lysine proceeds with a second-order rate constant of 13 $M^{-1} \cdot s^{-1}$, which is 380 times lower than the second-order rate constant for hydrolysis of N-phenylacetyl-D-norleucine. When the amino group of the side chain radical is acylated and the positive charge is extinguished, the second-order rate constant for di-α,ε-N,N-phenylacetyl-D-lysine hydrolysis is increased by more than 18,000-fold.

Hence, the chiral discrimination of the substrate in the penicillin acylase active center is based on the balance of the electrostatic interactions of the substrate with the positive charge in subsite ρ3 and sterically controlled hydrophobic interactions at subsite ρ2.

PENICILLIN ACYLASE–CATALYZED PREPARATION OF ENANTIOMERS

In general, penicillin acylase–catalyzed hydrolysis of N-phenylacetylated α- and β-amino acids is characterized by a rather high stereospecificity (TABLE 6). It should be mentioned that the stereospecificity in enzymatic hydrolysis of N-phenylacetyl-β-amino acids is lower, with the exception of N-phenylacetyl-β-phenylalanine and its derivatives. Because of the high stereospecificity, penicillin acylase can be used for preparative synthesis of the enantiomers of different amino acids.

In some cases, penicillin acylase possesses high stereospecificity and good catalytic activity in the hydrolysis of both enantiomers of the substrate. It is especially
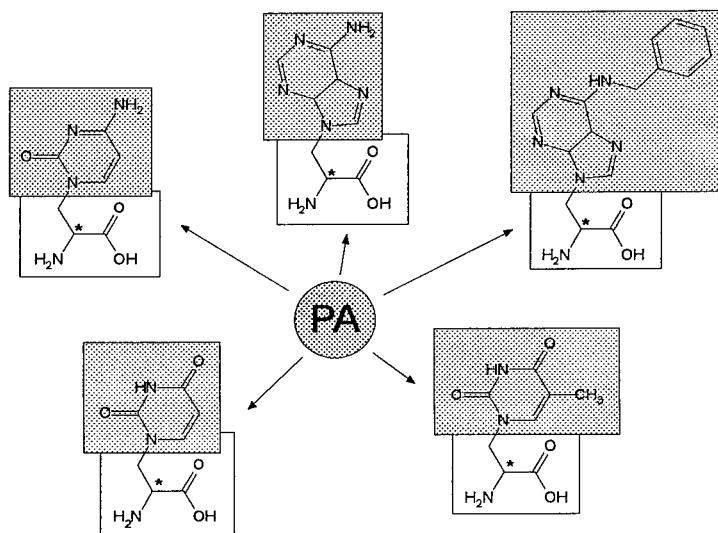
FIGURE 9. Structures of nucleo-amino acids prepared in optically pure form using penicillin acylase.

important when acidic hydrolysis of the D-enantiomer of the substrate proceeds with remarkable racemization (FIGURE 6).

The combination of the stereoselective synthesis of diastereomers and the consequent biocatalytic resolution of pure diastereomers into the pair of enantiomers provided a basis for the synthesis of each of the four isomers of the compounds with two chiral centers. α-Alkyl-β-fluoroalkyl-substituted β-amino acids represented a visual example for such a chemoenzymatic approach.[23] Diastereomers of free α-methyl-β-trifluoromethyl-β-alanine were synthesized and isolated in diastereomerically pure form by recrystallization (FIGURE 7). Phenylacetyl derivatives were synthesized with a good yield and the preparative enzymatic resolution of the four isomers was performed (FIGURE 8).
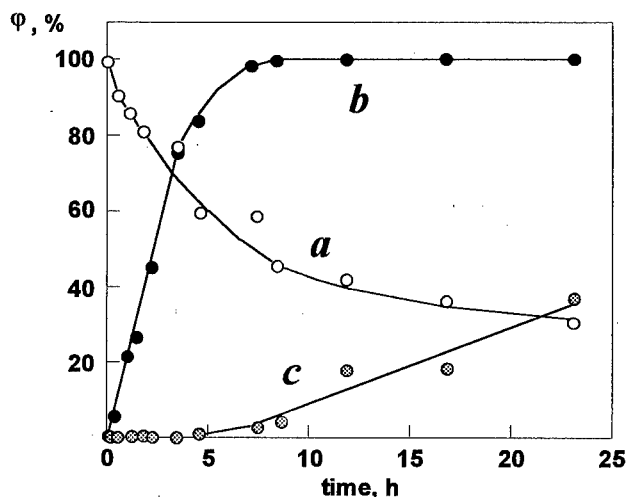
FIGURE 10. Progress curves of penicillin acylase–catalyzed hydrolysis of D,L-N-phenylacetyl-β-(Cytozinyl-N^1)-α-alanine (a) and accumulation of L-enantiomer (b) and D-enantiomer (c) of the nucleo-amino acid. Conditions: pH 7.5, 0.1 M phosphate, 25 °C.

Nucleo-amino acids represent a new field for application of penicillin acylase in preparation of enantiomers (FIGURE 9). Enzymatic hydrolysis of N-phenylacetylated nucleo-amino acids is quite a stereospecific reaction, leading to the consequent hydrolysis of both enantiomers (FIGURE 10). Enantiomers of four synthetic nucleo-amino acids and the natural nucleo-amino acid, 3-(6-benzylaminopurin-9-yl)alanine, were prepared with high optical purity.[24]

REFERENCES

1. VANDAMME, E. J. 1980. Microbial enzymes and bioconversions. *In* Economic Microbiology. Volume 5. A. A. Rose, Ed.: 467–522. Academic Press. New York.
2. ABBOTT, B. J. 1976. Adv. Appl. Microbiol. **20:** 203–257.
3. SHEWALE, J. G. & H. SIVARAMAN. 1989. Proc. Biochem. **24:** 146–154.
4. VIRDEN, R. 1990. Biotechnol. Genet. Eng. Rev. **8:** 189–218.

5. DUGGLEBY, H. J., S. P. TOLLEY, C. P. HILL, E. J. DODSON, G. DODSON & P. C. E. MOODY. 1995. Nature **373:** 264–268.
6. ŠVEDAS, V. K., I. YU. GALAEV, YU. A. SEMILETOV & G. A. KORSHUNOVA. 1983. Bioorg. Chem. **9:** 1139–1141.
7. WALDMANN, H. & D. SEBASTIAN. 1994. Chem. Rev. **94:** 911–937.
8. SOLOSHONOK, V. A., V. K. ŠVEDAS, V. P. KUKHAR, I. YU. GALAEV, E. V. KOZLOVA & N. YU. SVISTUNOVA. 1993. Bioorg. Khim. **19(4):** 478–483.
9. WALDMANN, H. 1989. Tetrahedron Lett. **30(23):** 3057–3058.
10. FUGANTI, C., C. M. ROSELL, S. SERVI, A. TAGLIANI & M. TERRENI. 1992. Tetrahedron Asymmetry **3(3):** 383–386.
11. BALDARO, E., P. D'ARRIGO, G. PEDROCCHI-FANTONI, C. M. ROSELL, S. SERVI, A. TAGLIANI & M. TERRENI. 1993. Tetrahedron Asymmetry **4(5):** 1031–1034.
12. ZMIJEWSKI, M. J., B. S. BRIGGS, A. R. THOMPSON & I. G. WRIGHT. 1991. Tetrahedron Lett. **32(13):** 1621–1622.
13. SOLODENKO, V. A., T. N. KASHEVA, V. P. KUKHAR, E. V. KOZLOVA, D. A. MIRONENKO & V. K. ŠVEDAS. 1991. Tetrahedron **47(24):** 3989–3998.
14. SOLODENKO, V. A., M. Y. BELIK, S. V. GALUSHKO, V. P. KUKHAR, E. V. KOZLOVA, D. A. MIRONENKO & V. K. ŠVEDAS. 1993. Tetrahedron Asymmetry **4(9):** 1965–1968.
15. SOLOSHONOK, V. A., A. G. KIRILENKO, N. A. FOKINA, I. P. SHISHKINA, S. V. GALUSHKO, V. P. KUKHAR, V. K. ŠVEDAS & E. V. KOZLOVA. 1994. Tetrahedron Asymmetry **5(6):** 1119–1126.
16. SOLOSHONOK, V. A., N. A. FOKINA, A. V. RYBAKOVA, I. P. SHISHKINA, S. V. GALUSHKO, A. E. SOROCHINSKY, V. P. KUKHAR, V. K. ŠVEDAS & M. V. SAVCHENKO. 1995. Tetrahedron Asymmetry **6(7):** 1601–1610.
17. COLE, M. 1969. Biochem. J. **115:** 733–739.
18. KUTZBACH, C. & E. RAUENBUSCH. 1974. Hoppe-Seyler's Z. Physiol. Chem. **354:** 45–53.
19. FUGANTI, C., P. GRASSELLI, S. SERVI, A. LAZZARINI & P. CASATI. 1987. J. Chem. Soc. Chem. Commun., p. 538–539.
20. MARGOLIN, A. I., V. K. ŠVEDAS & I. V. BEREZIN. 1980. Biochim. Biophys. Acta **616:** 283–289.
21. ŠVEDAS, V. K. 1976. Ph.D. thesis. Department of Chemistry, Moscow State University.
22. BELTSER, A. I. 1995. Diploma work. Department of Chemistry, Moscow State University.
23. SOLOSHONOK, V. A., A. G. KIRILENKO, N. A. FOKINA, V. P. KUKHAR, S. V. GALUSHKO, V. K. ŠVEDAS & G. RESNATI. 1994. Tetrahedron Asymmetry **5(7):** 1225–1228.
24. BAGERZADEH, G., A. A. KOZLOVSKY, N. V. SUMBATIAN, G. A. KORSHUNOVA, M. V. SAVCHENKO & V. K. ŠVEDAS. 1995. In preparation.

Enzymatic Preparation of Monoglycerides via Glycerolysis of Fats and Oils Catalyzed by Lipase from *Pseudomonas* Species[a]

SHU-GUI CAO,[b] XIU-GONG GAO,[c]
AND KE-CHANG ZHANG[c]

[b]*National Laboratory of Enzyme Engineering*
Jilin University
Changchun 130023, People's Republic of China

[c]*Department of Biotechnology*
Wuxi University of Light Industry
Wuxi 214036, People's Republic of China

INTRODUCTION

Monoglycerides (MG) are broadly applied as emulsifiers in foods, cosmetics, and pharmaceuticals.[1] At present, they are manufactured commercially via glycerolysis of fats and oils by a chemical method, which involves the reaction of fat with glycerol catalyzed by an inorganic catalyst at a temperature higher than 220 °C.[2] In addition to the lower MG yield (only about 40%), the chemical process also results in the formation of brown degradation products with an undesirable flavor from unsaturated fatty acids due to the high temperature employed.[2]

To obtain a product with higher quality and yield, and also to minimize energy costs, several attempts have been made to synthesize MG at low temperature using lipases as catalysts. Among them, the most efficient one was that developed by Yamane and coworkers,[3] in which a high yield of MG was achieved by carefully controlling the reaction temperature. It was found that lipases from *Pseudomonas* sp. were most effective. Surprisingly, the rate of MG production varied considerably among enzymes produced by different strains of this genus.[3] Herein, we present our investigation on the application of a new lipase from *Pseudomonas* sp. to the synthesis of MG from several fats and oils under a variety of conditions via solid-phase enzymatic glycerolysis.

MATERIALS AND METHODS

Materials

Pseudomonas sp. lipase (PSL) was produced from *Pseudomonas* sp. 2106, a wild strain newly isolated from soil by our laboratory. Refined deodorized fats and oils

were provided as gifts by the Department of Cereals and Oils of Wuxi University of Light Industry (Wuxi, China). Glycerol and all other chemicals were purchased from commercial sources and were of analytical grade.

Glycerolysis Reaction

A small amount of distilled water was dissolved in 1.8 g of glycerol to give a final concentration of 3.6% water in glycerol. Then, 8.2 g of fat and the lipase powder (500 IU/g oil) were added into the reactor and were stirred magnetically (800 rpm) to homogeneity. The aforementioned glycerol preparation was added dropwise over 5 min. Temperature control was achieved with the water bath jacket of the reactor.

Analysis

MG yield was monitored throughout the experiments by the chemical method of periodic acid oxidation according to Hamilton and Rossell.[4] Changes in the composition of the reaction mixture during glycerolysis were followed by thin-layer chromatography/flame ionization detection (TLC/FID) (Iatroscan TH-10, Iatron Laboratories, Tokyo, Japan) with Chromarod S III quartz rods according to the method of Yamane *et al.*[3] Water content in glycerol was measured by the optimized Fischer titration.[5]

RESULTS AND DISCUSSION

Effect of Temperature

The time course of MG formation during glycerolysis of palm oil catalyzed by *Pseudomonas* sp. lipase (PSL) in the temperature range of 36–44 °C is shown in FIGURE 1. It is evident that temperature has a critical effect on the equilibrium yield of MG. Above 40 °C, only about 30% MG was obtained; at 40 °C or lower, approximately 60% MG was produced. The maximum MG yield, 63%, was obtained at 38 °C. When the reaction was conducted at 40 °C or lower, the reaction mixture became solidified after 3 h and further stirring was impossible; however, the reaction was allowed to continue.

The above phenomenon might be accounted for by enzyme inactivation at higher temperatures. To check this possibility, the glycerolysis reaction was first carried out at 44 °C until equilibrium was achieved; then, the temperature was quickly adjusted to 38 °C and a new equilibrium was set up with a higher MG yield (FIGURE 2). This indicates that lower MG yields were not caused by enzyme inactivation at higher temperatures. Therefore, we hypothesize that there exists a critical temperature (T_c) for the glycerolysis. At or below T_c, relatively higher MG yield can be obtained at equilibrium, whereas the MG yield above T_c is reduced substantially; that is, a sharp transition exists between the two states and T_c is the temperature at which the transition occurs. For palm oil, T_c is 40 °C.
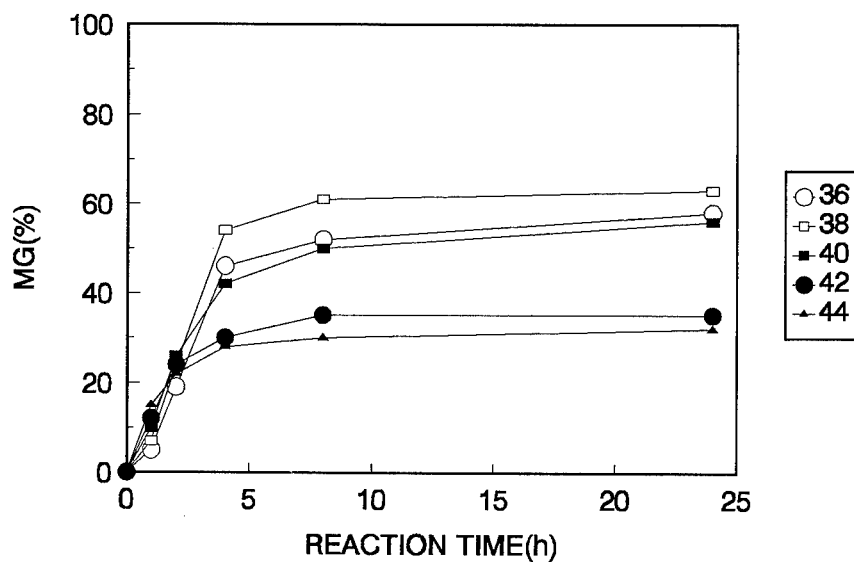
FIGURE 1. Effect of temperature on monoglyceride (MG) production during enzymatic glycerolysis of palm oil catalyzed by *Pseudomonas* sp. lipase at the various temperatures indicated.
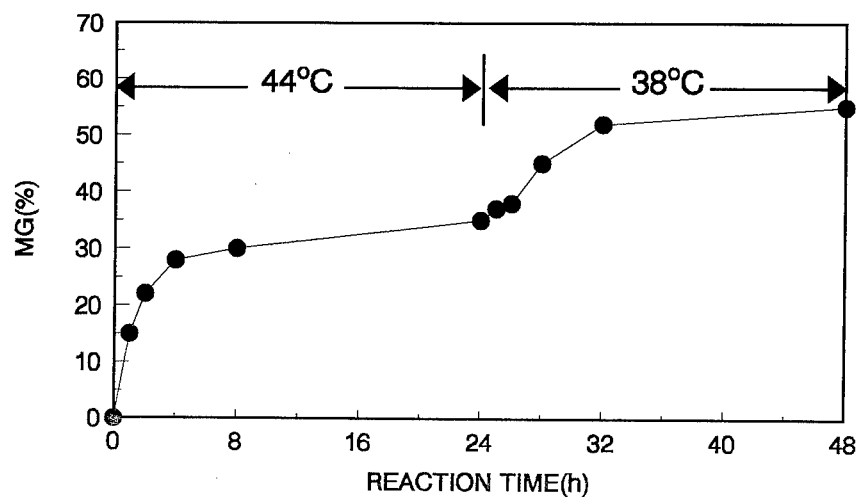
FIGURE 2. Monoglyceride (MG) production during enzymatic glycerolysis of palm oil catalyzed by *Pseudomonas* sp. lipase at 44 °C for 24 h and then at 38 °C.

Determination of T$_c$ for Various Fats and Oils

To verify the validity of the above hypothesis and to understand the nature of the critical temperature, we carried out the glycerolysis reaction of several typical fats and oils and determined the T_c for them (TABLE 1). It can be found that the value of T_c depends strongly on the type of fat/oil used. In general, a high value of T_c was found for fat/oil with a high melting point and a low T_c was found for low-melting-point fat/oil. In addition, for each fat/oil, T_c and the melting point are close to each other. It is noteworthy that, in all cases, the reaction mixture became solid after about 3 h at T_c or lower, whereas it remained liquid (an emulsion) at temperatures higher than T_c. The maximum yield of MG below T_c also depends on the fat/oil type, and the highest yield was obtained with palm oil (73%) among the fats/oils investigated (see TABLE 1).

Time Course of Glycerolysis

In FIGURE 3, the change in composition of the reaction mixture during glycerolysis of palm oil at 38 °C is shown. Initially, a linear decrease in triglyceride (TG)

TABLE 1. Critical Temperature (T_c), Optimum Temperature (T_o),[a] and Equilibrium MG Yield for Various Fats and Oils in Enzymatic Glycerolysis Catalyzed by PSL

Fat or Oil	Melting Point (°C)	T_c (°C)	T_o (°C)	MG Yield (%) at Equilibrium	Time (h) Required for Equilibrium
beef tallow	46	46	42	65	8–12
lard	33	32	30	62	8–12
palm oil	38	40	38	63	8–12
palm stearin	52	44	40	67	8–12
olive oil	<5	10	10	73	96
rapeseed oil	<5	10	5	57	120

[a]Temperature at which the maximum MG equilibrium yield was obtained.

concentration and a linear increase in 1,3-diglyceride (1,3-DG), 1,2-diglyceride (1,2-DG), and MG concentrations were found. After 2–3 h, the DG fractions began to decrease, whereas MG continued to increase linearly. It is noteworthy that, at the beginning of the reaction, 1,3-DG and 1,2-DG were produced in approximately equal amounts, indicating that the lipase is not 1,3-positionally specific in the glycerolysis reaction. In addition, after 2 h of reaction, the main component of the DG fraction was the 1,3-isomer, and 1,2-DG remained lower throughout the reaction, presumably due to acyl migration from the 2-position to the 3-position.[6]

Effect of Water Content

FIGURE 4 shows the dependence of the initial rate of MG formation on the water content in the glycerol phase ranging from 0.5% to 12.0% during glycerolysis of palm oil at 38 °C. The initial rate of MG formation increased linearly with water content
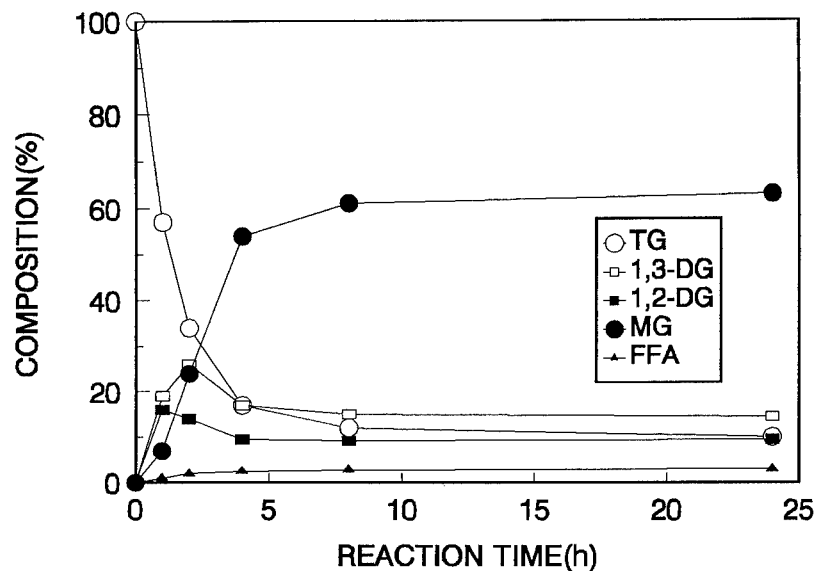
FIGURE 3. Changes in the composition of the reaction mixture during enzymatic glycerolysis of palm oil catalyzed by *Pseudomonas* sp. lipase at 38 °C. Abbreviations: triglyceride (TG); 1,3-diglyceride (1,3-DG); 1,2-diglyceride (1,2-DG); monoglyceride (MG); free fatty acid (FFA).
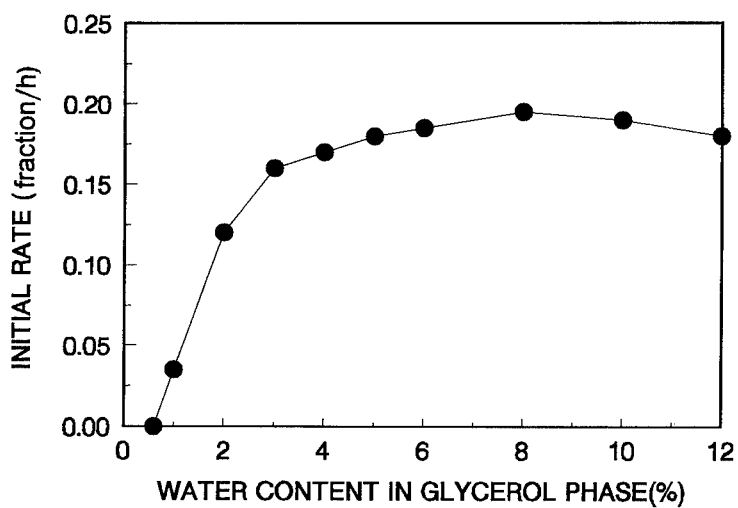
FIGURE 4. Effect of water content in the glycerol phase on the initial rate of monoglyceride (MG) formation during enzymatic glycerolysis of palm oil catalyzed by *Pseudomonas* sp. lipase at 38 °C. The initial rate of MG formation is defined as the change in the fractional content of MG per hour, and the fractional content is defined as wt%/100.

from 0.5% to 2.0%. Above 2.0%, the rate of increase slowed down and, above 4.0%, the water content had no evident effect on the rate of MG formation. These results indicate that it is essential for the enzyme to gain a trace amount of water in order to exhibit activity in nonaqueous media. This conclusion is shared by all enzymatic processes in neat organic phase.[7] The effect of water content on the equilibrium yield of MG is shown in FIGURE 5. The maximum MG yield was obtained at a water content of about 3.6%. In fact, water content had no significant influence on MG yield in the range of 2.0–6.0%. Above 6.0%, MG yield began to decrease, presumably due to the occurrence of a side reaction (hydrolysis) induced by the increased water content.
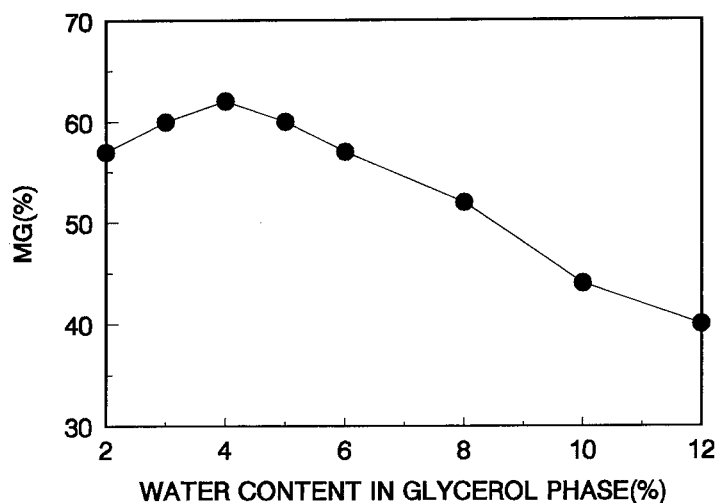
FIGURE 5. Effect of water content in glycerol phase on the equilibrium yield of monoglyceride (MG) during enzymatic glycerolysis of palm oil catalyzed by *Pseudomonas* sp. lipase at 38 °C.

Effect of Varying Glycerol:Oil Ratio

The optimum amount of glycerol required was determined by varying the molar ratio of glycerol to oil from 1:1 to 3:1 (FIGURE 6). The highest MG yield was obtained at 2:1, which corresponds with the reaction stoichiometry.

Separation of Reaction Mixture by Silica Gel Column Chromatography

Glycerolysis of palm oil catalyzed by PSL was carried out on a gram scale at the optimum conditions determined above—that is, temperature, 38 °C; water content in glycerol, 3.6%; glycerol:oil (molar ratio), 2:1—and the equilibrium yield of MG attained was 73%. The glyceride fractions were separated out on a silica gel column and the results are outlined in TABLE 2. The weight percentage of MG among the
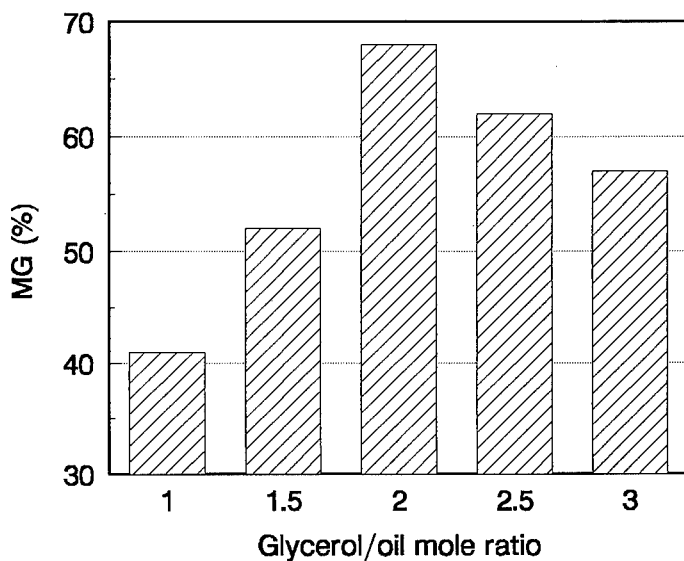
FIGURE 6. Effect of the molar ratio of glycerol to oil on the equilibrium yield of monoglyceride (MG) during enzymatic glycerolysis of palm oil catalyzed by *Pseudomonas* sp. lipase at 38 °C.

three glycerides, 63.9%, is lower than the result of chemical measurement, presumably due to operation losses.

CONCLUSIONS

The potential for catalysis of glycerolysis using *Pseudomonas* sp. lipase (PSL) and the conditions for obtaining MG-enriched products have been evaluated. The enzymatic glycerolysis reaction described here employed a nonsolvent system that avoided the use of organic solvents or emulsifiers. It is simple, but efficient, for MG production. Upon controlling the temperature at or below the critical temperature (T_c), high MG yield could be obtained. Under optimum conditions, a maximum of 73% MG yield was achieved from palm oil. The method presented here is expected

TABLE 2. Separation of Reaction Mixture by Silica Gel Column Chromatography[a]

	Sample	TG	DG	MG	Sum[b]
weight (g)	1.0548	0.0966	0.2549	0.5925	0.9440
percentage	100	9.15	24.16	56.17	89.50

[a]TG, DG, and MG were separated out from the reaction mixture by silica gel column chromatography using three different eluting solvent systems, respectively, according to Hamilton and Rossell.[4] The amount of each component was obtained after evaporating the eluting solvent(s) from it and the weight percentage was calculated.

[b]The total weight of the three fractions, TG, DG, and MG.

to provide a high-quality, inexpensive alternative to the conventional chemical process currently used in commercial MG production.

REFERENCES

1. SONNTAG, N. O. V. 1982. *In* Bailey's Industrial Oil and Fat Products. Fourth edition. Volume 2. D. Swern, Ed.: 134. Wiley. New York.
2. LAURIDSEN, J. B. 1976. J. Am. Oil Chem. Soc. **53:** 400.
3. MCNEILL, G. P., S. SHIMIZU & T. YAMANE. 1990. J. Am. Oil Chem. Soc. **67:** 779.
4. HAMILTON, R. J. & J. B. ROSSELL, Eds. 1986. Analysis of Oils and Fats. Elsevier. Amsterdam/New York.
5. LAITINEN, H. A. & W. E. HARRIS. 1975. *In* Chemical Analysis. Second edition, p. 361. McGraw–Hill. New York.
6. MATTSON, F. H. & R. A. VOLPENHEIM. 1962. J. Lipid Res. **3:** 281.
7. DORDICK, J. S. 1991. *In* Applied Biocatalysis. Volume 1. H. W. Blanch & D. S. Clark, Eds.: 1. Dekker. New York.

Enzymatic Transesterification
of a Triacylglycerol Mixture

Application to Butterfat Modification

L. LAMBOURSAIN,[a] A. MARTY,[a] S. KERMASHA,[b]
J. S. CONDORET,[a] AND D. COMBES[a]

[a]*Centre de Bioingénierie Gilbert Durand*
Institut National des Sciences Appliquées
Complexe Scientifique de Rangueil
31077 Toulouse, France

[b]*Faculty of Agricultural and Environmental Sciences*
McGill University
Sainte Anne de Bellevue, Québec, Canada H9X 1CO

INTRODUCTION

Butter has been identified for years as a hypercholesterolemic fat, inducing heart problems.[1] Because heart disease is today the major cause of death in industrial countries, it is of interest to identify why butter induces hypercholesterolemia and to propose solutions.

It was demonstrated that a saturated fatty acid located at position *sn*-2 of the glycerol backbone leads to cholesterolemia.[2] In butter, oleic acid, a monounsaturated acid, is the most present fatty acid (33%), but it is mostly present at positions 1 and 3 of the glycerol backbone.[3] However, in cacao butter, that is, a noninducing hypercholesterolemia fat, oleic acid is present at 87% at the 2-position.[4] We therefore might expect, by interchanging fatty acids within the triacylglycerol molecule, a decrease of the atherogenic potency of butter due to the increase of the oleic acid ratio at the 2-position.

A better way to catalyze this exchange, by interesterification, is the use of a specific hydrolytic enzyme in an organic solvent with low water activity. Such an enzymatic catalyst will allow the production of very specific reactions and consequently will minimize the formation of secondary products. The use of an organic solvent with low water activity is very suitable for catalyzing synthesis reactions. Indeed, in this case, it is crucial to minimize the formation of free fatty acids, which are considered to be compounds hazardous to health.

Butter appears to be a very complex substrate. Indeed, it is composed of at least 40 different triacylglycerols. Its water content is about 15% (g/g). This complexity leads to great difficulties in quantifying the results of a reaction. This is enhanced by the fact that the analysis needs to take into account isomers of position on the glycerol backbone. In order to determine the main parameters that influence the reaction, we have chosen to study a model reaction medium composed of a synthetic mixture of triolein and tripalmitin. *n*-Hexane was used as solvent because it is a very conventional organic solvent, deeply studied in our laboratory. For similar reasons,

we have chosen an efficient immobilized lipase, Lipozyme™, to catalyze this reaction.

This work presents the feasibility of acyl-exchange, with the optimization of the water content as a crucial parameter.

MATERIALS AND METHODS

Materials

Immobilized lipase, Lipozyme™, from *Mucor miehei*, supported on macroporous anionic beads (Duolite), was kindly provided by Novo Industri, Denmark.

Triolein and tripalmitin, with an approximate purity of 99%, and *n*-hexane were supplied by Sigma Chemical (St. Louis, Missouri) and Prolabo, respectively.

Methods

The hydration of the enzymatic support was realized in closed vessels containing hydrated salt solutions. A given saturated hydrated salt solution was able to give a fixed thermodynamic water activity in the aqueous phase that was in equilibrium with the inner atmosphere of the vessel, itself in equilibrium with the solid support. This method was efficient for obtaining a homogeneous hydration of the enzymatic support at a given activity. After long and sufficient equilibration, the water content of the support was determined using the Karl-Fisher method. The enzymatic support (50 mg) was then placed in *n*-hexane (10 mL) and the partition of water between the enzymatic support and the solvent was calculated using isotherms of adsorption.[5,6] Triolein (40 mM) and tripalmitin (40 mM) were added to the reaction medium, giving the zero time of the reaction.

Monoacylglycerol, diacylglycerol, and triacylglycerol concentrations were determined by high-performance liquid chromatography (HPLC) using a laser light scattering detector, in accordance with the method described previously in reference 7. Elution was conducted at 35 °C. The column is Spherisorb C18, 5 μm (250 × 4 mm), from Hewlett Packard and the eluant is a mixture of acetonitrile/chloroform (80/20 and 98/2 v/v, respectively, for triacylglycerols and for monoglycerides and diglycerides). Detection was done at 125 °C under a nitrogen pressure of 14.8 MPa.

Free fatty acids, oleic and palmitic acids, were derivatized to phenacyl esters as indicated by Christie in 1987.[8] Phenacyl esters were analyzed by HPLC with UV detection at 246 nm.

RESULTS AND DISCUSSION

It was pointed out in numerous works[5,6,9] that the control of the water content during synthesis reactions in hydrophobic organic solvents is crucial. On one side, water is necessary to maintain the optimal hydration and consequently the optimal conformation of the protein. On the other side, too much water induces negative effects. Indeed, water participates in the phenomenon of thermal deactivation of

proteins. It can also induce hydrophobic hindrance for nonpolar substrates in their transfer towards the protein.[6] Moreover, even when water is not involved in the main reaction, great values of water activity lead to secondary reactions of hydrolysis. In this work, a great value of water activity may lead to the hydrolysis of triacylglycerols into monoacylglycerols, diacylglycerols, and free fatty acids. The formation of these secondary products must be minimized. Finally, Miller *et al.*[10] showed that the initial step for the acyl-exchange is the hydrolysis and it is the limiting step. Consequently, it is important to determine the effect of water content on the transesterification reaction.

In order to quantify the evolution of the transesterification reaction, we have defined two parameters. First, the transesterification rate is given by

$$T(\%) = \frac{[OOP]_t + [OPO]_t + [PPO]_t + [POP]_t}{[OOO]_0 + [PPP]_0}$$

where $[\ldots]_t$ represents the concentration of the corresponding regioisomers at time t and $[\ldots]_0$ represents the initial concentration of triolein and tripalmitin. Second, the hydrolysis rate is defined as

$$H(\%) = \frac{[Mono]_t + [Di]_t}{3[Tri]_0} = \frac{\text{ester bonds broken at } t}{\text{initial ester bonds}}.$$

FIGURE 1 demonstrates the evolution of these two parameters versus the initial hydration of the enzymatic support. As the amount of water increases from 5% to 15%, both parameters demonstrate a slight increase to reach a maximum of 64% for
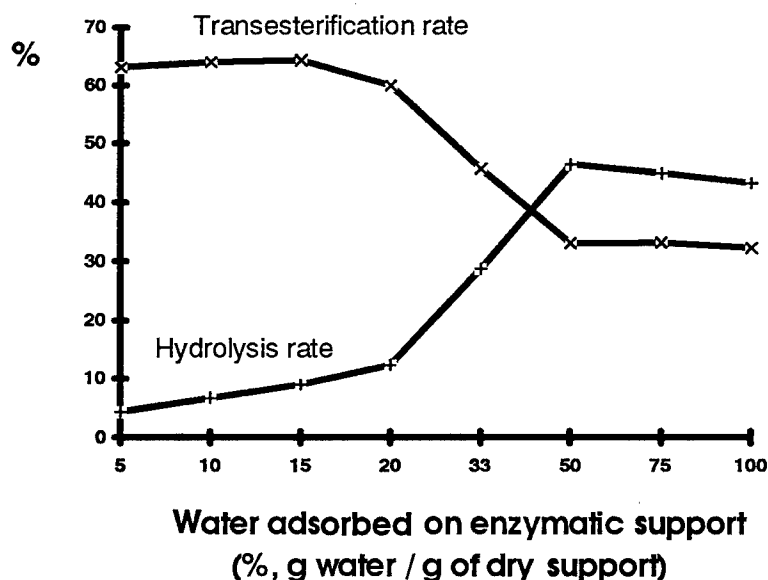
FIGURE 1. Influence of the water adsorbed on the enzymatic support on the transesterification and hydrolysis rates.
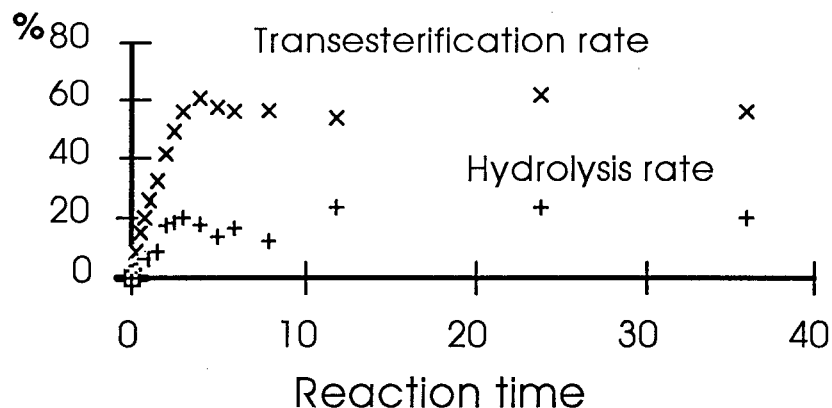
FIGURE 2. Transesterification and hydrolysis rates versus time.

transesterification and a value of 7% for the hydrolysis. In another part of the curve, between 15% and 50% (g/g) of adsorbed water on the support, the hydrolysis rate dramatically increases to 47%, whereas the transesterification rate drops to 33%. When water activity of the system increases, one can assume that the thermodynamic equilibrium is shifted towards hydrolysis. Beyond 50% (g/g) of adsorbed water on the support, both rates stabilize.

These results show that the optimum hydration of the enzymatic support is reached at between 4% and 15% of the water absorbed (g/g). In the following experiments, we used 10% of hydration, which corresponds to the initial water content of the commercial Lipozyme™.

TIME EVOLUTION OF THE TRANSESTERIFICATION RATE

Values obtained for the transesterification and hydrolysis rates, with 10% optimum water content of the enzymatic support, are presented in FIGURE 2.

The acyl-exchange reaction occurs with a great efficiency in the first 4 hours before the transesterification rate stabilizes at a value of 60%. The profile of the hydrolysis curve is very similar, but with a value at the plateau of 20%.

At equilibrium, the observed percentages of OOO/OOP/PPO/PPP (13.6/37.7/37.6/11.1) are close to those calculated, assuming that the phenomenon is following random exchange rules (12.5/37.5/37.5/12.5). The best incorporation rate (56% versus 50% initially) of oleic acid in the 2-position is obtained after 12 hours.

CONCLUSIONS

This work demonstrated that immobilized Lipozyme™ was an efficient catalyst for the acyl-exchange between triolein and tripalmitin in *n*-hexane, although its selectivity towards the desired incorporation of oleate was not achieved.

The optimization of water content was also carried out. The results showed that a value of 10% (g/g of support) maximized the transesterification rate by 60% and minimized the hydrolysis by 10–20%.

Currently, we are working on the accurate determination of intermediary product concentrations and time evolutions. The choice of a suitable enzyme that would more selectively catalyze the desired specific acyl-exchange is also under investigation.

REFERENCES

1. GURR, M. I. 1983. The nutritional significance of lipids. *In* Development in Dairy Chemistry. Volume 2. P. F. Fox, Ed.: 365–417. Applied Science Pub. London.
2. MARX, J. L. 1976. Atherosclerosis: the cholesterol connection. Science **194:** 711–755.
3. CHRISTIE, W. W. 1983. The composition and structure of milk lipids. *In* Development in Dairy Chemistry. Volume 2. P. F. Fox, Ed.: 1–35. Applied Science Pub. London.
4. HAYES, C., A. PRONCZUK, S. LINDSEY & D. DIERSON-SHADE. 1991. Dietary saturated fatty acids (12:0, 14:0, 16:0) differ in their impact on plasma cholesterol and lipoproteins. Am. J. Clin. Nutr. **53:** 491–498.
5. CHULALAKSANANUKUL, W., J. S. CONDORET, P. DELORME & R. M. WILLEMOT. 1990. Kinetic study of esterification by immobilized lipase in *n*-hexane. FEBS Lett. **276:** 181–184.
6. MARTY, A., W. CHULALAKSANANUKUL, R. M. WILLEMOT & J. S. CONDORET. 1992. Kinetics of lipase-catalyzed esterification in supercritical CO_2. Biotechnol. Bioeng. **39:** 273–280.
7. KERMASHA, S., S. KUBOW, M. SAFARI & A. REID. 1993. Determination of the positional distribution of fatty acids in butterfat triacylglycerols. J. Am. Chem. Soc. **70:** 169–173.
8. CHRISTIE, W. W. 1987. High Performance Chromatography and Lipids—A Practical Guide. Pergamon. Elmsford, New York.
9. HALLING, P. J. 1994. Thermodynamic predictions for biocatalysis in nonconventional media. Enzyme Microb. Technol. **16:** 178–206.
10. MILLER, D. A., J. M. PRAUSNITZ & H. W. BLANCH. 1991. Kinetics of lipase-catalyzed interesterification of triacylglycerols in cyclohexane. Enzyme Microb. Technol. **13:** 98–103.

Microbial D-Amino Acid Oxidases (EC 1.4.3.3)[a]

LUTZ FISCHER, MATTHIAS GABLER, ROY HÖRNER,
AND FRITZ WAGNER

Institute of Biochemistry and Biotechnology
Technical University of Braunschweig
D-38106 Braunschweig, Germany

INTRODUCTION

Today, the flavoprotein D-amino acid oxidase (D-AO) is used at industrial scale as one of the two biocatalysts taking part in the enzymatic two-step conversion of cephalosporin C to 7-aminocephalosporanic acid.[1] The latter is a key compound for the production of many semisynthetic, cephalosporin-based β-lactam drugs ($31 billion world market). Other important fields of application for the enantioselective D-AO are the production of α-keto acids[2] and pure L-amino acids.[3] The most-known D-AOs in the literature[4–6] originate from the yeasts, *Trigonopsis variabilis* and *Rhodotorula gracilis*, and pig kidney, but comprehensive, comparative data about their enzyme activities have not been published nor could they be exactly calculated based on published results.

This is due to the different, and sometimes unreliable, methods and conditions used for the determination of D-AO activity. This report describes the investigation and further development of D-AO assays with regard to reproducibility, specificity, side reactions, and sensitivity and, moreover, the determination and comparison of the comprehensive substrate spectra from known and new D-AOs.

MATERIALS AND METHODS

Microorganisms and Enzymes

The used microorganisms were *Trigonopsis variabilis* DSM 70714, *Rhodotorula gracilis* ATCC 26217, and the following isolates from soil samples, which were identified as *Alcaligenes denitrificans*, *Candida parapsilosis*, *Fusarium oxysporum*, and *Verticillium luteoalbum*. Pig kidney D-AO was purchased commercially from Boehringer Mannheim, Germany.

Media and Culture Conditions

The microorganisms, except *Trigonopsis variabilis*, were cultivated aerobically under shaking (100 rpm) at 30 °C in 2-L flasks with baffles containing a final volume

of 500 mL. The basal medium contained D-alanine (2 g/L) as the inducer, glucose (10 g/L), $(NH_4)_2SO_4$ (2 g/L), yeast extract (2 g/L), K_2HPO_4 (4 g/L), vitamins (40 μg/L biotin; 200 μg/L thiamine; 400 μg/L nicotinic acid; 200 μg/L 4-aminobenzoate), and the following metal salts: $MgSO_4 \cdot 7H_2O$ (1 g/L); $CaCl_2 \cdot 2H_2O$ (0.5 g/L); H_3BO_4 (0.1 g/L); $ZnSO_4 \cdot 7H_2O$ (40 mg/L); $NaMoO_4$ (40 mg/L); $CuSO_4 \cdot 5H_2O$ (45 mg/L); $FeSO_4 \cdot 7H_2O$ (25 mg/L). The pH of the medium was set to 7.0 without any further adjustment during growth. *Trigonopsis variabilis* was cultivated with $(NH_4)_2SO_4$ (4 g/L) as the nitrogen source and with *N*-carbamoyl-D,L-alanine (5 mM) as the inducer.[7] During cultivation, the D-AO activity was determined every 3 hours. The cells were harvested at their optimal point of activity (usually at the beginning of the stationary phase) by centrifugation at 4 °C and 12,000g for 30 min and were used immediately for the preparation of the cell-free extract.

Preparation of the Cell-free Extracts

The cell pastes of these microorganisms (3 g wet biomass) were suspended in 7 mL of potassium phosphate buffer (50 mM, pH 8.0) containing 3 mM EDTA and 0.1 M sucrose. The cells were disrupted by a mixer mill (MM 2, Retsch GmbH, Haan, Germany) with glass beads of $\sim$0.7-mm diameter at 4 °C for 20 min. The homogenate was centrifuged and the clear supernatant was used for further experiments.

Enzyme Assays

All assays were done in air-saturated solutions at 30 °C.

Peroxidase/o-Dianisidine Method

The reaction mixture contained 50 mM D-amino acid, 50 mM potassium phosphate buffer (pH 8.0), *o*-dianisidine (0.86 mM), peroxidase (3000 U), and enzyme solution in a final volume of 1 mL. The mixture was preincubated and started by adding the enzyme solution. After 1–5 min, the reaction was stopped with 500 μL of H_2SO_4 (30%). The activity was calculated by photometric measurements at 540 nm using an H_2O_2 calibration curve. The concentration of the amino acids for the substrate spectra was 50 mM, except for Tyr (2.5 mM).

Consumption of O_2 by a Clark Electrode

D-Amino acid oxidase was assayed by following the rate of oxygen consumption with a Clark electrode (WTW, Riomatic EO 200, Weilheim, Germany). The assay mixture contained 50 mM D-amino acid, 50 mM potassium phosphate buffer (pH 8.0), and enzyme solution in a final volume of 6 mL. This mixture was preincubated and started by adding the enzyme solution. The concentration of the amino acids for the substrate spectra was 50 mM, except for Tyr (2.5 mM).

Lactate Dehydrogenase/NADH Method

Using D-alanine as the substrate, the activity of D-AO was estimated photometrically in a coupled enzyme test. In a solution containing D-alanine (37.5 mM), potassium phosphate buffer (pH 8.0), lactate dehydrogenase (LDH) (9 U/mL), and NADH + H⁺ (0.23 mM), the decrease in absorption at 340 nm was monitored (molar absorption coefficient of NADH = 6300 mol/L-cm).

Dinitrophenylhydrazine Method

D-AO activity was assayed by measuring the production of keto acid. The reaction mixture contained 50 mM D-amino acid, 50 mM potassium phosphate buffer (pH 8.0), and enzyme solution in a final volume of 1 mL. After incubation for 10 min, the amount of keto acid produced was determined by adding 1 mL of 2,4-dinitrophenylhydrazine (final concentration, 2.5 mM). After 10 min, 1.4 mL of 3 M NaOH was added and the sample was photometrically measured at 550 nm using a pyruvate calibration curve.

TABLE 1. Enzyme Activities and Inducers for the Investigated Microbial D-AOs[a]

Microorganism	*Verticillium luteoalbum*	*Fusarium oxysporum*	*Candida parapsilosis*	*Rhodotorula gracilis*	*Trigonopsis variabilis*	*Alcaligenes denitrificans*
inducer	D-alanine	D-alanine	D-alanine	D-alanine	*N*-carbamoyl-D,L-alanine	D-alanine
activity (nkat/g wet biomass)	14	868	3	108	1809	40[b]

[a]D-Alanine was used as the substrate; measured by the peroxidase/*o*-dianisidine method.
[b]Assay by the oxygen electrode method; see TABLE 2.

RESULTS AND DISCUSSION

The new microorganisms were the yeast *Candida parapsilosis*, the two fungi *Fusarium oxysporum* and *Verticillium luteoalbum*, and the bacterium *Alcaligenes denitrificans*. The absolute activities of the new and known microorganisms and the used inducers are presented in TABLE 1. *Trigonopsis variabilis* was the best D-AO producer, and the amount of activity observed for *Fusarium oxysporum* was considerably high (not optimized).

The cell-free enzyme solutions were tested for D-AO activity by various assays (see FIGURE 1). The results are shown in TABLE 2. Depending on which assay was used, the values deviated up to 300%, although in each case the same stock enzyme solution was taken under the same conditions. Generally, the highest values were obtained by the LDH/NADH method and the lowest values by the dinitrophenylhydrazine method.

Each assay was influenced by individual factors and properties:

1. The peroxidase/*o*-dianisidine method was specific for oxidases and was highly sensitive, and the resulting chromogene was very stable over time. Catalase
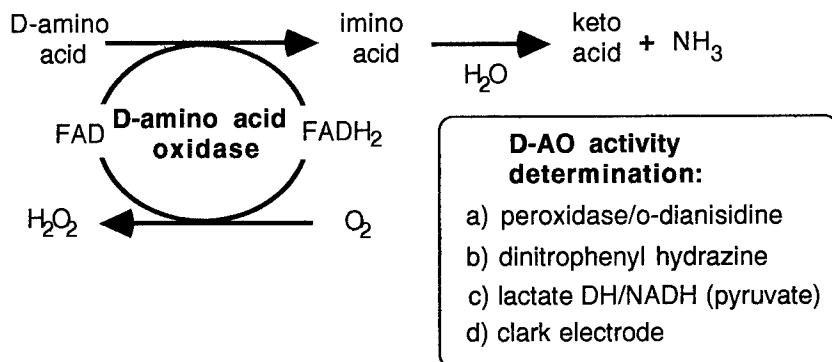
FIGURE 1. Reaction mechanism and possible methods to determine D-AO activity.

activities were inhibited by the chromogene o-dianisidine and were additionally suppressed through a high excess of peroxidase. The method was disturbed when direct oxidation of the chromogene, caused by unknown side activities in the crude enzyme solution, took place (in case of A. denitrificans).

2. Measurement of oxygen consumption using an oxygen electrode was less specific and less sensitive. The assay was crucially disturbed by catalase activity. Additionally, the true oxygen concentration at the beginning of the reaction can only be estimated chemically because the value published in reference tables and taken for calculations is valid for pure water at 30 °C.

3. The lactate dehydrogenase/NADH method could only be used when D-alanine was the substrate. It was sometimes significantly disturbed by side reactions (dehydrogenase, transferase, etc.). Depending on the origin of the crude enzyme solution, overly high blank activities were observed.

4. The dinitrophenylhydrazine method was less specific and less sensitive, and the resulting dye was unstable under the necessary alkaline conditions. With regard to the calibration standards, another disadvantage emerges because most of the corresponding α-keto acids are not commercially available.

TABLE 2. Results of Various D-AO Assays (nkat/mg protein)[a]

Microorganism	H_2O_2 (Peroxidase/ o-Dianisidine)	α-Keto Acid (Hydrazine)	Pyruvate (LDH/NADH)	O_2 (Oxygen Electrode)
Verticillium luteoalbum	0.84	0.60	0.80	0.62
Fusarium oxysporum	21.42	16.63	32.51	20.35
Alcaligenes denitrificans	?[b]	2.19	3.77	2.13
Candida parapsilosis	0.12	0.18	0.20	0.14
Trigonopsis variabilis	29.52	13.93	41.76	36.46[c]
Rhodotorula gracilis	5.62	4.27	9.21	7.19

[a]D-Alanine; air-saturated solution; 30 °C.
[b]Not applicable due to direct chromogene oxidation.
[c]Activity with pure oxygen: 98.44.

In summary, the most-suitable assay for measuring D-AO activities was the peroxidase/
o-dianisidine method.

Hence, except for *A. denitrificans* (oxygen electrode method), the peroxidase/*o*-
dianisidine assay was used for establishing the substrate spectrum of each D-AO,
including the well-known pig kidney oxidase. As shown in FIGURE 2, *T. variabilis* was
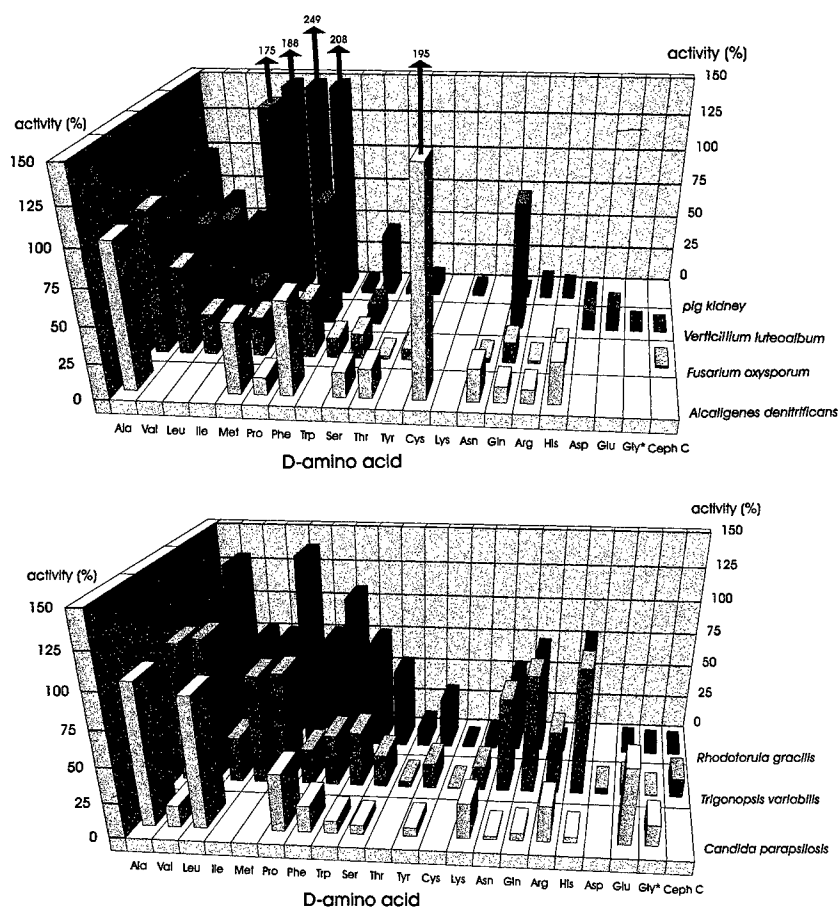
FIGURE 2. Substrate spectra of the D-AOs (* = not chiral).

still the best biocatalyst for the conversion of cephalosporin C. Only two of the four
new D-AO producers accepted cephalosporin C (about 1–2% relative activity). All
eukaryotic oxidases demonstrated a high acceptance of the hydrophobic D-amino
acids. However, the bacterial D-AO showed a unique high activity versus D-cysteine.
Generally, no L-amino acids were substrates for the tested enzymes.

ACKNOWLEDGMENTS

REFERENCES

1. CONLON, H. D., J. BAQAL, K. BAKER, Y. Q. SHEN, B. L. WONG, R. NOLLES & C. W. RAUSCH. 1995. Two-step immobilized enzyme conversion of cephalosporin C to 7-aminocephalo-sporanic acid. Biotechnol. Bioeng. **46:** 510–513.
2. BUTÓ, S., L. POLLEGIONI, L. D'ANGIURO & M. S. PILONE. 1994. Evaluation of D-amino acid oxidase from *Rhodotorula gracilis* for the production of α-keto acids: a reactor system. Biotechnol. Bioeng. **44:** 1288–1294.
3. FISCHER, L., R. HÖRNER & F. WAGNER. 1995. Production of L-amino acids by applying D-amino acid oxidases. Ann. N.Y. Acad. Sci. **750:** 415–420.
4. CURTI, B., S. RONCHI & M. S. PILONE. 1992. D- and L-amino acid oxidases. *In* Chemistry and Biochemistry of Flavoenzymes. Volume III. F. Müller, Ed.: 69–94. CRC Press. Boca Raton, Florida.
5. FAOTTO, L., L. POLLEGIONI, F. CECILIANI, S. RONCHI & M. S. PILONE. 1995. The primary structure of D-amino acid oxidase from *Rhodotorula gracilis.* Biotechnol. Lett. **17:** 193–198.
6. POLLEGIONI, L., S. BUTÓ, W. TISCHER, S. GHISLA & M. S. PILONE. 1993. Characterization of D-amino acid oxidase from *Trigonopsis variabilis.* Biochem. Mol. Biol. Int. **31:** 709–717.
7. HÖRNER, R., L. FISCHER & F. WAGNER. 1996. Induction of the D-amino acid oxidase from *Trigonopsis variabilis.* Appl. Environ. Microbiol. **62**(6): 2106–2110.

Enzymatic Resolution of (R,S)-2-Octanol Catalyzed by Lipase from Pseudomonas Species[a]

XIU-GONG GAO,[b] SHU-GUI CAO,[c] HONG YANG,[c]
NI-NI GUO,[c] AND KE-CHANG ZHANG[b]

[b]Department of Biotechnology
Wuxi University of Light Industry
Wuxi 214036, People's Republic of China

[c]National Laboratory of Enzyme Engineering
Jilin University
Changchun 130023, People's Republic of China

INTRODUCTION

Racemate resolution has long been a hard nut to crack for organic chemists. The recent advent of nonaqueous enzymology has led to the realization that enzymes can function in nonaqueous media as practical catalysts, and asymmetric esterifications or transesterifications catalyzed by lipases in organic solvents are now becoming a powerful method of choice for facile kinetic resolutions of racemic alcohols, acids, and their derivatives.[1] In the present paper, we report the results of our studies on enzymatic resolution of racemic 2-octanol catalyzed by a lipase from *Pseudomonas* sp. in organic solvents. The effects of acyl donors, solvents, and enzyme microenvironment were investigated. Treatment of the enzyme with amphipathic A afforded a preparation that exhibited a marked improvement in its enantioselectivity.

MATERIALS AND METHODS

Materials

Pseudomonas sp. lipase (PSL) was produced from *Pseudomonas* sp. 2106, a wild strain newly isolated from soil by our laboratory. The chiral reagents, (R)-(−)- and (S)-(+)-1-(1-naphthyl) ethyl isocyanates [(R)-NEI and (S)-NEI], were obtained commercially from Aldrich (Milwaukee, Wisconsin). Amphipathic A was a kind present from the Department of Chemistry of Northeast Normal University (Changchun, China), and its structure is shown in FIGURE 1. All other reagents and solvents were obtained from commercial sources and were of analytical grade. Prior to use, they were dehydrated by shaking with 4-Å molecular sieves and contained less than 0.02% (v/v) water.

Methods

A typical experimental procedure is as follows: The lipase powder was added to a mixture of (R,S)-2-octanol and a carboxylic acid dissolved in cyclohexane. The suspension was vigorously shaken at 37 °C and, periodically, aliquots were withdrawn. The conversion rate of 2-octanol and the enantiomeric excess of the remaining 2-octanol were determined by HPLC analysis according to the method of Hirata et al.[2] using a 3.9 × 300 mm (μBorasil Silica, 10 μm) column, which was eluted with a solvent system of 0.3% (v/v) ethanol in cyclohexane at a rate of 1.0 mL/min. The absorbance at 254 nm was monitored with a Waters Model 440 detector and a Hewlett-Packard 3390A integrator.

RESULTS AND DISCUSSION

Effect of Acyl Chain Length

PSL was found to catalyze the esterification of (R)-2-octanol more efficiently than the S-isomer in cyclohexane with all carboxylic acids tested (ranging from C_2 to C_{18}). The effect of the acid chain length is depicted in FIGURE 2. A clear minimum of both reactivity and enantioselectivity was observed for the six-carbon acid and a maximum for the eight-carbon one. This may be well elucidated by an acyl binding model similar to that proposed by Parida and Dordick:[4] there exist two acyl binding "pockets" or regions in PSL's active site—one small, in which acids with carbon chain lengths of less than six bind well; the other large, in which acids with carbon chain lengths of greater than six bind well and which is optimal for the eight-carbon acid. The acids that bind well in the pockets exhibit high catalytic efficiency. The fitness of binding of acids also influences the interaction of the resulting acyl-enzyme intermediate with the two enantiomers of 2-octanol, and high enantioselectivity is obtained for acids that bind fitly.

Effect of Solvents

The activity of PSL in different solvents was found to correlate well with the hydrophobicity (log P value) of the solvents (FIGURE 3). A plausible explanation is that the stripping of water from the enzyme in hydrophilic solvents (low log P values) is more severe than in hydrophobic solvents (high log P values). The loss of enzyme-bound water affects the structure and dynamics of the active site and results in poor values of V_{max}/K_m.[6]
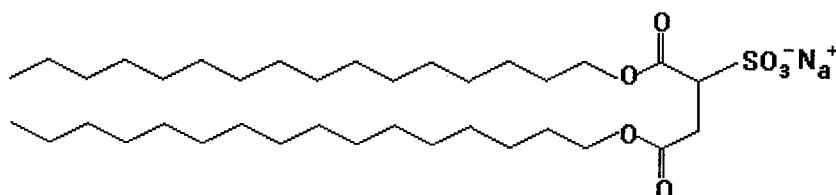
FIGURE 1. The chemical structure of the amphipathic A molecule.
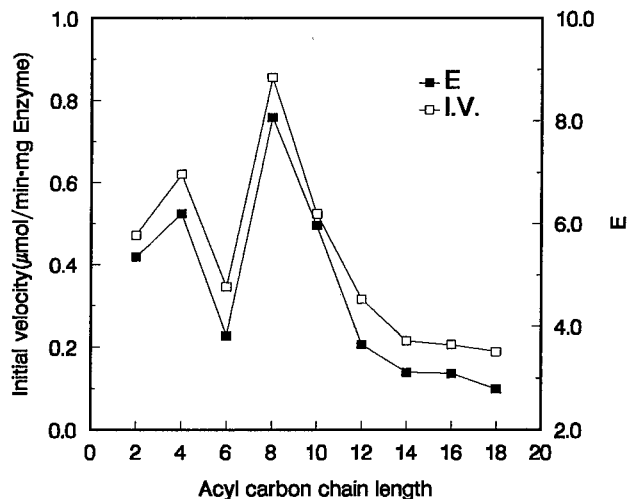
FIGURE 2. Dependence of initial velocity and enantiomeric ratio (E value) of the PSL-catalyzed enantioselective esterification of racemic 2-octanol in cyclohexane on the carbon chain length of the carboxylic acids. Conditions: 20 mg/mL PSL, 0.28 M racemic 2-octanol, 0.40 M acid, shaken at 150 rpm at 37 °C; for other conditions and procedures, see the text. No esterification was observed without enzyme. The E value was calculated from the following equation according to Chen *et al.*:[3] $E = \ln[(1 - c)(1 - ee_s)]/\ln[(1 - c)(1 + ee_s)]$, where c is the conversion rate of the substrate, racemic 2-octanol, and ee_s represents the enantiomeric excess of the remaining substrate, 2-octanol.

The enantioselectivity of PSL in various solvents was found to be an unequivocal function of the dielectric constant and dipole moment of the solvents (FIGURES 4A and 4B). To rationalize this phenomenon, we carried out a kinetic investigation to measure the V_{max} and K_m values for each enantiomer of 2-octanol in six representative solvents by the method of Gu and Sih,[8] and the V_{max}/K_m values were calculated and normalized according to Fitzpatrick and Klibanov.[9] The resultant values in TABLE 1 indicate that most of the relaxation of enantioselectivity in solvents with a high dielectric constant or dipole moment is due to an increase in the reactivity of the slow-reacting S-isomer.

The above conclusion leads to the development of a binding model for the R- and S-enantiomers of 2-octanol in the binding site of acyl-lipase (FIGURE 5). The model predicts that the nucleophile binding site of PSL contains two "pockets"—large and small. The binding fashion conducive to the deacylation reaction for the R-enantiomer of 2-octanol is shown in the left portion of FIGURE 5, in which the hexyl group occupies the large pocket and the methyl group occupies the small one. The binding for the S-enantiomer is shown in the right portion, which illustrates that the hexyl and the methyl groups substitute for each other in the two binding pockets and the hexyl group experiences severe steric hindrances in fitting into the small pocket. Consequently, the R-isomer is much more reactive in the esterification than the S-isomer. A dominant feature of enzymes in anhydrous media is their high conformational rigidity. The lipase should be much more rigid in anhydrous solvents of low dielectric constants or dipole moments than in those of high dielectric constants or

dipole moments.[9] Clearly, when the protein flexibility increases (as a result of high dielectric constant or dipole moment of the solvent), the steric constraints for the S-isomer become more forgiving, thereby relaxing the enantioselectivity. These reasonings could explain the aforementioned dependence of the lipase enantioselectivity on the solvents employed.

Effect of Enzyme Microenvironment

The results are shown in FIGURES 6A, 6B, and 6C. The water content of the reaction mixture has a significant impact on both reactivity and enantioselectivity,
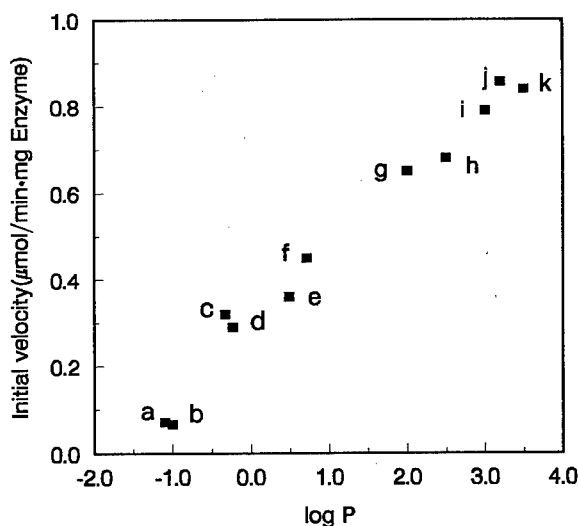
FIGURE 3. Catalytic efficiency of PSL in esterification of racemic 2-octanol with octanoic acid in anhydrous solvents as a function of the hydrophobicity (log P) of the solvents. Experimental conditions were the same as in FIGURE 2. No esterification was observed without enzyme. Solvents: a, 1,4-dioxane; b, dimethylformamide; c, acetonitrile; d, acetone; e, tetrahydrofuran; f, pyridine; g, benzene; h, toluene; i, tetrachloromethane; j, cyclohexane; k, hexane. For the definition of log P and its values for the above solvents, see Laane *et al.*[5]

with an optimum value of 0.4% (v/v). Although the pH value of the buffer solution from which the enzyme was lyophilized affects the former to some extent (with an optimal value of 9.0, coinciding with that for lipase activity in aqueous solution), it does not influence the latter much. The ionic strength of the buffer has no evident effect on either in the range of 0.01–0.05 M.

Effect of Amphipathics

PSL was treated with certain kinds of amphipathics, including lecithin, AOT, sodium deoxycholate, and amphipathic A, in an attempt to improve its enantioselec-
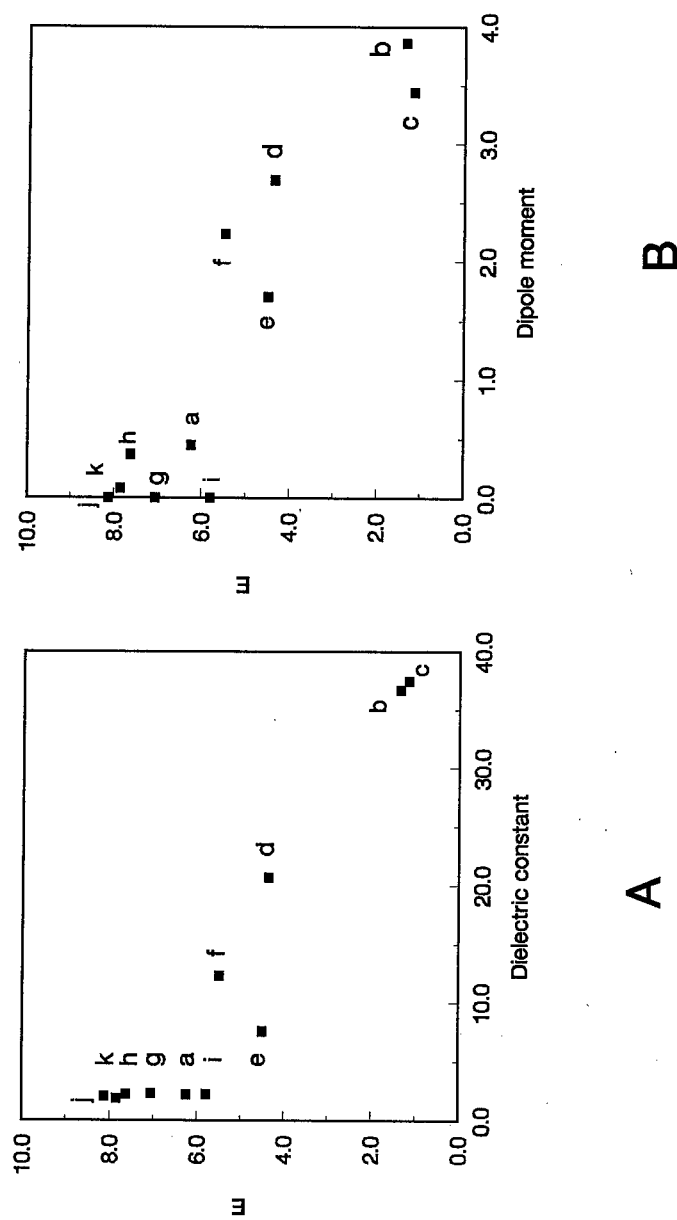
FIGURE 4. Enantioselectivity (E value) of PSL in asymmetric esterification of racemic 2-octanol with octanoic acid in anhydrous solvents as a function of the dielectric constant (A) and dipole moment (B) of the solvents. Experimental conditions were the same as in FIGURE 2 and the solvents employed were the same as in FIGURE 3. The values for the dielectric constant and dipole moment were taken from Reichardt.[7]

TABLE 1. Normalized Kinetic Parameters of the Enantioselectivity of PSL in Asymmetric Esterification of Racemic 2-Octanol in Anhydrous Solvents[a]

| | Normalized V_{max}/K_m[b] | | Enantioselectivity[c] |
Solvent	R Isomer	S Isomer	(E Value)
cyclohexane	0.42	0.052	8.12
benzene	0.46	0.065	7.05
1,4-dioxane	0.45	0.072	6.23
pyridine	0.36	0.066	5.48
tetrahydrofuran	0.52	0.120	4.50
dimethylformamide	0.34	0.251	1.35

[a]Experimental conditions were the same as in FIGURE 2. V_{max} and K_m values for each enantiomer of 2-octanol were measured by the method of Gu and Sih,[8] and the resultant V_{max}/K_m values (data not shown) were normalized according to Fitzpatrick and Klibanov[9] to subtract the solvent effect on the reactivity of both enantiomers.

[b]n-Octanol was substituted for 2-octanol in the esterification reaction with octanoic acid under identical conditions in various solvents. The aforementioned values of V_{max}/K_m for each enantiomer of 2-octanol were divided by the V_{max}/K_m values for n-octanol in the same solvents.

[c]Obtained as in FIGURE 2.

tivity. Although the former three molecules have no evident effects (data not shown), it is striking that amphipathic A can enhance the lipase enantioselectivity substantially (FIGURE 7). A possible explanation is that amphipathic A can modify the enzyme noncovalently, leading to a protein conformation that exhibits markedly enhanced enantioselectivity. Further investigation is needed to verify this hypothesis.

CONCLUSIONS

The chain length of the acyl donors and the nature of the organic solvents affect the catalytic efficiency and enantioselectivity of the PSL-catalyzed asymmetric
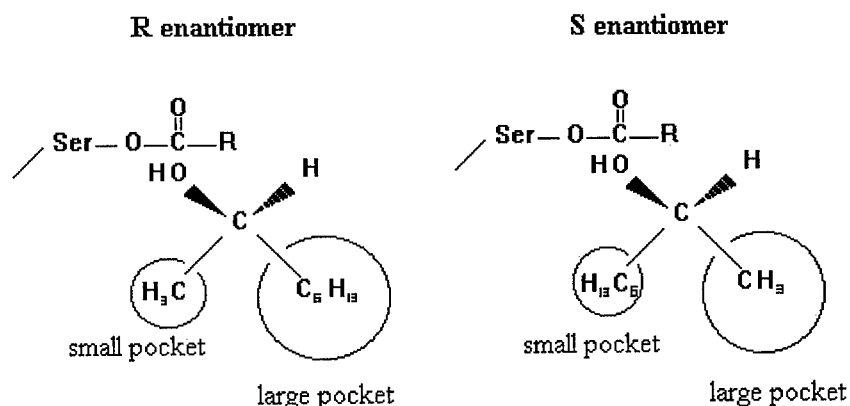
FIGURE 5. Schematic representation of the modes of binding of the R- and S-enantiomers of 2-octanol to the binding site of the acyl-lipase (PSL). Ser refers to the serine residue in the catalytic site of PSL with which the acyl donor reacts to form the acyl-enzyme.
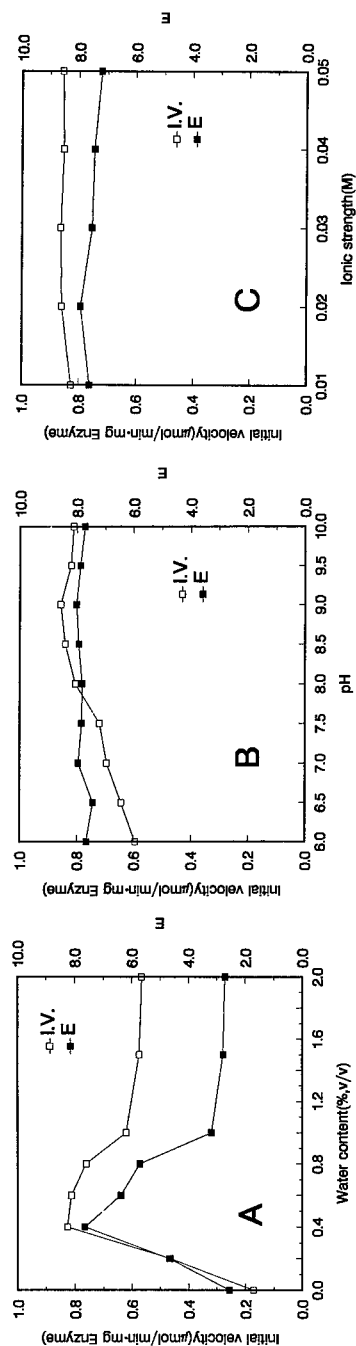
FIGURE 6. Effects of the enzyme microenvironment on the activity and enantioselectivity of PSL in the esterification reaction of racemic 2-octanol with octanoic acid in cyclohexane. (A) Effect of water content. (B) Effect of the pH value of the buffer solution from which the enzyme was lyophilized. PSL was dissolved in 0.02 M phosphate buffers with varying pH values (6.0–10.0) and then lyophilized. The resultant enzyme preparations were used to catalyze the esterification reaction. (C) Effect of ionic strength of the buffer solution from which the enzyme was lyophilized. PSL was dissolved in phosphate buffers with a pH of 9.0 and varying salt concentrations (0.01–0.05 M) and then lyophilized. The resultant enzyme preparations were used to catalyze the esterification reaction. Other conditions were the same as in FIGURE 2.
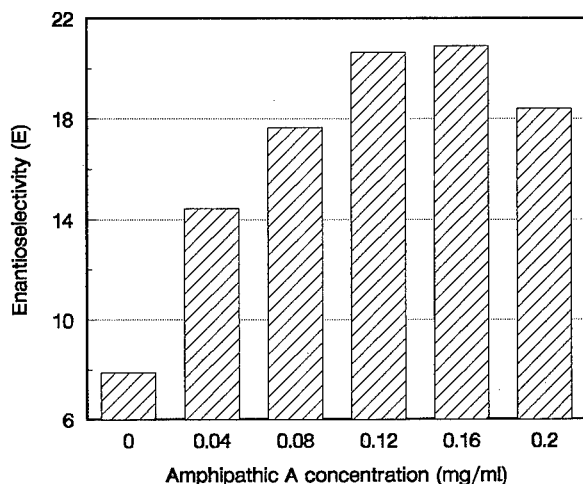
FIGURE 7. Effect of amphipathic A on the enantioselectivity of PSL in asymmetric esterification of racemic 2-octanol with octanoic acid. Amphipathic A was added at the indicated concentrations. Other conditions were the same as in FIGURE 2.

esterification of racemic 2-octanol. To our knowledge, this report represents the first demonstration that enzyme activity and enantioselectivity are controlled by different physicochemical parameters of the solvents, that is, hydrophobicity and dielectric constant (or dipole moment), respectively.

Our results also clearly show that enantioselectivity of PSL is markedly enhanced by treatment of the enzyme with an amphipathic. This furnishes chemists with an alternative approach for extending the usefulness of known enzymes for racemate separation. Because the discovery of new enzymes is a slow painstaking process, the treatment of known enzymes with amphipathics provides a rapid means of generating enzyme preparations with enhanced enantioselective properties.

REFERENCES

1. KLIBANOV, A. M. 1990. Acc. Chem. Res. **23:** 114–120.
2. HIRATA, H., T. YAMASHINA, K. HIGUCHI, K. SAKAKI & I. IIDA. 1991. J. Jpn. Oil Chem. Soc. **40:** 995–1000.
3. CHEN, C. S., Y. FUJIMOTO, G. GIRDAUKAS & C. J. SIH. 1982. J. Am. Chem. Soc. **104:** 7294–7299.
4. PARIDA, S. & J. S. DORDICK. 1993. J. Org. Chem. **58:** 3238–3244.
5. LAANE, C., S. BOEREN, K. VOS & C. VEEGER. 1987. Biotechnol. Bioeng. **30:** 81–87.
6. GORMAN, L. S. & J. S. DORDICK. 1992. Biotechnol. Bioeng. **39:** 392–397.
7. REICHARDT, C. 1988. Solvents and Solvent Effects in Organic Chemistry. Second edition, p. 408–410. Verlag Chemie. Weinheim.
8. GU, Q-M. & C. J. SIH. 1992. Biocatalysis **6:** 115–126.
9. FITZPATRICK, P. A. & A. M. KLIBANOV. 1991. J. Am. Chem. Soc. **113:** 3166–3171.

Novel Sol-Gel Matrices for the Immobilization of Enzymes[a]

IQBAL GILL AND ANTONIO BALLESTEROS

Instituto de Catalisis
CSIC
Campus Universidad Autonoma
28049 Madrid, Spain

INTRODUCTION

Sol-gel glasses have been examined as matrices for the immobilization of cells, organelles, proteins, and enzymes such as lipases, trypsin, phosphatase, and glucose oxidase.[1-4] Sol-gel entrapment possesses a number of desirable attributes: (i) the enzyme is physically entrapped in a rigid glass framework that provides a matrix of stabilizing interactions and virtually abolishes leaching phenomena; (ii) the high degree of biomolecule rigidity reduces denaturation phenomena; (iii) the hydrophilicity of the matrix can be readily controlled; (iv) the inorganic matrix imparts high mechanical and chemical stability; (v) optically transparent glasses are easily fabricated in a variety of geometries.

Although this technology has been successfully applied to the preparation of biocatalysts and biosensor elements,[1-4] a number of problems inherent to conventional sol-gel fabrication have come to light: (i) prevailing protocols rely on the hydrolysis of alkyl silicates in aqueous-organic media and this can result in solvent-induced denaturation of the enzyme; (ii) the low hydrolytic reactivity of simple alkyl silicate esters necessitates acid, base, or fluoride catalysts in order to initiate polymerization; (iii) severe shrinkage and pore collapse are typically encountered during the hydrogel to xerogel transition.

We now report the application of a novel range of activated, hydrophilic sol-gel intermediates with the following properties: (i) high degree of solubility/miscibility with water, thereby avoiding the use of cosolvents; (ii) the compounds autohydrolyze in aqueous media; (iii) hydrolysis releases lyoprotectants, which act as enzyme stabilizers; (iv) significantly less collapse is seen during xerogel formation and this allows the preparation of mesoporous and macroporous materials. A range of enzymes, including subtilisin and rabbit muscle aldolase (RAMA), have been entrapped in monosilicate- and polysilicate-derived glasses under mild conditions using this methodology. The resulting biocatalysts exhibited a high degree of activity and stability in aqueous-organic and low-water media and readily effected model biotransformations under these conditions.

MATERIALS AND METHODS

Subtilisin, rabbit muscle aldolase (RAMA), *N*-Cbz-L-tyrosine, L-leucinamide, dihydroxy-acetone phosphate (DHAP), *N*-acetyl-L-tyrosine ethyl ester (ATEE),

fructose-1,6-diphosphate (FDP), and biological buffers were obtained from Sigma. Tetramethyl silicate, metal alkoxides, 2-phenyl-ethanal, and all organic solvents were purchased from Aldrich. Poly(alkyl silicate) esters were acquired from Fluorochem Limited (Derbyshire, England).

The synthesis of the monosilicate and polysilicate precursors and the doped intermediates will be described elsewhere.[5] Enzymes were typically immobilized as follows: Silicate precursor (1.0 g) was mixed with ice-cold water (0.2–0.5 mL) in a sealed vial and the mixture was stirred in an ice bath for 1–15 min until homogeneity was achieved. Enzyme (1–100 mg) in buffer (0.2–0.5 mL of 100–200 mM) was then added and stirring continued for 5 min. The mixture was then allowed to gel and mature at 5 °C for 15–20 h, and the resultant hydrogel was dried at room temperature for 20 h or alternatively freeze-dried. The xerogel product was then extracted with a suitable buffer solution for 1–2 h and dried. In the case of RAMA, immobilization was carried out under helium, in the presence of 10 mM dithiothreitol to prevent oxidation of the enzyme. The fraction of enzyme immobilized was determined by measuring the amount of protein leached from the glass during the washing step, using the Lowry method. The activities of the biocatalysts were measured using standard reactions: ATEE hydrolysis for subtilisin and FDP hydrolysis for RAMA.

The subtilisin-mediated synthesis of N-Cbz-L-tyrosyl-leucinamide was implemented by incubating the immobilized enzyme (100 mg of biocatalyst with an enzyme loading of 50 mg/g) with a solution of N-Cbz-L-tyrosine ethyl ester (0.3 M) and L-leucinamide (0.3 M) in acetonitrile:ethanol containing 2–5% v/v of water. The RAMA-catalyzed synthesis of (3S,4R)-1,3,4-trihydroxy-5-phenyl-pentan-2-one-1-phosphate (THPP) was carried out by incubating the immobilized enzyme (100 mg of catalyst with an enzyme loading of 5 mg/g) with a solution of DHAP (30 mM) and 2-phenyl-ethanal (20 mM) in 7:3 50 mM MOPS buffer, pH 7.0, containing 0.5 mM magnesium chloride and 0.5 mM dithiothreitol/acetonitrile, under a helium atmosphere. After 10 h, the catalyst was pressure-filtered under nitrogen and washed with 5 mL of 7:3 buffer/acetonitrile, and the reaction was repeated. All reactions were carried out in sealed vials at 37 °C using a reciprocal shaker-incubator.

Reactions were analyzed by HPLC, using an LDC Milton Roy CM4000 pump connected to a Spectra Physics SP8450 UV/VIS detector or an ACS light scattering detector II, an LDC Marathon autosampler, and an HP Chemstation. Samples were quenched with pure methanol and then analyzed on a 0.46 × 15 cm Hichrom RPB5 column or a 0.46 × 15 cm Hypercarb column, operated at a flow rate of 1 mL/min and maintained at 40 °C. Methanol, acetonitrile, 2:8 methanol/water, and 1:9 acetonitrile/water were used as the mobile phases.

RESULTS AND DISCUSSION

The enzymes examined were readily immobilized at loadings of 1–100 mg/g, with protein retentions of 91–97% and with immobilization efficiencies of 73–93%. The entrapped enzymes were efficient catalysts for effecting model reactions performed in aqueous-organic and low-water organic media, and a superior degree of stability and activity was observed for these biocatalysts as compared with the native enzymes or those immobilized on supports such as Celite. For example, RAMA, which is
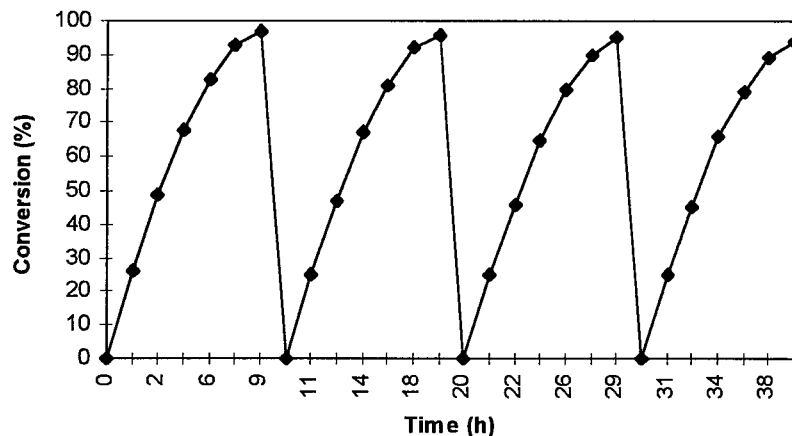
FIGURE 1. Cycles of THPP synthesis catalyzed by silicate-entrapped RAMA.

rapidly inactivated in a matter of hours ($t_{1/2}$ is 2–3 h) in aqueous media, was found to be very stable when entrapped in a pure silicate glass and readily performed the synthesis of THPP in a 7:3 acetonitrile/buffer mixture (FIGURE 1).

Indeed, negligible loss of activity was observed over six cycles of biocatalyst reuse and the high product yield was essentially maintained unchanged. In addition, the inclusion of approximately 10–15% w/w of titania or zirconia led to an increase in RAMA activity due to an increase in matrix porosity and an enhanced activity retention during entrapment (FIGURE 2).
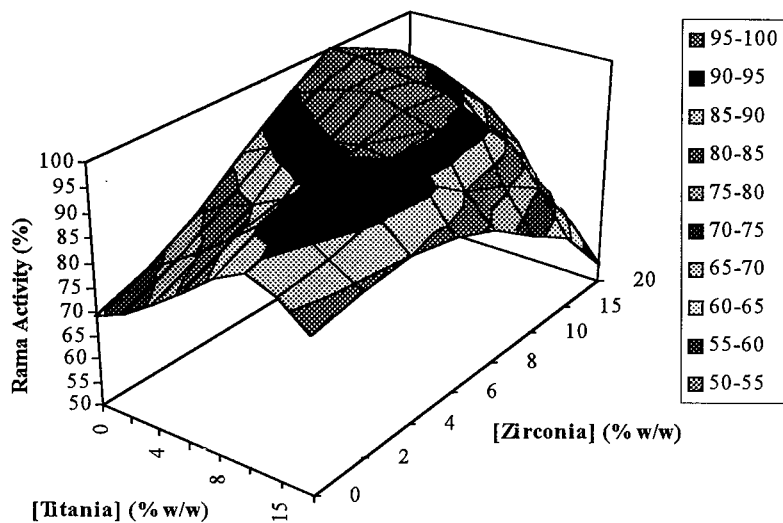
FIGURE 2. Effect of metal oxide doping on the activity of silicate-entrapped RAMA.
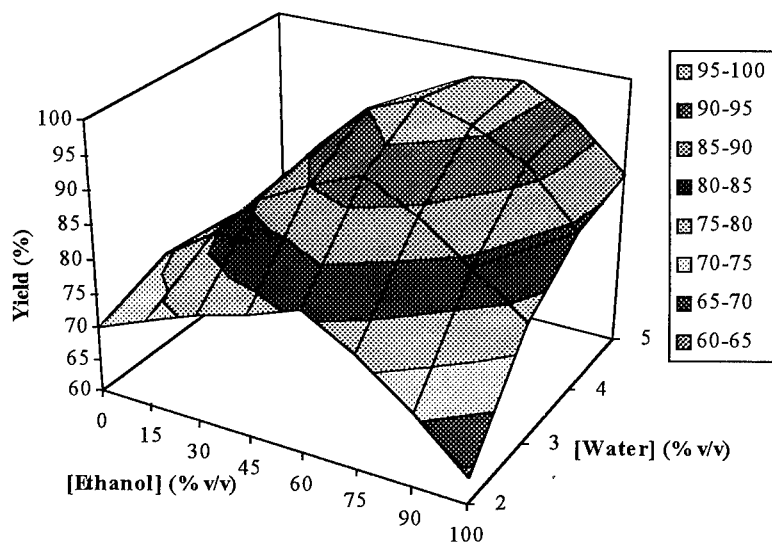
FIGURE 3. Effect of water and ethanol concentrations on dipeptide synthesis catalyzed by silica-entrapped subtilisin.

In addition, the glass-entrapped enzymes were found to tolerate high concentrations of polar/hydrophilic organic solvents, without undue deterioration in enzyme activity/stability. Thus, in the case of subtilisin (FIGURE 3), ethanol, DMF, and DMSO concentrations of up to 80%, 40%, and 40% v/v, respectively, could be employed, without greatly affecting the dipeptide yield. Similarly, immobilized RAMA was observed to perform efficiently in aqueous-organic mixtures in the presence of 40% v/v of dioxane or 20% v/v of DMF or DMSO.

These results indicate that the described methodology offers a facile and mild approach to sol-gel immobilization, which should be readily applicable to a range of enzymes of interest.

REFERENCES

1. ELLERBY, L. M., C. R. NISHIDA, F. NISHIDA, F. A. YAMANAKA, B. DUNN, J. S. VALENTINE & J. I. ZINK. 1992. Science **255:** 1113.
2. AVNIR, D., S. BRAUN, O. LEV & M. OTTOLENGHI. 1994. Chem. Mater. **6:** 1605.
3. DAVE, B. C., B. DUNN, J. S. VALENTINE & J. I. ZINK. 1994. Anal. Chem. **66:** 1120A.
4. REETZ, M. T., A. ZONTA & J. SIMPELKAMP. 1995. Angew. Chem. Int. Ed. Engl. **34:** 301.
5. GILL, I. & A. BALLESTEROS. 1996. In preparation.

Production and Stabilization of Pure Maltose Phosphorylase from *Lactobacillus brevis* for Sensing Inorganic Phosphate[a]

S. HÜWEL, L. HAALCK,[b] N. CONRATH, AND F. SPENER

Institute of Chemical and Biochemical Sensor Research
and
Department of Biochemistry
University of Münster
D-48149 Münster, Germany

INTRODUCTION

The determination of inorganic phosphate is especially important in environmental, food, and clinical analyses. As an alternative to common methods for the determination of inorganic phosphate, for example, colorimetric assays[1] or HPLC, we developed an amperometric biosensor based on an enzyme sequence using maltose phosphorylase as the key enzyme[2,3] (FIGURE 1). Maltose phosphorylase catalyzes the phosphorolysis of maltose to β-D-glucose-1-phosphate and α-D-glucose using inorganic phosphate as the cosubstrate. The enzyme was isolated from various microbial sources, but in all cases the purification procedure was laborious and resulted in a small recovery of enzyme activity. In the field of application, the enzyme was used, for example, to determine the enzyme activity of α-amylase,[4] utilizing the release of maltose during this reaction, or for the detection of maltose in the presence of other oligosaccharides.[5]

In this paper, we describe an effective and rapid purification procedure for maltose phosphorylase (MP) from *Lactobacillus brevis* and its further characterization. Moreover, the impact of buffers, carbohydrates, polyhydric alcohols, and polymers on the storage as well as thermal stability of the purified enzyme will be discussed.

MATERIALS AND METHODS

Maltose phosphorylase (MP) was isolated from *Lactobacillus brevis* ATCC 8287 as described elsewhere.[6] For storage stability experiments, pure MP was dialyzed against distilled water. An aliquot of this stock solution was added to a solution of buffer, carbohydrate, polyhydric alcohol (10 mM each), and polymer [0.1% (w/w) each]. The final concentration of MP was 66 μg/mL. The initial enzyme activity of

[b]To whom all correspondence should be addressed.

each preparation was determined under standard test conditions.[6] Prior to lyophilization, samples of 200 μL were placed in 1.5-mL Eppendorf test tubes and frozen rapidly in a precooled (−40 °C) ethanol bath. The samples were lyophilized for 18 h at a pressure of 0.3 mbar and a shelf temperature of 30 °C. The residual activity of the samples was determined after rehydration in 200 μL of distilled water and is defined as the difference in enzyme activity before and after lyophilization.

RESULTS AND DISCUSSION

The purification procedure for maltose phosphorylase included anion exchange chromatography on Fractogel TMAE™ as the capturizing step, Sephacryl S 300™ gel filtration, and hydroxyapatite chromatography according to reference 6. The gel
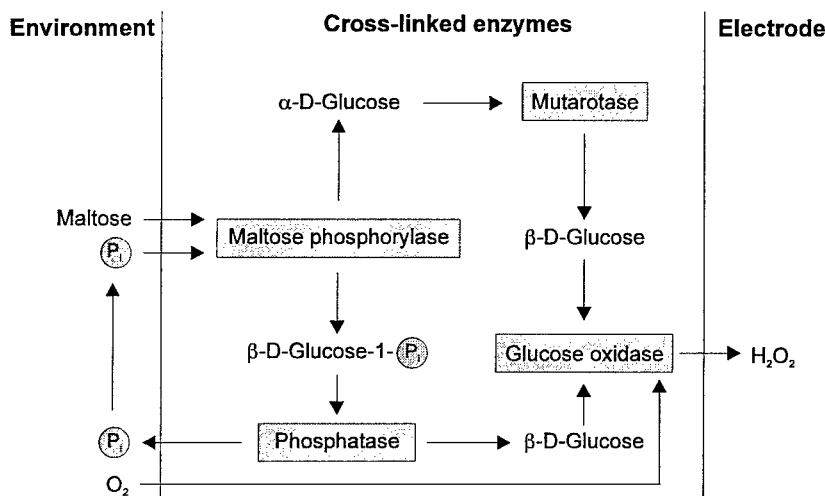
FIGURE 1. Enzyme sequence for the determination of inorganic phosphate.

filtration was mainly used to transfer maltose phosphorylase smoothly into 1 mM phosphate buffer for the subsequent hydroxyapatite chromatography. The purification procedure resulted in 24% recovery of the enzyme activity and a 49-fold enrichment of MP compared to the crude extract as shown in TABLE 1. The purified enzyme exhibited one band corresponding to a molecular mass of about 86 kDa in SDS-PAGE. In addition, a relative molecular mass of $M_r = 88,700$ was determined by matrix-assisted laser desorption ionization mass spectrometry. The molecular mass of the native enzyme was calculated to approximately 196 kDa as judged by gel filtration. These results support the idea that the native enzyme is a dimeric protein consisting of two subunits and are in line with data published for other microbial phosphorylases, such as sucrose phosphorylase from *Pseudomonas saccharophila*,[7] laminaribose phosphorylase from *Euglena gracilis* Z,[8] and maltodextrin phosphorylase from *Escherichia coli*.[9]

TABLE 1. Purification Protocol of Maltose Phosphorylase

Step	Protein (mg)	Enzyme Activity (units)	Specific Activity (units/mg)	Recovery (%)	Purification Factor
Crude extract	1700	941	0.55	100	1
Anion exchange	138	515	3.73	55	8
Gel filtration	37	300	8.11	32	15
Hydroxyapatite chromatography	8.8	228	27.1	24	49

Storage Stability

The effect of pH on the storage stability of maltose phosphorylase was investigated in 40 mM citrate buffer at a range between pH 4.5 to 5.5 and in 40 mM phosphate buffer, pH 6.0 to 8.5. After 24 h at room temperature (20 °C), a total recovery of enzyme activity was observed within a pH range from 6.0 to 7.0. However, the storage of MP in the presence of inorganic phosphate prior to the application in this biosensor is not recommended. We therefore investigated the effect of various buffers and soluble additives on the stability of MP during lyophilization. It is worthwhile to mention that a higher residual activity was obtained when MP was dialyzed against distilled water (70%) as compared to that in the presence of phosphate buffer (52%). Imidazole and acetate buffer had a strongly inactivating effect on the enzyme activity. As summarized in TABLE 2, carbohydrates, polyhydroxy alcohols, and polymers generally improved the stability of MP during freeze-drying. It is noteworthy that the addition of PEG did not result in a further improvement of the stability. The best results were obtained with sucrose, trehalose, lactitol, and sorbitol, giving rise to high residual activities ranging from 92% to 97%.

TABLE 2. Effect of Various Additives on the Stability of Maltose Phosphorylase during Lyophilization

Additive	Concentration	Residual Activity[a] (%)
Sorbitol	10 mM	92 ± 1.7
Lactitol	10 mM	97 ± 0.8
Trehalose (Tre)	10 mM	96 ± 1.9
Inositol	10 mM	73 ± 2.1
Sucrose (Suc)	10 mM	97 ± 2.2
DEAE-Dextran	0.1%	85 ± 0.9
HP-β-CD[b]	0.1%	87 ± 5.8
PVP[c]	0.1%	85 ± 2.2
PEG[d]	0.1%	61 ± 5.7
Tre + HP-β-CD	10 mM + 0.1%	92 ± 4.9
Tre + PVP	10 mM + 0.1%	94 ± 3.4
Suc + HP-β-CD	10 mM + 0.1%	96 ± 2.9
Suc + PVP	10 mM + 0.1%	95 ± 2.2

[a]Mean values from at least three experiments.
[b]Hydroxypropyl-β-cyclodextrin.
[c]Polyvinylpyrrolidone.
[d]Polyethylene glycol.

A synergistic effect of mixtures containing both carbohydrates and polymers on the activity could not be observed. However, sufficient results were obtained in long-term experiments, using a mixture of 10 mM trehalose and 0.1% polyvinylpyrrolidone as stabilizers (FIGURE 2). After storage of the enzyme preparation for 60 days at 25 °C, the activity was recovered to more than 90%. MP obtained from the purification could be stored for months now at −20 °C without any loss of activity. These results are in line with those obtained by other investigators using similar mixtures.[10,11]

Thermal Stability

In order to improve the stability of maltose phosphorylase with respect to its application in biosensors, particularly in a flow-injection analysis system (FIA), where an increase of viscosity due to additives is not recommended, the impact of different buffers was investigated. Test samples were incubated for 30 min at 45 °C and thermal stability was calculated as glucose liberation from maltose before and after incubation (data not shown). Remarkably, acetate, phosphate, and imidazole, which turned out to destabilize MP during lyophilization, exhibited stabilizing effects in aqueous solution. In contrast to the results obtained with sucrose phosphorylase, divalent cations like Mg^{2+} and Ca^{2+} had no beneficial effect on the enzyme stability.[7]

Enzyme Sensor

The enhancing effect of phosphatase in the enzyme sequence is demonstrated in FIGURE 3. Taking glucose oxidase (GOD) and MP, the response of this bienzyme
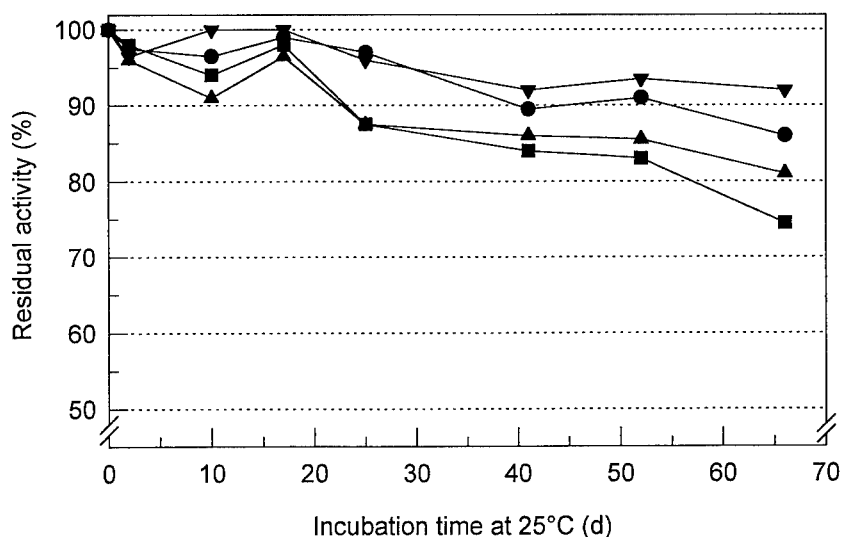
FIGURE 2. Stabilization of maltose phosphorylase by mixtures of carbohydrates (10 mM) and polymers (0.1%): ▼, trehalose and polyvinylpyrrolidone (PVP); ●, sucrose and hydroxypropyl-β-cyclodextrin (HP-β-CD); ▲, trehalose and HP-β-CD; ■, sucrose and PVP.
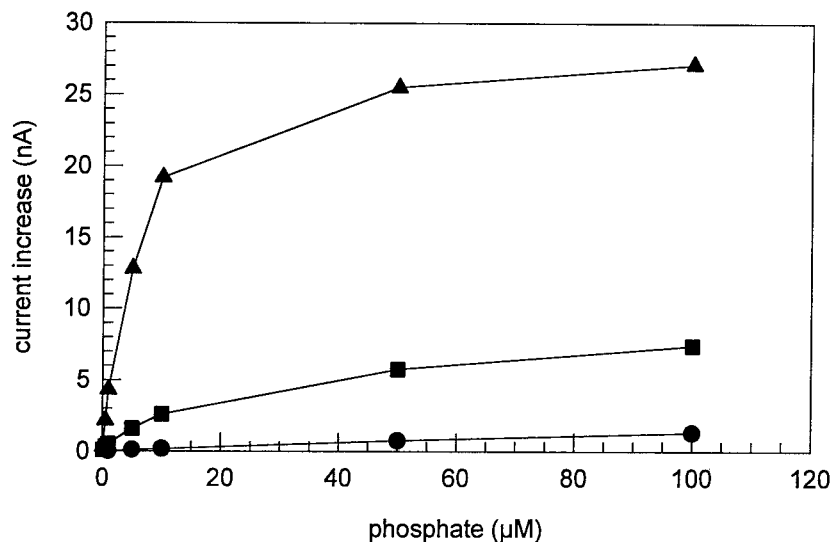
FIGURE 3. Sensitivity enhancement by signal amplification: ●, glucose oxidase and maltose phosphorylase; ■, glucose oxidase, maltose phosphorylase, and mutarotase; ▲, glucose oxidase, maltose phosphorylase, mutarotase, and acid phosphatase.

sensor was linear up to 100 μM phosphate with a sensitivity of 14 nA/mM phosphate. Introducing mutarotase (MR) to the immobilization layer led to a 20-fold higher response. Finally, addition of acid phosphatase (aP) increased the sensitivity towards phosphate significantly (up to 4 μA/mM). The calibration graph was linear between 0.1 and 1 μM phosphate. Compared to previously described biosensors for phosphate,[12-14] a 10-fold lower detection limit of 10 nM was obtained, allowing for the determination of phosphate in environmental monitoring.

REFERENCES

1. FISKE, C. H. & Y. SUBBAROW. 1925. The colorimetric determination of inorganic phosphorus. J. Biol. Chem. **66:** 375–382.
2. WARSINKE, A. & B. GRÜNDIG. 1992. Verfahren zum empfindlichen enzymatischen Nachweis von anorganischem Phosphat. German patent no. DE 4227569.
3. CONRATH, N., B. GRÜNDIG, S. HÜWEL & K. CAMMANN. 1995. A novel enzyme sensor for the determination of inorganic phosphate. Anal. Chim. Acta **309:** 47–52.
4. POUDRIER, S. M. & M. T. OYEN. Stable reagent and kinetic assay for α-amylase. Beckman Instruments. United States patent no. US 4990445 A 910205.
5. KAMOGAWA, A., K. YOKOBAYASHI & T. FUKUI. 1974. An enzymatic method for the determination of maltose in the presence of other oligosaccharides. Anal. Biochem. **54:** 303–305.
6. HÜWEL, S., L. HAALCK, N. CONRATH & F. SPENER. 1996. Maltose phosphorylase from *Lactobacillus brevis*: purification, characterization, and application in a biosensor for *ortho*-phosphate. Enzyme Microb. Technol. Submitted.
7. SILVERSTEIN, R., J. VOET, D. REED & R. H. ABELES. 1967. Purification and mechanism of action of sucrose phosphorylase. J. Biol. Chem. **242:** 1338–1346.
8. KITAOKA, M., T. SASAKI & H. TANIGUCHI. 1993. Purification and properties of lamina-

ribose phosphorylase (EC 2.4.1.31) from *Euglena gracilis* Z. Arch. Biochem. Biophys. **304:** 508–514.

9. SCHINZEL, R. & P. DRUECKES. 1991. The phosphate recognition site of *Escherichia coli* maltodextrin phosphorylase. FEBS Lett. **286:** 125–128.

10. IZUTSU, K., S. YOSHIOKA & T. TERAO. 1993. Stabilizing effect of amphiphilic excipients on the freeze-thawing and freeze-drying of lactate dehydrogenase. Biotechnol. Bioeng. **43:** 1102–1107.

11. GIBSON, T., I. J. HIGGINS & J. R. WOODWARD. 1992. Stabilization of analytical enzymes using a novel polymer-carbohydrate system and the production of a stabilized single reagent for alcohol analysis. Analyst **117:** 1293–1297.

12. LUQUE DE CASTRO, M. D., R. QUILES, J. M. FERNÁNDEZ-ROMERO & E. FERNÁNDEZ. 1995. Continuous-flow assay with immobilized enzymes for determination of inorganic phosphate in serum. Clin. Chem. **41:** 99–102.

13. MALE, K. B. & J. H. T. LUONG. 1991. An FIA biosensor system for the determination of phosphate. Biosens. Bioelectronics **6:** 581–587.

14. SCHUBERT, F., R. RENNEBERG, F. W. SCHELLER & L. KIRSTEIN. 1984. Plant tissue hybrid electrode for determination of phosphate and fluoride. Anal. Chem. **56:** 167–168.

(S)-Hydroxynitrile Lyase from *Hevea brasiliensis*

MEINHARD HASSLACHER,[a] MICHAEL SCHALL,[b]
MARIANNE HAYN,[b] HERFRIED GRIENGL,[c]
SEPP D. KOHLWEIN,[a] AND HELMUT SCHWAB[d]

[a]*Institut für Biochemie*
Technische Universität Graz
A-8010 Graz, Austria

[b]*Institut für Biochemie*
Karl-Franzens Universität
Graz, Austria

[c]*Institut für Organische Chemie*
[d]*Institut für Biotechnologie*
Technische Universität Graz
A-8010 Graz, Austria

INTRODUCTION

Hydroxynitrile lyases (Hnl) are plant enzymes involved in cyanogenesis, a process liberating HCN from cyanogenic glycosides, to protect the plant against predators.[1] α-Hydroxynitriles, which are produced by cleavage of cyanogenic glycosides by β-glycosidases, are converted by Hnl into the corresponding aldehyde or ketone and HCN. The high enantioselectivities of Hnls can be exploited for the synthesis of chiral cyanohydrins; these can then be transformed into optically active α-hydroxyketones or α-hydroxycarbonic acids, which are important intermediates for pharmaceuticals.[2]

This work describes the molecular cloning, characterization, and heterologous production of an (S)-hydroxynitrile lyase from *Hevea brasiliensis* (tropical rubber tree) in microorganisms. In order to identify putative active sites in Hnl from *H. brasiliensis*, we have conducted a detailed computational analysis of the deduced protein sequence. Participation of the identified residues was verified by *in vitro* mutagenesis. Based on these data, a model for the enzymatic reaction is proposed.

Hnl was expressed in *Escherichia coli*, *Saccharomyces cerevisiae*, and *Pichia pastoris*.

ISOLATION OF HNL cDNA FROM *H. BRASILIENSIS*

Hnl cDNA was isolated by immunoscreening from an *H. brasiliensis* cDNA library. The open reading frame contained in the isolated 1150-bp cDNA fragment had the capacity to code for a protein of 29.2 kDa, which was identical to the size of the isolated protein.[3] Authenticity of the cloned gene was demonstrated by peptide sequencing of proteolytic fragments and comparison to the deduced sequence.[4]
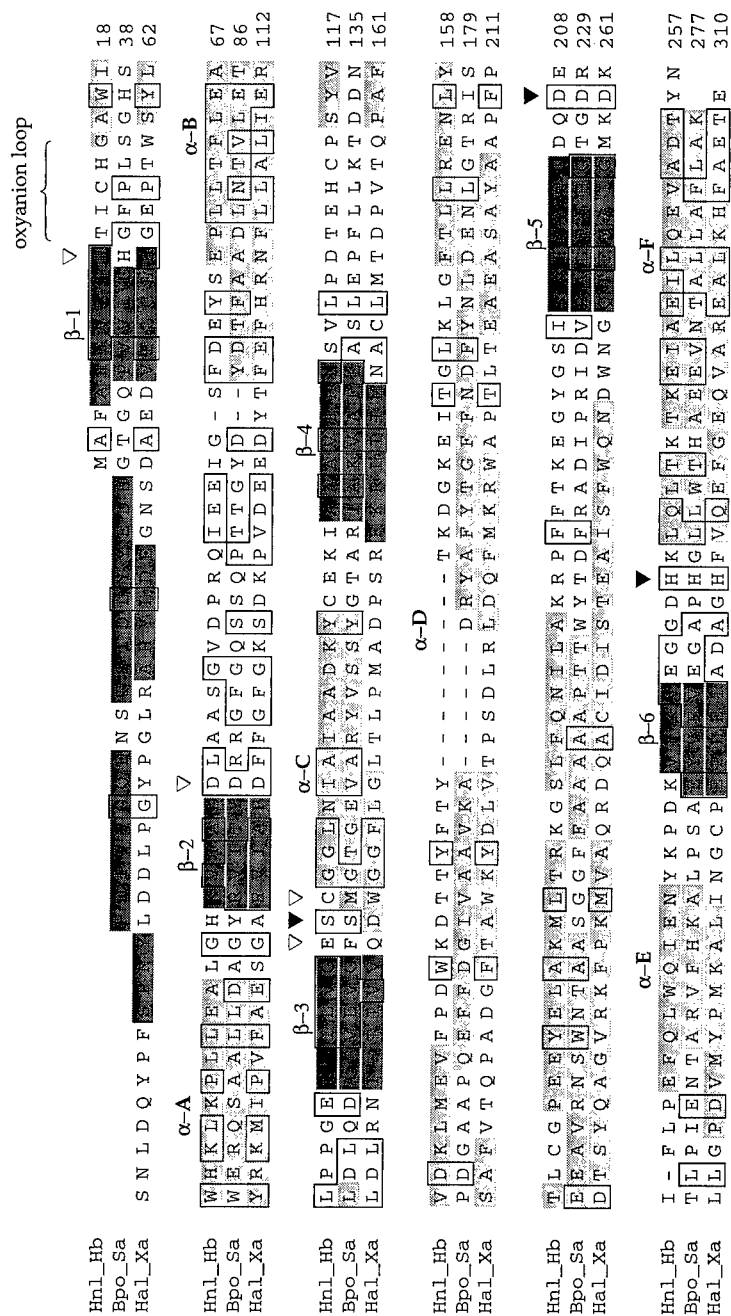
FIGURE 1. Multiple sequence alignment of hydroxynitrile lyase (Hnl), bromoperoxidase A2 (Bpo), and haloalkane dehalogenase (Hal). Secondary structure elements are obtained from the crystal structures of Hal and Bpo and are predicted for Hnl. Terms: (light gray) alpha-helix; (dark gray) beta-strand; (no shading) loop region; (▼) amino acids of the catalytic triad; (▽) amino acids changed by site-directed mutagenesis.

COMPUTATIONAL ANALYSIS OF HNL

A multiple sequence alignment of enzymes identified by homology searches with Hnl is presented in FIGURE 1. The identified enzymes are members of the α/β-hydrolase fold superfamily,[5] suggesting that Hnl from *H. brasiliensis* might be structurally related to this family of proteins. Several amino acid residues are highly conserved, leading to the suggestion of a catalytic triad that consists of Ser^{80}, Asp^{207}, and His^{235} in the Hnl protein. In addition, amino acid residues His^{10} and Asp^{37} of Hnl are conserved, based on the multiple sequence alignment.

IDENTIFICATION OF AMINO ACID RESIDUES INVOLVED IN ENZYMATIC FUNCTION

The predicted functional role of the indicated amino acid residues in catalytic activity was verified by *in vitro* mutagenesis (TABLE 1) and by expression of the modified enzymes in a heterologous host (*S. cerevisiae*). Changes of $His^{10} \rightarrow$ Ala and $Asp^{37} \rightarrow$ Ala did not significantly affect the activity of the enzyme, whereas substitution of other residues, suggested to be involved in catalysis, led to a dramatic decrease of activity.

TABLE 1. Relative Activities of Mutated Hnls Expressed in *Saccharomyces cerevisiae*

Hnl	Relative Activity (%)
wild type	100
Hnl-$His^{10} \rightarrow$ Ala	> 90
Hnl-$Asp^{37} \rightarrow$ Ala	> 90
Hnl-$Glu^{79} \rightarrow$ Ala	< 10
Hnl-$Ser^{80} \rightarrow$ Ala	0
Hnl-$Cys^{81} \rightarrow$ Ser	< 5
Hnl-$Asp^{207} \rightarrow$ Ala	< 15
Hnl-$His^{235} \rightarrow$ Ala	< 5

PROPOSED REACTION MECHANISM FOR HNL

Based on these data, the following model for the formation of cyanohydrins can be postulated (FIGURE 2): The reaction is initiated by nucleophilic attack of an amino acid residue of the nucleophilic loop (most likely Ser^{80}) on the substrate carbonyl residue, forming a hemiketal or hemiacetal tetrahedral transition state. Hydrocyanic acid, which might be activated by interaction with Cys^{81} and His^{235}, is added and the product is released.

HETEROLOGOUS EXPRESSION OF HNL FROM *H. BRASILIENSIS* IN MICROORGANISMS

In order to identify a host for heterologous production, we have analyzed three different expression systems for their efficiency in expressing enzymatically active Hnl.
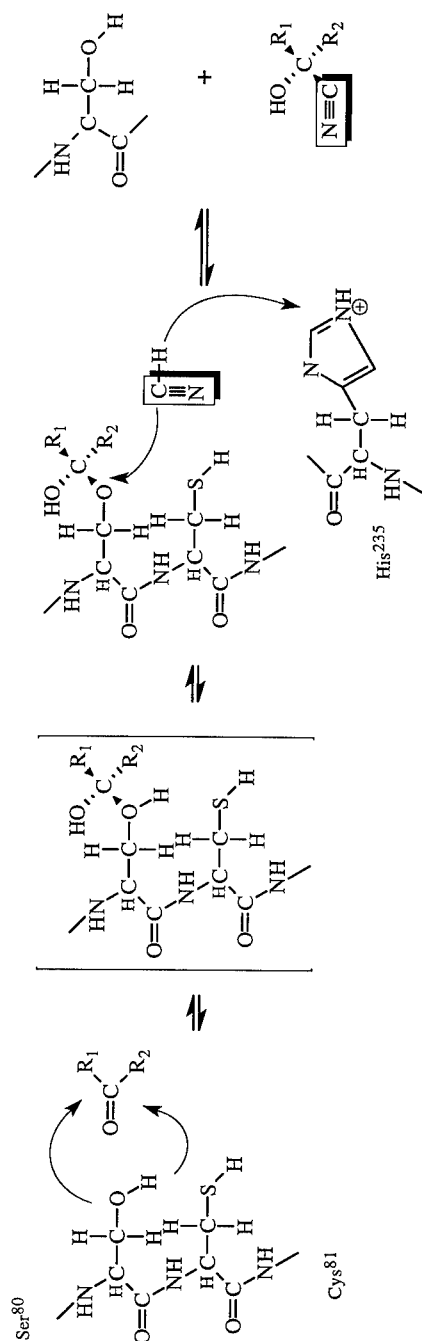
FIGURE 2. Model for the formation of cyanohydrins catalyzed by Hnl from *Hevea brasiliensis.*

Escherichia coli: An IPTG inducible trc-promoter[6] with a two-cistron-based enhanced translational efficiency system was used. Induction was performed at various temperatures (22 °C, 28 °C, and 37 °C) for two hours. Soluble and insoluble fractions were obtained by sonication of the cells following centrifugation.

Hnl expressed in *E. coli* had the tendency to aggregate and to form insoluble inclusion bodies that did not exhibit enzyme activity.

Saccharomyces cerevisiae: A pMA91-based vector with a constitutive phosphoglycerate kinase promoter and the LEU2-d gene for selection was used.[7] Because the Leu2-d marker is a promoterless version of the LEU2 gene, only high-copy-number transformants were obtained. Cytosolic fractions were prepared by the glass-bead method[8] and tested for Hnl activity (TABLE 2). Given a specific activity of 22 ± 3 IU/mg of heterologous Hnl, approximately 20% of the *Saccharomyces cerevisiae* soluble cytosolic crude extract was composed of Hnl. This was considerably high for a nonoptimized system.

Pichia pastoris: In this system, the strength of the AOX1 promoter was exploited; this promoter allows the production of alcohol oxidase of up to 30% of the soluble proteins in extracts of cells grown on methanol.[9] The expression cassette was inserted

TABLE 2. Hnl Yield and Specific Activity in Plant Leaves and Heterologous Hosts

	Cytosolic Activity (IU/mg)	Fraction of Cytosolic Protein (%)	Specific Activity (IU/mg)	Yield per Volume Flask Culture (IU/mL)
H. brasiliensis	0.42	2.3	15–20	0.5 (IU/g leaves)
E. coli	0.60	≈2.6	—	0.1 (OD = 4.0)
S. cerevisiae	4.6	20	20–25	1.2 (OD = 4.0)
P. pastoris	15.7	40	40–45	6.2 (OD = 4.0)

into the AOX1 chromosomal locus by PEG-spheroplast transformation according to the instruction manual of the "Pichia Expression Kit" (Invitrogen Corporation, San Diego, California). The cytosolic Hnl activity in the most efficiently expressing *Pichia pastoris* system was 3.5 times higher than the activity measured in the *Saccharomyces cerevisiae* system and represented more than 40% of the cytosolic protein (TABLE 2).

REFERENCES

1. CONN, E. E. 1981. Cyanogenic glycosides. *In* The Biochemistry of Plants: A Comprehensive Treatise. Volume 7. Secondary Plant Products. P. K. Stumpf & E. E. Conn, Eds.: 479–500. Academic Press. New York.
2. KRUSE, C. G. 1992. Chiral cyanohydrins—their manufacture and utility as chiral building blocks. *In* Chirality in Industry. A. N. Collins, G. N. Sheldrake & J. Crosby, Eds.: 279–299. Wiley. New York.
3. SCHALL, M. 1996. Isolation and characterization of a (*S*)-hydroxynitrile lyase from *Hevea brasiliensis*. Ph.D. thesis. University of Graz, Austria.
4. HASSLACHER, M., M. SCHALL, M. HAYN, H. GRIENGL, S. D. KOHLWEIN & H. SCHWAB. 1996. Molecular cloning of the full-length cDNA of (*S*)-hydroxynitrile lyase from *Hevea brasiliensis*. J. Biol. Chem. **271:** 5884–5891.
5. OLLIS, D. L. *et al.* 1992. The α/β hydrolase fold. Protein Eng. **5:** 197–211.

6. AMANN, E., J. BROSIUS & M. PTASHNE. 1983. Vectors bearing a hybrid *trp-lac* promoter
    useful for regulated expression of cloned genes in *Escherichia coli.* Gene **25:** 167–178.
7. KINGSMAN, S. M. *et al.* 1990. High-efficiency yeast expression vectors based on the promoter
    of the phosphoglycerate kinase gene. Methods Enzymol. **185:** 329–341.
8. AUSUBEL, F. *et al.* 1990. Current Protocols in Molecular Biology. Greene/Wiley–
    Interscience. New York.
9. CREGG, J. M., K. J. BARRINGER, A. Y. HESSLER & K. R. MADEN. 1985. *Pichia pastoris* as
    host system for transformation. Mol. Cell. Biol. **5:** 3376–3385.

Chiral Alcohols by Enantioselective Enzymatic Oxidation[a]

W. HUMMEL AND B. RIEBEL

Institut für Enzymtechnologie
Heinrich-Heine-Universität
Forschungszentrum Jülich
D-52404 Jülich, Germany

INTRODUCTION

The stereoselective synthesis of chiral compounds can be achieved by fermentation or enzyme-catalyzed processes. For the production of chiral alcohols, the route most frequently applied utilizes the reductive capability of dehydrogenases, coupled to an efficient method for the regeneration of the reduced coenzymes NADH or NADPH.[1]

Alternatively, the racemic mixture of an alcohol can be subject to the oxidative capacity of enantioselective alcohol dehydrogenases (ADH) or other oxidizing enzymes. This route is advantageous, for example, if the corresponding ketones are difficult to prepare, such as hydroxyketones, or for the use of enzymes with low enantioselectivity. A highly efficient method for the regeneration of the oxidized coenzyme is an inevitable prerequisite for this route.

In this contribution, we present methods for the preparation of chiral alcohols by applying enantioselective enzymatic oxidation reactions on racemic alcohols.

NEW ALCOHOL DEHYDROGENASES

Two new alcohol dehydrogenases were found and characterized: an *R*-specific ADH from *Lactobacillus kefir* and an *S*-specific enzyme from *Rhodococcus erythropolis*.[2–4] Each enzyme accepts a broad variety of substrates, for example, ketones with bulky side chains, such as acetophenone or halogen-substituted acetophenones, as well as ketoesters.[5,6] Both enzymes were purified to homogeneity. TABLE 1 summarizes the most important biochemical properties of these new catalysts.

ENZYME-CATALYZED REDUCTION OF THE PROCHIRAL KETO COMPOUND

Each of the new enzymes can be applied for the enantioselective reduction of prochiral ketones or ketoesters; each product was found to be enantiomerically pure.[6,7] The reduced coenzymes can be regenerated easily: NADPH (*L. kefir*) by addition of isopropanol and NADH (*R. erythropolis*) by coupling to formate and

713

TABLE 1. Biochemical Properties of the Novel Alcohol Dehydrogenases from *Lactobacillus kefir* and *Rhodococcus erythropolis*

Properties	ADH from *L. kefir*	ADH from *R. erythropolis*
Enantioselectivity	*R*-specific	*S*-specific
Coenzyme	NADP	NAD
pH optimum	pH 7.0 for reduction	pH 6.0 for reduction
Temperature optimum	about 40 °C for reduction	40 °C for reduction
Molecular weight	108 kDa, tetramer, SU 28, 5 kDa	95 kDa, dimer, SU 45/48 kDa
Ion dependence	Mg^{2+}	none
K_m value for substrate[a]	0.36 mM	0.5 mM
K_m value for coenzyme	0.058 mM	0.026 mM
Amino acid (aa) sequence	N-terminal, 45 aa	N-terminal, 24 aa
	C-terminal, 15 aa	

[a]Substrates: *L. kefir*-ADH, acetophenone; *R. erythropolis*-ADH, *p*-Cl-acetophenone.

formate dehydrogenase. Several products such as (*S*)-ethyl-3-hydroxybutyrate, (*S*)-1-phenyl-2-propanol, (*S*)-sulcatol, (*S*)-4-phenyl-2-butanol, and 6-methyl-5-hepten-2-ol were prepared along with these enzymes on a multigram scale.[6]

ENZYME-CATALYZED OXIDATION OF ALCOHOLS

In case that the ketone compound is difficult to prepare, it is easier to start with the racemic mixture and to use the enantioselective oxidation of one isomer. In principle, this route can be carried out with the new alcohol dehydrogenases as well.
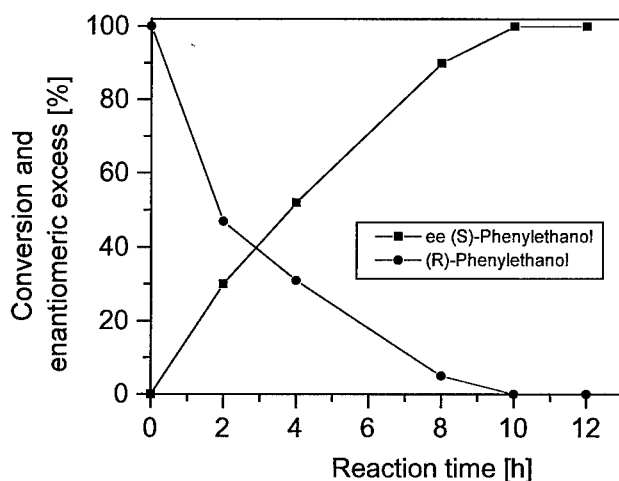
FIGURE 1. Time dependence of the oxidative conversion of 10 mM (*R,S*)-phenylethanol by applying (*R*)-specific alcohol dehydrogenase from *Lactobacillus kefir*, NADH oxidase, and catalase. The enantiomeric excess ([*S*] − [*R*]/[*S*] + [*R*]) was determined by measuring the concentrations of (*R*)- and (*S*)-phenylethanol by gas chromatography [cyclodextrin column (Lipodex E; Macherey and Nagel, Düren, Germany)].

In order to obtain an enantiomeric pure product, this reaction requires the complete regeneration of the oxidized coenzymes. We studied the use of NADH oxidase from *Thermus thermophilus*[8] for this purpose. This enzyme oxidizes NADH as well as NADPH with low K_m values. The product of this reaction is peroxide, which tends to deactivate enzymes, but can be destroyed easily by addition of catalase. Actually, a batch reaction with R-ADH and NADH oxidase starting with 10 mM R,S-phenylethanol resulted in a product solution containing 5 mM S-phenylethanol and 5 mM acetophenone (FIGURE 1).

This reaction principle can be used as well for the complete conversion of a racemic mixture into an enantiomeric pure alcohol because, in this case, enzymes of both types of enantioselectivity are available. As an example, TABLE 2 summarizes the oxidation of R,S-phenylethanol in a two-step reaction: After the S-ADH-catalyzed oxidation of one enantiomer of the racemate, the solution contains pure R-alcohol and the ketone as the oxidation product. The S-ADH is separated, for

TABLE 2. Batchwise Conversion of a Racemic Mixture of Phenylethanol into Enantiomerically Pure R-Phenylethanol at 100% Yield[a]

Reaction Step	Substrate/Product	ee Value	Yield
(1) Start	10 mM R,S-phenylethanol	0%	—
(2) Addition of S-ADH, NADH oxidase; 2-h reaction time	5 mM R-phenylethanol, 5 mM ketone	100%	50%
(3) Ultrafiltration			
(4) Addition of R-ADH, isopropanol; 1-h reaction time	10 mM R-phenylethanol	100%	100%

[a]In this experiment, 0.5 units of S- or R-ADH per mL was used. Product solution was analyzed by GC.

example, by ultrafiltration, followed by the addition of R-ADH for the reduction of the ketone. As a whole, this reaction system completely converts R,S-phenylethanol into pure R-phenylethanol (100% ee; 100% yield).

REFERENCES

1. HUMMEL, W. & M-R. KULA. 1989. Dehydrogenases for the synthesis of chiral compound. Eur. J. Biochem. **184:** 1–13.
2. HUMMEL, W. 1990. Enzyme-catalyzed synthesis of optically pure R(+)-phenylethanol. Biotechnol. Lett. **12:** 403–408.
3. HUMMEL, W. 1990. Reduction of acetophenone to R(+)-phenylethanol by a new alcohol dehydrogenase from *Lactobacillus kefir*. Appl. Microbiol. Biotechnol. **34:** 15–19.
4. TARHAN, L. & W. HUMMEL. 1995. Immobilisation and characterisation of phenylethanol dehydrogenase from *Lactobacillus kefir* and its application in a flow-injection-analysis system. Process Biochem. **30:** 49–55.
5. KRAGL, U., W. KRUSE, W. HUMMEL & C. WANDREY. 1996. Enzyme engineering aspects of biocatalysis: cofactor regeneration as an example. Biotechnol. Bioeng. In press.
6. KRUSE, W., W. HUMMEL & U. KRAGL. 1996. Alcohol dehydrogenase catalyzed production

of chiral hydrophobic alcohols—a new approach leading to a nearly wasteless process. Recl. Trav. Chim. Pays-Bas **115:** 239–243.

7. BRADSHAW, C. W., W. HUMMEL & C-H. WONG. 1992. *Lactobacillus kefir* alcohol dehydroge-nase: a useful catalyst for synthesis. J. Org. Chem. **57:** 1532–1536.

8. PARK, H-J., C. O. A. REISER, S. KONDRUWEIT, H. ERDMANN, R. D. SCHMID & M. SPRINZL. 1992. Purification and characterization of an NADH oxidase from the thermophile *Thermus thermophilus* HB8. Eur. J. Biochem. **205:** 881–885.

Optical Resolution of Racemic 1-Phenylethylamine Catalyzed by Aminotransferase and Dehydrogenase

JONG-SHIK SHIN AND BYUNG-GEE KIM[a]

Institute for Molecular Biology and Genetics
and
Department of Chemical Technology
Seoul National University
Seoul, Korea 151-742

INTRODUCTION

Reflecting the growing need for chiral intermediates for agrochemicals and pharmaceuticals, new approaches for chemical and biochemical resolution or asymmetric synthesis of chiral intermediates are under investigation. Because enzymes have frequently shown a very high enantioselectivity and provide simple reaction systems, biochemical approaches appear to hold promise for industrial use.

To resolve amine compounds using enzymes, several strategies can be considered: enantioselective amide synthesis or amide hydrolysis using commercial protease; enantioselective amino-transfer reaction using ω-aminotransferase;[1] and enantioselective oxidative deamination or reductive amination using dehydrogenase.[2] Each strategy has its advantages and drawbacks as follows. Although the amide synthesis reaction with protease in nonaqueous solvent has great potential due to the commercial availability of the enzyme, the relatively low enzyme reaction rate in solvent, the screening of solvents, and the cost of solvents and active ester as the cosubstrate pose major problems. Furthermore, the aminotransferase reaction requires an expensive amino-acceptor as a cosubstrate as well as extensive enzyme screening. Similarly, amination and deamination with dehydrogenase require an expensive cofactor regeneration system and extensive enzyme screening. However, both aminotransferase and dehydrogenase reactions occur in aqueous phase, and their reaction rates are much higher than that in the protease reaction in organic solvent.

It would appear, then, on average, that the advantages of the aminotransferase and dehydrogenase reactions outweigh their disadvantages. As an initial step in comparing the three enzyme systems with regard to the kinetic resolution of amine compounds, we screened aminotransferase and dehydrogenase using an enrichment technique and chose racemic 1-phenylethylamine (1-PEA) as a model compound. In this study, (S)-specific ω-aminotransferase and (R)-specific FAD-dependent dehydrogenase were identified in *Bacillus thuringiensis* JS64 and in *Acinetobacter baumannii* JS616, respectively. To further optimize the aminotransferase reaction, a biphasic reaction system was devised and compared with a monophasic system.

[a]To whom all correspondence should be addressed.

MATERIALS AND METHODS

Enrichment and Culture Conditions

A mixture of soil samples from several industrial sites where amine compounds are produced was used for the enrichment culture. The enrichment culture was carried out in test tubes, with the dilution rate changed up to twice per day with the replacement of new culture media. The composition of the enrichment culture media is as follows: phosphate buffer, 50 mM (pH 7.0); glycerol, 50 mM; citric acid, 30 mM; racemic 1-PEA or one enantiomer of 1-PEA, 30 mM; $MgSO_4$, 1.0 g/L; $CuSO_4$, 0.1 mg/L; $CaCl_2$, 0.02 mg/L; $CoCl_2$, 0.05 mg/L; $ZnCl_2$, 0.1 mg/L; $NiSO_4$, 0.1 mg/L; $MnSO_4$, 0.1 mg/L; Na_2MoO_4, 2.0 mg/L; H_3BO_4, 0.02 mg/L; and $FeSO_4$, 4.0 mg/L. The same media composition was used for cell growth, except for the concentration of carbon (glycerol, 100 mM) and the nitrogen (1-PEA, 10 mM) source. Cells grown over five days in the culture media (optical density ≅ 1.0 at 600 nm) were harvested and used in the enzyme reactions.

Enzyme Reaction and Assay

To identify different enzyme reactions, we used whole cells, cell extract, and dialyzed cell extract as necessary. Aminotransferase activity was measured either by quantifying the remaining pyruvate using lactate dehydrogenase and NADH with a UV spectrophotometer or by analyzing (R)- and (S)-1-PEA using HPLC with a chiral column [Crownpak CR(+), Daicel, Japan]. The reaction solution (reaction volume = 1 mL) consisted of phosphate buffer (pH 7.0), 50 mM; 1-PEA, 15 mM; sodium pyruvate, 50 mM; and pyridoxal phosphate, 0.5 mM. NAD-dependent dehydrogenase activity was measured by adding 20 mM NAD and 10 mM 1-PEA in 100 mM $NaHCO_3$/NaOH buffer (pH 10.0). FAD-dependent dehydrogenase activity was measured by adding 100 mM of electron acceptors, such as 2,6-dichlorophenol-indophenol (DPIP), methylene blue, and $K_3Fe(CN)_6$. Acetophenone was analyzed by either GC or HPLC.

RESULTS AND DISCUSSION

ω-Aminotransferase and Dehydrogenase

After several rounds of enrichment culture with each enantiomer of 1-PEA as a sole nitrogen source, we could identify many colonies on agar plates. We found that the cells grown in (R)-1-PEA could also grow in (S)-1-PEA, but the reverse was not true. This result suggests that it was very hard to select the cells containing only (R)-specific enzymes. To explain this result, we examined the possibilities of the presence of racemase[3] or of amine oxidase[4] requiring O_2 as an electron acceptor and of NAD-dependent dehydrogenase[5] activities, but none of them could be detected. We also examined aminotransferase and dehydrogenase activity using the different reaction assays (FIGURE 1) as mentioned in the previous section. Several colonies showing high enantioselective (S)-ω-aminotransferase activity were identified among
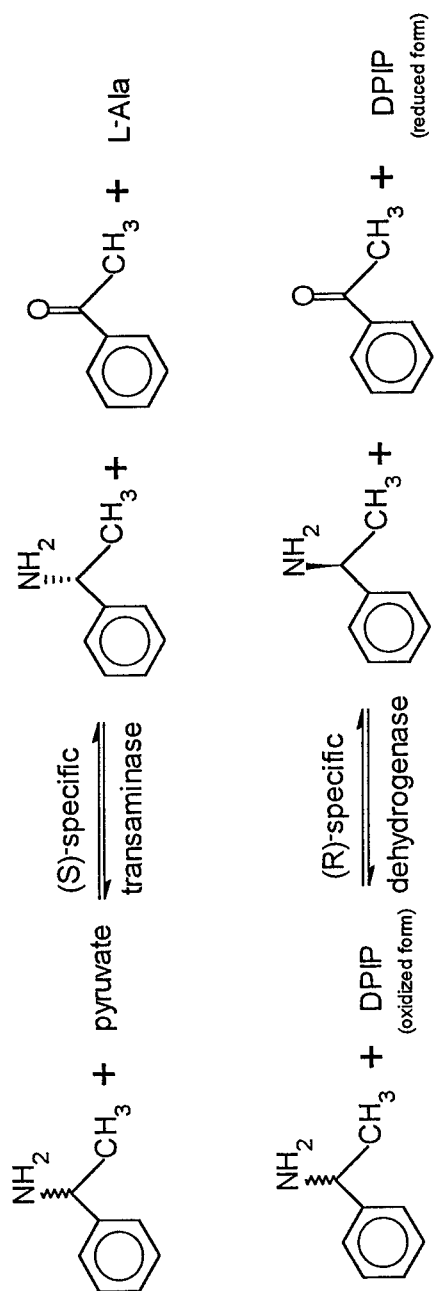
FIGURE 1. Resolution schemes for racemic 1-PEA using ω-aminotransferase and dehydrogenase.

TABLE 1. Properties of (R)-specific FAD-dependent Dehydrogenase

source	*A. baumannii* JS616
reaction conditions	phosphate buffer (50 mM, pH 7.0), 37 °C
growth conditions for induction	carbon source: glycerol (100 mM) nitrogen source: (R)-1-PEA (10 mM)
relative activity for substrates	(R)-1-PEA: 100% D-Trp: 137% D-Phe: 91%
electron acceptors	2,6-dichlorophenol-indophenol: reactive methylene blue: nonreactive $K_3Fe(CN)_6$: nonreactive
enantioselectivity (E)	75.9

the colonies selected from the media with (S)-1-PEA, but (S)-specific dehydrogenase activity was not detected among the cells. None of the strains from the media with (R)-1-PEA showed any (R)-specific aminotransferase activity; instead, the strains displayed both (S)-specific ω-aminotransferase activity and (R)-specific FAD-

TABLE 2. Properties of (S)-specific ω-Aminotransferase

source	*B. thuringiensis* JS64		
optimal reaction conditions	phosphate buffer (50 mM, pH 7.0), 37 °C		
growth conditions for induction	carbon source: glycerol (100 mM) nitrogen source: (S)-1-PEA (10 mM)		
		% ee(R)	% conversion
amino-donor specificity	1-PEA	>99	52
	Trp	98	59
	Phe	95	63
relative activity for amino-acceptors	pyruvate: 100% butanal: 330% propanal: 133%		
relative activity for inhibitors (3 mM)	(aminooxy)acetic acid: 17% hydroxylamine: 69% gabaculine: 0%		
Michaelis constants	1-PEA: 35.03 mM pyruvate: 9.60 mM		
product inhibition constants	acetophenone: 0.13 mM L-alanine: 2.85 mM		
enantioselectivity (E)	71.4		

dependent dehydrogenase activity. The results explain completely the growth behavior of the cells in media with (R)- and (S)-1-PEA.

FAD-dependent dehydrogenase activity was only detected coupled with DPIP (TABLE 1) among the three electron acceptors examined. This kind of oxidatively
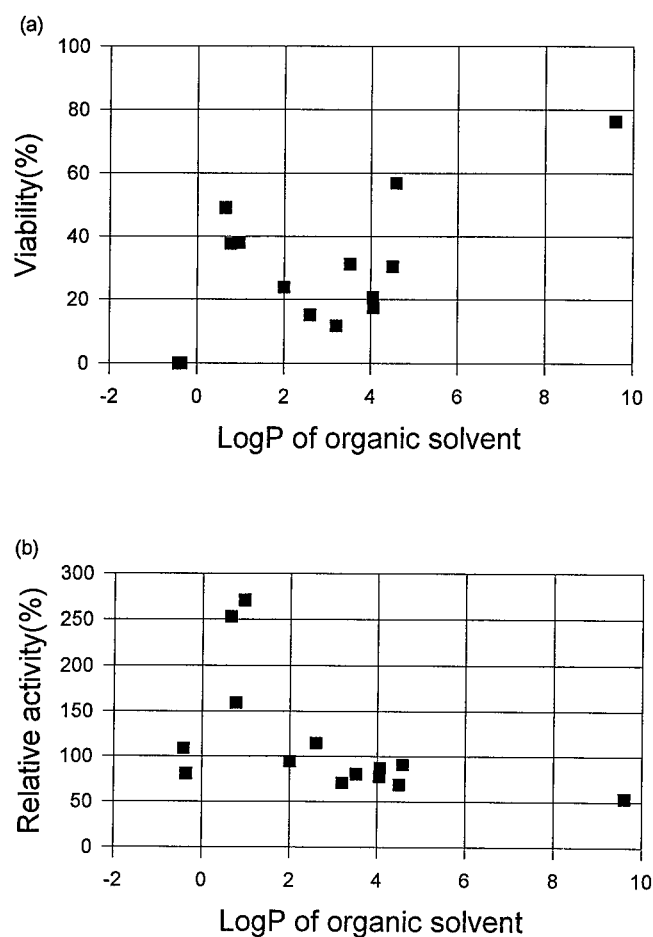
FIGURE 2. Relative (a) cell viability and (b) ω-aminotransferase activity in the biphasic system depending upon the log P value of various solvents. Solvents comprised one-fifth of the reaction volume in the biphasic system.

deaminating dehydrogenase appears to be somewhat different from D-amino acid oxidases that require O_2. Further characterization of the enzyme is under way. We also examined the characteristics of (S)-specific ω-aminotransferase and a summary of the results appears in TABLE 2. The reaction rate of FAD-dependent dehydrogenase was quite comparable with that of aminotransferase. However, because the
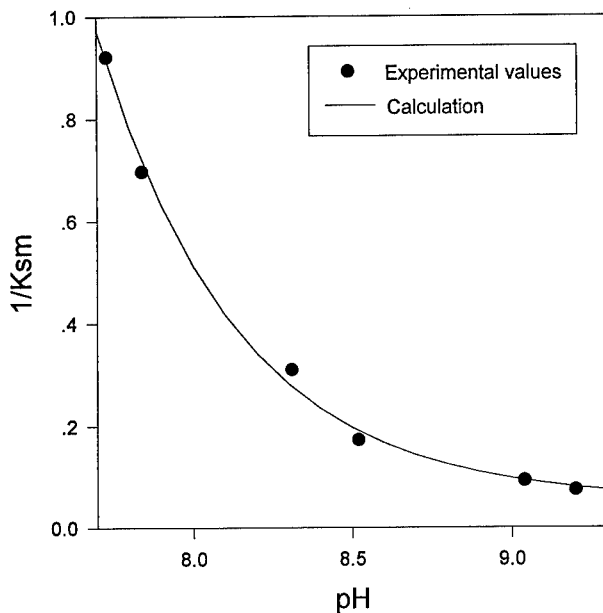
FIGURE 3. Dependence of the overall partition coefficient, K_{sm} = [1-PEA]$_{organic}$/ ([1-PEA]$_{aqueous}$ + [1-PEA$^+$]$_{aqueous}$), on the pH of the aqueous phase. The simulation results according to the Henderson-Hasselbalch equation are shown as a solid line.

dehydrogenase system requires the coupling of an electron acceptor to regenerate the FAD-enzyme complex, the ω-aminotransferase system was examined to achieve a desirable reaction rate and conversion yield.

Biphasic Reaction of ω-Aminotransferase

The ω-aminotransferase reaction showed severe product inhibition[6] with an increase in 1-PEA concentration. Although the product, acetophenone, has low solubility (ca. 60 mM) in water, even 5 mM of acetophenone added to the reaction medium reduced the relative enzyme activity by 50%. This means that any increase in 1-PEA concentration above 10 mM would result in a great loss of enzyme activity. In this situation, the selections of the reaction system (whole cell versus purified enzyme) and of the bioreactor operation mode (biphasic versus monophasic) are critical to obtaining a high reaction rate and a high conversion yield. In order to achieve good partitioning of acetophenone into solvent and less cell lysis during the bioconversion, solvent screening was carried out based upon log P. We found that cell viability has nothing to do with the enzyme reaction rate. FIGURE 2 indicates that there is no correlation between solvent hydrophobicity and cell viability, but solvents whose log P is around 1.0 generally show the highest reaction rates. This suggests that a good partitioning of acetophenone would be a key factor in increasing the reaction rate. In fact, the log P value of acetophenone was quite similar to that of the solvent

showing the highest reaction rate. Here, cyclohexanone was chosen as the best solvent.

In the biphasic system, the partitioning of both 1-PEA and acetophenone is affected significantly by environmental factors, such as pH, salt, and solvent properties, and hence, so too, is the reaction rate. The amount of 1-PEA partitioned into the cyclohexanone phase increased as the amine group was unprotonated. Accordingly, the amount of 1-PEA in aqueous phase decreased rapidly with a pH greater than 7.0 (FIGURE 3) and the decrease reduced the enzyme reaction rate. However, as the enzyme reaction proceeded, the pH of the reaction solution increased due to the amine group partitioned from the cyclohexanone to the aqueous phase. Therefore, adjusting the pH of the reaction buffer was very important with high concentrations of 1-PEA in the biphasic system.

We next compared the conversion and ee(S) (%) of the resolution reaction of 1-PEA using the monophasic and biphasic systems (FIGURE 4). We could clearly observe the advantages of using the biphasic system in terms of both conversion and ee (%) as the 1-PEA concentration increased. When 100 mM 1-PEA and 2 units/mL of cell extract dialysate were used in the biphasic system, 50% of conversion and 98% ee were achieved within 30 h. This enzyme reaction rate was several times higher
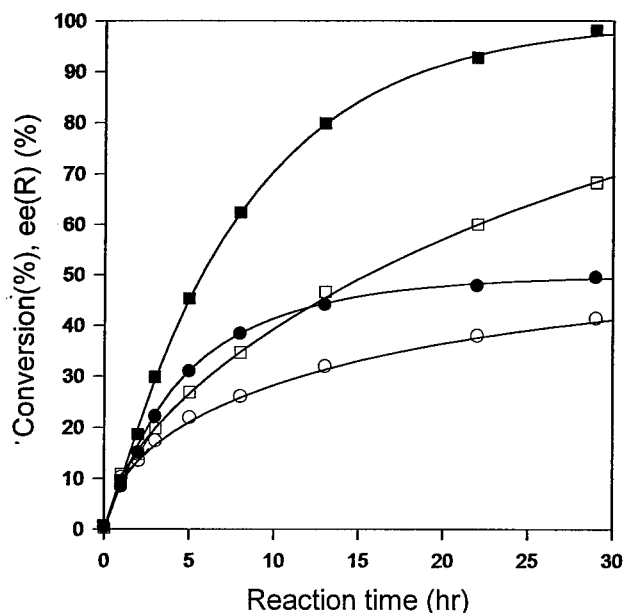
FIGURE 4. Comparison of the resolution of racemic 1-PEA (100 mM) between monophasic and biphasic (water-cyclohexanone) systems using (S)-aminotransferase from *B. thuringiensis* JS64 cell extract dialysate. Both reactions were carried out at 37 °C. Cyclohexanone comprised one-fifth of the reaction volume in the biphasic system. Closed symbols [●: conversions (%); ■: ee(R) (%)] and open symbols [○: conversions (%); □: ee(R) (%)] indicate reactions in the biphasic system and monophasic system, respectively.

than the best results obtained in our laboratory by using protease for the resolution of racemic 1-PEA in organic phase.

REFERENCES

1. STERLING, D. I. & G. W. MATCHAM. 1990. *In* Proceedings of the Chiral '90 Symposium, p. 111–113. Manchester, England.
2. OLSIEWSKI, P. J., G. J. KACZOROWSKI & C. WALSH. 1980. J. Biol. Chem. **255:** 4487–4494.
3. MOCHIZUKI, K., K. HOSONO & H. KOBAYASHI. 1994. Biochim. Biophys. Acta **1200:** 27–33.
4. POLLEGIONI, L., A. FALBO & M. S. PILONE. 1992. Biochim. Biophys. Acta **1120:** 11–16.
5. OHSHIMA, T., H. TAKADA, T. YOSHIMURA, N. ESAKI & K. SODA. 1991. J. Bacteriol. **173:** 3943–3948.
6. BULOS, B. & P. HANDLER. 1965. J. Biol. Chem. **240:** 3283–3294.

New Microbial Amidases[a]

M-R. KULA, U. JOERES, AND U. STELKES-RITTER

Institute of Enzyme Technology
Heinrich-Heine University
D-52404 Jülich, Germany

INTRODUCTION

Amides are rather stable intermediates, often readily obtained by partial hydrolysis of nitriles. There has been considerable interest to find specific enzymes to hydrolyze amides stereoselectively to yield chiral acids.[1] We discuss here a new enzyme highly stereoselective for L-carnitine amide that can be applied for the production of L-carnitine.

In addition, we report a new bacterial enzyme hydrolyzing exclusively C-terminal amides in peptides or N-protected amino acids. The peptide amidase is highly stereoselective and regioselective and is devoid of peptidase/protease activity. These properties make it feasible to use amino acid amides as superior nucleophiles in peptide synthesis, allowing the selective removal of the protecting group, which is impossible to achieve by chemical means.

L-CARNITINE AMIDASE

In a microbial screening with racemic carnitine amide as the carbon and/or nitrogen source, we isolated approximately 1400 single strains. In 65 strains, carnitine amidase activity could be clearly demonstrated. Ultimately, 1 strain was found to possess a highly stereoselective enzyme hydrolyzing exclusively L-carnitine amide to yield L-carnitine with an enantiomeric excess of >99%. All other strains did not exhibit such high stereospecificity. The L-amide was always the preferred substrate. Although the screening did not select against it, no D-carnitine amidase was found among the isolates.[2]

L-Carnitine amidase activity is barely detectable in the absence of an inducer possessing carnitine structure. Unlike other amidases, enzyme production was not repressed upon addition of ammonium ions to the medium. The purification of the enzyme and its molecular properties have been described.[3]

The L-carnitine amidase has a very narrow substrate range; out of 60 other amides tested, none was hydrolyzed. D-Carnitine amide was not converted during prolonged incubation times, but was found to be a strong competitive inhibitor. Besides, L-carnitine as well as D-carnitine inhibited the amidase. The following model was derived to describe the time course of the batch hydrolysis:

$$\frac{d[S]}{dt} = \frac{E \cdot V_{max} \cdot [S]}{K_m \left(1 + \frac{[I]}{K_I}\right)\left(1 + \frac{[P]}{K_P}\right) + [S]}.$$

The kinetic constants were determined as K_m = 11.3 mM, K_P = 19.7 mM, and K_I = 29.7 mM. In FIGURE 1, the conversion of 500 mM D,L-carnitine amide in a batch reaction is shown as a function of time. The model describes the complex reaction system quite well.

During continuous conversions in an enzyme-membrane reactor, the half-life of the catalyst was estimated to be around 55 hours under unoptimized conditions. The optical purity of the L-carnitine obtained from the racemate was very high, ee > 99%, and did not depend on the degree of conversion, the method of pH control, or the purity of the enzyme employed. Despite the complex inhibition pattern, total conversion of the substrate can be achieved, even at an initial concentration as high as 1 M racemate.[4] These properties make L-carnitine amidase a valuable tool for L-carnitine production.

PEPTIDE AMIDASE

We described first an enzyme hydrolyzing the C-terminal amide groups in peptides from the flavedo of oranges.[5] The enzyme can be detected also in fruits and leaves of various species of the Rutaceae family; however, its natural substrate and function are still unknown. The peptide amidase is highly regioselective and stereo-selective and can be used with advantage in peptide chemistry.[6] This new enzyme allows the selective removal of the amide group in the C-terminal position. A technically useful catalyst may be extracted from orange peels, using an aqueous two-phase system composed of polyethylene glycol and sodium citrate as summarized in TABLE 1.
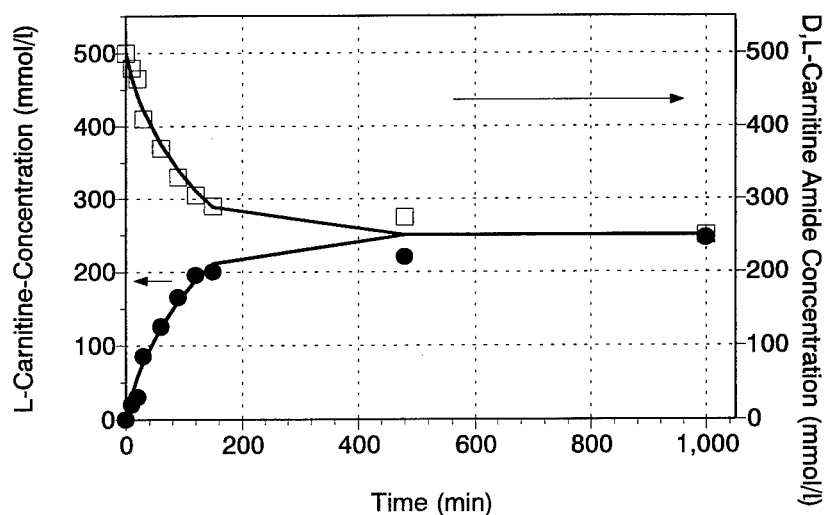
FIGURE 1. Batch conversion of racemic carnitine amidase (starting concentration, 500 mM; points = measurements; lines = simulation; 16.7 U/mL; 30 °C; pH 8.5).

TABLE 1. Purification of Plant Peptide Amidase by Aqueous Two-Phase Systems

	Specific Activity (U/mg BSA equiv.)	Purification (fold)	Yield (%)
Crude extract	0.14	1	100
Phase system I (16% PEG 1550, 10.8% citrate)	0.65	4.6	100
Phase system II (50% top-phase from system I, 7.2% citrate, 12% PEG 20,000)	1.84	13.1	98
Ultrafiltration	2.02	14.4	85

The enzyme from oranges (*Citrus sinensis*) could be purified to a specific activity of 100 U/mg by pseudoaffinity methods, but it still exhibited a complex band pattern in native and SDS electrophoresis, apparently due to glycosylation and proteolytic modification of the protein, which frustrated further purification efforts. Because the activity available from peels varies with season and other uncontrollable factors, we searched for an alternate enzyme source, preferentially from microorganisms.

MICROBIAL PEPTIDE AMIDASE

Limited Screening

We selected at random 45 strains of our collection of single colonies obtained by screening for growth on D,L-carnitine amide as the sole nitrogen source.[2] The cells were cultivated and the cell-free extracts were assayed for peptide amidase activity using Z-Gly-Tyr-NH$_2$ as the substrate. Peptide amidase activity of >3 mU/mg was found in 6 strains; 5 strains were later identified as isolates of *Stenotrophomonas maltophilia* by the German Culture Collection.[7]

The peptide amidase appears to be constitutively expressed in *S. maltophilia*. No significant increase in activity was observed by adding various amides (Leu-NH$_2$, carnitine amide, N-Ac-Met-NH$_2$) to the growth medium. The enzyme could be purified about 500-fold to homogeneity. After ion exchange chromatography followed by gel filtration, the peptide can be used for a deprotection step in peptide synthesis. The properties of the microbial and plant enzymes are compared in TABLE 2.

Substrate Range

The substrate range of the microbial peptide amidase[7] is remarkably similar to that of the plant enzyme.[8] With the exception of proline, all proteinaceous amino acids are accepted in the C-terminal position of peptide amides. The C-terminal amino acid has to have the L-configuration; peptides with D-amino acids in internal positions are accepted as long as the terminal residue has the correct L-configuration. The peptide amidase does not hydrolyze amide functions in the side chain of Asn or Gln. The smallest substrates recognized are N-protected amino acids. Some nonpro-

TABLE 2. Comparison of the Microbial Peptide Amidases from the Flavedo of *Citrus sinensis* (PAF) and *Xanthomonas maltophilia* (PAX)

	PAF	PAX
Specific activity (U/mg)	100.1	2.13
Activity of amino acid amidase	0	0
Activity of proteases/peptidases	0	0
Molecular weight (gel filtration) [Da]	27,000	38,000
Optimum pH	6.5–8.7	5.6–6.5
Optimum temperature [°C]	30–35	37–45
Isoelectric point	9.5	5.8

teinaceous amino acid amide derivatives are also substrates for the enzyme, which opens a way for resolution of racemates if the conventional acylase process is not efficient.[9]

REFERENCES

1. KAMPHUIS, J. *et al.* 1992. The production and uses of optically pure natural and unnatural amino acids. *In* Chirality in Industry. A. N. Collins, G. N. Sheldrake & J. Crosby, Eds.: 187–208. Wiley. New York.
2. JOERES, U. & M-R. KULA. 1994. Purification and characterization of a microbial L-carnitine amidase. Appl. Microbiol. Biotechnol. **40:** 606–610.
3. JOERES, U. & M-R. KULA. 1994. Screening for a novel enzyme hydrolyzing L-carnitine amide. Appl. Microbiol. Biotechnol. **40:** 599–605.
4. JOERES, U., A. S. BOMMARIUS, J. THÖMMES & M-R. KULA. 1995. Studies on the kinetics and application of L-carnitine amidase for the production of L-carnitine. Biocatalysis **12:** 27–36.
5. STEINKE, D. & M-R. KULA. 1990. Selektive deamidierung von peptidamiden. Angew. Chem. **102:** 1204–1206; Angew. Chem. Int. Ed. Engl. **29:** 1139–1140.
6. SCHWARZ, A., D. STEINKE, M-R. KULA & C. WANDREY. 1992. A two-step enzymatic synthesis of dipeptides. Biotechnol. Bioeng. **39:** 132–140.
7. STELKES-RITTER, U., K. WYZGOL & M-R. KULA. 1995. Purification and characterization of a newly screened microbial peptide amidase. Appl. Microbiol. Biotechnol. **44:** 393–398.
8. KAMMERMEIER-STEINKE, D., A. SCHWARZ, C. WANDREY & M-R. KULA. 1993. Studies on the substrate specificity of a peptide amidase partially purified from orange flavedo. Enzyme Microb. Technol. **15:** 764–769.
9. STELKES-RITTER, U., K. WYZGOL, A. S. BOMMARIUS, M. SCHWARM, K. DRAUZ & M-R. KULA. 1994. Characterization of a newly screened microbial peptide amidase. *In* Proceedings of the Fifth Akabori Conference. E. Wünsch, Ed.: 66–69. Max Planck Gesellschaft. Munich, Germany.

Carbon-Carbon Bond Synthesis

Preparation and Use of Immobilized Transketolase[a]

SIMON P. BROCKLEBANK, ROBIN K. MITRA,
JOHN M. WOODLEY, AND MALCOLM D. LILLY[b]

Advanced Center for Biochemical Engineering
Department of Chemical and Biochemical Engineering
University College London
London WC1E 7JE, United Kingdom

INTRODUCTION

Stereospecific carbon-carbon bond synthesis is potentially an important reaction in synthetic organic chemistry. Among other enzymes, carbon-carbon bond synthesis can be catalyzed by transketolase [EC 2.2.1.1]. Transketolase is a dimer with identical subunits of 70 kDa, which requires thiamine pyrophosphate (TPP) and a divalent metal ion (Mg^{2+}) as cofactors.[1] Unlike other enzymes involved in carbon-carbon bond synthesis, transketolase does not require phosphorylated substrates.[2]

The structural gene and promoter for the *Escherichia coli* enzyme have been cloned in that organism to give a high expression system[3] and the enzyme has been purified.[4] The structure of the *E. coli* enzyme crystal has been elucidated[5] and recently resolved to 1.9 Å.[6] Its substrate specificity[4] and performance in a model biotransformation producing erythrulose have also been evaluated.[7] In addition, significant quantities of the enzyme have been produced on a large scale[8] and we are now at the stage of developing a suitable biotransformation process.

The form of the biocatalyst can have a considerable impact upon the bioreactor design, product purification, productivity, and economics of a biotransformation process.[9] Therefore, the development of a biocatalyst is a critical stage in the development of an integrated biotransformation process.[10]

Because *E. coli* transketolase can be produced in large quantities at pilot scale, the cost of producing the enzyme is sufficiently low that its use in commercial biotransformations can be contemplated. The TPP and metal ion cofactors are not directly consumed in the biotransformation and, hence, cofactor recycling is unnecessary. Many of the most useful aldehydes are insoluble in water and may not be able to enter the intact cell unless its membrane has been made more permeable. With these characteristics in mind, we have chosen to use the isolated enzyme as the biocatalyst.

Due to the potential benefits of immobilization, immobilized enzymes have seen increasing use in the bioprocessing industry.[11,12] As such, immobilization allows the enzyme to be retained in the bioreactor, reclaimed, or used in a continuous process. The immobilization of an enzyme may also result in its stabilization.[13,14] In this study,

[b]To whom all correspondence should be addressed.

729
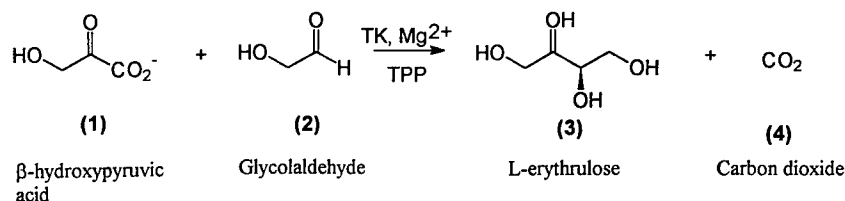
FIGURE 1. Transketolase-catalyzed transfer of the ketol group from hydroxypyruvic acid (**1**) to glycolaldehyde (**2**), liberating L-erythrulose (**3**) and carbon dioxide (**4**).

we describe the preparation of transketolase immobilized by covalent binding to epoxy-activated polymethylacrylamide beads (Eupergit-C®) and the performance of this biocatalyst in a model reaction.

The use of β-hydroxypyruvic acid (HPA) (**1**) as a ketol donor yields carbon dioxide as a by-product and consequently leads to complete aldehyde conversion. Glycolaldehyde (GA) (**2**) is the simplest aldol acceptor and the enzyme has the greatest affinity for this substrate.[15] The transfer of a ketol group from β-hydroxypyruvic acid (supplied as the lithium salt) to glycolaldehyde yields L-erythrulose (**3**) and carbon dioxide (**4**) as shown in FIGURE 1.

The product, L-erythrulose, is a competitive inhibitor of transketolase.[16] It also is believed to act as a ketol donor and can subsequently cause a futile cycle when bound to transketolase.[17] The use of hydroxypyruvic acid results in a pH change, and soluble bicarbonate, in equilibrium with the carbon dioxide by-product, is produced as the HPA is consumed during the reaction. There is thus a net requirement for acid addition to maintain pH.

IMMOBILIZATION

Immobilization can be achieved in several ways: physical entrapment within a polymer gel, adsorption, ionic binding, and covalent binding to the support. Covalent binding is achieved by the formation of one or more tight bonds between functional groups on the support and on the surface of the enzyme. The covalent bond produces a strong link between the enzyme and its supporting matrix that prevents the protein from leaching from the surface of the support. This is especially advantageous where regulations prohibit the presence of biological compounds in the product stream.

The support may be activated by the addition of electrophilic groups and, in the case of Eupergit-C®, these are oxirane groups. This makes the support more reactive towards the nucleophilic groups present on the enzyme.[18] The groups on the enzyme available for binding can be the terminal amine, other amines, or hydroxyl or thiol groups. In order to promote the reaction, the nucleophiles on the enzyme's surface need to be deprotonated; hence, high pH values are normally required. Because the resolution of the TPP and Mg^{2+} cofactors from the holoenzyme and the stability of the enzyme are both affected by the pH of the binding buffer solution,[7,19] it is logical to use a binding pH that causes minimal denaturation of the enzyme. Epoxide groups are strong electrophiles and therefore can react readily with amine groups at pH

values approaching neutrality. Eupergit-C® is a commercially available epoxy-activated polymethylacrylamide support.

Binding of Transketolase to Eupergit-C®

FIGURE 2 shows the binding of transketolase to Eupergit-C® beads at pH 7.5 in 1 M phosphate buffer. The binding of protein follows a similar profile to that of transketolase. During the first hour of incubation, 70% of the transketolase disappeared from solution. However, when the support was washed, only 40% of the enzyme remained bound to the support, indicating that the remainder of the enzyme was merely trapped in the pore volume of the support and could be washed off. As the immobilization time increased, more enzyme remained bound to the support, as indicated by the reduced amount removed during washing. This suggested that the initial rapid disappearance of the enzyme may be due to the adsorption of the enzyme to the support or to entrapment of the enzyme in the pore volume rather than due to covalent binding. The amount of enzyme washed off the support decreased over the immobilization period, implying that the reaction between the enzyme and the epoxide groups is slower than the rate of disappearance of the enzyme from solution. After 24 hours, 90% of the enzyme had bound to the support and little of the enzyme could be washed off. A 48-hour preparation was stored in 10 mM buffer at pH 7.5 and no transketolase activity was observed in the supernatant after 3 days of incubation, indicating complete binding of the enzyme to the support.

FIGURE 3 shows the effect of varying the amount of enzyme presented to Eupergit-C®. At an enzyme loading of up to 700 U/g (wet), over 90% of the enzyme was bound to the support. The specific activity (expressed as U/g wet Eupergit-C®), measured as an initial rate, in a biotransformation at pH 7 with 100 mM hydroxypyruvate and glycolaldehyde, approached a maximum value of 100 U/g (wet) at an
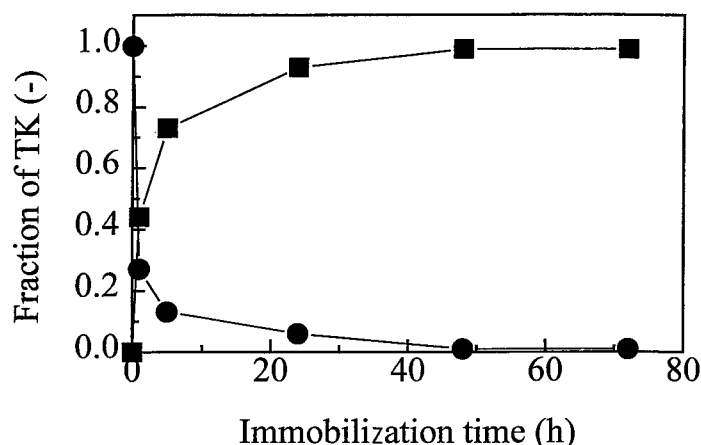
FIGURE 2. Immobilization of transketolase to Eupergit-C® in 1 M phosphate buffer at pH 7.5, showing the fraction of transketolase activity bound (■) and the fraction of transketolase activity remaining in solution (●).

enzyme loading of 600 U/g (wet). This is reflected in the decrease in retained activity (defined as the observed activity expressed as a percentage of the activity bound) as the enzyme load is increased. When a 900-U/g (wet) preparation was ground to decrease the particle size and therefore increase the rate of diffusion of substrates, cofactors, and products, increases in biotransformation activity and retained activity were observed.

BIOTRANSFORMATION

Use of Soluble Transketolase

The conversion by soluble transketolase (5.8 U/mL) of 100 mM hydroxypyruvic acid and glycolaldehyde into erythrulose and carbon dioxide is shown in FIGURE 4.
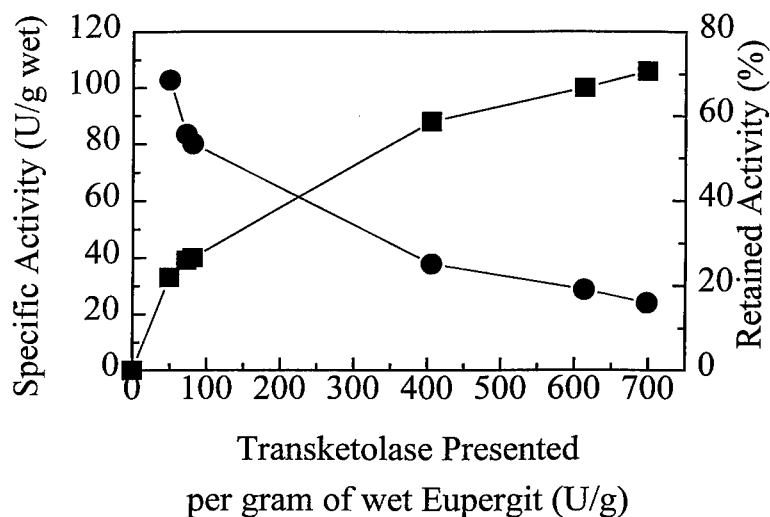
FIGURE 3. Effect of enzyme loading upon the specific activity and the percentage of retained activity of immobilized transketolase: specific activity of the biocatalyst measured in the biotransformation with 100 mM reactants (■) and the percentage of retained activity (●).

There was a stoichiometric yield of product. As the hydroxypyruvic acid was consumed, HCl was added to maintain the pH at 7.0. However, the amount of HCl added was less than the product formed on a molar basis due to the formation of bicarbonate in equilibrium with the carbon dioxide produced.

Use of Immobilized Transketolase

The progress of a biotransformation with initial reactant concentrations of 100 mM, catalyzed by immobilized transketolase (80 U/g wet wt), is shown in FIGURE 5.
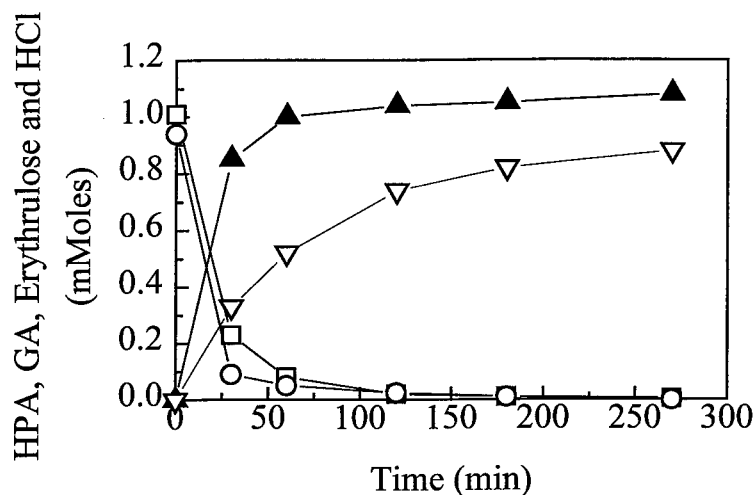
FIGURE 4. Mass balance for a biotransformation with initial reactant concentrations of 100 mM using soluble transketolase (5.8 U/mL), showing the number of moles of hydroxypyruvate (□), glycolaldehyde (○), erythrulose (▲), and HCl (▽) in the reactor.

Again, there was a stoichiometric conversion of reactants to products. In order to give an indication of the operational stability of the immobilized enzyme, a second biotransformation was carried out with each immobilized preparation. The immobilization time can affect the number of interactions between the support and the
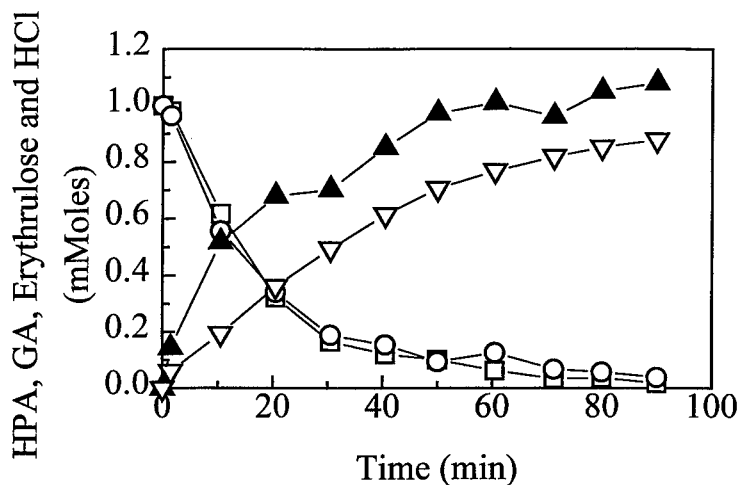
FIGURE 5. Mass balance for a biotransformation with initial reactant concentrations of 100 mM using immobilized transketolase (80 U/g), showing the number of moles of hydroxypyruvate (□), glycolaldehyde (○), erythrulose (▲), and HCl (▽) in the reactor.

enzyme and thereby the stability of the biocatalyst.[20] There was an improvement in the operational stability of the preparation allowed to react with Eupergit-C® for 72 hours compared with that allowed to react for 24 hours. However, when the immobilized holoenzyme was stored overnight in 10 mM phosphate buffer at pH 7.5, little activity was recovered. Conversely, the immobilized apoenzyme can be stored under the same conditions without loss of activity. When a preparation of the immobilized holoenzyme was exposed to pH 9.5 to resolve any bound cofactors, an improvement in the storage stability was observed.

When compared with that for the free enzyme, the erythrulose production and HCl addition profiles with the immobilized enzyme were different. This indicated that some mass-transfer limitation was probably occurring within the particles. This conclusion was supported by the improvement in activity when the beads were ground.

DISCUSSION

Transketolase has been successfully bound to Eupergit-C® to give active preparations of the immobilized enzyme. As the immobilization time is increased, more bonds between the enzyme and the support are made. Blanco and coworkers[20] showed that an increase in the reaction time between trypsin and an aldehyde-activated agarose support resulted in an increase in the thermal stability of the enzyme. A longer immobilization time did enhance the operational stability of immobilized transketolase, but there is still a need for further improvement. Initial results indicate that the immobilized apoenzyme is more stable than the holoenzyme. When the immobilized holoenzyme was washed and stored in buffer at pH 9.5, the activity was recovered. This indicates that the reduction of activity between batch reactions is due to the inactivation of the holo-form. The free apoenzyme has also been shown to be more stable than the free holoenzyme. Recently, the free enzyme has been shown to be susceptible to an oxidizing environment during the biotransformation, which can be alleviated by addition of mercaptoethanol or by removal of oxygen via nitrogen sparging.[21]

As the enzyme loading was increased, the fraction of the activity retained fell. It can be expected that more enzyme will penetrate deeper into the support, increasing the likelihood of mass-transfer limitation. Borchert and Buchholz[22] demonstrated that a nonuniform distribution of enzyme within the support can increase the effectiveness of the biocatalyst. Carleysmith and coworkers[23] demonstrated that the activity of immobilized penicillin acylase increased following grinding and a similar observation was made with immobilized transketolase. Internal mass-transfer limitation of the rate of reaction can be especially disadvantageous for a product-inhibited enzyme such as transketolase as the product concentration within the support may be at an inhibitory level even if the concentration in the bulk of the reactor is low. *In situ* product removal (ISPR) may be integrated with the immobilized enzyme biotransformation to reduce the bulk erythrulose concentration and therefore increase the rate of mass transfer of product out of the particle.[24]

Protein engineering is being undertaken to modify the transketolase to influence the orientation of the protein during immobilization and therefore improve the accessibility of the active sites to reactants.[25]

Throughout the work described here, Eupergit-C® has been used as the support material. It is one of a few commercially available materials with properties suitable for large-scale operations, but is relatively expensive. Other work is being done, therefore, using cheaper materials such as Amberlite resins[23] to immobilize transketolase.

REFERENCES

1. LINDQVIST, Y., G. SCHNEIDER, U. ERMLER & M. SUNDSTRÖM. 1992. Three-dimensional structure of transketolase, a thiamine diphosphate–dependent enzyme, at 2.5 Å resolution. EMBO J. **11:** 2373–2379.
2. VILLAFRANCA, J. J. & B. AXELROD. 1971. Heptulose synthesis from nonphosphorylated aldoses and ketoses by spinach transketolase. J. Biol. Chem. **246:** 3126–3131.
3. FRENCH, C. & J. M. WARD. 1995. Improved production and stability of *E. coli* recombinants expressing transketolase for large-scale biotransformation. Biotechnol. Lett. **17:** 247–252.
4. HOBBS, G., M. D. LILLY, N. J. TURNER, J. M. WARD, A. J. WILLETTS & J. M. WOODLEY. 1993. Enzyme-catalyzed carbon-carbon bond formation: use of transketolase from *Escherichia coli.* J. Chem. Soc. Perkin Trans. **I:** 165–166.
5. LITTLECHILD, J., N. J. TURNER, G. HOBBS, M. D. LILLY, A. RAWAS & H. WATSON. 1995. Crystallisation and preliminary X-ray crystallographic data with *E. coli* transketolase. Acta Crystallogr. **D51:** 1074–1076.
6. ISUPOV, M., M. RUPPRECHT, Z. DAUTER, K. WILSON & J. LITTLECHILD. 1996. 1.9 Å resolution structure of *Escherichia coli* transketolase. Structure. Submitted.
7. WOODLEY, J. M., R. K. MITRA & M. D. LILLY. 1995. Carbon-carbon bond synthesis: reactor design and operation for transketolase-catalyzed biotransformations. This volume.
8. HOBBS, G. R., R. K. MITRA, R. P. CHAUHAN, J. M. WOODLEY & M. D. LILLY. 1996. Enzyme-catalyzed carbon-carbon bond formation: large-scale production of *Escherichia coli* transketolase. J. Biotechnol., p. 173–179.
9. WOODLEY, J. M., A. J. HARROP & M. D. LILLY. 1990. The impact of biocatalyst selection on the design of aqueous-organic biphasic biocatalytic processes. Ann. N.Y. Acad. Sci. **613:** 191–200.
10. WOODLEY, J. M. & M. D. LILLY. 1994. Biotransformation reactor selection and design. *In* Applied Biocatalysis. J. M. S. Cabral, D. Best, L. Boross & J. Tramper, Eds.: 371–393. Harwood. Chur, Switzerland.
11. CHEETHAM, P. S. J. 1994. Case studies in applied biocatalysis. *In* Applied Biocatalysis. J. M. S. Cabral, D. Best, L. Boross & J. Tramper, Eds.: 47–108. Harwood. Chur, Switzerland.
12. CHIBATA, I., T. TOSA & T. SHIBATANI. 1992. The industrial production of optically active compounds by immobilized biocatalysts. *In* Chirality in Industry. A. N. Collins, G. N. Sheldrake & J. Crosby, Eds.: 352–370. Wiley. New York.
13. GABEL, D. 1973. The denaturation by urea and GuCl of trypsin and *N*-acetylated trypsin derivatives bound to sephadex and agar. Eur. J. Biochem. **33:** 348–356.
14. ULTHRICH, R., A. SCHELLENBERGER & W. DEMERAU. 1986. Studies on the thermal inactivation of immobilized enzymes. Biotechnol. Bioeng. **28:** 511–522.
15. BOLTE, J., C. DEMUYNCK & H. SAMAKI. 1987. Utilization of enzymes in organic chemistry: transketolase-catalyzed synthesis of ketoses. Tetrahedron Lett. **28:** 5525–5528.
16. GYEMARAH, M., R. K. MITRA & A. J. WILLETTS. 1995. Kinetics of overexpressed transketolase from *Escherichia coli* JM107/pQR700. Presented at BIOTRANS '95, Warwick, United Kingdom.
17. HOBBS, G. R. 1994. Ph.D. thesis. University of London.
18. PORATH, J. & R. AXEN. 1976. Immobilization of enzymes to agar, agarose, and sephadex supports. Methods Enzymol. **44:** 19–46.
19. HEINRICH, P. C., H. STEFFEN, P. JENSER & O. WISS. 1972. Studies on the reconstitution of

apotransketolase with thiamine pyrophosphate and analogs of the coenzyme. Eur. J. Biochem. **30:** 533–541.

20. BLANCO, R., J. CALVETE & J. GUISAN. 1989. Immobilization-stabilization of enzymes: variables that control the intensity of trypsin-agarose multipoint attachment. Enzyme Microb. Technol. **11:** 353–359.

21. MITRA, R. K., J. M. WOODLEY & M. D. LILLY. 1996. Transketolase-catalyzed carbon-carbon bond formation: biotransformation characterization for process evaluation and selection. Enzyme Microb. Technol. Submitted.

22. BORCHERT, A. & K. BUCHHOLZ. 1984. Improved biocatalyst effectiveness by controlled immobilization of enzymes. Biotechnol. Bioeng. **24:** 727–736.

23. CARLEYSMITH, S. M., P. DUNNILL & M. D. LILLY. 1980. Kinetic behavior of immobilized penicillin acylase. Biotechnol. Bioeng. **22:** 735–756.

24. CHAUHAN, R., J. M. WOODLEY & L. W. POWELL. 1996. *In situ* product removal from *E. coli* transketolase-catalyzed biotransformations. This volume.

25. LILLY, M. D., R. CHAUHAN, C. FRENCH, M. GYEMARAH, G. R. HOBBS, A. HUMPHREY, M. ISUPOV, J. A. LITTLECHILD, R. K. MITRA, K. G. MORRIS, M. RUPPRECHT, N. J. TURNER, J. M. WARD, A. J. WILLETTS & J. M. WOODLEY. 1996. Carbon-carbon bond synthesis: the impact of rDNA technology on the production and use of *E. coli* transketolase. Ann. N.Y. Acad. Sci. **782:** 513–525.

Lipase-catalyzed Ester Synthesis[a]

YU-YEN LINKO,[b] ZHUO-LIN WANG,[b] MERJA LÄMSÄ,[c]
AND JUKKA SEPPÄLÄ[d]

[b]*Laboratory of Biotechnology and Food Engineering*
Helsinki University of Technology
FIN-02150 Espoo, Finland

[c]*Raisio Group Oil Milling Industry*
FIN-21200 Raisio, Finland

[d]*Laboratory of Industrial Chemistry and Polymer Technology*
Helsinki University of Technology
FIN-02150 Espoo, Finland

INTRODUCTION

The use of lipases (EC 3.1.1.3, triacylglycerol acyl hydrolases) as biocatalysts in ester[1,2] and polyester[3,4] synthesis has recently been the object of increasing interest. In addition to glycerol ester hydrolysis, lipases can catalyze a wide variety of esterification, transesterification, polyesterification, and polytransesterification reactions. The transesterifications include acidolysis, alcoholysis, interesterification, and aminolysis. The present paper discusses the applications of lipases both in the upgrading of rapeseed oil, a renewable raw material, by transesterification without additional organic solvent to obtain environmentally acceptable, biodegradable useful products and in the production of high-molar-mass biodegradable polyesters. Transesterification of rapeseed oil fatty acids and 2-ethyl-1-hexanol, polyesterification of diacids with diols, and polytransesterification of derivatized diacids with diols are used as example cases.

MATERIALS AND METHODS

Lipases

Crude, commercial lipases in powdered form from *Pseudomonas fluorescens*, *Rhizomucor miehei*, and *Candida rugosa* (ex. *cylindracea*) were obtained from Biocatalysts Limited (Wales, United Kingdom) and that of porcine pancreas was from Sigma Chemical (St. Louis, Missouri).

Chemicals

Rapeseed oil was obtained from the Raisio Group Oil Milling Industry (Raisio, Finland) and 2-ethyl-1-hexanol was from Fluka Chemie (Buchs, Switzerland). All

diacids and diols used were obtained from Aldrich-Chemie (Steinheim, Germany). Derivatized diacids were synthesized as previously described.[5] Organic solvents were stored over a 4-Å (0.4-nm) molecular sieve.

2-Ethyl-1-hexyl Ester of Rapeseed Oil

Lipase-catalyzed transesterification (alcoholysis) of 2-ethyl-1-hexanol and rapeseed oil was carried out in stirred-batch bioreactors without additional organic solvent, in up to 2-kg scale, basically as described in reference 6.

Polyesterification and Polytransesterification

A suitable quantity of lipase powder was added to the reaction mixture of a diacid (polyesterification) or derivatized diacid (polytransesterification) and a diol in an organic solvent. The polymerization was carried out under magnetic stirring and, when appropriate, under vacuum.

Analytical Methods

Rapeseed oil conversion (% rapeseed oil used) and ester yield (% of theoretical) were determined using reversed-phase high-performance liquid chromatography (HPLC), employing a Perkin-Elmer (Norwalk, Connecticut) four-pump module, an ISS-100 sampler, a 101 oven, a Novapack C18 3.9×150 mm column with 4-μm silica particles, an HP 1047A refractive index detector, a PE 316 integrator, and a PE 7500 professional computer. The running solvent was acetone:acetonitrile (1:1) at 1.0 mL/min, 37 °C, for 30 min.

The mass-average molar mass $(\overline{M}_w)$ of the polymer was determined by gel permeation chromatography (GPC), using three serially connected μ-Styragel columns (0.01 μm, 0.05 μm, and 0.1 μm). HPLC-grade chloroform (Rathburn Chemicals, Walkerburn, Scotland) was used as the eluant at a rate of 1.0 mL/min. The peaks were detected by a UV detector at 254 nm.

Infrared spectroscopy analysis was performed on a Philips Pye Unicam SP3-100 infrared spectrophotometer (Pye Unicam, Cambridge, United Kingdom) equipped with a Philips P3150 computer with a double-beam ratio recording mode and a scan time of 8 minutes. The sample pellet contained 0.8% of the oligomer mixture in potassium bromide.

^{13}C-NMR spectra were measured with a Varian Unity-400 NMR spectrometer at 100.577 MHz. The proton-decoupled ^{13}C-NMR spectrum was recorded at room temperature in a $CDCl_3$ solution of the polyester (0.15 g in 0.7 mL) with an 82° pulse (8.7 μs), 25,000-Hz spectrum width, 1.199-s acquisition time, and 2000 scans. [13]C chemical shifts were related to the 77-ppm peak of deuterated chloroform.

Differential scanning calorimeter (DSC) measurements were carried out by a PL Thermal Sciences DSC (Rheometric Scientific, formerly Polymer Laboratories, Epsom, United Kingdom). Nitrogen was used as the sweeping gas, and 6.6-mg samples were heated twice at a rate of 10 °C/min in order to ensure similar thermal history. The scanning temperature range was from -100 to 100 °C.

RESULTS AND DISCUSSION

Transesterification

Among the various commercial lipases investigated, best results were obtained with lipase from *Candida rugosa*. As could be expected, an increase in lipase quantity markedly increased the rapeseed oil conversion during the first few hours, but in about 7 to 12 hours the differences almost leveled off. FIGURE 1 illustrates the rapeseed oil conversion as a function of time with 0.3%, 3.3%, and 14.6% lipase, a substrate molar ratio of 2.8, and 3.0% added water. With the highest lipase quantity used, the reaction was nearly complete in 1 hour and, with 3.3% lipase, it took 7 h; in contrast, conversions of only about 26% and 88% with 0.3% lipase were obtained in 1 and 7 h, respectively. Interestingly, Goldberg *et al.*[7] reported that an increase in the
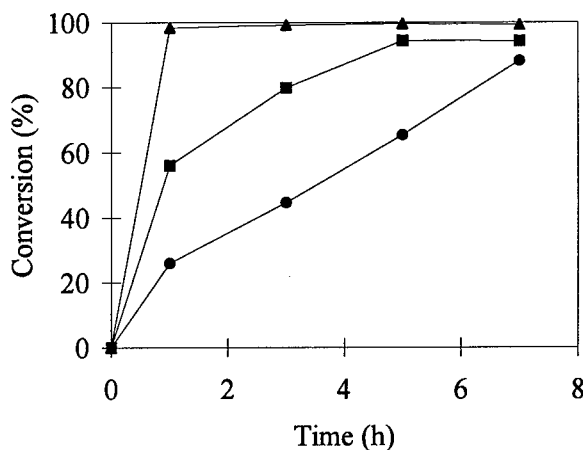
FIGURE 1. Effect of *Candida rugosa* lipase (●, 0.3%; ■, 3.3%; and ▲, 14.6%, w/w) on the transesterification between rapeseed oil and 2-ethyl-1-hexanol (substrate molar ratio, 2.8; 3.0%, w/w, added water).

quantity of powdered *C. rugosa* lipase results in a decrease in the apparent enzyme activity in the production of heptyl oleate, owing to an increase in diffusion limitation, a problem that in large-scale experiments may be minimized by optimal biocatalyst and bioreactor design.

While investigating the effects of added carriers and adsorbents on transesterification, we also found that an approximately 95% (100% of theoretical) rapeseed oil conversion (50 g of oil) was achieved in 75 h in the presence of 7.5 g of Amberlite XAD-7 resin per 2.5 g of lipase. Furthermore, the optimal conditions for a 2-kg batch operation were 2000 g of rapeseed oil, 1 L (829 g) of 2-ethyl-1-hexanol, 3% added water, 100 g of lipase with 300 g of XAD-7 resin, 170 rpm, and 37 °C. An example time course of the small pilot-scale transesterification is shown in FIGURE 2. About 90% conversion (97% of theoretical) was obtained in 8 h, equal to 22.4 g ester per g lipase or 112 g ester per 100 g rapeseed oil. Although the total reaction time

increased somewhat in the presence of the Amberlite XAD-7 carrier, the final conversion was increased by at least about 20% to nearly theoretical.

Polyesterification and Polytransesterification

When bis(2,2,2-trifluoroethyl) sebacate was polymerized with 1,4-butanediol at ambient pressure to form poly(1,4-butyl sebacate) using *Rhizomucor miehei* lipase as the biocatalyst, the mass-average molar mass of the polyester obtained in 72 hours was only 7800 g/mol (DP = 31) or less, as compared with the 27,700 g/mol (DP = 110) obtained in a vacuum system for the removal of the 2,2,2-trifluoroethanol formed during the transesterification. In general, up to four times higher mass-average molar masses were obtained with the underivatized diacids in vacuum than at the atmospheric pressure and they were of the same order of magnitude as
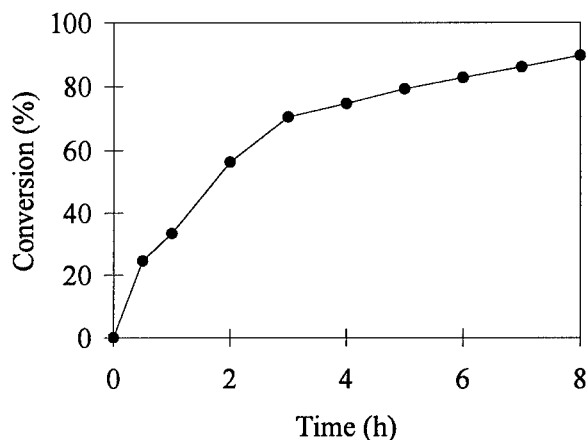
FIGURE 2. Time course of the transesterification between 2 kg of rapeseed oil and 829 g of 2-ethyl-1-hexanol (molar ratio, 2.8) with 100 g (3%) of *Candida rugosa* lipase, 300 g of Amberlite XAD-7 resin as carrier, and 3% added water, at 170 rpm and 37 °C.

that obtained in the polytransesterification of the derivatized acid. Under optimal conditions at 37 °C, the polymerization with both the derivatized sebacate and dodecanedioate progressed with time up to 168 hours (7 days), at which time a maximum average molar mass of 46,410 g/mol (DP = 184) or 34,750 g/mol (DP = 128), respectively, was obtained (FIGURE 2). This compares favorably with the approximately 40,000 g/mol (DP = 190) reported by Morrow[8] on polytransesterification of bis(2,2,2-trifluoroethyl) glutarate with 1,4-butanediol in veratrole, catalyzed by porcine pancreatic lipase for 432 hours (18 days).

Even with the underivatized sebacic acid and 1,4-butanediol in vacuum at 37 °C, a mass-average molar mass of 46,130 g/mol (DP = 183) was obtained; with hexanedioic acid and hexanediol, up to 70,430 g/mol (DP = 279), with the maximum molar mass of 126,510 g/mol (DP = 501), was obtained. The effect of chain length of the dicarboxylic acid and diol on the molar mass of the polyester at 37 °C is shown in

TABLE 1. Effect of Chain Length of Dicarboxylic Acid and Diol on the Molar Mass of Polyester

	C_2-diol	C_3-diol	C_4-diol	C_5-diol	C_6-diol
C_4-diacid					
$\overline{M}_n$	710	920	1560	1850	1880
$\overline{M}_w$	980	1150	2140	5290	3740
DP	6.8	7.3	12.4	28.4	18.7
C_6-diacid					
$\overline{M}_n$	1890	3590	4530	5340	6770
$\overline{M}_w$	6420	26,830	38,970	37,270	70,430
DP	37.3	114.3	194.8	174.2	308.9
C_8-diacid					
$\overline{M}_n$	1510	5570	3930	5190	5880
$\overline{M}_w$	2090	51,730	48,590	55,020	43,480
DP	10.4	241.7	213.1	227.3	169.8
C_{10}-diacid					
$\overline{M}_n$	2160	4100	3790	4580	5960
$\overline{M}_w$	9760	35,550	46,130	53,680	62,480
DP	42.8	146.9	180.2	198.8	219.9
C_{12}-diacid					
$\overline{M}_n$	1990	3620	3990	5090	4550
$\overline{M}_w$	8960	26,070	21,450	28,320	16,220
DP	35.0	96.6	75.5	95.0	52.0

[a]Conditions: 1.5 mM dicarboxylic acid with 1.5 mM diol at 37 °C; 7 days with programmed vacuum catalyzed by 0.25 g of *Rhizomucor miehei* lipase in 2.25 mL of diphenyl ether; yield: 85–93%.
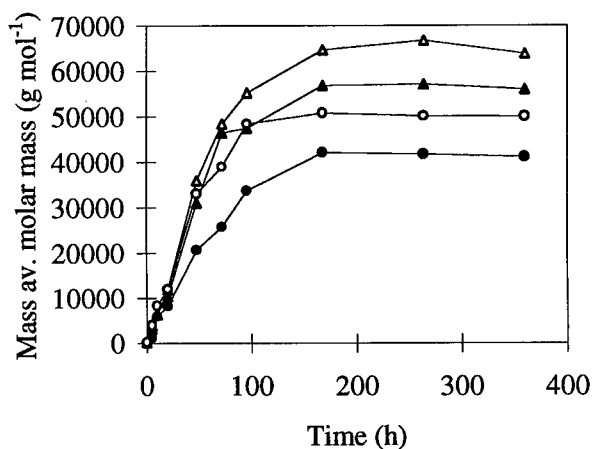
FIGURE 3. Effect of reaction temperature (●, 37 °C; △, 45 °C; ▲, 53 °C; and ○, 60 °C) on the polyesterification between sebacic acid (1.5 mmol) and 1,4-butanediol (1.5 mmol) with programmed vacuum, using 0.25 g of *Rhizomucor miehei* lipase as the biocatalyst and 2.25 mL of diphenyl ether as the solvent.

TABLE 1. The effect of reaction temperature is illustrated in FIGURE 3. When the reaction temperature was increased to 45 °C, the highest mass-average molar mass increased to 66,740 g/mol (DP = 264); when the polymer was reprecipitated from methanol at an 82% yield, the mass-average molar mass of the partially purified poly(1,4-butyl sebacate) increased further to 77,440 g/mol [DP = 339.6, Pd $(\overline{M}_w/\overline{M}_n)$ = 4.4, and a melting temperature of 66.8 °C as determined by DSC], with the maximum molar mass of 131,190 g/mol (DP = 520). This is believed to be the highest molar mass reported by lipase-catalyzed polyesterification between a diacid and a diol. The partially purified white solid was shown to be linear poly(1,4-butyl sebacate) by ^{13}C-NMR.

REFERENCES

1. LINKO, Y-Y., M. LÄMSÄ, A. HUHTALA & O. RANTANEN. 1995. Lipase biocatalysis in the production of esters. J. Am. Oil Chem. Soc. 72(11): 1293–1299.
2. LÄMSÄ, M., A. HUHTALA, Y-Y. LINKO & P. LINKO. 1994. 2-Ethyl-1-hexanol fatty acid esters from rapeseed oil by transesterification. Biotechnol. Tech. 8: 451–456.
3. LINKO, Y-Y., Z-L. WANG & J. SEPPÄLÄ. 1995. Lipase-catalyzed linear aliphatic polyester synthesis in organic solvent. Enzyme Microb. Technol. 17: 506–511.
4. LINKO, Y-Y., Z-L. WANG & J. SEPPÄLÄ. 1995. Lipase-catalyzed synthesis of poly(1,4-butyl sebacate) from sebacic acid or its derivatives with 1,4-butanediol. J. Biotechnol. 40: 133–138.
5. WANG, Z-L., K. HILTUNEN, P. ORAVA, J. SEPPÄLÄ & Y-Y. LINKO. 1996. Lipase-catalyzed polyester synthesis. J. Macromol. Sci. Pure Appl. Chem. A33: 599–612.
6. LINKO, Y-Y., M. LÄMSÄ, A. HUHTALA & P. LINKO. 1994. Lipase-catalyzed transesterification of rapeseed oil and 2-ethyl-1-hexanol. J. Am. Oil Chem. Soc. 71: 1411–1414.
7. GOLDBERG, M., D. THOMAS & M-D. LEGOY. 1990. Water activity as a key parameter of synthetic reactions: the example of lipase in biphasic (lipid/solid) media. Enzyme Microb. Technol. 12: 976–981.
8. MORROW, C. J. 1992. Biocatalytic synthesis of polyesters using enzymes. MRS Bull. November: 43–47.

Acceptor Reactions of Levansucrase
from *Bacillus circulans*[a]

M. A. PÉREZ OSEGUERA, G. L. GUERECA,
AND A. LÓPEZ-MUNGUÍA

Instituto de Biotecnología
UNAM
Cuernavaca, Morelos 62271, Mexico

INTRODUCTION

Levansucrase (LS) (EC 2.4.1.10) is an enzyme known for its transfructosylase activity product, levan, a β(2-6)-fructan. However, the enzyme is also capable of transferring fructose from sucrose to water and to other nucleophiles. Therefore, if the enzyme is used for the synthesis of fructosides in the presence of an acceptor, it has the disadvantage of producing levan and hydrolyzing sucrose. The factors affecting these three simultaneous activities of LS have not been extensively studied.

As early as 1961, Dedonder reviewed the properties of transfructosylases, reporting that *Bacillus subtilis* LS was able to transfer fructose from raffinose to glucose, D-xylose, L-arabinose, D-galactose, melibiose, and lactose.[1] Recently, the same enzyme has been reported for the synthesis of noncaloric sweeteners such as cellobiofructoside and gentobiofructoside.[2] In a recent report, Ohtsuka *et al.*,[3] working with *Rahnella aquatilis* LS, screened a wide variety of sugars and sugar alcohols as acceptors. These investigators found that D-xylose and L-arabinose, among other monosaccharides, were good acceptors, as were lactose, melibiose, maltose, and cellobiose among the oligosaccharides. However, the enzyme was not able to transfer fructose to sugar alcohols such as xylitol, sorbitol, maltitol, etc. The potential applications of LS in the synthesis of useful fructosides are demonstrated by patents recently granted in Japan for products such as theanderose [o-α-D-glucopyranosyl(1-6)-o-α-glucopyranosyl-1(1,2)β-fructofuranoside] with LS from *B. subtilis*, lactosyl fructoside with LS from *B. megaterium*, and galactooligosaccharides with LS from *R. aquatilis.*

In this paper, we report the transferase properties of a levansucrase from a strain of *Bacillus circulans* isolated from cane sugar.

MATERIALS AND METHODS

The enzyme was produced in a culture medium containing sucrose as inducer and as carbon source. After fermentation, the enzyme was extracted with 25% PEG (M_w = 1500). It has been previously shown that hydrolase and transferase activities are associated with a single enzyme.[4] Reaction mixtures contained 60 g/L sucrose in

50 mM (pH 7) phosphate buffer at 30 °C. Total glucose released was measured in a Biochemistry Analyzer YSI (YS, Ohio), whereas fructose was measured enzymatically (Boehringer Mannheim). The hydrolase and transferase rates as well as the total LS activity were determined as already described.[4] In the presence of acceptors, the products were measured by HPLC in a Waters 410 differential refractometer with a Waters Carbohydrate Analysis 125 A (10 μm) column (3.9 × 300 mm) using a 75:25 mixture of acetonitrile:water as the mobile phase at a flow rate of 1.0 mL/min.

RESULTS AND DISCUSSION

The effect of reaction conditions on the relative hydrolase and transferase activities of LS has been thoroughly studied only for a few cases. In LS from *B. circulans*, the relative proportion of transferase/hydrolase rates may be modulated by varying the temperature and the pH, as already shown for other levansucrases.[5-7] Optimal conditions for the transferase reaction are 35 °C and pH 5–7. Also, the transferase activity increased as the amount of levan added to the reaction medium was increased, showing a saturation-type behavior with the maximum transferase found when 5 mg of levan was added per unit of total LS activity. However, it is interesting to point out that the increase in transferase activity was not at the expense of the hydrolase activity as there was also an increase of 60% in the total LS activity. The specific hydrolase rate remained almost constant and independent of the levan concentration. In contrast, high sucrose concentrations (above 0.6 M) were found to inhibit the transferase activity, with no effect on the maximum initial hydrolysis rate observed in the range of 0.3–1.7 M sucrose. Tanaka *et al.*[8] showed that levan acts as an activator, but not as an acceptor, of the enzyme; this was because there was no change in the molecular weight of the activator, but only an increase in concentration. Robyt *et al.*[9] observed the same activating effect on *S. mutans* dextransucrase and more recently in a constitutive mutant of *Leuconostoc mesenteroides*, demonstrating at the same time that no dextran was required as primer.[10] Based also on studies on *Leuconostoc* dextransucrases, Kobayashi *et al.*[11] proposed a scheme for the activity in which dextran binds to an acceptor site, while sucrose binds to a donor. Robyt *et al.*[9] also demonstrated the existence of more than one site in dextransucrase. The fact that transferase and hydrolase activities may be modulated is an element in favor of a second site for levan. As shown here, the presence of levan increases the transferase activity, whereas sucrose in excess may bind to both sites, inhibiting mainly the transferase activity. This is a new element supporting the hypothesis of a site for levan binding, which may also show a weaker affinity for sucrose.

LS from *B. circulans* transfers fructose from sucrose to maltose, galactose, lactose, methanol, sorbitol, and glycerol. In TABLE 1, it is shown that the three reactions occur in different proportions depending on the acceptor. Sorbitol was selected to exemplify the effect of reaction conditions on the transferring efficiency. In FIGURE 1A, the effect of sorbitol concentration in the reaction medium is shown. The reduction in water activity results in a net increase in the total reaction rate, which is a result of an increase in the transferase reaction rate. However, the hydrolysis rate remains constant and, in the range studied, independent of water activity. High concentrations of sorbitol and/or sucrose modify considerably the

TABLE 1. Acceptor Reactions of Levansucrase from *B. circulans* IBT-MB[a]

Acceptor	Fructose Transferred to Levan (%)	Fructose Transferred to Acceptor (%)	Fructose from Hydrolysis (%)
maltose	0	76	24
galactose	0	63	37
sorbitol	29	21	50
lactose	38	33	29
glycerol	—	—	50
control	43	0	57

[a]All reactions were carried out at 30 °C and pH 7 with 0.66 U/mL of total levansucrase activity and a sucrose-to-acceptor weight ratio of 1.

rheological properties of the reaction medium. Also, the solubility of sucrose is reduced as the sorbitol concentration is increased. At 60% sorbitol, sucrose concentrations higher than 10% could not be obtained. Therefore, the sorbitol concentration was reduced to 50% in order to increase the concentrations of sucrose as shown in FIGURE 1B. It is possible to inhibit the hydrolytic activity to levels of only 10% of the total LS activity from 50% in the original experiments reported in TABLE 1. The highest transferase rate was obtained with 50% sorbitol and 30% sucrose; at 50% sorbitol and 40% sucrose, the hydrolytic rate was the lowest. The reaction medium in the selected conditions presents a non-Newtonian behavior and, furthermore, a pronounced Wissenberg effect that consists of a fluid climbing through the glass impeller. As the reaction proceeds, the medium becomes more non-Newtonian. It is interesting to point out that the reaction medium (sorbitol 50%, sucrose 40%) behaves like a Newtonian fluid with a viscosity of 13 Pa, whereas purified levan in solution behaves like a non-Newtonian fluid. Therefore, levan confers non-Newtonian properties to the fluid.
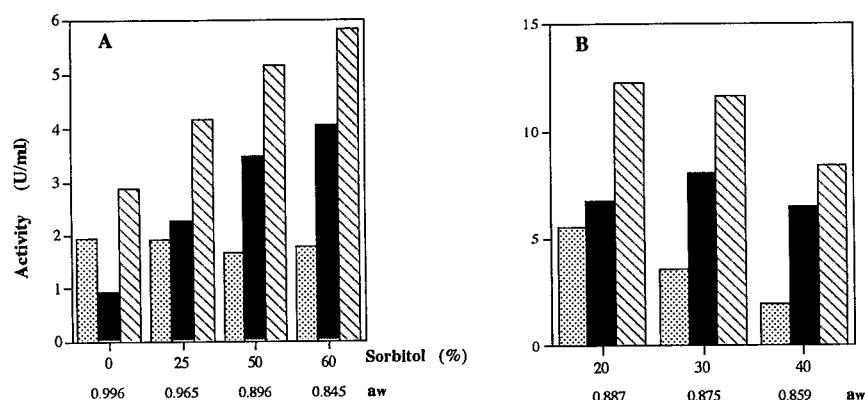
FIGURE 1. Effect of sorbitol and sucrose concentrations on the activities of *B. circulans* IBT-MB levansucrase. Reaction conditions: pH 7, 30 °C. (A) Effect of sorbitol (sucrose, 6%). (B) Effect of sucrose (sorbitol, 50%). In the absence of sorbitol, the total activity is 3 U/mL. Terms: (stippled) invertase activity; (solid) transferase activity; (hatched) total activity.

ACKNOWLEDGMENTS

REFERENCES

1. CHAMBERT, R., G. GONZY-TRÉBOUL & R. DEDONDER. 1974. Eur. J. Biochem. **41:** 285–300.
2. BITON, J., J. M. MICHEL, D. LE BELLER, V. PELENC, F. PAUL, P. F. MONSAN & G. GELLF. 1995. Ann. N.Y. Acad. Sci. **750:** 321–324.
3. OHTSUKA, K., S. HINO, T. FUKUSHIMA, O. OZAWA, T. KANEMATSU & T. UCHIDA. 1992. Biosci. Biotechnol. Biochem. **56:** 1373–1377.
4. PÉREZ, A., L. GUERECA & A. LÓPEZ-MUNGUÍA. 1996. Appl. Microbiol. Biotechnol. **45:** 465–471.
5. CRITTENDEN, R. G. & H. W. DOELLE. 1994. Appl. Microbiol. Biotechnol. **41:** 302–308.
6. VAN BALKEN, J. A. M., J. G. M. VAN DOOREN, W. J. J. VAN DEN TWEEL, J. KAMPHUIS & E. M. MEIJER. 1991. Appl. Microbiol. Biotechnol. **35:** 216–221.
7. YANASE, H., M. IWATA, R. NAKAHIGASHI, K. KITA, N. KATO & K. TONOMURA. 1992. Biosci. Biotechnol. Biochem. **56:** 1335–1337.
8. TANAKA, T., S. OI & T. YAMAMOTO. 1979. J. Biochem. **85:** 287–293.
9. ROBYT, J. F. & A. J. CORRIGAN. 1977. Arch. Biochem. Biophys. **183:** 726–731.
10. KIM, D. & J. F. ROBYT. 1994. Enzyme Microb. Technol. **16:** 1011–1015.
11. KOBAYASHI, M., I. YOKOYAMA & K. MATSUDA. 1986. Agric. Biol. Chem. **50:** 2585–2590.

Lipase-catalyzed Selective Esterification of Ibuprofen

A. DUCRET, P. PEPIN, M. TRANI, AND R. LORTIE

Bioprocess Research and Development Group
Biotechnology Research Institute
National Research Council
Montreal, Canada H4P 2R2

INTRODUCTION

The advent of nonaqueous enzymology has opened new horizons for process development as well as for fundamental research. The influence of parameters such as water content and nature of the solvent on the stability, activity, and selectivity of enzymes is not well understood yet. This information, of course, is of paramount importance in the design of a process based on enzymatic reactions in nonaqueous media, but it can also give very useful information on the functioning of enzymes.

In the work presented here, the enzymatic resolution of racemic ibuprofen in pure molten substrates or in solvent media was used as a model system to evaluate the influence of water content (measured as a_w) and nature of the solvent (characterized by log P) on the activity and enantioselectivity of *Candida antarctica* Type B lipase.

MATERIALS AND METHODS

Two different systems were used:

1. a solventless system with pure molten substrates with control of water activity;
2. a solvent system with control of water activity.

In all cases, the esterification reaction was catalyzed by *Candida antarctica* Type B lipase, immobilized on acrylic resin (NOVOZYM 435), a gracious gift from Novo Industri (Denmark).

The racemic mixture as well as the pure enantiomers of ibuprofen [2-(4-isobutylphenyl)propionic acid] were gifts from the Ethyl Corporation (Baton Rouge, Louisiana).

The reactions with pure molten substrates were run at 55 °C in a closed chamber in which the water activity was controlled using saturated salt solutions.

The reactions in solvent were run at room temperature in closed vessels that also contained, in separate vials, a saturated salt solution (LiBr, $a_w = 0.09$) or molecular sieves ($a_w = 0.04$) to control the water activity. The value of a_w was measured in test reactions with a Hanna Instruments (Padova, Italy) HI 9065 hygrometer. The reactants, 1.963 mmol ibuprofen and 1.472 mmol dodecanol, were dissolved in 15 mL

of the appropriate solvent, and 150 or 750 mg of enzyme, depending on the rate of reaction, was used.

The analysis of the reaction products was performed by HPLC using either a chiral column (Hypersil HSA, Shandon, United Kingdom; or Chiralcel OD, Chiral Technologies, Pennsylvania) or a chiral monitor (ChiraMonitor 2000, Applied Chromatography Systems, United Kingdom) with a C18 column.[1] The rate constants were determined from the initial reaction rates. Previous work showed that the reaction is first order with respect to ibuprofen and zero order with respect to alcohol.[2]
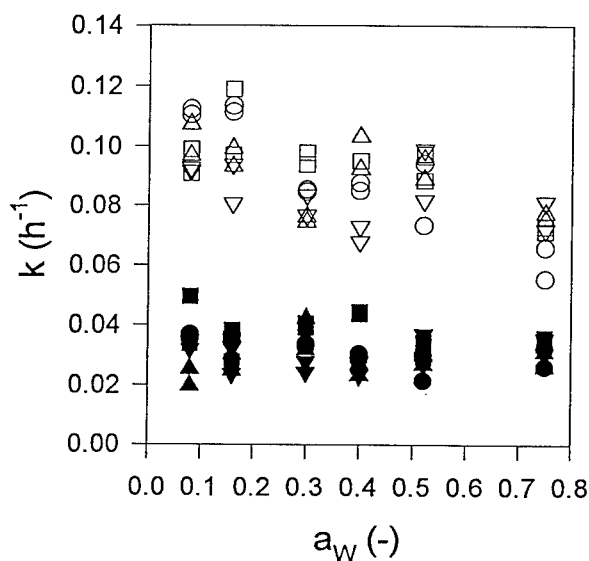
FIGURE 1. Apparent first-order esterification rate constant as a function of the water activity: 0.73 mmol (R, S)-ibuprofen with 0.55 mmol alcohol and 0.025 g enzyme. Symbols: O, decanol; □, dodecanol; △, tetradecanol; ▽, hexadecanol; filled: k_S; open: k_R.

RESULTS

As can be seen in FIGURE 1, in the case of molten racemic ibuprofen, the water activity has an influence on the rate of esterification of (R)-ibuprofen and the chain length of the alcohol has no effect. The value of a_w has another effect in solventless reactions, as shown in FIGURE 2. When the water activity diminishes, it induces a substrate inhibition for (S)-ibuprofen; however, the kinetics for (R)-ibuprofen remain linear and the reaction rate increases when the water activity diminishes. This explains why, in the process reported earlier[2,3] for the resolution of ibuprofen under vacuum, a good enantiomeric excess could be obtained, even with an enzyme
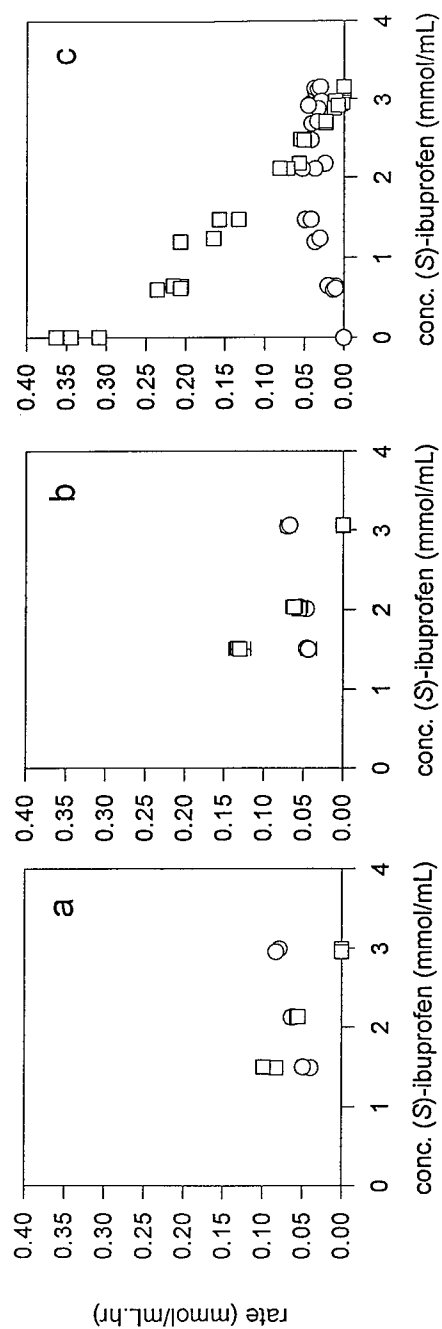
FIGURE 2. Initial reaction rate as a function of the concentration of (*S*)-ibuprofen for various water activities (a: 0.74; b: 0.41; c: 0.09). Total ibuprofen: 0.73 mmol; decanol: 0.55 mmol; 0.025 g enzyme. Symbols: $\bigcirc$, k_S; $\square$, k_R.

having a relatively low enantioselectivity when assayed with the racemate. When the competing substrate, (R)-ibuprofen, disappears, the rate of esterification of (S)-ibuprofen does not increase as much as it would without inhibition, preventing an excessive consumption of the desired product.

Water activity also has an effect on the reaction in solvents, combined with a strong effect of the hydrophobicity of the solvent, as can be seen in FIGURE 3. Low hydrophobicity favors enantioselectivity; however, reaction rates are much lower in these conditions. It is possible to design an effective resolution process in solvent media, although a compromise must be made between selectivity and the rate of reaction.
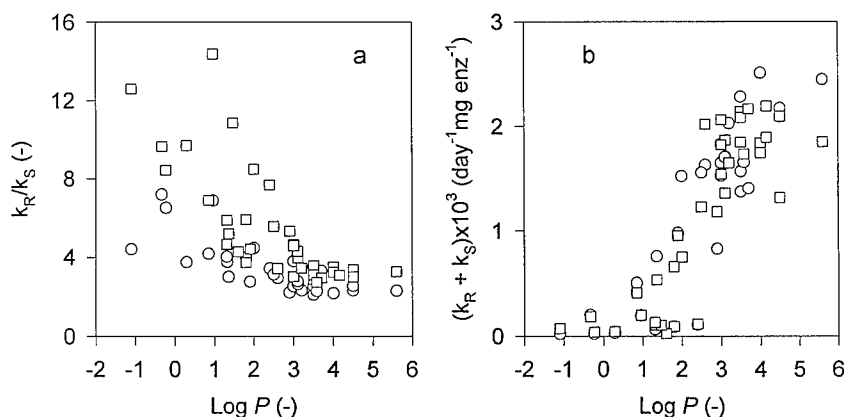
FIGURE 3. Selectivity (a) and total reaction rate constant (b) as a function of log P of the solvent used. Symbols: $\square$, $a_w = 0.04$; $\bigcirc$, $a_w = 0.09$. Solvents and log P: dioxane (-1.1), acetonitrile (-0.3), acetone (-0.2), 2-butanone (0.3), diethyl ether (0.8), cyclohexanone (1.0), 2-methyl-2-butanol (1.3), 4-methyl-2-pentanone (1.3), methyl $tert$-butyl ether (1.4), dichloromethane (1.5), triethyl amine (1.6), acetophenone (1.8), 4-heptanone (1.8), diisopropyl ether (1.9), benzene (2.0), 2-octanone (2.4), toluene (2.5), cyclopentane (2.6), diisobutyl ether (2.9), tetrachloromethane (3.0), 2-methyl butane (3), pentane (3), xylene (3.1), methyl cyclopentane (3.1), cyclohexane (3.2), 2,2-dimethyl butane (3.5), 3-methyl pentane (3.5), hexane (3.5), mesitylene (3.6), methyl cyclohexane (3.7), 2,3-dimethyl pentane (4), heptane (4), ethyl cyclohexane (4.1), 1,3-dimethyl cyclohexane (4.1), isooctane (4.5), octane (4.5), and decane (5.6).

CONCLUSIONS

From the results presented above, it can be concluded that the enantioselectivity is not a simple intrinsic property of the enzyme and that more work is needed to fully understand the influence of the environment on this key property, which is essential for the proper design of an enzymatic resolution process.

REFERENCES

1. DUCRET, A., M. TRANI, P. PEPIN & R. LORTIE. 1995. Comparison of two HPLC techniques for monitoring enantioselective reactions for the resolution of (R, S)-ibuprofen: chiral HPLC versus achiral HPLC linked to an optical rotation detector. Biotechnol. Tech. **9:** 591–596.
2. ERGAN, F., M. TRANI & R. LORTIE. 1995. Selective esterification of racemic ibuprofen. Ann. N.Y. Acad. Sci. **750:** 228–231.
3. TRANI, M., A. DUCRET, P. PEPIN & R. LORTIE. 1995. Scale-up of the enantioselective reaction for the enzymatic resolution of (R, S)-ibuprofen. Biotechnol. Lett. **17:** 1095–1098.

Inactivation of Glucose-Fructose Oxidoreductase from *Zymomonas mobilis* during Its Catalytic Action[a]

MONIKA FÜRLINGER,[b] BERND NIDETZKY,[b,c]
ROBERT K. SCOPES,[d] DIETMAR HALTRICH,[b] AND
KLAUS D. KULBE[b]

[b]*Division of Biochemical Engineering*
Institute of Food Technology
Universität für Bodenkultur Wien (BOKU)
1190 Vienna, Austria

[d]*Department of Biochemistry*
La Trobe University
Bundoora, Victoria 3083, Australia

INTRODUCTION

Glucose-fructose oxidoreductase (GFOR)—an enzyme yet found only in *Zymomonas mobilis*—is capable of simultaneously converting mixtures of glucose and fructose. Tightly bound NADP(H), whose interaction with GFOR remains enigmatic, acts as the hydrogen carrier in the simultaneous redox process (FIGURE 1).

The reaction catalyzed by GFOR is almost irreversible *in vitro* and *in vivo* as even without the addition of gluconolactonase (GL) the hydrolysis of glucono-1,5-lactone to gluconic acid represents a spontaneous process.[1] GFOR operates by a classical ping-pong kinetic mechanism and consequently has a single binding site for all substrates. The specific activity of the enzyme is high (350–400 U/mg),[1] whereas the affinity for fructose is exceptionally low ($K_m \sim 400$ mM).[2]

The advantages of GFOR in view of producing sorbitol and gluconic acid are as follows: The enzyme activity does not depend on exogenously added cofactor and two products—widely used in the food industry—are synthesized by only one enzyme.[3,4] Protocols for the permeabilization of *Zymomonas* cells have been developed and nonviable cells have been used in continuous conversion processes with excellent operational stability.[4]

Being interested in employing the cell-free enzyme for product synthesis, we have recently found that a drastic inactivation of GFOR during catalysis occurred. The present paper deals with the approach that we have chosen to overcome the low operational stability of GFOR during substrate conversion.

[c]To whom all correspondence should be addressed.

Glucose ——————▶ Glucono-δ ——— $\overset{GL}{\longrightarrow}$ ▶ Gluconic
lactone   acid

GFOR⋯NADP⁺   GFOR⋯NADPH + H⁺

Sorbitol◀——————— Fructose
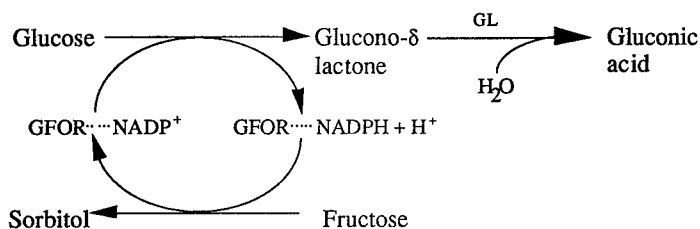
FIGURE 1. Simultaneous conversion of glucose and fructose by glucose-fructose oxidoreductase (GFOR) from *Zymomonas mobilis* (GL: gluconolactonase).

MATERIALS AND METHODS

Enzymes

GFOR was partly purified by a two-step purification procedure. Ammonium sulfate precipitation [30% saturation] and, subsequently, purification by hydrophobic interaction chromatography on Phenylsepharose were used. The obtained enzyme preparation had a specific activity of 20 U/mg.

Sufficient quantities of gluconolactonase (GL) were obtained from an *E. coli* strain overexpressing the lactonase gene from *Zymomonas*.[5] GL was partly purified by applying a positive dye column (Yellow MX-GR coupled to Sepharose Cl-4B).

Assays/Analysis

GFOR and GL activities were determined according to reported procedures.[1] The decolorization of *p*-nitrophenol solutions due to acid production (gluconic acid) by enzyme action was measured.

Sugar conversion was analyzed by HPLC as described in reference 3.
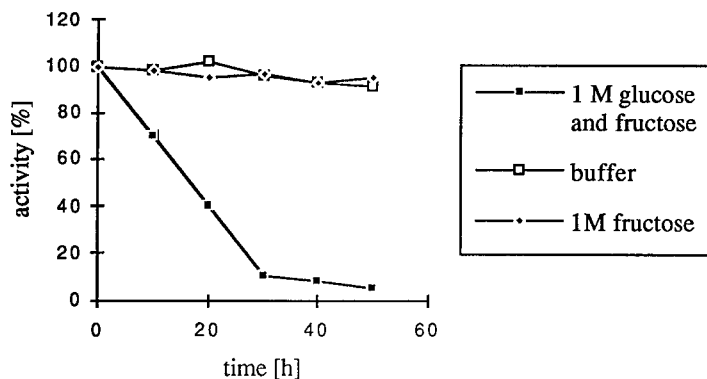
FIGURE 2. Stability of GFOR in phosphate buffer, in the presence of 1 M fructose, and in the presence of both substrates (glucose and fructose).

Discontinuous and Continuous Conversion Experiments

Discontinuous conversions of substrate mixtures in the concentration range from 0.1 to 1 M were carried out at 25 °C at a constant pH of 6.4 (controlled by titration with 2 M KOH). At the times indicated, samples were taken (0.2 mL) and used for the determination of the residual enzyme activity and of the degree of substrate conversion.

Continuous conversions were performed in a laboratory-scale reactor equipped with a flat 10-kDa ultrafiltration membrane and fitted with a pH and conductivity electrode. Enzymes were injected through a septic seal to initiate the reaction and the substrate solution was fed continuously at an average residence time of 17 h.

RESULTS AND DISCUSSION

Stability of GFOR

As described previously,[3] a significant deactivation of GFOR was found during conversion of mixtures of glucose and fructose. Various buffer systems (phosphate, propionate, citrate, and MES) in a pH range from 5.5 to 6.8 have been tested and the corresponding stability of GFOR has been evaluated. At 35 °C, a maximal 10% of enzyme activity was lost after an incubation period of 52 h.

Aiming at identifying the major factors governing the stability of GFOR, three cases had to be considered: (a) stability in buffer, (b) stability in the presence of one
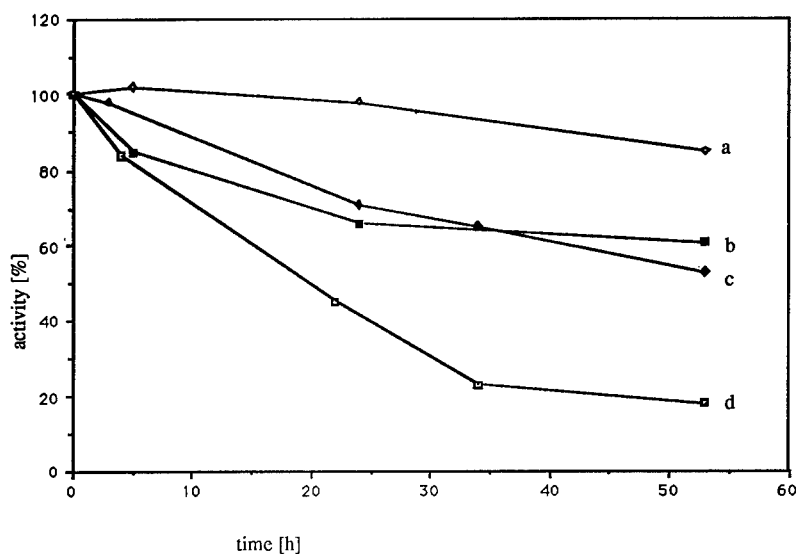
FIGURE 3. Stabilization of GFOR during conversion of 1 M glucose and fructose by 10 mM DTT (a), 10 mM cysteine (b), 10 mM GSH (c), and 10 mM thioglycolate (d).
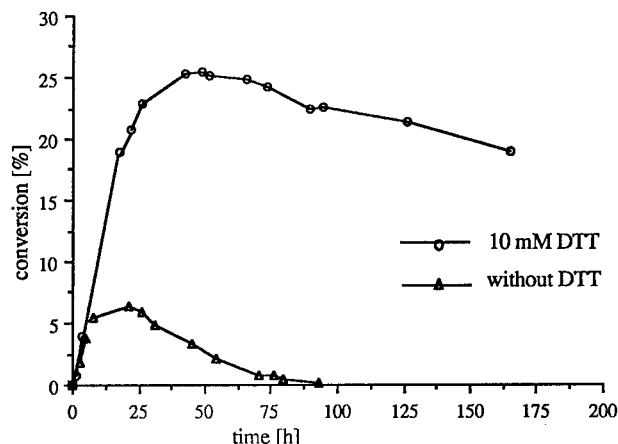
FIGURE 4. Continuous conversion of 1 M glucose and fructose using 1.0 U/mL GFOR at an average residence time of 17 h with or without the addition of 10 mM DTT. Titration was with 2 M KOH.

substrate (glucose or fructose), and (c) stability under catalytic conditions in the presence of both substrates, glucose and fructose.

Results are shown in FIGURE 2 and clearly demonstrate that the loss of GFOR activity is linked to its catalytic action. This conclusion was corroborated further by finding that partially inactivated GFOR remained stable once a complete substrate conversion had been obtained. In the presence of no substrate or only one substrate (either fructose or glucose), GFOR is fully stable.

Other factors that might possibly account for GFOR inactivation can be ruled out: shear stress (because of stirring) and thermal instability (at 35 °C). It is noteworthy that GFOR is quite sensitive to alkaline pH values. An inactivation caused by titration with base thus had to be considered. Addition of gluconolactone to a GFOR solution and subsequent titration of gluconic acid with 2 M KOH did not affect the enzyme's activity. Although no explanation or model is currently available that would explain the unusual inactivation of GFOR, a similar type of so-called autoinactivation has been described for a glucose-oxidase as well, whose loss of activity was found to be dependent on the number of catalytic cycles carried out by the enzyme.[6]

Stabilization of GFOR

The rapid inactivation of GFOR during catalysis seems to make the enzyme rather unsuitable for conversion processes. Consequently, we have sought for strategies to enhance the stability of the enzyme under operational conditions. A series of possible stabilizing components such as salts, polyols, and polymers were found ineffective.

In contrast, the addition of thiol reagents proved to exhibit a significant beneficial effect on GFOR stability. Among all SH-compounds tested so far (dithiothreitol, mercaptoethanol, cysteine, thioglycolate, glutathione), dithiothreitol (DTT) was the most efficient reagent with regard to the avoidance of GFOR inactivation (FIGURE 3). The stabilizing effect is dependent on the concentration of the thiol reagents, and molarities of DTT between 5 and 15 mM were shown to be the most striking.

In FIGURE 4, where the results of two continuous conversions in a membrane reactor with and without the addition of 10 mM DTT are compared, the improved stability of GFOR with DTT being present is clearly demonstrated. In the absence of DTT, the degree of substrate conversion was much lower than expected (~ 40%) and did not exceed 7%. Moreover, because no equilibrium of substrate fed and converted is seen during the reaction, the constant decay of GFOR activity becomes evident. In contrast, when 10 mM DTT was added, a significantly improved substrate conversion could be obtained and maintained for at least 50 h of reaction time. The decrease in substrate conversion even in the presence of DTT indicates an incomplete stability of GFOR. For technical exploitation, further improvement of the stability of cell-free GFOR will be necessary, especially when the long-term operational stabilities of the cell-bound enzyme in permeabilized cells of *Zymomonas* are considered.

Our results, though, lead us to propose that cysteines might be important for catalysis or for maintaining the correct structure of the enzyme. However, to elucidate the role of cysteine residues in more detail, further investigations will be needed.

REFERENCES

1. ZACHARIOU, M. & R. K. SCOPES. 1986. Glucose-fructose oxidoreductase, a new enzyme isolated from *Zymomonas mobilis* that is responsible for sorbitol production. J. Bacteriol. **167:** 863–869.
2. HARDMAN, M. J. & R. K. SCOPES. 1988. The kinetics of glucose-fructose oxidoreductase from *Zymomonas mobilis*. Eur. J. Biochem. **173:** 203–209.
3. GOLLHOFER, D., B. NIDETZKY, M. FÜRLINGER & K. D. KULBE. 1995. Efficient protection of glucose-fructose oxidoreductase from *Zymomonas mobilis* against irreversible inactivation during its catalytic action. Enzyme Microb. Technol. **17:** 235–240.
4. REHR, B., C. WILHELM & H. SAHM. 1991. Production of sorbitol and gluconic acid by permeabilized cells of *Zymomonas mobilis*. Appl. Microbiol. Biotechnol. **35:** 144–148.
5. KANAGASUNDARAM, V. & R. K. SCOPES. 1992. Isolation and characterization of the gene encoding gluconolactonase from *Zymomonas mobilis*. Biochim. Biophys. Acta **1171:** 198–200.
6. BOURDILLON, D., C. HERVAGAULT & D. THOMAS. 1985. Increase in operational stability of glucose oxidase by the use of an artificial cosubstrate. Biotechnol. Bioeng. **27:** 1619–1622.

Application of Vinyl Esters for the Lipase-catalyzed High-Yield Synthesis of Monoacylglycerols

U. BORNSCHEUER, L. GAZIOLA, AND R. D. SCHMID[a]

Institut für Technische Biochemie
Universität Stuttgart
70569 Stuttgart, Germany

INTRODUCTION

Monoacylglycerols (MAG) are the most widely used emulsifiers in food, pharmaceutical, and cosmetic industries. At present, they are manufactured by continuous chemical glycerolysis of fats and oils at high temperatures (220–250 °C) using inorganic alkaline catalysts. A potential alternative is the enzymatic synthesis of MAG by selective hydrolysis of triacylglycerols (TAG), by esterification of free fatty acids with glycerol, or by glycerolysis of TAG. Unfortunately, enzymatic methods give low to moderate yields of MAG because they reach equilibrium and because the diacylglycerols (DAG) form as a by-product.[1] To increase the equilibrium constant, we used vinyl esters of fatty acids. Vinyl alcohol generated during the reaction tautomerizes irreversibly to acetaldehyde. To increase the regioselectivity, we used protected glycerols such as 1,2-*O*-isopropylidene glycerol (IPG, solketal).[2] Furthermore, we investigated the influence of the structure of different protective groups on the enantioselectivity of the reaction.

MATERIALS AND METHODS

All chemicals were purchased from commercial suppliers at the highest purity available. Protected glycerols (except IPG) were synthesized from glycerol (130 mmol) and the corresponding ketone (100 mmol) in toluene (100 mL) using *p*-toluene sulfonic acid (1 mmol) as the catalyst under reflux in a Dean-Stark trap and were purified by standard procedures. The structures were confirmed by NMR and MS spectra. Lipase from *Pseudomonas cepacia* (PCL, lipase PS from Amano, Nagoya, Japan) was used in its crude form. Lipase activity was determined using a pH-stat assay system (Metrohm, Herisau, Switzerland). A 20-mL assay solution [5% (w/v) olive oil, 2% (w/v) gum arabicum, mixed in an ultraturrax for 5 min] and a 470-μL $CaCl_2$ solution (22% w/v) were incubated at 37 °C. A known amount of lipase was dissolved in phosphate buffer and centrifuged, and an aliquot of the supernatant was assayed. Released fatty acids were titrated automatically with sodium hydroxide solution (0.1 N). One unit (U) of activity is defined as the amount of lipase that liberates 1 μmol of fatty acid from olive oil in 1 min at 37 °C. Enzymatic

reactions were performed in 10-mL glass-stoppered flasks thermostated in an oil bath to 40 °C. In a typical experiment, 1.5 mmol protected glycerol and 1.5 mmol vinyl ester were dissolved in 3 mL of toluene, and 50 units of lipase was added. Samples withdrawn from the reaction mixture were centrifuged and the supernatant was derivatized with trifluoroacetic acid anhydride (TFAA) as described previously.[3] No racemization during this step was observed, as confirmed by the derivatization of pure (R)-isopropylidene glycerol with TFAA. Analysis was performed on a gas chromatograph (HRGC Mega 2 series, Autosampler A 200S, software package Chrom Card for Windows, Fisons Instruments, Mainz-Kastel, Germany) equipped with a chiral stationary phase [Hydrodex β-3P = heptakis-(2,3,6-tri-O-methyl)-β-cyclodextrin; 25 m; i.d. = 0.25 mm; Macherey & Nagel, Düren, Germany] and a flame ionization detector (FID). The analysis conditions were as follows: injector temperature, 200 °C; FID temperature, 200 °C; carrier gas, hydrogen, 60 kPa; split ratio, 1:100 mL/min. From the enantiomeric excess determined by GC analysis, the conversion was calculated according to Chen et al.[4] The absolute configuration was determined from the reaction of (R)-isopropylidene glycerol with vinyl acetate followed by GC analysis. Isolation of pure MAG was possible by selective cleavage of the protective group with boric acid in methoxyethanol as described previously.[5]

RESULTS AND DISCUSSION

Reaction of Glycerol or IPG with Vinyl Esters

Transesterification of the vinyl esters with glycerol catalyzed by PCL gave a mixture of MAG, DAG, and TAG. Only 45% MAG will be synthesized under
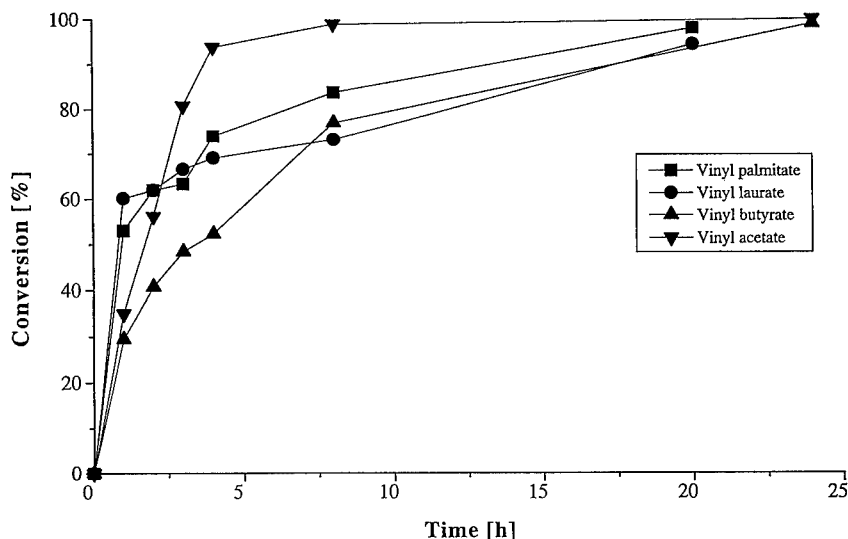
FIGURE 1. Conversion/time course for the acylation of IPG with vinyl esters catalyzed by crude PCL in toluene.
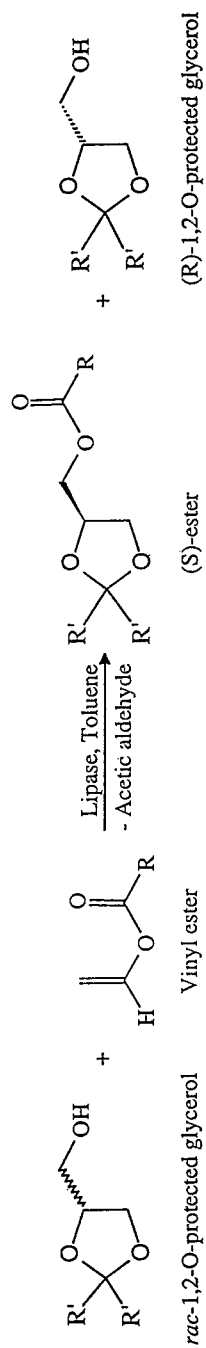
FIGURE 2. Lipase-catalyzed biotransformation using 1,2-*O*-protected glycerols and vinyl esters in toluene.

optimized conditions.[5] In contrast, PCL catalyzed the complete conversion of 1,2-*O*-isopropylidene glycerol to the monoester in less than 24 h (FIGURE 1). With vinyl acetate, acetylation was complete within only 8 h. In the absence of toluene, the reaction was considerably slower (data not shown).

Enantioselectivity

The enantioselectivity of the acylation was studied using various protected glycerol derivatives (FIGURE 2 and TABLE 1). In all cases, acylation was fast and favored the *S*-enantiomer. Gas chromatography did not separate the enantiomers of glycerol esters of laurate and palmitate, but efficiently separated the acetates and butyrates.[6] Both the acylating agent (vinyl acetate or butyrate) and the nature of the protective group influenced the enantioselectivity. The highest enantiomeric excess (79% eeS) and the highest enantioselectivity (8.5) were found for the derivative with isopropyl groups. An increase in the chain length of the aliphatic residue R'

TABLE 1. Influence of the Protective Group and the Acyl Donor on the Enantiomeric Excess of the Substrate (eeS) and on the Enantioselectivity (E)

Compound[a] R'	Vinyl Acetate		Vinyl Butyrate	
	% eeS	E	% eeS	E
methyl	78	2.3	42	3.9
ethyl	63	1.7	35	1.7
propyl	51	5.5	29	1.4
isopropyl	79	5.5	46	8.5

[a]For R', see FIGURE 2.

decreased the enantiomeric excess in the order of methyl > ethyl > propyl. Acylations with vinyl acetate were considerably more enantioselective than those with vinyl butyrate. In all cases, the E values were too low to isolate optically pure product. This lack of chiral recognition of the lipase from *Pseudomonas cepacia* was also found for many other primary alcohols, especially when an oxygen is attached to the stereocenter as in the case of chiral glycerol derivatives.[7]

SUMMARY

The lipase-catalyzed acylation of protected glycerol derivatives with vinyl esters is a fast and regioselective route to MAG. The structures of both the acyl donor and the protective group affected the enantioselectivity of the reaction, but in all cases the enantioselectivity was too low to isolate optically pure product. Further variations of the structure of the protective group may increase the enantioselectivity to practical levels.

REFERENCES

1. BORNSCHEUER, U. T. 1995. Enzyme Microb. Technol. **17:** 578–586.
2. BORNSCHEUER, U., H. STAMATIS, A. XENAKIS, T. YAMANE & F. N. KOLISIS. 1994. Biotechnol. Lett. **16:** 697–702.
3. BORNSCHEUER, U., A. HERAR, L. KREYE, V. WENDEL, A. CAPEWELL, H. H. MEYER, T. SCHEPER & F. N. KOLISIS. 1995. Tetrahedron Asymmetry **4:** 1007–1016.
4. CHEN, C. S., Y. FUJIMOTO, G. GIRDAUKAS & C. J. SIH. 1982. J. Am. Chem. Soc. **104:** 7294–7299.
5. BORNSCHEUER, U. T. & T. YAMANE. 1995. J. Am. Oil Chem. Soc. **72:** 193–197.
6. GAZIOLA, L., U. BORNSCHEUER & R. D. SCHMID. 1996. Enantiomer **1:** 49–53.
7. WEISSFLOCH, A. N. E. & R. J. KAZLAUSKAS. 1995. J. Org. Chem. **60:** 6959–6969.

Enzymatic Preparation of Optically Active Silicon-containing Amino Acids

ATSUO TANAKA, HAYATO YAMANAKA,
AND TAKUO KAWAMOTO

Department of Synthetic Chemistry and Biological Chemistry
Graduate School of Engineering
Kyoto University
Kyoto 606-01, Japan

In practical processes, employment of unconventional compounds as enzyme substrates has become more and more important in the field of biotechnology to increase the potential and expand the application of biocatalysts. Organosilicon compounds may be one type of these unconventional substrates because these compounds have never been known in nature. However, organosilicon compounds play important roles in organic chemistry and these compounds, especially those having optical activity, are interesting as biologically active compounds or their precursors.[1] Therefore, we have tried to prepare optically active silicon-containing amino acids, 3-trimethylsilylalanine and *p*-trimethylsilylphenylalanine, via enzymatic processes.

PREPARATION OF OPTICALLY ACTIVE 3-TRIMETHYLSILYLALANINE (TMS-ALA)

Optically active 3-trimethylsilylalanine (TMS-Ala) was prepared through enantioselective enzymatic hydrolysis of chemically synthesized *N*-acetyl-D,L-TMS-Ala (FIGURE 1).[2] Aminoacylase from porcine kidney (PKA) was found to be more effective than that from *Aspergillus melleus* in the preparation of L-TMS-Ala, although the activity of PKA on *N*-acetyl-D,L-TMS-Ala was far lower compared to that on *N*-acetyl-D,L-methionine. PKA showed an optimum pH at 7.5 and its activity was stimulated by the addition of cobaltous ion. When 2.436 g (12 mmol) of *N*-acetyl-D,L-TMS-Ala was deacylated for 3.5 h to reach 50% hydrolysis with 30 mg of PKA in 60 mL of the optimized reaction mixture (pH 7.5 and presence of 0.5 mM Co^{2+}), 700 mg of the recrystallized L-amino acid of more than 99% ee was obtained at a yield of 72%. The residual *N*-acetyl-D-TMS-Ala was subjected to acid hydrolysis with HCl and 734 mg (yield, 76%) of the recrystallized D-amino acid was recovered at 96% ee (TABLE 1). TMS-Ala, especially its L-isomer, will be useful as an analogue of leucine in the synthesis of various biologically active peptides.

Recently, we have found that L-TMS-Ala serves as a substrate in the synthesis of dipeptides with thermolysin in an organic solvent system. When benzyloxycarbonyl(Z)-L-amino acids and L-amino acid methyl esters were used as the carboxyl and amino components, respectively, thermolysin catalyzed the synthesis of Z-(TMS-Ala)-X-OMe (X = Leu, Ile, Phe, Tyr, etc.), whereas L-TMS-Ala-OMe was inactive as an

Acylase I

N-Acetyl-DL-TMS-Ala $\xrightarrow{\text{Acylase I}}$ L-TMS-Ala + *N*-Acetyl-D-TMS-Ala

$\downarrow$ 3N HCl
100 ℃

D-TMS-Ala

$$
\begin{array}{c}
CH_3 \\
| \\
H_3C\text{-}Si\text{-}CH_3 \\
| \\
CH_2 \\
| \\
H_2N\text{-}C\text{-}COOH \\
| \\
H
\end{array}
$$

3-Trimethylsilylalanine
(TMS-Ala)
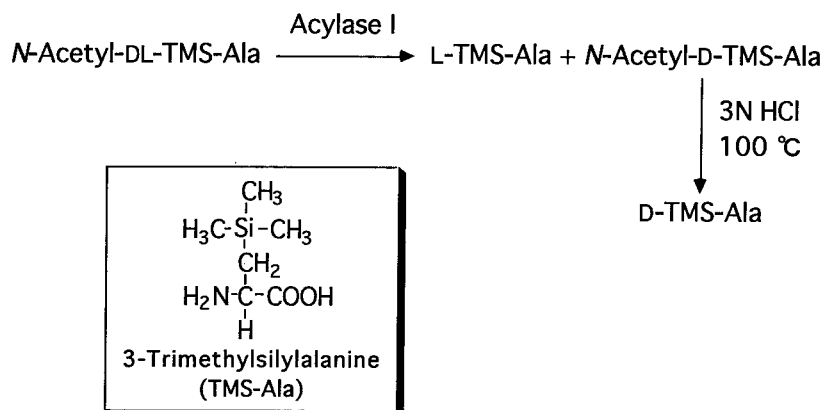
FIGURE 1. Preparation of optically active 3-trimethylsilylalanine (TMS-Ala).

amino component. Now, we are investigating the biological activities of these peptides containing TMS-Ala.

PREPARATION OF OPTICALLY ACTIVE
p-TRIMETHYLSILYLPHENYLALANINE (TMS-PHE)

Chemically synthesized D,L-5-(*p*-trimethylsilylphenylmethyl)hydantoin (D,L-TMS-Phe-Hyd) was subjected to bacterial hydrolysis to obtain optically active *p*-trimethylsilylphenylalanine (TMS-Phe) through the *N*-carbamoyl derivative, but all strains examined did not show the sufficient hydantoinase activity on this compound. However, several strains were found to have an activity of *N*-carbamoyl amino acid amidohydrolase and to be able to hydrolyze *N*-carbamoyl-D,L-5-*p*-trimethylsilylphenylalanine (C-D,L-TMS-Phe) chemically prepared from the hydantoin (FIGURE 2). Although *Blastobacter* sp. A17p-4[2] exhibited the highest enzyme activity, the optical yield of D-TMS-Phe with the cell-free extract was low. In fact, two kinds of enzymes, that is, D-specific (DCase) and L-specific (LCase) *N*-carbamoyl amino acid amidohydrolases, were present in this bacterial strain. These enzymes in the cell-free extract could be separated by DEAE-Sephacel column chromatography. Partially purified DCase showed an optimum pH at 8.0 and addition of 2.5% *N*,*N*-dimethylformamide was proved to be effective for dissolving the substrate without inactivation of the enzyme. When 1.12 g (4.0 mmol) of the C-D,L-TMS-Phe was subjected to the

TABLE 1. Optical Resolution of *N*-Acetyl-D,L-TMS-Ala

	Yield[a]	% ee[b]
L-TMS-Ala	700 mg (72%)	> 99
D-TMS-Ala	734 mg (76%)	96

[a]Yield was calculated on the recrystallized product.
[b]% ee was determined with HPLC.
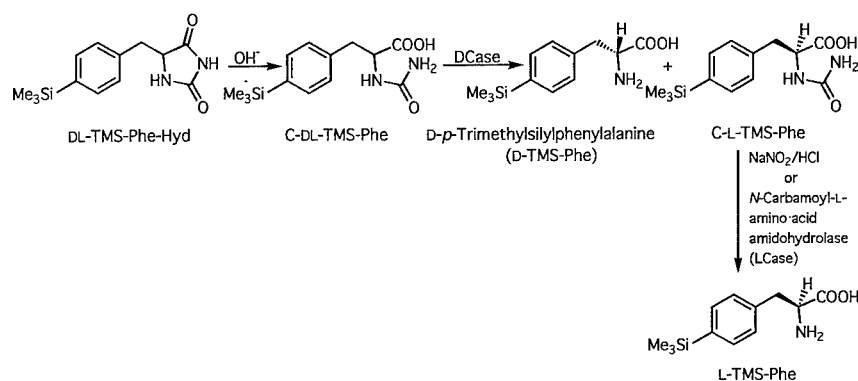
FIGURE 2. Preparation of optically active *p*-trimethylsilylphenylalanine (TMS-Phe).

hydrolysis for 120 h to reach 49% hydrolysis with 50 U of partially purified DCase in 800 mL of the optimized reaction mixture (pH 8.0 and presence of 2.5% *N,N*-dimethylformamide), 160 mg of D-TMS-Phe was obtained at a yield of 34% and with 98% ee of the optical purity after column chromatographic separation and recrystallization (TABLE 2). L-TMS-Phe will be prepared from the residual *N*-carbamoyl-L-amino acid by chemical or biochemical hydrolysis.

To improve the process by using the cell-free extract of *Blastobacter* sp. A17p-4 as an enzyme source, we have tried to inactivate LCase by heat treatment of the cell-free extract because DCase was reported to be thermostable.[3] In fact, when the cell-free extract was subjected to the heat treatment at 50 °C and pH 7.0, DCase retained its full activity even after 60 min, whereas LCase completely lost its activity after 40 min.

Therefore, the cell-free extract of the bacterium was treated for 40 min at 50 °C and pH 7.0 followed by dialysis at pH 8.0 (the optimum reaction pH) to prepare the efficient DCase preparation. This enzyme preparation gave an excellent result in the enantioselective hydrolysis of C-D,L-TMS-Phe, yielding D-TMS-Phe of more than 99% ee at a hydrolysis ratio of 25% after 24 h of reaction.

Preparation of the heat-treated cell-free extract is far simpler and more convenient compared with that of the partially purified enzyme by column chromatography, allowing a large-scale production of D-TMS-Phe and, subsequently, its L-enantiomer. These optically active silicon-containing amino acids may become interesting components of antibiotics and biologically active peptides.

TABLE 2. Optical Resolution of *N*-Carbamoyl-D,L-TMS-Phe

	Yield[a]	% ee[b]
D-TMS-Phe	160 mg (34%)	98

[a]Yield was calculated on the recrystallized product.
[b]% ee was determined with HPLC.

REFERENCES

1. TANAKA, A. & T. KAWAMOTO. 1994. Organosilicon biochemistry. Chim. Oggi **July/August:** 63–69.
2. YAMANAKA, H., T. FUKUI, T. KAWAMOTO & A. TANAKA. 1996. Enzymatic preparation of optically active 3-trimethylsilylalanine. Appl. Microbiol. Biotechnol. **45:** 51–55.
3. OGAWA, J., M. C-M. CHUNG, S. HIDA, H. YAMADA & S. SHIMIZU. 1994. Thermostable *N*-carbamoyl-D-amino acid amidohydrolase: screening, purification, and characterization. J. Biotechnol. **38:** 11–19.

Synthesis of Adenosine 5′-Triphosphate Derivatives and Their Substrate Activities to Some Glucokinases

KOSUKE TOMITA, KANEHISA KOJOH,
AND ATSUSHI SUZUKI

Department of Chemistry
College of Engineering
Kanto Gakuin University
Yokohama 236, Japan

INTRODUCTION

Glucokinase (GlcK) (EC 2.7.1.2) is well known as an important enzyme located at the entrance of the glycolytic pathway and is distinguished from hexokinase (HK) (EC 2.7.1.1) in its high substrate specificity for glucose. We[1-4] have been investigating the characteristics of two kinds of bacterial thermostable GlcKs, one from *Bacillus stearothermophilus* (BS), a thermophilic bacterium, and another from *Zymomonas mobilis* (ZM), a mesophilic bacterium. The former ferments by the typical glycolytic pathway, whereas the latter does so by the Entner-Doudoroff pathway.

Adenosine 5′-triphosphate (ATP) derivative is important as a precursor of immobilized ATP in an ATP-related enzyme reactor and as a ligand of biospecific affinity adsorbent, etc.

In the present study, two kinds of ATP derivatives were synthesized with our method and their substrate activities to both GlcKs were compared with those of ATP itself.

SYNTHESIS OF ATP DERIVATIVES

In the synthesis of ATP derivatives, it is necessary to dissolve ATP in a suitable solvent. Water is considered to be the only solvent for ATP, which limits the method of the synthesis of ATP derivatives; that is, it is impossible to use reagents unstable in water. However, we[5] have already discovered an aprotic nonaqueous dipolar solvent for ATP, which was applied to the present synthesis.

Solubilization of ATP in Aprotic Nonaqueous Solvent

We investigated the solubility of ATP in some aprotic dipolar solvents, that is, dimethyl sulfoxide (DMSO), dimethyl formamide, and hexamethyl phosphoramide, and found that DMSO containing LiCl is a good solvent for ATP. FIGURE 1 illustrates the effect of LiCl on the solubility of ATP in DMSO. LiCl is shown to be effective even at a low concentration.

Synthesis of N⁶-(Succinyl)ATP

One gram of ATP was dissolved in 60 mL of DMSO containing 3 g of LiCl, and 15 g of succinic anhydride was added to the solution. The solution was kept at 30 °C with stirring. After 50 h, an excess amount of ice-cold ethanol/acetone (1/1) was added to the solution. The precipitate was collected and then dissolved in 5 mL of water. The solution was applied to a Dowex 1-X8 column (Cl⁻), which was washed with 0.1 M LiCl, pH 2.75. A linear LiCl gradient was applied: the mixing chamber contained 0.1 M LiCl, pH 2.75, and the reservoir contained 0.5 M LiCl, pH 2.0. The pooled
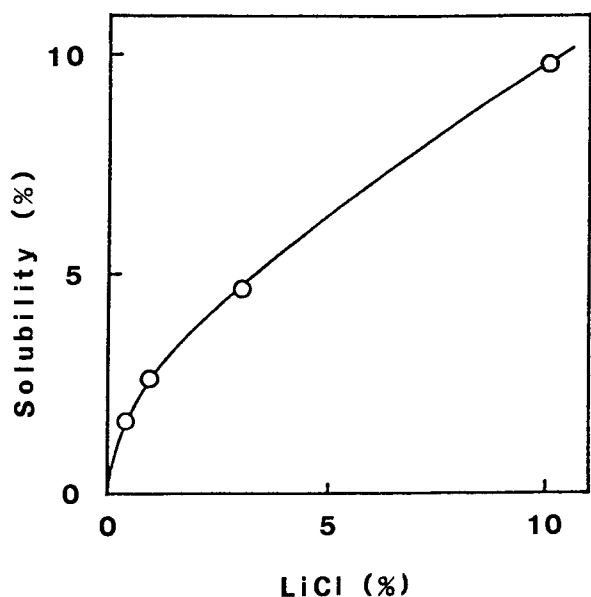
FIGURE 1. Solubility of ATP in DMSO containing LiCl.[5] Excess ATP was added to DMSO containing different concentrations of LiCl, the mixture was stirred at 30 °C for three days, and the solubility was determined with removal of insoluble ATP by centrifugation.

fractions comprising the main peak were concentrated, and the product was precipitated with an excess amount of ice-cold ethanol/acetone (1/1) to give 0.44 g (44% yield) of N^6-(succinyl)ATP (6-S-T)—R_f: 0.59 (solvent A), 0.54 (solvent B); UV: λ_{max} (pH 7.0) nm (ϵ) = 274 (16.7 mM⁻¹ cm⁻¹); ¹H-NMR spectrum: δ = 2.56 (2H, t, CH_2COO), 2.87 (2H, t, N^6-$COCH_2$), 6.27 (1H, d, H-1′), 8.67 (1H, s, H-2), and 8.72 (1H, s, H-8).

Synthesis of N⁶-[N-(6-Aminohexyl)carbamoyl]ATP

One gram of ATP was dissolved in 60 mL of DMSO containing 3 g of LiCl, and 14 g of hexamethylene diisocyanate was added to the solution. The solution was kept at

30 °C with stirring. After 20 h, the reaction mixture was poured into ice-cold acetone. The precipitate was collected and dissolved in 500 mL of water (pH 2 with HCl) and allowed to stand overnight at 4 °C. The solution was neutralized with 1 M LiOH, and the product was precipitated with an excess amount of ice-cold ethanol/acetone (1/1). The precipitate was collected and then dissolved in 5 mL of water. The solution was applied to a Dowex 1-X8 column (Cl$^-$). The column was washed with 0.01 M LiCl, pH 6.0. A linear LiCl gradient was then applied: the mixing chamber contained 0.01 M LiCl, pH 6.0, and the reservoir contained 0.5 M LiCl, pH 2.0. The pooled fractions comprising the main peak were concentrated, and the product was precipitated with an excess amount of ice-cold ethanol/acetone (1/1) to give 0.48 g (48% yield) of N^6-[N-(6-aminohexyl)carbamoyl]ATP (6-AHC-T)—R_f: 0.38 (A), 0.33 (B); UV: λ_{max} (pH 7.0) nm (ϵ) = 271 (17.6 mM^{-1} cm^{-1}); ^{1}H-NMR spectrum: δ = 1.18 (8H, m, C$_4$H$_8$), 2.89 (2H, t, CH$_2$NH$_2$), 3.63 (2H, t, N^6-CONHCH$_2$), 6.12 (1H, d, H-1'), 8.24 (1H, s, H-2), and 8.53 (1H, s, H-8).

Analytical Procedure

Thin-layer chromatography was performed on Funacel SF cellulose (Funakoshi Pharmaceutical Company) in the following solvent systems: A, isobutyric acid–1 M aqueous ammonia (5:3, v/v), solvent saturated with disodium EDTA; B, 0.1 M potassium phosphate (pH 6.8)–ammonium sulfate–1-propanol (100:60:2, v/w/v). Spots were located by viewing under an ultraviolet lamp. Ultraviolet spectra were obtained with a Shimadzu UV 2200 Spectrophotometer. ^{1}H-NMR spectra were obtained at 25 °C with a JEOL GSX 270 NMR Spectrometer at 270 MHz using a 15% w/v solution in D$_2$O containing sodium 2,2-dimethyl-2-silapentane-5-sulfonate (DSS) as an external standard.

SUBSTRATE ACTIVITIES OF ATP DERIVATIVES TO BOTH GLUCOKINASES

The substrate activities of the above ATP derivatives were kinetically examined with respect to both GlcKs; that is, the GlcK activity in each case was determined as the increase in the absorbance at 340 nm due to the production of NADH according to the following equations:

$$\text{glucose + ATP derivative} \xrightarrow{\text{GlcK}} \text{glucose 6-phosphate (G6P) + ADP}$$

$$\text{G6P + NAD}^+ \xrightarrow{\text{G6PD}} \text{6-phosphogluconolactone + NADH + H}^+$$
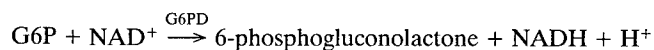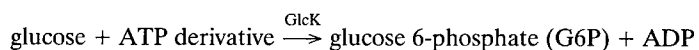
where G6PD stands for glucose 6-phosphate dehydrogenase.

This assay procedure was carried out at 30 °C with the Shimadzu UV 2200

Spectrophotometer. The results are shown in TABLE 1 and are summarized as follows:

- 6-S-T Activities: 6-S-T has a V_{max} value similar to that of ATP itself with respect to GlcK (BS), but a much larger K_m value. With respect to GlcK (ZM), the K_m value is similar to that of ATP itself, but the V_{max} value is much less.
- 6-AHC-T Activities: 6-AHC-T has a similar activity to that of ATP itself with respect to both GlcKs, judging from its V_{max} and K_m values.

CONCLUSIONS

Two kinds of ATP derivatives, 6-S-T and 6-AHC-T, were synthesized. Although the necessary reagents for the synthesis, succinic anhydride and hexamethylene diisocyanate, are very unstable in water, the discovery of a new solvent system made it possible to use such unstable reagents.

Their substrate activities to two kinds of GlcK, namely, GlcK (BS) and (ZM), were kinetically examined and they showed a different tendency from each other

TABLE 1. Substrate Activities of Two ATP Derivatives to Two GlcKs

	BS[a]		ZM[b]	
	V_{max} (%)	K_m (mM)	V_{max} (%)	K_m (mM)
6-S-T	125	1.00	12	0.38
6-AHC-T	100	0.50	83	1.25
ATP	100	0.13	100	0.50

[a]GlcK from BS.
[b]GlcK from ZM.

depending on the enzyme origin. These facts may be relative to the difference between the functional groups of both derivatives, that is, the free carboxyl group in 6-S-T and the free amino group in 6-AHC-T.

These data should be useful for the investigation of the enzymatic function and the design of immobilized ATP for GlcK.

ACKNOWLEDGMENTS

REFERENCES

1. KAMEI, S., K. TOMITA, K. NAGATA, H. OKUNO, T. SHIRAISHI, A. MOTOYAMA, A. OHKUBO & M. YAMANAKA. 1987. A stable glucokinase from a thermophilic bacterium. I. Purification and some properties. J. Clin. Biochem. Nutr. **3:** 1–9.
2. TOMITA, K., K. NAGATA, H. KONDO, T. SHIRAISHI, H. TSUBOTA, H. SUZUKI & H. OCHI. 1990. Thermostable glucokinase from *Bacillus stearothermophilus* and its analytical application. Ann. N.Y. Acad. Sci. **613:** 421–425.

3. TOMITA, K., A. SHIMIZU & M. MORINO. 1994. Some characteristics of glucokinase from
    Zymomonas mobilis. J. Technol. Res. Kanto Gakuin Univ. **37:** 111–114.
4. TOMITA, K. & K. NOMURA. 1995. Enzymes from *Zymomonas mobilis* and their application
    to glucose determination. Ann. N.Y. Acad. Sci. **750:** 338–343.
5. TOMITA, K. & K. IMAHORI. 1982. Synthesis of adenosine 5′-triphosphate derivatives in
    nonaqueous solvent and their substrate activities to kinases. J. Appl. Biochem. **4:** 234–
    238.

Enantioselective Synthesis of Aliphatic (*S*)-Cyanohydrins in Organic Solvents Using Hydroxynitrile Lyase from *Manihot esculenta*

HARALD WAJANT,[a] SIEGFRIED FÖRSTER,[b]
ACHIM SPRAUER,[c] FRANZ EFFENBERGER,[b]
AND KLAUS PFIZENMAIER[a]

[a] *Institut für Zellbiologie und Immunologie*
[b] *Institut für Organische Chemie und Isotopenforschung*
[c] *Institut für Technische Biochemie*
Universität Stuttgart
70569 Stuttgart, Germany

INTRODUCTION

(*S*)-Hydroxynitrile lyases [*S*-HNLs] have been employed as catalysts for enantio-selective addition of HCN to aldehydes or ketones, yielding (*S*)-α-hydroxynitriles in very high enantiomeric purity.[1,2] Optically active α-hydroxynitriles are interesting intermediates for the synthesis of α-hydroxy-acids, α-hydroxy-ketones, or β-ethanol-amines, all of which are important building blocks in organic synthesis.[2] A problem of all (*S*)-HNLs is the restricted availability. Therefore, expression cloning of (*S*)-HNLs will be necessary to establish HNL-catalyzed synthesis of (*S*)-cyanohydrins on a technical scale.

In the present study, we describe the purification and expression cloning of acetone cyanohydrin lyase from *Manihot esculenta* Crantz (cassava) (EC 4.1.2.37; MeHNL) and we demonstrate the potential use of MeHNL as a chiral catalyst for the synthesis of a broad range of optically active α-hydroxynitriles including keto-(*S*)-cyanohydrins.

MATERIALS AND METHODS

Molecular Cloning of MeHNL

The MeHNL gene was cloned in the expression vector pQE3 (Quiagen). For this purpose, the coding region of the MeHNL gene was amplified from oligo(dT)-primed first-strand cDNA from *Manihot esculenta* using a primer with 5′-overhangs encompassing BamH I restriction sites (forward primer: GCA GGG CCG GAT CCC ATT TCC AAA ATG GTA ACT GCA CA; rewind primer: GCA GGG CCG GAT CCA CC AAC GTG GAA CTC TCC CAT ATT—underlined sequences correspond to positions 16–39 and 933–910 of the MeHNL gene[3]). The in-frame insertion of the BamH I–digested PCR fragment into the BamH I site of pQE3

results in the plasmid pQE3-MeHNLwt, which was transformed in *E. coli* M15[pREP4] cells (Quiagen) for overexpression of MeHNL.

MeHNL Expression in E. coli M15[REP4] Cells

An overnight culture of a single colony in LB media containing ampicillin (100 μg/mL) and kanamycin (25 μg/mL) was used to inoculate 8 L of prewarmed LB media (+ antibiotics) and was grown again overnight at 37 °C. On the next day, this culture was diluted ten times in LB media (+ antibiotics) in a 100-L fermentor (Bioengineering). The cells were stirred at 30 °C for 1 hour and expression of recombinant MeHNL was induced by adding IPTG to a final concentration of 1 mM. The cells were grown for an additional 4 hours and harvested by cross-flow concentration (Maxisette system) using a 0.3-μm membrane (0.46 m^2) (Filtron). To remove the remaining LB media, the cells were centrifuged for 10 min at 8000 rpm in a JA14 rotor (Beckmann) and the supernatant was discarded. Then, the pellet was resuspended in 50 mM sodium acetate, pH 5.4 (1.5–2 L), and the cells were disrupted using high-pressure homogenization (500 bar, 3 cycles; Rannie-APV Mini-Lab). The temperature of the lysate was kept below 30 °C during the disruption. To destroy chromosomal DNA, which can interfere with the subsequent purification, benzoase (Merck) was added to a final concentration of 400 μg/L for 60 min at room temperature. Subsequently, the lysate was cleared by centrifugation at 8000 rpm in a JA14 rotor for 15 min and applied to a Q-sepharose FF XK 16/20 column, equilibrated in 20 mM sodium acetate, pH 5.4. The column was rinsed with buffer until the extinction reached the initial baseline. Bound protein was eluted with a linear gradient of NaCl at a flow rate of 5 mL/min. The fractions were assayed for acetone cyanohydrin lyase activity and samples were pooled based on their specific activity.

Five- to 10-mL aliquots of the protein sample were applied to a HiLoad 26/60 Superdex 200 prep grade column (Pharmacia), equilibrated in 20 mM Tris, pH 7.5, and 200 mM NaCl. Proteins were eluted at a flow rate of 1 mL/min and fractions with high specific activity were pooled.

Pooled fractions from gel filtration were diluted 1:4 with 20 mM Tris, pH 7.5, and were applied to Q-sepharose HP HR 10/10, equilibrated in 20 mM Tris, pH 7.5. After sample application, the column was washed with 30 mL of starting buffer. Elution of MeHNL was carried out with a 200-mL linear gradient of 0–500 mM NaCl in 20 mM Tris, pH 7.5, at a flow rate of 3 mL/min.

SDS-PAGE

Electrophoresis was performed according to Laemmli.[4] Acrylamide gels were silver-stained using the procedure described by Blum et al.[5]

Enzyme Assays

The activity of MeHNL was assayed by measuring the HCN liberated during decomposition of acetone cyanohydrin according to Selmar et al.[6] The amount of

MeHNL that decomposes 1 μmol acetone cyanohydrin in 60 s is defined as 1 unit. Specific activity was expressed in U/mg. Protein concentrations were measured by a modified Lowry assay (BCA assay kit, Pierce, Rockford, Illinois) with bovine serum albumin as standard.

RESULTS AND DISCUSSION

Purification of MeHNL from Cassava Leaves

The purification of MeHNL from leaves of *Manihot esculenta* was essentially performed as previously described.[7] About 1.2 mg of purified MeHNL with an activity of 110 was obtained from 800 g of fresh leaves.

Overexpression of MeHNL

To obtain large amounts of MeHNL, the cDNA of MeHNL was cloned into pQE3 and overexpressed in *E. coli* M15[pREP4] cells. Activity measurements of the lysates of IPTG-induced pQE3-MeHNLwt-transformed cells showed an activity of 0.5 U per mL of culture, whereas uninduced cells exerted no MeHNL activity.

Lysates from mock-transformed, uninduced, and IPTG-induced pQE3-MeHNLwt-transformed cells were analyzed on 13.5% SDS-PAGE. As compared to control cells, induced cells transformed with pQE3-MeHNLwt showed the appearance of an additional bright band at $M_r = 30,000$ that comigrated with purified MeHNL isolated from leaves of *Manihot esculenta* (data not shown).

Purification of Recombinant MeHNL

IPTG-induced cells transformed with pQE3-MeHNLwt were lysed in 50 mM sodium acetate, pH 5.4, and treated with benzoase. Cleared supernatants obtained by centrifugation were applied to a Q-sepharose FF XK 16/20 column. MeHNL was eluted from Q-sepharose FF with a linear NaCl gradient. Only a single peak of MeHNL activity was detected. The fractions with MeHNL activity were combined, concentrated, and applied to gel filtration chromatography. Final purification of MeHNL was performed using anion exchange chromatography on Q-sepharose HP (pH 7.5) (see TABLE 1). MeHNL began to elute at a sodium concentration of 160 mM. Analysis of active fractions in SDS-PAGE reveals MeHNL of high purity (FIGURE 1). The specific activity of purified MeHNL was 80 U/mg, which is in good accordance with 91.6 U/mg described for MeHNL isolated from leaves of *Manihot esculenta*. A typical 80-L culture of induced cells yields about 0.5 g (calculated, based on enzyme activity) of soluble MeHNL in the lysate and about 150 mg of pure enzyme after purification. Several fractions of enriched preparations of MeHNL were also obtained during the purification. The cellular debris contains a high amount of unsoluble, mainly inactivated, MeHNL (data not shown).

TABLE 1. Purification of Recombinant MeHNL

Step	Total Protein (mg)	Total Activity (units)	Specific Activity (units/mg)	Yield (%)	Purification (fold)
crude extract	180	3000	16.7	100	—
Q-sepharose FF, pH 5.4	30	2025	67.5	67.5	4.1
gel filtration	25	1900	76	63	4.6
Q-sepharose FF, pH 7.5	19	1634	86	54	5.1

Synthesis of (S)-Cyanohydrins Using Recombinant MeHNL

In our experiments, the reaction was carried out in organic media by using diisopropyl ether as an organic solvent and HCN as a cyanide source. In standard reactions, a 5-fold molar excess of cyanide over the carbonyl compound was used (0.5 mmol versus 2.5 mmol in 5 mL). As described elsewhere,[7] experiments with MeHNL isolated from the natural source suggest a broad substrate range of MeHNL. However, the ee values obtained in these initial experiments were rather poor. Thorough optimization of the MeHNL-catalyzed synthesis of (S)-cyanohydrins was hampered through the limited availability of the enzyme.
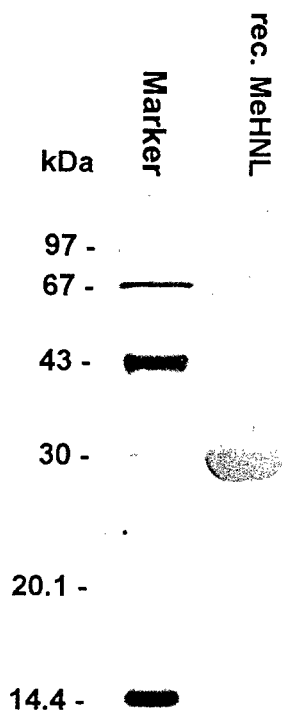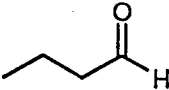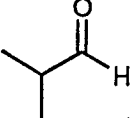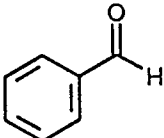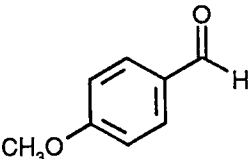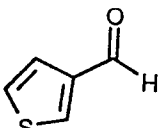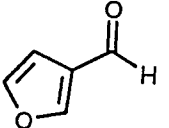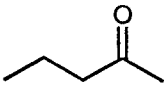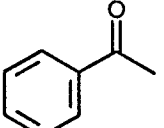
FIGURE 1. Analysis of purified recombinant MeHNL: 500 ng of recombinant MeHNL was treated with 40 mM dithiothreitol and subjected to SDS-PAGE (13.5% polyacrylamide gel, silver-stained).

TABLE 2. Synthesis of (*S*)-Cyanohydrins Using MeHNL

Carbonyl	MeHNL from Leaves (25 U/mL)		MeHNL from *E. coli* (900 U/mL)	
	Yield (%)	ee (%)	Yield (%)	ee (%)
	70	80	92	90
	—	—	91	95
	34	90	100	98
	—	—	82	98
	90	38	98	98
	—	—	98	92
	n.d.	74	36	69
	—	—	13	78

Using the aforementioned recombinant enzyme, which is easily available in large amounts from *E. coli* cultures, we have improved the reactions significantly. Usage of a high-concentrated MeHNL preparation for immobilization increases the enzyme activity in a standard reaction by 4–10 times (data not shown). As shown in TABLE 2, MeHNL can utilize a broad range of carbonyls for synthesis of (*S*)-cyanohydrins. Aliphatic, aromatic, and heteroaromatic aldehydes as well as ketones can be converted in the corresponding (*S*)-cyanohydrins with high enantiomeric excess, without alterations in the reaction conditions.

REFERENCES

1. EFFENBERGER, F., B. HÖRSCH, S. FÖRSTER & T. ZIEGLER. 1990. Enzyme-catalyzed synthesis of (*S*)-cyanohydrins and subsequent hydrolysis to (*S*)-α-hydroxy-carboxylic acids. Tetrahedron Lett. **31:** 1249–1252.
2. SMITSKAMPS-WILMS, E., J. BRUSSEE, G. J. M. VAN SCHARRENBURG, J. B. SLOOTHAAK & A. VAN DER GEN. 1991. Hydroxynitrile lyases from almond and sorghum as biocatalysts. Recl. Trav. Chim. Pays-Bas **110:** 209–215.
3. HUGHES, J., F. J. P. DE C. CARVALHO & M. A. HUGHES. 1994. Purification, characterization, and cloning of α-hydroxynitrile lyase from cassava (*Manihot esculenta* Crantz). Arch. Biochem. Biophys. **311:** 496–502.
4. LAEMMLI, U. K. 1970. Cleavage of structural proteins during the assembly of the head of bacteriophage T4. Nature **227:** 680–685.
5. BLUM, H., H. BEIER & H. J. GROSS. 1987. Improved silver staining of plant proteins, RNA, and DNA in polyacrylamide gels. Electrophoresis **8:** 93–99.
6. SELMAR, D., F. J. P. DE C. CARVALHO & E. E. CONN. 1987. A colorimetric assay for α-hydroxynitrile lyase. Anal. Biochem. **166:** 208–211.
7. WAJANT, H., S. FÖRSTER, H. BÖTTINGER, F. EFFENBERGER & K. PFIZENMAIER. 1995. Acetone cyanohydrin lyase from *Manihot esculenta* (cassava) is serologically distinct from other hydroxynitrile lyases. Plant Sci. **108:** 1–11.

Cross-Linked Crystals of Subtilisin

Versatile Catalysts for Organic Synthesis

YI-FONG WANG, KIRILL YAKOVLEVSKY,
NAZER KHALAF, BAILING ZHANG,
AND ALEXEY L. MARGOLIN

Altus Biologics Incorporated
Cambridge, Massachusetts 02139

Enzyme-catalyzed reactions have long been recognized as useful technology for organic synthesis. Currently, almost 3000 enzymes, which catalyze nearly all types of organic reactions, are known. In the last two decades, more than 5000 papers related to enzyme-catalyzed reactions have been published.[1] Despite the enormous potential and many benefits of enzymatic catalysis, only a few enzymatic processes are used in the syntheses of fine chemicals and pharmaceuticals on an industrial scale.[2] The reasons for the limited industrial use of enzymes are the poor stability of enzymes, the variability in performance, and the difficulties in handling.

We have found that a recently developed technology, cross-linked enzyme crystals (CLECs™), successfully addresses all of these problems.[3] CLECs are prepared by growing enzyme microcrystals followed by cross-linking with a bifunctional agent such as glutaraldehyde. CLECs exhibit remarkable characteristics that are superior to both soluble and immobilized enzymes. CLECs are pure and highly stable heterogeneous catalysts. They remain active in environments where conventional enzymes often do not, including prolonged exposure to elevated temperature, aqueous-organic mixtures, and neat organic solvents. They are also stable against autolysis and exogenous proteolytic degradation. They are insoluble, but active, in both aqueous and organic solvents. They can be easily separated from the reaction mixture and reused. We have applied CLEC technology to the protease subtilisin. Herein, we describe the stability, activity, and versatile synthetic utility of subtilisin CLECs.

STABILITY

Subtilisin is one of the serine proteases. It has been used in organic synthesis for the coupling of amino acid derivatives and oligopeptides. In enzymatic peptide synthesis, neat organic or high concentrations of organic solvents are advantageous to manipulate reaction kinetics and equilibria to increase product yield.[4] Unfortunately, soluble subtilisin is intrinsically unstable and has low catalytic activity in neat or high concentrations of organic solvents.[5] Furthermore, the contamination of products with autolyzed peptide fragments increases the difficulty in the product purification, especially in peptide synthesis. We have found that the cross-linked enzyme crystals of subtilisin are highly stable both at elevated temperature and in high concentrations of organic solvents. Subtilisin CLEC retains full activity after 7

days of incubation at 60 °C and in high concentrations of organic solvents, including 50% acetone, 50% DMF, and 70% DMF. This solid catalyst is also stable against autolysis: after 5 days of incubation at 40 °C, no degraded peptide fragments were detected.

ACTIVITY IN ORGANIC SOLVENTS

Subtilisin CLEC (ChiroCLEC™-BL) is highly active in both hydrophobic (isooctane, toluene, and *t*-butyl methyl ether) and polar organic solvents (alcohols, acetone, THF, DMF, and pyridine) (FIGURE 1). As for monomeric protein catalysts, CLECs required a small amount of water when used in neat organics,[6] especially in polar solvents such as acetone and DMF. The complete absence of water resulted in the loss of catalyst selectivity and, ultimately, in the complete loss of activity in solvents such as DMF (FIGURE 1). The activity in acetone with 1% water was much higher than in dry acetone. For nonpolar organic solvents such as isooctane, toluene, or *t*-butyl methyl ether, however, we found that it was not necessary to add water. The catalyst exhibited high activity in these hydrophobic solvents.

VERSATILE SYNTHETIC UTILITY

Resolution of Natural and Unnatural Amino Acids

ChiroCLEC-BL accepts both natural and unnatural amino acids as substrates.[7] It exhibits high activity and enantioselectivity in the resolution of amino acids. *N*-Acetyl-
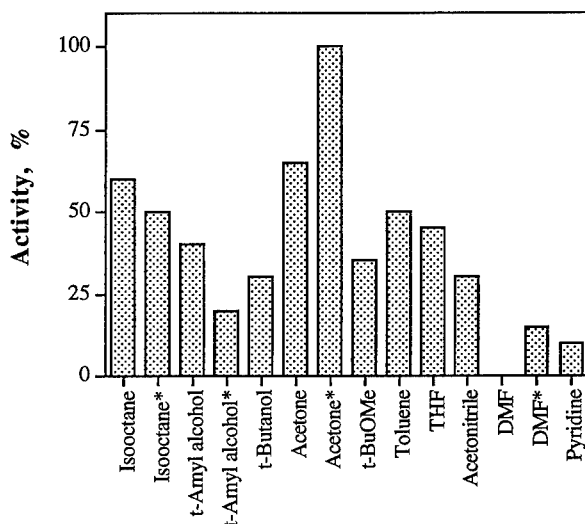
FIGURE 1. Relative activity of ChiroCLEC-BL in organic solvents. Assay: transesterification of *N*-Ac-L-Phe-OEt with 1-propanol in isooctane; 2.5-h incubation at 40 °C; (*) with 1% water.
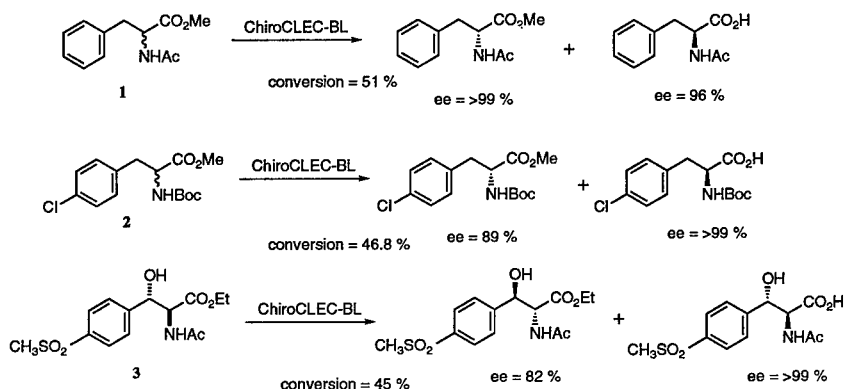
FIGURE 2. Resolution of amino acids.

phenylalanine methyl ester **1** was resolved to give L-acid product and the remaining D-ester in 96% and >99% optical purity, respectively (FIGURE 2). The unnatural acids, *N*-Boc-*p*-chlorophenylalanine methyl ester **2** and *threo*-*N*-acetyl-*p*-sulfonylphenylalanine ethyl ester **3**, were also resolved by this catalyst with high enantioselectivity.

Resolution of meso-*Diester* and pro-*Chiral Diester*

ChiroCLEC-BL also accepted simple organic esters as substrates.[8] The *meso*-diester **4** was resolved to give a monoester with 96% optical purity (FIGURE 3). In this reaction, the diester **4** was first hydrolyzed to its corresponding monoacid **4a**, which underwent further hydrolysis by the same enzyme to form a diacid. The optical purity of monoacid **4a** was increased in the second step. This indicates that the catalyst has the same enantiopreference towards the monoacid as towards the diester.[9] The *pro*-chiral diester, diethyl acetylamino (methyl) malonate **5**, was enantioselectively hydrolyzed to give 97% of the corresponding monoacid with 80% optical purity.

Resolution of Amine and Alcohol Compounds

ChiroCLEC-BL also was used to perform resolutions in neat organic solvents. Both amine and alcohol compounds[10] were resolved via transesterification in neat organic solvents. α-(1-Naphthyl)ethylamine **6** was resolved to give the corresponding butyramide and the remaining amine with 97% and 74% ee, respectively (FIGURE 4). α-Methyltryptamine **7** was resolved by this catalyst to give the *R*-amine with an ee greater than 99% at 54% conversion. The optical purity of the amide product was 94% when the conversion was 20%. The alcohol, *sec*-phenethyl alcohol **8**, was also resolved with high enantioselectivity. The optical purity of the ester product and the remaining alcohol was 51% and >99% at 65% conversion, respectively. Surprisingly, the catalyst showed no enantioselectivity in the hydrolysis resolution of the corresponding butyrate in aqueous buffer.
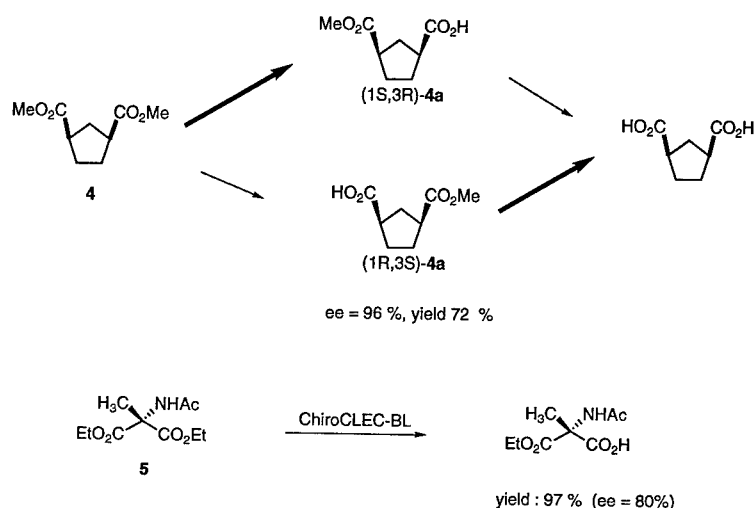
FIGURE 3. Resolution of diesters.

Regioselective Reactions

ChiroCLEC-BL could also perform regioselective hydrolysis and transesterification. Multifunctional amino acid diesters, sugar derivatives, and steroid derivatives were selectively hydrolyzed or esterified.[11] The α-ester of aspartic dibenzyl ester 9 was selectively hydrolyzed to give 97% corresponding monoacid (FIGURE 5). The 3-hydroxyl group of castanospermine 11 and the 17-hydroxyl group of 5α-androstane-3β,17β-diol 10 were selectively esterified to give their corresponding monoesters.
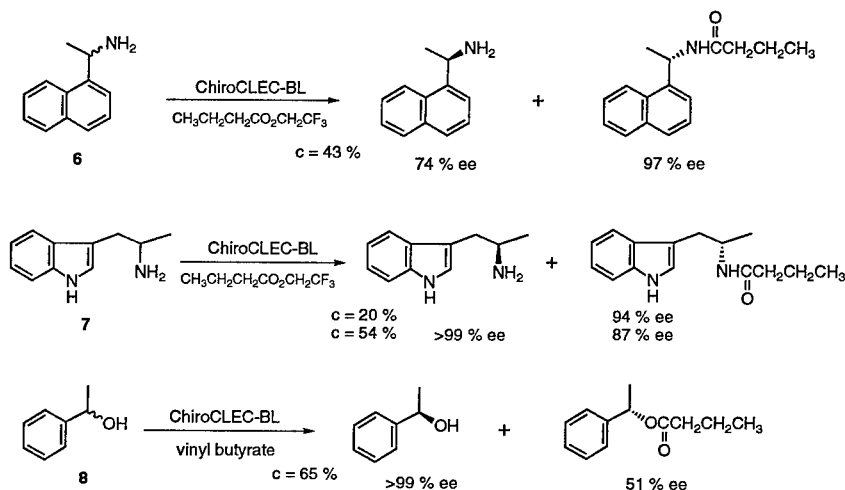
FIGURE 4. Resolution of amine and alcohol compounds.
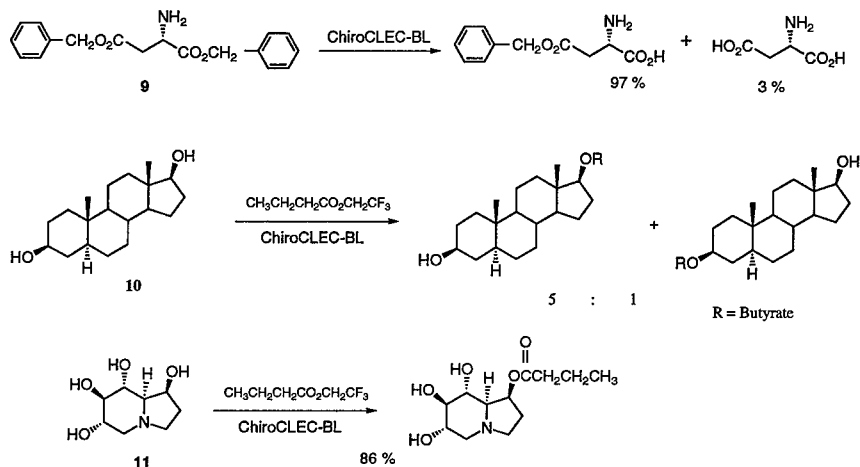
FIGURE 5. Regioselective reactions.

Mild Hydrolysis of Amino Acid Amides and Peptide Amides

One of the major problems in the chemical hydrolysis of amino acid amides is racemization. We found that ChiroCLEC-BL can hydrolyze amino acid amides under mild reaction conditions without racemization. The amino acid amides can be both protected and unprotected. For example, both protected (including Ac, Boc, and Cbz) and unprotected tyrosinamide **12** were hydrolyzed to give their corresponding acids in quantitative yield (FIGURE 6). Furthermore, not only the tyrosinamide, but also other amides (such as phenylalaninamide and tryptophanamide) and the
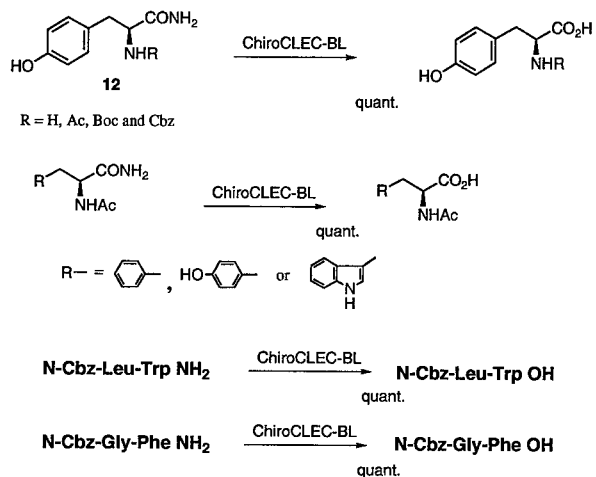
FIGURE 6. Mild hydrolysis of amides.

Transesterification
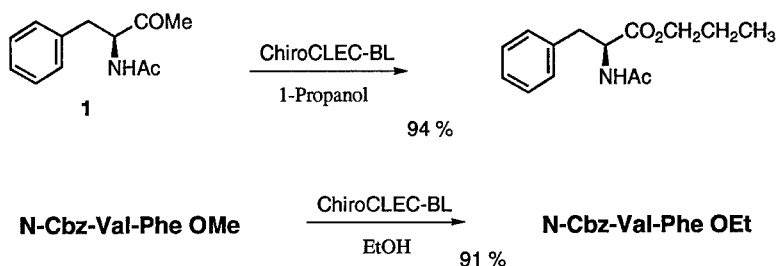
FIGURE 7. Transesterification.

terminal amide of peptide amides (such as N-Cbz-Leu-Trp-NH$_2$ and N-Cbz-Gly-Phe-NH$_2$) were hydrolyzed with high chemical yield.

Transesterification of Amino Acid Esters

ChiroCLEC-BL could also perform the transesterification of amino acid esters and peptide esters (FIGURE 7). For example, N-acetyl-phenylalanine methyl ester and N-Cbz-Val-Phe methyl ester were converted with high yield to the corresponding propyl ester and ethyl ester, respectively.

PRODUCTIVITY

The productivity of ChiroCLEC-BL was quite impressive in typical hydrolysis and transesterification reactions. The minimal productivity based on the weight ratio of substrate to catalyst was 2000:1 in the resolution of N-acetyl-phenylalanine methyl ester, 600:1 in the transesterification of N-acetyl-L-phenylalanine ethyl ester, and 300:1 in the hydrolysis of N-acetyl-L-tyrosinamide (FIGURE 8). In all of these examples, the catalyst was still fully active and functioning on completion of the reaction. As such, the productivity indicated is a lower limit.
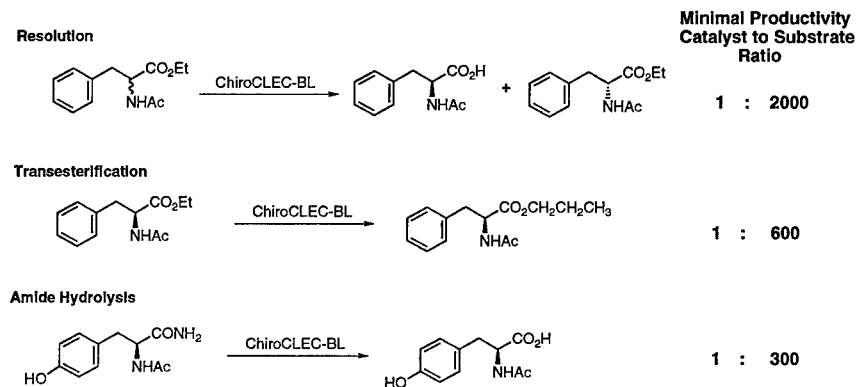
FIGURE 8. Minimal productivity.

CONCLUSIONS

Subtilisin CLEC is a versatile catalyst. It can be used for chiral resolution, regioselective reactions, mild amide hydrolysis, and transesterification. The catalyst is highly stable and active in both aqueous and organic solvents. It is also resistant to inactivation by elevated temperature and proteolysis. By virtue of these characteristics, subtilisin CLEC is a useful catalyst for organic synthesis both in the laboratory and in large-scale applications.

REFERENCES

1. (a) SANTANIELLO, E., P. FERRABOSCHI, P. GRISENTI & A. MANZOCCHI. 1992. Chem. Rev. **92:** 1071; (b) BOLAND, W., C. FROL & M. LORENZ. 1991. Synthesis, p. 1049; (c) CROUT, D. H. G. & M. CHRISTEN. 1989. *In* Modern Synthetic Methods, p. 1–114. Springer-Verlag. Berlin/New York; (d) FABER, K. & M. C. R. FRANSSEN. 1993. Trends Biochem. Technol. **11:** 461; (e) WONG, C. H. & G. M. WHITESIDES. 1994. Enzymes in Synthetic Organic Chemistry. Pergamon. Elmsford, New York; (f) POPPE, L. & L. NOVAK. 1992. Selective Biocatalysis. Verlag Chemie. Weinheim; (g) FABER, K. 1995. Biotransformations in Organic Chemistry—A Textbook. Second edition. Springer-Verlag. Berlin/New York.
2. (a) MATSUMOTO, K. 1993. *In* Industrial Application of Immobilized Biocatalysis. A. Tanaka, T. Tosa & T. Kobayashi, Eds.: 67–88. Dekker. New York; (b) GERHARTZ, W., Ed. 1990. Enzyme in Industry. Verlag Chemie. Weinheim; (c) FABER, K. & M. C. R. FRANSSEN. 1993. TIBTECH **11:** 461.
3. (a) ST. CLAIR, N. L. & M. NAVIA. 1992. J. Am. Chem. Soc. **114:** 7314; (b) PERSICHETTI, R. A., N. L. ST. CLAIR, J. P. GRIFFITH, M. A. NAVIA & A. L. MARGOLIN. 1995. J. Am. Chem. Soc. **117:** 2732; (c) LALONDE, J. J., C. GOVARDHAN, N. KHALAF, A. G. MARTINEZ, K. VISURI & A. L. MARGOLIN. 1995. J. Am. Chem. Soc. **117:** 6845.
4. (a) HOMANDBERG, G. A., J. A. MATTIS & M. LASKOVSKI, JR. 1978. Biochemistry **17:** 5220; (b) MARGOLIN, A. L. & A. M. KLIBANOV. 1987. J. Am. Chem. Soc. **109:** 3802; (c) BARBAS, C. F., J. R. MATOS, J. B. WEST & C. H. WONG. 1988. J. Am. Chem. Soc. **110:** 5162; (d) CHEN, S. T., S. Y. CHEN & K. T. WANG. 1992. J. Org. Chem. **57:** 6960.
5. (a) WONG, C. H. 1989. Science **244:** 1145; (b) TOONE, E. J., E. S. SIMON, M. D. BEDNARSKI & G. M. WHITESIDES. 1989. Tetrahedron **45:** 5365; (c) SEARS, P., M. SCHUSTER, P. WANG, K. WITTE & C. H. WONG. 1994. J. Am. Chem. Soc. **116:** 6521.
6. (a) HALLING, P. J. 1994. Enzyme Microb. Technol. **16:** 178; (b) KLIBANOV, A. M. 1989. TIBS **14:** 141–144.
7. (a) WONG, C. H., S. T. CHEN, W. J. HENNEN, J. A. BIBBS, Y-F. WANG, J. L. C. LIU, M. W. PANTOLIANO, M. WHITLOW & P. N. BRYAN. 1990. J. Am. Chem. Soc. **112:** 945; (b) IMPERIALI, B., T. J. PRINS & S. L. FISHER. 1993. J. Org. Chem. **58:** 1613; (c) CHENEVERT, R., M. LETOURNEAU & S. THIBOUTOT. 1990. Can. J. Chem. **68:** 960; (d) LEANNA, M. R. & H. E. MORTON. 1993. Tetrahedron Lett. **34:** 4485.
8. (a) MAZDIYASNI, H., D. B. KONOPACKI, D. A. DICKMAN & T. M. ZYDOWSKY. 1993. Tetrahedron Lett. **34:** 435; (b) CHENEVERT, R. & R. MARTIN. 1992. Tetrahedron Asymmetry **3:** 199.
9. WANG, Y-F., C-S. CHEN, G. GIRDAUKAS & C. J. SIH. 1984. J. Am. Chem. Soc. **106:** 3695.
10. KITAGUCHI, H., P. A. FITZPATRICK, J. E. HUBER & A. M. KLIBANOV. 1989. J. Am. Chem. Soc. **111:** 3094.
11. (a) WU, S-H., L-C. LO, S-T. CHEN & K-T. WANG. 1989. J. Org. Chem. **54:** 4220; (b) RIVA, S., J. CHOPINEAU, A. P. G. KIEBOON & A. M. KLIBANOV. 1988. J. Am. Chem. Soc. **110:** 584; (c) MARGOLIN, A. L., D. L. DELINCK & M. R. WHALON. 1990. J. Am. Chem. Soc. **112:** 2849.

Enzymatic Preparation of D(−)-Tartaric Acid from *cis*-Epoxysuccinic Acid by *Pseudomonas putida* MCI3037

KENJI YAMAGISHI AND HIROSHI CHO

Mitsubishi Chemical Corporation
Yokohama Research Center
Yokohama 227, Japan

D(−)-Tartaric acid is a useful compound as a chiral auxiliary in asymmetric synthesis. Although the opposite enantiomer, L(+)-tartaric acid, is a cheap by-product of the wine industry, D(−)-tartaric acid occurs only rarely in nature.

D(−)-Tartaric acid is obtained by optical resolution of its racemic form with *Aerobacter* sp.[1] and also can be synthesized from *cis*-epoxysuccinic acid (CES) by *Alcaligenes levotartaricus*.[2]

In this paper, we report the isolation of a new microbial strain, identified as a *Pseudomonas putida,* which produces D(−)-tartaric acid from CES in high yield. The purification and initial characterization of CES-hydratase, which produces D(−)-tartaric acid from CES, are also described.

ISOLATION OF THE NEW MICROORGANISM AND ITS PRODUCTIVITY

To produce D(−)-tartaric acid from CES that was obtained by epoxidizing maleic acid with hydrogen peroxide, we screened a number of CES-utilizing microorganisms for D(−)-tartaric acid–producing activity in an intact cell system. Only a few microorganisms were capable of hydrolyzing the epoxy-ring of CES. One stain, MCI3037, which produced D(−)-tartaric acid from CES, was identified taxonomically as *Pseudomonas putida* according to *Bergey's Manual of Systematic Bacteriology*.[3] The culture and reaction conditions for this strain were investigated. Under the best conditions, 98.0 g/L of D(−)-tartaric acid was produced from 88.0 g/L of CES with a molar yield of 98% in the presence of *Pseudomonas putida* (FIGURE 1). The enantiomeric purity of D(−)-tartaric acid produced by this strain was more than 99%.

PURIFICATION AND CHARACTERIZATION OF CES-HYDRATASE

The enzyme was purified 321-fold, with a total yield of 20.7%. SDS-PAGE revealed a single band, corresponding to a protein with a molecular weight of 34.2 kDa, and showed that the enzyme was electrophoretically homogeneous. The molecular weight of the native protein was estimated to be 69 kDa by gel filtration through Asahipak GS-520. These results suggest that the enzyme consists of two subunits.

Maximal enzyme activity was observed at approximately 47 °C. At temperatures above 50 °C, inactivation of the enzyme was observed during the time of the activity assay (60 min). The enzyme had a pH optimum of around 7.5, and citrate buffer (100 mM) inhibited the enzyme activity.

The activity of this enzyme toward CES and seven related organic acids (D,L-*trans*-epoxysuccinic acid, acetylenedicarboxylic acid, fumaric acid, maleic acid, *cis*-aconic acid, *trans*-aconic acid, and mesaconic acid) was examined. Only CES was active as a substrate for the enzyme, and the Michaelis constant of the enzyme for CES was 273 mM in phosphate buffer (pH 7.5). Among various organic acids tested [D,L-*trans*-epoxysuccinic acid, acetylenedicarboxylic acid, fumaric acid, maleic acid, L(+)-tartaric acid, D(−)-tartaric acid, *meso*-tartaric acid, L-malic acid, D-malic acid], *meso*-tartaric acid and *trans*-epoxysuccinic acid were effective inhibitors of the enzyme.

FIGURE 1. Formation of D(−)-tartaric acid from *cis*-epoxysuccinic acid by *Pseudomonas putida* MCI3037. The reaction was carried out at 30 °C in 10 mL of a reaction mixture (pH 7.5) containing 6 mM *cis*-epoxysuccinic acid and intact cells harvested from 10 mL of the culture of *Pseudomonas putida* MCI3037. Symbols: (O) D(−)-tartaric acid; (●) *cis*-epoxysuccinic acid.
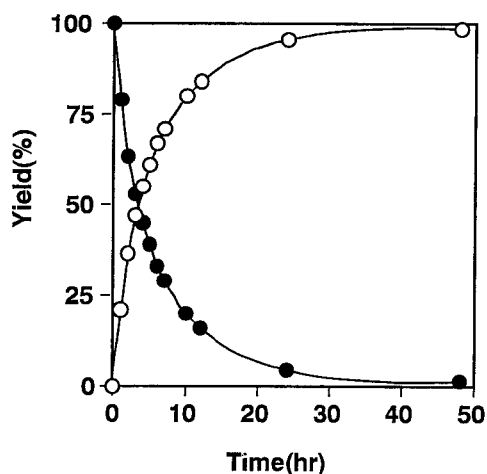
CONCLUSIONS

The findings of this preliminary study are promising with regard to the potential commercial production of D(−)-tartaric acid from CES. The major results of this study can be summarized as follows:

1. isolation of a new microorganism that produces D(−)-tartaric acid from CES;
2. the enantiomeric purity of D(−)-tartaric acid produced by this strain is more than 99%;
3. purification of CES-hydratase, which produces D(−)-tartaric acid from CES.

REFERENCES

1. TAKEDA, H. 1975. Jpn. Kokai Tokkyo JP 48-76579.
2. SATO, K. & K. YAUTI. 1982. Jpn. Kokai Tokkyo JP 57-1990.
3. NORBERTO PALLERONI, J. 1981. *In* Bergey's Manual of Systematic Bacteriology. Volume 1, p. 141–199. Williams & Wilkins. Baltimore.

Index of Contributors

787